Mathematical Problems in Engineering

New Developments in Mathematical Control and Information for Fuzzy Systems

Guest Editors: Hamid Reza Karimi, Mohammed Chadli, and Peng Shi

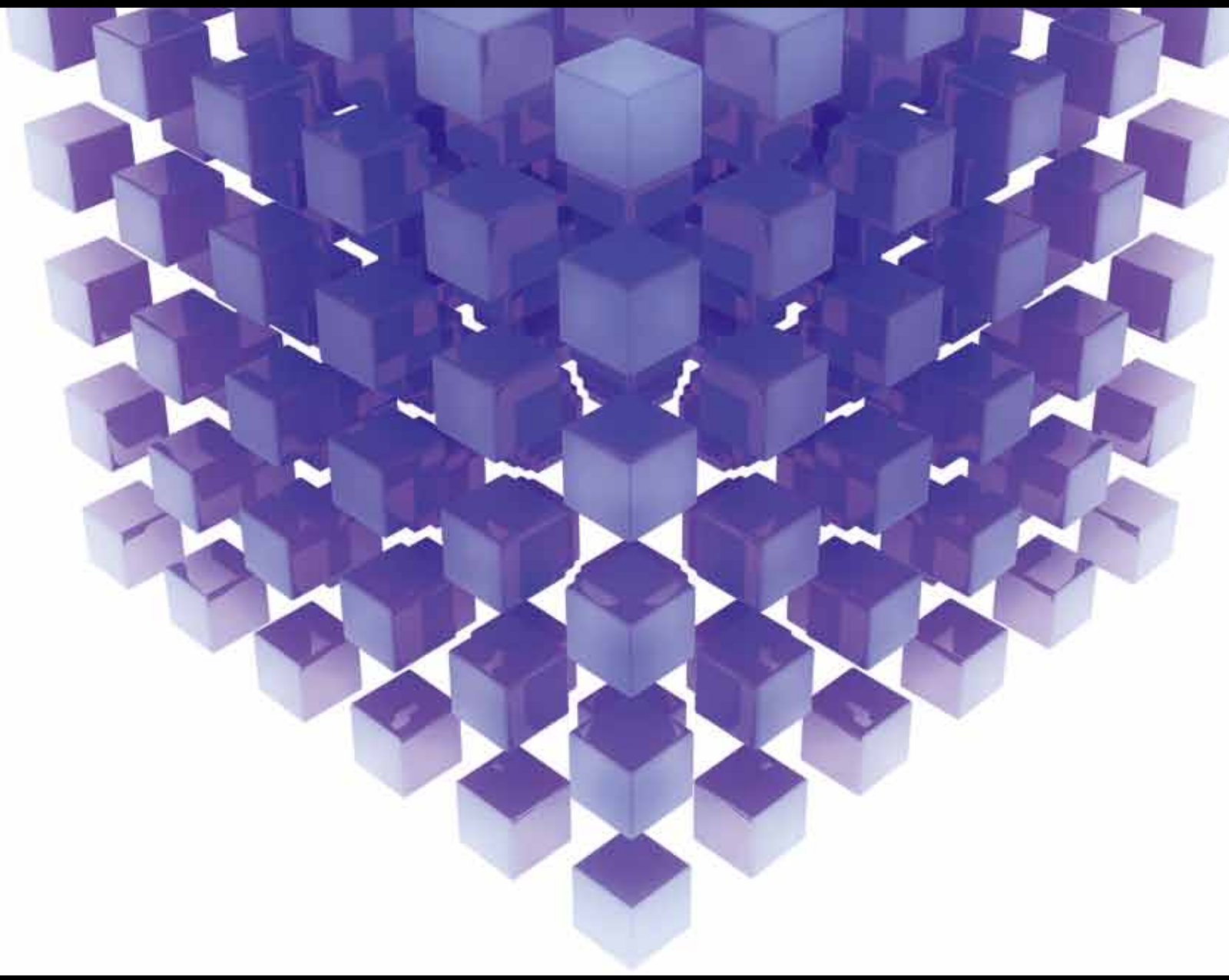

New Developments in Mathematical Control and Information for Fuzzy Systems

Mathematical Problems in Engineering

New Developments in Mathematical Control and Information for Fuzzy Systems

Guest Editors: Hamid Reza Karimi, Mohammed Chadli, and Peng Shi

Copyright © 2013 Hindawi Publishing Corporation. All rights reserved.

This is a special issue published in "Mathematical Problems in Engineering." All articles are open access articles distributed under the Creative Commons Attribution License, which permits unrestricted use, distribution, and reproduction in any medium, provided the original work is properly cited.

Editorial Board

Mohamed Abd El Aziz, Egypt
Eihab M. Abdel-Rahman, Canada
Rashid K. Abu Al-Rub, USA
Sarp Adali, South Africa
Salvatore Alfonzetti, Italy
Igor Andrianov, Germany
Sebastian Anita, Romania
W. Assawinchaichote, Thailand
Erwei Bai, USA
Ezzat G. Bakhoum, USA
José Manoel Balthazar, Brazil
R. K. Bera, India
Christophe Bérenguer, France
Jonathan N. Blakely, USA
Stefano Boccaletti, Spain
Stephane P. A. Bordas, USA
Daniela Boso, Italy
M. Boutayeb, France
Michael J. Brennan, UK
Salvatore Caddemi, Italy
Piermarco Cannarsa, Italy
Jose E. Capilla, Spain
Carlo Cattani, Italy
Marcelo Cavalcanti, Brazil
Diego J. Celentano, Chile
Mohammed Chadli, France
Arindam Chakraborty, USA
Yong-Kui Chang, China
Michael J. Chappell, UK
Xinkai Chen, Japan
Kui Fu Chen, China
Kue-Hong Chen, Taiwan
Jyh-Hong Chou, Taiwan
Slim Choura, Tunisia
Cesar Cruz-Hernandez, Mexico
Swagatam Das, India
Filippo de Monte, Italy
Maria de Pinho, Portugal
Antonio Desimone, Italy
Yannis Dimakopoulos, Greece
Baocang Ding, China
Joao B. R. Do Val, Brazil
Daoyi Dong, Australia
B. Dubey, India
Horst Ecker, Austria
M. Onder Efe, Turkey
Elmetwally Elabbasy, Egypt
Alex Elias-Zuniga, Mexico
Anders Eriksson, Sweden
Vedat S. Erturk, Turkey
Qi Fan, USA
Moez Feki, Tunisia
Ricardo Femat, Mexico
Robertt Fontes Valente, Portugal
Claudio Fuerte-Esquivel, Mexico
Zoran Gajic, USA
Ugo Galvanetto, Italy
Furong Gao, Hong Kong
Xin-Lin Gao, USA
Behrouz Gatmiri, Iran
Oleg V. Gendelman, Israel
Didier Georges, France
Paulo Batista Gonçalves, Brazil
Oded Gottlieb, Israel
Fabrizio Greco, Italy
Quang Phuc Ha, Australia
M. R. Hajj, USA
Thomas Hanne, Switzerland
Katica Hedrih, Serbia
M. I. Herreros, Spain
Wei-Chiang Hong, Taiwan
Jaromir Horacek, Czech Republic
Gordon Huang, Canada
Chuangxia Huang, China
Huabing Huang, China
Yi Feng Hung, Taiwan
Hai-Feng Huo, China
Asier Ibeas, Spain
Anuar Ishak, Malaysia
Reza Jazar, Australia
Zhijian Ji, China
Jun Jiang, China
J. J. Judice, Portugal
Tadeusz Kaczorek, Poland
Tamas Kalmar-Nagy, USA
Tomasz Kapitaniak, Poland
Hamid Reza Karimi, Norway
Metin O. Kaya, Turkey
Nikolaos Kazantzis, USA
Farzad Khani, Iran
Kristian Krabbenhoft, Australia
Ren-Jieh Kuo, Taiwan
Jurgen Kurths, Germany
Claude Lamarque, France
Marek Lefik, Poland
Stefano Lenci, Italy
Roman Lewandowski, Poland
Shanling Li, Canada
Ming Li, China
Jian Li, China
Shihua Li, China
Teh-Lu Liao, Taiwan
Panos Liatsis, UK
Jui-Sheng Lin, Taiwan
Yi-Kuei Lin, Taiwan
Shueei M. Lin, Taiwan
Wanquan Liu, Australia
Bin Liu, Australia
Yuji Liu, China
Paolo Lonetti, Italy
Vassilios C. Loukopoulos, Greece
Chien-Yu Lu, Taiwan
Junguo Lu, China
Alexei Mailybaev, Brazil
Manoranjan K. Maiti, India
Oluwole Daniel Makinde, South Africa
Rafael Martinez-Guerra, Mexico
Driss Mehdi, France
Roderick Melnik, Canada
Xinzhu Meng, China
Yuri V. Mikhlin, Ukraine
Gradimir Milovanovic, Serbia
Ebrahim Momoniat, South Africa
Trung Nguyen Thoi, Vietnam
Hung Nguyen-Xuan, Vietnam
Ben T. Nohara, Japan
Sotiris Ntouyas, Greece
Gerard Olivar, Colombia
Claudio Padra, Argentina
Bijaya Ketan Panigrahi, India
Francesco Pellicano, Italy
Matjaz Perc, Slovenia
Vu Ngoc Phat, Vietnam
Alexander Pogromsky, The Netherlands
Seppo Pohjolainen, Finland

Stanislav Potapenko, Canada
Sergio Preidikman, USA
Carsten Proppe, Germany
Hector Puebla, Mexico
Justo Puerto, Spain
Dane Quinn, USA
Kumbakonam Rajagopal, USA
Gianluca Ranzi, Australia
Sivaguru Ravindran, USA
G. Rega, Italy
Pedro Ribeiro, Portugal
J. Rodellar, Spain
Rosana Rodriguez-Lopez, Spain
Alejandro J. Rodriguez-Luis, Spain
Ignacio Romero, Spain
Hamid Ronagh, Australia
Carla Roque, Portugal
Rubén Ruiz García, Spain
Manouchehr Salehi, Iran
Miguel A. F. Sanjuán, Spain
Ilmar Ferreira Santos, Denmark
Nickolas S. Sapidis, Greece
Evangelos J. Sapountzakis, Greece
Bozidar Sarler, Slovenia
Andrey V. Savkin, Australia
Massimo Scalia, Italy
Mohamed A. Seddeek, Egypt
Alexander P. Seyranian, Russia
Leonid Shaikhet, Ukraine
Cheng Shao, China
Bo Shen, Germany
Daichao Sheng, Australia
Tony Sheu, Taiwan
Jian-Jun Shu, Singapore
Zhan Shu, UK
Dan Simon, USA
Luciano Simoni, Italy
Grigori M. Sisoev, UK
Christos H. Skiadas, Greece
Davide Spinello, Canada
Sri Sridharan, USA
Rolf Stenberg, Finland
Jitao Sun, China
Xi-Ming Sun, China
Changyin Sun, China
Andrzej Swierniak, Poland
Yang Tang, Germany
Allen Tannenbaum, USA
Cristian Toma, Romania
Irina N. Trendafilova, UK
Alberto Trevisani, Italy
Jung-Fa Tsai, Taiwan
Kuppalapalle Vajravelu, USA
Victoria Vampa, Argentina
Josep Vehi, Spain
Stefano Vidoli, Italy
Dan Wang, China
Youqing Wang, China
Yongqi Wang, Germany
Moran Wang, China
Cheng C. Wang, Taiwan
Yijing Wang, China
Xiaojun Wang, China
Gerhard-Wilhelm Weber, Turkey
Jeroen Witteveen, USA
Kwok-Wo Wong, Hong Kong
Zheng-Guang Wu, China
Ligang Wu, China
Wang Xing-yuan, China
X. Frank Xu, USA
Xuping Xu, USA
Xing-Gang Yan, UK
Jun-Juh Yan, Taiwan
Suh-Yuh Yang, Taiwan
Mahmoud T. Yassen, Egypt
Mohammad I. Younis, USA
Huang Yuan, Germany
S. P. Yung, Hong Kong
Ion Zaballa, Spain
Ashraf Zenkour, Saudi Arabia
Jianming Zhan, China
Yingwei Zhang, China
Xu Zhang, China
Lu Zhen, China
Liancun Zheng, China
Jian Guo Zhou, UK
Zexuan Zhu, China
Mustapha Zidi, France

Contents

New Developments in Mathematical Control and Information for Fuzzy Systems, Hamid Reza Karimi, Mohammed Chadli, and Peng Shi
Volume 2013, Article ID 126878, 6 pages

Switched Two-Level H_∞ and Robust Fuzzy Learning Control of an Overhead Crane, Kao-Ting Hung, Zhi-Ren Tsai, and Yau-Zen Chang
Volume 2013, Article ID 712615, 12 pages

Delay-Dependent Stability Analysis of Uncertain Fuzzy Systems with State and Input Delays under Imperfect Premise Matching, Zejian Zhang, Xiao-Zhi Gao, Kai Zenger, and Xianlin Huang
Volume 2013, Article ID 324738, 13 pages

Filtering for Discrete Fuzzy Stochastic Time-Delay Systems with Sensor Saturation, Jia You, Shen Yin, and Hamid R. Karimi
Volume 2013, Article ID 146325, 10 pages

Observer-Based Robust Adaptive Fuzzy Control for MIMO Nonlinear Uncertain Systems with Delayed Output, Chiang Cheng Chiang
Volume 2013, Article ID 215201, 12 pages

A Compound Fuzzy Disturbance Observer Based on Sliding Modes and Its Application on Flight Simulator, Yunjie Wu, Youmin Liu, and Dapeng Tian
Volume 2013, Article ID 913538, 8 pages

Terminal Sliding Mode Control Using Adaptive Fuzzy-Neural Observer, Dezhi Xu, Bin Jiang, Moshu Qian, and Jing Zhao
Volume 2013, Article ID 958958, 8 pages

Fuzzy Formation Control and Collision Avoidance for Multiagent Systems, Yeong-Hwa Chang, Chun-Lin Chen, Wei-Shou Chan, Hung-Wei Lin, and Chia-Wen Chang
Volume 2013, Article ID 908180, 18 pages

Fuzzy Sliding Mode Controller Design Using Takagi-Sugeno Modelled Nonlinear Systems, S. Bououden, M. Chadli, and H. R. Karimi
Volume 2013, Article ID 734094, 7 pages

An Iterative Procedure for Optimizing the Performance of the Fuzzy-Neural Job Cycle Time Estimation Approach in a Wafer Fabrication Factory, Toly Chen and Yi-Chi Wang
Volume 2013, Article ID 740478, 15 pages

Stability Analysis and Stabilization of T-S Fuzzy Delta Operator Systems with Time-Varying Delay via an Input-Output Approach, Zhixiong Zhong, Guanghui Sun, Hamid Reza Karimi, and Jianbin Qiu
Volume 2013, Article ID 913234, 14 pages

Adaptive Fuzzy Tracking Control for Uncertain Nonlinear Time-Delay Systems with Unknown Dead-Zone Input, Chiang-Cheng Chiang
Volume 2013, Article ID 363748, 13 pages

Robust H_∞ Control for a Class of Uncertain Switched Fuzzy Time-Delay Systems Based on T-S Models, Yang Cui, Kaiqing Liu, Yang Zhao, and Xue Wang
Volume 2013, Article ID 234612, 8 pages

Using Metaheuristic and Fuzzy System for the Optimization of Material Pull in a Push-Pull Flow Logistics Network, Afshin Mehrsai, Hamid-Reza Karimi, Klaus-Dieter Thoben, and Bernd Scholz-Reiter
Volume 2013, Article ID 359074, 19 pages

A Reduced-Order TS Fuzzy Observer Scheme with Application to Actuator Faults Reconstruction, Dušan Krokavec and Anna Filasová
Volume 2012, Article ID 951953, 25 pages

A Fuzzy Approach to Robust Control of Stochastic Nonaffine Nonlinear Systems, Ting-Ting Gang, Jun Yang, Qing Gao, Yu Zhao, and Jianbin Qiu
Volume 2012, Article ID 439805, 17 pages

Fuzzy PD Control of Networked Control Systems Based on CMAC Neural Network, Li-lian Huang and Jin Chen
Volume 2012, Article ID 347217, 10 pages

On Interval-Valued Supra-Fuzzy Syntopogenous Structure, F. M. Sleim and Heba I. Mustafa
Volume 2012, Article ID 854942, 8 pages

Bi-Objective Optimization Method and Application of Mechanism Design Based on Pigs' Payoff Game Behavior, Lu Wang, Jian-gang Wang, Rui Meng, and Neng-gang Xie
Volume 2012, Article ID 808161, 15 pages

Direct Adaptive Fuzzy Sliding Mode Control with Variable Universe Fuzzy Switching Term for a Class of MIMO Nonlinear Systems, Guo Haigang, Li Hongxing, Zhao Weijing, and Song Zhankui
Volume 2012, Article ID 543039, 21 pages

Low-Speed Control of Heavy-Load Transfer Robot with Long Telescopic Boom Based on Stribeck Friction Model, Bo You, Ming Qiao, Jiazhong Xu, and Dan Liu
Volume 2012, Article ID 432129, 12 pages

Fuzzy Investment Portfolio Selection Models Based on Interval Analysis Approach, Haifeng Guo, BaiQing Sun, Hamid Reza Karimi, Yuanjing Ge, and Weiquan Jin
Volume 2012, Article ID 628295, 15 pages

Robust Observer Design for Takagi-Sugeno Fuzzy Systems with Mixed Neutral and Discrete Delays and Unknown Inputs, Hamid Reza Karimi and Mohammed Chadli
Volume 2012, Article ID 635709, 13 pages

Fuzzy Variable Structure Control for Uncertain Systems with Disturbance, Bo Wang, Peng Shi, Hamid Reza Karimi, Jun Wang, and Yongduan Song
Volume 2012, Article ID 105074, 12 pages

Unknown Input Observer Design for Fuzzy Bilinear System: An LMI Approach, D. Saoudi, M. Chadli, C. Mechmeche, and N. Benhadj Braiek
Volume 2012, Article ID 794581, 21 pages

A Two-Wheeled Self-Balancing Robot with the Fuzzy PD Control Method, Junfeng Wu, Wanying Zhang, and Shengda Wang
Volume 2012, Article ID 469491, 13 pages

Approximate Analytic and Numerical Solutions to Lane-Emden Equation via Fuzzy Modeling Method, De-Gang Wang, Wen-Yan Song, Peng Shi, and Hamid Reza Karimi
Volume 2012, Article ID 259494, 15 pages

Fuzzy Control and Connected Region Marking Algorithm-Based SEM Nanomanipulation, Dongjie Li, Weibin Rong, Lining Sun, Bo You, Yu Zou, and Wanzhe Xiao
Volume 2012, Article ID 803912, 16 pages

A Novel Identification Method for Generalized T-S Fuzzy Systems, Ling Huang, Kai Wang, Peng Shi, and Hamid Reza Karimi
Volume 2012, Article ID 893807, 12 pages

A Novel Evaluation Model for Hybrid Power System Based on Vague Set and Dempster-Shafer Evidence Theory, Dongxiao Niu, Yanan Wei, Yan Shi, and Hamid Reza Karimi
Volume 2012, Article ID 784389, 12 pages

Robust Stabilization for Continuous Takagi-Sugeno Fuzzy System Based on Observer Design, Yassine Manai and Mohamed Benrejeb
Volume 2012, Article ID 836814, 18 pages

H_∞ **Fuzzy Control of DC-DC Converters with Input Constraint**, D. Saifia, M. Chadli, S. Labiod, and H. R. Karimi
Volume 2012, Article ID 973082, 18 pages

Hindawi Publishing Corporation
Mathematical Problems in Engineering
Volume 2013, Article ID 126878, 6 pages
http://dx.doi.org/10.1155/2013/126878

Editorial

New Developments in Mathematical Control and Information for Fuzzy Systems

Hamid Reza Karimi,[1] Mohammed Chadli,[2] and Peng Shi[3,4]

[1] *Department of Engineering, Faculty of Engineering and Science, University of Agder, 4898 Grimstad, Norway*
[2] *Laboratory of Modeling, Information and Systems, University of Picardie Jules Verne, 80039 Amiens, France*
[3] *College of Engineering and Science, Victoria University, Melbourne, VIC 8001, Australia*
[4] *School of Electrical and Electronic Engineering, The University of Adelaide, Adelaide, SA 5005, Australia*

Correspondence should be addressed to Hamid Reza Karimi; hamid.r.karimi@uia.no

Received 14 March 2013; Accepted 14 March 2013

Copyright © 2013 Hamid Reza Karimi et al. This is an open access article distributed under the Creative Commons Attribution License, which permits unrestricted use, distribution, and reproduction in any medium, provided the original work is properly cited.

1. Discussion and Up-To-Date Overview

Intelligence techniques, such as fuzzy logic approaches, have long been applied to dynamical systems with many important theoretical solutions and successful applications. The overall aim of this special issue is both to promote discussion among researchers actively working on applied fuzzy systems and to provide an up-to-date overview of the research directions and advance observer and controllers methods in the field. Of particular interest, the papers in this special issue are devoted to the development of mathematical methodologies analysis, control and observer problems of fuzzy systems, including nonlinear dynamics, fuzzy logic, and interdisciplinary topics with artificial intelligence. Potential topics include, but are not limited to (1) fuzzy controller design (robust control, adaptive control, and supervisory control), (2) fuzzy observer design (adaptive observers, sliding mode observers, and unknown inputs observers), (3) cascaded fuzzy systems and observers, (4) synchronization in fuzzy systems, (5) stochastic fuzzy systems, (6) robust fault detection and isolation, fault diagnosis, and fault-tolerant control of fuzzy systems, (7) applications of fuzzy controllers and observers to complex systems (including hardware and software development environments for fuzzy systems), (8) fuzzy logics, and (9) fuzzy modeling and optimization. For this special issue we solicit submissions from mathematicians, electrical/control/mechanical engineers, and computer scientists. After a rigorous peer review process, 31 papers have been selected. These papers have covered both the theoretical and practical aspects of fuzzy systems in the broad areas of dynamical systems, mathematics, statistics, operational research, and engineering.

During the past decades, the problem of stability analysis of fuzzy systems has received significant attentions. In the paper entitled "*Delay-dependent stability analysis of uncertain fuzzy systems with state and input delays under imperfect premise matching*" by Z. Zhang et al., the robust stability and stabilization problems are studied for general nonlinear fuzzy systems with time-varying state and input delays. For obtaining a less conservative delay-dependent robust stability criterion, the authors introduce a novel augmented Lyapunov function with an additional triple-integral term to the stability analysis for the systems. Moreover, for improving the design flexibility and reducing the implementation cost of the fuzzy controller, they propose a new design approach different from the traditional PDC design technique, which means that the fuzzy model and the fuzzy controllers share different membership functions. Some less conservative stability conditions are obtained, and a new design approach is also proposed. The proposed stability conditions are less conservative in the sense of getting larger allowable time-delay and obtaining smaller feedback control gains, and the design flexibility is enhanced by arbitrarily selecting simple fuzzy membership functions. In the paper entitled "*Stability analysis and stabilization of T-S fuzzy*

delta operator systems with time-varying delay via an input-output approach" by Z. Zhong et al., the stability analysis and stabilization problems are investigated for fuzzy delta operator systems with time-varying delay. The delta operator method is introduced to transform T-S fuzzy continuous-time systems into discrete-time systems, and the input-output (IO) approach is employed to deal with the stability analysis and control design of T-S fuzzy delta operator systems with time-varying delay. The main contribution of the paper is that the stability analysis and stabilization problems for fuzzy delta operator systems with time-varying delay are investigated by the IO Approach. A model approximation method is employed to transform the original system into an equivalent interconnected system, which is comprised of a forward subsystem with constant time-delays and a feedback one with delayed uncertainties, such that less conservative results are ensured.

The problems of modeling and identification have long been the main stream of research topics, and much effort has been made for fuzzy systems. In order to approximate any nonlinear systems, not just affine nonlinear systems, generalized T-S fuzzy systems where the control variables and the state variables are all premise variables are introduced in the paper entitled "*A novel identification method for generalized T-S fuzzy systems*" by L. Huang et al.. In order to improving the identification effect, a new method combined colony algorithm and genetic algorithm is proposed. Firstly, fuzzy spaces and rules are determined by using ant colony cluster algorithm to get the best one, and colony cluster algorithm has general optimizing capability, which is better than general cluster algorithm. Secondly, the state-space model parameters are optimized by genetic algorithm based on the least square method, which provided the better consequence parameters. In the paper entitled "*Approximate analytic and numerical solutions to Lane-Emden equation via fuzzy modeling method*" by D. Wang et al., a novel algorithm, called variable weight fuzzy marginal linearization (VWFML) method, is proposed to obtain the approximate analytic and numerical solutions to Lane-Emden equations. The main ideas of the VWFML method are as follows. Firstly, the authors need to transfer a group of data into fuzzy rules. Then, they, respectively, use two partition methods to divide the input universes and utilize fuzzy marginal linearization method to obtain the corresponding fuzzy system. By transferring initial value technology, the authors can solve these two fuzzy systems. Finally, they take weighted sum of these two solutions and obtain the approximate solutions of the Lane-Emden equations. When the Lane-Emden equation is unknown and only data information can obtained, many traditional numerical approximation methods could not solve it. The main contribution of this paper is that the authors can only use some data information to obtain the approximate analytic and numerical solutions to Lane-Emden equation with high accuracy. And this method is easy to be implemented and extended for solving other nonlinear differential equations. In the paper entitled "*Bi-objective optimization method and application of mechanism design based on pigs' payoff game behavior*" by L. Wang et al., a new bi-objective optimization game method is proposed. Two design goals can be regarded as two game players, the design variables set can be regarded as strategy subsets named S_1 and S_2, and the constraints in multiobjective problems can be regarded as constraints in the game method. Through the specific technological means, the design variables can be divided into each game players strategy subsets (S_1 and S_2), and two payoff functions u are constructed based on pigs' payoff game behavior. For optimization problems with preferred target, the designers need to emphasize one design goal. For this problem, there exist traditional methods such as weighting method (by adjusting the weight of each goal), hierarchical sequence method (by adjusting the objective optimization order), and goal programming method. In this paper, one new bi-objective optimization game method is proposed based on pigs' payoff game behavior for solving optimization problems with preferred target. It takes bi-objective optimization of luffing mechanism of compensative shave block; for example, the results show that the method can effectively solve the bi-objective optimization problems with preferred target (designers need to take the preferred target as the small pig side and take another target as the big pig side), the efficiency and accuracy are well, and the solution is obtained only through fewer game rounds. Although the Markowitz mean-variance (MV) portfolio optimization theory has been widely used, which leads the investment theory to a new era, in the paper entitled "*Fuzzy investment portfolio selection models based on interval analysis approach*" by H. Guo et al., the authors found that this model has unintuitive problem in investment portfolio selection in economic decision. Thus this paper employs fuzzy set theory and extends it to a fuzzy investment portfolio selection model to solve this problem. Our model establishes intervals for expected returns and risk preference, which can take into account investors' different investment appetite and thus can find the optimal resolution for each interval. In the empirical part, we test this model in Chinese stocks investment and find that this model can fulfill different kinds of investors' objectives. Furthermore, investment risk can be decreased when we add investment limit to each stock in our model. The results indicate that fuzzy set theory is useful to avoid the problems of Markowitz mean-variance portfolio model and takes into account different expected return levels and risk preference levels. In the paper entitled "*On interval valued supra fuzzy syntopogenous structure*" by F. Sleim and H. Mustafa, the authors generalize the concept of supra fuzzy syntopogenous space by using the notion of interval valued set. Topology and its generalization proximity and syntopogenous are branches of mathematics which have many real life applications. They believe that the generalized topological structure suggested in this paper will be important base for modification of medical diagnosis, decision making, and knowledge discovery.

In the past decades, the issue of control design for fuzzy systems has received considerable research interests and has found successful applications in a variety of areas. An adaptive fuzzy sliding mode controller for a class of uncertain nonlinear systems is proposed in the paper entitled "*Fuzzy sliding mode controller design using Takagi-Sugeno modelled nonlinear systems*" by S. Bououden et al.. The unknown system dynamics and upper bounds of the minimum approximation

errors are adaptively updated with stabilizing adaptive laws. The closed-loop system driven by the proposed controllers is shown to be stable with all the adaptation parameters being bounded. The performance and stability of the proposed control system is achieved analytically using the Lyapunov stability theory. In the paper entitled "*Fuzzy variable structure control for uncertain systems with disturbance*" by B. Wang et al., the authors focus on the fuzzy variable structure control for uncertain systems with disturbance. Specifically, the fuzzy control is introduced to estimate the control disturbance, and the switching control is included to compensate the approximation error and possess the characteristic of simpleness in design and effectiveness in attenuating the control chattering. In the paper entitled "*Robust H_∞ control for a class of uncertain switched fuzzy time-delay systems based on T-S models*" by Y. Cui et al., the authors have developed a robust H_∞ control with disturbance attenuation level γ approach for a class of uncertain switched fuzzy time-delay systems based on T-S models. Each and every subsystem of the switched systems is an uncertain fuzzy one to which the PDC (parallel distributed compensation) controller of every subfuzzy system is proposed with its main condition given in a more solvable form of convex combinations. The closed-loop stability of the proposed robust H_∞ control scheme is rigorously proved using Lyapunov theory. Finally, switching law of the state-dependent form achieving system quadratic stability of the switched fuzzy system is given. In the paper entitled "*direct adaptive fuzzy sliding mode control with variable universe fuzzy switching term for a class of MIMO nonlinear systems*" by G. Haigang et al., the authors developed a novel framework for the control of the MIMO nonlinear with model uncertainty and external disturbances. They also proposed a high-precision controller by the variable universe fuzzy control theory. In the paper entitled "*A Fuzzy approach to robust control of stochastic nonaffine nonlinear systems*" by T. Gang et al., the authors investigate the stabilization problem for a class of discrete-time stochastic nonaffine nonlinear systems (SNNS) based on generalized stochastic T-S fuzzy models. By using the function approximation capability of the stochastic T-S fuzzy models, the original SNNS can be exactly represented by a stochastic T-S fuzzy model with some norm bounded approximation errors as the uncertainty term on any compact set. In this way, the stabilization problem of the SNNS can be solved as a robust stabilization problem of the obtained uncertain stochastic T-S fuzzy models. By using a class of piecewise dynamic feedback fuzzy controllers and piecewise quadratic Lyapunov functions, robust semiglobally stabilization of SNNS can be formulated in terms of linear matrix inequalities. In the paper entitled "*adaptive fuzzy tracking control for uncertain nonlinear time-delay systems with unknown dead-zone input*" by C. Chiang, the problem of output tracking control is investigated for a class of uncertain nonlinear state time-delay systems containing unknown dead-zone input and unmatched uncertainties. In general systems, there exist some nonsmooth nonlinearities in the actuators, such as dead zone, saturation, and backlash. However, the dead-zone characteristics in actuators may severely limit the performance of the systems. Also, time-delay characteristic and the existence of uncertain elements usually confronted in engineering systems may degrade the control performance and make the systems unstable. The main features of the proposed robust adaptive fuzzy controller are summarized as follows. (i) An adaptive law is used to estimate the properties of the dead-zone model intuitively and mathematically, without constructing a dead-zone inverse. (ii) Fuzzy logic systems with some appropriate learning laws are applied to approximate the nonlinear gain function and the upper bounded functions of uncertainties. (iii) The unknown upper bound of the uncertainties caused by approximation (or fuzzy modeling) error is estimated by a simple adaptive law. (iv) By means of Lyapunov stability theorem, the proposed controller cannot only guarantee the robust stability of the whole closed-loop system, but also obtain the good tracking performance. In this paper entitled "*Fuzzy PD control of networked control systems based on CMAC neural network*" by L. Huang and J. Chen, the main problem is how to design the fuzzy PD controller and combine with the cerebellar model articulation controller to compose a integral controller which used in the networked control systems effectively. In order to solve this problem, the switching control system between fuzzy PD and PD control is proposed. PD control in the small deviation is applied to obtain higher static control accuracy, and fuzzy PD control in large deviations is applied to obtain faster dynamic response and smaller overshoot. The paper entitled "*Fuzzy control and connected region marking algorithm-based SEM nanomanipulation*" by D. Li et al. is motivated for manipulating the nanocomponent in SEM with telepresence as in macroscale. With the help of virtual reality and haptic technology, the SEM-based master-slave telenanomanipulation platform is established having the performance of security, reliable, and real time without force sensor. The CRM algorithm is introduced to process the 2D SEM image which provides effective position data of the objects for updating the virtual environment. The fuzzy control algorithm is adopted in the master-slave control to obtain relatively stable control variable to avoid damage of platform.

Over the past decades, the observer/filter problems of fuzzy systems have been investigated extensively, since they are very useful in signal processing and engineering applications. In the paper entiled "*Robust observer design for Takagi-Sugeno fuzzy systems with mixed neutral and discrete delays and unknown inputs*" by H. Karimi and M. Chadli, a robust observer design is proposed for Takagi-Sugeno fuzzy neutral models with unknown inputs. The model consists of a mixed neutral and discrete delay, and the disturbances are imposed on both state and output signals. Delay-dependent sufficient conditions for the design of an unknown input T-S observer with time delays are given in terms of linear matrix inequalities. In the paper entitled "*Observer-based robust adaptive fuzzy control for MIMO nonlinear uncertain systems with delayed output*" by C. Chiang, the problem of controller design is considered for a class of MIMO nonlinear uncertain output-delay systems whose states are not available. The common feature of most previous results is the assumption that the controlled systems are free of uncertainties, or the uncertainties are assumed to be a bounded external

disturbance. Therefore, the motivation of this paper is to synthesize an observer-based robust adaptive fuzzy control scheme to deal with the tracking control problem for a class of MIMO nonlinear uncertain systems with delayed output in the presence of uncertainties including the structural uncertainty. In the paper entitled "*Unknown input observer design for fuzzy bilinear system: an LMI approach*" by D. Saoudi et al., a new method to design a Fuzzy Bilinear Observer (FBO) with unknown inputs is developed for a class of nonlinear systems. The nonlinear system is modeled as a fuzzy bilinear model (FBM). This kind of T-S fuzzy model is especially suitable for a nonlinear system with a bilinear term. The proposed fuzzy bilinear observer subject to unknown inputs is developed to ensure the asymptotic convergence of the error dynamic using the Lyapunov method. An unknown input fuzzy bilinear fault diagnosis observer design is also proposed. Specifying for a class of nonlinear systems described by Takagi-Sugeno (T-S) model, in the paper, entitled "*A reduced-order TS fuzzy observer scheme with application to actuator faults reconstruction*" by D. Krokavec and A. Filasova, is newly defined the reduced-order T-S fuzzy observer, and it is demonstrated that the matching requirement, under which it can be disposed to actuator faults estimation, can be reflected in the observer design stipulation. The stability conditions, relying on the feasibility of an associated system of linear matrix inequalities (LMI), are derived and guarantee that the observer scheme asymptotically estimates actuator faults. In terms of fuzzy systems, the article provides a suitable new methodology and expands the theoretical basis of TS fuzzy model applications in control system design. The paper entitled "*Terminal sliding mode control using adaptive fuzzy-neural observer*" by D. Xu et al. proposed a dynamic approximation algorithm which is used to simplify the nonaffine nonlinear systems as affine nonlinear systems with time-varying parameters. And the time-varying parameters can be obtained by a filter. Next, an adaptive fuzzy-neural observer is designed to estimate the signals of position, velocity, and unknown functions. Terminal sliding mode control is used to design based on the observer. Stability analysis and simulations can show that the method is effective. The paper entitled "*Filtering for discrete fuzzy stochastic time-delay systems with sensor saturation*" by J. You et al. investigates the H_∞ filtering problem for T-S fuzzy systems with time varying delay and sensor saturation. The communication channel between the plant and the filer is supposed to be imperfect, and random noise depending on the state and external disturbance is taken into account. The key method employed to handle with the time-varying delay is to develop the Scaled Small Gain (SSG) theorem to the stochastic systems. The main contribution is that this paper establishes a research approach that could handle with time varying delay and sensor saturation together, and both characteristics are always involved in many theoretical and practical problems. The paper entitled "*Robust stabilization for continuous Takagi-Sugeno fuzzy system based on observer design*" by Y. Manai and M. Benrejeb investigates the influence of new Parallel Distributed Controller (PDC) on the stabilization region of continuous Takagi-Sugeno (T-S) fuzzy models. Using a nonquadratic Lyapunov function, new sufficient stabilization criterion is established in terms of linear matrix inequality. The criterion examines the derivative membership function; an approach to determine state variables is given based on observer design.

The applications of various control schemes have received considerable research interests in the past decades. In the work entitled "*An iterative procedure for optimizing the performance of the fuzzy-neural job cycle time estimation approach in a wafer fabrication factory*" by T. Chen and Y. Wang, a classifying fuzzy-neural approach, based on the combination of principal component analysis (PCA), fuzzy c-means (FCM), and back propagation network (BPN), is proposed to estimate the cycle time of a job in a wafer fabrication factory. The paper entitled "*Switched two-level H_∞ and robust fuzzy learning control of an overhead crane*" by K. Hung et al. investigates the use of fuzzy techniques for modeling nonlinear plants as a combination of a nominal linear system and a T-S fuzzy blending of affine terms. This type of dynamic model significantly simplifies subsequent analysis and control designs, because assumptions on the plant dynamics can be significantly reduced. In the paper entitled "*A two-wheeled self-balancing robot with the fuzzy PD control method*" by J. Wu et al., the utility and effectiveness of soft computing approaches for a two-wheeled self-balancing robot with structured and unstructured uncertainties are presented. In this approach, precompensation of a hybrid fuzzy PD controller is proposed. The control scheme consists of a fuzzy logic-based precompensator followed by fuzzy PD control. Moreover, a fuzzy supervisory controller is used to supervise conventional proportional and derivative actions, such that the conventional gains are adapted online through fuzzy reasoning. Due to the influence of nonlinear friction, creep phenomenon occurs when the moving speed is low in the telescopic boom system of heavy-load transfer robot. To solve this problem and to improve control precision, B. You et al. in the paper entitled "*Low-speed control of heavy-load transfer robot with long telescopic boom based on stribeck friction model*" built a three-loop control nonlinear model of the system with the Stribeck friction disturbance model to simulate the motion of the telescopic boom in low speed. Fuzzy PID control was used to solve the problem of "flat-top" position tracking and "dead-zone" speed tracking. The creep phenomenon was eliminated, and the tracking accuracy and robustness of the system were also improved. The paper entitled "*Using metaheuristic and fuzzy system for optimization of material-pull in a push pull flow logistics network*" by A. Mehrsai et al. generally complies with a known problem in manufacturing environment, which is the coordination of heterogeneous material flows throughout supply chains and within every production plant. Alternative flows of material, following push and pull principles of control cause collection of inventory and WIP of materials as well as lags in delivery times. Model-based control of material flows regarding the interference of human in the entire process seems relatively very complex to practitioners in industries. In contrast, in this paper some material flow strategies are recommended to simplify and improve the flows throughout. Besides, some heuristics (i.e., genetic algorithm and simulated annealing)

to solve the flow coordination are experimented here as well. Fuzzy logic as a suitable solution for solving human centered operations is reasonably explained and experimented in two applications, that is, control of pallets within an assembly system as well as normalization of multiobjective optimization problem. In the paper entitled "*A novel evaluation model for hybrid power system based on vague set and dempster-shafer evidence theory*" by D. Niu et al., due to advantages of vague set processing abundant uncertain and fuzzy information, it is chosen to determine basic decision matrix of evaluation model. Combining vague set with D-S evidence theory, a novel evaluation algorithm is established and applied into the comprehensive benefit evaluation of hybrid power system. In the paper entitled "H_∞ *fuzzy control of DC-DC converters with input constraint*," D. Saifia et al. study fuzzy control of DC-DC converters under actuator saturation. Because linear control design methods do not take into account the nonlinearity of the system, a T-S fuzzy models and a controller design approach are used. The input constraint is first transformed into a symmetric saturation which is represented by a polytopic model. Stabilization conditions for the H_∞ state feedback system of DC-DC converters under actuator saturation are established using the Lyapunov approach. In the paper entitled "*A compound fuzzy disturbance observer based on sliding modes and its application on flight simulator*," Y. Wu et al. present a compound fuzzy disturbance observer based on sliding modes. The proposed method improves the performance of the disturbance inhibition when there exists huge modeling mismatch. Traditional methods use high-gain control, which may cause resonance in controlling elastic electromechanical systems, to inhibit equivalent disturbance. The proposed method employs fuzzy tools to deal with the primary part of the disturbance, and the residual disturbance is compensated by sliding mode control. The proposed method improves the robustness and performance of the system while avoiding the disadvantages of traditional methods. Finally, the paper entitled "*Fuzzy formation control and collision avoidance for multiagent systems*" by Y. Chang et al. investigates the formation control of leader-follower multiagent systems, where the problem of collision avoidance is considered. Based on the graph-theoretic concepts and locally distributed information, a neural fuzzy formation controller is designed with the capability of online learning. The learning rules of controller parameters can be derived from the gradient descent method. To avoid collisions between neighboring agents, a fuzzy separation controller is proposed such that the local minimum problem can be solved.

Appendix

A. Accepted Papers According to Classified Topics

A.1. Papers on the Topic of Stability

(1) Delay-dependent Stability Analysis of Uncertain Fuzzy Systems with State and Input Delays under Imperfect Premise Matching.

(2) Stability Analysis and Stabilization of T-S Fuzzy Delta Operator Systems with Time-Varying Delay via an Input-Output Approach.

A.2. Papers on the Topic of Modeling/Identification

(3) A Novel Identification Method for Generalized T-S Fuzzy Systems.

(4) Approximate analytic and numerical solutions to Lane-Emden equation via fuzzy modeling method.

(5) Bi-objective Optimization Method and Application of Mechanism Design Based on Pigs' Payoff Game Behavior.

(6) Fuzzy investment portfolio selection models based on interval analysis approach.

(7) On interval valued supra fuzzy syntopogenous structure.

A.3. Papers on the Topic of Control for Fuzzy Systems

(8) Fuzzy Sliding Mode Controller Design Using Takagi-Sugeno modelled Nonlinear Systems.

(9) Fuzzy variable structure control for uncertain systems with disturbance.

(10) Robust H_∞ Control for A Class of Uncertain Switched Fuzzy Time-Delay Systems based on T-S Models.

(11) Direct Adaptive Fuzzy Sliding Mode Control with Variable Universe Fuzzy Switching Term for a class of MIMO Nonlinear Systems.

(12) A Fuzzy Approach to Robust Control of Stochastic Non-Affine Nonlinear Systems.

(13) Adaptive Fuzzy Tracking Control for Uncertain Nonlinear Time-Delay Systems with Unknown Dead-Zone Input.

(14) Fuzzy PD Control of Networked Control Systems Based on CMAC Neural Network.

(15) Fuzzy Control and Connected Region Marking Algorithm-based SEM Nanomanipulation.

A.4. Papers on the Topic of Observer/Filter Design for Complex Systems

(16) Robust Observer Design for Takagi-Sugeno Fuzzy Systems with Mixed Neutral and Discrete delays and Unknown Inputs.

(17) Observer-based Robust Adaptive Fuzzy Control for MIMO Nonlinear Uncertain Systems with Delayed Output.

(18) Unknown Input Observer Design for Fuzzy Bilinear System: an LMI Approach.

(19) A reduced-order TS fuzzy observer scheme with application to actuator faults reconstruction.

(20) Terminal Sliding Mode Control using Adaptive Fuzzy-Neural Observer.

(21) Filtering for Discrete Fuzzy Stochastic Time-Delay Systems with Sensor Saturation.

(22) Robust Stabilization for Continuous Takagi-Sugeno Fuzzy System based on Observer Design.

A.5. Papers on the Topic of Applications

(23) An Iterative Procedure for Optimizing the Performance of the Fuzzy-neural Job Cycle Time Estimation Approach in a Wafer Fabrication Factory.

(24) Switched Two-Level H_∞ and Robust Fuzzy Learning Control of an Overhead Crane.

(25) A Two-Wheeled Self-Balancing Robot with the Fuzzy PD Control Method.

(26) Low-Speed Control of Heavy-Load Transfer Robot with Long Telescopic Boom Based on Stribeck Friction Model.

(27) Using Meta-Heuristic and Fuzzy System for Optimization of Material-Pull In A Push-Pull Flow Logistics Network.

(28) A Novel Evaluation Model for Hybrid Power System Based on Vague Set and Dempster-Shafer Evidence Theory.

(29) H_∞ Fuzzy Control of DC-DC Converters with Input Constraint.

(30) A Compound Fuzzy Disturbance Observer based on Sliding Modes and Its Application on Flight Simulator.

(31) Fuzzy Formation Control and Collision Avoidance for Multi-Agent Systems.

Acknowledgments

The guest editors would like to thank all the authors of this special issue for contributing the high quality papers, and we hope the reader will share our joy and find this special issue very useful. We are also very grateful to the reviewers for their efforts in reviewing the papers on time.

Hamid Reza Karimi
Mohammed Chadli
Peng Shi

Hindawi Publishing Corporation
Mathematical Problems in Engineering
Volume 2013, Article ID 712615, 12 pages
http://dx.doi.org/10.1155/2013/712615

Research Article

Switched Two-Level H_∞ and Robust Fuzzy Learning Control of an Overhead Crane

Kao-Ting Hung,[1] Zhi-Ren Tsai,[2] and Yau-Zen Chang[1]

[1] *Department of Mechanical Engineering, Chang Gung University, Taoyuan 33302, Taiwan*
[2] *Department of Computer Science & Information Engineering, Asia University, Taichung 41354, Taiwan*

Correspondence should be addressed to Yau-Zen Chang; zen@mail.cgu.edu.tw

Received 30 November 2012; Revised 9 February 2013; Accepted 25 February 2013

Academic Editor: Peng Shi

Copyright © 2013 Kao-Ting Hung et al. This is an open access article distributed under the Creative Commons Attribution License, which permits unrestricted use, distribution, and reproduction in any medium, provided the original work is properly cited.

Overhead cranes are typical dynamic systems which can be modeled as a combination of a nominal linear part and a highly nonlinear part. For such kind of systems, we propose a control scheme that deals with each part separately, yet ensures global Lyapunov stability. The former part is readily controllable by the H_∞ PDC techniques, and the latter part is compensated by fuzzy mixture of affine constants, leaving the remaining unmodeled dynamics or modeling error under robust learning control using the Nelder-Mead simplex algorithm. Comparison with the adaptive fuzzy control method is given via simulation studies, and the validity of the proposed control scheme is demonstrated by experiments on a prototype crane system.

1. Introduction

Overhead cranes are used in workshops or harbors to transport massive goods within short distance. The manipulation of overhead cranes is affected by the existence of unavoidable disturbances, such as friction, winds, unbalanced load, and accidental collision. Besides, change of payloads and string length can result in tremendous variations in system dynamics. Due to these inherent problems, most of the overhead cranes are still operated by skilled labors.

An automatic crane system should be able to accurately carry payloads to the desired position as fast as possible without swing. Many works have been focused on automatic control of the overhead crane in the literature. For instance, Park et al. and Singhose et al. [1, 2] investigated the input shaping control of the crane systems. [3–5] used the variable structure control with sliding modes to control the overhead crane. Moreno et al. [6] used neural networks to tune the parameters of state feedback control law to improve the performance of an overhead crane. Lee and Cho [7] proposed an antiswing fuzzy controller to enhance a servo controller that was used for positioning. Moreover, Nalley and Trabia [8] adopted fuzzy control for both positioning control and swing damping. Moreover, a standard discrete-time fuzzy model [9–13] and continuous-time fuzzy controller [14] have been proposed in the literature. While the controllers of [15–20] are based on the so-called Single Input Rule Modules (SIRMs) and [21] focused on the construction of a reduced-order model to approximate the original system.

In the above researches, [1, 2] lack robustness consideration for external disturbances and plant uncertainty, while stability is not guaranteed in [6–8]. Successful implementation of these schemes might depend on unreliable and hard-to-obtain consequent parts (linguistic value), such as the schemes of [3, 14] and the dynamic importance degree defined in [15], respectively.

In this paper, we model the nonlinear plant as a combination of a continuous-time linear nominal model and fuzzily blended supplemental affine terms. These terms are added mainly to account for dominant friction effects and residual nonlinear dynamics. The model not only simplifies subsequent control design but also enhances system robustness, because assumptions on the plant dynamics are significantly reduced. The nominal model allows linear control techniques, specifically, the H_∞ linear control technique [22, 23], to be applied to the nonlinear plant.

In the closely related literature of [15–20, 24–31], fuzzy controllers are developed to simultaneously stabilize these fuzzy linear models using the parallel distributed control (PDC) scheme that satisfies the linear matrix inequality

(LMI) relations. However, these control design strategies rely on accurate fuzzy modeling of the plant, which usually results in a large number of fuzzy rules and, hence, complex and conservative designs.

To further alleviate the requirement for accurate fuzzy modeling of the plant, a two-level H_∞ robust nonlinear control scheme is proposed. The inner-level controller is responsible for accurate servo control, while the outer-level controller compensates for unmodeled system dynamics and bounded disturbances. Besides, each part of the proposed control laws can be independently designed satisfying its own specification. This incremental design procedure avoids solving the problem at one time and allows each part to be designed with different guidelines. Also, global stability of the closed-loop system is ensured against bounded disturbances with guaranteed disturbance attenuation level.

A particular switching controller is proposed in [32] for nonlinear systems with unknown parameters based on a fuzzy logic approach. The major difference between our proposed scheme and the controller of [32] is that the switching of our scheme is between the inner-loop and the outer-loop controllers, while the controller of [32] is switched constantly between many (which is 8 in the simulation example) linear controllers. Furthermore, the fuzzy terms in our controller are dedicated for the compensation of highly nonlinear effects that deviate from the nominal linear dynamics. Nevertheless, in [32], a fuzzy plant model is required for the construction of the switching plant model, which is then used for the model-based design of the switching controller. The switching Takagi-Sugeno fuzzy control proposed in [33] also requires the plant to be accurately represented by a fuzzy system.

As the closed-loop stability is ensured by the outer-level controller, we are able to optimize the inner-level controller by the Nelder-Mead simplex algorithm [34] based on actual closed-loop control performance, rather than deriving from the plant model. The optimization algorithm converges faster than particle swarm optimization (PSO) [35], which is adequate for online applications. This scheme, which incorporates online trials, can be applied to many applications such as self-guided robot and evolvable systems. Furthermore, considering that the swing dynamics depend on both string length and load mass, fuzzy rules are created to interpolate control gains obtained from trial experiments [36–38].

In the following sections, this paper is divided into four parts. Section 2 describes the plant model and the problem, Section 3 proposes the two-level control scheme, and Section 4 evaluates the effectiveness of the proposed scheme using both simulation comparison with a recently proposed strategy in the literature and experimental studies. Finally, Section 5 concludes the results.

2. Problem Formulation

The plant under consideration is assumed to be a disturbed nonlinear system which is affine in the input and contains uncertain dynamics:

$$\dot{x} = f(x) + \Delta f(x,t) + [g(x) + \Delta g(t)] \cdot u + w, \quad (1)$$

where $\Delta f(x,t)$ and $\Delta g(t)$ are unknown system dynamics, which are bounded in x and t; $x = [x_1, x_2, \ldots, x_n]^T \in R^{n\times 1}$ is the state vector, $u = [u_1, u_2, \ldots, u_m]^T \in R^{m\times 1}$ is the nonlinear input vector, and $w \in R^{n\times 1}$ denotes unknown and bounded disturbance. Furthermore, nonlinear functions $f(x)$ and $g(x)$ are Lipschitz in x.

Next, we approximate the nonlinear system as a nominal linear system augmented with Takagi-Sugeno type fuzzy blending of affine terms. Note that these affine terms, which are usually dominated by friction in many mechatronic systems, are added to the control-input term, rather than being added directly. This form closely reflects the practical effects of friction on system dynamics. Specifically, the ith rule of the affine T-S fuzzy model is in the following form:

Plant rule i:

IF $z_1(t)$ is M_{i1} and $\cdots$ and $z_p(t)$ is M_{ip}

$$\text{THEN } \dot{x} = A \cdot x + \Delta A(t) \cdot x + [B + \Delta B(t)] \cdot [u + c_i] \quad \text{for } i = 1, 2, \ldots, L. \quad (2)$$

In each rule, $z_1(t)$, $z_2(t)$, ... and $z_p(t)$ are the p premise variables, which can be state variables or functions of state variables, M_{ij} is the fuzzy set corresponding to the jth premise variable, $A \in R^{n\times n}$ is the system matrix, and $B \in R^{n\times m}$ denotes the control input matrix. Moreover, $c_i \in R^{m\times 1}$ is the ith bias vector, $\Delta A(t) \in R^{n\times n}$ is the system uncertainty, and $\Delta B(t) \in R^{n\times m}$ denotes the control input uncertainty.

Defining $\mu_{ij}(\cdot)$ as the membership function corresponding to fuzzy set M_{ij}, we have that $\mu_{ij}(z_j(t))$ is the grade of membership of $z_j(t)$ in M_{ij}. Using the sum-product composition, the firing strength of the ith fuzzy rule is represented as $\varpi_i = \varpi_i(z) \equiv \prod_{j=1}^{p} \mu_{ij}(z_j(t))$ with $z \equiv [z_1(t), z_1(t), \ldots, z_p(t)]^T$.

By defining $h_i(z) = \varpi_i / \sum_{j=1}^{L} \varpi_j$ as the normalized firing strength of the ith rule, hence $\sum_{i=1}^{L} h_i(z) = 1$, the overall fuzzy system model is then inferred as the weighted average of the consequent parts:

$$\dot{x} = Ax + \Delta A(t)\, x + [B + \Delta B(t)] \cdot \left[u + \sum_{i=1}^{L} h_i(z) \cdot c_i \right]. \quad (3)$$

The proposed control scheme is of a two-level switching structure where the control input is composed of three parts, u_S, u_H, and u_f, defined as follows:

$$\begin{aligned} u &= (1 - I^*) \cdot u_S + I^* \cdot u_H + u_f \\ &= (1 - I^*) \cdot K_S \cdot e - I^* \cdot K_H \cdot x - \sum_{i=1}^{L} h_i(z) \cdot c_i, \end{aligned} \quad (4)$$

where $I^* \in \{0, 1\}$ is a switching function to be defined in Section 3. In (4), the first term, $u_S = K_S \cdot e$, is a servo controller located in the inner loop responsible for accurate tracking, where $e = x_r - x$ is the tracking error with x_r denoting the reference state trajectory. The second term,

$u_H = -K_H \cdot x$, is an H_∞ robust controller in the outer loop to ensure system stability. And $u_f = -\sum_{i=1}^{L} h_i(z) \cdot c_i$ is a fuzzy-combination term that compensates for nonlinear dynamics, such as friction and other effects that deviate from nominal linear dynamics.

Next, let us define the modeling error $\bar{e}_{\text{mod}}$ as

$$\bar{e}_{\text{mod}} \equiv f(x) + \Delta f(x,t) + [g(x) + \Delta g(t)] \cdot u + w - y, \quad (5)$$

where $y = A \cdot x + \Delta A(t) \cdot x + [B + \Delta B(t)] \cdot [u + \sum_{i=1}^{L} h_i(z) \cdot c_i]$. Hence the closed-loop system, formed by applying (4) to (1), can be expressed concisely as follows:

$$\begin{aligned} \dot{x} &= A \cdot x + \Delta A(t) \cdot x + [B + \Delta B(t)] \\ &\quad \cdot \left[(1 - I^*) \cdot u_S + I^* \cdot u_H + u_f + \sum_{i=1}^{L} h_i(z) \cdot c_i \right] + \bar{e}_{\text{mod}} \\ &= A \cdot x + \Delta A(t) \cdot x + [B + \Delta B(t)] \cdot [(1 - I^*) \cdot u_S + I^* \cdot u_H] \\ &\quad + \bar{e}_{\text{mod}}. \end{aligned} \quad (6)$$

3. The Proposed Two-Level Control Scheme

As shown in Figure 1, the overall control scheme is composed of an outer-level stabilizing controller and an inner-level servo controller. Each of the controllers is designed according to a switching condition defined by the deviation of tracking errors from a prescribed reference vector $x_r(t)$. That is,

$$\text{If } \|e\| = \|x_r - x\| \le \varepsilon_E \quad \text{then } I^* = 0, \text{ otherwise } I^* = 1. \quad (7)$$

In the condition, the threshold ε_E is a user-defined positive number. The value of it, for instance, may be designed as $0.1 \times \max_t(\|x_r(t)\|)$.

The closed-loop system dynamics when $\|e\| > \varepsilon_E$ is formed by assigning $I^* = 1$ in (6), as follows:

$$\dot{x} = [A + \Delta A(t)] \cdot x - [B + \Delta B(t)] \cdot K_H \cdot x + \bar{e}_{\text{mod}}. \quad (8)$$

If uncertainties in the plant dynamic matrices, $\Delta A(t)$ and $\Delta B(t)$, are bounded, we may introduce a time-varying matrix, $F(t)$ with $0 \le \|F(t)\| \le 1$, and constant matrices, D, E_1, and E_2, such that

$$\begin{aligned} [\Delta A(t) \quad \Delta B(t) K_H] \cdot x &= D \cdot F(t) \cdot [E_1 \quad E_2 K_H] \cdot x \\ &\quad + [\delta(t) \quad 0], \end{aligned} \quad (9)$$

with $\delta(t)$ being a bounded function in x:

$$\|\delta(t)\| \le a \cdot \|x\|, \quad \text{where } a \text{ is a positive constant.} \quad (10)$$

Using (9), the closed-loop system dynamics, (8), can then be written as

$$\dot{x} = (A - B \cdot K_H) \cdot x + D \cdot F(t) \cdot (E_1 - E_2 \cdot K_H) \cdot x + e_{\text{mod}}, \quad (11)$$

where $e_{\text{mod}} = \bar{e}_{\text{mod}} + \delta(t)$.

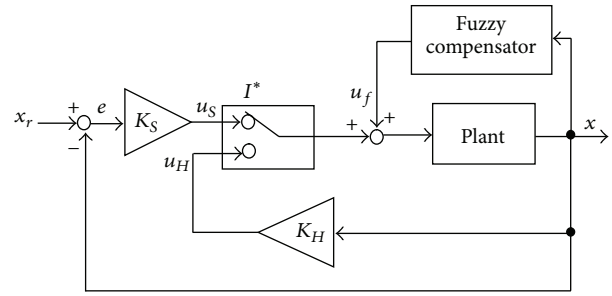

Figure 1: The proposed two-level switching control scheme.

When the system is under acceptable tracking, that is, $\|e\| \le \varepsilon_E$, only the servo controller is in charge. The closed-loop system dynamics is then formed by assigning $I^* = 0$ in (6), as follows:

$$\dot{x} = [A + \Delta A(t)] \cdot x + [B + \Delta B(t)] \cdot K_S \cdot e + e_{\text{mod}}. \quad (12)$$

3.1. Design of the Outer-Level H_∞ Stabilization Controller. The H_∞ stabilization performance of u_H is defined as follows:

$$\frac{\int_0^{t_f} [x(t)^T \cdot Q \cdot x(t)] \cdot dt}{E_{\text{mod}}} \le \rho^2, \quad (13)$$

where

$$E_{\text{mod}} = \int_0^{t_f} e_{\text{mod}}^T \cdot e_{\text{mod}} \cdot dt, \quad (14)$$

t_f is terminal time of control, Q is a positive definite weighting matrix, and ρ denotes prescribed attenuation level with ρ^2 being the attenuation disturbance level. From the energy viewpoint, (13) confines the effect of e_{mod} on state, $x(t)$, to be attenuated below a desired level. If initial conditions are also considered, the H_∞ performance in (13) can be modified as follows:

$$\int_0^{t_f} (x^T \cdot Q \cdot x)\, dt \le x^T(0) \cdot P \cdot x(0) + \rho^2 \cdot E_{\text{mod}}, \quad (15)$$

where Q and P are symmetric and positive definite weighting matrices. The design of the stabilizing controller in the outer level corresponds to find a linear controller in the form of $u_H = -K_H \cdot x$, such that the H_∞ performance (15) is guaranteed to stabilize the closed-loop system (11).

Theorem 1. *Assuming that the modeling error is bounded such that $\|e_{\text{mod}}\| \le e_U$, with e_U being a positive constant, the H_∞ control performance, defined in* (15) *is guaranteed for the closed-loop system* (11) *via the stabilizing control law, $u_H = -K_H \cdot x$, and the feed-forward fuzzy compensator $u_f = -\sum_{i=1}^{L} h_i(z) \cdot c_i$, if there exist constant positive values v, ρ, positive-definite matrix P, and matrix K_H, such that the following linear matrix inequality is satisfied*

$$\Phi \equiv \begin{bmatrix} \phi & (E_1 \cdot W - E_2 \cdot Y)^T \\ (E_1 \cdot W - E_2 \cdot Y) & -v^2 \cdot I \end{bmatrix} < 0, \quad (16)$$

where

$$W \equiv P^{-1}, \qquad Y \equiv K_H \cdot W, \tag{17}$$

$$\phi \equiv (A \cdot W - B \cdot Y)^T + A \cdot W - B \cdot Y + \frac{1}{\rho^2} \cdot I + \nu^2 \cdot D \cdot D^T. \tag{18}$$

The proof of Theorem 1 requires the following lemma.

Lemma 2 (see [31, 39]). *Given constant matrices D and E and a symmetric constant matrix S of appropriate dimensions, the following inequality holds:*

$$S + D \cdot F(t) \cdot E + E^T \cdot F^T(t) \cdot D^T < 0, \tag{19}$$

if and only if for some $\nu > 0$

$$S + \begin{bmatrix} \nu^{-1} \cdot E^T & \nu \cdot D \end{bmatrix} \cdot \begin{bmatrix} R & 0 \\ 0 & I \end{bmatrix} \cdot \begin{bmatrix} \nu^{-1} \cdot E \\ \nu \cdot D^T \end{bmatrix} < 0, \tag{20}$$

where $F(t)$ *satisfies* $F(t)^T \cdot F(t) \le R$.

Proof of Theorem 1. Considering a Lyapunov function candidate composed of the Lyapunov function:

$$V(t) = x^T(t) \cdot P \cdot x(t), \tag{21}$$

its time derivative, $\dot{V}$, can be obtained as

$$\begin{aligned} \dot{V}(x(t)) &= \dot{x}^T \cdot P \cdot x + x^T \cdot P \cdot \dot{x} \\ &= x^T \cdot \left\{ (A - B \cdot K_H)^T \cdot P + P \cdot (A - B \cdot K_H) \right\} \cdot x \\ &\quad + x^T \cdot \left\{ [D \cdot F(t) \cdot (E_1 - E_2 \cdot K_H)]^T \cdot P \right. \\ &\qquad \left. + P \cdot D \cdot F(t) \cdot (E_1 - E_2 \cdot K_H) \right\} \cdot x \\ &\quad + e_{\text{mod}}^T \cdot P \cdot x + x^T \cdot P \cdot e_{\text{mod}}. \end{aligned} \tag{22}$$

By Lemma 2, we have

$$\begin{aligned} \dot{V} &\le x^T \cdot \left\{ (A - B \cdot K_H)^T \cdot P + P \cdot (A - B \cdot K_H) + \frac{1}{\rho^2} \cdot P^T \cdot P \right. \\ &\quad + \begin{bmatrix} \nu^{-1} \cdot (E_1 - E_2 \cdot K_H)^T & \nu \cdot P \cdot D \end{bmatrix} \\ &\quad \left. \cdot \begin{bmatrix} \nu^{-1} \cdot (E_1 - E_2 \cdot K_H) \\ \nu \cdot D^T \cdot P \end{bmatrix} \right\} \cdot x + \rho^2 \cdot e_{\text{mod}}^T \cdot e_{\text{mod}} \\ &= -x^T \cdot Q \cdot x + \rho^2 \cdot e_{\text{mod}}^T \cdot e_{\text{mod}}, \end{aligned} \tag{23}$$

where

$$\begin{aligned} Q \equiv -\Bigg\{ &(A - B \cdot K_H)^T \cdot P + P \cdot (A - B \cdot K_H) + \frac{1}{\rho^2} \cdot P^T \cdot P \\ &+ \begin{bmatrix} \nu^{-1} \cdot (E_1 - E_2 \cdot K_H)^T & \nu \cdot P \cdot D \end{bmatrix} \\ &\cdot \begin{bmatrix} \nu^{-1} \cdot (E_1 - E_2 \cdot K_H) \\ \nu \cdot D^T \cdot P \end{bmatrix} \Bigg\}. \end{aligned} \tag{24}$$

According to (16) and (24), we have

$$\begin{aligned} W^T \cdot Q \cdot W = -\Bigg\{ &(A \cdot W - B \cdot Y)^T + A \cdot W - B \cdot Y + \frac{1}{\rho^2} \cdot I \\ &+ \begin{bmatrix} \nu^{-1} \cdot (E_1 \cdot W - E_2 \cdot Y)^T & \nu \cdot D \end{bmatrix} \\ &\cdot \begin{bmatrix} \nu^{-1} \cdot (E_1 \cdot W - E_2 \cdot Y) \\ \nu \cdot D^T \end{bmatrix} \Bigg\}. \end{aligned} \tag{25}$$

From (18) and (25), we have

$$\phi + \nu^{-2} \cdot (E_1 \cdot W - E_2 \cdot Y)^T \cdot (E_1 \cdot W - E_2 \cdot Y) < 0. \tag{26}$$

Equation (26) can be represented in the standard LMI form:

$$\begin{bmatrix} \phi & (E_1 \cdot W - E_2 \cdot Y)^T \\ (E_1 \cdot W - E_2 \cdot Y) & -\nu^2 \cdot I \end{bmatrix} < 0. \tag{27}$$

If (16) holds, then $Q > 0$. Equation (23) can be rewritten as

$$\begin{aligned} \dot{V} &\le -x^T \cdot Q \cdot x + \rho^2 \cdot e_{\text{mod}}^T \cdot e_{\text{mod}} \le -\lambda_{\min}(Q) \cdot \|x\|^2 \\ &\quad + \rho^2 \cdot \|e_{\text{mod}}\|^2 \le -\lambda_{\min}(Q) \cdot \|x\|^2 + \rho^2 \cdot e_U^2, \end{aligned} \tag{28}$$

where the property $\|e_{\text{mod}}\| \le e_U$ is applied.

Whenever $\|x\| > (\rho \cdot e_U)/\sqrt{\lambda_{\min}(Q)}$, we have that $\dot{V} < 0$. It is clear that if (16) is satisfied, then the system (11) is UUB stable. This completes the proof. □

3.2. Design of the Inner-Level Tracking Controller. Once the outer-level stabilization controller, $u_H = -K_H \cdot x$, has been designed, we are able to put the system undergoing safe trials. Taking tracking performance together with control effort into consideration, the overall performance index, J, is defined as a weighted sum of the indices

$$J = \frac{1}{t_f} \cdot \int_0^{t_f} \|u(t)\| \cdot dt + \frac{\omega_1}{t_f} \cdot \int_0^{t_f} \|e(t)\| \cdot dt, \tag{29}$$

where ω_1 is a weighting factor, which is defined according to practical trade-offs between desired tracking performance and physical constrains.

The inner-level controller, $u_S = K_S \cdot e$, is designed by searching for the gain matrix K_S such that the overall performance index, J, is minimized. We propose to use the Nelder-Mead simplex method [34] to guide the minimization procedure in this paper. The method deals with nonlinear optimization problems without derivative information, which normally requires fewer steps to find a solution close to global optimum, when proper initial values are given, in comparison with the more powerful DIRECT (DIviding RECTangle) algorithm or evolutionary computation techniques.

The Nelder-Mead simplex method uses the concept of a simplex, which has $N + 1$ vertices in N dimensions for an optimization problem with N design parameters. In each

step of the algorithm, one of the four possible operations is conducted: reflection, expansion, contraction, and shrink. As the method is sensitive to initial guess, for an N-dimensional problem we may start the algorithm with $N+1$ simplexes with $(N+1)^2$ randomly generated parameter sets for the vertices, and, after several steps, collect the $N+1$ best solutions of the simplexes to form a simplex for final convergence. With this strategy, we have more initial guesses to avoid being trapped at local minimum. Details are presented in the subsequent case study.

4. Case Study

In order to verify performance of the proposed control scheme, case studies of simulations and experiments are conducted. In the simulations, a comparison with the adaptive fuzzy control method (AFCM) of [40] is made. In experimental studies, a two-dimensional prototype crane system is used.

4.1. Simulation Study. The crane system under control is composed of a motor-driven cart running along a horizontal rail, a payload, and a string carrying the payload, which is attached to a joint on the cart. We assume that the cart and the load can move only in the vertical plane. In the following study, the cart is of mass $M = 6.78$ kg, the payload is of mass $m = 1.5$ kg, and the string is of length $l = 0.5$ m. Furthermore, x_1 is the cart position, θ is the swing angle, u is the control signal applied to the cart, and $x_r = [1, 0, 0, 0]^T$ is the reference input. The position of payload, y, can be calculated from the relation: $y = x_1 + l \cdot \sin(\theta)$. Besides, we assume that the viscous friction coefficient between the cart and the rail is D_1, and the wind resistance coefficient between the air and the string is D_2.

Lagrange analysis of the simplified two-dimensional crane system gives the dynamic equation

$$\begin{aligned}
\ddot{x}_1 = {} & \left(u + m \cdot l \cdot \dot{\theta}^2 \cdot \sin(\theta) + m \cdot g \cdot \sin(\theta) \cdot \cos(\theta)\right. \\
& \left. - D_1 \cdot \dot{x}_1 + D_2 \cdot \dot{\theta} \cdot \cos(\theta)\right)\left(M + m - m \cdot \cos^2(\theta)\right)^{-1} \\
\ddot{\theta} = {} & \left(\left(m \cdot \cos(\theta) \cdot u + m^2 \cdot l \cdot \dot{\theta}^2 \cdot \sin(\theta) \cdot \cos(\theta)\right.\right. \\
& \left. + (M + m) \cdot m \cdot g \cdot \sin(\theta)\right) \\
& \times\left(m^2 \cdot l \cdot \cos^2(\theta) - m \cdot l \cdot (M + m)\right)^{-1}\Big) \\
& + \Big(\left(-D_1 \cdot \dot{x}_1 \cdot m \cdot \cos(\theta) + D_2 \cdot l\right. \\
& \left. \cdot \left[(M + m) - m \cdot \cos^2(\theta)\right] \cdot \dot{\theta}\right) \\
& \times\left(m^2 \cdot l \cdot \cos^2(\theta) - m \cdot l \cdot (M + m)\right)^{-1}\Big) + w_4,
\end{aligned} \tag{30}$$

where g is the gravitational acceleration and w_4 represents the external disturbance.

(1) Controller Design of the Proposed Control Strategy. From (3), the overall fuzzy model of the overhead crane system (30) is inferred to be

$$\dot{x} = Ax + \Delta A(t)\, x + [B + \Delta B(t)] \cdot \left[u + \sum_{i=1}^{2} h_i(z) \cdot c_i\right], \tag{31}$$

where $x = [x_1,\ x_2,\ x_3,\ x_4]^T = [x_1,\ \dot{x}_1,\ \theta,\ \dot{\theta}]^T$ is the state vector. And the matrices are

$$A = \begin{bmatrix} 0 & 1 & 0 & 0 \\ 0 & -\dfrac{D_1}{M} & \dfrac{m \cdot g}{M} & \dfrac{D_2}{M} \\ 0 & 0 & 0 & 1 \\ 0 & \dfrac{D_1}{(l \cdot M)} & \dfrac{-(M+m) \cdot g}{l \cdot M} & \dfrac{(M+m) \cdot D_2}{m^2 \cdot l - m \cdot l \cdot (M+m)} \end{bmatrix},$$

$$B = \begin{bmatrix} 0 \\ \dfrac{1}{M} \\ 0 \\ -\dfrac{1}{(l \cdot M)} \end{bmatrix}, \tag{32}$$

with $D_1 = 588$, $D_2 = 0.01$, $g = 9.81$, $z = m \cdot l \cdot \sin(x_3) \cdot x_4^2$, $h_1 = 0.5(1+z)$, $h_2 = 0.5(1-z)$, $c_1 = 1$, and $c_2 = -1$. And $[\ \Delta A(t)\ \ \Delta B(t)\ ] = D \cdot F(t) \cdot [\ E_1\ \ E_2\ ]$, where $F(t) = \sin(t)$, $D = [0, -0.01, 0, 0.01]^T$, $E_1 = [2, 0, 0, 0]$, and $E_2 = 0.02$.

By selecting $\nu = 3$ and $\rho = 18$, we are able to obtain

$$P = \begin{bmatrix} 90.3667 & 18.8347 & 13.0680 & 9.0783 \\ 18.8347 & 14.5588 & 0.3778 & 7.1938 \\ 13.0680 & 0.3778 & 51.4426 & 0.6680 \\ 9.0783 & 7.1938 & 0.6680 & 3.5618 \end{bmatrix}, \tag{33}$$

and $K_H = [1250,\ 315.7,\ -1766.5,\ 129.5]$ using the standard LMI techniques. The optimal servo control gains are found to be $K_S = [1140.47,\ 230.47,\ 69.97,\ 315.22]$ by the simplex method.

(2) Controller Design of [40]. For comparison purpose, the adaptive fuzzy controller of [40], abbreviated as AFCM, is implemented. Design parameters of the AFCM include membership functions of the antecedents in the fuzzy rules, values of the consequent forces, and the fuzzy rule map. Detailed values obtained by the procedures described in [40] are shown in Figure 2.

In the fuzzy rules, each of the universe of discourse of the variables is divided into 6 linguistic values as {NB, NS, ZO, PS, PM, PB}, which represent Negative Big,

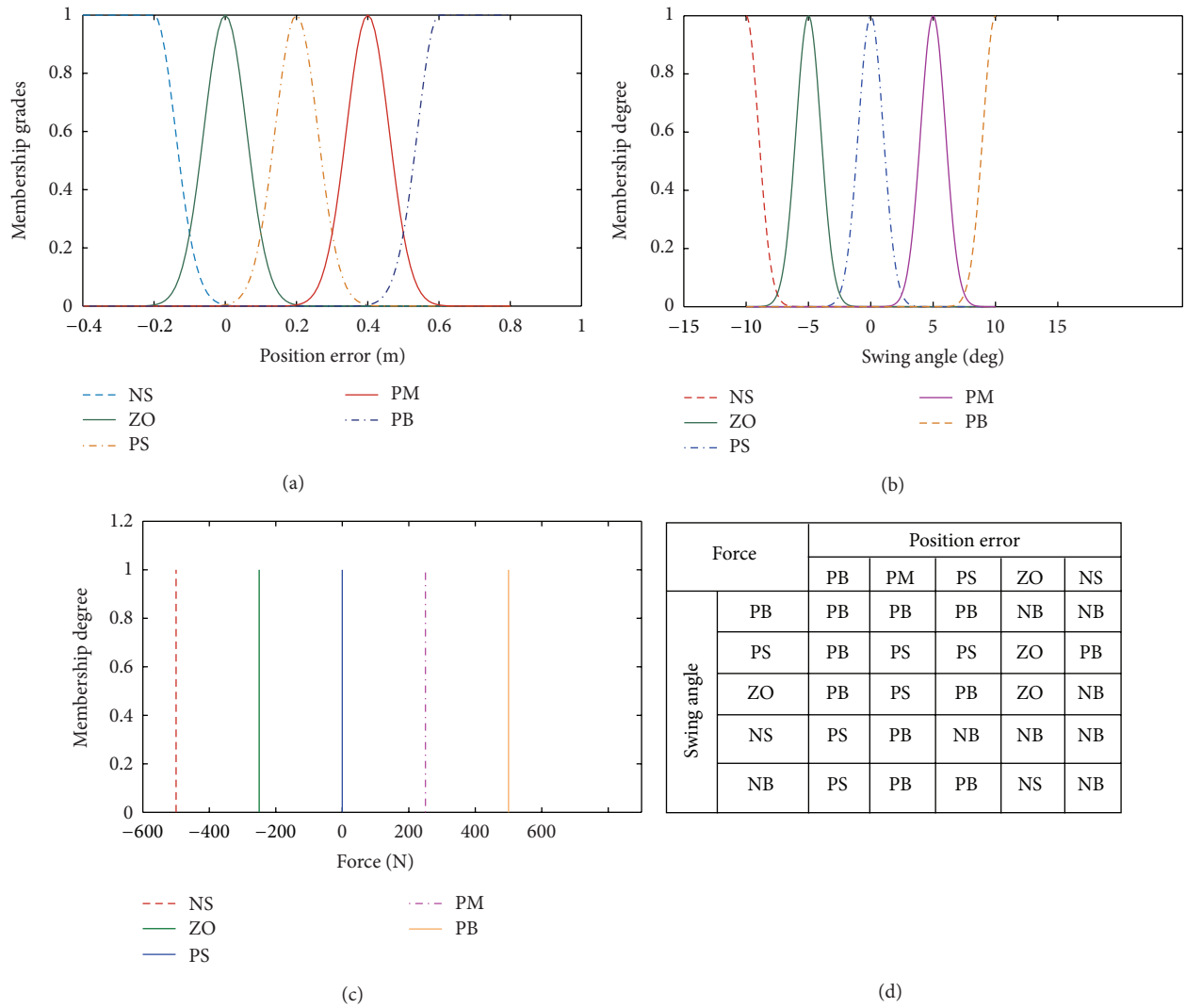

Force		Position error				
		PB	PM	PS	ZO	NS
Swing angle	PB	PB	PB	PB	NB	NB
	PS	PB	PS	PS	ZO	PB
	ZO	PB	PS	PB	ZO	NB
	NS	PS	PB	NB	NB	NB
	NB	PS	PB	PB	NS	NB

FIGURE 2: Linguistic terms, membership functions, and rule table of the fuzzy control rules for AFCM. (a) Definition of membership functions of position error; (b) definition of membership functions of swing angle; (c) consequent part membership function of control input $u(t)$; and (d) fuzzy rule map.

Negative Small, Zero, Positive Small, and Positive Big, respectively.

(3) Performance Comparison. In order to compare relative performance of the two approaches, a significant disturbance of $w = [0, 0, 0, w_4]^T$ with

$$w_4 = \begin{cases} \dfrac{\pi}{3}, & 4.5 \le t \le 6.5, \\ 0, & \text{otherwise} \end{cases} \tag{34}$$

is applied to the crane model.

From the time history of the payload position of these two approaches, shown in Figure 3(a), it is clear that both can successfully demonstrate stable tracking during $0 \le t < 4.5$. However, while the proposed approach remains stable and exhibits accurate tracking after $t \ge 4.5$, the controller of AFCM cannot effectively compensate the applied disturbance w_4, shown in Figure 3(b), and eventually goes unstable. Note also that the control signal $u(t)$ generated by the proposed controller is much smoother and less violent than that of AFCM, further justifying it as a more efficient control strategy.

4.2. Experimental Study. A prototype crane system, shown in Figure 4(a), is built to test the proposed control strategy. As shown in the pictures of Figures 4(b) and 4(c), an encoder with resolution of 2000 pulse/rev is installed in the hanging joint to measure the swing angle θ. To investigate robustness of the control system, the string length can vary between 0.5 to 0.6 m, and the payload weight has three choices: 0.531, 1.041, and 1.484 kg.

The system is firstly identified using the parallel genetic algorithms [41] as T-S type fuzzy combination of the following two rules.

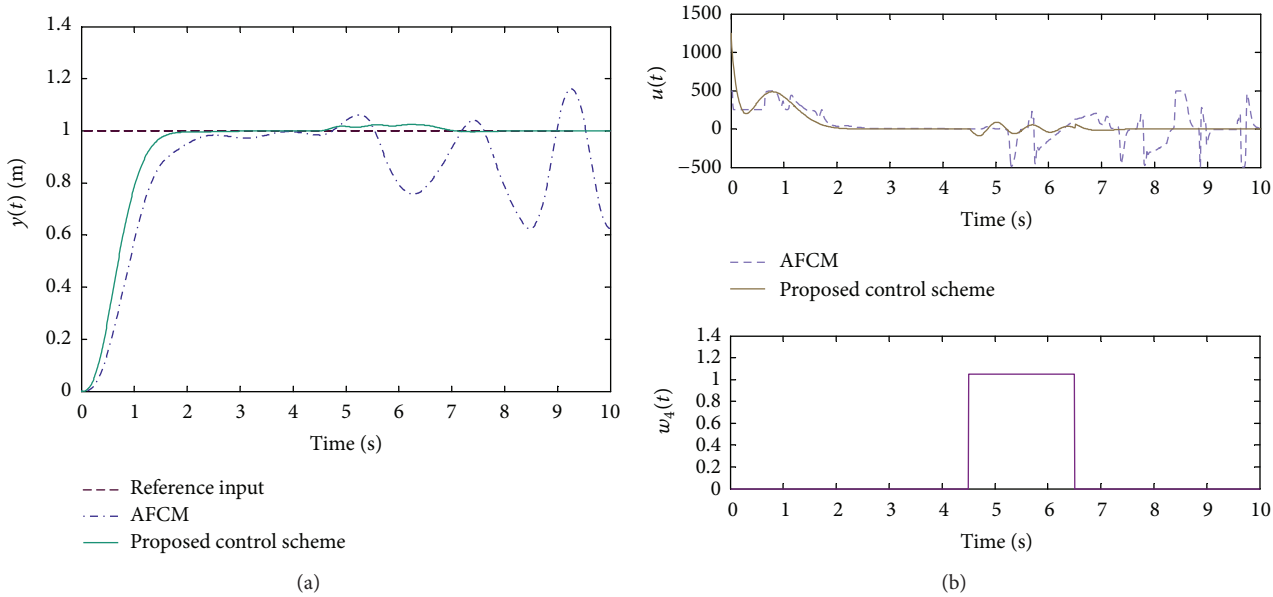

FIGURE 3: Comparative simulation for the proposed control strategy and the AFCM. (a) Position of payload, $y(t)$; (b) control input, $u(t)$, and the external disturbance, $w_4(t)$.

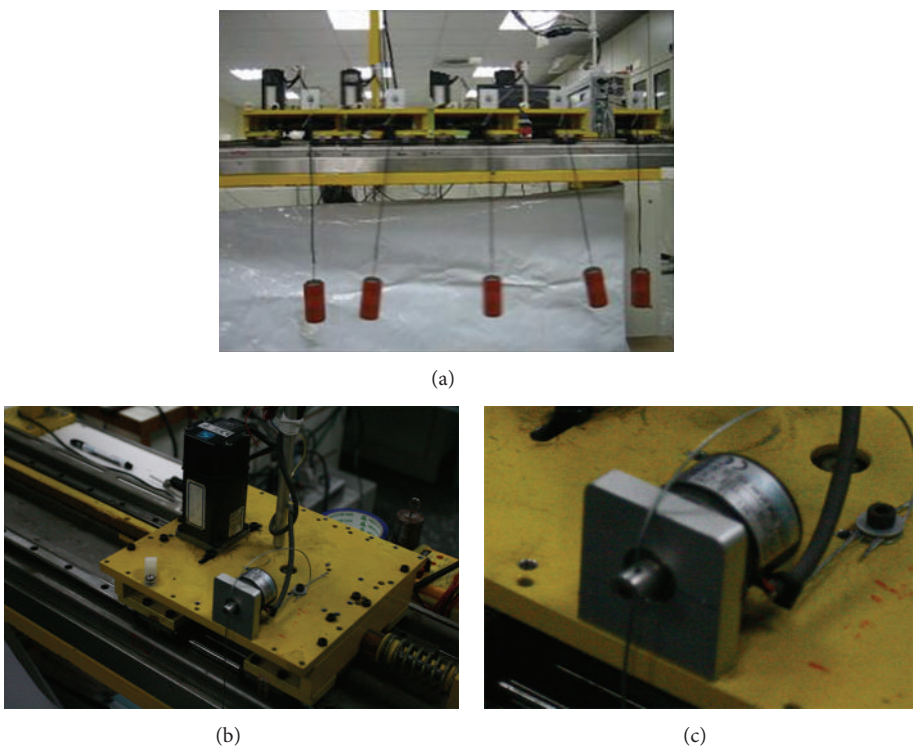

FIGURE 4: Pictures of the experimental crane system. (a) A whole view of the system. The image was generated by overlapping five snapshots taken during operation. (b) An upper view of the cart showing a servo motor to drive the cart and a bearing-supported shaft to hang the payload. (c) Close view of an encoder, also shown in (b), which is attached to the shaft for swing angle measurement.

(i) Plant rule 1:

If x_2 is M_{11},

$$\text{then } \dot{x} = A \cdot x + \Delta A(t) \cdot x + [B + \Delta B(t)] \cdot [u + c_1]. \quad (35)$$

(ii) Plant rule 2:

If x_2 is M_{21},

$$\text{then } \dot{x} = A \cdot x + \Delta A(t) \cdot x + [B + \Delta B(t)] \cdot [u + c_2]. \quad (36)$$

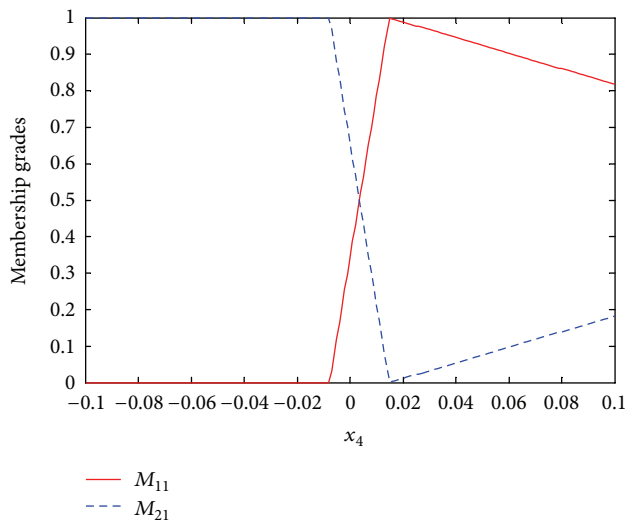

FIGURE 5: The antecedent membership functions, M_{11} and M_{21}, of the fuzzy control law u_f.

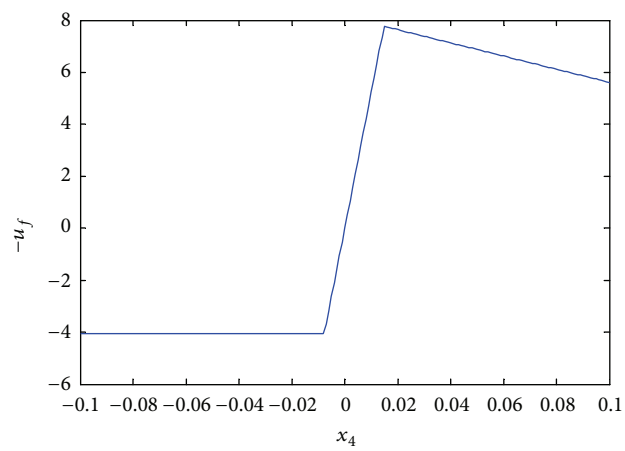

FIGURE 6: The magnitude of $-u_f$ as a function of x_4 (cart velocity).

In the identification, a set of commands are designed to perform various maneuvers satisfying persistent excitation requirements for system identification. The identified two antecedent membership functions of these two rules, M_{11} and M_{21}, are shown in Figure 5, with

$$A = \begin{bmatrix} 0 & 1 & 0 & 0 \\ -23.9363 & 0 & 0 & 0 \\ 0 & 0 & 0 & 1 \\ 2.1681 & 0 & 0 & 0 \end{bmatrix}, \qquad B = \begin{bmatrix} 0 \\ -0.295 \\ 0 \\ 0.1475 \end{bmatrix}. \tag{37}$$

Furthermore,

$$D = \begin{bmatrix} 0 \\ -0.1 \\ 0 \\ 0.01 \end{bmatrix}, \qquad E_1 = \begin{bmatrix} 2 & 0 & 0 & 0 \end{bmatrix}, \qquad E_2 = 0.02 \quad \text{with } F(t) \in [-1, 1]. \tag{38}$$

These are used to define $\Delta A(t)$ and $\Delta B(t)$ according to (9). Interesting enough, if we draw the magnitude of $\sum_{i=1}^{L} h_i(z) \cdot c_i$ versus x_4, the velocity of the cart, we are able to obtain the relationship of Figure 6, which shows the behavior similar to a combination of Coulomb friction with Stribeck effects [42].

Next, by selecting $\nu = 1$ and $\rho = 0.54$, we are able to obtain

$$P = \begin{bmatrix} 1.7070 & 0.3014 & -0.1362 & -0.2631 \\ 0.3014 & 0.0869 & -0.0188 & -0.0444 \\ -0.1362 & -0.0188 & 0.0298 & 0.0269 \\ -0.2631 & -0.0444 & 0.0269 & 0.0658 \end{bmatrix}, \tag{39}$$

$c_1 = -7.772$, $c_2 = 4.0561$, and $K_H = [26.23, 8.02, 23.44, 14.92]$ by the standard LMI techniques.

Figure 7 shows the performance of the outer-level stabilizing controller, u_H. In this figure, three cases were recorded where impacts were applied to the payload at 1.72, 1.45, and 0.38 sec, respectively. The string length and payload weight, [length, weight], of these cases were [0.5, 0.531], [0.55, 1.041], and [0.6, 1.484], respectively. According to these experimental results, the stabilizing controller applied at the outer level exhibits H_∞ robustness against significant disturbances, in spite of variations in the plant dynamics.

Next, considering that string length and payload weight dominate system dynamics, we implemented the servo control law, $u_S = K_S \cdot e$, as a fuzzy controller composed of four fuzzy rules:

Servo control rule ij

If string length is A_i and payload weight is B_j,

$$\text{then } u_S = K_{Sij} \cdot e. \tag{40}$$

That is, both string length and payload weight are fuzzified with two membership functions, A_1, A_2, B_1, and B_2, respectively. The corresponding membership grades of these four fuzzy sets are shown in Figure 8.

Furthermore, by assigning $\omega_1 = 10$ in the definition of the overall performance index J, defined in (29), the Nelder-Mead simplex method was applied to search for the best gains K_{Sij} in the four rules. The learning history of gains is depicted in Figure 9. Note that only the gains corresponding to [length, weight] = [0.5, 0.531] underwent 116 steps; all the other gains were initiated with the gains of fuzzy rule 1, hence less than 30 steps were required. According to considerations

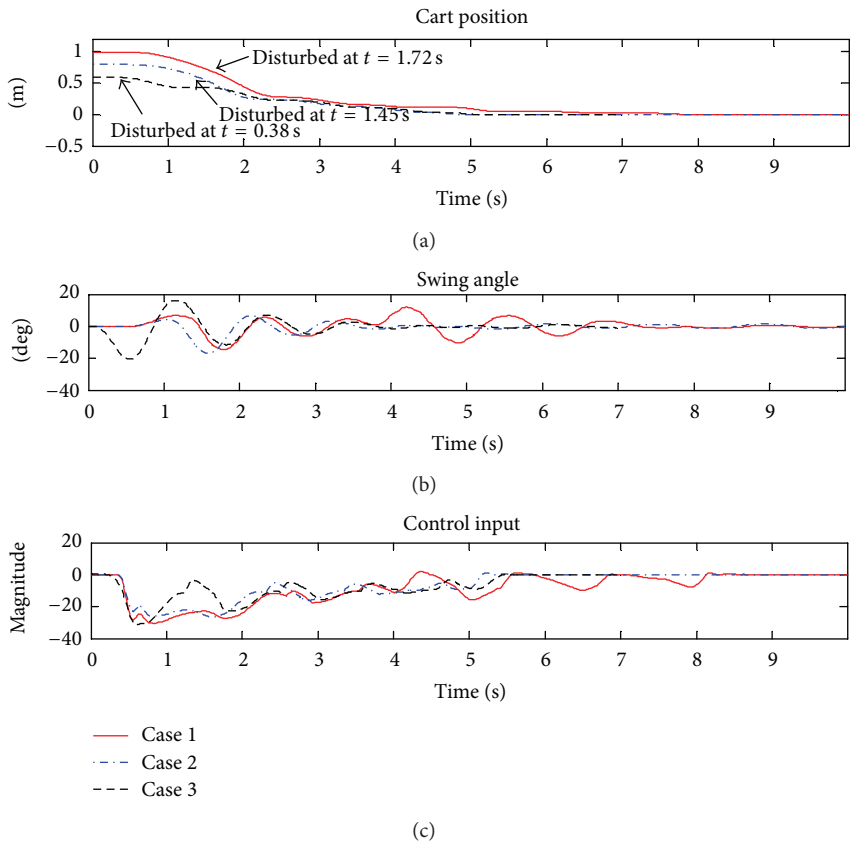

FIGURE 7: Performance of u_H in the face of impact during manipulation. The values of string length and payload weight, [length, weight], are: Case 1: [0.5, 0.531], Case 2: [0.55, 1.041], and Case 3: [0.6, 1.484], respectively.

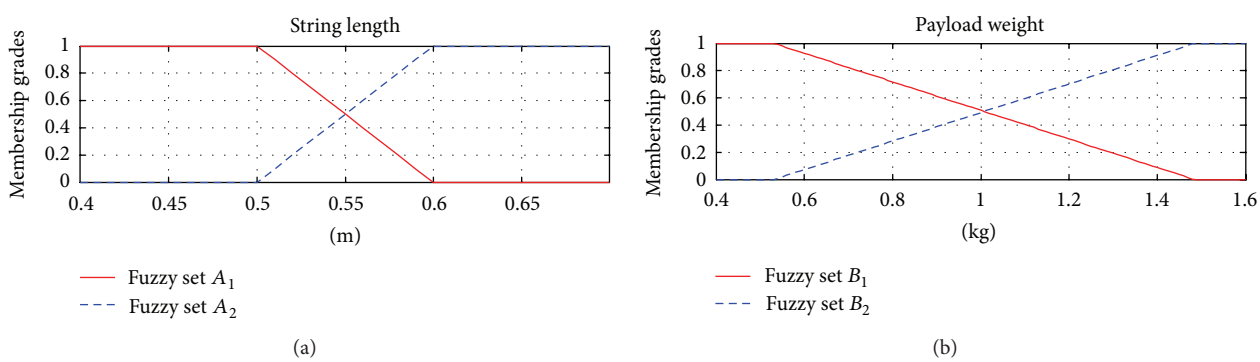

FIGURE 8: The antecedent membership functions of the fuzzy sets, A_1, A_2, B_1, and B_2.

and procedures detailed in Remark 3, the gains are found to be of the following values:

$$\begin{aligned} K_{S11} &= [56, 44, 34, 23] \text{ for } [\text{length}, \text{weight}] = [0.5, 0.531], \\ K_{S21} &= [62, 40, 53, 39] \text{ for } [\text{length}, \text{weight}] = [0.6, 0.531], \\ K_{S12} &= [53, 48, 42, 24] \text{ for } [\text{length}, \text{weight}] = [0.5, 1.484], \\ K_{S22} &= [56, 41, 46, 38] \text{ for } [\text{length}, \text{weight}] = [0.6, 1.484]. \end{aligned} \tag{41}$$

Remark 3. Four fuzzy rules defined in (40), each of them contains a set of optimized control gains, are designed to compensate for the uncertainties in the weight of payload and string length. As shown in the learning history of Figure 10, the gains of rule 1 took 50 iterations and those of the rest of the rules took only 12 iterations. That is, only the first gain set requires complete search. This is because the performance of the Nelder-Mead simplex algorithm is sensitive to initial trial values, and the optimal control gains are close to each other. If the search for the other sets begin with the optimized first set, less iteration is required. Also, an iteration of Figure 10

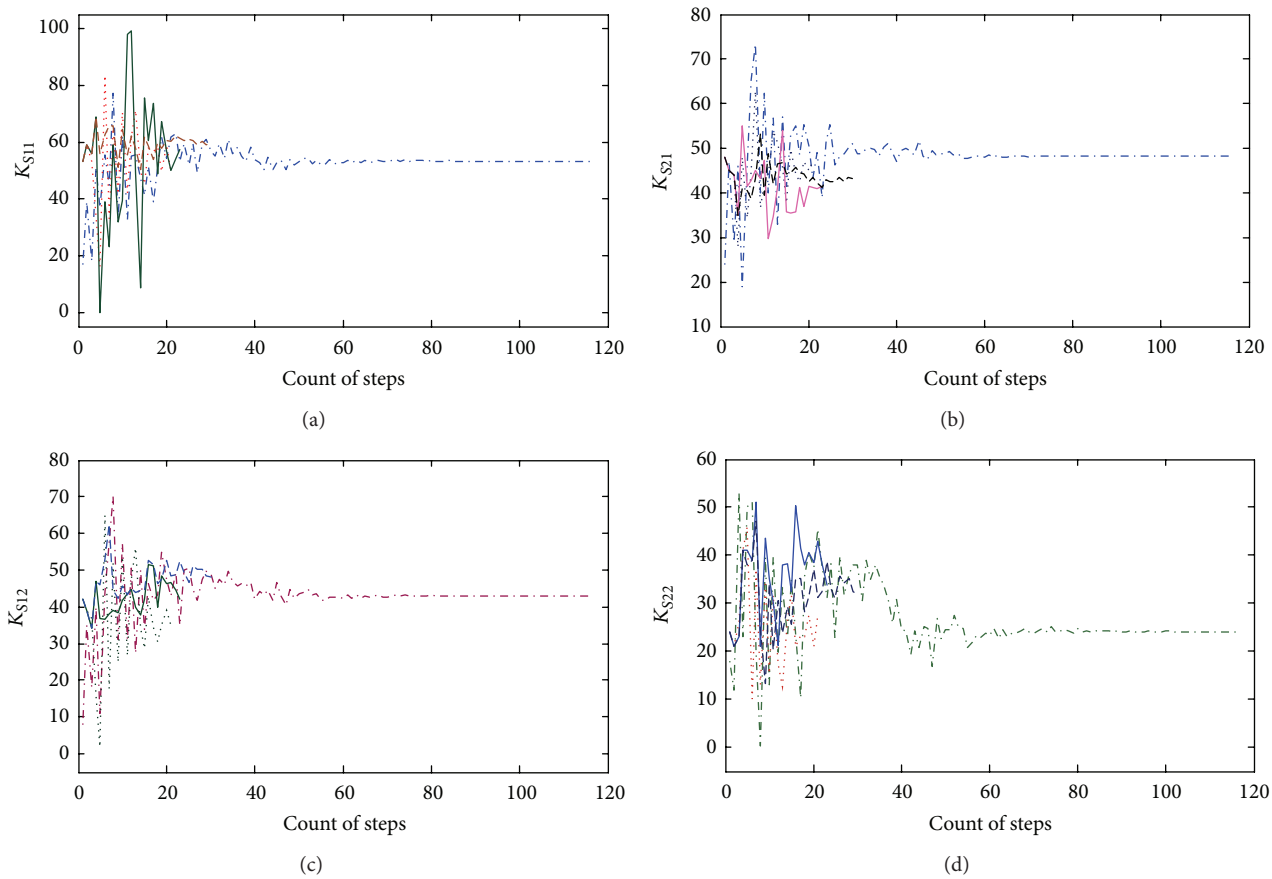

FIGURE 9: The learning history of gains guided by the simplex method showing convergence of the gain parameters. In each of the 3 dimensional cases, the method starts with 4 simplexes and a new simplex, is formed for the following steps by collecting the 4 best solutions so far at the 30th step.

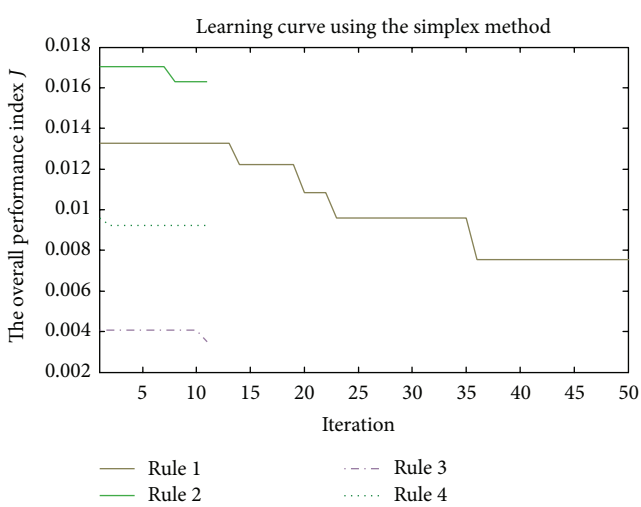

FIGURE 10: The simplex convergence history of the overall performance index, J, in the four rules.

corresponds to 1 to 3 steps in Figure 9, since only improved step is regarded as an effective iteration.

In the experiments of automatic repetitive trials to find the optimal gains, reference state trajectories were designed such that the payload moves smoothly forward without swinging back. In fulfilling the requirement, the reference trajectories should be a function of the nature frequency that, in turn, depends on both the string length and the load weight. Specifically, for the payload position $y = x_1 + l \cdot \sin\theta$ to move in this way, the trajectory of θ should contain integer multiple of a full nature-frequency cycle.

Finally, experiments were conducted to justify the control performance. Three experiments were designed: Case 1: [length, weight, distance] = [0.6, 1.484, 1.0], Case 2: [length, weight, distance] = [0.6, 1.041, 0.8], and Case 3: [length, weight, distance] = [0.5, 0.531, 0.6]. The gains of Case 2 are interpolated from four fuzzy rules to be: K_S = [58.7891, 40.5352, 49.2539, 38.4648]. The performance of the crane control system is demonstrated in Figure 11. According to the experimental results, the proposed control strategy can guide the payload smoothly forward without swinging back in a reasonable period of time.

5. Conclusions

By the antiswing control approach, a two-level control scheme is proposed for crane systems. The plant is modeled as a combination of a nominal linear system and a T-S fuzzy blending of affine terms. This type of dynamic model

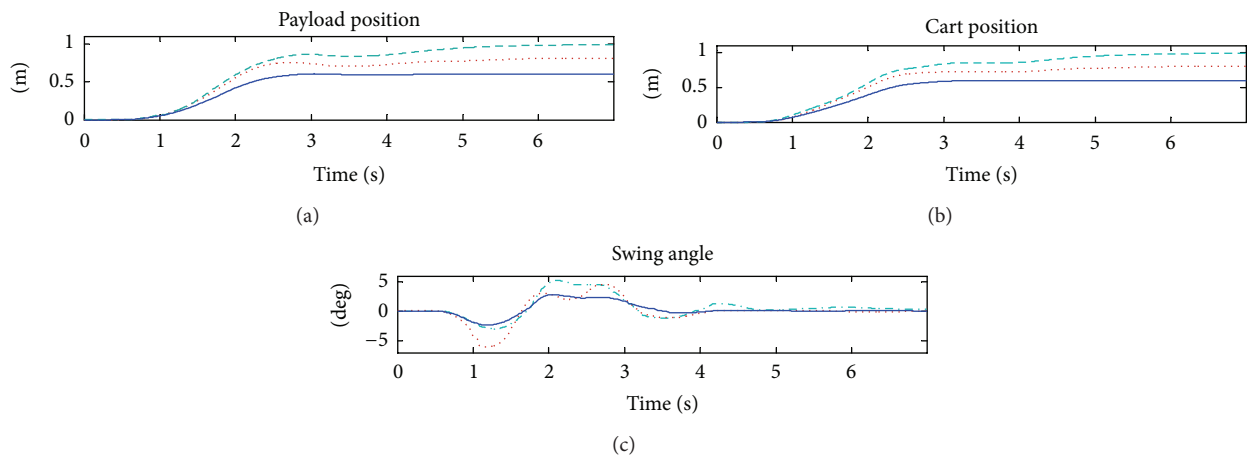

Figure 11: Experimental results of the crane control system. Case 1: [length, weight, distance] = [0.6, 1.484, 1.0], Case 2: [length, weight, distance] = [0.6, 1.041, 0.8], Case 3: [length, weight, distance] = [0.5, 0.531, 0.6].

significantly simplifies the subsequent analysis and control designs, because assumptions on the plant dynamics can be significantly reduced. The proposed control scheme can also be applied to other nonlinear plants, such as ships, mobile robots, and aircrafts, but is not applicable for systems with considerable time delay, which is the issue to be addressed in our future investigation.

In the scheme, the outer-level control law serves as an H_∞ robust controller, which is responsible for closed-loop stability in the face of disturbances and plant dynamic variations. Optimal gains of the inner-loop servo control law are obtained using the Nelder-Mead simplex algorithm in a learning control manner. Close observation of the obtained fuzzy model reveals that the fuzzy compensator mainly counteracts the effects of friction. The dynamics of Coulomb friction, viscous friction, and Stribeck effects are distinguishable as functions of relative velocity.

A simulation study shows superior performance of the proposed control strategy in compensating significant disturbances. Experimental results of a prototype two-dimensional crane control system also demonstrate smooth manipulation of the payload with H_∞ robust stability. The control strategy can be extended to full dimensional crane systems and is within our plans of future research.

Acknowledgments

The authors would like to express their sincere appreciation to the editor and all the reviewers for their helpful and constructive comments. Besides, the authors are enormously grateful for the supports from the National Science Council of Taiwan, under Grants nos. NSC 101-2221-E-182-006 and 100-2221-E-182-008.

References

[1] B. J. Park, K. S. Hong, and C. D. Huh, "Time-efficient input shaping control of container crane systems," in *Proceedings of IEEE International Conference on Control Applications*, pp. 80–85, 2000.

[2] W. Singhose, L. Porter, M. Kenison, and E. Kriikku, "Effects of hoisting on the input shaping control of gantry cranes," *Control Engineering Practice*, vol. 8, no. 10, pp. 1159–1165, 2000.

[3] D. Liu, J. Yi, D. Zhao, and W. Wang, "Adaptive sliding mode fuzzy control for a two-dimensional overhead crane," *Mechatronics*, vol. 15, no. 5, pp. 505–522, 2005.

[4] M. J. Er, M. Zribi, and K. L. Lee, "Variable structure control of an overhead crane," in *Proceedings of IEEE International Conference on Control Applocations*, pp. 398–402, September 1998.

[5] A. M. H. Basher, "Swing-free transport using variable structure model reference control," in *Proceedings of IEEE SoutheastCon*, pp. 85–92, April 2001.

[6] L. Moreno, L. Acosta, J. A. Méndez, S. Torres, A. Hamilton, and G. N. Marichal, "A self-tuning neuromorphic controller: application to the crane problem," *Control Engineering Practice*, vol. 6, no. 12, pp. 1475–1483, 1998.

[7] H. H. Lee and S. K. Cho, "A new fuzzy-logic anti-swing control for industrial three-dimensional overhead cranes," in *Proceedings of IEEE International Conference on Robotics and Automation*, pp. 2956–2961, May 2001.

[8] M. J. Nalley and M. B. Trabia, "Control of overhead cranes using a fuzzy logic controller," *Journal of Intelligent and Fuzzy Systems*, vol. 8, no. 1, pp. 1–18, 2000.

[9] L. Wu, X. Su, P. Shi, and J. Qiu, "Model approximation for discrete-time state-delay systems in the TS fuzzy framework," *IEEE Transactions on Fuzzy Systems*, vol. 19, no. 2, pp. 366–378, 2011.

[10] X. Su, P. Shi, L. Wu, and Y. D. Song, "A novel approach to filter design for T-S fuzzy discrete-time systems with time-varying delay," *IEEE Transactions on Fuzzy Systems*, vol. 20, pp. 1114–1129, 2012.

[11] C. H. Sun, S. W. Lin, and Y. T. Wang, "Relaxed stabilization conditions for switching T-S fuzzy systems with practical constraints," *International Journal of Innovative Computing, Information and Control*, vol. 8, pp. 4133–4145, 2012.

[12] X. Su, P. Shi, L. Wu, and Y. D. Song, "A novel control design on discrete-time Takagi-Sugeno fuzzy systems with time-varying delays," *IEEE Transactions on Fuzzy Systems*.

[13] R. Yang, P. Shi, G.-P. Liu, and H. Gao, "Network-based feedback control for systems with mixed delays based on quantization and dropout compensation," *Automatica*, vol. 47, no. 12, pp. 2805–2809, 2011.

[14] A. Benhidjeb and G. L. Gissinger, "Fuzzy control of an overhead crane performance comparison with classic control," *Control Engineering Practice*, vol. 3, no. 12, pp. 1687–1696, 1995.

[15] J. Yi, N. Yubazaki, and K. Hirota, "Anti-swing and positioning control of overhead traveling crane," *Information Sciences*, vol. 155, no. 1-2, pp. 19–42, 2003.

[16] X. H. Chang and G. H. Yang, "Relaxed results on stabilization and state feedback H_∞ control conditions for T-S fuzzy systems," *International Journal of Innovative Computing, Information and Control*, vol. 7, no. 4, pp. 1753–1764, 2011.

[17] A. Schwung, T. Gusner, and J. Adamy, "Stability analysis of recurrent fuzzy systems: a hybrid system and sos approach," *IEEE Transactions on Fuzzy Systems*, vol. 19, no. 3, pp. 423–431, 2011.

[18] H. K. Lam, "Polynomial fuzzy-model-based control systems: Stability analysis via piecewise-linear membership functions," *IEEE Transactions on Fuzzy Systems*, vol. 19, no. 3, pp. 588–593, 2011.

[19] J. C. Lo, Y. T. Lin, and W. C. Liao, "Generalized stabilizing controllers for fuzzy systems via circle criterion-LMI and SOS," in *Proceedings of IEEE International Conference on Fuzzy Systems*, pp. 1294–1298, 2011.

[20] K. Tanaka, H. Ohtake, T. Seo, and H. O. Wang, "An SOS-based observer design for polynomial fuzzy systems," in *American Control Conference*, pp. 4953–4958, 2011.

[21] X. Su, L. Wu, P. Shi, and Y. D. Song, "H_∞ model reduction of T-S fuzzy stochastic systems," *IEEE Transactions on Systems, Man, and Cybernetics Part B*, vol. 42, pp. 1574–1585, 2012.

[22] F. Li and X. Zhang, "Delay-range-dependent robust H_∞ filtering for singular LPV systems with time variant delay," *International Journal of Innovative Computing, Information and Control*, vol. 9, pp. 339–353, 2013.

[23] R. Yang, H. Gao, and P. Shi, "Delay-dependent robust H_∞ control for uncertain stochastic time-delay systems," *International Journal of Robust and Nonlinear Control*, vol. 20, no. 16, pp. 1852–1865, 2010.

[24] K. Tanaka and H. O. Wang, *Fuzzy Control Systems Design and Analysis: A Linear Matrix Inequality Approach*, Wiley, New York, NY, USA, 2001.

[25] K. Tanaka, T. Hori, and H. O. Wang, "A multiple Lyapunov function approach to stabilization of fuzzy control systems," *IEEE Transactions on Fuzzy Systems*, vol. 11, no. 4, pp. 582–589, 2003.

[26] K. Tanaka, T. Ikeda, and H. O. Wang, "Robust stabilization of a class of uncertain nonlinear systems via fuzzy control: quadratic stabilizability, H_∞ control theory, and linear matrix inequalities," *IEEE Transactions on Fuzzy Systems*, vol. 4, no. 1, pp. 1–13, 1996.

[27] K. Tanaka and M. Sugeno, "Stability analysis and design of fuzzy control systems," *Fuzzy Sets and Systems*, vol. 45, no. 2, pp. 135–156, 1992.

[28] H. O. Wang, K. Tanaka, and M. F. Griffin, "An approach to fuzzy control of nonlinear systems: Stability and design issues," *IEEE Transactions on Fuzzy Systems*, vol. 4, no. 1, pp. 14–23, 1996.

[29] B. S. Chen, C. S. Tseng, and H. J. Uang, "Robustness design of nonlinear dynamic systems via fuzzy linear control," *IEEE Transactions on Fuzzy Systems*, vol. 7, no. 5, pp. 571–585, 1999.

[30] C. S. Tseng, B. S. Chen, and H. J. Uang, "Fuzzy tracking control design for nonlinear dynamic systems via T-S fuzzy model," *IEEE Transactions on Fuzzy Systems*, vol. 9, no. 3, pp. 381–392, 2001.

[31] K. R. Lee, E. T. Jeung, and H. B. Park, "Robust fuzzy H_∞ control for uncertain nonlinear systems via state feedback: an LMI approach," *Fuzzy Sets and Systems*, vol. 120, no. 1, pp. 123–134, 2001.

[32] H. K. Lam, F. H. F. Leung, and Y. S. Lee, "Design of a switching controller for nonlinear systems with unknown parameters based on a fuzzy logic approach," *IEEE Transactions on Systems, Man, and Cybernetics, Part B*, vol. 34, no. 2, pp. 1068–1074, 2004.

[33] C. H. Sun, Y. T. Wang, and C. C. Chang, "Switching T-S fuzzy model-based guaranteed cost control for two-wheeled mobile robots," *International Journal of Innovative Computing, Information and Control*, vol. 8, pp. 3015–3028, 2012.

[34] J. A. Nelder and R. Mead, "A simplex method for function minimization," *Computer Journal*, vol. 7, pp. 308–313, 1965.

[35] T. Niknam, H. D. Mojarrad, and M. Nayeripour, "A new hybrid fuzzy adaptive particle swarm optimization for non-convex economic dispatch," *International Journal of Innovative Computing, Information and Control*, vol. 7, no. 1, pp. 189–202, 2011.

[36] Y. C. Ho, W. C. Hsu, and C. C. Chang, "Multi-category and multi-standard project selection with fuzzy value-based time limit," *International Journal of Innovative Computing, Information and Control*, vol. 9, pp. 971–989, 2013.

[37] C. M. Lin, C. F. Hsu, and R. G. Yeh, "Adaptive fuzzy sliding-mode control system design for brushless DC motors," *International Journal of Innovative Computing, Information and Control*, vol. 9, pp. 1259–1270, 2013.

[38] H. M. Lee, C. F. Fuh, and J. S. Su, "Fuzzy parallel system reliability analysis based on level (λ, ρ) interval-valued fuzzy numbers," *International Journal of Innovative Computing, Information and Control*, vol. 8, no. 8, pp. 5703–5713, 2012.

[39] L. K. Wong, F. H. F. Leung, and P. K. S. Tarn, "Lyapunov-function-based design of fuzzy logic controllers and its application on combining controllers," *IEEE Transactions on Industrial Electronics*, vol. 45, no. 3, pp. 502–509, 1998.

[40] C. Y. Chang, "Adaptive fuzzy controller of the overhead cranes with nonlinear disturbance," *IEEE Transactions on Industrial Informatics*, vol. 3, no. 2, pp. 164–172, 2007.

[41] Y. Z. Chang, J. Chang, and C. K. Huang, "Parallel genetic algorithms for a neurocontrol problem," in *International Joint Conference on Neural Networks (IJCNN '99)*, pp. 4151–4155, July 1999.

[42] P. A. Bliman and M. Sorine, "Friction modelling by hysteresis operators application to Dahl, sticktion and Stribeck effects," in *Proceedings of the Conference on Models of Hysteresis*, 1991.

Hindawi Publishing Corporation
Mathematical Problems in Engineering
Volume 2013, Article ID 324738, 13 pages
http://dx.doi.org/10.1155/2013/324738

Research Article

Delay-Dependent Stability Analysis of Uncertain Fuzzy Systems with State and Input Delays under Imperfect Premise Matching

Zejian Zhang,[1,2] Xiao-Zhi Gao,[2] Kai Zenger,[2] and Xianlin Huang[1]

[1] *Center for Control Theory and Guidance Technology, Harbin Institute of Technology, Harbin 150001, China*
[2] *Department of Automation and Systems Technology, Aalto University School of Electrical Engineering, 00076 Aalto, Finland*

Correspondence should be addressed to Zejian Zhang; zzhanghit@gmail.com

Received 1 December 2012; Accepted 4 February 2013

Academic Editor: Peng Shi

Copyright © 2013 Zejian Zhang et al. This is an open access article distributed under the Creative Commons Attribution License, which permits unrestricted use, distribution, and reproduction in any medium, provided the original work is properly cited.

This paper discusses the stability and stabilization problem for uncertain T-S fuzzy systems with time-varying state and input delays. A new augmented Lyapunov function with an additional triple-integral term and different membership functions of the fuzzy models and fuzzy controllers are introduced to derive the stability criterion, which is less conservative than the existing results. Moreover, a new flexibility design method is also provided. Some numerical examples are given to demonstrate the effectiveness and less conservativeness of the proposed method.

1. Introduction

Since the Takagi-Sugeno (T-S) [1] fuzzy systems were firstly proposed in 1985, their stability analysis has received considerable research attention [2, 3]. However, most of the existing results are only for the T-S fuzzy systems free of time delay. Actually, time delay often occurs in many practical systems, such as [4, 5]. It has been shown that the existence of time delay usually becomes the source of instability and deteriorated performance of systems. Therefore, study of the time delay is important in both theory and practice [6]. The first stability analysis work on the T-S fuzzy systems with time delay is done in [7, 8] by using the Lyapunov-Razumikhin functional approach. If some uncertainties exist in a T-S fuzzy time delay system, they may also significantly affect the system performances and even cause unstable system outputs. Therefore, the issue of the stability for the uncertain T-S fuzzy time delay systems has been widely explored [9–11]. In the literature, two basic approaches have been utilized, that is, delay-independent approach [12] and delay-dependent approach. The latter makes use of the information on the length of the delays, and it is less conservative than the former one. A lot of stability analysis results have been reported based on the delay-dependent approach [13, 14].

During the recent years, some research work for different types of the delays of the T-S fuzzy systems has been published, such as constant delay [15, 16], bounded time delay [17], time varying delay [18], and interval time varying delay [19, 20]. However, all these results are only for the T-S fuzzy systems with state delays. Thus, they may be invalid when applied to the systems with input delays. As we know, input delays extensively exist in industrial processes and can cause instability or serious performance deterioration. In fact, in modern industrial systems, sensors, controllers, and plants are often connected together, and the sampled data and controller signals are transmitted through networks. In view of this, the input delays should be taken into consideration for robust controller design. Intensive results on the stabilization for the T-S fuzzy systems with state and input delays are reported in [21–28]. For example, the work in [21] is based on the linear systems with input delays. In [22, 24], the authors only consider the fuzzy systems with constant input delays, and their results are conservative. In [23], the authors study the fuzzy systems with both the state and input delays. Unfortunately, the results are obtained without any uncertainty, and the state delay is assumed to be equal to the input delay. In [26], the uncertainty has been considered in the analysis, but the state delay is also assumed

to be the same as the input delay. Some interesting results for the uncertain fuzzy systems with state and input delays have been obtained in [25, 27, 28], most of which introduce some Lyapunov-Krasovskii functions containing integral terms, for example, $\int_{t-\tau}^{t} x^T(s)Qx(s)ds$, and double-integral terms, $\int_{-\tau}^{0}\int_{t+\theta}^{t} \dot{x}^T(s)Q\dot{x}(s)ds\,d\theta$. Several triple-integral terms are used in the Lyapunov function [29] to yield less conservative results for the fuzzy systems with state delay. A large portion of robust controller design topics have been investigated on the basis of the Parallel Distribution Compensation (PDC) design technique, where the fuzzy controller shares the same premise membership functions as those of the T-S fuzzy time delay model [7–11, 15–20, 22–28]. As a matter of fact, if the membership functions in the premise of the fuzzy rules of the fuzzy controllers are allowed to be designed arbitrarily, we can even achieve better design flexibility. For instance, a fuzzy controller not sharing the same premise rules as those of the T-S fuzzy model referred to as imperfect premise matching is employed to control the nonlinear plants [30, 31], and [12] extends the available results to the T-S fuzzy time-delay systems with only the state delay.

In this paper, an augmented Lyapunov-Krasovskii function that contains a triple-integral term is introduced to investigate the stability and stabilization problem for uncertain T-S fuzzy systems with the state and input delays under the imperfect premise matching, in which the fuzzy time delay model and fuzzy controller are with different premise. Some less conservative delay-dependent stability and robust stability conditions are obtained by two integral inequalities and a parameterized model transformation method. Moreover, different from the general PDC design technique, a new design approach of robust stable controllers is proposed. Two simulation examples are further given to illustrate that the proposed design methods are less conservative and more flexible.

2. System Description and Preliminaries

Let r be the number of the fuzzy rules describing the time delay nonlinear plant. The ith rule can be represented as follows.

If $f_1(x(t))$ is M_1^i and ... and $f_p(x(t))$ is M_p^i

$$\begin{aligned}\dot{x}(t) = {} & \left(A_{1i} + \Delta A_{1i}(t)\right)x(t) + \left(A_{2i} + \Delta A_{2i}(t)\right) \\ & \times x\left(t - d_1(t)\right) + \left(B_i + \Delta B_i(t)\right)u\left(t - d_2(t)\right), \\ x(t) = {} & \varphi(t), \quad t \in \left[-\max\left(h_1, h_2\right), 0\right],\end{aligned} \tag{1}$$

where M_α^i is a fuzzy term of rule i corresponding to the function $f_\alpha(x(t))$, $\alpha = 1, 2, \ldots, p$; $i = 1, 2, \ldots, r$. $x(t) \in R^n$ is the system state vector, and $u(t) \in R^m$ is the input vector. The matrices A_{1i}, A_{2i}, and B_i, $i = 1, 2, \ldots, r$, are of appropriate dimensions. The initial condition $\varphi(t)$ is a continuous vector-valued function. The delays $d_1(t)$ and $d_2(t)$ are time varying, and satisfy

$$\begin{aligned} 0 \le d_1(t) \le h_1, \qquad \dot{d}_1(t) \le \mu_1, \\ 0 \le d_2(t) \le h_2, \qquad \dot{d}_2(t) \le \mu_2, \end{aligned} \tag{2}$$

where h_i are constants representing the upper bound of the delay. μ is a positive constant. ΔA_{1i}, ΔA_{2i}, and ΔB_i denote the uncertainties in the system, and they are the form of

$$\begin{aligned}\left[\Delta A_{1i} \quad \Delta A_{2i} \quad \Delta B_i\right] = D_i K_i(t)\left[E_{1i} \quad E_{2i} \quad E_{bi}\right], \\ i = 1, 2, \ldots, r,\end{aligned} \tag{3}$$

where D_i, E_{1i}, E_{2i}, and E_{bi} are known constant matrices of appropriate dimensions, and $K_i(t)$ is unknown matrix function satisfying $K_i^T(t)K_i(t) \le I$. I is an appropriately dimensioned identity matrix. Hence, the overall fuzzy model can be formulized as follows:

$$\begin{aligned}\dot{x}(t) = \sum_{i=1}^{r} w_i(x(t))\left[\left(A_{1i} + \Delta A_{1i}(t)\right)x(t) + \left(A_{2i} + \Delta A_{2i}(t)\right)\right. \\ \times x\left(t - d_1(t)\right) + \left(B_i + \Delta B_i(t)\right) \\ \left.\times u\left(t - d_2(t)\right)\right],\end{aligned} \tag{4}$$

where

$$\begin{aligned}\sum_{i=1}^{r} w_i(x(t)) = 1, \quad w_i(x(t)) \ge 0, \\ w_i(x(t)) = \frac{\mu_i(x(t))}{\sum_{i=1}^{r}\mu_i(x(t))}, \\ \mu_i(x(t)) = \prod_{\alpha=1}^{p}\mu_{M_\alpha^i}\left(f_\alpha(x(t))\right).\end{aligned} \tag{5}$$

$w_i(x(t))$ is the normalized grade of membership function that is a nonlinear function of $x(t)$. $\mu_{M_\alpha^i}(f_\alpha(x(t)))$ is the grade of the membership corresponding to the fuzzy term of M_α^i.

Different from the popular PDC design technique, the following fuzzy control law under imperfect premise matching is employed to deal with the problem of stabilization via state feedback. Under the imperfect premise matching, the jth rule of the fuzzy controller is defined as follows.

If $g_1(x(t))$ is N_1^i and ... and $g_q(x(t))$ is N_q^i

$$u(t) = F_j x(t), \quad j = 1, 2, \ldots, r, \tag{6}$$

where N_β^j denotes the fuzzy set. q is a positive integer, and $F_j \in R^{m\times n}$ is the feedback gain of rule j. The state feedback fuzzy control law is represented by

$$u(t) = \sum_{j=1}^{r} m_j(x(t))F_j x(t), \tag{7}$$

where

$$\sum_{j=1}^{r} m_j(x(t)) = 1, \quad m_j(x(t)) \geq 0,$$

$$m_j(x(t)) = \frac{v_j(x(t))}{\sum_{j=1}^{r} v_j(x(t))}, \tag{8}$$

$$v_j(x(t)) = \prod_{\beta=1}^{q} v_{N_\beta^j}\left(g_\beta(x(t))\right).$$

$m_j(x(t))$ is the normalized grade of membership function that is a nonlinear function of $x(t)$. $v_{N_\beta^j}(g_\beta(x(t)))$ is the grade of the membership corresponding to the fuzzy term of N_β^j.

As the time varying delay is included in the control input, we have

$$u(t-d_2(t)) = \sum_{j=1}^{r} m_j(x(t-d_2(t)))F_j x(t-d_2(t)), \tag{9}$$

where

$$\sum_{j=1}^{r} m_j(x(t-d_2(t))) = 1, \quad m_j(x(t-d_2(t))) \geq 0. \tag{10}$$

Lemma 1 (see [32] (Schur complement)). *Given constant matrices Ω_1, Ω_2, and Ω_3, where $\Omega_1 = \Omega_1^T$ and $\Omega_2 = \Omega_2^T$, there is $\Omega_1 + \Omega_3^T\Omega_2^{-1}\Omega_3 < 0$, if and only if*

$$\begin{bmatrix} \Omega_1 & \Omega_3^T \\ * & -\Omega_2 \end{bmatrix} < 0 \quad or \quad \begin{bmatrix} -\Omega_2 & \Omega_3 \\ * & -\Omega_1 \end{bmatrix} < 0. \tag{11}$$

Lemma 2 (see [33]). *Let $Q = Q^T$, D, E, and $K(t)$ satisfies $K^T(t)K(t) \leq I$; the following inequality holds*

$$Q + DK(t)E + E^T K^T(t) D^T < 0, \tag{12}$$

if and only if the following inequality holds for any smaller $\varepsilon > 0$:

$$Q + \varepsilon^{-1} DD^T + \varepsilon E^T E < 0. \tag{13}$$

Lemma 3 (see [34]). *For any constant matrix $\Sigma = \Sigma^T > 0$ and a scalar $\tau > 0$ such that the following integrations are well defined, we have*

$$\begin{aligned} &-\int_{t-\tau}^{t} x^T(s)\Sigma x(s)\,ds \\ &\quad \leq -\frac{1}{\tau}\left(\int_{t-\tau}^{t} x(s)\,ds\right)^T \Sigma \left(\int_{t-\tau}^{t} x(s)\,ds\right), \\ &-\int_{-\tau}^{0}\int_{t+\theta}^{t} x^T(s)\Sigma x(s)\,ds\,d\theta \\ &\quad \leq -\frac{1}{\tau^2}\left(\int_{-\tau}^{0}\int_{t+\theta}^{t} x(s)\,ds\,d\theta\right)^T \Sigma \left(\int_{-\tau}^{0}\int_{t+\theta}^{t} x(s)\,ds\,d\theta\right). \end{aligned} \tag{14}$$

3. Main Results

In this section, some new delay-dependent criteria for the T-S fuzzy systems with state and input delays are proposed by introducing a novel Lyapunov function with an additional triple-integral term under the imperfect premise matching. Moreover, a robust stabilization criterion is also investigated.

3.1. Stability of Nominal Fuzzy Systems. Firstly, we consider the control design of a state feedback control law under the imperfect premise matching that stabilizes the following nominal fuzzy time varying delay system:

$$\begin{aligned} \dot{x}(t) = &\sum_{i=1}^{r}\sum_{j=1}^{r} w_i(x(t)) m_j(x(t-d_2(t))) \\ &\times \left[A_{1i}x(t) + A_{2i}x(t-d_1(t)) + B_i F_j x \right. \\ &\left. \times (t-d_2(t))\right], \\ x(t) = &\varphi(t), \quad t \in [-\max(h_1, h_2), 0]. \end{aligned} \tag{15}$$

Theorem 4. *Given scalars $h_1 \geq 0, h_2 \geq 0$, μ_1, μ_2, and t_i $(i = 2, \ldots, 8)$, the closed-loop system (15) is asymptotically stable for any $0 \leq d_i(t) \leq h_i$ $(i = 1, 2)$ via the imperfect premise matching controller design technique, if the membership functions of the fuzzy model and fuzzy controller satisfy $m_j(x(t-d_2(t))) - \rho_j w_j(x(t)) \geq 0$ for all j, $x(t)$ and $x(t-d_2(t))$, where $0 < \rho_j < 1$, and there exist matrices $\overline{P}_{11} > 0, \overline{P}_{22} > 0$, $\overline{W}_{11} > 0$, $\overline{W}_{22} > 0$, $\overline{Z}_{11} > 0$, $\overline{Z}_{22} > 0$, $\overline{N}_{11} > 0$, $\overline{N}_{22} > 0$, $\overline{Q}_i > 0$, $\overline{M}_i > 0$, $\overline{R}_i > 0$ $(i = 1, 2)$, $\Lambda_i = \Lambda_i^T \in R^{8n\times 8n} > 0$ $(i = 1, 2, \ldots, r)$, and*

$$\begin{aligned} \overline{P} &= \begin{bmatrix} \overline{P}_{11} & \overline{P}_{12} \\ * & \overline{P}_{22} \end{bmatrix} > 0, \qquad \overline{W} = \begin{bmatrix} \overline{W}_{11} & \overline{W}_{12} \\ * & \overline{W}_{22} \end{bmatrix} > 0, \\ \overline{Z} &= \begin{bmatrix} \overline{Z}_{11} & \overline{Z}_{12} \\ * & \overline{Z}_{22} \end{bmatrix} > 0, \qquad \overline{N} = \begin{bmatrix} \overline{N}_{11} & \overline{N}_{12} \\ * & \overline{N}_{22} \end{bmatrix} > 0, \end{aligned} \tag{16}$$

and real matrices Y_j $(j = 1, 2, \ldots, r)$, $\overline{P}_{12}\,\overline{W}_{12}\,\overline{Z}_{12}\,\overline{N}_{12}$, and X such that (30)–(32) hold. In addition, the stabilizing control law is given by

$$u(t) = \sum_{j=1}^{r} m_j(x(t-d_2(t)))Y_j X^{-T} x(t). \tag{17}$$

Proof. Choose a fuzzy weighting-dependent Lyapunov-Krasovskii functional candidate as

$$\begin{aligned} V(x(t)) = &V_1(x(t)) + V_2(x(t)) + V_3(x(t)) + V_4(x(t)) \\ &+ V_5(x(t)), \end{aligned}$$

$$\begin{aligned}
V_1(x(t)) &= \xi_1^T(t)P\xi_1(t) + \xi_2^T(t)W\xi_2(t),\\
V_2(x(t)) &= \int_{-h_1}^{0}\int_{t+\theta}^{t}\xi^T(s)Z\xi(s)\,ds\,d\theta\\
&\quad+\int_{-h_2}^{0}\int_{t+\theta}^{t}\xi^T(s)N\xi(s)\,ds\,d\theta,\\
V_3(x(t)) &= \int_{t-d_1(t)}^{t}x^T(s)Q_1x(s)\,ds\\
&\quad+\int_{t-d_2(t)}^{t}x^T(s)Q_2x(s)\,ds,\\
V_4(x(t)) &= \int_{t-h_1}^{t}x^T(s)M_1x(s)\,ds+\int_{t-h_2}^{t}x^T(s)M_2x(s)\,ds,\\
V_5(x(t)) &= \int_{-h_1}^{0}\int_{\theta}^{0}\int_{t+\lambda}^{t}\dot{x}^T(s)R_1\dot{x}(s)\,ds\,d\lambda\,d\theta\\
&\quad+\int_{-h_2}^{0}\int_{\theta}^{0}\int_{t+\lambda}^{t}\dot{x}^T(s)R_2\dot{x}(s)\,ds\,d\lambda\,d\theta,
\end{aligned} \tag{18}$$

where

$$\begin{aligned}
\xi_1^T(t) &= \left[x^T(t)\quad\left(\int_{t-h_1}^{t}x(s)\,ds\right)^T\right],\\
\xi_2^T(t) &= \left[x^T(t)\quad\left(\int_{t-h_2}^{t}x(s)\,ds\right)^T\right],\\
\xi^T(t) &= \left[x^T(t)\quad\dot{x}^T(t)\right],\\
P &= \begin{bmatrix}P_{11} & P_{12}\\ * & P_{22}\end{bmatrix}>0,\qquad W=\begin{bmatrix}W_{11} & W_{12}\\ * & W_{22}\end{bmatrix}>0,\\
Z &= \begin{bmatrix}Z_{11} & Z_{12}\\ * & Z_{22}\end{bmatrix}>0,\qquad N=\begin{bmatrix}N_{11} & N_{12}\\ * & N_{22}\end{bmatrix}>0,
\end{aligned} \tag{19}$$

and Q_i, M_i, and R_i $(i = 1,2)$ are the positive-definite matrices to be determined.

The derivatives of $V(x(t))$ along the trajectories of system (15) are as follows:

$$\begin{aligned}
\dot{V}_1(x(t)) &= 2\xi_1^T(t)P\dot{\xi}_1(t)+2\xi_2^T(t)W\dot{\xi}_2(t)\\
&= 2\left[x^T(t)\quad\left(\int_{t-h_1}^{t}x(s)\,ds\right)^T\right]\begin{bmatrix}P_{11} & P_{12}\\ * & P_{22}\end{bmatrix}\\
&\quad\times\begin{bmatrix}\dot{x}(t)\\ x(t)-x(t-h_1)\end{bmatrix}\\
&\quad+2\left[x^T(t)\left(\int_{t-h_2}^{t}x(s)\,ds\right)^T\right]\begin{bmatrix}W_{11} & W_{12}\\ * & W_{22}\end{bmatrix}\\
&\quad\times\begin{bmatrix}\dot{x}(t)\\ x(t)-x(t-h_2)\end{bmatrix},\\
\dot{V}_2(x(t)) &= h_1\left[x^T(t)\quad\dot{x}^T(t)\right]\begin{bmatrix}Z_{11} & Z_{12}\\ * & Z_{22}\end{bmatrix}\begin{bmatrix}x(t)\\ \dot{x}(t)\end{bmatrix}\\
&\quad-\int_{t-h_1}^{t}\left[x^T(s)\quad\dot{x}^T(s)\right]\begin{bmatrix}Z_{11} & Z_{12}\\ * & Z_{22}\end{bmatrix}\begin{bmatrix}x(s)\\ \dot{x}(s)\end{bmatrix}ds\\
&\quad+h_2\left[x^T(t)\quad\dot{x}^T(t)\right]\begin{bmatrix}N_{11} & N_{12}\\ * & N_{22}\end{bmatrix}\begin{bmatrix}x(t)\\ \dot{x}(t)\end{bmatrix}\\
&\quad-\int_{t-h_2}^{t}\left[x^T(s)\quad\dot{x}^T(s)\right]\begin{bmatrix}N_{11} & N_{12}\\ * & N_{22}\end{bmatrix}\begin{bmatrix}x(s)\\ \dot{x}(s)\end{bmatrix}ds,\\
\dot{V}_3(x(t)) &= x^T(t)Q_1x(t)-\left(1-\dot{d}_1(t)\right)x^T(t-d_1(t))\\
&\quad\times Q_1x(t-d_1(t))+x^T(t)Q_2x(t)\\
&\quad-\left(1-\dot{d}_2(t)\right)x^T(t-d_2(t))Q_2x(t-d_2(t))\\
&\le x^T(t)Q_1x(t)+x^T(t)Q_2x(t)-(1-\mu_1)\\
&\quad\times x^T(t-d_1(t))Q_1x(t-d_1(t))-(1-\mu_2)\\
&\quad\times x^T(t-d_2(t))Q_2x(t-d_2(t)),\\
\dot{V}_4(x(t)) &= x^T(t)M_1x(t)-x^T(t-h_1)M_1x(t-h_1)\\
&\quad+x^T(t)M_2x(t)-x^T(t-h_2)M_2x(t-h_2),\\
\dot{V}_5(x(t)) &= \frac{1}{2}h_1^2\dot{x}^T(t)R_1\dot{x}(t)-\int_{-h}^{0}\int_{t+\theta}^{t}\dot{x}^T(s)\\
&\quad\times R_1\dot{x}(s)\,ds\,d\theta+\frac{1}{2}h_2^2\dot{x}^T(t)R_2\dot{x}(t)\\
&\quad-\int_{-h}^{0}\int_{t+\theta}^{t}\dot{x}^T(s)R_2\dot{x}(s)\,ds\,d\theta.
\end{aligned} \tag{20}$$

From (15), the following equation can be obtained for any matrices T_i, $i = 1,2,\ldots,8$,

$$\begin{aligned}
&2\sum_{i=1}^{r}\sum_{j=1}^{r}w_i(x(t))m_j(x(t-d_2(t)))\\
&\quad\times\Bigg[x^T(t)T_1+x^T(t-d_1(t))T_2+x^T(t-h_1)T_3\\
&\qquad+\left(\int_{t-h_1}^{t}x(s)\,ds\right)^TT_4+x^T(t-d_2(t))T_5+x^T\\
&\qquad\times(t-h_2)T_6+\left(\int_{t-h_2}^{t}x(s)\,ds\right)^TT_7+\dot{x}^T(t)T_8\Bigg]\\
&\quad\times\left[A_{1i}x(t)-A_{2i}x(t-d_1(t))\right.\\
&\qquad\left.-B_iF_jx(t-d_2(t))-\dot{x}(t)\right]=0.
\end{aligned} \tag{21}$$

By Lemma 3, we have

$$
\begin{aligned}
&-\int_{t-h_1}^{t}\left[x^t(s)\quad \dot{x}^T(s)\right]\begin{bmatrix} Z_{11} & Z_{12}\\ * & Z_{22}\end{bmatrix}\begin{bmatrix} x(s)\\ \dot{x}(s)\end{bmatrix}ds\\
&\quad\le -\frac{1}{h_1}\left[\left(\int_{t-h_1}^{t} x(s)\,ds\right)^T\quad x^T(t)-x^T(t-h_1)\right]\\
&\qquad\times\begin{bmatrix} Z_{11} & Z_{12}\\ * & Z_{22}\end{bmatrix}\begin{bmatrix}\int_{t-h_1}^{t} x(s)\,ds\\ x(t)-x(t-h_1)\end{bmatrix},\\
&-\int_{t-h_2}^{t}\left[x^T(s)\quad \dot{x}^T(s)\right]\begin{bmatrix} N_{11} & N_{12}\\ * & N_{22}\end{bmatrix}\begin{bmatrix} x(s)\\ \dot{x}(s)\end{bmatrix}ds\\
&\quad\le -\frac{1}{h_2}\left[\left(\int_{t-h_2}^{t} x(s)\,ds\right)^T\quad x^T(t)-x^T(t-h_1)\right]\\
&\qquad\times\begin{bmatrix} N_{11} & N_{12}\\ * & N_{22}\end{bmatrix}\begin{bmatrix}\int_{t-h_2}^{t} x(s)\,ds\\ x(t)-x(t-h_2)\end{bmatrix},\\
&-\int_{-h_i}^{0}\int_{t+\theta}^{t}\dot{x}^T(s)R_i\dot{x}(s)\,ds\,d\theta\\
&\quad\le -\frac{2}{h_i^2}\left(\int_{-h_i}^{0}\int_{t+\theta}^{t}\dot{x}(s)\,ds\,d\theta\right)^T R_i\left(\int_{-h_i}^{0}\int_{t+\theta}^{t}\dot{x}(s)\,ds\,d\theta\right)\\
&\quad= -\frac{2}{h_i^2}\left(h_i x(t)-\int_{t-h_i}^{t} x(s)\,ds\right)^T\\
&\qquad\times R_i\left(h_i x(t)-\int_{t-h_i}^{t} x(s)\,ds\right)\quad i=1,2.
\end{aligned}
\tag{22}
$$

Using the above inequalities, and with the zero quantities (21), we can obtain

$$
\begin{aligned}
&\dot{V}(x_t)\\
&\quad\le 2\left[x^T(t)\quad\left(\int_{t-h_1}^{t} x(s)\,ds\right)^T\right]\begin{bmatrix} P_{11} & P_{12}\\ * & P_{22}\end{bmatrix}\\
&\qquad\times\begin{bmatrix}\dot{x}(t)\\ x(t)-x(t-h_1)\end{bmatrix}+h_1\left[x^T(t)\quad\dot{x}^T(t)\right]\\
&\qquad\times\begin{bmatrix} Z_{11} & Z_{12}\\ * & Z_{22}\end{bmatrix}\begin{bmatrix} x(t)\\ \dot{x}(t)\end{bmatrix}+h_2\left[x^T(t)\quad\dot{x}^T(t)\right]\begin{bmatrix} N_{11} & N_{12}\\ * & N_{22}\end{bmatrix}\\
&\qquad\times\begin{bmatrix} x(t)\\ \dot{x}(t)\end{bmatrix}-\frac{1}{h_1}\left[\left(\int_{t-h_1}^{t} x(s)\,ds\right)^T\quad x^T(t)-x^T(t-h_1)\right]\\
&\qquad\times\begin{bmatrix} Z_{11} & Z_{12}\\ * & Z_{22}\end{bmatrix}\begin{bmatrix}\int_{t-h_1}^{t} x(s)\,ds\\ x(t)-x(t-h_1)\end{bmatrix}\\
&\qquad-\frac{1}{h_2}\left[\left(\int_{t-h_2}^{t} x(s)\,ds\right)^T\quad x^T(t)-x^T(t-h_2)\right]\\
&\qquad\times\begin{bmatrix} N_{11} & N_{12}\\ * & N_{22}\end{bmatrix}\begin{bmatrix}\int_{t-h_2}^{t} x(s)\,ds\\ x(t)-x(t-h_2)\end{bmatrix}+x^T(t)Q_1x(t)\\
&\qquad+x^T(t)Q_2x(t)-(1-\mu_1)x^T(t-d_1(t))Q_1x\\
&\qquad\times(t-d_1(t))-(1-\mu_2)x^T(t-d_2(t))Q_2x\\
&\qquad\times(t-d_2(t))+x^T(t)M_1x(t)-x^T(t-h_1)M_1x\\
&\qquad\times(t-h_1)+x^T(t)M_2x(t)-x^T(t-h_2)M_2x\\
&\qquad\times(t-h_2)+\frac{1}{2}h_1^2\dot{x}^T(t)R_1\dot{x}(t)-\frac{2}{h_1^2}\\
&\qquad\times\left(h_1x(t)-\int_{t-h_1}^{t} x(s)\,ds\right)^T R_1\left(h_1x(t)-\int_{t-h_1}^{t} x(s)\,ds\right)\\
&\qquad+\frac{1}{2}h_2^2\dot{x}^T(t)R_2\dot{x}(t)-\frac{2}{h_2^2}\left(h_2x(t)-\int_{t-h_2}^{t} x(s)\,ds\right)^T\\
&\qquad\times R_2\left(h_2x(t)-\int_{t-h_2}^{t} x(s)\,ds\right)\\
&\qquad+2\left[x^T(t)\quad\left(\int_{t-h_2}^{t} x(s)\,ds\right)^T\right]\\
&\qquad\times\begin{bmatrix} W_{11} & W_{12}\\ * & W_{22}\end{bmatrix}\begin{bmatrix}\dot{x}(t)\\ x(t)-x(t-h_2)\end{bmatrix}\\
&\qquad+2\sum_{i=1}^{r}\sum_{j=1}^{r}w_i(x(t))m_j(x(t-d_2(t)))\\
&\qquad\times\left[x^T(t)T_1+x^T(t-d_1(t))T_2+x^T(t-h_1)T_3\right.\\
&\qquad\quad+\left(\int_{t-h_1}^{t} x(s)\,ds\right)^T T_4+x^T(t-d_2(t))T_5+x^T\\
&\qquad\quad\left.\times(t-h_2)T_6+\left(\int_{t-h_2}^{t} x(s)\,ds\right)^T T_7+\dot{x}^T(t)T_8\right]\\
&\qquad\times\left[A_{1i}x(t)-A_{2i}x(t-d_1(t))\right.\\
&\qquad\quad\left.-B_iF_jx(t-d_2(t))-\dot{x}(t)\right]\\
&\quad=\zeta^T(t)\left(\sum_{i=1}^{r}\sum_{j=1}^{r}w_i(x(t))m_j(x(t-d_2(t)))\Phi_{ij}\right)\zeta(t),
\end{aligned}
\tag{23}
$$

$$\zeta^T(t) = \left[x^T(t) \;\; x^T(t-d_1(t)) \;\; x^T(t-h_1) \;\; \left(\int_{t-h_1}^{t} x(s)\,ds\right)^T \;\; x^T(t-d_2(t)) \;\; x^T(t-h_2) \;\; \left(\int_{t-h_2}^{t} x(s)\,ds\right)^T \;\; \dot{x}^T(t) \right]. \quad (24)$$

where

$$\Phi_{ij} = \begin{bmatrix} \Phi_{11i} & \Phi_{12i} & \Phi_{13} & \Phi_{14} & \Phi_{15ij} & \Phi_{16} & \Phi_{17} & \Phi_{18} \\ * & \Phi_{22i} & A_{2i}^T T_3^T & A_{2i}^T T_4^T & \Phi_{25ij} & A_{2i}^T T_6^T & A_{2i}^T T_7^T & \Phi_{28i} \\ * & * & \Phi_{33i} & -P_{22} & T_3 B_i F_j & 0 & 0 & -T_3 \\ * & * & * & \Phi_{44} & T_4 B_i F_j & 0 & 0 & \Phi_{48} \\ * & * & * & * & \Phi_{55ij} & F_j^T B_i^T T_6^T & F_j^T B_i^T T_7^T & \Phi_{58i} \\ * & * & * & * & * & \Phi_{66} & \Phi_{67} & -T_6 \\ * & * & * & * & * & * & \Phi_{77} & \Phi_{78} \\ * & * & * & * & * & * & * & \Phi_{88} \end{bmatrix},$$

$$\begin{aligned}
\Phi_{11i} &= P_{12} + P_{12}^T + W_{12} + W_{12}^T + h_1 Z_{11} + h_2 N_{11} \\
&\quad - \frac{1}{h_1} Z_{22} - \frac{1}{h_2} N_{22} + Q_1 + Q_2 + M_1 + M_2 \\
&\quad - 2R_1 - 2R_2 + T_1 A_{1i} + A_{1i}^T T_1^T, \\
\Phi_{12i} &= T_1 A_{2i} + A_{1i}^T T_2^T, \\
\Phi_{13} &= -P_{12} - \frac{1}{h_1} Z_{22} + A_{1i}^T T_3^T, \\
\Phi_{14} &= P_{22} - \frac{1}{h_2} Z_{12}^T + \frac{1}{h_1} R_1 + A_{1i}^T T_4^T, \\
\Phi_{15ij} &= T_1 B_i F_j + A_{1i}^T T_5^T, \\
\Phi_{16} &= -W_{12} - \frac{1}{h_2} N_{22} + A_{1i}^T T_6^T, \\
\Phi_{17} &= W_{22} - \frac{1}{h_2} N_{12}^T + \frac{2}{h_2^2} R_2 + A_{1i}^T T_7^T, \\
\Phi_{18} &= P_{11} + W_{11} + h_1 Z_{12} + h_2 N_{12} - T_1 + A_{1i}^T T_8^T, \\
\Phi_{22i} &= -(1-\mu_1) Q_1 + T_2 A_{2i} + A_{2i}^T T_2^T, \\
\Phi_{25ij} &= T_2 B_i F_j + A_{2i}^T T_5^T, \\
\Phi_{28i} &= -T_2 + A_{2i}^T T_8^T, \\
\Phi_{33} &= -\frac{1}{h} Z_{22} - M_1, \\
\Phi_{44} &= -\frac{1}{h_1} Z_{11} - \frac{2}{h_1^2} R_1, \\
\Phi_{48} &= P_{12}^T - T_4, \\
\Phi_{55i} &= -(1-\mu_2) Q_2 + T_5 B_i F_j + F_j^T B_i^T T_5^T, \\
\Phi_{58i} &= -T_5 + F_j^T B_i^T T_8^T, \\
\Phi_{66} &= -\frac{1}{h_2} N_{22} - M_2, \\
\Phi_{67} &= -\frac{1}{h_2} N_{12}^T - W_{22}, \\
\Phi_{77} &= -\frac{1}{h_2} N_{11} - \frac{2}{h_2^2} R_2, \\
\Phi_{78} &= W_{12}^T - T_7, \\
\Phi_{88} &= h_1 Z_{22} + h_2 N_{22} + \frac{1}{2} h_1^2 R_1 + \frac{1}{2} h_2^2 R_2 - T_8.
\end{aligned} \quad (25)$$

From (25), it is obvious that if

$$\sum_{i=1}^{r} \sum_{j=1}^{r} w_i(x(t))\, m_j(x(t-d_2(t)))\, \Phi_{ij} < 0, \quad (26)$$

$\dot{V}(x(t)) < 0$.

From (26), we can discover that the feedback gains are predefined. The following proof presents the controller design method. We first pre- and postmultiply both the diag $[\, X \; X \; X \; X \; X \; X \; X \; X \,]$ and transpose to both sides of (25) and pre- and postmultiply the diag $[\, X \; X \,]$ transpose to both sides of P, W, Z, and N and the X and transpose to both sides of Q_i, M_i, and R_i, $i = 1, 2$. Let $T_i = t_i T_1 (i = 2, \ldots, 8)$, and denote new variables $X = T_1^{-1}$, $\overline{R}_1 = XR_1X^T$, $\overline{Q}_1 = XQ_1X^T$, $\overline{M}_1 = XM_1X^T$, $\overline{R}_2 = XR_2X^T$, $\overline{Q}_2 = XQ_2X^T$, $\overline{M}_2 = XM_2X^T$, $\overline{\Lambda}_i = X\Lambda_i X^T$, $\overline{\Lambda}_j = X\Lambda_j X^T$, $i = 1, 2, \ldots, r$, $\overline{P}_{11} = XP_{11}X^T$, $\overline{P}_{12} = XP_{12}X^T$, $\overline{P}_{22} = XP_{22}X^T$, $\overline{W}_{11} = XW_{11}X^T$, $\overline{W}_{12} = XW_{12}X^T$, $\overline{W}_{22} = XW_{22}X^T$, $\overline{Z}_{11} = XZ_{11}X^T$, $\overline{Z}_{12} = XZ_{12}X^T$, $\overline{Z}_{22} = XZ_{22}X^T$, $\overline{N}_{11} = XN_{11}X^T$, $\overline{N}_{12} = XN_{12}X^T$, and $\overline{N}_{22} = XN_{22}X^T$. With $F_i = Y_i X^{-T}$, $i = 1, 2 \ldots, r$, we next get

$$\sum_{i=1}^{r} \sum_{j=1}^{r} w_i(x(t))\, m_j(x(t-d_2(t)))\, \overline{\Phi}_{ij} < 0, \quad (27)$$

where

$$\overline{\Phi}_{ij} = \begin{bmatrix} \overline{\Phi}_{11i} & \overline{\Phi}_{12i} & \overline{\Phi}_{13} & \overline{\Phi}_{14} & \overline{\Phi}_{15ij} & \overline{\Phi}_{16} & \overline{\Phi}_{17} & \overline{\Phi}_{18} \\ * & \overline{\Phi}_{22i} & t_3XA_{2i}^T & t_4XA_{2i}^T & \overline{\Phi}_{25ij} & t_6XA_{2i}^T & t_7XA_{2i}^T & \overline{\Phi}_{28i} \\ * & * & \overline{\Phi}_{33i} & -\overline{P}_{22} & t_3B_iY_j & 0 & 0 & -t_3X^T \\ * & * & * & \overline{\Phi}_{44} & t_4B_iY_j & 0 & 0 & \overline{\Phi}_{48} \\ * & * & * & * & \overline{\Phi}_{55ij} & t_6Y_j^TB_i^T & t_7Y_j^TB_i^T & \overline{\Phi}_{58i} \\ * & * & * & * & * & \overline{\Phi}_{66} & \overline{\Phi}_{67} & -t_6X^T \\ * & * & * & * & * & * & \overline{\Phi}_{77} & \overline{\Phi}_{78} \\ * & * & * & * & * & * & * & \overline{\Phi}_{88} \end{bmatrix},$$

$$\begin{aligned}
\overline{\Phi}_{11i} &= \overline{P}_{12} + \overline{P}_{12}^T + \overline{W}_{12} + \overline{W}_{12}^T + h_1\overline{Z}_{11} \\
&\quad + h_2\overline{N}_{11} - \frac{1}{h_1}\overline{Z}_{22} - \frac{1}{h_2}\overline{N}_{22} + \overline{Q}_1 + \overline{Q}_2 \\
&\quad + \overline{M}_1 + \overline{M}_2 - 2\overline{R}_1 - 2\overline{R}_2 + A_{1i}X^T + XA_{1i}^T, \\
\overline{\Phi}_{12i} &= A_{2i}X^T + t_2XA_{1i}^T, \\
\overline{\Phi}_{13} &= -\overline{P}_{12} - \frac{1}{h_1}\overline{Z}_{22} + t_3XA_{1i}^T, \\
\overline{\Phi}_{14} &= \overline{P}_{22} - \frac{1}{h_1}\overline{Z}_{12}^T + \frac{1}{h_1}\overline{R}_1 + t_4XA_{1i}^T, \\
\overline{\Phi}_{15ij} &= B_iY_j + t_5XA_{1i}^T, \\
\overline{\Phi}_{16} &= -\overline{W}_{12} - \frac{1}{h_2}\overline{N}_{22} + t_6XA_{1i}^T, \\
\overline{\Phi}_{17} &= \overline{W}_{22} - \frac{1}{h_2}\overline{N}_{12}^T + \frac{2}{h_2^2}\overline{R}_2 + t_7XA_{1i}^T, \\
\overline{\Phi}_{18} &= \overline{P}_{11} + \overline{W}_{11} + h_1\overline{Z}_{12} + h_2\overline{N}_{12} - X^T + t_8XA_{1i}^T, \\
\overline{\Phi}_{22i} &= -(1-\mu_1)\overline{Q}_1 + t_2A_{2i}X^T + t_2XA_{2i}^T, \\
\overline{\Phi}_{25ij} &= t_2B_iY_j + t_5XA_{2i}^T, \\
\Phi_{28i} &= -t_2X^T + t_8XA_{2i}^T, \\
\overline{\Phi}_{33} &= -\frac{1}{h_1}\overline{Z}_{22} - \overline{M}_1, \\
\overline{\Phi}_{44} &= -\frac{1}{h_1}\overline{Z}_{11} - \frac{2}{h_1^2}\overline{R}_1, \\
\overline{\Phi}_{48} &= \overline{P}_{12}^T - t_4X^T, \\
\overline{\Phi}_{55i} &= -(1-\mu_2)\overline{Q}_2 + t_5B_iY_j + t_5Y_j^TB_i^T, \\
\overline{\Phi}_{58i} &= -t_5X^T + t_8Y_j^TB_i^T, \\
\overline{\Phi}_{66} &= -\frac{1}{h_2}\overline{N}_{22} - \overline{M}_2, \\
\overline{\Phi}_{67} &= -\frac{1}{h_2}\overline{N}_{12}^T - \overline{W}_{22}, \\
\overline{\Phi}_{77} &= -\frac{1}{h_2}\overline{N}_{11} - \frac{2}{h_2^2}\overline{R}_2, \\
\overline{\Phi}_{78} &= \overline{W}_{12}^T - t_7X^T, \\
\overline{\Phi}_{88} &= h_1\overline{Z}_{22} + h_2\overline{N}_{22} + \frac{1}{2}h_1^2\overline{R}_1 + \frac{1}{2}h_2^2\overline{R}_2 - t_8X^T.
\end{aligned} \tag{28}$$

Here, "$*$" denotes the transpose elements in the symmetric positions.

If (27) holds, then $\dot{V}(x(t)) < 0$. Consider $\sum_{i=1}^r\sum_{j=1}^r w_i(x(t))(w_j(x(t)) - m_j(x(t-d_2(t))))\Lambda_i = 0$, where $\Lambda_i = \Lambda_i^T \in R^{8n\times 8n} > 0$, $i = 1,2,\ldots,r$, are arbitrary matrices. These terms are introduced to (27) to alleviate the conservativeness. From (27), we also have

$$\begin{aligned}
\overline{\Phi} &= \sum_{i=1}^r\sum_{j=1}^r w_i(x(t))\, m_j(x(t-d_2(t)))\,\overline{\Phi}_{ij} \\
&= \sum_{i=1}^r\sum_{j=1}^r w_i(x(t))\big(w_j(x(t)) - m_j(x(t-d_2(t))) \\
&\qquad + \rho_j w_j(x(t)) - \rho_j w_j(x(t))\big)\Lambda_i \\
&\quad + \sum_{i=1}^r\sum_{j=1}^r w_i(x(t))\, m_j(x(t-d_2(t)))\,\overline{\Phi}_{ij} \\
&= \sum_{i=1}^r\sum_{j=1}^r w_i(x(t))\, w_j(x(t))\big(\rho_j\Phi_{ij} - \rho_j\Lambda_i + \Lambda_i\big) \\
&\quad + \sum_{i=1}^r\sum_{j=1}^r w_i(x(t))\big(m_j(x(t-d_2(t))) - \rho_j w_j(x(t))\big) \\
&\quad \times\big(\overline{\Phi}_{ij} - \Lambda_i\big) \\
&\le \sum_{i=1}^r w_i^2\big(\rho_i\overline{\Phi}_{ii} - \rho_i\Lambda_i + \Lambda_i\big) \\
&\quad + \sum_{i=1}^r\sum_{j=1}^r w_i\big(m_j - \rho_j w_j\big)\big(\overline{\Phi}_{ij} - \Lambda_i\big) \\
&\quad + \sum_{i=1}^r\sum_{i<j} w_iw_j\big(\rho_j\overline{\Phi}_{ij} + \rho_i\overline{\Phi}_{ji} - \rho_j\Lambda_i - \rho_i\Lambda_j \\
&\qquad + \Lambda_i + \Lambda_j\big)
\end{aligned} \tag{29}$$

with $m_j(x(t-d_2(t))) - \rho_j w_j(x(t)) \ge 0$ for all j, $x(t)$ and $x(t-d_2(t))$. Let

$$\overline{\Phi}_{ij} - \Lambda_i < 0, \tag{30}$$

$$\rho_i\overline{\Phi}_{ii} - \rho_i\Lambda_i + \Lambda_i < 0, \tag{31}$$

$$\rho_j\overline{\Phi}_{ij} + \rho_i\overline{\Phi}_{ji} - \rho_j\Lambda_i - \rho_i\Lambda_j + \Lambda_i + \Lambda_j \le 0, \quad i < j, \tag{32}$$

for all $i, j = 1,2,\ldots,r$.

Since $\dot{V}(x(t)) < 0$, the fuzzy control system with the time varying state and input delays (15) is asymptotically stable with the state feedback control law (17). □

3.2. Robust Stability of Uncertain Fuzzy Systems. We also examine the design of a robust stable controller for the uncertain system (4) under the imperfect premise matching. Consider the following uncertain fuzzy time varying delay control system:

$$\begin{aligned}\dot{x}(t) = \sum_{i=1}^{r}\sum_{j=1}^{r} w_i(x(t))\, m_j(x(t-d_2(t)))\\ \times\left[\left(A_{1i}+\Delta A_{1i}(t)\right)x(t)+\left(A_{2i}+\Delta A_{2i}(t)\right)\right.\\ \times x(t-d_1(t))+\left(B_i+\Delta B_i(t)\right)\\ \left.\times u(t-d_2(t))\right],\\ x(t)=\varphi(t), \quad t\in\left[-\max(h_1,h_2),0\right].\end{aligned} \tag{33}$$

Based on the above results of Theorem 4, a robust stabilization criterion for the T-S fuzzy systems with time varying state and input delays is investigated. The following result can be obtained.

Theorem 5. *Given scalars $h_1 \geq 0$, $h_2 \geq 0$, μ_1, μ_2, and t_i $(i = 2,\ldots,8)$, the uncertain fuzzy control systems with the time varying state and input delays* (33) *is robustly stable for any $0 \leq d_i(t) \leq h_i$ $(i = 1,2)$ via the imperfect premise matching controller design technique, if the membership functions of the fuzzy model and fuzzy controller satisfy $m_j(x(t-d_2(t))) - \rho_j w_j(x(t)) \geq 0$ for all j, $x(t)$, and $x(t-d_2(t))$, where $0 < \rho_j < 1$, and there exist common matrices $\overline{P}_{11} > 0$, $\overline{P}_{22} > 0$, $\overline{W}_{11} > 0$, $\overline{W}_{22} > 0$, $\overline{Z}_{11} > 0$, $\overline{Z}_{22} > 0$, $\overline{N}_{11} > 0$, $\overline{N}_{22} > 0$, $\overline{Q}_i > 0$, $\overline{M}_i > 0$, $\overline{R}_i > 0$ $(i = 1,2)$ and $\Lambda_i = \Lambda_i^T \in R^{8n\times 8n} > 0$ $(i = 1,2,\ldots,r)$, $\overline{P} > 0$, $\overline{W} > 0$, $\overline{Z} > 0$, $\overline{N} > 0$ and some matrices Y_j $(j = 1,2,\ldots,r)$, X and scalars $\varepsilon_{1i} > 0$, $\varepsilon_{2i} > 0$, $\varepsilon_{bij} > 0$ satisfy the following LMIs:*

$$\Psi_{ij} - \overline{\Lambda}_i < 0, \tag{34}$$

$$\rho_i\Psi_{ii} - \rho_i\overline{\Lambda}_i + \overline{\Lambda}_i < 0, \tag{35}$$

$$\rho_j\Psi_{ij} + \rho_i\Psi_{ji} - \rho_j\overline{\Lambda}_i - \rho_i\overline{\Lambda}_j + \overline{\Lambda}_i + \overline{\Lambda}_j, \leq 0 \quad i < j, \tag{36}$$

where Ψ_{ij} is defined as in (44). *The state feedback gains can be constructed as $F_i = Y_i X^{-T}$.*

Proof. If A_{1i}, A_{2i}, and B_i in $\overline{\Phi}_{ij}$ are replaced with $A_{1i} + D_iK_i(t)E_{1i}$, $A_{2i} + D_iK_i(t)E_{2i}$, and $B_i + D_iK_i(t)E_{bi}$ in (28) of Theorem 4, respectively, (27) for system (33) can be rewritten as

$$\sum_{i=1}^{r}\sum_{j=1}^{r} w_i(x(t))\, m_j(x(t-d(t)))\,\Omega_{ij} < 0, \tag{37}$$

where

$$\begin{aligned}\Omega_{ij} = \overline{\Phi}_{ij} + \widehat{D}_{1i}^T K_i(t)\widehat{E}_i + \widehat{E}_i^T K_i^T(t)\widehat{D}_{1i} + \widehat{D}_{2i}^T K_i(t)\widehat{E}_{2ij}\\ + \widehat{E}_{2ij}^T K_i^T(t)\widehat{D}_{2i} + \widehat{D}_{bi}^T K_i(t)\widehat{E}_{bij} + \widehat{E}_{bij}^T K_i^T(t)\widehat{D}_{bi},\\ \widehat{D}_{1i} = \left[D_i^T \;\; 0 \;\; 0 \;\; 0 \;\; 0 \;\; 0 \;\; 0 \;\; 0\right],\\ \widehat{D}_{2i} = \left[0 \;\; D_i^T \;\; 0 \;\; 0 \;\; 0 \;\; 0 \;\; 0 \;\; 0\right],\\ \widehat{D}_{bi} = \left[0 \;\; 0 \;\; 0 \;\; 0 \;\; D_i^T \;\; 0 \;\; 0 \;\; 0\right],\end{aligned} \tag{38}$$

$$\begin{aligned}\widehat{E}_{1i} &= \left[E_{1i}X^T \;\; t_2E_{1i}X^T \;\; t_3E_{1i}X^T \;\; t_4E_{1i}X^T \;\; t_5E_{1i}X^T \;\; t_6E_{1i}X^T \;\; t_7E_{1i}X^T \;\; t_8E_{1i}X^T\right],\\ \widehat{E}_{2i} &= \left[E_{2i}X^T \;\; t_2E_{2i}X^T \;\; t_3E_{2i}X^T \;\; t_4E_{2i}X^T \;\; t_5E_{2i}X^T \;\; t_6E_{2i}X^T \;\; t_7E_{2i}X^T \;\; t_8E_{2i}X^T\right],\\ \widehat{E}_{bij} &= \left[E_{bi}Y_j \;\; t_2E_{bi}Y_j \;\; t_3E_{bi}Y_j \;\; t_4E_{bi}Y_j \;\; t_5E_{bi}Y_j \;\; t_6E_{bi}Y_j \;\; t_7E_{bi}Y_j \;\; t_8E_{bi}Y_j\right].\end{aligned} \tag{39}$$

If $\Omega_{ij} < 0$, (37) holds. According to Lemma 2, it is straightforward to know that $\Omega_{ij} < 0$ is true, if for each i, j, there exists scalars $\varepsilon_{1i} > 0$, $\varepsilon_{2i} > 0$, and $\varepsilon_{bij} > 0$ such that the following inequality holds:

$$\begin{aligned}\overline{\Phi}_{ij} + \varepsilon_{1i}\widehat{D}_{1i}^T\widehat{D}_{1i} + \varepsilon_{1i}^{-1}\widehat{E}_{1i}^T\widehat{E}_{1i} + \varepsilon_{2i}\widehat{D}_{2i}^T\widehat{D}_{2i}\\ + \varepsilon_{2i}^{-1}\widehat{E}_{2i}^T\widehat{E}_{2i} + \varepsilon_{bij}\widehat{D}_{bi}^T\widehat{D}_{bi} + \varepsilon_{bij}^{-1}\widehat{E}_{bij}^T\widehat{E}_{bij} < 0.\end{aligned} \tag{40}$$

Based on Schur complement, (40) is equivalent to the following inequality:

$$\Psi_{ij} = \begin{bmatrix}\widehat{\Phi}_{ij} & \widehat{E}_{1i}^T & \widehat{E}_{2i}^T & \widehat{E}_{bij}^T\\ * & -\varepsilon_{1i}I & 0 & 0\\ * & * & -\varepsilon_{2i}I & 0\\ * & * & * & -\varepsilon_{bij}I\end{bmatrix} < 0, \tag{41}$$

where

$$\widehat{\Phi}_{ij} = \begin{bmatrix} \widehat{\Phi}_{11i} & \overline{\Phi}_{12i} & \overline{\Phi}_{13} & \overline{\Phi}_{14} & \overline{\Phi}_{15ij} & \overline{\Phi}_{16} & \overline{\Phi}_{17} & \overline{\Phi}_{18} \\ * & \widehat{\Phi}_{22i} & t_3XA_{2i}^T & t_4XA_{2i}^T & \overline{\Phi}_{25ij} & t_6XA_{2i}^T & t_7XA_{2i}^T & \overline{\Phi}_{28i} \\ * & * & \overline{\Phi}_{33i} & -\overline{P}_{22} & t_3B_iY_j & 0 & 0 & -t_3X^T \\ * & * & * & \overline{\Phi}_{44} & t_4B_iY_j & 0 & 0 & \overline{\Phi}_{48} \\ * & * & * & * & \widehat{\Phi}_{55ij} & t_6Y_j^TB_i^T & t_7Y_j^TB_i^T & \overline{\Phi}_{58i} \\ * & * & * & * & * & \overline{\Phi}_{66} & \overline{\Phi}_{67} & -t_6X^T \\ * & * & * & * & * & * & \overline{\Phi}_{77} & \overline{\Phi}_{78} \\ * & * & * & * & * & * & * & \overline{\Phi}_{88} \end{bmatrix} < 0,$$

$$\widehat{\Phi}_{11i} = \overline{\Phi}_{11i} + \varepsilon_{1i}D_iD_i^T,$$
$$\widehat{\Phi}_{22i} = \overline{\Phi}_{22i} + \varepsilon_{2i}D_iD_i^T,$$
$$\widehat{\Phi}_{55ij} = \overline{\Phi}_{55ij} + \varepsilon_{bi}D_iD_i^T, \tag{42}$$

and $\overline{\Phi}$ are the same as in Theorem 4. Therefore, (41) holds, if and only if the following inequality holds:

$$\sum_{i=1}^{r}\sum_{j=1}^{r} w_i(x(t))\, m_j(x(t-d(t)))\, \Psi_{ij} < 0. \tag{43}$$

To alleviate the conservativeness of our robust stability analysis, similar to the analysis approach of Theorem 4, we introduce $\sum_{i=1}^{r}\sum_{j=1}^{r} w_i(w_j - m_j)\overline{\Lambda}_i = 0$ to (43), and the following proof is the same as in Theorem 4. We can obtain the conditions and (34)–(36). Thus, the fuzzy control system with the time varying state and input delays (34) is robust stable on the basis of the control law $F_i = Y_iX^{-T}$ under these conditions, and (34)–(36) hold. □

Remark 6. If we set $w_i(x(t)) = m_j(x(t))$, $d_1(t) = d_2(t)$, the closed-loop system in this paper has the same structure as that of paper [26]. On the other hand, let $w_i(x(t)) = m_j(x(t))$ and $d_1(t) = d_2(t) = d$; we can obtain the system in [16]. Therefore, the system studied in this paper is more general. Additionally, the information of the membership functions of the fuzzy time delay models and controllers are all considered in the stability analysis. If the fuzzy models and fuzzy controllers share the same fuzzy membership functions, that is, $w_i(x(t)) = m_j(x(t))$, the stability analysis can be referred to [25, 27, 28]. In other words, the problem in [25, 27, 28] is actually a special case of the one investigated in this paper.

Remark 7. The augmented Lyapunov function with an additional triple-integral term is introduced in analyzing the stability problem for the T-S fuzzy systems with time varying state and input delays. In addition, two integral inequalities are used to derive Theorem 4, and less free-weighting matrices are introduced, which lead to get less conservative results. It can be observed that some existing results are the special cases of this paper. For example, the method in [25] is from (18) with $P_{12} = 0$, $P_{22} = 0$, $Z_{12} = Z_{22} = 0$, $N_{12} = N_{22} = 0$, and $R_1 = R_2 = 0$ in Theorem 4. The results in [22] are based on system (33) with $d_2(t) = 0$ and (18) with $M_2 = 0$, $Z_{12} = Z_{22} = 0$, $Q_1 = Q_2 = 0$, and $R_1 = R_2 = 0$.

Remark 8. Different from the general PDC technique, the design method under the imperfect premise matching is much more flexible, because the membership functions of the fuzzy controllers do not need to be chosen the same as those of the fuzzy time delay models. Instead, they can be designed arbitrarily. Thus, the design flexibility is significantly enhanced. On the other hand, some simple membership functions of the fuzzy controllers might be employed, which can reduce the implementation cost.

Remark 9. In [7–11, 15–20], the authors have considered the robust control for uncertain T-S fuzzy systems with state delays. Some delay-dependent conditions and fuzzy controllers are obtained with a traditional Lyapunov-Krasovskii functional method and PDC method, which all are the special cases of Theorem 5 in this paper.

4. Numerical Examples

In this section, two numerical examples are given to illustrate the conservativeness and effectiveness of the proposed methods. The first example compares our techniques with the existing ones in the literature for stability analysis, which shows that Theorem 4 in this paper is less conservative than the other results. The second example is used to illustrate the advantage of the robust stability conditions of Theorem 5 and demonstrate how to design robust fuzzy controllers by using our approach.

Example 10. Consider the following fuzzy system with state and input delays:

$$\dot{x}(t) = \sum_{i=1}^{2} w_i(\theta(t))\left[A_{1i}x(t) + A_{2i}x(t-d_1(t)) + B_iu(t-d_2(t))\right],$$
$$A_{11} = \begin{bmatrix} 0 & 0.6 \\ 0 & 1 \end{bmatrix}, \quad A_{21} = \begin{bmatrix} 0.5 & 0.9 \\ 0 & 2 \end{bmatrix},$$
$$A_{12} = \begin{bmatrix} 1 & 0 \\ 1 & 0 \end{bmatrix}, \quad A_{22} = \begin{bmatrix} 0.9 & 0 \\ 1 & 1.6 \end{bmatrix},$$
$$B_1 = B_2 = \begin{bmatrix} 1 \\ 1 \end{bmatrix}. \tag{44}$$

The fuzzy membership functions are selected as [31]

$$w_1(x_1(t)) = \left(1 - \frac{c(t)\sin\left(\left|x_1(t)\right|^{-4}\right)^5}{1+\exp^{-100x_1(t)^3(1-x_1(t))}}\right) \times \frac{\cos(x_1(t))^2}{1+\exp^{-2.5x_1(t)(3+(x_1(t)/0.42))}} \times w_2(x_1(t)) = 1 - w_1(x_1(t)), \tag{45}$$

Table 1: The maximum allowable time delay and feedback gains ($\mu_1 = 0, \mu_2 = 0$).

Paper	h_1	h_2	Feedback gains
[26]	0.3120	0.3120	$F_1 = \begin{bmatrix} 1.0598 & -5.6598 \end{bmatrix}$ $F_2 = \begin{bmatrix} -1.3068 & -4.1167 \end{bmatrix}$
Theorem 4	0.33	0.57	$F_1 = \begin{bmatrix} -0.0042 & -0.0449 \end{bmatrix}$ $F_2 = \begin{bmatrix} 0.0048 & 0.0717 \end{bmatrix}$

where

$$x_1(t) \in \left[-\frac{\pi}{2} \quad \frac{\pi}{2}\right],$$
$$c(t) = \frac{\sin(x_1(t)) + 1}{40} \in [-0.05 \quad 0.05]. \tag{46}$$

If we set $d_1(t) = d_2(t)$ in system (44), we can obtain the system in [26], which implies that our system is more general. Employing the LMIs in [26] and those in Theorem 4 yields the maximum state and input delays h_1, and h_2, which guarantee the stability of system (44) and the feedback gains for $\mu_1 = 0$, and $\mu_2 = 0$, when $\rho_1 = 0.75$, $\rho_2 = 0.95$, $t_2 = 0.1$, $t_3 = 0.2$, $t_4 = 0.7$, $t_5 = 0.1$, $t_6 = 0.4$, $t_7 = 0.1$, and $t_8 = 1.3$ as given in Table 1, which clearly shows the superiority of the results derived in this paper over those obtained from [26].

Example 11. Consider the well-known truck-trailer system, which can be described by the following T-S fuzzy system:

$$\dot{x}(t) = \sum_{i=1}^{2} w_i(\theta(t)) \left[(A_{1i} + \Delta A_{1i}) x(t) + A_{2i} x(t - d_1(t)) + (B_i + \Delta B_i) u(t - d_2(t)) \right], \tag{47}$$

$$A_{11} = \begin{bmatrix} -a\dfrac{v\bar{t}}{Lt_0} & 0 & 0 \\ a\dfrac{v\bar{t}}{Lt_0} & 0 & 0 \\ a\dfrac{v^2\bar{t}^2}{2Lt_0} & \dfrac{v\bar{t}}{t_0} & 0 \end{bmatrix},$$

$$A_{21} = \begin{bmatrix} -(1-a)\dfrac{v\bar{t}}{Lt_0} & 0 & 0 \\ (1-a)\dfrac{v\bar{t}}{Lt_0} & 0 & 0 \\ (1-a)\dfrac{v^2\bar{t}^2}{2Lt_0} & 0 & 0 \end{bmatrix},$$

$$B_1 = \begin{bmatrix} \dfrac{v\bar{t}}{lt_0} \\ 0 \\ 0 \end{bmatrix},$$

$$A_{12} = \begin{bmatrix} -a\dfrac{v\bar{t}}{Lt_0} & 0 & 0 \\ a\dfrac{v\bar{t}}{Lt_0} & 0 & 0 \\ a\dfrac{dv^2\bar{t}^2}{2Lt_0} & \dfrac{dv\bar{t}}{t_0} & 0 \end{bmatrix},$$

$$A_{22} = \begin{bmatrix} -(1-a)\dfrac{v\bar{t}}{Lt_0} & 0 & 0 \\ (1-a)\dfrac{v\bar{t}}{Lt_0} & 0 & 0 \\ (1-a)\dfrac{dv^2\bar{t}^2}{2Lt_0} & 0 & 0 \end{bmatrix}, \tag{48}$$

$$B_2 = \begin{bmatrix} \dfrac{v\bar{t}}{lt_0} \\ 0 \\ 0 \end{bmatrix}, \tag{49}$$

where $l = 2.8$, $L = 5.5$, $v = -1.0$, $\bar{t} = 2.0$, $t_0 = 0.5$, $d = 10t_0/\pi$, $D_i = [0.2555 \quad 0.2555 \quad 0.2555]^T$, $E_{1i} = E_{2i} = [0.1 \quad 0 \quad 0]^T$, $E_{bi} = [0.1 \quad 0 \quad 0]^T$ $(i = 1, 2)$, and the fuzzy membership functions are selected the same as in Example 10.

(1) Let $a = 1$, system (47) is the same as the fuzzy system of [22], which implies that our system is more general. Table 2 gives the maximum input delay value of h_2, for which the stabilization is guaranteed by Theorem 5 as well as the state feedback gains, when $\rho_1 = 0.75$, $\rho_2 = 0.95$ $t_2 = 0.1$, $t_3 = 0.2$, $t_4 = 0.7$, $t_5 = 0.1$, $t_6 = 0.4$, $t_7 = 0.8$, and $t_8 = 2$. It is clearly visible that the results derived in this paper are better than those from [22, 28].

(2) In the case of $a \neq 1$, the state and input delays of system (47) are all exist. The approach proposed in [22] can not be used to get the maximum of state delay h_1, as the system in [22] only contains the input delay. However, the method in [28] and Theorem 5 can be used. Here, let $a = 0.7$, $\rho_1 = 0.75$, $\rho_2 = 0.95$, $t_2 = 0.1$, $t_3 = 0.2$, $t_4 = 0.7$, $t_5 = 0.1$, $t_6 = 0.4$, $t_7 = 0.8$, and $t_8 = 3$, and Table 3 provides the maximum upper bounds of h_1 and h_2 and the state feedback gains for which the robust stabilization is guaranteed by Theorem 5.

By Theorem 5, we can conclude that the uncertain fuzzy model (47) is robust stable based on the following fuzzy control law:

$$u(t - h_2) = \sum_{j=1}^{2} m_j(x_1(t - h_2)) F_j x(t - h_2). \tag{50}$$

With the PDC design technique, it is required that the fuzzy controller must share the same fuzzy membership functions as those of the fuzzy time delay model. Under such

Table 2: The maximum allowable time delay and feedback gains ($\mu_2 = 0$).

Paper	h_2	Feedback gains
[22]	0.75	$F_1 = [3.4227 \quad -0.3535 \quad 0.0045]$ $F_2 = [3.5215 \quad -0.3617 \quad 0.0056]$
[28]	0.86	$F_1 = [3.3219 \quad -0.2406 \quad 0.0025]$ $F_2 = [3.3272 \quad -0.2494 \quad 0.0026]$
Theorem 5	1.2	$F_1 = [-0.0212 \quad 0.0093 \quad -0.0024]$ $F_2 = [-0.0250 \quad 0.0044 \quad 0.0014]$

Table 3: The maximum allowable time delay and feedback gains ($\mu_1 = \mu_2 = 0$).

Paper	h_1	h_2	Feedback gains
[28]	0.1	0.55	$F_1 = [3.3219 \quad -0.2406 \quad 0.0025]$ $F_2 = [3.3272 \quad -0.2494 \quad 0.0026]$
Theorem 5	0.4	1.7	$F_1 = [-0.0128 \quad 0.0090 \quad -0.0017]$ $F_2 = [-0.0194 \quad 0.0012 \quad 0.0009]$

a condition, the implementation cost of the fuzzy controller is high by employing these complex membership functions. However, from Theorem 5, the membership functions do not need to be chosen the same as $w_1(x_1(t))$ and $w_2(x_1(t))$. Thus, we can select some simple membership functions instead, such as

$$m_1(x_1(t-h_2)) = 0.75 \exp \frac{(-x_1(t-h_2)-0.38)^2}{2\times 0.38^2} + 0.05,$$
$$m_2(x_1(t-h_2)) = 1 - m_1(x_1(t-h_2)). \tag{51}$$

We also assume that $\rho_1 = 0.75$, and $\rho_2 = 0.95$, such that $m_j(x_1(t-h_2)) - \rho_j w_j(x_1(t)) > 0$ for $j = 1, 2$ and $x_1(t-h_2)$. The fuzzy control law $u(t-h_2) = m_1[-0.0128 \quad 0.0090 \quad -0.0017]x + m_2[-0.0194 \quad 0.0012 \quad 0.0009]x$ can be employed to stabilize the uncertain fuzzy control systems in (47) with the state and input delays. Figures 1 and 2 illustrate the stable state response and control input under the initial condition of $x(0) = [4 \quad -1 \quad 2]^T$.

Remark 12. In Example 11, our method offers less conservative results in the sense of allowing longer time delay and obtaining smaller feedback control gains. Moreover, compared with [22–28], where the fuzzy controller must have the same fuzzy membership functions as those of the fuzzy time delay model, the above membership functions of our fuzzy controller are much simper, which can considerably lower the implementation cost of the fuzzy controller and enhance the design flexibility.

Remark 13. If the function of $c(t)$ in $w_1(x_1(t))$ is unknown, on the basis of the PDC design technique [7–11, 15–20, 22–28], the fuzzy controller cannot be implemented as $c(t)$ is not available. However, using the proposed design method,

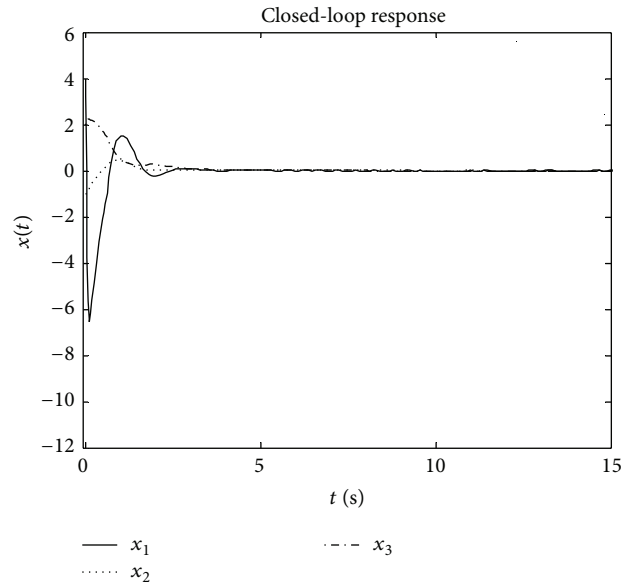

Figure 1: The state responses of system (47) with $h_1 = 0.4$, $h_2 = 1.7$.

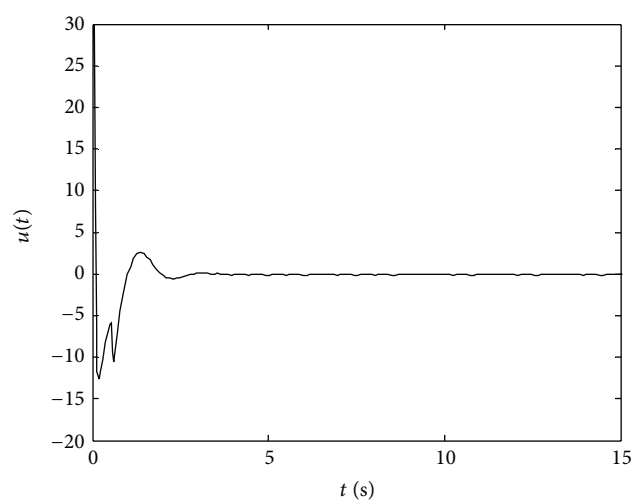

Figure 2: The control input of system (47) with $h_1 = 0.4$, $h_2 = 1.7$.

we can select some simper and well-known membership functions that are different from those of the fuzzy time delay models, for example, $m_1(x_1(t))$ and $m_2(x_1(t))$, so as to realize the fuzzy controller. In other words, the proposed design approach can be applied even for the fuzzy time delay models with uncertain grades of membership.

5. Conclusions

In this paper, we study the robust stability and stabilization problems for general nonlinear fuzzy systems with time varying state and input delays. A less conservative delay-dependent robust stability criterion has been obtained by introducing a novel augmented Lyapunov function with an additional triple-integral term. Moreover, a new design

approach different from the traditional PDC design technique is proposed, which can significantly improve the design flexibility and reduce the implementation cost of the fuzzy controller by arbitrarily selecting simple fuzzy membership functions. Two numerical examples are used to illustrate the conservativeness and effectiveness of our proposed methods.

Acknowledgments

This research work was funded by the NSFC under Grant no. 61273095 and the Academy of Finland under Grants no. 135225 and no. 127299.

References

[1] T. Takagi and M. Sugeno, "Fuzzy identification of systems and its applications to modeling and control," *IEEE Transactions on Systems, Man and Cybernetics*, vol. 15, no. 1, pp. 116–132, 1985.

[2] W. H. Ho, S. H. Chen, I. T. Chen, J. H. Chou, and C. C. Shu, "Design of stable and quadratic-optimal static output feedback controllers for T-S-fuzzy-model-based control systems: an integrative computational approach," *International Journal of Innovative Computing, Information and Control*, vol. 8, no. 1A, pp. 403–418, 2012.

[3] X. J. Su, L. G. Wu, P. Shi, and Y. D. Song, "H_∞ model reduction of T-S fuzzy stochastic systems," *IEEE Transactions on Systems, Man, and Cybermetics B*, vol. 42, no. 6, pp. 1574–1585, 2012.

[4] R. Yang, P. Shi, G.-P. Liu, and H. Gao, "Network-based feedback control for systems with mixed delays based on quantization and dropout compensation," *Automatica*, vol. 47, no. 12, pp. 2805–2809, 2011.

[5] X. M. Zhang, Z. J. Zhang, and G. P. Lu, "Fault detection for state-delay fuzzy systems subject to random communication delay," *International Journal of Innovative Computing, Information and Control*, vol. 8, no. 4, pp. 2439–2451, 2012.

[6] F. B. Li and X. Zhang, "Delay-range-dependent robust H_∞ filtering for singuar LPV systems with time variant delay," *International Journal of Innovative Computing, Information and Control*, vol. 9, no. 1, pp. 339–353, 2013.

[7] Y. Y. Cao and P. M. Frank, "Analysis and synthesis of nonlinear time-delay systems via fuzzy control approach," *IEEE Transactions on Fuzzy Systems*, vol. 8, no. 2, pp. 200–211, 2000.

[8] Y.-Y. Cao and P. M. Frank, "Stability analysis and synthesis of nonlinear time-delay systems via linear Takagi-Sugeno fuzzy models," *Fuzzy Sets and Systems*, vol. 124, no. 2, pp. 213–229, 2001.

[9] O. M. Kwon and J. H. Park, "Delay-range-dependent stabilization of uncertain dynamic systems with interval time-varying delays," *Applied Mathematics and Computation*, vol. 208, no. 1, pp. 58–68, 2009.

[10] E. Tian, D. Yue, and Y. Zhang, "Delay-dependent robust H_∞ control for T-S fuzzy system with interval time-varying delay," *Fuzzy Sets and Systems*, vol. 160, no. 12, pp. 1708–1719, 2009.

[11] J. Y. An, T. Li, G. L. Wen, and R. Li, "New stability conditions for uncertain T-S fuzzy systems with interval time-varying delay," *International Journal of Control, Automation and Systems*, vol. 10, no. 3, pp. 490–497, 2012.

[12] Z. J. Zhang, X. L. Huang, X. J. Ban, and X. Z. Gao, "Stability analysis and controller design of T-S fuzzy systems with time-delay under imperfect premise matching," *Journal of Beijing Institute of Technology*, vol. 21, no. 3, pp. 387–393, 2012.

[13] O. M. Kwon, M. J. Park, S. M. Lee, and J. H. Park, "Augmented Lyapunov-Krasovskii functional approaches to robust stability criteria for uncertain Takagi-Sugeno fuzzy systems with time-varying delays," *Fuzzy Sets and Systems*, vol. 201, no. 16, pp. 1–19, 2012.

[14] F. Liu, M. Wu, Y. He, and R. Yokoyama, "New delay-dependent stability criteria for T-S fuzzy systems with time-varying delay," *Fuzzy Sets and Systems*, vol. 161, no. 15, pp. 2033–2042, 2010.

[15] B. Chen, X. Liu, and S. Tong, "New delay-dependent stabilization conditions of T-S fuzzy systems with constant delay," *Fuzzy Sets and Systems*, vol. 158, no. 20, pp. 2209–2224, 2007.

[16] J. Yoneyama, "Robust stability and stabilization for uncertain Takagi-Sugeno fuzzy time-delay systems," *Fuzzy Sets and Systems*, vol. 158, no. 2, pp. 115–134, 2007.

[17] C. Lin, Q.-G. Wang, and T. H. Lee, "Delay-dependent LMI conditions for stability and stabilization of T-S fuzzy systems with bounded time-delay," *Fuzzy Sets and Systems*, vol. 157, no. 9, pp. 1229–1247, 2006.

[18] X. J. Su, P. Shi, L. G. Wu, and Y. D. Song, "A novel approach to filter design for T-S fuzzy discrete-time systems with time-varying delay," *IEEE Transactions on Fuzzy Systems*, vol. 20, no. 6, pp. 1114–1129, 2012.

[19] C. Peng and Q.-L. Han, "Delay-range-dependent robust stabilization for uncertain T-S fuzzy control systems with interval time-varying delays," *Information Sciences*, vol. 181, no. 19, pp. 4287–4299, 2011.

[20] S. T. Li, Y. W. Jing, and X. M. Liu, "Robust control for a class of T-S fuzzy systems with interval time-varying delay," *Internatinal Journal of Control, Automation and Systems*, vol. 10, no. 4, pp. 737–743, 2012.

[21] X.-M. Zhang, M. Wu, J.-H. She, and Y. He, "Delay-dependent stabilization of linear systems with time-varying state and input delays," *Automatica*, vol. 41, no. 8, pp. 1405–1412, 2005.

[22] B. Chen, X. Liu, and S. Tong, "Robust fuzzy control of nonlinear systems with input delay," *Chaos, Solitons & Fractals*, vol. 37, no. 3, pp. 894–901, 2008.

[23] C. Lin, Q.-G. Wang, and T. H. Lee, "Delay-dependent LMI conditions for stability and stabilization of T-S fuzzy systems with bounded time-delay," *Fuzzy Sets and Systems*, vol. 157, no. 9, pp. 1229–1247, 2006.

[24] H. J. Lee, J. B. Park, and Y. H. Joo, "Robust control for uncertain Takagi-Sugeno fuzzy systems with time-varying input delay," *Journal of Dynamic Systems, Measurement and Control, Transactions of the ASME*, vol. 127, no. 2, pp. 302–306, 2005.

[25] C.-H. Lien and K.-W. Yu, "Robust control for Takagi-Sugeno fuzzy systems with time-varying state and input delays," *Chaos, Solitons and Fractals*, vol. 35, no. 5, pp. 1003–1008, 2008.

[26] Y. K. Su, B. Chen, S. Y. Zhang, and C. Lin, "Delay-dependent stabilization of T-S fuzzy systems with time delay," *Control and Decision. Kongzhi yu Juece*, vol. 24, no. 6, pp. 921–927, 2009.

[27] B. Chen, X. Liu, C. Lin, and K. Liu, "Robust H_∞ control of Takagi-Sugeno fuzzy systems with state and input time delays," *Fuzzy Sets and Systems*, vol. 160, no. 4, pp. 403–422, 2009.

[28] L. Li and X. Liu, "New results on delay-dependent robust stability criteria of uncertain fuzzy systems with state and input delays," *Information Sciences*, vol. 179, no. 8, pp. 1134–1148, 2009.

[29] Z. J. Zhang, X. J. Ban, X. L. Huang, and X. Z. Gao, "New delay-dependent robust stablity for T-S fuzzy systems with interveval time-varying delay," in *Proccedings of the 5th International Joint Conference on Computational Science and Optimization*, pp. 826–830, Harbin, China, 2012.

[30] H. K. Lam and F. H. F. Leung, "LMI-based stability and performance design of fuzzy control systems: fuzzy models and controllers with different premises," in *Proceedings of the International Conference on Fuzzy Systerm*, pp. 9599–9506, Vancouver, Canada, 2006.

[31] H. K. Lam and M. Narimani, "Stability analysis and perfomance design for fuzzy-model-based control system under imperfect premise matching," *IEEE Transactions on Fuzzy Systems*, vol. 17, no. 4, pp. 949–961, 2009.

[32] S. Boyd, L. E. Ghaoui, and E. Feron, *Linear Matrix Inequality in Systems and Control Theory*, SIAM, Philadelphia, Pa, USA, 1994.

[33] I. R. Petersen and C. V. Hollot, "A Riccati equation approach to the stabilization of uncertain linear systems," *Automatica*, vol. 22, no. 4, pp. 397–411, 1986.

[34] J. Sun, G. P. Liu, and J. Chen, "Delay-dependent stability and stabilization of neutral time-delay systems," *International Journal of Robust and Nonlinear Control*, vol. 19, no. 12, pp. 1364–1375, 2009.

Hindawi Publishing Corporation
Mathematical Problems in Engineering
Volume 2013, Article ID 146325, 10 pages
http://dx.doi.org/10.1155/2013/146325

Research Article

Filtering for Discrete Fuzzy Stochastic Time-Delay Systems with Sensor Saturation

Jia You,[1] Shen Yin,[2] and Hamid R. Karimi[3]

[1] *Research Institute of Intelligent Control and Systems, Harbin Institute of Technology, Heilongjiang 150001, China*
[2] *College of Information Science and Technology, Bohai University, Jinzhou, Liaoning 121013, China*
[3] *Department of Engineering, Faculty of Engineering and Science, University of Agder, 4879 Grimstad, Norway*

Correspondence should be addressed to Shen Yin; shen.yin2011@googlemail.com

Received 29 November 2012; Accepted 4 February 2013

Academic Editor: Peng Shi

Copyright © 2013 Jia You et al. This is an open access article distributed under the Creative Commons Attribution License, which permits unrestricted use, distribution, and reproduction in any medium, provided the original work is properly cited.

This paper addresses the $\mathscr{H}_\infty$ filtering problem for discrete fuzzy stochastic systems with time-varying delay and sensor saturation. Random noise depending on state and external disturbance is also taken into account. A decomposition approach is employed to solve the characteristic of sensor saturation. The scaled small gain (SSG) theorem is extended to the stochastic systems, which is employed to handle with the time-varying delay by transforming the original system into the form of an interconnected system consisting of two subsystems. By the proposed Lyapunov-Krasovskii function, the scaled small gains of the subsystems are analyzed, respectively. Sufficient conditions for the stochastic stability of the filtering error system with a prescribed $\mathscr{H}_\infty$ level are established such that the gains of the $\mathscr{H}_\infty$ filter can be obtained explicitly. Finally, simulation results are presented to demonstrate the effectiveness of the proposed approach.

1. Introduction

In recent years, the control and filtering problems for Takagi-Sugeno (T-S) fuzzy systems, which have been employed to solve a great deal of issues in control and filtering fields, have drawn a great attention of many researchers [1–4]. Described by a set of If-Then rules, the T-S fuzzy system can approximate any given continuous function in a compact set of $\mathscr{R}^n$ at any preciseness [5–7]. Consequently, it has become one of the most useful and popular research platforms in fuzzy logic control (FLC), since many nonlinear systems can be analyzed by using the properties of conventional linear systems via T-S fuzzy model. A great number of significant results have been reported in the literatures [8–11]. In particular, a great effort has been devoted to the filtering problems for T-S fuzzy systems. Among the existing filtering approaches, the Kalman filtering is popular and useful due to its easy implementing and good performance in many engineering problems [12]. However, the Kalman filtering has strict constraints that a precise model of the system is available and all error terms and measurements have Gaussian distributions, which are hard to reach in many practical dynamics. Meanwhile, $\mathscr{H}_\infty$ filtering, which only requires that the noise sources to be arbitrary signals with bounded energy or bounded average power instead of Gaussian noises, has arguably become another useful and important filtering method for T-S fuzzy systems.

On the other hand, a large number of practical engineering problems encounter time-delay phenomenon, which is always a source of poor performance and even instability of the systems [13, 14]. Over the past few years, a great interest has been devoted to time-delay systems, and many significant results have been reported by the Lyapunov method [3, 15–17]. On the other hand, an input-output (IO) approach developed from the SSG theorem that has been introduced for constant delay [18, 19] and then extended to time-varying delay [20]. In contrast to the time-independent methods [15], less conservative results could be achieved by this approach, which analyzes the stability of the system by transforming the system into the form of two interconnected subsystems [20, 21], especially for small time delays [22]. It should be noted that a proper approximation to the time delay plays the key role in this method, and many approximation approaches are proposed to pursue smaller approximation error. Recently,

a method for estimating the time-varying delay by the upper and lower delay bounds was introduced in [23], which has a much smaller resulting error than the other one-term ones [24–26]. This motivates this research to extend this approach to $\mathscr{H}_\infty$ filtering problems for T-S fuzzy systems.

In practical engineering, sensor saturation is one of the most popular phenomena that limits the performance of sensors on various aspects significantly. When sensors cannot provide the enough amplitude signals due to the physical or safety constraints [18, 27], a complicated controller is needed for a good resulting performance. In recent years, researchers have paid a great attention to filtering problems with sensor saturation [28, 29]. However, it should be noted that in [28] the output of the system is only the sum of a linear term and a nonlinear one, which means that the output model is a special class of nonlinear sensor model, rather than a general form, and the filtering method in [28] cannot be utilized for the stochastic systems directly [30, 31].

Motivated by the above reasons, we investigate the $\mathscr{H}_\infty$ filtering problem for discrete-time T-S fuzzy stochastic systems with time-varying delay and senor saturation. A decomposition approach is applied to handle with the characteristic of the sensor saturation, and random noise subject to state and external-disturbance is also considered. A new model transformation is employed to transform the original system into a form of two interconnected subsystems. Based on the SSG theorem developed to stochastic systems and the proposed Lyapunov-Krasovskii function, the SSG of each subsystem is analyzed to establish the sufficient conditions under which the filtering error system is stochastically stable with a prescribed $\mathscr{H}_\infty$ performance level γ. Then, the corresponding $\mathscr{H}_\infty$ filter design technique is proposed. Finally, an illustrative example is presented to show the effectiveness of the proposed method.

The remainder of this paper is organized as follows. In Section 2, the problem of $\mathscr{H}_\infty$ filtering is formulated for T-S fuzzy stochastic systems with time-varying delay and sensor saturation. Section 3 presents the results for $\mathscr{H}_\infty$ performance analysis and $\mathscr{H}_\infty$ filter design. A numerical example is provided to demonstrate the effectiveness of the designed filtering technique in Section 4, and we conclude the paper with Section 5.

Notation. Throughout this paper, $\mathbb{R}^n$ represents the n-dimensional Euclidean space, $\mathbb{R}^{n\times m}$ is the set of all $n \times m$ real matrices, and the superscripts "-1" and "T", respectively, stand for the matrix inverse and matrix transpose. $\mathrm{Sym}\{A\}$ is the shortened notation for $A + A^T$, and the notation $P > 0$ (resp., $P \geq 0$), for $P \in \mathbb{R}^{n\times n}$, means that P is real symmetric and positive definite (resp., semidefinite). The symmetric elements of the symmetric matrix are represented by an asterisk ($*$), and the block diagonal matrices are denoted by $\mathrm{diag}\{\cdots\}$. $\mathbf{G}_1 \circ \mathbf{G}_2$ means the series connection of mapping $\mathbf{G}_1$ and $\mathbf{G}_2$ $\cdot$ $\mathbf{E}\{\cdot\}$ denotes the expectation operator with respect to probability measure, and for vector $x(k)$, $\|x\|_{E_2} = \mathbf{E}\{\sum_{n=0}^{\infty} \|x(n)\|^2\}^{1/2}$.

2. Problem Formulation

We consider the following nonlinear fuzzy dynamic described by a Takagi-Sugeno (T-S) stochastic model:

R^i: If $\zeta_1(k)$ is F_1^i, $\zeta_2(k)$ *is* F_2^i and $\ldots$, and $\zeta_s(k)$ is F_s^i, Then

$$\begin{aligned} x(k+1) &= A_i x(k) + A_{di} x(k-\tau_k) + B_i v(k) \\ &\quad + [E_i x(k) + G_i v(k)]\, w(k), \\ y(k) &= \phi(C_i x(k)) + D_i v(k), \\ z(k) &= L_i x(k), \end{aligned} \tag{1}$$

where $R^i, i \in \{1, 2, \ldots, \overline{n}\}$, denotes the ith fuzzy inference rule, $\overline{n}$ is the number of the inference rules, F_j^i, $j \in \{1, 2, \ldots, s\}$, are fuzzy sets, and $\zeta(k) = [\zeta_1(k), \zeta_2(k), \ldots, \zeta_s(k)]$ are some measurable premise variables of the system. $x(k) \in \mathbb{R}^n$ is the state vector, $y(k) \in \mathbb{R}^m$ is the measured output, and $z(k) \in \mathbb{R}^p$ is the signal to be estimated. $A_i \in \mathbb{R}^{n\times n}$, $A_{di} \in \mathbb{R}^{n\times n}$, $B_i \in \mathbb{R}^{n\times q}$, $C_i \in \mathbb{R}^{m\times n}$, $D_i \in \mathbb{R}^{m\times q}$, $L_i \in \mathbb{R}^{p\times n}$, $E_i \in \mathbb{R}^{n\times n}$, and $G_i \in \mathbb{R}^{n\times q}$ are known constant matrices. τ_k is the time-varying delay satisfying

$$d_1 \leq \tau_k \leq d_2, \tag{2}$$

where $d_1 > 0$ and $d_2 > 0$ denote the lower and upper bounds of the delays, respectively. We define the delay interval as $d_{12} = d_2 - d_1$.

In the system (1), $w(k)$ is a random process with standard one dimension on a probability space $(\Omega, \mathscr{F}, \mathscr{P})$, where Ω denotes the sample space, and $\mathscr{P}$ is the probability measure on $\mathscr{F}$, which is the σ-algebra of subsets of the sample space. The sequence of $w(k)$ is generated by $(w(k))_{k\in\mathbf{N}}$, where $\mathbf{N}$ is the set of natural numbers, such that $\mathbf{E}\{w(k)\} = 0$, $\mathbf{E}\{w(k)^2\} = 1$, and $\mathbf{E}\{w(i)w(j)\} = 0$ for $i \neq j$.

The exogenous disturbance $v(k) \in \mathbb{R}^q$ is assumed to belong to $\mathscr{L}_{E_2}([0,\infty); \mathbb{R}^q)$, which denotes the space of k-dimensional nonanticipatory square-integrable process $f(\cdot) = (f(k))_{k\in\mathbf{N}}$ on $\mathbf{N}$ with respect to $(\mathscr{F}_{k\in\mathbf{N}})$, such that

$$\|f\|_{E_2}^2 = \mathbf{E}\left\{\sum_{k=0}^{\infty} \|f(k)\|^2\right\} = \sum_{k=0}^{\infty} \mathbf{E}\left\{\|f(k)\|^2\right\} < \infty. \tag{3}$$

The defuzzified output of the T-S fuzzy system (1) is inferred as

$$\begin{aligned} \Sigma : x(k+1) &= \sum_{i=1}^{r} h_i(\theta_k) \{A_i x(k) + A_{di} x(k-\tau_k) + B_i v(k) \\ &\qquad + [E_i x(k) + G_i v(k)]\, w(k)\}, \\ y(k) &= \sum_{i=1}^{r} h_i(\theta_k) \{\phi(C_i x(k)) + D_i v(k)\}, \\ z(k) &= \sum_{i=1}^{r} h_i(\theta_k) L_i x(k), \end{aligned} \tag{4}$$

where

$$h_i(\theta_k) = \frac{\mu_i(\theta_k)}{\sum_{j=1}^{r}\mu_j(\theta_k)}, \qquad \mu_i(\theta_k) = \prod_{i=1}^{s} F_j^i(\theta_{jk}). \tag{5}$$

Then, we have $\mu_i(\theta_k) \geq 0$, $(i = 1, 2, \ldots, r)$ and $\sum_{i=1}^{r}\mu_i(\theta_k) > 0$, which implies that $h_i(\theta_k) \geq 0$ $(i = 1, 2, \ldots, r)$ and $\sum_{i=1}^{r} h_i(\theta_k) = 1$.

In this paper, the sensor saturation is described by the saturation function $\phi(\cdot) : \mathbb{R}^m \to \mathbb{R}^m$ satisfying $\phi \in [K_1, K_2]$, for some given diagonal matrices $K_1 \geq 0$, $K_2 \geq 0$ with $K_2 > K_1$, such that

$$(\phi(\zeta) - K_1\zeta)^T(\phi(\zeta) - K_2\zeta) \leq 0, \quad \forall \zeta \in \mathbb{R}^m. \tag{6}$$

Furthermore, the nonlinear function $\phi(\zeta)$ can be decomposed into a linear and a nonlinear part

$$\phi(\zeta) = \phi_s(\zeta) + K_1\zeta, \tag{7}$$

where the nonlinearity $\phi_s(\zeta)$ belongs to Φ_s, where

$$\Phi_s = \left\{\phi_s : \phi_s^T(\zeta)(\phi_s(\zeta) - K\zeta) \leq 0\right\}, \quad K \triangleq K_2 - K_1. \tag{8}$$

For the fuzzy system (1), we construct the following filter with full order to estimate the system states $x(k)$ from measured output $y(k)$:

$$\mathscr{F} : \begin{cases} \hat{x}(k+1) = \sum_{i=1}^{r} h_i(\theta_k)\{A_{\mathrm{F}i}\hat{x}(k) + B_{\mathrm{F}i}y(k)\}, \\ \hat{z}(k) = \sum_{i=1}^{r} h_i(\theta_k) L_i\hat{x}(k), \end{cases} \tag{9}$$

where $\hat{x}(k) \in \mathbb{R}^n$ is the filter state vector, $\hat{z}(k) \in \mathbb{R}^p$ is the estimate of $z(k)$, and $A_F \in \mathbb{R}^{n\times n}$ and $B_F \in \mathbb{R}^{n\times m}$ are the filter gains to be determined.

Define the following error variables:

$$e_x(k) = x(k) - \hat{x}(k), \qquad e(k) = \left[x^T(k) \;\; e_x^T(k)\right]^T, \qquad e_z(k) = z(k) - \hat{z}(k). \tag{10}$$

Combining the system (1) and the filter (9) yields the filtering error system as follows:

$$\mathscr{E} : \begin{cases} e(k+1) = \sum_{i=1}^{r}\sum_{j=1}^{r}\{\overline{A}_{ij}e(k) + \overline{A}_{di}I_K e(k-\tau_k) \\ \qquad + \overline{B}_{ij}v(k)\left[\overline{E}_i I_K e(k) + \overline{G}_i v(k)\right]w(k) \\ \qquad + \overline{B}_{\mathrm{F}i}\phi\left(C_j e(k)\right)\}, \\ e_z(k) = \sum_{i=1}^{r} h_i(\theta_k)\overline{L}_i e(k), \end{cases} \tag{11}$$

where

$$\overline{A}_{ij} = \begin{bmatrix} A_i & 0 \\ A_i - A_{\mathrm{F}i} - B_{\mathrm{F}i}K_1C_j & A_{\mathrm{F}i} \end{bmatrix}, \qquad \overline{A}_{di} = \begin{bmatrix} A_{di} \\ A_{di} \end{bmatrix},$$
$$\overline{B}_{ij} = \begin{bmatrix} B_i \\ B_i - B_{\mathrm{F}i}D_j \end{bmatrix}, \qquad \overline{E}_i = \begin{bmatrix} E_i \\ E_i \end{bmatrix}, \qquad \overline{G}_i = \begin{bmatrix} G_i \\ G_i \end{bmatrix},$$
$$\overline{B}_{\mathrm{F}i} = \begin{bmatrix} 0 \\ -B_{\mathrm{F}i} \end{bmatrix}, \qquad \overline{C}_j = \begin{bmatrix} C_j & 0 \end{bmatrix},$$
$$\overline{L}_i = \begin{bmatrix} 0 & L_i \end{bmatrix}, \qquad I_K = \begin{bmatrix} I_n & 0 \end{bmatrix}. \tag{12}$$

Furthermore, the following definitions will be used in this paper.

Definition 1 (see [32]). For the system in (1) with $\omega(k) = 0$, the system is stochastically stable if for any $\psi(k) \in \mathbb{R}^n$,

$$\mathbf{E}\left\{\sum_{k=0}^{\infty}\|x(k)\|^2\right\} \leq \theta\mathbf{E}\left\{\|x(0)\|^2\right\}. \tag{13}$$

Definition 2 (see [33]). A mapping $\mathbf{G} : u(k) \to y(k)$ is said to be input-output stable in the mean square if there exists $\gamma \geq 0$, such that

$$\|y(k)\|_{E_2} = \|\mathbf{G}(u)\|_{E_2} \leq \gamma\|u(k)\|_{E_2}. \tag{14}$$

Then, the main objective of this paper is as follows.

$\mathscr{H}_\infty$ *Filtering Problem*. Given a scalar $\gamma > 0$, the gains $A_{\mathrm{F}i}$ and $B_{\mathrm{F}i}$ of the filter (9) are designed such that for any time-delay $\tau(k)$ satisfying (2), the filter error system (11) is stochastically stable under $v(k) = 0$, and for any given integer γ, the following $\mathscr{H}_\infty$ performance index

$$\|z(k) - \hat{z}(k)\|_{E_2} \leq \gamma\|v(k)\|_{E_2} \tag{15}$$

holds for any function $\phi(\cdot) \in [K_1, K_2]$.

3. Filtering Performance Analysis

In this section, we focus on the filter performance analysis based on the developed SSG theorem. By the developed SSG theorem to the stochastic systems and a new model transformation to the system $\mathscr{E}$ in (11), the sufficient conditions are proposed, under which the system $\mathscr{E}$ is stochastically stable with a prescribed $\mathscr{H}_\infty$ performance index.

3.1. SSG Theorem for Stochastic Systems

Lemma 3 (stochastic small gain theorem [34]). *Consider the following interconnected system consisting of two subsystems in Figure 1:*

$$\mathscr{S}_1 : \varepsilon(t) = \mathbf{G}\epsilon(t), \qquad \mathscr{S}_2 : \epsilon(t) = \mathbf{\Delta}\varepsilon(t). \tag{16}$$

Then, the closed loop systems are input-output stable in mean square for all the subsystems $\mathbf{G}$ *and* $\mathbf{\Delta}$ *satisfying*

$$\|\mathbf{G}(u_1)\|_{E_2} \leq k_1\|u_1\|_{E_2}, \quad k_1 > 0,$$
$$\|\mathbf{\Delta}(u_2)\|_{E_2} \leq k_2\|u_2\|_{E_2}, \quad k_2 > 0 \tag{17}$$

if $k_1k_2 < 1$.

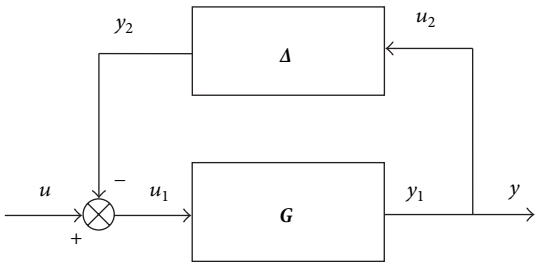

Figure 1: The interconnection subsystems.

Proof. Considering (16) yields

$$\begin{aligned}\|y\|_{E_2} &\le k_1\|u_1\|_{E_2} = k_1\|u-\Delta(y)\|_{E_2}\\ &\le k_1\left(\|u\|_{E_2}+k_2\|y\|_{E_2}\right).\end{aligned} \tag{18}$$

Obviously,

$$\|y\|_{E_2} \le \frac{k_1}{1-k_1k_2}\|u\|_{E_2}, \tag{19}$$

which implies that the closed loop is input-output stable in mean square. □

Corollary 4 (stochastic SSG theorem [34]). *Consider the system described in* (16). *The system is input-output stable in mean square if* $\|T_\epsilon \circ \mathbf{G} \circ T_\varepsilon\| < 1$ *holds for some nonsingular matrices* T_y *and* T_δ *with* $\|T_\varepsilon \circ \Delta \circ T_\epsilon\| \le 1$.

The proof of Corollary 4 can be readily obtained by following the similar lines of Lemma 3.

3.2. A New Model Transformation. To transform the systems (11) into the form of (16), we express $x(k-\tau_k)$ as

$$x(k-\tau_k) = \frac{1}{2}x(k-d_1)+\frac{1}{2}x(k-d_2)+\frac{d_{12}}{2}\epsilon(k), \tag{20}$$

where $(1/2)[x(k-d_1)+x(k-d_2)]$ is the approximation of $x(k-\tau_k)$, and $(d_{12}/2)\epsilon(k)$ denotes the approximation error. Then, the system $\mathscr{E}$ can be rewritten as follows:

$$\mathscr{E}: \begin{cases} e(k+1) = \displaystyle\sum_{i=1}^{r}\sum_{j=1}^{r}\Big\{\overline{A}_{ij}e(k)+\frac{1}{2}\overline{A}_{di}\\ \qquad\qquad \times\left[x(k-d_1)+x(k-d_2)+d_{12}\epsilon(k)\right]\\ \qquad\qquad +\overline{B}_{ij}v(k)+\left[\overline{E}_iI_Ke(k)+\overline{G}_iv(k)\right]\\ \qquad\qquad \times w(k),+\overline{B}_{\mathrm{Fi}}\phi\left(C_je(k)\right)\Big\},\\ e_z(k) = \displaystyle\sum_{i=1}^{r}h_i(\theta_k)\overline{L}_ie(k).\end{cases} \tag{21}$$

Define $\varepsilon(k) = \mathbf{E}\{x(k+1)\}-x(k)$, and we have

$$\begin{aligned}\epsilon(k) &= \frac{2}{d_{12}}\left[x(k-\tau_k)-\frac{1}{2}x(k-d_1)-\frac{1}{2}x(k-d_2)\right]\\ &= \frac{1}{d_{12}}\left[\sum_{i=k-d_2}^{k-\tau_k-1}\varepsilon(i)-\sum_{i=k-\tau_k}^{k-d_1-1}\varepsilon(i)\right]\\ &= \frac{1}{d_{12}}\left[\sum_{i=k-d_2}^{k-d_1-1}\beta(i)\varepsilon(i)\right],\end{aligned} \tag{22}$$

where

$$\beta(i) \triangleq \begin{cases}1, & \text{when } i \leqslant k-\tau_k-1,\\ -1, & \text{when } i > k-\tau_k-1.\end{cases} \tag{23}$$

Then, obviously the system (21) can be rewritten in the form as follows:

$$\mathscr{E}_1: \sigma(k) = \sum_{i=1}^{r}\sum_{j=1}^{r}\mathbf{G}\xi(k), \qquad \mathscr{E}_2: \epsilon(k) = \Delta\varepsilon(k), \tag{24}$$

where

$$\begin{gathered}\xi(k) = \left[e^T(k)\ \ x^T(k-d_1)\ \ x^T(k-d_2)\ \ \epsilon(k)\ \ v(k)\ \ \phi_s(C_jx(k))\right]^T,\\ \sigma(k) = \left[e^T(k+1)\ \ \varepsilon^T(k)\ \ e_z^T(k)\right]^T, \qquad \mathbf{G} = \left[\mathbf{G}_1^T\ \ \mathbf{G}^T\ \ \mathbf{G}_3^T\right]^T,\\ \mathbf{G}_1 = \left[\overline{A}_{ij}\ \ \frac{1}{2}\overline{A}_{di}\ \ \frac{1}{2}\overline{A}_{di}\ \ \frac{d_{12}}{2}\overline{A}_{di}\ \ \overline{B}_{ij}\ \ \overline{B}_{\mathrm{Fi}}\right],\\ \mathbf{G}_2 = \left[A_i-I\ \ 0\ \ \frac{1}{2}A_{di}\ \ \frac{1}{2}A_{di}\ \ \frac{d_{12}}{2}A_{di}\ \ B_i\ \ 0\right],\\ \mathbf{G}_3 = \left[\overline{L}_i\ \ 0_{p\times(3n+m+q)}\right].\end{gathered} \tag{25}$$

Furthermore, the SSG of the mapping Δ denoted by $\gamma(\Delta_T)$ has an upper bound.

Lemma 5. $\gamma(\Delta_T)$ *has an upper bound*

$$\gamma(\Delta_T) = \sup\frac{\|T\epsilon(k)\|_{E_2}}{\|T\varepsilon(k)\|_{E_2}} \le 1. \tag{26}$$

Proof. According to the fact that $|\beta(i)| = 1$, by using Jensen's inequality, it can be derived under zero initial condition

$$\begin{aligned}\|T\epsilon(k)\|_{E_2}^2 &= \mathbf{E}\left\{\sum_{j=0}^{\infty}\left[\epsilon^T(j)Z\epsilon(j)\right]\right\}\\ &\le \frac{2}{d_{12}^2}\mathbf{E}\left\{\sum_{i=0}^{\infty}\left[d_{12}\sum_{j=i-d_2}^{i-d_1-1}\beta^2(j)\epsilon^T(j)\epsilon(j)\right]\right\}\end{aligned}$$

$$= \frac{1}{d_{12}}\mathbf{E}\left\{\sum_{j=-d_2}^{-d_1-1}\sum_{i=0}^{\infty}\epsilon^T(i+j)\,\epsilon(i+j)\right\}$$
$$\leq \frac{1}{d_{12}}\mathbf{E}\left\{\sum_{j=-d_2}^{-d_1-1}\sum_{i=0}^{\infty}\epsilon^T(i)\,\epsilon(i)\right\}$$
$$\leq \mathbf{E}\left\{\sum_{j=0}^{\infty}\left[\varepsilon^T(j)\,Z\varepsilon(j)\right]\right\} = \|T\varepsilon(k)\|_{E_2}^2, \tag{27}$$

where $Z = T^TT$, which implies $\gamma(\mathbf{\Delta}_T) \leq 1$. The proof is completed. □

From Lemmas 3 and 5, the system $\mathscr{E}$ in (11) is input-output stable in mean square if the SSG of the subsystem $\mathscr{E}_1$ satisfies the conditions in Lemma 3, which will be investigated in the following section.

3.3. $\mathscr{H}_\infty$ Performance Analysis. In this section, the $\mathscr{H}_\infty$ performance of the filtering error system is analyzed by the SSG of the subsystem $\mathscr{E}_1$ in (24) in order to establish the conditions under which the $\mathscr{H}_\infty$ performance index is guaranteed for the filtering error system (11).

Theorem 6. *Suppose that the system matrices A_i, A_{di}, B_i, C_i, D_i, and L_i represent a fixed system. Given the filter matrices A_{Fi}, B_{Fi} and integers $d_2 > d_1 \geq 0$ and a constant $\gamma > 0$, the filtering error system* (21) *is input-output stable in mean square with an $\mathscr{H}_\infty$ performance attention level γ for any time-varying delay satisfying* (2) *if there exist matrices $P > 0$, $Q_i > 0$, $i = 1, 2$, such that*

$$\Psi_{ij} \triangleq \begin{bmatrix} \Xi_1 & \left[\Gamma_2^T Z \;\; \Gamma_3^T \;\; \Gamma_1^T P\right] \\ * & \operatorname{diag}\left\{-Z, -I_p, -P\right\}\end{bmatrix} < 0, \tag{28}$$

where

$$\Xi_1 = \begin{bmatrix} \Xi_{11} & \left[0 \;\; 0 \;\; 0 \;\; I_k^T\overline{E}_i^T P\overline{G}_i \;\; I_k^T C_j^T K^T\right] \\ * & \operatorname{diag}\left\{-Q_1, -Q_2, -Z, \alpha_i, -2I_m\right\}\end{bmatrix},$$
$$\Gamma_1 = \left[\overline{A}_{ij} \;\; \frac{1}{2}\overline{A}_{di} \;\; \frac{1}{2}\overline{A}_{di} \;\; \frac{1}{2}d_{12}\overline{A}_{di} \;\; \overline{B}_{ij} \;\; \overline{B}_{Fi}\right],$$
$$\Gamma_2 = \left[\overline{A}_i - I \;\; 0 \;\; \frac{1}{2}\overline{A}_{di} \;\; \frac{1}{2}\overline{A}_{di} \;\; \frac{1}{2}d_{12}\overline{A}_{di} \;\; \overline{B}_i \;\; 0\right], \tag{29}$$
$$\Gamma_3 = \left[\overline{L}_i \;\; 0_{p\times(3n+m+q)}\right], \qquad \alpha_i = -\gamma^2 I_q + \overline{G}_i^T P\overline{G}_i,$$
$$\Xi_{11} = -P + I_K^T\left(Q_1 + Q_2 + \overline{E}_i^T P\overline{E}_i\right)I_K.$$

Proof. Choose the following Lyapunov-Krasovskii functional:

$$V(k) = V_1(k) + V_2(k) \tag{30}$$

with

$$V_1(k) = e^T(k)\,Pe(k),$$
$$V_2(k) = \sum_{i=k-d_1}^{k-1} x^T(i)\,Q_1x(i) + \sum_{i=k-d_2}^{k-1} x^T(i)\,Q_2x(i), \tag{31}$$

where $P > 0$ and $Q_i > 0$, $i = 1, 2$ are the matrices to be determined.

Define $\Delta V(k) = \mathbf{E}\{V(k+1)\} - V(k)$, then we have

$$\Delta V_1(k)$$
$$= \mathbf{E}\left\{e^T(k+1)\,Pe(k+1)\right\} - e^T(k)\,Pe(k)$$
$$\leq \sum_{i=1}^{r}\sum_{j=1}^{r}\left\{\begin{pmatrix} \xi^T(k)\,\Gamma_1^T P\Gamma_1\xi(k) - e^T(k)\,Pe(k) \\ -2\phi_s\left(C_jx(k)\right)\left[\phi_s\left(C_jx(k)\right) - KC_jx(k)\right]\end{pmatrix}\right\},$$
$$\Delta V_2(k) = x^T(k)\,Q_1x(k) - x^T(k-d_1)\,Q_1x(k-d_1)$$
$$+ x^T(k)\,Q_2x(k) - x^T(k-d_2)\,Q_2x(k-d_2). \tag{32}$$

Then, define

$$J_s = \mathbf{E}\left\{\sum_{k=0}^{\infty}\left[\varepsilon^T(k)\,Z\varepsilon(k) - \epsilon^T(k)\,Z\epsilon(k) + e_z^T(k)\,e_z(k) - \gamma^2 v^T(k)\,v(k)\right]\right\}, \tag{33}$$

which together with (30) yields

$$J_s \leq J_s + V(\infty) - V(0)$$
$$= \mathbf{E}\left\{\sum_{k=0}^{\infty}\begin{pmatrix} \Delta V(k) + \varepsilon^T(k)\,Z\varepsilon(k) - \epsilon^T(k)\,Z\epsilon(k) \\ + e_z^T(k)\,e_z(k) - \gamma^2 v^T(k)\,v(k)\end{pmatrix}\right\}$$
$$= \mathbf{E}\left\{\sum_{k=0}^{\infty}\sum_{i=1}^{r}\sum_{j=1}^{r}\left[\xi^T(k)\begin{pmatrix} \Xi_1 + \Gamma_1^T P\Gamma_1 \\ + \Gamma_2^T Z\Gamma_2 + \Gamma_3^T\Gamma_3\end{pmatrix}\xi(k)\right]\right\}. \tag{34}$$

By the Schur complement, it can be verified that $J_s < 0$ is guaranteed by $\Psi_{ij} < 0$, which implies that if $Z = T^TT$, we have $\gamma(\mathbf{G}_T) < 1$, where $\mathbf{G}$ is defined in (24). According to Lemmas 3 and 5, it is shown that the system $\mathscr{E}$ in (11) is input-output stable in mean square.

Furthermore, $J_s < 0$ implies that

$$\|T\varepsilon(k)\|_{E_2}^2 + \|e_z(k)\|_{E_2}^2 < \|T\epsilon(k)\|_{E_2}^2 + \gamma^2\|v(k)\|_{E_2}^2, \tag{35}$$

which together with (30) yields $\|e_z(k)\|_{E_2}^2 < \gamma^2\|v(k)\|_{E_2}^2$. The proof is completed. □

Theorem 6 shows the conditions under which the system $\mathscr{E}$ in (11) is input-output stable in mean square with a prescribed $\mathscr{H}_\infty$ performance index. Moreover, the conditions for stochastic stability of the system $\mathscr{E}$ can be reached by the Lyapunov-Krasovskii functional method, which will be discussed in the following theorem.

Theorem 7. *For the forward system $\mathscr{E}$ in* (24)*, if Theorem 6 holds, then, the system $\mathscr{E}$ is stochastically stable for $v(k) = 0$.*

Proof. For the LKF defined in (30), we have

$$\begin{aligned}\Delta V_c(k) &= \Delta V(k) + \varepsilon^T(k) Z\varepsilon(k) - \epsilon^T(k) Z\epsilon(k)\\ &= \xi_1^T(k)\left(\widetilde{\Xi}_1 + \widetilde{\Gamma}_1^T P\widetilde{\Gamma}_1 + \widetilde{\Gamma}_2^T Z\widetilde{\Gamma}_2\right)\xi_1(k),\end{aligned} \tag{36}$$

with

$$\begin{aligned}\xi_1(k) &= \left[e^T(k)\ \ x^T(k-d_1)\ \ x^T(k-d_2)\ \ \epsilon(k)\ \ \phi_s(C_j x(k))\right]^T,\\ \widetilde{\Xi}_1 &= \begin{bmatrix}\Xi_{11} & \left[0\ \ 0\ \ 0\ \ I_k^T C_j^T K^T\right]\\ * & \operatorname{diag}\{-Q_1, -Q_2, -Z, -2I_m\}\end{bmatrix},\\ \widetilde{\Gamma}_1 &= \left[\overline{A}_{ij}\ \ \frac{1}{2}\overline{A}_{di}\ \ \frac{1}{2}\overline{A}_{di}\ \ \frac{d_{12}}{2}\overline{A}_{di}\ \ \overline{B}_{\mathrm{Fi}}\right],\\ \widetilde{\Gamma}_2 &= \left[A_i - I\ \ 0\ \ \frac{1}{2}A_{di}\ \ \frac{1}{2}A_{di}\ \ \frac{d_{12}}{2}A_{di}\ \ 0\right],\end{aligned} \tag{37}$$

where Ξ_{11} is defined in (28). □

Define $(\widetilde{\Xi}_1 + \widetilde{\Gamma}_1^T P\widetilde{\Gamma}_1 + \widetilde{\Gamma}_2^T Z\widetilde{\Gamma}_2)$ as Φ_{ij}. It can be shown that $\Phi_{ij} < 0$, if Theorem 6 holds. Then, we can always find a small scalar $\lambda > 0$, such that

$$\Phi_{ij} < \begin{bmatrix}-\lambda I_n & 0\\ 0 & 0\end{bmatrix}, \tag{38}$$

which implies that

$$\mathbf{E}\{V_c(k+1) - V_c(k)\} \le -\lambda x^T(k)x(k) < 0. \tag{39}$$

For any positive integer R, by summing up the inequality on both sides from $k = 0, \ldots, R$, we obtain

$$\mathbf{E}\{V_c(R) - V_c(0)\} \le -\lambda\sum_{k=0}^{R} x^T(k)x(k) < 0, \tag{40}$$

which implies that when $R \to \infty$,

$$\begin{aligned}\sum_{k=0}^{\infty}\mathbf{E}\left\{x^T(k)x(k)\right\} &\le \frac{1}{\lambda}\mathbf{E}\{V_c(0) - V_c(\infty)\}\\ &\le \frac{1}{\lambda}\mathbf{E}\{V_c(0)\} < \theta\mathbf{E}\left\{\|x(0)\|^2\right\},\end{aligned} \tag{41}$$

which indicates that the systems in (24) are stochastically stable according to Definition 1. The proof is completed.

Remark 8. It is well known that free-weighting matrices are introduced a lot to estimate the upper bound of the term $(1/d_{12})\sum_{i=-d_2}^{-d_1-1}\epsilon^T(k+i)Z\epsilon(k+i)$, while in this paper, Jensen's inequality is employed instead of such weighting matrices, which reduce the NoV of the proposed conditions to $3n^2+3n$. It is remarkably smaller than the results in some existing literatures, such as $9n^2 + 3n$ [35], and $11n^2 + 2.5n$ [16], $13n^2 + 5n$ [36], and $31n^2 + 7n$ [17], which demonstrates the computational advantage of the proposed approach obviously [24].

4. $\mathscr{H}_\infty$ Filter Design

This section is devoted to the $\mathscr{H}_\infty$ filter design problem for the system (1) based on Theorem 6. Sufficient conditions for the existence of the $\mathscr{H}_\infty$ filter are provided in the following theorem.

Theorem 9. *Consider the discrete-time fuzzy stochastic system in* (1)*, for a given constant $\gamma > 0$, if there exist matrices $0 < X \in \mathbb{R}^{n\times n}$, $0 < Y \in \mathbb{R}^{n\times n}$, $\overline{A}_{Fi} \in \mathbb{R}^{n\times n}$, and $\overline{B}_{Fi} \in \mathbb{R}^{n\times m}$, such that the following LMI holds:*

$$\widetilde{\Psi}_{ij} \triangleq \begin{bmatrix}\widetilde{\Xi}_1 & \left[\Gamma_2^T Z\ \ \Gamma_3^T\ \ \Gamma_C^T X\ \ \Gamma_C^T Y + \Gamma_F^T\right]\\ * & \operatorname{diag}\left\{-Z, -I_p, -X, -Y\right\}\end{bmatrix} < 0, \tag{42}$$

where

$$\begin{aligned}\widetilde{\Xi}_1 &= \begin{bmatrix}\widetilde{\Xi}_{11} & \left[0_{n\times 4n}\ \ E_i^T(X+Y)G_i\ \ C_j^T K^T\right]\\ * & \operatorname{diag}\{Y, -Q_1, -Q_2, -Z, \widetilde{\alpha}_i, -2I_m\}\end{bmatrix},\\ \Gamma_C &= \left[\overline{A}_i\ \ 0\ \ \frac{1}{2}\overline{A}_{di}\ \ \frac{1}{2}\overline{A}_{di}\ \ \frac{1}{2}d_{12}\overline{A}_{di}\ \ \overline{B}_i\ \ 0\right],\\ \Gamma_F &= \left[-\overline{B}_{Fi}K_1C_j - \overline{A}_{Fi}\ \ \overline{A}_{Fi}\ \ 0_{n\times 3n}\ \ -\overline{B}_{Fi}D_j\ \ -\overline{B}_{Fi}\right],\\ \widetilde{\alpha}_i &= -\gamma^2 I_q + G_i^T(X+Y)G_i,\\ \widetilde{\Xi}_{11} &= -X + Q_1 + Q_2 + E_i^T(X+Y)E_i,\end{aligned} \tag{43}$$

then, the system $\mathscr{E}$ in (11) *is stochastically stable with $\mathscr{H}_\infty$ performance level γ, and the filter gains are given by*

$$A_{Fi} = Y^{-1}\overline{A}_{Fi}, \qquad B_{Fi} = Y^{-1}\overline{B}_{Fi}. \tag{44}$$

Proof. Define P introduced in Theorem 6 as

$$P = \begin{bmatrix}X & 0\\ 0 & Y\end{bmatrix}, \tag{45}$$

where $0 < X \in \mathbb{R}^{n\times n}$ and $0 < Y \in \mathbb{R}^{n\times n}$ are to be determined such that solvability of (28) is satisfied.

Then, we have

$$\begin{aligned}&\begin{bmatrix}A_i^T & A_i^T - A_{\mathrm{Fi}}^T - C_j^T K_1^T B_{\mathrm{Fi}}^T\\ 0 & A_{\mathrm{Fi}}^T\end{bmatrix}\begin{bmatrix}X & 0\\ 0 & Y\end{bmatrix}\\ &\quad = \begin{bmatrix}A_i^T X & A_i^T Y - A_{\mathrm{Fi}}^T Y - C_j^T K_1^T B_{\mathrm{Fi}}^T Y\\ 0 & A_{\mathrm{Fi}}^T Y\end{bmatrix},\\ &\left[B_i^T\ \ B_i^T - D_j^T B_{\mathrm{Fi}}^T\right]\begin{bmatrix}X & 0\\ 0 & Y\end{bmatrix}\\ &\quad = \left[B_i^T X\ \ B_i^T Y - D_j^T B_{\mathrm{Fi}}^T Y\right].\end{aligned} \tag{46}$$

Define $\overline{A}_{\mathrm{Fi}} = YA_{\mathrm{Fi}}$, $\overline{B}_{\mathrm{Fi}} = YB_{\mathrm{Fi}}$, which together with (28) yields (42). The proof is completed. □

5. Numerical Example

In this section, an example is provided to demonstrate effectiveness of the filter design method proposed in the preceding sections.

Example 10. Consider the system (1) with the following parameters:

$$A_1 = \begin{bmatrix} -0.28 & -0.01 & -0.02 \\ -0.2 & -0.25 & -0.29 \\ 0.03 & -0.04 & -0.23 \end{bmatrix},$$

$$A_{d1} = \begin{bmatrix} 0.01 & 0.02 & 0 \\ 0.01 & 0 & 0.01 \\ 0 & 0 & -0.01 \end{bmatrix},$$

$$E_1 = \begin{bmatrix} -0.11 & 0.1 & 1.66 \\ 0 & 0.46 & -0.47 \\ 0.47 & -0.11 & -0.43 \end{bmatrix}, \qquad B_1 = \begin{bmatrix} -2.02 \\ 3.83 \\ 1.39 \end{bmatrix},$$

$$C_1 = \begin{bmatrix} -0.11 & 0.05 & -0.1 \\ 0.69 & 0.35 & 0.48 \end{bmatrix}, \qquad L_1 = \begin{bmatrix} 0.1 & 0.1 & 0.1 \\ 0.12 & 0.1 & 0.19 \end{bmatrix},$$

$$G_1 = \begin{bmatrix} -0.21 & 0.61 & 0.15 \end{bmatrix}^T, \qquad D_1 = \begin{bmatrix} 0.3 & -0.3 \end{bmatrix}^T,$$

$$A_2 = \begin{bmatrix} -0.35 & 0.0 & 0.01 \\ -0.59 & -0.24 & 0.02 \\ 0.1 & -0.06 & -0.72 \end{bmatrix},$$

$$A_{d2} = \begin{bmatrix} 0.01 & 0.02 & 0 \\ 0.01 & 0 & 0.01 \\ 0 & 0 & 0.01 \end{bmatrix},$$

$$E_2 = \begin{bmatrix} -0.12 & -0.11 & 0.38 \\ 0.11 & 0.64 & -0.18 \\ -0.31 & -0.63 & -0.6 \end{bmatrix}, \qquad B_2 = \begin{bmatrix} 2.04 \\ -3.25 \\ -0.93 \end{bmatrix},$$

$$C_2 = \begin{bmatrix} -0.2 & -0.1 & -0.2 \\ 0.5 & 0.2 & 0.21 \end{bmatrix}, \qquad L_2 = \begin{bmatrix} 0.2 & 0.19 & 0.2 \\ 0.1 & 0.1 & 0.2 \end{bmatrix},$$

$$G_2 = \begin{bmatrix} -0.43 & 2.11 & 0.51 \end{bmatrix}^T, \qquad D_2 = \begin{bmatrix} 0.1 & 0.47 \end{bmatrix}^T, \tag{47}$$

and the saturation parameters are selected as

$$K_1 = \begin{bmatrix} 0.6 & 0 \\ 0 & 0.7 \end{bmatrix}, \qquad K_2 = \begin{bmatrix} 0.8 & 0 \\ 0 & 0.8 \end{bmatrix}, \tag{48}$$

the membership functions are

$$h_1(\theta) = \frac{1 - \sin(x_1)}{2}, \qquad h_1(\theta) = \frac{1 + \sin(x_1)}{2}, \tag{49}$$

and the noises $v(k)$ are assumed to be $v(k) = 1/(0.1 + k^2)$, which satisfy the constraint in (3), and set $d_1 = 1$ and $d_2 = 2$.

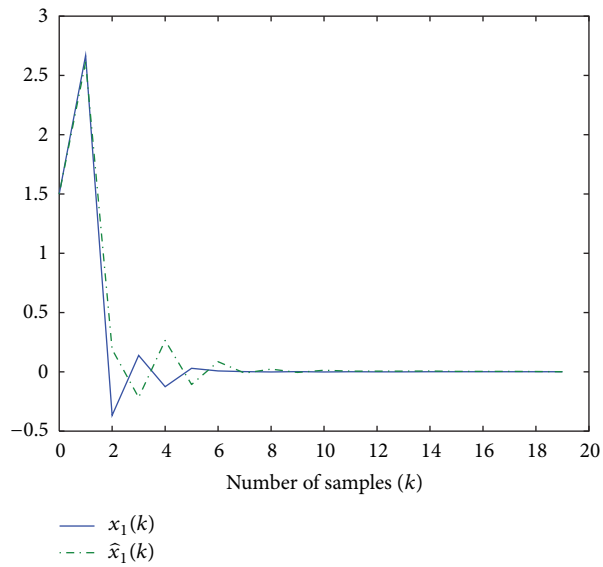

Figure 2: $x_1(k)$ and $\hat{x}_1(k)$.

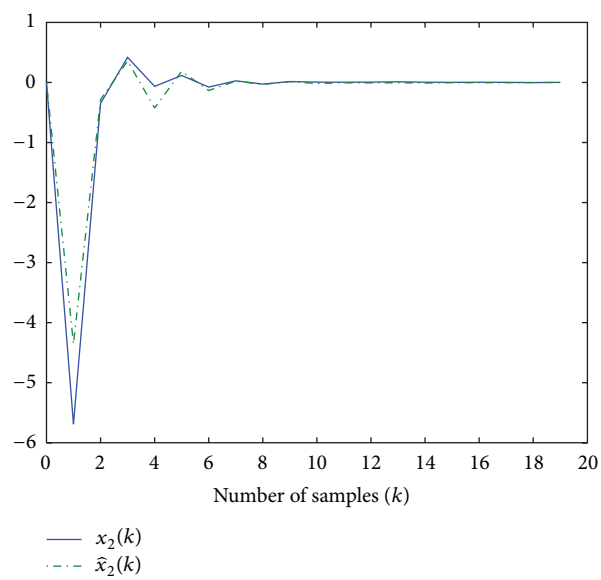

Figure 3: $x_2(k)$ and $\hat{x}_2(k)$.

To design the $\mathscr{H}_\infty$ filter, by solving the LMI condition (42) under the prescribed disturbance level $\gamma = 1.2$, it can be obtained that

$$\overline{A}_{F1} = \begin{bmatrix} -0.0001 & -0.0008 & 0.0021 \\ 0.0001 & 0.0005 & -0.0013 \\ 0.0000 & 0.0002 & -0.0006 \end{bmatrix},$$

$$\overline{B}_{F1} = \begin{bmatrix} -0.5877 & 1.4425 \\ 1.2489 & -2.1186 \\ 0.5082 & -0.5446 \end{bmatrix},$$

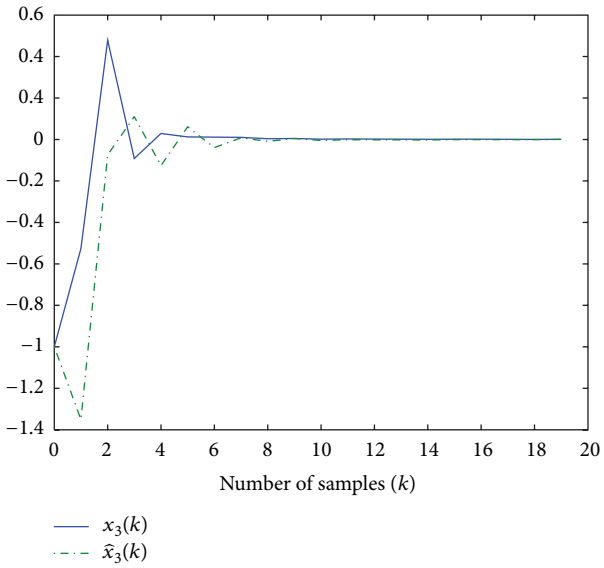

FIGURE 4: $x_3(k)$ and $\hat{x}_3(k)$.

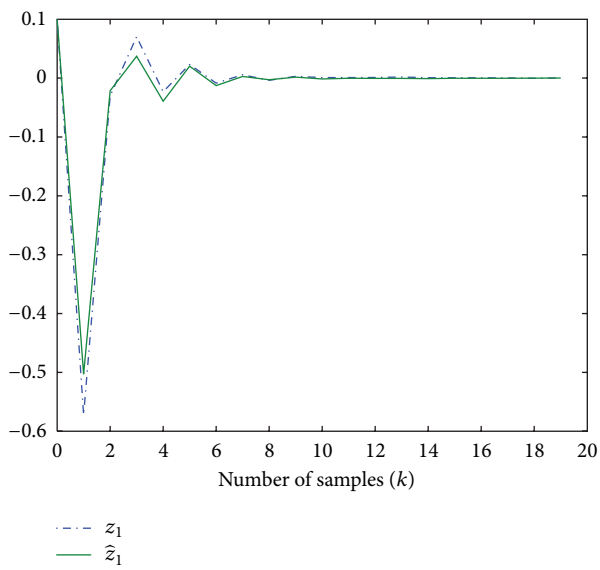

FIGURE 5: $z_1(k)$ and $\hat{z}_1(k)$.

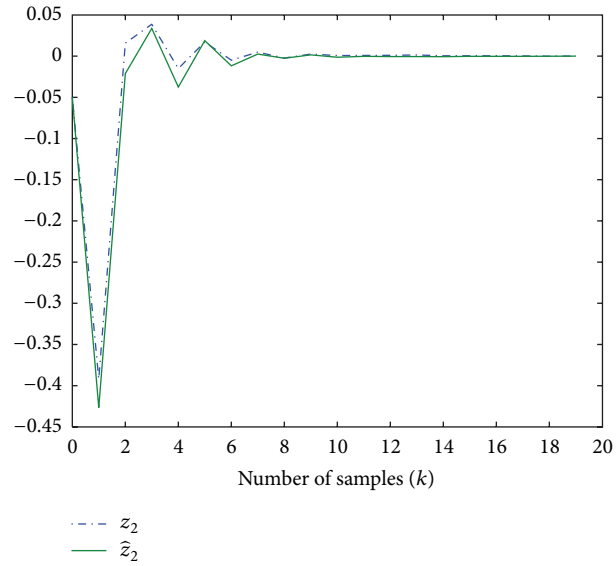

FIGURE 6: $z_2(k)$ and $\hat{z}_2(k)$.

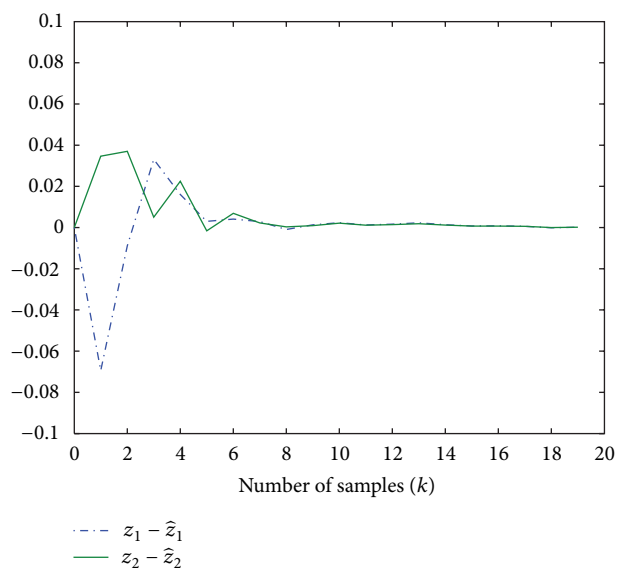

FIGURE 7: $e_{z1}(k)$ and $e_{z2}(k)$.

$$\overline{A}_{F2} = \begin{bmatrix} -0.0002 & -0.0005 & 0.0012 \\ 0.0002 & 0.0000 & 0.0002 \\ 0.0000 & 0.0001 & -0.0002 \end{bmatrix},$$

$$\overline{B}_{F2} = \begin{bmatrix} 1.0949 & 2.0782 \\ -0.9802 & -3.5244 \\ 0.0898 & -1.1212 \end{bmatrix}. \tag{50}$$

Assume the sensor saturation as

$$\phi(y) = \frac{K_1 + K_2}{2} y + \frac{K_2 - K_1}{2} \sin(y), \tag{51}$$

which satisfies (8), and the initial conditions as $x(0) = [1.5 \;\; 0 \;\; -1]^T$, $x(-1) = x(-2) = [1 \;\; 0.1 \;\; -0.6]^T$. By calculation, it can be obtained that the $\|e_z(k)\|_{E_2}^2 = 0.0095$ and $\|v(k)\|_{E_2}^2 = 3.0810$ that yields $\gamma = 0.0555$ which is below the given $\gamma = 1.2$, which demonstrates effectiveness of the proposed filter design. In addition, the trajectories of state variable $x(k)$ and its estimate $\hat{x}(k)$ are shown in Figures 2, 3, and 4, $z(k)$ and its estimate $\hat{z}(k)$ are given in Figures 5 and 6, and $e_z(k) = z(k) - \hat{z}(k)$ is provided in Figure 7.

6. Conclusion

This paper addresses the $\mathscr{H}_\infty$ filtering problem for T-S fuzzy systems subject to sensor saturation. The plant is considered with random noise depending on state and external-disturbance. The system is transformed into an input-output

form consisted of two interconnected subsystems. Based on the SSG theorem developed to stochastic systems and the proposed Lyapunov-Krasovskii function, sufficient conditions under which the $\mathscr{H}_\infty$ filter can be achieved with the prescribed $\mathscr{H}_\infty$ performance index are established. Finally, a numerical example is presented to demonstrate the effectiveness of the proposed filter design scheme.

References

[1] H. R. Karimi, "Observer-based mixed H_2/H_∞ control design of linear systems with time-varying delays: an LMI approach," *International Journal of Control, Automation and Systems*, vol. 6, no. 1, pp. 1–14, 2008.

[2] H. R. Karimi and H. Gao, "New delay-dependent exponential H_∞ synchronization for uncertain neural networks with mixed time delays," *IEEE Transactions on Systems, Man, and Cybernetics, Part B*, vol. 40, no. 1, pp. 173–185, 2010.

[3] M. Liu, D. W. C. Ho, and Y. Niu, "Stabilization of Markovian jump linear system over networks with random communication delay," *Automatica*, vol. 45, no. 2, pp. 416–421, 2009.

[4] M. Liu, D. W. C. Ho, and Y. Niu, "Robust filtering design for stochastic system with mode-dependent output quantization," *IEEE Transactions on Signal Processing*, vol. 58, no. 12, pp. 6410–6416, 2010.

[5] R. Yang, P. Shi, and G.-P. Liu, "Filtering for discrete-time networked nonlinear systems with mixed random delays and packet dropouts," *IEEE Transactions on Automatic Control*, vol. 56, no. 11, pp. 2655–2660, 2011.

[6] R. Yang, Z. Zhang, and P. Shi, "Exponential stability on stochastic neural networks with discrete interval and distributed delays," *IEEE Transactions on Neural Networks*, vol. 21, no. 1, pp. 169–175, 2010.

[7] H. R. Karimi and H. Gao, "Mixed H_2/H_∞ output-feedback control of second-order neutral systems with time-varying state and input delays," *ISA Transactions*, vol. 47, no. 3, pp. 311–324, 2008.

[8] H. R. Karimi, "Optimal vibration control of vehicle engine-body system using Haar functions," *International Journal of Control, Automation and Systems*, vol. 4, no. 6, pp. 714–724, 2006.

[9] M. J. Wang and M. F. Yang, "Application of signed distances method to integrate linear programming for fuzzy multi-objective project management," *International Journal of Innovative Computing, Information and Control*, vol. 7, no. 1, pp. 237–252, 2011.

[10] H. Li, H. Liu, H. Gao, and P. Shi, "Reliable fuzzy control for active suspension systems with actuator delay and fault," *IEEE Transactions on Fuzzy Systems*, vol. 20, no. 2, pp. 342–357, 2012.

[11] H. Li, B. Chen, Q. Zhou, and W. Qian, "Robust stability for uncertain delayed fuzzy Hopfield neural networks with Markovian jumping parameters," *IEEE Transactions on Systems, Man, and Cybernetics, Part B*, vol. 39, no. 1, pp. 94–102, 2009.

[12] T. Niknam, H. D. Mojarrad, and M. Nayeripour, "A new hybrid fuzzy adaptive particle swarm optimization for non-convex economic dispatch," *International Journal of Innovative Computing, Information and Control*, vol. 7, no. 1, pp. 189–202, 2011.

[13] F. Li and X. Zhang, "Delay-range-dependent robust H_∞ filtering for singular LPV systems with variant delay," *International Journal of Innovative Computing, Information and Control*, vol. 9, no. 1, pp. 339–353, 2013.

[14] T.-C. Lin, S.-W. Chang, and C.-H. Hsu, "Robust adaptive fuzzy sliding mode control for a class of uncertain discrete-time nonlinear systems," *International Journal of Innovative Computing, Information and Control*, vol. 8, no. 1 A, pp. 347–359, 2012.

[15] H. Gao and C. Wang, "A delay-dependent approach to robust H_∞ filtering for uncertain discrete-time state-delayed systems," *IEEE Transactions on Signal Processing*, vol. 52, no. 6, pp. 1631–1640, 2004.

[16] H. Gao and T. Chen, "New results on stability of discrete-time systems with time-varying state delay," *IEEE Transactions on Automatic Control*, vol. 52, no. 2, pp. 328–334, 2007.

[17] X. Meng, J. Lam, B. Du, and H. Gao, "A delay-partitioning approach to the stability analysis of discrete-time systems," *Automatica*, vol. 46, no. 3, pp. 610–614, 2010.

[18] X. Su, P. Shi, L. Wu, and Y. D. Song, "A novel control design on discrete-time takagisugeno fuzzy systems with time-varying delays," *IEEE Transactions on Fuzzy Systems*, no. 99, p. 9, 2012.

[19] Y.-P. Huang and K. Zhou, "Robust stability of uncertain time-delay systems," *IEEE Transactions on Automatic Control*, vol. 45, no. 11, pp. 2169–2173, 2000.

[20] C.-Y. Kao and B. Lincoln, "Simple stability criteria for systems with time-varying delays," *Automatica*, vol. 40, no. 8, pp. 1429–1434, 2004.

[21] H. R. Karimi, M. Zapateiro, and N. Luo, "Stability analysis and control synthesis of neutral systems with time-varying delays and nonlinear uncertainties," *Chaos, Solitons & Fractals*, vol. 42, no. 1, pp. 595–603, 2009.

[22] X. M. Zhang and Q. L. Han, "Delay-dependent robust H_∞ filtering for uncertain discrete-time systems with time-varying delay based on a finite sum inequality," *IEEE Transactions on Circuits and Systems II*, vol. 53, no. 12, pp. 1466–1470, 2006.

[23] K. Gu, Y. Zhang, and S. Xu, "Small gain problem in coupled differential-difference equations, time-varying delays, and direct Lyapunov method," *International Journal of Robust and Nonlinear Control*, vol. 21, no. 4, pp. 429–451, 2011.

[24] X. Li and H. Gao, "A new model transformation of discrete-time systems with time-varying delay and its application to stability analysis," *IEEE Transactions on Automatic Control*, vol. 56, no. 9, pp. 2172–2178, 2011.

[25] L. Wu, X. Su, P. Shi, and J. Qiu, "Model approximation for discrete-time state-delay systems in the T-S fuzzy framework," *IEEE Transactions on Fuzzy Systems*, vol. 19, no. 2, pp. 366–378, 2011.

[26] L. Wu, X. Su, P. Shi, and J. Qiu, "A new approach to stability analysis and stabilization of discrete-time T-S fuzzy time-varying delay systems," *IEEE Transactions on Systems, Man, and Cybernetics, Part B*, vol. 41, no. 1, pp. 273–286, 2011.

[27] W. H. Ho, S. H. Chen, I. T. Chen, J. H. Chou, and C. C. Shu, "Design of stable and quadraticoptimal static output feedback controllers for TS-fuzzy-model-based control systems: an integrative computational approach," *International Journal of Innovative Computing, Information and Control*, vol. 20, no. 6, pp. 403–418, 2012.

[28] L. Wu and Z. Wang, "Fuzzy filtering of nonlinear fuzzy stochastic systems with time-varying delay," *Signal Processing*, vol. 89, no. 9, pp. 1739–1753, 2009.

[29] D. Zhang, H. Wang, B. Lu, and Z. Wang, "LMI-based fault detection fuzzy observer design with multiple performance constraints for a class of non-linear systems: comparative study," *International Journal of Innovative Computing, Information and Control*, vol. 8, no. 1, pp. 633–645, 2012.

[30] X. Su, L. Wu, and P. Shi, "H_∞ model reduction of Takagi-Sugeno fuzzy stochastic systems," *IEEE Transactions on Systems, Man, and Cybernetics, Part B*, vol. 42, no. 6, pp. 1574–1585, 2012.

[31] W. Yang and M. Liu, "H_∞ filtering for nonlinear stochastic systems with sensor saturation, quantization and random packet losses," *Signal Processing*, vol. 92, no. 6, pp. 1387–1396, 2012.

[32] S. Xu, J. Lam, and T. Chen, "Robust H_∞ control for uncertain discrete stochastic time-delay systems," *Systems & Control Letters*, vol. 51, no. 3-4, pp. 203–215, 2004.

[33] P. Seiler and R. Sengupta, "An H_∞ approach to networked control," *IEEE Transactions on Automatic Control*, vol. 50, no. 3, pp. 356–364, 2005.

[34] S. Sastry, *Nonlinear Systems*, vol. 10 of *Interdisciplinary Applied Mathematics*, Springer, New York, NY, USA, 1999.

[35] B. Zhang, S. Xu, and Y. Zou, "Improved stability criterion and its applications in delayed controller design for discrete-time systems," *Automatica*, vol. 44, no. 11, pp. 2963–2967, 2008.

[36] Y. He, G. P. Liu, D. Rees, and M. Wu, "H_∞ filtering for discrete-time systems with time-varying delay," *Signal Processing*, vol. 89, no. 3, pp. 275–282, 2009.

Hindawi Publishing Corporation
Mathematical Problems in Engineering
Volume 2013, Article ID 215201, 12 pages
http://dx.doi.org/10.1155/2013/215201

Research Article

Observer-Based Robust Adaptive Fuzzy Control for MIMO Nonlinear Uncertain Systems with Delayed Output

Chiang Cheng Chiang

Department of Electrical Engineering, Tatung University, 40 Chung-Shan North Road, Sec. 3, Taipei, Taiwan

Correspondence should be addressed to Chiang Cheng Chiang; ccchiang@ttu.edu.tw

Received 29 October 2012; Revised 20 January 2013; Accepted 22 January 2013

Academic Editor: Peng Shi

Copyright © 2013 Chiang Cheng Chiang. This is an open access article distributed under the Creative Commons Attribution License, which permits unrestricted use, distribution, and reproduction in any medium, provided the original work is properly cited.

An observer-based robust adaptive fuzzy control scheme is presented to tackle the problem of the robust stability and the tracking control for a class of multiinput multioutput (MIMO) nonlinear uncertain systems with delayed output. Because the nonlinear system functions and the uncertainties of the controlled system including structural uncertainties are supposed to be unknown, fuzzy logic systems are utilized to approximate these nonlinear system functions and the upper bounded functions of the uncertainties. Moreover, the upper bound of uncertainties caused by these fuzzy modeling errors is also estimated. In addition, the state observer based on state variable filters is designed to estimate all states which are not available for measurement in the controlled system. By constructing an appropriate Lyapunov function and using strictly positive-real (SPR) stability theorem, the proposed robust adaptive fuzzy controller not only guarantees the robust stability of a class of multivariable nonlinear uncertain systems with delayed output but also maintains a good tracking performance. Finally, some simulation results are illustrated to verify the effectiveness of the proposed control approach.

1. Introduction

Controller design for nonlinear systems has been given a lot of attention in the control community during the last two decades. Recently, the methods of feedback linearization have been successfully applied in the development of controllers for a class of nonlinear systems [1, 2]. However, the above techniques can be only applied to nonlinear systems whose dynamics are exactly known. Actually, it is difficult to obtain the exact construction of the systems in most of industrial and engineering systems because of the complexity of systems. In addition, the existence of uncertainties such as parameter uncertainties, modeling errors, and external disturbances may lead to poor performance and instability [3–8]. Hence, the study of robust stability of nonlinear uncertain systems in the presence of uncertainties is an important topic for the control design engineer.

Recently, fuzzy control technique has been considered extensively in the control problems of complex and ill-defined nonlinear systems in the presence of incomplete knowledge of the plant [3, 9–15]. However, the above adaptive fuzzy controllers are only limited to the systems under the conservative assumption that system states are available for measurement. In order to relax this restriction, an observer-based fuzzy adaptive output feedback control for the SISO nonlinear systems is presented to tackle the nonlinear systems whose states are not available [16–23]. So far, few research results have been extended to MIMO nonlinear systems [24, 25]. The common feature of most previous results [16, 19, 24, 25] is the assumption that the controlled systems are free of uncertainties. Although the above restrictive assumption can be relaxed in [17, 18, 20–23], the uncertainties are assumed to be a bounded external disturbance. Therefore, the motivation of this paper is to synthesize an observer-based robust adaptive fuzzy control scheme to deal with the tracking control problem for a class of MIMO nonlinear uncertain systems with delayed output in the presence of uncertainties including the structural uncertainty.

On the other hand, the design problem of nonlinear time-delay systems has received considerable attention in [26–31] because time-delay characteristic often encountered in

various engineering systems may not only cause instability but also lead to serious deterioration in the performance of the plants. By employing the input-output approach and the scaled small gain theorem, the filtering problem for discrete-time T-S fuzzy systems with time-varying delay has been studied [26]. The robust H_∞ control problem for stochastic systems with a delay in the state is investigated in [28], and the results are further extended to the stochastic time-delay systems with parameter uncertainties. The problems of stability analysis and robust control for uncertain systems with input delay were examined in [29, 31]. In [27], the design scheme of output feedback controller for a class of SISO nonlinear systems with delayed output was proposed to construct a delay-dependent controller making the closed-loop system globally asymptotically stable. In [30], a new approach for the construction of a state observer for SISO nonlinear systems with delayed output was presented to ensure the global exponential convergence to zero of the observation error. It should be pointed out that the uncertainty was not taken into account in [27, 30]. Therefore, the robust control problem of MIMO nonlinear systems with delayed output in the presence of uncertainties will be considered in this paper.

In this paper, the problem of controller design for a class of MIMO nonlinear uncertain output-delay systems whose states are not available is considered. The main features of the proposed observer-based robust adaptive fuzzy controller are summarized as follows. (i) Fuzzy logic systems with some appropriate learning laws are applied to approximate the nonlinear system functions and the upper bounded functions of the uncertainties including the structural uncertainty. (ii) The unknown upper bound of the uncertainties caused by approximation (or fuzzy modeling) error is estimated by a simple adaptive law. (iii) The state observer based on state variable filters is designed to estimate all states which are not available for measurement in the controlled system. (iv) By constructing an appropriate Lyapunov function and using strictly positive-real (SPR) stability theorem, the proposed robust adaptive fuzzy output feedback controller can not only guarantee the robust stability of the whole closed-loop system but also obtain the good tracking performance.

This paper is organized as follows: the description of the system and the concept of fuzzy logic systems are given together in Section 2. Section 3 proposes an observer-based robust adaptive fuzzy output feedback controller to achieve the purpose of asymptotic stabilization and output tracking performance of the whole closed-loop MIMO nonlinear uncertain systems with delayed output. In Section 4, a series of simulation results are illustrated to show the effectiveness of the proposed control scheme. Finally, a conclusion is given in Section 5.

2. Problem Formulation and Preliminaries

2.1. Problem Formulation. Consider a class of MIMO nonlinear uncertain systems with delayed output in the following form:

$$\begin{gathered}
\dot{x}_{11}(t) = x_{12}(t), \\
\dot{x}_{12}(t) = x_{13}(t), \\
\vdots \\
\dot{x}_{1(n_1-1)}(t) = x_{1n_1}(t), \\
\dot{x}_{1n_1}(t) = f_1(\mathbf{x}(t)) + \sum_{j=1}^{p} g_{1j}(\mathbf{x}(t))\, u_j(t) + \Delta\phi_1(\mathbf{x}(t)), \\
\vdots \\
\dot{x}_{p1}(t) = x_{p2}(t), \\
\dot{x}_{p2}(t) = x_{p3}(t), \\
\vdots \\
\dot{x}_{p(n_p-1)}(t) = x_{pn_p}(t), \\
\dot{x}_{pn_p}(t) = f_p(\mathbf{x}(t)) + \sum_{j=1}^{P} g_{pj}(\mathbf{x}(t))\, u_j(t) + \Delta\phi_p(\mathbf{x}(t)), \\
y_1(t) = x_{11}(t-\tau), \\
\vdots \\
y_p(t) = x_{p1}(t-\tau),
\end{gathered} \tag{1}$$

or equivalently

$$\begin{gathered}
\dot{\mathbf{x}}(t) = \mathbf{A}\mathbf{x}(t) + \mathbf{B}\left[\mathbf{F}(\mathbf{x}(t)) + \mathbf{G}(\mathbf{x}(t))\,\mathbf{u}(t) + \Delta\mathbf{\Phi}(\mathbf{x}(t))\right], \\
\mathbf{y}(t) = \mathbf{C}\mathbf{x}(t-\tau),
\end{gathered} \tag{2}$$

where

$$\begin{gathered}
\mathbf{F}(\mathbf{x}) = \left[f_1(\mathbf{x}), \ldots, f_p(\mathbf{x})\right]^T \in R^p, \\
\mathbf{G}(\mathbf{x}) = \left[\mathbf{G}_1(\mathbf{x}), \ldots, \mathbf{G}_p(\mathbf{x})\right] \in R^{p\times p}, \\
\mathbf{G}_i(\mathbf{x}) = \left[g_{1i}(\mathbf{x}), \ldots, g_{pi}(\mathbf{x})\right]^T \in R^p, \quad i = 1, 2, \ldots, p, \\
\mathbf{A} = \operatorname{diag}\left[\mathbf{A}_1, \ldots, \mathbf{A}_p\right] \in R^{n\times n}, \\
\mathbf{B} = \operatorname{diag}\left[\mathbf{B}_1, \ldots, \mathbf{B}_p\right] \in R^{n\times p}, \\
\mathbf{C} = \operatorname{diag}\left[\mathbf{C}_1, \ldots, \mathbf{C}_p\right] \in R^{p\times n},
\end{gathered}$$

$$\mathbf{A}_i = \begin{bmatrix} 0 & 1 & 0 & \cdots & 0 \\ 0 & 0 & 1 & \cdots & 0 \\ \vdots & \vdots & \vdots & \cdots & 1 \\ 0 & 0 & 0 & \cdots & 0 \end{bmatrix} \in R^{n_i \times n_i},$$

$$\mathbf{B}_i = \begin{bmatrix} 0 \\ 0 \\ \vdots \\ 1 \end{bmatrix} \in R^{n_i}, \qquad \mathbf{C}_i^T = \begin{bmatrix} 1 \\ 0 \\ \vdots \\ 0 \end{bmatrix} \in R^{n_i}, \tag{3}$$

where $\mathbf{x} = [x_{11}, x_{12}, \ldots, x_{1n_1}, \ldots, x_{p1}, x_{p2}, \ldots, x_{pn_p}]^T \in R^n$ is the system state vector which is assumed to be unavailable for measurement, $\mathbf{u} = [u_1, \ldots, u_p]^T \in R^p$ is the control input, $\mathbf{y} = [y_1, \ldots, y_p]^T \in R^p$ is the output vector, $n_1 + n_2 + \cdots + n_p = n$, $\tau > 0$ is a known time delay of the system, $f_i(\mathbf{x}(t))$ and $g_{ij}(\mathbf{x}(t))$ are the unknown nonlinear system functions, and $\Delta\mathbf{\Phi}(\mathbf{x}(t)) = [\Delta\phi_1(\mathbf{x}(t), \Delta\phi_2(\mathbf{x}(t), \ldots, \Delta\phi_p(\mathbf{x}(t)]^T \in R^p$ is the vector of uncertainties.

Now let the output of the system and its derivatives be expressed as follows:

$$\begin{aligned} y_i(t) &= x_{i1}(t-\tau), \\ \dot{y}_i(t) &= \dot{x}_{i1}(t-\tau) = x_{i2}(t-\tau), \\ &\vdots \\ y_i^{(n_i-1)}(t) &= \dot{x}_{i(n_i-1)}(t-\tau) = x_{in_i}(t-\tau), \\ y_i^{(n_i)}(t) &= \dot{x}_{in_i}(t-\tau) \\ &= f_i(\mathbf{x}(t-\tau)) + \sum_{j=1}^{p} g_{ij}(\mathbf{x}(t-\tau))\, u_j(t-\tau) \\ &\quad + \Delta\phi_i(\mathbf{x}(t-\tau)). \end{aligned} \tag{4}$$

Then, let $\mathbf{y}_d = [y_{1d}, \ldots, y_{pd}]^T \in R^p$ be the given bounded output desired signal and contain finite derivatives up to the nth order. The tracking errors of the system can be defined as $e_{ij}(t) = y_i^{(j-1)}(t) - y_{id}^{(j-1)}(t)$, for $i = 1, 2, \ldots, p$ and $j = 1, 2, \ldots, n_i$, and its derivatives can be obtained as

$$\begin{aligned} \dot{e}_{i1}(t) &= \dot{y}_i(t) - \dot{y}_{id}(t) = e_{i2}(t), \\ \dot{e}_{i2}(t) &= y_i^{(2)}(t) - y_{id}^{(2)}(t) = e_{i3}(t), \\ &\vdots \\ \dot{e}_{i(n_i-1)}(t) &= y_i^{(n_i-1)}(t) - y_{id}^{(n_i-1)}(t) = e_{1n_i}(t), \\ \dot{e}_{in_i}(t) &= y_i^{(n_i)}(t) - y_{id}^{(n_i)}(t) \\ &= f_i(\mathbf{x}(t-\tau)) + \sum_{j=1}^{p} g_{ij}(\mathbf{x}(t-\tau))\, u_j(t-\tau) \\ &\quad + \Delta\phi_i(\mathbf{x}(t-\tau)) - y_{id}^{(n_i)}(t) \\ &= f_i(\mathbf{x}(t-\tau)) + \sum_{j=1}^{p} g_{ij}(\mathbf{x}(t-\tau))\, u_j(t) \\ &\quad - y_{id}^{(n_i)}(t) + \Delta\psi_i(\mathbf{x}, \mathbf{u}), \end{aligned} \tag{5}$$

where the uncertainty $\Delta\psi_i(\mathbf{x}, \mathbf{u})$ including the structural uncertainty is defined as

$$\begin{aligned} \Delta\psi_i(\mathbf{x}, \mathbf{u}) &= \sum_{j=1}^{p} g_{ij}(\mathbf{x}(t-\tau)) \left[u_j(t-\tau) - u_j(t)\right] \\ &\quad + \Delta\phi_i(\mathbf{x}(t-\tau)). \end{aligned} \tag{6}$$

Thus, (5) can be expressed as

$$\begin{aligned} \dot{\mathbf{e}}_i(t) = \mathbf{A}_i\mathbf{e}_i(t) + \mathbf{B}_i \Bigg[& f_i(\mathbf{x}(t-\tau)) + \sum_{j=1}^{p} g_{ij}(\mathbf{x}(t-\tau))\, u_j(t) \\ & - y_{id}^{(n_i)}(t) + \Delta\psi_i(\mathbf{x}, \mathbf{u}) \Bigg]. \end{aligned} \tag{7}$$

From (7), it is easy to verify that the tracking error dynamics of the system (2) can be represented in the following form:

$$\begin{aligned} \dot{\mathbf{e}}(t) = \mathbf{A}\mathbf{e}(t) + \mathbf{B}\Big[& \mathbf{F}(\mathbf{x}(t-\tau)) + \mathbf{G}(\mathbf{x}(t-\tau))\, \mathbf{u}(t) \\ & - \underline{\mathbf{Y}_d}(t) + \Delta\mathbf{\Psi}(\mathbf{x}, \mathbf{u}) \Big]. \end{aligned} \tag{8}$$

$$\underline{\mathbf{e}_1}(t) = \mathbf{C}\mathbf{e}(t),$$

where

$$\begin{aligned} \mathbf{e} &= \left[\mathbf{e}_1^T, \mathbf{e}_2^T, \ldots, \mathbf{e}_p^T\right]^T \\ &= \left[e_{11}, \ldots, e_{1n_1}, \ldots, e_{p1}, \ldots, e_{pn_p}\right]^T \in R^n, \\ \underline{\mathbf{e}_1} &= \left[e_{11}, e_{21}, \ldots, e_{p1}\right]^T \in R^p, \\ \Delta\mathbf{\Psi} &= \left[\Delta\psi_1, \Delta\psi_2, \ldots, \Delta\psi_p\right]^T \in R^p, \\ \mathbf{e}_i &= \left[e_{i1}, e_{i2}, \ldots, e_{in_i}\right]^T \in R^{n_i}, \\ \underline{\mathbf{Y}_d} &= \left[y_{1d}^{(n_1)}, y_{2d}^{(n_2)}, \ldots, y_{pd}^{(n_p)}\right]^T \in R^p, \\ \mathbf{Y}_d &= \left[y_{1d}, \ldots, y_{1d}^{(n_1-1)}, \ldots, y_{pd}, \ldots, y_{pd}^{(n_p-1)}\right]^T \in R^n. \end{aligned} \tag{9}$$

Based on the above discussion, the following assumptions should be made for the controller design.

Assumption 1. The matrix $\mathbf{G}(\mathbf{x})$ is nonsingular (i.e., $\mathbf{G}(\mathbf{x})^{-1}$ exists) for all $\mathbf{x} \in U_x$ where U_x is a compact set in R^n.

Assumption 2. $\|\Delta\boldsymbol{\Psi}(\mathbf{x},\mathbf{u})\| \le h_1(\mathbf{x})+h_2(\mathbf{x}(t-\tau))$, where $h_1(\mathbf{x})$ and $h_2(\mathbf{x}(t-\tau))$ are the unknown positive smooth continuous functions.

Remark 3. Compared with the previous results [27, 30], the uncertainties including the structural uncertainty are taken into account in this paper. In addition, the uncertainties considered in this paper are not supposed to be a bounded external disturbance unlike the previous results [17, 18, 20–23].

The control objective of this paper is to design a control law $\mathbf{u}(t)$ such that $\mathbf{y}(t)$ can follow a given desired reference signal $\mathbf{y}_m(t)$ and guarantee that all the signals involved in the whole closed-loop system are bounded.

2.2. Description of Fuzzy Logic Systems. The basic configuration of the fuzzy logic system consists of four main components: fuzzy rule base, fuzzy inference engine, fuzzifier and defuzzifier [12, 16]. The fuzzy logic system performs a mapping from $U \subset R^n$ to $V \subset R$. Let $U = U_1 \times \cdots \times U_n$ where $U_i \subset R$, $i = 1, 2, \ldots, n$. The fuzzifier maps a crisp point in U into a fuzzy set in U. The fuzzy rule base consists of a collection of fuzzy IF-THEN rules:

$$\begin{aligned} R^{(l)} &: \text{IF } x_1 \text{ is } F_1^l, \text{ and } x_2 \text{ is } F_2^l, \ldots, x_n \text{ is } F_n^l \\ &\quad \text{THEN } y_j \text{ is } G_j^l, \quad j = 1, \ldots, p, \; l = 1, \ldots, N, \end{aligned} \tag{10}$$

in which $\mathbf{x} = [x_1, x_2, \ldots, x_n]^T \in U$ and $y \in V \subset R$ are the input and output of the fuzzy logic system, F_i^l and G_j^l are fuzzy sets in U_i and V_j, respectively. N is the number of rules. The fuzzy inference engine performs a mapping from fuzzy sets in U to fuzzy sets in V, based upon the fuzzy IF-THEN rules in the fuzzy rule base and the compositional rule of inference. The defuzzifier maps a fuzzy set in V to a crisp point in V. Through singleton fuzzification, center average defuzzification, and product inference, the output of the fuzzy logic system can be expressed as

$$y_j = \theta_j^T \xi(x), \quad j = 1, \ldots, p, \tag{11}$$

where $\theta_j^T = [\theta_j^1, \ldots, \theta_j^N]$ with each variable θ_j^l as the point at which the fuzzy membership function of G_j^l achieves the maximum value, and $\xi(x) = [\xi_1(x), \ldots, \xi_N(x)]^T$ with each variable ξ_l as the fuzzy basis function defined as

$$\xi_l(x) = \frac{\prod_{i=1}^n \mu_{F_i^l}(x_i)}{\sum_{l=1}^N \left(\prod_{i=1}^n \mu_{F_i^l}(x_i)\right)}, \tag{12}$$

where $\mu_{F_i^l}(x_i)$ is the membership function of the fuzzy set.

Now let MIMO fuzzy logic systems be expressed as follows:

$$\mathbf{y} = \boldsymbol{\Phi}(\mathbf{x})\boldsymbol{\theta}, \tag{13}$$

where

$$\begin{gathered} \boldsymbol{\theta}^T = \left[\theta_1{}^T, \ldots, \theta_p{}^T\right], \\ \theta_i^T = \left[\theta_i^1, \ldots, \theta_i^N\right] \quad \text{for } i = 1, 2, \ldots, p, \\ \boldsymbol{\Phi}(\mathbf{x}) = \operatorname{diag}\left[\xi^T(\mathbf{x}), \ldots, \xi^T(\mathbf{x})\right]. \end{gathered} \tag{14}$$

3. Observer-Based Robust Adaptive Fuzzy Controller Design and Stability Analysis

According to the description of the fuzzy logic systems presented in Section 2.2, we can construct the following fuzzy logic systems, over a compact set $\Omega_{\mathbf{x}}$, to approximate the unknown nonlinear functions $f_i(\mathbf{x}(t))$ and $g_{ij}(\mathbf{x}(t))$ and the unknown upper bounded functions $h_1(\mathbf{x})$, $h_2(\mathbf{x}(t-\tau))$ as follows:

$$\begin{gathered} \widehat{f}_i\left(\mathbf{x} \mid \theta_{f_1}\right) = \theta_{f_i}^T \xi(\mathbf{x}), \quad i = 1, \ldots, p, \\ \widehat{g}_{ij}\left(\mathbf{x} \mid \theta_{g_{ij}}\right) = \theta_{g_{ij}}^T \xi(\mathbf{x}), \quad i, j = 1, \ldots, p, \\ \widehat{h}_1(\mathbf{x}) = \theta_{h_1}^T \xi(\mathbf{x}), \\ \widehat{h}_2(\mathbf{x}(t-\tau)) = \theta_{h_2}^T \xi(\mathbf{x}(t-\tau)). \end{gathered} \tag{15}$$

Based on the above statements, it can be easily shown that

$$\begin{aligned} \widehat{\mathbf{F}}(\mathbf{x} \mid \boldsymbol{\theta}_1) &= \left[\widehat{f}_1\left(\mathbf{x} \mid \theta_{f_1}\right), \ldots, \widehat{f}_p\left(\mathbf{x} \mid \theta_{f_p}\right)\right]^T = \boldsymbol{\Phi}(\mathbf{x})\boldsymbol{\theta}_1, \\ \widehat{\mathbf{G}}(\mathbf{x} \mid \boldsymbol{\theta}_2) &= \begin{bmatrix} \widehat{g}_{11}\left(\mathbf{x} \mid \theta_{g_{11}}\right), & \ldots, & \widehat{g}_{1p}\left(\mathbf{x} \mid \theta_{g_{1p}}\right) \\ \vdots & \ddots & \vdots \\ \widehat{g}_{p1}\left(\mathbf{x} \mid \theta_{g_{p1}}\right), & \ldots, & \widehat{g}_{pp}\left(\mathbf{x} \mid \theta_{g_{pp}}\right) \end{bmatrix} \\ &= \boldsymbol{\Phi}(\mathbf{x})\boldsymbol{\theta}_2, \end{aligned} \tag{16}$$

where

$$\begin{gathered} \boldsymbol{\theta}_1^T = \left[\theta_{f1}^T, \ldots, \theta_{fp}^T\right], \qquad \theta_{fi}^T = \left[\theta_{fi}^1, \ldots, \theta_{fi}^N\right], \\ \boldsymbol{\theta}_2 = \begin{bmatrix} \theta_{g_{11}}, \ldots, \theta_{g_{1p}} \\ \vdots \quad \ddots \quad \vdots \\ \theta_{g_{p1}}, \ldots, \theta_{g_{pp}} \end{bmatrix}, \qquad \theta_{g_{ij}}^T = \left[\theta_{g_{ij}}^1, \ldots, \theta_{g_{ij}}^N\right], \\ \theta_{h_1}^T = \left[\theta_{h_1}^1, \ldots, \theta_{h_1}^N\right], \qquad \theta_{h_2}^T = \left[\theta_{h_2}^1, \ldots, \theta_{h_2}^N\right], \\ \boldsymbol{\Phi}(\mathbf{x}) = \operatorname{diag}\left[\xi^T(\mathbf{x}), \ldots, \xi^T(\mathbf{x})\right]. \end{gathered} \tag{17}$$

Suppose the state variables of the controlled system (1) are available for measurement, then the following robust adaptive fuzzy controller $\mathbf{u}(t)$ can be adopted to let the system achieve the above control objective and can be defined as follows:

$$\begin{aligned} \mathbf{u}(t) = \widehat{\mathbf{G}}(\mathbf{x}(t-\tau))^{-1} &\left[-\widehat{\mathbf{F}}(\mathbf{x}(t-\tau)) - \mathbf{K}_c\mathbf{e}(t)\right. \\ &\left. + \underline{\mathbf{Y}_d}(t) + \mathbf{u}_s(t)\right], \end{aligned} \tag{18}$$

where $\mathbf{K}_c = \mathrm{diag}[\mathbf{K}_{c1}, \ldots, \mathbf{K}_{cp}] \in R^{p\times n}$, where $\mathbf{K}_{ci} = [k_{i1}^c, \ldots, k_{in_i}^c] \in R^{1\times n_i}$ for $i = 1, 2, \ldots, p$, is the control gain matrix such that the characteristic polynomial of $\mathbf{A} - \mathbf{B}\mathbf{K}_c$ is Hurwitz. The robust compensator $\mathbf{u}_s(t)$ will be designed to compensate the fuzzy approximation errors and the uncertainties.

However, the state variables of the system are unavailable for measurement in many engineering systems. In addition, although the tracking error vector $\mathbf{e}$ can be obtained ideally by successive differentiation of e_{i1} $(i = 1, 2, \ldots, p)$, ideal differentiators are physically unrealizable. Obviously, we must employ a state observer to estimate $\mathbf{x}$ and $\mathbf{e}$ and let $\hat{\mathbf{x}}$ and $\hat{\mathbf{e}}$ be the estimates of $\mathbf{x}$ and $\mathbf{e}$, respectively. Then replacing $\hat{\mathbf{F}}(\mathbf{x} \mid \boldsymbol{\theta}_1)$, $\hat{\mathbf{G}}(\mathbf{x} \mid \boldsymbol{\theta}_2)$, $\hat{h}_1(\mathbf{x} \mid \boldsymbol{\theta}_h)$, $\hat{h}_2(\mathbf{x}(t-\tau))$, $\mathbf{x}$, and $\mathbf{e}$ by $\hat{\mathbf{F}}(\hat{\mathbf{x}} \mid \boldsymbol{\theta}_1)$, $\hat{\mathbf{G}}(\hat{\mathbf{x}} \mid \boldsymbol{\theta}_2)$, $\hat{h}_1(\hat{\mathbf{x}} \mid \boldsymbol{\theta}_h)$, $\hat{h}_2(\hat{\mathbf{x}}(t-\tau))$, $\hat{\mathbf{x}}$, and $\hat{\mathbf{e}}$, respectively, the robust adaptive fuzzy controller (18) cannot be used to control the nonlinear system (2) and will be modified as the following form:

$$\begin{aligned}\mathbf{u}(t) = \hat{\mathbf{G}}(\hat{\mathbf{x}}(t-\tau))^{-1}\big[&-\hat{\mathbf{F}}(\hat{\mathbf{x}}(t-\tau)) - \mathbf{K}_c\hat{\mathbf{e}}(t)\\ &+\underline{\mathbf{Y}_d}(t) + \mathbf{u}_s(t)\big],\end{aligned} \tag{19}$$

where

$$\hat{\mathbf{F}}(\hat{\mathbf{x}} \mid \boldsymbol{\theta}_1) = \left[\hat{f}_1\left(\hat{\mathbf{x}} \mid \theta_{f_1}\right), \ldots, \hat{f}_p\left(\hat{\mathbf{x}} \mid \theta_{f_p}\right)\right]^T = \boldsymbol{\Phi}(\hat{\mathbf{x}})\boldsymbol{\theta}_1, \tag{20}$$

$$\begin{aligned}\hat{\mathbf{G}}(\hat{\mathbf{x}} \mid \boldsymbol{\theta}_2) &= \begin{bmatrix} \hat{g}_{11}\left(\hat{\mathbf{x}} \mid \theta_{g_{11}}\right), & \ldots, & \hat{g}_{1p}\left(\hat{\mathbf{x}} \mid \theta_{g_{1p}}\right)\\ \vdots & \ddots & \vdots\\ \hat{g}_{p1}\left(\hat{\mathbf{x}} \mid \theta_{g_{p1}}\right), & \ldots, & \hat{g}_{pp}\left(\hat{\mathbf{x}} \mid \theta_{g_{pp}}\right)\end{bmatrix}\\ &= \boldsymbol{\Phi}(\hat{\mathbf{x}})\boldsymbol{\theta}_2,\end{aligned} \tag{21}$$

$$\hat{h}_1(\hat{\mathbf{x}}) = \theta_{h_1}^T\xi(\hat{\mathbf{x}}); \qquad \hat{h}_2(\hat{\mathbf{x}}(t-\tau)) = \theta_{h_2}^T\xi(\hat{\mathbf{x}}(t-\tau)). \tag{22}$$

Substituting (19) into (8) yields

$$\begin{aligned}\dot{\mathbf{e}}(t) = {}& \mathbf{A}\mathbf{e}(t) - \mathbf{B}\mathbf{K}_c\hat{\mathbf{e}}(t)\\ &+ \mathbf{B}\Big\{\mathbf{F}(\mathbf{x}(t-\tau)) - \hat{\mathbf{F}}(\hat{\mathbf{x}}(t-\tau) \mid \boldsymbol{\theta}_1)\\ &\quad + \left[\mathbf{G}(\mathbf{x}(t-\tau)) - \hat{\mathbf{G}}(\hat{\mathbf{x}}(t-\tau) \mid \boldsymbol{\theta}_2)\right]\mathbf{u}(t)\\ &\quad + \mathbf{u}_s(t) + \Delta\boldsymbol{\Psi}(\mathbf{x}, \mathbf{u})\Big\},\\ &\underline{\mathbf{e}_1}(t) = \mathbf{C}\mathbf{e}(t).\end{aligned} \tag{23}$$

In order to estimate the output tracking error vector, we design the observer as follows:

$$\begin{aligned}\dot{\hat{\mathbf{e}}}(t) &= (\mathbf{A} - \mathbf{B}\mathbf{K}_c)\hat{\mathbf{e}}(t) + \mathbf{K}_o\left(\underline{\mathbf{e}_1}(t) - \underline{\hat{\mathbf{e}}_1}(t)\right),\\ \underline{\hat{\mathbf{e}}_1}(t) &= \mathbf{C}\hat{\mathbf{e}}(t),\end{aligned} \tag{24}$$

where $\mathbf{K}_o = \mathrm{diag}[\mathbf{K}_{o1}, \ldots, \mathbf{K}_{op}] \in R^{n\times p}$, where $\mathbf{K}_{oi} = [k_{1i}^o, \ldots, k_{n_i i}^o]^T$ for $i = 1, 2, \ldots, p$, is the observer gain matrix such that the characteristic polynomial of $\mathbf{A} - \mathbf{K}_o\mathbf{C}$ is Hurwitz. Let us define the observation error vector as

$$\tilde{\mathbf{e}}(t) = \mathbf{e}(t) - \hat{\mathbf{e}}(t). \tag{25}$$

Then by (23) and (24), we obtain

$$\begin{aligned}\dot{\tilde{\mathbf{e}}}(t) = {}& (\mathbf{A} - \mathbf{K}_o\mathbf{C})\tilde{\mathbf{e}}(t)\\ &+ \mathbf{B}\Big\{\mathbf{F}(\mathbf{x}(t-\tau)) - \hat{\mathbf{F}}(\hat{\mathbf{x}}(t-\tau) \mid \boldsymbol{\theta}_1)\\ &\quad + \left[\mathbf{G}(\mathbf{x}(t-\tau)) - \hat{\mathbf{G}}(\hat{\mathbf{x}}(t-\tau) \mid \boldsymbol{\theta}_2)\right]\mathbf{u}(t)\\ &\quad + \mathbf{u}_s(t) + \Delta\boldsymbol{\Psi}(\mathbf{x}, \mathbf{u})\Big\},\\ &\underline{\tilde{\mathbf{e}}_1}(t) = \mathbf{C}\tilde{\mathbf{e}}(t).\end{aligned} \tag{26}$$

It is assumed that $\boldsymbol{\theta}_1, \boldsymbol{\theta}_2, \theta_{h_1}$, and θ_{h_2} belong to compact sets $\Omega_{\boldsymbol{\theta}_1}$, $\Omega_{\boldsymbol{\theta}_2}$, $\Omega_{\theta_{h_1}}$, and $\Omega_{\theta_{h_2}}$, respectively, which are defined as

$$\begin{aligned}\Omega_{\boldsymbol{\theta}_1} &= \left\{\boldsymbol{\theta}_1 \in R^{N\times p} : \|\boldsymbol{\theta}_1\| \le M_{\boldsymbol{\theta}_1} < \infty\right\},\\ \Omega_{\boldsymbol{\theta}_2} &= \left\{\boldsymbol{\theta}_2 \in R^{pN\times p} : \|\boldsymbol{\theta}_2\| \le M_{\boldsymbol{\theta}_2} < \infty\right\},\\ \Omega_{\theta_{h_1}} &= \left\{\theta_{h_1} \in R^{N} : \|\theta_{h_1}\| \le M_{\theta_{h_1}} < \infty\right\},\\ \Omega_{\theta_{h_2}} &= \left\{\theta_{h_2} \in R^{N} : \|\theta_{h_2}\| \le M_{\theta_{h_2}} < \infty\right\},\end{aligned} \tag{27}$$

where $M_{\boldsymbol{\theta}_1}$, $M_{\boldsymbol{\theta}_2}$, $M_{\theta_{h_1}}$, and $M_{\theta_{h_2}}$ are the designed parameters by the designer, and N is the number of fuzzy inference rules.

Now let us define the optimal parameter vectors $\boldsymbol{\theta}_1^*$, $\boldsymbol{\theta}_2^*$, $\theta_{h_1}^*$, and $\theta_{h_2}^*$ as follows:

$$\begin{aligned}\boldsymbol{\theta}_1^* &= \arg\min_{\boldsymbol{\theta}_1\in\Omega_{\boldsymbol{\theta}_1}}\left\{\sup_{\mathbf{x}\in\Omega_{\mathbf{x}}, \hat{\mathbf{x}}\in\Omega_{\hat{\mathbf{x}}}}\left|\mathbf{F}(\mathbf{x}) - \hat{\mathbf{F}}(\hat{\mathbf{x}} \mid \boldsymbol{\theta}_1)\right|\right\},\\ \boldsymbol{\theta}_2^* &= \arg\min_{\boldsymbol{\theta}_2\in\Omega_{\boldsymbol{\theta}_2}}\left\{\sup_{\mathbf{x}\in\Omega_{\mathbf{x}}, \hat{\mathbf{x}}\in\Omega_{\hat{\mathbf{x}}}}\left|\mathbf{G}(\mathbf{x}) - \hat{\mathbf{G}}(\hat{\mathbf{x}} \mid \boldsymbol{\theta}_2)\right|\right\},\\ \theta_{h_1}^* &= \arg\min_{\boldsymbol{\theta}_{h_1}\in\Omega_{\theta_{h_1}}}\left\{\sup_{\mathbf{x}\in\Omega_{\mathbf{x}}, \hat{\mathbf{x}}\in\Omega_{\hat{\mathbf{x}}}}\left|h_1(\mathbf{x}) - \hat{h}_1(\hat{\mathbf{x}} \mid \theta_{h_1})\right|\right\},\\ \theta_{h_2}^* &= \arg\min_{\boldsymbol{\theta}_{h_2}\in\Omega_{\theta_{h2}}}\left\{\sup_{\mathbf{x}\in\Omega_{\mathbf{x}}, \hat{\mathbf{x}}\in\Omega_{\hat{\mathbf{x}}}}\left|h_2(\mathbf{x}(t-\tau))\right.\right.\\ &\qquad\qquad \left.\left. - \hat{h}_2(\hat{\mathbf{x}}(t-\tau)) \mid \theta_{h_2})\right|\right\},\end{aligned} \tag{28}$$

where $\boldsymbol{\theta}_1^*$, $\boldsymbol{\theta}_2^*$, $\theta_{h_1}^*$, and $\theta_{h_2}^*$ are bounded in the suitable closed sets $\Omega_{\boldsymbol{\theta}_1}$, $\Omega_{\boldsymbol{\theta}_2}$, $\Omega_{\theta_{h_1}}$, and $\Omega_{\theta_{h_2}}$, respectively. Also the parameter estimation errors are defined as

$$\tilde{\boldsymbol{\theta}}_1 = \boldsymbol{\theta}_1^* - \boldsymbol{\theta}_1, \tag{29}$$

$$\tilde{\boldsymbol{\theta}}_2 = \boldsymbol{\theta}_2^* - \boldsymbol{\theta}_2, \tag{30}$$

$$\tilde{\theta}_{h_1} = \theta_{h_1}^* - \theta_{h_1}; \qquad \tilde{\theta}_{h_2} = \theta_{h_2}^* - \theta_{h_2}. \tag{31}$$

Then, the minimum approximation errors which correspond to the optimal parameter vectors are defined as

$$\begin{aligned}\boldsymbol{\omega}_1 &= \mathbf{F}(\mathbf{x}(t-\tau)) - \widehat{\mathbf{F}}(\widehat{\mathbf{x}}(t-\tau) \mid \boldsymbol{\theta}_1^*) \\ &\quad + \left(\mathbf{G}(\mathbf{x}(t-\tau)) - \widehat{\mathbf{G}}(\widehat{\mathbf{x}}(t-\tau) \mid \boldsymbol{\theta}_2^*)\right)\mathbf{u},\end{aligned} \tag{32}$$

$$\begin{aligned}\omega_2 &= h_1(\mathbf{x}) - \widehat{h}_1\left(\widehat{\mathbf{x}} \mid \theta_{h_1}^*\right) \\ &\quad + h_2(\mathbf{x}(t-\tau)) - \widehat{h}_2\left(\widehat{\mathbf{x}}(t-\tau) \mid \theta_{h_2}^*\right).\end{aligned} \tag{33}$$

Applying (29), (30), and (32), (26) can be rewritten as

$$\begin{aligned}\dot{\widetilde{\mathbf{e}}}(t) &= (\mathbf{A} - \mathbf{K}_o\mathbf{C})\widetilde{\mathbf{e}}(t) \\ &\quad + \mathbf{B}\Big\{\boldsymbol{\Phi}(\widehat{\mathbf{x}})\widetilde{\boldsymbol{\theta}}_1 + \boldsymbol{\Phi}(\widehat{\mathbf{x}})\widetilde{\boldsymbol{\theta}}_2\mathbf{u}(t) \\ &\quad + \mathbf{F}(\mathbf{x}(t-\tau)) - \widehat{\mathbf{F}}(\widehat{\mathbf{x}}(t-\tau) \mid \boldsymbol{\theta}_1^*) \\ &\quad + \left[\mathbf{G}(\mathbf{x}(t-\tau)) - \widehat{\mathbf{G}}(\widehat{\mathbf{x}}(t-\tau) \mid \boldsymbol{\theta}_2^*)\right]\mathbf{u}(t) \\ &\quad + \mathbf{u}_s(t) + \Delta\boldsymbol{\Psi}(\mathbf{x},\mathbf{u})\Big\} \\ &= (\mathbf{A} - \mathbf{K}_o\mathbf{C})\widetilde{\mathbf{e}}(t) + \mathbf{B}\Big[\boldsymbol{\Phi}(\widehat{\mathbf{x}})\widetilde{\boldsymbol{\theta}}_1 + \boldsymbol{\Phi}(\widehat{\mathbf{x}})\widetilde{\boldsymbol{\theta}}_2\mathbf{u}(t) \\ &\quad + \boldsymbol{\omega}_1 + \mathbf{u}_s(t) + \Delta\boldsymbol{\Psi}(\mathbf{x},\mathbf{u})\Big], \\ \underline{\widetilde{\mathbf{e}}_1}(t) &= \mathbf{C}\widetilde{\mathbf{e}}(t).\end{aligned} \tag{34}$$

Then, the output error dynamics in (34) can be expressed as follows:

$$\begin{aligned}\underline{\widetilde{\mathbf{e}}_1} &= \mathbf{H}(\mathbf{s})\Big[\boldsymbol{\Phi}(\widehat{\mathbf{x}})\widetilde{\boldsymbol{\theta}}_1 + \boldsymbol{\Phi}(\widehat{\mathbf{x}})\widetilde{\boldsymbol{\theta}}_2\mathbf{u}(t) + \boldsymbol{\omega}_1 + \mathbf{u}_s(t) \\ &\quad + \Delta\boldsymbol{\Psi}(\mathbf{x},\mathbf{u})\Big],\end{aligned} \tag{35}$$

where

$$\mathbf{H}(\mathbf{s}) = \mathbf{C}(\mathbf{s}\mathbf{I} - (\mathbf{A} - \mathbf{K}_o\mathbf{C}))^{-1}\mathbf{B}. \tag{36}$$

Obviously, the transfer function $\mathbf{H}(\mathbf{s})$ is a known stable transfer function matrix. In order to utilize the SPR-Lyapunov design approach, (35) can be represented as

$$\begin{aligned}\underline{\widetilde{\mathbf{e}}_1} &= \mathbf{H}(\mathbf{s})\mathbf{L}(\mathbf{s})\Big[\mathbf{L}(\mathbf{s})^{-1}\boldsymbol{\Phi}(\widehat{\mathbf{x}})\widetilde{\boldsymbol{\theta}}_1 + \mathbf{L}(\mathbf{s})^{-1}\boldsymbol{\Phi}(\widehat{\mathbf{x}})\widetilde{\boldsymbol{\theta}}_2\mathbf{u}(t) \\ &\quad + \mathbf{L}(\mathbf{s})^{-1}\left(\boldsymbol{\omega}_1 + \mathbf{u}_s(t) + \Delta\boldsymbol{\Psi}(\mathbf{x},\mathbf{u})\right)\Big],\end{aligned} \tag{37}$$

with

$$\begin{aligned}\mathbf{L}(s) &= \operatorname{diag}\left[L_i(s), \ldots, L_p(s)\right], \\ L_i(s) &= s^{m_i} + b_{i1}s^{m_i-1} + \cdots + b_{im_i} \\ &\quad (m_i = n_i - 1),\ i = 1, 2, \ldots, p.\end{aligned} \tag{38}$$

It is worth noting that $\mathbf{L}(s)$ is chosen to be a proper stable transfer function matrix and to make $\mathbf{H}(\mathbf{s})\mathbf{L}(\mathbf{s})$ to be a proper SPR transfer function matrix. Then the state-space realization of (37) can be written as

$$\begin{aligned}\dot{\widetilde{\mathbf{e}}}_c(t) &= (\mathbf{A} - \mathbf{K}_o\mathbf{C})\widetilde{\mathbf{e}}_c + \mathbf{B}_c\Big[\boldsymbol{\Phi}_f(\widehat{\mathbf{x}})\widetilde{\boldsymbol{\theta}}_1 + \boldsymbol{\Phi}_f(\widehat{\mathbf{x}})\widetilde{\boldsymbol{\theta}}_2\mathbf{u}(t) \\ &\quad + \boldsymbol{\omega}_{1f} + \mathbf{u}_{sf}(t) + \Delta\boldsymbol{\Psi}_f(\mathbf{x},\mathbf{u})\Big], \\ \underline{\widetilde{\mathbf{e}}_1}(t) &= \mathbf{C}\widetilde{\mathbf{e}}_c(t),\end{aligned} \tag{39}$$

with

$$\mathbf{B}_c = \operatorname{diag}\left[\mathbf{B}_{c1}, \ldots, \mathbf{B}_{cp}\right] \in R^{n\times p}, \tag{40}$$

$$\mathbf{B}_{ci} = \left[1, b_{i1}, b_{i2}, \ldots, b_{im_i}\right]^T \in R^{n_i\times 1}, \quad i = 1, 2, \ldots, p, \tag{41}$$

$$\boldsymbol{\Phi}_f(\widehat{\mathbf{x}}) = \mathbf{L}(\mathbf{s})^{-1}\boldsymbol{\Phi}(\widehat{\mathbf{x}}), \tag{42a}$$

$$\boldsymbol{\omega}_{1f} = \mathbf{L}(\mathbf{s})^{-1}\boldsymbol{\omega}_1, \tag{42b}$$

$$\mathbf{u}_{sf} = \mathbf{L}(\mathbf{s})^{-1}\mathbf{u}_s, \tag{42c}$$

$$\Delta\boldsymbol{\Psi}_f(\mathbf{x},\mathbf{u}) = \mathbf{L}(\mathbf{s})^{-1}\Delta\boldsymbol{\Psi}(\mathbf{x},\mathbf{u}). \tag{42d}$$

We define

$$\begin{aligned}\left\|\boldsymbol{\omega}_{1f}\right\| + \left|\omega_2\right| &\le \omega_f, \\ \widetilde{\omega}_f &= \omega_f - \widehat{\omega}_f,\end{aligned} \tag{43}$$

where $\widehat{\omega}_f$ is the estimate of an unknown positive constant ω_f.

Remark 4. Since $\mathbf{L}(\mathbf{s})$ is chosen as a proper stable transfer function matrix, it is obvious that the norm of $\Delta\boldsymbol{\Psi}_f(\mathbf{x},\mathbf{u})$ also satisfies the inequality in Assumption 2. Moreover, the upper bound functions will be replaced by $\widehat{h}_1(\widehat{\mathbf{x}} \mid \boldsymbol{\theta}_h)$ and $\widehat{h}_2(\widehat{\mathbf{x}}(t-\tau))$ because the state variables are unavailable for measurement.

Based on the Lyapunov stability theorem, we can obtain the robust compensator $\mathbf{u}_{sf}(t)$ as follows:

$$\mathbf{u}_{sf}(t) = \mathbf{u}_1(t) + \mathbf{u}_2(t), \tag{44}$$

where

$$\begin{aligned}\mathbf{u}_1(t) &= -\frac{\mathbf{B}_c^T\mathbf{P}_1\widetilde{\mathbf{e}}_c}{\left\|\widetilde{\mathbf{e}}_c^T\mathbf{P}_1\mathbf{B}_c\right\|} \\ &\quad \times\left[\widehat{\omega}_f + \widehat{h}_1\left(\widehat{\mathbf{x}} \mid \theta_{h_1}\right) + \widehat{h}_2\left(\widehat{\mathbf{x}}(t-\tau) \mid \theta_{h_2}\right)\right], \\ \mathbf{u}_2(t) &= -\frac{\mathbf{B}_c^T\mathbf{P}_1\widetilde{\mathbf{e}}_c}{\left\|\widetilde{\mathbf{e}}_c^T\mathbf{P}_1\mathbf{B}_c\right\|^2}\left[\widetilde{\mathbf{e}}^T\mathbf{P}_2\mathbf{K}_o\underline{\widetilde{\mathbf{e}}_1}\right],\end{aligned} \tag{45}$$

where $\mathbf{K}_c$ is the control gain matrix, $\mathbf{K}_o$ is the observer gain matrix, and $\mathbf{P}_1$ and $\mathbf{P}_2$ are the symmetric positive definite matrices and will be solved later.

Then, the parameter adaptive learning laws are chosen as

$$\dot{\boldsymbol{\theta}}_1 = \gamma_1\boldsymbol{\Phi}_f^T(\widehat{\mathbf{x}})\mathbf{B}_c^T\mathbf{P}_1\widetilde{\mathbf{e}}_c, \tag{46}$$

$$\dot{\boldsymbol{\theta}}_2 = \gamma_2\boldsymbol{\Phi}_f^T(\widehat{\mathbf{x}})\mathbf{B}_c^T\mathbf{P}_1\widetilde{\mathbf{e}}_c\mathbf{u}^T, \tag{47}$$

$$\dot{\theta}_{h_1} = \gamma_3 \left\| \tilde{\mathbf{e}}_c^T \mathbf{P}_1 \mathbf{B}_c \right\| \boldsymbol{\xi}(\hat{\mathbf{x}}), \tag{48a}$$

$$\dot{\theta}_{h_2} = \gamma_4 \left\| \tilde{\mathbf{e}}_c^T \mathbf{P}_1 \mathbf{B}_c \right\| \boldsymbol{\xi}(\hat{\mathbf{x}}(t-\tau)), \tag{48b}$$

$$\dot{\hat{\omega}}_f = \gamma_5 \left\| \tilde{\mathbf{e}}_c^T \mathbf{P}_1 \mathbf{B}_c \right\|, \tag{49}$$

where $\gamma_1 > 0$, $\gamma_2 > 0$, $\gamma_3 > 0$, $\gamma_4 > 0$, and $\gamma_5 > 0$ are the positive adaptive gain constants and can be chosen by the designer.

Remark 5. Without loss of generality, the adaptive laws used in this paper are assumed such that the parameter vectors are within the constraint sets or on the boundaries of the constraint sets but moving toward the inside of the constraint sets. If the parameter vectors are on the boundaries of the constraint sets but moving toward the outside of the constraint sets, we have to use the projection algorithm [12] to modify the adaptive laws such that the parameter vectors will remain inside of the constraint sets. The proposed adaptive laws (46)–(49) can be modified as the following form:

$$\dot{\boldsymbol{\theta}}_1 = \begin{cases} \gamma_1 \boldsymbol{\Phi}_f^T(\hat{\mathbf{x}}) \mathbf{B}_c^T \mathbf{P}_1 \tilde{\mathbf{e}}_c, & \text{if } \left(\|\boldsymbol{\theta}_1\| < M_{\theta_1}\right) \\ & \text{or } \left(\|\boldsymbol{\theta}_1\| = M_{\theta_1}, \right. \\ & \qquad \left. \boldsymbol{\theta}_1^T \boldsymbol{\Phi}_f^T(\hat{\mathbf{x}}) \mathbf{B}_c^T \mathbf{P}_1 \tilde{\mathbf{e}}_c \le 0\right), \\ P\left\{\gamma_1 \boldsymbol{\Phi}_f^T(\hat{\mathbf{x}}) \mathbf{B}_c^T \mathbf{P}_1 \tilde{\mathbf{e}}_c\right\}, & \text{if } \left(\|\boldsymbol{\theta}_1\| = M_{\theta_1}, \right. \\ & \qquad \left. \boldsymbol{\theta}_1^T \boldsymbol{\Phi}_f^T(\hat{\mathbf{x}}) \mathbf{B}_c^T \mathbf{P}_1 \tilde{\mathbf{e}}_c > 0\right), \end{cases} \tag{50}$$

where $P\{\gamma_1 \boldsymbol{\Phi}_f^T(\hat{\mathbf{x}}) \mathbf{B}_c^T \mathbf{P}_1 \tilde{\mathbf{e}}_c\}$ is defined as

$$\begin{aligned} P\left\{\gamma_1 \boldsymbol{\Phi}_f^T(\hat{\mathbf{x}}) \mathbf{B}_c^T \mathbf{P}_1 \tilde{\mathbf{e}}_c\right\} &= \gamma_1 \boldsymbol{\Phi}_f^T(\hat{\mathbf{x}}) \mathbf{B}_c^T \mathbf{P}_1 \tilde{\mathbf{e}}_c \\ &\quad - \gamma_1 \frac{\boldsymbol{\theta}_1 \boldsymbol{\theta}_1^T}{\|\boldsymbol{\theta}_1\|^2} \boldsymbol{\Phi}_f^T(\hat{\mathbf{x}}) \mathbf{B}_c^T \mathbf{P}_1 \tilde{\mathbf{e}}_c, \end{aligned} \tag{51}$$

$$\dot{\boldsymbol{\theta}}_2 = \begin{cases} \gamma_2 \boldsymbol{\Phi}_f^T(\hat{\mathbf{x}}) \mathbf{B}_c^T \mathbf{P}_1 \tilde{\mathbf{e}}_c \mathbf{u}^T, & \text{if } \left(\|\boldsymbol{\theta}_2\| < M_{\theta_2}\right) \\ & \text{or } \left(\|\boldsymbol{\theta}_2\| = M_{\theta_2}, \right. \\ & \qquad \left. \boldsymbol{\theta}_2^T \boldsymbol{\Phi}_f^T(\hat{\mathbf{x}}) \mathbf{B}_c^T \mathbf{P}_1 \tilde{\mathbf{e}}_c \mathbf{u}^T \le 0\right), \\ P\left\{\gamma_2 \boldsymbol{\Phi}_f^T(\hat{\mathbf{x}}) \mathbf{B}_c^T \mathbf{P}_1 \tilde{\mathbf{e}}_c \mathbf{u}^T\right\}, & \text{if } \left(\|\boldsymbol{\theta}_2\| = M_{\theta_2}, \right. \\ & \qquad \left. \boldsymbol{\theta}_2^T \boldsymbol{\Phi}_f^T(\hat{\mathbf{x}}) \mathbf{B}_c^T \mathbf{P}_1 \tilde{\mathbf{e}}_c \mathbf{u}^T > 0\right), \end{cases} \tag{52}$$

where $P\{\gamma_2 \boldsymbol{\Phi}_f^T(\hat{\mathbf{x}}) \mathbf{B}_c^T \mathbf{P}_1 \tilde{\mathbf{e}}_c \mathbf{u}^T\}$ is defined as

$$\begin{aligned} P\left\{\gamma_2 \boldsymbol{\Phi}_f^T(\hat{\mathbf{x}}) \mathbf{B}_c^T \mathbf{P}_1 \tilde{\mathbf{e}}_c \mathbf{u}^T\right\} &= \gamma_2 \boldsymbol{\Phi}_f^T(\hat{\mathbf{x}}) \mathbf{B}_c^T \mathbf{P}_1 \tilde{\mathbf{e}}_c \mathbf{u}^T \\ &\quad - \gamma_2 \frac{\boldsymbol{\theta}_2 \boldsymbol{\theta}_2^T}{\|\boldsymbol{\theta}_2\|^2} \boldsymbol{\Phi}_f^T(\hat{\mathbf{x}}) \mathbf{B}_c^T \mathbf{P}_1 \tilde{\mathbf{e}}_c \mathbf{u}^T, \end{aligned} \tag{53}$$

$$\dot{\theta}_{h_1} = \begin{cases} \gamma_3 \left\| \tilde{\mathbf{e}}_c^T \mathbf{P}_1 \mathbf{B}_c \right\| \boldsymbol{\xi}(\hat{\mathbf{x}}), & \text{if } \left(\|\theta_{h_1}\| < M_{\theta_{h_1}}\right) \\ & \text{or } \left(\|\theta_{h_1}\| = M_{\theta_{h_1}}, \right. \\ & \qquad \left. \left\| \tilde{\mathbf{e}}_c^T \mathbf{P}_1 \mathbf{B}_c \right\| \cdot \theta_{h_1}^T \boldsymbol{\xi}(\hat{\mathbf{x}}) \le 0\right), \\ P\left\{\gamma_3 \left\| \tilde{\mathbf{e}}_c^T \mathbf{P}_1 \mathbf{B}_c \right\| \boldsymbol{\xi}(\hat{\mathbf{x}})\right\}, & \text{if } \left(\|\theta_{h_1}\| = M_{\theta_{h_1}}, \right. \\ & \qquad \left. \left\| \tilde{\mathbf{e}}_c^T \mathbf{P}_1 \mathbf{B}_c \right\| \cdot \theta_{h_1}^T \boldsymbol{\xi}(\hat{\mathbf{x}}) > 0\right), \end{cases} \tag{54a}$$

where $P\{\gamma_3 \|\tilde{\mathbf{e}}_c^T \mathbf{P}_1 \mathbf{B}_c\| \boldsymbol{\xi}(\hat{\mathbf{x}})\}$ is defined as

$$\begin{aligned} P\left\{\gamma_3 \left\| \tilde{\mathbf{e}}_c^T \mathbf{P}_1 \mathbf{B}_c \right\| \boldsymbol{\xi}(\hat{\mathbf{x}})\right\} &= \gamma_3 \left\| \tilde{\mathbf{e}}_c^T \mathbf{P}_1 \mathbf{B}_c \right\| \boldsymbol{\xi}(\hat{\mathbf{x}}) \\ &\quad - \gamma_3 \frac{\theta_{h_1} \theta_{h_1}^T}{\|\theta_{h_1}\|^2} \left\| \tilde{\mathbf{e}}_c^T \mathbf{P}_1 \mathbf{B}_c \right\| \boldsymbol{\xi}(\hat{\mathbf{x}}), \end{aligned} \tag{54b}$$

$$\dot{\theta}_{h_2} = \begin{cases} \gamma_4 \left\| \tilde{\mathbf{e}}_c^T \mathbf{P}_1 \mathbf{B}_c \right\| \boldsymbol{\xi}(\hat{\mathbf{x}}(t-\tau)), & \text{if } \left(\|\theta_{h_2}\| < M_{\theta_{h_2}}\right) \\ & \text{or } \left(\|\theta_{h_2}\| = M_{\theta_{h_2}}, \right. \\ & \qquad \left. \left\| \tilde{\mathbf{e}}_c^T \mathbf{P}_1 \mathbf{B}_c \right\| \cdot \theta_{h_2}^T \boldsymbol{\xi}(\hat{\mathbf{x}}(t-\tau)) \le 0\right), \\ P\left\{\gamma_4 \left\| \tilde{\mathbf{e}}_c^T \mathbf{P}_1 \mathbf{B}_c \right\| \boldsymbol{\xi}(\hat{\mathbf{x}})\right\}, & \text{if } \left(\|\theta_{h_2}\| = M_{\theta_{h_2}}, \right. \\ & \qquad \left. \left\| \tilde{\mathbf{e}}_c^T \mathbf{P}_1 \mathbf{B}_c \right\| \cdot \theta_{h_2}^T \boldsymbol{\xi}(\hat{\mathbf{x}}(t-\tau)) > 0\right), \end{cases} \tag{55a}$$

where $P\{\gamma_4 \|\tilde{\mathbf{e}}_c^T \mathbf{P}_1 \mathbf{B}_c\| \boldsymbol{\xi}(\hat{\mathbf{x}}(t-\tau))\}$ is defined as

$$\begin{aligned} &P\left\{\gamma_4 \left\| \tilde{\mathbf{e}}_c^T \mathbf{P}_1 \mathbf{B}_c \right\| \boldsymbol{\xi}(\hat{\mathbf{x}}(t-\tau))\right\} \\ &\quad = \gamma_4 \left\| \tilde{\mathbf{e}}_c^T \mathbf{P}_1 \mathbf{B}_c \right\| \boldsymbol{\xi}(\hat{\mathbf{x}}(t-\tau)) \\ &\qquad - \gamma_4 \frac{\theta_{h_2} \theta_{h_2}^T}{\|\theta_{h_2}\|^2} \left\| \tilde{\mathbf{e}}_c^T \mathbf{P}_1 \mathbf{B}_c \right\| \boldsymbol{\xi}(\hat{\mathbf{x}}(t-\tau)). \end{aligned} \tag{55b}$$

The main result of the proposed observer-based robust adaptive fuzzy control scheme is summarized in the following theorem.

Theorem 6. *Consider the MIMO nonlinear system* (2) *in the presence of output delay and the uncertainties subject to Assumptions 1-2. The observer-based robust adaptive fuzzy controller is defined by* (19) *and* (44)-(45) *with adaptation laws given by* (46)–(49). *For the given positive definite matrices* $\mathbf{Q}_1$ *and* $\mathbf{Q}_2$, *if there exist symmetric positive definite matrices* $\mathbf{P}_1$ *and* $\mathbf{P}_2$ *such that the following Lyapunov equations*

$$\left(\mathbf{A} - \mathbf{K}_o \mathbf{C}\right)^T \mathbf{P}_1 + \mathbf{P}_1 \left(\mathbf{A} - \mathbf{K}_o \mathbf{C}\right) = -\mathbf{Q}_1, \tag{56}$$

$$\left(\mathbf{A} - \mathbf{B}\mathbf{K}_c\right)^T \mathbf{P}_2 + \mathbf{P}_2 \left(\mathbf{A} - \mathbf{B}\mathbf{K}_c\right) = -\mathbf{Q}_2, \tag{57}$$

$$\mathbf{P}_1 \mathbf{B}_c = \mathbf{C}^T, \tag{58}$$

are satisfied, then all the closed-loop signals are bounded, and the tracking errors converge to a neighborhood of zero.

Proof. Consider the Lyapunov function candidate

$$\begin{aligned} V &= \frac{1}{2} \tilde{\mathbf{e}}_c^T \mathbf{P}_1 \tilde{\mathbf{e}}_c + \frac{1}{2} \hat{\mathbf{e}}^T \mathbf{P}_2 \hat{\mathbf{e}} + \frac{1}{2\gamma_1} \left(\tilde{\boldsymbol{\theta}}_1^T \tilde{\boldsymbol{\theta}}_1\right) + \frac{1}{2\gamma_2} \operatorname{tr}\left(\tilde{\boldsymbol{\theta}}_2^T \tilde{\boldsymbol{\theta}}_2\right) \\ &\quad + \frac{1}{2\gamma_3} \left(\tilde{\theta}_{h_1}^T \tilde{\theta}_{h_1}\right) + \frac{1}{2\gamma_4} \left(\tilde{\theta}_{h_2}^T \tilde{\theta}_{h_2}\right) + \frac{1}{2\gamma_5} \tilde{\omega}_f^2. \end{aligned} \tag{59}$$

By the time derivative of V and the facts that $\dot{\tilde{\boldsymbol{\theta}}}_1 = -\dot{\boldsymbol{\theta}}_1$, $\dot{\tilde{\boldsymbol{\theta}}}_2 = -\dot{\boldsymbol{\theta}}_2$, $\dot{\tilde{\theta}}_{h_1} = -\dot{\theta}_{h_1}$, $\dot{\tilde{\theta}}_{h_2} = -\dot{\theta}_{h_2}$ and $\dot{\tilde{\omega}}_f = -\dot{\hat{\omega}}_f$, it can be easily shown from (24) and (39) that

$$\begin{aligned}
\dot{V} = {} & \frac{1}{2}\dot{\tilde{\mathbf{e}}}_c^T\mathbf{P}_1\tilde{\mathbf{e}}_c + \frac{1}{2}\tilde{\mathbf{e}}_c^T\mathbf{P}_1\dot{\tilde{\mathbf{e}}}_c + \frac{1}{2}\dot{\hat{\mathbf{e}}}^T\mathbf{P}_2\hat{\mathbf{e}} + \frac{1}{2}\hat{\mathbf{e}}^T\mathbf{P}_2\dot{\hat{\mathbf{e}}} \\
& - \frac{1}{\gamma_1}\left(\tilde{\boldsymbol{\theta}}_1^T\dot{\boldsymbol{\theta}}_1\right) - \frac{1}{\gamma_2}\operatorname{tr}\left(\tilde{\boldsymbol{\theta}}_2^T\dot{\boldsymbol{\theta}}_2\right) - \frac{1}{2\gamma_3}\left(\tilde{\theta}_{h_1}^T\dot{\theta}_{h_1}\right) \\
& - \frac{1}{2\gamma_4}\left(\tilde{\theta}_{h_2}^T\dot{\theta}_{h_2}\right) - \frac{1}{\gamma_5}\tilde{\omega}_f\dot{\hat{\omega}}_f \\
= {} & \frac{1}{2}\tilde{\mathbf{e}}_c^T\left[(\mathbf{A}-\mathbf{K}_o\mathbf{C})^T\mathbf{P}_1 + \mathbf{P}_1(\mathbf{A}-\mathbf{K}_o\mathbf{C})\right]\tilde{\mathbf{e}}_c \\
& + \frac{1}{2}\hat{\mathbf{e}}^T\left[(\mathbf{A}-\mathbf{B}\mathbf{K}_c)^T\mathbf{P}_2 + \mathbf{P}_2(\mathbf{A}-\mathbf{B}\mathbf{K}_c)\right]\hat{\mathbf{e}} \\
& + \tilde{\mathbf{e}}_c^T\mathbf{P}_1\mathbf{B}_c\left[\boldsymbol{\Phi}_f(\hat{\mathbf{x}})\tilde{\boldsymbol{\theta}}_1 + \boldsymbol{\Phi}_f(\hat{\mathbf{x}})\tilde{\boldsymbol{\theta}}_2\mathbf{u}(t) + \omega_{1f}\right. \\
& \qquad \left. + \mathbf{u}_{sf}(t) + \Delta\boldsymbol{\Psi}_f(\mathbf{x},\mathbf{u})\right] + \hat{\mathbf{e}}^T\mathbf{P}_2\mathbf{K}_o\underline{\tilde{\mathbf{e}}_1} \\
& - \frac{1}{\gamma_1}\left(\tilde{\boldsymbol{\theta}}_1^T\dot{\boldsymbol{\theta}}_1\right) - \frac{1}{\gamma_2}\operatorname{tr}\left(\tilde{\boldsymbol{\theta}}_2^T\dot{\boldsymbol{\theta}}_2\right) - \frac{1}{2\gamma_3}\left(\tilde{\theta}_{h_1}^T\dot{\theta}_{h_1}\right) \\
& - \frac{1}{2\gamma_4}\left(\tilde{\theta}_{h_2}^T\dot{\theta}_{h_2}\right) - \frac{1}{\gamma_5}\tilde{\omega}_f\dot{\hat{\omega}}_f \\
\le {} & \frac{1}{2}\tilde{\mathbf{e}}_c^T\left[(\mathbf{A}-\mathbf{K}_o\mathbf{C})^T\mathbf{P}_1 + \mathbf{P}_1(\mathbf{A}-\mathbf{K}_o\mathbf{C})\right]\tilde{\mathbf{e}}_c \\
& + \frac{1}{2}\hat{\mathbf{e}}^T\left[(\mathbf{A}-\mathbf{B}\mathbf{K}_c)^T\mathbf{P}_2 + \mathbf{P}_2(\mathbf{A}-\mathbf{B}\mathbf{K}_c)\right]\hat{\mathbf{e}} \\
& + \tilde{\mathbf{e}}_c^T\mathbf{P}_1\mathbf{B}_c\boldsymbol{\Phi}_f(\hat{\mathbf{x}})\tilde{\boldsymbol{\theta}}_1 + \tilde{\mathbf{e}}_c^T\mathbf{P}_1\mathbf{B}_c\boldsymbol{\Phi}_f(\hat{\mathbf{x}})\tilde{\boldsymbol{\theta}}_2\mathbf{u} \\
& + \tilde{\mathbf{e}}_c^T\mathbf{P}_1\mathbf{B}_c\mathbf{u}_{sf} + \left\|\tilde{\mathbf{e}}_c^T\mathbf{P}_1\mathbf{B}_c\right\|\left\|\boldsymbol{\omega}_{1f}\right\| \\
& + \left\|\tilde{\mathbf{e}}_c^T\mathbf{P}_1\mathbf{B}_c\right\|\cdot\left\|\Delta\Psi_f(\mathbf{x},\mathbf{u})\right\| + \hat{\mathbf{e}}^T\mathbf{P}_2\mathbf{K}_o\underline{\tilde{\mathbf{e}}_1} \\
& - \frac{1}{\gamma_1}\left(\tilde{\boldsymbol{\theta}}_1^T\dot{\boldsymbol{\theta}}_1\right) - \frac{1}{\gamma_2}\operatorname{tr}\left(\tilde{\boldsymbol{\theta}}_2^T\dot{\boldsymbol{\theta}}_2\right) - \frac{1}{2\gamma_3}\left(\tilde{\theta}_{h_1}^T\dot{\theta}_{h_1}\right) \\
& - \frac{1}{2\gamma_4}\left(\tilde{\theta}_{h_2}^T\dot{\theta}_{h_2}\right) - \frac{1}{\gamma_5}\tilde{\omega}_f\dot{\hat{\omega}}_f.
\end{aligned} \tag{60}$$

Applying Assumption 2, (56), and (57), it yields

$$\begin{aligned}
\dot{V} \le {} & -\frac{1}{2}\tilde{\mathbf{e}}_c^T\mathbf{Q}_1\tilde{\mathbf{e}}_c - \frac{1}{2}\hat{\mathbf{e}}^T\mathbf{Q}_2\hat{\mathbf{e}} + \tilde{\mathbf{e}}_c^T\mathbf{P}_1\mathbf{B}_c\boldsymbol{\Phi}_f(\hat{\mathbf{x}})\tilde{\boldsymbol{\theta}}_1 \\
& + \tilde{\mathbf{e}}_c^T\mathbf{P}_1\mathbf{B}_c\boldsymbol{\Phi}_f(\hat{\mathbf{x}})\tilde{\boldsymbol{\theta}}_2\mathbf{u} + \tilde{\mathbf{e}}_c^T\mathbf{P}_1\mathbf{B}_c\mathbf{u}_{sf} + \left\|\tilde{\mathbf{e}}_c^T\mathbf{P}_1\mathbf{B}_c\right\|\left\|\boldsymbol{\omega}_{1f}\right\| \\
& + \left\|\tilde{\mathbf{e}}_c^T\mathbf{P}_1\mathbf{B}_c\right\|\cdot\left(h_1(\mathbf{x}) + h_2(\mathbf{x}(t-\tau))\right) + \hat{\mathbf{e}}^T\mathbf{P}_2\mathbf{K}_o\underline{\tilde{\mathbf{e}}_1} \\
& - \frac{1}{\gamma_1}\left(\tilde{\boldsymbol{\theta}}_1^T\dot{\boldsymbol{\theta}}_1\right) - \frac{1}{\gamma_2}\operatorname{tr}\left(\tilde{\boldsymbol{\theta}}_2^T\dot{\boldsymbol{\theta}}_2\right) - \frac{1}{2\gamma_3}\left(\tilde{\theta}_{h_1}^T\dot{\theta}_{h_1}\right) \\
& - \frac{1}{2\gamma_4}\left(\tilde{\theta}_{h_2}^T\dot{\theta}_{h_2}\right) - \frac{1}{\gamma_5}\tilde{\omega}_f\dot{\hat{\omega}}_f \\
= {} & -\frac{1}{2}\tilde{\mathbf{e}}_c^T\mathbf{Q}_1\tilde{\mathbf{e}}_c - \frac{1}{2}\hat{\mathbf{e}}^T\mathbf{Q}_2\hat{\mathbf{e}} + \tilde{\mathbf{e}}_c^T\mathbf{P}_1\mathbf{B}_c\boldsymbol{\Phi}_f(\hat{\mathbf{x}})\tilde{\boldsymbol{\theta}}_1 \\
& + \tilde{\mathbf{e}}_c^T\mathbf{P}_1\mathbf{B}_c\boldsymbol{\Phi}_f(\hat{\mathbf{x}})\tilde{\boldsymbol{\theta}}_2\mathbf{u} + \tilde{\mathbf{e}}_c^T\mathbf{P}_1\mathbf{B}_c\mathbf{u}_{sf} + \left\|\tilde{\mathbf{e}}_c^T\mathbf{P}_1\mathbf{B}_c\right\|\left\|\boldsymbol{\omega}_{1f}\right\| \\
& + \left\|\tilde{\mathbf{e}}_c^T\mathbf{P}_1\mathbf{B}_c\right\|\cdot\left[h_1(\mathbf{x}) - \hat{h}_1\left(\hat{\mathbf{x}} \mid \theta_{h_1}^*\right) + \hat{h}_1\left(\hat{\mathbf{x}} \mid \theta_{h_1}^*\right)\right. \\
& \qquad \left. - \hat{h}_1\left(\hat{\mathbf{x}} \mid \theta_{h_1}\right) + \hat{h}_1\left(\hat{\mathbf{x}} \mid \theta_{h_1}\right)\right] \\
& + \left\|\tilde{\mathbf{e}}_c^T\mathbf{P}_1\mathbf{B}_c\right\|\cdot\left[h_2(\mathbf{x}(t-\tau)) - \hat{h}_2\left(\hat{\mathbf{x}}(t-\tau) \mid \theta_{h_2}^*\right)\right. \\
& \qquad + \hat{h}_2\left(\hat{\mathbf{x}}(t-\tau) \mid \theta_{h_2}^*\right) \\
& \qquad - \hat{h}_2\left(\hat{\mathbf{x}}(t-\tau) \mid \theta_{h_2}\right) \\
& \qquad \left. + \hat{h}_2\left((t-\tau)\hat{\mathbf{x}} \mid \theta_{h_2}\right)\right] \\
& + \hat{\mathbf{e}}^T\mathbf{P}_2\mathbf{K}_o\underline{\tilde{\mathbf{e}}_1} - \frac{1}{\gamma_1}\left(\tilde{\boldsymbol{\theta}}_1^T\dot{\boldsymbol{\theta}}_1\right) - \frac{1}{\gamma_2}\operatorname{tr}\left(\tilde{\boldsymbol{\theta}}_2^T\dot{\boldsymbol{\theta}}_2\right) \\
& - \frac{1}{2\gamma_3}\left(\tilde{\theta}_{h_1}^T\dot{\theta}_{h_1}\right) - \frac{1}{2\gamma_4}\left(\tilde{\theta}_{h_2}^T\dot{\theta}_{h_2}\right) - \frac{1}{\gamma_5}\tilde{\omega}_f\dot{\hat{\omega}}_f.
\end{aligned} \tag{61}$$

According to (33) and (43), we have

$$\begin{aligned}
\dot{V} \le {} & -\frac{1}{2}\tilde{\mathbf{e}}_c^T\mathbf{Q}_1\tilde{\mathbf{e}}_c - \frac{1}{2}\hat{\mathbf{e}}^T\mathbf{Q}_2\hat{\mathbf{e}} + \tilde{\mathbf{e}}_c^T\mathbf{P}_1\mathbf{B}_c\boldsymbol{\Phi}_f(\hat{\mathbf{x}})\tilde{\boldsymbol{\theta}}_1 \\
& + \tilde{\mathbf{e}}_c^T\mathbf{P}_1\mathbf{B}_c\boldsymbol{\Phi}_f(\hat{\mathbf{x}})\tilde{\boldsymbol{\theta}}_2\mathbf{u} + \tilde{\mathbf{e}}_c^T\mathbf{P}_1\mathbf{B}_c\mathbf{u}_{sf} + \left\|\tilde{\mathbf{e}}_c^T\mathbf{P}_1\mathbf{B}_c\right\|\left\|\boldsymbol{\omega}_{1f}\right\| \\
& + \left\|\tilde{\mathbf{e}}_c^T\mathbf{P}_1\mathbf{B}_c\right\|\cdot\hat{h}_1\left(\hat{\mathbf{x}} \mid \theta_{h_1}\right) + \left\|\tilde{\mathbf{e}}_c^T\mathbf{P}_1\mathbf{B}_c\right\|\cdot\tilde{\theta}_{h_1}^T\xi(\hat{\mathbf{x}}) \\
& + \left\|\tilde{\mathbf{e}}_c^T\mathbf{P}_1\mathbf{B}_c\right\|\cdot\hat{h}_2\left(\hat{\mathbf{x}}(t-\tau) \mid \theta_{h_2}\right) \\
& + \left\|\tilde{\mathbf{e}}_c^T\mathbf{P}_1\mathbf{B}_c\right\|\cdot\tilde{\theta}_{h_2}^T\xi(\hat{\mathbf{x}}(t-\tau)) \\
& + \left\|\tilde{\mathbf{e}}_c^T\mathbf{P}_1\mathbf{B}_c\right\|\cdot|\omega_2| + \hat{\mathbf{e}}^T\mathbf{P}_2\mathbf{K}_o\underline{\tilde{\mathbf{e}}_1} - \frac{1}{\gamma_1}\left(\tilde{\boldsymbol{\theta}}_1^T\dot{\boldsymbol{\theta}}_1\right) \\
& - \frac{1}{\gamma_2}\operatorname{tr}\left(\tilde{\boldsymbol{\theta}}_2^T\dot{\boldsymbol{\theta}}_2\right) - \frac{1}{2\gamma_3}\left(\tilde{\theta}_{h_1}^T\dot{\theta}_{h_1}\right) - \frac{1}{2\gamma_4}\left(\tilde{\theta}_{h_2}^T\dot{\theta}_{h_2}\right) \\
& - \frac{1}{\gamma_5}\tilde{\omega}_f\dot{\hat{\omega}}_f \\
\le {} & -\frac{1}{2}\tilde{\mathbf{e}}_c^T\mathbf{Q}_1\tilde{\mathbf{e}}_c - \frac{1}{2}\hat{\mathbf{e}}^T\mathbf{Q}_2\hat{\mathbf{e}} + \tilde{\mathbf{e}}_c^T\mathbf{P}_1\mathbf{B}_c\boldsymbol{\Phi}_f(\hat{\mathbf{x}})\tilde{\boldsymbol{\theta}}_1 \\
& + \tilde{\mathbf{e}}_c^T\mathbf{P}_1\mathbf{B}_c\boldsymbol{\Phi}_f(\hat{\mathbf{x}})\tilde{\boldsymbol{\theta}}_2\mathbf{u} + \tilde{\mathbf{e}}_c^T\mathbf{P}_1\mathbf{B}_c\mathbf{u}_{sf} + \left\|\tilde{\mathbf{e}}_c^T\mathbf{P}_1\mathbf{B}_c\right\|\hat{\omega}_f \\
& + \left\|\tilde{\mathbf{e}}_c^T\mathbf{P}_1\mathbf{B}_c\right\|\cdot\hat{h}_1\left(\hat{\mathbf{x}} \mid \theta_{h_1}\right) + \left\|\tilde{\mathbf{e}}_c^T\mathbf{P}_1\mathbf{B}_c\right\|\cdot\tilde{\theta}_{h_1}^T\xi(\hat{\mathbf{x}}) \\
& + \left\|\tilde{\mathbf{e}}_c^T\mathbf{P}_1\mathbf{B}_c\right\|\cdot\hat{h}_2\left(\hat{\mathbf{x}}(t-\tau) \mid \theta_{h_2}\right) \\
& + \left\|\tilde{\mathbf{e}}_c^T\mathbf{P}_1\mathbf{B}_c\right\|\cdot\tilde{\theta}_{h_2}^T\xi(\hat{\mathbf{x}}(t-\tau))
\end{aligned}$$

$$
\begin{aligned}
&+ \left\|\tilde{\mathbf{e}}_c^T \mathbf{P}_1 \mathbf{B}_c\right\| \cdot \tilde{\omega}_f + \hat{\mathbf{e}}^T \mathbf{P}_2 \mathbf{K}_o \underline{\tilde{\mathbf{e}}_1} - \frac{1}{\gamma_1}\left(\tilde{\boldsymbol{\theta}}_1^T \dot{\boldsymbol{\theta}}_1\right) \\
&- \frac{1}{\gamma_2}\operatorname{tr}\left(\tilde{\boldsymbol{\theta}}_2^T \dot{\boldsymbol{\theta}}_2\right) - \frac{1}{2\gamma_3}\left(\tilde{\theta}_{h_1}^T \dot{\theta}_{h_1}\right) \\
&- \frac{1}{2\gamma_4}\left(\tilde{\theta}_{h_2}^T \dot{\theta}_{h_2}\right) - \frac{1}{\gamma_5}\tilde{\omega}_f \dot{\tilde{\omega}}_f \\
= &- \frac{1}{2}\tilde{\mathbf{e}}_c^T \mathbf{Q}_1 \tilde{\mathbf{e}}_c - \frac{1}{2}\hat{\mathbf{e}}^T \mathbf{Q}_2 \hat{\mathbf{e}} + \tilde{\mathbf{e}}_c^T \mathbf{P}_1 \mathbf{B}_c \mathbf{u}_{sf} \\
&+ \left\|\tilde{\mathbf{e}}_c^T \mathbf{P}_1 \mathbf{B}_c\right\| \hat{\omega}_f + \left\|\tilde{\mathbf{e}}_c^T \mathbf{P}_1 \mathbf{B}_c\right\| \cdot \hat{h}_1\left(\hat{\mathbf{x}} \mid \theta_{h_1}\right) \\
&+ \left\|\tilde{\mathbf{e}}_c^T \mathbf{P}_1 \mathbf{B}_c\right\| \cdot \hat{h}_2\left(\hat{\mathbf{x}}(t-\tau) \mid \theta_{h_2}\right) + \hat{\mathbf{e}}^T \mathbf{P}_2 \mathbf{K}_o \underline{\tilde{\mathbf{e}}_1} \\
&+ \left[\tilde{\mathbf{e}}_c^T \mathbf{P}_1 \mathbf{B}_c \boldsymbol{\Phi}_f(\hat{\mathbf{x}}) \tilde{\boldsymbol{\theta}}_1 - \frac{1}{\gamma_1}\left(\tilde{\boldsymbol{\theta}}_1^T \dot{\boldsymbol{\theta}}_1\right)\right] \\
&+ \left[\tilde{\mathbf{e}}_c^T \mathbf{P}_1 \mathbf{B}_c \boldsymbol{\Phi}_f(\hat{\mathbf{x}}) \tilde{\boldsymbol{\theta}}_2 \mathbf{u} - \frac{1}{\gamma_2}\operatorname{tr}\left(\tilde{\boldsymbol{\theta}}_2^T \dot{\boldsymbol{\theta}}_2\right)\right] \\
&+ \left[\left\|\tilde{\mathbf{e}}_c^T \mathbf{P}_1 \mathbf{B}_c\right\| \cdot \tilde{\theta}_{h_1}^T \xi(\hat{\mathbf{x}}) - \frac{1}{\gamma_3}\left(\tilde{\theta}_{h_1}^T \dot{\theta}_{h_1}\right)\right] \\
&+ \left[\left\|\tilde{\mathbf{e}}_c^T \mathbf{P}_1 \mathbf{B}_c\right\| \cdot \tilde{\theta}_{h_2}^T \xi(\hat{\mathbf{x}}(t-\tau)) - \frac{1}{\gamma_4}\left(\tilde{\theta}_{h_2}^T \dot{\theta}_{h_2}\right)\right] \\
&+ \left[\left\|\tilde{\mathbf{e}}_c^T \mathbf{P}_1 \mathbf{B}_c\right\| \tilde{\omega}_f - \frac{1}{\gamma_5}\tilde{\omega}_f \dot{\tilde{\omega}}_f\right].
\end{aligned}
\tag{62}
$$

By employing (46)–(49) and using the control laws (44)-(45), we can obtain

$$
\dot{V} \le -\frac{1}{2}\tilde{\mathbf{e}}_c^T \mathbf{Q}_1 \tilde{\mathbf{e}}_c - \frac{1}{2}\hat{\mathbf{e}}^T \mathbf{Q}_2 \hat{\mathbf{e}}. \tag{63}
$$

Therefore, it can be concluded that $\dot{V} \le 0$ from (63), and the output tracking error of the closed-loop system converges asymptotically to a neighborhood of zero based on the Lyapunov synthesis approach. This completes the proof. □

4. An Example and Simulation Results

In this paper, a numerical example is illustrated to verify the performance of the proposed observer-based robust adaptive fuzzy controller. Consider the following MIMO nonlinear uncertain system with delayed output:

$$
\begin{aligned}
\dot{x}_{11}(t) &= x_{12}(t), \\
\dot{x}_{12}(t) &= f_1(\mathbf{x}) + g_{11}(\mathbf{x}) u_1(t) + g_{12}(\mathbf{x}) u_2(t) + \Delta\phi_1(\mathbf{x}), \\
\dot{x}_{21}(t) &= x_{22}(t), \\
\dot{x}_{22}(t) &= f_2(\mathbf{x}) + g_{21}(\mathbf{x}) u_1(t) + g_{22}(\mathbf{x}) u_2(t) + \Delta\phi_2(\mathbf{x}), \\
y_1(t) &= x_{11}(t-\tau), \\
y_2(t) &= x_{21}(t-\tau).
\end{aligned}
\tag{64}
$$

According to (2), the above equation can be rewritten as the following compact form:

$$
\begin{aligned}
\begin{bmatrix} \dot{x}_{11}(t) \\ \dot{x}_{12}(t) \\ \dot{x}_{21}(t) \\ \dot{x}_{22}(t) \end{bmatrix} &= \begin{bmatrix} 0 & 1 & 0 & 0 \\ 0 & 0 & 0 & 0 \\ 0 & 0 & 0 & 1 \\ 0 & 0 & 0 & 0 \end{bmatrix} \begin{bmatrix} x_{11}(t) \\ x_{12}(t) \\ x_{21}(t) \\ x_{22}(t) \end{bmatrix} + \begin{bmatrix} 0 & 0 \\ 1 & 0 \\ 0 & 0 \\ 0 & 1 \end{bmatrix} \\
&\times \left(\begin{bmatrix} f_1(\mathbf{x}) \\ f_2(\mathbf{x}) \end{bmatrix} + \begin{bmatrix} g_{11}(\mathbf{x}) & g_{12}(\mathbf{x}) \\ g_{21}(\mathbf{x}) & g_{22}(\mathbf{x}) \end{bmatrix} \begin{bmatrix} u_1(t) \\ u_2(t) \end{bmatrix} \right. \\
&\left. + \begin{bmatrix} \Delta\phi_1(\mathbf{x}) \\ \Delta\phi_2(\mathbf{x}) \end{bmatrix} \right), \\
\begin{bmatrix} y_1(t) \\ y_2(t) \end{bmatrix} &= \begin{bmatrix} 1 & 0 & 0 & 0 \\ 0 & 0 & 1 & 0 \end{bmatrix} \begin{bmatrix} x_{11}(t-\tau) \\ x_{12}(t-\tau) \\ x_{21}(t-\tau) \\ x_{22}(t-\tau) \end{bmatrix},
\end{aligned}
\tag{65}
$$

where $\mathbf{A}_1 = \mathbf{A}_2 = \left[\begin{smallmatrix} 0 & 1 \\ 0 & 0 \end{smallmatrix}\right]$, $\mathbf{B}_1 = \mathbf{B}_2 = \left[\begin{smallmatrix} 0 \\ 1 \end{smallmatrix}\right]$, $\mathbf{C}_1 = \mathbf{C}_2 = \left[\begin{smallmatrix} 1 & 0 \end{smallmatrix}\right]$, the nonlinear system functions $f_1(\mathbf{x}) = (1 - e^{-x_{11}})/(1 + e^{-x_{11}})$, $f_2(\mathbf{x}) = (1 - e^{-x_{21}})/(1 + e^{-x_{21}})$, $g_{12}(\mathbf{x}) = g_{21}(\mathbf{x}) = 0$, and $g_{11}(\mathbf{x}) = g_{22}(\mathbf{x}) = 1$, and the uncertainties $\Delta\boldsymbol{\Phi} = \left[\begin{smallmatrix} 0.1x_{21}\sin(t) \\ 0.1x_{12}\cos(t) \end{smallmatrix}\right]$ and the delay time is $\tau = 0.1$. In the simulation, these nonlinear system functions and uncertainties are assumed to be unknown and are estimated by the fuzzy logic systems. The fuzzy membership functions are chosen as follows:

$$
\begin{aligned}
\mu_{F_i^1}(\hat{x}_i) &= \frac{1}{1 + \exp\left(5\left(\hat{x}_i + 0.8\right)\right)}, \\
\mu_{F_i^2}(\hat{x}_i) &= \exp\left(-\left(\hat{x}_i + 0.6\right)^2\right), \\
\mu_{F_i^3}(\hat{x}_i) &= \exp\left(-\left(\hat{x}_i + 0.4\right)^2\right), \\
\mu_{F_i^4}(\hat{x}_i) &= \exp\left(-\hat{x}_i^{\,2}\right), \\
\mu_{F_i^5}(\hat{x}_i) &= \exp\left(-\left(\hat{x}_i - 0.4\right)^2\right), \\
\mu_{F_i^6}(\hat{x}_i) &= \exp\left(-\left(\hat{x}_i - 0.6\right)^2\right), \\
\mu_{F_i^7}(\hat{x}_i) &= \frac{1}{1 + \exp\left(-5\left(\hat{x}_i - 0.8\right)\right)}, \quad i = 1, 2, 3, 4.
\end{aligned}
\tag{66}
$$

Let

$$
\begin{aligned}
\xi^l(\hat{x}) &= \frac{\mu_{F_1^l}(\hat{x}_1)\,\mu_{F_2^l}(\hat{x}_2)\,\mu_{F_3^l}(\hat{x}_3)\,\mu_{F_4^l}(\hat{x}_4)}{\sum_{l=1}^{7}\mu_{F_1^l}(\hat{x}_1)\,\mu_{F_2^l}(\hat{x}_2)\,\mu_{F_3^l}(\hat{x}_3)\,\mu_{F_4^l}(\hat{x}_4)}, \\
\xi(\hat{x}) &= \left(\xi^1(\hat{x}), \xi^2(\hat{x}), \xi^3(\hat{x}), \xi^4(\hat{x}), \xi^5(\hat{x}), \xi^6(\hat{x}), \xi^7(\hat{x})\right)^T.
\end{aligned}
\tag{67}
$$

In this section, we apply the observer-based robust adaptive fuzzy controller proposed in Section 3 to deal with the output tracking control problem of an MIMO nonlinear uncertain system with delayed output in (65).

The control objective is to force the system output to track the given desired trajectories $y_{1d} = y_{2d} = 0.5\sin(2\pi/10)$.

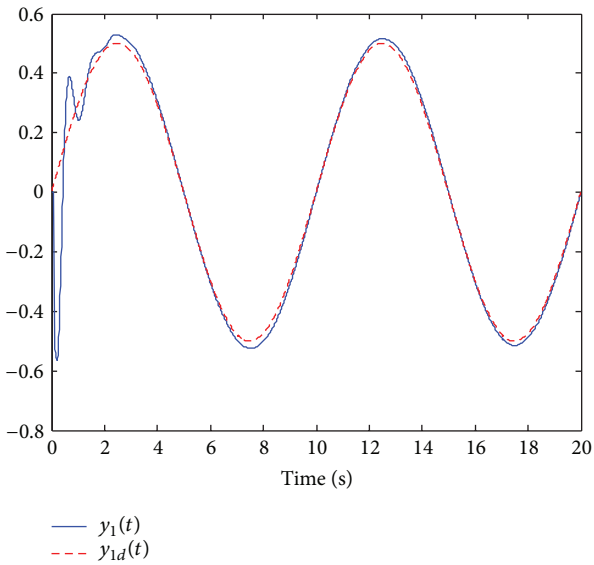

FIGURE 1: The trajectories of y_1 and y_{1d}.

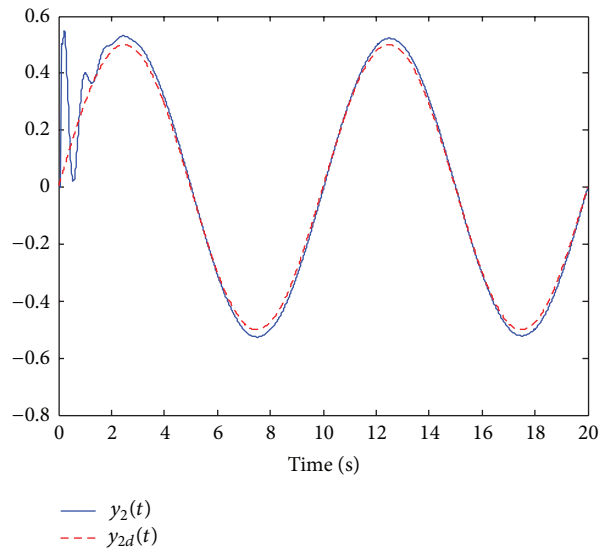

FIGURE 2: The trajectories of y_2 and y_{2d}.

First, we select the control and observer gain matrices as $\mathbf{K}_c = \begin{bmatrix} 170 & 40 & 0 & 0 \\ 0 & 0 & 180 & 30 \end{bmatrix}$ and $\mathbf{K}_o = \begin{bmatrix} 50 & 100 & 0 & 0 \\ 0 & 0 & 75 & 100 \end{bmatrix}^T$, using (20) and (21) to approximate the unknown $\mathbf{F}(\mathbf{x})$ and $\mathbf{G}(\mathbf{x})$, respectively. Given the positive definite matrices $\mathbf{Q}_1 = \operatorname{diag}[1, 1, 1, 1]$ and $\mathbf{Q}_2 = \operatorname{diag}[1, 1, 1, 1]$, and solving the Lyapunov equations (56), we can get

$$\mathbf{P}_1 = \begin{bmatrix} 0.0101 & 0.005 & 0 & 0 \\ 0.005 & 1.26 & 0 & 0 \\ 0 & 0 & 0.0067 & 0.005 \\ 0 & 0 & 0.005 & 1.0483 \end{bmatrix},$$
$$\mathbf{P}_2 = \begin{bmatrix} 0.1302 & -0.5 & 0 & 0 \\ -0.5 & 2.1375 & 0 & 0 \\ 0 & 0 & 0.1 & -0.5 \\ 0 & 0 & -0.5 & 3.0167 \end{bmatrix}. \tag{68}$$

The initial conditions are chosen as $\mathbf{x}(0) = [-0.5, -0.5, 0.5, 0.5]^T$, $\widehat{\mathbf{e}}(0) = [0.3, 0.3, 0.3, 0.3]^T$, $\boldsymbol{\theta}_h(0) = \mathbf{0}$, $\theta_{f1}(0) = \theta_{f2}(0) = 0$, $\gamma_1 = \gamma_2 = 0.13$, $\gamma_3 = 0.1$, $\gamma_4 = 0.01$, $\theta_{g11}(0) = 1$, $\theta_{g12}(0) = 0$, $\theta_{g21}(0) = 0$, $\theta_{g22}(0) = 1$. The Simulation results are shown in Figures 1, 2, 3, 4, 5, 6, and 7. Figures 1 and 2 show the output tracking performance of the system output. Figures 3, 4, 5, and 6 show the trajectories of the system states and their estimation states. Figure 7 shows the control signal. Obviously, the proposed controller can not only ensure that all the signals of the resulting closed-loop system are bounded but also obtain that the good tracking performance of an MIMO nonlinear uncertain output-delay system is achieved.

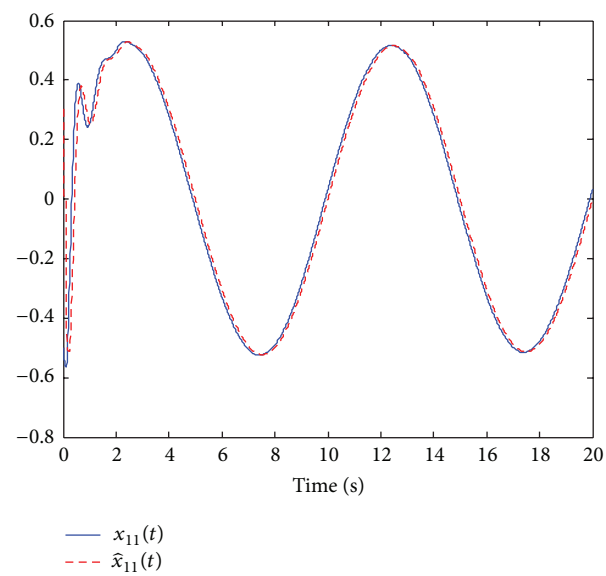

FIGURE 3: The trajectories of x_{11} and $\widehat{x}_{11}$.

5. Conclusion

For a class of multiinput multioutput (MIMO) nonlinear systems with output delay and uncertainties, a robust adaptive fuzzy output feedback controller is proposed to deal with the problem of robust stability and output tracking control. Since the system states are unavailable for measurement, the elements of the observation error vector cannot be obtained completely. Hence, by means of the strictly positive-real (SPR) theory, all elements of the observation error vector will be obtained completely. Moreover, the fuzzy logic systems and some parameter adaptive laws are used to approximate the unknown nonlinear functions and the unknown upper bounds of the uncertainties including the structural uncertainty. By constructing an appropriate Lyapunov function, the proposed observer-based robust adaptive fuzzy controller can not only guarantee that all the signals in the whole closed-loop system are bounded but also obtain that the

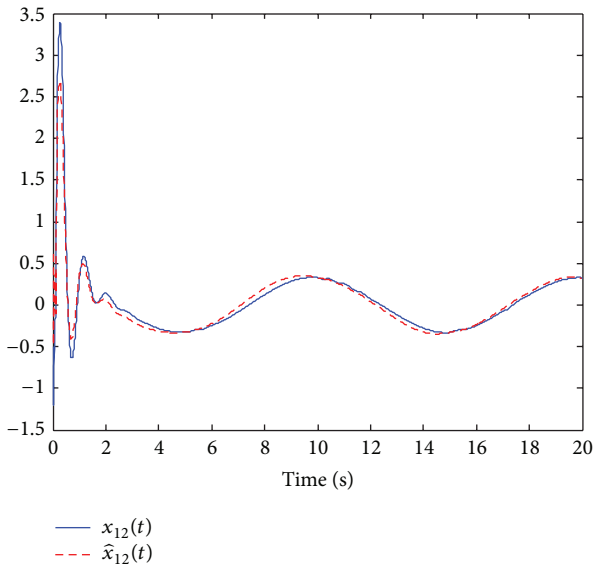

FIGURE 4: The trajectories of x_{12} and $\widehat{x}_{12}$.

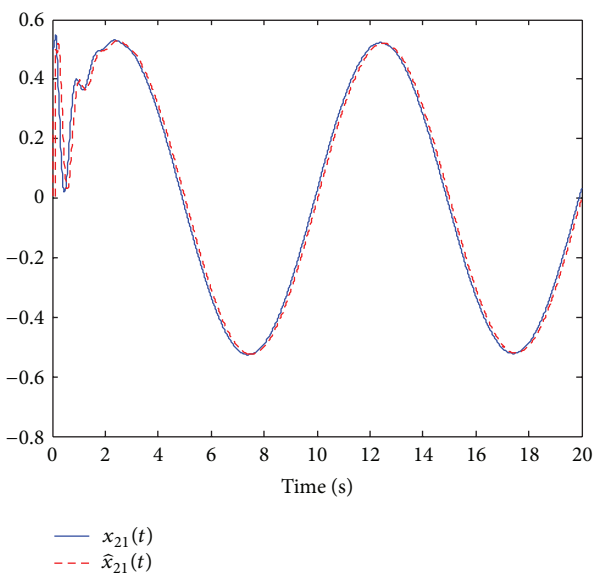

FIGURE 5: The trajectories of x_{21} and $\widehat{x}_{21}$.

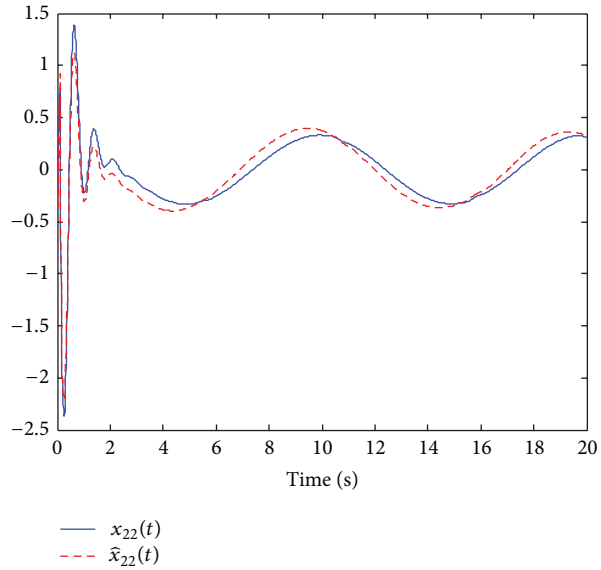

FIGURE 6: The trajectories of x_{22} and $\widehat{x}_{22}$.

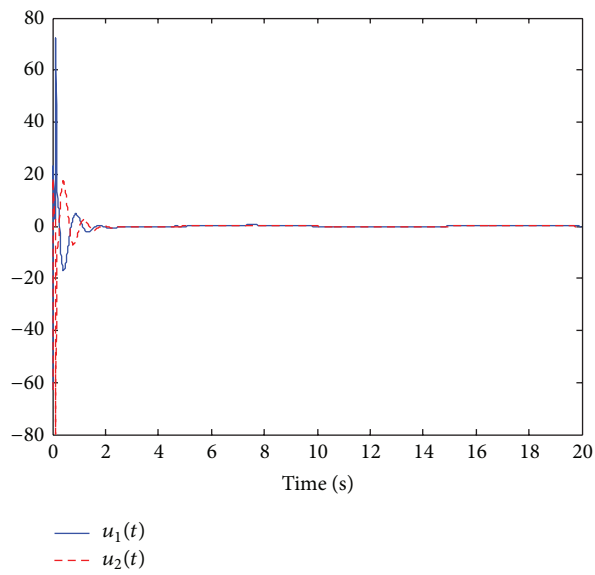

FIGURE 7: The control signals u_1 and u_2.

output tracking performance of the controlled system with delayed output and uncertainties can be achieved. Finally, some simulation results are provided to illustrate the validity of the proposed approach.

References

[1] A. Isidori, *Nonlinear Control Systems*, Springer, New York, NY, USA, 2nd edition, 1989.

[2] J. E. Slotine and W. Li, *Applied Nonlinear Control*, Prentice-Hall, Englewood Cliffs, NJ, USA, 1991.

[3] C. P. Huang, "Model based fuzzy control with affine T-S delayed models applied to nonlinear systems," *International Journal of Innovative Computing Information and Control*, vol. 8, no. 5, pp. 2979–2993, 2012.

[4] Y. Yang, "Direct robust adaptive fuzzy control (DRAFC) for uncertain nonlinear systems using small gain theorem," *Fuzzy Sets and Systems*, vol. 151, no. 1, pp. 79–97, 2005.

[5] C. C. Chiang and Z. H. Kuo, "Output tracking controller design for MIMO nonlinear systems with higher-order and unmatched uncertainties," in *Proceedings of the 39th IEEE Confernce on Decision and Control*, pp. 1315–1320, December 2000.

[6] Y. Wang, Y. Feng, X. Yu, and N. Zhang, "Terminal sliding mode control of MIMO linear systems with unmatched uncertainties,"

in *Proceedings of the 29th Annual Conference of the IEEE Industrial Electronics Society*, pp. 1146–1151, November 2003.

[7] C. C. Chiang and T. C. Tung, "Robust tracking control of uncertain nonlinear systems with an input time elay," in *Proceedings of the International Joint Conference on Neural Networks*, pp. 2394–2399, July 2003.

[8] C. Qian and W. Lin, "Output feedback control of a class of nonlinear systems: a nonseparation principle paradigm," *IEEE Transactions on Automatic Control*, vol. 47, no. 10, pp. 1710–1715, 2002.

[9] L. Wu and W. X. Zheng, "L_2-L_∞ control of nonlinear fuzzy itô stochastic delay systems via dynamic output feedback," *IEEE Transactions on Systems, Man, and Cybernetics B*, vol. 39, no. 5, pp. 1308–1315, 2009.

[10] C. S. Chiu, "Robust adaptive control of uncertain MIMO nonlinear system—feedforward Takagi-Sugeno fuzzy approximation based approach," *IEE Proceedings Control Theory and Applications*, vol. 152, no. 2, pp. 157–164, 2005.

[11] S. Labiod, M. S. Boucherit, and T. M. Guerra, "Adaptive fuzzy control of a class of MIMO nonlinear systems," *Fuzzy Sets and Systems*, vol. 151, no. 1, pp. 59–77, 2005.

[12] L. X. Wang, *Adaptive Fuzzy Systems and Control: Design and Stability Analysis*, Prentice-Hill, Englewood Cliffs, NJ, USA, 1994.

[13] B. S. Chen, C. H. Lee, and Y. C. Chang, "H_∞ tracking design of uncertain nonlinear SISO systems: adaptive fuzzy approach," *IEEE Transactions on Fuzzy Systems*, vol. 4, no. 1, pp. 32–43, 1996.

[14] S. Tong, J. Tang, and T. Wang, "Fuzzy adaptive control of multivariable nonlinear systems," *Fuzzy Sets and Systems*, vol. 111, no. 2, pp. 153–167, 2000.

[15] W. Ma, D. Geng, and Y. Yan, "Multi-phase fuzzy control of single intersection in traffic system based on genetic algorithm," *International Journal of Innovative Computing Information and Control*, vol. 8, no. 5, pp. 3387–3397, 2012.

[16] S. Tong, T. Wang, and J. T. Tang, "Fuzzy adaptive output tracking control of nonlinear systems," *Fuzzy Sets and Systems*, vol. 111, no. 2, pp. 169–182, 2000.

[17] Y. G. Leu, T. T. Lee, and W. Y. Wang, "Observer-based adaptive fuzzy-neural control for unknown nonlinear dynamical systems," *IEEE Transactions on Systems, Man, and Cybernetics B*, vol. 29, no. 5, pp. 583–591, 1999.

[18] C.-C. Kung and T.-H. Chen, "Observer-based indirect adaptive fuzzy sliding mode control with state variable filters for unknown nonlinear dynamical systems," *Fuzzy Sets and Systems*, vol. 155, no. 2, pp. 292–308, 2005.

[19] S. Tong, H.-X. Li, and W. Wang, "Observer-based adaptive fuzzy control for SISO nonlinear systems," *Fuzzy Sets and Systems*, vol. 148, no. 3, pp. 355–376, 2004.

[20] C. H. Wang, H. L. Liu, and T. C. Lin, "Direct adaptive fuzzy-neural control with state observer and supervisory controller for unknown nonlinear dynamical systems," *IEEE Transactions on Fuzzy Systems*, vol. 10, no. 1, pp. 39–49, 2002.

[21] C.-S. Tseng and C.-K. Hwang, "Fuzzy observer-based fuzzy control design for nonlinear systems with persistent bounded disturbances," *Fuzzy Sets and Systems*, vol. 158, no. 2, pp. 164–179, 2007.

[22] J. H. Park and G. T. Park, "Adaptive fuzzy observer with minimal dynamic order for uncertain nonlinear systems," *IEE Proceedings Control Theory and Applications*, vol. 150, no. 2, pp. 189–197, 2003.

[23] A. Wu and P. K. S. Tam, "Stable fuzzy neural tracking control of a class of unknown nonlinear systems based on fuzzy hierarchy error approach," *IEEE Transactions on Fuzzy Systems*, vol. 10, no. 6, pp. 779–789, 2002.

[24] H. X. Li and S. Tong, "A hybrid adaptive fuzzy control for a class of nonlinear MIMO systems," *IEEE Transactions on Fuzzy Systems*, vol. 11, no. 1, pp. 24–34, 2003.

[25] T. Shaocheng, C. Bin, and W. Yongfu, "Fuzzy adaptive output feedback control for MIMO nonlinear systems," *Fuzzy Sets and Systems*, vol. 156, no. 2, pp. 285–299, 2005.

[26] X. Su, P. Shi, L. Wu, and Y. D. Song, "A novel approach to filter design for T-S fuzzy discrete-time systems with time-varying delay," *IEEE Transactions on Fuzzy Systems*, vol. 20, no. 6, pp. 1114–1129, 2012.

[27] X. Zhang, C. Zhang, and Z. Cheng, "Asymptotic stabilization via output feedback for nonlinear systems with delayed output," *International Journal of Systems Science*, vol. 37, no. 9, pp. 599–607, 2006.

[28] R. Yang, H. Gao, and P. Shi, "Delay-dependent robust H_∞ control for uncertain stochastic time-delay systems," *International Journal of Robust and Nonlinear Control*, vol. 20, no. 16, pp. 1852–1865, 2010.

[29] Y. S. Moon, P. Park, and W. H. Kwon, "Robust stabilization of uncertain input-delayed systems using reduction method," *Automatica*, vol. 37, no. 2, pp. 307–312, 2001.

[30] A. Germani, C. Manes, and P. Pepe, "A new approach to state observation of nonlinear systems with delayed output," *IEEE Transactions on Automatic Control*, vol. 47, no. 1, pp. 96–101, 2002.

[31] D. Yue and J. Lam, "Stabilizing controller design for uncertain systems with time-varying input delay," *IEE Proceedings Control Theory and Applications*, vol. 151, no. 6, pp. 699–705, 2004.

Hindawi Publishing Corporation
Mathematical Problems in Engineering
Volume 2013, Article ID 913538, 8 pages
http://dx.doi.org/10.1155/2013/913538

Research Article

A Compound Fuzzy Disturbance Observer Based on Sliding Modes and Its Application on Flight Simulator

Yunjie Wu,[1] Youmin Liu,[1] and Dapeng Tian[2]

[1] *School of Automation Science and Electrical Engineering, Beihang University, Beijing 100191, China*
[2] *Changchun Institute of Optics, Fine Mechanics and Physics, Chinese Academy of Science, Jilin 130033, China*

Correspondence should be addressed to Youmin Liu; snakelym1985@163.com

Received 2 December 2012; Accepted 28 January 2013

Academic Editor: Peng Shi

Copyright © 2013 Yunjie Wu et al. This is an open access article distributed under the Creative Commons Attribution License, which permits unrestricted use, distribution, and reproduction in any medium, provided the original work is properly cited.

A compound fuzzy disturbance observer based on sliding modes is developed, and its application on flight simulator is presented. Fuzzy disturbance observer (FDO) is an effective method in nonlinear control. However, traditional FDO is confined to monitor dynamic disturbance, and the frequency bandwidth of the system is restricted. Sliding mode control (SMC) compensates the high-frequency component of disturbance while it is limited by the chattering phenomenon. The proposed method uses the sliding mode technique to deal with the uncompensated dynamic equivalent disturbance. The switching gain of sliding mode control designed according to the error of disturbance estimation is a small value. Therefore, the proposal also helps to decrease the chattering. The validity of the proposal method is confirmed by experiments on flight simulator.

1. Introduction

Flight simulator simulates the attitude of aircraft and helps the ground experiments. High precision motion control is the key of a flight simulator, which influences the accuracy of simulation experiments. As a typical kind of servomotor system, the robustness against external nonlinear disturbances, time-varied characters, and modeling uncertainties is urgently required [1]. The disturbance observer (DOB) approach has been widely used as an effective robust method to compensate the disturbance and parameter variations from both environment and system [2, 3]. The disturbance observer, which makes the system dynamics same as the nominal model in ideal condition, can absolutely compensate the equivalent disturbance regarding the external disturbance torque, modeling error, and other uncertain factors. However, this method is a linear one and equivalent to high-gain control, which may cause resonance in controlling elastic electromechanical systems [4]. Moreover, there exists huge modeling mismatch if the nonlinear characters of the system are ignored and the performance of the system is limited as the two elements are contradictive in stable controller designing.

Fuzzy method, as a nonlinear method, has been studied with the basic idea that a fuzzy logic system can well approximate arbitrary highly nonlinear system [5, 6]. In previous work, fuzzy approach has been used in complex nonlinear areas such as facial pattern recognition [7], project management [8], and economic dispatch [9] and obtained good effect. Facing to the difficulties caused by nonlinear factors in control area, an apparent view is to use fuzzy tools to monitor and compensate these uncertainties. In some investigations, fuzzy method has been used in controller design [10, 11], filter design [12, 13], and observer design [14, 15]. Thereinto, a fuzzy-disturbance-observer- (FDO-) based control suggested by Kim [14] inherits the advantages of disturbance observer and avoids the unstable factors when there exists huge difference between the nominal model and the actual system. Compared with the indirect and direct adaptive fuzzy approaches suggested by Chen et al. [15] and Ordonez and Passino [16], the FDO-based method guarantees the uniformly ultimately bounded of the disturbance observation error within a sufficiently small region by appropriate choice of the design parameter without the requirement of a supervisory or a robustifying controller. FDO deals with nonlinear problems in motion control

systems and is optimal to industrial application. However, FDO still has difficulty in compensating high-frequency component of a nonlinear disturbance sufficiently.

Sliding mode control (SMC) can inhibit high-frequency disturbance by switching control value, which also causes chattering phenomenon. SMC is an effective approach to deal with nonlinear systems [17, 18]; therefore, an apparent solution is to combine SMC and disturbance observer together. SMC is used as an outer loop controller in some investigations while disturbance observer deals with the compensation of disturbance [19, 20]. In these conditions, the SMC needs to improve the tracking performance as well as inhibiting the disturbance simultaneous. As a result, the chattering phenomenon is hardly decreased as the switching gain keeps affecting. Meanwhile, the upper bound on unknown disturbances is generally considered as constant estimation in order to meet the conditions for the existence of generalized sliding mode [21, 22]. Therefore, if the upper bound is underestimated, the tracking performance of motor servo system is difficult to improve and the system is possibly unstable. Moreover, the switching gain of SMC is designed conservatively and the chattering alleviation is also limited. In previous work, sliding mode disturbance observer has also been proposed as an independent branch which employs the sliding mode technique to estimate the lumped disturbance rather than to do the position control directly [23, 24], and some intelligent methods have also been employed to observe the varying disturbances and estimate the upper bound accordingly [25, 26]. However, the conservative is still a great problem as the switching gain should be larger than the unknown upper bound, and most of intelligent units are not sufficiently sensitive to the chattering in the output of the controller.

In this paper, a compound fuzzy disturbance observer (CFDO) based on sliding modes is proposed, and the task of disturbance compensation is divided into two parts. Low-frequency disturbance is compensated by FDO while high-frequency disturbance is treated by SMC. As low-frequency component is the main part of equivalent disturbance, SMC deals with only the secondary part of the disturbance. Consequently, the switching gain of SMC may be designed as a relative small value, and the chattering alleviation is achieved. The proposed method comprehended the advantages of both FDO and SMC. By using this method, the equivalent disturbance can be compensated more accurately, and the resonance caused by traditional methods in controlling elastic electromechanical systems can be avoided. Compared with the traditional proposed DOB and FDO schemes, CFDO has better robustness when there exists large nonlinear factors, decreases the modeling mismatch, and extends the frequency bandwidth of the systems. The model of disturbance is not required when the CFDO is designed. As a typical kind of servo motor system, the theoretic results in flight simulator can be used in other servo motion control systems.

The brief outline of the paper is as follows. In Section 2, the fuzzy disturbance observer is introduced. In Section 3, the control problem is formulated. Then, the structure and design of CFDO are proposed. In Section 4, experimental results are included to support the theoretical work. Finally, the paper is concluded in Section 5.

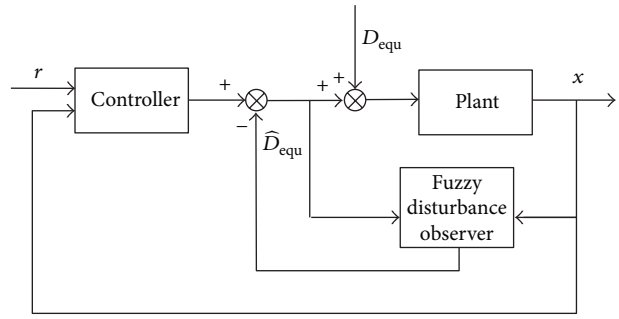

Figure 1: Structure of the control system with fuzzy disturbance observer.

2. Fuzzy Disturbance Observer

Consider a system described as

$$\dot{x}_1 = x_2, \tag{1}$$

$$\dot{x}_2 = [\alpha(x_2) + \Delta A(x)] + [\beta(x_2) + \Delta B(x)]\, u + d_{\text{ext}}, \tag{2}$$

where u denotes controller output, $x = (x_1, x_2)^T$ denotes state vector of the system, $\alpha(x_2)$ and $\beta(x_2)$ are decided by nominal model, $\Delta A(x)$ and $\Delta B(x)$ denote the internal unknown time-varying nonlinear dynamics, and d_{ext} denotes generalized external disturbance. In the viewpoint of disturbance observer, both internal uncertainty and external disturbance can be defined as equivalent disturbance, and the system can be written as

$$\dot{x}_2 = \alpha(x_2) + \beta(x_2)\left(u + D_{\text{equ}}\right), \tag{3}$$

where $D_{\text{equ}} = [\Delta A(x) + \Delta B(x)u + d_{\text{ext}}]/\beta(x_2)$ is the nonlinear equivalent disturbance in controller output terminal and cannot be described by mathematical expressions in general. A fuzzy logic is used as a solution to approximate the nonlinear disturbance as an FDO.

Figure 1 shows the structure of FDO. From the structure, the equivalent disturbance can be compensated sufficiently, and the system has the same dynamics as the nominal model in the case of the fuzzy system $\widehat{D}_{\text{equ}}$ follows the disturbance D_{equ} completely.

In order to achieve the compensation, the estimated value can be obtained by fuzzy logic system, which is described briefly here. The fuzzy inference engine uses the fuzzy IF-THEN rules to perform a mapping from an input compact set $x = (x_1, x_2, \ldots, x_n)^T \in R^n$ to an output variable $z \in R$. The fuzzy rules can be described as

$$R^i : \text{If } x_1 \text{ is } K_1^i \text{ and} \cdots \text{and } x_n \text{ is } K_n^i, \text{then } z \text{ is } z_i, \tag{4}$$

where $K_1^i, K_2^i, \ldots, K_n^i$ are fuzzy variables and z_i is a singleton number. By using product inference engine, center-average

defuzzifier, and singleton fuzzifier, the output of the fuzzy system can be expressed as

$$z(x) = \frac{\sum_{i=1}^{M} z_i \left(\prod_{j=1}^{n} \mu_{K_j^i}(x_j)\right)}{\sum_{i=1}^{M} \left(\prod_{j=1}^{n} \mu_{K_j^i}(x_j)\right)} = \widehat{\theta}^T \xi(x), \tag{5}$$

where $\mu_{K_j^i}(x_j)$ is membership function value of the fuzzy variable x_j, M is the number of fuzzy rules, $\widehat{\theta}^T = (z_1, z_2, \ldots, z_M)$ denote adjustable parameter vector, and $\xi(x) = (\xi_1(x), \xi_2(x), \ldots, \xi_M(x))^T$ denote fuzzy basis functions defined by

$$\xi^i = \frac{\prod_{j=1}^{n} \mu_{K_j^i}(x_j)}{\sum_{i=1}^{M} \left(\prod_{j=1}^{n} \mu_{K_j^i}(x_j)\right)}. \tag{6}$$

In order to design an FDO, a tuning method must be developed for the adjustable parameter vector. Consider the following dynamic system (7):

$$\dot{\mu} = -\sigma\mu + \sigma x_2 + \alpha(x_2) + \beta(x_2)\left(u + \widehat{D}_{\text{equ}}\right). \tag{7}$$

Define disturbance observation error as $\varsigma \equiv x_2 - \mu$. Obviously, $\varsigma \to 0 (\mu \to x_2)$ implies that the estimated disturbance value $\widehat{D}_{\text{equ}}$ approaches the actual but unknown disturbance D_{equ}.

The disturbance observation error ς is uniformly ultimately bounded within a region, which size can be kept arbitrarily small, if the adjustable parameter vector of the FDO is tuned by (8) and bounded. To ensure the FDO outputs zero signal in case of $D_{\text{equ}} = 0$ (perfect matching), the adjustable parameter vector is set to zero as (9). The correlated proof can be found in [14]. Consider

$$\dot{\widehat{\theta}} = \gamma\varsigma\xi(x, u), \tag{8}$$

$$\widehat{\theta}(0) = 0, \tag{9}$$

As a typical servo system, a flight simulator system can be described as

$$J_n\ddot{\theta} + B_n\dot{\theta} = u + d, \tag{10}$$

where d is the nonlinear equivalent disturbance in controller output terminal, J_n is the nominal inertia, and B_n is the nominal damping. Define $x_1 = \theta$, $x_2 = \dot{\theta}$, it is significant that the system (10) is a special case of system (2), and the FDO can be designed as is stated previously.

The FDO makes system response the same as the nominal model. Compared with DOB, FDO-based control has advantages on the robust stability and static performance when the system lacks mechanical stiffness. Unfortunately, some flight simulator systems are elastic electromechanical systems, and the use of DOB is restricted. Therefore, the FDO helps to improve the static performance and robustness of these flight simulators.

However, the nonlinear disturbance, such as friction, is composed of the components of many frequencies. The high-frequency components limit the system performance and the effect of FDO is limited in practice [27]. Therefore, disturbance compensation method with better effect is expected.

3. Compound Fuzzy Disturbance Observer

Consider the flight simulator system (10) with the help of FDO, it can be described as (11), where $\widehat{d}$ is the estimated disturbance by FDO. The difference between the observer value d and the equivalent disturbance $\widehat{d}$ should be compensated. Define a secondary system as (12), where u_c is the objective control value to make $e \to 0$. In this case, u_c is expected to $d - \widehat{d}$. Consider

$$J_n\ddot{\theta} + B_n\dot{\theta} = u + d - \widehat{d}, \tag{11}$$

$$J_n\ddot{\theta}_n + B_n\dot{\theta}_n = u + u_c, \tag{12}$$

$$e = \theta - \theta_n. \tag{13}$$

Define the sliding surface as (14), where $c = B_n/J_n$. Then the objective turns into making $w \to 0$. The control value is designed as (15), where κ is a positive constant gain, ψ is the positive switching gain, ε is a small constant that communicates with the boundary layer near the sliding mode surface, and sat($\bullet$) is the saturation function defined as (16):

$$w = \dot{e} + ce, \tag{14}$$

$$u_c = \kappa w + \psi \operatorname{sat}\left(\frac{\psi w}{4\varepsilon}\right), \tag{15}$$

$$\operatorname{sat}(\bullet) = \begin{cases} 1, & \bullet \geq 1 \\ \bullet, & |\bullet| < 1 \\ -1, & \bullet \leq -1. \end{cases} \tag{16}$$

According to (11)~(15), there is (17). Define a positive definite Lyapunov candidate (18); its time derivative is obtained as (19):

$$\begin{aligned} J_n\dot{w} &= J_n\ddot{\theta}_n + B_n\dot{\theta}_n - \left(J_n\ddot{\theta} + B_n\dot{\theta}\right) \\ &= -\kappa w - \psi \operatorname{sat}\left(\frac{\psi w}{4\varepsilon}\right) + \widehat{d} - d, \end{aligned} \tag{17}$$

$$V(w) = \frac{1}{2}J_n w^2, \tag{18}$$

$$\dot{V}(w) = wJ_n\dot{w} \leq -\kappa w^2 - w\psi \operatorname{sat}\left(\frac{\psi w}{4\varepsilon}\right) + |w|\left|\widehat{d} - d\right|, \tag{19}$$

$$\psi \geq \left|\widehat{d} - d\right|. \tag{20}$$

Suppose that (20) is satisfied; the analysis of (19) is discussed as follows.

If $|w| \geq 4\varepsilon/\psi$ and $\psi \geq |\widehat{d} - d|$, there is (21). From (21) and considering $|w| \geq 4\varepsilon/\psi$, there is (22):

$$\begin{aligned} \dot{V}(w) &= -\kappa w^2 - |w|\left(\psi - \left|\widehat{d} - d\right|\right) \\ &\leq -\kappa w^2 = -2\frac{\kappa}{J_n}V(w) \leq 0, \end{aligned} \tag{21}$$

$$\lim_{t\to\infty} |w(t)| \leq \frac{4\varepsilon}{\left|\widehat{d} - d\right|}. \tag{22}$$

If $|w| \le 4\varepsilon/\psi$ and $\psi \ge |\widehat{d} - d|$, there is (23). According to the solution of the differential inequality, there is (24) and (25):

$$\begin{aligned}\dot{V}(w) &= -\kappa w^2 - \frac{\psi^2|w|^2}{4\varepsilon} + |w|\left|\widehat{d} - d\right| \\ &\le -\kappa w^2 - \frac{\psi^2|w|^2}{4\varepsilon} + |w|\psi \\ &= -\kappa w^2 - \frac{1}{\varepsilon}\left(\frac{\psi|w|}{2} - \varepsilon\right)^2 + \varepsilon \\ &\le -\kappa w^2 + \varepsilon = -2\frac{\kappa}{J_n}V(w) + \varepsilon,\end{aligned} \tag{23}$$

$$w^2(t) \le w^2(0)\exp\left(-\frac{2\kappa}{J_n}t\right) + \frac{\varepsilon}{\kappa}\left[1 - \exp\left(-\frac{2\kappa}{J_n}t\right)\right], \tag{24}$$

$$\lim_{t\to\infty}|w(t)| \le \sqrt{\frac{\varepsilon}{\kappa}}. \tag{25}$$

Consequently, if (20) is satisfied, w exponentially converges and satisfied (25). By the definition of w, e exponentially converges and satisfied (26). Therefore, the compound disturbance observer can be designed if (20) is satisfied:

$$\lim_{t\to\infty}|e(t)| \le \frac{1}{c}\sqrt{\frac{\varepsilon}{\kappa}}. \tag{26}$$

The expression (20) should be satisfied; that is, the switching gain is related to the difference between equivalent disturbance and observer value of FDO. From the process of FDO design, the difference aforementioned are decided by the disturbance observation error ς. Therefore, the estimation of upper bound which is used to design sliding mode controller can be got by ς. When the disturbance observation error disappears after some time, the switching gain of the SMC can be kept in a small value. And further, the chattering phenomenon can be decreased. The expression (27) gives the description of the switching gain in this paper, where η is the magnification coefficient that can be tried in practice. The whole structure of CFDO is showed in Figure 2. Consider

$$\psi = \eta\varsigma. \tag{27}$$

4. Experiment Results

In order to test the effect of the proposed method, an experiment is implemented by using a three-axis flight simulator shown in Figure 3. The optical-electrical encoder with resolution of 0.0007 degrees is employed as the position sensor. The program of control algorithm is written with C language based on Windows-RTX real-time system in an industrial computer (Advantech IPC 610), which connects with the servo drivers by a 16-bit D/A convertor of PCI bus. The control cycle is 0.001s.

As in the previous discussion, FDO monitors both the internal and the external disturbance so that each axis of the flight simulator can be designed independently. Therefore, the pitch axis is chosen herein to verify the method. The controller design is based on the parameters which are acquired by identifying the flight simulator. The parameters of the nominal model are identified as $J_n = 0.0172$, $B_n = 0.0948$. The fitting curves for frequency characteristics of actual plant and nominal model are shown in Figure 4. A PD controller is used as a position controller and $K_p = 0.65$, $K_d = 0.03$. The membership functions shown in Figure 5 are selected for the premise parts of the FDO. Other factors employed in the experiment are given as follows: $\sigma = 15$, $\gamma = 350$, $\kappa = 10$, and $\eta = 1.1$. A nonlinear tracking differential estimator is used to get differential value [28], and the nonlinear tracking differential gain is $g_v = 400$. The accuracy of the static position, the stationarity of the static velocity, and the dynamic frequency are the most important indexes to a flight simulator. Generally, the static position accuracy can be guaranteed by a stable disturbance observer.

Figure 6 shows the curves of the steady-state speed under DOB, FDO, and CFDO schemes, respectively. In this case, the reference signal is constant and the response curves tracking with the velocity of 1°/s as well. All of the systems can reach the position command value ultimately.

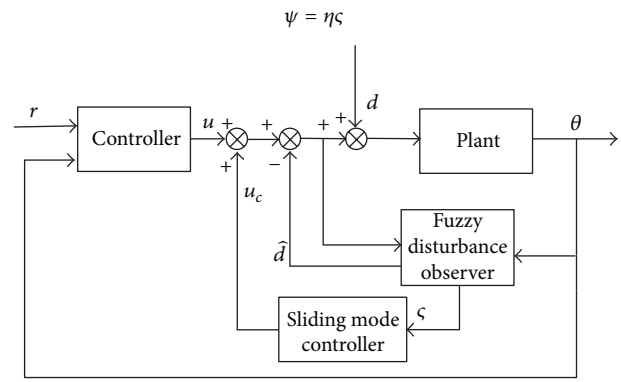

Figure 2: Structure of the control system with compound fuzzy disturbance observer.

Figure 3: The three-axis flight simulator.

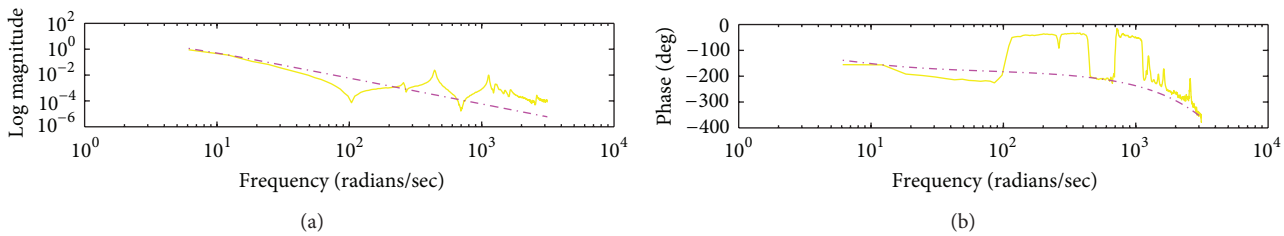

(a) (b)

Figure 4: The fitting curves for frequency characteristics of actual plant and nominal model.

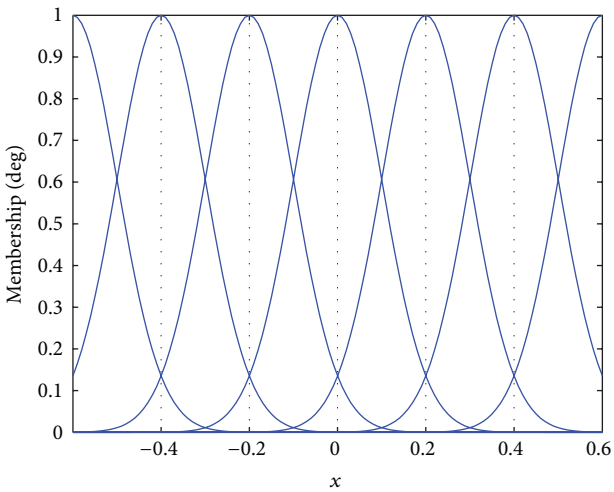

Figure 5: Gaussian membership functions.

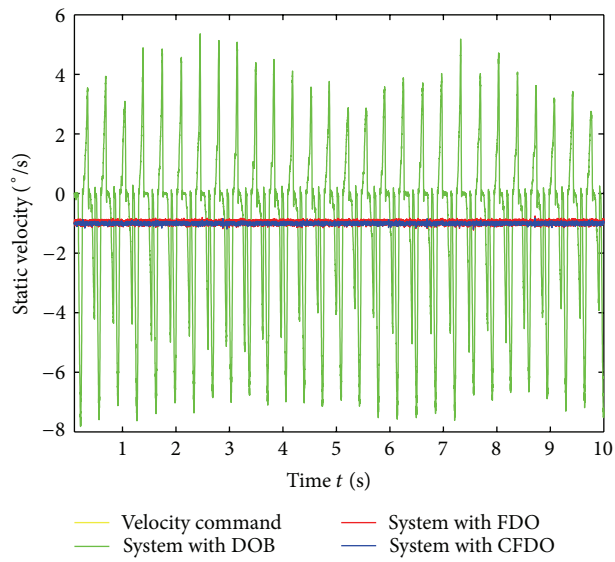

Figure 6: The curves of the steady-state speed under DOB, FDO, and CFDO schemes.

However, the DOB scheme has a oscillatory speed because of the influence of elasticity. The FDO and CFDO schemes can keep a stable speed while tracking and it is the effect of FDO as the sliding mode part almost has no effect in static condition. Compared with traditional DOB scheme, the proposed method has better robustness as FDO is a nonlinear approach and decreases the modeling mismatch. Evidently, reducing the effect of DOB helps to decrease the oscillation while restricting the performance of the system.

Figure 7 compares the tracking error and the control value of the FDO and CFDO schemes when the reference signal is described as $2\sin(2\pi \cdot 0.5t)$. The figure shows that the maximum tracking error under the FDO scheme approximately equals 0.037 deg while that decreases to 0.028 deg using the proposed CFDO. The tracking error indicates that the system with CFDO has better dynamic performance than the system with only FDO. Furthermore, the control value of the CFDO system does not exhibit obvious chattering phenomenon compared with the value of the FDO system. The system performance is effected by FDO primarily, and the sliding mode controller whose switching gain is restricted in a small range only assists secondarily.

Figure 8 shows the tracking error and the control value of the two systems when the reference signal is described as $2\sin(2\pi \cdot 4t)$. High-frequency disturbance, treated by SMC, is the main problem in this environment. The figure shows that the maximum tracking error under the FDO scheme approximately equals 0.652 deg while that decreases to 0.203 deg using the proposed CFDO. From the comparison of the two error curves, the CFDO system has better dynamic performance and the frequency range is extended with the help of SMC. Inevitably, chattering phenomenon can hardly be alleviated for the SMC need to recover rapidly.

Neither the steady-state error of FDO nor the error of CFDO is influenced by the extra constant disturbance, as FDO compensates the constant disturbance over time. However, under the condition of small time-varying disturbance like Figure 8, CFDO has better performance than FDO as the sliding mode controller deals with the high-frequency disturbance rapidly. According to Figures 7 and 8, changes of working frequency have less influence under CFDO scheme than under FDO scheme; that is, the system with CFDO has better robustness than the system with FDO.

The part of sliding mode controller compensates the high-frequency component of disturbance and improves not only the robustness but also the dynamic performance of the system, meanwhile, the FDO deals with the low-frequency

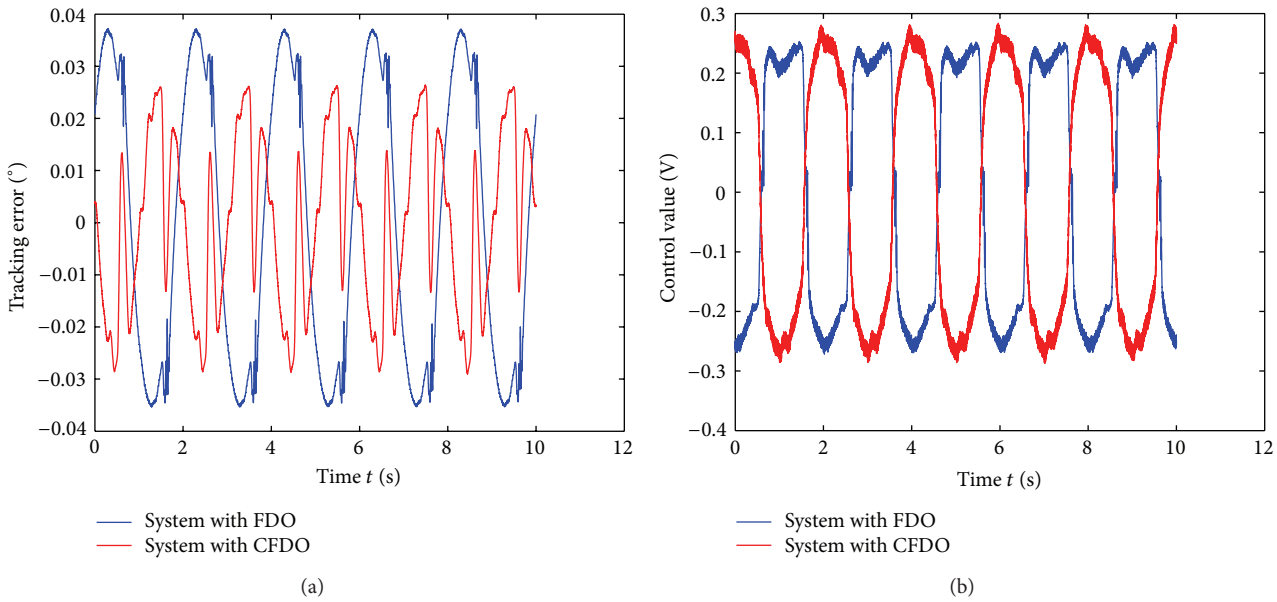

FIGURE 7: The comparison of error curves and control value in the case of sin input ($A = 2$, $f = 0.5$).

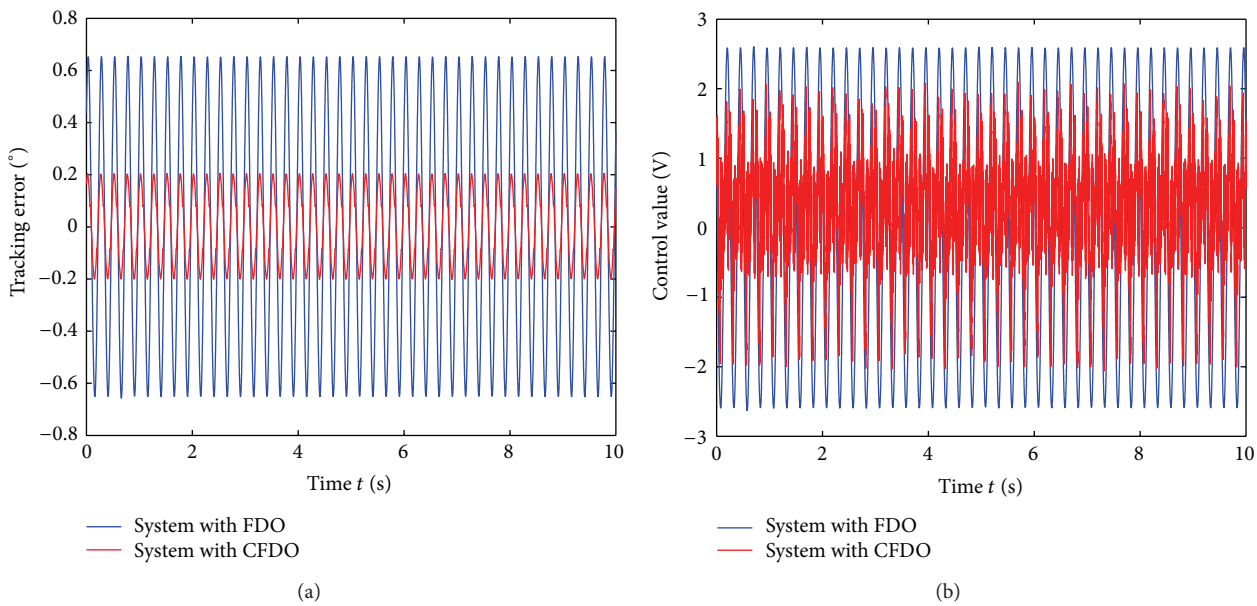

FIGURE 8: The comparison of error curves and control value in the case of sin input ($A = 2$, $f = 4$).

component of disturbance and helps to weaken the chattering. In consequence, they help each other to compensate the equivalent disturbance.

To a flight simulator system, the references are often slow-varying signals, which can be seen as static signals, in most part of an aircraft trajectory. In the last part of the trajectory, there will be fast-varying signals. CFDO meets the demand of these systems perfectly: FDO guarantees the accuracy, chattering is limited in most part of time, and SMC helps the system to respond fast while facing enormous variations.

5. Conclusion

This paper proposes a compound fuzzy disturbance observer based on sliding modes. The equivalent disturbance is sufficiently compensated by using the proposed CFDO when there exists huge modeling mismatch, and the disadvantages of FDO and SMC are avoided. The performance, especially the accuracy, of the system is improved. The switching gain of sliding mode controller is designed by disturbance estimation error, and the reduction of switching gain helps to weaken the chattering.

The method has been validated by experiments. By using the proposed method, the maximum tracking error decreases from 0.037 deg to 0.028 deg in low-frequency condition with the reference of $2\sin(2\pi \cdot 0.5t)$, and from 0.652 deg to 0.203 deg in high-frequency condition with the reference of $2\sin(2\pi \cdot 4t)$. Most servo motion control systems have similar characteristics as flight simulator; therefore, the theoretic results are able to be extended to other relational fields such as mechanical arm systems, camera tracking systems, and other servo motion control systems, especially those with high-precision requirement and deficient mechanical stiffness.

However, the coefficient about the fuzzy disturbance observer error can only be decided by trying in practice and an unsuitable parameter may lead to performance degradation or make the system unstable. In future work, better ways to decide switching gain will be studied and the fuzzy adjustable method will be optimized.

Acknowledgment

This work was supported by the National Natural Science Foundation of China (Grant no. 91216304).

References

[1] Q. Liu and L. Er, "Disturbance observer based robust tracking control of high precision flight simulator," *Journal of Beijing University of Aeronautics and Astronautics*, vol. 29, no. 2, pp. 181–184, 2003 (Chinese).

[2] T. R. Grochmal and A. F. Lynch, "Precision tracking of a rotating shaft with magnetic bearings by nonlinear decoupled disturbance observers," *IEEE Transactions on Control Systems Technology*, vol. 15, no. 6, pp. 1112–1121, 2007.

[3] K.-S. Kim, K.-H. Rew, and S. Kim, "Disturbance observer for estimating higher order disturbances in time series expansion," *IEEE Transactions on Automatic Control*, vol. 55, no. 8, pp. 1905–1911, 2010.

[4] T. Umeno, T. Kaneko, and Y. Hori, "Robust servosystem design with two degrees of freedom and its application of novel motion control of robot manipulators," *IEEE Transactions on Industrial Electronics*, vol. 40, no. 5, pp. 473–485, 1993.

[5] X. Zeng and M. G. Singh, "Approximation theory of fuzzy systems-MIMO case," *IEEE Transactions on Fuzzy Systems*, vol. 3, no. 2, pp. 219–235, 1995.

[6] L. Wu, X. Su, P. Shi, and J. Qiu, "Model approximation for discrete-time state-delay systems in the TS fuzzy framework," *IEEE Transactions on Fuzzy Systems*, vol. 19, no. 2, pp. 366–378, 2011.

[7] S. Y. Cho, C. W. Ting, and C. Quek, "Thermal facial pattern recognition for personal verification using fuzzy cmac model," *International Journal of Innovative Computing, Information and Control*, vol. 7, no. 1, pp. 203–222, 2011.

[8] M. J. Wang and M. F. Yang, "Application of signed distances method to integrate linear programming for fuzzy multi-objective project management," *International Journal of Innovative Computing, Information and Control*, vol. 7, no. 1, pp. 237–252, 2011.

[9] T. Niknam, H. D. Mojarrad, and M. Nayeripour, "A new hybrid fuzzy adaptive particle swarm optimization for non-convex economic dispatch," *International Journal of Innovative Computing, Information and Control*, vol. 7, no. 1, pp. 189–202, 2011.

[10] X. Su, P. Shi, L. Wu, and Y.-D. Song, "A novel control design on discrete-time Takagi-Sugeno fuzzy systems with time-varying delays," *IEEE Transactions on Fuzzy Systems*, 2012.

[11] L. Wu, X. Su, P. Shi, and J. Qiu, "A new approach to stability analysis and stabilization of discrete-time T-S fuzzy time-varying delay systems," *IEEE Transactions on Systems, Man, and Cybernetics B*, vol. 41, no. 1, pp. 273–286, 2011.

[12] M. H. Bahari, A. Karsaz, and N. Pariz, "High maneuvering target tracking using a novel hybrid Kalman filter-fuzzy logic architecture," *International Journal of Innovative Computing, Information and Control*, vol. 7, no. 2, pp. 501–510, 2011.

[13] X. Su, P. Shi, L. Wu, and Y.-D. Song, "A novel approach to filter design for T-S fuzzy discrete-time systems with time-varying delay," *IEEE Transactions on Fuzzy Systems*, vol. 20, no. 6, pp. 1114–1129, 2012.

[14] E. Kim, "A fuzzy disturbance observer and its application to control," *IEEE Transactions on Fuzzy Systems*, vol. 10, no. 1, pp. 77–84, 2002.

[15] B. S. Chen, H. J. Uang, and C. S. Tseng, "Robust tracking enhancement of robot systems including motor dynamics: a fuzzy-based dynamic game approach," *IEEE Transactions on Fuzzy Systems*, vol. 6, no. 4, pp. 538–552, 1998.

[16] R. Ordonez and K. M. Passino, "Stable multi-input multi-output adaptive fuzzy/neural control," *IEEE Transactions on Fuzzy Systems*, vol. 7, no. 3, pp. 345–353, 1999.

[17] T. C. Lin, S. W. Chang, and C. H. Hsu, "Robust adaptive fuzzy sliding mode control for a class of uncertain discrete-time nonlinear systems," *International Journal of Innovative Computing, Information and Control*, vol. 8, no. 1, pp. 347–359, 2012.

[18] Q. Khan, A. I. Bhatti, M. Iqbal, and Q. Ahmed, "Dynamic integral sliding mode control for SISO uncertain nonlinear systems," *International Journal of Innovative Computing, Information and Control*, vol. 8, no. 7, pp. 4621–4633, 2012.

[19] Y. Wu, W. Le, and D. Tian, "Application of sliding mode control based on disturbance observer on high performance flight motion simulator," in *Proceedings of the IEEE International Conference on Automation and Logistics (ICAL '07)*, pp. 2695–2699, August 2007.

[20] A. Hace, K. Jezernik, and A. Sabanovic, "SMC with disturbance observer for a linear belt drive," *IEEE Transactions on Industrial Electronics*, vol. 54, no. 6, pp. 3402–3412, 2007.

[21] Z. L. He, J. F. Wu, G. H. Sun, and C. Gao, "State estimation and sliding mode control of uncertain switched hybrid systems," *International Journal of Innovative Computing, Information and Control*, vol. 8, no. 10, pp. 7143–7156, 2012.

[22] K. D. Young, V. I. Utkin, and U. Ozguner, "A control engineer's guide to sliding mode control," *IEEE Transactions on Control Systems Technology*, vol. 7, no. 3, pp. 328–342, 1999.

[23] X. Chen, S. Komada, and T. Fukuda, "Design of a nonlinear disturbance observer," *IEEE Transactions on Industrial Electronics*, vol. 47, no. 2, pp. 429–437, 2000.

[24] S. J. Lopez, O. C. Nieto, and J. I. C. Oria, "Non-parametric modeling of uncertain hyperbolic partial differential equations using pseudo-high order sliding mode observers," *International Journal of Innovative Computing, Information and Control*, vol. 8, no. 3, pp. 1501–1521, 2012.

[25] M. Zhihong, X. H. Yu, K. Eshraghian, and M. Palaniswami, "A robust adaptive sliding mode tracking control using an RBF

neural network for robotic manipulators," in *Proceedings of the IEEE International Conference on Neural Networks*, pp. 2403–2408, December 1995.

[26] V. Panwar, "Asymptotic trajectory tracking for a robot manipulator using RBF neural network and adaptive bound on disturbances," in *Proceedings of the International Conference on Mechanical and Electrical Technology (ICMET '10)*, pp. 156–160, September 2010.

[27] Z. Jamaludin, H. van Brussel, and J. Swevers, "Friction compensation of an XY feed table using friction-model-based feedforward and an inverse-model-based disturbance observer," *IEEE Transactions on Industrial Electronics*, vol. 56, no. 10, pp. 3848–3853, 2009.

[28] D. Tian, D. Yashiro, and K. Ohnishi, "New nonlinear tracking differential-estimators: theory and practice," *International Journal of Innovative Computing, Information and Control*, vol. 8, no. 12, pp. 8257–8271, 2012.

Hindawi Publishing Corporation
Mathematical Problems in Engineering
Volume 2013, Article ID 958958, 8 pages
http://dx.doi.org/10.1155/2013/958958

Research Article

Terminal Sliding Mode Control Using Adaptive Fuzzy-Neural Observer

Dezhi Xu, Bin Jiang, Moshu Qian, and Jing Zhao

College of Automation Engineering, Nanjing University of Aeronautics and Astronautics, Nanjing 210016, China

Correspondence should be addressed to Bin Jiang; ebjiang@yahoo.com

Received 31 October 2012; Revised 27 December 2012; Accepted 27 December 2012

Academic Editor: Peng Shi

Copyright © 2013 Dezhi Xu et al. This is an open access article distributed under the Creative Commons Attribution License, which permits unrestricted use, distribution, and reproduction in any medium, provided the original work is properly cited.

We propose a terminal sliding mode control (SMC) law based on adaptive fuzzy-neural observer for nonaffine nonlinear uncertain system. First, a novel nonaffine nonlinear approximation algorithm is proposed for observer and controller design. Then, an adaptive fuzzy-neural observer is introduced to identify the simplified model and resolve the problem of the unavailability of the state variables. Moreover, based on the information of the adaptive observer, the terminal SMC law is designed. The Lyapunov synthesis approach is used to guarantee a global uniform ultimate boundedness property of the state estimation error and the asymptotic output tracking of the closed-loop control systems in spite of unknown uncertainties/disturbances, as well as all the other signals in the closed-loop system. Finally, using the designed terminal sliding mode controller, the simulation results on the dynamic model demonstrate the effectiveness of the proposed new control techniques.

1. Introduction

Sliding mode control (SMC) is known to be a robust control scheme applicable for controlling uncertain systems. Great robustness is provided against various categories of uncertainties such as external disturbances and measurement errors [1–7]. It is also straightforward to execute the resulting algorithms. The dynamics performance of a SMC system is affected by the suggested sliding manifolds upon which the control structure is switched. The most normally used sliding manifolds are linear hyperplanes. Such hyperplanes ensure the asymptotic stability of the sliding mode. Nonlinear switching manifolds may give increase to a better control performance, provided the nonlinearity is added purposefully. The terminal sliding mode concept has been suggested to focus the finite time control [8]. However, SMC techniques cannot provide satisfactory results when suffering poorly modeling unless the designers know the bounds of uncertainty.

Since fuzzy logic systems (FLSs) and neural networks (NNs) are universal function approximators [9–16], the adaptive control methods of nonlinear systems that integrate the universal function approximators have developed quickly [2, 13, 17]. The main improvement of using universal function approximators is to eliminate the linear-in-the-parameters form on unknown nonlinearities of the controlled pant. Thus, the class of nonlinear systems to which the adaptive control technique can be employed is improved by using universal function approximators. Another benefit is that we can use conventional and advanced adaptive techniques with a novel robust action which compensates the errors.

In fact, most of the works in the fuzzy/neural control are dedicated to the control problem for the affine nonlinear systems, that is, systems characterized by inputs appearing linearly in the system input-output equation. Few results are accessible for nonaffine nonlinear systems in which the control input occurs in a nonlinear fashion. In this paper, a novel dynamic model approximation method is first proposed to approximate the nonaffine nonlinear dynamics, which is a solution that bridges the gap between affine and nonaffine control systems. Then we combine the FLSs and NNs, and adaptive techniques proposed an adaptive fuzzy-neural observer for nonaffine nonlinear systems. Because in many control problems, state variables may be partly unavailable. So an adaptive observer is designed, and it entails simultaneous estimation of parameters and unknown state variables. The update laws of fuzzy-neural network (FNN) parameters provide the Lyapunov stability for the closed-loop

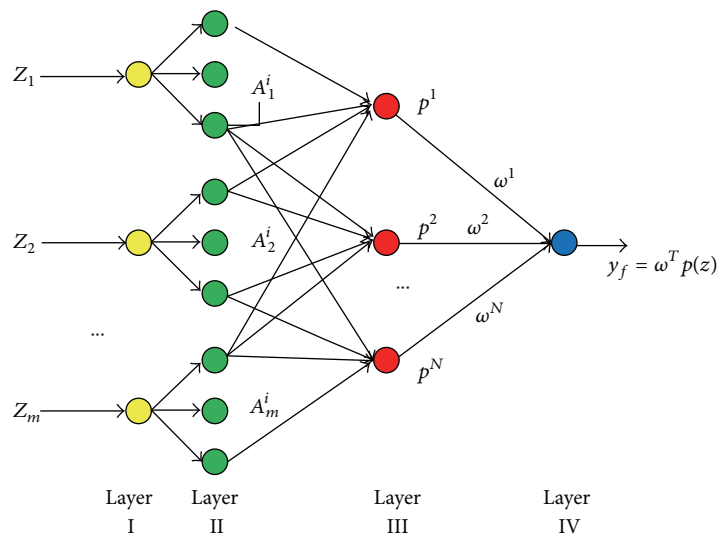

Figure 1: Functional link of a fuzzy-neural network structure.

system and guarantee that all signals involved are globally uniformly ultimately bounded. Using terminal SMC, based on the adaptive FNN observer, the robust tracking controller is designed.

The rest of this paper is organized as follows. First, a brief descriptions of the fuzzy-neural network system. Main results include a novel dynamic model approximation technique, adaptive fuzzy-neural observer, and an SMC control algorithm which are proposed in Section 3. In Section 4, simulation results are presented to show the effectiveness of the proposed technique. Finally, some conclusions are made at the end of this paper.

2. Background

2.1. Fuzzy-Neural Network for Approximation. Figure 1 depicts a functional link FNN which consists of fuzzy logic and neural network. The FLS can be divided into two parts: some fuzzy IF-THEN rules and a fuzzy inference engine. The fuzzy inference engine uses the fuzzy IF-THEN rules to perform a mapping from an input linguistic vector $z = [z_1, \ldots, z_m]^T \in \Re^m$ to a scalar output variable $y_f \in \Re$. The ith fuzzy IF-THEN rule can be characterized by the following form [16]:

$$\begin{aligned} &\text{IF } z_1 \text{ is } A_1^i \text{ and} \cdots \text{and} \quad z_m \text{ is } A_m^i \\ &\text{THEN } y_f \text{ is } B^i \quad (i = 1, \ldots, N), \end{aligned} \tag{1}$$

where A_j^i, B^i are fuzzy sets. By using product inference, center-average and singleton fuzzifier, N is the total number of rules. Then the output of the FNN can be expressed as

$$y_f = \frac{\sum_{i=1}^N \omega^i \left[\prod_j^m \mu_{A_j^i}(z_j)\right]}{\sum_{i=1}^N \left[\prod_j^m \mu_{A_j^i}(z_j)\right]} = W^T P(z), \tag{2}$$

where $\mu_{A_j^i}(z_j)$ is the membership function value of the fuzzy variable, ω^i is the point at which $\mu_{B^i}(\omega^i) = 1$, and $W = [\omega^1, \omega^2, \ldots, \omega^N]$ is an adjustable parameter vector. We assume that an upper limit $\|\varepsilon(z)\| \le \varepsilon_M$ of the functional reconstruction error is known. $P = [p^1, p^2, \ldots, p^N]$ is a fuzzy basis vector, where p^i is defined as

$$p^i(z) = \frac{\prod_j^m \mu_{A_j^i}(z_j)}{\sum_{i=1}^N \left[\prod_j^m \mu_{A_j^i}(z_j)\right]}. \tag{3}$$

The truth value p^i (layer III) of the antecedent part of the ith implication is calculated by (3). Among the commonly used defuzzification strategies, the output (layer IV) of the FNN is expressed as (2). The fuzzy logic approximator based on the neural network can be established. The approximator has four layers. At layer I, nodes, which are input ones, stand for the input linguistic variables. At layer II, nodes represent the values of the membership function value. At layer III, nodes are the values of the fuzzy basis vector. Each node of layer III performs a fuzzy rule. The links between layer III and layer IV are full connected by the weighting vector. ω, that is, the adjusted parameters. At layer IV, the output stands for the value of y_f.

3. Main Results

Consider the nonaffine nonlinear system represented in the following normal form:

$$\begin{aligned} \dot{x}_i &= x_{i+1}, \quad i = 1, 2, \ldots, n-1, \\ \dot{x}_n &= f(x, u) + d(t), \\ y &= x_1, \end{aligned} \tag{4}$$

or equivalently in observer canonical form given by

$$\dot{x} = Ax + b\left[f(x,u) + d(t)\right],$$
$$y = c^T x, \tag{5}$$

where

$$A = \begin{bmatrix} 0 & 1 & 0 & \cdots & 0 \\ 0 & 0 & 1 & \cdots & 0 \\ & & & \cdots & \\ 0 & 0 & 0 & \cdots & 1 \\ 0 & 0 & 0 & \cdots & 0 \end{bmatrix}, \quad b = \begin{bmatrix} 0 \\ 0 \\ \vdots \\ 0 \\ 1 \end{bmatrix}, \quad c = \begin{bmatrix} 1 \\ 0 \\ \vdots \\ 0 \\ 0 \end{bmatrix}, \tag{6}$$

and $x = [x_1, \ldots, x_n]^T \in \mathfrak{R}^n$ is the state vector of the system in the normal form which is assumed to be available for measurement, $u \in \mathfrak{R}$ is the control input assumed to have an upper bound $\overline{u}$ (i.e., $|u| \le \overline{u}$), $y \in \mathfrak{R}$ is the system output, and $f(x,u)$ is an unknown smooth nonlinear function. $d(t)$ denotes the external disturbance.

Observer-based model identification methods have been proposed in affine nonlinear systems in [18, 19]. However, using such observers to identify for nonaffine nonlinear systems is not an easy thing. And in many practical situations, state variables are often unavailable in nonlinear systems. Thus, observer-based adaptive fuzzy control is required for such complicated applications. In this section, in order to design robust tracking controller for unknown nonaffine nonlinear uncertain systems, a new model-free control design method is firstly proposed based on sliding mode technology.

3.1. Novel Nonaffine Nonlinear Approximation. The problem of controlling the plants characterized by models that are nonaffine in the control input vector is a difficult one. For the tracking control especially, the linearization may result in the design of sufficiently accurate controllers in the case of stabilization around the operating point; in the case of tracking of desired trajectories, the problem becomes much more difficult because the linearized model is time-varying. Hence, there is a clear need for the development of systematic control design techniques for nonlinear models that are nonaffine in u and that are suitable for the case of tracking of desired trajectories.

For the nonaffine nonlinear model (4), the Taylor expansion of the nonlinear function $f[x(t), u(t)]$ with respect to $u(t)$ around $u(t-\tau)$ can result in

$$\dot{x}_i = x_{i+1},$$
$$\dot{x}_n = f(x, u(t-\tau)) + f_d(x, u(t-\tau))\Delta u + R_p + d, \tag{7}$$

where $\Delta u = u - u(t-\tau)$, $f_d(x, u(t-\tau)) = \partial f(x,u)/\partial u|_{u=u(t-\tau)}$, and the remainder $R_p = f_{dd}\Delta u^2/2$ is bounded by

$$\left|R_p\right| \le \frac{r_p \Delta u^2}{2}, \tag{8}$$

where $f_{dd} = \partial^2 f(x,u)/\partial^2 u|_{u=\zeta}$, ζ is a point between u and $u(t-\tau)$. Let $0 \le |f_{dd}| \le r_p$ with r_p be a finite positive number. The parameter $\tau > 0$ is the updating input. It may be chosen as the sampling time in a sampled-data control system or as an integer multiple of the sampling time. A better choice of the parameter τ is the sampling because a larger τ may lead to an inaccurate approximation when the system function $f(x,u)$ varies quickly.

It is easy that (7) can be representation as the following form:

$$\dot{x}_i = x_{i+1},$$
$$\dot{x}_n = f_n(x, u(t-\tau)) + f_d(x, u(t-\tau))u + d_\xi(t), \tag{9}$$

where $d_\xi(t) = R_p + d(t)$ and

$$f_n(x, u(t-\tau)) = f(x, u(t-\tau)) - f_d(x, u(t-\tau))u(t-\tau). \tag{10}$$

In this paper, we assume that $|d_\xi(t)| \le d_M$. To approximation accuracy, control input must satisfy the following assumption.

Assumption 1. Consider that $|\Delta u| \in [0, \delta]$ and $0 < |\partial f/\partial u| \le \beta$; δ and β are two finite positive constants.

In Assumption 1, $0 < |\partial f/\partial u| \le \beta$ means that the system (4) has a well-defined relative degree. $|\Delta u|$ should not be too large in order to limit the approximation error of the model (9) for a computed $u(t)$. In many actual process control systems and flight control systems, $|\Delta u(t)| \in [0, \delta]$ is a physical restriction of many practical systems because their states and outputs (actuators) cannot change too fast because of system "inertia".

Convenient for the following statements, $u(t-\tau)$ is defined as $v(t)$, then (9) can be described as follows:

$$\dot{x}_i = x_{i+1},$$
$$\dot{x}_n = f_n(x, v) + f_d(x, v)u + d_\xi(t). \tag{11}$$

Remark 1. By (9) and Assumption 1, it can be seen that $u(t-\tau)$ should be around the input u. If the time-delay τ is selected too large, the precision of approximation of simplified model will be reduced. So the selection of τ often requires experience. Theoretically, the smaller τ the better precision of global approximation, the best precision of global approximation if $\tau = 0$. But u is a control law to be solved, so it is unable to be realized. In order to obtain exact time-varying trim point, here, further improvement of the above-proposed method is given as follows. Considering lag property of the filtering as

$$\dot{v} = -\lambda v + \lambda u, \tag{12}$$

then $\lim_{\lambda\to\infty} v = u$. This is a very good solution to the problem that $u(t-\tau)$ may be not around u. Here, $\lambda \to \infty$ is only a rigorous expression for mathematics meanings, in general, $\lambda \in [5, 50]$. The filter (12) is not unique. The filtering v can be completely replaced by an other filtering equation, such as higher-order differentiator.

Remark 2. The traditional model simplification method is not global, mainly due to that the simplified model is fixed rather than time-varying model. It can be seen that (11) is a time-varying simplified model. The method which is proposed in this subsection can achieve the global approximation for nonlinear systems (4). So the proposed simplified model method can effectively solve the tracking control problem using affine nonlinear control strategy, such as sliding mode control, output-feedback control, and so on. backstepping control.

3.2. Adaptive Fuzzy-Neural Observer Design. The simplified model (11) can be described as

$$\begin{aligned} \dot{x} &= Ax + b\left[f_n(x,v) + f_d(x,v)u + d_\xi(t)\right], \\ y &= cx. \end{aligned} \tag{13}$$

In order to ascertain subject for further elaboration, we shall use the following vectors, they are $\mathbb{x} = [x^T, v]^T$ and $\widehat{\mathbb{x}} = [\widehat{x}^T, v]^T$.

We approximate the functions $f_n(\mathbb{x})$, $f_d(\mathbb{x})$ by using two fuzzy systems with their input being estimated by $\mathbb{x}$ as follows:

$$f_n(\widehat{\mathbb{x}}) = W_{f_n}^T P_{f_n}(\widehat{\mathbb{x}}), \qquad f_d(\widehat{\mathbb{x}}) = W_{f_d}^T P_{f_d}(\widehat{\mathbb{x}}). \tag{14}$$

The original functions $f_n(\mathbb{x})$ and $f_d(\mathbb{x})$ in (24) can be expressed as

$$\begin{aligned} f_n(\mathbb{x}) &= W_{f_n}^{*T} P_{f_n}(\mathbb{x}) + \varepsilon_{f_n}, \\ f_d(\mathbb{x}) &= W_{f_d}^{*T} P_{f_d}(\mathbb{x}) + \varepsilon_{f_d}, \end{aligned} \tag{15}$$

where ε_{f_n} and ε_{f_d} are the FNN functional reconstruction errors. In general, even given the best possible weight values, the given nonlinear function is not exactly approximated, and functional reconstruction error is remaining. $W_{f_n}^*$ and $W_{f_d}^*$ are the optimal parameter vectors required for analytical purpose satisfying

$$\begin{aligned} W_{f_n}^* &= \arg\min_{W_{f_n}}\left[\sup_{\mathbb{x}\in\Re^{n+1}}\left|f_n(\widehat{\mathbb{x}}) - f_n(\mathbb{x})\right|\right], \\ W_{f_d}^* &= \arg\min_{W_{f_d}}\left[\sup_{\mathbb{x}\in\Re^{n+1}}\left|f_d(\widehat{\mathbb{x}}) - f_d(\mathbb{x})\right|\right] \end{aligned} \tag{16}$$

bounded as $\|W_{f_n}^*\| \le M_{f_n}$, $\|W_{f_d}^*\| \le M_{f_d}$.

Using the FNN approximations, the dynamic equation of a fuzzy-neural observer that estimates the states in (13) is given as follows:

$$\begin{aligned} \dot{\widehat{x}} &= A\widehat{x} + b_0\left[f_n(\widehat{\mathbb{x}}) + f_d(\widehat{\mathbb{x}})u\right] + L\left(y - c^T\widehat{x}\right), \\ \widehat{y} &= c^T\widehat{x}, \end{aligned} \tag{17}$$

where $L = [l_1, l_2, \ldots, l_n]^T$ is the observer gain vector, and b_0 will be designed later.

Defining the state and output estimate errors as $\widetilde{x} = x - \widehat{x}$ and $\widetilde{y} = y - \widehat{y}$ yields the error dynamics from (13) and (17):

$$\begin{aligned} \dot{\widetilde{x}} &= \overline{A}\widetilde{x} + b_0\left[\widetilde{W}_{f_n}^T P_{f_n}(\widehat{\mathbb{x}}) + \widetilde{W}_{f_d}^T P_{f_d}(\widehat{\mathbb{x}})u\right] \\ &\quad + (b - b_0)\left[W_{f_n}^{*T} P_{f_n}(\mathbb{x}) + W_{f_d}^{*T} P_{f_d}(\mathbb{x})u\right] \\ &\quad + b_0\left(d_{f_n} + d_{f_d}u\right) + b\left[d_\xi(t) + \varepsilon_{f_n} + \varepsilon_{f_d}u\right], \end{aligned} \tag{18}$$

where $\overline{A} = A - Lc^T$, $\widetilde{W}_{f_n} = W_{f_n}^* - W_{f_n}$, $\widetilde{W}_{f_d} = W_{f_d}^* - W_{f_d}$, $d_{f_n} = W_{f_n}^{*T}[P_{f_n}(\mathbb{x}) - P_{f_n}(\widehat{\mathbb{x}})]$, and $d_{f_d} = W_{f_d}^{*T}[P_{f_d}(\mathbb{x}) - P_{f_d}(\widehat{\mathbb{x}})]$. In general, the FNN basis function is bounded, for example, radial basis activation function, sigmoidal function, and spline function. This implies that every element of $P(\mathbb{x}) - P(\widehat{\mathbb{x}})$ is bounded, that is, $\|P_{f_n}(\mathbb{x}) - P_{f_n}(\widehat{\mathbb{x}})\| \le \widetilde{P}_{f_n}^M$ and $\|P_{f_d}(\mathbb{x}) - P_{f_d}(\widehat{\mathbb{x}})\| \le \widetilde{P}_{f_d}^M$ with $\widetilde{P}^M$ constant.

In order to construct the vector b_0, the algebraic Ricati-like equation $\overline{A}^T\Gamma + \Gamma\overline{A} + \Gamma^2 \le -Q$ for $Q > 0$ is considered [20]. Using the positive definite matrix Γ, the vector b_0 is chosen as $b_0 = \Gamma^{-1}c$. It is shown below that this choice will guarantee the stability of the observer.

Theorem 3. *Consider the observer system* (17). *Let the update laws for the parameters of fuzzy-neural systems be*

$$\begin{aligned} \dot{W}_{f_n} &= \widetilde{y}\,\Gamma_{f_n} P_{f_n}(\widehat{\mathbb{x}}) - k_{f_n} W_{f_n}, \\ \dot{W}_{f_d} &= \widetilde{y}\,\Gamma_{f_d} P_{f_d}(\widehat{\mathbb{x}})u - k_{f_d} W_{f_d}, \end{aligned} \tag{19}$$

where $\Gamma_{f_n} = \Gamma_{f_n}^T > 0$, $\Gamma_{f_d} = \Gamma_{f_d}^T > 0$ *and* $k_{f_n} > 0$, $k_{f_d} > 0$. *Then, the state estimation error and parameter estimation errors are uniformly ultimately bounded.*

Proof. Consider the Lyapunov-function candidate

$$V = \underbrace{\widetilde{x}^T\Gamma\widetilde{x}}_{V_1} + \underbrace{\widetilde{W}_{f_n}^T\Gamma_{f_n}^{-1}\widetilde{W}_{f_n} + \widetilde{W}_{f_d}^T\Gamma_{f_d}^{-1}\widetilde{W}_{f_d}}_{V_2}. \tag{20}$$

The time derivative of V_1 is

$$\begin{aligned} \dot{V}_1 &= \widetilde{x}^T\left(\overline{A}^T\Gamma + \Gamma\overline{A}\right)\widetilde{x} + 2\widetilde{y}\left[\widetilde{W}_{f_n}^T P_{f_n}(\widehat{\mathbb{x}}) + \widetilde{W}_{f_d}^T P_{f_d}(\widehat{\mathbb{x}})u\right] \\ &\quad + 2\widetilde{x}^T\Gamma\left\{(b - b_0)\left[W_{f_n}^{*T} P_{f_n}(\mathbb{x}) + W_{f_d}^{*T} P_{f_d}(\mathbb{x})u\right]\right. \\ &\quad \left. + b_0\left(d_{f_n} + d_{f_d}u\right) + b\left[d_\xi(t) + \varepsilon_{f_n} + \varepsilon_{f_d}u\right]\right\}. \end{aligned} \tag{21}$$

Since the P_{f_n} and P_{f_d} are bounded, that is, $\|P_{f_n}(\mathbb{x})\| \le P_{f_n}^M$ and $\|P_{f_d}(\mathbb{x})\| \le P_{f_d}^M$ with $P_{f_n}^M$ and $P_{f_d}^M$ as constants, thus,

$$\begin{aligned} &(b - b_0)\left[W_{f_n}^{*T} P_{f_n}(\mathbb{x}) + W_{f_d}^{*T} P_{f_d}(\mathbb{x})u\right] + b_0\left(d_{f_n} + d_{f_d}u\right) \\ &\quad + b\left[d_\xi(t) + \varepsilon_{f_n} + \varepsilon_{f_d}u\right] \le \Upsilon \end{aligned} \tag{22}$$

with

$$\begin{aligned}\Upsilon = &\ \|(b-b_0)\|\left[M_{f_n}P_{f_n}^M + M_{f_d}P_{f_d}^M\overline{u}\right] \\ &+ \|b_0\|\left(M_{f_n}\widetilde{P}_{f_n}^M + M_{f_d}\widetilde{P}_{f_d}^M\overline{u}\right) \\ &+ b\left[d_M + \varepsilon_{f_nM} + \varepsilon_{f_dM}\overline{u}\right].\end{aligned} \tag{23}$$

By using $2a_1^Tb_1 \le a_1^Ta_1 + b_1^Tb_1$, it can be shown that

$$\begin{aligned}&2\widetilde{x}^T\Gamma\left\{(b-b_0)\left[W_{f_n}^{*T}P_{f_n}(\mathbb{x}) + W_{f_d}^{*T}P_{f_d}(\mathbb{x})u\right] + b_0\left(d_{f_n} + d_{f_d}u\right)\right. \\ &\qquad \left. + b\left[d_\xi(t) + \varepsilon_{f_n} + \varepsilon_{f_d}u\right]\right\} \\ &\quad \le \widetilde{x}^T\Gamma^2\widetilde{x} + \Upsilon^2.\end{aligned} \tag{24}$$

Substituting (24) into (21) yields

$$\dot{V}_1 \le -\widetilde{x}^TQ\widetilde{x} + 2\widetilde{y}\left[\widetilde{W}_{f_n}^TP_{f_n}(\widehat{\mathbb{x}}) + \widetilde{W}_{f_d}^TP_{f_d}(\widehat{\mathbb{x}})u\right] + \Upsilon^2. \tag{25}$$

Then, $\dot{V}$ follows as

$$\dot{V} \le -\widetilde{x}^TQ\widetilde{x} + 2k_{f_n}\widetilde{W}_{f_n}^TW_{f_n} + 2k_{f_g}\widetilde{W}_{f_g}^TW_{f_g} + \Upsilon^2, \tag{26}$$

where the update laws (19) have been used. By completion of squares, it follows that

$$\begin{aligned}\dot{V} \le &\ -\lambda_{\min}(Q)\left\{\|\widetilde{x}\|^2 + \frac{2k_{f_n}}{\lambda_{\min}(Q)}\left(\left\|\widetilde{W}_{f_n}^T\right\| - \frac{1}{2}\left\|W_{f_n}^*\right\|\right)^2\right. \\ &+ \frac{2k_{f_d}}{\lambda_{\min}(Q)}\left(\left\|\widetilde{W}_{f_d}^T\right\| - \frac{1}{2}\left\|W_{f_d}^*\right\|\right)^2 \\ &- \left[\frac{k_{f_n}}{2\lambda_{\min}(Q)}\left\|W_{f_n}^*\right\|^2 + \frac{k_{f_d}}{2\lambda_{\min}(Q)}\left\|W_{f_d}^*\right\|^2\right. \\ &\left.\left. + \frac{1}{\lambda_{\min}(Q)}\Upsilon^2\right]\right\},\end{aligned} \tag{27}$$

which is guaranteed negative as long as either

$$\|\widetilde{x}\| > \sqrt{\frac{k_{f_n}\left\|W_{f_n}^*\right\|^2}{2\lambda_{\min}(Q)} + \frac{k_{f_d}\left\|W_{f_d}^*\right\|^2}{2\lambda_{\min}(Q)} + \frac{\Upsilon^2}{\lambda_{\min}(Q)}} = B_x \tag{28}$$

or

$$\left\|\widetilde{W}_{f_n}^T\right\| > \sqrt{\frac{\left\|W_{f_n}^*\right\|^2}{4} + \frac{\left\|W_{f_d}^*\right\|^2}{4} + \frac{\Upsilon^2}{2}} + \frac{\left\|W_{f_n}^*\right\|}{2} = B_{f_n}, \tag{29}$$

$$\left\|\widetilde{W}_{f_d}^T\right\| > \sqrt{\frac{\left\|W_{f_n}^*\right\|^2}{4} + \frac{\left\|W_{f_d}^*\right\|^2}{4} + \frac{\Upsilon^2}{2}} + \frac{\left\|W_{f_d}^*\right\|}{2} = B_{f_d}. \tag{30}$$

Defining a vector $\mathbb{z} = [\widetilde{x}^T, \widetilde{W}_{f_n}^T, \widetilde{W}_{f_d}^T]^T$, thus, $\dot{V}$ is negative outside the compact set: $M_\sigma = \{\mathbb{z} \in M_z \mid \|\mathbb{z}\| \le \sigma\}$, where $\sigma = \max(B_x, B_{f_n}, B_{f_d})$. We can guarantee that $\alpha < \beta$ which can be made by increasing $\lambda_{\min}(Q)$, and therefore ultimate boundedness of $\mathbb{z}$, where $\alpha = \max_{\|\mathbb{z}\|=\sigma}V$ and $\beta = \min_{\|\mathbb{z}\|=R}V$. □

3.3. Controller Design and Stability Analysis. Define tracking error as

$$E = x - x_d = \left[e, \dot{e}, \ldots, e^{(n-1)}\right]^T, \tag{31}$$

where $e = x_1 - x_{1d}$. Define the following terminal sliding mode surface:

$$\sigma(x,t) = CE - W(t), \tag{32}$$

where $C = [c_1, c_2, \ldots, c_n]$, c_i $(i = 1, \ldots, n)$ is positive constant, and $c_n = 1$. And $W(t) = CP(t)$, where $P(t) = [p(t), \dot{p}(t), \ldots, p^{(n-1)}(t)]^T$.

Assumption 2. Consider terminal function $p(t) : \mathscr{R}_+ \to \mathscr{R}$, $p(t) \in C^n[0,\infty)$, $p, \dot{p}, \ldots, p^{(n)} \in L^\infty$, $p(t)$ is finite in interval $[0,T]$, $E(0) = P(0)$, $\dot{E}(0) = \dot{P}(0)$, that is, $p(0) = e(0)$, $\dot{p}(0) = \dot{e}(0), \ldots, p^{(n)}(0) = e^{(n)}(0)$. Moreover, $p = 0, \dot{p} = 0, \cdots, p^{(n)} = 0$, for $t \ge T$. $C^n[0,\infty)$ represents the set of all n rank differentiable continuous functions defined in $[0,\infty)$.

Define terminal function $p(t)$ for (4) as

$$p(t) = \begin{cases}\displaystyle\sum_{j=0}^{n}\left(\sum_{l=0}^{n}\frac{a_{jl}}{T^{j-l+n+1}}e_i(0)^{(l)}\right)t^{j+n+1} \\ \displaystyle\quad + \sum_{k=0}^{n}\frac{1}{k!}e_i(0)^{(k)}t^k & t \le T \\ 0 & t > T,\end{cases} \tag{33}$$

where a_{jl} can be defined by using Assumption 3.

Theorem 4. *Suppose that the control law is*

$$\begin{aligned}u(t) = &\ -\frac{1}{b_0f_d(\widehat{\mathbb{x}})}\left\{b_0f_n(\widehat{\mathbb{x}}) + l_n\widetilde{y} - x_{1d}^{(n)} - p^{(n)}(t)\right. \\ &\left. + c_n^{-1}\sum_{k=1}^{n-1}\left[\widehat{e}^{(k)} - p^{(k)}(t)\right]\right\} \\ &- \frac{1}{b_0f_d(\widehat{\mathbb{x}})}\frac{c_n\sigma(x,t)}{\|c_n\sigma(x,t)\|}\{D(t) + K\},\end{aligned} \tag{34}$$

where $K > 0$, then $\sigma(x,t)$ will reach zero in finite time T. Furthermore, the sates x will converge to zero in finite time T, and D is a positive constant value designed as below.

Proof. Consider a Lyapunov-function candidate as follows:

$$V_3(t) = \frac{1}{2}\sigma^T\sigma. \tag{35}$$

The derivative of $\sigma(x,t)$ is

$$\begin{aligned}\dot{\sigma}(x,t) &= C\dot{E} - C\dot{P}(t)\\ &= C\cdot\left[\dot{e}^T\cdots e^{(n-1)T}\right]^T - C\cdot\left[\dot{p}(t)^T\cdots p^{(n-1)}(t)^T\right]^T\\ &= c_n\left[x_1^{(n)} - x_{1d}^{(n)} - p^{(n)}(t)\right] + \sum_{k=1}^{n-1} c_k\left[e^{(k)} - p^{(k)}(t)\right]\\ &= c_n\left[\widehat{x}_1^{(n)} - x_{1d}^{(n)} - p^{(n)}(t)\right] + \sum_{k=1}^{n-1} c_k\left[\widehat{e}^{(k)} - p^{(k)}(t)\right]\\ &\quad + \sum_{k=2}^{n} c_k\widetilde{x}_k\\ &= c_n\left[b_0 f_n(\widehat{\mathbb{x}}) + b_0 f_d(\widehat{\mathbb{x}})u + l_n\widetilde{y} - x_{1d}^{(n)} - p^{(n)}(t)\right]\\ &\quad + \sum_{k=1}^{n-1} c_k\left[\widehat{e}^{(k)} - p^{(k)}(t)\right] + \sum_{k=2}^{n} c_k\widetilde{x}_k,\end{aligned} \tag{36}$$

where $\widehat{e} = \widehat{x} - x_d$, $\dot{\widehat{e}} = \widehat{x}_2 - \dot{x}_d, \ldots, \widehat{e}^{(n-1)} = \widehat{x}_n = \widehat{x}_d^{(n-1)}$. Then

$$\begin{aligned}\dot{V}_3(t) &= \sigma^T\dot{\sigma}\\ &= \sigma^T c_n\left\{b_0 f_n(\widehat{\mathbb{x}}) + l_n\widetilde{y} - x_{1d}^{(n)} - p^{(n)}(t)\right.\\ &\qquad \left. + c_n^{-1}\sum_{k=1}^{n-1}\left[\widehat{e}^{(k)} - p^{(k)}(t)\right]\right\} + \sigma^T c_n b_0 f_d(\widehat{\mathbb{x}})u\\ &\quad + \sigma^T c_n c_n^{-1}\sum_{k=2}^{n} c_k\widetilde{x}_k\\ &\le \sigma^T c_n\left\{b_0 f_n(\widehat{\mathbb{x}}) + l_n\widetilde{y} - x_{1d}^{(n)} - p^{(n)}(t)\right.\\ &\qquad \left. + c_n^{-1}\sum_{k=1}^{n-1}\left[\widehat{e}^{(k)} - p^{(k)}(t)\right]\right\} + \sigma^T c_n b_0 f_d(\widehat{\mathbb{x}})u\\ &\quad + \left\|\sigma^T c_n\right\|\left\|c_n^{-1}\sum_{k=2}^{n} c_k\widetilde{x}_k\right\|.\end{aligned} \tag{37}$$

By Theorem 3, it is easily get that $|c_n^{-1}\sum_{k=2}^{n} c_k\widetilde{x}_k| \le D(t)$.

Substituting the control law (34) into $\dot{V}_3(t)$ yields

$$\dot{V}_3(t) \le -\frac{\sigma^T c_n c_n^T\sigma}{\|c_n\sigma\|}\{D(t) + K\} \tag{38}$$

because of

$$\sigma^T c_n c_n^T\sigma = \|c_n\sigma\|^2, \tag{39}$$

so

$$\dot{V}_3(t) \le 0. \tag{40}$$

If $|\sigma| \ne 0$, then $\dot{V}_3(t) < 0$. This means that this Lyapunov function will decrease gradually, and the sliding surface $\sigma(x,t)$ will converge to zero. The proof is completed. □

Remark 5. It follows from Assumption 2 that

$$\sigma(x,0) = CE(0) - W(0) = C[E(0) - P(0)] = 0. \tag{41}$$

According to Lyapunov analysis, $\sigma(x,t) = 0$ can be achieved all the time. This indicates that the reaching phase in terminal sliding mode control can be eliminated, and global robustness can be guaranteed.

Remark 6. In order to reduce chattering which is caused by discontinuous control signal, a continuous function vector is used to the controller design. In control law (34), $c_n^T\sigma(x,t)/\|c_n\sigma(x,t)\|$ is replaced by the continuous function vector S_δ defined by

$$S_\delta = \frac{c_n^T\sigma(x,t)}{\|c_n\sigma(x,t)\| + \delta} \tag{42}$$

with $\delta = \delta_0 + \delta_1\|e\|$, where δ_0, δ_1 are two positive constants.

4. Simulation Results

This section presents the simulation results of the proposed tracking controller to illustrate that the stability of the closed-loop system is guaranteed, and all signal involved are bounded. Consider the nonlinear system

$$\begin{aligned}\dot{x}_1 &= x_2,\\ \dot{x}_2 &= 0.2\left(1 + e^{x_1x_2}\right)\left(2 + \sin(x_2)\right)\left(u + e^u - 1\right) + d(t),\\ y &= x_1,\end{aligned} \tag{43}$$

where external disturbance $d(t) = 5\sin(7\pi t)$. Define terminal function $p(t)$ for dynamics of (43) as

$$p(t) = \begin{cases}\displaystyle\sum_{j=0}^{2}\left(\sum_{l=0}^{2}\frac{a_{jl}}{T^{j-l+3}}e_i(0)^{(l)}\right)t^{j+3} + \sum_{k=0}^{2}\frac{1}{k!}e_i(0)^k t^k & t \le T\\ 0 & t > T\end{cases} \tag{44}$$

according to Assumption 3; function $p(t)$, $\dot{p}(t)$, and $\ddot{p}(t)$ can be equal to zero at time $t = T$ by designing a_{jl} ($j = 0,1,2, l = 0,1,2$). That is, if we design a_{jl} according to the following

equations, $p(t)$, $\dot{p}(t)$, and $\ddot{p}(t)$ can all be equal to zero at time $t = T$:

$$\begin{aligned} a_{00} + a_{10} + a_{20} &= -1, \\ 3a_{00} + 4a_{10} + 5a_{20} &= 0, \\ 6a_{00} + 12a_{10} + 20a_{20} &= 0, \\ a_{01} + a_{11} + a_{21} &= -1, \\ 3a_{01} + 4a_{11} + 5a_{21} &= -1, \\ 6a_{01} + 12a_{11} + 20a_{21} &= 0, \\ a_{02} + a_{12} + a_{22} &= -\frac{1}{2}, \\ 3a_{02} + 4a_{12} + 5a_{22} &= -1, \\ 6a_{02} + 12a_{12} + 20a_{22} &= -1. \end{aligned} \tag{45}$$

Based on the three groups of (45), parameters a_{jl} can be solved as

$$\begin{aligned} a_{00} &= -10, & a_{01} &= -6, & a_{02} &= -1.5, \\ a_{10} &= 15, & a_{11} &= 8, & a_{12} &= 1.5, \\ a_{20} &= -6, & a_{21} &= -3, & a_{22} &= -0.5. \end{aligned} \tag{46}$$

From (44)–(46), $p(t)$ can be written as

$$p(t) = \begin{cases} e_0 + \dot{e}_0 t + \frac{1}{2}\ddot{e}_0 t^2 + \left(\frac{a_{00}}{T^3}e_0 + \frac{a_{01}}{T^2}\dot{e}_0 + \frac{a_{02}}{T}\ddot{e}_0\right)t^3 \\ \quad + \left(\frac{a_{10}}{T^4}e_0 + \frac{a_{11}}{T^3}\dot{e}_0 + \frac{a_{12}}{T^2}\ddot{e}_0\right)t^4 \\ \quad + \left(\frac{a_{20}}{T^5}e_0 + \frac{a_{21}}{T^4}\dot{e}_0 + \frac{a_{22}}{T^3}\ddot{e}_0\right)t^5, & t \le T \\ 0, & t > T. \end{cases} \tag{47}$$

We choose control parameters as $c_2 = 50$, $c_1 = 1$, and $K = 0$, and terminal time is chosen as $T = 1.0$. The control law is now chosen as

$$\begin{aligned} u(t) = &-\frac{1}{b_0 f_d(\hat{\mathbb{x}})}\left\{b_0 f_n(\hat{\mathbb{x}}) + l_n\tilde{y} - \ddot{x}_{1d} - \ddot{p}(t) + c_2^{-1}\dot{\tilde{e}} - c_2^{-1}\dot{p}(t)\right\} \\ &- \frac{1}{b_0 f_d(\hat{\mathbb{x}})}\frac{c_2\sigma(x,t)}{\|c_2\sigma(x,t)\|}\{D(t) + K\}. \end{aligned} \tag{48}$$

Then the observer for the system (43) is given by (17). We can apply Theorem 3 with the following simulation parameters: observer gain $L = [1000, 8000]$, weight-tuning parameters $\Gamma_{f_n} = \mathrm{diag}[5 \times 10^4]$, and $\Gamma_{f_d} = \mathrm{diag}[5 \times 10^3]$. And $k_{f_n} = k_{f_d} = 0.001$.

The desired output is $x_{1d} = \sin t$. The initial conditions are $x(0) = [0, 0.5]^T$. $\hat{\mathbb{x}}(0) = [0.1, 0, 0]^T$. The response of the system (43) and adaptive fuzzy-neural observer with the terminal SMC law is shown in Figure 2. From Figure 2, we can obtain a better tracking ability by terminal SMC than output feedback control (OFC) method of [21, 22]. Figure 3 shows the states and observer values, and Figure 4 shows the errors of observer.

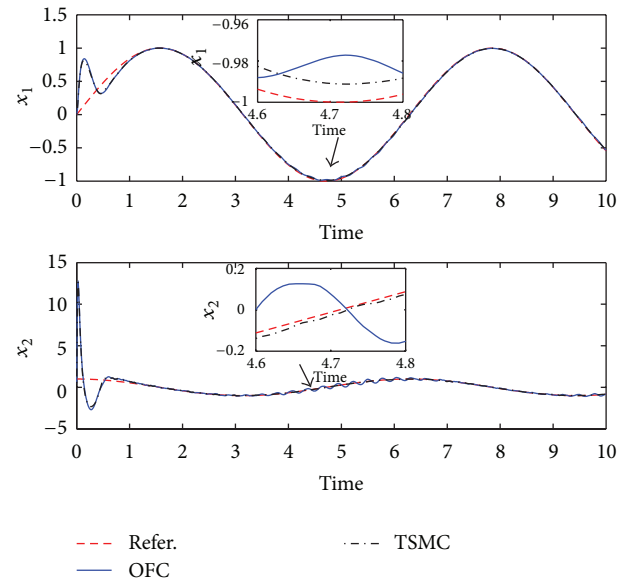

Figure 2: System response with the proposed tracking controller.

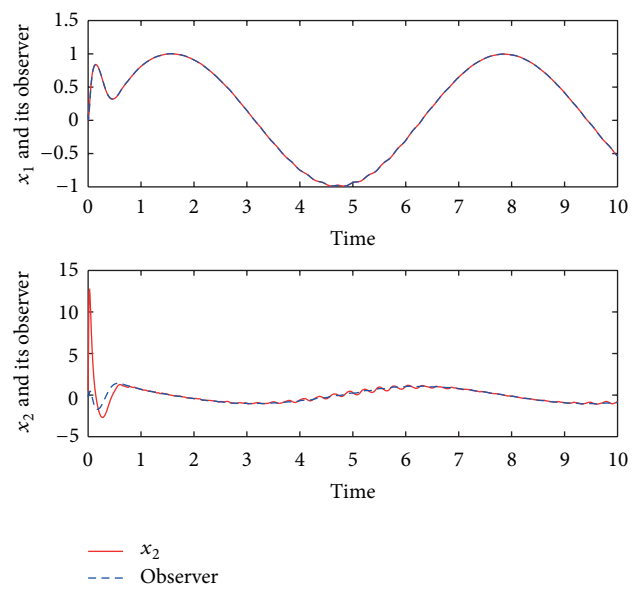

Figure 3: System states and observer values.

5. Conclusion

We have carried out a systematic study on fuzzy-neural observer-based terminal SMC in this paper, based on an adaptive fuzzy-neural observer which is used to identify the model and estimate the states. So the information of mathematical model and states does not require to know,

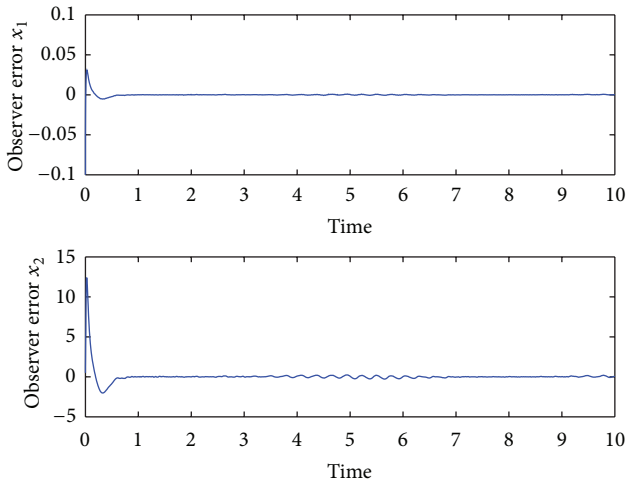

Figure 4: Observer error of states.

only using the measurable output. The proposed nonlinear tracking control scheme can guarantee the asymptotic output tracking of the closed-loop control systems in spite of unknown uncertainties/disturbances. Finally, simulation results are provided on a nonaffine nonlinear system to show the effective and advantages of the new control strategy.

Acknowledgments

This work was partially supported by the National Natural Science Foundation of China (61273171, 61034005, and 61174058), the National Aerospace Science Foundation of China (2011ZA52009, 2012ZA52017), PAPD, Funding of Jiangsu Innovation Program for Graduate Education (CXZZ11-0213), and funding for Outstanding Doctoral Dissertation in NUAA (BCXJ12-04).

References

[1] P. Shi, Y. Xia, G. P. Liu, and D. Rees, "On designing of sliding-mode control for stochastic jump systems," *IEEE Transactions on Automatic Control*, vol. 51, no. 1, pp. 97–103, 2006.

[2] J. Zhang, P. Shi, and Y. Xia, "Robust adaptive sliding-mode control for fuzzy systems with mismatched uncertainties," *IEEE Transactions on Fuzzy Systems*, vol. 18, no. 4, pp. 700–711, 2010.

[3] L. Wu, P. Shi, and H. Gao, "State estimation and sliding-mode control of Markovian jump singular systems," *IEEE Transactions on Automatic Control*, vol. 55, no. 5, pp. 1213–1219, 2010.

[4] Q. Khan, A. I. Bhatti, M. Iqbal, and Q. Ahmed, "Dynamic integral sliding mode control for SISO uncertain nonlinear systems," *International Journal of Innovative Computing, Information and Control*, vol. 8, no. 7, pp. 4621–4633, 2012.

[5] L. Wu and D. W. C. Ho, "Sliding mode control of singular stochastic hybrid systems," *Automatica*, vol. 46, no. 4, pp. 779–783, 2010.

[6] J. Fei and M. Xin, "Robust adaptive sliding mode controller for semi-active vehicle suspension system," *International Journal of Innovative Computing, Information and Control*, vol. 8, no. 1, pp. 691–700, 2012.

[7] L. Wu and W. X. Zheng, "Passivity-based sliding mode control of uncertain singular time-delay systems," *Automatica*, vol. 45, no. 9, pp. 2120–2127, 2009.

[8] Y. Wu, X. Yu, and Z. Man, "Terminal sliding mode control design for uncertain dynamic systems," *Systems & Control Letters*, vol. 34, no. 5, pp. 281–287, 1998.

[9] J. Wang, L. Zou, H. Peng, and G. Zhang, "An extended spiking neural P system for fuzzy knowledge representation," *International Journal of Innovative Computing, Information and Control*, vol. 7, no. 7, pp. 3709–3724, 2011.

[10] W. Pawlus, H. R. Karimi, and K. G. Robbersmyr, "Data-based modeling of vehicle collisions by nonlinear autoregressive model and feedforward neural network," *Information Sciences*, 2012.

[11] D. Jia and B. You, "Study on novel plasma arc cutting technology based on PIDNN-FUZZY controller," *International Journal of Innovative Computing, Information and Control*, vol. 7, no. 7, pp. 4171–4182, 2011.

[12] L. Wu, X. Su, P. Shi, and J. Qiu, "Model approximation for discrete-time state-delay systems in the T–S fuzzy framework," *IEEE Transactions on Fuzzy Systems*, vol. 19, no. 2, pp. 366–378, 2011.

[13] T.-C. Lin, S.-W. Chang, and C.-H. Hsu, "Robust adaptive fuzzy sliding mode control for a class of uncertain discrete-time nonlinear systems," *International Journal of Innovative Computing, Information and Control*, vol. 8, no. 1, pp. 347–359, 2012.

[14] X. Su, P. Shi, L. Wu, and Y.-D. Song, "A novel approach to filter design for T–S fuzzy discrete-time systems with time-varying delay," *IEEE Transactions on Fuzzy Systems*, vol. 20, no. 6, Article ID 6189779, pp. 1114–1129, 2012.

[15] C. M. Lin and C. F. Hsu, "Supervisory recurrent fuzzy neural network control of wing rock for slender delta wings," *IEEE Transactions on Fuzzy Systems*, vol. 12, no. 5, pp. 733–742, 2004.

[16] C. M. Lin and C. F. Hsu, "Supervisory recurrent fuzzy neural network control of wing rock for slender delta wings," *IEEE Transactions on Fuzzy Systems*, vol. 12, no. 5, pp. 733–742, 2004.

[17] B. Jiang, Z. Gao, P. Shi, and Y. Xu, "Adaptive fault-tolerant tracking control of near-space vehicle using TakagiSugeno fuzzy models," *IEEE Transactions on Fuzzy Systems*, vol. 18, no. 5, pp. 1000–1007, 2010.

[18] S. J. Lopez, O. C. Nieto, and J. I. C. Oria, "Non-parametric modeling of uncertain hyperbolic partial differential equations using pseudo-high order sliding mode observers," *International Journal of Innovative Computing, Information and Control*, vol. 8, no. 3, pp. 1501–1521, 2012.

[19] Y. H. Kim, L. Frank, and C. T. Abdallah, "A dynamic recurrent neural-network-based adaptive observer for a class of nonlinear systems," *Automatica*, vol. 33, no. 8, pp. 1539–1543, 1997.

[20] M.-L. Ni and M. J. Er, "Stability of linear systems with delayed perturbations: an LMI approach," *IEEE Transactions on Circuits and Systems. I*, vol. 49, no. 1, pp. 108–112, 2002.

[21] S. K. Nguang and P. Shi, "H_∞ fuzzy output feedback control design for nonlinear systems: an LMI approach," *IEEE Transactions on Fuzzy Systems*, vol. 11, no. 3, pp. 331–340, 2003.

[22] Y. Wang, T. Chai, and Y. Zhang, "State observer-based adaptive fuzzy output-feedback control for a class of uncertain nonlinear systems," *Information Sciences*, vol. 180, no. 24, pp. 5029–5040, 2010.

Hindawi Publishing Corporation
Mathematical Problems in Engineering
Volume 2013, Article ID 908180, 18 pages
http://dx.doi.org/10.1155/2013/908180

Research Article

Fuzzy Formation Control and Collision Avoidance for Multiagent Systems

Yeong-Hwa Chang,[1] Chun-Lin Chen,[1] Wei-Shou Chan,[1] Hung-Wei Lin,[2] and Chia-Wen Chang[3]

[1] *Department of Electrical Engineering, Chang Gung University, Kwei-Shan, Tao-Yuan 333, Taiwan*
[2] *Department of Electrical Engineering, Lee-Ming Institute of Technology, Taishan, Taipei 243, Taiwan*
[3] *Department of Information and Telecommunication Engineering, Ming Chuan University, Kwei-Shan, Tao-Yuan 333, Taiwan*

Correspondence should be addressed to Yeong-Hwa Chang; yhchang@mail.cgu.edu.tw

Received 2 December 2012; Accepted 12 January 2013

Academic Editor: Peng Shi

Copyright © 2013 Yeong-Hwa Chang et al. This is an open access article distributed under the Creative Commons Attribution License, which permits unrestricted use, distribution, and reproduction in any medium, provided the original work is properly cited.

This paper aims to investigate the formation control of leader-follower multiagent systems, where the problem of collision avoidance is considered. Based on the graph-theoretic concepts and locally distributed information, a neural fuzzy formation controller is designed with the capability of online learning. The learning rules of controller parameters can be derived from the gradient descent method. To avoid collisions between neighboring agents, a fuzzy separation controller is proposed such that the local minimum problem can be solved. In order to highlight the advantages of this fuzzy logic based collision-free formation control, both of the static and dynamic leaders are discussed for performance comparisons. Simulation results indicate that the proposed fuzzy formation and separation control can provide better formation responses compared to conventional consensus formation and potential-based collision-avoidance algorithms.

1. Introduction

Recently, distributed multiagent coordination has attracted much attention in many fields, where only the information available locally from its neighbors is required for each agent [1–6]. There are many applications of multiagent systems, such as autonomous unmanned aerial vehicles [7], autonomous formation flight [8], congestion-controlled communication network [9], wireless sensor network [10], and autonomous multivehicle formations [11]. Graph theory has been used to characterize network topologies for consensus studies. A general consensus problem solving is to find a distributed control strategy such that the states of agents converge to a common value. Average-consensus problem was investigated for distributed networks with fixed and switching topologies [12]. Relying on graph theory, matrix theory, and control theory, the analysis of consensus protocols was thoroughly discussed. In [13], an impulsive control protocol was presented for multiagent linear dynamic systems with fixed topology based on the local information of agents. A fuzzy sliding-mode controller was proposed to investigate the formation control problem in directed graphs [14]. Cai et al. [15] addressed the controllability improvement problem for two types of linear time-invariant dynamic multiagent systems by adjusting the configuration of graphs. A general case of leader-following consensus problems under fixed and switching topologies was discussed in [16]. The second-order agents under switching topology were concerned in [17], where the condition of communication delays was determined for achieving consensus. The consensus problem for a group of high-order dynamic agents with switching topology and time-varying communication delays was discussed in [18]. In the work of [19], linear consensus protocol and saturated consensus protocol were presented for the consensus problem of heterogeneous multiagent system. The heterogeneous multiagent system consists of first-order and second-order integrator agents.

Lately, the fuzzy logic control which consists of linguistic control rules is a technique to design controllers based on human expert knowledge and experience. This technique

is a good alternative to overcome the difficulties in the requirement of exact mathematics models for plants with unexpected complex dynamics and external disturbances. Although the method has been practically successful, it has proved extremely difficult to develop a general analysis and design theory for conventional fuzzy control systems. Recently, based on Takagi-Sugeno (T-S) fuzzy techniques, there have appeared in the literature a great number of results concerning stability analysis and design. T-S fuzzy techniques have been applied to many applications of interest [20–25]. However, the membership functions of the above method are through manual adjustment. Lately, neural fuzzy control, combining with the capability of fuzzy reasoning to handle uncertain information and the capability of artificial neural networks to learn from processes, has been popularly addressed. In [26], a robust fuzzy neural network control (FNN) scheme including a parameter tuning algorithm was designed for a linear Maglev rail system to achieve the objective of model-free control. A neural network-based self-learning control strategy including an FNN controller and a recurrent neural network identifier was proposed for electronic throttle valves [27]. Lin and Shen [28] proposed an adaptive fuzzy neural network control scheme for a field-oriented control permanent magnet linear synchronous motor servo-drive system to track periodic reference trajectories. In [29], an adaptive network based fuzzy inference system was presented for speed and position estimations of a permanent-magnet synchronous generator. In [30], an adaptive neurofuzzy controller was presented for the tracking control of dynamic systems with unknown nonlinearities. A recurrent fuzzy neural controller for the robust tracking of a robot manipulator with adaptive observers was addressed in [31]. A robust self-organizing neural fuzzy control scheme was proposed for a class of uncertain nonlinear MIMO systems [32]. In the study of [33], an adaptive neurofuzzy inference system was employed to identify hand motion commands based on surface electromyogram signals. In [34], a new approach was proposed for machine health condition prognosis with the integration of neurofuzzy system and Bayesian algorithms. Moreover, a T-S fuzzy-neural model was adopted for identification and robust adaptive control of an antilock braking system [35]. In addition, a hybrid evolutionary algorithm using fuzzy rules to adjust optimization parameters was proposed in [36].

In multiagent networks, the problem of collision avoidance is also an important and interesting topic that is worthy of being discussed. A cooperative control law was proposed for general nonlinear dynamic models to guarantee collision-free conflict resolution [37]. In [38], a fuzzy logic was designed for potential functions to achieve the separation control with input constrains. In the work of [39], a flocking algorithm was presented for separation forces generated to avoid collisions with external obstacles. A modified avoidance function was proposed for nonlinear Lagrange systems to achieve collision avoidance with bounded disturbances [40]. In [41], a potential field method was discussed for mobile robots to solve the local minimum problem. In addition, Wang and Gu [42] presented a fuzzy potential force for the separating potential function in flocking control. However, only few of existing results have been presented to solve the problem of local minima in multiagent systems.

This paper aims to investigate the formation control of leader-follower multiagent systems, where the problem of collision avoidance is also considered. The graph theory is used to model the communication topology between agents. To improve the control performance, a novel formation algorithm, neural-fuzzy formation controller, is proposed for multiagent systems in directed graphs. The neural-fuzzy control parameter consists of input Gaussian membership functions and output fuzzy singletons, where the parameters of input and output membership functions can be adaptively adjusted. The proposed neural-fuzzy formation controller has the capability of on-line learning, and the adaptive rules can be derived using the gradient descent method. Moreover, a fuzzy based separation control is presented for collision avoidance, and the local minimum problem of traditional potential-based separation control can be solved. The fuzzy based separation control consists of triangular input membership functions and singleton output membership functions, where the control output provides an alternative moving direction for agents to achieve collision-free tasks. Numerical simulations are provided to validate the collision-free formation responses.

This paper is organized as follows. In Section 2, some essential graph-theoretic concepts and a network of single-integrator agents are introduced. In Section 3, the framework of a neural-fuzzy formation controller is investigated, where the updating rules for controller parameters are derived. In Section 4, the conventional potential-based collision avoidance is introduced. Moreover, a novel fuzzy-oriented separation control is presented. In Section 5, simulation results are provided for performance validations. Some concluding remarks are given in Section 6.

2. Preliminaries

2.1. Graph Theory. Considering a multiagent system of n agents, let $G = (V, \Xi)$ be a directed graph (digraph), consisting of a vertex set $V = \{v_1, v_2, \ldots, v_n\}$ and an edge set $\Xi \subseteq V \times V$. The vertexes v_i and v_j represent the ith and jth agents, respectively. In digraphs, an edge of G is an ordered pair of distinct nodes $(v_j, v_i) \in \Xi$, in which v_i and v_j are the head and tail of the edge, respectively [43]. The weighted adjacency matrix of a digraph G is denoted as

$$A = \begin{bmatrix} a_{11} & a_{12} & \cdots & a_{1n} \\ a_{21} & a_{22} & \cdots & a_{2n} \\ \vdots & \vdots & \ddots & \vdots \\ a_{n1} & a_{n2} & \cdots & a_{nn} \end{bmatrix} \in R^{n\times n}, \tag{1}$$

where a_{ij} is the link weight; $a_{ij} = 1$, if $(v_j, v_i) \in \Xi$, and $a_{ij} = 0$, if $(v_j, v_i) \notin \Xi$.

In this paper, a leader-follower problem will be dealt with, where the multiagent system consists of n agents, one leader, and $n-1$ followers. In notations, the agents indexed by $1, 2, \ldots, n-1$ are followers and the item n is the leader. Assume that the leader agent has only transmitting capability, that is, the leader acquires no information from followers,

$a_{nj} = 0,\ \ j = 1, \ldots, n$. In this case, let the topology relationship of follower agents be denoted as $\overline{G}$, a subgraph of G. Then, the associated adjacency matrix of $\overline{G}$ is represented as

$$\overline{A} = \begin{bmatrix} a_{11} & a_{12} & \cdots & a_{1(n-1)} \\ a_{21} & a_{22} & \cdots & a_{2(n-1)} \\ \vdots & \vdots & \ddots & \vdots \\ a_{(n-1)1} & a_{(n-1)2} & \cdots & a_{(n-1)(n-1)} \end{bmatrix} \in R^{(n-1)\times(n-1)}. \quad (2)$$

Consequently, the connection relationship between the leader and followers can be described as $\overline{B} = \operatorname{diag}\{\overline{b}_1, \overline{b}_2, \ldots, \overline{b}_{n-1}\}$, where $\overline{b}_i = a_{in}$, $i = 1, 2, \ldots, n-1$.

2.2. Single-Integrator Multiagent System. In this paper, a single-integrator network is considered as

$$\dot{r}_i(t) = u_i(t), \quad (3)$$

where $r_i(t) = [x_i(t)\ \ y_i(t)]^T \in R^2$ is the position vector and $u_i(t) = [u_{xi}(t)\ \ u_{yi}(t)]^T \in R^2$ is the control input vector of the ith agent, $i = 1, 2, \ldots, n$. It is assumed that all agents have the same environment sensing capability. In addition to formation keeping, each agent is not allowed to collide with other agents during the whole moving process.

The geometric relationship between agents is shown in Figure 1, where R_s is the sensing radius. The node j is a neighboring agent of the ith node if the Euclidean distance between two agents is less or equal to the sensing radius, $d_{ij} = \|r_i - r_j\| \le R_s$. Let N_i stand for the neighbor set of the ith agent. Once the jth agent moves inside the sensing radius of the ith agent, the collision-avoidance mechanism starts to work. In Figure 1, the notation r_a denotes the avoidance radius of which the minimum distance allowed between two agents is $2r_a$. In this case, it is reasonable that $R_s > 2r_a$ for preventing collisions.

Table 1: Fuzzy rule base.

S_{xi} (S_{yi})	NB	NM	NS	PS	PM	PB
u_{xi} (u_{yi})	PB	PM	PS	NS	NM	NB

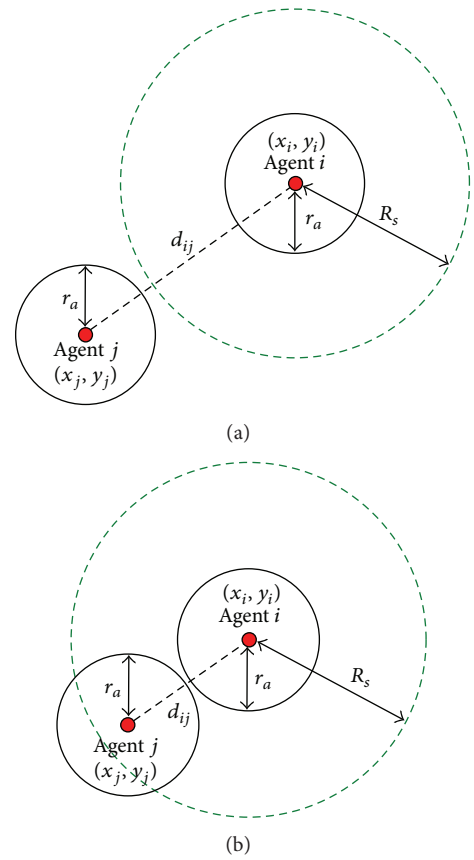

Figure 1: Geometric relationship between agents: (a) node j is not a neigh-boring agent of node i; (b) node j is a neighboring agent of node i.

3. Neural Fuzzy Formation Control

3.1. Structure of Neural Fuzzy Controller. In this section, a neural fuzzy control (NFC) is proposed to deal with the leader-following formation problem, where the single-integrator model of (3) is considered. First, let the x- and y-axis error functions be, respectively, defined as

$$e_{xi}(t) = \sum_{j=1, j\neq i}^{n-1} a_{ij}\left[\left(x_i(t) - p_{xi}\right) - \left(x_j(t) - p_{xj}\right)\right] + \overline{b}_i\left[\left(x_i(t) - p_{xi}\right) - \left(x_n(t) - p_{xn}\right)\right], \quad (4)$$

$$e_{yi}(t) = \sum_{j=1, j\neq i}^{n-1} a_{ij}\left[\left(y_i(t) - p_{yi}\right) - \left(y_j(t) - p_{yj}\right)\right] + \overline{b}_i\left[\left(y_i(t) - p_{yi}\right) - \left(y_n(t) - p_{yn}\right)\right], \quad (5)$$

where p_{xi}, p_{xn}, p_{yi}, and p_{yn} are coordinate positions regarding a desired formation pattern in x- and y-axes. It is noticed that $a_{ij} = 1$ means that the jth agent can send position information to the ith agent, and $\overline{b}_i = 1$ means that the ith agent can receive position information from the leader. In this study, the leader is maneuvered along a prespecified trajectory, and the design of formation controller is focused on followers. Let the controller inputs of the ith follower agent be designated as follows

$$S_{xi} = c_1 \cdot e_{xi} + c_2 \cdot \int_0^t e_{xi}dt,$$
$$S_{yi} = c_1 \cdot e_{yi} + c_2 \cdot \int_0^t e_{yi}dt, \quad (6)$$

where c_1 and c_2 are positive constants, $i = 1, 2, \ldots, n-1$.

The network structure of NFC is shown in Figure 2. The fuzzy rules are given in Table 1, where the input and output spaces are fuzzily partitioned into six fuzzy sets, Negative Big (NB), Negative Medium (NM), Negative Small (NS), Positive Small (PS), Positive Medium (PM), and Positive Big (PB). The input and output membership functions are depicted in

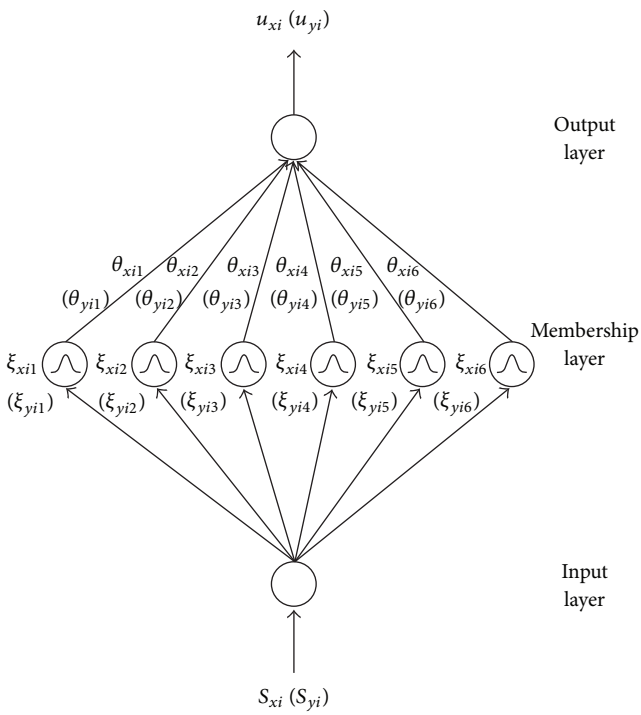

Figure 2: Structure of NFC.

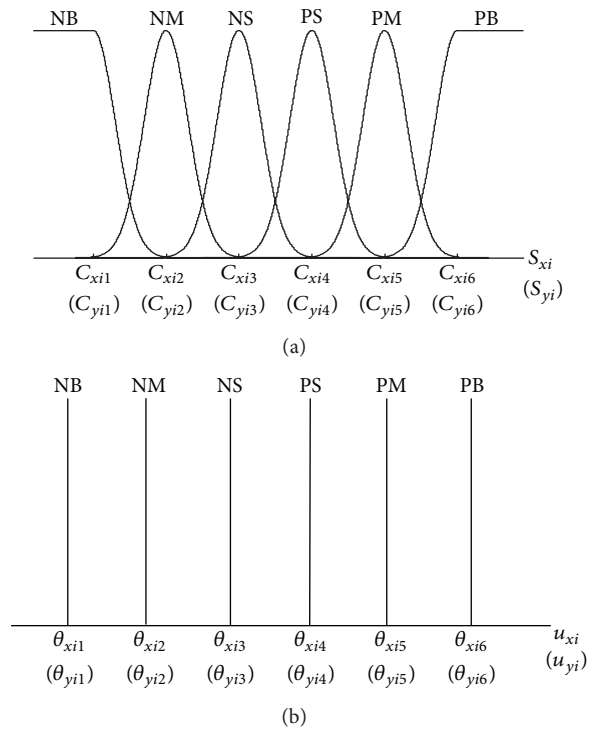

Figure 3: Membership functions of NFC.

Figure 3. The corresponding if-then fuzzy rules for the ith agent are expressed as

$$\begin{aligned} R_{ik}: &\ \text{IF } S_{xi}\left(S_{yi}\right) \text{ is } \xi_{xik}\left(\xi_{yik}\right) \\ &\text{THEN } u_{xi}\left(u_{yi}\right) \text{ is } \theta_{xik}\left(\theta_{yik}\right), \end{aligned} \tag{7}$$

where $\xi_{xik}(\xi_{yik})$ and $\theta_{xik}(\theta_{yik})$ are the fuzzy sets of the antecedent and consequence parts, respectively, $i = 1, 2, \ldots, n-1$, $k = 1, 2, \ldots, 6$. In Figure 3, the kth nodes of the membership layer are Gaussian functions,

$$\xi_{xik}\left(S_{xi}, \sigma_{xi}, C_{xi}\right) = \exp\left[\frac{-1}{2}\left(\frac{S_{xi} - c_{xik}}{\sigma_{xik}}\right)^2\right], \tag{8}$$

$$\xi_{yik}\left(S_{yi}, \sigma_{yi}, C_{yi}\right) = \exp\left[\frac{-1}{2}\left(\frac{S_{yi} - c_{yik}}{\sigma_{yik}}\right)^2\right], \tag{9}$$

where

$$\begin{aligned} \sigma_{xi} &= \left[\sigma_{xi1} \ \ \sigma_{xi2} \ \ \sigma_{xi3} \ \ \sigma_{xi4} \ \ \sigma_{xi5} \ \ \sigma_{xi6}\right]^T, \\ \sigma_{yi} &= \left[\sigma_{yi1} \ \ \sigma_{yi2} \ \ \sigma_{yi3} \ \ \sigma_{yi4} \ \ \sigma_{yi5} \ \ \sigma_{yi6}\right]^T, \\ C_{xi} &= \left[c_{xi1} \ \ c_{xi2} \ \ c_{xi3} \ \ c_{xi4} \ \ c_{xi5} \ \ c_{xi6}\right]^T, \\ C_{yi} &= \left[c_{yi1} \ \ c_{yi2} \ \ c_{yi3} \ \ c_{yi4} \ \ c_{yi5} \ \ c_{yi6}\right]^T, \end{aligned} \tag{10}$$

$i = 1, 2, \ldots, n-1$. In (8) and (9), $c_{xik}(c_{yik})$ and $\sigma_{xik}(\sigma_{yik})$ are means and standard deviations, respectively, $k = 1, 2, \ldots, 6$.

By using the centroid defuzzification technique, the NFC output can be calculated as follows:

$$\begin{aligned} u_{xi}\left(S_{xi}, \xi_{xi}, \theta_{xi}\right) &= \frac{\sum_{k=1}^{6} \xi_{xik}\theta_{xik}}{\sum_{k=1}^{6} \xi_{xik}} = \theta_{xi}^T \xi_{xi}, \\ u_{yi}\left(S_{yi}, \xi_{yi}, \theta_{yi}\right) &= \frac{\sum_{k=1}^{6} \xi_{yik}\theta_{yik}}{\sum_{k=1}^{6} \xi_{yik}} = \theta_{yi}^T \xi_{yi}, \end{aligned} \tag{11}$$

where $\theta_{xik}(\theta_{yik})$ are the values corresponding to singleton outputs,

$$\begin{aligned} \theta_{xi} &= \left[\theta_{xi1} \ \ \theta_{xi2} \ \ \theta_{xi3} \ \ \theta_{xi4} \ \ \theta_{xi5} \ \ \theta_{xi6}\right]^T, \\ \theta_{yi} &= \left[\theta_{yi1} \ \ \theta_{yi2} \ \ \theta_{yi3} \ \ \theta_{yi4} \ \ \theta_{yi5} \ \ \theta_{yi6}\right]^T, \\ \xi_{xi} &= \left[\frac{\xi_{xi1}}{\xi'_{xi}} \ \ \frac{\xi_{xi2}}{\xi'_{xi}} \ \ \frac{\xi_{xi3}}{\xi'_{xi}} \ \ \frac{\xi_{xi4}}{\xi'_{xi}} \ \ \frac{\xi_{xi5}}{\xi'_{xi}} \ \ \frac{\xi_{xi6}}{\xi'_{xi}}\right]^T, \\ \xi_{yi} &= \left[\frac{\xi_{yi1}}{\xi'_{yi}} \ \ \frac{\xi_{yi2}}{\xi'_{yi}} \ \ \frac{\xi_{yi3}}{\xi'_{yi}} \ \ \frac{\xi_{yi4}}{\xi'_{yi}} \ \ \frac{\xi_{yi5}}{\xi'_{yi}} \ \ \frac{\xi_{yi6}}{\xi'_{yi}}\right]^T, \end{aligned} \tag{12}$$

in which $\xi'_{xi} = \sum_{k=1}^{6} \xi_{xik}$ and $\xi'_{yi} = \sum_{k=1}^{6} \xi_{yik}$.

3.2. Parameter-Learning Algorithms. In this section, the idea of gradient descent will be adopted to derive on-line learning

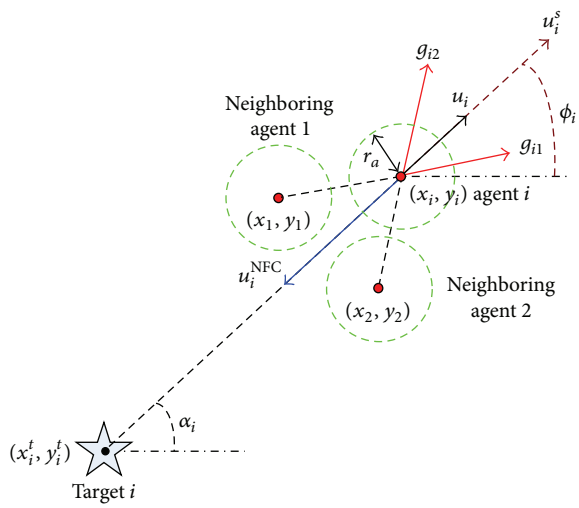

Figure 4: Schematic diagram of local minima problem.

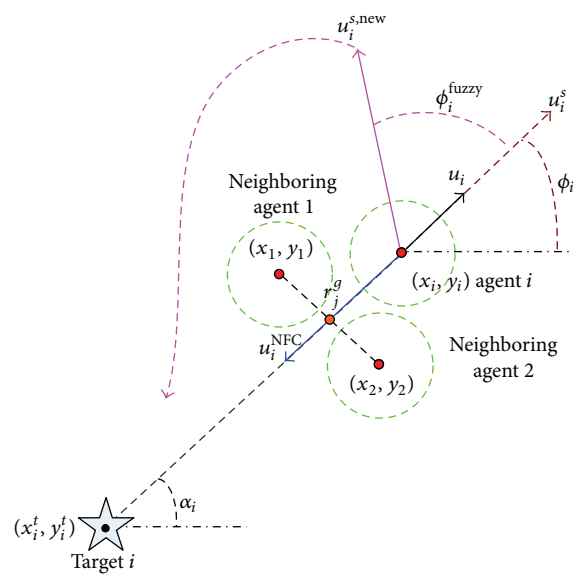

Figure 5: Schematic diagram of improved avoidance functions.

algorithms to update NFC parameters. First, energy functions E_{xi} and E_{yi} are defined as follows:

$$E_{xi} = \frac{1}{2}(S_{xi})^2,$$
$$E_{yi} = \frac{1}{2}(S_{yi})^2, \tag{13}$$

where $i = 1, 2, \ldots, n-1$. Then, the update laws of layer parameters are described in the following.

(1) Output Layer. According to the gradient decent method [44], θ_{xik} and θ_{yik} are updated by the following rules:

$$\Delta\theta_{xik} = -\eta_1 \frac{\partial E_{xi}}{\partial \theta_{xik}} = -\eta_1 \frac{\partial E_{xi}}{\partial u_{xi}} \frac{\partial u_{xi}}{\partial \theta_{xik}},$$
$$\Delta\theta_{yik} = -\eta_1 \frac{\partial E_{yi}}{\partial \theta_{yik}} = -\eta_1 \frac{\partial E_{yi}}{\partial u_{yi}} \frac{\partial u_{yi}}{\partial \theta_{yik}}, \tag{14}$$

where $\eta_1 > 0$ is a learning rate, $i = 1, 2, \ldots, n-1$, $k = 1, 2, \ldots, 6$. From (11), it can be obtained that

$$\frac{\partial u_{xi}}{\partial \theta_{xik}} = \frac{\xi_{xik}}{\sum_{k=1}^{6} \xi_{xik}},$$
$$\frac{\partial u_{yi}}{\partial \theta_{yik}} = \frac{\xi_{yik}}{\sum_{k=1}^{6} \xi_{yik}}. \tag{15}$$

In (14), the error term to be propagated can be reformulated as

$$\frac{\partial E_{xi}}{\partial u_{xi}} = \frac{\partial E_{xi}}{\partial S_{xi}} \frac{\partial S_{xi}}{\partial u_{xi}},$$
$$\frac{\partial E_{yi}}{\partial u_{yi}} = \frac{\partial E_{yi}}{\partial S_{yi}} \frac{\partial S_{yi}}{\partial u_{yi}}. \tag{16}$$

However, the terms $\partial S_{xi}/\partial u_{xi}$ and $\partial S_{yi}/\partial u_{yi}$ in (16) cannot be analytically determined. To overcome this problem, the following adaptive laws are adopted [45]:

$$-\frac{\partial E_{xi}}{\partial u_{xi}} \approx k_1 \cdot S_{xi} + k_2 \cdot \dot{S}_{xi},$$
$$-\frac{\partial E_{yi}}{\partial u_{yi}} \approx k_1 \cdot S_{yi} + k_2 \cdot \dot{S}_{yi}, \tag{17}$$

where k_1 and k_2 are positive constants.

In summary, from (15) and (17), the parameters of the output layer can be adaptively updated.

(2) Membership Layer. The parameters c_{xik} and c_{yik} are updated by the following rules:

$$\Delta c_{xik} = -\eta_2 \frac{\partial E_{xi}}{\partial c_{xik}} = -\eta_2 \frac{\partial E_{xi}}{\partial u_{xi}} \frac{\partial u_{xi}}{\partial \xi_{xik}} \frac{\partial \xi_{xik}}{\partial c_{xik}},$$
$$\Delta c_{yik} = -\eta_2 \frac{\partial E_{yi}}{\partial c_{yik}} = -\eta_2 \frac{\partial E_{yi}}{\partial u_{yi}} \frac{\partial u_{yi}}{\partial \xi_{yik}} \frac{\partial \xi_{yik}}{\partial c_{yik}}, \tag{18}$$

where $\eta_2 > 0$ is a learning rate, $i = 1, 2, \ldots, n-1$, $k = 1, 2, \ldots, 6$. From (8), (9), and (11), it can be obtained that

$$\frac{\partial u_{xi}}{\partial \xi_{xik}} \frac{\partial \xi_{xik}}{\partial c_{xik}} = \frac{\theta_{xik} \cdot \left(\sum_{k=1}^{6} \xi_{xik}\right) - \sum_{k=1}^{6} \xi_{xik}\theta_{xik}}{\left(\sum_{k=1}^{6} \xi_{xik}\right)^2} \cdot \exp\left[\frac{-1}{2}\left(\frac{S_{xi} - c_{xik}}{\sigma_{xik}}\right)^2\right] \cdot \left(\frac{S_{xi} - c_{xik}}{\sigma_{xik}^2}\right),$$
$$\frac{\partial u_{yi}}{\partial \xi_{yik}} \frac{\partial \xi_{yik}}{\partial c_{yik}} = \frac{\theta_{yik} \cdot \left(\sum_{k=1}^{6} \xi_{yik}\right) - \sum_{k=1}^{6} \xi_{yik}\theta_{yik}}{\left(\sum_{k=1}^{6} \xi_{yik}\right)^2} \cdot \exp\left[\frac{-1}{2}\left(\frac{S_{yi} - c_{yik}}{\sigma_{yik}}\right)^2\right] \cdot \left(\frac{S_{yi} - c_{yik}}{\sigma_{yik}^2}\right). \tag{19}$$

Table 2: Fuzzy rule base.

Rule	1	2	3	4	5	6	7	8	9	10	11	12	13	14	15	16	17	18	19	20	21	22	23	24	25
z_i^1	NB	NB	NB	NB	NB	NS	NS	NS	NS	NS	ZO	ZO	ZO	ZO	ZO	PS	PS	PS	PS	PS	PB	PB	PB	PB	PB
z_i^2	VC	C	M	F	VF	VC	C	M	F	VF	VC	C	M	F	VF	VC	C	M	F	VF	VC	C	M	F	VF
ϕ_i^{fuzzy}	PS	PS	PS	ZO	ZO	PB	PB	PS	PS	PS	PB	PB	PB	PB	PB	PB	PB	PS	PS	PS	PS	PS	PS	ZO	ZO

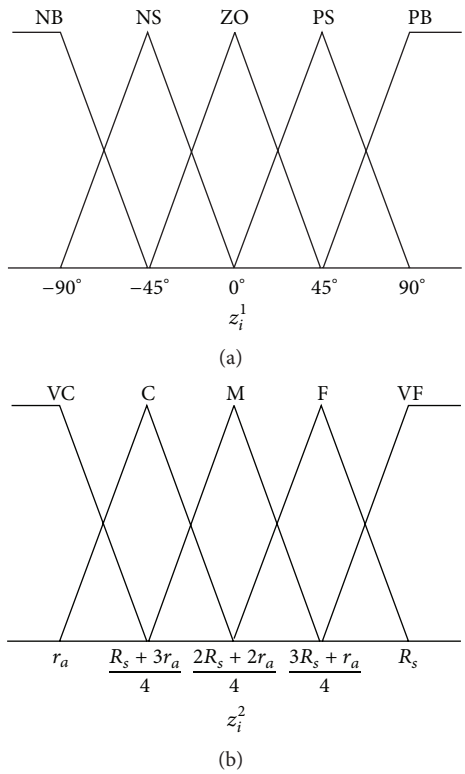

Figure 6: The input membership functions.

Similarly, σ_{xik} and the σ_{yik} are updated by the following amounts:

$$\begin{aligned} \Delta\sigma_{xik} &= -\eta_3 \frac{\partial E_{xi}}{\partial \sigma_{xik}} = -\eta_3 \frac{\partial E_{xi}}{\partial u_{xi}} \frac{\partial u_{xi}}{\partial \xi_{xik}} \frac{\partial \xi_{xik}}{\partial \sigma_{xik}}, \\ \Delta\sigma_{yik} &= -\eta_3 \frac{\partial E_{yi}}{\partial \sigma_{yik}} = -\eta_3 \frac{\partial E_{yi}}{\partial u_{yi}} \frac{\partial u_{yi}}{\partial \xi_{yik}} \frac{\partial \xi_{yik}}{\partial \sigma_{yik}}, \end{aligned} \tag{20}$$

where $\eta_3 > 0$ is a learning rate, $i = 1, 2, \ldots, n$, $k = 1, 2, \ldots, 6$. From (8), (9), and (11), it can be obtained that

$$\begin{aligned} \frac{\partial u_{xi}}{\partial \xi_{xik}} \frac{\partial \xi_{xik}}{\partial \sigma_{xik}} &= \frac{\theta_{xik} \cdot \left(\sum_{k=1}^{6} \xi_{xik}\right) - \sum_{k=1}^{6} \xi_{xik}\theta_{xik}}{\left(\sum_{k=1}^{6} \xi_{xik}\right)^2} \\ &\quad \cdot \exp\left[\frac{-1}{2}\left(\frac{S_{xi} - c_{xik}}{\sigma_{xik}}\right)^2\right] \cdot \frac{\left(S_{xi} - c_{xik}\right)^2}{\left(\sigma_{xik}\right)^3}, \end{aligned}$$

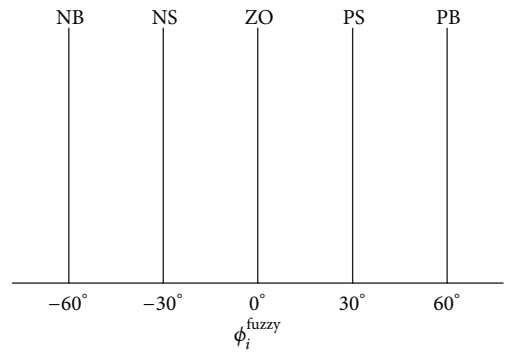

Figure 7: The output membership functions.

$$\begin{aligned} \frac{\partial u_{yi}}{\partial \xi_{yik}} \frac{\partial \xi_{yik}}{\partial \sigma_{yik}} &= \frac{\theta_{yik} \cdot \left(\sum_{k=1}^{6} \xi_{yik}\right) - \sum_{k=1}^{6} \xi_{yik}\theta_{yik}}{\left(\sum_{k=1}^{6} \xi_{yik}\right)^2} \\ &\quad \cdot \exp\left[\frac{-1}{2}\left(\frac{S_{yi} - c_{yik}}{\sigma_{yik}}\right)^2\right] \cdot \frac{\left(S_{yi} - c_{yik}\right)^2}{\left(\sigma_{yik}\right)^3}. \end{aligned} \tag{21}$$

In summary, from (18)–(21), the parameters of the input layer can be adaptively updated.

4. Separation Control for Collision Avoidance

4.1. Potential-Based Separation Control. Let g_{ij} be the separation force between the ith and jth agents. Then, the integrated separation force from all its neighboring agents can be formulated as

$$u_i^s = -\sum_{j \in N_i} g_{ij}\left(r_i, r_j\right). \tag{22}$$

To derive a proper separation force between two connected agents, a smooth potential function V_{ij} is considered,

$$V_{ij}\left(d_{ij}\right) = \left[\min\left(0, \frac{d_{ij}^2 - R_s^2}{d_{ij}^2 - 4r_a^2}\right)\right]^2, \tag{23}$$

such that

$$g_{ij} = \nabla_{r_i} V_{ij}. \tag{24}$$

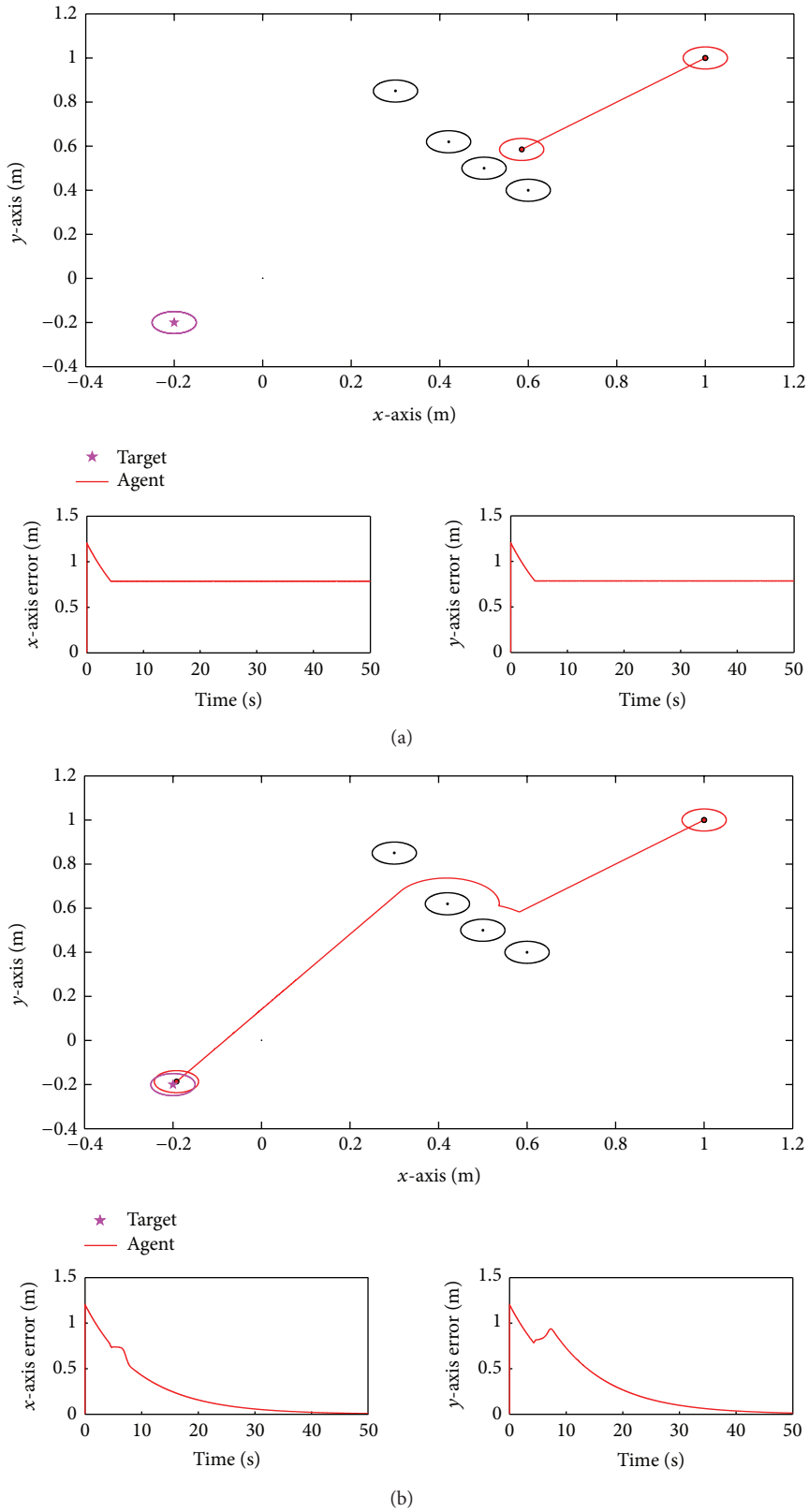

Figure 8: Simulation results of collision avoidance: (a) linger in local minimum (PSC) and (b) bypass neighboring agents (FSC).

In a two-dimensional case, $r_i = [x_i \quad y_i]^T$, the gradient computations of V_{ij} can be obtained as follows:

$$\frac{\partial V_{ij}}{\partial x_i} = \begin{cases} 0, & \text{if } R_s \le d_{ij}, \\ V_{gij}\left(x_i - x_j\right), & \text{if } 2r_a < d_{ij} < R_s, \\ V_{\max}, & \text{if } d_{ij} < 2r_a, \end{cases}$$

$$\frac{\partial V_{ij}}{\partial y_i} = \begin{cases} 0, & \text{if } R_s \le d_{ij}, \\ V_{gij}\left(y_i - y_j\right), & \text{if } 2r_a < d_{ij} < R_s, \\ V_{\max}, & \text{if } d_{ij} < 2r_a, \end{cases} \tag{25}$$

$$V_{gij} = \frac{4\left(R_s^2 - 4r_a^2\right)\left(d_{ij}^2 - R_s^2\right)}{\left(d_{ij}^2 - 4r_a^2\right)^3},$$

where $V_{\max}$ is the maximum allowable separation force. Integrating the formation and separation forces, the net control action to an agent can be obtained as

$$u_i = u_i^{\mathrm{NFC}} + u_i^s, \tag{26}$$

where $u_i^{\mathrm{NFC}} = [u_{xi} \quad u_{yi}]^T$ is the neural fuzzy formation action.

4.2. Fuzzy Separation Control. In a multiagent system, an agent could be standstill or move back and forth if the net force acting on this agent is balanced. This phenomenon is known as the local minimum problem. In Figure 4, the case of agent i with two neighboring agents is considered, where (x_1, y_1) and (x_2, y_2) are neighboring agents, and the related target is located at (x_i^t, y_i^t). The notation u_i^{NFC} is denoted as the attractive force to the target, and g_{i1} and g_{i2} are separation forces corresponding to neighboring agents. Then, the integrated separation force to the ith agent is the vector sum of g_{i1} and g_{i2}, where ϕ_i is the related direction of u_i^s to the x-axis. In addition, u_i is the net force of the ith agent, and α_i is angle between the agent i and its target. In case $\phi_i = \alpha_i$, the direction of u_i^s is opposite to the attractive action u_i^{NFC}. Moreover, if the magnitude of u_i^{NFC} is less or equal to the magnitude of u_i^s, the ith agent will be stuck in the local minimum. To solve this problem, a fuzzy separation control method will be presented, and the key idea is depicted in Figure 5, where an extra angle ϕ_i^{fuzzy} is added to the original separation force, $\phi_i^{\mathrm{new}} = \phi_i + \phi_i^{\mathrm{fuzzy}}$. In Figure 5, $u_i^{s,\mathrm{new}}$ is the modified separation force, of which the magnitude keeps unchanged but the direction is changed because of ϕ_i^{fuzzy}. Consequently, the integrated net force of attractive force and separation force can be represented as

$$u_i = u_i^{\mathrm{NFC}} + u_i^{s,\mathrm{new}}. \tag{27}$$

Basically, $u_i^{s,\mathrm{new}}$ can provide a new route to bypass the neighboring agents when a local minimum situation happens. It is noticed that the target of a follower is its temporary destination for next movement during the process of avoiding collision. For those follower agents, communication-connected to the leader, their respective targets can be obtained according to the leader position and designated formation pattern; however, a substitute solution is required for other followers. Alternatively, from (4) and (5), targets can be equivalently viewed as the propagated errors from other followers,

$$\begin{aligned} x_i^t &= x_i - e_{xi}, \\ y_i^t &= y_i - e_{yi}, \end{aligned} \tag{28}$$

where follower i is not communicated to the leader, $\bar{b}_i = 0$, $i = 1, 2, \ldots, n-1$.

The design of fuzzy separation controller will be illustrated in the following. First, let the fuzzy inputs of the ith agent be

$$\begin{aligned} z_i^1 &= \phi_i - \alpha_i, \\ z_i^2 &= \left\| r_i - r_j^g \right\|, \end{aligned} \tag{29}$$

where $r_j^g = [x_j^g \quad y_j^g]^T \in R^2$ is the position of the center gravity of neighboring agents,

$$\begin{aligned} x_j^g &= \frac{\sum_{j \in N_i} x_j}{|N_i|}, \\ y_j^g &= \frac{\sum_{j \in N_i} y_j}{|N_i|}, \end{aligned} \tag{30}$$

where $|\cdot|$ is the cardinality of a set, that is, $|N_i|$ is the number of neighboring agents of the ith agent.

The fuzzy rules are given in Table 2, where the input and output spaces are fuzzily partitioned into ten fuzzy sets, Negative Big (NB), Negative Small (NS), Zero (ZO), Positive Small (PS), Positive Big (PB), Very Close (VC), Close (C), Medium (M), Far (F), and Very Far (VF). The input and output membership functions are depicted in Figures 6 and 7, respectively. The corresponding if-then fuzzy rules for the ith agent are expressed as

$$R_i: \text{ IF } z_i^1 \text{ is } M_{ik}^1 \text{ AND } z_i^2 \text{ is } M_{ik}^2 \text{ THEN } \phi_i^{\mathrm{fuzzy}} \text{ is } G_{ik}, \tag{31}$$

where M_{ik}^1 and M_{ik}^2 are the fuzzy sets of the antecedent part, and G_{ik} is the fuzzy set of the consequence part, $i = 1, 2, \ldots, n-1$, and $k = 1, 2, \ldots, 5$. By using the centroid defuzzification technique, the defuzzified fuzzy output is calculated as

$$\phi_i^{\mathrm{fuzzy}} = \frac{\sum_{k=1}^{5} \mu_{ik}\left(G_{ik}\right) \cdot G_{ik}}{\sum_{k=1}^{5} \mu_{ik}\left(G_{ik}\right)}, \tag{32}$$

where a min-max operation is performed over all rules mapping to the same output fuzzy set:

$$\mu_{ik}\left(G_{ik}\right) = \max_{G_{ik}} \left\{ \min\left(\mu_{M_{ik}^1}\left(G_{ik}\right), \mu_{M_{ik}^2}\left(G_{ik}\right) \right) \right\}. \tag{33}$$

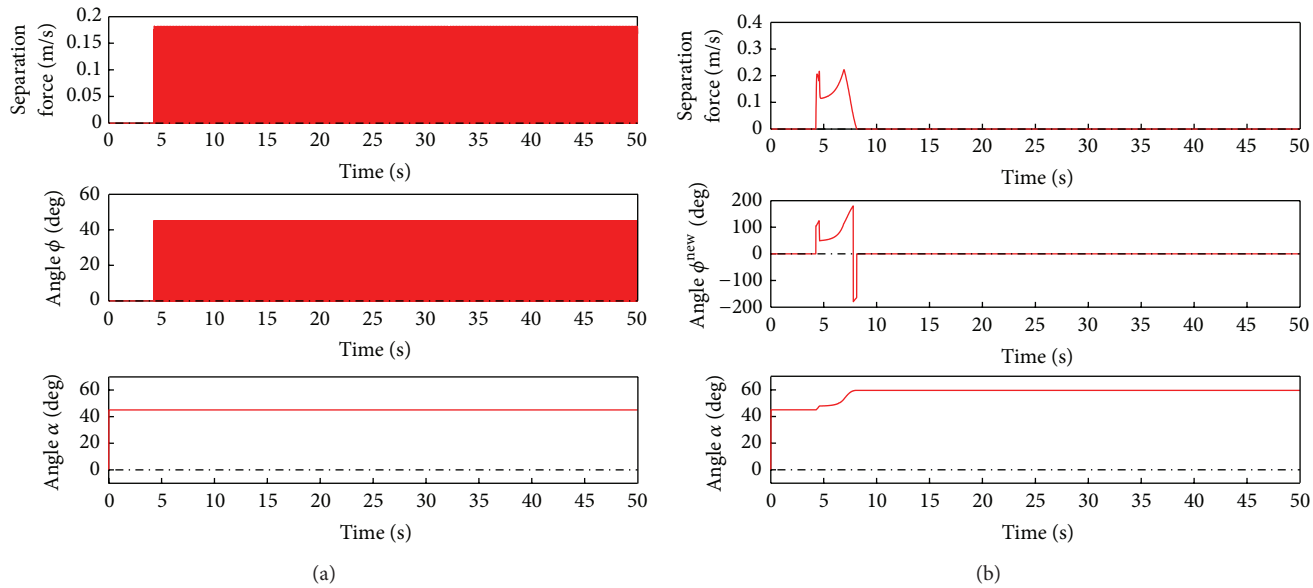

FIGURE 9: Separation force and angle of collision avoidance: (a) PSC and (b) FSC.

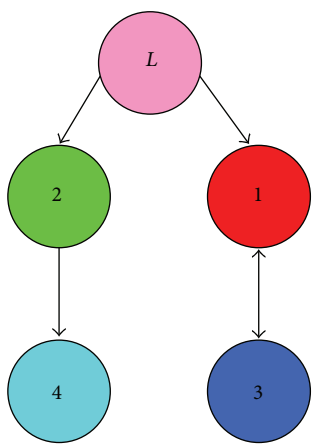

FIGURE 10: Communication topology of multiagent systems.

5. Simulation Results

In the following, all the agents are assumed to be homogeneous with the same specifications, $r_a = 0.05$ (m) and $R_s = 0.15$ (m). To verify the feasibility of proposed neuro-fuzzy formation controller and fuzzy separation controller, both the collision avoidance and formation preservation are considered.

5.1. Collision Avoidance with Static Target. One dynamical agent is initially placed at the point $(1, 1)$ (m), and four fixed agents are located at $(0.5, 0.5)$, $(0.6, 0.4)$, $(0.42, 0.62)$, and $(0.3, 0.85)$ (m), respectively. The target position is given as $(-0.2, -0.2)$ (m). It is desired that the dynamic agent can reach the designated target without colliding with fixed agents. Figures 8 and 9 illustrate the collision-avoidance responses corresponding to potential-based separation control (PSC) and the proposed fuzzy separation control (FSC), where the formation control of each case is the conventional consensus algorithm [46]. In Figure 8, it can be seen that the agent lingers in front of neighboring agents with PSC. On the other hand, the agent can successfully bypass neighboring agents with the proposed FSC. The responses of position errors, shown in the bottom two subplots of Figure 8, indicate that the desired target can be asymptotically achieved with the proposed FSC. However, a local-minimum behavior exists by using the PSC, and the related separation force keeps oscillation. The oscillation behavior of the separation force is coincided with the response of ϕ, shown in Figure 9(a). In Figure 9(b), the angle $\phi = 0$ after 8.26 (sec) means that the dynamic agent successfully bypasses the fixed agents, and thus, there is no separation force.

5.2. Formation Control and Collision Avoidance with Static Leader. In leader-follower formation control, the case of five agents, one static leader and four followers, is considered. The communication topology is shown in Figure 10, where the circles labelled 1 to 4 denote the follower agents and the circle L represents the leader agent. From (2), the information exchanges between leader and followers can be modelled as

$$\overline{A} = \begin{bmatrix} 0 & 0 & 1 & 0 \\ 0 & 0 & 0 & 0 \\ 1 & 0 & 0 & 0 \\ 0 & 1 & 0 & 0 \end{bmatrix}, \qquad \overline{B} = \begin{bmatrix} 1 & 0 & 0 & 0 \\ 0 & 1 & 0 & 0 \\ 0 & 0 & 0 & 0 \\ 0 & 0 & 0 & 0 \end{bmatrix}. \tag{34}$$

The followers are initially placed at the points $(0, -0.25)$, $(0.25, 0)$, $(0, 0.25)$, and $(-0.25, 0)$ (m), respectively, and the position of the leader is $(0.5, 0)$ (m). The formation pattern is designated as $(p_{x1}, p_{y1}) = (-0.5, 0.25)$, $(p_{x2}, p_{y2}) = (-0.75, 0)$, $(p_{x3}, p_{y3}) = (-0.5, -0.25)$, $(p_{x4}, p_{y4}) = (-0.25, 0)$, and $(p_{x5}, p_{y5}) = (0, 0)$ (m). The parameters of the NFC are

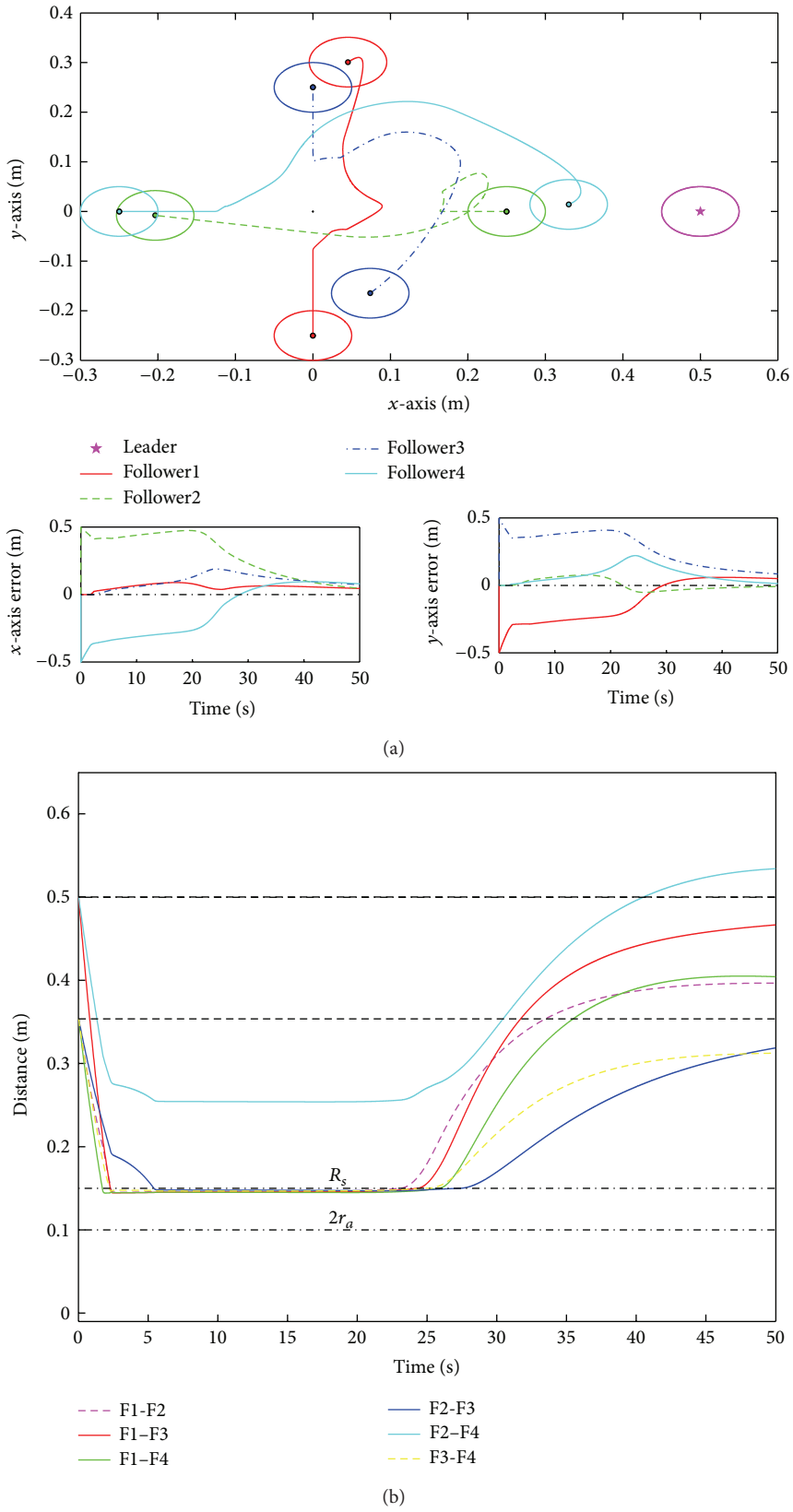

Figure 11: Simulation results of formation and collision avoidance control with static leader (CA + PSC): (a) agents' trajectories and formation errors and (b) the distance between agents.

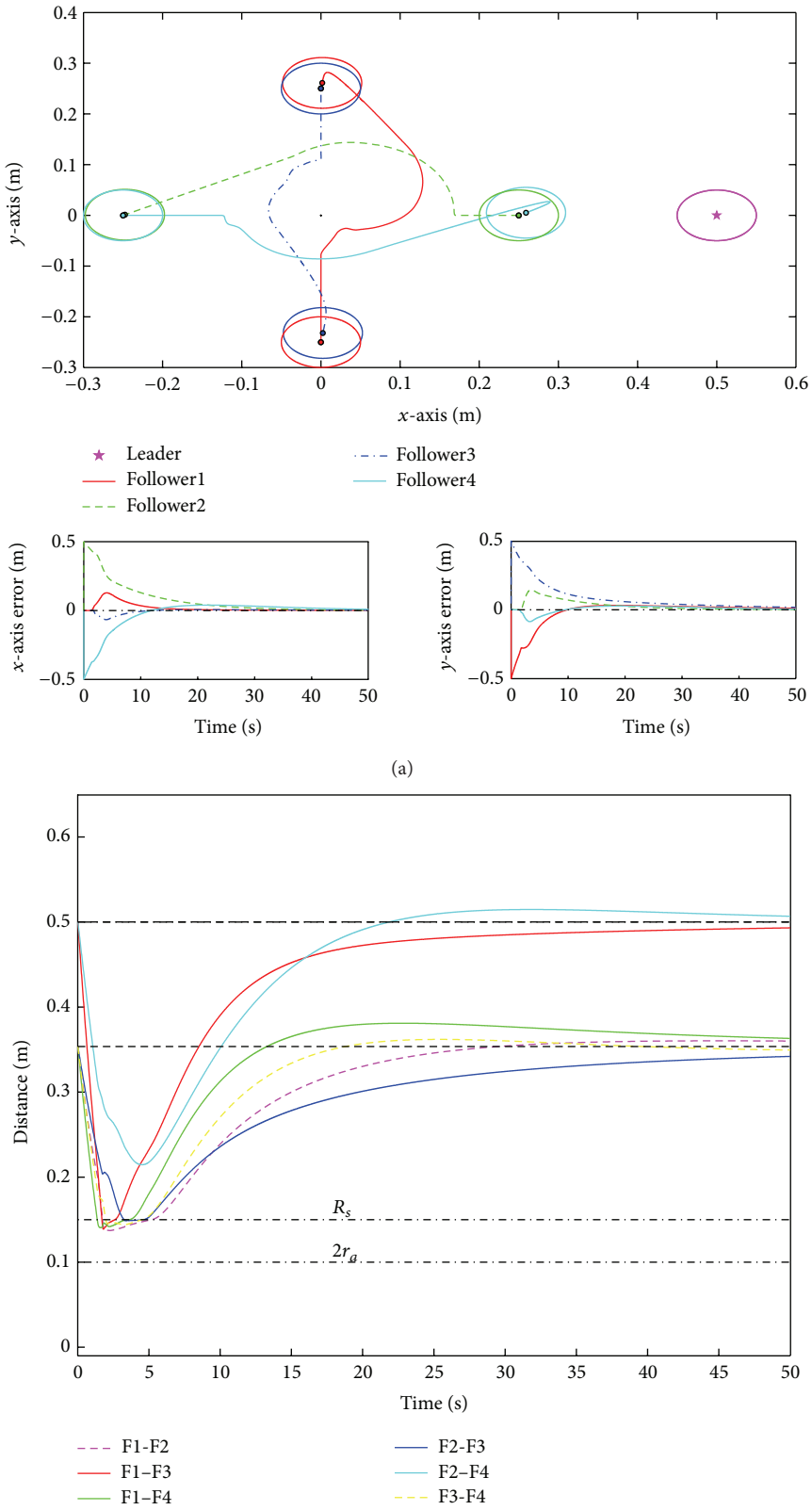

FIGURE 12: Simulation results of formation and collision-avoidance control with static leader (CA + FSC): (a) agents' trajectories and formation errors and (b) the distance between agents.

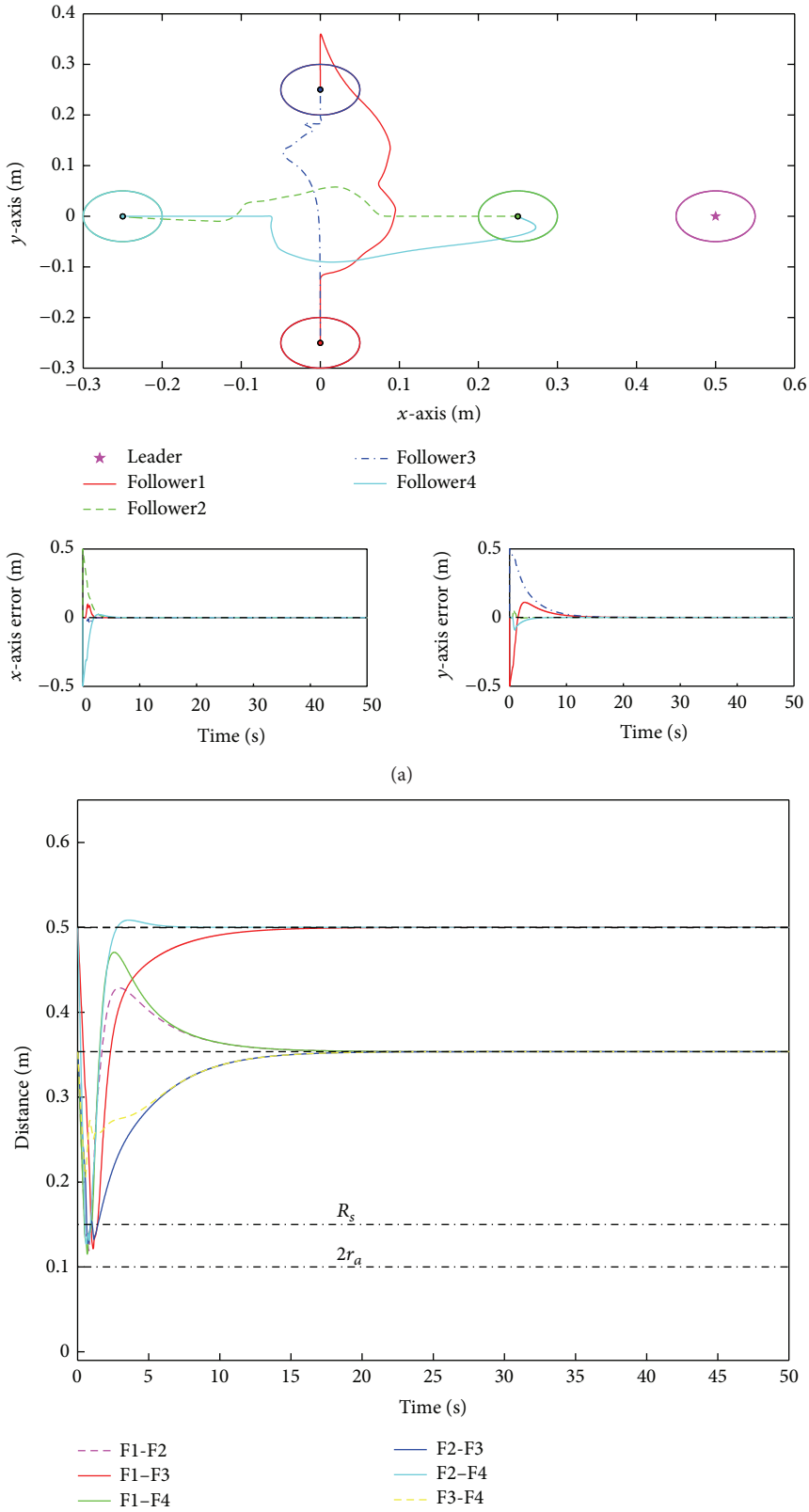

Figure 13: Simulation results of formation and collision-avoidance control with static leader (NFC + FSC): (a) agents' trajectories and formation errors and (b) the distance between agents.

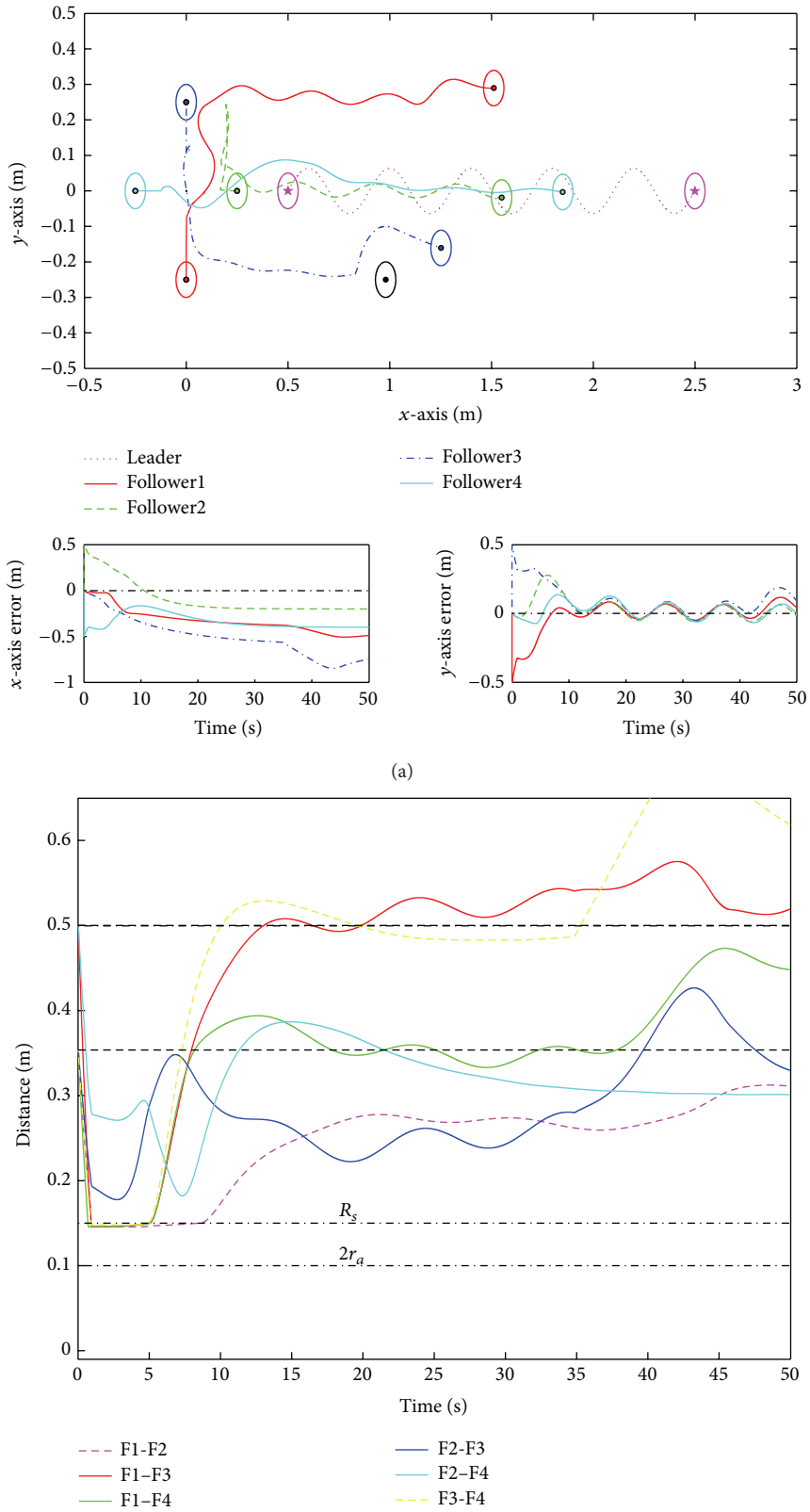

Figure 14: Simulation results of formation and collision-avoidance control with dynamic leader (CA + PSC): (a) agents' trajectories and formation errors and (b) the distance between agents.

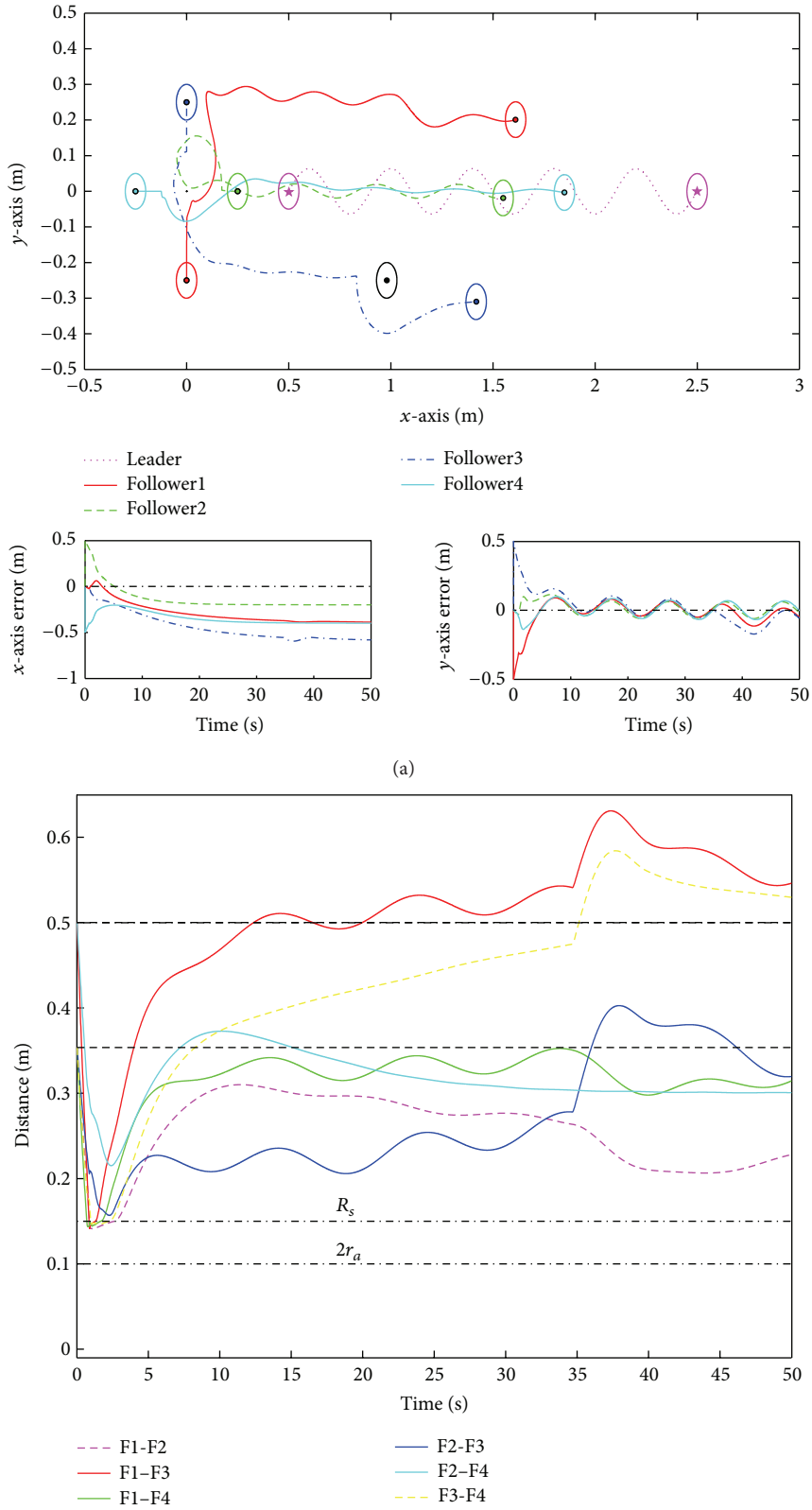

Figure 15: Simulation results of formation and collision-avoidance control with dynamic leader (CA + FSC): (a) agents' trajectories and formation errors and (b) the distance between agents.

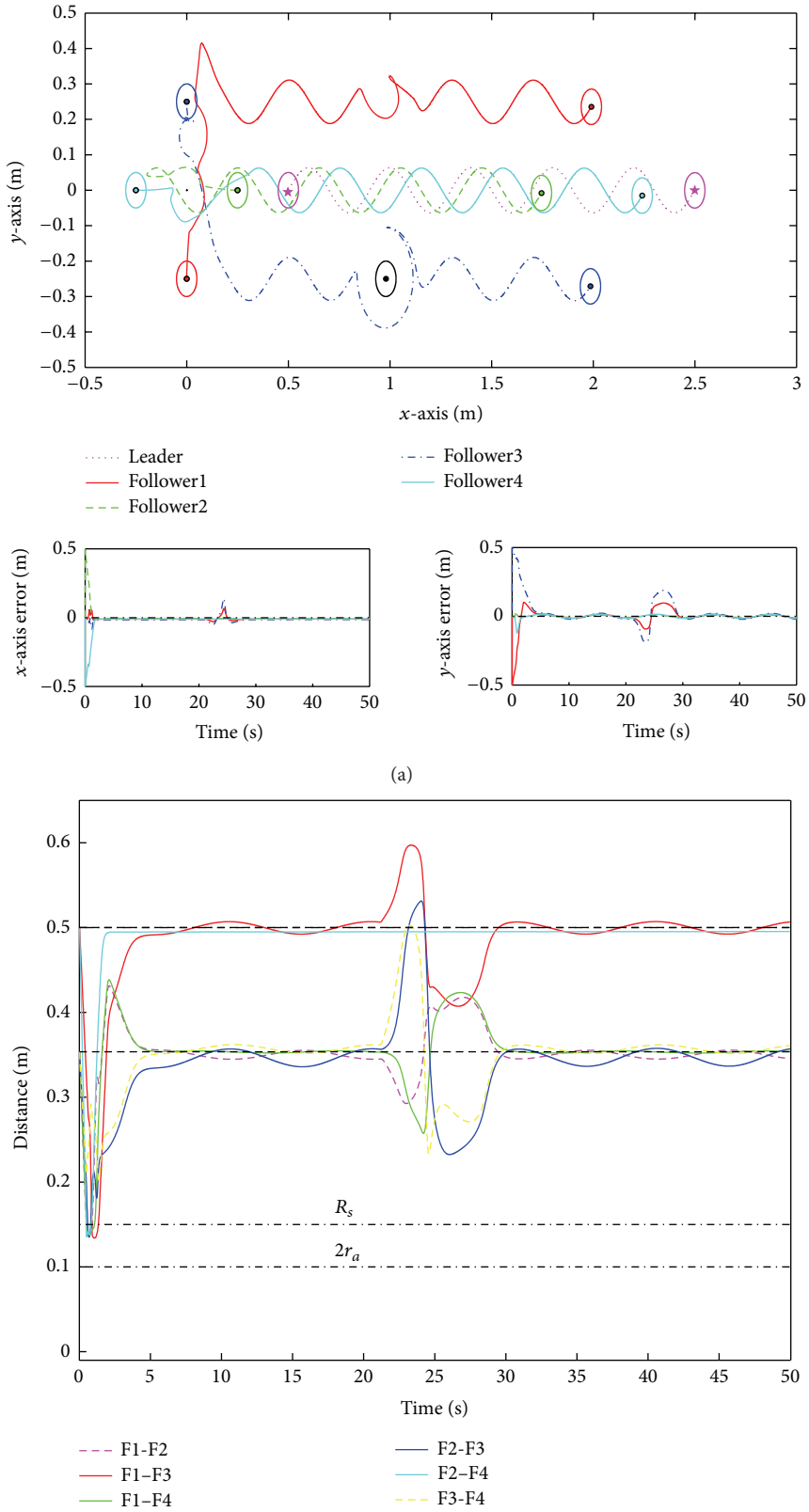

Figure 16: Simulation results of formation and collision-avoidance control with dynamic leader (NFC + FSC): (a) agents' trajectories and formation errors and (b) the distance between agents.

Table 3: Formation errors: formation and separation control with static leader.

	IAE	ISE	ITAE	ITSE
CA + PSC	5887.77	1580.74	114492.31	23911.31
CA + FSC	1746.77	304.78	20183.14	1249.37
NFC + FSC	382.47	90.12	967.88	103.77

Table 4: Formation errors: formation and separation control with dynamic leader.

	IAE	ISE	ITAE	ITSE
CA + PSC	8214.19	3156.40	223875.11	96814.34
CA + FSC	7477.28	2528.48	204209.46	75349.76
NFC + FSC	765.87	99.88	13552.16	700.71

originally chosen as $c_1 = 3$, $c_2 = 2$, $C_{xi}(0) = C_{yi}(0) = \theta_{xi}(0) = \theta_{yi}(0) = [-1 \quad -0.67 \quad -0.33 \quad 0.33 \quad 0.67 \quad 1]^T$, $i = 1, 2, 3, 4$, $\sigma_{xi}(0) = \sigma_{yi}(0) = [0.5 \quad 0.5 \quad 0.5 \quad 0.5 \quad 0.5 \quad 0.5]^T$, $\eta_1 = 0.022$, $\eta_2 = 0.01$, and $\eta_3 = 0.012$. Three unique distributed strategies, consensus algorithm with potential-based separation control (CA + PSC), consensus algorithm with fuzzy separation control (CA + FSC), and neurofuzzy formation control with fuzzy separation control (NFC + FSC), are considered. Accordingly, simulation results are shown in Figures 11, 12, and 13, including the error trajectories of x- and y-axis, and the relative distances between a pair of agents. Since the relative distance between any two agents is greater than $2r_a$, shown in Figures 11(b), 12(b), and 13(b), the desired collision avoidance can be accomplished using these three control strategies. In addition, the formation responses are shown in Figures 11(a), 12(a), and 13(a). It can be seen that there exist significant steady-state errors using CA + PSC. Conversely, the formation pattern can be asymptotically achieved with the use of NFC + FSC. The position errors, $|e_{xi}| + |e_{yi}|$, are summarized in Table 3, where IAE is the integral absolute error, ISE is the integral square error, ITAE is the integral time absolute error, and ITAE stands for the integral time square error. In summary, the proposed NFC + FSC can provide better performance than the counterparts of the other two methods.

5.3. Formation Control and Collision Avoidance with Dynamic Leader. In the following, previous leader-follower system is addressed, where all initial settings are the same except that one fixed agent is added at the position (0.95, −0.25) (m). This fixed agent can be viewed as a standstill obstacle. Besides, a time-varying leader is considered, where the velocity vector is $(0.06, 0.08 \ \sin(0.002\pi t))$ (m/s). The formation responses are shown in Figures 14, 15, and 16, where the methods of CA + PSC, CA + FSC, and NFC + FSC are considered. Similar to the previously mentioned illustrations, the moving trajectories and the relative distances between two follower agents are depicted in Figures 14, 15, and 16. It can be seen that even the collision avoidance can be achieved with CA + PSC and CA + FSC; however, these two strategies eventually fail to preserve the desired formation pattern. On the other hand, from Figure 16, collision-free formation can be obtained by using the proposed NFC + FSC control scheme. In particular, it can be seen that the third follower can successfully bypass the fixed agent and keep its way to form a designated pattern. The formation errors of different control strategies are summarized in Table 4. It can be concluded that the proposed neurofuzzy formation and fuzzy separation combined controller can provide better responses than the counterparts of conventional consensus algorithm with potential-based separation control.

Remark 1. From simulation results, it can be seen that the collision-free formation task can be achieved for single-integrator agents. In particular, the local minimum problem can be overcome using the proposed fuzzy separation control. It is promising that the proposed works can be applied to some practical applications, such as multirobot systems and unmanned vehicle systems.

6. Conclusion

This paper presents a neural fuzzy formation controller for multiagent systems. The learning rules for controller parameters can be derived from the use of gradient decent method. In addition, a fuzzy separation control is proposed to achieve collision avoidance such that the problem of local minima can be solved. Simulation results are provided for the cases of static leader and dynamic leader. The collision-free leader-follower formation can be accomplished by the proposed fuzzy formation and separation control strategy. Performance comparisons indicate that the proposed fuzzy-based control scheme has better formation responses compared to the counterparts of conventional consensus algorithm and potential-based separation control. The current results are mainly limited in single-integrator multiagent systems. It should be challenging and interesting to investigate the collision avoidance problem for high-order agents with nonlinear dynamics. For example, a fuzzy based separation control for kinematic agents will be undertaken in our future work.

Acknowledgments

This work is partially supported by the Taiwan National Science Council under the Grants NSC 101-2221-E-182-041-MY2 and NSC 100-2918-I-182-002. The authors also want to appreciate the High Speed Intelligent Communication Research Center, Chang Gung University, Taiwan, for continuing support in the study of multiagent systems.

References

[1] Z. G. Hou, L. Cheng, and M. Tan, "Decentralized robust adaptive control for the multiagent system consensus problem using neural networks," *IEEE Transactions on Systems, Man, and Cybernetics, Part B*, vol. 39, no. 3, pp. 636–647, 2009.

[2] H. Zhang and F. L. Lewis, "Adaptive cooperative tracking control of higher-order nonlinear systems with unknown dynamics," *Automatica*, vol. 48, no. 7, pp. 1432–1439, 2012.

[3] M. E. Valcher and P. Misra, "On the controllability and stabilizability of non-homogeneous multi-agent dynamical systems," *Systems & Control Letters*, vol. 61, no. 7, pp. 780–787, 2012.

[4] B. Ranjbar-Sahraei, F. Shabaninia, A. Nemati, and S.-D. Stan, "A novel robust decentralized adaptive fuzzy control for swarm formation of multiagent systems," *IEEE Transactions on Industrial Electronics*, vol. 59, no. 8, pp. 3124–3134, 2012.

[5] R. Cui, B. Ren, and S. S. Ge, "Synchronised tracking control of multi-agent system with high-order dynamics," *IET Control Theory & Applications*, vol. 6, no. 5, pp. 603–614, 2012.

[6] X. Luo, D. Liu, X. Guan, and S. Li, "Flocking in target pursuit for multi-agent systems with partial informed agents," *IET Control Theory & Applications*, vol. 6, no. 4, pp. 560–569, 2012.

[7] D. J. Pack, P. DeLima, G. J. Toussaint, and G. York, "Cooperative control of UAVs for localization of intermittently emitting mobile targets," *IEEE Transactions on Systems, Man, and Cybernetics, Part B*, vol. 16, no. 1, pp. 19–33, 2009.

[8] T. Keviczky, F. Borrelli, K. Fregene, D. Godbole, and G. J. Balas, "Decentralized receding horizon control and coordination of autonomous vehicle formations," *IEEE Transactions on Control Systems Technology*, vol. 16, no. 1, pp. 19–33, 2008.

[9] K. S. Hwang, S. W. Tan, M. C. Hsiao, and C. S. Wu, "Cooperative multiagent congestion control for high-speed networks," *IEEE Transactions on Systems, Man, and Cybernetics, Part B*, vol. 35, no. 2, pp. 255–268, 2005.

[10] L. Shi, A. Capponi, K. H. Johansson, and R. M. Murray, "Resource optimisation in a wireless sensor network with guaranteed estimator performance," *IET Control Theory and Applications*, vol. 4, no. 5, pp. 710–723, 2010.

[11] B. Fidan, C. Yu, and B. D. O. Anderson, "Acquiring and maintaining persistence of autonomous multi-vehicle formations," *IET Control Theory and Applications*, vol. 1, no. 2, pp. 452–460, 2007.

[12] R. Olfati-Saber and R. M. Murray, "Consensus problems in networks of agents with switching topology and time-delays," *IEEE Transactions on Automatic Control*, vol. 49, no. 9, pp. 1520–1533, 2004.

[13] H. Jiang, J. Yu, and C. Zhou, "Consensus of multi-agent linear dynamic systems via impulsive control protocols," *International Journal of Systems Science*, vol. 42, no. 6, pp. 967–976, 2011.

[14] Y.-H. Chang, C.-W. Chang, C.-L. Chen, and C.-W. Tao, "Fuzzy sliding-mode formation control for multi-robot systems: design and implementation," *IEEE Transactions on Systems, Man and Cybernetics, Part B*, vol. 42, no. 2, pp. 444–457, 2012.

[15] N. Cai, J.-X. Xi, Y.-S. Zhong, and H.-Y. Ma, "Controllability improvement for linear time-invariant dynamic multi-agent systems," *International Journal of Innovative Computing, Information and Control*, vol. 8, no. 5, pp. 3315–3328, 2012.

[16] W. Ni and D. Cheng, "Leader-following consensus of multi-agent systems under fixed and switching topologies," *Systems and Control Letters*, vol. 59, no. 3-4, pp. 209–217, 2010.

[17] J. Qin, H. Gao, and W. X. Zheng, "Second-order consensus for multi-agent systems with switching topology and communication delay," *Systems and Control Letters*, vol. 60, no. 6, pp. 390–397, 2011.

[18] F. Jiang, L. Wang, and G. Xie, "Consensus of high-order dynamic multi-agent systems with switching topology and time-varying delays," *Journal of Control Theory and Applications*, vol. 8, no. 1, pp. 52–60, 2010.

[19] Y. Zheng, Y. Zhu, and L. Wang, "Consensus of heterogeneous multi-agent systems," *IET Control Theory & Applications*, vol. 5, no. 16, pp. 1881–1888, 2011.

[20] X. Su, P. Shi, L. Wu, and Y.-D. Song, "A novel control design on discrete-time Takagi-Sugeno fuzzy systems with time-varying delays," *IEEE Transactions on Fuzzy Systems*, 2012.

[21] X. Su, P. Shi, L. Wu, and Y.-D. Song, "A novel approach to filter design for T-S fuzzy discrete-time systems with time-varying delay," *IEEE Transactions on Fuzzy Systems*, vol. 20, no. 6, pp. 1114–1129, 2012.

[22] X. Su, P. Shi, L. Wu, and S. K. Nguang, "Induced ℓ_2 filtering of fuzzy stochastic systems with time-varying delays," *IEEE Transactions on Systems, Man and Cybernetics, Part B*, 2012.

[23] L. Wu, X. Su, P. Shi, and J. Qiu, "Model approximation for discrete-time state-delay systems in the TS fuzzy framework," *IEEE Transactions on Fuzzy Systems*, vol. 19, no. 2, pp. 366–378, 2011.

[24] L. Wu and W. X. Zheng, "$L_2 - L_\infty$ control of nonlinear fuzzy itô stochastic delay systems via dynamic output feedback," *IEEE Transactions on Systems, Man, and Cybernetics, Part B*, vol. 39, no. 5, pp. 1308–1315, 2009.

[25] L. Wu, X. Su, P. Shi, and J. Qiu, "A new approach to stability analysis and stabilization of discrete-time T-S fuzzy time-varying delay systems," *IEEE Transactions on Systems, Man, and Cybernetics, Part B*, vol. 41, no. 1, pp. 273–286, 2011.

[26] R. J. Wai and J. D. Lee, "Robust levitation control for linear Maglev rail system using fuzzy neural network," *IEEE Transactions on Control Systems Technology*, vol. 17, no. 1, pp. 4–14, 2009.

[27] X. Yuan, Y. Wang, L. Wu, X. Zhang, and W. Sun, "Neural network based self-learning control strategy for electronic throttle valve," *IEEE Transactions on Vehicular Technology*, vol. 59, no. 8, pp. 3757–3765, 2010.

[28] F. J. Lin and P. H. Shen, "Adaptive fuzzy-neural-network control for a DSP-based permanent magnet linear synchronous motor servo drive," *IEEE Transactions on Fuzzy Systems*, vol. 14, no. 4, pp. 481–495, 2006.

[29] M. Singh and A. Chandra, "Application of adaptive network-based fuzzy inference system for sensorless control of PMSG-based wind turbine with nonlinear-load-compensation capabilities," *IEEE Transactions on Power Electronics*, vol. 26, no. 1, pp. 165–175, 2011.

[30] S. P. Moustakidis, G. A. Rovithakis, and J. B. Theocharis, "An adaptive neuro-fuzzy tracking control for multi-input nonlinear dynamic systems," *Automatica*, vol. 44, no. 5, pp. 1418–1425, 2008.

[31] S. H. Park and S. I. Han, "Robust-tracking control for robot manipulator with deadzone and friction using backstepping and RFNN controller," *IET Control Theory & Applications*, vol. 5, no. 12, pp. 1397–1417, 2011.

[32] C.-S. Chen, "Robust self-organizing neural-fuzzy control with uncertainty observer for MIMO nonlinear systems," *IEEE Transactions on Fuzzy Systems*, vol. 19, no. 4, pp. 694–706, 2011.

[33] M. Khezri and M. Jahed, "A neuro-fuzzy inference system for sEMG-based identification of hand motion commands," *IEEE Transactions on Industrial Electronics*, vol. 58, no. 5, pp. 1952–1960, 2011.

[34] C. Chen, B. Zhang, and G. Vachtsevanos, "Prediction of machine health condition using neuro-fuzzy and Bayesian algorithm," *IEEE Transactions on Instrumentation and Measurement*, vol. 61, no. 2, pp. 297–306, 2012.

[35] W.-Y. Wang, M.-C. Chen, and S.-F. Su, "Hierarchical T-S fuzzy-neural control of anti-lock braking system and active suspension in a vehicle," *Automatica*, vol. 48, no. 8, pp. 1698–1706, 2012.

[36] T. Niknam, H. D. Mojarrad, and M. Nayeripour, "A new hybrid fuzzy adaptive particle swarm optimization for non-convex economic dispatch," *International Journal of Innovative*

Computing, Information and Control, vol. 7, no. 1, pp. 189–202, 2011.

[37] D. M. Stipanović, P. F. Hokayem, M. W. Spong, and D. D. Šiljak, "Cooperative avoidance control for multiagent systems," *Journal of Dynamic Systems, Measurement and Control, Transactions of the ASME*, vol. 129, no. 5, pp. 699–707, 2007.

[38] D. Gu and H. Hu, "Using fuzzy logic to design separation function in flocking algorithms," *IEEE Transactions on Fuzzy Systems*, vol. 16, no. 4, pp. 826–838, 2008.

[39] D. Gu and Z. Wang, "Leader-follower flocking: algorithms and experiments," *IEEE Transactions on Control Systems Technology*, vol. 17, no. 5, pp. 1211–1219, 2009.

[40] P. F. Hokayem, D. M. Stipanović, and M. W. Spong, "Coordination and collision avoidance for Lagrangian systems with disturbances," *Applied Mathematics and Computation*, vol. 217, no. 3, pp. 1085–1094, 2010.

[41] S. S. Ge and Y. J. Cui, "Dynamic motion planning for mobile robots using potential field method," *Autonomous Robots*, vol. 13, no. 3, pp. 207–222, 2002.

[42] Z. Wang and D. Gu, "Cooperative target tracking control of multiple robots," *IEEE Transactions on Industrial Electronics*, vol. 59, no. 8, pp. 3232–3240, 2012.

[43] M. Mesbahi and M. Egerstedt, *Graph Theoretic Methods in Multiagent Networks*, Princeton University Press, Princeton, NJ, USA, 2010.

[44] L. Khan, S. Anjum, and R. Badar, "Standard fuzzy model identification using gradient methods," *World Applied Sciences Journal*, vol. 8, no. 1, pp. 1–9, 2010.

[45] F. J. Lin, R. J. Wai, and C. C. Lee, "Fuzzy neural network position controller for ultrasonic motor drive using push-pull DC-DC converter," *IEE Proceedings: Control Theory and Applications*, vol. 146, no. 1, pp. 99–107, 1999.

[46] W. Ren and R. Beard, *Distributed Consensus in Multi-Vehicle Cooperative Control: Theory and Applications*, Springer, 2007.

Hindawi Publishing Corporation
Mathematical Problems in Engineering
Volume 2013, Article ID 734094, 7 pages
http://dx.doi.org/10.1155/2013/734094

Research Article

Fuzzy Sliding Mode Controller Design Using Takagi-Sugeno Modelled Nonlinear Systems

S. Bououden,[1] M. Chadli,[2] and H. R. Karimi[3]

[1] *Laboratoire d'Automatique et de Robotique, Université de Constantine, Route d'Ain El Bey, Constantine, Algeria*
[2] *MIS (EA 4290), University of Picardie Jules Verne, 33 rue Saint-Leu, 80039 Amiens, France*
[3] *Department of Engineering, Faculty of Engineering and Science, University of Agder, 4898 Grimstad, Norway*

Correspondence should be addressed to M. Chadli; mohammed.chadli@u-picardie.fr

Received 4 September 2012; Accepted 4 October 2012

Academic Editor: Peng Shi

Copyright © 2013 S. Bououden et al. This is an open access article distributed under the Creative Commons Attribution License, which permits unrestricted use, distribution, and reproduction in any medium, provided the original work is properly cited.

Adaptive fuzzy sliding mode controller for a class of uncertain nonlinear systems is proposed in this paper. The unknown system dynamics and upper bounds of the minimum approximation errors are adaptively updated with stabilizing adaptive laws. The closed-loop system driven by the proposed controllers is shown to be stable with all the adaptation parameters being bounded. The performance and stability of the proposed control system are achieved analytically using the Lyapunov stability theory. Simulations show that the proposed controller performs well and exhibits good performance.

1. Introduction

Recent research on fuzzy logic control has, therefore, been devoted to model based fuzzy control systems that guarantee not only stability, but also performance of closed-loop fuzzy control systems [1–6]. For a systematic control design of nonlinear systems, the Takagi-Sugeno (T-S) fuzzy model [4, 5, 7–12] has been a popular choice in industrial processes due to its ability to represent the nonlinear system only for input-output data without complex mathematical equations.

In an effort to improve the robustness of the adaptive fuzzy control system, many works have been published on the design of adaptive fuzzy sliding mode controller [13–18], which integrates the sliding mode controller [16, 19–23] design technique into the adaptive fuzzy control to improve the stability and the robustness of the control system. Conventionally, adaptive fuzzy sliding control systems (AFSCSs) design is based on the assumption that the system states are available for measurement, so the adaptive laws of AFSCS are formulated as functions of the tracking error of the system [21, 24–27].

However, some problems on the algorithm convergence and conditions stabilities remain with no response. To resolve this problem, first is the need for accurate information on the evolution of the system in the state space, upper bounds of uncertainties and disturbances. The second is the knowledge of the upper bound of the minimum approximation error. We know that the uncertain nature of nonlinear systems makes it difficult to have an analytical description of the dynamics of the system. Moreover, the knowledge of the upper bound of the minimum approximation error leaves the control law still restrictive. In the further study involving a perturbed large-scale system with a time-varying interconnection, an adaptive algorithm for estimating an uncertain upper bound based on a variable sliding control frame was proposed in [28].

In this note, based on the variable surface, a fuzzy sliding model controller is developed for guaranteeing the tracking performance, in particular, time-varying uncertain parameters are approximated by fuzzy system, and the adaptive sliding mode control is designed so as to compensate for any unknown reconstruction error, through parameter adaptation law. In this way, the actual system can follow the reference signal even in the event of a hard nonlinearity, and fuzzy sliding mode control gives the unknown upper bound of uncertainties that are adaptively updated with stabilizing adaptive laws. It is proved that the closed-loop system is

globally stable in the Lyapunov sense if the signals involved are bounded and the system output can track the desired reference input asymptotically.

This paper is organized as follows: some preliminaries are provided in Section 2. Following the introduction, the fuzzy logic system is reviewed briefly in Section 3. The design and stability analysis for the proposed adaptive fuzzy sliding mode controller is included in Section 4. Simulation examples to demonstrate the performance of the proposed method are provided in Section 5. Finally, in Section 6, we give a brief conclusion.

2. Preliminaries

Consider the nth-order nonlinear dynamical system of the form:

$$\begin{aligned} x^n &= f(\mathbf{x}) + g(\mathbf{x})u + d_s, \\ y &= x, \end{aligned} \tag{1}$$

where $\mathbf{x} = [x, \dot{x}, \ldots, x^{n-1}]^T = [x_1, x_2, \ldots, x_n]^T \in R^n$ is vector of the system that is assumed to be available for measurements, f and g are unknown but bounded nonlinear functions, $u \in R$ and $y \in R$ control input and output of the system, respectively, and d_s is external disturbance. As system (1) is required to be controllable, the nonzero condition of input gain $g(\mathbf{x}) \neq 0$ is necessary.

The system (1) can be rewritten in the following form:

$$0 = -g^{-1}(\mathbf{x})x^n + g^{-1}(\mathbf{x})f(\mathbf{x}) + u + g^{-1}(\mathbf{x})d_s. \tag{2}$$

By adding x^n to both sides, we get

$$x^n = x^n - g^{-1}(\mathbf{x})x^n + g^{-1}(\mathbf{x})f(\mathbf{x}) + u + g^{-1}(\mathbf{x})d_s. \tag{3}$$

Equation (3) can be rewritten as

$$x^n = F(\mathbf{x}) + u + d(\mathbf{x}) \tag{4}$$

such that

$$\begin{aligned} F(\mathbf{x}) &= \left(1 - g^{-1}(\mathbf{x})\right)x^n + g^{-1}(\mathbf{x})f(\mathbf{x}), \\ d(\mathbf{x}) &= g^{-1}(\mathbf{x})d_s. \end{aligned} \tag{5}$$

Assumption 1 (see [29, 30]). Assume that $f(\mathbf{x})$, $g(\mathbf{x})$, and d_s satisfy $|f(\mathbf{x})| \leq \mu < \infty$, $0 < g_{\min} \leq g(\mathbf{x}) \leq g_{\max} < \infty$, and $|d| \leq \kappa$, respectively, for all $\mathbf{x} \in \mathbf{U}_{\mathbf{x}} \subset \Re^n$.

Where μ, $g_{\min}$, $g_{\max}$, and κ are known constants. The control problem is to force the system output y to follow a given bounded reference signal y_d.

Define the tracking error as

$$e = y_d - y. \tag{6}$$

3. Takagi-Sugeno (T-S) Fuzzy Model

Fuzzy logic systems address the imprecision of the input and output variables directly by defining them with fuzzy numbers (and fuzzy sets) that can be expressed in linguistic terms. The basic configuration of the Takagi and Sugeno [5, 8, 31] system includes a rule base, which consists of a collection of fuzzy IF-THEN rules in the following form:

Plant Rule r:

IF x_1 is B_1^r and $\cdots$ and x_n is B_n^r,

$$\text{THEN} \quad y_r = a_0^r + a_1^r x_1 + \cdots + a_n^r x_n = \theta_r^T \mathbf{x}, \tag{7}$$

where B_i^r are fuzzy sets and $\theta_r^T = [a_0^r, a_1^r, \ldots, a_n^r]$ is a vector of the adjustable factors on the consequence part of the fuzzy rule, and the input vector $\mathbf{x} = [1, x_1, \ldots, x_n] \in R^n$. Let $i = 1, 2, \ldots, n$ denote the number of input for fuzzy logic system, and let $r = 1, 2, \ldots, m$ denote the number of the fuzzy IF-THEN rules. By using the singleton fuzzification, product inference and centre average defuzzication, the output value of the fuzzy system is

$$y(\mathbf{x}) = \frac{\sum_{r=1}^m y^r \left(\prod_{i=1}^n \mu_{B_i^r}(x_i)\right)}{\sum_{r=1}^m \left(\prod_{i=1}^n \mu_{B_i^r}(x_i)\right)}, \tag{8}$$

where $\mu_{B_i^r}(x_i)$ is the membership function value of the fuzzy variable x_i and $\prod_{i=1}^n \mu_{B_i^r}(x_i)$ is the true value of the rth implication. Equation (8) can be rewritten as

$$y(\mathbf{x}) = \theta^T \xi(\mathbf{x}), \tag{9}$$

where $\theta^T = [\theta_1^T, \theta_2^T, \ldots, \theta_m]$ is an adjustable parameter vector, $\xi(\mathbf{x})^T = [\xi^1(\mathbf{x}), \ldots, \xi^m(\mathbf{x})]$ is a fuzzy basis function vector in which, $\xi^r(\mathbf{x})$, $r = 1, 2, \ldots, m$,

$$\xi^r(\mathbf{x}) = \frac{\prod_{i=1}^n \mu_{B_i^r}(x_i)}{\sum_{r=1}^m \prod_{i=1}^n \mu_{B_i^r}(x_i)}. \tag{10}$$

The aforementioned fuzzy system has been shown to be capable of universally approximating well-defined functions over a compact set to arbitrary degree of accuracy. For smooth nonlinear functions $F(\mathbf{x})$, $d(\mathbf{x})$, they can be approximated by

$$\begin{aligned} F(\mathbf{x}) &= \theta_f^{*T}\Psi(\mathbf{x}) + \varepsilon, \\ d(\mathbf{x}) &= \theta_d^{*T}\Xi(\mathbf{x}) + \sigma, \end{aligned} \tag{11}$$

where ε and σ are the fuzzy approximations and θ_f^*, and θ_d^* are optimal weight vectors.

And whose estimates are given by

$$\begin{aligned} F\left(\frac{\mathbf{x}}{\widehat{\theta}_f}\right) &= \widehat{\theta}_f^T \Psi(\mathbf{x}), \\ d\left(\frac{\mathbf{x}}{\widehat{\theta}_d}\right) &= \widehat{\theta}_d^T \Xi(\mathbf{x}). \end{aligned} \tag{12}$$

4. Adaptive Fuzzy Sliding Mode Controller Design

In this section, a systematic methodology is presented for the design of stable adaptive fuzzy sliding mode controller,

the control law and the weight adaptation rules are developed, guaranteeing the uniform ultimate boundedness of the tracking error with respect to an arbitrary small set around the origin. Additionally, the boundedness of all signals involved in the closed-loop configuration is ensured. The resetting scheme is introduced, performing on the weight estimates θ_f, θ_d to guarantee the validity of the control law.

If we consider the system given by (4), the sliding surface can be defined by

$$S = a_{n-1}e + \cdots + a_1 e^{n-2} + e^{n-1}. \tag{13}$$

The elements of the sliding surface are chosen such that the polynomial $a_{n-1}\, p^{n-1} + a_{n-2}\, p^{n-2} + \cdots + a_0$ is strictly Hurwitz [32] (here p denotes the complex Laplace transform variable).

We propose to choose "a" as follows [33]:

$$a_i = \frac{M_i}{\left|e^{n-1-i}\right| + \eta_i}; \quad i = 1, \ldots, n-1, \tag{14}$$

where M_i is a given positive scalar, and η_i is positive constant low value.

Note that M/η represents the slope of sliding along the surface when it is reached by the system.

By using the tracking error defined by (6), the time derivative of (13) is

$$\begin{aligned}
\dot{S} &= \sum_{i=1}^{n-1} a_{n-i}e^{i} + \sum_{i=1}^{n-1} \dot{a}_{n-i}e^{i-1} + e^{n}, \\
\dot{S} &= y_d^n - y^n + \sum_{i=1}^{n-1} a_{n-i}e^{i} + \sum_{i=1}^{n-1} \dot{a}_{n-i}e^{i-1} \\
&= y_d^n - F(\mathbf{x}) - u - d(\mathbf{x}) + \sum_{i=1}^{n-1} a_{n-i}e^{i} + \sum_{i=1}^{n-1} \dot{a}_{n-i}e^{i-1} \\
&= y_d^n - F(\mathbf{x}) - u - d(\mathbf{x}) + \mathbf{Ae},
\end{aligned} \tag{15}$$

where n is the nth derivative of the system, and $\mathbf{A} = [\dot{a}_{n-1}, a_{n-1}, \dot{a}_{n-2}, \ldots, \dot{a}_1, a_1]$, $\mathbf{e} = [e, \ldots, e^{n-3}; e^{n-2}, e^{n-2}; e^{n-1}]^T$.

Assumption 2. Let $\mathbf{x}$ belong to a compact set Ω_x. The optimal weight vectors θ_f^* and θ_d^* are defined as

$$\begin{aligned}
\theta_f^* &= \arg\min_{\widehat{\theta}_f \in \Omega_f} \left[\sup_{x \in \Omega_x} \left[F\left(\frac{\mathbf{x}}{\widehat{\theta}_f}\right) - F(\mathbf{x}) \right] \right], \\
\theta_d^* &= \arg\min_{\widehat{\theta}_d \in \Omega_d} \left[\sup_{x \in \Omega_x} \left[d\left(\frac{\mathbf{x}}{\widehat{\theta}_d}\right) - d(\mathbf{x}) \right] \right].
\end{aligned} \tag{16}$$

And define the constraint sets that the parameters concerned belong to

$$\begin{aligned}
\Omega_f &= \left\{\theta_f \mid \left\|\theta_f\right\| \le M_f\right\}, \\
\Omega_d &= \left\{\theta_d \mid \left\|\theta_d\right\| \le M_d\right\},
\end{aligned} \tag{17}$$

where M_f and M_g are design parameters.

We assume that $\widehat{\theta}_f$, $\widehat{\theta}_d$, and x never reach the boundaries Ω_f, Ω_d, and Ω_x. We can define the minimum approximation errors as

$$\begin{aligned}
\varepsilon &= F(\mathbf{x}) - F\left(\frac{\mathbf{x}}{\theta_f^*}\right), \\
\sigma &= d(\mathbf{x}) - d\left(\frac{\mathbf{x}}{\theta_d^*}\right).
\end{aligned} \tag{18}$$

It is assumed that minimum approximation errors are bounded for all $x \in \Omega_x$:

$$|\varepsilon| \le \overline{\varepsilon}, \quad |\sigma| \le \overline{\sigma}, \quad \forall x \in \Omega_x. \tag{19}$$

The upper bound $\overline{\varepsilon}$, $\overline{\sigma}$ can be reduced arbitrarily. But this choice is not always easy, that is our aim in this work to estimate them by adaptive laws, which guarantee the stability of the closed loop system.

The role of the fuzzy systems $F(\mathbf{x}/\widehat{\theta}_f)$ and $d(\mathbf{x}/\widehat{\theta}_d)$ is to represent the unknown functions using the input-output measurement of the target system. Also, a corrective controller is defined to guarantee the stability of the closed-loop control system and compensate the approximation errors. A direct adaptive control law can be chosen as

$$u = \left(\left| F\left(\frac{\mathbf{x}}{\widehat{\theta}_f}\right) \right| + \left| d\left(\frac{\mathbf{x}}{\widehat{\theta}_d}\right) \right| + y_d^n + \lambda + \mathbf{Ae} + \widehat{\overline{\varepsilon}} + \widehat{\overline{\sigma}} \right) \operatorname{sgn}(S), \tag{20}$$

where λ is a strictly positive constant, and $\widehat{\overline{\varepsilon}}$, $\widehat{\overline{\sigma}}$ are estimates of $\overline{\varepsilon}, \overline{\sigma}$, and

$$\operatorname{sgn}(S) = \begin{cases} 1 & \text{if } S > 0 \\ 0 & \text{if } S = 0 \\ -1 & \text{if } S < 0. \end{cases} \tag{21}$$

Theorem 1. *Consider the nonlinear system described by* (4), *and suppose that Assumptions 1 and 2 are satisfied. The control law is provided by* (20), *and the parameters adaptation laws are given by*

$$\begin{aligned}
\dot{\widehat{\theta}}_f &= \gamma_f \Psi_f(\mathbf{x}) S, \\
\dot{\widehat{\theta}}_d &= \gamma_d \Xi_d(\mathbf{x}) S, \\
\dot{\widehat{\overline{\varepsilon}}} &= S\gamma_\varepsilon, \\
\dot{\widehat{\overline{\sigma}}} &= S\gamma_\sigma.
\end{aligned} \tag{22}$$

Then, the desired tracking performance can be achieved as S becomes asymptotically stable and all adaptation parameters remain bounded.

Proof. Taking into account the minimum approximation errors (18) and control law (20), the sliding surface (15) can be rewritten as

$$\begin{aligned}\dot{S} = {} & y_d^n - \left(\left|F\left(\frac{\mathbf{x}}{\widehat{\theta}_f}\right)\right| + \left|d\left(\frac{\mathbf{x}}{\widehat{\theta}_d}\right)\right| \right. \\ & \left. + y_d^n + l + \mathbf{Ae} + \widehat{\bar{e}} + \widehat{\bar{s}}\right) \operatorname{sgn}(S) \\ & - F(\mathbf{x}) - d(\mathbf{x}) + \mathbf{Ae}.\end{aligned} \tag{23}$$

Defining the parameters errors $\widetilde{\theta}_f = \widehat{\theta}_f - \theta_f^*$, $\widetilde{\theta}_d = \widehat{\theta}_d - \theta_d^*$.

We choose the Lyapunov function candidate as follows:

$$\begin{aligned} V = {} & \frac{1}{2}S^2 + \frac{1}{2\gamma_f}\widehat{\theta}_f^T\widehat{\theta}_f + \frac{1}{2\gamma_d}\widehat{\theta}_d^T\widehat{\theta}_d + \frac{1}{2\gamma_e}\widehat{\bar{e}}^2 + \frac{1}{2\gamma_s}\widehat{\bar{s}}^2 \\ & \widetilde{\bar{\varepsilon}} = \bar{\varepsilon} - \widehat{\bar{\varepsilon}}, \qquad \widetilde{\bar{\sigma}} = \bar{\sigma} - \widehat{\bar{\sigma}},\end{aligned} \tag{24}$$

where γ_f, γ_d, γ_ε, and γ_σ are positive constants. The time derivative of (24) can be obtained as follows:

$$\begin{aligned}\dot{V} = {} & S\dot{S} + \frac{1}{\gamma_f}\widetilde{\theta}_f^T\dot{\widetilde{\theta}}_f + \frac{1}{\gamma_d}\widetilde{\theta}_d^T\dot{\widetilde{\theta}}_d + \frac{1}{\gamma_\varepsilon}\widetilde{\bar{\varepsilon}}\dot{\widetilde{\bar{\varepsilon}}} + \frac{1}{\gamma_\sigma}\widetilde{\bar{\sigma}}\dot{\widetilde{\bar{\sigma}}} \\ = {} & S\left(y_d^n - F(\mathbf{x}) - \left(\left|F\left(\frac{\mathbf{x}}{\widehat{\theta}_f}\right)\right| + \left|d\left(\frac{\mathbf{x}}{\widehat{\theta}_d}\right)\right| + y_d^n + \lambda + \mathbf{Ae} \right.\right. \\ & \left.\left. + \widehat{\bar{\varepsilon}} + \widehat{\bar{\sigma}}\right) \operatorname{sgn}(S) - d(\mathbf{x}) + \mathbf{Ae}\right) \\ & + \frac{1}{\gamma_f}\widetilde{\theta}_f^T\dot{\widetilde{\theta}}_f + \frac{1}{\gamma_d}\widetilde{\theta}_d^T\dot{\widetilde{\theta}}_d + \frac{1}{\gamma_\varepsilon}\widetilde{\bar{\varepsilon}}\dot{\widetilde{\bar{\varepsilon}}} + \frac{1}{\gamma_\sigma}\widetilde{\bar{\sigma}}\dot{\widetilde{\bar{\sigma}}} \\ \le {} & |S|\,|\mathbf{Ae}| + |S|\,y_d^n - S\left(\left|F\left(\frac{\mathbf{x}}{\widehat{\theta}_f}\right)\right| + \left|d\left(\frac{\mathbf{x}}{\widehat{\theta}_d}\right)\right| + \ddot{y}_d \right. \\ & \left. + \lambda + \mathbf{Ae} + \widehat{\bar{\varepsilon}} + \widehat{\bar{\sigma}}\right) \operatorname{sgn}(S) \\ & - SF(\mathbf{x}) - Sd(\mathbf{x}) + \frac{1}{\gamma_f}\widetilde{\theta}_f^T\dot{\widetilde{\theta}}_f + \frac{1}{\gamma_d}\widetilde{\theta}_d^T\dot{\widetilde{\theta}}_d + \frac{1}{\gamma_\varepsilon}\widetilde{\bar{\varepsilon}}\dot{\widetilde{\bar{\varepsilon}}} + \frac{1}{\gamma_\sigma}\widetilde{\bar{\sigma}}\dot{\widetilde{\bar{\sigma}}} \\ = {} & -\lambda|S| - |S|\left|F\left(\frac{\mathbf{x}}{\widehat{\theta}_f}\right)\right| - |S|\left|d\left(\frac{\mathbf{x}}{\widehat{\theta}_d}\right)\right| - |S|\,\widehat{\bar{\varepsilon}} \\ & - |S|\,\widehat{\bar{\sigma}} - SF(\mathbf{x}) - Sd(\mathbf{x}) \\ & + \frac{1}{\gamma_f}\widetilde{\theta}_f^T\dot{\widetilde{\theta}}_f + \frac{1}{\gamma_d}\widetilde{\theta}_d^T\dot{\widetilde{\theta}}_d + \frac{1}{\gamma_\varepsilon}\widetilde{\bar{\varepsilon}}\dot{\widetilde{\bar{\varepsilon}}} + \frac{1}{\gamma_\sigma}\widetilde{\bar{\sigma}}\dot{\widetilde{\bar{\sigma}}} \\ = {} & -\lambda|S| - |S|\left|F\left(\frac{\mathbf{x}}{\widehat{\theta}_f}\right)\right| - |S|\left|d\left(\frac{\mathbf{x}}{\widehat{\theta}_d}\right)\right| - |S|\,\widehat{\bar{\varepsilon}} \\ & - |S|\,\widehat{\bar{\sigma}} - S\left(F\left(\frac{\mathbf{x}}{\theta_f^*}\right) + \varepsilon\right) \\ & - S\left(d\left(\frac{\mathbf{x}}{\theta_d^*}\right) + \sigma\right) + \frac{1}{\gamma_f}\widetilde{\theta}_f^T\dot{\widetilde{\theta}}_f + \frac{1}{\gamma_d}\widetilde{\theta}_d^T\dot{\widetilde{\theta}}_d \\ & + \frac{1}{\gamma_\varepsilon}\widetilde{\bar{\varepsilon}}\dot{\widetilde{\bar{\varepsilon}}} + \frac{1}{\gamma_\sigma}\widetilde{\bar{\sigma}}\dot{\widetilde{\bar{\sigma}}} \\ \le {} & -\lambda|S| - |S|\left|F\left(\frac{\mathbf{x}}{\widehat{\theta}_f}\right)\right| - |S|\left|d\left(\frac{\mathbf{x}}{\widehat{\theta}_d}\right)\right| - |S|\,\widehat{\bar{\varepsilon}} - |S|\,\widehat{\bar{\sigma}} \\ & + |S|\left|F\left(\frac{\mathbf{x}}{\widehat{\theta}_f}\right)\right| - |S|\left|d\left(\frac{\mathbf{x}}{\widehat{\theta}_d}\right)\right| \\ & - S\widetilde{\theta}_f\Psi(\mathbf{x}) - S\widetilde{\theta}_d\Xi(\mathbf{x}) + |S|\,\bar{\varepsilon} + |S|\,\bar{\sigma} + \frac{1}{\gamma_f}\widetilde{\theta}_f^T\dot{\widetilde{\theta}}_f \\ & + \frac{1}{\gamma_d}\widetilde{\theta}_d^T\dot{\widetilde{\theta}}_d + \frac{1}{\gamma_\varepsilon}\widetilde{\bar{\varepsilon}}\dot{\widetilde{\bar{\varepsilon}}} + \frac{1}{\gamma_\sigma}\widetilde{\bar{\sigma}}\dot{\widetilde{\bar{\sigma}}} \\ = {} & -\lambda|S| - S\widetilde{\theta}_f\Psi(\mathbf{x}) - S\widetilde{\theta}_d\Xi(\mathbf{x}) + |S|\,\widetilde{\bar{\varepsilon}} + |S|\,\widetilde{\bar{\sigma}} \\ & + \frac{1}{\gamma_f}\widetilde{\theta}_f^T\dot{\widetilde{\theta}}_f + \frac{1}{\gamma_d}\widetilde{\theta}_d^T\dot{\widetilde{\theta}}_d + \frac{1}{\gamma_\varepsilon}\widetilde{\bar{\varepsilon}}\dot{\widetilde{\bar{\varepsilon}}} + \frac{1}{\gamma_\sigma}\widetilde{\bar{\sigma}}\dot{\widetilde{\bar{\sigma}}} \\ = {} & -\lambda|S| + \widetilde{\theta}_f^T\left(-S\Psi_f(\mathbf{x}) + \frac{1}{\gamma_f}\dot{\widetilde{\theta}}_f\right) \\ & + \widetilde{\theta}_d^T\left(-S\Xi_d(\mathbf{x})\,u + \frac{1}{\gamma_d}\dot{\widetilde{\theta}}_d\right) \\ & + \widetilde{\bar{\varepsilon}}\left(S + \frac{1}{\gamma_\varepsilon}\dot{\widetilde{\bar{\varepsilon}}}\right) + \widetilde{\bar{\sigma}}\left(S + \frac{1}{\gamma_d}\dot{\widetilde{\bar{\sigma}}}\right).\end{aligned} \tag{25}$$

Choosing a fuzzy rule adaptive method as

$$\begin{aligned}\dot{\widetilde{\theta}}_f &= \gamma_f\Psi_f(\mathbf{x})\,S, \\ \dot{\widetilde{\theta}}_g &= \gamma_d\Xi_d(\mathbf{x})\,S, \\ \dot{\widetilde{\bar{\varepsilon}}} &= -S\gamma_\varepsilon, \\ \dot{\widetilde{\bar{\sigma}}} &= -S\gamma_\sigma\end{aligned} \tag{26}$$

or equivalently, by definition

$$\begin{aligned} \dot{\hat{\theta}}_f &= \gamma_f \Psi_f(\mathbf{x}) S, \\ \dot{\hat{\theta}}_g &= \gamma_d \Xi_d(\mathbf{x}) S, \\ \dot{\hat{\varepsilon}} &= S\gamma_\varepsilon, \\ \dot{\hat{\sigma}} &= S\gamma_\sigma \end{aligned} \tag{27}$$

yields

$$\dot{V} = -\lambda |S|. \tag{28}$$

Integrating both sides of (28), we have $\int_0^\infty \dot{V} dt \leq -\int_0^\infty (1/2)|S| dt$, and thus, the following equation holds:

$$\int_0^\infty |S| \, dt \leq 2(V(0) - V(\infty)). \tag{29}$$

As $V(0)$ is bounded and also $0 \leq V(\infty) \leq V(0)$ from (28), $\int_0^\infty |S| dt$ is also bounded from (29). Using Barbalat's lemma, [19, 34] $|S| \to 0$ for $t \to \infty$.

From the moment where the sliding surface is designed and constructed to be attractive, we can also see that $\lim_{t\to\infty} e = 0$. Therefore, the closed-loop system is asymptotically stable and the position tracking objective is achieved. The modified projection adaptive laws are given in [7]. □

5. Simulation Example

We illustrate the validity of the design approach by an example of robot arm tracking control with a single degree of freedom as Figure 1 shows.

The dynamic equations of such a system are given by

$$\begin{aligned} x^{(3)} &= f(\mathbf{x}) + g(\mathbf{x}) u + d, \\ y &= x, \end{aligned} \tag{30}$$

where

$$\begin{aligned} f(\mathbf{x}) &= -\frac{r}{L} x_3 - \left(\frac{g}{l} \cos(x_1) + \frac{K_b N^2 K_t}{Lml^2} \right) x_2 - \frac{rg}{Ll} \sin(x_1), \\ g(\mathbf{x}) &= \frac{K_t N}{Lml^2}, \\ \mathbf{x} &= [x_1, x_2, x_3]^T, \end{aligned} \tag{31}$$

where x_1 is the angular position (rad), x_2 is the angular velocity (rad/s), x_3 is the angular acceleration (rad/s^2), $u(t)$ is the applied force (control signal) (N), and d is the external disturbance. The simulation parameters are given in Table 1.

According to (30), we choose the sliding surface as $S = e^{(2)} + a_2 e^{(1)} + a_1 e$. The following parameters are chosen so that the characteristic function of the surface is the negative real part

$$M_1 = 8, \qquad \eta_1 = 1, \qquad M_2 = 15 \qquad \eta_2 = 1. \tag{32}$$

To construct two fuzzy logic systems, $F(\mathbf{x}/\hat{\theta}_f)$ and $d(\mathbf{x}/\hat{\theta}_d)$ as given in (12), the initial consequent parameters of fuzzy rules are chosen randomly in the interval $[-1.2, 1.2]$. The initial values of $\mathbf{x}$ are given as $[0\ 0\ 0]^T$.

This interval will be sufficiently covered by three membership functions for position, velocity, and angular acceleration. Then, we have 27 rules.

Let the learning rate $\gamma_f = 0.05$, $\gamma_d = 20$, $\gamma_\varepsilon = 100$, $\gamma_\sigma = 500$, $k_d = 6$, and $M = 40$.

The control objective is to maintain the system to track the desired angle trajectory, $y_d = \sin(t)$, and to test the proposed control, we introduced parametric variations and external disturbances given by $\Delta m = 0.1 \sin(x)$, $d = 0.125 \times \sin(2t)$, respectively.

Figures 2–5 show the simulation results obtained in the case where the system is subjected to external disturbances and parametric variations. Figures 2, 3, and 4 show the rapid convergence of the system output to the reference signal. In Figure 5, we can see that the control signal is smooth and that the actual and desired trajectories are superposed, after a short transitional arrangement whereby the error is significant between the two outputs, this is due to disturbances, initial conditions, and initialization of adjustable parameters.

Figures 2–4 show that the effect of parametric perturbations is negligible, with less stress to the control level despite greater external disturbances. Similarly, the results obtained in [35] show that the tracking error is about 8% whereas it is less than 2, 5% in our case.

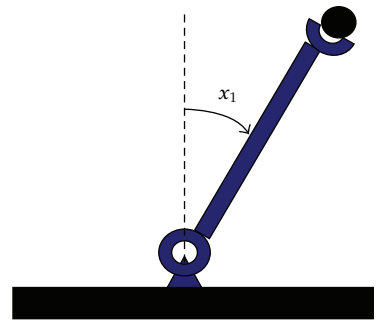

Figure 1: Robot arm.

Table 1: Simulation parameters.

Mass of the pole	$m = 5$ kg
The half-length of the pole	$l = 0.5$ m
The acceleration due to gravity	$G = 9.8$
Resistance	$r = 1.5$
Inductance	$L = 0.5$
Electromotive force constant	$K_b = 0.2$
Constant torque motor	$K_t = 0.3$
Reduction ratio	$N = 60$

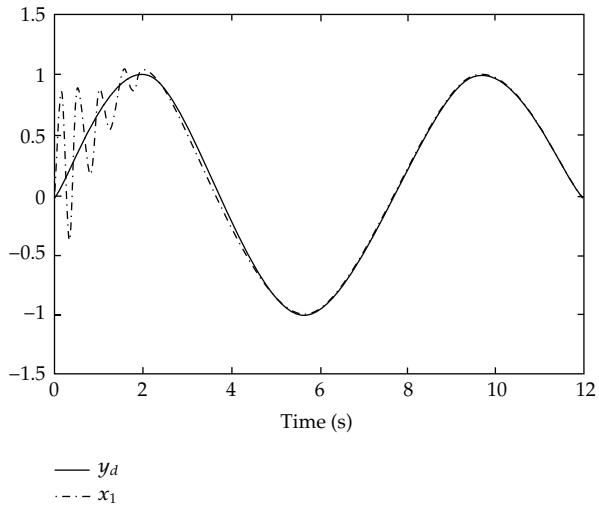

Figure 2: Trajectories of the state $x_1(t)$ of tracking control of the desired $y_d(t)$ for the robot arms.

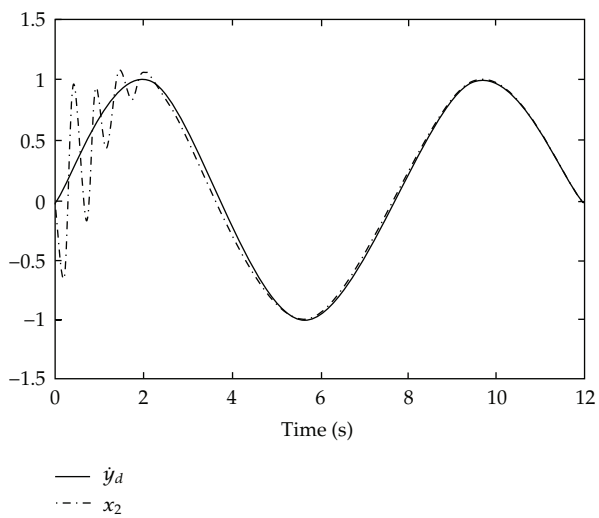

Figure 3: Trajectories of the state $x_2(t)$ of tracking control of the desired $\dot{y}_d(t)$ for the robot arm.

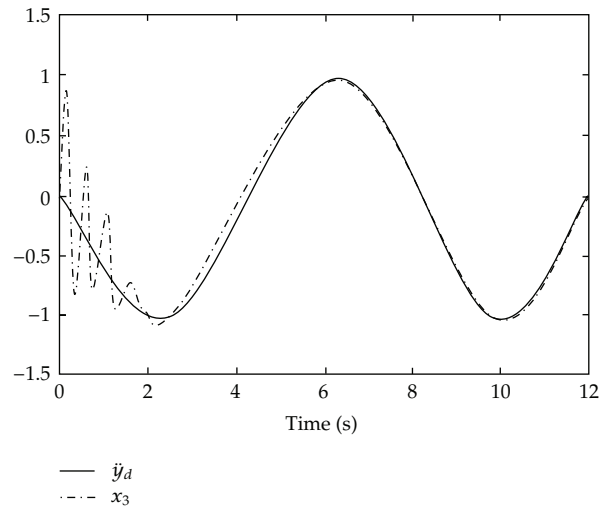

Figure 4: Trajectories of the state $x_3(t)$ of tracking control of the desired $\ddot{y}_d(t)$ for the robot arm.

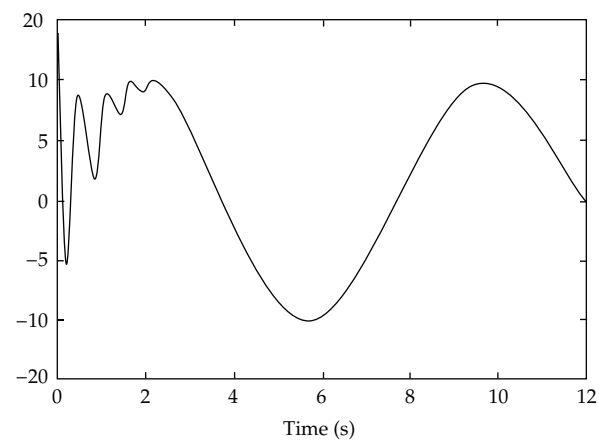

Figure 5: Trajectories of the control input $u(t)$ of the tracking control for robot arm.

It can be seen in Figures 2–5 that the advantage of our controller is its ability to eliminate the effect of fluctuations in the transient response with less effort on the control law; moreover, an estimation of the upper bound of error is performed without needing their prior knowledge, which allows the control law to be less restrictive regarding the conditions of stability.

6. Conclusion

In this paper, the output tracking control problem has been considered for a class of uncertain nonlinear systems. The unknown functions in systems are not linearly parameterized and have no a priori knowledge of the bounded functions. Fuzzy logic systems are used to approximate these unknown nonlinear functions. By sliding mode design technique, the adaptive fuzzy tracking control scheme has been developed for nonlinear systems. The proposed controllers guarantee that the outputs of the closed-loop system follow the reference signals, and achieve uniform ultimate boundedness of all the signals in the closed-loop system. It is proved in theory and shown in simulation that the closed-loop system is stable and the output tracks the given reference signal satisfactorily. Future work will deal with the delay systems in the type 2 fuzzy systems taking into account uncertainties and a novel nonlinearity sliding mode surface and an application to a real process.

References

[1] S. Bououden, S. Filali, and K. Kemih, "Adaptive fuzzy tracking control for unknown nonlinear systems," *International Journal of Innovative Computing, Information and Control*, vol. 6, no. 2, pp. 541–549, 2010.

[2] M. Chadli and A. El Hajjaji, "observer-based robust fuzzy control of nonlinear systems with parametric uncertainties," *Fuzzy Sets and Systems*, vol. 157, no. 9, pp. 1276–1281, 2006.

[3] M. Chadli, "On the stability analysis of uncertain fuzzy models," *International Journal of Fuzzy Systems*, vol. 8, no. 4, pp. 224–231, 2006.

[4] Y. J. Liu, W. Wang, S. C. Tong, and Y. S. Liu, "Robust adaptive tracking control for nonlinear systems based on bounds of fuzzy approximation parameters," *IEEE Transactions on Systems, Man, and Cybernetics A*, vol. 40, no. 1, pp. 170–184, 2010.

[5] K. Tanaka, H. Ohtake, and H. O. Wang, "A descriptor system approach to fuzzy control system design via fuzzy Lyapunov functions," *IEEE Transactions on Fuzzy Systems*, vol. 15, no. 3, pp. 333–341, 2007.

[6] L. Wu, X. Su, P. Shi, and J. Qiu, "Model approximation for discrete-time state-delay systems in the TS fuzzy framework," *IEEE Transactions on Fuzzy Systems*, vol. 19, no. 2, pp. 366–378, 2011.

[7] Y. C. Chang, "Robust tracking control for nonlinear MIMO systems via fuzzy approaches," *Automatica*, vol. 36, no. 10, pp. 1535–1545, 2000.

[8] Y. H. Chien, W. Y. Wang, Y. G. Leu, and T. T. Lee, "Robust adaptive controller design for a class of uncertain nonlinear systems using online T-S fuzzy-neural modeling approach," *IEEE Transactions on Systems, Man, and Cybernetics B*, vol. 41, no. 2, pp. 542–552, 2011.

[9] M. Krstic, I. Kanellakopoulos, and P. Koktovic, *Nolinear and Adaptive Control*, Wiley, New York, NY, USA, 1995.

[10] X. Zhang, C. Wang, D. Li, X. Zhou, and D. Yang, "Robust stability of impulsive Takagi-Sugeno fuzzy systems with parametric uncertainties," *Information Sciences*, vol. 181, no. 23, pp. 5278–5290, 2011.

[11] R. Yang, Z. Zhang, and P. Shi, "Exponential stability on stochastic neural networks with discrete interval and distributed delays," *IEEE Transactions on Neural Networks*, vol. 21, no. 1, pp. 169–175, 2010.

[12] L. Wu, X. Su, P. Shi, and J. Qiu, "A new approach to stability analysis and stabilization of discrete-time T-S fuzzy time-varying delay systems," *IEEE Transactions on Systems, Man, and Cybernetics B*, vol. 41, no. 1, pp. 273–286, 2011.

[13] S. Islam and X. P. Liu, "Robust sliding mode control for robot manipulators," *IEEE Transactions on Industrial Electronics*, vol. 58, no. 6, pp. 2444–2453, 2011.

[14] C. C. Kung and T. H. Chen, "Observer-based indirect adaptive fuzzy sliding mode control with state variable filters for unknown nonlinear dynamical systems," *Fuzzy Sets and Systems*, vol. 155, no. 2, pp. 292–308, 2005.

[15] T. C. Kuo, Y. J. Huang, and S. H. Chang, "Sliding mode control with self-tuning law for uncertain nonlinear systems," *ISA Transactions*, vol. 47, no. 2, pp. 171–178, 2008.

[16] T. R. Oliveira, A. J. Peixoto, and L. Hsu, "Sliding mode control of uncertain multivariable nonlinear systems with unknown control direction via switching and monitoring function," *IEEE Transactions on Automatic Control*, vol. 55, no. 4, pp. 1028–1034, 2010.

[17] V. I. Utkin, *Sliding Modes and Their Application in Variable Structure Systems*, MIR Publishers, Moscow, Russia, 1978.

[18] W. Y. Wang, M. L. Chan, C. C. J. Hsu, and T. T. Lee, "H∞ tracking-based sliding mode control for uncertain nonlinear systems via an adaptive fuzzy-neural approach," *IEEE Transactions on Systems, Man, and Cybernetics B*, vol. 32, no. 4, pp. 483–492, 2002.

[19] J. Fei and C. Batur, "A novel adaptive sliding mode control with application to MEMS gyroscope," *ISA Transactions*, vol. 48, no. 1, pp. 73–78, 2009.

[20] Y. J. Huang, T. C. Kuo, and S. H. Chang, "Adaptive sliding-mode control for nonlinear systems with uncertain parameters," *IEEE Transactions on Systems, Man, and Cybernetics B*, vol. 38, no. 2, pp. 534–539, 2008.

[21] V. Nekoukar and A. Erfanian, "Adaptive fuzzy terminal sliding mode control for a class of MIMO uncertain nonlinear systems," *Fuzzy Sets and Systems*, vol. 179, no. 1, pp. 34–49, 2011.

[22] Z. Xi, G. Feng, and T. Hesketh, "Piecewise integral sliding-mode control for TS fuzzy systems," *IEEE Transactions on Fuzzy Systems*, vol. 19, no. 1, pp. 65–74, 2011.

[23] M. Yue, W. Sun, and P. Hu, "Sliding mode robust control for two-wheeled mobile robot with lower center of gravity," *International Journal of Innovative Computing, Information and Control*, vol. 7, no. 2, pp. 637–646, 2011.

[24] T. C. Lin and M. C. Chen, "Adaptive hybrid type-2 intelligent sliding mode control for uncertain nonlinear multivariable dynamical systems," *Fuzzy Sets and Systems*, vol. 171, no. 1, pp. 44–71, 2011.

[25] J. Zhang, P. Shi, and Y. Xia, "Robust adaptive sliding-mode control for fuzzy systems with mismatched uncertainties," *IEEE Transactions on Fuzzy Systems*, vol. 18, no. 4, pp. 700–711, 2010.

[26] Z. He, J. Wu, G. Sun, and C. Gao, "State estimation and sliding mode control of uncertain switched hybrid systems," *International Journal of Innovative Computing Information and Control*, vol. 8, no. 10, pp. 7143–7156, 2012.

[27] T. C. Lin, S. W. Chang, and C. H. Hsu, "Robust adaptive fuzzy sliding mode control for a class of uncertain discrete-time nonlinear systems," *International Journal of Innovative Computing Information and Control*, vol. 8, no. 1, pp. 347–359, 2012.

[28] M. A. Demetriou and I. G. Rosen, "Variable structure model reference adaptive control of parabolic distributed parameter systems," in *Proceedings of the American Control Conference*, pp. 4371–4376, May 2002.

[29] L. X. Wang, *A Course in Fuzzy Systems and Control*, Prentice-Hall, Englewood Cliffs, NJ, USA, 1997.

[30] C. H. Wang, H. L. Liu, and T. C. Lin, "Direct adaptive fuzzy-neural control with state observer and supervisory controller for unknown nonlinear dynamical systems," *IEEE Transactions on Fuzzy Systems*, vol. 10, no. 1, pp. 39–49, 2002.

[31] A. Sala, T. M. Guerra, and R. Babuška, "Perspectives of fuzzy systems and control," *Fuzzy Sets and Systems*, vol. 156, no. 3, pp. 432–444, 2005.

[32] J. Wang and J. Hu, "Robust adaptive neural control for a class of uncertain non-linear time-delay systems with unknown dead-zone non-linearity," *IET Control Theory & Applications*, vol. 5, no. 15, pp. 1782–1795, 2011.

[33] Z. L. Liu, "Reinforcement adaptive fuzzy control of wing rock phenomena," *IEE Proceedings: Control Theory and Applications*, vol. 152, no. 6, pp. 615–620, 2005.

[34] J. E. Slotine and W. Li, *Applied Nonlinear Control*, Prentice-Hall, Upper Saddle River, NJ, USA, 1991.

[35] F. J. Lin, P. H. Shieh, and Y. C. Hung, "An intelligent control for linear ultrasonic motor using interval type-2 fuzzy neural network," *IET Electric Power Applications*, vol. 2, no. 1, pp. 32–41, 2008.

Hindawi Publishing Corporation
Mathematical Problems in Engineering
Volume 2013, Article ID 740478, 15 pages
http://dx.doi.org/10.1155/2013/740478

Research Article

An Iterative Procedure for Optimizing the Performance of the Fuzzy-Neural Job Cycle Time Estimation Approach in a Wafer Fabrication Factory

Toly Chen and Yi-Chi Wang

Department of Industrial Engineering and Systems Management, Feng Chia University, 100 Wenhwa Road, Seatwen, Taichung 408, Taiwan

Correspondence should be addressed to Toly Chen; tcchen@fcu.edu.tw

Received 28 October 2012; Accepted 27 December 2012

Academic Editor: Peng Shi

Copyright © 2013 T. Chen and Y.-C. Wang. This is an open access article distributed under the Creative Commons Attribution License, which permits unrestricted use, distribution, and reproduction in any medium, provided the original work is properly cited.

Estimating the cycle time of each job in a wafer fabrication factory is a critical task to every wafer manufacturer. In recent years, a number of hybrid approaches based on job classification (either preclassification or postclassification) for cycle time estimation have been proposed. However, the problem with these methods is that the input variables are not independent. In order to solve this problem, principal component analysis (PCA) is considered useful. In this study, a classifying fuzzy-neural approach, based on the combination of PCA, fuzzy c-means (FCM), and back propagation network (BPN), is proposed to estimate the cycle time of a job in a wafer fabrication factory. Since job classification is an important part of the proposed methodology, a new index is proposed to assess the validity of the classification of jobs. The empirical relationship between the S value and the estimation performance is also found. Finally, an iterative process is employed to deal with the outliers and to optimize the overall estimation performance. A real case is used to evaluate the effectiveness of the proposed methodology. Based on the experimental results, the estimation accuracy of the proposed methodology was significantly better than those of the existing approaches.

1. Introduction

The competition in the semiconductor industry has been very intense. How to obtain and maintain the competitive edge is an important task for all manufacturers in this industry. Quick response and on-time delivery are obviously pressing needs for any modern enterprise. To this end, accurate estimating and shortening the cycle time (flow time or manufacturing lead time) of each job in the factory is a prerequisite [1–9]. In a wafer fabrication factory, a job is usually composed of about 25 pieces of wafers and has hundreds of steps to be processed. In addition, a job may visit the same workstation more than once because the same operation may be needed multiple times. A wafer fabrication factory is therefore classified as a complicated reentrant production system.

Estimating the cycle time of each job in a wafer fabrication factory is very important to the factory because it can signal the manager if the orders are progressed as they were expected. For example, if the estimated cycle time of a job is longer than as it was expected, then this order may not be completed to the customer before its due date. Some production control actions should then immediately be taken to accelerate the progress of the job [10]. That is why this paper studies the estimation of job cycle time in a wafer fabrication factory.

The existing approaches for the job cycle time estimation in a wafer fabrication factory can be classified into six categories: statistical analysis, production simulation (PS), back propagation network (BPN), case-based reasoning (CBR), fuzzy modeling methods, and hybrid approaches [9]. Among the six approaches, statistical analysis is the easiest, quickest, and most prevalent in practical applications. Most of the statistical analyses used linear regression equations to estimate the job cycle time (e.g., [11, 12]). Pearn et al. [13] fitted the distribution of the waiting time of a job with

a gamma distribution and then used a linear equation to estimate the job cycle time. Recently, Chien et al. [14] used nonlinear regression equations instead and then found out the relationship between the estimation error and some factory conditions and job attributes with a BPN to further improve the estimation accuracy. The major disadvantage of statistical analysis is the lack of estimation accuracy [9]. Conversely, a huge amount of data and lengthy simulation time required are two disadvantages of PS. Nevertheless, theoretically PS is the most accurate job cycle time estimation approach if the simulation model is completely valid and is continuously updated.

Considering effectiveness (estimation accuracy) and efficiency (execution time) simultaneously, Chang et al. [8], Chang and Hsieh [15], and Sha and Hsu [16] estimated the cycle time of a job in a wafer fabrication factory using a BPN with a single hidden layer. A BPN is an effective tool in modeling complex physical systems described by sets of different equations for prediction, control, and design purposes. Compared with some statistical analysis approaches, the average estimation accuracy measured with root mean squared error (RMSE) was considerably improved with the BPNs. For example, an improvement of about 40% in RMSE was achieved in the study of Chang et al. [8]. Chen [17] incorporated the job releasing plan of the wafer fabrication factory into a BPN, and constructed a "look-ahead" BPN for the same purpose, which led to an average reduction of 12% in RMSE. On the other hand, much less time and fewer data are required with a BPN than with PS. Chen et al. [18] and Beeg [19] estimated the cycle time of a job in a ramping up wafer fabrication factory. In their studies, Chen et al. used a BPN-based method, while Beeg tried to find out the impact of utilization for the cycle time.

Chiu et al. [20] established an expert system based on CBR for the job cycle time estimation. To effectively consider the uncertainty in the job cycle time, fuzzy logic was used in a number of studies. For example, Chang et al. [8] modified the first step (i.e., partitioning the range of each input variable into several fuzzy intervals) of the fuzzy modeling method proposed by Wang and Mendel [21], called the WM method, with a simple genetic algorithm (GA) and proposed the evolving fuzzy rule (EFR) approach to estimate the cycle time of a job in a wafer fabrication factory. Their EFR approach outperformed CBR and BPN in the estimation accuracy. Chen [9] constructed a fuzzy back propagation network (FBPN) that incorporated expert opinions to modify the inputs of the FBPN. Chen's FBPN surpassed the crisp BPN especially with respect to efficiency.

In recent years, a number of hybrid approaches have been proposed, most of which classified jobs before estimating the cycle times. For example, Chen [7] combined self-organization map (SOM) and WM, in which jobs were classified using a SOM before estimating the cycle times of the jobs with WM. Chen and Wang [22] constructed a look-ahead k-means- (kM-) FBPN for the same purpose and discussed in detail the effects of using different look-ahead functions. More recently, Chen [17] proposed the look-ahead SOM-FBPN approach for the job cycle time estimation in a semiconductor factory [23]. Besides, a set of fuzzy inference rules were also developed to evaluate the achievability of a cycle time forecast. Subsequently, Chen [24] added a selective allowance to the cycle time estimated using the look-ahead SOM-FBPN approach to determine the intermediate due date. Further, Chen et al. [23] showed that the suitability of combining the SOM and FBPN for the data could be improved with the feedback of the estimation error by the FBPN to adjust the classification results of the SOM. Chen et al. [25] proposed a postclassification fuzzy-neural approach in which a job was not pre-classified but rather postclassified after estimating the cycle time. Experimental results showed that the postclassification approach was better than the preclassification approaches in certain cases. In order to combine the advantages of preclassifying and post-classifying approaches, Chen [26] proposed a bi-directional classifying approach, in which jobs are not only pre-classified but also postclassified. Except few studies in which the historical data of a real semiconductor factory were collected, most studies in this field used simulated data [27].

In short, the followings have not done before:

(1) Some factors used to estimate the cycle time are dependent on each other, which may cause problems in classifying jobs and in fitting the relationship between the job cycle time and these factors. However, this issue has rarely been addressed in previous studies of this field.

(2) Job classification has been shown to be conducive to the estimation performance. However, most past studies chose classifiers subjectively and did not evaluate the performance of the classifier. Needless to say optimizing the classifier for the subsequent estimation task.

Principal component analysis (PCA) is a multivariate statistical analysis method. This method constructs a series of linear combinations of the original variables to form a new variable, so that these new variables are unrelated to each other as much as possible, and the relationship among them can be reflected in a better way. In this study, a fuzzy-neural approach, based on the combination of PCA, FCM, and BPN, is proposed to estimate the cycle time of a job in a wafer fabrication factory. The motivation of this study is explained as follows.

(1) While in the past some studies combined PCA and FCM, the references on the combination of PCA, FCM, and BPN are still very limited. Chen [28] applied PCA to modify the inputs to a BPN for the job cycle time estimation. The estimation accuracy of PCA-BPN was slightly better than that of BPN alone. It seems that BPN can solve the dependencies of the input variables for the job cycle time estimation problems. PCA seems to be more important for the classification of jobs. This provides us with a motivation to improve the existing job cycle time estimation methods based on job classification.

(2) FCM, as a part of the preclassifying approach, cannot be evaluated alone. Its success depends on the

performance of the subsequent estimation task. This provides us with a motivation to assess the validity of the classification of jobs from this point of view.

(3) The S test is a commonly used method to determine the best number of categories in FCM. However, whether this way directly favors the estimation performance has not been confirmed.

The contribution compared with some previous works in the literature includes the following.

(1) With factors that are dependent on each other, jobs may be misclassified if FCM is used alone. This may be harmful to the estimation accuracy of BPN, because incorrect examples are used to train the BPN. The fuzzy-neural approach replaces the original factors with new independent factors and is expected to be able to generate the correct classification results. The correctness of the classification results must be judged from the estimation performance. In order to measure that, two new indexes are defined.

(2) It is anticipated that the new factors found out by PCA have a more explicit relationship with the job cycle time. As a result, the training of BPN may be accelerated. This also means that a more accurate relationship between the factors and the cycle time can also be generated with the same time.

(3) A new index is proposed to assess the validity of the classification of jobs.

(4) The empirical relationship between the S value and the estimation performance is found.

(5) Outliers, that is, jobs that cannot be classified definitely, have not been dealt with properly in the past. However, the overall estimation performance is often affected by the outliers. For this reason, an iterative process is established in this study, which can optimize the overall estimation performance.

The differences between the proposed methodology and the previous methods are summarized in Table 1.

The remainder of this paper is organized as follows. Section 2 introduces the proposed PCA-FCM-BPN approach. An example is employed to illustrate the proposed methodology. A case with the real data from a wafer fabrication factory is investigated in Section 3. The performance of the proposed methodology is compared with those of the existing approaches for this real case. Based on the results, some points are made in analysis. Finally, the concluded remarks with a view to the future are given in Section 4.

2. Methodology

Two characteristics of the proposed methodology are input replacement and job classification. These features not are mathematical skills, but also have implications for the operations of a wafer fabrication factory. First, in the useful information for the estimation of the job cycle time, many factors are in fact mutually dependent. For example, it is well known that the utilization of a factory increases when the work-in-process (WIP) level in the factory rises. Both utilization and the WIP level are important factors considered in some job cycle time estimation approaches. Whether the dependence of the factors will lead to problems in the classification of jobs needs to be checked. Therefore, the replacement of these factors with new independent variables is worth a try.

On the other hand, a number of job cycle time estimation approaches in this field classify jobs. A well-known concept is that the cycle time of a job is proportional to the WIP level of the factory, according to Little's law; however, that only holds when the factory utilization is 100%. Therefore, it is reasonable to divide jobs into two categories: jobs that are released into the factory when the factory utilization is 100% and jobs released when the factory utilization is less than 100%.

The architecture of the proposed methodology is shown in Figure 1.

2.1. Variable Replacement Using PCA. First, PCA is used to replace the inputs to the FCM-BPN. The combination of PCA and FCM has proven to be a more effective classifier than FCM alone [29]. PCA consists of the following steps.

(1) Raw data standardization: to eliminate the difference between the dimensions and the impact of large numerical difference in the original variables, The original variables are standardized as the following:

$$x_{ji}^{*} = \frac{x_{ji} - \overline{x}_i}{\sigma_i}, \quad \overline{x}_i = \frac{\sum_{j=1}^{n} x_{ji}}{n}, \quad \sigma_i = \sqrt{\frac{\sum_{j=1}^{n} \left(x_{ji} - \overline{x}_i\right)^2}{n-1}}, \tag{1}$$

where x_{ji} is the ith attribute of job j, $j = 1 \sim n$; $\overline{x}_i$ and σ_i indicate the mean and standard deviation of variable i, respectively.

(2) Establishment of the correlation matrix R:

$$R = \frac{1}{n-1} X^{*T} X^{*}, \tag{2}$$

where X^{*} is the standardized data matrix. The eigenvalues and eigenvectors of R are calculated and represented as $\lambda_1 \sim \lambda_m$ and $u_1 \sim u_m$, respectively, $\lambda_1 \geq \lambda_2 \geq \ldots \geq \lambda_m$.

(3) Determination of the number of principal components: the variance contribution rate is calculated as:

$$\eta_q = \frac{\lambda_q}{\sum_{r=1}^{m} \lambda_r} \cdot 100\%, \tag{3}$$

Table 1: The differences between the proposed methodology and the previous methods.

Method	SOM-WM [7], SOM-FBPN [17], kM-FBPN [22–24]	BPN-BPN [25]	FCM-FBPN-RBF [26]	The proposed methodology
Job preclassification	Yes	No	Yes	Yes
Job post/reclassification	No	Yes	Yes	Yes
Parameter replacement	No	No	No	Yes
Dealing with outliers	No	No	No	Yes
Iteration	No	No	No	Yes

* RBF is radial basis function network.

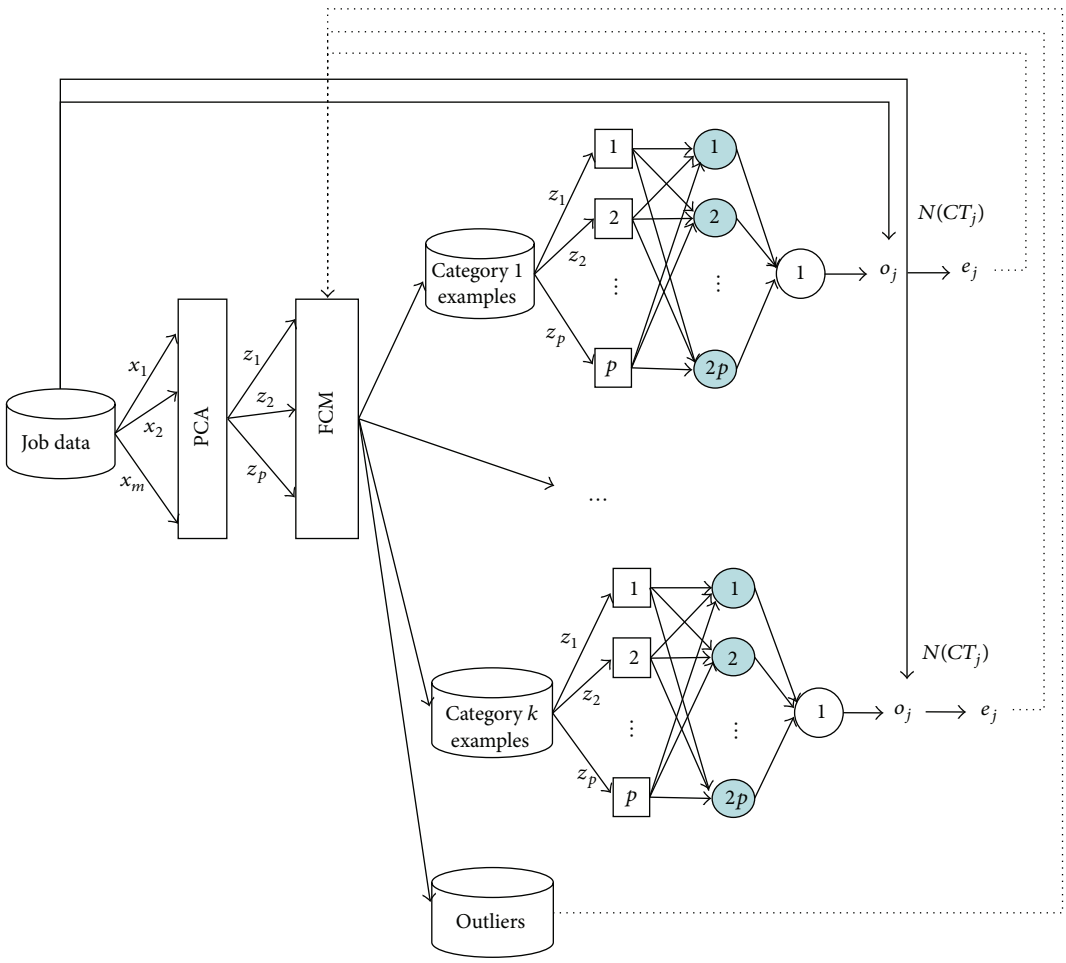

Figure 1: The architecture of the proposed methodology.

where $q = 1 \sim m$, and the accumulated variance contribution rate is

$$\eta_{\Sigma}(p) = \sum_{q=1}^{p} \eta_q, \tag{4}$$

where $p = 1 \sim m$. Choose the smallest p value such that $\eta_{\Sigma}(p) \geq 85\% \sim 90\%$. A Pareto analysis chart can be used to compare the percent variability explained by each principal component.

(4) Formation of the following matrixes:

$$U_{m\times p} = \left[u_1, u_2, \ldots, u_p\right],$$
$$Z_{n\times p} = X^{*}_{n\times m} U_{m\times p}. \tag{5}$$

$Z_{n\times p} = [z_{jq}]$ $(j = 1 \sim n;\ q = 1 \sim p)$ is the component scores, which contain the coordinates of the original data in the new coordinate system defined by the principal components, and will be used as the new inputs to the FFNN.

Table 2: An example.

j	x_{j1}	x_{j2}	x_{j3}	x_{j4}	x_{j5}	x_{j6}
1	24	1261	181	781	112	0.92
2	24	1263	181	762	127	0.90
3	24	1220	176	761	127	0.89
4	23	1282	178	802	127	0.94
5	23	1303	180	780	175	0.93
6	23	1281	183	782	175	0.93
7	23	1242	184	741	163	0.89
8	24	1262	182	681	139	0.86
9	22	1260	182	701	98	0.86
10	22	1260	179	700	257	0.87
11	24	1301	163	722	99	0.84
12	22	1221	184	641	131	0.82
13	23	1323	159	740	247	0.87
14	24	1362	181	782	191	0.95
15	24	1261	181	762	219	0.91
16	23	1321	177	801	219	0.96
17	22	1343	180	822	219	0.97
18	24	1321	177	762	54	0.93
19	25	1343	179	781	54	0.96
20	25	1300	180	740	54	0.92
21	22	1320	181	721	54	0.91
22	24	1321	182	742	49	0.92
23	23	1262	165	680	201	0.80
24	22	1240	161	722	103	0.82
25	23	1183	183	661	53	0.82
26	23	1282	184	701	53	0.88
27	22	1202	177	680	248	0.84
28	23	1202	178	681	248	0.85
29	24	1202	185	701	82	0.86
30	23	1202	158	721	98	0.81
31	24	1343	181	760	67	0.94
32	24	1381	185	801	67	0.97
33	22	1362	156	780	67	0.91
34	23	1282	179	782	223	0.92
35	23	1320	180	782	176	0.93
36	25	1340	176	801	462	0.97
37	23	1320	182	781	168	0.95
38	22	1361	181	781	141	0.94
39	22	1381	179	781	95	0.97
40	23	1363	178	802	179	0.97

To illustrate the application of the proposed methodology, an example is given in Table 2. To get a quick impression of the data, a box plot is made in Figure 2. Note that there is substantially more variability in x_{j2}, x_{j4}, and x_{j5} than in the remaining variables.

Subsequently, we standardize the data (see Table 3) and obtain the correlation matrix as

$$R = \begin{bmatrix} 0.97 & 0.10 & 0.16 & 0.21 & -0.03 & 0.25 \\ 0.10 & 0.98 & 0.01 & 0.70 & -0.01 & 0.78 \\ 0.16 & 0.01 & 0.98 & 0.05 & -0.07 & 0.37 \\ 0.21 & 0.70 & 0.05 & 0.98 & 0.15 & 0.86 \\ -0.03 & -0.01 & -0.07 & 0.15 & 0.98 & 0.10 \\ 0.25 & 0.78 & 0.37 & 0.86 & 0.10 & 0.98 \end{bmatrix}. \quad (6)$$

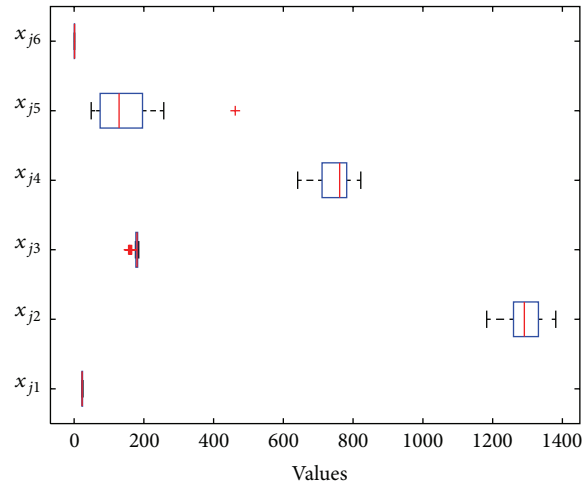

Figure 2: The box plot.

The eigenvalues and eigenvectors of R are calculated as the following:

$$\begin{aligned} &\lambda_1 = 2.66, \quad \lambda_2 = 1.15, \\ &\lambda_3 = 0.94, \quad \lambda_4 = 0.83, \\ &\lambda_5 = 0.25, \quad \lambda_6 = 0.02, \\ &u_1 = \begin{bmatrix} 0.20 \\ 0.52 \\ 0.16 \\ 0.56 \\ 0.07 \\ 0.59 \end{bmatrix}, \quad u_2 = \begin{bmatrix} 0.47 \\ -0.19 \\ 0.68 \\ -0.19 \\ -0.49 \\ 0.05 \end{bmatrix}, \\ &u_3 = \begin{bmatrix} -0.27 \\ 0.31 \\ -0.32 \\ 0.03 \\ -0.85 \\ -0.02 \end{bmatrix}, \quad u_4 = \begin{bmatrix} 0.81 \\ -0.02 \\ -0.57 \\ 0.06 \\ -0.04 \\ -0.15 \end{bmatrix}, \\ &u_5 = \begin{bmatrix} -0.12 \\ -0.72 \\ -0.07 \\ 0.65 \\ -0.18 \\ 0.09 \end{bmatrix}, \quad u_6 = \begin{bmatrix} 0.02 \\ 0.29 \\ 0.28 \\ 0.47 \\ 0.03 \\ -0.78 \end{bmatrix}, \end{aligned} \quad (7)$$

respectively. The variance contribution rates are

$$\begin{aligned} &\eta_1 = 46\%, \quad \eta_2 = 20\%, \quad \eta_3 = 16\%, \\ &\eta_4 = 14\%, \quad \eta_5 = 4\%, \quad \eta_6 = 0\%. \end{aligned} \quad (8)$$

Table 3: The standardized data.

j	x_{j1}	x_{j2}	x_{j3}	x_{j4}	x_{j5}	x_{j6}
1	0.88	−0.53	0.40	0.74	−0.40	0.37
2	0.88	−0.49	0.48	0.30	−0.22	−0.05
3	0.88	−1.27	−0.17	0.29	−0.22	−0.31
4	−0.22	−0.15	0.07	1.18	−0.22	0.65
5	−0.22	0.24	0.37	0.71	0.35	0.58
6	−0.22	−0.17	0.78	0.74	0.35	0.45
7	−0.22	−0.87	0.90	−0.14	0.21	−0.19
8	0.88	−0.51	0.53	−1.45	−0.08	−0.87
9	−1.32	−0.55	0.60	−1.01	−0.56	−0.81
10	−1.32	−0.54	0.23	−1.03	1.34	−0.55
11	0.88	0.20	−1.87	−0.57	−0.56	−1.19
12	−1.32	−1.25	0.80	−2.33	−0.18	−1.64
13	−0.22	0.60	−2.40	−0.16	1.22	−0.60
14	0.88	1.31	0.47	0.75	0.55	0.94
15	0.88	−0.53	0.40	0.31	0.88	0.19
16	−0.22	0.57	−0.05	1.17	0.88	1.13
17	−1.32	0.97	0.33	1.62	0.88	1.38
18	0.88	0.56	−0.01	0.31	−1.09	0.62
19	1.97	0.96	0.15	0.74	−1.09	1.06
20	1.97	0.19	0.38	−0.16	−1.09	0.36
21	−1.32	0.55	0.51	−0.57	−1.09	0.10
22	0.88	0.55	0.54	−0.13	−1.16	0.32
23	−0.22	−0.52	−1.59	−1.47	0.67	−2.00
24	−1.32	−0.91	−2.11	−0.57	−0.51	−1.54
25	−0.22	−1.95	0.72	−1.89	−1.11	−1.64
26	−0.22	−0.15	0.89	−1.01	−1.11	−0.36
27	−1.32	−1.59	−0.07	−1.47	1.23	−1.26
28	−0.22	−1.60	0.07	−1.47	1.23	−1.11
29	0.88	−1.60	0.93	−1.03	−0.76	−0.87
30	−0.22	−1.59	−2.57	−0.58	−0.56	−1.86
31	0.88	0.97	0.41	0.27	−0.94	0.70
32	0.88	1.65	1.00	1.16	−0.94	1.27
33	−1.32	1.30	−2.73	0.71	−0.94	0.10
34	−0.22	−0.14	0.16	0.74	0.92	0.33
35	−0.22	0.55	0.34	0.75	0.36	0.54
36	1.97	0.91	−0.23	1.17	3.79	1.28
37	−0.22	0.55	0.61	0.73	0.27	0.91
38	−1.32	1.28	0.42	0.72	−0.05	0.81
39	−1.32	1.66	0.14	0.72	−0.60	1.36
40	−0.22	1.33	0.13	1.18	0.40	1.42

Summing up η_q's, we obtain the following

$$\begin{aligned} &\eta_\Sigma(1) = 46\%, \qquad \eta_\Sigma(2) = 65\%, \\ &\eta_\Sigma(3) = 81\%, \qquad \eta_\Sigma(4) = 95\%, \\ &\eta_\Sigma(5) = 100\%, \qquad \eta_\Sigma(6) = 100\%. \end{aligned} \tag{9}$$

A Pareto analysis chart is used to compare the percent variability explained by each principal component (see Figure 3). There is a clear break in the amount of variance accounted for by each component between the first and the second components. However, that component by itself can only explain less than 50% of the variance, so more components may be needed. To meet the requirement $\eta_\Sigma(p) \geq 85\% \sim 90\%$, p is chosen as 3. We can see that the first three principal components explain roughly 80% of the total variability in the standardized data, so that might be a reasonable way to reduce the dimensions in order to visualize the data.

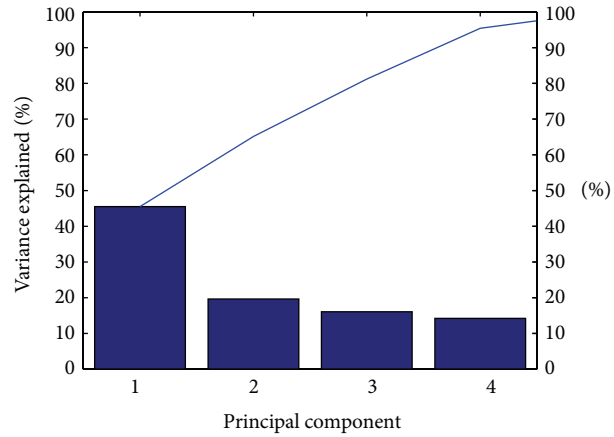

Figure 3: The Pareto analysis chart.

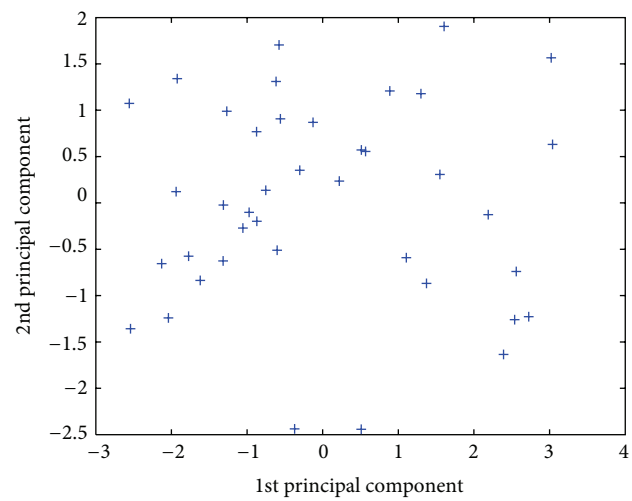

Figure 4: The component scores.

Subsequently, the component scores are computed (see Table 4), which contain the coordinates of the original data in the new coordinate system defined by the principal components and will be used as the new inputs to the FCM-BPN. In Figure 4, the first two columns of the component scores are plotted, showing the data projected onto the first two principal components.

2.2. Classifying Jobs Using FCM. After employing PCA, examples are then classified using FCM. If a crisp clustering method is applied instead, then it is very likely that some clusters will have very few examples. In contrast, an example belongs to multiple clusters to different degrees in FCM,

Table 4: New inputs to the FCM-BPN.

z_{j1}	z_{j2}	z_{j3}
−0.56	0.91	−0.19
−0.13	0.87	−0.34
0.51	0.57	−0.37
−0.97	−0.10	0.20
−0.87	−0.20	−0.26
−0.75	0.14	−0.51
0.57	0.56	−0.66
1.30	1.18	−0.55
1.55	0.31	0.47
1.37	−0.87	−1.04
1.11	−0.59	0.91
3.04	0.63	−0.20
0.51	−2.44	−0.02
−1.94	0.12	−0.43
−0.30	0.35	−1.29
−1.62	−0.84	−0.48
−2.04	−1.24	−0.17
−0.87	0.77	0.89
−1.92	1.34	0.64
−0.58	1.70	0.34
0.22	0.23	1.29
−0.62	1.31	0.73
2.54	−1.26	−0.16
2.39	−1.64	1.20
3.02	1.57	0.14
0.89	1.21	0.66
2.56	−0.74	−1.19
2.19	−0.13	−1.54
1.61	1.90	−0.42
2.72	−1.23	0.87
−1.27	0.99	0.71
−2.56	1.07	0.78
−0.37	−2.44	2.47
−0.60	−0.51	−0.82
−1.06	−0.27	−0.17
−2.54	−1.36	−3.41
−1.31	−0.02	−0.18
−1.32	−0.63	0.67
−1.77	−0.58	1.32
−2.13	−0.66	0.12

which provides a solution to this problem. Similarly, in probability theory, the naïve Bayes method provides the probability that the item belongs to each class. However, the application of FCM can consider subjective factors in classifying the jobs. Algorithm 1.

FCM classifies jobs by minimizing the following objective function:

$$\text{Min} \sum_{k=1}^{K} \sum_{j=1}^{n} \mu_{j(k)}^{m} e_{j(k)}^{2}, \tag{10}$$

where K is the required number of categories; n is the number of jobs; $\mu_{j(k)}$ indicates the membership that job j belongs to category k; $e_{j(k)}$ measures the distance from job j to the centroid of category k; $m \in [1, \infty)$ is a parameter to adjust the fuzziness and is usually set to 2. The procedure of FCM is described as follows.

(1) Normalize the input data.

(2) Produce a preliminary clustering result.

(3) (Iterations) Calculate the centroid of each category as the following:

$$\begin{gathered}
\overline{z}_{(k)} = \left\{\overline{z}_{(k)q}\right\}, \quad k = 1 \sim K, \\
\overline{z}_{(k)q} = \frac{\sum_{j=1}^{n} \mu_{j(k)}^{m} z_{jq}}{\sum_{j=1}^{n} \mu_{j(k)}^{m}}, \quad k = 1 \sim K,\ q = 1 \sim p, \\
\mu_{j(k)} = \frac{1}{\sum_{g=1}^{K} \left(e_{j(k)}/e_{j(g)}\right)^{2/(m-1)}}, \quad j = 1 \sim n,\ k = 1 \sim K, \\
e_{j(k)} = \sqrt{\sum_{q=1}^{p} \left(z_{jp} - \overline{z}_{(k)p}\right)^{2}}, \quad j = 1 \sim n,\ k = 1 \sim K,
\end{gathered} \tag{11}$$

where $\overline{z}_{(k)}$ is the centroid of category k. $\mu_{j(k)}^{(t)}$ is the membership that job j belongs to category k after the tth iteration.

(4) Remeasure the distance from each job to the centroid of each category and then recalculate the corresponding membership.

(5) Stop if the following condition is met. Otherwise, return to step (3):

$$\max_{k} \max_{j} \left|\mu_{j(k)}^{(t)} - \mu_{j(k)}^{(t-1)}\right| < d. \tag{12}$$

where d is a real number representing the threshold for the convergence of membership.

The performance of FCM is highly affected by the settings for the initial values, and therefore can be repeated multiple times in order to find the optimal solution. Finally, the separate distance test (S test) proposed by Xie and Beni [30] can be applied to determine the optimal number of categories K as follows:

$$\text{Min } S \tag{13}$$

subject to

$$\begin{gathered}
J_m = \sum_{k=1}^{K} \sum_{j=1}^{n} \mu_{j(k)}^{m} e_{j(k)}^{2}, \\
e_{\min}^{2} = \min_{k_1 \neq k_2} \left(\sum_{q=1}^{p} \left(\overline{z}_{(k_1)q} - \overline{z}_{(k_2)q}\right)^{2} \right), \\
S = \frac{J_m}{n \times e_{\min}^{2}}, \\
K \in Z^{+}.
\end{gathered} \tag{14}$$

```
A=[0.3857 7175 0.5381;...; 0.1614 0.4281 0.5803]
c=2
[center, U, obj_fun]=fcm(A, c);
Jm=min(obj_fun)
e2_min=9999;
for i=1:c
  for j=i+1:c
    e2_sum=0;
    for k=1: 3
      e2_sum=e2_sum+(center(i, k)−center(j, k))^ 2;
    end
    if e2_sum<e2_min
      e2_min=e2_sum;
    end
  end
end
e2_min
S=min(Jm)/(40∗e2_min)
```

Algorithm 1: The sample MATLAB code for the FCM approach.

Table 5: The results of the S test.

Number of categories (K)	J_m	$e^2_{\min}$	S
2	1.96	0.14	0.34
3	1.21	0.09	0.34
4	0.86	0.07	0.30
5	0.67	0.06	0.26
6	0.53	0.03	0.43

Table 6: The classifying results ($\mu_L = 0.5$).

Category	Jobs
1	1, 2, 18, 19, 20, 22, 31, 32
2	3, 7, 8, 9, 12, 25, 26, 29
3	4, 5, 6, 14, 16, 17, 34, 35, 37, 38, 39, 40
4	10, 11, 23, 24, 27, 30

Table 7: The classifying results ($\mu_L = 0.3$).

Category	Jobs
1	1, 2, 18, 19, 20, 21, 22, 31, 32
2	2, 3, 7, 8, 9, 12, 25, 26, 28, 29
3	4, 5, 6, 14, 15, 16, 17, 33, 34, 35, 36, 37, 38, 39, 40
4	10, 11, 13, 23, 24, 27, 28, 30, 33

The K value minimizing S determines the optimal number of categories.

The Fuzzy Logic Toolbox of MATLAB can be used to implement the FCM approach. A sample code is shown in

In the illustrative example, the data have been standardized and therefore are not normalized again. The results of the S test are summarized in Table 5. In this case, the optimal number of job categories was 5. However, there will be some categories with very few jobs. For this reason, the second best solution is used, that is, 4 categories. A common practice is to set a threshold of membership μ_L to determine whether a job belongs to each category. For example, if $\mu_L = 0.5$, then the classifying results are shown in Table 6. With the decrease in the threshold, each category will contain more jobs. For example, if $\mu_L = 0.3$, then the classifying results are shown in Table 7. Such a property can solve the problem of an insufficient number of examples.

We also note that the classification results are very different according to the new variables, compared with the results based on the original variables. In other words, the results of FCM and PCA-FCM are not the same.

(1) The optimal number of categories in FCM is 6, while that in PCA-FCM is 5.

(2) If jobs are divided into four categories in these two methods, then the results are compared in Figure 5. Many jobs have been reclassified, which means that the misclassification problem has been resolved after variable replacement.

In Figure 5, there are also some outliers that cannot be classified into any category.

2.3. Estimating the Cycle Time Using BPN. Finally, the jobs/examples of a category are learned with the same BPN. Artificial neural networks have been proposed to solve a wide variety of problems usually characterized by sets of different equations. Although there have been some more advanced artificial neural networks, such as compositional pattern-producing network, cascading neural network, and dynamic neural network, a well-trained BPN with an optimized structure can still produce very good results. The configuration of the BPN is established as follows.

(1) Inputs: the new factors determined by PCA associated with the jth example/job. These factors have to be partially normalized so that their values fall within [0.1, 0.9] [18].

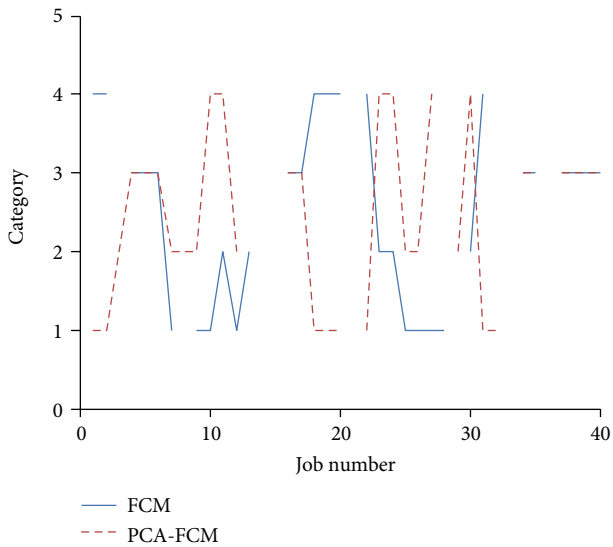

Figure 5: Comparison of the classification results by PCA-FCM and FCM.

(2) Single hidden layer: generally one or two hidden layers are more beneficial for the convergence property of the BPN.

(3) For simplicity, the number of neurons in the hidden layer is twice that in the input layer. An increase in the number of hidden-layer nodes lessens the output errors for the training examples, but increases the errors for novel examples. Such a phenomena is often called "over-fitting." There has been some research considering the relation among the complexity of a BPN, the performance for the training data and the number of examples, for example using Akaike's information criterion (AIC) or the minimum description length (MDL).

(4) Output: the (normalized) cycle time estimate of the example.

The procedure for determining the parameter values is now described. After preclassification, a portion of the adopted examples in each category is fed as "training examples" into the BPN to determine the parameter values for the category. Two phases are involved at the training stage. At first, in the forward phase, inputs are multiplied with weights, summated, and transferred to the hidden layer. Then activated signals h_{jl} are outputted from the hidden layer as:

$$h_{jl} = \frac{1}{1 + e^{-n_{jl}^h}}, \tag{15}$$

where

$$n_{jl}^h = I_{jl}^h - \theta_l^h,$$
$$I_{jl}^h = \sum_{q=1}^{p} w_{ql}^h z_{jq} \tag{16}$$

h_{jl}'s are also transferred to the output layer with the same procedure. Finally, the output of the BPN is generated as:

$$o_j = \frac{1}{1 + e^{-n_j^o}}, \tag{17}$$

where

$$n_j^o = I_j^o - \theta^o,$$
$$I_j^o = \sum_{l=1}^{L} w_l^o h_{jl}. \tag{18}$$

The output o_j is compared with the normalized step flow time $N(CT_j)$, for which RMSE is calculated as the following:

$$\text{RMSE} = \sqrt{\frac{\sum_{j=1}^{n} \left(o_j - N\left(CT_j\right)\right)^2}{n}}. \tag{19}$$

Subsequently in the backward phase, some algorithms are applicable for training a BPN, such as the gradient descent algorithms, the conjugate gradient algorithms, the Levenberg-Marquardt algorithm, and others. In this study, the Levenberg-Marquardt algorithm is applied. The Levenberg-Marquardt algorithm was designed for training with the second-order speed without having to compute the Hessian matrix. It uses approximation and updates the network parameters in a Newton-like way, as described below.

The network parameters are placed in vector $\boldsymbol{\beta} = [w_{11}^h, \ldots, w_{pL}^h, \theta_1^h, \ldots, \theta_L^h, w_1^o, \ldots, w_L^o, \theta^o]$. The network output o_j can be represented with $f(\mathbf{x}_j, \boldsymbol{\beta})$. The objective function of the BPN is to minimize RMSE or equivalently the sum of squared error (SSE):

$$\text{SSE}\left(\boldsymbol{\beta}\right) = \sum_{j=1}^{n} \left(N(CT_j) - f\left(\mathbf{x}_j, \boldsymbol{\beta}\right)\right)^2. \tag{20}$$

The Levenberg-Marquardt algorithm is an iterative procedure. In the beginning, the user should specify the initial values of the network parameters $\boldsymbol{\beta}$. Let $\boldsymbol{\beta}^{\mathbf{T}} = (1, 1, \ldots, 1)$ be a common practice. In each step, the parameter vector $\boldsymbol{\beta}$ is replaced by a new estimate $\boldsymbol{\beta} + \boldsymbol{\delta}$, where $\boldsymbol{\delta} = [\Delta w_{11}^h, \ldots, \Delta w_{pL}^h, \Delta\theta_1^h, \ldots, \Delta\theta_L^h, \Delta w_1^o, \ldots, \Delta w_L^o, \Delta\theta^o]$. The network output becomes $f(\mathbf{x}_j, \boldsymbol{\beta} + \boldsymbol{\delta})$ that is approximated by its linearization as

$$f\left(\mathbf{x}_j, \boldsymbol{\beta} + \boldsymbol{\delta}\right) \approx f\left(\mathbf{x}_j, \boldsymbol{\beta}\right) + \mathbf{J}_j \boldsymbol{\delta}, \tag{21}$$

where

$$\mathbf{J}_j = \partial \frac{f\left(\mathbf{x}_j, \boldsymbol{\beta}\right)}{\partial \boldsymbol{\beta}} \tag{22}$$

is the gradient vector of f with respect to $\boldsymbol{\beta}$. Substituting (21) into (20) leads to.

$$\text{SSE}\left(\boldsymbol{\beta}+\boldsymbol{\delta}\right) \approx \sum_{j=1}^{n} \left(N\left(CT_j\right) - f\left(\mathbf{x}_j, \boldsymbol{\beta}\right) - \mathbf{J}_j \boldsymbol{\delta}\right)^2. \tag{23}$$

```
tn_input=[0.843 0.831 ···; 0.839 0.859 ···; 0.9 0.9 ···; 0.878 0.889 ···; 0.875 0.858 ···;
0.822 0.827 ···]
tn_target=[0.849 0.849 ···]
net=newff([0 1; 0 1; 0 1; 0 1; 0 1; 0 1], [12, 1], {"logsig" , "logsig"}, "trainlm");
net=init(net);
net. trainParam. show=10;
net. trainParam. lr=0.1;
net. trainParam. epochs=1000;
net. trainParam. goal=1e−4;
[net, tr]=train(net, tn_input, tn_target);
tn_output=sim(net, tn_input)
te_input=[0.825 0.844···; 0.824 0.835 ···; 0.9 0.9 ···; 0.878 0.889 ···; 0.883 0.875 ···;
0.807 0.820 ···]
te_output=sim(net, te_input)
```

Algorithm 2: The sample MATLAB code for the BPN approach.

When the network reaches the optimal solution, the gradient of SSE with respect to $\boldsymbol{\delta}$ will be zero. Taking the derivative of SSE($\boldsymbol{\beta}+\boldsymbol{\delta}$) with respect to $\boldsymbol{\delta}$ and setting the result to zero gives the following:

$$\left(\mathbf{J}^{\mathbf{T}}\mathbf{J}\right)\boldsymbol{\delta} = \mathbf{J}^{\mathbf{T}}\left(N\left(CT_j\right) - f\left(\mathbf{x}_j, \boldsymbol{\beta}\right)\right), \tag{24}$$

where $\mathbf{J}$ is the Jacobian matrix containing the first derivative of network error with respect to the weights and biases. Equation (24) includes a set of linear equations that can be solved for $\boldsymbol{\delta}$.

In the illustrative example, 3/4 of the examples in each category are used as the training example. The remaining 1/4 is left for testing. A three-layer BPN is then used to estimate the cycle time of jobs in each category according to the new variables with the following setting.

Single hidden layer.

The number of neurons in the hidden layer: $2 * 3 = 6$.

Convergence criterion: SSE $< 10^{-6}$ or 10000 epochs have been run.

For an outlier, the BPNs of all categories are applied to estimate the cycle time. The Neural Network Toolbox of MATLAB is used to implement the BPN approach. The sample code is shown in Algorithm 2. The estimation accuracy can be evaluated with mean absolute error (MAE), mean absolute percentage error (MAPE), and RMSE. The estimation performances are summarized in Table 8.

Obviously, the overall estimation performance is affected by the outliers. If the outliers can be dealt with properly, the overall estimation will be improved. To this end, an iterative feedback control procedure is established in the next subsection (see Figure 6), which can optimize the overall estimation performance. In the literature, there have been a few control mechanisms for various types of fuzzy systems [31–39]. On the other hand, we also compare the performances of the gradient descent algorithm and the Levenberg-Marquardt algorithm, as shown in Table 9.

Table 8: The estimation performances.

Category	MAE (hrs)	MAPE	RMSE (hrs)
1	18	1.6%	42
2	1	0.1%	3
3	6	0.4%	12
4	23	1.8%	53
Outliers	149	11.9%	152
Total	42	3.5%	85

Table 9: Comparing the performances of two training algorithms (group 4, convergence criterion: SSE $< 10^{-6}$).

Algorithm	Number of epochs	MAE	MAPE	RMSE
Gradient descent	10000	79	6.7%	98
Levenberg-Marquardt	<100	23	1.8%	53

2.4. Iterative Optimization

2.4.1. The Effectiveness of the S Test. Job classification in the proposed methodology is based on the combination of FCM (or PCA-FCM) and the S test, according to which the best number of categories is chosen. This classification method takes into account only the similarity of the parameters of jobs. Whether it has a decisive impact for the subsequent cycle time estimation is not clear. For this reason, the cycle time estimation performances with different numbers of categories are compared to verify the results from the S test. The results are shown in Figure 7. Y-axis is provided in a logarithmic scale to make the relationship clearer. Clearly, when the S value becomes smaller, the estimation error (in terms of MAPE) is also reduced. Therefore, choosing the clustering results with the smallest S value is helpful to the estimation accuracy.

2.4.2. The Correctness of Job Classification. There are absolute rules for the classification of jobs in a wafer fabrication factory. It usually depends on the purpose of job classification, apparently to enhance the estimation accuracy in the

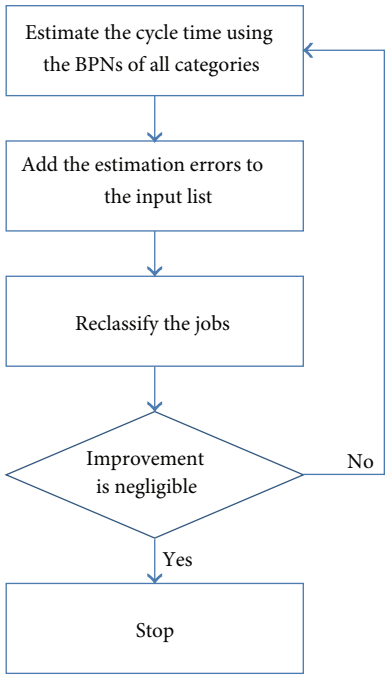

FIGURE 6: The iterative process of dealing with outliers.

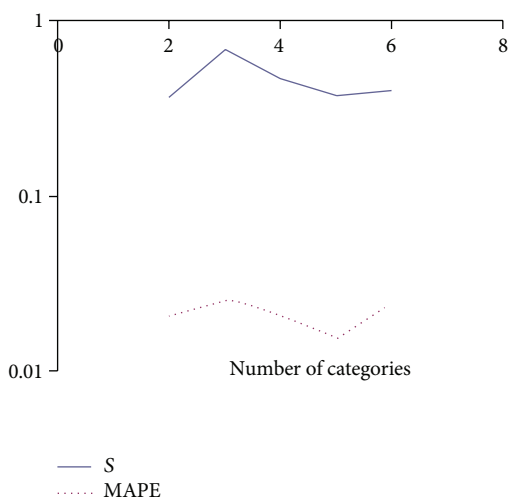

FIGURE 7: The relationship between the S value and MAPE.

proposed methodology. Therefore, a job is correctly classified if its cycle time is accurately estimated after classification. Otherwise, the job is misclassified.

Definition 1 (job misclassification). Assuming the cycle time of job j estimated by the BPN of category k is indicated with $o_j(k)$. The category of job j determined by classifier f is $f(j)$. Then, job j is correctly classified if

$$\begin{aligned} &\left|o_j\left(f\left(j\right)\right) - N\left(CT_j\right)\right| \\ &\quad \le \left|o_j\left(k\right) - N\left(CT_j\right)\right|, \quad \text{for any } k \ne f\left(j\right). \end{aligned} \tag{25}$$

A strong requirement of inequality (25) is

$$\left|o_j\left(f\left(j\right)\right) - N\left(CT_j\right)\right| \le \min_{k \ne f(j)} \left|o_j\left(k\right) - N\left(CT_j\right)\right|, \tag{26}$$

while a weak requirement of this inequality is

$$\left|o_j\left(f\left(j\right)\right) - N\left(CT_j\right)\right| \le \max_{k \ne f(j)} \left|o_j\left(k\right) - N\left(CT_j\right)\right|. \tag{27}$$

Definition 2 (the correctness of classifying a job). The degree that job j is correctly classified by classifier f is

$$\theta\left(f, j\right) = \begin{cases} 1 & \text{if } \left|o_j\left(f\left(j\right)\right) - N\left(CT_j\right)\right| \le \min\limits_{k \ne f(j)} \left|o_j\left(k\right) - N\left(CT_j\right)\right| \\ 0 & \text{if } \left|o_j\left(f\left(j\right)\right) - N\left(CT_j\right)\right| \ge \max\limits_{k \ne f(j)} \left|o_j\left(k\right) - N\left(CT_j\right)\right| \\ \dfrac{\left|o_j\left(f\left(j\right)\right) - N\left(CT_j\right)\right| - \max_{k \ne f(j)} \left|o_j\left(k\right) - N\left(CT_j\right)\right|}{\min_{k \ne f(j)} \left|o_j\left(k\right) - N\left(CT_j\right)\right| - \max_{k \ne f(j)} \left|o_j\left(k\right) - N\left(CT_j\right)\right|} & \text{otherwise.} \end{cases} \tag{28}$$

Definition 3 (the correctness/correct percentage of the classification results). The correctness/correct percentage of the classification results by classifier f is

$$\theta\left(f\right) = \frac{\sum_{j=1}^{n} \theta\left(f, j\right)}{n} \cdot 100\%. \tag{29}$$

In the illustrative example, the correctness of job classification is evaluated, and the results are summarized in Table 10. In this example, the correctness of the classification results is 94%.

2.4.3. Feeding Back the Estimation Error and Reclassification. Subsequently, the estimation error is fed back to the FCM classifier to adjust the classification results. The difference with Chen and Wang's method [40] is that in the proposed methodology the BPNs of all categories are applied to estimate the cycle time of a job [41], and then the estimation errors arising from these BPNs all become additional inputs to the FCM, and jobs are reclassified. The new classification results are shown and compared with that before error feedback in Figure 8. After job reclassification, some outliers are assigned to the existing categories, and the overall estimation performance is improved in this way (see Table 11). The correctness of job classification $\theta(f)$ is now 97%. Job reclassification continues until the improvement in the overall estimation performance or in the correctness of job classification becomes negligible.

3. Further Comparisons

To further evaluate the advantages and/or disadvantages of the proposed methodology, eight existing approaches, statistical analysis, CBR [20], BPN, SOM-WM [7], EFR [21], SOM-FBPN [17], the postclassifying FBPN [25], and the bidirectional classifying BPN approach [26] were all applied

Table 10: The correctness of the classification results.

j	$\theta(f, j)$
1	1.00
2	1.00
3	1.00
4	1.00
5	1.00
6	1.00
7	1.00
8	1.00
9	1.00
10	1.00
11	1.00
12	1.00
13	1.00
14	1.00
15	1.00
16	1.00
17	1.00
18	1.00
19	1.00
20	1.00
21	1.00
22	1.00
23	1.00
24	1.00
25	1.00
26	0.63
27	1.00
28	0.58
29	1.00
30	1.00
31	1.00
32	1.00
33	1.00
34	1.00
35	1.00
36	1.00
37	1.00
38	0.55
39	0.00
40	1.00

to the collected data. Three performance measures including MAE, MAPE, and the minimal RMSE were evaluated.

The proposed methodology was implemented on a PC with an Intel Dual CPU E2200 2.2 GHz and 2.0 G RAM. FCM

Table 11: The estimation performances.

Category	MAE (hrs)	MAPE	RMSE (hrs)
1	1	0.0%	1
2	1	0.1%	2
3	1	0.1%	2
4	2	0.2%	5
Outliers	56	4.5%	80
Total	15	1.2%	36

Table 12: Comparisons of the performances of various approaches.

	MAE (hours)	MAPE	RMSE (hours)
Statistical analysis	73	6.1%	99
CBR	81	6.5%	104
BPN	33	2.8%	71
SOM-WM	30	2.5%	64
EFR	30	2.6%	65
SOM-FBPN	22	2.0%	38
Postclassifying FBPN	40	2.7%	88
Bidirectional classifying BPN	19	1.9%	37
The proposed methodology	15	1.2%	36

was implemented with the Fuzzy toolbox of MATLAB 2006a. In addition, BPN was implemented with the Neural Network Toolbox under the following conditions.

(1) Number of epochs per replication: 10000.

(2) Number of initial conditions/replications: 10.

(3) Stop training if MSE $< 10^{-6}$ is satisfied or 10000 epochs have been run.

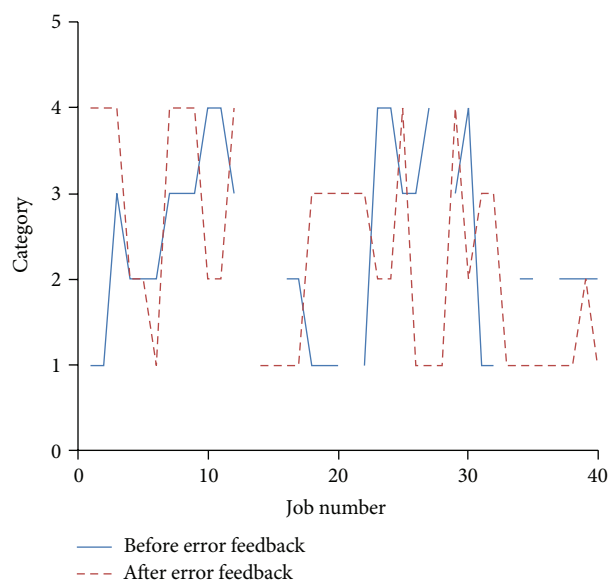

Figure 8: Comparison of the classification results.

Among the steps, PCA and FCM can be done instantaneously. The training of BPN usually takes less than 1 minute per replication.

The performances with the nine approaches are compared and summarized in Table 12.

In statistical analysis, a linear regression equation is used to estimate the job cycle time. In the CBR approach, the weights of factors (the cycle times of the previous cases) are proportional to the similarities of the new job with the previous cases. The optimal value of parameter k in the CBR approach was equal to the value that minimized the RMSE [8]. In the BPN approach, there was one hidden layer with 4~8 nodes, depending on the results of a preliminary analysis for establishing the best configuration. 3/4 of the collected data were used for training the BPN, while the remaining data were used for testing. In SOM-FBPN and SOM-WM, jobs were first classified with SOM. Subsequently, the examples of different categories were then learned with different FBPNs but with the same topology (or WM). In EFR, jobs are classified using fuzzy partition. In the post-classifying FBPN approach, a job was not pre-classified but rather post-classified after the estimation error has been generated. For this purpose, a BPN was used as the postclassification algorithm. In the bidirectional classifying approach, jobs are not only preclassified but also postclassified. The results of preclassification and postclassification are aggregated into a suitability index for each job. Each job is then assigned to the category to which its suitability index is the highest.

Statistical analysis was adopted as a comparison basis. According to experimental results, the following points are made.

(1) The combination of BPN and PCA could reduce about 50% of space for storing the input variables in the modeling of the wafer fabrication system.

(2) From the effectiveness viewpoint, the estimation accuracy (measured with the MAPE) of the proposed methodology was significantly better than those of the other approaches. The average advantage over statistical analysis is 80%.

(3) The standard deviation of the cycle time for this case is 100 hours. Compared with this, the accuracy of the proposed methodology is good.

(4) The estimation performance of the proposed methodology was also better than the existing classifying methods, such as SOM-WM, SOM-FBN, EFR, SOM-FBPN, the postclassifying FBPN, and the bidirectional classifying BPN approach. The advantage of the proposed methodology was reasonable due to the replacement of the variables and the iterative process of dealing with the outliers.

(5) In general, the performances with the preclassifying approaches are better than that with the postclassifying approach.

(6) The proposed methodology was also applied to other cases. The results are summarized in Table 13.

Table 13: Performances in other cases.

RMSE	Case I	Case II	Case III	Case IV
Statistical analysis	77	83	104	78
CBR	74	78	96	72
BPN	53	68	84	63
SOM-WM	49	71	86	66
EFR	50	50	62	47
SOM-FBPN	38	53	66	50
Postclassifying FBPN	62	93	113	86
Bidirectional classifying BPN	24	31	38	28
The proposed methodology	23	23	28	22

Wilcoxon signed-rank test [42] was then used to make sure whether or not the differences between the performance of the proposed methodology and those of the eight existing approaches are significant.

H_0 : When estimating the job cycle time the estimating performance of the proposed methodology is the same as that of the existing approach being compared.

H_1 : When estimating the job cycle time, the estimating performance of the proposed methodology is better than that of the existing approach being compared.

The results are summarized in Table 14. The null hypothesis H_0 was rejected at $\alpha = 0.05$, showing that the proposed methodology was superior to seven existing approaches in estimating the job cycle time.

(7) To ascertain the effect of each treatment taken in the proposed methodology, the performances of BPN, FCM-BPN, PCA-BPN, and PCA-FCM-BPN (the proposed methodology) are compared in Table 15. Obviously, job classification (FCM) did contribute to the effectiveness of the proposed methodology, while the effect of variable replacement (PCA) was not obvious. The simultaneous application of the two treatments further improved the estimation accuracy for the testing data.

4. Conclusions and Directions for Future Research

Estimating the cycle time of each job in a wafer fabrication factory is a critical task to the wafer fabrication factory and has been widely studied in recent years. In order to further enhance the accuracy of the job cycle time estimation, PCA is applied to the FCM-BPN approach in this study, which is an innovative treatment in this field. Through replacing the variables, job classification can be more accurate. In addition, the relationship between the factors and the cycle time can be clearly specified.

On the other hand, since job classification is the core for the proposed methodology, a new index is used to validate the classification of jobs. The empirical relationship between the S value and the estimation performance is also found. Finally,

Table 14: Results of the Wilcoxon sign-rank test.

	H_0
Statistical analysis	$Z = 1.83^*$
CBR	1.83^*
BPN	1.83^*
SOM-WM	1.83^*
EFR	1.64
SOM-FBPN	1.83^*
Postclassifying FBPN	1.83^*
Bidirectional classifying BPN	1.83^*

$^*P < 0.05$.
$^{**}P < 0.025$.
$^{***}P < 0.01$.

Table 15: The effects of the treatments taken in the proposed methodology.

RMSE (hrs)	BPN	FCM-BPN	PCA-BPN	PCA-FCM-BPN
Training data	73	58	71	36

an iterative process is established to deal with the outliers to optimize the overall estimation performance.

An example is used to illustrate the proposed methodology. According to the experimental results,

(1) the estimation accuracy (measured with MAE, MAPE, and RMSE) using the proposed methodology was significantly better than those with the existing approaches;

(2) the advantage of PCA is for improving the correctness of job classification. The simple combination of PCA and BPN does not show much advantage;

(3) after combining with PCA, the estimation accuracy of FCM-BPN was significantly improved;

(4) the overall estimation performance is often affected by the outliers. The iterative procedure tries to remove the outliers and gradually improves the overall estimation performance.

Some other issues for this topic can be further investigated. Most of the existing methods are based on the job clustering. The aim of this study is to provide positive impacts on certain measures for these methods. However, if there are the other variable replacement techniques that can be as effective is also worth exploring in future studies. In addition, the iterative procedure used to optimize the results of job classification is quite time consuming especially for a large-scale problem, and therefore a more efficient way should be found.

Acknowledgment

This work was supported by the National Science Council of Taiwan.

References

[1] T. Chen, "A hybrid look-ahead SOM-FBPN and FIR system for wafer-lot-output time prediction and achievability evaluation," *International Journal of Advanced Manufacturing Technology*, vol. 35, no. 5-6, pp. 575–586, 2007.

[2] T. Chen, Y. C. Wang, and H. C. Wu, "A fuzzy-neural approach for remaining cycle time estimation in a semiconductor manufacturing factory: a simulation study," *International Journal of Innovative Computing, Information and Control*, vol. 5, no. 8, pp. 2125–2139, 2009.

[3] T. Chen and Y. C. Lin, "A fuzzy back propagation network ensemble with example classification for lot output time prediction in a wafer fab," *Applied Soft Computing Journal*, vol. 9, no. 2, pp. 658–666, 2009.

[4] T. Chen, "A fuzzy-neural and multiple-bucket approach for estimating lot cycle time in a wafer fab with dynamic product mix," *Computers and Industrial Engineering*, vol. 55, pp. 423–438, 2008.

[5] T. Chen, "A hybrid fuzzy-neural approach to job completion time prediction in a semiconductor fabrication factory," *Neurocomputing*, vol. 71, no. 16–18, pp. 3193–3201, 2008.

[6] T. Chen, "A SOM-FBPN-ensemble approach with error feedback to adjust classification for wafer-lot completion time prediction," *International Journal of Advanced Manufacturing Technology*, vol. 37, no. 7-8, pp. 782–792, 2008.

[7] T. Chen, "A hybrid SOM-BPN approach to lot output time prediction in a wafer fab," *Neural Processing Letters*, vol. 24, no. 3, pp. 271–288, 2006.

[8] P. C. Chang, J. C. Hieh, and T. W. Liao, "Evolving fuzzy rules for due-date assignment problem in semiconductor manufacturing factory," *Journal of Intelligent Manufacturing*, vol. 16, no. 4-5, pp. 549–557, 2005.

[9] T. Chen, "A fuzzy back propagation network for output time prediction in a wafer fab," *Applied Soft Computing Journal*, vol. 2, no. 3, pp. 211–222, 2003.

[10] T. Chen, "A fuzzy-neural DBD approach for job scheduling in a wafer fabrication factory," *International Journal of Innovative Computing, Information and Control*, vol. 8, no. 6, pp. 4024–4044, 2012.

[11] S. L. Yang, M. Liu, and L. Li, "Forecasting of production cycle of engineer-to-order products," in *Proceedings of the IEEE 18th International Conference on Industrial Engineering and Engineering Management*, pp. 510–513, 2011.

[12] T. Chen, "A fuzzy-neural knowledge-based system for job completion time prediction and internal due date assignment in a wafer fabrication plant," *International Journal of Systems Science*, vol. 40, no. 8, pp. 889–902, 2009.

[13] W. L. Pearn, S. L. Chung, and C. M. Lai, "Due-date assignment for wafer fabrication under demand variate environment," *IEEE Transactions on Semiconductor Manufacturing*, vol. 20, no. 2, pp. 165–175, 2007.

[14] C. F. Chien, C. Y. Hsu, and C. W. Hsiao, "Manufacturing intelligence to forecast and reduce semiconductor cycle time," *Journal of Intelligent Manufacturing*, vol. 23, no. 6, pp. 2281–2294, 2011.

[15] P. C. Chang and J. C. Hsieh, "A neural networks approach for due-date assignment in a wafer fabrication factory," *International Journal of Industrial Engineering : Theory Applications and Practice*, vol. 10, no. 1, pp. 55–61, 2003.

[16] D. Y. Sha and S. Y. Hsu, "Due-date assignment in wafer fabrication using artificial neural networks," *International Journal of*

Advanced Manufacturing Technology, vol. 23, no. 9-10, pp. 768–775, 2004.

[17] T. Chen, "An intelligent hybrid system for wafer lot output time prediction," *Advanced Engineering Informatics*, vol. 21, no. 1, pp. 55–65, 2007.

[18] T. Chen, Y. C. Wang, and H. R. Tsai, "Lot cycle time prediction in a ramping-up semiconductor manufacturing factory with a SOM-FBPN-ensemble approach with multiple buckets and partial normalization," *International Journal of Advanced Manufacturing Technology*, vol. 42, no. 11-12, pp. 1206–1216, 2009.

[19] T. Beeg, "Wafer fab cycle time forecast under changing loading situations," in *Proceedings of the IEEE Conference and Workshop on Advanced Semiconductor Manufacturing*, pp. 339–343, May 2004.

[20] C. Chiu, P. C. Chang, and N. H. Chiu, "A case-based expert support system for due-date assignment in a wafer fabrication factory," *Journal of Intelligent Manufacturing*, vol. 14, no. 3-4, pp. 287–296, 2003.

[21] L. X. Wang and J. M. Mendel, "Generating fuzzy rules by learning from examples," *IEEE Transactions on Systems, Man and Cybernetics*, vol. 22, no. 6, pp. 1414–1427, 1992.

[22] T. Chen and Y. C. Wang, "Incorporating the FCM-BPN approach with nonlinear programming for internal due date assignment in a wafer fabrication plant," *Robotics and Computer-Integrated Manufacturing*, vol. 26, no. 1, pp. 83–91, 2010.

[23] T. Chen, A. Jeang, and Y. C. Wang, "A hybrid neural network and selective allowance approach for internal due date assignment in a wafer fabrication plant," *International Journal of Advanced Manufacturing Technology*, vol. 36, no. 5-6, pp. 570–581, 2008.

[24] T. Chen, "Incorporating fuzzy *c*-means and a back-propagation network ensemble to job completion time prediction in a semiconductor fabrication factory," *Fuzzy Sets and Systems*, vol. 158, no. 19, pp. 2153–2168, 2007.

[25] T. Chen, H. C. Wu, and Y. C. Wang, "Fuzzy-neural approaches with example post-classification for estimating job cycle time in a wafer fab," *Applied Soft Computing Journal*, vol. 9, no. 4, pp. 1225–1231, 2009.

[26] T. Chen, "Job cycle time estimation in a wafer fabrication factory with a bi-directional classifying fuzzy-neural approach," *International Journal of Advanced Manufacturing Technology*, vol. 56, no. 9–12, pp. 1007–1018, 2011.

[27] T. Chen, "Evaluating the mid-term competitiveness of a product in a semiconductor fabrication factory with a systematic procedure," *Computers and Industrial Engineering*, vol. 53, no. 3, pp. 499–513, 2007.

[28] T. Chen, "A PCA-FBPN approach for job cycle time estimation in a wafer fabrication factory," *International Journal of Fuzzy System Applications*, vol. 2, no. 2, pp. 50–67, 2012.

[29] X. He and Q. He, "Application of PCA method and FCM clustering to the fault diagnosis of excavator's hydraulic system," in *Proceedings of the IEEE International Conference on Automation and Logistics (ICAL '07)*, pp. 1635–1639, August 2007.

[30] X. L. Xie and G. Beni, "A validity measure for fuzzy clustering," *IEEE Transactions on Pattern Analysis and Machine Intelligence*, vol. 13, no. 8, pp. 841–847, 1991.

[31] H.-C. Chang, G.-S. Liang, C.-W. Chu, and C.-H. Chou, "Prioritizing service attributes for improvement using fuzzy zone of tolerance," *International Journal of Innovative Computing, Information and Control*, vol. 8, no. 1, pp. 75–89, 2012.

[32] X. Su, P. Shi, L. Wu, and Y. D. Song, "A novel control design on discrete-time Takagi-Sugeno fuzzy systems with time-varying delays," *IEEE Transactions on Fuzzy Systems*. In press.

[33] X. Su, P. Shi, L. Wu, and Y.-D. Song, "A novel approach to filter design for T-S fuzzy discrete-time systems with time-varying delay," *IEEE Transactions on Fuzzy Systems*, vol. 20, no. 6, Article ID 6189779, pp. 1114–1129, 2012.

[34] L. Wu, X. Su, P. Shi, and J. Qiu, "Model approximation for discrete-time state-delay systems in the T-S fuzzy framework," *IEEE Transactions on Fuzzy Systems*, vol. 19, no. 2, pp. 366–378, 2011.

[35] L. Wu and W. X. Zheng, "L2-L∞ control of nonlinear fuzzy itô stochastic delay systems via dynamic output feedback," *IEEE Transactions on Systems, Man, and Cybernetics, Part B: Cybernetics*, vol. 39, no. 5, pp. 1308–1315, 2009.

[36] T. Niknam, H. D. Mojarrad, and M. Nayeripour, "A new hybrid fuzzy adaptive particle swarm optimization for non-convex economic dispatch," *International Journal of Innovative Computing, Information and Control*, vol. 7, no. 1, pp. 189–202, 2011.

[37] S. Y. Cho, C. W. Ting, and C. Quek, "Thermal facial pattern recognition for personal verification using fuzzy cmac model," *International Journal of Innovative Computing, Information and Control*, vol. 7, no. 1, pp. 203–222, 2011.

[38] R. Yang, Z. Zhang, and P. Shi, "Exponential stability on stochastic neural networks with discrete interval and distributed delays," *IEEE Transactions on Neural Networks*, vol. 21, no. 1, pp. 169–175, 2010.

[39] R. Yang, H. Gao, and P. Shi, "Novel robust stability criteria for stochastic Hopfield neural networks with time delays," *IEEE Transactions on Systems, Man, and Cybernetics B*, vol. 39, no. 11, pp. 467–474, 2009.

[40] T. Chen and Y. C. Wang, "A fuzzy-neural system with error feedback to adjust classification for forecasting wafer lot flow time: a simulation study," *Proceedings of the Institution of Mechanical Engineers. Part I: Journal of Systems and Control Engineering*, vol. 221, no. 5, pp. 807–817, 2007.

[41] T. Chen, "A collaborative fuzzy-neural system for global CO_2 concentration forecasting," *International Journal of Innovative Computing, Information and Control*, vol. 8, no. 11, pp. 7679–7696, 2012.

[42] F. Wilcoxon, "Individual comparisons by ranking methods," *Biometrics Bulletin*, vol. 1, no. 6, pp. 80–83, 1945.

Hindawi Publishing Corporation
Mathematical Problems in Engineering
Volume 2013, Article ID 913234, 14 pages
http://dx.doi.org/10.1155/2013/913234

Research Article

Stability Analysis and Stabilization of T-S Fuzzy Delta Operator Systems with Time-Varying Delay via an Input-Output Approach

Zhixiong Zhong,[1] Guanghui Sun,[1] Hamid Reza Karimi,[2] and Jianbin Qiu[1]

[1] *Space Control and Inertial Technology Research Center, Harbin Institute of Technology, Harbin 150001, China*
[2] *Faculty of Engineering and Science, University of Agder, N-4898 Grimstad, Norway*

Correspondence should be addressed to Zhixiong Zhong; zhixiongzhong2012@gmail.com

Received 29 November 2012; Accepted 27 December 2012

Academic Editor: M. Chadli

Copyright © 2013 Zhixiong Zhong et al. This is an open access article distributed under the Creative Commons Attribution License, which permits unrestricted use, distribution, and reproduction in any medium, provided the original work is properly cited.

The stability analysis and stabilization of Takagi-Sugeno (T-S) fuzzy delta operator systems with time-varying delay are investigated via an input-output approach. A model transformation method is employed to approximate the time-varying delay. The original system is transformed into a feedback interconnection form which has a forward subsystem with constant delays and a feedback one with uncertainties. By applying the scaled small gain (SSG) theorem to deal with this new system, and based on a Lyapunov Krasovskii functional (LKF) in delta operator domain, less conservative stability analysis and stabilization conditions are obtained. Numerical examples are provided to illustrate the advantages of the proposed method.

1. Introduction

The T-S fuzzy modeling approach, as a simple and effective tool for nonlinear control systems, has been widely accepted and extensive studied for a few decades [1–8]. In addition, it is well known that time delay is a source of instability or performance degradation [9]. Hence, analysis and synthesis of time-delay systems and other relative studies have attracted much attention during the past years [10–17]. Moreover, high-speed digital processing methods are of increasing importance in modern industrial applications. However, most traditional signal processing and control algorithms are inherently ill-conditioned when data are taken at high sampling rates [18]. The delta operator model can be applied as a useful approach to deal with discrete-time systems under high sampling rates through the analysis methods of continuous-time systems [19–22]. In view of the above considerations, both T-S fuzzy modeling approach and delta operator modeling approach have been extended to tackle the analysis and synthesis of nonlinear systems with time delay [23–25].

Recently, some works on analysis and design of T-S fuzzy systems via delta operator approach were developed [26–28]. However, to the authors' best knowledge, few results on the stability analysis and stabilization for Takagi-Sugeno (T-S) fuzzy delta operator systems with time-varying delay are proposed.

In this paper, an indirect approach, namely, the *input-output* (IO) approach is introduced to deal with the stability analysis and control design of T-S fuzzy delta operator systems with time-varying delay. The main contribution of paper is that the stability analysis and stabilization problems for fuzzy delta operator systems with time-varying delay are investigated by the IO approach. A model approximation method is employed to transform the original system into an equivalent interconnected system, which is comprised of a forward subsystem with constant time delays and a feedback one with delayed uncertainties. The scaled small gain (SSG) method is applied and an LKF in delta domain is constructed to analyze and synthesize this system. Furthermore, a frequency sweeping method [9] is suggested to guarantee the internal stability for the forward subsystem, such that less conservative results are ensured. Finally, some comparisons are made with the existing results and control of a truck-trailer model is also presented to illustrate the effectiveness of our method.

This paper is organized as follows. A model transformation method and the proof of the SSG theorem for T-S fuzzy delta operator systems with time-varying delay are presented in Section 2. In Section 3, the stability analysis and stabilization results are provided. The simulation studies are given in Section 4 to illustrate the effectiveness of the proposed method. Finally, conclusions are drawn in Section 5.

Notations. The notations used throughout this paper are standard. $\mathbb{R}^n$ and $\mathbb{R}^{n\times m}$ represent the n-dimensional Euclidean space and $n \times m$ real matrices, respectively. $\mathbf{G}_1 \circ \mathbf{G}_2$ represents the series connection of mapping $\mathbf{G}_1$ and $\mathbf{G}_2$. The notation $P > 0$ (≥ 0) means that the matrix P is positive (semi) definite, I_n denotes an identity matrix with dimension n, and diag$\{\cdots\}$ denotes a block-diagonal matrix. The symbol "$*$" in a matrix stands for the transposed elements in the symmetric positions.

2. Model Description and Problem Formulation

In the following, we consider a fuzzy delta operator system with time-varying delay, which can be described by the following T-S fuzzy model.

Plant Rule i. **IF** $\theta_1(t)$ is M_{i1} and $\theta_2(t)$ is M_{i2} and ... and $\theta_p(t)$ is M_{ip}, **THEN**

$$\begin{aligned} \partial x(t) &= A_i x(t) + A_{di} x(t-nT) + B_i u(t), \\ x(t) &= \phi(t), \quad t \in [-h_2, 0], \ i = 1, 2, \ldots, r, \end{aligned} \tag{1}$$

where $x(t) \in \mathbb{R}^{n_x}$ is the state variable; $u(t) \in \mathbb{R}^m$ is control input; n is a time-varying integer; T is the sampling period; the bounded time-varying delay nT satisfies $0 < h_1 \leq nT \leq h_2$; $\phi(t) \in \mathbb{R}^{n_x}$ is the vector-valued initial condition; M_{ij} is the fuzzy set; r is the number of IF-THEN rules; $\theta(t) = [\theta_1(t), \theta_2(t), \ldots, \theta_p(t)]$ are the premise variables which do not depend on the control input; A_i, A_{di}, and B_i are known constant matrices with appropriate dimensions; $\partial x(t)$ is the delta operator of $x(t)$, which is defined by

$$\partial x(t) = \begin{cases} \dfrac{d}{dt} x(t), & T = 0, \\ \dfrac{x(t+T) - x(t)}{T}, & T \neq 0. \end{cases} \tag{2}$$

The overall T-S fuzzy delta operator system with time-varying delay is inferred as follows:

$$\partial x(t) = \sum_{i=1}^{r} \lambda_i(\theta(t)) \left[A_i x(t) + A_{di} x(t-nT) + B_i u(t) \right], \tag{3}$$

where $\sum_{i=1}^{r} \lambda_i(\theta(t)) = 1$, $\lambda_i(\theta(t)) = \omega_i(\theta(t)) / \sum_{i=1}^{r} \omega_i(\theta(t)) \geq 0$, and $\omega_i(\theta(t)) = \prod_{j=1}^{r} M_{ij}(\theta_j(t))$ with $M_{ij}(\theta_j(t))$ represent the grade of membership of $\theta_j(t)$ in M_{ij}.

The following control law is employed to deal with the problem of stabilization via state feedback, where the controller rule shares the same fuzzy sets with the T-S model.

Controller Rule i. **IF** $\theta_1(t)$ is M_{i1} and $\theta_2(t)$ is M_{i2} and ... and $\theta_p(t)$ is M_{ip}, **THEN**

$$\begin{aligned} u(t) = {} & K_{1i} x(t) + \frac{1}{2} K_{2i} x(t-h_1) \\ & + \frac{1}{2} K_{3i} x(t-h_2), \quad i = 1, 2, \ldots, r. \end{aligned} \tag{4}$$

The overall T-S fuzzy state feedback control law is inferred as

$$\begin{aligned} u(t) = {} & \sum_{i=1}^{r} \lambda_i(\theta(t)) \Big[K_{1i} x(t) + \frac{1}{2} K_{2i} x(t-h_1) \\ & + \frac{1}{2} K_{3i} x(t-h_2) \Big]. \end{aligned} \tag{5}$$

Remark 1. It is noted that the controller given in (5) covers the special cases of the memoryless controller when $K_{2i} = K_{3i} = 0$ and the purely delayed controller when $K_{1i} = 0$, respectively.

Combining system (3) with the control law (5), the resulting closed-loop system can be expressed as follows:

$$\begin{aligned} \partial x(t) = {} & \sum_{i=1}^{r} \sum_{j=1}^{r} \lambda_i(\theta(t)) \lambda_j(\theta(t)) \\ & \times \Big[\left(A_i + B_i K_{1j} \right) x(t) + A_{di} x(t-nT) \\ & + \frac{1}{2} B_i K_{2j} x(t-h_1) + \frac{1}{2} B_i K_{3j} x(t-h_2) \Big]. \end{aligned} \tag{6}$$

Before ending this section, we introduce the following lemmas as to be used to prove our main results in the following sections.

Lemma 2 (see [9]). *Consider an interconnected system with two subsystems $\widetilde{\mathcal{S}}_1$ and $\widetilde{\mathcal{S}}_2$:*

$$\begin{aligned} \widetilde{\mathcal{S}}_1 : \ & z(t) = \mathbf{G}\omega(t), \\ \widetilde{\mathcal{S}}_2 : \ & \omega(t) = \Delta z(t), \end{aligned} \tag{7}$$

where the forward subsystem $\widetilde{\mathcal{S}}_1$ is known, the feedback subsystem $\widetilde{\mathcal{S}}_2$ is unknown and time-varying, and assume that $\widetilde{\mathcal{S}}_1$ is internally stable. The closed-loop system formed by $\widetilde{\mathcal{S}}_1$ and $\widetilde{\mathcal{S}}_2$ is asymptotically stable for all $\Delta \in D \triangleq \{\Delta : \|\Delta\|_\infty \leq 1\}$

if there exist matrices $\{T_w, T_z\} \in \mathbb{T}$ *satisfied:*

$$\mathbb{T} \triangleq \left\{ \{T_w, T_z\} \in \mathbb{R}^{w\times w} \times \mathbb{R}^{z\times z} : T_w, T_z \text{ nonsigular}; \left\| T_w \circ \Delta \circ T_z^{-1} \right\|_\infty \le 1 \right\}, \tag{8}$$

such that the following SSG condition holds:

$$\left\| T_z \circ \mathbf{G} \circ T_w^{-1} \right\|_\infty \le 1. \tag{9}$$

Lemma 3 (see [29]). *For any constant positive semidefinite symmetric matrix W, two positive integers r and r_0 satifying $r \ge r_0 \ge 1$, the following inequality holds:*

$$\left[\sum_{i=r_0}^{r} x(i) \right]^T W \left[\sum_{i=r_0}^{r} x(i) \right] \le (r - r_0 + 1) \sum_{i=r_0}^{r} x^T(i) W x(i). \tag{10}$$

Lemma 4 (see [30]). *The property of delta operator: for any time function $x(t)$ and $y(t)$, it holds that*

$$\partial(x(t)\, y(t)) = \partial x(t)\, y(t) + x(t)\, \partial y(t) + T \partial x(t)\, \partial y(t), \tag{11}$$

where T is the sampling period.

3. Model Transformation

In this paper, the T-S fuzzy delta operator system with time-varying delay is investigated by an IO approach. By this method, the term $x(t - nT)$ is approximated and the error is written into the feedback path. The recent work in [31] proposed a two-term approximation method $(1/2)[x(t - h_1) + x(t - h_2)]$ for $x(t - nT)$, which results in a smaller approximation error bound. Inspired by this method, the approximation error of time-varying delay can be expressed as

$$\begin{aligned} \omega_t(t) &= x(t - nT) - \frac{1}{2}\left[x(t - h_1) + x(t - h_2) \right] \\ &= \frac{T}{2} \sum_{i=-h_2/T}^{-n-1} \partial x(t + iT) - \frac{T}{2} \sum_{i=-n}^{-(h_1/T)-1} \partial x(t + iT) \\ &= \frac{T}{2} \sum_{i=-h_2/T}^{-(h_1/T)-1} k(i)\, \partial x(t + iT), \end{aligned} \tag{12}$$

where $\partial x(t)$ is defined in (2), and

$$k(i) = \begin{cases} 1, & i < -n, \\ -1, & i \ge -n. \end{cases} \tag{13}$$

3.1. Open-Loop Case. Considering the fuzzy delta operator system (3) and setting $u(t) = 0$, we have

$$\partial x(t) = \sum_{i=1}^{r} \lambda_i(\theta(t)) \left[A_i x(t) + A_{di} x(t - nT) \right]. \tag{14}$$

Employing the two-term approximation method to pull out the uncertainties of time-varying delay, the open-loop system can be written as an interconnected system with a forward subsystem and a feedback one, which is described by

$$\begin{aligned} \mathcal{S}_1 : &\left[\frac{\partial x(t)}{z(t)} \right] \\ &= \sum_{i=1}^{r} \lambda_i(\theta(t)) \left[\begin{array}{c|c} \Theta_1 & \frac{h_{12}}{2} A_{di} X^{-1} \\ \hline X\Theta_1 & X \frac{h_{12}}{2} A_{di} X^{-1} \end{array} \right] \\ &\quad \times \left[\frac{\zeta(t)}{\omega(t)} \right], \\ \mathcal{S}_2 : &\, \omega(t) = X \Delta X^{-1} z(t), \end{aligned} \tag{15}$$

where $\Theta_1 = [A_i \;\; (1/2)A_{di} \;\; (1/2)A_{di}]$, $\zeta(t) = \mathrm{col}\{x(t) \;\; x(t - h_1) \;\; x(t - h_2)\}$, $h_{12} = h_2 - h_1$, $\omega(t) = (2/h_{12}) X \omega_t(t)$, the scaling matrix $\{X, X\} \in \mathbb{T}$ has the appropriate dimensions, and the operator Δ is the maping $z(t) \to \omega(t)$.

For convenience, we denote $\omega(t) = X\tilde{\omega}(t)$ and $z(t) = X\tilde{z}(t)$. The system (15) can be rewritten as

$$\begin{aligned} \mathcal{S}_3 : &\left[\frac{\partial x(t)}{\tilde{z}(t)} \right] \\ &= \sum_{i=1}^{r} \lambda_i(\theta(t)) \left[\begin{array}{c|c} \Theta_1 & \frac{h_{12}}{2} A_{di} \\ \hline \Theta_1 & \frac{h_{12}}{2} A_{di} \end{array} \right] \left[\frac{\zeta(t)}{\tilde{\omega}(t)} \right], \\ \mathcal{S}_4 : &\, \tilde{\omega}(t) = \Delta \tilde{z}(t). \end{aligned} \tag{16}$$

Now, the uncertainties of the time-varying delay have been pulled out from the system (14). Furthermore, the system has been transformed into the interconnection by the forward subsystem and the feedback subsystem. The following result shows that this reformulated system satisfies the following SSG condition.

Lemma 5. *The operator $\Delta : z(t) \to \omega(t)$ in system* (15) *satisfies the SSG theorem if there exists the nosingular matrix $\{X, X\} \in \mathbb{T}$, such that*

$$\left\| X \Delta X^{-1} \right\| \le 1. \tag{17}$$

Proof. Following the notations in (12), under the zero initial condition, we have the following inequalities by using the

discrete Jensen inequality in Lemma 3:

$$\begin{aligned}
&\sum_{t=0}^{\infty} \omega^T(t)\,\omega(t) \\
&\quad = \left(\frac{T}{h_{12}}\right)^2 \sum_{t=0}^{\infty} \left[\sum_{i=-h_2/T}^{-(h_1/T)-1} k(i)\,\partial x(t+iT)\right]^T \\
&\qquad \times X^T X \left[\sum_{i=-h_2/T}^{-(h_1/T)-1} k(i)\,\partial x(t+iT)\right] \\
&\quad \le \frac{T}{h_{12}} \sum_{i=-h_2/T}^{-(h_1/T)-1} \sum_{t=0}^{\infty} \left[\partial x^T(t+iT)\,X^T X \partial x(t+iT)\right] \\
&\quad \le \frac{T}{h_{12}} \sum_{i=-h_2/T}^{-(h_1/T)-1} \sum_{t=0}^{\infty} \left[\partial x^T(t)\,X^T X \partial x(t)\right] \\
&\quad = \sum_{t=0}^{\infty} z^T(t)\,z(t),
\end{aligned} \tag{18}$$

which implies that $\|X\Delta X^{-1}\| \le 1$. The proof is completed. □

3.2. Closed-Loop Case. Employing the two-term approximation method to pull out the uncertainties of time-varying delay, the closed-loop system (6) can also be written as an interconnected system with a forward subsystem and a feedback one, which is described by

$$\begin{aligned}
&\mathcal{S}_5: \left[\frac{\partial x(t)}{z(t)}\right] \\
&\quad = \sum_{i=1}^{r}\sum_{j=1}^{r} \lambda_i(\theta(t))\,\lambda_j(\theta(t)) \left[\begin{array}{c|c} \Theta_2 & \frac{h_{12}}{2} A_{di} X^{-1} \\ \hline X\Theta_2 & X \frac{h_{12}}{2} A_{di} X^{-1} \end{array}\right] \\
&\qquad \times \left[\frac{\zeta(t)}{\tilde{\omega}(t)}\right], \\
&\mathcal{S}_6: \omega(t) = X\Delta X^{-1} z(t),
\end{aligned} \tag{19}$$

where $\Theta_2 = [(A_i + B_i K_{1j}) \;\; (1/2)(A_{di} + B_i K_{2j}) \;\; (1/2)(A_{di} + B_i K_{3j})]$, and $\zeta(t)$, $\omega(t)$, and $z(t)$ are defined as the same as the open-loop case.

For convenience, we denote $\omega(t) = X\tilde{\omega}(t)$ and $z(t) = X\tilde{z}(t)$. The system (19) can be rewritten as

$$\begin{aligned}
&\mathcal{S}_7: \left[\frac{\partial x(t)}{\tilde{z}(t)}\right] \\
&\quad = \sum_{i=1}^{r}\sum_{j=1}^{r} \lambda_i(\theta(t))\,\lambda_j(\theta(t)) \left[\begin{array}{c|c} \Theta_2 & \frac{h_{12}}{2} A_{di} \\ \hline \Theta_2 & \frac{h_{12}}{2} A_{di} \end{array}\right] \left[\frac{\zeta(t)}{\tilde{\omega}(t)}\right], \\
&\mathcal{S}_8: \tilde{\omega}(t) = \Delta\tilde{z}(t).
\end{aligned} \tag{20}$$

Remark 6. The definitions of $\omega(t)$ and $z(t)$ for the closed-loop system are the same as the open-loop system, so it is easy to see that the closed-loop system (19) also satisfies the SSG condition.

Now the reformulated systems have been shown to satisfy the SSG condition in both the open-loop and closed-loop cases. Then the systems in (15) and (19) are asymptotically stable if both the forward subsystems are internally stable. Indeed, a frequency sweeping method is often used to check this condition [9].

Lemma 7 (see [9]). *Consider the following system:*

$$\begin{aligned}
&\tilde{\mathcal{S}}_1: z(t) = \mathbf{G}\omega(t), \\
&\tilde{\mathcal{S}}_2: \omega(t) = \Delta z(t).
\end{aligned} \tag{21}$$

The aforementioned system is internally asymptotically stable if there exist a scalar $\varepsilon > 0$ and a Lyapunov Krasovskii functional $V(t)$ satisfying

$$V(t) > \varepsilon\|x(t)\|^2, \tag{22}$$

such that the functional

$$w(t) = \dot{V}(t) + z^T(t)\,z(t) - \omega^T(t)\,\omega(t) \tag{23}$$

statisfies

$$w(t) \le -\varepsilon\|x(t)\|^2 - \varepsilon\|\omega(t)\|^2. \tag{24}$$

4. Stability Analysis

The previous section presents a model transformation for the original system (3). The open-loop system has been converted into an interconnected system in (15), and the closed-loop system has been converted into (19). In this section, we investigate the asymptotic stability of the system in (15). First, we present the following result for T-S fuzzy delta system with time-varying delay.

Theorem 8. *Consider T-S fuzzy delta operator system in* (14). *Then given scalars $h_2 > h_1 > 0$ and the sampling period $T > 0$,*

the fuzzy delta operator system (14) *with time-varying delay is asymptotically stable if there exist positive definite symmetric matrices U, P, R_1, R_2, Q_1, Q_2, and Z, such that the following LMIs hold for $i = 1, 2, \ldots, r$:*

$$\Phi_i = \begin{bmatrix} \Phi_i(1,1) & PA_i & \frac{1}{2}PA_{di} & \frac{1}{2}PA_{di} & \frac{h_{12}}{2}PA_{di} \\ * & \Phi_i(2,2) & \frac{1}{2}PA_{di} + \frac{R_1}{h_1} & \frac{1}{2}PA_{di} + \frac{R_2}{h_2} & \frac{h_{12}}{2}PA_{di} \\ * & * & -Q_1 - \frac{1}{4}Z - \frac{R_1}{h_1} & -\frac{1}{4}Z & -\frac{h_{12}}{4}Z \\ * & * & * & -Q_2 - \frac{1}{4}Z - \frac{R_2}{h_2} & -\frac{h_{12}}{4}Z \\ * & * & * & * & -\frac{h_{12}^2}{4}Z - U \end{bmatrix} < 0, \tag{25}$$

where

$$\begin{aligned} \Phi_i(1,1) &= TP + h_1R_1 + h_2R_2 - 2P + U, \\ \Phi_i(2,2) &= PA_i + A_i^TP + Z + \frac{h_{12}}{T}Z \\ &\quad + Q_1 + Q_2 - \frac{R_1}{h_1} - \frac{R_2}{h_2}. \end{aligned} \tag{26}$$

Proof. Firstly, choosing a Lyapunov-Krasovskii functional candidate in delta domain,

$$V(t) = V_1(t) + V_2(t) + V_3(t) + V_4(t), \tag{27}$$

where

$$\begin{aligned} V_1(t) &= x^T(t)Px(t), \\ V_2(t) &= T\sum_{i=h_1/T}^{h_2/T}\sum_{j=1}^{i} x^T(t-jT)Zx(t-jT), \\ V_3(t) &= T\sum_{i=1}^{h_1/T} x^T(t-iT)Q_1x(t-iT) \\ &\quad + T\sum_{i=1}^{h_2/T} x^T(t-iT)Q_2x(t-iT), \\ V_4(t) &= \sum_{i=1}^{h_1/T}\sum_{j=1}^{i} e^T(t-jT)R_1e(t-jT) \\ &\quad + \sum_{i=1}^{h_2/T}\sum_{j=1}^{i} e^T(t-jT)R_2e(t-jT), \end{aligned} \tag{28}$$

and T is the sampling period, $e(j) = x(j) - x(j+T)$, so that $\partial x(j) = -e(j)/T$ and $e(t-jT) = x(t-jT) - x(t-(j-1)T)$.

Taking the delta operator manipulations of $V_1(t)$ along the trajectory of systems $\mathcal{S}_1$ and $\mathcal{S}_2$, and using Lemma 4, it can be obtained that

$$\begin{aligned} \partial V_1(t) &= \partial^T(x(t))Px(t) + x^T(t)P\partial(x(t)) \\ &\quad + T\cdot\partial^T(x(t))P\partial(x(t)) \\ &= \begin{bmatrix} \partial x(t) \\ x(t) \\ x(t-h_1) \\ x(t-h_2) \\ \tilde{\omega}(t) \end{bmatrix}^T \\ &\quad \times \begin{bmatrix} TP & 0 & 0 & 0 & 0 \\ * & PA_i + A_i^TP & \frac{1}{2}PA_{di} & \frac{1}{2}PA_{di} & \frac{h_{12}}{2}PA_{di} \\ * & * & 0 & 0 & 0 \\ * & * & * & 0 & 0 \\ * & * & * & * & 0 \end{bmatrix} \\ &\quad \times \begin{bmatrix} \partial x(t) \\ x(t) \\ x(t-h_1) \\ x(t-h_2) \\ \tilde{\omega}(t) \end{bmatrix}. \end{aligned} \tag{29}$$

Taking the delta operator manipulation of $V_2(t)$, we have

$$\begin{aligned} \partial V_2(t) &= T\cdot\frac{1}{T}\sum_{i=h_1/T}^{h_2/T}\sum_{j=1}^{i} x^T(t-(j-1)T) \\ &\qquad \times Zx(t-(j-1)T) \\ &\quad - T\cdot\frac{1}{T}\sum_{i=h_1/T}^{h_2/T}\sum_{j=1}^{i} x^T(t-iT)Zx(t-iT) \\ &= \sum_{i=h_1/T}^{h_2/T} x^T(t)Zx(t) \\ &\quad - \sum_{i=h_1/T}^{h_2/T} x^T(t-iT)Zx(t-iT) \\ &\le \left(\frac{h_{12}}{T} + 1\right)x^T(t)Zx(t) \\ &\quad - x^T(t-nT)Zx(t-nT). \end{aligned} \tag{30}$$

Substituting (12) into (30), we have

$$\partial V_2(t) = \begin{bmatrix} x(t) \\ x(t-h_1) \\ x(t-h_2) \\ \tilde{\omega}(t) \end{bmatrix}^T \times \begin{bmatrix} Z + \frac{h_{12}}{T} Z & 0 & 0 & 0 \\ * & -\frac{1}{4} Z & -\frac{1}{4} Z & -\frac{h_{12}}{4} Z \\ * & * & -\frac{1}{4} Z & -\frac{h_{12}}{4} Z \\ * & * & * & -\frac{h_{12}^2}{4} Z \end{bmatrix} \times \begin{bmatrix} x(t) \\ x(t-h_1) \\ x(t-h_2) \\ \tilde{\omega}(t) \end{bmatrix}. \tag{31}$$

Taking the delta operator manipulation of $V_3(t)$, we have

$$\begin{aligned} \partial V_3(t) = \frac{1}{T} \cdot T \Bigg[& \sum_{i=1}^{h_1/T} x^T(t-(i-1)T) \times Q_1 x(t-(i-1)T) \\ & + \sum_{i=1}^{h_2/T} x^T(t-(i-1)T) \times Q_2 x(t-(i-1)T) \\ & - \sum_{i=1}^{h_1/T} x^T(t-iT) Q_1 x(t-iT) \\ & - \sum_{i=1}^{h_2/T} x^T(t-iT) Q_2 x(t-iT) \Bigg] \\ = {} & x^T(t)(Q_1+Q_2)x(t) \\ & - x^T(t-h_1) Q_1 x(t-h_1) \\ & - x^T(t-h_2) Q_2 x(t-h_2). \end{aligned} \tag{32}$$

Taking the delta operator manipulation of $V_4(t)$ and using Lemma 3, we have

$$\begin{aligned} \partial V_4(t) = \frac{1}{T} \Bigg[& \sum_{i=1}^{h_1/T} \sum_{j=1}^{i} e^T(t-(j-1)T) \times R_1 e(t-(j-1)T) \\ & + \sum_{i=1}^{h_2/T} \sum_{j=1}^{i} e^T(t-(j-1)T) \times R_2 e(t-(j-1)T) \\ & - \sum_{i=1}^{h_1/T} \sum_{j=1}^{i} e^T(t-jT) R_1 e(t-jT) \\ & - \sum_{i=1}^{h_2/T} \sum_{j=1}^{i} e^T(t-jT) R_2 e(t-jT) \Bigg] \\ \le {} & \frac{h_1}{T^2} e^T(t) R_1 e(t) \\ & - \frac{1}{h_1} \left(\sum_{i=1}^{h_1/T} e(t-iT) \right)^T R_1 \left(\sum_{i=1}^{h_1/T} e(t-iT) \right) \\ & + \frac{h_2}{T^2} e^T(t) R_2 e(t) \\ & - \frac{1}{h_2} \left(\sum_{i=1}^{h_2/T} e(t-iT) \right)^T R_2 \left(\sum_{i=1}^{h_2/T} e(t-iT) \right) \\ = {} & h_1 \partial x^T(t) R_1 \partial x(t) - \frac{1}{h_1} (x(t-h_1) - x(t))^T \\ & \times R_1 (x(t-h_1) - x(t)) + h_2 \partial x^T(t) R_2 \partial x(t) \\ & - \frac{1}{h_2} (x(t-h_2) - x(t))^T R_2 (x(t-h_2) - x(t)). \end{aligned} \tag{33}$$

For the positive definite symmetric matrix P, we have the following equation from (16):

$$\begin{aligned} 0 = - \sum_{i=1}^{r} \lambda_i(\theta(t)) 2\partial^T(x(t)) P \times \Bigg[& \partial x(t) - A_i x(t) - \frac{1}{2} A_{di} (x(t-h_1) + x(t-h_2)) \\ & - \frac{h_{12}}{2} A_{di} \tilde{\omega}(t) \Bigg]. \end{aligned} \tag{34}$$

Substituting (34) into $\partial V(t)$, we have

$$\partial V(t) = \sum_{i=1}^{r} \lambda_i(\theta(t)) \xi^T \Sigma_{1i} \xi, \tag{35}$$

where

$$\Sigma_{1i} = \begin{bmatrix} \Sigma_{1i}(1,1) & PA_i & \frac{1}{2}PA_{di} & \frac{1}{2}PA_{di} & \frac{h_{12}}{2}PA_{di} \\ * & \Sigma_{1i}(2,2) & \frac{1}{2}PA_{di}+\frac{R_1}{h_1} & \frac{1}{2}PA_{di}+\frac{R_2}{h_2} & \frac{h_{12}}{2}PA_{di} \\ * & * & -Q_1-\frac{1}{4}Z-\frac{R_1}{h_1} & -\frac{1}{4}Z & -\frac{h_{12}}{4}Z \\ * & * & * & -Q_2-\frac{1}{4}Z-\frac{R_2}{h_2} & -\frac{h_{12}}{4}Z \\ * & * & * & * & -\frac{h_{12}^2}{4}Z \end{bmatrix},$$

$$\Sigma_{1i}(1,1) = TP + h_1R_1 + h_2R_2 - 2P,$$

$$\Sigma_{1i}(2,2) = PA_i + A_i^TP + Z + \frac{h_{12}}{T}Z + Q_1 + Q_2 - \frac{R_1}{h_1} - \frac{R_2}{h_2},$$

$$\xi^T = \left[\partial^T(x(t))\, x^T(t)\, x^T(t-h_1)\, x^T(t-h_2)\, \tilde{\omega}^T(t)\right]. \tag{36}$$

Therefore if $\partial V(t) < 0$, there always exists a sufficiently small scalar ε, for $x(t) \neq 0$, such that $\partial V(t) \leq -\varepsilon\|x(t)\|^2$, which indicates that the systems $\mathcal{S}_1$ and $\mathcal{S}_2$ under $\omega(t) = 0$ are asymptotically stable.

Next, to consider the condition $\omega(t) \neq 0$, we denote $U = X^TX > 0$ and it can be expanded in Lemma 7 as

$$\begin{aligned} \mathscr{W} &\triangleq \partial V(t) + z^T(t)z(t) - \omega^T(t)\omega(t) \\ &= \sum_{i=1}^{r} \lambda_i(\theta(t))\, \xi^T\Sigma_{1i}\xi + \tilde{z}^T(t)X^TX\tilde{z}(t) \\ &\quad - \tilde{\omega}^T(t)X^TX\tilde{\omega}(t) \\ &= \sum_{i=1}^{r} \lambda_i(\theta(t))\, \xi^T\Sigma_{2i}\xi, \end{aligned} \tag{37}$$

where $\Sigma_{2i} = \Phi_i$. The proof is completed. □

To compare the results obtained by IO approach, we give the following corollary, which is obtained by a direct LKF-based method.

Corollary 9. *Consider T-S fuzzy delta operator system in* (14). *Then given scalars $h_2 > h_1 > 0$ and the sampling period $T > 0$, the fuzzy delta operator system* (14) *with time-varying delay is asymptotically stable if there exist positive definite symmetric matrices P, R_1, R_2, Q_1, Q_2, and Z, matrices $N = \begin{bmatrix} N_1 \\ N_2 \end{bmatrix}$, $M = \begin{bmatrix} M_1 \\ M_2 \end{bmatrix}$, $S = \begin{bmatrix} S_1 \\ S_2 \end{bmatrix}$, $\widetilde{X} = \begin{bmatrix} \widetilde{X}_{11} & \widetilde{X}_{12} \\ \widetilde{X}_{12}^T & \widetilde{X}_{22} \end{bmatrix}$, and $Y = \begin{bmatrix} Y_{11} & Y_{12} \\ Y_{12}^T & Y_{22} \end{bmatrix}$, such that the following LMIs* (38)-(39) *hold:*

$$\Psi_1 = \begin{bmatrix} -\widetilde{X}_{11} & -\widetilde{X}_{12} & N_1 \\ * & -\widetilde{X}_{22} & N_2 \\ * & * & -\frac{R_2}{T} \end{bmatrix} < 0,$$

$$\Psi_2 = \begin{bmatrix} -\widetilde{X}_{11} & -\widetilde{X}_{12} & M_1 \\ * & -\widetilde{X}_{22} & M_2 \\ * & * & -\frac{R_2}{T} \end{bmatrix} < 0,$$

$$\Psi_3 = \begin{bmatrix} -Y_{11} & -Y_{12} & S_1 \\ * & -Y_{22} & S_2 \\ * & * & -\frac{R_1}{T} \end{bmatrix} < 0, \tag{38}$$

$$\Psi_{4i} = \begin{bmatrix} \Psi_{4i}(1,1) & PA_i & PA_{di} & 0 & 0 \\ * & \Psi_{4i}(2,2) & \Psi_{4i}(2,3) & -S_1 & -M_1 \\ * & * & \Psi_{4i}(3,3) & -S_2 & -M_2 \\ * & * & * & -Q_1 & 0 \\ * & * & * & * & -Q_2 \end{bmatrix} < 0, \quad i = 1, 2, \ldots, r, \tag{39}$$

where

$$\begin{aligned} \Psi_{4i}(1,1) &= TP + h_1R_1 + h_2R_2 - 2P, \\ \Psi_{4i}(2,2) &= PA_i + A_i^TP + Z + \frac{h_{12}}{T}Z + Q_1 + Q_2 \\ &\quad + N_1 + N_1^T + S_1 + S_1^T + \frac{h_2}{T}\widetilde{X}_{11} + \frac{h_1}{T}Y_{11}, \\ \Psi_{4i}(2,3) &= PA_{di} - N_1 + N_2^T + M_1 + S_2^T \\ &\quad + \frac{h_2}{T}\widetilde{X}_{12} + \frac{h_1}{T}Y_{12}, \\ \Psi_{4i}(3,3) &= -Z - N_2 - N_2^T + M_2 + M_2^T \\ &\quad + \frac{h_2}{T}\widetilde{X}_{22} + \frac{h_1}{T}Y_{22}. \end{aligned} \tag{40}$$

Proof. To make a fair comparison, we choose the same LKF candidate as in the proof of Theorem 8.

Taking the delta operator manipulations of $V_1(t)$, $V_2(t)$, $V_3(t)$, and $V_4(t)$ along the trajectory of system (14), we have

$$\begin{aligned} \partial V_1(t) &= \partial^T(x(t))\, Px(t) + x^T(t)\, P\partial(x(t)) \\ &\quad + T\cdot\partial^T(x(t))\, P\partial(x(t)) \\ &= \begin{bmatrix} \partial x(t) \\ x(t) \\ x(t-nT) \end{bmatrix}^T \begin{bmatrix} TP & 0 & 0 \\ * & PA_i + A_i^TP & PA_{di} \\ * & * & 0 \end{bmatrix} \\ &\quad \times \begin{bmatrix} \partial x(t) \\ x(t) \\ x(t-nT) \end{bmatrix}, \end{aligned}$$

$$\begin{aligned}
\partial V_2(t) &\le \left(\frac{h_{12}}{T}+1\right)x^T(t)Zx(t) \\
&\quad - x^T(t-nT)Zx(t-nT), \\
\partial V_3(t) &= x^T(t)\left(Q_1+Q_2\right)x(t) \\
&\quad - x^T\left(t-h_1\right)Q_1x\left(t-h_1\right) \\
&\quad - x^T\left(t-h_2\right)Q_2x\left(t-h_2\right), \\
\partial V_4(t) &= h_1\partial^T(x(t))R_1\partial(x(t)) \\
&\quad - \frac{1}{T}\sum_{i=1}^{h_1/T} e^T(t-iT)R_1e(t-iT) \\
&\quad + h_2\partial^T(x(t))R_2\partial(x(t)) \\
&\quad - \frac{1}{T}\sum_{i=1}^{h_2/T} e^T(t-iT)R_2e(t-iT),
\end{aligned} \tag{41}$$

where $e(t-iT)$ is defined in (27).

For a positive definite symmetric matrix P, we have the following equation from (14):

$$\begin{aligned}
0 = &-\sum_{i=1}^{r}\lambda_i(\theta(t))2\partial^T(x(t))P \\
&\times\left[\partial x(t)-A_ix(t)-A_{di}x(t-nT)\right].
\end{aligned} \tag{42}$$

From the definition of $e(t-iT)$, the following equations hold for any matrices N, M, and S with appropriate dimensions:

$$\begin{aligned}
0 &= 2\Upsilon^T(t)N\left[x(t)-x(t-nT)+\sum_{i=1}^{n}e^T(t-iT)\right], \\
0 &= 2\Upsilon^T(t)M\left[x(t-nT)-x\left(t-h_2\right)\right. \\
&\qquad \left.+\sum_{i=n+1}^{h_2/T}e^T(t-iT)\right], \\
0 &= 2\Upsilon^T(t)S\left[x(t)-x\left(t-h_1\right)+\sum_{i=1}^{h_1/T}e^T(t-iT)\right],
\end{aligned} \tag{43}$$

where $\Upsilon^T(t)=[x^T(t)x^T(t-nT)]$.

For any appropriate dimensions matrices $\widetilde{X}=\widetilde{X}^T$ and $Y=Y^T$, we have

$$\begin{aligned}
0 &= \sum_{i=1}^{h_2/T}\Upsilon^T(t)\widetilde{X}\Upsilon(t)-\sum_{i=1}^{h_2/T}\Upsilon^T(t)\widetilde{X}\Upsilon(t) \\
&= \frac{h_2}{T}\Upsilon^T(t)\widetilde{X}\Upsilon(t)-\sum_{i=1}^{n}\Upsilon^T(t)\widetilde{X}\Upsilon(t) \\
&\quad -\sum_{i=n+1}^{h_2/T}\Upsilon^T(t)\widetilde{X}\Upsilon(t), \\
0 &= \sum_{i=1}^{h_1/T}\Upsilon^T(t)Y\Upsilon(t)-\sum_{i=1}^{h_1/T}\Upsilon^T(t)Y\Upsilon(t) \\
&= \frac{h_1}{T}\Upsilon^T(t)Y\Upsilon(t)-\sum_{i=1}^{h_1/T}\Upsilon^T(t)Y\Upsilon(t).
\end{aligned} \tag{44}$$

Substituting (42)–(44) into $\partial V(t)$, we have

$$\begin{aligned}
\partial V(t) = &\sum_{i=1}^{r}\lambda_i(t)\xi_1^T\Sigma_{3i}\xi_1+\sum_{i=1}^{n}\Upsilon_1^T(t)\Sigma_4\Upsilon_1(t) \\
&+\sum_{i=1}^{h_1/T}\Upsilon_1^T(t)\Sigma_5\Upsilon_1(t)+\sum_{i=n+1}^{h_2/T}\Upsilon_1^T(t)\Sigma_6\Upsilon_1(t),
\end{aligned} \tag{45}$$

where $\xi_1^T=[\partial x^T(t)\ \ x^T(t)\ \ x^T(t-nT)\ \ x^T(t-h_1)\ \ x^T(t-h_2)]$, $\Upsilon_1^T(t)=[x^T(t)\ \ x^T(t-nT)\ \ e^T(t-iT)]$, $\Sigma_{3i}=\Psi_{4i}$, $\Sigma_4=\Psi_1$, $\Sigma_5=\Psi_3$, and $\Sigma_6=\Psi_2$. Since $\Sigma_{3i}<0$, $\Sigma_4<0$, $\Sigma_5<0$, and $\Sigma_6<0$ hold, then $\partial V(t)<0$. The proof is completed. □

5. Stabilization

The previous section presents the criterion for asymptotic stability of fuzzy delta operator open-loop system. In this section, we are interested in designing a controller in (5). By employing the same LKF and applying IO method, the following criteria can be obtained.

Theorem 10. *Consider T-S fuzzy delta operator system* (3) *with the controller in* (5). *Then given scalars $h_2>h_1>0$ and the sampling period $T>0$, the fuzzy delta operator system with time-varying delay is asymptotically stable if there exist positive definite symmetric matrices G, $\overline{U}$, $\overline{R}_1$, $\overline{R}_2$, $\overline{Q}_1$, $\overline{Q}_2$, and $\overline{Z}$ and matrices $\widetilde{K}_{1i}$, $\widetilde{K}_{2i}$, and $\widetilde{K}_{3i}$, such that the following LMIs hold:*

$$\begin{aligned}
&\Phi_{ii}<0, \quad (1\le i\le r), \\
&\Phi_{ij}+\Phi_{ji}<0, \quad \left(1\le i<j\le r\right),
\end{aligned} \tag{46}$$

where

$$\Phi_{ij} = \begin{bmatrix} \Phi_{ij}(1,1) & \Phi_{ij}(1,2) & \Phi_{ij}(1,3) & \Phi_{ij}(1,4) & \frac{h_{12}}{2}A_{di}G \\ * & \Phi_{ij}(2,2) & \Phi_{ij}(2,3) & \Phi_{ij}(2,4) & \frac{h_{12}}{2}A_{di}G \\ * & * & \Phi_{ij}(3,3) & -\frac{1}{4}\overline{Z} & -\frac{h_{12}}{4}\overline{Z} \\ * & * & * & \Phi_{ij}(4,4) & -\frac{h_{12}}{4}\overline{Z} \\ * & * & * & * & -\frac{h_{12}^2}{4}\overline{Z}-\overline{U} \end{bmatrix},$$

$$\begin{aligned} \Phi_{ij}(1,1) &= TG + h_1\overline{R}_1 + h_2\overline{R}_2 - 2G + \overline{U}, \\ \Phi_{ij}(1,2) &= A_iG + B_i\widetilde{K}_{1j}, \\ \Phi_{ij}(1,3) &= \frac{1}{2}\left(A_{di}G + B_i\widetilde{K}_{2j}\right), \\ \Phi_{ij}(1,4) &= \frac{1}{2}\left(A_{di}G + B_i\widetilde{K}_{3j}\right), \\ \Phi_{ij}(2,2) &= A_iG + B_i\widetilde{K}_{1j} + GA_i^T + \widetilde{K}_{1j}^TB_i^T \\ &\quad + \overline{Z} + \frac{h_{12}}{T}\overline{Z} + \overline{Q}_1 + \overline{Q}_2 - \frac{\overline{R}_1}{h_1} - \frac{\overline{R}_2}{h_2}, \\ \Phi_{ij}(2,3) &= \frac{1}{2}\left(A_{di}G + B_i\widetilde{K}_{2j}\right) + \frac{\overline{R}_1}{h_1}, \\ \Phi_{ij}(2,4) &= \frac{1}{2}\left(A_{di}G + B_i\widetilde{K}_{3j}\right) + \frac{\overline{R}_2}{h_2}, \\ \Phi_{ij}(3,3) &= -\overline{Q}_1 - \frac{1}{4}\overline{Z} - \frac{\overline{R}_1}{h_1}, \\ \Phi_{ij}(4,4) &= -\overline{Q}_2 - \frac{1}{4}\overline{Z} - \frac{\overline{R}_2}{h_2}. \end{aligned} \tag{47}$$

Moreover, a suitable stabilizing fuzzy state feedback controller can be chosen by

$$\begin{aligned} u(t) = &\sum_{i=1}^{r}\lambda_i(\theta(t))\left[K_{1i}x(t) + \frac{1}{2}K_{2i}x(t-h_1)\right. \\ &\left. + \frac{1}{2}K_{3i}x(t-h_2)\right], \quad i = 1,2,\ldots,r, \end{aligned} \tag{48}$$

where $K_{1i} = \widetilde{K}_{1i}G^{-1}$, $K_{2i} = \widetilde{K}_{2i}G^{-1}$, $K_{3i} = \widetilde{K}_{3i}G^{-1}$.

Proof. Choosing the same LKF candidate as in the proof of Theorem 8, we have

$$\partial V(t) = \sum_{i=1}^{r}\sum_{j=1}^{r}\lambda_i(\theta(t))\lambda_j(\theta(t))\xi^T\Sigma_{1ij}\xi, \tag{49}$$

where

$$\Sigma_{1ij} = \begin{bmatrix} \Sigma_{1ij}(1,1) & \Sigma_{1ij}(1,2) & \Sigma_{1ij}(1,3) & \Sigma_{1ij}(1,4) & \frac{h_{12}}{2}PA_{di} \\ * & \Sigma_{1ij}(2,2) & \Sigma_{1ij}(2,3) & \Sigma_{1ij}(2,4) & \frac{h_{12}}{2}PA_{di} \\ * & * & \Sigma_{1ij}(3,3) & -\frac{1}{4}Z & -\frac{h_{12}}{4}Z \\ * & * & * & \Sigma_{1ij}(4,4) & -\frac{h_{12}}{4}Z \\ * & * & * & * & -\frac{h_{12}^2}{4}Z \end{bmatrix},$$

$$\begin{aligned} \Sigma_{1ij}(1,1) &= TP + h_1R_1 + h_2R_2 - 2P, \\ \Sigma_{1ij}(1,2) &= P\left(A_i + B_iK_{1j}\right), \\ \Sigma_{1ij}(1,3) &= \frac{1}{2}P\left(A_{di} + B_iK_{2j}\right), \\ \Sigma_{1ij}(1,4) &= \frac{1}{2}P\left(A_{di} + B_iK_{3j}\right), \\ \Sigma_{1ij}(2,2) &= P\left(A_i + B_iK_{1j}\right) + \left(A_i + B_iK_{1j}\right)^TP \\ &\quad + Z + \frac{h_{12}}{T}Z + Q_1 + Q_2 - \frac{R_1}{h_1} - \frac{R_2}{h_2}, \\ \Sigma_{1ij}(2,3) &= \frac{1}{2}P\left(A_{di} + B_iK_{2j}\right) + \frac{R_1}{h_1}, \\ \Sigma_{1ij}(2,4) &= \frac{1}{2}P\left(A_{di} + B_iK_{3j}\right) + \frac{R_2}{h_2}, \\ \Sigma_{1ij}(3,3) &= -Q_1 - \frac{1}{4}Z - \frac{R_1}{h_1}, \\ \Sigma_{1ij}(4,4) &= -Q_2 - \frac{1}{4}Z - \frac{R_2}{h_2}, \end{aligned} \tag{50}$$

and ξ is defined in (35).

Next, by applying Lemma 7, we have

$$\begin{aligned} \mathscr{W} &\triangleq \partial V(t) + z^T(t)z(t) - \omega^T(t)\omega(t) \\ &= \sum_{i=1}^{r}\sum_{j=1}^{r}\lambda_i(\theta(t))\lambda_j(\theta(t))\xi^T\Sigma_{1ij}\xi \\ &\quad + \widetilde{z}^T(t)X^TX\widetilde{z}(t) - \widetilde{\omega}^T(t)X^TX\widetilde{\omega}(t) \\ &= \sum_{i=1}^{r}\sum_{j=1}^{r}\lambda_i(\theta(t))\lambda_j(\theta(t))\xi^T\Sigma_{2ij}\xi, \end{aligned} \tag{51}$$

where

$$\Sigma_{2ij} = \begin{bmatrix} \Sigma_{1ij}(1,1)+U & \Sigma_{1ij}(1,2) & \Sigma_{1ij}(1,3) & \Sigma_{1ij}(1,4) & \frac{h_{12}}{2}PA_{di} \\ * & \Sigma_{1ij}(2,2) & \Sigma_{1ij}(2,3) & \Sigma_{1ij}(2,4) & \frac{h_{12}}{2}PA_{di} \\ * & * & \Sigma_{1ij}(3,3) & -\frac{1}{4}Z & -\frac{h_{12}}{4}Z \\ * & * & * & \Sigma_{1ij}(4,4) & -\frac{h_{12}}{4}Z \\ * & * & * & * & -\frac{h_{12}^2}{4}Z-U \end{bmatrix}. \tag{52}$$

It can be clearly shown that

$$\begin{aligned} \mathscr{W} \triangleq & \sum_{i=1}^{r} \lambda_i^2(\theta(t))\,\xi^T\Sigma_{2ii}\xi \\ & + \sum_{i=1}^{r}\sum_{i<j}^{r} \lambda_i(\theta(t))\,\lambda_j(\theta(t))\,\xi^T \times \left(\Sigma_{2ij}+\Sigma_{2ji}\right)\xi. \end{aligned} \tag{53}$$

Premultiplying and postmultiplying Σ_{2ii} by $\mathrm{diag}\{P^{-1}\ P^{-1}\ P^{-1}\ P^{-1}\ P^{-1}\}$, and letting $G = P^{-1}$, $\overline{R}_1 = P^{-1}R_1P^{-1}$, $\overline{R}_2 = P^{-1}R_2P^{-1}$, $\overline{Q}_1 = P^{-1}Q_1P^{-1}$, $\overline{Q}_2 = P^{-1}Q_2P^{-1}$, $\overline{U} = P^{-1}UP^{-1}$, $\widetilde{K}_{1i} = K_{1i}P^{-1}$, $\widetilde{K}_{2i} = K_{2i}P^{-1}$, and $\widetilde{K}_{3i} = K_{3i}P^{-1}$ yield Φ_{ii}. Following a similar line in the previous process to Σ_{2ij} and Σ_{2ji} yields Φ_{ij} and Φ_{ji}.

Since $\Phi_{ii} < 0$ holds for $1 \le i \le r$, and $(\Phi_{ij}+\Phi_{ji}) < 0$ holds for $1 \le i < j \le r$,then we have $\mathscr{W} < 0$. Then by using Lemma 7, the system (19) is internally asymptotically stable. Furthermore, from Lemma 2, the fuzzy delta operator system (3) under the controller (5) is asymptotically stable. Finally, the explicit expression of the state feedback controller is given by $K_{1i} = \widetilde{K}_{1i}G^{-1}$, $K_{2i} = \widetilde{K}_{2i}G^{-1}$, and $K_{3i} = \widetilde{K}_{3i}G^{-1}$. The proof is completed. □

To compare the results obtained by the IO approach, we give the following corollary, which is obtained by a direct LKF-based method.

Corollary 11. *Consider T-S fuzzy delta operator system* (3) *with the controller in* (5). *Then given scalars* $h_2 > h_1 > 0$ *and the sampling period* $T > 0$, *the fuzzy delta operator system with time-varying delay is asymptotically stable if there exist positive definite symmetric matrices* G, $\overline{R}_1$, $\overline{R}_2$, $\overline{Q}_1$, $\overline{Q}_2$, *and* $\overline{Z}$ *and matrices* $\overline{N} = \begin{bmatrix}\overline{N}_1\\ \overline{N}_2\end{bmatrix}$, $\overline{M} = \begin{bmatrix}\overline{M}_1\\ \overline{M}_2\end{bmatrix}$, $\overline{S} = \begin{bmatrix}\overline{S}_1\\ \overline{S}_2\end{bmatrix}$, $\overline{X} = \begin{bmatrix}\overline{X}_{11} & \overline{X}_{12}\\ \overline{X}_{12}^T & \overline{X}_{22}\end{bmatrix}$, $\overline{Y} = \begin{bmatrix}\overline{Y}_{11} & \overline{Y}_{12}\\ \overline{Y}_{12}^T & \overline{Y}_{22}\end{bmatrix}$ *and* $\widetilde{K}_{1i}$, *such that* (38) *and the following LMIs hold:*

$$\begin{aligned} \Psi_{4ii} < 0 \quad & (1 \le i \le r), \\ \Psi_{4ij}+\Psi_{4ji} < 0 \quad & (1 \le i < j \le r), \end{aligned} \tag{54}$$

where

$$\Psi_{4ij} = \begin{bmatrix} \Psi_{4ij}(1,1) & A_iG+B_i\widetilde{K}_{1j} & A_{di}G & 0 & 0 \\ * & \Psi_{4ij}(2,2) & \Psi_{4ij}(2,3) & -\overline{S}_1 & -\overline{M}_1 \\ * & * & \Psi_{4ij}(3,3) & -\overline{S}_2 & -\overline{M}_2 \\ * & * & * & -\overline{Q}_1 & 0 \\ * & * & * & * & -\overline{Q}_2 \end{bmatrix},$$

$$\begin{aligned} \Psi_{4ij}(1,1) &= TG + h_1\overline{R}_1 + h_2\overline{R}_2 - 2G, \\ \Psi_{4ij}(2,2) &= A_iG + B_i\widetilde{K}_{1j} + GA_i^T + \widetilde{K}_{1j}^TB_i^T + \overline{Z} \\ &\quad + \frac{h_{12}}{T}\overline{Z} + \overline{Q}_1 + \overline{Q}_2 + \overline{N}_1 + \overline{N}_1^T + \overline{S}_1 + \overline{S}_1^T \\ &\quad + \frac{h_2}{T}\overline{X}_{11} + \frac{h_1}{T}\overline{Y}_{11}, \\ \Psi_{4ij}(2,3) &= A_{di}G - \overline{N}_1 + \overline{N}_2^T + \overline{M}_1 + \overline{S}_2^T \\ &\quad + \frac{h_2}{T}\overline{X}_{12} + \frac{h_1}{T}\overline{Y}_{12}, \\ \Psi_{4ij}(3,3) &= -\overline{Z} - \overline{N}_2 - \overline{N}_2^T + \overline{M}_2 + \overline{M}_2^T \\ &\quad + \frac{h_2}{T}\overline{X}_{22} + \frac{h_1}{T}\overline{Y}_{22}. \end{aligned} \tag{55}$$

Moreover, a suitable stabilizing fuzzy state feedback controller is given by

$$u(t) = \sum_{i=1}^{r} \lambda_i(\theta(t))\,K_{1i}x(t), \quad i = 1,2,\ldots,r, \tag{56}$$

where $K_{1i} = \widetilde{K}_{1i}G^{-1}$.

Proof. Choosing the same LKF candidate as in the proof of Theorem 8, we have

$$\begin{aligned} \partial V(t) = & \sum_{i=1}^{r}\sum_{j=1}^{r} \lambda_i(\theta(t))\,\lambda_j(\theta(t))\,\xi_1^T\Sigma_{3ij}\xi_1 \\ & + \sum_{i=1}^{n} \Upsilon_1^T(t)\,\Sigma_4\Upsilon_1(t) + \sum_{i=1}^{h_1/T} \Upsilon_1^T(t)\,\Sigma_5\Upsilon_1(t) \\ & + \sum_{i=n+1}^{h_2/T} \Upsilon_1^T(t)\,\Sigma_6\Upsilon_1(t), \end{aligned} \tag{57}$$

where

$$\Sigma_{3ij}=\begin{bmatrix}\Sigma_{3ij}(1,1) & P\left(A_i+B_iK_{1j}\right) & PA_{di} & 0 & 0\\ * & \Sigma_{3ij}(2,2) & \Sigma_{3ij}(2,3) & -S_1 & -M_1\\ * & * & \Sigma_{3ij}(3,3) & -S_2 & -M_2\\ * & * & * & -Q_1 & 0\\ * & * & * & * & -Q_2\end{bmatrix},$$

$$\begin{aligned}\Sigma_{3ij}(1,1)&=TP+h_1R_1+h_2R_2-2P,\\ \Sigma_{3ij}(2,2)&=P\left(A_i+B_iK_{1j}\right)+\left(A_i+B_iK_{1j}\right)^TP+Z\\ &\quad+\frac{h_{12}}{T}Z+Q_1+Q_2+N_1+N_1^T+S_1+S_1^T\\ &\quad+\frac{h_2}{T}\widetilde{X}_{11}+\frac{h_1}{T}Y_{11},\\ \Sigma_{3ij}(2,3)&=PA_{di}-N_1+N_2^T+M_1+S_2^T\\ &\quad+\frac{h_2}{T}\widetilde{X}_{12}+\frac{h_1}{T}Y_{12},\\ \Sigma_{3ij}(3,3)&=-Z-N_2-N_2^T+M_2+M_2^T\\ &\quad+\frac{h_2}{T}\widetilde{X}_{22}+\frac{h_1}{T}Y_{22},\end{aligned}\tag{58}$$

and ξ_1^T, Υ_1^T, Σ_4, Σ_5, and Σ_6 are defined in (45).

It can be clearly shown that

$$\begin{aligned}\partial V(t)\triangleq&\sum_{i=1}^{r}\lambda_i^2(\theta(t))\,\xi_1^T\Sigma_{3ii}\xi_1\\ &+\sum_{i=1}^{r}\sum_{i<j}^{r}\lambda_i(\theta(t))\,\lambda_j(\theta(t))\,\xi_1^T\left(\Sigma_{3ij}+\Sigma_{3ji}\right)\xi_1\\ &+\sum_{i=1}^{n}\Upsilon_1^T(t)\,\Sigma_4\Upsilon_1(t)+\sum_{i=1}^{h_1/T}\Upsilon_1^T(t)\,\Sigma_5\Upsilon_1(t)\\ &+\sum_{i=n+1}^{h_2/T}\Upsilon_1^T(t)\,\Sigma_6\Upsilon_1(t).\end{aligned}\tag{59}$$

Premultiplying and postmultiplying Σ_{3ii} by $\mathrm{diag}\{P^{-1}\ P^{-1}\ P^{-1}\ P^{-1}\ P^{-1}\}$, premultiplying and postmultiplying $\Sigma_4, \Sigma_5, \Sigma_6$ by $\mathrm{diag}\{P^{-1}\ P^{-1}\ P^{-1}\}$, and letting $G=P^{-1}$, $\overline{R}_1=P^{-1}R_1P^{-1}$, $\overline{R}_2=P^{-1}R_2P^{-1}$, $\overline{Q}_1=P^{-1}Q_1P^{-1}$, $\overline{Q}_2=P^{-1}Q_2P^{-1}$, $\overline{Z}=P^{-1}ZP^{-1}$, $\overline{N}_1=P^{-1}N_1P^{-1}$, $\overline{N}_2=P^{-1}N_2P^{-1}$, $\overline{M}_1=P^{-1}M_1P^{-1}$, $\overline{M}_2=P^{-1}M_2P^{-1}$, $\overline{S}_1=P^{-1}S_1P^{-1}$, $\overline{S}_2=P^{-1}S_2P^{-1}$, $\overline{X}_{11}=P^{-1}\widetilde{X}_{11}P^{-1}$, $\overline{X}_{12}=P^{-1}\widetilde{X}_{12}P^{-1}$, $\overline{X}_{22}=P^{-1}\widetilde{X}_{22}P^{-1}$, $\overline{Y}_{11}=P^{-1}Y_{11}P^{-1}$, $\overline{Y}_{12}=P^{-1}Y_{12}P^{-1}$, $\overline{Y}_{22}=P^{-1}Y_{22}P^{-1}$, and $\widetilde{K}_{1i}=K_{1i}P^{-1}$ yield Ψ_{4ii}, Ψ_1, Ψ_2, and Ψ_3. Following a similar line of the previous process to Σ_{3ij} and Σ_{3ji} yields Ψ_{4ij} and Ψ_{4ji}.

Since $\Psi_{4ii}<0$ holds for $1\le i\le r$, and $(\Psi_{4ij}+\Psi_{4ji})<0$ holds for $1\le i<j\le r$, $\Sigma_4<0$, $\Sigma_5<0$, and $\Sigma_6<0$,then we have $\partial V(t)<0$. Therefore the fuzzy delta operator system (3) under the controller (59) is asymptotically stable. Finally, the explicit expression of the state feedback controller is given by $K_{1i}=\widetilde{K}_{1i}G^{-1}$. The proof is completed. □

Table 1: Comparisons of maximum allowed delay upper bound h_2 for Example 12 with $h_1=0.8$.

Method	h_2 ($T=0.01$)
Result of Corollary 9	Infeasible
Result of Theorem 8	0.933

6. Simulation Examples

In this section, three examples are provided to demonstrate the effectiveness of the proposed results.

Example 12 (Stability Analysis). Consider a T-S fuzzy delta operator system with time-varying delay in the form of (1) with parameters given by

$$\begin{aligned}A_1&=\begin{bmatrix}-2&0\\0&-0.9\end{bmatrix},\qquad A_2=\begin{bmatrix}-1&0.5\\0&-1\end{bmatrix},\\ A_{d1}&=\begin{bmatrix}-1&0\\-1&-1\end{bmatrix},\qquad A_{d2}=\begin{bmatrix}-1&0\\0.1&-1\end{bmatrix}.\end{aligned}\tag{60}$$

In this example, for a given delay lower bound $h_1=0.8$, we seek for the admissible upper bound h_2, which guarantees the asymptotic stability of the open-loop system. Choosing the sampling period $T=0.01$, the obtained results are listed in Table 1.

Table 1 shows that the proposed result in Theorem 8 is less conservative than that in Corollary 9, which demonstrates the advantages of our method. Table 2 shows the delay upper bound h_2 under different delay lower bound h_1 and different sampling period T. It is obvious that the delay upper bound h_2 increases gradually as the sampling rate rises, which indicates the advantage of the delta operator fuzzy system at high sampling rate.

Example 13 (Controller Design). To further illustrate the effectiveness of our method for controller design, we consider the following T-S fuzzy delta operator system with time-varying delay:

$$\partial V(t)=\sum_{i=1}^{r}\lambda_i(\theta(t))\left[A_ix(t)+A_{di}x(t-nT)+B_iu(t)\right],\tag{61}$$

where A_i, B_i, and A_{di} $(i=1,2)$ are given by

$$\begin{aligned}A_1&=\begin{bmatrix}0&0.6\\0&1\end{bmatrix},\qquad A_{d1}=\begin{bmatrix}0.5&0.9\\0&2\end{bmatrix},\\ B_1&=\begin{bmatrix}1\\1\end{bmatrix},\qquad A_2=\begin{bmatrix}1&0\\1&0\end{bmatrix},\\ A_{d2}&=\begin{bmatrix}0.9&0\\1&1.6\end{bmatrix},\qquad B_2=\begin{bmatrix}1\\1\end{bmatrix}.\end{aligned}\tag{62}$$

Table 2: Comparisons of maximum allowed delay upper bound h_2 by different h_1 and T for Example 12.

Method	$T = 0.01$			$T = 0.05$			$T = 0.1$		
h_1	0.1	0.4	0.8	0.1	0.4	0.8	0.1	0.4	0.8
Result of Theorem 8	0.732	0.790	0.933	0.685	0.749	0.901	0.626	0.700	0.863

Table 3: Comparisons of maximum allowed delay upper bound h_2 by different h_1 and T for Example 13.

Method	$T = 0.01$			$T = 0.05$			$T = 0.1$		
h_1	0.1	0.4	0.8	0.1	0.4	0.8	0.1	0.4	0.8
Result of Corollary 11	0.185	—	—	0.179	—	—	0.172	—	—
Result of Theorem 10	0.428	0.668	0.951	0.418	0.658	0.941	0.406	0.646	0.929

For different delay lower bounds h_1, the allowed delay upper bounds h_2 are listed in Table 3. It can be seen that the proposed results in Theorem 10 are less conservative than those in Corollary 11.

The fuzzy controller gains for $T = 0.01$, $h_1 = 0.8$, and $h_2 = 0.951$ by Theorem 10 are given as

$$\begin{aligned} K_{11} &= \begin{bmatrix} 1.2781 & -4.4103 \end{bmatrix}, \\ K_{12} &= \begin{bmatrix} 0.0812 & -2.9757 \end{bmatrix}, \\ K_{21} &= \begin{bmatrix} -0.1010 & -2.0993 \end{bmatrix}, \\ K_{22} &= \begin{bmatrix} -1.0592 & -2.5416 \end{bmatrix}, \\ K_{31} &= \begin{bmatrix} -0.1064 & -1.9295 \end{bmatrix}, \\ K_{32} &= \begin{bmatrix} -1.0592 & -2.5414 \end{bmatrix}. \end{aligned} \tag{63}$$

Example 14. To illustrate the application of our method, we consider the following truck-trailer system given in [32]:

$$\begin{aligned} \dot{x}_1(t) &= -c\frac{vt_1}{Lt_0}x_1(t) - (1-c)\frac{vt_1}{Lt_0}x_1(t-d(t)) + \frac{vt_1}{lt_0}u(t), \\ \dot{x}_2(t) &= c\frac{vt_1}{Lt_0}x_1(t) + (1-c)\frac{vt_1}{Lt_0}x_1(t-d(t)), \\ \dot{x}_3(t) &= \frac{vt_1}{t_0}\sin x_2(t) + c\frac{vt_1}{2L}x_1(t) \\ &\quad + (1-c)\frac{vt_1}{2L}x_1(t-d(t)), \end{aligned} \tag{64}$$

where $x_1(t)$ is the angular difference between the truck and trailer, $x_2(t)$ is the angle of the trailer, and $x_3(t)$ is the vertical position of rear end of the trailer.

The model parameters are given as $l = 2.8$, $L = 5.5$, $v = -1.0$, $t_1 = 2.0$, and $t_0 = 0.5$, and $c \in [0, 1]$ is a retarded coefficient with limits 0 and 1 corresponding to delay-free term and to a full-delay term. The premise variable is chosen as $\theta(t) = x_2(t) + c(vt_1/Lt_0)x_1(t) + (1-c)(vt_1/Lt_0)x_1(t-d(t))$, and the sampling period $T = 0.01$. The following fuzzy rules via delta operator are employed by

Plant Rule 1: IF $\theta(t)$ = is about 0 rad**, THEN**

$$\partial x(t) = A_1 x(t) + A_{d1} x(t-nT) + B_1 u(t), \tag{65}$$

Plant Rule 2: IF $\theta(t)$ = is about π rad or -π rad**, THEN**

$$\partial x(t) = A_2 x(t) + A_{d2} x(t-nT) + B_2 u(t). \tag{66}$$

The membership functions for Rule 1 and Rule 2 are given by

$$\lambda = \begin{cases} \lambda_1 = \left(1 - \dfrac{1}{1+\exp(-3(\theta(t)-0.5\pi))}\right) \\ \qquad \times \left(1 - \dfrac{1}{1+\exp(-3(\theta(t)+0.5\pi))}\right), \\ \lambda_2 = 1 - \lambda_1, \end{cases} \tag{67}$$

and with

$$\begin{aligned} A_1 &= \begin{bmatrix} 0.509 & 0 & 0 \\ -0.509 & 0 & 0 \\ 0.509 & -4 & 0 \end{bmatrix}, \\ A_{d1} &= \begin{bmatrix} 0.218 & 0 & 0 \\ -0.218 & 0 & 0 \\ 0.218 & 0 & 0 \end{bmatrix}, \\ B_1 &= \begin{bmatrix} -1.4286 \\ 0 \\ 0 \end{bmatrix}, \\ A_2 &= \begin{bmatrix} 0.509 & 0 & 0 \\ -0.509 & 0 & 0 \\ 0.810 & -6.366 & 0 \end{bmatrix}, \\ A_{d2} &= \begin{bmatrix} 0.218 & 0 & 0 \\ -0.218 & 0 & 0 \\ 0.347 & 0 & 0 \end{bmatrix}, \\ B_2 &= \begin{bmatrix} -1.4286 \\ 0 \\ 0 \end{bmatrix}. \end{aligned} \tag{68}$$

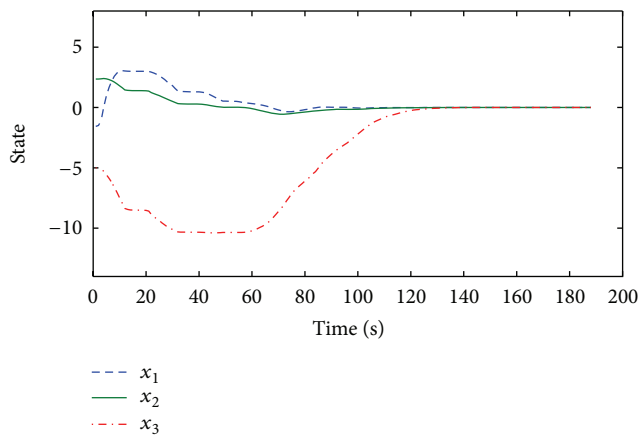

Figure 1: State responses for the closed-loop system in Example 14.

Assume the time-varying delay $1 \leq nT \leq 2$, and the initial condition $x(t_0) = [-0.5\pi \quad 0.75\pi \quad -5]^T$. The fuzzy delta operator controller gains by Theorem 10 are given as

$$\begin{aligned} K_{11} &= [2.2108 \quad -2.7252 \quad 0.1445], \\ K_{12} &= [2.2620 \quad -3.0776 \quad 0.1453], \\ K_{21} &= [0.5423 \quad 0.0608 \quad -0.0046], \\ K_{22} &= [0.5656 \quad 0.0503 \quad -0.0038], \\ K_{31} &= [0.5467 \quad 0.0095 \quad -0.0015], \\ K_{32} &= [0.5689 \quad 0.0079 \quad -0.0012]. \end{aligned} \tag{69}$$

As shown in Figure 1, the states of the closed-loop system converge to zero under the obtained fuzzy delta operator state-feedback controller, which demonstrates the effectiveness of our method.

7. Conclusion

This paper proposes an input-output method to analysis and synthesis of T-S fuzzy delta operator systems with time-varying delay. The two-term approximation method has been employed to transform the fuzzy delta operator system with time-varying delay into a feedback interconnection form. Based on a Lyapunov-Krasovskii functional in delta operator domain, the SSG method is suggested for the interconnected system. Numerical examples are given to demonstrate the advantages and less-conservatism of the proposed results.

Acknowledgments

The work described in this paper was supported in part by the National Natural Science Foundation of China (nos. 61104112 and 61004038), in part by the Fundamental Research Funds for the Central Universities (no. HIT. NSRIF. 201162), and the China Postdoctoral Science Foundation (no. 2012M510960).

References

[1] M. Sugeno, *Industrial Applications of Fuzzy Control*, Elsevier, New York, NY, USA, 1985.

[2] T. Tanaka and H. O. Wang, *Fuzzy Control Systems Design and Analysis: A Linear Matrix Inequality Approach*, John Wiley & Sons, New York, NY, USA, 2001.

[3] J. B. Qiu, G. Feng, and H. J. Gao, "Fuzzy-model-based piecewise $\mathscr{H}_\infty$ static-output-feedback controller design for networked nonlinear systems," *IEEE Transactions on Fuzzy Systems*, vol. 18, no. 5, pp. 919–934, 2010.

[4] J. B. Qiu, G. Feng, and H. J. Gao, "Nonsynchronized-state estimation of multichannel networked nonlinear systems with multiple packet dropouts via T-S fuzzy-affine dynamic models," *IEEE Transactions on Fuzzy Systems*, vol. 19, no. 1, pp. 75–90, 2011.

[5] S. G. Cao, N. W. Rees, and G. Feng, "Analysis and design for a class of complex control systems. II. Fuzzy controller design," *Automatica*, vol. 33, no. 6, pp. 1029–1039, 1997.

[6] M. Chadli and H. Karimi, "Robust observer design for unknown inputs Takagi-Sugeno models," *IEEE Transactions on Fuzzy Systems*, 2012.

[7] M. Chadli and T. M. Guerra, "LMI solution for robust static output feedback control of discrete Takagi-Sugeno fuzzy models," *IEEE Transactions on Fuzzy Systems*, vol. 20, no. 6, pp. 1160–1165, 2012.

[8] G. Feng, "A survey on analysis and design of model-based fuzzy control systems," *IEEE Transactions on Fuzzy Systems*, vol. 14, no. 5, pp. 676–697, 2006.

[9] K. Gu, V. Kharitonov, and J. Chen, *Stability of Time-Delay Systems*, Birkhauser, Boston, Mass, USA, 2003.

[10] S. Xu and J. Lam, "Robust $\mathscr{H}_\infty$ control for uncertain discrete-time-delay fuzzy systems via output feedback," *IEEE Transactions on Fuzzy Systems*, vol. 13, no. 1, pp. 82–93, 2005.

[11] Z. Zuo and Y. Wang, "Robust stability and stabilisation for nonlinear uncertain time-delay systems via fuzzy control approach," *IET Control Theory & Applications*, vol. 1, no. 1, pp. 422–429, 2007.

[12] H. N. Wu and H. X. Li, "New approach to delay-dependent stability analysis and stabilization for continuous-time fuzzy systems with time-varying delay," *IEEE Transactions on Fuzzy Systems*, vol. 15, no. 3, pp. 482–493, 2007.

[13] J. B. Qiu, G. Feng, and H. J. Gao, "Observer-based piecewise affine output feedback controller synthesis of continuous-time T-S fuzzy affine dynamic systems using quantized measurements," *IEEE Transactions on Fuzzy Systems*, vol. 20, no. 6, pp. 1046–1062, 2012.

[14] H. Y. Li, B. Chen, Q. Zhou, and W. Y. Qian, "Robust stability for uncertain delayed fuzzy hopfield neural networks with Markovian jumping parameters," *IEEE Transactions on Systems, Man, and Cybernetics B*, vol. 39, no. 1, pp. 94–102, 2009.

[15] H. Y. Li, H. H. Liu, H. J. Gao, and P. Shi, "Reliable fuzzy control for active suspension systems with actuator delay and fault," *IEEE Transactions on Fuzzy Systems*, vol. 20, no. 2, pp. 342–357, 2012.

[16] L. G. Wu and W. X. Zheng, "Weighted $\mathscr{H}_\infty$ model reduction for linear switched systems with time-varying delay," *Automatica*, vol. 45, no. 1, pp. 186–193, 2009.

[17] L. G. Wu, X. G. Su, and P. Shi, "Sliding mode control with bounded $\mathscr{L}_2$ gain performance of Markovian jump singular time-delay systems," *Automatica*, vol. 48, no. 8, pp. 1929–1933, 2012.

[18] R. Middleton and G. Goodwin, "Improved finite word length characteristics in digital control using delta operators," *IEEE Transactions on Automatic Control*, vol. 31, no. 11, pp. 1015–1021, 1986.

[19] M. A. Garnero, G. Thomas, B. Caron, J. F. Bourgeois, and E. Irving, "Pseudocontinuous identification application to adaptive pole placement control using the delta-operator," *Rairo-Automatique-Productique Informatique Industrielle-Automatic Control Production Systems*, vol. 26, no. 2, pp. 147–166, 1992.

[20] G. Li and M. Gevers, "Comparative study of finite wordlength effects in shift and delta operator parameterizations," *IEEE Transactions on Automatic Control*, vol. 38, no. 5, pp. 803–807, 1993.

[21] C. P. Neuman, "Transformations between delta and forward shift operator transfer-function models," *IEEE Transactions on Systems Man and Cybernetics*, vol. 23, no. 2, pp. 295–296, 1993.

[22] K. Premaratne, R. Salvi, N. R. Habib, and J. P. LeGall, "Delta-operator formulated discrete-time approximations of continuous-time systems," *IEEE Transactions on Automatic Control*, vol. 39, no. 3, pp. 581–585, 1994.

[23] S. Zhou and T. Li, "Robust stabilization for delayed discrete-time fuzzy systems via basis-dependent Lyapunov-Krasovskii function," *Fuzzy Sets and Systems*, vol. 151, no. 1, pp. 139–153, 2005.

[24] J. Qiu, G. Feng, and J. Yang, "A new design of delay-dependent robust H1 filtering for discrete-time T-S fuzzy systems with time-varying delay," *IEEE Transactions on Fuzzy Systems*, vol. 17, no. 5, pp. 1044–1058, 2009.

[25] H. Gao and T. Chen, "Stabilization of nonlinear systems under variable sampling: a fuzzy control approach," *IEEE Transactions on Fuzzy Systems*, vol. 15, no. 5, pp. 972–983, 2007.

[26] Z. R. Xiang, Q. W. Chen, W. L. Hu, and D. J. Zhang, "Robust stability analysis and control for fuzzy systems with uncertainties using the delta operator," *Control and Decision*, vol. 18, no. 6, pp. 720–723, 2003.

[27] D. Q. Li, C. Y. Sun, and S. M. Fei, "Stabilizing controller synthesis of delta-operator formulated fuzzy dynamic systems," *Proceedings of the International Conference on Machine Learning and Cybernetics*, no. 1, pp. 417–422, 2004.

[28] H. Yang, P. Shi, J. Zhang, and J. Qiu, "Robust $\mathscr{H}_\infty$ control for a class of discrete time fuzzy systems via delta operator approach," *Information Sciences*, vol. 184, pp. 230–245, 2012.

[29] X. Jiang, Q. L. Han, and X. Yu, "Stability criteria for linear discrete-time systems with interval-like time-varying delay," in *Proceedings of the American Control Conference*, pp. 2817–2822, 2005.

[30] J. Qiu, Y. Xia, H. Yang, and J. Zhang, "Robust stabilisation for a class of discrete-time systems with time-varying delays via delta operators," *IET Control Theory & Applications*, vol. 2, no. 1, pp. 87–93, 2008.

[31] K. Gu, Y. Zhang, and S. Xu, "Small gain problem in coupled differential-difference equations, time-varying delays, and direct Lyapunov method," *International Journal of Robust and Nonlinear Control*, vol. 21, no. 4, pp. 429–451, 2011.

[32] H. J. Gao, Z. D. Wang, and C. H. Wang, "Improved $\mathscr{H}_\infty$ control of discrete-time fuzzy systems: a cone complementarity linearization approach," *Information Sciences*, vol. 175, no. 1-2, pp. 57–77, 2005.

Hindawi Publishing Corporation
Mathematical Problems in Engineering
Volume 2013, Article ID 363748, 13 pages
http://dx.doi.org/10.1155/2013/363748

Research Article

Adaptive Fuzzy Tracking Control for Uncertain Nonlinear Time-Delay Systems with Unknown Dead-Zone Input

Chiang-Cheng Chiang

Department of Electrical Engineering, Tatung University, 40 Chung Shan North Road, Section 3, Taipei 104, Taiwan

Correspondence should be addressed to Chiang-Cheng Chiang; ccchiang@ttu.edu.tw

Received 2 November 2012; Revised 21 December 2012; Accepted 4 January 2013

Academic Editor: Peng Shi

Copyright © 2013 Chiang-Cheng Chiang. This is an open access article distributed under the Creative Commons Attribution License, which permits unrestricted use, distribution, and reproduction in any medium, provided the original work is properly cited.

The tracking control problem of uncertain nonlinear time-delay systems with unknown dead-zone input is tackled by a robust adaptive fuzzy control scheme. Because the nonlinear gain function and the uncertainties of the controlled system including matched and unmatched uncertainties are supposed to be unknown, fuzzy logic systems are employed to approximate the nonlinear gain function and the upper bounded functions of these uncertainties. Moreover, the upper bound of the uncertainty caused by the fuzzy modeling error is also estimated. According to these learning fuzzy models and some feasible adaptive laws, a robust adaptive fuzzy tracking controller is developed in this paper without constructing the dead-zone inverse. Based on the Lyapunov stability theorem, the proposed controller not only guarantees that the robust stability of the whole closed-loop system in the presence of uncertainties and unknown dead-zone input can be achieved, but it also obtains that the output tracking error can converge to a neighborhood of zero exponentially. Some simulation results are provided to demonstrate the effectiveness and performance of the proposed approach.

1. Introduction

In general systems, there exist some nonsmooth nonlinearities in the actuators, such as dead-zone, saturation, and backlash [1–7]. The information of the dead-zone is usually poorly known and time variant. Recently, high accuracy position control is required, such as DC servosystems, pressure control systems, power systems, chemical reactor systems, and machine tools [1–3, 8]. However, the dead-zone characteristics in actuators may severely limit the performance of the systems and let the output of the systems not reach our requirements. The robust adaptive control was proposed to deal with nonlinear systems with unknown dead-zone [2]. In Corradini and Orlando [3], the sliding mode controller was presented to robustly stabilize a nonlinear uncertain input. Robust adaptive dead-zone compensation method was used in a DC servo-motor control system [4]. Variable structure control laws were proposed for uncertain large-scale system with dead-zone input [5]. In [8, 9], adaptive control approach was used to cope with nonlinear systems with nonsymmetric dead-zone input. The proposed controllers in [10, 11] tackled the plants with unknown dead-zone via dead-zone inverse. However, the common feature of most previous results [1, 2, 4–6, 8, 9, 12] is the nonlinear gain function which is assumed to be a constant. Although the Previous restrictive assumption can be relaxed in [3, 7, 10, 11], the unmatched uncertainty is not taken into account. Therefore, the motivation of this paper is to synthesize a controller to handle the tracking control problem for a class of uncertain nonlinear state time-delay systems in the presence of an unknown dead-zone input and unmatched uncertainties without constructing the dead-zone inverse.

It is well known that a real system is difficult to be described by the exact mathematical model, owing to the existence of uncertain elements, such as parameter variation, modeling errors, unmodeled dynamics, and external disturbances. These uncertainties may affect the stability of the systems. Robust stabilization of the nonlinear uncertain system has widely been investigated [13–16]. In [13], the purpose of this direct robust adaptive fuzzy controller was to deal with a class of nonlinear systems containing both unconstructed state-dependent unknown nonlinear uncertain and gain

functions. Bartolini et al. [14] suggested the second-order sliding mode controller to cope with the uncertain system nonaffine in the control law and the presence of the unmodeled dynamic actuator. The methods of robust adaptive control [15, 16] were utilized to solve the nonlinear uncertain problem. In [15], the robust adaptive controller for SISO nonlinear uncertain system was presented by the input/output linearization approach. In the case where the nonlinear uncertain systems include constant linearly parameterized uncertainty and nonlinear state-dependent parametric uncertainty, the direct robust adaptive control framework was developed in [16].

In recent years, the design problem of nonlinear time-delay systems has received considerable attention in [17–23] because time-delay characteristic usually confronted in engineering systems may degrade the control performance and make the systems unstable. By employing the input-output approach and the scaled small gain theorem, the filtering problem for discrete-time T-S fuzzy systems with time-varying delay has been studied [17]. In [18], the stabilization of LTI systems with time delay was considered by using a low-order controller. The stability analysis and robust control for time-delay systems attracted a large number of researchers over the past years [19–21]. Recently, the problem of stability analysis for stochastic neural networks with discrete interval and distributed time-varying was investigated by applying the idea of delay partitioning method [23].

On the other hand, the fuzzy control techniques have been widely used in many control problems in recent years [24–26]. The fuzzy logic system is constructed from a collection of fuzzy IF-THEN rules. It becomes a useful way to approximate the unknown nonlinear functions and uncertainties in the nonlinear systems. An adaptive interval type-2 fuzzy sliding mode controller for a class of unknown nonlinear discrete-time systems corrupted by external disturbances was presented [24]. In [25], an adaptive neural-fuzzy control design was examined for tracking of nonlinear affine in the control dynamic systems with unknown nonlinearities. Based on a novel fuzzy Lyapunov-Krasovskii functional, a delay partitioning method has been developed for the delay-dependent stability analysis of fuzzy time-varying state delay systems [26].

In this paper, the problem of output tracking control is investigated for a class of uncertain nonlinear state time-delay systems containing unknown dead-zone input and unmatched uncertainties. The main features of the proposed robust adaptive fuzzy controller are summarized as follows. (i) By utilizing a description of a dead-zone feature, an adaptive law is used to estimate the properties of the dead-zone model intuitively and mathematically, without constructing a dead-zone inverse. (ii) Fuzzy logic systems with some appropriate learning laws are applied to approximate the nonlinear gain function and the upper bounded functions of matched and unmatched uncertainties. (iii) The unknown upper bound of the uncertainties caused by approximation (or fuzzy modeling) error is estimated by a simple adaptive law. (iv) By means of Lyapunov stability theorem, the proposed controller cannot only guarantee the robust stability of the whole closed-loop system but also obtain the good tracking performance.

This paper is organized as follows. In Section 2, the form of the uncertain nonlinear state time-delay system with unknown dead-zone input is described. The fuzzy logic systems and fuzzy basis functions are also reviewed. Section 3 presents the robust adaptive fuzzy tracking controller to deal with a class of nonlinear uncertain state time-delay systems containing unknown dead-zone input. By Lyapunov stability theorem, the presented controller can ensure the stability of the controlled systems. Simulation results are demonstrated along with the effectiveness and performance of the proposed controller in Section 4. Finally, a conclusion is given in Section 5.

2. Problem Statement and Preliminaries

2.1. Problem Statement. Consider a class of uncertain nonlinear state time-delay systems containing an unknown dead-zone in the following form:

$$\begin{aligned}
\dot{x}_1 &= x_2 + \Delta\phi_1(\mathbf{x}),\\
\dot{x}_2 &= x_3 + \Delta\phi_2(\mathbf{x}),\\
\dot{x}_3 &= x_4 + \Delta\phi_3(\mathbf{x}),\\
&\vdots\\
\dot{x}_{n-1} &= x_n + \Delta\phi_{n-1}(\mathbf{x}),\\
\dot{x}_n &= \sum_{i=1}^{M}\theta_{1i} f_{1i}(\mathbf{x}(t)) + \Delta f_1(\mathbf{x}(t))\\
&\quad + \sum_{j=1}^{N}\theta_{2j} f_{2j}(\mathbf{x}(t-\tau)) + \Delta f_2(\mathbf{x}(t-\tau))\\
&\quad + g(\mathbf{x}) Z(\upsilon(t)) + \Delta\phi_n(\mathbf{x}),\\
y &= x_1,
\end{aligned} \tag{1}$$

or equivalently,

$$\begin{aligned}
\dot{\mathbf{x}} &= \mathbf{A}\mathbf{x} + \mathbf{B}\left[\sum_{i=1}^{M}\theta_{1i} f_{1i}(\mathbf{x}(t)) + \Delta f_1(\mathbf{x}(t))\right.\\
&\quad + \sum_{j=1}^{N}\theta_{2j} f_{2j}(\mathbf{x}(t-\tau))\\
&\quad \left. + \Delta f_2(\mathbf{x}(t-\tau)) + g(\mathbf{x}) Z(\upsilon(t))\right] + \Theta(\mathbf{x}),\\
y &= \mathbf{C}\mathbf{x},
\end{aligned} \tag{2}$$

where

$$\mathbf{A} = \begin{bmatrix} 0 & 1 & 0 & \cdots & 0 \\ 0 & 0 & 1 & \ddots & \vdots \\ \vdots & \vdots & \ddots & \ddots & 0 \\ 0 & 0 & \cdots & 0 & 1 \\ 0 & 0 & \cdots & 0 & 0 \end{bmatrix} \in R^{n\times n}, \qquad \mathbf{B} = \begin{bmatrix} 0 \\ 0 \\ \vdots \\ 0 \\ 1 \end{bmatrix} \in R^{n\times 1},$$
$$\mathbf{C}^T = \begin{bmatrix} 1 \\ 0 \\ \vdots \\ 0 \\ 0 \end{bmatrix} \in R^{n\times 1}, \tag{3}$$

where $\mathbf{x}(t) = [x_1(t), x_2(t), \ldots, x_n(t)]^T \in R^n$ is the system state vector which is assumed to be available for measurement, and $v(t) \in R$ and $y(t) \in R$ are the input and output of the system, respectively. τ is the value of time delay. The unknown nonlinear system functions are assumed to be in the linearly parameterized form and consist of two parts: (i) the sum of $\theta_{1i} f_{1i}(\mathbf{x}(t))$ for $i = 1, 2, \ldots, M$; (ii) the sum of $\theta_{2j} f_{2j}(\mathbf{x}(t-\tau))$ for $j = 1, 2, \ldots, N$. The parameters θ_{1i} and θ_{2j} are unknown but constant. $f_{1i}(\mathbf{x}(t))$ and $f_{2j}(\mathbf{x}(t-\tau))$ are known continuous, linear or nonlinear functions. $\Delta f_1(\mathbf{x}(t))$ and $\Delta f_2(\mathbf{x}(t-\tau))$ are the unknown matched uncertainties. $g(\mathbf{x}(t))$ is the unknown nonlinear gain function, and $\Theta(\mathbf{x}) = [\Delta\phi_1(\mathbf{x}), \Delta\phi_2(\mathbf{x}), \ldots, \Delta\phi_n(\mathbf{x})]^T \in R^{n\times 1}$ is the vector of unknown unmatched uncertainties. Without loss of generality, it is assumed that the sign of $g(\mathbf{x}(t))$ is positive. $Z(v(t)) : R \to R$ is the nonlinear input function containing a dead-zone.

Now, let the output of the system and its derivatives be expressed as follows:

$$\begin{aligned}
y &= x_1, \\
y^{(1)} &= \dot{x}_1 = x_2 + \Delta\phi_1, \\
y^{(2)} &= \dot{x}_2 + (\Delta\phi_1)^{(1)} = x_3 + \Delta\phi_2 + (\Delta\phi_1)^{(1)}, \\
y^{(3)} &= \dot{x}_3 + (\Delta\phi_2)^{(1)} + (\Delta\phi_1)^{(2)} \\
&= x_4 + \Delta\phi_3 + (\Delta\phi_2)^{(1)} + (\Delta\phi_1)^{(2)}, \\
&\vdots \\
y^{(n-1)} &= \dot{x}_{(n-1)} + (\Delta\phi_{(n-2)})^{(1)} + (\Delta\phi_{(n-3)})^{(2)} \\
&\quad + \cdots + (\Delta\phi_2)^{(n-3)} + (\Delta\phi_1)^{(n-2)} \\
&= x_n + (\Delta\phi_{(n-1)}) + (\Delta\phi_{(n-2)})^{(1)} \\
&\quad + (\Delta\phi_{(n-3)})^{(2)} + \cdots + (\Delta\phi_2)^{(n-3)} + (\Delta\phi_1)^{(n-2)}, \\
y^{(n)} &= \dot{x}_n + (\Delta\phi_{(n-1)})^{(1)} + (\Delta\phi_{(n-2)})^{(2)} \\
&\quad + (\Delta\phi_{(n-3)})^{(3)} + \cdots + (\Delta\phi_2)^{(n-2)} + (\Delta\phi_1)^{(n-1)} \\
&= \sum_{i=1}^{M} \theta_{1i} f_{1i}(\mathbf{x}(t)) + \Delta f_1(\mathbf{x}(t)) \\
&\quad + \sum_{j=1}^{N} \theta_{2j} f_{2j}(\mathbf{x}(t-\tau)) + \Delta f_2(\mathbf{x}(t-\tau)) \\
&\quad + g(\mathbf{x}) Z(v(t)) + \Delta\phi_n + (\Delta\phi_{(n-1)})^{(1)} \\
&\quad + (\Delta\phi_{(n-2)})^{(2)} + (\Delta\phi_{(n-3)})^{(3)} \\
&\quad + \cdots + (\Delta\phi_2)^{(n-2)} + (\Delta\phi_1)^{(n-1)} \\
&= \sum_{i=1}^{M} \theta_{1i} f_{1i}(\mathbf{x}(t)) + \Delta f_1(\mathbf{x}(t)) \\
&\quad + \sum_{j=1}^{N} \theta_{2j} f_{2j}(\mathbf{x}(t-\tau)) + \Delta f_2(\mathbf{x}(t-\tau)) \\
&\quad + g(\mathbf{x}) Z(v(t)) + \Delta\Phi,
\end{aligned} \tag{4}$$

where

$$\Delta\Phi = \Delta\phi_1^{(n-1)} + \Delta\phi_2^{(n-2)} + \cdots + \Delta\phi_{n-1}^{(1)} + \Delta\phi_n. \tag{5}$$

The dead-zone with input $v(t)$ and output as shown in Figure 1 is described by

$$Z(v(t)) = \begin{cases} m_r(v(t) - c_a) & \text{for } v(t) \geq c_a, \\ 0 & \text{for } c_b < v(t) < c_a, \\ m_l(v(t) - c_b) & \text{for } v(t) \leq c_b, \end{cases} \tag{6}$$

where $c_a > 0, c_b < 0$ and $m_r > 0$, $m_l > 0$ are parameters and slopes of the dead-zone, respectively. In order to investigate the key features of the dead-zone in the control problems, the following assumptions should be made.

Assumption 1. The dead-zone output $Z(v(t))$ is not available to obtain.

Assumption 2. The dead-zone slopes are of the same value; that is, $m_r = m_l = m$.

Assumption 3. There exist known constants $c_{a\min}, c_{a\max}$, $c_{b\min}, c_{b\max}, m_{\min}$, and $m_{\max}$ such that the unknown dead-zone parameters c_a, c_b, and m are bounded; that is, $c_a \in [c_{a\min}, c_{a\max}]$, $c_b \in [c_{b\min}, c_{b\max}]$, and $m \in [m_{\min}, m_{\max}]$.

Based on the previous assumptions, the expression (6) can be represented as

$$Z(v(t)) = mv(t) + z(v(t)), \tag{7}$$

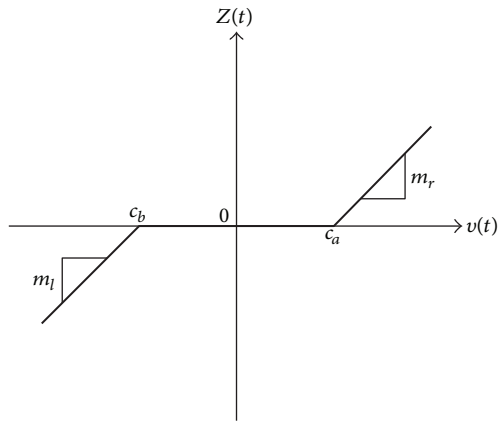

Figure 1: Dead-zone model.

where $z(v(t))$ can be calculated from (6) and (7) as

$$z(v(t)) = \begin{cases} -mc_a & \text{for } v(t) \geq c_a, \\ -mv(t) & \text{for } c_b < v(t) < c_a, \\ -mc_b & \text{for } v(t) \leq c_b. \end{cases} \tag{8}$$

From Assumptions 2 and 3, we can conclude that $z(v(t))$ is bounded and satisfies $|z(v(t))| \leq \rho$, where ρ is the upper bound which can be chosen as

$$\rho = \max\{m_{\max}c_{a\max}, -m_{\max}c_{b\max}\}, \tag{9}$$

where $c_{b\min}$ is a negative value.

Then, let y_m be a given bounded reference signal and contain finite derivatives up to the nth order, define the tracking error as

$$e_i = y_m{}^{(i-1)} - y^{(i-1)}, \quad \text{for } i = 1, 2, \ldots, n, \tag{10}$$

and denote $\mathbf{e} = [e_1, e_2, \ldots, e_n]^T$, $\mathbf{y} = [y, \dot{y}, \ldots, y^{(n-1)}]^T$, and $\mathbf{y}_m = [y_m, \dot{y}_m, \ldots, y_m{}^{(n-1)}]^T$.

The control objective of this paper is to design a control law $v(t)$ such that y can follow a given desired reference signal y_m and guarantee that all the signals involved in the whole closed-loop system are bounded.

2.2. Description of Fuzzy Logic Systems. The basic configuration of the fuzzy logic system consists of four main components: fuzzy rule base, fuzzy inference engine, fuzzifier, and defuzzifier [27]. The fuzzy logic system performs a mapping from $U \subset R^n$ to $V \subset R$. Let $U = U_1 \times \cdots \times U_n$, where $U_i \subset R, i = 1, 2, \ldots, n$. The fuzzy rule base consists of a collection of fuzzy IF-THEN rules as follows:

$$R^{(l)}\text{: IF } x_1 \text{ is } F_1^l \text{ and} \ldots \text{and } x_n \text{ is } F_n^l, \text{ THEN } y \text{ is } G^l, \tag{11}$$

where $\mathbf{x} = [x_1, x_2, \ldots, x_n]^T \in U$ and $y \in V \subset R$ are the input and output of the fuzzy logic system, and F_i^l and G^l are fuzzy sets in U_i and V, respectively. The fuzzifier maps a crisp point $\mathbf{x} = [x_1, x_2, \ldots, x_n]^T$ into a fuzzy set in U. The fuzzy inference engine performs a mapping from fuzzy sets in U to fuzzy sets in V, based upon the fuzzy IF-THEN rules in the fuzzy rule base and the compositional rule of inference. The defuzzifier maps a fuzzy set in V to a crisp point in V.

The fuzzy systems with center-average defuzzifier, product inference, and singleton fuzzifier are of the following form:

$$y(\mathbf{x}) = \frac{\sum_{l=1}^{M} \theta^l \left(\prod_{i=1}^{n} \mu_{F_i^l}(x_i)\right)}{\sum_{l=1}^{M} \left(\prod_{i=1}^{n} \mu_{F_i^l}(x_i)\right)}, \tag{12}$$

where M is the number of rules, θ^l is the point at which the fuzzy membership function $\mu_{G^l}(\theta^l)$ of fuzzy sets G^l achieves its maximum value, and it is assumed that $\mu_{G^l}(\theta^l) = 1$. Equation (12) can be rewritten as

$$y(\mathbf{x}) = \boldsymbol{\theta}^T \boldsymbol{\xi}(\mathbf{x}), \tag{13}$$

where $\boldsymbol{\theta} = [\theta^1, \theta^2, \ldots, \theta^M]^T$ is a parameter vector, and $\boldsymbol{\xi}(\mathbf{x}) = [\xi^1(\mathbf{x}), \ldots, \xi^M(\mathbf{x})]^T$ is a regressive vector with the regressor $\xi^l(\mathbf{x})$, which is defined as fuzzy basis function

$$\xi^l(\mathbf{x}) = \frac{\prod_{i=1}^{n} \mu_{F_i^l}(x_i)}{\sum_{l=1}^{n} \left(\prod_{i=1}^{n} \mu_{F_i^l}(x_i)\right)}. \tag{14}$$

3. Adaptive Fuzzy Tracking Controller Design and Stability Analysis

According to (2.1), (7), and (10), the tracking error dynamic equation can be expressed as

$$\begin{aligned} \dot{\mathbf{e}} = \mathbf{A}\mathbf{e} + \mathbf{B}\Bigg[& y_m^{(n)} - \sum_{i=1}^{M} \theta_{1i} f_{1i}(\mathbf{x}(t)) - \Delta f_1(\mathbf{x}(t)) \\ & - \sum_{j=1}^{N} \theta_{2j} f_{2j}(\mathbf{x}(t-\tau)) - \Delta f_2(\mathbf{x}(t-\tau)) \\ & - g(\mathbf{x}) m v(t) - g(\mathbf{x}) z(v(t)) - \Delta\Phi \Bigg]. \end{aligned} \tag{15}$$

Now, let us choose a vector $\mathbf{K} = [k_1, k_2, \ldots, k_n] \in R^{1\times n}$ such that $\mathbf{A}_m = \mathbf{A} - \mathbf{B}\mathbf{K}$ is Hurwitz; then, the tracking error dynamic equation (15) can be rewritten as

$$\begin{aligned} \dot{\mathbf{e}} = \mathbf{A}_m\mathbf{e} + \mathbf{B}\Bigg[& \mathbf{K}\mathbf{e} + y_m^{(n)} - \sum_{i=1}^{M} \theta_{1i} f_{1i}(\mathbf{x}(t)) - \Delta f_1(\mathbf{x}(t)) \\ & - \sum_{j=1}^{N} \theta_{2j} f_{2j}(\mathbf{x}(t-\tau)) - \Delta f_2(\mathbf{x}(t-\tau)) \\ & - g(\mathbf{x}) m v(t) - g(\mathbf{x}) z(v(t)) - \Delta\Phi \Bigg]. \end{aligned} \tag{16}$$

It is worth noting that $\Delta f_1(\mathbf{x}(t))$, $f_{2j}(\mathbf{x}(t-\tau))$, and $\Delta\Phi$ are unknown uncertainties and satisfy the following assumption.

Assumption 4. $|\Delta\Phi| \leq h_1(\mathbf{x}), |\Delta f_1(\mathbf{x}(t))| \leq h_2(\mathbf{x}(t))$, and $|\Delta f_2(\mathbf{x}(t-\tau))| \leq h_3(\mathbf{x}(t-\tau))$, where $h_1(\mathbf{x})$, $h_2(\mathbf{x}(t))$, and $h_3(\mathbf{x}(t-\tau))$ are unknown smooth positive functions and can be estimated by fuzzy logic systems with some adaptive laws which will be determined later.

First, the nonlinear gain function $g(\mathbf{x})$ and the upper bounded functions $h_1(\mathbf{x}), h_2(\mathbf{x}(t))$, and $h_3(\mathbf{x}(t-\tau))$ of unmatched and matched uncertainties can be approximated, over a compact set $\Omega_{\mathbf{x}}$, by the fuzzy logic systems as follows:

$$\begin{aligned} \widehat{g}\left(\mathbf{x} \mid \boldsymbol{\theta}_g\right) &= \boldsymbol{\theta}_g^T \boldsymbol{\xi}(\mathbf{x}), \\ \widehat{h}_1\left(\mathbf{x} \mid \boldsymbol{\theta}_{h1}\right) &= \boldsymbol{\theta}_{h1}^T \boldsymbol{\xi}(\mathbf{x}), \\ \widehat{h}_2\left(\mathbf{x} \mid \boldsymbol{\theta}_{h2}\right) &= \boldsymbol{\theta}_{h2}^T \boldsymbol{\xi}(\mathbf{x}), \\ \widehat{h}_3\left(\mathbf{x}(t-\tau) \mid \boldsymbol{\theta}_{h3}\right) &= \boldsymbol{\theta}_{h3}^T \boldsymbol{\xi}(\mathbf{x}(t-\tau)), \end{aligned} \tag{17}$$

where $\boldsymbol{\xi}(\mathbf{x})$ and $\boldsymbol{\xi}(\mathbf{x}(t-\tau))$ are the fuzzy basis vectors, and $\boldsymbol{\theta}_g, \boldsymbol{\theta}_{h1}, \boldsymbol{\theta}_{h2}$, and $\boldsymbol{\theta}_{h3}$ are the corresponding adjustable parameter vectors of each fuzzy logic system. It is assumed that $\boldsymbol{\theta}_g, \boldsymbol{\theta}_{h1}, \boldsymbol{\theta}_{h2}$, and $\boldsymbol{\theta}_{h3}$ belong to compact sets $\Omega_{\boldsymbol{\theta}_g}, \Omega_{\boldsymbol{\theta}_{h1}}, \Omega_{\boldsymbol{\theta}_{h2}}$, and $\Omega_{\boldsymbol{\theta}_{h3}}$, respectively, which are defined as

$$\begin{aligned} \Omega_{\boldsymbol{\theta}g} &= \left\{\boldsymbol{\theta}_g \in R^M : \left\|\boldsymbol{\theta}_g\right\| \leq N_1 < \infty\right\}, \\ \Omega_{\boldsymbol{\theta}_{h1}} &= \left\{\boldsymbol{\theta}_{h1} \in R^M : \left\|\boldsymbol{\theta}_{h1}\right\| \leq N_2 < \infty\right\}, \\ \Omega_{\boldsymbol{\theta}_{h2}} &= \left\{\boldsymbol{\theta}_{h2} \in R^M : \left\|\boldsymbol{\theta}_{h2}\right\| \leq N_3 < \infty\right\}, \\ \Omega_{\boldsymbol{\theta}_{h3}} &= \left\{\boldsymbol{\theta}_{h3} \in R^M : \left\|\boldsymbol{\theta}_{h3}\right\| \leq N_4 < \infty\right\}, \end{aligned} \tag{18}$$

where N_1, N_2, N_3, and N_4 are the designed parameters, and M is the number of fuzzy inference rules. Let us define the optimal parameter vectors $\boldsymbol{\theta}_g^*, \boldsymbol{\theta}_{h1}^*, \boldsymbol{\theta}_{h2}^*$, and $\boldsymbol{\theta}_{h3}^*$ as follows:

$$\begin{aligned} \boldsymbol{\theta}_g^* &= \arg \min_{\boldsymbol{\theta}_g \in \Omega_{\boldsymbol{\theta}_g}} \left\{\sup_{\mathbf{x} \in \Omega_{\mathbf{x}}} \left|g(\mathbf{x}) - \widehat{g}\left(\mathbf{x} \mid \boldsymbol{\theta}_g\right)\right|\right\}, \\ \boldsymbol{\theta}_{h1}^* &= \arg \min_{\boldsymbol{\theta}_{h1} \in \Omega_{\boldsymbol{\theta}_{h1}}} \left\{\sup_{\mathbf{x} \in \Omega_{\mathbf{x}}} \left|h_1(\mathbf{x}) - \widehat{h}_1\left(\mathbf{x} \mid \boldsymbol{\theta}_{h1}\right)\right|\right\}, \\ \boldsymbol{\theta}_{h2}^* &= \arg \min_{\boldsymbol{\theta}_{h2} \in \Omega_{\boldsymbol{\theta}_{h2}}} \left\{\sup_{\mathbf{x} \in \Omega_{\mathbf{x}}} \left|h_2(\mathbf{x}) - \widehat{h}_2\left(\mathbf{x} \mid \boldsymbol{\theta}_{h2}\right)\right|\right\}, \\ \boldsymbol{\theta}_{h3}^* &= \arg \min_{\boldsymbol{\theta}_{h3} \in \Omega_{\boldsymbol{\theta}_{h3}}} \left\{\sup_{\mathbf{x} \in \Omega_{\mathbf{x}}} \left|h_3(\mathbf{x}(t-\tau)) \right.\right. \\ &\qquad \left.\left. - \widehat{h}_1\left(\mathbf{x}(t-\tau) \mid \boldsymbol{\theta}_{h1}\right)\right|\right\}, \end{aligned} \tag{19}$$

where $\boldsymbol{\theta}_g^*, \boldsymbol{\theta}_{h1}^*, \boldsymbol{\theta}_{h2}^*$, and $\boldsymbol{\theta}_{h3}^*$ are bounded in the suitable closed sets $\Omega_{\boldsymbol{\theta}_g}, \Omega_{\boldsymbol{\theta}_{h1}}, \Omega_{\boldsymbol{\theta}_{h2}}$, and $\Omega_{\boldsymbol{\theta}_{h3}}$, respectively. The parameter estimation errors can be defined as

$$\begin{aligned} \widetilde{\boldsymbol{\theta}}_g &= \boldsymbol{\theta}_g - \boldsymbol{\theta}_g^*, \\ \widetilde{\boldsymbol{\theta}}_{h1} &= \boldsymbol{\theta}_{h1} - \boldsymbol{\theta}_{h1}^*, \\ \widetilde{\boldsymbol{\theta}}_{h2} &= \boldsymbol{\theta}_{h2} - \boldsymbol{\theta}_{h2}^*, \\ \widetilde{\boldsymbol{\theta}}_{h3} &= \boldsymbol{\theta}_{h3} - \boldsymbol{\theta}_{h3}^*, \\ \left|\omega_1\right| + \left|\omega_2\right| &\leq \omega, \end{aligned} \tag{20}$$

where ω is an unknown positive constant, and

$$\begin{aligned} \omega_1 &= \left(h_1(\mathbf{x}) - \widehat{h}_1\left(\mathbf{x} \mid \boldsymbol{\theta}_{h1}^*\right)\right) \\ &\quad + \left(h_2(\mathbf{x}(t)) - \widehat{h}_2\left(\mathbf{x} \mid \boldsymbol{\theta}_{h2}^*\right)\right) \\ &\quad + \left(h_3\mathbf{x}(\mathbf{x}(t-\tau)) - \widehat{h}_3\left(\mathbf{x} \mid \boldsymbol{\theta}_{h3}^*\right)\right), \\ \omega_2 &= \left(g(\mathbf{x}) - \widehat{g}\left(\mathbf{x} \mid \boldsymbol{\theta}_g^*\right)\right)(mv(t) + z(v(t))) \end{aligned} \tag{21}$$

as the minimum approximation errors, which correspond to approximation errors obtained when optimal parameters are used.

Secondly, we define

$$\begin{aligned} \widetilde{\phi} &= \widehat{\phi} - \phi, \\ \widetilde{\boldsymbol{\theta}}_1 &= \widehat{\boldsymbol{\theta}}_1 - \boldsymbol{\theta}_1, \\ \widetilde{\boldsymbol{\theta}}_2 &= \widehat{\boldsymbol{\theta}}_2 - \boldsymbol{\theta}_2, \\ \widetilde{\omega} &= \widehat{\omega} - \omega, \end{aligned} \tag{22}$$

where $\widehat{\phi}$ is an estimate of ϕ, which is defined as $\phi = (m)^{-1}$. $\widehat{\boldsymbol{\theta}}_1$ and $\widehat{\boldsymbol{\theta}}_2$ are the estimates of $\boldsymbol{\theta}_1$ and $\boldsymbol{\theta}_2$, respectively, which are defined as

$$\begin{aligned} \boldsymbol{\theta}_1 &= \left[(m)^{-1}\theta_{11}, (m)^{-1}\theta_{12}, \ldots, (m)^{-1}\theta_{1M}\right]^T \in R^M, \\ \boldsymbol{\theta}_2 &= \left[(m)^{-1}\theta_{21}, (m)^{-1}\theta_{22}, \ldots, (m)^{-1}\theta_{2N}\right]^T \in R^N, \end{aligned} \tag{23}$$

and $\widehat{\omega}$ is an estimate of ω.

Based on the previous discussion and under Assumptions 1–4, we are in a position to propose the robust adaptive fuzzy controller in the following form:

$$v = v_1 + v_2 + v_3 + v_4 + v_5, \tag{24}$$

where

$$\begin{aligned} v_1 = \frac{1}{\widehat{g}\left(\mathbf{x} \mid \boldsymbol{\theta}_g\right)} \widehat{\phi} \Bigg[& \mathbf{Ke} + y_m^{(n)} + \frac{\left(\mathbf{e}^T\mathbf{PB}\right)^T}{\left\|\mathbf{e}^T\mathbf{PB}\right\|} \\ & \times \left(\widehat{h}_1\left(\mathbf{x} \mid \boldsymbol{\theta}_{h1}\right) + \widehat{h}_2\left(\mathbf{x} \mid \boldsymbol{\theta}_{h2}\right)\right. \\ & \left. + \widehat{h}_3\left(\mathbf{x}(t-\tau) \mid \boldsymbol{\theta}_{h3}\right)\right) \Bigg], \end{aligned} \tag{25}$$

$$\begin{aligned} v_2 &= -\frac{1}{\widehat{g}\left(\mathbf{x} \mid \boldsymbol{\theta}_g\right)} \mathbf{f}_1^T(\mathbf{x}(t)) \widehat{\boldsymbol{\theta}}_1, \\ v_3 &= -\frac{1}{\widehat{g}\left(\mathbf{x} \mid \boldsymbol{\theta}_g\right)} \mathbf{f}_2^T(\mathbf{x}(t-\tau)) \widehat{\boldsymbol{\theta}}_2, \\ v_4 &= \frac{1}{m_{\min}} \frac{1}{\widehat{g}\left(\mathbf{x} \mid \boldsymbol{\theta}_g\right)} \frac{\left(\mathbf{e}^T\mathbf{PB}\right)^T}{\left\|\mathbf{e}^T\mathbf{PB}\right\|} \widehat{\omega}, \\ v_5 &= \frac{\rho}{m_{\min}} \tanh\left(\frac{\mathbf{e}^T\mathbf{PB}}{\varepsilon}\right), \end{aligned} \tag{26}$$

where $\mathbf{f}_1(\mathbf{x}(t)) = [f_{11}, f_{12}, \ldots, f_{1M}]^T \in R^M$ and $\mathbf{f}_2(\mathbf{x}(t-\tau)) = [f_{21}, f_{22}, \ldots, f_{2N}]^T \in R^N$, ρ is defined in (9), and $\mathbf{P}$ is a symmetric positive definite matrix, which is a solution of the following Lyapunov equation:

$$\mathbf{A}_m^T\mathbf{P} + \mathbf{PA}_m = -\mathbf{Q}, \tag{27}$$

where $\mathbf{Q}$ is a positive definite matrix, and the parameter update laws are as follows:

$$\dot{\boldsymbol{\theta}}_g = -\gamma_g \mathbf{e}^T\mathbf{PB}\boldsymbol{\xi}(\mathbf{x})\left(v(t) + z_1(v(t))\right), \tag{28}$$

$$\begin{aligned} \dot{\boldsymbol{\theta}}_{h1} &= \gamma_{h1}\left\|\mathbf{e}^T\mathbf{PB}\right\| \boldsymbol{\xi}(\mathbf{x}(t)), \\ \dot{\boldsymbol{\theta}}_{h2} &= \gamma_{h2}\left\|\mathbf{e}^T\mathbf{PB}\right\| \boldsymbol{\xi}(\mathbf{x}(t)), \end{aligned} \tag{29}$$

$$\dot{\boldsymbol{\theta}}_{h3} = \gamma_{h3}\left\|\mathbf{e}^T\mathbf{PB}\right\| \boldsymbol{\xi}(\mathbf{x}(t-\tau)), \tag{30}$$

$$\dot{\widehat{\boldsymbol{\theta}}}_1 = -\gamma_1 \mathbf{e}^T\mathbf{PBf}_1(\mathbf{x}(t)), \tag{31}$$

$$\dot{\widehat{\boldsymbol{\theta}}}_2 = -\gamma_2 \mathbf{e}^T\mathbf{PBf}_2(\mathbf{x}(t-\tau)), \tag{32}$$

$$\dot{\widehat{\omega}} = \gamma_\omega\left\|\mathbf{e}^T\mathbf{PB}\right\|, \tag{33}$$

$$\begin{aligned} \dot{\widehat{\phi}} = \eta\left(\mathbf{e}^T\mathbf{PB}\right) \Bigg\{ &\left[\mathbf{Ke} + y_m^{(n)}\right] + \frac{\left(\mathbf{e}^T\mathbf{PB}\right)}{\left\|\mathbf{e}^T\mathbf{PB}\right\|} \widehat{h}_1\left(\mathbf{x} \mid \boldsymbol{\theta}_{h1}\right) \\ &+ \frac{\left(\mathbf{e}^T\mathbf{PB}\right)}{\left\|\mathbf{e}^T\mathbf{PB}\right\|} \widehat{h}_2\left(\mathbf{x}(t) \mid \boldsymbol{\theta}_{h2}\right) \\ &+ \frac{\left(\mathbf{e}^T\mathbf{PB}\right)}{\left\|\mathbf{e}^T\mathbf{PB}\right\|} \widehat{h}_3\left(\mathbf{x}(t-\tau) \mid \boldsymbol{\theta}_{h3}\right) \Bigg\}, \end{aligned} \tag{34}$$

where the scalars $\gamma_{h1}, \gamma_{h2}, \gamma_{h3}, \gamma_g, \gamma_1, \gamma_2, \gamma_\omega$, and η are positive constants, determining the rates of adaptations, and

$$z_1(v(t)) = \begin{cases} -c_a & \text{for } v(t) \geq c_a, \\ -v(t) & \text{for } c_b < v(t) < c_a, \\ -c_b & \text{for } v(t) \leq c_b. \end{cases} \tag{35}$$

Remark 1. Without loss of generality, the adaptive laws used in this paper are assumed that the parameter vectors are within the constraint sets or on the boundaries of the constraint sets but moving toward the inside of the constraint sets. If the parameter vectors are on the boundaries of the constraint sets but moving toward the outside of the constraint sets, we have to use the projection algorithm [27] to modify the adaptive laws such that the parameter vectors will remain inside of the constraint sets. The proposed adaptive law (28)–(30) can be modified as the following form:

$$\dot{\boldsymbol{\theta}}_g = \begin{cases} -\gamma_g\left\|\mathbf{e}^T\mathbf{PB}\right\| \boldsymbol{\xi}(\mathbf{x}(t))\left(v(t) + z_1(v(t))\right), \\ \quad \text{if } \left(\left\|\boldsymbol{\theta}_g\right\| < N_1\right) \text{ or} \\ \quad \left(\begin{array}{c} \left\|\boldsymbol{\theta}_g\right\| = N_1 \text{ and} \\ \left\|\mathbf{e}^T\mathbf{PB}\right\| \boldsymbol{\theta}_g^T\boldsymbol{\xi}(\mathbf{x}(t))\left(v(t) + z_1(v(t))\right) \geq 0 \end{array}\right), \\ P\left\{-\gamma_g\left\|\mathbf{e}^T\mathbf{PB}\right\| \boldsymbol{\xi}(\mathbf{x}(t))\left(v(t) + z_1(v(t))\right)\right\}, \\ \quad \text{if } \left(\begin{array}{c} \left\|\boldsymbol{\theta}_g\right\| = N_1 \text{ and} \\ \left\|\mathbf{e}^T\mathbf{PB}\right\| \boldsymbol{\theta}_g^T\boldsymbol{\xi}(\mathbf{x}(t))\left(v(t) + z_1(v(t))\right) < 0 \end{array}\right), \end{cases} \tag{36}$$

where $P\{-\gamma_g\|\mathbf{e}^T\mathbf{PB}\|\boldsymbol{\xi}(\mathbf{x}(t))(v(t) + z_1(v(t)))\}$ is defined as

$$\begin{aligned} &P\left\{-\gamma_g\left\|\mathbf{e}^T\mathbf{PB}\right\| \boldsymbol{\xi}(\mathbf{x}(t))\left(v(t) + z_1(v(t))\right)\right\} \\ &\quad = -\gamma_g\left\|\mathbf{e}^T\mathbf{PB}\right\| \boldsymbol{\xi}(\mathbf{x}(t))\left(v(t) + z_1(v(t))\right) \\ &\qquad + \gamma_g\left\|\mathbf{e}^T\mathbf{PB}\right\| \frac{\boldsymbol{\theta}_g\boldsymbol{\theta}_g^T}{\left\|\boldsymbol{\theta}_g\right\|^2} \boldsymbol{\xi}(\mathbf{x}(t)) \\ &\qquad \times \left(v(t) + z_1(v(t))\right), \end{aligned}$$

$$\dot{\boldsymbol{\theta}}_{h1} = \begin{cases} \gamma_{h1}\left\|\mathbf{e}^T\mathbf{PB}\right\| \boldsymbol{\xi}(\mathbf{x}(t)), \\ \quad \text{if } \left(\left\|\boldsymbol{\theta}_{h1}\right\| < N_2\right) \text{ or} \\ \quad \left(\left\|\boldsymbol{\theta}_{h1}\right\| = N_2 \text{ and } \left\|\mathbf{e}^T\mathbf{PB}\right\| \boldsymbol{\theta}_{h1}^T\boldsymbol{\xi}(\mathbf{x}(t)) \leq 0\right), \\ P\left\{\gamma_{h1}\left\|\mathbf{e}^T\mathbf{PB}\right\| \boldsymbol{\xi}(\mathbf{x}(t))\right\}, \\ \quad \text{if } \left(\left\|\boldsymbol{\theta}_{h1}\right\| = N_2 \text{ and } \left\|\mathbf{e}^T\mathbf{PB}\right\| \boldsymbol{\theta}_{h1}^T\boldsymbol{\xi}(\mathbf{x}(t)) > 0\right), \end{cases} \tag{37}$$

where $P\{\gamma_{h1}\|\mathbf{e}^T\mathbf{PB}\|\boldsymbol{\xi}(\mathbf{x}(t))\}$ is defined as

$$\begin{aligned} &P\left\{\gamma_{h1}\left\|\mathbf{e}^T\mathbf{PB}\right\| \boldsymbol{\xi}(\mathbf{x}(t))\right\} \\ &\quad = \gamma_{h1}\left\|\mathbf{e}^T\mathbf{PB}\right\| \boldsymbol{\xi}(\mathbf{x}(t)) \\ &\qquad - \gamma_{h1}\left\|\mathbf{e}^T\mathbf{PB}\right\| \frac{\boldsymbol{\theta}_{h1}\boldsymbol{\theta}_{h1}^T}{\left\|\boldsymbol{\theta}_{h1}\right\|^2} \boldsymbol{\xi}(\mathbf{x}(t)), \end{aligned}$$

$$\dot{\boldsymbol{\theta}}_{h2} = \begin{cases} \gamma_{h2}\left\|\mathbf{e}^T\mathbf{PB}\right\| \boldsymbol{\xi}(\mathbf{x}(t)), \\ \quad \text{if } \left(\left\|\boldsymbol{\theta}_{h2}\right\| < N_3\right) \text{ or} \\ \quad \left(\left\|\boldsymbol{\theta}_{h2}\right\| = N_3 \text{ and } \left\|\mathbf{e}^T\mathbf{PB}\right\| \boldsymbol{\theta}_{h2}^T\boldsymbol{\xi}(\mathbf{x}(t)) \leq 0\right), \\ P\left\{\gamma_{h2}\left\|\mathbf{e}^T\mathbf{PB}\right\| \boldsymbol{\xi}(\mathbf{x}(t))\right\}, \\ \quad \text{if } \left(\left\|\boldsymbol{\theta}_{h2}\right\| = N_3 \text{ and } \left\|\mathbf{e}^T\mathbf{PB}\right\| \boldsymbol{\theta}_{h2}^T\boldsymbol{\xi}(\mathbf{x}(t)) > 0\right), \end{cases} \tag{38}$$

where $P\{\gamma_{h2}\|\mathbf{e}^T\mathbf{PB}\|\boldsymbol{\xi}(\mathbf{x}(t))\}$ is defined as

$$\begin{aligned} P\left\{\gamma_{h2}\left\|\mathbf{e}^T\mathbf{PB}\right\|\boldsymbol{\xi}\left(\mathbf{x}\left(t\right)\right)\right\} &= \gamma_{h2}\left\|\mathbf{e}^T\mathbf{PB}\right\|\boldsymbol{\xi}\left(\mathbf{x}\left(t\right)\right) \\ &\quad - \gamma_{h2}\left\|\mathbf{e}^T\mathbf{PB}\right\|\frac{\boldsymbol{\theta}_{h2}\boldsymbol{\theta}_{h2}^T}{\left\|\boldsymbol{\theta}_{h2}\right\|^2}\boldsymbol{\xi}\left(\mathbf{x}\left(t\right)\right), \end{aligned}$$

$$\dot{\boldsymbol{\theta}}_{h3} = \begin{cases} \gamma_{h3}\left\|\mathbf{e}^T\mathbf{PB}\right\|\boldsymbol{\xi}\left(\mathbf{x}\left(t-\tau\right)\right), \\ \quad \text{if } \left(\left\|\boldsymbol{\theta}_{h3}\right\| < N_4\right) \text{ or} \\ \quad \left(\left\|\boldsymbol{\theta}_{h3}\right\| = N_4 \text{ and } \left\|\mathbf{e}^T\mathbf{PB}\right\|\boldsymbol{\theta}_{h3}^T\boldsymbol{\xi}\left(\mathbf{x}\left(t-\tau\right)\right) \le 0\right), \\ P\left\{\gamma_{h3}\left\|\mathbf{e}^T\mathbf{PB}\right\|\boldsymbol{\xi}\left(\mathbf{x}\left(t-\tau\right)\right)\right\}, \\ \quad \text{if } \left(\left\|\boldsymbol{\theta}_{h3}\right\| = N_4 \text{ and} \right. \\ \qquad \left.\left\|\mathbf{e}^T\mathbf{PB}\right\|\boldsymbol{\theta}_{h3}^T\boldsymbol{\xi}\left(\mathbf{x}\left(t-\tau\right)\right) > 0\right), \end{cases} \tag{39}$$

where $P\{\gamma_{h3}\|\mathbf{e}^T\mathbf{PB}\|\boldsymbol{\xi}(\mathbf{x}(t-\tau))\}$ is defined as

$$\begin{aligned} P\left\{\gamma_{h3}\left\|\mathbf{e}^T\mathbf{PB}\right\|\boldsymbol{\xi}\left(\mathbf{x}\left(t-\tau\right)\right)\right\} &= \gamma_{h3}\left\|\mathbf{e}^T\mathbf{PB}\right\|\boldsymbol{\xi}\left(\mathbf{x}\left(t-\tau\right)\right) \\ &\quad - \gamma_{h3}\left\|\mathbf{e}^T\mathbf{PB}\right\|\frac{\boldsymbol{\theta}_{h3}\boldsymbol{\theta}_{h3}^T}{\left\|\boldsymbol{\theta}_{h3}\right\|^2}\boldsymbol{\xi}\left(\mathbf{x}\left(t-\tau\right)\right). \end{aligned} \tag{40}$$

The main result of the proposed robust adaptive fuzzy tracking control scheme is summarized in the following theorem.

Theorem 2. *Consider the uncertain nonlinear state time-delay system* (1) *with unknown dead-zone input* (7). *If Assumptions 1–4 are satisfied, then the proposed robust adaptive fuzzy tracking controller defined by* (24)–(3) *with some adaptation laws* (28)–(34) *ensures that all the signals of the whole closed-loop system are bounded, and the output tracking errors converge to a neighborhood of zero exponentially.*

Proof. Consider the Lyapunov function candidate

$$\begin{aligned} V = \frac{1}{2}\Bigg(&\frac{1}{m}\mathbf{e}^T\mathbf{Pe} + \frac{1}{\gamma_1}\tilde{\boldsymbol{\theta}}_1^T\tilde{\boldsymbol{\theta}}_1 + \frac{1}{\gamma_2}\tilde{\boldsymbol{\theta}}_2^T\tilde{\boldsymbol{\theta}}_2 + \frac{1}{m\cdot\gamma_{h1}}\tilde{\boldsymbol{\theta}}_{h1}^T\tilde{\boldsymbol{\theta}}_{h1} \\ &+ \frac{1}{m\cdot\gamma_{h2}}\tilde{\boldsymbol{\theta}}_{h2}^T\tilde{\boldsymbol{\theta}}_{h2} + \frac{1}{m\cdot\gamma_{h3}}\tilde{\boldsymbol{\theta}}_{h3}^T\tilde{\boldsymbol{\theta}}_{h3} \\ &+ \frac{1}{\gamma_g}\tilde{\boldsymbol{\theta}}_g^T\tilde{\boldsymbol{\theta}}_g + \frac{1}{\eta}\tilde{\phi}^2 + \frac{1}{m_{\min}\cdot\gamma_\omega}\tilde{\omega}^2\Bigg). \end{aligned} \tag{41}$$

Differentiating the Lyapunov function V with respect to time, we can obtain

$$\begin{aligned} \dot{V} = &\frac{1}{2m}\dot{\mathbf{e}}^T\mathbf{Pe} + \frac{1}{2m}\mathbf{e}^T\mathbf{P}\dot{\mathbf{e}} + \frac{1}{\gamma_1}\tilde{\boldsymbol{\theta}}_1^T\dot{\tilde{\boldsymbol{\theta}}}_1 \\ &+ \frac{1}{\gamma_2}\tilde{\boldsymbol{\theta}}_2^T\dot{\tilde{\boldsymbol{\theta}}}_2 + \frac{1}{m\gamma_{h1}}\tilde{\boldsymbol{\theta}}_{h1}^T\dot{\tilde{\boldsymbol{\theta}}}_{h1} \\ &+ \frac{1}{m\gamma_{h2}}\tilde{\boldsymbol{\theta}}_{h2}^T\dot{\tilde{\boldsymbol{\theta}}}_{h2} + \frac{1}{m\gamma_{h3}}\tilde{\boldsymbol{\theta}}_{h3}^T\dot{\tilde{\boldsymbol{\theta}}}_{h3} \\ &+ \frac{1}{\gamma_g}\tilde{\boldsymbol{\theta}}_g^T\dot{\tilde{\boldsymbol{\theta}}}_g + \frac{1}{\eta}\tilde{\phi}\dot{\tilde{\phi}} + \frac{1}{m_{\min}\cdot\gamma_\omega}\tilde{\omega}\dot{\tilde{\omega}}. \end{aligned} \tag{42}$$

From (16) and by the fact that $\dot{\tilde{\boldsymbol{\theta}}}_1 = \dot{\hat{\boldsymbol{\theta}}}_1$, $\dot{\tilde{\boldsymbol{\theta}}}_2 = \dot{\hat{\boldsymbol{\theta}}}_2$, $\dot{\tilde{\boldsymbol{\theta}}}_{h1} = \dot{\boldsymbol{\theta}}_{h1}$, $\dot{\tilde{\boldsymbol{\theta}}}_{h2} = \dot{\boldsymbol{\theta}}_{h2}$, $\dot{\tilde{\boldsymbol{\theta}}}_{h3} = \dot{\boldsymbol{\theta}}_{h3}$, $\dot{\tilde{\boldsymbol{\theta}}}_g = \dot{\boldsymbol{\theta}}_g$, $\dot{\tilde{\phi}} = \dot{\hat{\phi}}$, and $\dot{\tilde{\omega}} = \dot{\hat{\omega}}$, the previous equation becomes

$$\begin{aligned} \dot{V} = &\frac{1}{2m}\mathbf{e}^T\left[\mathbf{A}_m^T\mathbf{P} + \mathbf{PA}_m\right]\mathbf{e} \\ &+ \frac{1}{m}\mathbf{e}^T\mathbf{PB}\Bigg[\mathbf{Ke} + y_m^{(n)} - \sum_{i=1}^{M}\theta_{1i}f_{1i}\left(\mathbf{x}\left(t\right)\right) \\ &\qquad - \Delta f_1\left(\mathbf{x}\left(t\right)\right) - \sum_{j=1}^{N}\theta_{2j}f_{2j}\left(\mathbf{x}\left(t-\tau\right)\right) \\ &\qquad - \Delta f_2\left(\mathbf{x}\left(t-\tau\right)\right) - g\left(\mathbf{x}\right)m\upsilon\left(t\right) \\ &\qquad - g\left(\mathbf{x}\right)z\left(\upsilon\left(t\right)\right) - \Delta\Phi\Bigg] \\ &+ \frac{1}{\gamma_1}\tilde{\boldsymbol{\theta}}_1^T\dot{\hat{\boldsymbol{\theta}}}_1 + \frac{1}{\gamma_2}\tilde{\boldsymbol{\theta}}_2^T\dot{\hat{\boldsymbol{\theta}}}_2 + \frac{1}{m\gamma_{h1}}\tilde{\boldsymbol{\theta}}_{h1}^T\dot{\boldsymbol{\theta}}_{h1} \\ &+ \frac{1}{m\gamma_{h2}}\tilde{\boldsymbol{\theta}}_{h2}^T\dot{\boldsymbol{\theta}}_{h2} + \frac{1}{m\gamma_{h3}}\tilde{\boldsymbol{\theta}}_{h3}^T\dot{\boldsymbol{\theta}}_{h3} \\ &+ \frac{1}{\gamma_g}\tilde{\boldsymbol{\theta}}_g^T\dot{\boldsymbol{\theta}}_g + \frac{1}{\eta}\tilde{\phi}\dot{\hat{\phi}} + \frac{1}{m_{\min}\gamma_\omega}\tilde{\omega}\dot{\hat{\omega}}. \end{aligned} \tag{43}$$

Applying (27) and Assumption 4 to (43) yields

$$\begin{aligned} \dot{V} \le &-\frac{1}{2m}\mathbf{e}^T\mathbf{Qe} + \frac{1}{m}\mathbf{e}^T\mathbf{PB} \\ &\times\Bigg[\mathbf{Ke} + y_m^{(n)} - \sum_{i=1}^{M}\theta_{1i}f_{1i}\left(\mathbf{x}\left(t\right)\right) \\ &\qquad - \sum_{j=1}^{N}\theta_{2j}f_{2j}\left(\mathbf{x}\left(t-\tau\right)\right) \\ &\qquad - g\left(\mathbf{x}\right)m\upsilon\left(t\right) - g\left(\mathbf{x}\right)z\left(\upsilon\left(t\right)\right)\Bigg] \\ &+ \frac{1}{m}\left\|\mathbf{e}^T\mathbf{PB}\right\|h_1\left(\mathbf{x}\right) + \frac{1}{m}\left\|\mathbf{e}^T\mathbf{PB}\right\|h_2\left(\mathbf{x}\left(t\right)\right) \\ &+ \frac{1}{m}\left\|\mathbf{e}^T\mathbf{PB}\right\|h_3\left(\mathbf{x}\left(t-\tau\right)\right) + \frac{1}{\gamma_1}\tilde{\boldsymbol{\theta}}_1^T\dot{\hat{\boldsymbol{\theta}}}_1 \\ &+ \frac{1}{\gamma_2}\tilde{\boldsymbol{\theta}}_2^T\dot{\hat{\boldsymbol{\theta}}}_2 + \frac{1}{m\gamma_{h1}}\tilde{\boldsymbol{\theta}}_{h1}^T\dot{\boldsymbol{\theta}}_{h1} + \frac{1}{m\gamma_{h2}}\tilde{\boldsymbol{\theta}}_{h2}^T\dot{\boldsymbol{\theta}}_{h2} \end{aligned}$$

$$+\frac{1}{m\gamma_{h3}}\tilde{\boldsymbol{\theta}}_{h3}^{T}\dot{\boldsymbol{\theta}}_{h3}+\frac{1}{\gamma_g}\tilde{\boldsymbol{\theta}}_{g}^{T}\dot{\boldsymbol{\theta}}_{g}+\frac{1}{\eta}\tilde{\phi}\dot{\tilde{\phi}}+\frac{1}{m_{\min}\gamma_{\omega}}\tilde{\omega}\dot{\tilde{\omega}}. \tag{44}$$

Substituting (17) and (23) into (44), we obtain

$$\begin{aligned}
\dot{V}\le{}&-\frac{1}{2m}\mathbf{e}^{T}\mathbf{Q}\mathbf{e}+\mathbf{e}^{T}\mathbf{P}\mathbf{B}\\
&\times\left\{\frac{1}{m}\left[\mathbf{K}\mathbf{e}+y_m^{(n)}\right]-\mathbf{f}_1^{T}(\mathbf{x}(t))\boldsymbol{\theta}_1-\mathbf{f}_2^{T}(\mathbf{x}(t-\tau))\boldsymbol{\theta}_2\right\}\\
&+\frac{1}{m}\left\|\mathbf{e}^{T}\mathbf{P}\mathbf{B}\right\|(|\omega_1|+|\omega_2|)-\frac{1}{m}\mathbf{e}^{T}\mathbf{P}\mathbf{B}\\
&\times\left[\hat{g}(\mathbf{x}\mid\boldsymbol{\theta}_g)(mv(t)+z(v(t)))\right]\\
&+\frac{1}{m}\mathbf{e}^{T}\mathbf{P}\mathbf{B}\left[\tilde{\boldsymbol{\theta}}_g^{T}\boldsymbol{\xi}(\mathbf{x})(mv(t)+z(v(t)))\right]\\
&+\frac{1}{m}\left\|\mathbf{e}^{T}\mathbf{P}\mathbf{B}\right\|\left[\hat{h}_1(\mathbf{x}\mid\boldsymbol{\theta}_{h1})-\tilde{\boldsymbol{\theta}}_{h1}^{T}\boldsymbol{\xi}(\mathbf{x})\right]\\
&+\frac{1}{m}\left\|\mathbf{e}^{T}\mathbf{P}\mathbf{B}\right\|\left[\hat{h}_2(\mathbf{x}(t)\mid\boldsymbol{\theta}_{h2})-\tilde{\boldsymbol{\theta}}_{h2}^{T}\boldsymbol{\xi}(\mathbf{x}(t))\right]\\
&+\frac{1}{m}\left\|\mathbf{e}^{T}\mathbf{P}\mathbf{B}\right\|\left[\hat{h}_3(\mathbf{x}(t-\tau)\mid\boldsymbol{\theta}_{h3})-\tilde{\boldsymbol{\theta}}_{h3}^{T}\boldsymbol{\xi}(\mathbf{x}(t-\tau))\right]\\
&+\frac{1}{\gamma_1}\tilde{\boldsymbol{\theta}}_1^{T}\dot{\hat{\boldsymbol{\theta}}}_1+\frac{1}{\gamma_2}\tilde{\boldsymbol{\theta}}_2^{T}\dot{\hat{\boldsymbol{\theta}}}_2+\frac{1}{m\cdot\gamma_{h1}}\tilde{\boldsymbol{\theta}}_{h1}^{T}\dot{\boldsymbol{\theta}}_{h1}\\
&+\frac{1}{m\cdot\gamma_{h2}}\tilde{\boldsymbol{\theta}}_{h2}^{T}\dot{\boldsymbol{\theta}}_{h2}+\frac{1}{m\cdot\gamma_{h3}}\tilde{\boldsymbol{\theta}}_{h3}^{T}\dot{\boldsymbol{\theta}}_{h3}\\
&+\frac{1}{\gamma_g}\tilde{\boldsymbol{\theta}}_g^{T}\dot{\boldsymbol{\theta}}_g+\frac{1}{\eta}\tilde{\phi}\dot{\tilde{\phi}}+\frac{1}{m_{\min}\cdot\gamma_{\omega}}\tilde{\omega}\dot{\tilde{\omega}}\\
\le{}&-\frac{1}{2m}\mathbf{e}^{T}\mathbf{Q}\mathbf{e}+\mathbf{e}^{T}\mathbf{P}\mathbf{B}\\
&\times\left\{\frac{1}{m}\left[\mathbf{K}\mathbf{e}+y_m^{(n)}\right]-\mathbf{f}_1^{T}(\mathbf{x}(t))\boldsymbol{\theta}_1-\mathbf{f}_2^{T}(\mathbf{x}(t-\tau))\boldsymbol{\theta}_2\right\}\\
&+\frac{1}{m}\left\|\mathbf{e}^{T}\mathbf{P}\mathbf{B}\right\|\omega-\frac{1}{m}\mathbf{e}^{T}\mathbf{P}\mathbf{B}\\
&\times\left[\hat{g}(\mathbf{x}\mid\boldsymbol{\theta}_g)(mv(t)+z(v(t)))\right]\\
&+\frac{1}{m}\mathbf{e}^{T}\mathbf{P}\mathbf{B}\left[\tilde{\boldsymbol{\theta}}_g^{T}\boldsymbol{\xi}(\mathbf{x})(mv(t)+m\cdot z_1(v(t)))\right]\\
&+\frac{1}{m}\left\|\mathbf{e}^{T}\mathbf{P}\mathbf{B}\right\|\left[\hat{h}_1(\mathbf{x}\mid\boldsymbol{\theta}_{h1})-\tilde{\boldsymbol{\theta}}_{h1}^{T}\boldsymbol{\xi}(\mathbf{x})\right]\\
&+\frac{1}{m}\left\|\mathbf{e}^{T}\mathbf{P}\mathbf{B}\right\|\left[\hat{h}_2(\mathbf{x}(t)\mid\boldsymbol{\theta}_{h2})-\tilde{\boldsymbol{\theta}}_{h2}^{T}\boldsymbol{\xi}(\mathbf{x}(t))\right]\\
&+\frac{1}{m}\left\|\mathbf{e}^{T}\mathbf{P}\mathbf{B}\right\|\left[\hat{h}_3(\mathbf{x}(t-\tau)\mid\boldsymbol{\theta}_{h3})-\tilde{\boldsymbol{\theta}}_{h3}^{T}\boldsymbol{\xi}(\mathbf{x}(t-\tau))\right]\\
&+\frac{1}{\gamma_1}\tilde{\boldsymbol{\theta}}_1^{T}\dot{\hat{\boldsymbol{\theta}}}_1+\frac{1}{\gamma_2}\tilde{\boldsymbol{\theta}}_2^{T}\dot{\hat{\boldsymbol{\theta}}}_2+\frac{1}{m\cdot\gamma_{h1}}\tilde{\boldsymbol{\theta}}_{h1}^{T}\dot{\boldsymbol{\theta}}_{h1}\\
&+\frac{1}{m\cdot\gamma_{h2}}\tilde{\boldsymbol{\theta}}_{h2}^{T}\dot{\boldsymbol{\theta}}_{h2}+\frac{1}{m\cdot\gamma_{h3}}\tilde{\boldsymbol{\theta}}_{h3}^{T}\dot{\boldsymbol{\theta}}_{h3}\\
&+\frac{1}{\gamma_g}\tilde{\boldsymbol{\theta}}_g^{T}\dot{\boldsymbol{\theta}}_g+\frac{1}{\eta}\tilde{\phi}\dot{\tilde{\phi}}+\frac{1}{m_{\min}\cdot\gamma_{\omega}}\tilde{\omega}\dot{\tilde{\omega}}.
\end{aligned} \tag{45}$$

According to adaptive laws (28)–(30), (45) can be rewritten as

$$\begin{aligned}
\dot{V}\le{}&-\frac{1}{2m}\mathbf{e}^{T}\mathbf{Q}\mathbf{e}+\frac{1}{m}\left\|\mathbf{e}^{T}\mathbf{P}\mathbf{B}\right\|\omega\\
&+\frac{1}{m}\mathbf{e}^{T}\mathbf{P}\mathbf{B}\left\{\left[\mathbf{K}\mathbf{e}+y_m^{(n)}\right]\right.\\
&\qquad+\frac{\left(\mathbf{e}^{T}\mathbf{P}\mathbf{B}\right)^{T}}{\left\|\mathbf{e}^{T}\mathbf{P}\mathbf{B}\right\|}\hat{h}_1(\mathbf{x}\mid\boldsymbol{\theta}_{h1})\\
&\qquad+\frac{\left(\mathbf{e}^{T}\mathbf{P}\mathbf{B}\right)^{T}}{\left\|\mathbf{e}^{T}\mathbf{P}\mathbf{B}\right\|}\hat{h}_2(\mathbf{x}(t)\mid\boldsymbol{\theta}_{h2})\\
&\qquad\left.+\frac{\left(\mathbf{e}^{T}\mathbf{P}\mathbf{B}\right)^{T}}{\left\|\mathbf{e}^{T}\mathbf{P}\mathbf{B}\right\|}\hat{h}_3(\mathbf{x}(t-\tau)\mid\boldsymbol{\theta}_{h3})\right\}\\
&+\mathbf{e}^{T}\mathbf{P}\mathbf{B}\left\{-\hat{g}(\mathbf{x}\mid\boldsymbol{\theta}_g)v(t)-\hat{g}(\mathbf{x}\mid\boldsymbol{\theta}_g)\frac{z(v(t))}{m}\right\}\\
&-\mathbf{e}^{T}\mathbf{P}\mathbf{B}\mathbf{f}_1^{T}(\mathbf{x}(t))\boldsymbol{\theta}_1-\mathbf{e}^{T}\mathbf{P}\mathbf{B}\mathbf{f}_2^{T}(\mathbf{x}(t-\tau))\boldsymbol{\theta}_2\\
&+\frac{1}{\gamma_1}\tilde{\boldsymbol{\theta}}_1^{T}\dot{\hat{\boldsymbol{\theta}}}_1+\frac{1}{\gamma_2}\tilde{\boldsymbol{\theta}}_2^{T}\dot{\hat{\boldsymbol{\theta}}}_2+\frac{1}{\eta}\tilde{\phi}\dot{\tilde{\phi}}\\
&+\frac{1}{m_{\min}\cdot\gamma_{\omega}}\tilde{\omega}\dot{\tilde{\omega}}\\
\le{}&-\frac{1}{2m}\mathbf{e}^{T}\mathbf{Q}\mathbf{e}+\frac{1}{m}\left\|\mathbf{e}^{T}\mathbf{P}\mathbf{B}\right\|\omega+\frac{1}{m}\mathbf{e}^{T}\mathbf{P}\mathbf{B}\\
&\times\left\{\left[\mathbf{K}\mathbf{e}+y_m^{(n)}\right]+\frac{\left(\mathbf{e}^{T}\mathbf{P}\mathbf{B}\right)^{T}}{\left\|\mathbf{e}^{T}\mathbf{P}\mathbf{B}\right\|}\hat{h}_1(\mathbf{x}\mid\boldsymbol{\theta}_{h1})\right.\\
&\qquad+\frac{\left(\mathbf{e}^{T}\mathbf{P}\mathbf{B}\right)^{T}}{\left\|\mathbf{e}^{T}\mathbf{P}\mathbf{B}\right\|}\hat{h}_2(\mathbf{x}(t)\mid\boldsymbol{\theta}_{h2})\\
&\qquad\left.+\frac{\left(\mathbf{e}^{T}\mathbf{P}\mathbf{B}\right)^{T}}{\left\|\mathbf{e}^{T}\mathbf{P}\mathbf{B}\right\|}\hat{h}_3(\mathbf{x}(t-\tau)\mid\boldsymbol{\theta}_{h3})\right\}\\
&-\mathbf{e}^{T}\mathbf{P}\mathbf{B}\hat{g}(\mathbf{x}\mid\boldsymbol{\theta}_g)v(t)+\left\|\mathbf{e}^{T}\mathbf{P}\mathbf{B}\right\|\hat{g}(\mathbf{x}\mid\boldsymbol{\theta}_g)\\
&\times\frac{|z(v(t))|}{|m|}-\mathbf{e}^{T}\mathbf{P}\mathbf{B}\mathbf{f}_1^{T}(\mathbf{x}(t))\boldsymbol{\theta}_1\\
&-\mathbf{e}^{T}\mathbf{P}\mathbf{B}\mathbf{f}_2^{T}(\mathbf{x}(t-\tau))\boldsymbol{\theta}_2+\frac{1}{\gamma_1}\tilde{\boldsymbol{\theta}}_1^{T}\dot{\hat{\boldsymbol{\theta}}}_1\\
&+\frac{1}{\gamma_2}\tilde{\boldsymbol{\theta}}_2^{T}\dot{\hat{\boldsymbol{\theta}}}_2+\frac{1}{\eta}\tilde{\phi}\dot{\tilde{\phi}}+\frac{1}{m_{\min}\cdot\gamma_{\omega}}\tilde{\omega}\dot{\tilde{\omega}}.
\end{aligned} \tag{46}$$

Using the control laws (24)–(3), the previous equation can be rewritten as

$$\begin{aligned}
\dot{V} \le & -\frac{1}{2m}\mathbf{e}^T\mathbf{Q}\mathbf{e} + \frac{1}{m_{\min}}\left\|\mathbf{e}^T\mathbf{P}\mathbf{B}\right\| \cdot (\omega - \widehat{\omega}) \\
& + \mathbf{e}^T\mathbf{P}\mathbf{B}\left(\phi - \widehat{\phi}\right) \\
& \times \left\{ \left[\mathbf{K}\mathbf{e} + y_m^{(n)}\right] + \frac{\left(\mathbf{e}^T\mathbf{P}\mathbf{B}\right)^T}{\left\|\mathbf{e}^T\mathbf{P}\mathbf{B}\right\|}\widehat{h}_1\left(\mathbf{x} \mid \boldsymbol{\theta}_{h1}\right) \right. \\
& \quad + \frac{\left(\mathbf{e}^T\mathbf{P}\mathbf{B}\right)^T}{\left\|\mathbf{e}^T\mathbf{P}\mathbf{B}\right\|}\widehat{h}_2\left(\mathbf{x}(t) \mid \boldsymbol{\theta}_{h2}\right) \\
& \quad \left. + \frac{\left(\mathbf{e}^T\mathbf{P}\mathbf{B}\right)^T}{\left\|\mathbf{e}^T\mathbf{P}\mathbf{B}\right\|}\widehat{h}_3\left(\mathbf{x}(t-\tau) \mid \boldsymbol{\theta}_{h3}\right) \right\} \\
& + \left\|\mathbf{e}^T\mathbf{P}\mathbf{B}\right\| \widehat{g}\left(\mathbf{x} \mid \boldsymbol{\theta}_g\right) \frac{|z(\upsilon(t))|}{|m|} \\
& - \mathbf{e}^T\mathbf{P}\mathbf{B}\left(\boldsymbol{\theta}_1^T - \widehat{\boldsymbol{\theta}}_1^T\right) \cdot \mathbf{f}_1(\mathbf{x}(t)) \\
& - \mathbf{e}^T\mathbf{P}\mathbf{B}\left(\boldsymbol{\theta}_2^T - \widehat{\boldsymbol{\theta}}_2^T\right) \cdot \mathbf{f}_2(\mathbf{x}(t-\tau)) \\
& - \mathbf{e}^T\mathbf{P}\mathbf{B} \cdot \widehat{g}\left(\mathbf{x} \mid \boldsymbol{\theta}_g\right) \cdot \frac{\rho}{m_{\min}} \\
& \cdot \tanh\left(\frac{\mathbf{e}^T\mathbf{P}\mathbf{B}}{\varepsilon}\right) + \frac{1}{\gamma_1}\widetilde{\boldsymbol{\theta}}_1^T\dot{\widehat{\boldsymbol{\theta}}}_1 + \frac{1}{\gamma_2}\widetilde{\boldsymbol{\theta}}_2^T\dot{\widehat{\boldsymbol{\theta}}}_2 \\
& + \frac{1}{\eta}\widetilde{\phi}\dot{\widehat{\phi}} + \frac{1}{m_{\min}\cdot\gamma_\omega}\widetilde{\omega}\dot{\widehat{\omega}} \\
= & -\frac{1}{2m}\mathbf{e}^T\mathbf{Q}\mathbf{e} - \frac{1}{m_{\min}}\left\|\mathbf{e}^T\mathbf{P}\mathbf{B}\right\| \cdot \widetilde{\omega} \\
& - \mathbf{e}^T\mathbf{P}\mathbf{B}\widetilde{\phi}\left\{ \left[\mathbf{K}\mathbf{e} + y_m^{(n)}\right] + \frac{\left(\mathbf{e}^T\mathbf{P}\mathbf{B}\right)^T}{\left\|\mathbf{e}^T\mathbf{P}\mathbf{B}\right\|}\widehat{h}_1\left(\mathbf{x} \mid \boldsymbol{\theta}_{h1}\right) \right. \\
& \quad + \frac{\left(\mathbf{e}^T\mathbf{P}\mathbf{B}\right)^T}{\left\|\mathbf{e}^T\mathbf{P}\mathbf{B}\right\|}\widehat{h}_2\left(\mathbf{x}(t) \mid \boldsymbol{\theta}_{h2}\right) \\
& \quad \left. + \frac{\left(\mathbf{e}^T\mathbf{P}\mathbf{B}\right)^T}{\left\|\mathbf{e}^T\mathbf{P}\mathbf{B}\right\|}\widehat{h}_3\left(\mathbf{x}(t-\tau) \mid \boldsymbol{\theta}_{h3}\right) \right\} \\
& + \left\|\mathbf{e}^T\mathbf{P}\mathbf{B}\right\| \widehat{g}\left(\mathbf{x} \mid \theta_g\right) \frac{|z(\upsilon(t))|}{|m|} \\
& + \mathbf{e}^T\mathbf{P}\mathbf{B} \cdot \widetilde{\boldsymbol{\theta}}_1^T \cdot \mathbf{f}_1(\mathbf{x}(t)) + \mathbf{e}^T\mathbf{P}\mathbf{B} \cdot \widetilde{\boldsymbol{\theta}}_2^T \cdot \mathbf{f}_2(\mathbf{x}(t-\tau)) \\
& - \mathbf{e}^T\mathbf{P}\mathbf{B} \cdot \widehat{g}\left(\mathbf{x} \mid \boldsymbol{\theta}_g\right) \cdot \frac{\rho}{m_{\min}} \cdot \tanh\left(\frac{\mathbf{e}^T\mathbf{P}\mathbf{B}}{\varepsilon}\right) \\
& + \frac{1}{\gamma_1}\widetilde{\boldsymbol{\theta}}_1^T\dot{\widehat{\boldsymbol{\theta}}}_1 + \frac{1}{\gamma_2}\widetilde{\boldsymbol{\theta}}_2^T\dot{\widehat{\boldsymbol{\theta}}}_2 \\
& + \frac{1}{\eta}\widetilde{\phi}\dot{\widehat{\phi}} + \frac{1}{m_{\min}\cdot\gamma_\omega}\widetilde{\omega}\dot{\widehat{\omega}}.
\end{aligned} \tag{47}$$

According to adaptive laws (31)–(33), we have

$$\begin{aligned}
\dot{V} \le & -\frac{1}{2m}\mathbf{e}^T\mathbf{Q}\mathbf{e} + \left\|\mathbf{e}^T\mathbf{P}\mathbf{B}\right\| \widehat{g}\left(\mathbf{x} \mid \boldsymbol{\theta}_g\right) \frac{|z(\upsilon(t))|}{|m|} \\
& - \mathbf{e}^T\mathbf{P}\mathbf{B} \cdot \widehat{g}\left(\mathbf{x} \mid \boldsymbol{\theta}_g\right) \cdot \frac{\rho}{m_{\min}} \cdot \tanh\left(\frac{\mathbf{e}^T\mathbf{P}\mathbf{B}}{\varepsilon}\right) \\
\le & -\frac{1}{2m}\mathbf{e}^T\mathbf{Q}\mathbf{e} + \left\|\mathbf{e}^T\mathbf{P}\mathbf{B}\right\| \widehat{g}\left(\mathbf{x} \mid \boldsymbol{\theta}_g\right) \frac{\rho}{m_{\min}} \\
& - \mathbf{e}^T\mathbf{P}\mathbf{B} \cdot \widehat{g}\left(\mathbf{x} \mid \boldsymbol{\theta}_g\right) \cdot \frac{\rho}{m_{\min}} \cdot \tanh\left(\frac{\mathbf{e}^T\mathbf{P}\mathbf{B}}{\varepsilon}\right).
\end{aligned} \tag{48}$$

By considering the inequality $|\phi| - \phi\tanh(\phi/\varepsilon) \le 0.2785\varepsilon$. We obtain

$$\begin{aligned}
\dot{V} \le & -\frac{1}{2m}\mathbf{e}^T\mathbf{Q}\mathbf{e} + 0.2785\widehat{g}\left(\mathbf{x} \mid \boldsymbol{\theta}_g\right) \cdot \frac{\rho}{m_{\min}} \cdot \varepsilon \\
= & -\frac{1}{2m}\mathbf{e}^T\mathbf{Q}\mathbf{e} - \frac{1}{2\gamma_1}\widetilde{\boldsymbol{\theta}}_1^T\widetilde{\boldsymbol{\theta}}_1 - \frac{1}{2\gamma_2}\widetilde{\boldsymbol{\theta}}_2^T\widetilde{\boldsymbol{\theta}}_2 \\
& - \frac{1}{2m\gamma_{h1}}\widetilde{\boldsymbol{\theta}}_{h1}^T\widetilde{\boldsymbol{\theta}}_{h1} - \frac{1}{2m\gamma_{h2}}\widetilde{\boldsymbol{\theta}}_{h2}^T\widetilde{\boldsymbol{\theta}}_{h2} \\
& - \frac{1}{2m\gamma_{h3}}\widetilde{\boldsymbol{\theta}}_{h3}^T\widetilde{\boldsymbol{\theta}}_{h3} - \frac{1}{2\gamma_g}\widetilde{\boldsymbol{\theta}}_g^T\widetilde{\boldsymbol{\theta}}_g - \frac{1}{2\eta}\widetilde{\phi}^2 \\
& - \frac{1}{2m_{\min}\cdot\gamma_\omega}\widetilde{\omega}^2 + \frac{1}{2\gamma_1}\widetilde{\boldsymbol{\theta}}_1^T\widetilde{\boldsymbol{\theta}}_1 + \frac{1}{2\gamma_2}\widetilde{\boldsymbol{\theta}}_2^T\widetilde{\boldsymbol{\theta}}_2 \\
& + \frac{1}{2m\gamma_{h1}}\widetilde{\boldsymbol{\theta}}_{h1}^T\widetilde{\boldsymbol{\theta}}_{h1} + \frac{1}{2m\gamma_{h2}}\widetilde{\boldsymbol{\theta}}_{h2}^T\widetilde{\boldsymbol{\theta}}_{h2} \\
& + \frac{1}{2m\gamma_{h3}}\widetilde{\boldsymbol{\theta}}_{h3}^T\widetilde{\boldsymbol{\theta}}_{h3} + \frac{1}{2\gamma_g}\widetilde{\boldsymbol{\theta}}_g^T\widetilde{\boldsymbol{\theta}}_g + \frac{1}{2\eta}\widetilde{\phi}^2 \\
& + \frac{1}{2m_{\min}\cdot\gamma_\omega}\widetilde{\omega}^2 + 0.2785\widehat{g}\left(\mathbf{x} \mid \boldsymbol{\theta}_g\right) \cdot \frac{\rho}{m_{\min}} \cdot \varepsilon.
\end{aligned} \tag{49}$$

Let

$$\begin{aligned}
L = & \frac{1}{2\gamma_1}\widetilde{\boldsymbol{\theta}}_1^T\widetilde{\boldsymbol{\theta}}_1 + \frac{1}{2\gamma_2}\widetilde{\boldsymbol{\theta}}_2^T\widetilde{\boldsymbol{\theta}}_2 \\
& + \frac{1}{2m\gamma_{h1}}\widetilde{\boldsymbol{\theta}}_{h1}^T\widetilde{\boldsymbol{\theta}}_{h1} + \frac{1}{2m\gamma_{h2}}\widetilde{\boldsymbol{\theta}}_{h2}^T\widetilde{\boldsymbol{\theta}}_{h2} \\
& + \frac{1}{2m\gamma_{h3}}\widetilde{\boldsymbol{\theta}}_{h3}^T\widetilde{\boldsymbol{\theta}}_{h3} + \frac{1}{2\gamma_g}\widetilde{\boldsymbol{\theta}}_g^T\widetilde{\boldsymbol{\theta}}_g \\
& + \frac{1}{2\eta}\widetilde{\phi}^2 + \frac{1}{2m_{\min}\cdot\gamma_\omega}\widetilde{\omega}^2 \\
& + 0.2785\widehat{g}\left(\mathbf{x} \mid \theta_g\right) \cdot \frac{\rho}{m_{\min}} \cdot \varepsilon.
\end{aligned} \tag{50}$$

Then,

$$\begin{aligned}\dot{V} \le & -\frac{1}{2m}\mathbf{e}^T\mathbf{Q}\mathbf{e} - \frac{1}{2\gamma_1}\tilde{\boldsymbol{\theta}}_1^T\tilde{\boldsymbol{\theta}}_1 \\ & - \frac{1}{2\gamma_2}\tilde{\boldsymbol{\theta}}_2^T\tilde{\boldsymbol{\theta}}_2 - \frac{1}{2m\gamma_{h1}}\tilde{\boldsymbol{\theta}}_{h1}^T\tilde{\boldsymbol{\theta}}_{h1} \\ & - \frac{1}{2m\gamma_{h2}}\tilde{\boldsymbol{\theta}}_{h2}^T\tilde{\boldsymbol{\theta}}_{h2} - \frac{1}{2m\gamma_{h3}}\tilde{\boldsymbol{\theta}}_{h3}^T\tilde{\boldsymbol{\theta}}_{h3} \\ & - \frac{1}{2\gamma_g}\tilde{\boldsymbol{\theta}}_g^T\tilde{\boldsymbol{\theta}}_g - \frac{1}{2\eta}\tilde{\phi}^2 - \frac{1}{2m_{\min}\cdot\gamma_\omega}\tilde{\omega}^2 + L \\ \le & -\frac{1}{2m}\lambda_{\min}(\mathbf{Q})\,\mathbf{e}^T\mathbf{e} - \frac{1}{2\gamma_1}\tilde{\boldsymbol{\theta}}_1^T\tilde{\boldsymbol{\theta}}_1 \\ & - \frac{1}{2\gamma_2}\tilde{\boldsymbol{\theta}}_2^T\tilde{\boldsymbol{\theta}}_2 - \frac{1}{2m\gamma_{h1}}\tilde{\boldsymbol{\theta}}_{h1}^T\tilde{\boldsymbol{\theta}}_{h1} \\ & - \frac{1}{2m\gamma_{h2}}\tilde{\boldsymbol{\theta}}_{h2}^T\tilde{\boldsymbol{\theta}}_{h2} - \frac{1}{2m\gamma_{h3}}\tilde{\boldsymbol{\theta}}_{h3}^T\tilde{\boldsymbol{\theta}}_{h3} \\ & - \frac{1}{2\gamma_g}\tilde{\boldsymbol{\theta}}_g^T\tilde{\boldsymbol{\theta}}_g - \frac{1}{2\eta}\tilde{\phi}^2 - \frac{1}{2m_{\min}\cdot\gamma_\omega}\tilde{\omega}^2 + L \\ \le & -\frac{1}{2m}\frac{\lambda_{\min}(\mathbf{Q})}{\lambda_{\max}(\mathbf{P})}\mathbf{e}^T\mathbf{P}\mathbf{e} - \frac{1}{2\gamma_1}\tilde{\boldsymbol{\theta}}_1^T\tilde{\boldsymbol{\theta}}_1 \\ & - \frac{1}{2\gamma_2}\tilde{\boldsymbol{\theta}}_2^T\tilde{\boldsymbol{\theta}}_2 - \frac{1}{2m\gamma_{h1}}\tilde{\boldsymbol{\theta}}_{h1}^T\tilde{\boldsymbol{\theta}}_{h1} \\ & - \frac{1}{2m\gamma_{h2}}\tilde{\boldsymbol{\theta}}_{h2}^T\tilde{\boldsymbol{\theta}}_{h2} - \frac{1}{2m\gamma_{h3}}\tilde{\boldsymbol{\theta}}_{h3}^T\tilde{\boldsymbol{\theta}}_{h3} \\ & - \frac{1}{2\gamma_g}\tilde{\boldsymbol{\theta}}_g^T\tilde{\boldsymbol{\theta}}_g - \frac{1}{2\eta}\tilde{\phi}^2 - \frac{1}{2m_{\min}\cdot\gamma_\omega}\tilde{\omega}^2 + L.\end{aligned} \tag{51}$$

Let $\lambda_\upsilon = \lambda_{\min}(\mathbf{Q})/\lambda_{\max}(\mathbf{P})$. We obtain

$$\begin{aligned}\dot{V} \le & -\frac{1}{2m}\lambda_\upsilon\mathbf{e}^T\mathbf{P}\mathbf{e} - \frac{1}{2\gamma_1}\tilde{\boldsymbol{\theta}}_1^T\tilde{\boldsymbol{\theta}}_1 \\ & - \frac{1}{2\gamma_2}\tilde{\boldsymbol{\theta}}_2^T\tilde{\boldsymbol{\theta}}_2 - \frac{1}{2m\gamma_{h1}}\tilde{\boldsymbol{\theta}}_{h1}^T\tilde{\boldsymbol{\theta}}_{h1} \\ & - \frac{1}{2m\gamma_{h2}}\tilde{\boldsymbol{\theta}}_{h2}^T\tilde{\boldsymbol{\theta}}_{h2} - \frac{1}{2m\gamma_{h3}}\tilde{\boldsymbol{\theta}}_{h3}^T\tilde{\boldsymbol{\theta}}_{h3} \\ & - \frac{1}{2\gamma_g}\tilde{\boldsymbol{\theta}}_g^T\tilde{\boldsymbol{\theta}}_g - \frac{1}{2\eta}\tilde{\phi}^2 - \frac{1}{2m_{\min}\cdot\gamma_\omega}\tilde{\omega}^2 + L \\ \le & -\min\left\{\lambda_\upsilon, \frac{1}{\gamma_1}, \frac{1}{\gamma_2}, \frac{1}{m\cdot\gamma_{h1}}, \frac{1}{m\cdot\gamma_{h2}}, \right. \\ & \left. \frac{1}{m\cdot\gamma_{h3}}, \frac{1}{\gamma_g}, \frac{1}{\eta}, \frac{1}{m\cdot\gamma_\omega}\right\} \\ & \times\left[\frac{1}{2m}\mathbf{e}^T\mathbf{P}\mathbf{e} + \frac{1}{2\gamma_1}\tilde{\boldsymbol{\theta}}_1^T\tilde{\boldsymbol{\theta}}_1 + \frac{1}{2\gamma_2}\tilde{\boldsymbol{\theta}}_2^T\tilde{\boldsymbol{\theta}}_2 \right. \\ & + \frac{1}{2m\gamma_{h1}}\tilde{\boldsymbol{\theta}}_{h1}^T\tilde{\boldsymbol{\theta}}_{h1} + \frac{1}{2m\gamma_{h2}}\tilde{\boldsymbol{\theta}}_{h2}^T\tilde{\boldsymbol{\theta}}_{h2} \\ & + \frac{1}{2m\gamma_{h3}}\tilde{\boldsymbol{\theta}}_{h3}^T\tilde{\boldsymbol{\theta}}_{h3} + \frac{1}{2\gamma_g}\tilde{\boldsymbol{\theta}}_g^T\tilde{\boldsymbol{\theta}}_g \\ & \left. + \frac{1}{2\eta}\tilde{\phi}^2 + \frac{1}{2m_{\min}\cdot\gamma_\omega}\tilde{\omega}^2\right] + L.\end{aligned} \tag{52}$$

Setting $c = \min\{\lambda_\upsilon, 1/\gamma_1, 1/\gamma_2, 1/(m\cdot\gamma_{h1}), 1/(m\cdot\gamma_{h2}), 1/(m\cdot\gamma_{h3}), 1/\gamma_g, 1/\eta, 1/(m\cdot\gamma_\omega)\}$, it yields that

$$\dot{V} \le -cV + L. \tag{53}$$

Then, it is easy from (53) to show that

$$V(t) \le e^{-ct}V(0) + \frac{L}{c}. \tag{54}$$

Therefore, the output tracking error converges to a neighborhood of zero exponentially. □

Remark 3. In the future work, the control problem of uncertain T-S fuzzy time-varying delay systems with unknown dead-zone input is an important topic and is worth to be studied. Based on a novel fuzzy Lyapunov-Krasovskii functional, a delay partitioning method has been developed for the delay-dependent stability analysis of fuzzy time-varying state delay systems [26]. Obviously, it provides a useful idea to deal with the aforementioned future research.

4. An Example and Simulation Results

Consider the second-order uncertain nonlinear time-delay system containing an unknown dead-zone that is modified from the simulation example in [7] as follows:

$$\begin{aligned}\dot{x}_1 &= x_2 + \Delta\phi_1(\mathbf{x}), \\ \dot{x}_2 &= x_1 + f_{11}(\mathbf{x}(t)) + f_{22}(\mathbf{x}(t-\tau)) \\ &\quad + \Delta f_1(\mathbf{x}(t)) + \Delta f_2(\mathbf{x}(t-\tau)) \\ &\quad + g(\mathbf{x})Z(\upsilon(t)) + \Delta\phi_2(\mathbf{x}), \\ y &= x_1,\end{aligned} \tag{55}$$

where the nonlinear functions $f_{11}(\mathbf{x}(t)) = -0.3\sin x_1(t)$, $f_{12}(\mathbf{x}(t)) = 0, f_{21}(\mathbf{x}(t-\tau)) = 0$, and $f_{22}(\mathbf{x}(t-\tau)) = 0.1x_1^2(t-\tau)$ are assumed to be known, and $\Delta f_1(\mathbf{x}(t)) = -0.1x_1\sin(3x_2(t))$, $\Delta f_2(\mathbf{x}(t-\tau)) = -0.1x_1\sin(3x_2(t-\tau))$ are unknown system uncertainties with unknown upper bound functions, where τ is the time delay. $\Delta\phi_1(\mathbf{x}) = 0.1x_1\sin(t)$ and $\Delta\phi_2(\mathbf{x}) = 0.3x_2\sin(t)$ are unknown external disturbances, and $g(\mathbf{x}(t)) = 2 - \sin^2(x_1(t))$. $|\Delta f_1(\mathbf{x}(t))| \le h_2(\mathbf{x}(t)), |\Delta f_2(\mathbf{x}(t-\tau))| \le h_3(\mathbf{x}(t-\tau))$, and $Z(\upsilon(t))$ is an output of a dead-zone. The goal of control is to maintain the system output y to follow the reference signal $y_m = 0.5[\sin(t) + \sin(0.5t)]$.

In the simulation, parameters of the dead-zone are $m = 1$, $c_r = 0.5$, and $c_l = -0.5$. And their bounds are chosen as $m_{\max} = 1.5$, $m_{\min} = 0.6$, $c_{r\max} = 0.9$, $c_{r\min} = 0.1$, $c_{l\max} = -0.1$,

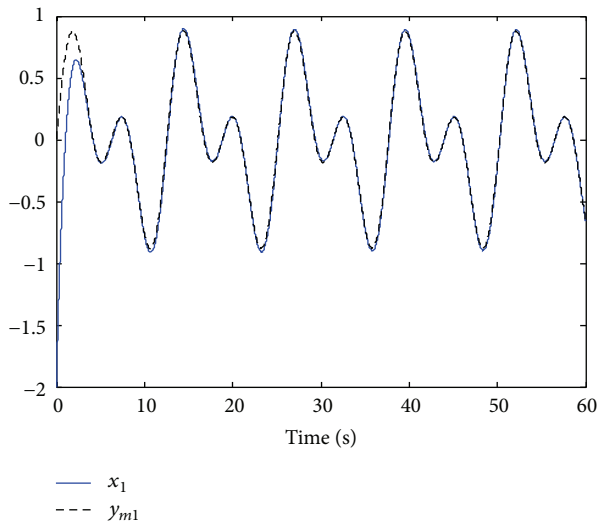

FIGURE 2: The trajectories of state x_1 and desired output y_{m1}.

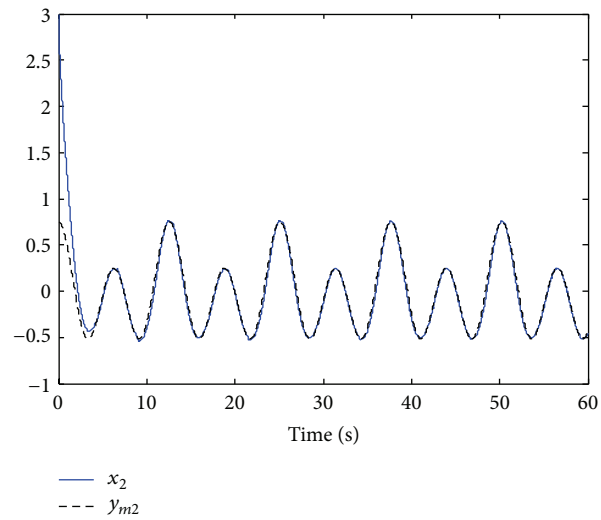

FIGURE 3: The trajectories of state x_2 and desired output y_{m2}.

and $c_{l\min} = -0.8$. In the implementation, six fuzzy sets are defined over interval $[-3, 3]$ for both x_1 and x_2, with labels $F1$, $F2$, $F3$, $F4$, $F5$, and $F6$, and their membership functions are

$$\begin{aligned}
\mu_{F1}(x_i) &= \frac{1}{1+\exp(5(x_i+2))}, \\
\mu_{F2}(x_i) &= \exp\left(-(x_i+1.5)^2\right), \\
\mu_{F3}(x_i) &= \exp\left(-(x_i+0.5)^2\right), \\
\mu_{F4}(x_i) &= \exp\left(-(x_i-0.5)^2\right), \\
\mu_{F5}(x_i) &= \exp\left(-(x_i-1.5)^2\right), \\
\mu_{F6}(x_i) &= \frac{1}{1+\exp(-5(x_i-2))}, \quad i = 1, 2.
\end{aligned} \tag{56}$$

In this section, we apply the proposed robust adaptive fuzzy tracking control approach in Section 3 to deal with the output tracking control problem of the second-order uncertain nonlinear time-delay system as shown in (55). Choose $\mathbf{K} = [10, 10]$ and $\mathbf{Q} = \mathrm{diag}[5, 5]$; then, we solve the Lyapunov equation (27) to obtain

$$\mathbf{P} = \begin{bmatrix} 5.25 & 0.25 \\ 0.25 & 0.275 \end{bmatrix}. \tag{57}$$

In this example, the sampling time is 0.01 sec. Initial values are chosen as $\mathbf{x}(0) = [-2, 3]^{\mathrm{T}}$, $\boldsymbol{\theta}_g(0) = 1$, $\boldsymbol{\theta}_{h1}(0) = 0$, $\boldsymbol{\theta}_{\mathbf{h}2}(0) = 0$, and $\boldsymbol{\theta}_{\mathbf{h}3}(0) = 0$. The initial values of the parameters to be estimated are selected as $\widehat{\phi}(0) = 0.85$, $\widehat{\boldsymbol{\theta}}_1(0) = [0\ 0]^T$, $\widehat{\boldsymbol{\theta}}_2(0) = [0\ 0]^T$. $\gamma_g = 2$, $\gamma_{h1} = 1.5$, $\gamma_{h2} = 1.5$, $\gamma_{h3} = 1.5$, $\gamma_1 = 1.5$, $\gamma_2 = 1.5$, $\gamma_\omega = 1.5$, $\eta = 1.0$, $\tau = 0.5$ s, and $\varepsilon = 0.06$. The simulation results are shown in Figures 2–5. Figures 2 and 3 show the trajectories of states x_1 and x_2 and the desired outputs y_{m1} and y_{m2}, respectively. The phase plane of tracking errors of e_1 and e_2 is shown in Figure 4. Figure 5 shows the trajectory of the control signal. Obviously, the proposed robust adaptive fuzzy tracking control scheme can achieve the objective of good tracking performance and robust stability simultaneously in spite of the controlled system containing an unknown dead-zone and uncertainties.

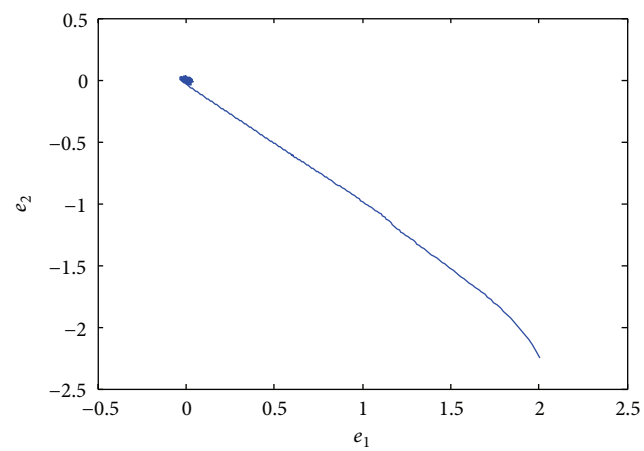

FIGURE 4: The phase plane of tracking errors e_1 and e_2.

5. Conclusion

The dead-zone input characteristics widely exist in the actuators of practical control systems, which are usually poorly known. The time-delay characteristics are usually confronted in engineering systems. The two characteristics may severely limit the performance of control. In this paper, the robust adaptive fuzzy tracking controller is designed to overcome the

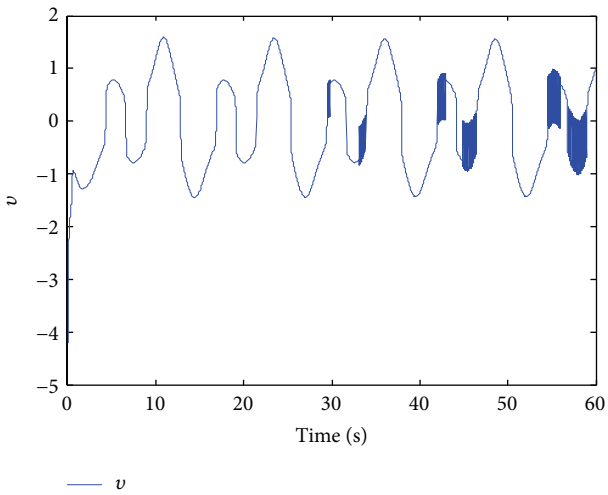

Figure 5: The trajectory of the control input $v(t)$.

stabilization problem of a class of uncertain nonlinear state time-delay systems containing unknown dead-zone input and unmatched uncertainties. By utilizing a description of a dead-zone feature to estimate the properties of the dead-zone model intuitively and mathematically, the adaptive fuzzy tracking controller is proposed without constructing the dead-zone inverse. The nonlinear uncertainties are approximated by the fuzzy logic system according to the adaptive laws. Based on the Lyapunov stability theorem, the proposed robust adaptive tracking fuzzy controller can ensure that the output tracking error of the resulting closed-loop system converges to a neighborhood of zero exponentially. Finally, some simulations results are illustrated to verify the effectiveness and performance of the proposed approach.

References

[1] J. Anthonis, A. Seuret, J. P. Richard, and H. Ramon, "Design of a pressure control system with dead band and time delay," *IEEE Transactions on Control Systems Technology*, vol. 15, no. 6, pp. 1103–1111, 2007.

[2] X.-S. Wang, C.-Y. Su, and H. Hong, "Robust adaptive control of a class of nonlinear systems with unknown dead-zone," *Automatica*, vol. 40, no. 3, pp. 407–413, 2004.

[3] M. L. Corradini and G. Orlando, "Robust stabilization of nonlinear uncertain plants with backlash or dead zone in the actuator," *IEEE Transactions on Control Systems Technology*, vol. 10, no. 1, pp. 158–166, 2002.

[4] W. Zhonghua, Y. Bo, C. Lin, and Z. Shusheng, "Robust adaptive deadzone compensation of DC servo system," *IEE Proceedings*, vol. 153, no. 6, pp. 709–713, 2006.

[5] K.-K. Shyu, W.-J. Liu, and K.-C. Hsu, "Design of large-scale time-delayed systems with dead-zone input via variable structure control," *Automatica*, vol. 41, no. 7, pp. 1239–1246, 2005.

[6] D. R. Seidl, L. Sui-Lun, J. A. Putman, and R. D. Lorenz, "Neural network compensation of gear backlash hysteresis in position-controlled mechanisms," *IEEE Transactions on Industry Applications*, vol. 31, no. 6, pp. 1475–1483, 1995.

[7] T. P. Zhang and S. S. Ge, "Adaptive neural control of MIMO nonlinear state time-varying delay systems with unknown dead-zones and gain signs," *Automatica*, vol. 43, no. 6, pp. 1021–1033, 2007.

[8] C.-C. Hua, Q.-G. Wang, and X.-P. Guan, "Adaptive tracking controller design of nonlinear systems with time delays and unknown dead-zone input," *IEEE Transactions on Automatic Control*, vol. 53, no. 7, pp. 1753–1759, 2008.

[9] S. Ibrir, W. F. Xie, and C.-Y. Su, "Adaptive tracking of nonlinear systems with non-symmetric dead-zone input," *Automatica*, vol. 43, no. 3, pp. 522–530, 2007.

[10] D. A. Recker, P. V. Kokotovic, D. Rhode, and J. Winkelman, "Adaptive nonlinear control of systems containing a deadzone," in *Proceedings of the 30th IEEE Conference on Decision and Control*, pp. 2111–2115, Brighton, UK, December 1991.

[11] G. Tao and P. V. Kokotović, "Adaptive control of plants with unknown dead-zones," *IEEE Transactions on Automatic Control*, vol. 39, no. 1, pp. 59–68, 1994.

[12] J. Zhou, C. Wen, and Y. Zhang, "Adaptive output control of nonlinear systems with uncertain dead-zone nonlinearity," *IEEE Transactions on Automatic Control*, vol. 51, no. 3, pp. 504–511, 2006.

[13] Y. Yang, "Direct robust adaptive fuzzy control (DRAFC) for uncertain nonlinear systems using small gain theorem," *Fuzzy Sets and Systems*, vol. 151, no. 1, pp. 79–97, 2005.

[14] G. Bartolini, A. Pisano, and E. Usai, "Global tracking control for a class of nonlinear uncertain systems," in *Proceedings of the 40th IEEE Conference on Decision and Control*, pp. 473–478, Orlando, Fla, USA, December 2001.

[15] Y. Hashimoto, H. Wu, and K. Mizukami, "Exponentially robust output tracking of SISO nonlinear systems with uncertainties," in *Proceedings of the 35th IEEE Conference on Decision and Control*, pp. 2077–2082, Kobe, Japan, December 1996.

[16] W. M. Haddad, T. Hayakawa, and V. Chellaboina, "Robust adaptive control for nonlinear uncertain systems," *Automatica*, vol. 39, no. 3, pp. 551–556, 2003.

[17] X. Su, P. Shi, L. Wu, and Y. D. Song, "A novel approach to filter design for T-S fuzzy discrete-time systems with time-varying delay," *IEEE Transactions on Fuzzy Systems*, vol. 20, no. 6, pp. 1114–1129, 2012.

[18] L.-L. Ou, W.-D. Zhang, and L. Yu, "Low-order stabilization of LTI systems with time delay," *IEEE Transactions on Automatic Control*, vol. 54, no. 4, pp. 774–787, 2009.

[19] W. J. Chang, C. C. Ku, and P. H. Huang, "Robust fuzzy control via observer feedback for passive stochastic fuzzy systems with time-delay and multiplicative noise," *International Journal of Innovative Computing, Information and Control*, vol. 7, no. 1, pp. 345–364, 2011.

[20] R. Yang, H. Gao, and P. Shi, "Delay-dependent robust H_∞ control for uncertain stochastic time-delay systems," *International Journal of Robust and Nonlinear Control*, vol. 20, no. 16, pp. 1852–1865, 2010.

[21] S. J. Yoo, J. B. Park, and Y. H. Choi, "Adaptive dynamic surface control for stabilization of parametric strict-feedback nonlinear systems with unknown time delays," *IEEE Transactions on Automatic Control*, vol. 52, no. 12, pp. 2360–2365, 2007.

[22] C. Lin, Q. G. Wang, and T. H. Lee, "Stabilization of uncertain fuzzy time-delay systems via variable structure control approach," *IEEE Transactions on Fuzzy Systems*, vol. 13, no. 6, pp. 787–798, 2005.

[23] R. Yang, Z. Zhang, and P. Shi, "Exponential stability on stochastic neural networks with discrete interval and distributed delays," *IEEE Transactions on Neural Networks*, vol. 21, no. 1, pp. 169–175, 2010.

[24] T. C. Lin, S. W. Chang, and C. H. Hsu, "Robust adaptive fuzzy sliding mode control for a class of uncertain discrete-time nonlinear systems," *International Journal of Innovative Computing Information and Control*, vol. 8, no. 1, pp. 347–359, 2012.

[25] S. P. Moustakidis, G. A. Rovithakis, and J. B. Theocharis, "An adaptive neuro-fuzzy tracking control for multi-input nonlinear dynamic systems," *Automatica*, vol. 44, no. 5, pp. 1418–1425, 2008.

[26] L. Wu, X. Su, P. Shi, and J. Qiu, "A new approach to stability analysis and stabilization of discrete-time T-S fuzzy time-varying delay systems," *IEEE Transactions on Systems, Man, and Cybernetics B*, vol. 41, no. 1, pp. 273–286, 2011.

[27] L. X. Wang, *Adaptive Fuzzy Systems and Control: Design and Stability Analysis*, Prentice Hall, Englewood Cliffs, NJ, USA, 1994.

Hindawi Publishing Corporation
Mathematical Problems in Engineering
Volume 2013, Article ID 234612, 8 pages
http://dx.doi.org/10.1155/2013/234612

Research Article

Robust H_∞ Control for a Class of Uncertain Switched Fuzzy Time-Delay Systems Based on T-S Models

Yang Cui,[1] Kaiqing Liu,[2] Yang Zhao,[2] and Xue Wang[2]

[1] *Teaching and Training Center of Electrical and Electronics Engineering, Harbin University of Science and Technology, Harbin, Heilongjiang 150080, China*
[2] *School of Automation, Harbin University of Science and Technology, Harbin, Heilongjiang 150080, China*

Correspondence should be addressed to Yang Cui; cuiyang97@126.com

Received 30 October 2012; Revised 28 December 2012; Accepted 28 December 2012

Academic Editor: Peng Shi

Copyright © 2013 Yang Cui et al. This is an open access article distributed under the Creative Commons Attribution License, which permits unrestricted use, distribution, and reproduction in any medium, provided the original work is properly cited.

The problem of robust H_∞ control for a class of uncertain switched fuzzy time-delay systems is discussed for system described by T-S fuzzy model with Lyapunov stable theory and linear matrix inequality approach. A sufficient condition in terms of the LMI is derived such that the stability of the closed-loop systems is guaranteed. The continuous state feedback controller is built to ensure the asymptotically stable closed-loop system for all allowable uncertainties, with the switching law designed to implement the global asymptotic stability of uncertain switched fuzzy time-delay systems. In this model, each and every subsystem of the switched systems is an uncertain fuzzy one to which the parallel distributed compensation (PDC) controller of each sub fuzzy system system is proposed with its main condition given in a more solvable form of convex combinations. Such a switched control system is highly robust to varying parameters. A simulation shows the feasibility and effectiveness of the design method.

1. Introduction

In recent years, as intelligent control method, the research of the fuzzy system has been paid extensive attention [1–3]. The T-S model which is a fuzzy system is the most effective system model. This paper is focused on a class of uncertain switched time-delay systems, in which each subsystem is T-S fuzzy model. The T-S fuzzy model is a kind of fuzzy system proposed by Sugeno et al. [4, 5], which is described by a set of fuzzy IF-THEN rules representing local linear input-output relations of a nonlinear system. The main idea of T-S fuzzy model is to express the local dynamics of each fuzzy rule by a linear system model and to express the overall system by fuzzy "blending" of the local linear system models. The stability studies based on this model fuzzy system have had yielded fruitful results [6–10]. Recently, considerable effort [11–13] has been contributed to the problem of H_∞ robust fuzzy control for a class of nonlinear systems that can be represented by T-S fuzzy models.

On the other hand, switched systems are an important class of hybrid systems. A switched system consists of a number of subsystems, both continuous time and discrete time dynamic systems, and a switching law, which orchestrates the switching between the subsystems. The applications in robot control systems, computer disc drives, and other engineering systems indicate that switched systems have extensive practice background. Therefore, it has the important theoretical significance and practical value, which has yielded fruitful research results [14–20]. A switched system is called a switched fuzzy system if all subsystems are fuzzy systems. This class of systems can often more precisely describe continuous dynamics and discrete dynamics as well as their interactions in actual systems. Compared with the results on stability of switched systems and those of fuzzy control systems, the results on switched fuzzy systems are very few. Reference [21] presents a novel switched T-S fuzzy control design approach based on control Lyapunov function. Reference [22] advances a fuzzy-basis-dependent and mode-dependent Lyapunov function to study the problems of stability analysis and H_∞ controller design for discrete-time switched fuzzy systems.

This paper will study the problem of designing state feedback H_∞ controllers for continuous-time T-S switched

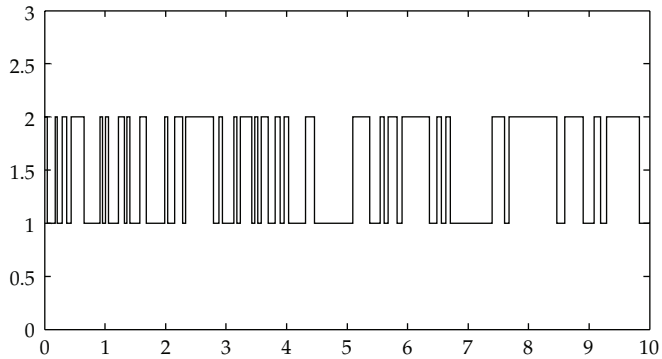

Figure 1: The switching signal.

fuzzy systems. A new type of state feedback controllers, namely, switched parallel distributed compensation (PDC) controllers, are proposed, which are switched based on the values of membership functions. The problem begins with the representation models for switched systems. The design method inherits some hybrid features and presents the information of fuzzy system. The delay-independent sufficient condition in terms of the LMI is derived such that the quadratic stability of the closed-loop systems is guaranteed. The state feedback controller is built to ensure the asymptotically stable closed-loop system for all allowable uncertainties, with the switching law designed to implement the global asymptotic stability of uncertain fuzzy time-delay switched systems. In this model, each and every subsystem of the switched systems is an uncertain fuzzy one to which the PDC controller of each sub fuzzy system system is proposed with its main condition given in a more solvable form of convex combinations. Numerical example is given to illustrate the effectiveness of the proposed method.

2. Problem Formulation

In this section, we consider the continuous uncertain switched fuzzy time-delay model; namely, every subsystem of switched systems is uncertain fuzzy time-delay system. Consider the following:

R_σ^l: if $\xi_1(t)$ is $M_{\sigma 1}^l \cdots$ and $\xi_p(t)$ is $M_{\sigma p}^l$, then

$$\begin{aligned}\dot{x}(t) &= \left[A_{\sigma l} + \Delta A_{\sigma l}(t)\right] x(t) + \left[A_{d\sigma l} + \Delta A_{d\sigma l}(t)\right] x(t-d) \\ &\quad + B_{\sigma l} u(t) + B_{1\sigma l} w(t), \\ z(t) &= C_{\sigma l} x(t), \quad x(t) = \varphi(t), \\ &\forall t \in [-d, 0], \ l = 1, 2, \ldots, N_\sigma,\end{aligned} \tag{1}$$

where $\sigma = \sigma(t) : [0, +\infty) \to \{1, 2, \ldots, N\} = \overline{N}$ is the switching signal to be designed (Figure 1).

$M_{\sigma 1}^l, \ldots, M_{\sigma p}^l$ denote fuzzy sets in the σth switched subsystem. R_σ^l denotes the lth fuzzy inference rule in the σth switched subsystem. N_σ is the number of inference rules in the σth switched subsystem, and fuzzy rules are selected in every switched subsystem. $x(t) \in R^n$ is the state variable vector, $u(t)$ is the input variable, $z(t)$ is output variable vector, $w(t)$ is external disturbance of the switched systems, and satisfies $w(t) \in L_2[0, T]$. d is the delay constant, and satisfies $d \geq 0$. $A_{\sigma l}$, $A_{d\sigma l}$, $B_{\sigma l}$, $B_{1\sigma l}$, and $C_{\sigma l}$ are known constant matrices of appropriate dimensions of the σth switched subsystem. $\Delta A_{\sigma l}$ and $\Delta A_{d\sigma l}$ are the uncertain matrices corresponding to the σth switched subsystem with appropriate dimensions. $\varphi(t)$ denotes a differentiable vector-valued initial function. $\xi_1(t), \xi_2(t), \ldots, \xi_n(t)$ are the premise variables.

In this paper, the switching signal $\sigma = \sigma(t)$ is state dependent; namely, $\sigma \in \overline{N}$, the switching signal $\sigma = \sigma(t) = i$, and the switching signal is totally described by $v_i = \begin{cases} 1, x(t) \in \widetilde{\Omega}_i \\ 0, x(t) \notin \widetilde{\Omega}_i \end{cases}$, that is, if and only $\sigma = \sigma(t) = i$, $v_i(x(t)) = 1$. $\widetilde{\Omega}_1, \widetilde{\Omega}_2, \ldots, \widetilde{\Omega}_n$ will be designed later.

Through the function $v_i(x(t))$, the global model of the ith switched subsystem is described by

$$\begin{aligned}\dot{x}(t) &= \sum_{i=1}^{n} v_i(t) \sum_{l=1}^{N_i} \eta_{il}(\xi(t)) \left[A_{il} + \Delta A_{il}(t)\right] x(t) \\ &\quad + \left[A_{dil} + \Delta A_{dil}(t)\right] x(t-d) \\ &\quad + B_{il} u(t) + B_{1il} w(t), \\ z(t) &= \sum_{i=1}^{n} v_i(t) \sum_{l=1}^{N_i} \eta_{il}(\xi(t)) C_{il} x(t), \quad x(t) = \varphi(t), \\ &\forall t \in [-d, 0], \quad i = 1, 2, \ldots, n, \quad l = 1, 2, \ldots, N_i,\end{aligned} \tag{2}$$

where $0 \leq \eta_{il}(\xi(t)) \leq 1$, and $\sum_{l=1}^{N_i} \eta_{il}(\xi(t)) = 1$.

Also, $\omega_{il}(\xi(t)) = \prod_{\rho=1}^{p} M_{i\rho}^l(\xi_\rho(t))$, and $\eta_{il} = \omega_{il}(\xi(t)) / \sum_{l=1}^{N_i} \omega_{il}(\xi(t))$, where $M_{i\rho}^l(\xi_\rho(t))$ denotes the membership function, and $\xi_\rho(t)$ belongs to the fuzzy set $M_{i\rho}^l$.

Definition 1. The H_∞ control problem for the switched fuzzy system (1) is stated as follows.

Let a constant $\gamma > 0$ be given. Find a continuous state feedback controller $u = u(x)$ for each subsystem and a switching law $i = \sigma(t)$ such that

(1) the closed-loop system is asymptotically stable when $w(t) = 0$,

(2) the output z satisfies $\|z\|_{L_2[0,T]} < \gamma\|w\|_{L_2[0,T]}$ under the zero initial condition.

3. Main Results

Assumption 2. The uncertainties can be represented and emulated as

$$[\Delta A_{il}, \Delta A_{dil}] = E_{il}\Sigma_{il}(t)[F_{1il}, F_{2il}], \quad i = 1, 2, \ldots, n, \ l = 1, 2, \ldots, N_i, \tag{3}$$

where, E_{il}, F_{1il}, and F_{2il} are known constant matrices, and $\Sigma_{il}(t)$ is an unknown time-varying matrix satisfying $\Sigma_{il}^T(t)\Sigma_{il}(t) < I$, for all $t \geq 0$.

Here, the PDC fuzzy controller design method is used for each sub fuzzy system namely, fuzzy controller and system (2) have the same fuzzy inference premise variables. Consider the following:

R_j^l: if $\xi_1(t)$ is $M_{j1}^l \cdots$ and $\xi_p(t)$ is M_{jp}^l, then

$$u(t) = K_{jl}x(t), \quad j = 1, 2, \ldots, n, \ l = 1, 2, \ldots, N_j. \tag{4}$$

Thus, the global controller is

$$u(t) = \sum_{i=1}^{n} \upsilon_i(t) \sum_{l=1}^{N_i} \eta_{il}(\xi(t)) K_{il}x(t). \tag{5}$$

The global closed-loop system can be expressed as follows:

$$\begin{aligned}\dot{x}(t) = {} & \sum_{i=1}^{n} \upsilon_i(t) \sum_{l=1}^{N_i} \eta_{il}(\xi(t)) \\ & \times \sum_{h=1}^{N_i} \eta_{ih}(\xi(t)) \big[(A_{il} + B_{il}K_{ih} + \Delta A_{il}(t))x(t) \\ & + (A_{dil} + \Delta A_{dil}(t))x(t-d) \\ & + B_{1il}w(t)\big],\end{aligned} \tag{6}$$

$$z(t) = \sum_{i=1}^{n} \upsilon_i(t) \sum_{l=1}^{N_i} \eta_{il}(\xi(t)) C_{il}x(t), \quad x(t) = \varphi(t),$$

$$\forall t \in [-d, 0], \ i = 1, 2, \ldots, n, \ h, l = 1, 2, \ldots, N_i.$$

Lemma 3 (see [23]). *Let R_1 and R_2 be real matrices of appropriate dimensions, with $\Sigma^T(t)\Sigma(t) \leq I$; then, one has that for any scalar $\alpha > 0$,*

$$R_1\Sigma(t)R_2 + R_2^T\Sigma^T(t)R_1^T \leq \alpha R_1R_1^T + \alpha^{-1}R_2^TR_2. \tag{7}$$

Lemma 4 (Lemma (Schur complement)). *The matrix $\begin{bmatrix} Q & R \\ R^T & S \end{bmatrix} < 0$ is symmetrical matrix, and then the following two functions are equivalent:*

$$S < 0, \quad Q - RS^{-1}R^T < 0, \quad or \quad Q < 0, \quad S - RQ^{-1}R^T < 0. \tag{8}$$

Theorem 5. *Let a constant $\gamma > 0$ be given. If there exist the symmetric positive definite matrices $X, Q_i \in R^{n\times n}$, scalar $\varepsilon, \varepsilon_1, \varepsilon_2 > 0$, α_i ($\alpha_i \in [0, 1]$, $\sum_{i=1}^n \alpha_i = 1$), and the matrices W_{ih} satisfying*

$$\sum_{i=1}^{n} \alpha_i \begin{bmatrix} \begin{matrix}(A_{il}X + B_{il}W_{ih})^T \\ + (A_{il}X + B_{il}W_{ih}) + Q_i\end{matrix} & * & * & * & * & * & 0 \\ E_{il}^T & -\varepsilon I & 0 & 0 & 0 & 0 & 0 \\ F_{1il}X & 0 & -\varepsilon_1^{-1}I & 0 & 0 & 0 & 0 \\ C_{il}X & 0 & 0 & -I & 0 & 0 & 0 \\ B_{1il}^T & 0 & 0 & 0 & -\gamma^2 I & 0 & 0 \\ 0 & 0 & 0 & 0 & 0 & -\varepsilon_2^{-1}I & * \\ XA_{dil}^T & 0 & 0 & 0 & 0 & XF_{2il}^T & -Q_i \end{bmatrix} < 0, \tag{9}$$

then system (6) is globally asymptotically stable, and H_∞ robust control problem is solvable under the switching law $\sigma(t)$, where $\varepsilon^{-1} = \varepsilon_1^{-1} + \varepsilon_2^{-1}$.

So, the gain matrices of switched fuzzy controllers and the switching law are given as follows:

$$K_{ih} = W_{ih}X^{-1}, \tag{10}$$

$$\sigma(t) = \arg\min_{i\in\overline{N}} \max_{l,h} \left\{ x^T \begin{bmatrix} R_{ilh} + \gamma^{-2}PB_{1il}B_{1il}^TP + C_{il}C_{il}^T & PA_{dil} \\ A_{dil}^TP & -S_i + \varepsilon_2F_{2il}^TF_{2il} \end{bmatrix} x, \quad l, h = 1, 2, \ldots, N_i \right\}, \tag{11}$$

where

$$\begin{aligned} P &= X^{-1}, \\ R_{ilh} &= (A_{il} + B_{il}K_{ih})^TP + P(A_{il} + B_{il}K_{ih}) \\ &\quad + S_i + \varepsilon^{-1}PE_{il}^TE_{il}P + \varepsilon_1F_{1il}^TF_{1il}. \end{aligned} \tag{12}$$

Proof. We define $K_{ih} = W_{ih}X^{-1}$ and $S_i = X^{-1}Q_iX^{-1}$.

So, choose the Lyapunov function as follows:

$$V(t) = x^T(t)Px(t) + \int_{t-d}^{t} x^T(\tau)S_ix(\tau)\,d\tau. \tag{13}$$

We now compute the time derivative of the function (13):

$$\begin{aligned}\dot{V}(t) = {} & \sum_{i=1}^{n} \upsilon_i(t) \sum_{l=1}^{N_i} \eta_{il}(\xi(t)) \\ & \times \sum_{i=1}^{n} \eta_{ih}(t) \big\{x^T \big[(A_{il} + B_{il}K_{il})^TP + P(A_{il} + B_{il}K_{il}) \\ & + \Delta A_{il}^T(t)P + P\Delta A_{il}(t) + S_i\big] x\end{aligned}$$

$$
\begin{aligned}
&+ x^T PB_{1il} w + w^T B_{1il}^T Px \\
&+ x(t-d)^T A_{dil}^T Px \\
&+ x^T PA_{dil} x(t-d) \\
&+ x(t-d)^T \Delta A_{dil}^T Px \\
&+ x^T \Delta PA_{dil} x(t-d) \\
&- x(t-d)^T S_i x(t-d) \Big\}. \qquad (14)
\end{aligned}
$$

It follows from Lemma 3 that for any of scalars $\varepsilon_1 > 0$ and $\varepsilon_2 > 0$, we have that

$$
\begin{aligned}
\Delta A_{il}^T(t) P + P\Delta A_{il}(t) &= F_{1il}^T \Sigma_i^T(t) E_{il}^T P + PE_{il}\Sigma_i(t) F_{1il} \\
&\le \varepsilon_1 F_{1il}^T F_{1il} + \varepsilon_1^{-1} PE_{il} E_{il}^T P, \\
x^T(t-d)\Delta A_{il}^T(t) Px + x^T P\Delta A_{il}(t) x(t-d) &= x^T(t-d) F_{2il}^T \Sigma_{ij}^T(t) E_{il}^T Px + x^T PE_{il}\Sigma_{il}(t) F_{2il} x(t-d) \\
&\le \varepsilon_2 x^T(t-d) F_{2il}^T F_{2il} x(t-d) + \varepsilon_2^{-1} x^T PE_{il} E_{il}^T Px. \qquad (15)
\end{aligned}
$$

When $w(t) = 0$, the function (14) can be given as follows:

$$
\begin{aligned}
\dot{V}(t) &\le \sum_{i=1}^{n} v_i(t) \sum_{l=1}^{N_i} \eta_{il}(\xi(t)) \\
&\quad \times \sum_{i=1}^{n} \eta_{ih}(\xi(t)) \Big\{ x^T \Big[(A_{il} + B_{il}K_{il})^T P \\
&\qquad + P(A_{il} + B_{il}K_{il}) \\
&\qquad + \varepsilon_1 F_{1il}^T F_{1il} + \varepsilon^{-1} PE_{il} E_{il}^T P + S_i \Big] x \\
&\qquad + x(t-d)^T A_{dil}^T Px + x^T PA_{dil} x(t-d) \\
&\qquad - x^T(t-d)\left(S_i - \varepsilon_2 F_{2il}^T F_{2il}\right) x(t-d) \Big\} \\
&= \sum_{i=1}^{n} v_i(t) \sum_{i=1}^{n} \eta_{il}(\xi(t)) \\
&\quad \times \sum_{i=1}^{n} \eta_{ih}(\xi(t)) \left[x^T x^T(t-d) \right] \begin{bmatrix} R_{ilh} & PA_{dil} \\ A_{dil}^T P & -S_i + \varepsilon_2 F_{2il}^T F_{2il} \end{bmatrix} \\
&\quad \times \begin{bmatrix} x \\ x(t-d) \end{bmatrix}. \qquad (16)
\end{aligned}
$$

That is,

$$
\begin{aligned}
\dot{V}(t) &\le \sum_{i=1}^{n} v_i(t) \sum_{i=1}^{n} \eta_{il}(\xi(t)) \\
&\quad \times \sum_{i=1}^{n} \eta_{ih}(\xi(t)) \zeta^T(t) \begin{bmatrix} R_{ilh} & PA_{dil} \\ A_{dil}^T P & -S_i + \varepsilon_2 F_{2il}^T F_{2il} \end{bmatrix} \zeta(t), \qquad (17)
\end{aligned}
$$

where $\zeta(t) = \left[\begin{smallmatrix} x \\ x(t-d) \end{smallmatrix} \right]$. So, we need to prove that $\left[\begin{smallmatrix} R_{ilh} & PA_{dil} \\ A_{dil}^T P & -S_i + \varepsilon_2 F_{2il}^T F_{2il} \end{smallmatrix} \right] < 0$, the closed-loop system (6) is asymptotically stable when $w(t) = 0$.

Inequalities (9) are pre- and postmultiplied by the transformation diag$\{P, I, I, I, I, I, P\}$, respectively. In turn, we have tha following:

$$
\sum_{i=1}^{n} \alpha_i \begin{bmatrix}
(A_{il} + B_{il}K_{ih})^T P & & & & & & \\
+P(A_{il} + B_{il}K_{ih}) + S_i & * & * & * & * & * & 0 \\
E_{il}^T P & -\varepsilon I & 0 & 0 & 0 & 0 & 0 \\
F_{1il} & 0 & -\varepsilon_1^{-1} I & 0 & 0 & 0 & 0 \\
C_{il} & 0 & 0 & -I & 0 & 0 & 0 \\
B_{1il}^T P & 0 & 0 & 0 & -\gamma^2 I & 0 & 0 \\
0 & 0 & 0 & 0 & 0 & -\varepsilon_2^{-1} I & * \\
A_{dil}^T P & 0 & 0 & 0 & 0 & F_{2il}^T & -S_i
\end{bmatrix} < 0. \qquad (18)
$$

Due to Lemma 4, inequality (18) can be changed as follows:

$$
\sum_{i=1}^{n} \alpha_i \begin{bmatrix} R_{ilh} + \gamma^{-2} PB_{1il} B_{1il}^T P + C_{il} C_{il}^T & PA_{dil} \\ A_{dil}^T P & -S_i + \varepsilon_2 F_{2il}^T F_{2il} \end{bmatrix} < 0. \qquad (19)
$$

So, for any $x \in R^n \setminus \{0\}$,

$$
\begin{aligned}
&\sum_{i=1}^{n} \alpha_i \left\{ x^T \begin{bmatrix} R_{ilh} + \gamma^{-2} PB_{1il} B_{1il}^T P + C_{il} C_{il}^T & PA_{dil} \\ A_{dil}^T P & -S_i + \varepsilon_2 F_{2il}^T F_{2il} \end{bmatrix} x \right\} \qquad (20) \\
&< 0.
\end{aligned}
$$

Due to the switching law (11), for all $t \ge 0$, the inequality is tenable as follows:

$$
x^T \begin{bmatrix} R_{ilh} + \gamma^{-2} PB_{1il} B_{1il}^T P + C_{il} C_{il}^T & PA_{dil} \\ A_{dil}^T P & -S_i + \varepsilon_2 F_{2il}^T F_{2il} \end{bmatrix} x < 0. \qquad (21)
$$

Let

$$
\begin{aligned}
\Omega_i = \Big\{ x \in R^n \mid x^T &\times \begin{bmatrix} R_{ilh} + \gamma^{-2} PB_{1il} B_{1il}^T P + C_{il} C_{il}^T & PA_{dil} \\ A_{dil}^T P & -S_i + \varepsilon_2 F_{2il}^T F_{2il} \end{bmatrix} x \\
&< 0 \Big\}. \qquad (22)
\end{aligned}
$$

Constructing the sets $\widetilde{\Omega}_1 = \Omega_1, \ldots, \widetilde{\Omega}_n = \Omega_n - \bigcup_{i=1}^{n-1} \widetilde{\Omega}_i$, obviously, we have $\bigcup_{i=1}^{n} \widetilde{\Omega}_i = R^n \setminus \{0\}$, and $\widetilde{\Omega}_i \cap \widetilde{\Omega}_j = \Phi$, $i \ne j$.

Now, we focus on designing a switching law as follows:

$$
\sigma = i, \qquad x(t) \in \widetilde{\Omega}_i. \qquad (23)
$$

When $w = 0$, $\sum_{i=1}^{n} \alpha_i \left[\begin{smallmatrix} R_{ilh} & PA_{dil} \\ A_{dil}^T P & -S_i + \varepsilon_2 F_{2il}^T F_{2il} \end{smallmatrix} \right] < 0$ is correct. So, we have that $\dot{V}(t) \le \sum_{i=1}^{n} v_i(t) \sum_{i=1}^{n} \eta_{il}(\xi(t)) \sum_{i=1}^{n} \eta_{ih}(\xi(t))$

$\zeta^T(t)\begin{bmatrix} R_{ilh} & PA_{dil} \\ A_{dil}^T P & -S_i + \varepsilon_2 F_{2il}^T F_{2il} \end{bmatrix}\zeta(t) < 0$; so, the system is asymptotically stable.

From the design of switching law, we can obtain that $\dot{V}(t) < 0$, for all $x(t) \neq 0$; that is, the switching fuzzy controllers can make the system (6) asymptotically stable, when $w = 0$.

To demonstrate that the H_∞ control problem of system is solvable, we define that

$$J = \int_0^\infty \left[z^T(t)z(t) - \gamma^2 w^T(t)w(t)\right]dt. \tag{24}$$

Thus, when the initial state is $x(t) = 0$, for any nonzero vector $w(t) \in L_2[0,\infty)$, the function J can be written as follows:

$$\begin{aligned} J &= \int_0^\infty \left[z^T(t)z(t) - \gamma^2 w^T(t)w(t) + \dot{V}(t)\right]dt \\ &\quad - [V(\infty) - V(0)] \\ &= \int_0^\infty \left[z^T(t)z(t) - \gamma^2 w^T(t)w(t) + \dot{V}(t)\right]dt - V(\infty) \\ &\le \int_0^\infty \left[z^T(t)z(t) - \gamma^2 w^T(t)w(t) + \dot{V}(t)\right]dt. \end{aligned} \tag{25}$$

Due to the Lemma 3, the function (14) can be changed as follows:

$$\begin{aligned} \dot{V}(t) \le &\sum_{i=1}^n \upsilon_i(t)\sum_{l=1}^{N_i}\eta_{il}(\xi(t)) \\ &\times \sum_{i=1}^n \eta_{ih}(\xi(t))\left\{x^T\left[\left(A_{il} + B_{il}K_{il}\right)^T P\right.\right. \\ &\qquad + P\left(A_{il} + B_{il}K_{il}\right) \\ &\qquad + \varepsilon_1 F_{1il}^T F_{1il} + \varepsilon^{-1} PE_{il}E_{il}^T P \\ &\qquad \left. + S_i + \gamma^{-2} PB_{1il}B_{1il}^T P\right] x \\ &\quad + \gamma^2 w^T w + x(t-d)^T A_{dil}^T Px \\ &\quad + x^T PA_{dil}x(t-d) - x^T(t-d) \\ &\quad \left.\times\left(S_i - \varepsilon_2 F_{2il}^T F_{2il}\right)x(t-d)\right\}. \end{aligned} \tag{26}$$

So, the function J can be further expressed as follows:

$$\begin{aligned} J \le &\sum_{i=1}^n \upsilon_i(t)\sum_{l=1}^{N_i}\eta_{il}(\xi(t))\sum_{i=1}^n \eta_{ih}(\xi(t)) \\ &\times \int_0^\infty \left\{x^T\left[\left(A_{il} + B_{il}K_{il}\right)^T P + P\left(A_{il} + B_{il}K_{il}\right)\right.\right. \\ &\qquad + \varepsilon_1 F_{1il}^T F_{1il} + \varepsilon^{-1} PE_{il}E_{il}^T P \\ &\qquad \left. + S_i + \gamma^{-2} PB_{1il}B_{1il}^T P + C_{il}^T C_{il}\right] x \\ &\quad + x(t-d)^T A_{dil}^T Px + x^T PA_{dil}x(t-d) \\ &\quad \left. - x^T(t-d)\left(S_i - \varepsilon_2 F_{2il}^T F_{2il}\right)x(t-d)\right\}dt \\ = &\sum_{i=1}^n \upsilon_i(t)\sum_{l=1}^{N_i}\eta_{il}(\xi(t))\sum_{i=1}^n \eta_{ih}(\xi(t)) \\ &\times \int_0^\infty \left[x^T \quad x^T(t-d)\right]\begin{bmatrix} R_{ilh} + \gamma^{-2}PB_{1il}B_{1il}^T P + C_{il}C_{il}^T & PA_{dil} \\ A_{dil}^T P & -S_i + \varepsilon_2 F_{2il}^T F_{2il} \end{bmatrix} \\ &\quad \times \begin{bmatrix} x \\ x(t-d) \end{bmatrix} dt \\ = &\sum_{i=1}^n \upsilon_i(t)\sum_{l=1}^{N_i}\eta_{il}(\xi(t))\sum_{i=1}^n \eta_{ih}(\xi(t)) \\ &\times \int_0^\infty \zeta^T(t)\begin{bmatrix} R_{ilh} + \gamma^{-2}PB_{1il}B_{1il}^T P + C_{il}C_{il}^T & PA_{dil} \\ A_{dil}^T P & -S_i + \varepsilon_2 F_{2il}^T F_{2il} \end{bmatrix} \\ &\quad \times \zeta(t)\,dt. \end{aligned} \tag{27}$$

□

From the design of switching law, we get that $J < 0$; that is, for any $w(t) \in L_2[0,\infty)$, $\|z\|_{L_2[0,T]} < \gamma\|w\|_{L_2[0,T]}$ holds.

4. Simulation Example

The switched systems (1) consists of two fuzzy subsystems, and each subsystem has two fuzzy rules; that is, $n = 2$, and $N_i = 2$, where $i = 1, 2$. Hence, we approximate the system by the following modes:

R_1^1: if $\xi_1(t)$ is M_{11}^1, then

$$\begin{aligned} \dot{x}(t) = &\left[A_{11} + \Delta A_{11}(t)\right]x(t) + \left[A_{d11} + \Delta A_{d11}(t)\right]x(t-d) \\ &+ B_{11}u(t) + B_{111}w(t), \qquad z(t) = C_{11}x(t), \end{aligned} \tag{28}$$

R_1^2: if $\xi_1(t)$ is M_{11}^2, then

$$\begin{aligned} \dot{x}(t) = &\left[A_{12} + \Delta A_{12}(t)\right]x(t) + \left[A_{d12} + \Delta A_{d12}(t)\right]x(t-d) \\ &+ B_{12}u(t) + B_{112}w(t), \qquad z(t) = C_{12}x(t), \end{aligned} \tag{29}$$

R_2^1: if $\xi_1(t)$ is M_{21}^1, then

$$\begin{aligned}\dot{x}(t) = {} & [A_{21} + \Delta A_{21}(t)]\, x(t) + [A_{d21} + \Delta A_{d21}(t)]\, x(t-d) \\ & + B_{21}u(t) + B_{121}w(t), \qquad z(t) = C_{21}x(t),\end{aligned} \tag{30}$$

R_2^2: if $\xi_1(t)$ is M_{21}^2, then

$$\begin{aligned}\dot{x}(t) = {} & [A_{22} + \Delta A_{22}(t)]\, x(t) + [A_{d22} + \Delta A_{d22}(t)]\, x(t-d) \\ & + B_{22}u(t) + B_{122}w(t), \qquad z(t) = C_{22}x(t),\end{aligned} \tag{31}$$

where

$$\begin{gathered}A_{11} = \begin{bmatrix}-5 & 1\\ 4 & -2\end{bmatrix}, \quad A_{12} = \begin{bmatrix}-6 & -2\\ 5 & -3\end{bmatrix}, \quad A_{21} = \begin{bmatrix}-6 & 1\\ 7 & -4\end{bmatrix}, \\ A_{22} = \begin{bmatrix}-4 & -3\\ 6 & -2\end{bmatrix}, \quad A_{d11} = \begin{bmatrix}0.1 & 0.6\\ 0.6 & 0.2\end{bmatrix}, \\ A_{d12} = \begin{bmatrix}0.3 & 0.4\\ 0.5 & 0.3\end{bmatrix}, \quad A_{d21} = \begin{bmatrix}0.4 & 0.3\\ 0.2 & 0.1\end{bmatrix}, \\ A_{d22} = \begin{bmatrix}0.5 & 0.1\\ 0.3 & 0.6\end{bmatrix}, \\ B_{11} = \begin{bmatrix}-1\\ -2\end{bmatrix}, \quad B_{12} = \begin{bmatrix}1\\ -2\end{bmatrix}, \\ B_{21} = \begin{bmatrix}-1\\ -2\end{bmatrix}, \quad B_{22} = \begin{bmatrix}1\\ -2\end{bmatrix}, \quad B_{111} = \begin{bmatrix}0.4654\\ 1.4937\end{bmatrix}, \\ B_{112} = \begin{bmatrix}0.3478\\ 1.5417\end{bmatrix}, \quad B_{121} = \begin{bmatrix}0.8324\\ 1.6574\end{bmatrix}, \\ B_{122} = \begin{bmatrix}0.6497\\ 1.8876\end{bmatrix}, \quad C_{11} = [-1 \;\; -1], \quad C_{12} = [1 \;\; -1], \\ C_{21} = [-1 \;\; -1], \quad C_{22} = [1 \;\; -1], \\ E_{11} = E_{12} = E_{21} = E_{22} = \begin{bmatrix}0.4\\ 0.2\end{bmatrix}, \\ F_{111} = F_{112} = F_{121} = F_{122} = [0.3 \;\; 0.2], \\ F_{111} = F_{212} = F_{221} = F_{222} = [0.2 \;\; 0.1], \\ \alpha_1 = \alpha_2 = 0.5, \\ \Sigma_{11}(t) = \Sigma_{12}(t) = \Sigma_{21}(t) = \Sigma_{22}(t) = 0.2\sin t, \\ w(t) = e^{-0.5t}\sin(2\pi t).\end{gathered} \tag{32}$$

The membership functions are, respectively,

$$\begin{gathered}\mu_{M_{11}^1}(x_1) = \mu_{M_{21}^1}(x_1) = 1 - \frac{1}{1+e^{-4x_1}}, \\ \mu_{M_{11}^2}(x_1) = \mu_{M_{21}^2}(x_1) = \frac{1}{1+e^{-4x_1}}.\end{gathered} \tag{33}$$

Let $\gamma = 1/\sqrt{2}$, choosing $u(t) = -\sum_{i=1}^{n} v_i(t) \sum_{l=1}^{N_i} \eta_{il}(\xi(t)) K_{il} x(t)$, where $i = 1, 2$ and $N_i = 2$.

For the linear matrix inequality (9) of Theorem 5, the following can be obtained with LMI toolbox:

$$\begin{gathered}X = \begin{bmatrix}6.3950 & -1.4630\\ -1.4630 & 4.1467\end{bmatrix}, \quad Q_1 = \begin{bmatrix}29.2473 & -21.0996\\ -21.0996 & 71.6683\end{bmatrix}, \\ Q_2 = \begin{bmatrix}26.7269 & -19.7250\\ -19.7250 & 69.5959\end{bmatrix}, \\ W_{11} = [22.5630 \;\; 34.4393], \quad W_{12} = [-30.4831 \;\; 48.9880], \\ W_{21} = [6.0884 \;\; 48.0289], \\ W_{22} = [-14.9545 \;\; 49.1351], \quad \omega_1 = 0.0087, \\ \omega_2 = 0.0086.\end{gathered} \tag{34}$$

Because $K_{ih} = W_{ih}X^{-1}$, we have that

$$\begin{gathered}K_{11} = [5.9048 \;\; 10.3884], \; K_{12} = [-2.2453 \;\; 11.0215], \\ K_{21} = [3.9180 \;\; 12.9647], \; K_{22} = [0.4050 \;\; 11.9920].\end{gathered} \tag{35}$$

Designing the switching law by (11), the system state responses with the initial condition $x(0) = \left[\begin{smallmatrix}1\\ -0.8\end{smallmatrix}\right]$ are depicted by Figure 2 which is obtained by the Matlab simulation.

Obviously, the closed-loop switched fuzzy system is stable under the corresponding switching laws and the robust fuzzy controllers in Figure 3, in spite of the influences by parameter uncertainties and time-delay, and possesses the strong robustness. Comparing their results with others, the simulation results indicate that the design controllers can satisfy the robust performance requirements under the corresponding switching laws.

5. Conclusions

In this paper, the problem of state feedback robust H_∞ control for a class of uncertain switched fuzzy time-delay systems based on T-S models is discussed. The sufficient condition in terms of the LMI is derived such that the quadratic stability of the closed-loop systems is guaranteed. A new type of continuous state feedback PDC controllers are built to ensure the asymptotically stable closed-loop system with H_∞ disturbance attenuation level γ, with the switching law designed to implement the global asymptotic stability of uncertain fuzzy time-delay switched systems. The results are also extended to the interval fuzzy time-delay systems. Simulation results demonstrate that a quality control performance has been achieved.

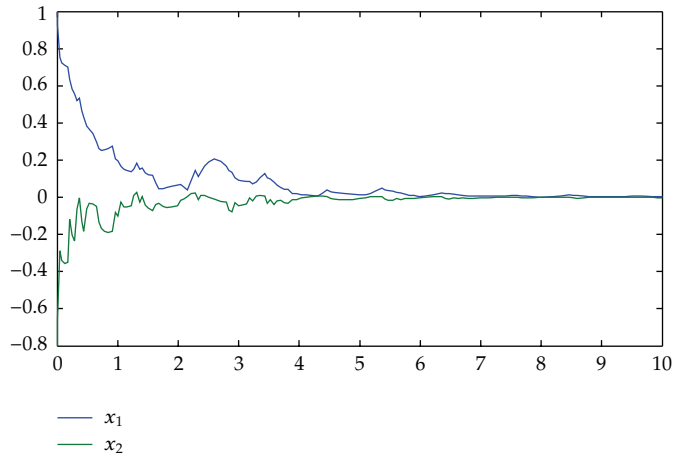

Figure 2: The system state responses.

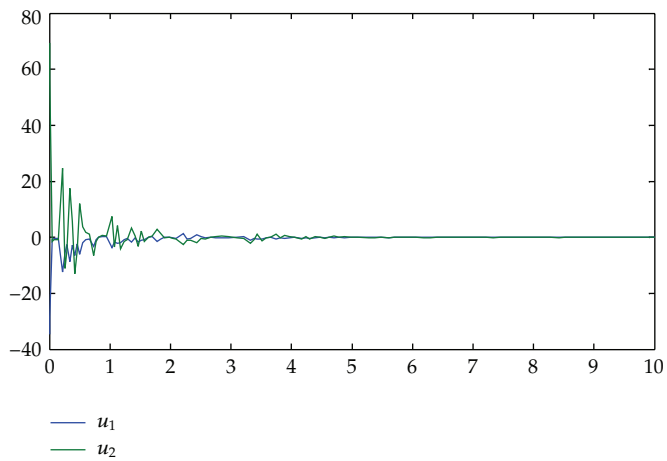

Figure 3: The system control inputs.

Acknowledgment

This work is partially supported by Scientific Research Fund of Heilongjiang Provincial Education Department 2010 (no. 11551092).

References

[1] K. Lee, E. T. Jeung, and H. B. Park, "Robust fuzzy H_∞ control for uncertain nonlinear systems via state feedback: an LMI approach," *Fuzzy Sets and Systems*, vol. 120, no. 1, pp. 123–134, 2001.

[2] M. J. Wang and M. F. Yang, "Application of signed distances method to integrate linear programming for fuzzy multi-objective project management," *International Journal of Innovative Computing, Information and Control*, vol. 7, no. 1, pp. 237–252, 2011.

[3] M. H. Bahari, A. Karsaz, and N. Pariz, "High maneuvering target tracking using a novel hybrid Kalman filter-fuzzy logic architecture," *International Journal of Innovative Computing, Information and Control*, vol. 7, no. 2, pp. 501–510, 2011.

[4] T. Takagi and M. Sugeno, "Fuzzy identification of systems and its applications to modeling and control," *IEEE Transactions on Systems, Man and Cybernetics*, vol. 15, no. 1, pp. 116–132, 1985.

[5] K. Tanaka and M. Sugeno, "Stability analysis and design of fuzzy control systems," *Fuzzy Sets and Systems*, vol. 45, no. 2, pp. 135–156, 1992.

[6] W. J. Wang and C. H. Sun, "Relaxed stability and stabilization conditions for a T-S fuzzy discrete system," *Fuzzy Sets and Systems*, vol. 156, no. 2, pp. 208–225, 2005.

[7] X. Liu and Q. Zhang, "Approaches to quadratic stability conditions and H_∞ control designs for T-S fuzzy systems," *IEEE Transactions on Fuzzy Systems*, vol. 11, no. 6, pp. 830–839, 2003.

[8] M. Wang, B. Chen, and S. Tong, "Adaptive fuzzy tracking control for strict-feedback nonlinear systems with unknown time delays," *International Journal of Innovative Computing, Information and Control*, vol. 4, no. 4, pp. 829–837, 2008.

[9] D. H. Lee, J. B. Park, Y. H. Joo, and H. S. Moon, "Further studies on stabilization conditions for discrete-time Takagi-Sugeno fuzzy systems," in *Proceedings of the IEEE International Conference on Fuzzy Systems (FUZZ-IEEE '09)*, pp. 831–835, August 2009.

[10] L. Wu, X. Su, P. Shi, and J. Qiu, "A new approach to stability analysis and stabilization of discrete-time T-S fuzzy time-varying delay systems," *IEEE Transactions on Systems, Man, and Cybernetics B*, vol. 41, no. 1, pp. 273–286, 2011.

[11] X. J. Su, L. G. Wu, P. Shi, and Y. D. Song, "H_∞ model reduction of T-S Fuzzy stochastic systems," *IEEE Transactions on Systems, Man, and Cybernetics B*, vol. 42, no. 2, pp. 1574–1585, 2012.

[12] L. Wu, X. Su, P. Shi, and J. Qiu, "Model approximation for discrete-time state-delay systems in the TS fuzzy framework," *IEEE Transactions on Fuzzy Systems*, vol. 19, no. 2, pp. 366–378, 2011.

[13] W. J. Chang, C. C. Ku, and P. H. Huang, "Robust fuzzy control via observer feedback for passive stochastic fuzzy systems with time-delay and multiplicative noise," *International Journal of Innovative Computing, Information and Control*, vol. 7, no. 1, pp. 345–364, 2011.

[14] J. Daafouz, P. Riedinger, and C. Iung, "Stability analysis and control synthesis for switched systems: a switched Lyapunov function approach," *IEEE Transactions on Automatic Control*, vol. 47, no. 11, pp. 1883–1887, 2002.

[15] Z. He, M. Wang, and S. Liu, "Discrete sliding mode prediction control of uncertain switched systems," *Journal of Systems Engineering and Electronics*, vol. 20, no. 5, pp. 1065–1071, 2009.

[16] F. Li and X. Zhang, "A delay-dependent bounded real lemma for singular LPV systems with time-variant delay," *International Journal of Robust and Nonlinear Control*, vol. 22, no. 5, pp. 559–574, 2012.

[17] Z. Wu, P. Shi, H. Su, and J. Chu, "Delay-dependent stability analysis for switched neural networks with time-varying delay," *IEEE Transactions on Systems, Man and Cybernetics B*, vol. 41, no. 6, pp. 1522–1530, 2011.

[18] Z. L. He, L. G. Wu, and X. J. Su, "H_∞ control of linear positive systems: continuous-and discrete-time cases," *International Journal of Innovative Computing, Information and Control*, vol. 5, no. 6, pp. 1747–1756, 2009.

[19] E. Fridman and U. Shaked, "Delay-dependent stability and H_∞ control: constant and time-varying delays," *International Journal of Control*, vol. 76, no. 1, pp. 48–60, 2003.

[20] Z. L. He, J. F. Wu, G. H. Sun, and C. Gao, "State estimation and sliding mode control of uncertain switched hybrid systems," *International Journal of Innovative Computing, Information and Control*, vol. 20, no. 5, pp. 1065–1071, 2009.

[21] S. S. Chen, Y. Chang, J. L. Wu, W. C. Cheng, and S. F. Su, "Fuzzy control design for switched nonlinear systems," in *Proceedings of the SICE Annual Conference of International Conference on Instrumentation, Control and Information Technology*, pp. 352–357, August 2008.

[22] Y. Chen, L. X. Zhang, H. R. Karimi, and X. D. Zhao, "Stability analysis and controller design of a class of switched discrete-time fuzzy systems," in *Proceedings of the 50th IEEE Conference on Decision and Control and European Control Conference*, pp. 6159–6164, 2011.

[23] I. R. Petersen, "A stabilization algorithm for a class of uncertain linear systems," *Systems and Control Letters*, vol. 8, no. 4, pp. 351–357, 1987.

Hindawi Publishing Corporation
Mathematical Problems in Engineering
Volume 2013, Article ID 359074, 19 pages
http://dx.doi.org/10.1155/2013/359074

Research Article

Using Metaheuristic and Fuzzy System for the Optimization of Material Pull in a Push-Pull Flow Logistics Network

Afshin Mehrsai,[1] Hamid-Reza Karimi,[2] Klaus-Dieter Thoben,[1] and Bernd Scholz-Reiter[1]

[1] *International Graduate School for Dynamics in Logistics, University of Bremen, c/o BIBA, Hochschulring 20, 28359 Bremen, Germany*
[2] *Department of Engineering, Faculty of Engineering and Science, University of Agder, 4879 Grimstad, Norway*

Correspondence should be addressed to Afshin Mehrsai; meh@biba.uni-bremen.de

Received 31 October 2012; Revised 5 December 2012; Accepted 6 December 2012

Academic Editor: M. Chadli

Copyright © 2013 Afshin Mehrsai et al. This is an open access article distributed under the Creative Commons Attribution License, which permits unrestricted use, distribution, and reproduction in any medium, provided the original work is properly cited.

Alternative material flow strategies in logistics networks have crucial influences on the overall performance of the networks. Material flows can follow push, pull, or hybrid systems. To get the advantages of both push and pull flows in networks, the decoupling-point strategy is used as coordination mean. At this point material pull has to get optimized concerning customer orders against pushed replenishment-rates. To compensate the ambiguity and uncertainty of both dynamic flows, fuzzy set theory can practically be applied. This paper has conceptual and mathematical parts to explain the performance of the push-pull flow strategy in a supply network and to give a novel solution for optimizing the pull side employing Conwip system. Alternative numbers of pallets and their lot-sizes circulating in the assembly system are getting optimized in accordance with a multi-objective problem; employing a hybrid approach out of meta-heuristics (genetic algorithm and simulated annealing) and fuzzy system. Two main fuzzy sets as triangular and trapezoidal are applied in this technique for estimating ill-defined waiting times. The configured technique leads to smoother flows between push and pull sides in complex networks. A discrete-event simulation model is developed to analyze this thesis in an exemplary logistics network with dynamics.

1. Introduction

Today, after spanning the extension phase from simple companies towards supply chains and correlated networks, more complex logistics processes have been burdened to industries [1]. Under the pressure of global competitions, continuously changing business environment, mass customized products, and transient demands, not only the individual plant, but also the logistics networks have rather acquired decisive roles for achieving excellence. Accordingly, planning and control of material flows within individual factories and supply networks have become one of the most complex tasks in practices. The complexities accompanied with collaborative logistics networks are the consequences of the paradox in integrating the members of a network, while they have their own requirements and performances [2]. Indeed, material flows, inside shop floors, besides integration, and coordination of flows throughout logistics networks have engaged the most planning and control potentials in manufacturing organizations. Concerning the changing business environment, more flexible systems are required to fulfill customers' demands more quickly [3]. Since being responsive to customers is an inevitable factor for sustainment in such markets [4], several material flow strategies and production systems can be employed, for example, flexible manufacturing systems, hybrid systems, and distributed and autonomous control systems [5–7]. Although mass production originally follows material push strategy by higher production rate and higher benefits, for some other production approaches material pull reflects better performance [8]. Appropriately selecting a material flow system directly contributes to the ultimate performance of production systems. Implementation of push, pull, or both strategies has a direct effect on performances of the overall logistics processes in a network.

Moreover, manufacturing enterprises are confronted with continuous changing conditions inside their processes, called dynamics, which are supposed to be handled by more intelligent strategies. For example, mass customized products force supply networks to follow make-to-order (MTO) or engineer-to-order (ETO) production strategies to comply

with individual demands. The recent production strategies burden more pressure on logistics networks to operate based on real demand and at the right time. This issue can result in real-time operations, which impose more agile systems by means of better regulated systems, for example, pull strategies. In the literature it is argued that push strategy, for example, MRP, results better when high variety exists and demand fluctuates [9]. On the contrary, traditional pull strategies, for example, Kanban, comply better with preferably stable demands and low variety in products [10]. Indeed, different material flow strategies have their own benefits and drawbacks. Shifting from totally push systems to Kanban system, that is, fully pull system, may result in some shortcomings in facing uncertainties in new business environments. Therefore, a clever strategy is required to deal with such conditions and to employ advantages of several material flow control strategies [11]. For this purpose, some hybrid systems have been practiced, for example, CONWIP, Polca, and G-Polca, in shop-floor as well as Leagility approach in supply networks [12, 13]. These flow control strategies compensate the potential drawbacks of merely using a strategy and, at the same time, protect production systems from getting failed or overproduction. Furthermore, employment of hybrid strategies supports the targets of responsiveness, quickness, flexibility, reliable delivery, and agility as well as leanness in logistics [11].

In general, most of the above-stated systems have emphasized production and shop-floor logistics, while they can be effectively applied by supply chains and logistics networks as well. For instance, a logistics network with application of material pushup to a specific point, called decoupling point (DC) [14], can have push planning and control systems (like MRP), whereas the downstream of DC can follow pull or hybrid push-pull control system. This is specifically useful for benefiting from both control concepts and still remaining flexible. Nevertheless, coordination of downstream, with pull system, along with upstream, by means of push flow, is a challenging issue in such networks. This specific hybrid system for complex logistics networks is selected to be studied in this paper. Although the current study is a part of a greater research project which proceeds with material flow control throughout supply networks, this paper only focuses on the pull section of hybrid system and tries to optimize the number of carrier carts (pallet) and their lot sizes for smoother flows. For this purpose, a discrete-event simulation scenario of a hybrid logistics network is developed facing dynamics in their processes (material replenishments and demands). In the pull side a CONWIP (constant work in process in pull environment) technique is developed to control the flow of materials and the pallets, representing the control means in CONWIP. Correspondingly, the recommended hybrid concept contributes to the improvement of logistics performance measures, for example, throughput time (TPT), throughput (TP), responsiveness, utilization, and work in process (WIP) [15]. The dynamics include stochastic demands, fluctuating supply, and uncertain processing times of operations that resemble real-world problems in logistics. Several stochastic variables affect material flow control both at shop floors [16] and, in a broader scale, throughout logistics networks. Abundance of dynamic factors and their causal effects on flows' performances make a complex optimization problem of flows in the pull side that aims at the least collection of stocks in the system.

The particular assumption in this paper is that the push side can be optimized by means of MRP system, while optimization of material pull is not straightforward regarding the real-time control and the required coordination of both sides of flows (demand and supply). Therefore, this study highlights the general strategies dealing with uncertainty and fluctuations in material flows over supply networks and at shop floors. Particularly, it complies with two main parts as theoretical comments on the material flow strategies in supply/logistics networks by focusing on better coordination of material pull from DC to final customer. In doing so, a brief introduction is given to possible material flow systems in supply networks, facing uncertain processing times. Then it directly proceeds with a practical solution in the optimization of material flows after DC in networks. In this way, the supply network for optimizing its pull control is developed that considers uncertainty of customer orders, stochastic material push replenishments in DC, and stochastic processing times. For finding the optimum combination of effective factors, genetic algorithm (GA) as a stochastic optimization method, known as metaheuristic, is chosen to solve the optimization problem of pull flows, as in [17]. This optimization procedure regards the number of pallets and lot sizes in the pull section. Besides, to prove the performance of metaheuristics in such a dynamic problem, simulated annealing (SA) is partially experimented too.

To recognize the uncertain and ill-defined processing times in flows control fuzzy set theory against the conventional crisp estimations is employed. In other words, control of distributed pallets in an optimum manner under an ill-defined circumstance requires more smart control techniques. Therefore, fuzzy system is applied to manage the ambiguous situations in locally decision makings for better routes. Besides, GA and SA are exploited to competently cover the huge range of combinations that a distributed control system may build under dynamics and uncertainty to meet specific demands. The target is to show the importance of metaheuristic methods and fuzzy system in dealing with complex as well as uncertain material flow systems. The main contributions are to show the privileges of fuzzy control system for smoothing the flow of distributed pallets, the contribution of heuristics in approximating the optimum combination values of just some key factors of pull flows in a logistics networks, for example, number of carts, and flexible lot sizes, and the simplicity and applicability of fuzzy set theory in solving multiobjective problems by means of defining satisfaction degrees.

The rest of the paper is organized as follows. Section 2 proceeds with a brief explanation about the types of material flow control systems. Section 3 refers to GA and its approach in solving stochastic optimization problems. Section 4 concisely describes the algorithm of SA as an alternative to GA. Section 5 shortly introduces the application of fuzzy set theory in production and logistics. The logistics network scenario is clearly given in Section 5. The problem solution

is displayed in Section 7 that represents the application of fuzzy control system and its set theory in material flow control and solving multiobjective optimization problems. Experimental results are depicted in Section 8 by means of several 3D graphs. The summary and further works are given in Section 9.

2. Material Flow Control System

Generally, the systems of material flow control can be classified into push and pull mechanisms [13]. Each of which systems has some advantages and drawbacks, for example, under control inventory for pull systems and profiting from forecast information for push systems are the advantages of both control mechanisms [18]. In case of uncertainty, that is, variability, and volatility in production networks these flow systems can be used to compensate the undesirable effects of uncertain supply and demand [19]. However, these two pure systems trigger a spectrum of flow strategies between two manufacturing points maybe two workstations or (in a macroscale) two members of a supply network. Below the two control systems and a hybrid approach of them are concisely explained.

2.1. Material Push Control. Conventionally, material flow systems have been worked in accordance to push-flow control, by means of pushing materials to next processing steps as soon as processing of them is finished at the current step. In other words, the production (flow) of materials is planned beforehand based on forecasted demand or some predefined information about demand. However, if the production line or workstations are not balanced together, work in process (WIP) may be collected everywhere as well as overproduction may occur, as the consequence of this performance. Indeed, push control mechanism is assumed more appropriate for mass production and make-to-forecast (MTF) strategies with balanced lines [20]. Nevertheless, line balancing is a challenging issue by itself when the production system (order, supply, processing-time) is unstable. Material requirement planning (MRPI) is a well-known method categorized as a push control system [18]. According to the MRPI mechanism, flow of materials is planned in advance based on forecasted demand and without any concern about real capacity or current demand. Despite the fact that capacity utilization is quite high with push specifications (in advance planning and predefined logistics operations), this control mechanism suffers from some shortcomings. These drawbacks are basically in opposite to logistics' targets, that is, they result in higher WIP and inventory level, blind production, and less flexibility in plan and schedule. Moreover, in spite of the specifications in pure push mechanisms, some authors partially classify drum-buffer-rope (DBR), starvation avoidance, G-Polca, and even CONWIP mechanisms as push control systems [13, 21, 22]. Nevertheless, classification of some of these systems as pure push mechanisms does not completely reflect their performances, for example, CONWIP.

2.2. Material Pull Control. In contrast, generally, material pull control usually operates based on current demand of the upstream customer. This control strategy is originated by Toyota production system (TPS) in the form of Kanban system [23]. The material pull mechanism in the context of TPS has made a breakthrough at Toyota and later at other adherent industries for a long time. Nonetheless, this flow mechanism encounters some difficulties when demand is oscillating and processes are inherently uncertain [24, 25]. The strategy of pull mechanism is simply to fulfill the required material of customer (internal/external) just in time (JIT), so that ideally no blockage and starvation occur. Normally, blockage and starvation happen to pull mechanism, while in push with infinite capacity only starvation can be realized [26]. In addition to Kanban and partially the CONWIP, the Paired-Cell Overlapping Loops of Cards with Authorization (Polca) [27] and in part the Synchro-MRP [28] can be categorized in the pull control system as well. However these two later mechanisms, like the other semipush mechanisms, exploit some aspects of push control. In this manner, several hybrid control systems have been developed to resolve the drawbacks accompanied with pure pull or push systems. Among them CONWIP and Polca mechanisms can be mentioned.

2.3. Hybrid Push-Pull Control. Contrary to MRP system, as a centralized control mechanism with push approach, pull mechanisms are categorized as distributed control systems. As mentioned before, pull control generally works based on WIP limitation and current demand of the local working area, whilst push systems perform based on predefined material flow plans with considering forecasts. However, simultaneous application of both push and pull systems reflects a twofold view by a seamless control of material flow, while it streams the flow. In developing a hybrid system following contributions occur. Firstly, by employing a push mechanism (by a central control) the release dates of operations in global context can be defined. Meanwhile, in contributing to the global context, the employed pull control performs based on local situations of WIP to facilitate smoother flows. Consequently, in this context, global and local factors interact with each other in a positive manner. This approach enhances the coordination of the entire logistic system facing dynamic challenges. However, simultaneous employment of the push and the pull systems is not necessarily required. Inspired by shop floors control systems, some suggested control strategies for logistic networks can be sorted as follows:

(i) dividing the entire logistic network into two parts as push and pull, which is broadly discussed as Leagile supply chains [29],

(ii) employing both the push and the pull control systems simultaneously within each member of the network or throughout the whole network, like: CONWIP and G-Polca (this type needs high flexibility entirely which is subject to have distributed and intelligent control system),

(iii) inspired by Polca, dividing the network into paired-cells and applying the material release date by push system as well as WIP limitation by pull cards.

These listed options are some assisting strategies for profiting from alternative material flow controls in case of fluctuations and variations in demand and supply. However, in realizing these three alternatives material flow scheduling, that is, work dispatching rules and workload balancing (particularly in shop floors echelon), is still a challenging issue in that order. Nevertheless, in this paper, the first proposed option is considered to be analyzed with regard to inventory control and work dispatching (assignment) concerns. Indeed, this hybrid flow system is being practiced in manufacturing industries like automotive [30, 31], for example, Daimler AG locates its DC before painting shop of bodies. Here, the downstream of a logistic network with material pull flow is optimized to coordinate the collision point (DC) of both push and pull flows close to the end customer. The flows in this point require to be optimized to avoid any condition of overloaded inventory. Respectively, the tasks of workloads balancing and job dispatching are assigned to an autonomous control system, which is briefly explained in the next section [32]. This autonomous control basically follows the bottleneck control rule, but is based on self-decisions of autonomous objects and less queue length estimation (QLE) [33].

3. Logistic Network Scenario

3.1. General Structure. Today, thanks to the achievements in simulation, complex problems, like material flow control in logistic networks with a broad solution space, can be solved easier and quicker. A combination out of simulation and heuristic methods with quick response time is preferred to those conventional model-based mathematical solutions with relatively long optimization time. This holds specifically true for alternating circumstances in industries. In this regard, an exemplary logistic network scenario is modeled by discrete-event simulation software to present the improvement of material pull flow in a push-pull flow mechanism throughout the network.

Plant-Simulation is a discrete-event based simulation package developed by Siemens. The inventory policy, service levels, and so forth are arbitrary adjustable. However, in the current simulation, the policy of entrance inventory at OEM is set to priority rules (depending on the availability of respective pallets for the products in the inventory), and the rest buffers and inventories are set to first-in-first-out (FIFO) policy. The service level of the simulated production network at the inventory is dependent on the transport means and sources production rates. But the geranial service level is reflected into the satisfaction degree of the manager by means of more total delivery (throughput) at the customer side. Moreover, the inputs of the simulation model are some distribution functions for generating production intervals at sources and also some stochastic demands for sinking these produced products at the exit of OEM. The general outputs of the simulation are several statistics of performance indicators of production systems that some are used by the optimization function.

However, the enhancement in material flows by means of this mechanism is achieved by simulating metaheuristics, that is, GA and SA, for flows in this study. It is shown that metaheuristic algorithms can just optimize two factors (out of several potential ones) at the pull side of the network to reflect a reasonable solution for smoothing the flows throughout the network. Indeed, this contribution directly coordinates the push-pull collision point just by optimizing the pull-side material flow. The simulation model is developed to apply an offline optimization approach, using GA as the main contribution and using SA as the justification of GA performance. However, metaheuristics may be employed as online or real-time control system. For example, in practice, this can be carried out by autonomous pallets within a pull principle production system [32, 34].

In material pull systems, pallets (or any means of transport like fixtures) circulate permanently within logistics systems; thus, such pallets can be used as pull signals [24]. Pallets as local and distributed logistic objects have the chance to concurrently evaluate the system and decide for optimizing the sequence of the next steps without a global controller. Since GA and SA are global search techniques [35], the optimization process is considered to be offline to have all data at once; so that it makes it possible to use the entire information at the original equipment manufacturer (OEM) in the exemplary network.

The simulated network is constructed out of three steps of processing plants. In step one, two source plants (P_{11}, P_{12}) are considered to produce three types of raw materials. Each plant produces the counterparts of the other raw materials at the other source plant. Every type of raw material has to be assembled with its counterpart in the next step. The step two has two assembly plants (P_{21}, P_{22}), which have comparable processing capabilities. Therefore, the plants in step one are fully connected to the plants in step two, so that the semifinished parts can be allocated to them based on bottleneck control concept; that is, the plant with less queuing in entrance inventory has priority. Finally, the plants in step two transfer their assembled products (which are now just three types) to the last plant (OEM). This specific structure of the network reflects several characteristics of a complex logistic network, for example, differentiation and alternation in supply of counterpart products from different suppliers, arrangement of DC close to the end customer, and smart allocation of pushed replenishments by considering the current requirement of either customer plant. DC can be shifted to customer side or supplier side depending to the production strategy; this issue is already experimented in [24]. Universally, from the sources up to the entrance of OEM products are pushed regarding the forecasted demands and existing plan, whilst just inside OEM (in downstream from the entrance inventory) pull principle is applied. This strategy is to meet fluctuations in demands of final customer for the three final-product types over the simulation time horizon. Figure 1 shows the overview of the exemplary network.

In order to reflect alternations in demand of each type of product, orders are triggered to OEM with time intervals

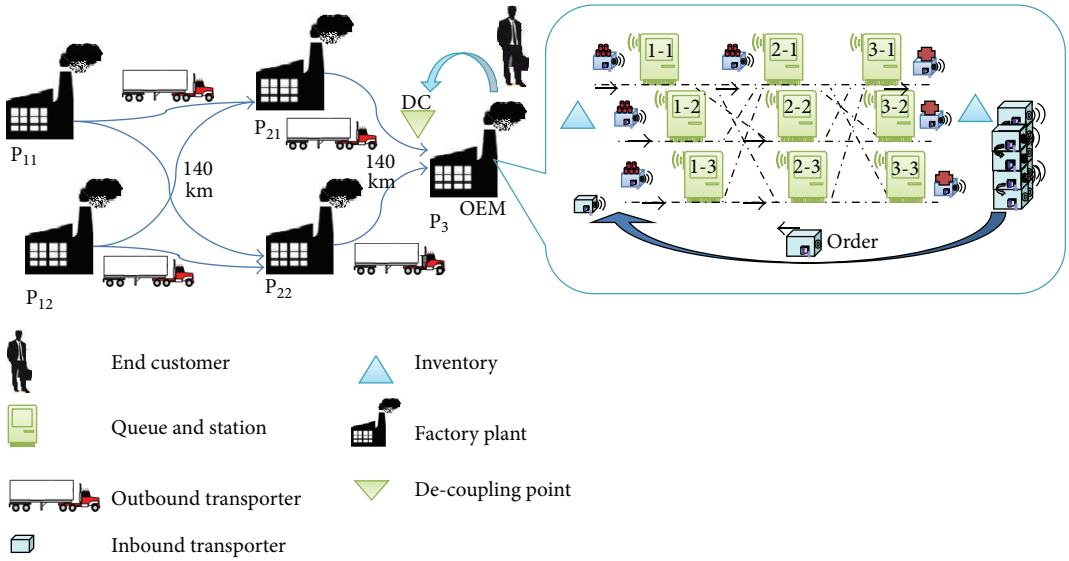

Figure 1: Exemplary push-pull network, with lasting each round trip 4 hours for transporters.

Table 1: Processing times for each product on each line.

Plant	Processing times [h:min] for each plant						
	P_{11}; P_{12}			P_{21}; P_{22} Line	P_3 (OEM)		
	Deterministic value				Mean value (μu)		
Product type	1	2	3	1	1	2	3
Type 1	2:00	3:00	2:30	0:50	2:00	2:40	2:20
Type 2	2:30	2:00	3:00	0:50	2:20	2:00	2:40
Type 3	3:00	2:30	2:00	0:50	2:40	2:20	2:00

following the exponential distribution in the first alternative and normal distribution in the second one. Hence, final demand is stochastic based on time intervals between each order of products. Equation (1) represents the used negative exponential distribution (Neg-Exp) for intervals. Neg-Exp is a common model for representing the intervals of customer random arrivals as Johnston and Boylan [36] say "... with a random arrival of independent customers, the order arrival process could be modeled as a Poisson stream and, therefore, a negative exponential distribution would be a realistic model for the inter-order interval." Moreover, consideration of normal distribution by practice oriented studies is also typical, for example, [37], and it is considered to be experimented against the first alternative. For the first alternative, the mean value (2 hours and 30 minutes βe = 2:30 for each type) is assumed a bit bigger than the mean supply rate to collect WIP at the entrance inventory of OEM. The mean value and the variance in (1) are respectively denoted by ($\mu u = 1/\beta e$ and $\sigma^2 = \beta e^2$). For the second alternative, the mean value is 2 hours and 30 minutes: μu = 2:30 and the standard deviation is (σ = 10 min):

$$f(x) = \frac{1}{\beta e} \cdot \exp\left(-\frac{x}{\beta e}\right). \quad (1)$$

It is noticeable that inside each plant, except the assembly ones in step 2, a 3 × 3 matrix of workstations is devised. This matrix configures three similar production lines in parallel, which are fully coupled to every workstation in the next column. This resembles the flexible flow shop problem in general and is selected based on a predefined problem at the research cluster CRC 637 about autonomy in logistics at the Bremen University (http://www.logdynamics.com/).

However, the purpose of this fully coupled system is to simulate a highly flexible logistic system with the capability of employing autonomous logistic objects for self-organizing material flow. As one alternative, autonomous objects by collecting local information about successive queues (buffers in front of each station) and by using bottleneck control rule decide which route has the least waiting time to proceed. This specific control system (called QLE) has been discussed in previous papers, for example, [7, 10, 11, 33]. Alternatively, without considering any autonomous carrier objects, a conventional flow control (Conv) can be developed to just proceed through the stations with the least predefined processing times without any updating. These are later experimented in the simulation. Table 1 shows the processing times of each workstation inside every plant of the network. Just for OEM the processing times are considered stochastic

Table 2: Applied notations in the problem.

Notation	Description
$\mu u = 1/\beta e$	Mean value of distribution
σ	Standard deviation
X	Random variable
P	Product type, $p = 1 \cdots P$; $P = 3$
T	Time, $t = 0 \cdots T$; $T = 80 \times 24$ hours
ALTPT_p	Average local throughput time (in OEM at T)
AGTPT_p	Average global throughput time at T
TD_p	Total delivery of product p at time T
$\mu_{\widetilde{A}}$	Membership value of fuzzy set $\widetilde{A}$
$Lsize$	Capacity of a pallet [1 10]
e	Upper bound of the fuzzy number μ
WIP_p	Maximum OEM inventory
φ, δ	Importance weights; may be chosen arbitrarily by decision-maker
f_i	Fitness value of chromosome i
Pr_i	Selection probability value of chromosome i
Te	Current temperature in SA
$\mathrm{Te}_{\min}$	The least temperature in SA
c	The cycle number in the loop of SA
$\widetilde{A}$	Fuzzy set
$NPallet$	Number of pallets in system [10 60]
b	Lower bound of the fuzzy number μ

with the normal distribution, where the standard deviation is equal to ($\sigma = \mu u/10$). Besides, the mean of processing times is identical to the mean intervals of products' replenishment. These values are empirically extracted from several simulation runs toward smoother and coordinated flows. Each simulation experiment is run for 80 days each 24 hours to make authentic results.

The used flow strategy in the simulation is as follows. In step 1, materials are discharged to the network based on release dates following normal distribution. The normal distribution is arbitrarily assumed for time intervals between each release with $\mu u = 50$ min and $\sigma = 5$ min. Correspondingly, the three product types are randomly released to the system and pushed forward to the next step. In contrast, in downstream of the network customer orders are triggered within a stochastic manner, using exponential time intervals. The downstream control of pull material at OEM operates based on a form of CONWIP system. In other words, the orders pull the semifinished products from the entrance inventory of OEM and then the pallets are pushed toward the exit of OEM. Availability of circulating pallets at the entrance of OEM is the signal of stated demand and the pull signal. In fact, pallets do the duty of CONWIP cards or signals here. They are pushed by the merit of autonomous control (self-selection of next station with least queue) to the downstream of the shop-floor after picking up their respective products [32]. Eventually, uncertainties in the pushed replenishments at the entrance inventory and the stochastic pulled orders result in a chaotic performance at the collision (decoupling) point of push-pull. Therefore, this chaotic system must get coordinated toward an optimum solution with less inventory quantity.

3.2. Problem Statement. The current network scenario resembles a multiobjective optimization problem that minimizes the average local throughput time (ATPT), the average global throughput time (AGTPT), and the entrance inventory (WIP) of OEM, as well as maximizing the total deliveries (TD) to the end customers. Since there are several stochastic and vague defined variables which directly or indirectly influence the performance of the model and the optimization process, this problem is very complex to be formulated and solved by conventional mathematical solutions. Thus, as an alternative solution it is decided to employ simulation with the assistance of metaheuristics to realize the objective of the problem without mathematically modeling the existing constraints. These multiobjectives can be compactly written in one objective form with minimization target like (2). The used notations for the multiobjectives are given in Table 2. However, the unique objective out of the multiobjectives can only be formulated in a compact equation when all single objectives have a unique unit or they all can be written without units. Therefore, further synthesis is required to achieve a uniform objective equation. This is broadly explained in the solution section:

$$\mathrm{Min} \sum_{P} \left(\frac{\mathrm{ALTPT}_p + \mathrm{AGTPT}_p + \mathrm{WIP}_p \times \varphi}{\mathrm{TD}_p \times \delta} \right). \quad (2)$$

To explain this optimization problem, material flow flexibility as well as push rate (uncertainty in replenishment time of semifinished products) has to be considered. On the other side, the stochastic time of customer orders on the pull side have to be taken into account as well. For this purpose, the flexibilities in the simulation are as considered as flexible lot sizes and number of cyclic pallets in carrying products, which are the optimization factors. Besides, the autonomous control for pallets in selecting their own routes is another flexibility factor. This issue is not heighted in this paper, for more information see [32]. However, one great accompanied complexity with this scenario is the on-time arrangement of empty pallets to be available at the entrance inventory to pick up the upcoming products. This arrangement has to regard the respective orders of each product pallet. It can be optimally achieved when supply, demand, and production rates at OEM are coordinated with each other as much as possible. Thus, an intelligent heuristic algorithm plus several experiments is required to find the optimality of the decisive variables in those regards.

Since the time of pushed replenishments as well as upcoming demands is uncertain (leading to fluctuations), the number of pallets (CONWIP carts) and lot sizes can be considered as optimizing factors for making tradeoffs in the oscillating flow problem. However, their exact contributions to the objective are mathematically difficult to be defined in advance. These characteristics of the problem make strong

reasons for employing simulation and heuristic methods for solving it in a proper way.

As aforementioned, the selected heuristics for the current problem are GA and SA. Here, the core target is to show the suitability of the metaheuristics (e.g., GA and SA) for optimization material flow throughout the network. For instance, in using GA it can be possible just to minimize a fitness function of a problem, like (2), to achieve the optimum objectives within an evolutionary procedure. Additionally, with regard to the vague information about processing and waiting times and other processes at the shop floor of OEM, the superiority of fuzzy sets in better distinguishing uncertain processing times is to be explored. Besides, application of fuzzy set theory can facilitate the normalization and unification of the disparate multiobjectives of the model, which is represented following.

4. Genetic Algorithm

In general, a number of optimization methodologies have been introduced to solve complex problems, for example, nonlinear and NP-hard. As a competent evolutionary technique, GA is defined as a stochastic optimization method based on heuristic procedures [38]. It has been shown that GA is able to approximately find the optimum solution for complex problems within a fairly quick time. Universally, optimization process of GA starts with randomly generating a population of solutions (individuals), which are in the format of genotype. The specification of a solution can be stored in one or more chromosomes that a chromosome by itself is made of an ordered sequence of single genes. In each gene a single parameter of a coded solution (genotype) is stored. In fact, a genotype carries the coded solution, whose decoded form to the original solution is called phenotype. Moreover, the position of a gene in a chromosome is named locus [39]. Frequently, to codify a problem the binary-based encoding procedure is selected; nonetheless, encoding is not limited to binary values, for example, integer values are used here.

Basically, the initial population, which is normally generated randomly, is subject to get improved to achieve the optimum solution. In doing so, GA employs two strong driving engines to produce new solutions without having any knowledge in prior, that is, selection and adaption operations, in which crossover and mutation functions are driving engines. Generally, for crossover function two individuals from a population are considered to be merged and produce either one child (offspring) or two children. Respectively, there are one-point or multipoint crossover procedures for running this function in GA. Similarly, mutation is also a function of optimization procedure which avoids local traps. For example, changing a gene in an individual and shifting one/some gene(s) from one locus to other one(s) are two ways of mutation procedure. Inversion of an individual's genes can be assumed as mutation as well. Basically, the procedure of GA applied in this paper can be reflected as in Figure 2.

Furthermore, optimization elements in GA are dependent on fitness function values, evolution of individuals, and selection method [40]. Fitness function is an objective function to evaluate individuals and assigning a fitness value to each of them. Accordingly, the fitness values of individuals in a generation define the chance (probability) of each individual in being selected for the next generation. Usually, the best individuals breed the next generation and eliminate the weak performing solutions. In doing so, after generating enough new individuals in a generation each fitness value of them is measured. Afterwards, depending on the type of selection operator, their selection probabilities, proportional to each other, can be calculated. Correspondingly, weak individuals are substituted by those with better performances in solving the problem as the parents for the next generation. Afterwards, the new population of solutions is produced by means of reproduction operator.

However, selection methods can have different mechanisms for selecting the parents of the next generation, for example, roulette-wheel selection, stochastic remainder selection, stochastic universal sampling, and tournament selection [41]. For the sake of simplicity in this paper and regarding the homogeneity merit in defining probabilities, the roulette-wheel selection method is employed to evaluate the solutions. Indeed, the roulette-wheel function measures a probability of selection for each individual by getting the mean value of the fitness (f_i) of an individual in proportion to all observations of the fitness values. Equation (3) defines the probability function of roulette-wheel selection. Here, N is the number of individuals in current population. The higher the probability value, the more chances the individuals have to get selected. Furthermore, SA as another metaheuristic technique can be used as an alternative to GA in some optimization problems. This technique can justify the performance of GA in the specific application at the current problem:

$$\mathrm{Pr}_i = \frac{f_i}{\sum_{j=1}^{N} f_j}. \tag{3}$$

5. Simulated Annealing

Simulated annealing is a stochastic search technique inspired by statistical mechanics. Similar to GA, the metaheuristic algorithm of SA is suitable for solving global optimization problems with large solution space. The algorithm is initially introduced by [41] based on the physical annealing process in metallurgy. Basically, SA performs according to the low-energy state principle in aligning metal atoms, which is dependent on gradually cooling the temperature in annealing process similar to thermodynamics. The general algorithm of this method is shown in Figure 3. In this work, the step function, in decreasing the temperature after each loop, follows (4), where Te notices the current temperature, $\mathrm{Te}_{\min}$ is the least temperature, and c denotes the cycle number in the loop. For more information about different strategies in SA see also [40, 42]:

$$\mathrm{Step} = \exp\left(\frac{c-1}{\ln\left(\mathrm{Te}/\mathrm{Te}_{\min}\right)}\right). \tag{4}$$

The special use of cooling procedure assists the algorithm to avoid local optimum solutions and optimistically escape

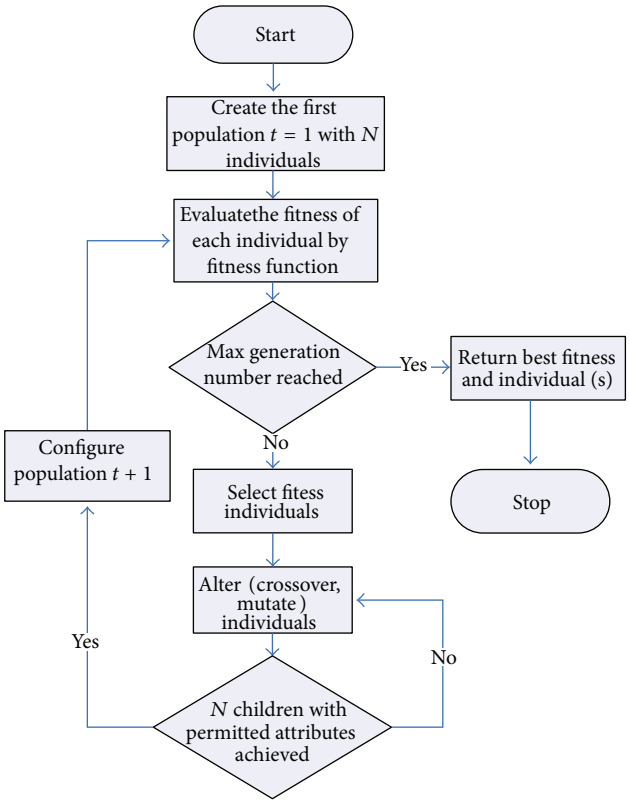

Figure 2: General genetic algorithm.

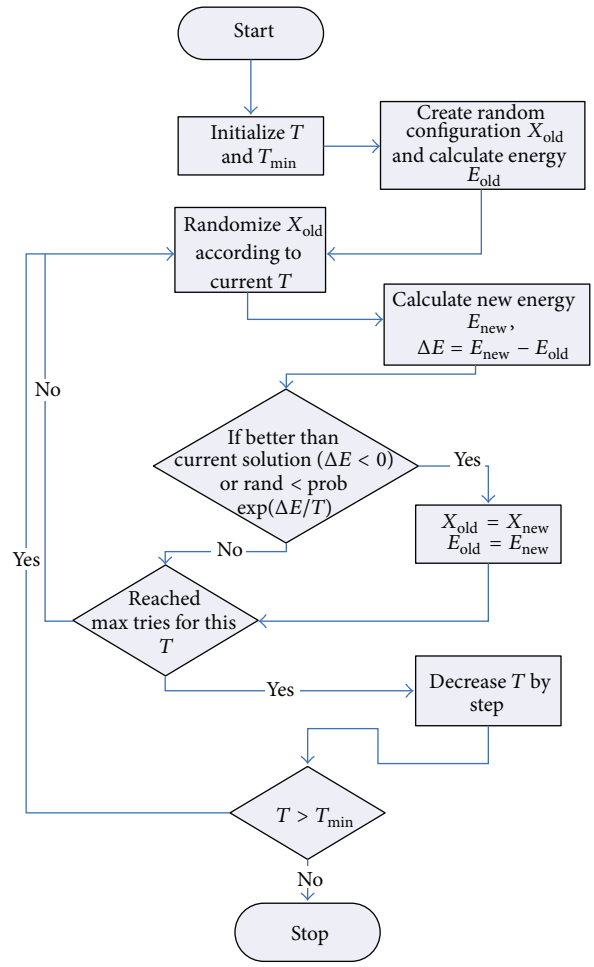

Figure 3: The flow chart of SA algorithm.

from local traps towards global optimum in a given amount of time.

6. Review on Fuzzy Set Application

Fuzzy set theory is considered as a powerful set theory for characterizing ill-defined, uncertain, and stochastic nature of practical operations in complex systems [43], like vagueness in logistics [44]. Practitioners are aware that any human-centered problems in industries, for example, processing times, due dates, and delivery time, forecasting, are uncertain and imprecise in nature [45]. Specially, in case of logistics operations it can be seen that customers' orders appear stochastically with ambiguity, so that the respective information is usually imprecise throughout supply networks. For this purpose, a fuzzy control system by employing fuzzy numbers, their membership functions, and defining fuzzy rules (fuzzy inferring) can distinguish the existing uncertainties as well as making tradeoffs in case of imprecision in practice.

In particular here, stochastic processing times, thanks to normal or exponential distribution, causes imprecise estimation over the waiting times in queues and, consequently, uncertain material flow scheduling and control. This problem can be better solved by taking into account the fuzzy nature of the operations and arranging fuzzy rules for inferring improved decisions. Respectively, IF-Then inference fuzzy rules reflect the policy of decision makers for the objectives of similar problems [46].

Desirably, fuzzy sets can directly assist the solution of normalizing multiobjective problems [47] with disparate and conflicting targets. Introduction of satisfaction degree by means of fuzzy sets theory enables decision makers to transform the multiobjectives of such problems into a normalized unique linear and unitless objective. This alternative reflects the satisfaction's amount of a decision maker in achieving (near)-/optimized values for each single objective and, thereupon, builds tradeoffs between them. This is briefly explained in the solution section. Depending on each objective, various fuzzy membership functions can be employed to reflect the satisfaction of decision maker. However, the functions should be simple for arithmetic operations. A good application of this solution is recently presented by [46].

In addition to the above privilege of fuzzy set theory in operational problems, estimation of imprecise waiting times at each buffer of stations can also be a suitable application of fuzzy sets in material flow control. In order to configure the best routing for each specific material with alternative processing times among several possibilities, different fuzzy functions can be employed for time estimation. Indeed, fuzzy numbers simulate the imprecise processing and waiting times of parts in each processing steps.

In General, several shapes can be applied for defining membership functions in fuzzy sets that amongst them are triangular, trapezoidal, Gaussian, and s-curve [48]. Each of these functions can be allocated to a specific application in industry; nonetheless, the arithmetic operations of them are usually not similar and easy handling. For instance, the triangular fuzzy membership function, because of its simple arithmetic operations, is often considered in the literature for modeling uncertain processing times. This membership function is represented by a triplet (a_1, a_2, a_3) as defined by (5); see Figure 4. While a_1 is the lower bound and a_3 is the upper bound of the fuzzy number $(\widetilde{A})$ with membership degrees of zero ($\mu_{\widetilde{A}} = 0$), a_2 is the modal point (middle range) with membership degree of one ($\mu_{\widetilde{A}} = 1$). However, the other simple function to be used in manufacturing operations is trapezoidal. This function is denoted by a quadruple (a_1, a_2, a_3, a_4) and can be defined by (6), see Figure 4. Trapezoidal function has almost the same arithmetic characteristics of triangular functions based on Zadeh extension principle [49]. Thus, it is also comfortable to be used in straightforward computations [50]. On this basis, these two functions are selected to be employed in this paper:

$$\mu_{\widetilde{A}} = \begin{cases} 0 \xrightarrow{\text{if}} x \le a_1 \vee x \ge a_2, \\ \dfrac{x - a_1}{a_2 - a_1} \xrightarrow{\text{if}} a_1 \le x \le a_2, \\ \dfrac{a_3 - x}{a_3 - a_2} \xrightarrow{\text{if}} a_2 \le x \le a_3,\ x, a_1, a_2, a_3 \in R, \end{cases} \tag{5}$$

$$\mu_{\widetilde{A}} = \begin{cases} 0 \xrightarrow{\text{if}} x \le a_1 \vee x \ge a_3, \\ \dfrac{x - a_1}{a_2 - a_1} \xrightarrow{\text{if}} a_1 \le x \le a_2, \\ 1 \xrightarrow{\text{if}} a_2 \le x \le a_3, \\ \dfrac{a_4 - x}{a_4 - a_3} \xrightarrow{\text{if}} a_3 \le x \le a_4,\ x, a_1, a_2, a_3, a_4 \in R. \end{cases} \tag{6}$$

The arithmetic operations of fuzzy numbers are also alternative according to the shape of the membership functions and the employed method. For instance, the addition of two triangular or trapezoidal numbers can be defined by (7) and (8), respectively, as defined by [45, 51–53]:

$$\widetilde{A} + \widetilde{B} = \left(a_1 + b_1, a_2 + b_2, a_3 + b_3; \min\left(\mu_{\widetilde{A}} + \mu_{\widetilde{B}}\right)\right), \tag{7}$$

$$\widetilde{A} + \widetilde{B} = \left(a_1 + b_1, a_2 + b_2, a_3 + b_3, a_4 + b_4; \min\left(\mu_{\widetilde{A}} + \mu_{\widetilde{B}}\right)\right). \tag{8}$$

However, ranking of fuzzy sets is not as simple as classical sets. Several methods are given in the literature, which aim at discriminating (ranking) fuzzy numbers; see [54]. However, most of the methods in the literature are computationally expensive for simulation with moderated capability for computing in a short time. Therefore, two practical and easy methods out of several are selected to rank the selected fuzzy sets (i.e., triangular and trapezoidal). For this purpose, [45] three simple ranking criteria were adopted to be sequentially used to discriminate triangular fuzzy sets. Firstly, criterion (9) is calculated as the greatest associate ordinary number; if the order of fuzzy numbers is cleared the criteria (10) and (11) are not required. Otherwise, (10) calculates the mode of the numbers to order them; if not criterion (11) is calculated to complete ranking procedure:

$$C_1\left(\widetilde{A}\right) = \frac{a_1 + 2a_2 + a_3}{4}, \tag{9}$$

$$C_2\left(\widetilde{A}\right) = a_2, \tag{10}$$

$$C_2\left(\widetilde{A}\right) = a_3 - a_1. \tag{11}$$

Similarly, to discriminate trapezoidal fuzzy numbers some criteria are needed. However, trapezoidal fuzzy numbers are not as easy as triangular ones to be ranked. Rao et al. [55] developed a "method for ranking fuzzy numbers based on the Circumcenter of Centroids and uses an index of optimism to reflect the decision maker's optimistic attitude and also an index of modality that represents the neutrality of the decision maker." Briefly explained, based on the Centroid of a trapezoid, as its balancing point, they divide the trapezoid into three plane figures as two triangles on two sides and one rectangle in the middle. Then, the Circumcenter of the Centroids of these three planes is considered as the reference point to rank generalized fuzzy numbers. Hence, the Circumcenter of the built triangle within a generalized trapezoidal fuzzy number $\widetilde{A} = (a_1, a_2, a_3, a_4; \mu)$ can be calculated by the following equation:

$$\begin{aligned} &S_{\widetilde{A}}\left(\overline{x}_0, \overline{y}_0\right) \\ &\quad = \left(\frac{a_1 + 2a_2 + 2a_3 + a_4}{6}, \right. \\ &\qquad \left. \frac{\left(2a_1 + a_2 - 3a_3\right)\left(2a_4 + a_3 - 3a_2\right) + 5\mu^2}{12\mu}\right). \end{aligned} \tag{12}$$

Accordingly, the associated index with the ranking is as (13), where $\alpha \in [0, 1]$ denotes the index of optimism. If $\alpha = 0$ the decision maker is pessimistic but if $\alpha = 1$ the decision maker is totally optimistic. In this paper moderated decision maker is chosen, that is, $\alpha = 0.5$:

$$I_\alpha\left(\widetilde{A}\right) = \alpha\overline{y}_0 + (1 - \alpha)\,\overline{x}_0. \tag{13}$$

However, Rao et al. [55] argue that this index dose not suffice the discrimination of fuzzy numbers, since it "uses only the extreme values of the Circumcenter of Centroids." Therefore, they add another index of modality to that as in (14). Here, $\beta \in [0, 1]$ is the index of modality to denote the importance weight of the central value versus the two extreme values of $(\overline{x}_0, \overline{y}_0)$. This value is taken as $\beta = 0.5$ in this paper:

$$I_{\alpha,\beta}\left(\widetilde{A}\right) = \beta\left(\frac{\left(\overline{x}_0 + \overline{y}_0\right)}{2}\right) + (1 - \beta)\, I_\alpha\left(\widetilde{A}\right). \tag{14}$$

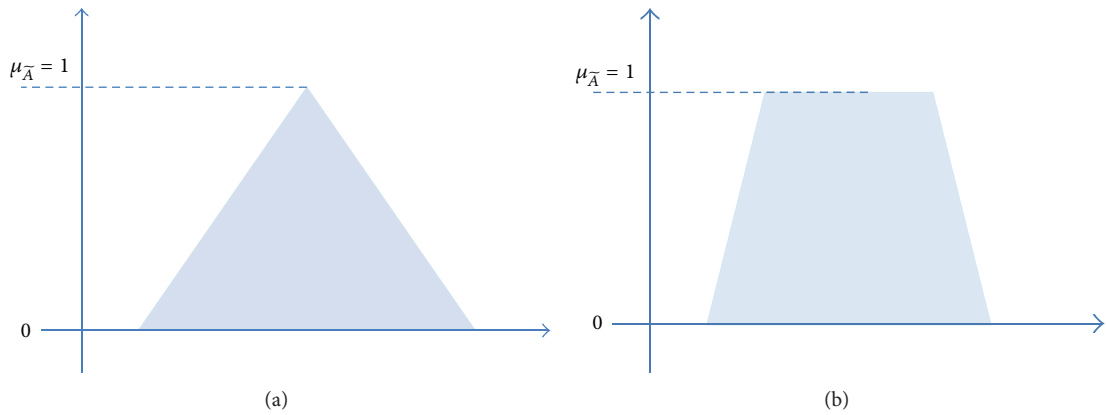

Figure 4: (a) Triangular membership function. (b) Trapezoidal membership function.

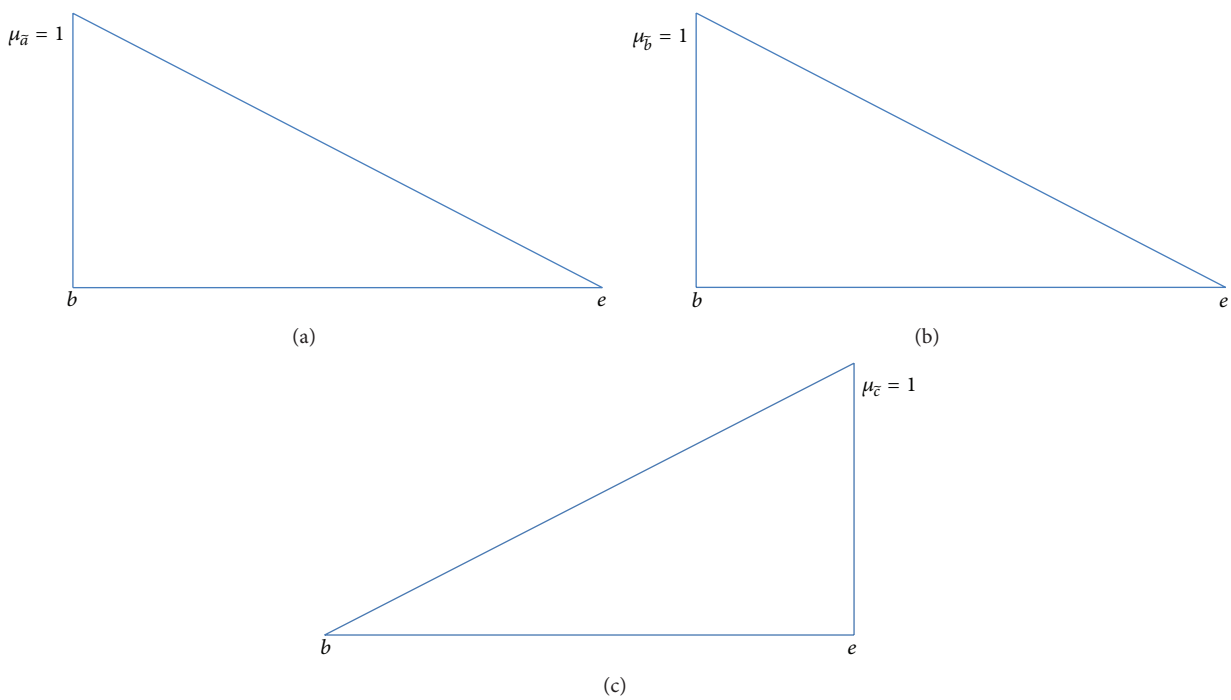

Figure 5: Membership functions for (a) minimization of TPT. (b) minimization of WIP. (c) maximization of TD.

Now, in order to rank the generalized trapezoidal fuzzy numbers the ranking function (15) has to be used, which defines the Euclidean distance from the Circumcenter of the Centroids and the original point:

$$R\left(\widetilde{A}\right) = \sqrt{\overline{x}_0^2 + \overline{y}_0^2}. \tag{15}$$

Each fuzzy number with bigger $R(\widetilde{A})$ is considered as greater number than the others. However, in case of equal values for this ranking function, the index of modality $I_{\alpha,\beta}(\widetilde{A})$ has to be subsequently calculated to rank the numbers. This method regarding its computational ease is adopted to compare trapezoidal fuzzy waiting times in material flow control.

7. Problem Formulation (Solution)

This section complies with formulating the exemplary problem of this study by taking into account the heuristics and fuzzy set theory. Since the objectives of this problem cover both directions of minimization (ATPT and WIP) as well as maximization (TD), besides consisting of two different units (time and number), these objectives must be properly homogenized (normalized). A suitable solution for making the objectives homogeneous is to transform them into their corresponding satisfaction degrees. Practitioners are aware of the contradictory nature of optimization problems and the realistic constraints accompanied with them. Therefore, it is quite common in practice to make some tradeoffs by managers between the goals to be optimized. The art of

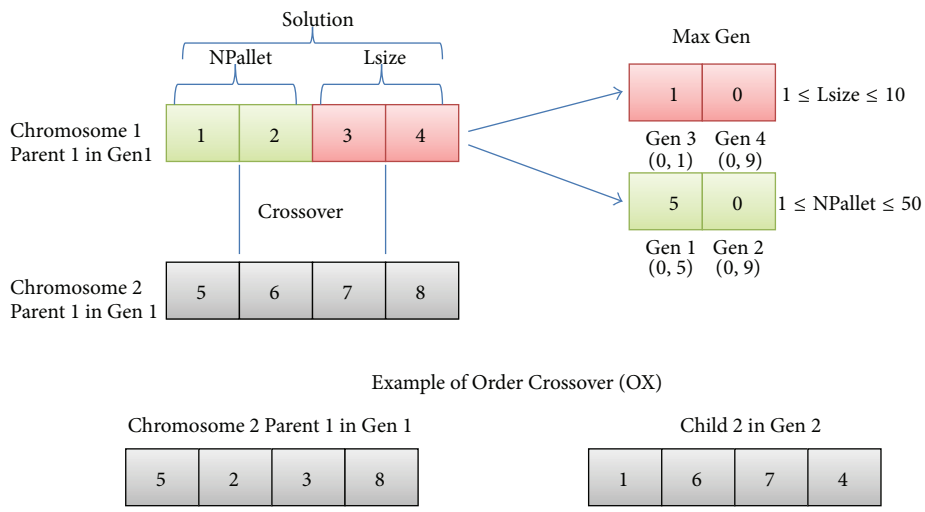

Figure 6: Satisfaction degrees in SA for two alternatives with NegExp supply in Source plants.

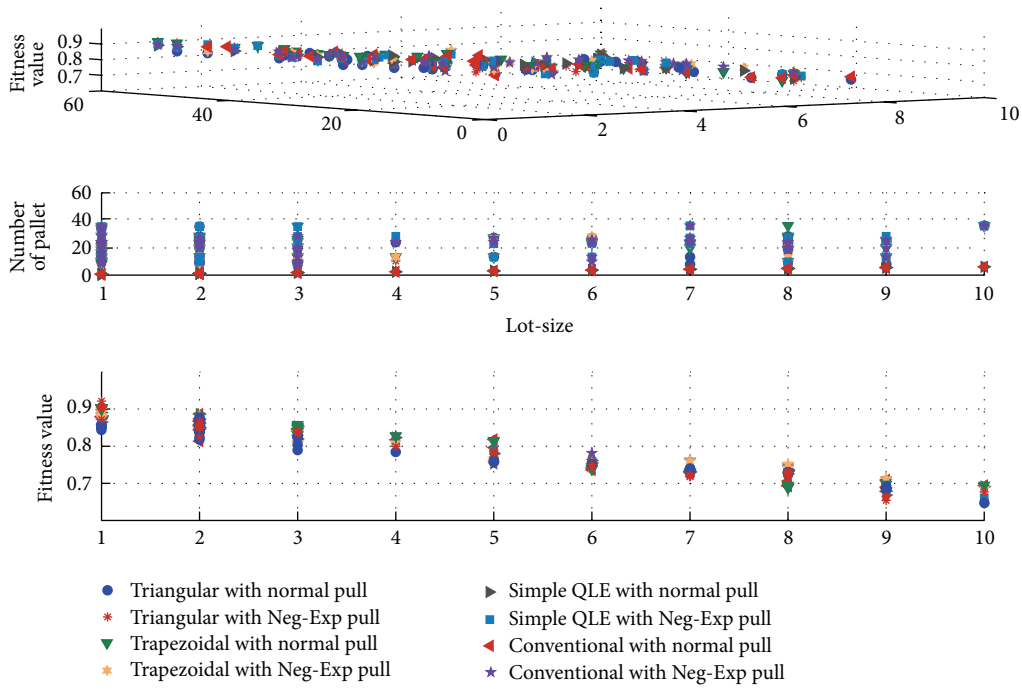

Figure 7: Fitness values of all eight alternatives from three views, showing normalized fitness values against various numbers of pallets and their lot sizes.

a professional manager is to define the best tradeoffs in accordance with the practical tolerances their organization can accept. There exists always a lower and an upper limit for a desired goal. This boundary builds a range for being satisfied with an achieved objective. Of course, the closer to their ideal value, the higher satisfaction can be obtained. However, this boundary may be applied to alternative goals differently by means of its function shape. On this basis, instead of optimizing some contradictory goals managers can subjectively optimize their multiobjective problems by converting them into a uniform problem (called a scalarized problem) of maximizing their satisfaction degrees for all objectives. Moreover, a very appropriate solution in operational research for solving multiobjective problems is the Pareto frontier. In general, the solutions of a multiobjective problem that any improvement in one objective results in decline of at least one other objective are called Pareto optimal solution. A set of these optimal solutions from different points of view is called Pareto optimal set. This is what the outputs of the satisfaction degree solution are going to depict in 3D figures. The drawn plot out of a set of Pareto optimal solution is called Pareto frontier.

There are always some challenges to solve a multiobjective problem, among them is scalarizing the multiobjectives and

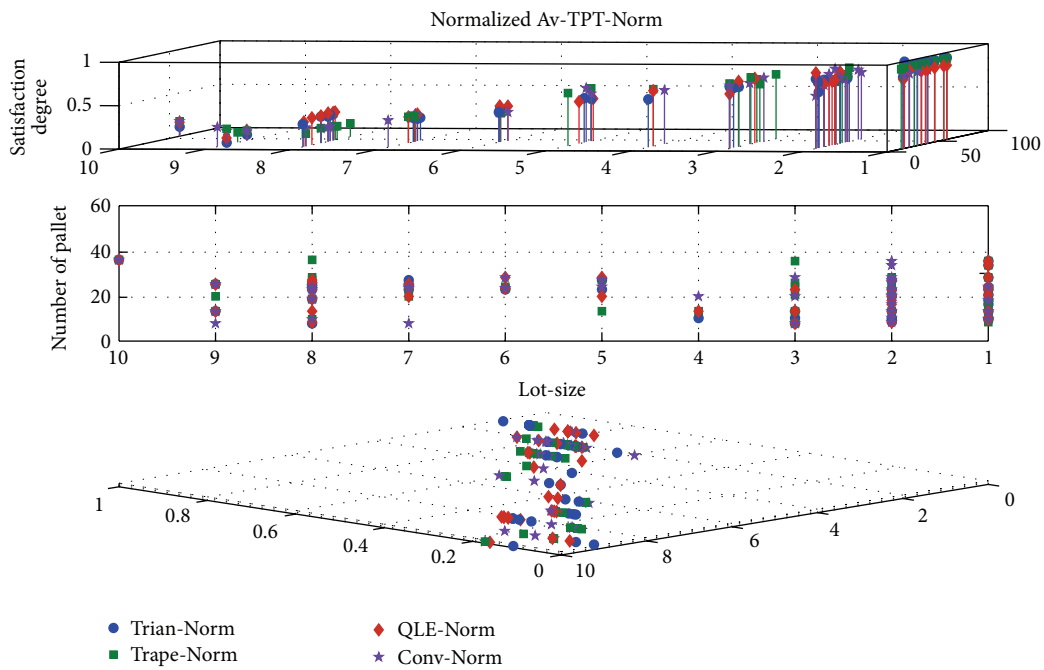

Figure 8: Satisfaction degrees of normalized average TPT (global and local TPT) with demands following normal distribution.

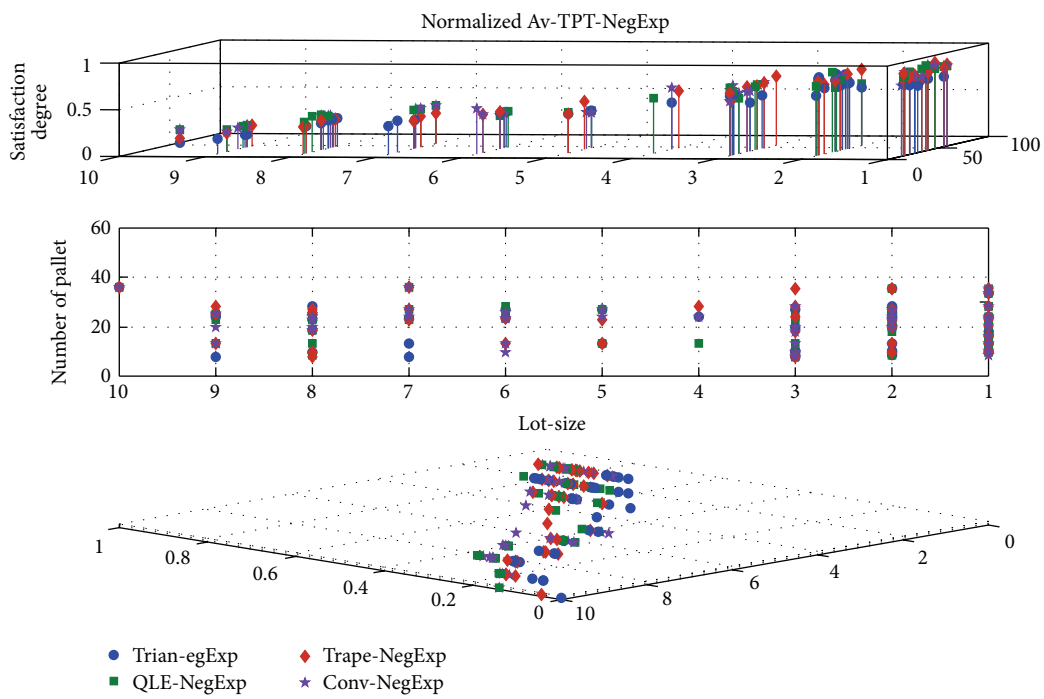

Figure 9: Satisfaction degrees of normalized average TPT with demands following negative exponential distribution.

selecting the best solution. There are different approaches and mathematical solutions for solving these challenges, for example, using a decision maker (like satisfaction degree), no decision maker (like no preference methods), a priori methods, a posteriori methods, interactive methods, and hybrid methods [56]. These all solutions are not covered by this paper, since the intention here is to introduce a simple and practical solution for practitioners to solve their multiobjective problems in a quick time. Nevertheless, the satisfaction degree solution is not distinct from Pareto frontier solution, the difference may be the exact formulation of the scalarized problem which can be also adopted by satisfaction degree and the later improvement iterations by decision maker which can be adopted as well.

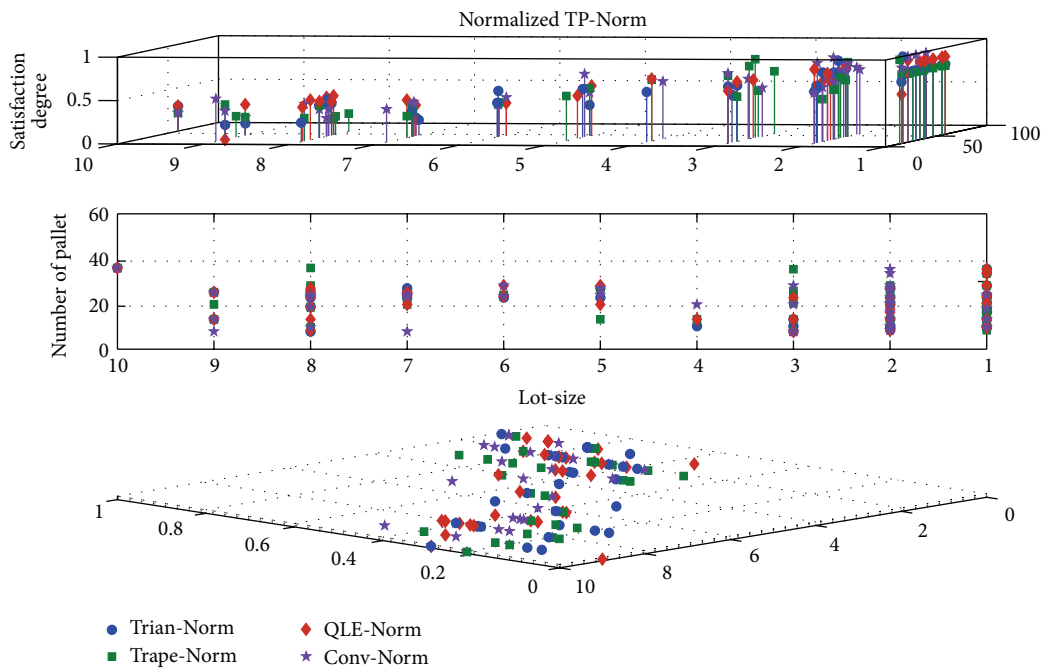

Figure 10: Satisfaction degrees of normalized throughputs with demands following normal distribution.

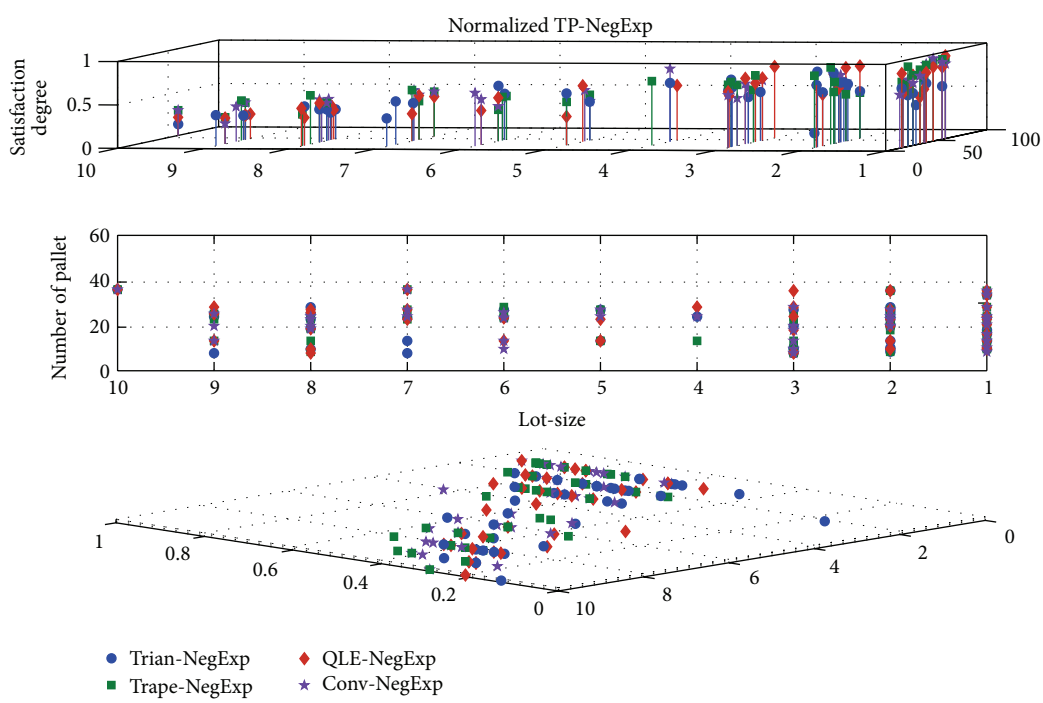

Figure 11: Satisfaction degrees of normalized throughputs with demands following negative exponential distribution.

For this purpose, all objectives together can simply be mapped into maximization of a linear membership function which takes the aggregation of every satisfaction degree within the range of [0 1]. Mapping of a real objective into the normalized satisfaction degree is a subjective process that can be applicable just by defining the lower (b) and upper (e) bounds, that is, [b e], of the corresponding objective by decision maker. Indeed, the boundaries are selected by the decision maker according to the system performance and his/her satisfaction from the operations. Explanation of this transformation process can better be illustrated by Figure 5. For this procedure, (17)–(20) hold true. It is noticeable that (17) $\mu_{\tilde{a}}$ reflects the satisfaction degree of the minimization objective of TPT, (18) calculates the satisfaction degree $\mu_{\tilde{b}}$ of

minimization of WIP, and (19) defines the satisfaction degree $\mu_{\tilde{c}}$ of maximization of TD. Then either by configuring some fuzzy rules, the minimum operator (16), or simply using the average aggregation operator for the satisfaction degrees, one unique linear satisfaction degree, representing all objectives, can be achieved:

$$\text{maximize } f = \text{Min}\left(\mu_{\tilde{a}}, \mu_{\tilde{b}}, \mu_{\tilde{c}}\right), \tag{16}$$

$$\mu_{\tilde{a}} = \begin{cases} \left\{\dfrac{e - x_1}{e - b}\right\} \xrightarrow{\text{if}} b < x_1 < e, \\ 0 \xrightarrow{\text{if}} e \le x_1, \\ 1 \xrightarrow{\text{if}} x_1 = b = 0, \end{cases} \tag{17}$$

$$\mu_{\tilde{b}} = \begin{cases} \left\{\dfrac{e - x_2}{e - b}\right\} \xrightarrow{\text{if}} b < x_2 < e, \\ 0 \xrightarrow{\text{if}} e \le x_2, \\ 1 \xrightarrow{\text{if}} x_2 = b = 0, \end{cases} \tag{18}$$

$$\mu_{\tilde{c}} = \begin{cases} \left\{\dfrac{x_3 - b}{e - b}\right\} \xrightarrow{\text{if}} b < x_3 < e, \\ 0 \xrightarrow{\text{if}} x_3 \le b, \\ 1 \xrightarrow{\text{if}} e \le x_3, \end{cases} \tag{19}$$

where

$$\begin{aligned} x_1 &= \sum_P \text{AGTPT}_p + \sum_P \text{ALTPT}_p, \\ x_2 &= \sum_P \text{WIP}_p, \\ x_3 &= \sum_T \sum_P \text{TD}_{tp}. \end{aligned} \tag{20}$$

In addition to the first application of fuzzy set theory, it can also contribute to the material flow control inside shop floors by means of self-controlled pallets. Each autonomous pallet is able to watch the size of parallel queues in front of parallel stations. This gives the pallet the ability to estimate the waiting time for each station (by aggregating the uncertain processing times of all waiting products in a queue) and to choose the one with the least waiting time [32]. This kind of autonomous control for pallets is called QLE. However, if the waiting and processing time of stations are not deterministic, this ambiguity leads to imprecise estimation of the waiting times in queues. Thus, the fuzzy set theory can assist the estimation process as follows.

Particularly, two alternatives as triangular and trapezoidal functions are considered for the fuzzy sets which approximate the waiting and processing times of products in queues and stations. In alternative one (Trian), the triangular fuzzy numbers for approximating the processing times of stations are considered as *1:48*, ***2:00***, *2:12; 2:06*, ***2:20***, *2:34;* and *2:24*, ***2:40***, *2:56* for the three product types. Here, the (mean $*$ 0.05) can be considered as standard deviation of the normal distribution $N \sim$ (mean, $(\text{mean} * 0.05)^2$). These values are exerted to recognize uncertain waiting times and, thereupon, choosing the best route with the least waiting time. This calculation happens by knowing the number and types of products in each parallel queue to choose the corresponding values for the triangular sets. In other words, the pallet adds the fuzzy set of its content to the fuzzy sets of all existing products in the queue as well as the successor station, by mean of the addition operator (7). After calculating the waiting times of all three parallel stations then by means of ranking criteria, say (9), (10), and (11), the pallet chooses the station with the least waiting time.

For the second alternative (Trape), the trapezoidal fuzzy numbers are differently calculated to the triangular ones. Since just the mean times (modal points in triangles) are given, they are taken as the reference values to estimate trapezoidal functions for each product type. The quadruple of each type are calculated as (mean − 2 (mean $*$ 0.05), mean − 1 (mean $*$ 0.05), mean + 1 (mean $*$ 0.05), mean + 2 (mean $*$ 0.05)), which means: *1:48, 1:54,* ***2:00***, *2:06, 2:12; 2:06, 2:13,* ***2:20***, *2:27, 2:34*; and *2:24, 2:32,* ***2:40***, *2:48, 2:56*, respectively, for each type on parallel stations. The process of waiting time estimation is comparable to the alternative one; again the pallet adds the trapezoidal set of its content to the fuzzy sets in the queue as well as the successor station by using (8) to achieve the entire waiting time. Accordingly, by means of the criteria (15) and (14) the least waiting time of parallel queues can be approximated.

Furthermore, the developed GA for this problem is supposed to optimize the fitness value, which is a maximization function. This importance is done by means of the following procedure. The fitness values (called observation too) for each individual, in the first generation, are originally calculated by (5). Then by means of (1) the selection's probabilities for each individual can be found. Derived from the probability values, ten individuals have to be randomly chosen for crossover and mutation operators. In the next generations the procedure is repeated the same until the termination value (sixth generation) is reached. Basically, GA by using (1) defines selection probabilities for individuals and then based on probabilities takes each successful couple of individuals to breed two children, by means of crossover and then mutation. In this experiment, the first created generation is configured by 10 individuals. The crossover operator (Figure 6) and mutation operators are applied according to their probability values as 0.8 and 0.1, respectively. Nevertheless, from the second generation to the last one, the populations are combined out of 20 individuals to cover a broader scope of the solution space. In the second generation, again 10 individuals with higher probabilities are selected to become parents for breeding new children. This repetitive procedure runs up to the termination value, which is set as six generations. All individuals in a new generation are evaluated; unless they have been seen in the previous generations. Universally, for seeking the excellent performance of the system, within the range of pallets number (*NPallet* = [10 60]) and lot size (*Lsize*

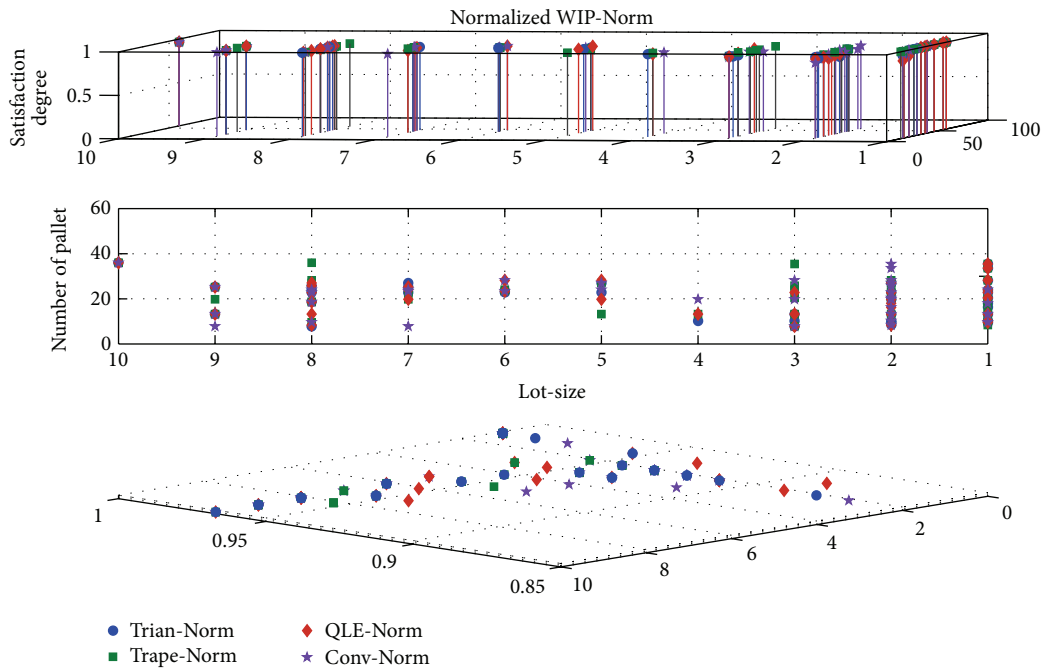

Figure 12: Satisfaction degrees of normalized WIP with demands following normal distribution.

= [1 10]), GA evaluates 110 individuals, that is, $(1 \times 10 + 5 \times 20 = 110$ out of $50 \times 10 = 500)$, see Figure 6 for more illustrations.

In general, two alternative pull-flow scenarios are considered to be experimented against four material flow control systems. In the first alternative, demands are triggered by following the negative exponential distribution (NegExp), whereas in the second alternative demands follow the normal distribution (Norm). Additionally, four variants are developed for material flow control as QLE with triangular fuzzy set (Trian), QLE with trapezoidal fuzzy set (Trape), QLE with crisp values (QLE), and conventional flow control (Conv). These alternatives and variants together configure eight experiment alternatives in the simulation which are presented in the next section. Moreover, to define the performance of each alternative some indicators are evaluated as throughput time (TPT), number of output products (TP), and work-in-processes (WIP).

8. Experimental Results

The eight alternatives include applying different fuzzy sets against conventional crisp numbers in estimation of waiting times for parallel queues are compared by scatter and surface graphs. Figure 7 shows a variety of values for fitness function in GA experiments against the two optimization factors. As it can be seen in different cases the fitness values of each alternative vary. This proves the compatibility of every control system for a specific flow circumstance. Additionally, the surface graphs in the appendix look smoother in case of using fuzzy sets than using crisp values in conventional and QLE control alternatives. Indeed, these results justify that when the system has high pressure of flow regarding number of pallets, lot size, and demand rate; besides existing some uncertain factors using fussy numbers brings more reasonable performance.

For better representation of the control alternatives against each performance indicator they are solely displayed in Figures 8, 9, 10, 11, 12, and 13. There, the alternatives against each performance indicator are easily analyzable for managers to decide over their flow control system.

Finally, application of metaheuristics gives the opportunity to decision maker for adapting its system to optimality through a broad range of available searched values. Moreover, to justify the performance of GA in seeking the near-optimum solutions, SA is employed as well. The results in Table 3 out of SA are quite comparable with those from GA; therefore, both are applicable for this problem with authenticity. However, because of SA essence, just the continuously improving results are shown to the simulator, according to the temperature and cooling system. Nevertheless, SA like GA requires several tunings to bring desirable results. Since GA has several operators (e.g., crossover or mutation probabilities) as well as SA (e.g., definition of step function) to proceed their evolutionary approaches towards optimum solutions there is no guarantee for such heuristics to get the global optimums. Therefore, tuning of the operator factors requires more efforts and experience. However, there lots of studies which aimed for tuning the factors of heuristics that can be directly applied for tuning. The tuning of the factors is subjective and may vary for alternative problems.

9. Summary and Discussion

In summary, the beginning sections of the paper gave some information about material flow control strategies. The strategies complying with material pull and material push

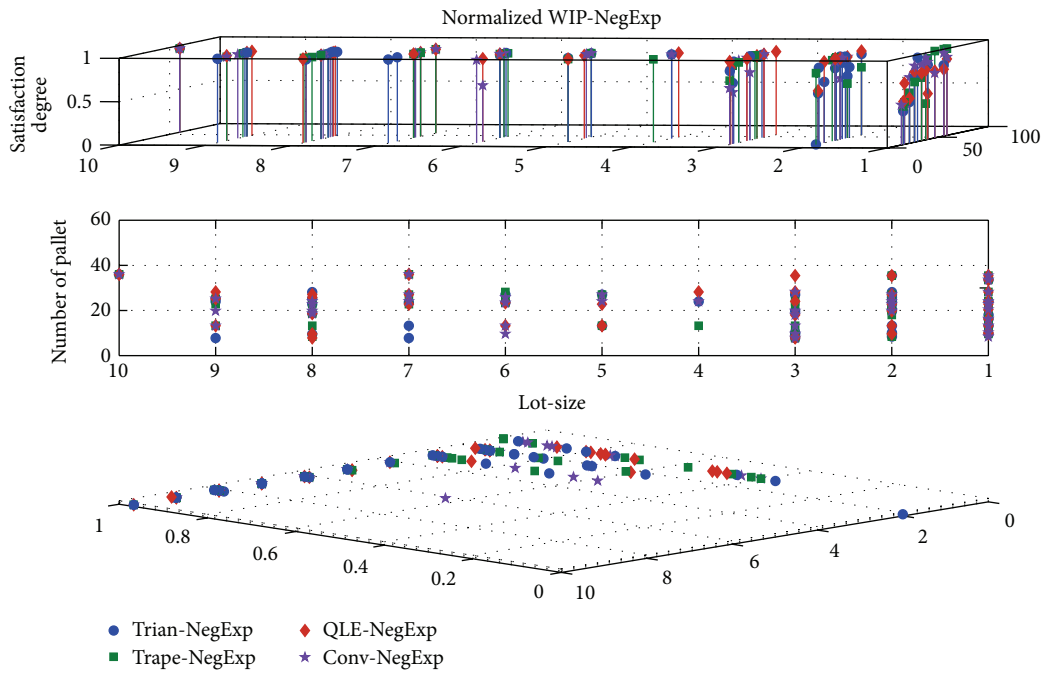

Figure 13: Satisfaction degrees of normalized WIP with demands following negative exponential distribution.

Table 3: Fitness values out of SA in three dimensions.

Fitness values out of SA results in a three dimension form									
Lot-size	Number of pallet	Trape_ Norm	Conv_ NegExp	Trian_ NegExp	Trian_ Norm	QLE_ Norm	QLE_ NegExp	Trape_ NegExp	Conv_ Norm
5	45	0.84	0.78	0.78	0.78			0.76	0.80
4	22	0.85				0.81		0.79	
3	33		0.82	0.79			0.77		0.84
3	17		0.79	0.83	0.84		0.81	0.83	
2	45	0.88	0.85	0.86	0.82	0.83	0.89	0.84	0.86
2	22	0.83		0.81	0.88	0.82	0.83		0.82
1	27	0.90	0.87	0.85	0.91		0.88	0.88	
1	16	0.92		0.84	0.85	0.86	0.90	0.88	0.87

were briefly explained and some theoretical examples were mentioned for them. The main emphasis in the conceptual sections was on the advantages of applying a hybrid control system out of push and pull concepts to exploit the advantages of both. This was inspired by Polca, CONWIP, Leagility, and other comparable hybrid systems to control a smooth and robust flow of material in dynamic systems (regarding uncertainty and fluctuating demands). In order to reflect the applicability of the recommended thesis on supply networks, an exemplary model is simulated with a discrete-event approach. The specifications of the model were given as well. After justifying the importance of coordinating (optimizing WIP and waiting time at) the collision point of push and pull flows, GA and SA as global optimization heuristics were concisely described and their procedures to get the optimum solution were defined. However, both methods may bring different results in case of varying their adjustment factors (e.g., crossover, selection function, cooling schedule, etc.). Later, a brief review is done on the application of fuzzy set theory in normalizing multiobjectives optimization problems and in defining uncertain processes. It was explained that by means of satisfaction degree of decision maker all single objectives can be converted into the range of [0 1] with a common unit to homogenize the heterogeneous multiobjectives. Moreover, the application of fuzzy sets in compensating uncertainty and ambiguity of processes, for example, processing and waiting times, by means of alternative membership functions was described and practiced. Correspondingly, triangular and trapezoidal fuzzy numbers with their selected ranking methods were elaborated.

It was shown that heuristic methods (e.g., GA, SA, and Tabu search) can be employed to find optimum values for coordinating factors (here number of pallets and lotsize) of stochastic flows (i.e., push and pull). Following the conceptual

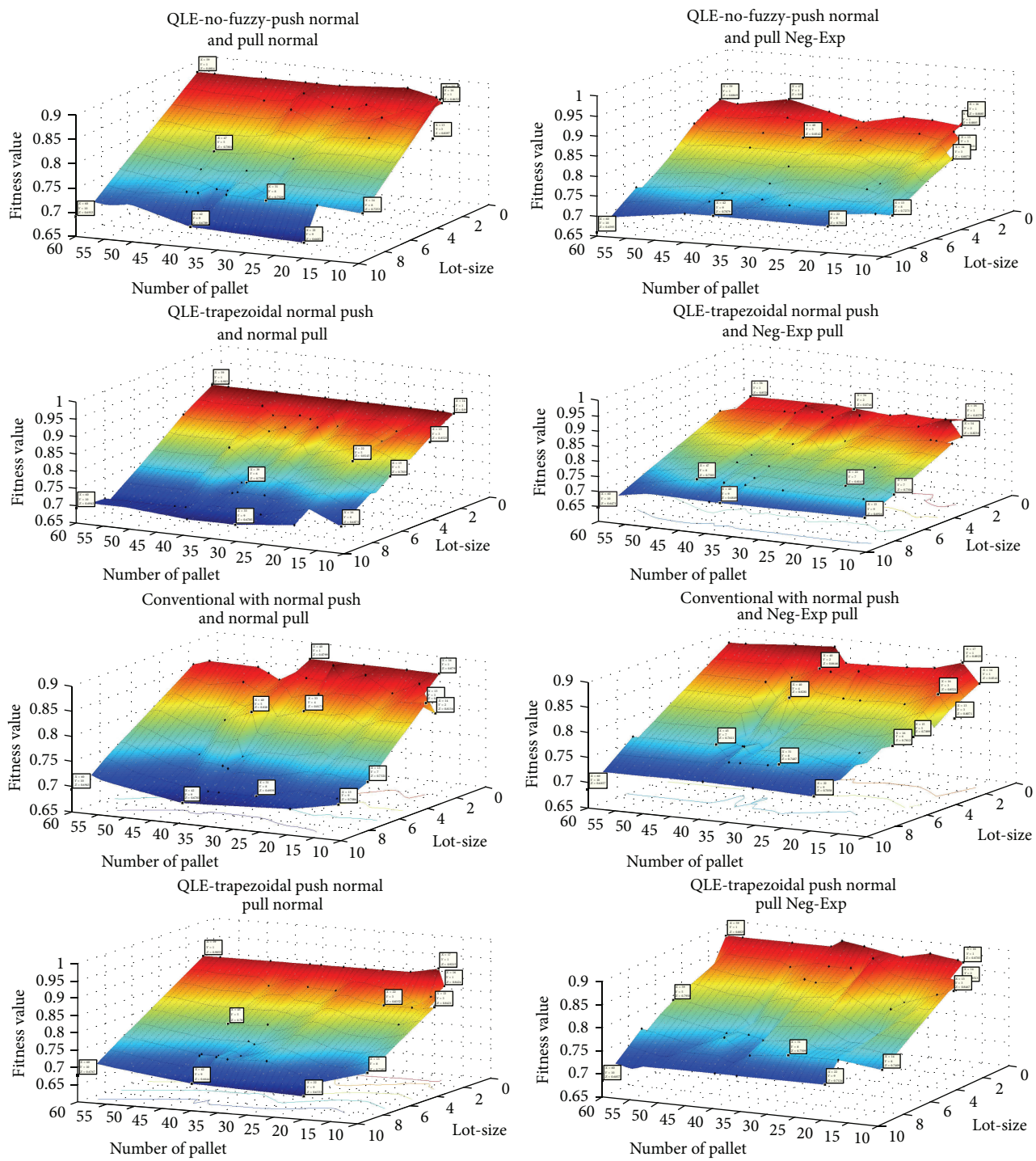

Figure 14

sections, the solution formulation for the simulated problem was fairly described. The results of the simulation experiments with alternative pull flows were depicted at the end. Conclusively, the enhancement of material flows with the assistance of fuzzy sets in alternative cases was proved against some performance indicators. Indeed, the graphs displayed a broad range of performances in case of alternative values for the two factors. The better flow of materials by use of fuzzy numbers was partially apparent in the graphs. However, in some cases the other alternatives as QLE and Conv without using fuzzy numbers outperformed the fuzzy sets. This fact reflects the necessity of adjusting the fuzzy sets to each specific simulation case. Moreover, the broad range of performances gives the opportunity to decision makers to fit their constraints to each performance circumstance in practice. Optimization of material flows throughout supply networks

(inbound as well as outbound) is a challenging task of practitioners. Experimental results showed that employment of optimizing factors in metaheuristics and using simulation contribute to the solution of complex flow controls. The broad scope of solution space investigated by heuristics gives the opportunity to managers to observe a broad range of single solutions (Pareto solutions) and exert those which suit the best to their constraints and requirements.

A very appropriate solution in operational research for solving multiobjective problems is the Pareto frontier. The precision of this solution is reflected by its strong mathematical models for finding the scalarized problem and solving them. This approach is considered to be experimented and compared against the applied approach in this paper (satisfaction degree) as further works in similar case studies. Moreover, in this study the optimization procedure was not run in real time of flows, but with the assistance of offline simulation's experiments. In further works, employment of some intelligent methodologies for example, data mining, artificial neural network (ANN), and Lamarckian learning for improving GA [35] are to be explored. Some learning methodologies can directly be assigned to distributed flow objects, so that they get the capability to locally control and improve their routes and decisions locally and globally in real time [32, 57].

Appendix

See Figure 14.

References

[1] P. Schönsleben, "With agility and adequate partnership strategies towards effective logistics networks," *Computers in Industry*, vol. 42, no. 1, pp. 33–42, 2000.

[2] J. Holstrom, K. Framling, J. Tuomi, M. Karkkainen, and T. Ala-Risku, "Implementing collaboration process networks," *International Journal of Logistics Management*, vol. 13, no. 2, pp. 39–50, 2002.

[3] R. Suri, *Quick Response Manufacturing: A Companywide Approach to Reducing Lead Times*, Productivity Pr, 1998.

[4] F. You and I. E. Grossmann, "Design of responsive supply chains under demand uncertainty," *Computers and Chemical Engineering*, vol. 32, no. 12, pp. 3090–3111, 2008.

[5] A. Yalcin and R. K. Namballa, "An object-oriented simulation framework for real-time control of automated flexible manufacturing systems," *Computers and Industrial Engineering*, vol. 48, no. 1, pp. 111–127, 2005.

[6] S. Zolfaghari and E. Roa, "Cellular manufacturing versus a hybrid system: a comparative study," *Journal of Manufacturing Technology Management*, vol. 17, no. 7, pp. 942–996, 2006.

[7] B. Scholz-Reiter and M. Freitag, "Autonomous processes in assembly systems," *CIRP Annals-Manufacturing Technology*, vol. 56, no. 2, pp. 712–729, 2007.

[8] T. Ozawa, *Institutions, Industrial Upgrading, and Economic Performance in Japan: The "Flying-Geese" Paradigm of Catch-Up Growth*, Edward Elgar Pub, Northampton, UK, 2006.

[9] W. Rocky and V. Sridharan, "Linking manufacturing planning and control to the manufacturing environment," *Integrated Manufacturing System*, vol. 6, no. 4, pp. 36–42, 1995.

[10] B. Scholz-Reiter, A. Mehrsai, and M. Görges, "Handling dynamics in logistics—adoption of dynamic behaviour and reduction of dynamic effects," *Asian International Journal of Science and Technology Production and Manufacturing Engineering*, vol. 2, no. 3, pp. 99–110, 2009.

[11] B. Scholz-Reiter and A. Mehrsai, "Integration of lean-agile experiments with autonomy in supply chains," in *Proceedings 7th International Conference on Manufacturing Research (ICMR09)*, pp. 60–66, University of Warwick, Warwick, UK, 2009.

[12] M. Spearman, D. Woodruff, and W. Hopp, "CONWIP: a pull alternative to kanban," *International Journal of Production Research*, vol. 28, no. 5, pp. 879–894, 1990.

[13] N. Fernandes and S. do Carmo-Silva, "Generic POLCA-A production and materials flow control mechanism for quick response manufacturing," *International Journal of Production Economics*, vol. 104, no. 1, pp. 74–84, 2006.

[14] X. Y. Sun, P. Ji, L. Y. Sun, and Y. L. Wang, "Positioning multiple decoupling points in a supply network," *International Journal of Production Economics*, vol. 113, no. 2, pp. 943–956, 2008.

[15] A. Gunasekaran, C. Patel, and R. E. McGaughey, "A framework for supply chain performance measurement," *International Journal of Production Economics*, vol. 87, no. 3, pp. 333–347, 2004.

[16] A. Petroni and A. Rizzi, "A fuzzy logic based methodology to rank shop floor dispatching rules," *International Journal of Production Economics*, vol. 76, no. 1, pp. 99–108, 2002.

[17] B. H. Wang and S. W. He, "Robust optimization model and algorithm for logistics center location and allocation under uncertain environment," *Journal of Transportation Systems Engineering and Information Technology*, vol. 9, no. 2, pp. 69–74, 2009.

[18] C. Karrer, "Engineering production control strategies: a guide to tailor strategies that unite the merits of push and pull," in *Engineering Production Control Strategies*, pp. 7–36, Springer, München, Germany, 2012.

[19] K. G. Kempf, "An overview of decision policies for production networks," in *Decision Policies for Production Networks*, D. Armbruster and K. G. Kempf, Eds., pp. 1–8, Springer, 2012.

[20] J. M. Tien, "Manufacturing and services: from mass production to mass customization," *Journal of Systems Science and Systems Engineering*, vol. 20, no. 2, pp. 129–154, 2011.

[21] J. Pahl, S. Voß, and D. L. Woodruff, "Production planning with load dependent lead times," *4OR Quarterly Journal of Operations Research*, vol. 3, no. 4, pp. 257–302, 2005.

[22] R. Germs and J. Riezebos, "Workload balancing capability of pull systems in MTO production," *International Journal of Production Research*, vol. 48, no. 8, pp. 2345–2360, 2010.

[23] F. T. S. Chan, "Effect of kanban size on just-in-time manufacturing systems," *Journal of Materials Processing Technology*, vol. 116, no. 2-3, pp. 146–160, 2001.

[24] B. Scholz-Reiter and A. Mehrsai, "Superior performance of leagile supply networks by application of autonomous control," *IFIP Advances in Information and Communication Technology*, vol. 338, pp. 333–341, 2010.

[25] R. G. Askin and S. Krishnan, "Defining inventory control points in multiproduct stochastic pull systems," *International Journal of Production Economics*, vol. 120, no. 2, pp. 418–429, 2009.

[26] A. Grosfeld-Nir and M. Magazine, "A simulation study of pull systems with ascending/descending buffers and stochastic processing times," *International Journal of Production Research*, vol. 43, no. 17, pp. 3529–3541, 2005.

[27] R. Suri and A. Krishnamurthy, "How to plan and implement POLCA—a material control system for high variety or custom-engineered products," Tech. Rep., Center for Quick Response Manufacturing, Madison University of Wisconsin, USA, 2003.

[28] J. Geraghty and C. Heavey, "A comparison of hybrid push/pull and CONWIP/pull production inventory control policies," *International Journal of Production Economics*, vol. 91, no. 1, pp. 75–90, 2004.

[29] R. Mason-Jones, B. Naylor, and D. Towill, "Engineering the leagile supply chain," *International Journal of Agile Management Systems*, vol. 2, no. 1, pp. 54–61, 2000.

[30] G. Stone, J. Miemczyk, and R. Esser, "Making build to order a reality: the 5-day car initiative," *Strengthening Competitiveness through Production Networks*, vol. 48, no. 16, pp. 4877–4899, 2010.

[31] W. Klingenberg and J. D. Boksma, "A conceptual framework for outsourcing of materials handling activities in automotive: differentiation and implementation," *International Journal of Production Research*, vol. 48, no. 16, pp. 4877–4899, 2010.

[32] A. Mehrsai, K. Hamid-Reza, K.-D. Thoben, and B. Scholz-Reiter, "Application of learning pallets for real-time scheduling by the use of radial basis function network," *Neurocomputing*, vol. 101, no. 4, pp. 82–93, 2013.

[33] B. Scholz-Reiter, M. Görges, and T. Philipp, "Autonomously controlled production systems-influence of autonomous control level on logistic performance," *CIRP Annals-Manufacturing Technology*, vol. 58, no. 1, pp. 395–398, 2009.

[34] A. Mehrsai and B. Scholz-Reiter, "Towards learning pallets applied in pull control job-open shop problem," in *Proceedings of IEEE International Symposium on Assembly and Manufacturing (ISAM '11)*, pp. 1–6, Tampere, Finland, 2011.

[35] Y. S. Ong and A. J. Keane, "Meta-Lamarckian learning in memetic algorithms," *IEEE Transactions on Evolutionary Computation*, vol. 8, no. 2, pp. 99–110, 2004.

[36] F. R. Johnston and J. E. Boylan, "Forecasting for items with intermittent demand," *The Journal of the Operational Research Society*, vol. 47, no. 1, pp. 113–121, 1996.

[37] S. Kumar and C. Chandra, "Managing multi-item common vendor inventory system with random demands," *International Journal of Physical Distribution & Logistics Management*, vol. 32, no. 3, pp. 188–202, 2002.

[38] N. Kubota and T. Fukuda, "Structured intelligence for self-organizing manufacturing systems," *Journal of Intelligent Manufacturing*, vol. 10, no. 2, pp. 121–133, 1999.

[39] J. Schönberger, "Operational freight carrier planning," in *Advanced Planning and Scheduling in Process Industry*, H. O. Günther and P. V. Beek, Eds., Springer, Heidelbelg, Germany, 2005.

[40] T. Weise, "Global Optimization Algorithms—Theory and Application," Abrufdatum, vol. 24, no. 1, 2008, http://www.it-weise.de/.

[41] E. Cantú-Paz, "Migration policies, selection pressure, and parallel evolutionary algorithms," *Journal of Heuristics*, vol. 7, no. 4, pp. 311–334, 2001.

[42] B. Naderi, M. Zandieh, A. Khaleghi Ghoshe Balagh, and V. Roshanaei, "An improved simulated annealing for hybrid flowshops with sequence-dependent setup and transportation times to minimize total completion time and total tardiness," *Expert Systems with Applications*, vol. 36, no. 6, pp. 9625–9633, 2009.

[43] A. Tarighat and A. Miyamoto, "Fuzzy concrete bridge deck condition rating method for practical bridge management system," *Expert Systems with Applications*, vol. 36, no. 10, pp. 112077–112085, 2009.

[44] B. K. Wong and V. S. Lai, "A survey of the application of fuzzy set theory in production and operations management," *International Journal of Production Economics*, vol. 129, no. 1, pp. 157–168, 2011.

[45] M. Sakawa and R. Kubota, "Fuzzy programming for multiobjective job shop scheduling with fuzzy processing time and fuzzy duedate through genetic algorithms," *European Journal of Operational Research*, vol. 120, no. 2, pp. 393–407, 2000.

[46] S. Petrovic, C. Fayad, D. Petrovic, E. Burke, and G. Kendall, "Fuzzy job shop scheduling with lot-sizing," *Annals of Operations Research*, vol. 159, no. 1, pp. 275–292, 2008.

[47] B. Y. Qu and P. N. Suganthan, "Multi-objective evolutionary algorithms based on the summation of normalized objectives and diversified selection," *Information Sciences*, vol. 180, no. 17, pp. 3170–3181, 2010.

[48] C. Fayad and S. Petrovic, "A fuzzy genetic algorithm for real-world job-shop scheduling," in *Innovations in Applied Artificial Intelligence*, M. Ali and F. Esposito, Eds., vol. 3533 of *Lecture Notes in Artificial Intelligence*, pp. 524–533, Springer, Berlin, Germany, 2005.

[49] L. Vermeiren, T. M. Guerra, and H. Lamara, "Application of practical fuzzy arithmetic to fuzzy internal model control," *Engineering Applications of Artificial Intelligence*, vol. 24, no. 6, pp. 1006–1017, 2011.

[50] Y. Thorani, P. P. B. Rao, and N. R. Shankar, "Ordering generalized trapezoidal fuzzy numbers using orthocentre of centroids," *International Journal of Algebra*, vol. 6, no. 22, pp. 1069–1085, 2012.

[51] P. Biswas and S. Pramanik, "Application of fuzzy ranking method to determine the replacement time for fuzzy replacement problem," *International Journal of Computer Applications*, vol. 25, no. 11, pp. 41–47, 2011.

[52] W. Jianqiang and Z. Zhong, "Aggregation operators on intuitionistic trapezoidal fuzzy number and its application to multi-criteria decision making problems," *Journal of Systems Engineering and Electronics*, vol. 20, no. 2, pp. 321–326, 2009.

[53] D. Chakraborty and D. Guha, "Addition of two generalized fuzzy numbers," *International Journal of Industrial Mathematics*, vol. 2, no. 1, pp. 9–20, 2010.

[54] S. M. Chen and J. H. Chen, "Fuzzy risk analysis based on ranking generalized fuzzy numbers with different heights and different spreads," *Expert Systems with Applications*, vol. 36, no. 3, pp. 6833–6842, 2009.

[55] P. Rao, P. Bushan, and N. R. Shankar, "Ranking fuzzy numbers with a distance method using circumcenter of centroids and an index of modality," *Advances in Fuzzy Systems*, vol. 2011, Article ID 178308, 7 pages, 2011.

[56] R. T. Marler and J. S. Arora, "Survey of multi-objective optimization methods for engineering," *Structural and Multidisciplinary Optimization*, vol. 26, no. 6, pp. 369–395, 2004.

[57] A. Mehrsai, K. Hamid-Reza, and B. Scholz-Reiter, "Toward learning autonomous pallets by using fuzzy rules, applied in a Conwip system," *The International Journal of Advanced Manufacturing Technology*, vol. 64, no. 5–8, pp. 1131–1150.

Hindawi Publishing Corporation
Mathematical Problems in Engineering
Volume 2012, Article ID 951953, 25 pages
doi:10.1155/2012/951953

Research Article

A Reduced-Order TS Fuzzy Observer Scheme with Application to Actuator Faults Reconstruction

Dušan Krokavec and Anna Filasová

Department of Cybernetics and Artificial Intelligence, Faculty of Electrical Engineering and Informatics, Technical University of Košice, Letná 9, 042 00 Košice, Slovakia

Correspondence should be addressed to Dušan Krokavec, dusan.krokavec@tuke.sk

Received 11 October 2012; Accepted 23 November 2012

Academic Editor: Peng Shi

Copyright © 2012 D. Krokavec and A. Filasová. This is an open access article distributed under the Creative Commons Attribution License, which permits unrestricted use, distribution, and reproduction in any medium, provided the original work is properly cited.

This paper focuses on the principle for designing reduced-order fuzzy-observer-based actuator fault reconstruction for a class of nonlinear systems. The problem addressed can be indicated as an approach for a kind of reduced-order fuzzy observer design with special gain matrix structure that depends on a given matching condition specification. Using the Lyapunov theory, the stability conditions are obtained and expressed in terms of linear matrix inequalities, and the conditions for asymptotic estimation of actuator faults are derived. Simulation results illustrate the observer design procedure and demonstrate the actuator fault reconstruction effectiveness and performance.

1. Introduction

Automated diagnosis has been one of the most fruitful applications in sophisticated control systems, with potential significance for domains in which systems diagnosis must proceed, while the system is operative and testing opportunities are limited by operational considerations. A real problem is usually to fix the system with faults so that it can continue its mission for some time with some limitations in functionality. Consequently, diagnosis is a part of a larger problem known as Fault Detection, Identification and Reconfiguration (FDIR). The classical principles include observer-based methods, parity space methods, and parameter identification based methods, which have been thoroughly studied (see, e.g., [1, 2] and the references therein).

Observer design is an actual research topic, important in the observer-based fault estimation, and in the fault detection and isolation [3–5]. The nonlinear system theory, exploiting Lipschitz condition, is emerged as an approach capable of use in the state estimation design for nonlinear systems [6], although Lipschitz condition is a restrictive

limitation and many classes of systems may not be satisfied. Application of this principle in state estimator design results only in a sufficient condition for the asymptotic stability of estimation error, and, in fact, there is no straightforward method for selecting the observer gain to satisfy such conditions [7]. Because of strong restrictions, an observer structure with adaptively adjusted parameters is proposed in [8], where Lipchitz constant can be unknown. Concerning fault detection, for example, in [9–11] there are proposed sliding-mode observers. Since they are conditioned by matching conditions, these approaches are not sufficient to ensure safe operation in all applications.

Recently, fault estimation and reconstruction are preferred as an option to fault detection, where, instead of generating residuals, observer-based methods are used to reconstruct sensor and actuator fault signals in nonlinear systems. These practices primarily use adaptive and unknown input observer structures (see e.g., [12–14]), ensuring disturbance rejection and robustness properties of fault estimation.

An alternative approach is the Takagi-Sugeno (TS) fuzzy approximation of the nonlinear system model equations. Since the TS fuzzy method provides the suitable model for a certain class of nonlinear dynamic systems [15], the well-known nonlinear observers are based on TS fuzzy system model. Using TS fuzzy model, a nonlinear system is represented by the fuzzy rules. Each rule utilizes the local system dynamics by a linear model, and the nonlinear system is represented by a collection of fuzzy rules. In this sense, the TS fuzzy model can be viewed as an expansion of piecewise linear partition for the nonlinear system. Since such description allows the utilization of system state representation, model order reduction and error approximation problems have to be solved using the projection methods [16], generally given in the form of linear matrix inequality (LMI) constraints.

System state observers based on TS fuzzy models are principally realized in the same structures as the linear observers [17–20], and design principles usually used techniques based on LMIs. Research in TS fuzzy observers application in fault detection and isolation has attracted many investigators and was the subject of widely scattered publications (see, e.g., [21–24]), mainly focused on the LMI-based observer design, to ensure the stability of the residuals and to optimize the quadratic performance of residual transfer matrix with respect to exogenous disturbance.

Because fault reconstruction provides a direct estimate of the size and severity of a fault, the location of the fault is so known, and the fault isolation step can be deleted. Establishing a general approach for fault reconstruction in systems described by TS models, or finding conditions under which fault reconstruction is well possible, is still an open task [25]. Sophisticated fault estimation schemes were proposed especially for systems with disturbances and uncertainties, where, for example, Gao et al. [26] propose the fuzzy descriptor observer, potentially applicable to sensor fault estimation. In contrast, Xu et al. [27] present an estimation algorithm, based on the integrated fuzzy observer and the inverse system model, for nonlinear actuator fault estimation. The principle of the inverse system model is combined with sliding mode also in [27], since sliding mode observers can be employed in fault estimation if systems are uncertain owing to their insensitivity to matched uncertainties or disturbances. Certainly, the basic approach to actuator faults estimation is based on TS adaptive observers [17], in spite of high-order observer dynamics. On the other hand, few results have been reported to reduced-order observer-based fault reconstruction [8, 28], despite the importance of relative-order dynamics of reduced-order observers for systems without disturbances.

Considering the author's previous work [29], the main contribution of the paper is to examine one principle for designing of reduced-order-observer-based actuator fault

estimation for a class of continuous-time nonlinear MIMO systems, approximated by TS models. Comparing with the approach given in [14], a new design method is proposed to construct a set of linear reduced-order observers, combined by fuzzy rules, to estimate unmeasurable part of the system state vector. Based on the stable observer set, the actuator fault estimation scheme is developed to guarantee asymptotic estimation of actuator faults. The structure of the design conditions is motivated by the need for feasibility, while under defined matching conditions the stability of the reduced-order observer is assured.

The remainder of this paper is organized as follows. Sections 2 and 3 describe TS fuzzy model properties for given class of nonlinear systems and the design principle of the reduced-order observer based on TS model, respectively. The actuator fault reconstruction, using reduced-order fuzzy observer, is outlined in Section 4, especially with respect to observer design principle, matching condition, and stability. In Section 5, one illustrative example is given, and simulation results are presented to confirm the validity of the proposed fault reconstruction scheme. Finally, Section 6 draws some concluding remarks.

Throughout the paper, the following notations are used: $\mathbf{x}^T$, $\mathbf{X}^T$ denotes the transpose of the vector $\mathbf{x}$ and matrix $\mathbf{X}$, respectively, diag$[\cdot]$ denotes a block diagonal matrix, for a square matrix $\mathbf{X} = \mathbf{X}^T > 0$ (resp., $\mathbf{X} = \mathbf{X}^T < 0$) means that $\mathbf{X}$ is a symmetric positive definite matrix (resp., symmetric negative definite matrix), the symbol $\mathbf{I}_n$ represents the nth order unit matrix, $\mathbb{R}$ denotes the set of real numbers, and $\mathbb{R}^{n\times r}$ denotes the set of all $n \times r$ real matrices.

2. Takagi-Sugeno Fuzzy Models

The systems under consideration fall in a class of multi-input and multioutput (MIMO) nonlinear dynamic systems, which in the state-space form are represented as

$$\begin{gathered}\dot{\mathbf{q}}(t) = \mathbf{a}(\mathbf{q}(t)) + \mathbf{B}(\mathbf{q}(t))\mathbf{u}(t) + \mathbf{B}_f\mathbf{f}(t),\\ \mathbf{y}(t) = \mathbf{C}\mathbf{q}(t),\end{gathered} \tag{2.1}$$

where $\mathbf{q}(t) \in \mathbb{R}^n$, $\mathbf{u}(t)$, $\mathbf{u}_f(t) \in \mathbb{R}^r$, and $\mathbf{y}(t) \in \mathbb{R}^m$ are vectors of the state, input, actuator fault, and output variables, respectively, $\mathbf{C} \in \mathbb{R}^{m\times n}$, $\mathbf{B}_f \in \mathbb{R}^{n\times r}$ are real matrices, $\mathbf{a}(\mathbf{q}(t)) \in \mathbb{R}^n$, $\mathbf{B}(\mathbf{q}(t)) \in \mathbb{R}^{n\times r}$ are bounded nonlinear functions of $\mathbf{q}(t)$, and $\mathbf{f}(t) \in \mathbb{R}^r$ is an actuator fault. It is assumed that $\mathbf{a}(\mathbf{q}(t))$ is bounded in associated sectors, that is, in the regions within the system will operate, $\mathbf{a}(0) = 0$, only actuator faults can occur, and if no actuator fault occurs then $\mathbf{u}_f(t) = \mathbf{0}$, for all $t \geq 0$.

It is considered that the number of the nonlinear terms in the vector function $\mathbf{a}(\mathbf{q}(t))$ is p and there exists the set of the nonlinear sector functions $\{w_{lj}(\theta_j(t)),\ l = 1,2,\ldots,p,\ j = 1,2,\ldots,k\}$ such that

$$w_{l1}(\boldsymbol{\theta}(t)) = 1 - \sum_{j=2}^{k} w_{lj}(\theta_j(t)), \tag{2.2}$$

where k is the number of sector functions, and

$$\boldsymbol{\theta}(t) = \begin{bmatrix}\theta_1(t) & \theta_2(t) & \cdots & \theta_q(t)\end{bmatrix} \tag{2.3}$$

is the vector of premise variables. A premise variable represents any measurable variable (in a simple case it can be directly a state variable) and none of the premise variables depend on the inputs $\mathbf{u}(t)$.

Thus, constructing the set of membership functions $w_i(\boldsymbol{\theta}(t)) = \prod_{l=1|j}^{p} w_{lj}(\theta_j(t))$, $i = 1, 2, \ldots s$, $s = 2^k$ from all combinations of the sector functions, the states of the system with an actuator fault are inferred as follows:

$$\dot{\mathbf{q}}(t) = \sum_{i=1}^{s} h_i(\boldsymbol{\theta}(t))(\mathbf{A}_i\mathbf{q}(t) + \mathbf{B}_i\mathbf{u}(t)) + \mathbf{B}_f\mathbf{f}(t), \tag{2.4}$$

$$\mathbf{y}(t) = \mathbf{C}\mathbf{q}(t), \tag{2.5}$$

where the system output is given by the relation (2.5) and

$$h_i(\boldsymbol{\theta}(t)) = \frac{w_i(\boldsymbol{\theta}(t))}{\sum_{i=1}^{s} w_i(\boldsymbol{\theta}(t))} \tag{2.6}$$

is the averaging weight for the ith rule, representing the normalized grade of membership (membership function). By definition, the membership functions satisfy the following convex sum properties:

$$0 \le h_i(\boldsymbol{\theta}(t)) \le 1, \quad \sum_{i=1}^{s} h_i(\boldsymbol{\theta}(t)) = 1, \quad \forall i \in \langle 1, \ldots, s \rangle, \tag{2.7}$$

$\mathbf{A}_i \in \mathbb{R}^{n\times n}$ is the Jacobian matrix of $\mathbf{a}(\mathbf{q}(t))$ with respect to $\mathbf{q}(t) = \mathbf{q}_i$, $\mathbf{B}_i \in \mathbb{R}^{n\times r}$ is the matrix equal to $\mathbf{B}(\mathbf{q}_i)$, and $\mathbf{q}_i$ is the center of the i-th fuzzy region, described by the associated sector function. It is evident that the fuzzy model is achieved by fuzzy amalgamation of the linear subsystem models.

Using a TS model, the conclusion part of a single rule consists no longer of a fuzzy set [19], but determines a function with state variables as arguments, and the corresponding function is a local function for the fuzzy region that is described by the premise part of the rule. Thus, using linear functions, a system state is described locally (in fuzzy regions) by linear models, and at the boundaries between regions the linear interpolation is used between the corresponding local models.

Note, the model (2.4), (2.5) is mostly considered for analysis, control, and state estimation of nonlinear systems.

It is supposed in the next that the aforementioned TS model does not include parameter uncertainties or external disturbances, and all premise and output variables are measurable.

3. Basic Preliminaries

Definition 3.1 (null space of the matrix). Let $\mathbf{E} \in \mathbb{R}^{h\times h}$, $\operatorname{rank}(\mathbf{E}) = k < h$ be a rank deficient matrix. Then the null space $N_{\mathbf{E}}$ of $\mathbf{E}$ is the orthogonal complement of the row space of $\mathbf{E}$.

Lemma 3.2 (orthogonal complement). *If* $\mathbf{E} \in \mathbb{R}^{h\times h}$, $\operatorname{rank}(\mathbf{E}) = k < h$, *is a rank deficient matrix, then an orthogonal complement* $\mathbf{E}^{\perp}$ *of* $\mathbf{E}$ *is*

$$\mathbf{E}^{\perp} = \mathbf{E}^{\circ}\mathbf{U}_{E2}^{T}, \tag{3.1}$$

where $\mathbf{U}_{E2}^{T}$ *is the null space of* $\mathbf{E}$ *and* $\mathbf{E}^{\circ}$ *is an arbitrary matrix of appropriate dimension.*

*Proof (*see, e.g., [30]*).* The singular value decomposition (SVD) of $\mathbf{E}$ gives

$$\mathbf{U}_{E}^{T}\mathbf{E}\mathbf{V}_{E} = \begin{bmatrix}\mathbf{U}_{E1}^{T}\\ \mathbf{U}_{E2}^{T}\end{bmatrix}\mathbf{E}\begin{bmatrix}\mathbf{V}_{E1} & \mathbf{V}_{E2}\end{bmatrix} = \begin{bmatrix}\mathbf{S}_{E} & \mathbf{0}_{12}\\ \mathbf{0}_{21} & \mathbf{0}_{22}\end{bmatrix}, \tag{3.2}$$

where $\mathbf{U}_{E}^{T} \in \mathbb{R}^{h\times h}$ is the orthogonal matrix of the left singular vectors of $\mathbf{E}$, $\mathbf{V}_{E} \in \mathbb{R}^{h\times h}$ is the orthogonal matrix of the right singular vectors of $\mathbf{E}$, and $\mathbf{S}_{E} \in \mathbb{R}^{k\times k}$ is the diagonal positive definite matrix of the form

$$\mathbf{S}_{E} = \operatorname{diag}\begin{bmatrix}\sigma_{E1} & \cdots & \sigma_{Ek}\end{bmatrix}, \quad \sigma_{E1} \geq \cdots \geq \sigma_{Ek} > 0, \tag{3.3}$$

which diagonal elements are the singular values of $\mathbf{E}$. Using orthogonal properties of $\mathbf{U}_{E}$ and $\mathbf{V}_{E}$, that is, $\mathbf{U}_{E}^{T}\mathbf{U}_{E} = \mathbf{I}_{h}$, $\mathbf{V}_{E}^{T}\mathbf{V}_{E} = \mathbf{I}_{h}$, and

$$\begin{bmatrix}\mathbf{U}_{E1}^{T}\\ \mathbf{U}_{E2}^{T}\end{bmatrix}\begin{bmatrix}\mathbf{U}_{E1} & \mathbf{U}_{E2}\end{bmatrix} = \begin{bmatrix}\mathbf{I}_{1} & \mathbf{0}\\ \mathbf{0} & \mathbf{I}_{2}\end{bmatrix}, \quad \mathbf{U}_{E2}^{T}\mathbf{U}_{E1} = \mathbf{0}, \tag{3.4}$$

respectively, where $\mathbf{I}_{h} \in \mathbb{R}^{h\times h}$ is the identity matrix, then $\mathbf{E}$ can be written as

$$\mathbf{E} = \mathbf{U}_{E}\mathbf{S}_{E}\mathbf{V}_{E}^{T} = \begin{bmatrix}\mathbf{U}_{E1} & \mathbf{U}_{E2}\end{bmatrix}\begin{bmatrix}\mathbf{S}_{E} & \mathbf{0}_{12}\\ \mathbf{0}_{21} & \mathbf{0}_{22}\end{bmatrix}\begin{bmatrix}\mathbf{V}_{E1}^{T}\\ \mathbf{V}_{E2}^{T}\end{bmatrix} = \begin{bmatrix}\mathbf{U}_{E1} & \mathbf{U}_{E2}\end{bmatrix}\begin{bmatrix}\mathbf{S}_{E1}\\ \mathbf{0}_{2}\end{bmatrix} = \mathbf{U}_{E1}\mathbf{S}_{E1}, \tag{3.5}$$

where $\mathbf{S}_{E1} = \mathbf{S}_{E}\mathbf{V}_{E1}^{T}$. Thus, (3.4) and (3.5) imply

$$\mathbf{U}_{E2}^{T}\mathbf{E} = \mathbf{U}_{E2}^{T}\begin{bmatrix}\mathbf{U}_{E1} & \mathbf{U}_{E2}\end{bmatrix}\begin{bmatrix}\mathbf{S}_{E1}\\ \mathbf{0}_{2}\end{bmatrix} = \mathbf{0}. \tag{3.6}$$

It is evident that for an arbitrary matrix $\mathbf{E}^{\circ}$ it is

$$\mathbf{E}^{\circ}\mathbf{U}_{E2}^{T}\mathbf{E} = \mathbf{E}^{\perp}\mathbf{E} = \mathbf{0}, \tag{3.7}$$

which implies (3.1). This concludes the proof. □

Lemma 3.3 (congruence transform). *Let the output matrix* $\mathbf{C}$ *be of full column rank,* $\operatorname{rank}\ \mathbf{C} = m$, *then there exists a new coordinate system such that* $\mathbf{C}$ *takes the structure* $\mathbf{C}_{a} = [\mathbf{I}_{m}\ \ 0]$.

Proof. Applying SVD to $\mathbf{C}$ gives

$$\mathbf{C} = \mathbf{U}\begin{bmatrix}\mathbf{S} & \mathbf{0}\end{bmatrix}\mathbf{V}^T = \mathbf{U}\mathbf{S}\begin{bmatrix}\mathbf{I}_m & \mathbf{0}\end{bmatrix}\mathbf{V}^T, \tag{3.8}$$

where rows of $\mathbf{U}^T \in \mathbb{R}^{m\times m}$ are left singular vectors of $\mathbf{C}$, and columns of $\mathbf{V} \in \mathbb{R}^{n\times n}$ are right singular vectors of $\mathbf{C}$, all ordered in such way to be associated with the singular values of $\mathbf{C}$, written as diagonal elements of $\mathbf{S} \in \mathbb{R}^{m\times m}$,

$$\mathbf{S} = \operatorname{diag}\begin{bmatrix}\sigma_1 & \cdots & \sigma_m\end{bmatrix}, \quad \sigma_1 \geq \cdots \geq \sigma_m > 0. \tag{3.9}$$

Using the notations

$$\mathbf{W}^{-1} = \mathbf{U}\mathbf{S}, \qquad \mathbf{T}_a = \mathbf{V}^T, \qquad \mathbf{C}_a = \begin{bmatrix}\mathbf{I}_m & \mathbf{0}\end{bmatrix}, \tag{3.10}$$

where

$$\mathbf{T}_a^T = \begin{bmatrix}\mathbf{T}_{a1}^T & \mathbf{T}_{a2}^T\end{bmatrix}, \quad \mathbf{T}_{a1}^T \in \mathbb{R}^{n\times m}, \tag{3.11}$$

then (3.8) implies

$$\mathbf{C} = \mathbf{W}^{-1}\mathbf{C}_a\mathbf{T}_a, \quad \mathbf{C}_a = \mathbf{W}\mathbf{C}\mathbf{T}_a^{-1}. \tag{3.12}$$

Note if $\mathbf{C}$ is of rank m, $\mathbf{W} \in \mathbb{R}^{m\times m}$ is a regular matrix, and $\mathbf{T}_a \in \mathbb{R}^{n\times n}$ is an orthogonal matrix such that $\mathbf{T}_a^{-1} = \mathbf{T}_a^T = \mathbf{V}$. This concludes the proof. □

Lemma 3.4. *Using the congruence transform* (3.12), *each linear submodel of fault-free TS fuzzy model* (2.4), (2.5) *can be partitioned such that*

$$\begin{bmatrix}\dot{\mathbf{q}}_{a1i}\\ \dot{\mathbf{q}}_{a2i}\end{bmatrix} = \begin{bmatrix}\mathbf{A}_{a11i} & \mathbf{A}_{a12i}\\ \mathbf{A}_{a21i} & \mathbf{A}_{a22i}\end{bmatrix}\begin{bmatrix}\mathbf{q}_{a1}(t)\\ \mathbf{q}_{a2}(t)\end{bmatrix} + \begin{bmatrix}\mathbf{B}_{a1i}\\ \mathbf{B}_{a2i}\end{bmatrix}\mathbf{u}(t) + \begin{bmatrix}\mathbf{B}_{af1}\\ \mathbf{B}_{af2}\end{bmatrix}\mathbf{f}(t), \tag{3.13}$$

$$\mathbf{y}(t) = \mathbf{W}^{-1}\mathbf{v}(t), \tag{3.14}$$

$$\mathbf{v}(t) = \begin{bmatrix}\mathbf{I}_m & \mathbf{0}\end{bmatrix}\mathbf{q}_a(t) = \begin{bmatrix}\mathbf{I}_m & \mathbf{0}\end{bmatrix}\begin{bmatrix}\mathbf{q}_{a1}(t)\\ \mathbf{q}_{a2}(t)\end{bmatrix}, \tag{3.15}$$

$$\mathbf{q}_a^T(t) = \begin{bmatrix}\mathbf{q}_{a1}^T(t) & \mathbf{q}_{a2}^T(t)\end{bmatrix}, \quad \mathbf{q}_a(t) = \mathbf{T}_a\mathbf{q}(t), \tag{3.16}$$

where $\mathbf{q}_{a1}(t) \in \mathbb{R}^m$, $\mathbf{q}_{a2}(t) \in \mathbb{R}^{n-m}$, $\mathbf{B}_{a1i} \in \mathbb{R}^{m\times r}$, $\mathbf{B}_{af1} \in \mathbb{R}^{m\times r}$, *respectively.*

Proof. Substituting (3.11) into (2.5) gives

$$\mathbf{y}(t) = \mathbf{W}^{-1}\mathbf{C}_a\mathbf{T}_a\mathbf{q}(t) = \mathbf{W}^{-1}\mathbf{C}_a\mathbf{q}_a(t). \tag{3.17}$$

Thus, using

$$\mathbf{v}(t) = \mathbf{C}_a \mathbf{q}_a(t), \tag{3.18}$$

(3.17) implies (3.14), and with (3.11), (3.12), then (3.18) implies (3.15).

Substituting (3.16) in (2.4), it can be obtained

$$\dot{\mathbf{q}}_a(t) = \sum_{i=1}^{s} h_i(\boldsymbol{\theta}(t))\mathbf{A}_{ai}\mathbf{q}_a(t) + \mathbf{B}_{ai}\mathbf{u}(t) + \mathbf{B}_{af}\mathbf{f}(t), \tag{3.19}$$

where

$$\mathbf{A}_{ai} = \mathbf{T}_a \mathbf{A}_i \mathbf{T}_a^{-1}, \qquad \mathbf{B}_{ai} = \mathbf{T}_a \mathbf{B}_i, \qquad \mathbf{B}_{af} = \mathbf{T}_a \mathbf{B}_f, \tag{3.20}$$

and partitioning accordingly to (3.15), (3.20) implies (3.13). This concludes the proof. □

Proposition 3.5 (matching condition). *The fault input matrix and the output matrix* $\mathbf{B}_{af}$, $\mathbf{C}$ *satisfies the conditions* rank $\mathbf{B}_{af} = r$, rank $\mathbf{C} >$ rank $\mathbf{B}_f$, *respectively, that is,* $m > r$, *and the matrix* $\mathbf{B}_{af}$ *takes the structure*

$$\mathbf{B}_{af} = \mathbf{C}_a^T \mathbf{B}_{af1}. \tag{3.21}$$

The matching condition, given in Proposition 3.5 seems to be restrictive theoretically, but fortunately, for many practical control systems it is satisfied. In addition, comparing with the static decoupling control principle [31], the condition reflects inserting at least one redundant output sensor into the sensor structure.

4. Full-Order TS Fuzzy Observer

Standard applications of TS fuzzy principle in nonlinear system fault diagnosis exploit the fuzzy observers as residual generators. The procedure of fault detection covers the residual generation by the fuzzy observers and their evaluation. Thus, the reconstruction error, or any function of it, is used as fault residual signal that is as a rule zero in the fault free case and nonzero otherwise [1, 2].

The fuzzy observer to the fault-free system (2.4), (2.5) is constructed as follows:

$$\dot{\mathbf{q}}_e(t) = \sum_{i=1}^{s} h_i(\boldsymbol{\theta}(t))(\mathbf{A}\mathbf{q}_e(t) + \mathbf{B}\mathbf{u}(t) + \mathbf{A}_i\mathbf{q}_e(t) + \mathbf{J}_i(\mathbf{y} - \mathbf{y}_e(t))), \tag{4.1}$$

$$\mathbf{y}_e(t) = \mathbf{C}\mathbf{q}_e(t), \tag{4.2}$$

where $\mathbf{q}_e(t) \in \mathbb{R}^n$ is the estimation of the system state vector, $\mathbf{J}_i \in \mathbb{R}^{n\times m}$, $i = 1, 2, \ldots, s$, is the set of the observer gain matrices. The design conditions are given by the next lemma.

Lemma 4.1. *The fuzzy observer* (4.1), (4.2) *is stable if there exist a positive definite symmetric matrix* $\mathbf{P} > 0$, $\mathbf{P} \in \mathbb{R}^{n\times n}$, *and matrices* $\mathbf{Z}_i \in \mathbb{R}^{n\times m}$, $i = 1, 2, \ldots, s$, *such that*

$$\mathbf{P} = \mathbf{P}^T > 0, \tag{4.3}$$

$$\mathbf{A}_i\mathbf{P} + \mathbf{P}\mathbf{A}_i - \mathbf{Z}_i^T\mathbf{C}^T - \mathbf{Z}_i\mathbf{C} < 0, \quad \forall i. \tag{4.4}$$

If the above conditions hold, the set of the observer gain matrices is given as

$$\mathbf{J}_i = \mathbf{P}^{-1}\mathbf{Z}_i. \tag{4.5}$$

Proof. Introducing the estimation error between the fault-free (2.4) and (4.1) as follows:

$$\mathbf{e}(t) = \mathbf{q}(t) - \mathbf{q}_e(t), \tag{4.6}$$

and taking into account the time derivative of $\mathbf{e}(t)$, it can be obtained

$$\dot{\mathbf{e}}(t) = \sum_{i=1}^{s} h_i(\boldsymbol{\theta}(t))(\mathbf{A}_i - \mathbf{J}_i\mathbf{C})\mathbf{e}(t) = \sum_{i=1}^{s} h_i(\boldsymbol{\theta}(t))\mathbf{A}_{ei}\mathbf{e}(t), \tag{4.7}$$

where the observer system matrices are

$$\mathbf{A}_{ei} = \mathbf{A}_i - \mathbf{J}_i\mathbf{C}, \quad i = 1, 2, \ldots, s. \tag{4.8}$$

Defining the quadratic positive definite Lyapunov function of the form

$$v(\mathbf{e}(t)) = \mathbf{e}^T(t)\mathbf{P}\mathbf{e}(t), \tag{4.9}$$

where $\mathbf{P} > 0$, then after evaluation of its derivative with respect to t it is obtained

$$\dot{v}(\mathbf{e}(t)) = \dot{\mathbf{e}}^T(t)\mathbf{P}\mathbf{e}(t) + \mathbf{e}^T(t)\mathbf{P}\dot{\mathbf{e}}(t). \tag{4.10}$$

Substituting (4.7) in (4.10) gives

$$\dot{v}(\mathbf{e}(t)) = \mathbf{e}^T(t)\mathbf{P}\sum_{i=1}^{s} h_i(\boldsymbol{\theta}(t))\mathbf{A}_{ei}\mathbf{e}(t) + \mathbf{e}^T(t)\sum_{i=1}^{s} h_i(\boldsymbol{\theta}(t))\mathbf{A}_{ei}^T\mathbf{P}\mathbf{e}(t), \tag{4.11}$$

$$\dot{v}(\mathbf{e}(t)) = \mathbf{e}^T(t)\sum_{i=1}^{s} h_i(\boldsymbol{\theta}(t))\left(\mathbf{P}\mathbf{A}_{ei} + \mathbf{A}_{ei}^T\mathbf{P}\right)\mathbf{e}(t), \tag{4.12}$$

respectively. It is evident that (4.12) is negative if there exist a set of gain matrices $\mathbf{J}_i \in \mathbb{R}^{n\times m}$, $i = 1, 2, \ldots, s$, and a symmetric positive definite matrix $\mathbf{P} \in \mathbb{R}^{n\times n}$ such that

$$(\mathbf{A}_i - \mathbf{J}_i\mathbf{C})^T\mathbf{P} + \mathbf{P}(\mathbf{A}_i - \mathbf{J}_i\mathbf{C}) < 0, \quad \forall i. \tag{4.13}$$

Setting

$$\mathbf{P}\mathbf{J}_i = \mathbf{Z}_i, \tag{4.14}$$

(4.13) implies (4.4). This concludes the proof. □

Note, to apply for actuator fault reconstruction, an adaptive structure of the full-order state observer can be used [12].

5. Reduced-Order TS Fuzzy Observer

Problem of the interest is to design the asymptotically stable reduced-order observer based on the TS fuzzy model of the fault-free nonlinear system (2.4), (2.5).

Theorem 5.1. *Considering the affine TS fuzzy system* (2.4), (2.5), *then the reduced-order TS fuzzy observer takes the form*

$$\dot{\mathbf{p}}_{2e}(t) = \sum_{i=1}^{s} h_i(\boldsymbol{\theta}(t))\mathbf{q}_{2ei}^{\circ}(t), \tag{5.1}$$

$$\mathbf{q}_{2ei}^{\circ}(t) = \mathbf{A}_{aei}\mathbf{p}_{2e}(t) + \mathbf{A}_{avi}\mathbf{v}(t) + \left[-\mathbf{J}_i \quad \mathbf{I}_{n-m}\right]\mathbf{B}_{ai}\mathbf{u}(t), \tag{5.2}$$

$$\mathbf{q}_{a2e}(t) = \mathbf{p}_{2e}(t) + \sum_{i=1}^{s} h_i(\boldsymbol{\theta}(t))\mathbf{J}_i\mathbf{v}(t), \tag{5.3}$$

where

$$\mathbf{A}_{avi} = \mathbf{A}_{a21i} - \mathbf{J}_i\mathbf{A}_{a11i} + (\mathbf{A}_{a22i} - \mathbf{J}_i\mathbf{A}_{a12i})\sum_{j=1}^{s} h_j(\boldsymbol{\theta}(t))\mathbf{J}_j, \tag{5.4}$$

$$\mathbf{A}_{aei} = \mathbf{A}_{a22i} - \mathbf{J}_i\mathbf{A}_{a12i}, \tag{5.5}$$

and $\mathbf{J}_i \in \mathbb{R}^{(n-m)\times m}$, $i = 1, 2, \ldots, s$ *is the set of gains.*

Proof. Since (3.13) can be partitioned as

$$\mathbf{A}_{a12i}\mathbf{q}_{a2}(t) = \dot{\mathbf{q}}_{a1i}(t) - \mathbf{A}_{a11i}\mathbf{v}(t) - \mathbf{B}_{a1i}\mathbf{u}(t), \tag{5.6}$$

$$\dot{\mathbf{q}}_{a2i}(t) = \mathbf{A}_{a21i}\mathbf{v}(t) + \mathbf{A}_{a22i}\mathbf{q}_{a2}(t) + \mathbf{B}_{a2i}\mathbf{u}(t), \tag{5.7}$$

then the TS fuzzy observer can be defined as follows:

$$\dot{\mathbf{q}}_{a2e}(t) = \sum_{i=1}^{s} h_i(\boldsymbol{\theta}(t))\mathbf{q}_{a2ei}^{\bullet}(t), \tag{5.8}$$

$$\mathbf{q}_{a2ei}^{\bullet}(t) = \mathbf{A}_{a21i}\mathbf{v}(t) + \mathbf{A}_{a22i}\mathbf{q}_{a2e}(t) + \mathbf{B}_{a2i}\mathbf{u}(t) + \mathbf{J}_i(\dot{\mathbf{q}}_{a1i}(t) - \mathbf{A}_{a11i}\mathbf{v}(t) - \mathbf{B}_{a1i}\mathbf{u}(t) - \mathbf{A}_{a12i}\mathbf{q}_{a2e}(t)), \tag{5.9}$$

where $\mathbf{q}_{a2e}(t) \in \mathbb{R}^{n-m}$ is an estimation of the unmeasurable part of system state vector, and $\mathbf{J}_i,\ i = 1, 2, \ldots, s,\ \mathbf{J}_i \in \mathbb{R}^{(n-m)\times m}$, is the set of the observer gain matrices. Now, (5.8), (5.9) can be rewritten as

$$\dot{\mathbf{q}}_{a2e}(t) - \sum_{i=1}^{s} h_i(\boldsymbol{\theta}(t))\mathbf{J}_i\dot{\mathbf{q}}_{a1i}(t) = \sum_{i=1}^{s} h_i(\boldsymbol{\theta}(t))\mathbf{q}^{\diamond}_{a2i}(t), \tag{5.10}$$

$$\begin{aligned}\mathbf{q}^{\diamond}_{a2i}(t) = {} & \mathbf{B}_{a2i}\mathbf{u}(t) + \mathbf{A}_{a21i}\mathbf{v}(t) + \mathbf{A}_{a22i}\left(\mathbf{q}_{a2e}(t) - \textstyle\sum_{j=1}^{s} h_j(\boldsymbol{\theta}(t))\mathbf{J}_j\mathbf{v}(t) + \sum_{j=1}^{s} h_j(\boldsymbol{\theta}(t))\mathbf{J}_j\mathbf{v}(t)\right) \\ & + \mathbf{J}_i\begin{pmatrix} -\mathbf{A}_{a11i}\mathbf{v}(t) - \mathbf{B}_{a1i}\mathbf{u}(t) \\ -\mathbf{A}_{a12i}\left(\mathbf{q}_{a2e}(t) - \sum_{j=1}^{s} h_j(\boldsymbol{\theta}(t))\mathbf{J}_j\mathbf{v}(t) + \sum_{j=1}^{s} h_j(\boldsymbol{\theta}(t))\mathbf{J}_j\mathbf{v}(t)\right)\end{pmatrix}.\end{aligned} \tag{5.11}$$

Defining the new state variable

$$\mathbf{p}_{2e}(t) = \mathbf{q}_{a2e}(t) - \sum_{i=1}^{s} h_i(\boldsymbol{\theta}(t))\mathbf{J}_i\mathbf{v}(t), \tag{5.12}$$

then (5.12) implies (5.3), and defining the left side of (5.10) as

$$\dot{\mathbf{p}}_{2e}(t) = \dot{\mathbf{q}}_{a2e}(t) - \sum_{i=1}^{s} h_i(\boldsymbol{\theta}(t))\mathbf{J}_i\dot{\mathbf{q}}_{a1i}(t), \tag{5.13}$$

it can be obtained

$$\dot{\mathbf{p}}_{2e}(t) = \sum_{i=1}^{s} h_i(\boldsymbol{\theta}(t))\mathbf{q}^{\circ}_{2ei} \tag{5.14}$$

$$\begin{aligned}\mathbf{q}^{\circ}_{2ei} = {} & (\mathbf{A}_{a22i} - \mathbf{J}_i\mathbf{A}_{a12i})\mathbf{p}_{2e}(t) + (\mathbf{B}_{a2i} - \mathbf{J}_i\mathbf{B}_{a1i})\mathbf{u}(t) \\ & + (\mathbf{A}_{a21i} - \mathbf{J}_i\mathbf{A}_{a11i})\mathbf{v}(t) + (\mathbf{A}_{a22i} - \mathbf{J}_i\mathbf{A}_{a12i})\sum_{j=1}^{s} h_j(\boldsymbol{\theta}(t))\mathbf{J}_j\mathbf{v}(t).\end{aligned} \tag{5.15}$$

Since

$$\mathbf{B}_{a2i} - \mathbf{J}_i\mathbf{B}_{a1i} = \begin{bmatrix}-\mathbf{J}_i & \mathbf{I}_{n-m}\end{bmatrix}\mathbf{B}_{ai} \tag{5.16}$$

with (5.4), (5.5), and (5.16) then (5.14), (5.15) implies (5.1), (5.2).

It is evident that

$$\mathbf{v}(t) = \mathbf{q}_{a1}(t) = \mathbf{p}_1(t). \tag{5.17}$$

This concludes the proof. □

Theorem 5.2 (reducer-order TS fuzzy observer stability). *The reduced-order TS fuzzy observer* (5.1), (5.2) *is asymptotically stable if there exist a symmetric positive definite matrix* $\mathbf{P}^{\circ} \in \mathbb{R}^{(n-m)\times(n-m)}$ *and matrices* $\mathbf{Z}_i^{\circ} \in \mathbb{R}^{(n-m)\times m}$, $i = 1, 2, \ldots, s$ *such that*

$$\mathbf{P}^{\circ} = \mathbf{P}^{\circ T} > 0, \tag{5.18}$$

$$\mathbf{A}_{a22i}^T \mathbf{P}^{\circ} + \mathbf{P}^{\circ} \mathbf{A}_{a22i} - \mathbf{A}_{a12i}^T \mathbf{Z}_i^{\circ T} - \mathbf{Z}_i^{\circ} \mathbf{A}_{a12i} < 0. \tag{5.19}$$

If the above conditions hold, the set of the observer gain matrices is given as

$$\mathbf{J}_i = (\mathbf{P}^{\circ})^{-1} \mathbf{Z}_i^{\circ}. \tag{5.20}$$

Proof. Using (5.1), (5.2), it can be rewritten as

$$\dot{\mathbf{p}}_{2e}(t) = \sum_{i=1}^{s} h_i(\boldsymbol{\theta}(t)) \left(\mathbf{A}_{aei} \mathbf{p}_{2e}(t) + \mathbf{A}_{avi} \mathbf{v}(t) + \left[-\mathbf{J}_i \;\; \mathbf{I}_{n-m} \right] \mathbf{B}_{ai} \mathbf{u}(t) \right), \tag{5.21}$$

and, with (5.4), the autonomous part of (5.21) takes the form

$$\dot{\mathbf{p}}_{2e}(t) = \sum_{i=1}^{s} h_i(\boldsymbol{\theta}(t)) (\mathbf{A}_{a22i} - \mathbf{J}_i \mathbf{A}_{a12i}) \mathbf{p}_{2e}(t). \tag{5.22}$$

Defining the quadratic positive definite Lyapunov function:

$$v(\mathbf{p}_{2e}(t)) = \mathbf{p}_{2e}^T(t) \mathbf{P}^{\circ} \mathbf{p}_{2e}(t), \tag{5.23}$$

where $\mathbf{P}^{\circ} = \mathbf{P}^{\circ T} > 0$, $\mathbf{P}^{\circ} \in \mathbb{R}^{(n-m)\times(n-m)}$ then, after evaluation of derivative with respect to t, it is obtained

$$\dot{v}(\mathbf{p}_{2e}(t)) = \mathbf{p}_{2e}^T(t) \mathbf{P}^{\circ} \dot{\mathbf{p}}_{2e}(t) + \dot{\mathbf{p}}_{2e}^T(t) \mathbf{P}^{\circ} \mathbf{p}_{2e}(t) < 0. \tag{5.24}$$

Substituting (5.22) into (5.24) gives

$$\dot{v}(\mathbf{p}_{2e}(t)) = \mathbf{p}_{2e}^T(t) \mathbf{P}^{\circ} \sum_{i=1}^{s} h_i(\boldsymbol{\theta}(t)) \mathbf{A}_{aei} \mathbf{p}_{2e}(t) + \mathbf{p}_{2e}^T(t) \sum_{i=1}^{s} h_i(\boldsymbol{\theta}(t)) \mathbf{A}_{aei}^T \mathbf{P}^{\circ} \mathbf{p}_{2e}(t) < 0, \tag{5.25}$$

$$\dot{v}(\mathbf{p}_{2e}(t)) = \mathbf{p}_{2e}^T(t) \sum_{i=1}^{s} h_i(\boldsymbol{\theta}(t)) \left(\mathbf{P}^{\circ} \mathbf{A}_{aei} + \mathbf{A}_{aei}^T \mathbf{P}^{\circ} \right) \mathbf{p}_{2e}(t) < 0, \tag{5.26}$$

respectively. Thus, (5.26) is negative, if there exist a set of matrices $\mathbf{J}_i$, $i = 1, 2, \ldots, s$, and a matrix $\mathbf{P}^{\circ}$ such that

$$(\mathbf{A}_{a22i} - \mathbf{J}_i \mathbf{A}_{a12i})^T \mathbf{P}^{\circ} + \mathbf{P}^{\circ} (\mathbf{A}_{a22i} - \mathbf{J}_i \mathbf{A}_{a12i}) < 0, \quad \forall i. \tag{5.27}$$

Setting

$$\mathbf{P}^{\circ}\mathbf{J}_i = \mathbf{Z}_i^{\circ} \tag{5.28}$$

(5.27) implies (5.19). This concludes the proof. □

Remark 5.3. If (5.19) is infeasible, then it can be set

$$\mathbf{A}_{a22i}^T\mathbf{P} + \mathbf{P}\mathbf{A}_{a22i} - \mathbf{A}_{a12i}^T\mathbf{Z}_i^T - \mathbf{Z}_i\mathbf{A}_{a12i} < -\mathbf{Q}, \tag{5.29}$$

where $\mathbf{Q} = \mathbf{Q}^T > 0$, $\mathbf{Q} \in \mathbb{R}^{(n-m)\times(n-m)}$ is a symmetric positive definite matrix. It is obvious, based on the inequality (5.29), such design condition implies inherently the more conservative solution.

Theorem 5.4 (stability condition equivalency). *The asymptotic stability condition of the autonomous part of* (5.22) *is the same as the asymptotic stability condition of the error reference model as follows:*

$$\dot{\mathbf{e}}_{aq2}(t) = \sum_{i=1}^{s} h_i(\boldsymbol{\theta}(t))(\mathbf{A}_{a22i} - \mathbf{J}_i\mathbf{A}_{a12i})\mathbf{e}_{aq2}(t), \tag{5.30}$$

where the estimation error of the unmeasurable part of state variables is

$$\mathbf{e}_{aq2}(t) = \mathbf{q}_{a2}(t) - \mathbf{q}_{a2e}(t). \tag{5.31}$$

Proof. Substituting (5.3) in (5.31) gives

$$\mathbf{e}_{a2}(t) = \mathbf{q}_{a2}(t) - \mathbf{p}_{2e}(t) - \sum_{i=1}^{s} h_i(\boldsymbol{\theta}(t))\mathbf{J}_i\mathbf{v}(t). \tag{5.32}$$

Defining, in analogy with (5.1)–(5.3), the reference variable $\mathbf{p}_2(t)$ is as follows:

$$\mathbf{p}_2(t) = \mathbf{q}_{a2}(t) - \sum_{i=1}^{s} h_i(\boldsymbol{\theta}(t))\mathbf{J}_i\mathbf{v}(t), \tag{5.33}$$

$$\dot{\mathbf{p}}_2(t) = \sum_{i=1}^{s} h_i(\boldsymbol{\theta}(t))\mathbf{q}_{2i}^{\circ}(t), \tag{5.34}$$

$$\mathbf{q}_{2i}^{\circ}(t) = \mathbf{A}_{aei}\mathbf{p}_2(t) + \mathbf{A}_{avi}\mathbf{v}(t) + \begin{bmatrix}-\mathbf{J}_i & \mathbf{I}_{n-m}\end{bmatrix}\mathbf{B}_{ai}\mathbf{u}(t), \tag{5.35}$$

and substituting (5.33) in (5.32) gives

$$\mathbf{e}_{aq2}(t) = \mathbf{p}_2(t) - \mathbf{p}_{2e}(t) = \mathbf{e}_{p2}(t), \tag{5.36}$$

$$\dot{\mathbf{e}}_{aq2}(t) = \dot{\mathbf{e}}_{p2}(t) = \dot{\mathbf{p}}_2(t) - \dot{\mathbf{p}}_{2e}(t), \tag{5.37}$$

respectively. Thus, inserting (5.1), (5.2) and (5.34), (5.35) into (5.37) results in

$$\dot{\mathbf{e}}_{aq2}(t) = \sum_{i=1}^{s} h_i(\boldsymbol{\theta}(t))\mathbf{A}_{aei}(\mathbf{p}_2(t) - \mathbf{p}_{2e}(t)), \tag{5.38}$$

and with (5.5), (5.36) then (5.38) implies (5.30).

Since (5.22) and (5.36) are associated with the same system matrix $\mathbf{A}_{aei}$, this concludes the proof. □

Note, the form of the time derivative (5.13) is given by the definition.

Corollary 5.5 (error reference model). *The equalities* (5.17), (5.33) *can be compactly written as*

$$\begin{bmatrix} \mathbf{p}_1(t) \\ \mathbf{p}_2(t) \end{bmatrix} = \sum_{i=1}^{s} h_i(\boldsymbol{\theta}(t))\mathbf{T}_i(\mathbf{A}_{ai}\mathbf{q}_{ai}(t) + \mathbf{B}_{ai}\mathbf{u}(t)), \tag{5.39}$$

where

$$\begin{gathered} \mathbf{T}_i = \begin{bmatrix} \mathbf{I}_m & \mathbf{0} \\ -\mathbf{J}_i & \mathbf{I}_{n-m} \end{bmatrix}, \\ \mathbf{T}_i\mathbf{B}_{ai}\mathbf{u}(t) = \begin{bmatrix} \mathbf{I}_m & \mathbf{0} \\ -\mathbf{J}_i & \mathbf{I}_{n-m} \end{bmatrix} \begin{bmatrix} \mathbf{B}_{a1i} \\ \mathbf{B}_{a2i} \end{bmatrix} \mathbf{u}(t), \\ \mathbf{T}_i\mathbf{A}_{ai}\mathbf{q}_a(t) = \begin{bmatrix} \mathbf{A}_{a11i} & \mathbf{A}_{a12i} \\ \mathbf{A}_{a21i} - \mathbf{J}_i\mathbf{A}_{a11i} & \mathbf{A}_{a22i} - \mathbf{J}_i\mathbf{A}_{a12i} \end{bmatrix} \begin{bmatrix} \mathbf{v}(t) \\ \mathbf{q}_{a2}(t) \end{bmatrix}. \end{gathered} \tag{5.40}$$

Ones explaining the variable $\mathbf{p}_2(t)$ *as a function of* $\mathbf{q}_{a2}(t)$ *using* (5.39), *then the time derivative of* $\mathbf{p}_2(t)$ *can be obtained by the substitution* (5.33), *that is,*

$$\dot{\mathbf{p}}_2(t) = \mathbf{p}_2(t)(\mathbf{q}_{a2}(t))_{\|\mathbf{q}_{a2}(t) \equiv \mathbf{p}_2(t) + \sum_{j=1}^{s} h_j(\boldsymbol{\theta}(t))\mathbf{J}_j\mathbf{v}(t)}. \tag{5.41}$$

Evidently, (5.39)–(5.41) can be adequately exploited to obtain the time derivative $\dot{\mathbf{p}}_{2e}(t)$ in the dependency on $\mathbf{p}_{2e}(t)$, $\mathbf{v}(t)$, and $\mathbf{u}(t)$.

Using the equivalency of the stability conditions, an actuator fault estimation structure based on reduced-order TS fuzzy observer can be discussed.

6. Estimation of Actuator Faults

To obtain an actuator fault estimation structure based on reduced-order TS fuzzy observer, the matching condition (3.21) has to be satisfied. This implies that a special observer gain matrices have to be chosen.

Theorem 6.1. *The estimation error dynamics of the reduced-order TS fuzzy observer* (5.1), (5.2) *is not affected by actuator faults if, with the matching condition* (3.21), *there exists a symmetric positive definite matrix* $\mathbf{P}^{\circ} \in \mathbb{R}^{(n-m)\times(n-m)}$ *such that*

$$\mathbf{P}^{\circ}\mathbf{J} = \mathbf{B}_{af1}^{\perp}, \tag{6.1}$$

where $\mathbf{B}_{af1}^{\perp}$ *is the orthogonal complement to* $\mathbf{B}_{af1}$, *and* $\mathbf{J}_i = \mathbf{J}$ *for all* $i = 1, 2, \ldots, s$.

Proof. The system with an actuator fault is described as

$$\dot{\mathbf{q}}_{afi}(t) = \mathbf{A}_{ai}\mathbf{q}_{afi}(t) + \mathbf{B}_{ai}\mathbf{u}(t) + \mathbf{B}_{af}\mathbf{u}_f(t). \tag{6.2}$$

Since (3.13), (5.1), (5.2), and (5.34), (5.35) now implies

$$\mathbf{B}_{af} = \mathbf{C}_a^T\mathbf{B}_{af1} = \begin{bmatrix}\mathbf{I}_m \\ \mathbf{0}\end{bmatrix}\mathbf{B}_{af1} = \begin{bmatrix}\mathbf{B}_{af1} \\ \mathbf{0}\end{bmatrix}, \tag{6.3}$$

$$\begin{aligned}\dot{\mathbf{p}}_{2e}(t) &= \sum_{i=1}^{s} h_i(\boldsymbol{\theta}(t))\mathbf{q}_{2efi}^{\circ}(t), \\ \dot{\mathbf{p}}_{2}(t) &= \sum_{i=1}^{s} h_i(\boldsymbol{\theta}(t))\mathbf{q}_{2i}^{\circ}(t),\end{aligned} \tag{6.4}$$

$$\mathbf{q}_{2efi}^{\circ}(t) = \mathbf{A}_{aei}\mathbf{p}_{2e}(t) + \mathbf{A}_{avi}\mathbf{v}(t) + \begin{bmatrix}-\mathbf{J}_i & \mathbf{I}_{n-m}\end{bmatrix}\left(\mathbf{B}_{ai}\mathbf{u}(t) + \mathbf{B}_{af}\mathbf{u}_f(t)\right), \tag{6.5}$$

$$\mathbf{q}_{2i}^{\circ}(t) = \mathbf{A}_{aei}\mathbf{p}_{2}(t) + \mathbf{A}_{avi}\mathbf{v}(t) + \begin{bmatrix}-\mathbf{J}_i & \mathbf{I}_{n-m}\end{bmatrix}\mathbf{B}_{ai}\mathbf{u}(t), \tag{6.6}$$

the dynamics of the error (5.37) can be rewritten as

$$\dot{\mathbf{e}}_{aq2}(t) = \dot{\mathbf{p}}_2(t) - \dot{\mathbf{p}}_{2e}(t) = \sum_{i=1}^{s} h_i(\boldsymbol{\theta}(t))\mathbf{A}_{aei}\mathbf{e}_{aq2}(t) + \sum_{i=1}^{s} h_i(\boldsymbol{\theta}(t))\begin{bmatrix}-\mathbf{J}_i & \mathbf{I}_{n-m}\end{bmatrix}\mathbf{B}_{af}\mathbf{u}_f(t) \tag{6.7}$$

Defining the quadratic positive definite Lyapunov function as follows:

$$v\left(\mathbf{e}_{aq2}(t)\right) = \mathbf{e}_{aq2}^T(t)\mathbf{P}^{\circ}\mathbf{e}_{aq2}(t), \tag{6.8}$$

where $\mathbf{P}^{\circ} = \mathbf{P}^{\circ T} > 0$, $\mathbf{P}^{\circ} \in \mathbb{R}^{(n-m)\times(n-m)}$, after evaluation of derivative of (6.7) with respect to t it is obtained

$$\dot{v}\left(\mathbf{e}_{aq2}(t)\right) = \dot{\mathbf{e}}_{aq2}^T(t)\mathbf{P}^{\circ}\mathbf{e}_{aq2}(t) + \mathbf{e}_{aq2}^T(t)\mathbf{P}^{\circ}\dot{\mathbf{e}}_{aq2}(t). \tag{6.9}$$

From the expression (6.7) it follows that

$$\begin{aligned}\dot{v}\left(\mathbf{e}_{aq2}(t)\right) &= \mathbf{e}_{aq2}^{T}(t)\mathbf{P}^{\circ}\sum_{i=1}^{s}h_i(\boldsymbol{\theta}(t))\mathbf{A}_{aei}\mathbf{e}_{aq2}(t) + \mathbf{e}_{aq2}^{T}(t)\sum_{i=1}^{s}h_i(\boldsymbol{\theta}(t))\mathbf{A}_{aei}^{T}\mathbf{P}^{\circ}\mathbf{e}_{a2}(t)\\ &\quad + \mathbf{e}_{aq2}^{T}(t)\mathbf{P}^{\circ}\sum_{i=1}^{s}h_i(\boldsymbol{\theta}(t))\left[-\mathbf{J}_i \;\; \mathbf{I}_{n-m}\right]\mathbf{B}_{af}\mathbf{u}_f(t)\\ &\quad + \mathbf{u}_f^{T}(t)\sum_{i=1}^{s}h_i(\boldsymbol{\theta}(t))\mathbf{B}_{af}^{T}\left[-\mathbf{J}_i \;\; \mathbf{I}_{n-m}\right]^{T}\mathbf{P}^{\circ}\mathbf{e}_{aq2}^{T}(t),\end{aligned} \tag{6.10}$$

and with respect to the matching condition (3.21), it can be set

$$\mathbf{P}^{\circ}\left[-\mathbf{J}_i \;\; \mathbf{I}_{n-m}\right]\mathbf{B}_{af} = \mathbf{P}^{\circ}\left[-\mathbf{J}_i\mathbf{B}_{af1} \;\; \mathbf{0}_{n-m}\right] = \mathbf{0}, \tag{6.11}$$

which results in the equality:

$$\mathbf{P}^{\circ}\mathbf{J}_i\mathbf{B}_{af1} = \mathbf{0}, \quad \forall i. \tag{6.12}$$

Evidently, (6.12) can be satisfied if and only if $\mathbf{J}_i = \mathbf{J}$ for all i. With such $\mathbf{J}$, the equality (6.12) will be satisfied if (6.1) is satisfied. This concludes the proof. □

Evidently, $\mathbf{B}_{af1}$ may not be a square matrix.

Theorem 6.2. *The estimation error dynamic* (6.7) *is asymptotically stable, if there exists a symmetric positive definite* matrix $\mathbf{P}^{\circ} \in \mathbb{R}^{(\mathrm{n-m})\times(\mathrm{n-m})}$ *such that for* $i = 1, 2, \ldots, s$

$$\mathbf{P}^{\circ} = \mathbf{P}^{\circ T} > 0, \tag{6.13}$$

$$\mathbf{A}_{a22i}^{T}\mathbf{P}^{\circ} + \mathbf{P}^{\circ}\mathbf{A}_{a22i} - \mathbf{A}_{a12i}^{T}\mathbf{B}_{af1}^{\perp T} - \mathbf{B}_{af1}^{\perp}\mathbf{A}_{a12i} < 0, \tag{6.14}$$

where $\mathbf{B}_{af1}^{\perp}$ *is the orthogonal complement to* $\mathbf{B}_{af1}$.

If the above conditions hold, the observer gain matrix is given as

$$\mathbf{J} = (\mathbf{P}^{\circ})^{-1}\mathbf{B}_{af1}^{\perp}. \tag{6.15}$$

Proof. Satisfying (6.11) then (6.10) implies

$$\dot{v}\left(\mathbf{e}_{aq2}(t)\right) = \mathbf{e}_{aq2}^{T}(t)\sum_{i=1}^{s}h_i(\boldsymbol{\theta}(t))\left(\mathbf{P}^{\circ}\mathbf{A}_{aei} + \mathbf{A}_{aei}^{T}\mathbf{P}^{\circ}\right)\mathbf{e}_{aq2}(t) < 0, \tag{6.16}$$

where $\mathbf{A}_{aei}$ is defined in (5.5). It is evident that (6.16) is negative if for all i

$$(\mathbf{A}_{a22i} - \mathbf{J}_i\mathbf{A}_{a12i})^T\mathbf{P}^\circ + \mathbf{P}^\circ(\mathbf{A}_{a22i} - \mathbf{J}_i\mathbf{A}_{a12i}) < 0. \tag{6.17}$$

Using (6.1) then (6.17) implies (5.19). This concludes the proof. □

Corollary 6.3. *Using* (5.20), *then one has*

$$\begin{bmatrix}-\mathbf{J} & \mathbf{I}_{n-m}\end{bmatrix}\mathbf{B}_{af} = (\mathbf{P}^\circ)^{-1}\begin{bmatrix}-\mathbf{B}_{af1}^{\perp} & \mathbf{P}^\circ\end{bmatrix}\mathbf{C}^T\mathbf{B}_{af1} = (\mathbf{P}^\circ)^{-1}\begin{bmatrix}-\mathbf{B}_{af1}^{\perp}\mathbf{B}_{af1} & \mathbf{0}\end{bmatrix} = \mathbf{0}. \tag{6.18}$$

Equality given above implies that neither estimation error (6.7), *nor reduced-order TS fuzzy observer equation* (6.5) *is affected by actuator faults.*

Corollary 6.4. *Since* $\mathbf{J}_i = \mathbf{J}$ *for all* i *and* $\sum_{j=1}^{s} h_j(\boldsymbol{\theta}(t)) = 1$, (5.12) *and* (5.19) *take the form*

$$\mathbf{p}_{2e}(t) = \mathbf{q}_{a2e}(t) - \mathbf{J}\mathbf{v}(t), \tag{6.19}$$

$$\mathbf{A}_{avi} = \mathbf{A}_{a21i} - \mathbf{J}\mathbf{A}_{a11i} + (\mathbf{A}_{a22i} - \mathbf{J}\mathbf{A}_{a12})\mathbf{J}. \tag{6.20}$$

Remark 6.5. If $\mathbf{B}_{ai} = \mathbf{B}_a = \mathbf{B}_{af}$ for all i, (6.18) implies that the reduced-order TS fuzzy observer will be independent on the input $\mathbf{u}(t)$ and will exploit only the vector variable $\mathbf{v}(t)$.

Considering the fact that the reduced-order TS fuzzy observer does not contain any information about actuator faults, the next reconstruction principle can be used.

Theorem 6.6. *Designed with respect to* $\mathbf{P}^\circ$ *satisfying* (5.18)–(5.20), *the reduced-order TS fuzzy observer* (5.1), (5.2) *asymptotically estimates actuator faults.*

Proof. Since (3.11), (3.14) implies

$$\mathbf{q}_e(t) = \mathbf{T}_a^T\mathbf{q}_{ae}(t) = \mathbf{T}_{a2}^T\mathbf{q}_{a2e}(t) + \mathbf{T}_{a1}^T\mathbf{v}(t), \tag{6.21}$$

substituting (6.19) in (6.21) leads to

$$\mathbf{q}_e(t) = \mathbf{T}_{a2}^T\mathbf{p}_{2e}(t) + \left(\mathbf{T}_{a1}^T + \mathbf{T}_{a2}^T\mathbf{J}\right)\mathbf{W}\mathbf{y}(t), \tag{6.22}$$

$$\dot{\mathbf{q}}_e(t) = \sum_{i=1}^{s} h_i(\boldsymbol{\theta}(t))(\mathbf{A}_i\mathbf{q}_e(t) + \mathbf{B}_i\mathbf{u}(t)) + \mathbf{B}_f\mathbf{u}_f(t). \tag{6.23}$$

Thus, using Moore-Penrose pseudoinverse $\mathbf{B}_f^{\ominus 1}$ of $\mathbf{B}_f$,

$$\mathbf{u}_{fe}(t) = \mathbf{B}_f^{\ominus 1}\sum_{i=1}^{s} h_i(\boldsymbol{\theta}(t))(\dot{\mathbf{q}}_e(t) - \mathbf{A}_i\mathbf{q}_e(t) - \mathbf{B}_i\mathbf{u}(t)). \tag{6.24}$$

Explaining $\mathbf{u}_f(t)$ as follows:

$$\mathbf{u}_f(t) = \mathbf{B}_f^{\ominus 1} \sum_{i=1}^{s} h_i(\boldsymbol{\theta}(t))(\dot{\mathbf{q}}(t) - \mathbf{A}_i \mathbf{q}_e(t) - \mathbf{B}_i \mathbf{u}(t)), \tag{6.25}$$

then for $\mathbf{e}_{uf}(t) = \mathbf{u}_f(t) - \mathbf{u}_{fe}(t)$ it yields

$$\mathbf{e}_{uf}(t) = \mathbf{B}_f^{\ominus 1} \sum_{i=1}^{s} h_i(\boldsymbol{\theta}(t))\left(\dot{\mathbf{e}}_q(t) - \mathbf{A}_i \mathbf{e}_q(t)\right). \tag{6.26}$$

Owing to that reduced-order observer is stable, $\mathbf{e}_{uf}(t)$ converges asymptotically to zero. This concludes the proof. □

Remark 6.7. Taking the actuator fault reconstructor as given by (6.24), it is necessary to note that $\dot{\mathbf{q}}_e(t)$ has to be computed numerically from (6.22), since (5.7) is affected by actuator faults and so cannot be used to the first state vector component derivative evaluation.

Note, matrix pseudoinverse in (6.24) is the reason that $\mathbf{B}_f$ has to be the same in all linear submodels of (2.4).

7. Illustrative Example

Referring to [32], a nonlinear hydrostatic transmission system is considered in this section for simulating the real environment. The proposed design method is applied to design an actuator fault estimation scheme based on a reduced-order fuzzy observer using TS model of this model. The hydrostatic transmission system is represented by the nonlinear state-space model of the form

$$\begin{aligned}
\dot{q}_1(t) &= -a_{11} q_1(t) + b_{11} u_1(t) \\
\dot{q}_2(t) &= -a_{22} q_2(t) + b_{22} u_2(t), \\
\dot{q}_3(t) &= a_{31} q_1(t) p(t) - a_{33} q_3(t) - a_{34} q_2(t) q_4(t), \\
\dot{q}_4(t) &= a_{43} q_2(t) q_3(t) - a_{44} q_4(t),
\end{aligned} \tag{7.1}$$

where $q_1(t)$ is the normalized hydraulic pump angle, $q_2(t)$ is the normalized hydraulic motor angle, $q_3(t)$ is the pressure difference [bar], $q_4(t)$ is the hydraulic motor speed [rad/s], $u_1(t)$ is the normalized control signal of the hydraulic pump, $u_2(t)$ is the normalized control signal of the hydraulic motor, and the external signal $p(t)$ represents speed of hydraulic pump [rad/s]. It is supposed that the external variable $p(t)$ and all state variables except $q_3(t)$ are measurable

and the model parameters are

$$\begin{aligned} a_{11} &= 7.6923, \quad a_{22} = 4.5455, \quad a_{33} = 7.6054 * 10^{-4}, \\ a_{31} &= 0.7877, \quad a_{34} = 0.9235, \quad b_{11} = 1.8590 * 10^{3}, \\ a_{43} &= 12.1967, \quad a_{44} = 0.4143, \quad b_{22} = 1.2879 * 10^{3}. \end{aligned} \tag{7.2}$$

Since the variables $p(t) \in \langle 105, 300 \rangle$ and $q_2(t) \in \langle 0, 1 \rangle$ are bounded on the prescribed sectors, the vector of premise variables was chosen as follows:

$$\boldsymbol{\theta}(t) = \left[\theta_1(t) \;\; \theta_2(t)\right] = \left[q_2(t) \;\; p(t)\right], \tag{7.3}$$

where the set of nonlinear sector functions:

$$\begin{aligned} w_{11}(q_2(t)) &= \frac{b_1 - q_2(t)}{b_1 - b_2}, \quad w_{12}(q_2(t)) = 1 - w_{11}(q_2(t)), \quad b_1 = 0, \; b_2 = 1, \\ w_{21}(p(t)) &= \frac{c_1 - p(t)}{c_1 - c_2}, \quad w_{22}(p(t)) = 1 - w_{21}(p(t)), \quad c_1 = 105, \quad c_2 = 300 \end{aligned} \tag{7.4}$$

implies the next set of normalized membership functions:

$$\begin{aligned} h_1(\boldsymbol{\theta}(t)) &= w_{11}(q_2(t))w_{21}(p(t)), \quad h_2(\boldsymbol{\theta}(t)) = w_{11}(q_2(t))w_{22}(p(t)), \\ h_3(\boldsymbol{\theta}(t)) &= w_{12}(q_2(t))w_{21}(p(t)), \quad h_4(\boldsymbol{\theta}(t)) = w_{12}(q_2(t))w_{22}(p(t)). \end{aligned} \tag{7.5}$$

The overall TS fuzzy model (2.4), (2.5) with an actuator fault is represented as follows:

$$\begin{aligned} \dot{\mathbf{q}}(t) &= \sum_{i=1}^{4} h_i(\boldsymbol{\theta}(t))(\mathbf{A}_i\mathbf{q}(t)) + \mathbf{B}(\mathbf{u}(t) + \mathbf{f}(t)), \\ \mathbf{y}(t) &= \mathbf{C}\mathbf{q}(t), \end{aligned} \tag{7.6}$$

where

$$\mathbf{A}_1 = \begin{bmatrix} -7.6923 & 0 & 0 & 0 \\ 0 & -4.5455 & 0 & 0 \\ 82.7086 & 0 & -0.0008 & 0 \\ 0 & 0 & 0 & -0.4143 \end{bmatrix},$$

$$\mathbf{A}_2 = \begin{bmatrix} -7.6923 & 0 & 0 & 0 \\ 0 & -4.5455 & 0 & 0 \\ 236.3103 & 0 & -0.0008 & 0 \\ 0 & 0 & 0 & -0.4143 \end{bmatrix},$$

$$\mathbf{A}_3 = \begin{bmatrix} -7.6923 & 0 & 0 & 0 \\ 0 & -4.5455 & 0 & 0 \\ 82.7086 & 0 & -0.0008 & -0.9235 \\ 0 & 0 & 12.1967 & -0.4143 \end{bmatrix}, \tag{7.7}$$

$$\mathbf{A}_4 = \begin{bmatrix} -7.6923 & 0 & 0 & 0 \\ 0 & -4.5455 & 0 & 0 \\ 236.3103 & 0 & -0.0008 & -0.9235 \\ 0 & 0 & 12.1967 & -0.4143 \end{bmatrix},$$

$$\mathbf{B}_i = \mathbf{B} = \mathbf{B}_f = \begin{bmatrix} 1.8590 & 0 \\ 0 & 1.2879 \\ 0 & 0 \\ 0 & 0 \end{bmatrix} \times 10^3, \quad i = 1, 2, 3, 4, \qquad \mathbf{C} = \begin{bmatrix} 1 & 0 & 0 & 0 \\ 0 & 1 & 0 & 0 \\ 0 & 0 & 0 & 1 \end{bmatrix}.$$

Note that rank($\mathbf{C}$) > rank($\mathbf{B}$) and Proposition 3.5 are satisfied.

Using SVD of the output matrix $\mathbf{C}$, (3.10) implies

$$\mathbf{U} = \mathbf{S} = \mathbf{W}^{-1} = \mathbf{I}_3, \qquad \mathbf{V} = \mathbf{T}_a = \operatorname{diag}\left[\mathbf{I}_2 \quad \begin{bmatrix} 0 & 1 \\ 1 & 0 \end{bmatrix}\right] = \begin{bmatrix} 1 & 0 & 0 & 0 \\ 0 & 1 & 0 & 0 \\ 0 & 0 & 0 & 1 \\ 0 & 0 & 1 & 0 \end{bmatrix},$$

$$\mathbf{T}_{a1} = \begin{bmatrix} 1 & 0 & 0 & 0 \\ 0 & 1 & 0 & 0 \\ 0 & 0 & 0 & 1 \end{bmatrix}, \qquad \mathbf{T}_{a2} = \begin{bmatrix} 0 & 0 & 1 & 0 \end{bmatrix}, \tag{7.8}$$

and with such defined $\mathbf{T}_a$, for $i = 1, 2, 3, 4$, it yields

$$\begin{gathered}
\mathbf{C}_a = \begin{bmatrix} 1 & 0 & 0 & 0 \\ 0 & 1 & 0 & 0 \\ 0 & 0 & 1 & 0 \end{bmatrix}, \qquad \mathbf{B}_{a1} = \begin{bmatrix} 1.8590 & 0 \\ 0 & 1.2879 \\ 0 & 0 \end{bmatrix} \times 10^3, \qquad \mathbf{B}_{a2} = \begin{bmatrix} 0 & 0 \end{bmatrix}, \\
\mathbf{A}_{a211} = \begin{bmatrix} 82.7086 & 0 & 0 \end{bmatrix}, \qquad \mathbf{A}_{a212} = \begin{bmatrix} 236.3103 & 0 & 0 \end{bmatrix}, \\
\mathbf{A}_{a213} = \begin{bmatrix} 82.7086 & 0 & -0.9235 \end{bmatrix}, \qquad \mathbf{A}_{a214} = \begin{bmatrix} 236.3103 & 0 & -0.9235 \end{bmatrix}, \\
\mathbf{A}_{a121} = \mathbf{A}_{a122} = \begin{bmatrix} 0 \\ 0 \\ 0 \end{bmatrix}, \qquad \mathbf{A}_{a123} = \mathbf{A}_{a124} = \begin{bmatrix} 0 \\ 0 \\ 12.1967 \end{bmatrix}, \\
\mathbf{A}_{a11i} = \begin{bmatrix} -7.6923 & 0 & 0 \\ 0 & -4.5455 & 0 \\ 0 & 0 & -0.4143 \end{bmatrix}, \quad \mathbf{A}_{a22i} = \begin{bmatrix} -0.0008 \end{bmatrix}, \quad i = 1, 2, 3, 4.
\end{gathered} \tag{7.9}$$

Considering the conditions given in Theorem 6.1, the reduced-order observer (5.1)–(5.5) takes now the form

$$\dot{\mathbf{p}}_{2e}(t) = \sum_{i=1}^{4} h_i(\boldsymbol{\theta}(t)) \left(\mathbf{A}_{aei} \mathbf{p}_{2e}(t) + \mathbf{A}_{avi} \mathbf{v}(t) + \begin{bmatrix} -\mathbf{J} & \mathbf{I}_{n-m} \end{bmatrix} \mathbf{B}_{ai} \mathbf{u}(t) \right), \tag{7.10}$$

where

$$\mathbf{A}_{avi} = \mathbf{A}_{a21i} - \mathbf{J}\mathbf{A}_{a11i} + (\mathbf{A}_{a22i} - \mathbf{J}\mathbf{A}_{a12i})\mathbf{J}, \qquad \mathbf{A}_{aei} = \mathbf{A}_{a22i} - \mathbf{J}\mathbf{A}_{a12i}, \tag{7.11}$$

and $\mathbf{J} \in \mathbb{R}^{1 \times 3}$ is given by (6.15) as follows:

$$\mathbf{J} = (\mathbf{P}^{\circ})^{-1} \mathbf{B}_{a1}^{\perp}, \tag{7.12}$$

where $\mathbf{B}_{a1}^{\perp}$ is an orthogonal complement to $\mathbf{B}_{a1}$.

The scalar LMI variable P° can be found by using the convex optimization techniques if $\mathbf{B}_{a1}^{\perp}$ is defined as a structured LM variable of the form

$$\mathbf{B}_{a1}^{\perp} = \begin{bmatrix} 0 & 0 & Z \end{bmatrix}, \quad Z \in \mathbb{R}, \tag{7.13}$$

where Z is an LMI variable. Note that a structured matrix variable can be specified only by including LMI matrix variables multiplied by a natural number or zero.

Thus, solving (6.13), (6.14) with respect to the LMI variables P°, Z using Self-Dual-Minimization (SeDuMi) package for Matlab [33], the reduced observer gain design problem was feasible with the results

$$P^{\circ} = 1.0832, \qquad \mathbf{B}_{a1}^{\perp} = \begin{bmatrix} 0 & 0 & 0.0410 \end{bmatrix}, \qquad \mathbf{J} = \begin{bmatrix} 0 & 0 & 0.0378 \end{bmatrix},$$
$$\mathbf{A}_{ae2} = \mathbf{A}_{ae1} = \mathbf{A}_{a22} - \mathbf{J}\mathbf{A}_{a121} = -7.6053 \times 10^{-4}, \tag{7.14}$$
$$\mathbf{A}_{ae4} = \mathbf{A}_{ae3} = \mathbf{A}_{b22} - \mathbf{J}\mathbf{A}_{a123} = -0.4610.$$

It is evident that the design of the stable reduced-order observer with suppressed input fault signals is now completely specified, and the system state can be reconstructed, using (6.22), from the estimated vector $\mathbf{p}_{2e}(t)$ and the output vector $\mathbf{y}(t)$ as

$$\mathbf{q}_e(t) = \begin{bmatrix} 0 \\ 0 \\ 1 \\ 0 \end{bmatrix} \mathbf{p}_{2e}(t) + \left(\begin{bmatrix} 1 & 0 & 0 \\ 0 & 1 & 0 \\ 0 & 0 & 0 \\ 0 & 0 & 1 \end{bmatrix} + \begin{bmatrix} 0 \\ 0 \\ 1 \\ 0 \end{bmatrix} \begin{bmatrix} 0 & 0 & 0.0378 \end{bmatrix} \right) \begin{bmatrix} 1 & 0 & 0 \\ 0 & 1 & 0 \\ 0 & 0 & 1 \end{bmatrix} \mathbf{y}(t). \tag{7.15}$$

Evidently, the final form of the state reconstruction equation is

$$\mathbf{q}_e(t) = \begin{bmatrix} 0 \\ 0 \\ 1 \\ 0 \end{bmatrix} \mathbf{p}_{2e}(t) + \begin{bmatrix} 1 & 0 & 0 \\ 0 & 1 & 0 \\ 0 & 0 & 0.0378 \\ 0 & 0 & 1 \end{bmatrix} \mathbf{y}(t), \tag{7.16}$$

and actuator faults, if were occurred, can be computed by (6.24) as

$$\mathbf{u}_{fe}(t) = \mathbf{B}^{\ominus 1} \sum_{i=1}^{4} h_i(\boldsymbol{\theta}(t))(\dot{\mathbf{q}}_e(t) - \mathbf{A}_i \mathbf{q}_e(t) - \mathbf{B}\mathbf{u}(t)), \tag{7.17}$$

where

$$\mathbf{B}^{\ominus 1} = \begin{bmatrix} 0.5379 & 0 & 0 & 0 \\ 0 & 0.7765 & 0 & 0 \end{bmatrix} \times 10^{-3}, \tag{7.18}$$

and $\boldsymbol{\theta}(t)$, $h_i(\boldsymbol{\theta}(t))(\dot{\mathbf{q}}_e(t))$, $\mathbf{A}_i$, and $\mathbf{B}$ are above specified. The derivative of the system state estimation $\dot{\mathbf{q}}_e(t)$ was computed by standard numerical method from the obtained $\mathbf{q}_e(t)$. Since the reduced-order observer is used only, for system without uncertainties no extra computation consumption is needed, comparing, for example, with the sliding mode approach.

For simulation purposes only, the equilibrium of the system was stabilized by the fuzzy feedback controller

$$\mathbf{u}(t) = -\sum_{j=1}^{4} h_j(\boldsymbol{\theta}(t)) \mathbf{K}_j \mathbf{q}(t), \tag{7.19}$$

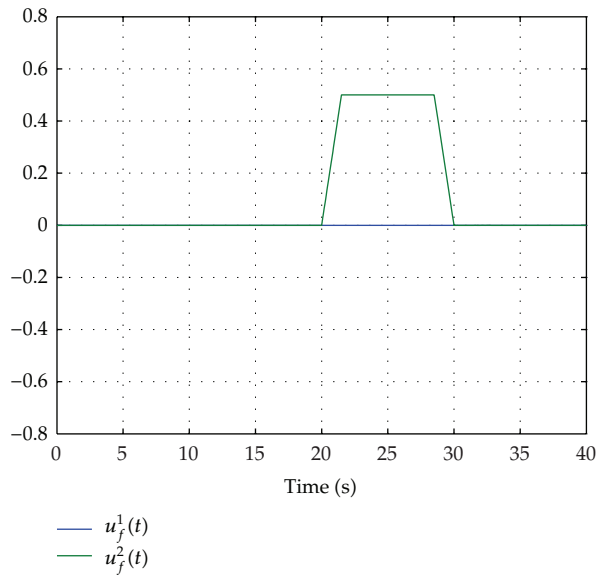

Figure 1: The second actuator fault signal.

where, using the method proposed in [34], offering the possibility to design the linear state controller for TS fuzzy system, the gain matrices were computed as

$$\mathbf{K} = \mathbf{K}_j = \begin{bmatrix} 0.2386 & 0.0000 & 0.0350 & 0.0075 \\ 0.0000 & 0.0207 & 0.0000 & 0.0000 \end{bmatrix}, \quad j = 1, 2, 3, 4. \tag{7.20}$$

In simulations was considered the fault which does not cause closed-loop system instability, modeled by a fault starting at any time instant in the system equilibrium state. Applying the above-designed reduced-order observer-based actuator fault estimation, the fault responses for the nonlinear system are given in Figures 1 and 2. Thus, Figure 1 presents the fault signal reflecting single actuator fault in the the second actuator, starting at the time instant $t = 20$ s and continuing during the time 10 s, and Figure 2 illustrates the signals u_f^1, u_f^2 obtained from (6.26) as a reconstruction of the single fault. Note that equivalent results are obtained for the system working in a forced regime.

From the simulation results of Figures 1 and 2, it can be found that the errors between the signals reflecting a single actuator fault and the observer approximate ones tend to zero. Moreover, the states of the system converge to the equilibrium when the actuator fault disappeared, via the used fuzzy controller.

8. Concluding Remarks

Generalized design method of a reduced-order observer-based actuator fault estimation scheme is developed, as augmentation of unknown observers synthesis for one class of nonlinear systems described by TS fuzzy model. This is achieved by manipulation of observer asymptotic stability with respect to the proposed matching conditions. Design conditions for asymptotic estimation of actuator faults are derived in terms of LMI, using standard

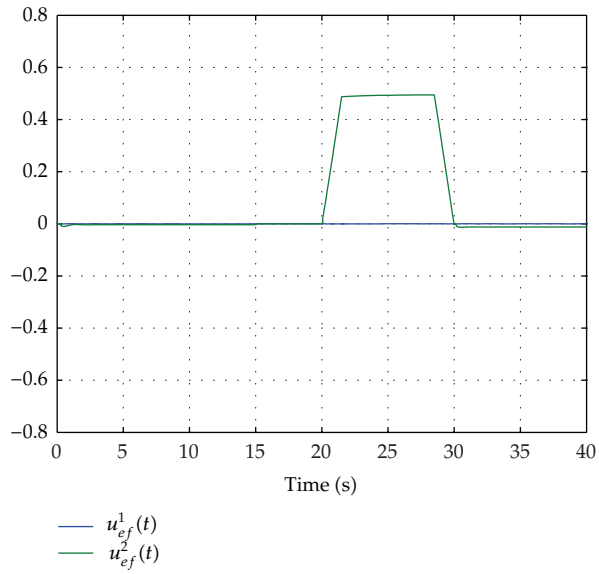

Figure 2: The reconstruction of the actuator fault signal.

LMI procedures to manipulate the reducer-order observer stability. Because of the specific observer gain matrix structure, the estimated unmeasurable part of the system state is free of actuators faults. By examining the estimated state vector, it is presented that using a numerical realization of time derivative of the state vector estimate, the actuator fault signals can be faithfully reconstructed.

Proposed scheme is able to simultaneously estimate the time-varying actuator faults, as well as the system state variables with a good accuracy, is easy to implement, and can be applied to a reasonably wide class of systems satisfying the matching condition. Presented simulations have shown that the proposed design task is feasible and effective.

Acknowledgment

The work, presented in this paper, was supported by VEGA, the Grant Agency of Ministry of Education and Academy of Sciences of Slovak Republic, under Grant no. 1/0256/11. This support is very gratefully acknowledged.

References

[1] J. Chen and R. J. Patton, *Robust Model-Based Fault Diagnosis for Dynamic Systems*, Kluwer Academic Publishers, Norwell, Mass, USA, 1999.

[2] S. Ding, *Model-Based Fault Diagnosis Techniques. Design Schemes, Algorithms, and Tools*, Springer, Berlin, Germany, 2008.

[3] W. Chen and M. Saif, "Observer-based strategies for actuator fault detection, isolation and estimation for certain class of uncertain nonlinear systems," *IET Control Theory and Applications*, vol. 1, no. 6, pp. 1672–1680, 2007.

[4] W. Chen, A. Q. Khan, M. Abid, and S. X. Ding, "Integrated design of observer based fault detection for a class of uncertain nonlinear systems," *International Journal of Applied Mathematics and Computer Science*, vol. 21, no. 3, pp. 423–430, 2011.

[5] A. Zolghadri, D. Henry, and M. Monsion, "Design of nonlinear observers for fault diagnosis: a case study," *Control Engineering Practice*, vol. 4, no. 11, pp. 1535–1544, 1996.
[6] F. E. Thau, "Observing the state of nonlinear dynamical systems," *International Journal of Control*, vol. 17, no. 3, pp. 471–479, 1973.
[7] A. J. Koshkouei and A. S. I. Zinober, "Partial Lipschitz nonlinear sliding mode observers," in *Proceedings of the 7th Mediterranean Conference on Control and Automation (MED '99)*, pp. 2350–2359, Haifa, Israel, 1999.
[8] F. Zhu and F. Cen, "Full-order observer-based actuator fault detection and reduced-order observer-based fault reconstruction for a class of uncertain nonlinear systems," *Journal of Process Control*, vol. 20, no. 10, pp. 1141–1149, 2010.
[9] X.-G. Yan and C. Edwards, "Nonlinear robust fault reconstruction and estimation using a sliding mode observer," *Automatica*, vol. 43, no. 9, pp. 1605–1614, 2007.
[10] J. Yu, G. Sun, and H. R. Karimi, "Fault-reconstruction-based cascaded sliding mode observers for descriptor linear systems," *Mathematical Problems in Engineering*, vol. 2012, Article ID 623426, 20 pages, 2012.
[11] F. Zhu, "State estimation and unknown input reconstruction via both reduced-order and high-order sliding mode observers," *Journal of Process Control*, vol. 22, no. 1, pp. 296–302, 2012.
[12] H. Wang and S. Daley, "Actuator fault diagnosis: an adaptive observer-based technique," *IEEE Transactions on Automatic Control*, vol. 41, no. 7, pp. 1073–1078, 1996.
[13] X. Zhang, M. M. Polycarpou, and T. Parisini, "Fault diagnosis of a class of nonlinear uncertain systems with Lipschitz nonlinearities using adaptive estimation," *Automatica*, vol. 46, no. 2, pp. 290–299, 2010.
[14] W. Zhang, H. Su, H. Wang, and Z. Han, "Full-order and reduced-order observers for one-sided Lipschitz nonlinear systems using Riccati equations," *Communications in Nonlinear Science and Numerical Simulation*, vol. 17, no. 12, pp. 4968–4977, 2012.
[15] T. Takagi and M. Sugeno, "Fuzzy identification of systems and its applications to modeling and control," *IEEE Transactions on Systems, Man and Cybernetics*, vol. 15, no. 1, pp. 116–132, 1985.
[16] L. Wu, X. Su, P. Shi, and J. Qiu, "Model approximation for discrete-time state-delay systems in the TS fuzzy framework," *IEEE Transactions on Fuzzy Systems*, vol. 19, no. 2, pp. 366–378, 2011.
[17] Z. Gao, B. Jiang, P. Shi, and Y. Xu, "Fault accommodation for near space vehicle attitude dynamics via T-S fuzzy models," *International Journal of Innovative Computing, Information and Control*, vol. 6, no. 11, pp. 4843–4856, 2010.
[18] Z. Lendek, T. M. Guerra, R. Babuška, and B. De Schutter, *Stability Analysis and Nonlinear Observer Design Using Takagi-Sugeno Fuzzy Models*, Springer, Berlin, Germany, 2010.
[19] K. M. Passino and S. Yurkovich, *Fuzzy Control*, Addison-Wesley Longman, Berkeley, Calif, USA, 1998.
[20] K. Tanaka and H. O. Wang, *Fuzzy Control Systems Design and Analysis. A Linear Matrix Inequality Approach*, John Wiley & Sons, New York, NY, USA, 2001.
[21] M. Chadli, "An LMI approach to design observer for unknown inputs Takagi-Sugeno fuzzy models," *Asian Journal of Control*, vol. 12, no. 4, pp. 524–530, 2010.
[22] D. Ichalal, B. Marx, J. Ragot, and D. Maquin, "Design of observers for Takagi-Sugeno discrete-time systems with unmeasurable premise variables," in *Proceedings of the 5th Workshop on Advanced Control and Diagnosis (ACD '07)*, Grenoble, France, 2007.
[23] A. M. Nagy Kiss, B. Marx, G. Mourot, G. Schutz, and J. Ragot, "Observers design for uncertain Takagi-Sugeno systems with unmeasurable premise variables and unknown inputs. Application to a wastewater treatment plant," *Journal of Process Control*, vol. 21, no. 7, pp. 1105–1114, 2011.
[24] D. Zhang, H. Wang, B. Lu, and Z. Wang, "LMI-based fault detection fuzzy observer design with multiple performance constraints for a class of non-linear systems: comparative study," *International Journal of Innovative Computing, Information and Control*, vol. 8, no. 1B, pp. 633–645, 2012.
[25] K. Zhang, B. Jiang, and P. Shi, *Observer-Based Fault Estimation and Accomodation for Dynamic Systems*, Springer, Berlin, Germany, 2012.
[26] Z. Gao, X. Shi, and S. X. Ding, "Fuzzy state/disturbance observer design for T-S fuzzy systems with application to sensor fault estimation," *IEEE Transactions on Systems, Man, and Cybernetics B*, vol. 38, no. 3, pp. 875–880, 2008.
[27] D. Xu, B. Jiang, and P. Shi, "Nonlinear actuator fault estimation observer: an inverse system approach via a T-S fuzzy model," *International Journal of Applied Mathematics and Computer Science*, vol. 22, no. 1, pp. 183–196, 2012.
[28] D. Krokavec and A. Filasová, "An approach to reconstruction of actuator faults for a class of nonlinear systems," in *Proceedings of the 8th IFAC Symposium on Fault Detection, Supervision and Safety of Technical Processes (SAFEPROCESS "12)*, pp. 216–221, Mexico City, Mexico, 2012.

[29] D. Krokavec and A. Filasová, "Reducer-order fuzzy-observer-based actuator fault reconstruction for a class of nonlinear systems," in *Proceedings of the 6th IASTED International Conference on Computational Intelligence and Bioinformatics (CIB '11)*, pp. 61–68, Pittsburgh, Pa, USA, 2011.
[30] D. Krokavec and A. Filasová, *Dynamic Systems Diagnosis*, Elfa, Kosice, Slovakia, 2007.
[31] Q.-G. Wang, *Decoupling Control*, vol. 285 of *Lecture Notes in Control and Information Sciences*, Springer, Berlin, Germany, 2003.
[32] P. Gerland, D. Groß, H. Schulte, and A. Kroll, "Robust adaptive fault detection using global state information and application to mobile working machines," in *Proceedings of the 1st Conference on Control and Fault-Tolerant Systems (SysTol '10)*, pp. 813–818, Nice, France, October 2010.
[33] D. Peaucelle, D. Henrion, Y. Labit, and K. Taitz, *User's Guide for SeDuMi Interface 1.04*, LAAS-CNRS, Toulouse, France, 2002.
[34] D. Krokavec and A. Filasová, "Optimal fuzzy control for a class of nonlinear systems," *Mathematical Problems in Engineering*, vol. 2012, Article ID 481942, 29 pages, 2012.

Hindawi Publishing Corporation
Mathematical Problems in Engineering
Volume 2012, Article ID 439805, 17 pages
doi:10.1155/2012/439805

Research Article

A Fuzzy Approach to Robust Control of Stochastic Nonaffine Nonlinear Systems

Ting-Ting Gang,[1] Jun Yang,[1] Qing Gao,[2,3] Yu Zhao,[1] and Jianbin Qiu[4]

[1] *School of Reliability and Systems Engineering, Beihang University, Beijing 100191, China*
[2] *Department of Automation, University of Science and Technology of China, Hefei 230027, China*
[3] *Department of Mechanical and Biomedical Engineering, City University of Hong Kong, 83 Tat Chee Avenue, Kowloon, Hong Kong*
[4] *Research Institute of Intelligent Control and Systems, Harbin Institute of Technology, Harbin 150001, China*

Correspondence should be addressed to Jun Yang, tomyj2001@buaa.edu.cn

Received 28 November 2012; Accepted 14 December 2012

Academic Editor: Peng Shi

Copyright © 2012 Ting-Ting Gang et al. This is an open access article distributed under the Creative Commons Attribution License, which permits unrestricted use, distribution, and reproduction in any medium, provided the original work is properly cited.

This paper investigates the stabilization problem for a class of discrete-time stochastic non-affine nonlinear systems based on T-S fuzzy models. Based on the function approximation capability of a class of stochastic T-S fuzzy models, it is shown that the stabilization problem of a stochastic non-affine nonlinear system can be solved as a robust stabilization problem of the stochastic T-S fuzzy system with the approximation errors as the uncertainty term. By using a class of piecewise dynamic feedback fuzzy controllers and piecewise quadratic Lyapunov functions, robust semiglobal stabilization condition of the stochastic non-affine nonlinear systems is formulated in terms of linear matrix inequalities. A simulation example illustrating the effectiveness of the proposed approach is provided in the end.

1. Introduction

In recent years, Takagi-Sugeno (T-S) type dynamic fuzzy model [1] based control methodologies have attracted great attention from control community. T-S fuzzy models describe a nonlinear system by the "blending" of a set of local linear dynamic models. This relatively simple structure facilitates the systematic stability analysis and controller design of T-S fuzzy control systems in view of the powerful linear systems control theory [2–13]. By using a common quadratic Lyapunov function and LMI techniques, control design of T-S fuzzy systems can be formulated in a convex optimization problem, which can be effectively solved

by various tools. However, common Lyapunov functions (CLFs) tend to be conservative and even might not exist for many highly complex nonlinear systems [3]. In order to reduce the conservatism of approaches based on CLFs, some results based on piecewise Lyapunov functions (PLFs) have been proposed [12, 13]. For the most recent advances on relevant topics, readers please refer to the book and the survey paper [2, 3] and the references therein for details.

Control design of nonlinear systems based on T-S fuzzy models can be typically summarized into two steps: (i) for a given nonlinear system, find its approximate T-S fuzzy model; and (ii) design a controller for the obtained T-S fuzzy model. It has been shown that T-S fuzzy models are universal function approximators in the sense that they are able to approximate any smooth nonlinear functions to any degree of accuracy in any convex compact region [14–16], which provides a theoretical foundation for utilizing the T-S fuzzy modeling method as an alternative approach to describing complex nonlinear systems approximately. However, it has been proved in [16] that the commonly used T-S fuzzy models where the control variables are not included in the premise variables are only able to approximate affine nonlinear systems to any degree of accuracy on any compact set. This implies that only the control design of affine nonlinear systems can be solved based on the commonly used T-S fuzzy models. To deal with more general nonlinear systems, that is, non-affine nonlinear systems, recently the coauthors proposed a class of generalized T-S fuzzy models which are universal function approximators of non-affine nonlinear systems [17, 18].

On another fruitful research frontier, stochastic control systems have been extensively studied because stochastic modeling plays a very important role in many branches of science and engineering [19–22]. Although many valuable results on stability analysis and controller synthesis of stochastic linear systems have been reported, most of the existing results on stochastic nonlinear control systems do not provide any systematic way of control design due to the difficulty in searching for suitable Lyapunov functions, especially for highly complex stochastic nonlinear systems. Motivated by the deterministic T-S fuzzy model based control techniques, the T-S fuzzy models have been extended to the stochastic case, where the local models are stochastic linear dynamic models instead of deterministic ones [23–26]. Especially, to deal with stochastic non-affine nonlinear systems (SNNS), the so-called generalized stochastic T-S fuzzy models were proposed in [26] by the co-authors.

In [26], the stabilization problem of continuous-time SNNS was studied based on the generalized stochastic T-S fuzzy models. However, it is noted that the approach proposed in [26] is based on common Lyapunov functions, which is very conservative. In this paper, we investigate the stabilization problem of discrete-time SNNS based on discrete-time generalized stochastic T-S fuzzy models. By using a piecewise Lyapunov function and a class of piecewise dynamic feedback fuzzy controllers, it is shown that the robust semiglobal stabilization condition of discrete-time SNNS can be formulated in terms of a set of linear matrix inequalities (LMIs) that are numerically efficient with commercially available software.

The rest of this paper is structured as follows. Section 2 is devoted to model description and problem formulation. In Section 3, robust controller design result for discrete-time stochastic non-affine nonlinear systems is presented. Simulation results are provided in Section 4 to demonstrate the effectiveness of the proposed approach. Conclusions are given in Section 5.

Notations. The notations used in this paper are fairly standard. The notation $\star$ is used to indicate the terms that can be induced by symmetry. "T" represents vector or matrix

transpose. $\mathbf{I}_n$ and $\mathbf{0}_{m\times n}$ are used to denote the $n \times n$ identity matrix and the $m \times n$ zero matrix, respectively. The subscripts n and $m \times n$ are omitted when the size is not relevant or can be determined from the context. $P > 0$ means that matrix P is real, symmetric, and positive definite. For a matrix A, $\lambda\{A\}$ is the eigenvalue of A. Let $\mathbb{E}\{\cdot\}$ be the mathematical expectation operator with respect to the given probability measure $\mathcal{P}$, and let $(\Omega, \mathcal{F}, \mathcal{P})$ be a complete probability space with a natural filtration $\{\mathcal{F}_t\}_{t\geq 0}$.

2. Model Description and Problem Formulation

2.1. T-S Fuzzy Model Description of SNNS

In this paper, we consider the following discrete-time stochastic non-affine nonlinear system:

$$x(t+1) = f(x(t), u(t)) + g(x(t), u(t))W(t), \tag{2.1}$$

where $x(t) = [x_1(t), \ldots, x_n(t)]^T \in X \subset \Re^n$, $u(t) = [u_1(t), \ldots, u_m(t)]^T \in U \subset \Re^m$, $X \times U$ is a compact set on $\Re^n \times \Re^m$ containing the origin, and $W(t) = [W_1(t), W_2(t), \ldots, W_q(t)]^T$ is a q-dimensional Wiener process defined on a complete probability space $(\Omega, \mathcal{F}, \mathcal{P})$ with

$$\mathbb{E}\{W_i(t)\} = 0, \qquad \mathbb{E}\left\{W_i^2(t)\right\} = 1. \tag{2.2}$$

Moreover, the noise processes $W_1(t), W_2(t), \ldots, W_q(t)$, the system state, and the control input are independent. It is assumed in this paper that the mappings $f \in \mathcal{C}^1$ and $g \in \mathcal{C}^1$ both vanish at zero, that is, $f(0,0) = 0$ and $g(0,0) = 0$. It is also assumed that f and g satisfy the usual linear growth and local Lipschitz conditions for existence and uniqueness of solutions to (2.1).

Our objective is to develop an approach to controlling the SNNS in (2.1) via T-S fuzzy modeling. In order to approximate the SNNS in (2.1), the following discrete-time generalized stochastic T-S fuzzy model is employed.

Plant rule $\mathcal{R}^l$

IF $x_1(t)$ is $\mathcal{U}_1^l$ AND... AND $x_n(t)$ is $\mathcal{U}_n^l$; $u_1(t)$ is $\mathcal{V}_1^l$ AND... AND $u_m(t)$ is $\mathcal{V}_m^l$; **THEN**

$$x(t+1) = A_l x(t) + B_l u(t) + \sum_{k=1}^{q} (C_{lk} x(t) + D_{lk} u(t)) W_k(t), \quad l \in \mathfrak{L} := \{1, 2, \ldots r\}, \tag{2.3}$$

where $\mathcal{R}^l$ denotes the lth rule, r the total number of rules, $\mathcal{U}_i^l$ and $\mathcal{V}_j^l$ the fuzzy sets, $x(t) \in \Re^n$ the state vector, $u(t) \in \Re^m$ the input vector, and $[A_l, B_l, C_{lk}, D_{lk}]$ the matrices of the lth local model.

Under the center-average defuzzifier, product inference, and singleton fuzzifier, the T-S fuzzy system in (2.3) can be expressed globally as

$$x(t+1) = \widehat{f}(x(t), u(t)) + \widehat{g}(x(t), u(t))W(t) \tag{2.4}$$

with

$$\begin{gathered}\hat{f}(x(t),u(t)) = \sum_{l=1}^{r}\mu_l(x,u)[A_l x(t) + B_l u(t)],\\ \hat{g}(x(t),u(t)) = \sum_{l=1}^{r}\mu_l(x,u) \times \left[C_{l1}x(t) + D_{l1}u(t),\ldots,C_{lq}x(t) + D_{lq}u(t)\right],\\ \mu_l(x,u) = \frac{\prod_{i=1}^{n}\mathcal{U}_i^l(x_i)\prod_{j=1}^{m}\mathcal{V}_j^l(u_j)}{\sum_{l=1}^{r}\prod_{i=1}^{n}\mathcal{U}_i^l(x_i)\prod_{j=1}^{m}\mathcal{V}_j^l(u_j)},\end{gathered} \tag{2.5}$$

where $\mu_l(x,u)$ are the so-called normalized fuzzy membership functions satisfying $\sum_{l=1}^{r}\mu_l(x,u) = 1$ and $\mu_l(x,u) \geq 0$.

In the co-authors' recent work [26], the continuous-time counterpart of the stochastic T-S fuzzy models in (2.4) has been proved to be the universal function approximator to continuous-time SNNS. It has been also shown in [26] that the function approximation capability also holds for the discrete-time case, which is summarized in the following lemma.

Lemma 2.1 (see [26]). *For any given SNNS described by* (2.1) *and any two positive constants* ϵ_1 *and* ϵ_2*, there exist a set of fuzzy basis functions* $\mu_l(x,u)$ *and constant matrices* A_l*,* B_l*,* C_{lk}*, and* D_{lk}*,* $l \in \{1,\ldots,r\}$*,* $k \in \{1,\ldots,q\}$ *such that*

$$\begin{gathered}\hat{f}(x,u) = \sum_{l=1}^{r}\mu_l(x,u)[A_l x + B_l u] = f(x,u) + \epsilon_f(x,u),\\ \hat{g}(x,u) = \sum_{l=1}^{r}\mu_l(x,u)\left[C_{l1}x + D_{l1}u,\ldots,C_{lq}x + D_{lq}u\right] = g(x,u) + \epsilon_g(x,u),\end{gathered} \tag{2.6}$$

where

$$\begin{gathered}\epsilon_f(x,u) = \Delta E_f(x,u)\overline{x},\\ \epsilon_g(x,u) = \left[\epsilon_{g1}(x,u),\ldots,\epsilon_{gq}(x,u)\right] = \left[\Delta E_{g1}(x,u)\overline{x},\ldots,\Delta E_{gq}(x,u)\overline{x}\right],\end{gathered} \tag{2.7}$$

with

$$\left\|\Delta E_f(x,u)\right\| < \epsilon_1, \quad \left\|\Delta E_{gk}(x,u)\right\| < \epsilon_2, \quad k = \{1,\ldots,q\}. \tag{2.8}$$

From (2.6) in Lemma 2.1, an SNNS described by (2.1) can be exactly expressed in a compact set by a generalized stochastic T-S fuzzy model in (2.4) with the approximation errors as some norm-bounded uncertainties as follows:

$$x(t+1) = \sum_{l=1}^{r} \mu_l(x,u) \Bigg\{ A_l x(t) + B_l u(t) + \epsilon_f(x(t),u(t)) + \sum_{k=1}^{q} \big(C_{lk} x(t) + D_{lk} u(t) + \epsilon_{gk}(x(t),u(t))\big) W_k(t) \Bigg\}, \tag{2.9}$$

where

$$\epsilon_f(x(t),u(t)) = \Delta E_f(x,u) \begin{bmatrix} x(t) \\ u(t) \end{bmatrix}, \qquad \epsilon_{gk}(x(t),u(t)) = \Delta E_{gk}(x,u) \begin{bmatrix} x(t) \\ u(t) \end{bmatrix}. \tag{2.10}$$

Therefore, one can easily conclude that the stabilization of an SNNS given in (2.1) can be actually solved as a robust stabilization problem of its corresponding stochastic generalized T-S fuzzy model with the approximation errors as the uncertainty terms.

2.2. System Formulation and Dynamic Fuzzy Controllers

It is noted that fuzzy system (2.4) induces a polyhedral partition of the premise space, which is dependent on both the system state x and control input u. As a result, the global fuzzy system can be viewed as a number of subsystems in a number of individual regions.

In this paper, the premise space is divided into a set of crisp regions and fuzzy regions. Denote the partitioned regions as $\{S_i\}_{i\in\Im}$ with $\Im$ as the set of region indices and define $\mathcal{J}(i)$ the indices of fired rules in each region S_i, then the crisp regions and fuzzy regions can be defined respectively by

$$\begin{aligned} S_i &:= \{(x,u) \mid \mu_m(x,u) = 1,\ m \in \mathcal{J}(i)\}, \\ S_j &:= \{(x,u) \mid 0 \le \mu_m(x,u) < 1,\ m \in \mathcal{J}(j)\}, \end{aligned} \tag{2.11}$$

where $i, j \in \Im$.

Based on such a partition method, the fuzzy model (2.4), or the original SNNS (2.1), in each region can be rewritten by a blending of $m \in \mathcal{J}(i)$ subsystems,

$$\begin{aligned} x(t+1) = {} & \sum_{m\in\mathcal{J}(i)} \mu_m(x(t),u(t)) \\ & \times \Bigg\{ A_m x(t) + B_m u(t) + \epsilon_f(x(t),u(t)) \\ & + \sum_{k=1}^{q} \big(C_{mk} x(t) + D_{mk} u(t) + \epsilon_{gk}(x(t),u(t))\big) W_k(t) \Bigg\}, \quad (x,u) \in S_i,\ i \in \Im. \end{aligned} \tag{2.12}$$

In order to stabilize the nonlinear system in (2.12), we employ the following piecewise dynamic state feedback fuzzy controller:

$$u(t+1) = \sum_{m\in\mathcal{J}(i)} \mu_m(x,u)\{F_{mi}x(t) + G_{mi}u(t)\}, \quad (x,u) \in S_i,\ i \in \Im. \tag{2.13}$$

Remark 2.2. As it has been argued in [17], because the premise variables of the generalized stochastic T-S fuzzy system in (2.12) contain the system control input, the commonly used parallel distributed compensation (PDC) scheme cannot be directly applied. Instead, the dynamic fuzzy controller in (2.13) is proposed. It is noted that by using the dynamic state feedback controller in (2.13), the closed-loop control system can be expressed in the summation of one index which is different from the traditional static state feedback case where indices are used. This will lead to much less number of LMIs in controller design which will be shown subsequently.

Remark 2.3. When the local gains of the piecewise dynamic fuzzy controller (PDFC) in (2.13) are equal, that is, $[F_{mi}, G_{mi}] = [F_i, G_i]$, for $m \in \mathcal{J}(i)$, the fuzzy controller in (2.13) reduces to the so-called piecewise dynamic crisp controller (PDCC). It will be shown in Section 4 that the fuzzy controller in (2.13) achieves better performance than the piecewise dynamic state feedback controller.

Then the closed-loop control system consisting of (2.12) and (2.13) is given by

$$\begin{aligned}\overline{x}(t+1) &= \sum_{m\in\mathcal{J}(i)} \mu_m(\overline{x}(t)) \\ &\quad\times \Bigg\{ \left(\mathcal{A}_{mi} + R\Delta E_f(\overline{x}(t))\right)\overline{x}(t) \\ &\qquad + \sum_{k=1}^{q} \left(\mathcal{C}_{mk} + R\Delta E_{gk}(\overline{x}(t))\right)\overline{x}(t)W_k(t) \Bigg\}, \quad \overline{x}(t) \in S_i,\end{aligned} \tag{2.14}$$

where $\mathcal{A}_{mi} = \overline{A}_m + \overline{B}\,\overline{K}_{mi}$, ΔE_f and ΔE_{gk} are defined in (2.10), and

$$\begin{gathered}\overline{x}(t) = \begin{bmatrix} x(t) \\ u(t) \end{bmatrix}, \qquad \overline{A}_m = \begin{bmatrix} A_m & B_m \\ \mathbf{0}_{m\times n} & \mathbf{0}_{m\times m} \end{bmatrix}, \\ \overline{B} = \begin{bmatrix} \mathbf{0}_{n\times m} \\ \mathbf{I}_m \end{bmatrix}, \qquad R = \begin{bmatrix} \mathbf{I}_n \\ \mathbf{0}_{m\times n} \end{bmatrix}, \\ \overline{K}_{mi} = \begin{bmatrix} F_{mi} & G_{mi} \end{bmatrix}, \qquad \mathcal{C}_{mk} = \begin{bmatrix} C_{mk} & D_{mk} \\ \mathbf{0}_{m\times n} & \mathbf{0}_{m\times m} \end{bmatrix}.\end{gathered} \tag{2.15}$$

In addition, we define a new set that represents all possible state transitions among regions of the closed-loop T-S fuzzy system in (2.15) as follows:

$$\Omega := \left\{ (i,j) \mid \overline{x}(t) \in S_i,\ \overline{x}(t+1) \in S_j,\ i,j \in \Im \right\}. \tag{2.16}$$

In the case of $(i, j) \in \Omega$ and $i = j$, the state trajectories evolve in the same region S_i at the time t. Otherwise, the state trajectories will transit from the region S_i to S_j at that time.

3. Robust Controller Design for SNNS

In this section, an LMI approach will be developed to solve the stabilization problem of the SNNS in (2.1) based on the generalized stochastic T-S fuzzy models in (2.4).

The following definitions are introduced first.

Definition 3.1. The closed-loop control system in (2.14) is said to be stochastically asymptotically stable in the mean square sense, if for any initial conditions $\overline{x}(0)$, the solution $\overline{x}(t)$ of (2.14) exists for all $t \geq 0$ and $\lim_{t\to\infty}\mathbb{E}\{\|\overline{x}(t)\|^2\} = 0$.

Definition 3.2. The closed-loop control system in (2.14) is said to be stochastically exponentially stable in the mean square sense, if there exist a set of positive constants C, $0 < \sigma < 1$ and $\lambda > 0$, such that given any initial states $\overline{x}(0)$, the solution $\overline{x}(t)$ of (2.14) exists for all $t \geq 0$ and $\mathbb{E}\{\|\overline{x}(t)\|\} \leq C\|\overline{x}(0)\|\sigma^t$.

Denote $\mathcal{M}_m = [(\mathcal{C}_{m1})^T, \ldots, (\mathcal{C}_{mq})^T]^T$ and $\Delta E_g(\overline{x}(t)) = [(R\Delta E_{g1}^T(\overline{x}(t))), \ldots, (R\Delta E_{gq}^T(\overline{x}(t)))]^T$. For the sake of simplicity, we denote $\mu_i(\overline{x}(t))$, $\Delta E_f(\overline{x}(t))$, $\Delta E_{gi}(\overline{x}(t))$, and $\Delta E_g(\overline{x}(t))$ as μ_i, ΔE_f, ΔE_{gi}, and ΔE_g, respectively.

Suppose that the upper bounds of the uncertainties ΔE_f and ΔE_g are given by

$$\Delta E_f^T \Delta E_f \leq \epsilon_1^2 \mathbf{I}_{(m+n)}, \qquad \Delta E_g^T \Delta E_g \leq \overline{\epsilon}_2^2 \mathbf{I}_{(m+n)}, \tag{3.1}$$

respectively.

Then the stochastic stability analysis result for the closed-loop control system (2.14) is provided in the following theorem.

Theorem 3.3. *The closed-loop stochastic fuzzy control system* (2.14) *is stochastically asymptotically stable in the mean square sense if there exist a set of positive definite matrices P_i, $i \in \Im$, two sets of positive constants ε_{1i} and ε_{2i}, and a positive constant δ such that the following matrix inequalities hold for all $(i, j) \in \Omega$, $m \in \mathcal{J}(i)$,*

$$\begin{bmatrix} \Xi_{ij} + \left(\dfrac{\overline{\epsilon}_1^2}{\varepsilon_{1i}} + \dfrac{\overline{\epsilon}_2^2}{\varepsilon_{2i}}\right)\mathbf{I} & \star & \star \\ R^T P_j \mathcal{A}_{mi} & R^T P_j R - \dfrac{1}{\varepsilon_{1i}}\mathbf{I} & \star \\ \mathbf{I}_q \otimes P_j \mathcal{M}_m & 0 & \mathbf{I}_q \otimes P_j - \dfrac{1}{\varepsilon_{2i}}\mathbf{I} \end{bmatrix} < -\delta\mathbf{I}, \tag{3.2}$$

where

$$\Xi_{ij} = \mathcal{A}_{mi}^T P_j \mathcal{A}_{mi} + \mathcal{M}_m^T (I_q \otimes P_j)\mathcal{M}_m - P_i. \tag{3.3}$$

Proof. Consider the following piecewise Lyapunov function candidate:

$$V(\overline{x}(t)) = \overline{x}^T(t)P_i\overline{x}(t), \quad \overline{x}(t) \in S_i. \tag{3.4}$$

For a given set of given positive definite matrices P_i, from (2.2) one has

$$\begin{aligned}
&\mathbb{E}\left\{\left(\sum_{m\in\mathcal{I}(i)}\mu_m(\mathcal{A}_{mi}+R\Delta E_f)\overline{x}(t)\right)^T P_j\left(\sum_{m\in\mathcal{I}(i)}\mu_m\sum_{k=1}^{q}(\mathcal{C}_{mk}+R\Delta E_{gk})\overline{x}(t)W_k(t)\right)\right\}\\
&\quad=\mathbb{E}\left\{\left(\sum_{m\in\mathcal{I}(i)}\mu_m\sum_{k=1}^{q}(\mathcal{C}_{mk}+R\Delta E_{gk})\overline{x}(t)W_k(t)\right)^T P_j\left(\sum_{m\in\mathcal{I}(i)}\mu_m(\mathcal{A}_{mi}+R\Delta E_f)\overline{x}(t)\right)\right\}\\
&\quad=0.
\end{aligned} \tag{3.5}$$

Based on Lemmas A.1 and A.2, one has that

$$\begin{aligned}
&\left\{\sum_{m\in\mathcal{I}(i)}\mu_m(\mathcal{A}_{mi}+R\Delta E_f)\overline{x}(t)\right\}^T P_j\left\{\sum_{m\in\mathcal{I}(i)}\mu_m(\mathcal{A}_{mi}+R\Delta E_f)\overline{x}(t)\right\}\\
&\quad\le\sum_{m\in\mathcal{I}(i)}\mu_m\overline{x}^T(t)(\mathcal{A}_{mi}+R\Delta E_f)^T P_j(\mathcal{A}_{mi}+R\Delta E_f)\overline{x}(t),\\
&\mathbb{E}\left\{\left(\sum_{m\in\mathcal{I}(i)}\mu_m\sum_{k=1}^{q}(\mathcal{C}_{mk}+R\Delta E_{gk})\overline{x}(t)W_k(t)\right)^T P_j\right.\\
&\quad\left.\times\left(\sum_{m\in\mathcal{I}(i)}\mu_m\sum_{k=1}^{q}(\mathcal{C}_{mk}+R\Delta E_{gk})\overline{x}(t)W_k(t)\right)\right\}\\
&\quad\le\sum_{m\in\mathcal{I}(i)}\mu_m\mathbb{E}\left\{\left(\sum_{k=1}^{q}(\mathcal{C}_{mk}+R\Delta E_{gk})\overline{x}(t)W_k(t)\right)^T P_j\times\left(\sum_{k=1}^{q}(\mathcal{C}_{mk}+R\Delta E_{gk})\overline{x}(t)W_k(t)\right)\right\}\\
&\quad=\sum_{m\in\mathcal{I}(i)}\mu_m\sum_{k=1}^{q}\overline{x}^T(t)(\mathcal{C}_{mk}+R\Delta E_{gk})^T P_j(\mathcal{C}_{mk}+R\Delta E_{gk})\overline{x}(t)\\
&\quad=\sum_{m\in\mathcal{I}(i)}\mu_m\overline{x}^T(t)(\mathcal{M}_m+\Delta E_g)^T(\mathbf{I}_q\otimes P_j)(\mathcal{M}_m+\Delta E_g)\overline{x}(t).
\end{aligned} \tag{3.6}$$

Then one has that along the system trajectories of (2.14),

$$\begin{aligned}
&\mathbb{E}\{V(\overline{x}(t+1) \mid \overline{x}(t))\} - V(\overline{x}(t)) \\
&\quad \leq \sum_{m\in\mathcal{O}(i)} \mu_m \overline{x}^T(t)\Big\{\left(\mathcal{A}_{mi} + R\Delta E_f\right)^T P_j\left(\mathcal{A}_{mi} + R\Delta E_f\right) \\
&\qquad\qquad + \left(\mathcal{M}_m + \Delta E_g\right)^T \left(\mathbf{I}_q \otimes P_j\right)\left(\mathcal{M}_m + \Delta E_g\right) - P_i\Big\}\overline{x}(t).
\end{aligned} \tag{3.7}$$

Therefore one has that $\mathbb{E}\{V(\overline{x}(t+1) \mid \overline{x}(t))\} - V(\overline{x}(t)) < -\delta\overline{x}^T(t)\overline{x}(t)$ if

$$\begin{aligned}
&\left(\mathcal{A}_{mi} + R\Delta E_f\right)^T P_j\left(\mathcal{A}_{mi} + R\Delta E_f\right) - P_i \\
&\quad + \left(\mathcal{M}_m + \Delta E_g\right)^T \left(\mathbf{I}_{\mathbf{q}} \otimes P_j\right)\left(\mathcal{M}_m + \Delta E_g\right) < -\delta\mathbf{I}.
\end{aligned} \tag{3.8}$$

Denote $\zeta = [\mathbf{I}_{(m+n)}, \Delta E_f^T, \Delta E_g^T]^T$. Then it can be seen that the inequality (3.8) is equivalent to

$$\zeta^T \begin{bmatrix} \Xi_{ij} & \star & \star \\ R^T P_j \mathcal{A}_{mi} & R^T P_j R & \star \\ \mathbf{I}_q \otimes P_j \mathcal{M}_m & 0 & \mathbf{I}_q \otimes P_j \end{bmatrix} \zeta < -\delta\mathbf{I}, \tag{3.9}$$

where Ξ_{ij} is defined in (3.3).

The upper bounds defined in (3.1) can be rewritten, respectively, as

$$\zeta^T \begin{bmatrix} -\overline{\epsilon}_1^2\mathbf{I}_{(m+n)} & \star & \star \\ 0 & \mathbf{I}_{(m+n)} & \star \\ 0 & 0 & 0 \end{bmatrix} \zeta < 0, \qquad \zeta^T \begin{bmatrix} -\overline{\epsilon}_2^2\mathbf{I}_{(m+n)} & \star & \star \\ 0 & 0 & \star \\ 0 & 0 & \mathbf{I}_{(m+n)} \end{bmatrix} \zeta < 0. \tag{3.10}$$

Then by applying Lemma A.3 (S-procedure) in the appendix, one can conclude that (3.8) holds if there exist two sets of positive constants ε_{1i} and ε_{2i} such that (3.2) holds.

Therefore, if (3.2) holds, one has that

$$\mathbb{E}\{V(\overline{x}(t+1) \mid \overline{x}(t))\} - V(\overline{x}(t)) < -\delta\overline{x}^T(t)\overline{x}(t). \tag{3.11}$$

Taking expectation of both sides of (3.11) yields

$$\mathbb{E}\{V(\overline{x}(t+1))\} - \mathbb{E}\{V(\overline{x}(t))\} < -\delta\mathbb{E}\left\{\|\overline{x}(t)\|^2\right\}, \tag{3.12}$$

which implies

$$\mathbb{E}\left\{\sum_{t=0}^{N}\|\overline{x}(t)\|^2\right\} < \frac{1}{\delta}\left(\mathbb{E}\{V(\overline{x}(0))\} - \mathbb{E}\{V(\overline{x}(N+1))\}\right) \leq \frac{1}{\delta}\mathbb{E}\{V(\overline{x}(0))\} < \infty. \tag{3.13}$$

Then one has that $\lim_{t\to\infty}\mathbb{E}\{\|\overline{x}(t)\|^2\} = 0$. From Definition 3.1, the closed-loop fuzzy system (2.14) is stochastically asymptotically stable in the mean square sense. The proof is thus completed. □

Corollary 3.4. *Under the conditions of Theorem 3.3, the closed-loop stochastic fuzzy control system* (2.14) *is also stochastically exponentially stable in the mean square sense.*

Proof. From (3.4) one has that

$$\lambda_1\|\overline{x}(t)\|^2 \le V(\overline{x}(t)) \le \lambda_2\|\overline{x}(t)\|^2, \tag{3.14}$$

where $\lambda_1 = \min_i \lambda\{P_i\}$ and $\lambda_2 = \max_i \lambda\{P_i\}$.

Then from (3.12), one has

$$\mathbb{E}\{V(\overline{x}(t+1))\} < \left(1-\frac{\delta}{\lambda_2}\right)\mathbb{E}\{V(\overline{x}(t))\}, \tag{3.15}$$

which implies

$$\lambda_1\mathbb{E}\left\{\|\overline{x}(t)\|^2\right\} \le V(\overline{x}(t)) \le \left(1-\frac{\delta}{\lambda_2}\right)^t\mathbb{E}\{V(\overline{x}(0))\}. \tag{3.16}$$

Thus one has that $\mathbb{E}\{\|\overline{x}(t)\|^2\} \le C\|\overline{x}(0)\|\sigma^t$, where $C = \lambda_2/\lambda_1 > 0$ and $0 < \sigma = 1-\delta/\lambda_2 < 1$. From Definition 3.2, one can conclude that the closed-loop fuzzy control system (2.14) is stochastically exponentially stable in the mean square sense. The proof is thus completed. □

Remark 3.5. It is noted that $\sigma = 1-\delta/\lambda_2$ represents the convergence rate of the closed-loop control system.

Based on Theorem 3.3, the following controller design results can be obtained.

Theorem 3.6. *The SNNS* (2.1) *can be semiglobally stochastically asymptotically stabilized in the mean square sense by the dynamic fuzzy controller in* (2.13)*, if there exist a set of positive definite matrices X_i, $i \in \Im$, two sets of positive constants ε_{1i} and ε_{2i}, and a positive constant λ such that the following matrix inequalities hold for all $(i,j) \in \Omega$, $m \in \mathcal{O}(i)$,*

$$\begin{bmatrix} -X_i & \star & \star & \star & \star & \star \\ \overline{\epsilon}_1 X_i & -\varepsilon_{1i}\mathbf{I} & \star & \star & \star & \star \\ \overline{\epsilon}_2 X_i & 0 & -\varepsilon_{2i}\mathbf{I} & \star & \star & \star \\ X_i & 0 & 0 & -\lambda\mathbf{I} & \star & \star \\ \overline{A}_m X_i + \overline{B}\,\overline{Q}_{mi} & 0 & 0 & 0 & X_j - \varepsilon_{1i}\mathbf{I} & \star \\ \mathcal{M}_m X_i & 0 & 0 & 0 & 0 & \mathbf{I}_q \otimes X_j - \varepsilon_{2i}\mathbf{I}_{q(m+n)} \end{bmatrix} < 0. \tag{3.17}$$

Moreover, the controller gain matrices $\overline{K}_{mi}$ are given by $\overline{K}_{mi} = \overline{Q}_{mi}X_i^{-1}$.

Proof. It is noted that the SNNS (2.1) can be expressed by the generalized stochastic T-S fuzzy model in any compact set. It is also noted that the system (4.2) can be expressed by (2.12)

in each local region of interest. Thus if the system (2.12) can be stochastically asymptotically stabilized in the mean square sense by the controller (2.13), with the bounded initial condition on the state $x(0)$ and the control $u(0)$, the original SNNS (2.1) can be shown to be semi-globally stochastically asymptotically stabilized in the mean square sense.

By using Schur's complement, (3.2) is equivalent to

$$\begin{aligned}&\mathcal{A}_{mi}^T P_j \mathcal{A}_{mi} - \mathcal{A}_{mi}^T P_j R\left(R^T P_j R - \frac{1}{\varepsilon_{1i}}\mathbf{I}\right)^{-1} R^T P_j \mathcal{A}_{mi} - P_i + \left(\frac{\overline{e}_1^2}{\varepsilon_{1i}} + \frac{\overline{e}_2^2}{\varepsilon_{2i}}\right)\mathbf{I} \\ &\quad + \mathcal{M}_m^T(\mathbf{I}_q \otimes P_j)\mathcal{M}_m - \mathcal{M}_m^T(\mathbf{I}_q \otimes P_j)\left(\mathbf{I}_q \otimes P_j - \frac{1}{\varepsilon_{2i}}\mathbf{I}\right)^{-1}(\mathbf{I}_q \otimes P_j)\mathcal{M}_m < -\delta\mathbf{I}.\end{aligned} \tag{3.18}$$

By matrix inverse lemma, (3.18) becomes

$$\mathcal{A}_{mi}^T\left(P_j^{-1} - \varepsilon_{1i}\mathbf{I}\right)^{-1}\mathcal{A}_{mi} - P_i + \left(\frac{\overline{e}_1^2}{\varepsilon_{1i}} + \frac{\overline{e}_2^2}{\varepsilon_{2i}}\right)\mathbf{I} + \mathcal{M}_m^T\left((\mathbf{I}_q \otimes P_j)^{-1} - \varepsilon_{2i}\mathbf{I}\right)^{-1}\mathcal{M}_m < -\delta\mathbf{I}. \tag{3.19}$$

Multiplying $X_i = P_i^{-1}$ from both sides to (3.19), one has

$$\begin{aligned}&X_i\mathcal{A}_{mi}^T(X_j - \varepsilon_{1i}\mathbf{I})^{-1}\mathcal{A}_{mi}X_i - X_i + \left(\frac{\overline{e}_1^2}{\varepsilon_{1i}} + \frac{\overline{e}_2^2}{\varepsilon_{2i}}\right)X_iX_i \\ &\quad + X_i\mathcal{M}_m^T(\mathbf{I}_q \otimes X_j - \varepsilon_{2i}\mathbf{I})^{-1}\mathcal{M}_mX_i < -\delta X_iX_i\end{aligned} \tag{3.20}$$

which is equivalent to (3.17) by using Schur's complement with the fact that $\overline{Q}_{mi} = \overline{K}_{mi}X_i$ and $\lambda = 1/\delta$.

Thus it follows from Theorem 3.3 that the closed-loop fuzzy system (2.14) is stochastically asymptotically stable in the mean square sense. Thus one has shown that the original SNNS (2.1) can be semi-globally stochastically asymptotically stabilized by the controller in (2.13). Thus the proof is completed. □

Remark 3.7. From (3.19), one can see that the LMIs in (3.17) are not easy to be satisfied if the upper bounds of the approximation errors, that is, $\overline{e}_1$ and $\overline{e}_2$, are too large. In order to achieve better approximation performance one has to use larger number of fuzzy rules, which, based on Theorems 3.3 and 3.6, leads to much higher computation cost of control design. However, this problem can be lessened to some extent due to the robustness of the proposed approach. In other words, the smaller number of fuzzy rules can be chosen since the robustness of the proposed approach allows larger approximation errors.

Remark 3.8. Theorems 3.3 and 3.6 are based on a piecewise quadratic Lyapunov function. When the positive definite matrices X_i are chosen as common ones, that is, $X_i = X$, $i \in \Im$, then the results of Theorems 3.3 and 3.6 reduce to those based on common Lyapunov functions. It will be shown in Section 4 that the results based on piecewise Lyapunov functions (FLPs) are less conservative than those based on common Lyapunov functions (CLFs).

4. Simulation Studies

In this section, to show the performance of the proposed controller design results, we consider the balancing problem of an inverted pendulum on a cart. The following discretized inverted pendulum plant with non-affine mathematical model [26] is used:

$$\begin{aligned} x_1(t+1) &= x_1(t) + Tx_2(t), \\ x_2(t+1) &= x_2(t) + T\left(f(x(t), v(t)) + [10x_1 + 10u, 15x_2 - 10u]\begin{bmatrix} W_1(t) \\ W_2(t) \end{bmatrix}\right), \end{aligned} \tag{4.1}$$

where $f(x,v) = (g\sin(x_1) - amlx_2^2\sin(2x_1)/2 - a\cos(x_1)v)/(4l/3 - aml\cos^2(x_1))$, $v(t) = (\arctan(u(t)) + 0.55u(t)) * 10^2$, x_1 denotes the angle of pendulum from the vertical, and x_2 is the angular velocity. $g = 9.8\,\mathrm{m/s^2}$ is the gravity constant, m is the mass of pendulum, M is the mass of the cart, $a = 1/(M+m)$, $T = 0.01\,\mathrm{s}$ is the sampling time in this study, and $2l$ is the length of the pendulum. Note that the input force is given by $\arctan(u) + 0.15u$ with an amplifier of gain 1000 connected. In this simulation, we choose $m = 2.0\,\mathrm{kg}$, $M = 8.0\,\mathrm{kg}$, and $2l = 1.0\,\mathrm{m}$.

We linearize the plant around the following operating points, $(x;u) = (0;0;0)$, $(0;0;3)$, $(\pm 88^\circ;0;0)$, and $(\pm 88^\circ;0;\pm 3)$, respectively, and consider the approximation errors between the linearized local model and the original nonlinear models as norm-bounded uncertainties. Then the following uncertain discrete-time dynamic T-S fuzzy model can be obtained:

$$\begin{aligned} x(t+1) = \sum_{l=1}^{4}\mu_l(x,u)\Big\{ &\big(A_l x(t) + B_l u(t) + \epsilon_f(x(t),u(t))\big) \\ &+ \sum_{k=1}^{2}\big(C_{lk}x(t) + D_{lk}u(t) + \epsilon_{gk}(x(t),u(t))\big)W_k(t)\Big\}, \end{aligned} \tag{4.2}$$

where the membership functions are shown in Figure 1,

$$\begin{gathered} A_1 = A_2 = \begin{bmatrix} 0 & 1 \\ 17.2941 & 0 \end{bmatrix}, \qquad A_3 = A_4 = \begin{bmatrix} 0 & 1 \\ 0.3593 & 0 \end{bmatrix}, \\ B_1 = \begin{bmatrix} 0 \\ -27.36 \end{bmatrix}, \qquad B_2 = \begin{bmatrix} 0 \\ -15.56 \end{bmatrix}, \\ B_3 = \begin{bmatrix} 0 \\ -0.81 \end{bmatrix}, \qquad B_4 = \begin{bmatrix} 0 \\ -0.46 \end{bmatrix}, \\ C_{l1} = \begin{bmatrix} 0 & 0 \\ 10 & 0 \end{bmatrix}, \qquad D_{l1} = \begin{bmatrix} 0 \\ 10 \end{bmatrix}, \qquad C_{l2} = \begin{bmatrix} 0 & 0 \\ 0 & 15 \end{bmatrix}, \\ D_{l2} = \begin{bmatrix} 0 \\ -10 \end{bmatrix}, \quad l \in \mathfrak{L} := \{1,2,\ldots,4\}. \end{gathered} \tag{4.3}$$

As it has been defined in Section 2, the indices of fired rules in each local region are given in Table 1.

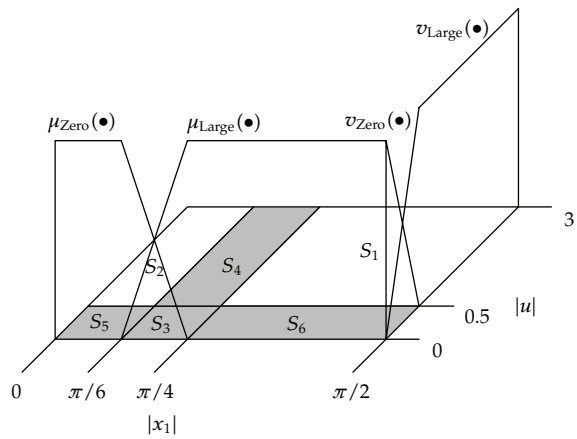

Figure 1: Membership functions.

Table 1: Indices of rules fired in each local region.

Local region S_i	Indices of rules fired $\mathcal{O}(i)$
S_1	$\{4\}$
S_2	$\{2\}$
S_3	$\{1,2,3,4\}$
S_4	$\{2,4\}$
S_5	$\{1,2\}$
S_6	$\{3,4\}$

It is noted that the exact or tightest upper bounds of the approximation errors are difficult to identify. However, one can apply the method shown in [26] to obtain the approximate upper bounds, which are $\overline{e}_1 = 0.3$ and $\overline{e}_2 = 0$, respectively. Then by applying Theorem 3.6, the controller gains with respect to each partitioned regions are obtained as

$$\begin{aligned}
\text{Region } S_1\text{: } \overline{K}_{41} &= \begin{bmatrix}-0.0147 & 0.0615 & 0.0191\end{bmatrix},\\
\text{Region } S_2\text{: } \overline{K}_{22} &= \begin{bmatrix}-0.0147 & 0.0615 & 0.0191\end{bmatrix},\\
\text{Region } S_3\text{: } \overline{K}_{13} &= \begin{bmatrix}-0.3471 & 0.0333 & 0.5511\end{bmatrix},\\
\overline{K}_{23} &= \begin{bmatrix}-0.3437 & 0.0296 & 0.3024\end{bmatrix},\\
\overline{K}_{33} &= \begin{bmatrix}-0.0065 & 0.0279 & 0.0152\end{bmatrix},\\
\overline{K}_{43} &= \begin{bmatrix}-0.0066 & 0.0279 & 0.0085\end{bmatrix},\\
\text{Region } S_4\text{: } \overline{K}_{24} &= \begin{bmatrix}-0.3738 & 0.0341 & 0.3357\end{bmatrix},\\
\overline{K}_{44} &= \begin{bmatrix}-0.0069 & 0.0300 & 0.0093\end{bmatrix},\\
\text{Region } S_5\text{: } \overline{K}_{15} &= \begin{bmatrix}-0.0210 & -0.0010 & 0.0332\end{bmatrix},\\
\overline{K}_{25} &= \begin{bmatrix}-0.0210 & -0.0010 & 0.0189\end{bmatrix},\\
\text{Region } S_6\text{: } \overline{K}_{36} &= \begin{bmatrix}-0.0145 & 0.0611 & 0.0336\end{bmatrix},\\
\overline{K}_{46} &= \begin{bmatrix}-0.0145 & 0.0608 & 0.0188\end{bmatrix}.
\end{aligned} \tag{4.4}$$

Table 2: Comparison of the convergence rate for different cases.

Methods	The convergence rate $\sigma = 1 - (\delta/\lambda_2)$
Theorem 3.6	0.8317
Results based on PDCC and PLFs as indicated in Remark 2.3	0.9117
Results based on PDCC and CLFs as indicated in Remark 3.8	0.9991

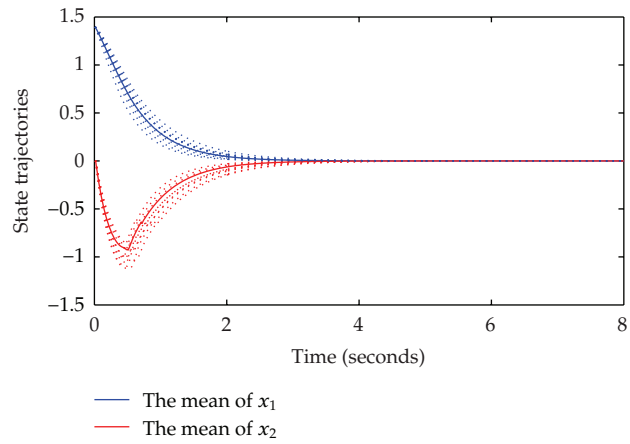

Figure 2: State trajectories.

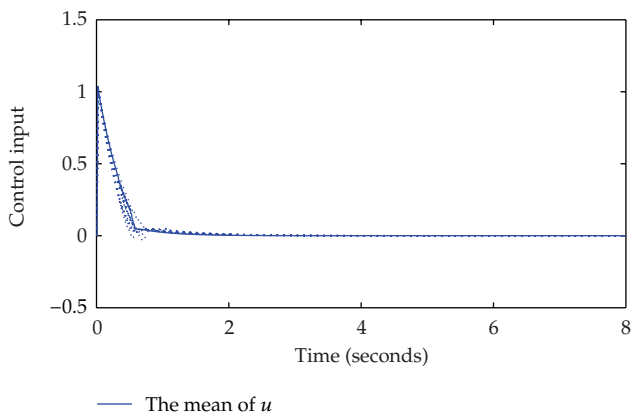

Figure 3: Control input.

To illustrate the performance of the approach proposed in this paper, the state trajectories and control input of the closed-loop system under initial condition $x(0) = (80°, 0)$ along 10 individual Wiener process paths are shown in Figures 2 and 3, respectively. One can observe that both the means of the system states and control input converge to zero as time approaches infinity.

To compare the proposed approach with results based on piecewise dynamic controller and piecewise/common Lyapunov functions, respectively, the convergence rates under different cases are presented in Table 2. It can be observed from Table 2 that the approaches based on piecewise quadratic Lyapunov functions are less conservative than those based on

common Lyapunov functions, and the piecewise dynamic *fuzzy* controller (PDFC) has better performance than the piecewise dynamic *crisp* controller.

5. Conclusion

In this paper, T-S fuzzy model based control design of discrete-time stochastic non-affine nonlinear systems (SNNS) has been investigated. By using a piecewise Lyapunov function, it is shown that a discrete-time SNNS can be stochastically asymptotically stabilized in the mean square sense by solving a set of linear matrix equalities. Simulation results are provided to demonstrate the effectiveness of the approaches proposed in this paper. Some interesting future topics include filtering design and fault detection problems for complex discrete-time *SNNS* based on piecewise Lyapunov functions.

Appendix

Lemma A.1. *Given a set of independent stochastic processes $W_1(t), \ldots, W_q(t)$ satisfying*

$$\mathbb{E}\{W_i(t)\} = 0, \qquad \mathbb{E}\left\{W_i^2(t)\right\} = w_i, \tag{A.1}$$

a set of vectors $X_i \in \Re^{n\times 1}$, and a symmetric matrix $H \in \Re^{n\times n}$, one has that

$$\mathbb{E}\left\{\left(\sum_{i=1}^{q} W_i(t)X_i\right)^T H\left(\sum_{i=1}^{q} W_i(t)X_i\right)\right\} = \sum_{i=1}^{q} w_i X_i^T H X_i. \tag{A.2}$$

Proof. One has

$$\begin{aligned}
&\mathbb{E}\left\{\left(\sum_{i=1}^{q} W_i(t)X_i\right)^T H\left(\sum_{i=1}^{q} W_i(t)X_i\right)\right\} \\
&\quad = \mathbb{E}\left\{\sum_{i=1}^{q} W_i^2 X_i^T H X_i\right\} + \mathbb{E}\left\{\sum_{i\neq j} W_i W_j X_i^T H X_j\right\} = \sum_{i=1}^{q} w_i X_i^T H X_i.
\end{aligned} \tag{A.3}$$

□

Lemma A.2 (see [27]). *For any real matrices X_i and $P > 0$ with compatible dimensions, then*

$$\left\{\sum_{i=1}^{r} \gamma_i X_i\right\}^T P \left\{\sum_{i=1}^{r} \gamma_i X_i\right\} \leq \sum_{i=1}^{r} \gamma_i X_i^T P X_i, \tag{A.4}$$

where γ_i, $(i = 1, \ldots, r)$, are nonnegative scalars with $\sum_{i=1}^{r} \gamma_i = 1$.

Lemma A.3 (S-procedure [28]). *Let $T_0, \ldots, T_p \in \mathbb{R}^{n\times n}$ be symmetric matrices. Then the following condition on $T_0, \ldots, T_p$*

$$\xi^T T_0 \xi > 0, \quad \forall \xi \neq 0, \tag{A.5}$$

such that

$$\xi^T T_i \xi \geq 0, \quad i = 1, \ldots, p, \tag{A.6}$$

holds if there exists

$$\tau_1 \geq 0, \ldots, \tau_p \geq 0 \quad \text{such that } T_0 - \sum_{i=1}^{p} \tau_i T_i > 0. \tag{A.7}$$

Acknowledgment

The work described in this paper was supported by the National Natural Science Foundation of China under Grant 11001005.

References

[1] T. Takagi and M. Sugeno, "Fuzzy identification of systems and its applications to modeling and control," *IEEE Transactions on Systems, Man and Cybernetics B*, vol. 15, no. 1, pp. 116–132, 1985.

[2] G. Feng, *Analysis and Synthesis of Fuzzy Control Systems: A Model-Based Approach*, CRC Press, Boca Raton, Fla, USA, 2010.

[3] G. Feng, "A survey on analysis and design of model-based fuzzy control systems," *IEEE Transactions on Fuzzy Systems*, vol. 14, no. 5, pp. 676–697, 2006.

[4] J. Qiu, G. Feng, and J. Yang, "A new design of delay-dependent robust H_∞ filtering for discrete-time T-S fuzzy systems with time-varying delay," *IEEE Transactions on Fuzzy Systems*, vol. 17, no. 5, pp. 1044–1058, 2009.

[5] J. Qiu, G. Feng, and H. Gao, "Fuzzy-model-based piecewise H_∞ static-output-feedback controller design for networked nonlinear systems," *IEEE Transactions on Fuzzy Systems*, vol. 18, no. 5, pp. 919–934, 2010.

[6] L. Wu, X. Su, P. Shi, and J. Qiu, "A new approach to stability analysis and stabilization of discrete-time T-S fuzzy time-varying delay systems," *IEEE Transactions on Systems, Man, and Cybernetics, Part B*, vol. 41, no. 1, pp. 273–286, 2011.

[7] H. R. Karimi, B. Moshiri, and C. Lucas, "Robust fuzzy linear control of a class of stochastic nonlinear time-delay systems," *Nonlinear Dynamics and Systems Theory*, vol. 4, no. 3, pp. 317–332, 2004.

[8] D. Saifia, M. Chadli, S. Labiod, and H. R. Karimi, "H_∞ fuzzy control of DC-DC converters with input constraint," *Mathematical Problems in Engineering*, vol. 2012, Article ID 973082, 18 pages, 2012.

[9] M. Chadli and H. R. Karimi, "Robust observer design for unknown inputs Takagi-Sugeno models," *IEEE Transactions on Fuzzy Systems*. In press.

[10] Z. -G. Wu, P. Shi, H. Su, and J. Chu, "Reliable H_∞ control for discrete-time fuzzy systems with infinite-distributed delay," *IEEE Transactions on Fuzzy Systems*, vol. 20, no. 1, pp. 22–31, 2012.

[11] H. Ohtake, K. Tanaka, and H. O. Wang, "Fuzzy model-based servo and model following control for nonlinear systems," *IEEE Transactions on Systems, Man, and Cybernetics B*, vol. 39, no. 6, pp. 1634–1639, 2009.

[12] G. Feng, "Stability analysis of discrete-time fuzzy dynamic systems based on piecewise lyapunov functions," *IEEE Transactions on Fuzzy Systems*, vol. 12, no. 1, pp. 22–28, 2004.

[13] M. Johansson, A. Rantzer, and K. E. Årzén, "Piecewise quadratic stability of fuzzy systems," *IEEE Transactions on Fuzzy Systems*, vol. 7, no. 6, pp. 713–722, 1999.

[14] X.-J. Zeng and M. G. Singh, "Approximation theory of fuzzy systems-SISO case," *IEEE Transactions on Fuzzy Systems*, vol. 2, no. 2, pp. 162–176, 1994.
[15] X.-J. Zeng and M. G. Singh, "Approximation theory of fuzzy systems-MIMO case," *IEEE Transactions on Fuzzy Systems*, vol. 3, no. 2, pp. 219–235, 1995.
[16] X. J. Zeng, J. A. Keane, and D. Wang, "Fuzzy systems approach to approximation and stabilization of conventional affine nonlinear systems," in *Proceedings of the IEEE International Conference on Fuzzy Systems*, pp. 277–284, Vancouver, Canada, July 2006.
[17] Q. Gao, X. -J. Zeng, G. Feng, Y. Wang, and J. Qiu, "T-S-Fuzzy-Model-Based approximation and controller design for general nonlinear systems," *IEEE Transactions on Systems, Man, and Cybernetics B*, vol. 42, no. 4, pp. 1131–1142, 2012.
[18] Q. Gao, G. Feng, Y. Wang, and J. Qiu, "Universal fuzzy controllers based on generalized T-S fuzzy models," *Fuzzy Sets and Systems*, vol. 201, pp. 55–70, 2012.
[19] X. Mao, *Stochastic Differential Equations and Applications*, Horwood, Chichester, UK, 2nd edition, 2008.
[20] C. X. Zhu and W. Q. Zhu, "Feedback control of nonlinear stochastic systems for targeting a specified stationary probability density," *Automatica*, vol. 47, no. 3, pp. 539–544, 2011.
[21] G. Chen and Y. Shen, "Robust reliable H_∞ control for nonlinear stochastic markovian jump systems," *Mathematical Problems in Engineering*, vol. 2012, Article ID 431576, 16 pages, 2012.
[22] X.-J. Xie and J. Tian, "Adaptive state-feedback stabilization of high-order stochastic systems with nonlinear parameterization," *Automatica*, vol. 45, no. 1, pp. 126–133, 2009.
[23] S. Zhou, W. Ren, and J. Lam, "Stabilization for T-S model based uncertain stochastic systems," *Information Sciences*, vol. 181, no. 4, pp. 779–791, 2011.
[24] B. Zhang, S. Xu, G. Zong, and Y. Zou, "Delay-dependent stabilization for stochastic fuzzy systems with time delays," *Fuzzy Sets and Systems*, vol. 158, no. 20, pp. 2238–2250, 2007.
[25] L. Hu and A. Yang, "Fuzzy model-based control of nonlinear stochastic systems with time-delay," *Nonlinear Analysis. Theory, Methods & Applications*, vol. 71, no. 12, pp. e2855–e2865, 2009.
[26] Q. Gao, G. Feng, Y. Wang, and J. Qiu, "Universal fuzzymodels and universal fuzzy controllers for stochastic non-affine nonlinear systems," *IEEE Transactions on Fuzzy Systems*. In press.
[27] X. P. Guan and C. L. Chen, "Delay-dependent guaranteed cost control for T-S fuzzy systems with time delays," *IEEE Transactions on Fuzzy Systems*, vol. 12, no. 2, pp. 236–249, 2004.
[28] S. Boyd, L. El Ghaoui, E. Feron, and V. Balakrishnan, *Linear Matrix Inequalities in System and Control Theory*, Society for Industrial and Applied Mathematics (SIAM), Philadelphia, Pa, USA, 1994.

Hindawi Publishing Corporation
Mathematical Problems in Engineering
Volume 2012, Article ID 347217, 10 pages
doi:10.1155/2012/347217

Research Article

Fuzzy PD Control of Networked Control Systems Based on CMAC Neural Network

Li-lian Huang and Jin Chen

College of Information and Communication Engineering, Harbin Engineering University, Harbin, Heilongjiang 150001, China

Correspondence should be addressed to Li-lian Huang, lilian_huang@163.com

Received 16 November 2012; Revised 4 December 2012; Accepted 5 December 2012

Academic Editor: Peng Shi

Copyright © 2012 L.-l. Huang and J. Chen. This is an open access article distributed under the Creative Commons Attribution License, which permits unrestricted use, distribution, and reproduction in any medium, provided the original work is properly cited.

The network and plant can be regarded as a controlled time-varying system because of the random induced delay in the networked control systems. The cerebellar model articulation controller (CMAC) neural network and a PD controller are combined to achieve the forward feedback control. The PD controller parameters are adjusted adaptively by fuzzy reasoning mechanism, which can optimize the control effect by reducing the uncertainty caused by the network-induced delay. Finally, the simulations show that the control method proposed can improve the performance effectively.

1. Introduction

Networked control system (NCS) is a distributed and networked real-time feedback control system which combine communication network and control system [1]. Due to the irregularly multiple nodes shared network and data flowing change, information exchange time delay occurred inevitably, which is the network-induced delay [2]. The network-induced delay will cause system poor control quality and bad performance, even unstable [3–5]. Therefore, the induced delay is one of the most issues in the network control system [6–9].

Based on the influence of the induced delay in the network control system, a cycle time delay network using augmented deterministic discrete time model method is proposed by [10] to control the linear continuous controlled object. In [11] based on the queue management network, the queuing methodology is put forward to turn random time delay into fixed-length time delay. The buffer queue method is designed based on probability predictor delay compensation, according to the problem of random delay in the network

control system [12]. Zhang et al. [13] studied the stability of network control system with constant delay. Wu et al. [14] propose a delay-dependent sufficient condition by applying the delay partitioning approach for the asymptotic stability with an $H\infty$ error performance for the error system. Wu and Zheng [15] addressed the L_2-L_∞ dynamic output feedback (DOF) control problem for a class of nonlinear fuzzy ItO stochastic systems with time-varying delay. Yue et al. [16] established the new network control system model considering network-varying delay, packet loss, and wrong sequence. Peng et al. [17] researched on network control system with interval variable delay and reduced complexity by introducing Jessen inequality. Wu et al. [18] investigated the problems of stability analysis and stabilization for a class of discrete-time Takagi-Sugeno fuzzy systems with time-varying state delay. Wu et al. [19] proposed sufficient conditions to guarantee the exponential stability for the switched neural networks with constant and time-varying delays by using the average dwell time approach together with the piecewise Lyapunov function technique and by combining a novel Lyapunov-Krasovskii functional, which benefits from the delay partitioning method, with the free-weighting matrix technique. In [20] the impact of the network-induced delay is described as a system of continuous-time nonlinear perturbation using nonlinear perturbation theory by assuming no observation noise. Yang et al. introduced a new class of discrete-time networked nonlinear systems with mixed random delays and packet dropouts [21] and discussed the problem of feedback control for networked systems with discrete and distributed delays subject to quantization and packet dropout [22]. Xie et al. [23] discussed the problem of robust $H\infty$ fault-tolerant control for uncertain networked control system with random delays and actuator faults.

In this paper, the PD control with CMAC (cerebellar model articulation controller, CMAC) is proposed. The transmission network and the controlled object are regarded as the time-varying controlled system, in which CMAC neural network implements the forward feedback, while the fuzzy PD composite switching model is applied and adaptive on-line parameters by using fuzzy inference engine are set. The method proposed can reduce the impact of network-induced delay and the uncertainties, so it optimize the control effect and improve the control performance of the system.

The rest of the paper is organized as follows. In Section 2, the problem of time delay in NCS is described. The CMAC neural network-based fuzzy PD controller is put forward in Section 3. Simulation results are shown in Section 4. Finally, a conclusion is provided in Section 5.

2. The Description of Network Control System with Time Delay

In network control system, there are three kinds of delay, namely, sensor-controller delay τ_{sc}, controller computation delay τ_c, and controller-actuator delay τ_{ca}, where the τ_{sc} and τ_{ca} are caused by the transmission delay generated by the forward channel and feedback channel, and the τ_c is caused by the hardware structure and software code. The controller computation delay τ_c used is to be neglected because it is smaller than τ_{sc} and τ_{ca}. So the total delay of the kth sampling period can be represented as $\tau^k = \tau_{sc}^k + \tau_{ca}^k$ [24]. The network control system block diagram is shown in Figure 1.

3. The Design of CMAC Neural Network-Based Fuzzy PD Controller

Network control system is time varying because of the network random delay, and the general PID controller will make the control performance worse. But intelligent control has

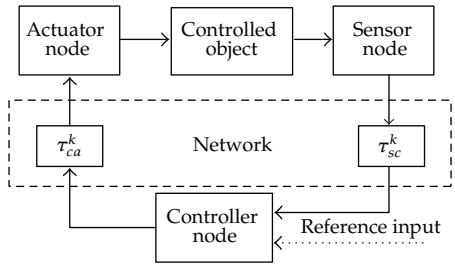

Figure 1: Networked control system.

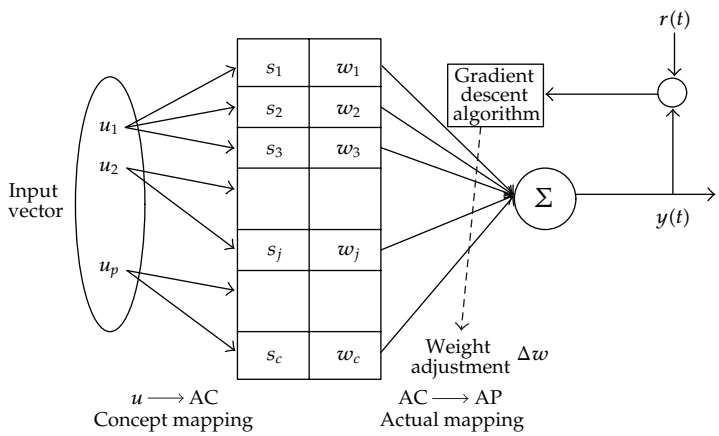

Figure 2: Structure of CMAC network.

a better adaptive ability and is an effective method to improve the system performance [25–28], therefore intelligent control is applied to improve the robustness of the system [29–33]. In this paper, CMAC neural network-based fuzzy PD is applied to control the system. We use the PD algorithm instead of the PID, so that the learning of CMAC neural network only depends on the measured and varying values of errors.

3.1. CMAC Neural Network

CMAC is a neural network model which can simulate the function of the cerebellar and has the ability to express and inquire complex nonlinear forms adaptively. The network can change the form's information through the learning algorithm and can also store information by category [34]. CMAC consists of input layer, middle layer, and output layer, and its structure is shown in Figure 2.

$\mathbf{u}_p = [\mathbf{u}_{1p}, \mathbf{u}_{2p}, \ldots, \mathbf{u}_{np}]^T$ and $[u_p]$ are respectively input space vector and quantization coding, and the input space is mapped to the c memory cells, and c is generalization parameters. The mapping vector is as follows:

$$\mathbf{R}_p = S([u_p]) = [s_1(u_p), s_2(u_p), \ldots, s_c(u_p)]^T, \tag{3.1}$$

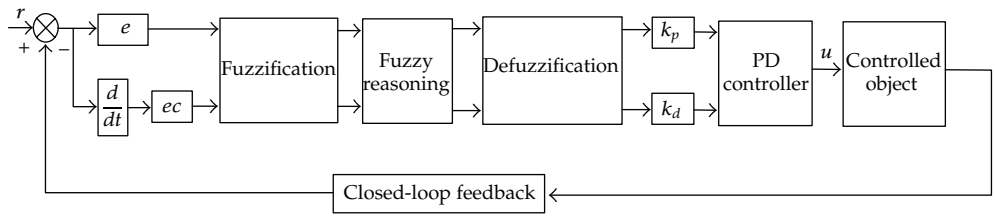

Figure 3: Diagram of fuzzy PD controller.

where $s_j([u_p]) = 1, j = 1, 2, \ldots, c$. The network's output is the sum of the weights of the c units.

Now only thinking of the single input, the output is

$$y = \sum_{j=1}^{c} w_j s_j([u_p]), \tag{3.2}$$

so

$$y = \sum_{j=1}^{c} w_j. \tag{3.3}$$

The learning algorithm is as follows.
The δ learning rule is adapted to adjust the weights, and the norm of weight adjustment is

$$E = \frac{1}{2c} e(t)^2, \tag{3.4}$$

where $e(t) = r(t) - y(t)$.

According to the gradient descent, the weights are adjusted as follows:

$$\begin{gathered} \Delta w_j(k) = -\eta \frac{\partial E}{\partial w} = \eta \frac{r(t) - y(t)}{c} \cdot \frac{\partial y}{\partial w} = \eta \frac{e(t)}{c}, \\ w_j(t) = w_j(t-1) + \Delta w_j(t) + \beta\big(w_j(t-1) - w_j(t-2)\big), \end{gathered} \tag{3.5}$$

where $w = [w_1, w_2, \ldots, w_c]^T$, and β is inertial coefficient.

3.2. *Fuzzy PD Controller*

Fuzzy PD controller takes fuzzy reasoning to adjust the real-time PD parameters. The design of the fuzzy controller includes the fuzzy rules, fuzzy domain, and defuzzification. In this paper, fuzzy algorithm applies the dual-input-output, where signal difference e and difference rate ec are the input, meanwhile, the PD controller proportion coefficient k_p and differential coefficient k_d are the output, respectively. The structure is shown in Figure 3.

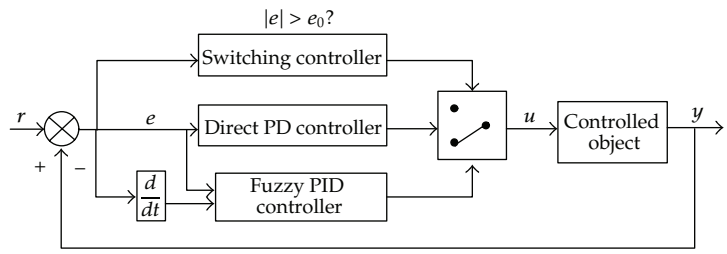

Figure 4: Structure of fuzzy PD switching controller.

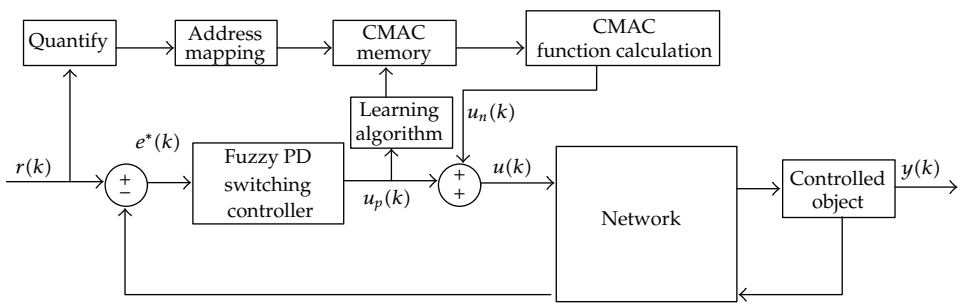

Figure 5: Compound control structure based on CMAC and fuzzy PD.

The fuzzy PD control in a wide range can improve the dynamic response speed, while PD control in a small scale can improve the static control accuracy. So in this paper switching control system between fuzzy PD and PD control is proposed, PD control in the small deviation is applied to obtain higher static control accuracy, and fuzzy PD control in large deviations is applied to obtain faster dynamic response and smaller overshoot. Its structure is shown in Figure 4. The PD control is applied when $|e| \leq e_0$ and the fuzzy PD control is applied when $|e| > e_0$, where e_0 is threshold value.

3.3. Fuzzy PD Composite Controller Based on CMAC Neural Network

In general, CMAC network is a nonlinear mapping, which is very suitable for online applications because it takes a simple δ algorithm as learning algorithm. This algorithm has a fast convergence speed and avoids local minimum value problem. The fuzzy PD switching controller is a nonlinear control, which has faster dynamic response, smaller overshoot, and strong robustness. So the CAMC-fuzzy PD controller is designed, which has the advantages of CMAC neural network and fuzzy PD controller. Also it is applied in the network control system with delay. The structure is shown in Figure 5.

The input of CMAC neural network is command signal $\mathrm{rin}(k)$. Using the study algorithm with tutor, calculate the relative neural network output $u_n(k)$ of CMAC, compare with the total control input $u(k)$ at the end of each control cycle, then correct weights, and go to the process of learning.

At the beginning of the operating system, fuzzy PD controller plays a major role, while the neural network of CMAC does not work. After a while, the output of CMAC neural network gradually plays a key role by continuous learning the actual output and the expected output values to modify weights.

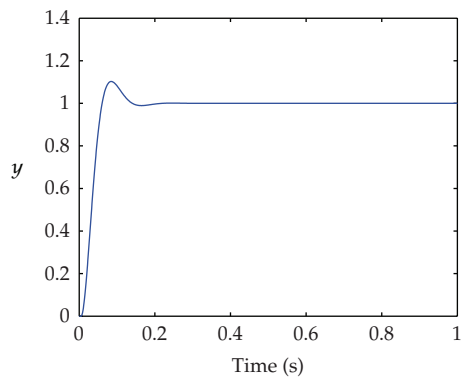

(a) Step response controlled by fuzzy PD

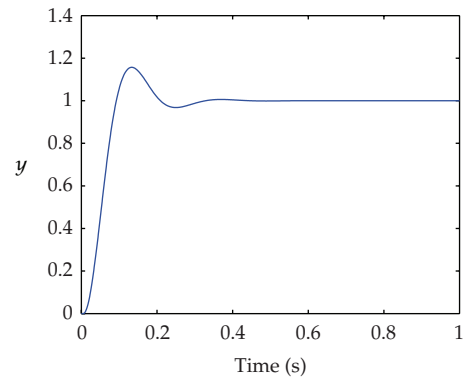

(b) Step response controlled by CMAC-PD

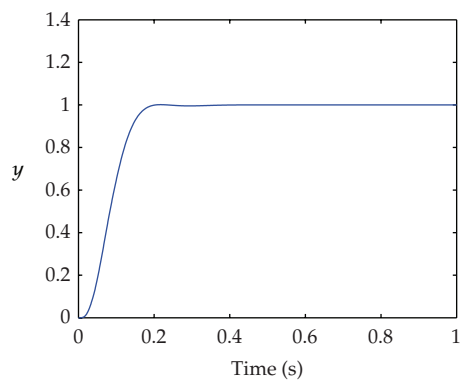

(c) Step response controlled by CMAC-fuzzy PD

Figure 6: Step responses when the mean of time delay is 5 ms.

The control algorithm is

$$u_n(k) = \sum_{i=1}^{c} w_i \mathbf{a}_i, \tag{3.6}$$

where $\mathbf{a}_i$ is binary choice vector, and c is a generalization parameter.

Consider the following:

$$u_p(k) = \begin{cases} k_P * e(k) + k_d * ec(k), & |e| \le e_0, \\ k'_p * e(k) + k'_d * ec(k), & |e| > e_0, \end{cases} \tag{3.7}$$

where k_P and k_d are parameters preset by PD controller, meanwhile k'_p and k'_d are parameters adjusted online by fuzzy PD controller.

The output of system is

$$u(k) = u_n(k) + u_p(k), \tag{3.8}$$

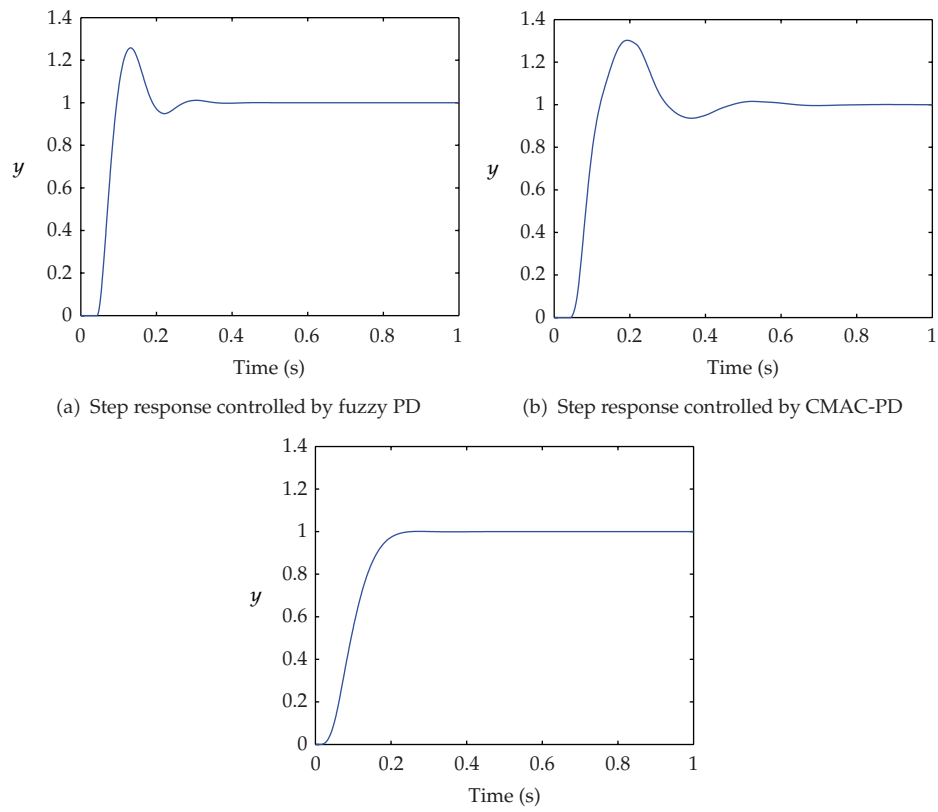

(a) Step response controlled by fuzzy PD

(b) Step response controlled by CMAC-PD

(c) Step response controlled by CMAC-fuzzy PD

Figure 7: Step responses when the mean of time delay is 50 ms.

where $u_n(k)$ is the output of CMAC neural network, and $u_p(k)$ is the output of the fuzzy PD composites switching controller.

The mapping of CMAC neural network is that the input space is S and the range of $[S_{\min}, S_{\max}]$ is divided into $N + 2c$ quantization intervals, that is,

$$\begin{gathered} v_1 \cdots v_c = S_{\min}, \\ v_j = v_{j-1} + \Delta v_j \quad (j = c+1, \ldots, c+N), \\ v_{N+c+1} \cdots v_{N+2c} = S_{\max}. \end{gathered} \tag{3.9}$$

The mapping of CMAC is

$$a_j = \begin{cases} 1, & \text{if } S_j \in [v_j v_{j+c}], j = c+1, \ldots, c+N, \\ 0, & \text{other.} \end{cases} \tag{3.10}$$

Adjusted index in the learning process is

$$E = \frac{1}{2c}(u_n(k) - u(k))^2,$$
$$\Delta w(k) = -\eta \frac{\partial E}{\partial w} = \eta \frac{u(k) - u_n(k)}{c} \cdot a_i = \eta \frac{u_p(k)}{c} a_i, \tag{3.11}$$
$$w(k) = w(k-1) + \Delta w(k) + \beta(w(k-1) - w(k-2)),$$

where η is the rate of network learning, $\eta \in (0,1)$, and β is inertial, $\beta \in (0,1)$.

4. Simulation

In simulation, the input is the unit step, and the transfer function of controlled object is $(0.0008674z + 0.0008503)/(z^2 - 1.94z + 0.9418)$. Parameters $N = 100$, $c = 5$, $\eta = 0.1$, $\beta = 0.04$, and $k_p = 0.02$, $k_d = 0.06$, and switching threshold e is 0.2.

The domain of fuzzy algorithm input e and ec is, respectively, $[-6, 6]$ and $[-30, 30]$. If the actual value of e exceeds the set domain, the value will be limited. The membership function is Gaussian bell-shaped function, which is N, Z, P (negative, zero, positive), respectively; the domain of k'_p and k'_d is, respectively, [0, 0.001] and [0, 0.1], and membership function is also Gaussian bell-shaped function, which is Z, S, M, P (zero, small, medium, large) respectively; Mamdani-type reasoning is adopted and gravity method is defuzzification. Fuzzy lut of k'_p and k'_d is, respectively, shown as Tables 1 and 2.

Due to the network delay varies randomly during continuous-time. In simulation, system network delay is generated by Gaussian random signal source, and step responses means for 5 ms and 50 ms under Gaussian distribution random delay network. Compared with the traditional CMAC-PD composite control and fuzzy PD control, step response charts are shown in Figures 6 and 7, where sampling time is 1 ms.

From Figure 6(a), we can see that the result is not very good because of the time delay. Under traditional fuzzy PD controller, the step responses of the system show great overshot, long rising time, and large steady state error. In Figure 7(a) especially, when the time delay increases, the fuzzy PD control overshoot of the system is also increased. Otherwise, the result is not ideal under traditional CMAC-PD controller from Figures 6–7(b). Compared with the first two kinds of methods, the CMAC-fuzzy PD controller proposed in this paper is more ideal, especially in the long-delay network. Figures 6–7(c) show that the system has the virtue of stability, precision, fastness, and strong robustness.

5. Conclusions

Network control system is the time varying because of the random-induced delay, which results in worse control effects. But the intelligent control has better adaptation and can be used to improve the control performance. This paper regards transmission network and the controlled objects as a time-varying system, combines CMAC neural network algorithm with PD controller to achieve forward feedback control, and adopts the intelligent control strategy. The PD controller introduces fuzzy PD complex switching model. According to the size of the error signal, switching-controller switches between directly PD controller and fuzzy PD

Table 1: Fuzzy lut of $k_p^{'}$.

e/ec	N	Z	P
N	S	M	Z
Z	P	P	P
P	P	P	P

Table 2: Fuzzy lut of $k_d^{'}$.

e/ec	N	Z	P
N	Z	M	M
Z	P	Z	P
P	M	Z	S

controller, in order to improve the speed of dynamic response of the system and accuracy of steady-state control. Simulation results show that the system has the virtue of stability, precision, fastness, and strong robustness. So that this method can achieve a better effect and can also improve the system's performance effectively.

Acknowledgments

This work is supported by the Chinese National Science Foundation (no. 61203004), the Natural Science Foundation of Heilongjiang province (no. 42400621-1-12201), and the Fundamental Research Funds for the Central Universities (no. HEUCFT1203).

References

[1] B. Tang, G. P. Liu, and W. H. Gui, "Improvement of state feedback controller design for networked control systems," *IEEE Transactions on Circuits and Systems II*, vol. 55, no. 5, pp. 464–468, 2008.

[2] N. Vatanski, J. P. Georges, C. Aubrun, E. Rondeau, and S. L. Jämsä-Jounela, "Networked control with delay measurement and estimation," *Control Engineering Practice*, vol. 17, no. 2, pp. 231–244, 2009.

[3] I. Hideaki, "Control with limited communication and message losses," *Systems and Control Letters*, vol. 57, pp. 322–331, 2008.

[4] X. Su, P. Shi, L. Wu et al., "Induced L_2 filtering of fuzzy stochastic systems withtime-varying delays,: cybernetics," *IEEE Transactions on Systems, Man and Cybernetics B*. In press.

[5] R. S. Gau, C. H. Lien, and J. G. Hsieh, "Novel stability conditions for interval delayed neural networks with multiple time-varying delays," *International Journal of Innovative Computing, Information and Control*, vol. 7, no. 1, pp. 433–444, 2011.

[6] M. B. G. Cloosterman, N. van de Wouw, W. P. M. H. Heemels, and H. Nijmeijer, "Stability of networked control systems with uncertain time-varying delays," *IEEE Transactions on Automatic Control*, vol. 54, no. 7, pp. 1575–1580, 2009.

[7] Y. Shi and B. Yu, "Output feedback stabilization of networked control systems with random delays modeled by Markov chains," *IEEE Transactions on Automatic Control*, vol. 54, no. 7, pp. 1668–1674, 2009.

[8] X. Su, P. Shi, L. Wu et al., "A novel control design on discrete-time takagi-sugeno fuzzysystems with time-varying delays," *IEEE Transactions on Fuzzy Systems*. In press.

[9] X. Su, P. Shi, L. Wu et al., "A novel approach to filter design for T-S fuzzy discrete-time systems with time-varying delay," *IEEE Transactions on Fuzzy Systems*, vol. 20, no. 6, pp. 1114–1129, 2012.

[10] Y. Halevi and A. Ray, "Integrated communication and control systems. Part 1—analysis," *Journal of Dynamic Systems, Measurement and Control, Transactions of the ASME*, vol. 110, no. 4, pp. 367–373, 1988.

[11] R. Luck and A. Ray, "An observer-based compensator for distributed delays," *Automatica*, vol. 26, no. 5, pp. 903–908, 1990.

[12] H. Chan, "Closed-loop control of systems over a communications network with queues," *International Journal of Control*, vol. 62, no. 3, pp. 493–510, 1995.
[13] W. Zhang, M. S. Branicky, and S. M. Phillips, "Stability of networked control systems," *IEEE Control Systems Magazine*, vol. 21, no. 1, pp. 84–97, 2001.
[14] L. Wu, X. Su, P. Shi, and J. Qiu, "Model approximation for discrete-time state-delay systems in the TS fuzzy framework," *IEEE Transactions on Fuzzy Systems*, vol. 19, no. 2, pp. 366–378, 2011.
[15] L. Wu and W. X. Zheng, "L_2-L^∞ control of nonlinear fuzzy itô stochastic delay systems via dynamic output feedback," *IEEE Transactions on Systems, Man, and Cybernetics B*, vol. 39, no. 5, pp. 1308–1315, 2009.
[16] D. Yue, Q. L. Han, and C. Peng, "State feedback controller design of networked control systems," *IEEE Transactions on Circuits and Systems II*, vol. 51, no. 11, pp. 640–644, 2004.
[17] C. Peng, Y. C. Tian, and M. O. Tadé, "State feedback controller design of networked control systems with interval time-varying delay and nonlinearity," *International Journal of Robust and Nonlinear Control*, vol. 18, no. 12, pp. 1285–1301, 2008.
[18] L. Wu, X. Su, P. Shi, and J. Qiu, "A new approach to stability analysis and stabilization of discrete-time T-S fuzzy time-varying delay systems," *IEEE Transactions on Systems, Man, and Cybernetics B*, vol. 41, no. 1, pp. 273–286, 2011.
[19] L. Wu, Z. Feng, and W. X. Zheng, "Exponential stability analysis for delayed neural networks with switching parameters: average dwell time approach," *IEEE Transactions on Neural Networks*, vol. 21, no. 9, pp. 1396–1407, 2010.
[20] G. C. Walsh, O. Beldiman, and L. G. Bushnell, "Asymptotic behavior of nonlinear networked control systems," *IEEE Transactions on Automatic Control*, vol. 46, no. 7, pp. 1093–1097, 2001.
[21] R. N. Yang, P. Shi, and G. P. Liu, "Filtering for discrete-time networked nonlinear systems with mixed random delays and packet dropouts," *IEEE Transactions on Automatic Control*, vol. 56, no. 11, pp. 2655–2660, 2011.
[22] R. N. Yang, P. Shi, and G. P. Liu, "Network-based feedback control for systems with mixed delays based on quantization and dropout compensation," *Automatic*, vol. 47, no. 12, pp. 2805–2809, 2011.
[23] D. Xie, D. Zhang, and Z. Wang, "Robust H^∞ faulttolerant control for uncertain networked control system with two additive random delays," *International Journal of Innovative Computing, Information and Control*, vol. 7, no. 1, pp. 315–326, 2011.
[24] L. Fu and G. Z. Dai, "A survey of networked control systems," *Computer Engineering and Applications*, vol. 41, no. 25, pp. 221–225, 2005.
[25] L. Wu and D. W. C. Ho, "Fuzzy filter design for Itô stochastic systems with application to sensor fault detection," *IEEE Transactions on Fuzzy Systems*, vol. 17, no. 1, pp. 233–242, 2009.
[26] F. Q. Liu and X. P. Xue, "Constructing kernels by fuzzy rules for support vector regressions," *International Journal of Innovative Computing, Information and Control*, vol. 8, no. 7, pp. 4811–4822, 2012.
[27] K. Z. Ghafoor, K. A. Bakar, S. Salleh et al., "Fuzzy logic-assisted geographical routing over Vehicular AD HOC Networks," *International Journal of Innovative Computing, Information and Control*, vol. 8, no. 7, pp. 5095–5120, 2012.
[28] J. Botzheim and F. Példesi, "Parametric approximation of fuzzy exponent for computationally intensive problems," *International Journal of Innovative Computing, Information and Control*, vol. 8, no. 8, pp. 5725–5744, 2012.
[29] S. Lee, S. H. Lee, K. C. Lee, M. H. Lee, and F. Harashima, "Intelligent performance management of networks for advanced manufacturing systems," *IEEE Transactions on Industrial Electronics*, vol. 48, no. 4, pp. 731–741, 2001.
[30] S. E. Shafiei and M. R. Soltanpour, "Neural network sliding-mode-PID controller design for electrically driven robot manipulators," *International Journal of Innovative Computing, Information and Control*, vol. 7, no. 2, pp. 511–524, 2011.
[31] T. Chaiyatham and I. Ngamroo, "A bee colony optimization based-fuzzy logic-pid control design of electrolyzer for microgrid stabilization," *International Journal of Innovative Computing, Information and Control*, vol. 8, no. 9, pp. 6049–6066, 2012.
[32] X. Su, L. Wu, P. Shi et al., "H^∞ model reduction of takagi-sugeno fuzzy stochastic systems," *IEEE Transactions on Systems, Man, and Cybernetics B*, vol. 42, no. 6, pp. 1574–1585, 2012.
[33] H. M. Feng and H. C. Chou, "Evolutionary fuzzy stock prediction system design and its application to the Taiwan stock index," *International Journal of Innovative Computing, Information and Control*, vol. 8, no. 9, pp. 6173–6190, 2012.
[34] C. Y. Leng and J. P. Yu, "The application of CMAC neural network to DTC control system," *Machine Building and Automation*, no. 12, pp. 78–83, 2004.

Hindawi Publishing Corporation
Mathematical Problems in Engineering
Volume 2012, Article ID 854942, 8 pages
doi:10.1155/2012/854942

Research Article

On Interval-Valued Supra-Fuzzy Syntopogenous Structure

F. M. Sleim and Heba I. Mustafa

Mathematics Department, Faculty of Science, Zagazig University, Zagazig 44519, Egypt

Correspondence should be addressed to Heba I. Mustafa, dr_heba_ibrahim@yahoo.com

Received 12 August 2012; Accepted 1 November 2012

Academic Editor: Hamid Reza Karimi

Copyright © 2012 F. M. Sleim and H. I. Mustafa. This is an open access article distributed under the Creative Commons Attribution License, which permits unrestricted use, distribution, and reproduction in any medium, provided the original work is properly cited.

A new definition of interval-valued supra-fuzzy syntopogenous (resp., supra-fuzzy proximity) space is given. We show that for any interval-valued fuzzy syntopogenous structure S, there is another interval-valued fuzzy syntopogenous structure S^c called the conjugate of S. This leads to introducing the concept of interval-valued bifuzzy syntopogenous space. Finally, we show every interval-valued bifuzzy syntopogenous space induces an interval-valued fuzzy supra-syntopogenous space. Throughout this paper, the family of all fuzzy sets on nonempty set X will be denoted by I^X and the family of all interval-valued fuzzy sets on a nonempty set X will be denoted by π^X.

1. Introduction

In [1], Csaszar introduced the concept of a syntopogenous structure to develop a unified approach to the three main structures of set-theoretic-topology: topologies, uniformities, and proximities. This enables him to evolve a theory including the foundations of the three classical theories of topological spaces, uniform spaces, and proximity spaces. In the case of the fuzzy structures, there are at least three notions of fuzzy syntopogenous structures. The first notion worked out in [2–4] presents a unified approach to the theories of Chang fuzzy topological spaces [5], Hutton fuzzy uniform spaces [6], and Liu fuzzy proximity spaces [7]. The second notion worked out in [8] agrees very well with Lowen fuzzy topological spaces [9], Lowen-Hohle fuzzy uniform spaces [10], and Artico-Moresco fuzzy proximity spaces [11]. The third notion worked out in [12] agrees with the framework of a fuzzifying topology [13]. In [14], Kandil et al. introduced the concepts of a supra-fuzzy topological space and supra-fuzzy proximity space. In [15], Ghanim et al. introduced the concepts of supra-fuzzy syntopogenous space as a generalization of the concepts of supra-fuzzy proximity and supra-fuzzy topology.

Interval-valued fuzzy sets were introduced independently by Zadeh [16], Grattan-Guiness [17], Jahn [18], and Sambuc [19], in the seventies, in the same year. An interval-valued fuzzy set (IVF) is defined by an interval-valued membership function. As a generalization of fuzzy, the concept of intuitionistic fuzzy sets was introduced by Atanassov [20]. In [21], it is shown that the concepts of interval-valued fuzzy sets and intuitionistic fuzzy sets are equivalent and they are extensions of fuzzy sets.

Interval-valued fuzzy sets can be viewed as a generalization of fuzzy sets (Zadeh [22]) that may better model imperfect information which is omnipresent in any conscious decision making [23]. It can be considered as a tool for a more human consistent reasoning under imperfectly defined facts and imprecise knowledge, with an application in supporting medical diagnosis [24, 25]. In [26] new notions of interval-valued supra-fuzzy topology (resp., supra-fuzzy proximity) were introduced by using the notions of interval-valued fuzzy sets.

In this paper, we generalize the concept of supra-fuzzy syntopogenous space by using the notion of interval-valued set. Topology and its generalization proximity and syntopogenous are branches of mathematics which have many real life applications. We believe that the generalized topological structure suggested in this paper will be important base for modification of medical diagnosis, decision making, and knowledge discovery. The other parts of this paper are arranged as follows. In Section 2, We recall and develop some notions and notations concerning supra-fuzzy topological space, interval-valued fuzzy set, interval-valued fuzzy topology, interval-valued supra-fuzzy topology, and interval-valued supra-fuzzy proximity. In Section 3, we introduce the concept of interval-valued supra-fuzzy syntopogenous (resp., supra-fuzzy proximity) space. We show that there is one-to-one correspondence between family of all interval-valued supra-fuzzy topological spaces and the family of all perfect interval-valued supra-fuzzy topogenous spaces. Also, we prove that there is one-to-one correspondence between the family of all interval-valued supra-fuzzy proximity spaces and the family of all symmetrical interval-valued supra-fuzzy topogenous spaces. We show that for any interval-valued fuzzy topogenous order R on π^X there is another interval-valued fuzzy topogenous structure R^c in Section 3. In Section 4, we introduce the concept of interval-valued bifuzzy syntopogenous structure by using two interval-valued fuzzy syntopogenous spaces. In the last section we show that with every interval-valued bifuzzy syntopogenous space there is an interval-valued supra-fuzzy syntopogenous associated with this space.

2. Preliminaries

The concept of a supra-fuzzy topological space has been introduced as follows.

Definition 2.1 (see [27]). A collection $\tau^* \subset I^X$ is a supra-fuzzy topology on X if $0, 1 \in \tau^*$ and τ^* is closed under arbitrary supremum. The pair (X, τ^*) is a supra-fuzzy topological space.

Definition 2.2 (see [20]). An interval-valued fuzzy set (IVF set for short) is a set $\underline{A} = (A_1, A_2) \in I^X \times I^X$ such that $A_1 \leq A_2$. The family of all interval-valued fuzzy sets on a given nonempty set X will be denoted by π^X.

The IVF set $\underline{1} = (1, 1)$ is called the universal IVF set and the IVF set $\underline{0} = (0, 0)$ is called the empty IVF set.

Proposition 2.3 (see [20]). *The operations on π^X are given by the following: Let $\underline{A}, \underline{B} \in \pi^X$:*

(1) $\underline{A} = \underline{B} \Leftrightarrow A_1 = B_1, A_2 = B_2$,

(2) $\underline{A} \leq \underline{B} \Leftrightarrow A_1 \leq B_1,\ A_2 \leq B_2$,

(3) $\underline{A} \vee \underline{B} = (A_1 \vee B_1, A_2 \vee B_2)$,

(4) $\underline{A} \wedge \underline{B} = (A_1 \wedge B_1, A_2 \wedge B_2)$,

(5) $\underline{A}^c = (A_2^c, A_1^c)$.

Definition 2.4 (see [26]). The family $\eta \subseteq \pi^X$ is called an interval-valued fuzzy topology (IVF tpology for short) on X if and only if η contains $\underline{1}$, $\underline{0}$, and it is closed under finite intersection and arbitrary union. The pair (X, η) is called an interval-valued fuzzy topological space (IVF top. space for short). Any IVF set $\underline{A} \in \eta$ is called an open IVF set and the complement of $\underline{A}$ denoted by $\underline{A}^c$ is called a closed IVF set. The family of all closed interval-valued fuzzy sets is denoted by η^c.

Definition 2.5 (see [26]). A non empty family $\eta^* \subseteq \pi^X$ is called an interval-valued supra-fuzzy topology (IVSF top. for short) on X if it contains $\underline{0}$, $\underline{1}$ and it is closed under arbitrary unions.

Definition 2.6 (see [26]). A binary relation $\delta \subseteq \pi^X \times \pi^X$ is called an interval-valued supra-fuzzy (IVSF) proximity on X if it satisfies the following conditions:

(1) $\underline{A}\delta\underline{B} \Rightarrow \underline{B}\delta\underline{A}$,

(2) $\underline{A}\delta\underline{B}$ or $\underline{A}\delta\underline{C} \Rightarrow \underline{A}\delta(\underline{B} \vee \underline{C})$,

(3) $\underline{0} \not\delta \underline{1}$,

(4) $\underline{A} \not\delta \underline{B} \Rightarrow \underline{A} \leq 1 - \underline{B}$,

(5) $\underline{A} \not\delta \underline{B} \Rightarrow \exists\, C \in \pi^X$ s.t. $\underline{A} \not\delta \underline{C}$ and $(1 - \underline{C}) \not\delta \underline{B}$.

3. Interval-Valued Fuzzy Topogenous Order

In this article, we define a new concept of topogenous structure by using the concept of interval-valued fuzzy sets.

Definition 3.1. Let R be a binary relation on π^X. Consider the following axioms:

(1) $\underline{0}R\underline{0}$,

(2) $\underline{A}R\underline{B} \Rightarrow \underline{A} \subseteq \underline{B}$,

(3) $\underline{A}_1 \leq \underline{A}R\underline{B} \leq \underline{B}_1 \Rightarrow \underline{A}_1 R \underline{B}_1$,

(4) $\underline{A}_1 R \underline{B}_1$ and $\underline{A}_2 R \underline{B}_2 \Rightarrow (\underline{A}_1 \vee \underline{A}_2) R (\underline{B}_1 \vee \underline{B}_2)$ and $(\underline{A}_1 \wedge \underline{A}_2) R (\underline{B}_1 \wedge \underline{B}_2)$,

(5) $\underline{A}_i R \underline{B}_i$ for all $i \Rightarrow (\vee \underline{A}_i) R (\vee \underline{B}_i)$,

(6) $\underline{A}_i R \underline{B}_i$ for all $i \Rightarrow (\wedge \underline{A}_i) R (\wedge \underline{B}_i)$,

(7) $\underline{A}R\underline{B} \Leftrightarrow (1 - \underline{B}) R (1 - \underline{A})$.

If R satisfies (1)–(4) then it is called an interval-valued fuzzy topogenous order (IVF topogenous order for short) on X.

If R satisfies (1)–(3) then it is called an interval-valued supra-fuzzy topogenous order (IVSF topogenous order for short) on X.

The interval-valued fuzzy topogenous order is called perfect (resp., biperfect, symmetrical) if it satisfies the condition (5) (resp., (6), (7)).

Definition 3.2. Let $X \neq \phi$ and S be a nonempty family of IVF topogenous orders on X satisfy the following conditions:

(s_1) $R_1, R_2 \in S \Rightarrow \exists R \in S$ s.t. $R_1 \leq R$ and $R_2 \leq R$,

(s_2) $R \in S \Rightarrow \exists L \in S$ s.t. $R \leq L \circ L$.

Then S is said to be interval-valued fuzzy (IVF) syntopogenous structure on X. The pair (X, S) is called an interval-valued fuzzy syntopogenous (IVF syntopogenous for short) space. If S satisfy the single element, then S is called an IVF topogenous structure on X and the pair (X, S) is called an IVF topogenous space.

Definition 3.3. Let $X \neq \phi$ and S^* be a nonempty family of IVSF topogenous orders on X satisfy the conditions (s_1) and (s_2). Then S^* is called an IVSF syntopogenous space. If S^* consists of single element, then it is called an IVSF topogenous structure. If each element of S^* is perfect (resp., biperfect symmetrical), then it is called a perfect (resp., biperfect symmetrical) IVSF structure on X.

The following proposition investigates the relation between the family of all IVSF topological spaces and the family of all perfect IVSF topogenous spaces.

Proposition 3.4. *There is one-to-one correspondence between the family of all IVSF topological spaces and the family of all perfect IVSF topogenous spaces.*

Proof. Let (X, τ^*) be an IVSF topological space. Define a relation R_{τ^*} by $\underline{A} R_{\tau^*} \underline{B} \Leftrightarrow \exists C \in \tau^*$ s.t. $\underline{A} \leq \underline{C} \leq \underline{B}$. Then R_{τ^*} is a perfect IVSF topogenous order on X. In fact, since $\underline{0}, \underline{1} \in \tau^*$, $\underline{0} \leq \underline{0} \leq \underline{0}$, and $\underline{1} \leq \underline{1} \leq \underline{1}$, then $\underline{0} R_{\tau^*} \underline{0}$ and $\underline{1} R_{\tau^*} \underline{1}$. Let $\underline{A} R_{\tau^*} \underline{B} \Rightarrow \exists C \in \tau^*$ s.t. $\underline{A} \leq \underline{C} \leq \underline{B} \Rightarrow \underline{A} \leq \underline{B}$. Assume that $A_1 \leq \underline{A} R_{\tau^*} \underline{B} \leq B_1 \Rightarrow \exists E \in \tau^*$ s.t. $\underline{A_1} \leq \underline{A} \leq \underline{E} \leq \underline{B} \leq \underline{B_1} \Rightarrow \underline{A_1} R_{\tau^*} \underline{B_1}$. Thus, R_{τ^*} is an IVSF topogenous order on X. We show that R_{τ^*} is perfect. Let $\underline{A_i} R_{\tau^*} \underline{B_i} \Rightarrow \exists \underline{C_i} \in \tau^*$ s.t. $\underline{A_i} \leq \underline{C_i} \leq \underline{B_i}$. Hence $\vee \underline{C_i} \in \tau^*$ and $\vee \underline{A_i} \leq \vee \underline{C_i} \leq \vee \underline{B_i}$. Thus, $(\vee \underline{A_i}) R_{\tau^*} (\vee \underline{B_i})$ and consequently R_{τ^*} is perfect. Thus R_{τ^*} is an IVSF topogenous order. Consequently, $S_{\tau^*} = \{R_{\tau^*}\}$ is a perfect IVSF topogenous structure.

Conversely, let (X, S^*) be a perfect IVSF topogenous space. Then $S^* = \{R^*\}$, where R^* is a perfect IVSF order. Define $\tau_{R^*} \subseteq \pi^X$ by $\underline{A} \in \tau_{R^*} \Leftrightarrow \underline{A} R^* \underline{A}$. We show that τ_{R^*} is an IVSF topology on X. Since $\underline{0} R^* \underline{0}$ and $\underline{1} R^* \underline{1}$, then $\underline{0}, \underline{1} \in \tau_{R^*}$. Also, $\underline{A_i} \in \tau_{R^*}$ for all $i \Rightarrow \underline{A_i} R^* \underline{A_i}$ for all $i \Rightarrow \vee \underline{A_i} R^* \vee \underline{A_i}$, because R^* is perfect. Hence $\vee \underline{A_i} \in \tau_{R^*}$ and, consequently, τ_{R^*} is an IVSF topology on X. □

Remark 3.5. One can easily show that $R_{\tau_{R^*}} = R^*$ and $\tau_{R_{\tau^*}} = \tau^*$.

Example 3.6. This example is a small form of interval-valued information table of a file containing some patients $X = \{Li, Wang, Zhang, Sun\}$. We consider the set of symptoms $S = \{$*Chest-pain*, *Cough*, *Stomach-pain*, *Headache*, *Temperature*$\}$. Each symptom is described by an interval fuzzy sets on X. The symptoms are given in Table 1. Define a binary relation R on π^X by $A, B \in \pi^X ARB$ if and only if $x \leq y$ implies $A(x) \leq B(y)$ for all $x \in X$. Therefore, R is biperfect IVSF topogenous order on X. The set of patients are ordered by $Li \leq Wang \leq Zhang \leq Sun$. So, we have chest-pain R Cough.

The following proposition shows the relation between the family of all IVSF proximity spaces and the family of all symmetrical IVSF topogenous spaces.

Table 1

	Chest-pain	Cough	Stomach-pain	Headache	Temperature
Li	[0.1, 0.2]	[0.1, 0.3]	[0, 0.2]	[0.3, 0.9]	[0.1, 0.9]
Wang	[0.1, 0.2]	[0.2, 0.3]	[0.3, 0.9]	[0.3, 0.6]	[0.2, 0.2]
Zhang	[0.5, 0.5]	[0.2, 0.3]	[0.4, 0.4]	[0.1, 0.9]	[0.1, 0.9]
Sun	[0.3, 0.6]	[0.7, 0.8]	[0.3, 0.6]	[0.1, 0.6]	[0.3, 0.4]

Proposition 3.7. *There is one-to-one correspondence between the family of all IVSF proximity spaces and the family of all symmetrical IVSF topogenous spaces.*

Proof. Let δ^* be an IVSF proximity. Define $\underline{A}R_{\delta^*}\underline{B} \Leftrightarrow \underline{A}\not\delta^*(1-\underline{B})$. Then R_{δ^*} is a symmetrical IVSF topogenous order. In fact, since $\underline{0}\not\delta\underline{1}$ and $\underline{1}\not\delta\underline{0}$, then $\underline{0}R_{\delta^*}\underline{0}$ and $\underline{1}R_{\delta^*}\underline{1}$. Also $\underline{A}R_{\delta^*}\underline{B} \Rightarrow \underline{A}\not\delta^*1-\underline{B} \Rightarrow \underline{A} \leq \underline{B}$. Finally, $\underline{A}_1 \leq \underline{A}R_{\delta^*}\underline{B} \leq \underline{B}_1 \Rightarrow \underline{A}_1 \leq \underline{A}$, $\underline{A}\not\delta^*1-\underline{B}$ and $1-\underline{B} \geq 1-\underline{B}_1$. Thus $\underline{A}_1\not\delta^*1-\underline{B}_1$ and therefore $\underline{A}_1R_{\delta^*}\underline{B}_1$. Consequently (X, S^*), where $S^* = \{R_{\delta^*}\}$ is IVSF topogenous space.

Conversely, let (X, S^*) a symmetrical IVSF topogenous space. Then $S^* = \{R^*\}$, where R^* is a symmetrical IVSF topogenous order on X. Define δ_{R^*} by $\underline{A}\delta_{R^*}\underline{B} \Leftrightarrow \underline{A}\not{R}^*1-\underline{B}$. We show that δ_{R^*} is an IVSF topogenous order on X. Assume that $\underline{A}\delta_{R^*}\underline{B}$, then $\underline{A}\not{R}^*(1-\underline{B})$. Therefore $\underline{B}\not{R}^*(1-\underline{A})$ because R^* is symmetric. Hence $\underline{B}\delta_{R^*}\underline{A}$. Since $0R^*0$ and $1R^*1$, then $0\not\delta_{R^*}0$. Assume that $\underline{A}\delta_{R^*}\underline{B}$ or $\underline{A}\delta_{R^*}\underline{C}$. Then $\underline{A}\not{R}^*(1-\underline{B})$ or $\underline{A}\not{R}^*(1-\underline{C})$. Suppose that $\underline{A}\delta\not{R}^*\underline{B}\vee\underline{C}$, then $\underline{A}\not{R}^*(1-(\underline{B}\vee\underline{C}))$. Thus $\underline{A}\not{R}^*(1-\underline{B})\wedge(1-\underline{C})$. Consequently $\underline{A}\not{R}^*(1-\underline{B})$ and $\underline{A}\not{R}^*(1-\underline{C})$. So, $\underline{A}\not\delta_{R^*}\underline{B}$ and $\underline{A}\not\delta_{R^*}\underline{C}$ a contradiction. Now $\underline{A}\not\delta_{R^*}\underline{B}$ implies $\underline{A}\not{R}^*(1-\underline{B})$ and hence $\underline{A} \leq (1-\underline{B})$. □

4. Interval-Valued Bifuzzy Syntopogenous Space

Proposition 4.1. *Let R be an IVF topogenous order on X. Then the relation R^c on π^X defined by $\underline{A}R^c\underline{B} \Leftrightarrow (1-\underline{B})R(1-\underline{A})$ is an IVF topogenous order on X.*

Proof. Since $\underline{0}R\underline{0}$ and $\underline{1}R\underline{1}$, then $\underline{1}R^c\underline{1}$ and $\underline{0}R^c\underline{0}$. Also, $\underline{A}R^c\underline{B} \Rightarrow (1-\underline{B})R(1-\underline{A}) \Rightarrow 1-\underline{B} \leq 1-\underline{A} \Rightarrow \underline{A} \leq \underline{B}$. Furthermore, $A_1 \leq \underline{A}R^c\underline{B} \leq \underline{B}_1 \Rightarrow (1-\underline{B})R(1-\underline{A})$, $1-\underline{B}_1 \leq 1-\underline{B}$, $1-\underline{A} \leq 1-\underline{A}_1 \Rightarrow (1-\underline{B}_1)R(1-\underline{A}_1) \Rightarrow \underline{A}_1R^c\underline{B}_1$. Finally, $\underline{A}_1R^c\underline{B}_1$ and $\underline{A}_2R^cB_2 \Rightarrow (1-\underline{B}_1)R(1-\underline{A}_1)$ and $(1-\underline{B}_2)R(1-\underline{A}_2)$. Since R is a topogenous order, then $(1-\underline{B}_1)\wedge(1-\underline{B}_2)R(1-\underline{A}_1)\wedge(1-\underline{A}_2)$ and hence $(1-(\underline{B}_1\vee\underline{B}_2))R(1-(\underline{A}_1\vee\underline{A}_2))$. Consequently, $(\underline{A}_1\vee\underline{A}_2)R^c(\underline{B}_1\vee\underline{B}_2)$. Similarly, we can show that $(\underline{A}_1\wedge\underline{A}_2)R^c(\underline{B}_1\wedge\underline{B}_2)$. Thus R^c is an IVF topogenous order on X. □

Remark 4.2. (1) The relation R^c defined in the previous proposition is called the conjugate of R.

(2) If R is perfect or biperfect, then R^c is also.

Proposition 4.3. *Let R_1 and R_2 be two IVF topogenous orders on X. If $R_1 \subseteq R_2$, then ${R_1}^c \subseteq {R_2}^c$ and $(R_1\circ R_2)^c = {R_2}^c\circ{R_1}^c$.*

Proof. Assume that, $R_1 \subseteq R_2$. Then $\underline{A}{R_1}^c\underline{B} \Rightarrow (1-\underline{B})R_1(1-\underline{A}) \Rightarrow (1-\underline{B})R_2(1-\underline{A}) \Rightarrow \underline{A}{R_2}^c\underline{B}$. Hence, ${R_1}^c \subseteq {R_2}^c$. Also, $\underline{A}(R_1\circ R_2)^cB \Rightarrow (1-\underline{B})(R_1\circ R_2)(1-\underline{A}) \Rightarrow \exists\underline{C}\in\pi^X$ s.t. $(1-\underline{B})R_1\underline{C}\wedge\underline{C}R_2(1-\underline{A}) \Rightarrow \exists\underline{C}\in\pi^X$ s.t. $(1-\underline{C}){R_1}^c\underline{B}\wedge\underline{A}{R_2}^c(1-\underline{C}) \Rightarrow \exists 1-\underline{C}\in\pi^X$ s.t. $\underline{A}{R_2}^c1-\underline{C}\wedge(1-\underline{C}){R_1}^c\underline{B} \Rightarrow \underline{A}({R_2}^c\circ{R_1}^c)\underline{B} \Rightarrow (R_1\circ R_2)^c \leq {R_2}^c\circ{R_1}^c$. Similarly, we can show that ${R_2}^c\circ{R_1}^c \leq (R_1\circ R_2)^c$. Consequently, $(R_1\circ R_2)^c = {R_2}^c\circ{R_1}^c$. □

Proposition 4.4. *Let S be an IVF syntopogenous structure on X. Then the family $S^c = \{R^c : R \in S\}$ is also an IVF syntopogenous structure.*

Proof. Since $S \neq \phi$, then $S^c \neq \phi$. Let ${R_1}^c, {R_2}^c \in S^c$, then $R_1, R_2 \in S$. Hence $\exists R \in S$ s.t. $R_1 \leq R$ and $R_2 \leq R$. Therefore $\exists R^c \in S^c$ s.t. ${R_1}^c \leq R^c$ and ${R_2}^c \leq R^c$. Also, $R^c \in S^c \Rightarrow R \in S \Rightarrow \exists R_1 \in S$ s.t. $R \leq (R_1 \circ R_1) \Rightarrow R^c \leq (R_1 \circ R_1)^c = {R_1}^c \circ {R_1}^c$. Thus $\exists R_1^c \in S^c$ s.t. $R^c \leq {R_1}^c \circ {R_1}^c$. Consequently, S^c is also IVF syntopogenous structure on X.

Hence, we have the result that on a nonempty set X we have two interval-valued fuzzy syntopogenous structures. □

Definition 4.5. Let X a nonempty set. Let S_1, S_2 be two IVF syntopogenous structures on X. The triple (X, S_1, S_2) is called an interval-valued bifuzzy syntopogenous space. If each S_1, S_2 is perfect (resp., biperfect symmetrical), then the space (X, S_1, S_2) is perfect (resp. biperfect symmetrical).

The following proposition shows that two IVF topogenous orders on X can induce an IVSF topogenous order on X.

Proposition 4.6. *Let R_1, R_2 be two interval-valued fuzzy topogenous orders on X. Then the order $R = R_1 \vee R_2$ defined by*

$$ARB \Longleftrightarrow AR_1B \quad or \quad AR_2B \tag{4.1}$$

is IVSF topogenous order on π^X.

Proof. Since, $\underline{0}R_i\underline{0}$ and $\underline{1}R_i\underline{1}$ for all $i = 1, 2$, then $\underline{0}R\underline{0}$ and $\underline{1}R\underline{1}$. Also, $\underline{A}_1 \leq \underline{A}R\underline{B} \leq \underline{B}_1 \Rightarrow \underline{A}_1 \leq \underline{A}R_i\underline{B} \leq \underline{B}_1$ for some $i = 1, 2 \Rightarrow \underline{A}_1 R_i \underline{B}_1$ for some $i = 1, 2 \Rightarrow \underline{A}_1 R \underline{B}_1$. Finally, $\underline{A}R\underline{B} \Rightarrow \underline{A}R_i\underline{B}$ for some $i = 1, 2 \Rightarrow \underline{A} \leq \underline{B}$. Thus, R is an IVSF topogenous order on π^X. □

5. Interval-Valued Supra-Fuzzy Syntopogenous Space Associated with Interval-Valued Bifuzzy Syntopogenous Spaces

Proposition 5.1. *Let (X, S_1, S_2) be interval-valued bifuzzy syntopogenous space. Then the family $S_{12}^* = \{R = R_1 \vee R_2 : R_1 \in S_1, R_2 \in S_2\}$ is an IVSF syntopogenous structure on X.*

Proof. (s_1) Let $R, L \in S_{12}^* \Rightarrow R = R_1 \vee R_2$ and $L = L_1 \vee L_2 R_i$ and $L_i \in S_i$ for some $i = 1, 2 \Rightarrow \exists K_1 \in S_1$ s.t. $R_1 \vee L_1 = K_1$ and $\exists K_2 \in S_1$ s.t. $R_2 \vee L_2 = K_2$. So, $\exists K = K_1 \vee K_2 \in S_{12}^*$ s.t. $R \vee L \leq K_1 \vee K_2 = K$.

(s_2) $R \in S_{12}^* \Rightarrow \exists R_1 \in S_1$, $R_2 \in S_2$ s.t. $R = R_1 \vee R_2 \Rightarrow \exists L_1 \in S_1$ s.t. $R_1 \leq L_1 \circ L_1$ and $\exists L_2 \in S_2$ s.t. $R_2 \leq L_2 \circ L_2$. Since $L_1, L_2 \leq L_1 \vee L_2$, then $L_1 \circ L_1 \leq L_1 \vee L_2 \circ L_1 \vee L_2$ and $L_2 \circ L_2 \leq L_1 \vee L_2 \circ L_1 \vee L_2$. Therefore $R_1 \leq L_1 \circ L_1 \leq L_1 \vee L_2 \circ L_1 \vee L_2$ and $R_2 \leq L_2 \circ L_2 \leq L_1 \vee L_2 \circ L_1 \vee L_2$. So $R_1 \vee R_2 \leq (L_1 \vee L_2) \circ (L_1 \vee L_2)$ and consequently S_{12}^* is an IVSF syntopogenous structure on X. □

Remark 5.2. The structure S_{12}^* is called the interval-valued supra-fuzzy syntopogenous associated with the space (X, S_1, S_2).

Proposition 5.3. *Let $(X, T_i) i = 1, 2$ be an IVF topological spaces. Then the family $T_{12}^* = \{\underline{A} = \underline{A}_1 \vee \underline{A}_2 : \underline{A}_i \in T_i \quad i = 1, 2\}$ is an IVSF topology on X.*

Proof. Since $\underline{0}, \underline{1} \in T_i$ for all $i = 1, 2$, then $\underline{0}, \underline{1} \in T_{12}^*$ Also, $\underline{A}_i \in T_{12}^* \Rightarrow \underline{A}_i = \underline{B}_1^i \vee \underline{B}_2^i$, $\underline{B}_1^i \in T_1, \underline{B}_2^i \in T_2 \Rightarrow \vee_i \underline{A}_i = \vee_i(\underline{B}_1^i \vee \underline{B}_2^i) = (\vee_i \underline{B}_1^i) \vee (\vee_i \underline{B}_2^i)$. Since, $T_i \quad i = 1, 2$ is an IVSF topology, then $(\vee_i \underline{B}_1^i) \in T_1$ and $(\vee_i \underline{B}_2^i) \in T_2$. Therefore, $\vee_i \underline{A}_i \in T_{12}^*$ and consequently, T_{12}^* is an IVSF topology on X. □

Proposition 5.4. *Let (X, S_1, S_2) be an interval-valued bifuzzy syntopogenous space. Assume that T_i is the interval-valued fuzzy topology associated with S_i for all $i = 1, 2$ and T_{12}^* is interval-valued supra-fuzzy topology associated with the space (X, T_1, T_2). Then T_{12}^* is the IVSF topology associated with the space (X, S_{12}^*), that is, $T_{12}^* = T_{S_{12}^*}$.*

Proof. The proof is obvious. □

Remark 5.5. In crisp case, let R be a fuzzy topogenous order on I^X. Define a binary relation R^p as follows:

$$\mu R^p \rho \Longleftrightarrow \exists \text{ family } \{\mu_i : i \in I\} \quad \text{s.t. } \mu = \vee_i \mu_i, \ \mu_i R \rho \quad \forall i. \tag{5.1}$$

Then, R^p is a perfect fuzzy topogenous order on X finer than R and coarser than any perfect fuzzy semitopogenous order on I^X which is finer than R.

Let S be a fuzzy syntopogenous structure on X. Define a relation R_S on I^X by

$$\mu R^S \rho \Longleftrightarrow \mu R \rho \quad \text{for some } R \in S. \tag{5.2}$$

The binary relation R^S as defined above is a perfect topogenous order on I^X. Let R^p be the coarsest perfect topogenous order on I^X finer than each member of S. (X, R_S^p) is the topogenous space. Let $R_o = R_S^p$.

6. Conclusion

Computer scientists used the relation concepts in many areas of life such as artificial intelligence, knowledge discovery, decision making and medical diagnosis [28]. One of the important theories depend on relations is the rough set theory [29]. Many authors studied the topological properties of rough set [30, 31]. In this paper we generalized the topological concepts by introducing the notions of IVSF syntopogenous structures. We can use the relations obtained from an interval-valued information systems to generate an IVSF syntopogenous structure and use the mathematical properties of these structures to discover the knowledge in the information modelings.

Acknowledgment

The authors are thankful to both the referees for their valuable suggestions for correcting this paper.

References

[1] A. Csaszar, *Foundations of General Topology*, A Pergamon Press Book, Pergamon Press, New York, NY, USA, 1963.

[2] A. K. Katsaras, "On fuzzy syntopogenous structures," *Revue Roumaine de Mathématiques Pures et Appliquées*, vol. 30, no. 6, pp. 419–431, 1985.

[3] M. Z. Wen, L. W. Jin, and S. Lan, "On fuzzy syntopogenous structures and preorder," *Fuzzy Sets and Systems*, vol. 90, no. 3, pp. 355–359, 1997.
[4] K. A. Hashem, "T-syntopogenous spaces," *Annals of Fuzzy Mathematics and Informatics*, vol. 4, no. 1, pp. 25–48, 2012.
[5] C. L. Chang, "Fuzzy topological spaces," *Journal of Mathematical Analysis and Applications*, vol. 24, pp. 182–190, 1968.
[6] B. Hutton, "Uniformities on fuzzy topological spaces," *Journal of Mathematical Analysis and Applications*, vol. 58, no. 3, pp. 559–571, 1977.
[7] L. Wang-Jin, "Fuzzy proximity spaces redefined," *Fuzzy Sets and Systems*, vol. 15, no. 3, pp. 241–248, 1985.
[8] A. K. Katsaras, "Operations on fuzzy syntopogenous structures," *Fuzzy Sets and Systems*, vol. 43, no. 2, pp. 199–217, 1991.
[9] R. Lowen, "Fuzzy topological spaces and fuzzy compactness," *Journal of Mathematical Analysis and Applications*, vol. 56, no. 3, pp. 621–633, 1976.
[10] R. Lowen, "Fuzzy uniform spaces," *Journal of Mathematical Analysis and Applications*, vol. 82, no. 2, pp. 370–385, 1981.
[11] G. Artico and R. Moresco, "Fuzzy proximities compatible with Lowen fuzzy uniformities," *Fuzzy Sets and Systems*, vol. 21, no. 1, pp. 85–98, 1987.
[12] A. A. Ramadan, S. N. El-Deeb, M.-S. Saif, and M. El-Dardery, "Fuzzifying syntopogenous structures," *Journal of Fuzzy Mathematics*, vol. 7, no. 3, pp. 535–546, 1999.
[13] M. S. Ying, "A new approach for fuzzy topology," *Fuzzy Sets and Systems*, vol. 53, no. 1, pp. 93–104, 1993.
[14] A. Kandil, A. A. Nouh, and S. A. El-Sheikh, "On fuzzy bitopological spaces," *Fuzzy Sets and Systems*, vol. 74, no. 3, pp. 353–363, 1995.
[15] M. H. Ghanim, O. A. Tantawy, and F. M. Salem, "On supra fuzzy syntopogenous space," in *Proceeding of the Conference on Geometry Topology and Application*, Cairo University, December 1997.
[16] L. A. Zadeh, "The concept of a linguistic variable and its application to approximate reasoning. I," *Information Sciences*, vol. 8, pp. 199–249, 1975.
[17] I. Grattan-Guiness, "Fuzzy membership mapped onto interval and many-valued quantities," *Zeitschrift für Mathematische Logik und Grundlagen der Mathematik*, vol. 22, pp. 149–160, 1975.
[18] K. U. Jahn, "Intervall-wertige Mengen," *Mathematische Nachrichten*, vol. 68, pp. 115–132, 1975.
[19] R. Sambuc, *Function Φ-flous, application a l'aide au diagnostic en pathologie thyroidienne [Ph.D. thesis]*, University of Marseille, Marseille, France, 1975.
[20] K. T. Atanassov, "Intuitionistic fuzzy sets," *Fuzzy Sets and Systems*, vol. 20, no. 1, pp. 87–96, 1986.
[21] D. Dubois, P. Hájek, and H. Prade, "Knowledge-driven versus data-driven logics," *Journal of Logic, Language and Information*, vol. 9, no. 1, pp. 65–89, 2000.
[22] L. A. Zadeh, "Fuzzy sets," *Information and Computation*, vol. 8, pp. 338–353, 1965.
[23] J. Hongmei, "Multicriteria fuzzy decision-making methods based on interval-valued fuzzy sets," in *Proceedings of the 5th International Conference on Intelligent Computation Technology and Automation (ICICTA'12)*, pp. 217–220, Hunan, China, January 2012.
[24] J. Hong and F. Wang, "A similarity measure for interval-valued fuzzy sets and its application in supporting medical diagnostic reasoning," in *Proceedings of the 10th International Symposium on Operations Research and Its Applications (ISORA'11)*, pp. 251–257, Dunhuang, China, August 2011.
[25] H. Choi, G. Mun, J. Ahn, and C. Korea, "A medical diagnosis based on interval valued fuzzy set," *Biomedical Engineering: Applications, Basis and Communications*, vol. 24, no. 4, p. 349, 2012.
[26] F. M. Sleim, "Oninterval valued-supra-openness," submitted for publication to the acta mathematica sinica journal.
[27] A. S. Mashhour, A. A. Allam, F. S. Mahmoud, and F. H. Khedr, "On supratopological spaces," *Indian Journal of Pure and Applied Mathematics*, vol. 14, no. 4, pp. 502–510, 1983.
[28] A. E. Samuel and M. Balamurugan, "Fuzzy max-min composition technique in medical diagnosis," *Applied Mathematical Sciences*, vol. 6, no. 35, pp. 1741–1746, 2012.
[29] Z. Pawlak, "Rough sets," *International Journal of Computer and Information Sciences*, vol. 11, no. 5, pp. 341–356, 1982.
[30] A. S. Salama, "Some topological properties of rough sets with tools for data mining," *International Journal of Computer Science Issues*, vol. 8, no. 3, part 2, pp. 1694–0814, 2011.
[31] R. Raghavan and B. K. Tripathy, "On some topological properties of multigranular rough sets," *Advances in Applied Science Research*, vol. 2, no. 3, pp. 536–543, 2011.

Hindawi Publishing Corporation
Mathematical Problems in Engineering
Volume 2012, Article ID 808161, 15 pages
doi:10.1155/2012/808161

Research Article

Bi-Objective Optimization Method and Application of Mechanism Design Based on Pigs' Payoff Game Behavior

Lu Wang, Jian-gang Wang, Rui Meng, and Neng-gang Xie

School of Mechanical Engineering, Anhui University of Technology, Maanshan, Anhui Province 243002, China

Correspondence should be addressed to Neng-gang Xie, xienenggang@yahoo.com.cn

Received 13 August 2012; Revised 24 October 2012; Accepted 25 October 2012

Academic Editor: Peng Shi

Copyright © 2012 Lu Wang et al. This is an open access article distributed under the Creative Commons Attribution License, which permits unrestricted use, distribution, and reproduction in any medium, provided the original work is properly cited.

It takes two design goals as different game players and design variables are divided into strategy spaces owned by corresponding game player by calculating the impact factor and fuzzy clustering. By the analysis of behavior characteristics of two kinds of intelligent pigs, the big pig's behavior is cooperative and collective, but the small pig's behavior is noncooperative, which are endowed with corresponding game player. Two game players establish the mapping relationship between game players payoff functions and objective functions. In their own strategy space, each game player takes their payoff function as monoobjective for optimization. It gives the best strategy upon other players. All the best strategies are combined to be a game strategy set. With convergence and multiround game, the final game solution is obtained. Taking bi-objective optimization of luffing mechanism of compensative shave block, for example, the results show that the method can effectively solve bi-objective optimization problems with preferred target and the efficiency and accuracy are also well.

1. Introduction

Multiobjective optimization problem in actual engineering design is very common. The essential characteristics of multiobjective optimization are as follows: (1) there exist several objective interests; (2) the status of the various objectives are different and have conflicts. The solution methods are diverse; the latest research is as follows: Akbari and Ziarati [1] applied a novel bee swarm optimization method to obtain a uniformly distributed Pareto front. Ismail et al. [2] proposed a new self-organizing genetic algorithm for multiobjective optimization problems to obtain a better value as compared to the existing weighted-sum methods. Lee et al. [3] used the multiobjective fuzzy optimization method to obtain the optimal parameters of rotor experimental apparatus. Ding et al. [4] proposed a new multiobjective

optimization algorithm named KSVC-SPEA to effectively achieve the overall performance of injection molding machine.

In recent years, considering the similarity between multiobjective design and the game, game theory has been used to solve multiobjective design problems, especially for practical problems in engineering fields. According to the different behaviors of each game player seeking for benefit, the game can be divided into noncooperative game and cooperative game. In a noncooperative game, each player benefits from competitive behavior patterns and the typical models are Nash equilibrium game model and the Stackelberg oligopoly game model. A cooperative game is defined as game players abiding by a binding agreement, benefiting from cooperative behavior patterns. The typical binding agreements contain three types, which are known as the "self-interest do not harm the others" (competitive and cooperative game model), "You have me, I have you" (coalition cooperative game model), and "all for one and one for all" (unselfish cooperative game model). About noncooperative game to solve multiobjective design, Spallino and Rizzo [5] proposed a noncooperative game optimization method based on evolutionary strategy in the multiobjective design of the composite laminate, which treated each game player as an equal body and eventually found a Nash equilibrium point through negotiation functions. Neng-gang et al. [6] established a multiobjective game design technology roadmap and key indicators based on the Nash equilibrium model and the Stackelberg oligopoly game model and successfully applied to multiobjective optimization design such as gravity dam, structure of arch-arch ring, and luff mechanism of compensative sheave block. In the use of cooperative games to solve multiobjective design, Chen and Li [7] proposed three-tier two-objective optimization method and applied this method to the manufacture of concurrent product and process optimization; Neng-gang et al. [8] adopted a competitive-cooperative game model to conduct a multi-objective optimization design and obtained a good design. However, whether the non-cooperative game methods or the cooperative game methods are used to solve multi-objective design problems, if the game method is selected, behavior modes of all players remain unchanged during the whole process. But this is an ideal situation. Each player's behavior is diverse in many survival games in nature. Neng-gang et al. [9] proposed a mixed game model according to the diversity of behavior patterns caused by differences in resources and endowment of each player. Through the bionics of the survival mechanisms of reproduction of lizard species, a typical mixed game model is presented, which consists of both competitive behavior patterns and cooperative behavior patterns of "all for one and one for all" and "benefits oneself but do not harm other people". This method is very good to solve the oneness problem of constructing payoff functions, but there exist two shortcomings as follows. (1) It can only be applied to three objectives or more than three objectives and cannot solve two-objective optimization problems. (2) It cannot solve "principal and subordinate" optimization problems. That is, it cannot solve the optimization problem with target preference. To compensate this deficiency and improve the game method for solving optimization problems, bi-objective optimization method is proposed based on pigs' payoff behavior, which can be applied in two-objective optimization problem with target preference.

2. The Basic Idea

2.1. Pigs' Payoff Game Model

American economist named Nash (the Nobel economic prize winner) has proposed "Pigs' Payoff". It is shown in Figure 1 and is as follows: there are a big pig and a small pig in

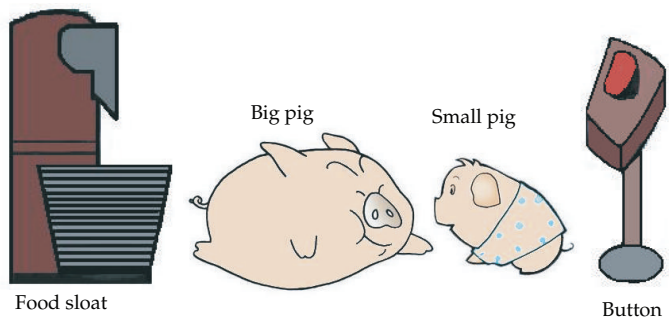

Figure 1: The picture of pigs' payoff.

Table 1: The payoff matrix.

Pigs' payoff	Small pig	
	Pressing the button	Waiting
Big pig		
Pressing the button	(5, 1)	(4, 4)
Waiting	(9, −1)	(0, 0)

the pigsty. One side of the pigsty has food slot and the other side has food control button. Whether the big pig or the small pig will pay 2-unit energy cost if it presses the food control button and 10-unit food will fall into food slot in return. If the big pig first arrives in the food slot, the benefit ratio of the big pig to the small pig is 9 : 1. If the big pig and the small pig arrive in the food slot at the same time, the benefit ratio of the big pig to the small pig is 7 : 3. If the small pig first arrives in the food slot, the benefit ratio of the big pig to the small pig is 6 : 4. The payoff matrix is shown in Table 1. In premise of both the big pig and small pig having intelligence, the final game result is that the big pig presses the button and the small pig dose not press the button but chooses to wait [10].

From the result of the behavior, the strategy of waiting is a selfish behavior of non-cooperation and the strategy of pressing the button is a collective behavior of cooperation. Hence, two game players (the big pig and the small pig) adopt two different behavior modes and constitute a hybrid game mode. The equilibrium solution (4, 4) is Pareto solution.

2.2. The Technology Principle

$$\begin{aligned}
&\text{The design variables: } \mathbf{X} = (x_1, x_2, \ldots, x_n) \in \Omega^n, \\
&\text{let the objective functions be minimized: } F(\mathbf{X}) = (F_1(\mathbf{X}), F_2(\mathbf{X})) \longrightarrow \min, \\
&\text{subject to constraint conditions: } g_k(\mathbf{X}) \leq 0 \quad (k = 1, 2, \ldots, q),
\end{aligned} \tag{2.1}$$

where n is the number of design variables. q is the number of constraint conditions. Ω^n is the feasible space of design variables.

Meanwhile, the definition of game is as follows: G_m represents one game. If G_m has 2 players (Illustration: the implication of number of players is equal to the number of objective

functions), the sets of available strategies are denoted by $\mathbf{S}_1$, $\mathbf{S}_2$. The payoff functions are u_1, u_2. Hence, the game with 2 players can be written as $G_m = (\mathbf{S}_1, \mathbf{S}_2; u_1, u_2)$.

The basic idea for bi-objective optimization method based on game is as follows: (1) there are 2 design objectives, which are seen as 2 players and the design variables $\mathbf{X}$ are divided into strategy subsets $\mathbf{S}_1$, $\mathbf{S}_2$ of the corresponding players by certain technical methods. (2) According to the specific game model, mapping relationships are established between the payoff functions u and objective functions F. (3) Each player takes its own payoff function as its objective and gets a single-objective optimal solution in its own strategy subset. So this player obtains the best strategy versus other players. The best strategies of all players form the group strategy in this round. The final equilibrium solutions can be obtained through multiround game according to the convergence criterion.

The payoff function u is closely related to the game model. The different behavior characteristics of the big pig and small pig, respectively, are assigned to the corresponding game players based on pigs' payoff game behavior model; then, the payoff functions u is constructed according to the corresponding behavior characteristics.

3. The Key Technology and Structure of the Algorithm

3.1. Game Player's Strategy Subset Computation

Fuzzy mathematics has been successfully used in the related design fields with the multidisciplinary cross research. Fuzzy mathematics has been successfully applied in filter design [11], T-S fuzzy systems [12, 13], and T-S fuzzy stochastic systems [14] and abundant research results are obtained. In this paper, the design variables are divided into each game players strategy subsets ($\mathbf{S}_1$, $\mathbf{S}_2$) by calculating the impact factor and fuzzy clustering based on fuzzy mathematics.

Computation steps are as follows.

(1) Optimize 2 mono-objectives; then obtain optimal solution $F_1(\mathbf{X}_1^*)$, $F_2(\mathbf{X}_2^*)$, where

$$\mathbf{X}_i^* = \left\{x_{1i}^*, x_{2i}^*, \ldots, x_{ni}^*\right\} \quad (i = 1, 2). \tag{3.1}$$

(2) Every x_j is divided into T fragments with step length Δx_j in its feasible space; Δ_{ji} is an impact factor (x_j affecting the objective f_i) and is shown as

$$\Delta_{ji} = \frac{\sum_{t=1}^{T}\left|F_i\left(x_{1i}^*, \ldots, x_{(j-1)i}^*, x_j(t), x_{(j+1)i}^*, \ldots, x_{ni}^*\right) - F_i\left(x_{1i}^*, \ldots, x_{(j-1)i}^*, x_j(t-1), x_{(j+1)i}^*, \ldots, x_{ni}^*\right)\right|}{T \cdot \Delta x_j}. \tag{3.2}$$

To avoid the different functions' self-affecting, make impact factors dimensionless:

$$\Delta_{ji} = \frac{\Delta_{ji}}{\left|F_i(\mathbf{X}_i^*)\right|}. \tag{3.3}$$

(3) All samples classification $\Delta = \{\Delta_1, \Delta_2, \ldots, \Delta_n\}$, the classification of j is $\Delta_j = \{\Delta_{j1}, \ldots, \Delta_{j2}\}$ $(j = 1, \ldots, n)$, and Δ_j means the impact factor set of j on all the players. The purpose is classifying highly similar samples as one classification; this paper uses a similar degree approach to reflect the samples' similarity relation. Select any two samples Δ_k and Δ_l and analyze their similarity relation; define a fuzzy relation function by normal distribution:

$$\mu_i(\Delta_k, \Delta_l) = \exp\left(-\frac{|\Delta_{ki} - \Delta_{li}|}{(1/m)\sum_{i=1}^{m}|\Delta_{ki} - \Delta_{li}|}\right) \quad (k, l = 1, 2, \ldots, n;\ k \neq l;\ i = 1, 2), \tag{3.4}$$

where $\mu_i(\Delta_k, \Delta_l)$ is the fuzzy relation between Δ_k and Δ_l in the ith objective function.

The correlation degree of Δ_k and Δ_l is

$$r_{kl} = \frac{1}{2}\sum_{i=1}^{2}\frac{\min_{i\in\{1,2\}}|\Delta_{ki} - \Delta_{li}| + 0.5\max_{i\in\{1,2\}}|\Delta_{ki} - \Delta_{li}|}{|\Delta_{ki} - \Delta_{li}| + 0.5\max_{i\in\{1,2\}}|\Delta_{ki} - \Delta_{li}|}. \tag{3.5}$$

(4) Establish the matrix $\mathbf{R}$ based on r_{kl} and do fuzzy clustering to matrix $\mathbf{R}$:

$$\mathbf{R} = \begin{vmatrix} r_{11} & r_{12} & \cdots & r_{1n} \\ r_{21} & r_{22} & \cdots & r_{2n} \\ \vdots & \vdots & \vdots & \vdots \\ r_{n1} & r_{n2} & \cdots & r_{nn} \end{vmatrix}. \tag{3.6}$$

Classification results of Δ represent the classification results of $\mathbf{X}$ because of a one-to-one relationship between $\Delta = \{\Delta_1, \Delta_2, \ldots, \Delta_n\}$ and $\mathbf{X} = \{x_1, x_2, \ldots, x_n\}$.

(5) According to fuzzy clustering, divide the design variables $\mathbf{X}$ into strategy subsets $\mathbf{S}_1, \ldots, \mathbf{S}_m$ and assign the strategy subset to the corresponding player by the average value of impact factors. According to a statistical viewpoint [15], when the number of design variables and objective functions is small, we can directly divide variable sets $\mathbf{X}$ into strategy space $\mathbf{S}_1$, $\mathbf{S}_2$ according to the value of impact factor. When the number design variables and objective functions are large, fuzzy clusterings are needed. Meanwhile, according to experience, we can first classify variables with strong correlation as a sample to reduce the complexity of clustering analysis.

Input system's classification control value is M and maximal sample number is P; each with sample as one classification, the system is $\Delta_1, \Delta_2, \ldots, \Delta_n$.

The steps of clustering are as follows.

(1) Calculate the correlation degree r_{kl} and build matrix $\mathbf{R}^{(0)}$; attention: $r_{kl} = r_{lk}$, $r_{kl} > 0$.

(2) Set maximum value of matrix $\mathbf{R}^{(0)}$ to be r_{ab}, $r_{ab} = \max_{k,l\in\{1,2,\ldots,n\}} r_{kl}$ and classify Δ_a and Δ_b into a new classification Δ_s; if the sample number is larger than P, then combine the second maximal value of $\mathbf{R}^{(0)}$.

(3) Combine $\Delta_c (c = 1, 2, \ldots, n; c \neq a, c \neq b)$ and Δ_s into a new classification system, calculate its correlation degree, and build a new matrix $\mathbf{R}^{(1)}$; the correlation degree of any classification Δ_c and Δ_s is $r_{cs} = \min\{r_{ca}, r_{cb}\}$.

(4) Repeat procedures (1), (2), and (3) until the system classification number equals control value M.

3.2. Behavior Modes and Construction of Game Payoff Functions

The characteristic of the small pig is competitive behavior mode and its corresponding game payoff function is as follows:

$$u_i = \frac{F_i}{\overline{F}_i} \quad (i = 1, 2), \tag{3.7}$$

where $\overline{F}$ is a reference value, which can eliminate the differences in the magnitude for each objective function. In this paper, the initial objective function value is chosen to be $\overline{F}$.

The characteristic of the big pig is cooperative behavior mode and its corresponding game payoff function is as follows:

$$u_i = w_{ii} \frac{F_i}{\overline{F}_i} + \sum_{j=1 (j \neq i)}^{m} w_{ij} \frac{F_j}{\overline{F}_j} \quad (i = 1, 2), \tag{3.8}$$

where $\sum_{j=1}^{m} w_{ij} = 1$ value of w_{ii} reflects the degree of considering its own interest. The greater the value is, the lower the cooperative degree is.

3.3. Algorithm Procedures and Flow Chart

(1) Obtain strategy subset $\mathbf{S}_1$, $\mathbf{S}_2$ attached to each player through calculating the impact factor and fuzzy clustering.

(2) Payoff functions u_i to any ith player ($i = 1, 2$) is constructed according to the characteristic of the small pig and big pig proposed by Section 3.2 above.

(3) Generate the initial feasible strategies in the strategy set of each player randomly and then form a strategy permutation $s^{(0)} = \{s_1^{(0)}, s_2^{(0)}\}$.

(4) Let $\overline{s}_1^{(0)}$, $\overline{s}_2^{(0)}$ be the corresponding complementary set of $s_1^{(0)}$, $s_2^{(0)}$ in $s^{(0)}$. For any player i ($i = 1, 2$), solve the optimal strategy $s_i^* \in \mathbf{S}_i$, and make payoff minimum $u_i(s_i^*, \overline{s}_i^{(0)}) \to \min (i = 1, 2)$;

(5) Define optimal strategy permutation $s^{(1)} = s_1^* \cup s_2^*$. Then judge the feasibility of $s^{(1)}$. If $g_k(s^{(1)}) \leq 0$ $(k = 1, 2, \ldots, q)$ does not satisfy, turn to step (3). Otherwise, compute the distance between $s^{(1)}$ and $s^{(0)}$ which is called the Euclidean norm. Then examine whether the distance satisfies the convergence criterion $\|s^{(1)} - s^{(0)}\| \leq \varepsilon$ or not (ε is a decimal parameter given in advance). If it satisfies, the game is over; if not, let $s^{(1)}$ displace $s^{(0)}$ and turn to step (4) to repeat.

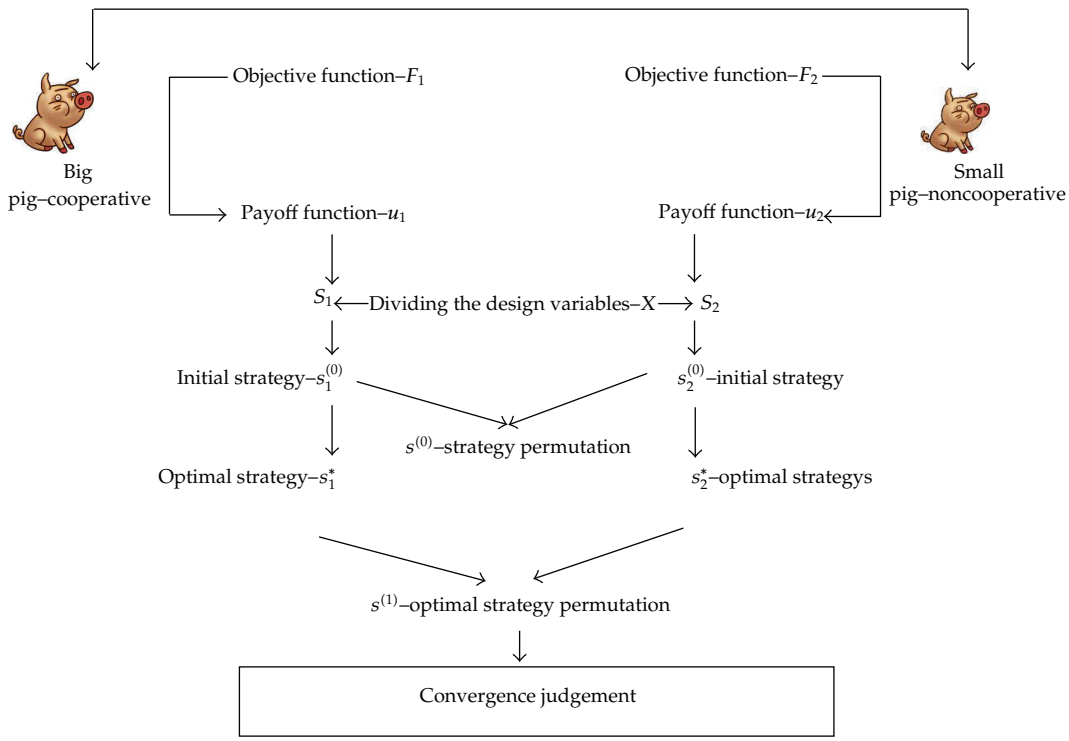

Figure 2: The algorithm chart.

The algorithm chart is shown in Figure 2 (illustration: if the big pig stands for F_1, then the small pig stands for F_2 and if the big pig stands for F_2, then the small pig stands for F_1).

4. Bi-Objective Optimization Model of Luff Mechanism of Compensative Sheave Block

4.1. The Design Model

The luff mechanism of compensative sheave block is a working device, which can realize mechanical loading range and is widely used in hoisting machinery. In its working process, there exists the stability goal; namely, the goods need to move along the horizontal path. On the other hand, there also exists the economic goal; namely, it needs less energy consumption. So, design problems have multiobjective optimization issues.

The luff mechanism of compensative sheave block is shown in Figure 3. The design variables are $\mathbf{X} = (x_1, x_2, x_3, x_4, x_5)$. Constraints need to meet upper and lower limits of design variables and amplitude range cannot exceed the prescribed range. The objective functions are F_1 (stability index) and F_2 (economic index).

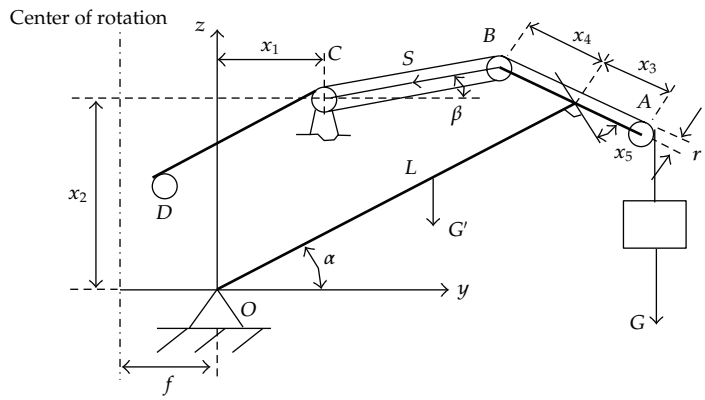

Figure 3: The luff mechanism of compensative sheave block.

4.2. The Objective Function of the Stability Index

Consider

$$R = L\cos\alpha + x_3\sin(\alpha + x_5) + f + r, \tag{4.1}$$

where R is the amplitude of fluctuation and α is the elevation.

The mechanism in the biggest amplitude is the starting point and the rise quantity relative to the starting point is $\Delta z(t)$ in any time t,

$$\Delta z(t) = L(\sin\omega t - \sin\alpha_1) + x_3[\cos(\alpha_1 + x_5) - \cos(\omega t + x_5)], \tag{4.2}$$

where $\omega = (\alpha_2 - \alpha_1)/T$ is angular velocity, T is the total time of the fluctuation, α_1 is the elevation in $R_{\max}$ (the maximum luffing), and α_2 is the elevation in $R_{\min}$ (the minimum luffing).

The fall quantity relative to the starting point is $\Delta l(t)$ in any time t due to the rope releasing:

$$\Delta l(t) = \frac{m_b}{m_q}(l_1 - l(t)), \tag{4.3}$$

where m_q is the number of wire rope of lifting pulley and m_b is the number of wire rope of compensation pulley, where

$$\begin{aligned} l_1 &= \sqrt{[L\cos\alpha_1 - x_4\sin(\alpha_1 + x_5) - x_1]^2 + [L\sin\alpha_1 + x_4\cos(\alpha_1 + x_5) - x_2]^2}, \\ l(t) &= \sqrt{[L\cos\omega t - x_4\sin(\omega t + x_5) - x_1]^2 + [L\sin\omega t + x_4\cos(\omega t + x_5) - x_2]^2}, \\ \Delta h(t) &= \Delta z(t) - \Delta l(t), \end{aligned} \tag{4.4}$$

where $\Delta h(t)$ is the deviation relative to the starting point in any time t.

So, the objective function of the stability index is as follows:

$$F_1 = \sup_{t\in[0,T]} \Delta h(t) - \inf_{t\in[0,T]} \Delta h(t). \tag{4.5}$$

4.3. The Objective Function of the Economic Index

The energy consumption is $P(t)$ in any time t.

$$P(t) = M_q(t)\omega, \tag{4.6}$$

where $M_q(t)$ is the torque. For no frame balance system, it is as follows:

$$M_q(t) = \frac{G}{9.8}[L\cos\omega t + x_3\sin(\omega t + x_5) + r] - \frac{m_b}{m_q}\frac{G}{9.8}(z_B\cos\beta - y_B\sin\beta) + \frac{G'}{9.8}L\xi\cos\omega t, \tag{4.7}$$

where $y_B = L\cos\omega t - x_4\sin(\omega t + x_5)$, $z_B = L\sin\omega t + x_4\cos(\omega t + x_5)$, G is the gravity of the goods, $\beta = \mathrm{arctg}((z_B - x_2)/(y_B - x_1))$, G' is the gravity of the arm frame, and ξ is the ratio of the distance (center of gravity of the arm frame from O point in Figure 3) to arm length-L.

So, the objective function of the economic index is as follows:

$$F_2 = \int_0^T P(t)dt = \omega\int_0^T M_q(t)dt. \tag{4.8}$$

5. The Application in Mechanism Design

5.1. Calculation Statement

The paper takes the luff mechanism of compensative sheave block (shown in Figure 3) as application object. $G = 31360\,\mathrm{N}$, $G' = 13720\,\mathrm{N}$, $L = 14\,\mathrm{m}$, $f = 0.7\,\mathrm{m}$, $\xi = 0.5$, $r = 0.2\,\mathrm{m}$, $m_b = 6$, $m_q = 2$. $R_{\max} = 12\,\mathrm{m}$, $R_{\min} = 5.8\,\mathrm{m}$, $-0.4 \le x_1 \le 0.5$, $3 \le x_2 \le 8$, $0.4 \le x_3 \le 0.8$, $0.3 \le x_4 \le 0.7$, $0 \le x_5 \le 0.43633$. The total fluctuation time is 40 seconds ($T = 40$ seconds). The smallest unit time is 1 second. The more-detailed mechanism instructions can refer to [16]. Meanwhile, a group of realistic optimization design parameters ($x_1 = -0.030$, $x_2 = 4.040$, $x_3 = 0.550$, $x_4 = 0.370$, $x_5 = 0.160$) is listed [16].

5.2. Single-Objective Optimization Results

Consider

$$\begin{aligned} \mathbf{X}_1^* &= (0.01897, 4.08848, 0.51854, 0.53969, 0.33220), \qquad F_1(\mathbf{X}_1^*) = 0.01558\,\mathrm{m}, \\ \mathbf{X}_2^* &= (0.00954, 4.83460, 0.77453, 0.57673, 0.31204), \qquad F_2(\mathbf{X}_2^*) = 2.946\,\mathrm{kJ}. \end{aligned} \tag{5.1}$$

The impact factors are shown in Table 2.

Table 2: The impact factors.

Impact factors Δ_{ji}	Design variables				
	x_1	x_2	x_3	x_4	x_5
Objective functions					
F_1	95.53	85.86	29.75	21.57	1.78
F_2	17.12	13.99	5.34	5.27	0.36

Table 3: The impact factors of strategy subsets to objection functions.

Impact factors	Strategy subsets	
	$\mathbf{S}_a$	$\mathbf{S}_b$
Objection functions		
F_1	90.695	17.700
F_2	15.555	3.657

5.3. Fuzzy Clustering

Consider $\Delta_1 = (95.53, 17.12)$, $\Delta_2 = (85.86, 13.99)$, $\Delta_3 = (29.75, 5.34)$, $\Delta_4 = (21.57, 5.27)$, $\Delta_5 = (1.78, 0.36)$,

$$\mathbf{R} = \begin{pmatrix} * & 1.66393 & 1.54728 & 1.52919 & 1.54697 \\ & * & 1.52336 & 1.50450 & 1.53111 \\ & & * & 1.34602 & 1.54624 \\ & & \text{Symmetry} & * & 1.60735 \\ & & & & * \end{pmatrix}, \tag{5.2}$$

$M = 2$, and $P = 3$. Because $r_{12} = 1.66393$ is the maximum value of matrix $\mathbf{R}$, x_1 and x_2 belong to one class. Namely, $\mathbf{S}_a = \{x_1, x_2\}$ and $\mathbf{S}_b = \{x_3, x_4, x_5\}$. The impact factors bof strategy subsets to objection functions are shown in Table 3.

According to Table 3, because the maximum value is 90.695, $\mathbf{S}_a = \mathbf{S}_1 = \{x_1, x_2\}$ is the strategy subset of F_1. $\mathbf{S}_b = \mathbf{S}_2 = \{x_3, x_4, x_5\}$ is the strategy subset of F_2.

5.4. Calculation Results

There exist two kinds of cases. Case 1 is that the big pig stands for F_2 and the small pig stands for F_1. Case 2 is that the big pig stands for F_1 and the small pig stands for F_2.

We take case 1; for example, the detailed calculation steps are as follows.

(1) Take the corresponding values of the initial design in strategy subsets $\mathbf{S}_1$, $\mathbf{S}_2$ as the initial feasible strategies $s_1^{(0)}$, $s_2^{(0)}$. Then, form a strategy permutation $s^{(0)} = \{s_1^{(0)}, s_2^{(0)}\}$.

(2) Perform the following two single-objective optimization.

Table 4: The iterative process of Case 1.

Game round	Design variables					Objective functions	
	x_1/m	x_2/m	x_3/m	x_4/m	x_5/rad	F_1/m	F_2/KJ
Initial strategy	0.02968	4.09656	0.59710	0.56809	0.04602	0.06290	34.819
Bout 1	−0.02685	4.06819	0.68734	0.30528	0.35235	0.04682	30.382
Bout 2	0.06769	4.15154	0.63034	0.46589	0.30726	0.03309	32.764
Bout 3	−0.01810	4.07167	0.69530	0.32966	0.41033	0.03157	30.829
Bout 4	0.00422	4.09241	0.72985	0.30224	0.40272	0.02267	31.060
Bout 5	−0.00605	4.06225	0.58250	0.49698	0.02102	0.01581	33.438
Bout 6	−0.00605	4.06225	0.58250	0.49698	0.02102	0.01581	33.438

(a) Seek the optimal strategy $s_1^* \in \mathbf{S}_1$ and minimize the payoff function,

$$u_1\left(s_1^*, s_2^{(0)}\right) = \frac{F_1\left(s_1^*, s_2^{(0)}\right)}{F_1\left(s_1^{(0)}, s_2^{(0)}\right)} \longrightarrow \min. \tag{5.3}$$

(b) Seek the optimal strategy $s_2^* \in \mathbf{S}_2$ and minimize the payoff function,

$$u_2\left(s_1^{(0)}, s_2^*\right) = w_{22} \times \frac{F_2\left(s_1^{(0)}, s_2^*\right)}{F_2\left(s_1^{(0)}, s_2^{(0)}\right)} + w_{21} \times \frac{F_1\left(s_1^{(0)}, s_2^*\right)}{F_1\left(s_1^{(0)}, s_2^{(0)}\right)} \longrightarrow \min. \tag{5.4}$$

(3) Define strategy permutation $s^{(1)} = s_1^* \cup s_2^*$. Then, justify the feasibility of $s^{(1)}$. If $s^{(1)}$ does not satisfy constraint conditions, turn to step (1). Otherwise, compute $\sqrt{\sum_{j=1}^{5}(((x_j^{(1)} - x_j^{(0)})/x_j^{(0)})^2/5)}$ and examine whether it satisfies the convergence precision ε (ε is 0.0001 in this paper). If it satisfies, the game is over; if not, let $s^{(0)} = s^{(1)}$ and turn to step (2) to iteration loop.

Illustration: for case 2, u_1 is constructed according to cooperative behavior mode and u_2 is constructed according to noncooperative behavior mode.

(1) For case 1, $w_{22} = 0.5$, $w_{21} = 0.5$, calculation starts from the initial strategy $\mathbf{X}^0 = (0.02968, 4.09656, 0.59710, 0.56809, 0.04602)$ and obtains convergence value $\mathbf{X}^* = (-0.00605, 4.06225, 0.58250, 0.49698, 0.02102)$ after six rounds game and $F_1 = 0.01581$ m, $F_2 = 33.438$ KJ. Iterative process is shown in Table 4.

(2) For case 2, $w_{11} = 0.5$, $w_{12} = 0.5$, calculation starts from the initial strategy $\mathbf{X}^0 = (0.19247, 4.17230, 0.42101, 0.31284, 0.31592)$ and obtains convergence value $\mathbf{X}^* = (0.01724, 4.08923, 0.40303, 0.30493, 0.43130)$ after four rounds game and $F_1 = 0.14471$ m, $F_2 = 28.255$ KJ. Iterative process is shown in Table 5.

The compared results are shown in Table 6. (Illustration: multiobjective fuzzy optimization method is adopted in [17] and multiobjective Nash equilibrium game method is adopted in [6]).

Table 5: The iterative process of Case 2.

Game round	Design variables					Objective functions	
	x_1/m	x_2/m	x_3/m	x_4/m	x_5/rad	F_1/m	F_2/KJ
Initial strategy	0.19247	4.17230	0.42101	0.31284	0.31592	0.03357	33.212
Bout 1	0.05860	4.02781	0.40414	0.30544	0.40052	0.02428	32.968
Bout 2	0.18459	4.17053	0.41018	0.30223	0.39318	0.03514	32.457
Bout 3	0.01724	4.08923	0.40303	0.30493	0.43130	0.14471	28.225
Bout 4	0.01724	4.08923	0.40303	0.30493	0.43130	0.14471	28.225

Table 6: The compared results.

Reference	Design variables					Objective functions	
	x_1/m	x_2/m	x_3/m	x_4/m	x_5/rad	F_1/m	F_2/KJ
[16]	−0.030	4.040	0.550	0.370	0.160	0.05935	31.166
[17]	−0.02199	4.14131	0.76369	0.44838	0.32446	0.04325	30.174
[6]	0.11480	4.08089	0.40800	0.30067	0.41340	0.01604	33.140
Method in this paper							
Case 1	−0.00605	4.06225	0.58250	0.49698	0.02102	0.01581	33.438
Case 2	0.01724	4.08923	0.40303	0.30493	0.43130	0.14471	28.225

The comparison of deviation trajectory (cases 1 and 2, [6, 16, 17]) is shown in Figure 4.

According to Table 6, we can know that F_1 in case 1 is better than [6, 16, 17] and case 2, and that F_1 in case 2 is the worst. According to Figure 4, the deviation trajectory in case 1 is better than [6, 16, 17] and case 2. F_2 in case 2 is better than [6, 16, 17] and case 1. F_2 in case 1 is the worst. The results show that the method can effectively solve bi-objective optimization problems with preferred target and that multiobjective fuzzy optimization method [17] is an effective method without preferred target (both F_1 and F_2 are better than realistic optimization results [16]).

By analyzing the results, we can know three conclusions as follows. (1) The game player with noncooperative characteristic of the small pig has greater advantage in the pursuit of its own interests than the game player with cooperative characteristic of the big pig. (2) If the designers have target preference, they need to take the preferred target as the small pig side and take another target as the big pig side. (3) The satisfactory equilibrium solution can be obtained through less iteration rounds because the design variables are decomposed into the strategy subset owned by 2 game players.

To reveal the influence of w_{ii} on the final solutions, w_{ii} = 0.1, 0.3, 0.5, 0.7, respectively. The results are shown in Tables 7 and 8. In case 1, the big pig stands for F_2 and the greater the value of w_{22} is (the cooperative degree is lower), the better the final value of F_2 is. In case 2, the big pig stands for F_1 and the greater the value of w_{11} is (the cooperative degree is lower), the better the final value of F_1 is.

6. Conclusions

(1) One new bi-objective optimization game method is proposed. Two design goals can be regarded as two game players, the design variables set can be regarded as

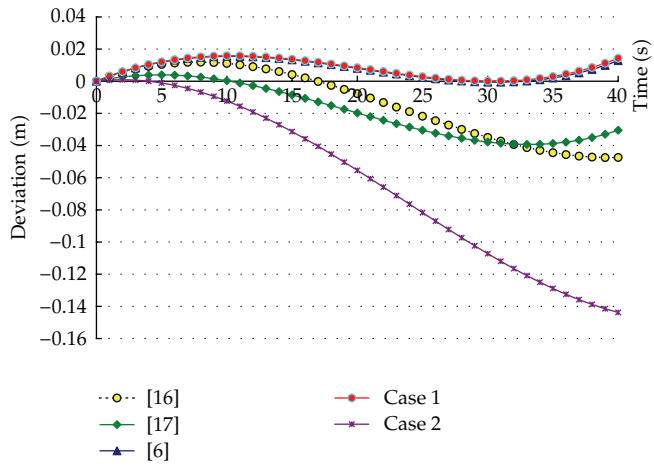

Figure 4: The comparison of deviation trajectory.

Table 7: The influence of w_{22} on the final solutions in Case 1.

w_{22}	Design variables					Objective functions	
	x_1/m	x_2/m	x_3/m	x_4/m	x_5/rad	F_1/m	F_2/KJ
0.1	0.00034	4.06904	0.49224	0.57956	0.07845	0.01569	33.585
0.3	−0.00605	4.06225	0.59757	0.48890	0.00316	0.01574	33.481
0.5	−0.00605	4.06225	0.58250	0.49698	0.02102	0.01581	33.438
0.7	0.01812	4.09616	0.58756	0.48979	0.37132	0.01588	32.383

Table 8: The influence of w_{11} on the final solutions in Case 2.

w_{11}	Design variables					Objective functions	
	x_1/m	x_2/m	x_3/m	x_4/m	x_5/rad	F_1/m	F_2/KJ
0.1	0.03455	4.11824	0.40770	0.30283	0.39273	0.15709	27.850
0.3	0.00833	4.08878	0.40770	0.30283	0.39273	0.15380	27.973
0.5	0.01724	4.08923	0.40303	0.30493	0.43130	0.14471	28.225
0.7	0.02928	4.10112	0.40770	0.30283	0.39273	0.14075	28.377

strategy subsets named $\mathbf{S}_1$, $\mathbf{S}_2$, and the constraints in multiobjective problems can be regarded as constraints in the game method. Through the specific technological means, the design variables can be divided into each game players strategy subsets ($\mathbf{S}_1$, $\mathbf{S}_2$) and two payoff functions u are constructed based on pigs' payoff game behavior.

(2) The solution step of game player's strategy subset is presented. The design variables are divided into strategy spaces owned by the corresponding game player by calculating the impact factor and fuzzy clustering.

(3) The big pig's behavior is cooperative but the small pig's behavior is noncooperative. The different behavior characteristics of the big pig and small pig, respectively, are assigned to the corresponding game players based on pigs' payoff game behavior.

The paper constitutes a hybrid game mode and proposes the detailed solution steps.

(4) For optimization problems with preferred target, the designers need to emphasize one design goal. For this problem, there exist traditional methods such as weighting method (by adjusting the weight of each goal), hierarchical sequence method (by adjusting the objective optimization order), and goal programming method. In this paper, one new bi-objective optimization game method is proposed based on pigs' payoff game behavior for solving optimization problems with preferred target. It takes bi-objective optimization of luffing mechanism of compensative shave block; for example, the results show that the method can effectively solve the bi-objective optimization problems with preferred target (designers need to take the preferred target as the small pig side and take another target as the big pig side), the efficiency and accuracy are well, and the solution is obtained only through fewer game rounds.

Acknowledgments

The project was supported by the Natural Science Foundation of Anhui Province of China (Grant no. 11040606 M119), State Key Laboratory of Hydrology-Water Resources and Hydraulic Engineering (Grant no. 2010491011), and the Foundation for Young Talents in College of Anhui Province (Grant no. 2011SQRL034).

References

[1] R. Akbari and K. Ziarati, "A cooperative approach to bee swarm optimization," *Journal of Information Science and Engineering*, vol. 27, no. 3, pp. 799–818, 2011.

[2] F. S. Ismail, R. Yusof, and M. Khalid, "Self organizing multi-objective optimization problem," *International Journal of Innovative Computing, Information and Control*, vol. 7, no. 1, pp. 301–314, 2011.

[3] T. E. Lee, J. P. Su, K. W. Yu, and K. H. Hsia, "Multi-objective fuzzy optimal design of alpha-beta estimators for nonlinear variable structure control," *International Journal of Innovative Computing, Information and Control*, vol. 7, no. 5, pp. 2123–2140, 2011.

[4] L. P. Ding, J. R. Tan, Z. Wei, W. L. Chen, and Z. Gao, "Multi-objective performance design of injection molding machine via a new multi-objective optimization algorithm," *International Journal of Innovative Computing, Information and Control*, vol. 7, no. 7, pp. 3939–3949, 2011.

[5] R. Spallino and S. Rizzo, "Multi-objective discrete optimization of laminated structures," *Mechanics Research Communications*, vol. 29, no. 1, pp. 17–25, 2002.

[6] X. Neng-gang, F. Hao, B. Jiahan, and Z. Lei, "Game analysis of multi-objective design on luff mechanism of compensative sheave block," *Journal of Mechanical Strength*, vol. 27, no. 2, pp. 202–206, 2005.

[7] L. Chen and S. Li, "A computerized team approach for concurrent product and process design optimization," *Computer-Aided Design*, vol. 34, no. 1, pp. 57–69, 2002.

[8] X. Neng-gang, S. Lin-song, B. Jiahan, and F. Hao, "Multi-objective game design of arch dam shape," *Acta Mechanica Solida Sinica*, vol. 27, no. 2, pp. 200–206, 2007.

[9] X. Neng-gang, C. Yu-wan, W. Lu, and L. Rui, "Tri-objective co-evolutionary algorithms and application of mechanism design based on bionics of lizard behavior," *Journal of Mechanical Engineering*, vol. 45, no. 5, pp. 62–68, 2009.

[10] X. Wei and F. Kun, "Based on game theory framework for thinking of remolding the relationship between government and enterprises-From the, "Prisoners Dilemma" to, "Pigs Payoffs" strategy of choice," *Journal of Huazhong Agricultural University*, no. 1, pp. 60–63, 2009.

[11] X. Su, P. Shi, L. Wu, and Y.-D. Song, "A novel approach to filter design for T-S fuzzy discrete-time dystems with time-varyingdelay," *IEEE Transactions on Fuzzy Systems*, vol. 20, no. 6, pp. 1114–1129, 2012.

[12] L. Wu, X. Su, P. Shi, and J. Qiu, "Model approximation for discrete-time state-delay systems in the TS fuzzy framework," *IEEE Transactions on Fuzzy Systems*, vol. 19, no. 2, pp. 366–378, 2011.

[13] L. Wu, X. Su, P. Shi, and J. Qiu, "A new approach to stability analysis and stabilization of discrete-time T-S fuzzy time-varying delay systems," *IEEE Transactions on Systems, Man, and Cybernetics B*, vol. 41, no. 1, pp. 273–286, 2011.

[14] X. Su, L. Wu, P. Shi, and Y. D. Song, "H∞ model reduction of T-S fuzzy stochastic systems," *IEEE Transactions on Systems, Man,and Cybernetics*, vol. 42, no. 6, pp. 1574–1585, 2012.

[15] M. Murshed, A. Ramirez, J. Kim, and O. Chae, "Statistical binary edge frequency accumulation model for moving object detection," *International Journal of InNovative Computing, Information and Control*, vol. 8, no. 7, pp. 4943–4957, 2012.

[16] S. Guozheng, *Optimization Design and Application*, People's Transportation Press, Beijing, China, 1992.

[17] X. Neng-gang and W. Qi-ping, "Multi-objective fuzzy optimum design of tackle-block mechanism compensating amplitude of variation based on genetic algorithm," *Journal of Mechanical Transmission*, vol. 27, no. 1, pp. 30–32, 2003.

Hindawi Publishing Corporation
Mathematical Problems in Engineering
Volume 2012, Article ID 543039, 21 pages
doi:10.1155/2012/543039

Research Article

Direct Adaptive Fuzzy Sliding Mode Control with Variable Universe Fuzzy Switching Term for a Class of MIMO Nonlinear Systems

Guo Haigang,[1,2] Li Hongxing,[1] Zhao Weijing,[1] and Song Zhankui[1]

[1] *Faculty of Electronic Information and Electrical Engineering, Dalian University of Technology, Dalian 116024, China*
[2] *School of Mathematics and Statistics, Henan University of Science and Technology, Luoyang 471039, China*

Correspondence should be addressed to Guo Haigang, ghgxsygzy@mail.dlut.edu.cn

Received 8 October 2012; Accepted 18 November 2012

Academic Editor: Hamid Reza Karimi

Copyright © 2012 Guo Haigang et al. This is an open access article distributed under the Creative Commons Attribution License, which permits unrestricted use, distribution, and reproduction in any medium, provided the original work is properly cited.

Combining adaptive fuzzy sliding mode control with fuzzy or variable universe fuzzy switching technique, this study develops two novel direct adaptive schemes for a class of MIMO nonlinear systems with uncertainties and external disturbances. The proposed control schemes consist of fuzzy equivalent control terms, fuzzy switching control terms (in scheme one) or variable universe fuzzy switching control terms (in scheme two), and compensation control terms. The compensation control terms are used to relax the assumption on fuzzy approximation error. Based on Lyapunov stability theory, the parameters update laws are adaptively tuned online and the global asymptotic stability of the closed-loop system can be guaranteed. The major contribution of this study is to develop a novel framework for designing direct adaptive fuzzy sliding mode control scheme facing model uncertainties and external disturbances. The derived schemes can effectively solve the chattering problem and the equivalent control calculation in that environment. Simulation results performed on a two-link robotic manipulator demonstrate the feasibility of the proposed control schemes.

1. Introduction

Some nonlinear systems, such as robotic manipulator, inverted pendulum, and electrical machines, not only are often highly coupled and time-varying systems, but also suffer from structured and unstructured uncertainties [1, 2]. The control of these systems is an important topic in the field of control. Sliding mode control (SMC) is an effective control scheme to deal with these problems [3–6]. However, this control scheme suffers mainly from two disadvantages. One is the chattering due to discontinuous switching term. The other is

the difficulty involved in the calculation of the equivalent control [7]. A thorough knowledge of the plant dynamics is required for this purpose. But in the real world, there are many complex industrial processes whose accurate mathematical models are not available or difficult to formulate.

In recent decades, fuzzy control methodology has emerged as a promising way to approach nonlinear control problems since it can incorporate linguistic information from human experts into control strategy [8–13]. Considerable efforts have been done to combine fuzzy system with SMC to overcome the disadvantages of general SMC [1, 14–30]. For example, fuzzy switching technique [15–17] and fuzzy boundary layer technique [18–20] have been developed to eliminate chattering problem. Both the techniques are built on the condition that the equivalent control has already existed. There exist some difficulties for the techniques to obtain a suitable equivalent control if the nominal mathematics model is unknown. In this case, there are generally two kinds of adaptive fuzzy SMC approaches to calculate the equivalent control in the existing literatures: direct [1, 21, 22] and indirect approaches [23–27]. Direct approach is to use fuzzy system directly to approximate the equivalent control term. Indirect approach is first to utilize fuzzy systems to approximate the unknown system functions, then to design the equivalent control based on these estimates. Both the approaches can effectively deal with the calculation of the equivalent control in the presence of model uncertainties and unknown disturbance. But the chattering problem might be encountered no matter what type of adaptive fuzzy SMC.

Several indirect schemes which combined adaptive fuzzy SMC with fuzzy switching technique have been reported for SISO nonlinear systems in [28–30]. The proposed schemes can simultaneously overcome the two disadvantages of SMC mentioned above despite of model uncertainties and unknown disturbances. Unfortunately, convergence of the tracking error to zero is guaranteed by assuming that the fuzzy approximation error is very small if not equal to zero and square integrable. This, however, is difficult to show for any given plant [31]. Besides, direct approach may be of more interest not only because of its simple design and easy implementation, but also because it does not need to consider any possible controller singularity problem [32]. However, the constraints on control gain present difficulties for the design of direct adaptive control. Therefore, it will be a challenge for the direct control of MIMO nonlinear systems with model uncertainties and unknown disturbances.

Combining adaptive fuzzy SMC with fuzzy or variable universe fuzzy switching technique, this paper proposes two novel direct adaptive control schemes for a class of MIMO nonlinear systems with uncertainties and external disturbances. The difference between them lies in that one scheme employs fuzzy system to estimate the switching control gain and the other uses the variable universe fuzzy system proposed in [33] to do it. Motivated by paper [21], this study relaxes the constraint on the gain matrix and only requires it to be positive definite symmetric besides the inverse of its derivative is bounded by an unknown function. To relax the assumption on fuzzy approximation error [28–30], we append an adaptive compensation term to compensate the effect of fuzzy approximation error [34]. The overall closed-loop systems stability and the online adjustment laws of the updated parameters are built based on Lyapunov stability theory. Lastly, the proposed schemes are utilized to deal with the trajectory tracking problem of robotic manipulators. Simulation results demonstrate that the proposed schemes are effective for a class of MIMO nonlinear systems. The two control schemes cannot only achieve the asymptotical tracking for ideal input signal, but also effectively eliminate the chattering of the general SMC.

The rest of this paper is organized as follows. In Sections 2 and 3, brief statements about the control system and variable universe fuzzy system are provided, respectively.

Section 4 develops two novel direct adaptive fuzzy SMC schemes. Computer simulation results are illustrated in Section 5. Section 6 concludes this paper.

2. Problem Statement

Consider the following MIMO nonlinear system [21, 25]:

$$\begin{aligned} y_1^{(r_1)} &= f_1(x) + \sum_{j=1}^{p} g_{1j}(x)u_j + d_1, \\ &\vdots \\ y_p^{(r_p)} &= f_p(x) + \sum_{j=1}^{p} g_{pj}(x)u_j + d_p, \end{aligned} \tag{2.1}$$

where $x = [y_1, \ldots, y_1^{(r_1-1)}, y_2, \ldots, y_2^{(r_2-1)}, \ldots, y_p, \ldots, y_p^{(r_p-1)}]^T$ is the state vector which is available for measurement and $r = [r_1, r_2, \ldots, r_p]^T$, $u = [u_1, u_2, \ldots, u_p]^T$ is the control input vector, $y = [y_1, y_2, \ldots, y_p]^T$ is the output vector, $f_i(x)$ $(i = 1, 2, \ldots, p)$ are unknown continuous nonlinear functions, $g_{ij}(x)$ $(i, j = 1, 2, \ldots, p)$ are smooth unknown nonlinear functions, and $D(t) = [d_1, d_2, \ldots, d_p]^T$ are unknown external disturbances.

Define $y = [y_1^{(r_1)}, y_2^{(r_2)}, \ldots, y_p^{(r_p)}]^T$, $F(x) = [f_1(x), f_2(x), \ldots, f_p(x)]^T$, and

$$G(x) = \begin{bmatrix} g_{11}(x), & \ldots, & g_{1p}(x) \\ \vdots & \ldots, & \vdots \\ g_{p1}(x), & \ldots, & g_{pp}(x) \end{bmatrix}. \tag{2.2}$$

Then the dynamic system equation (2.1) can be rewritten as

$$y^{(r)} = F(x) + G(x)u + D(t). \tag{2.3}$$

Define reference trajectory $x_d = [x_{d1}, x_{d2}, \ldots, x_{dp}]^T$ and the tracking error

$$\begin{aligned} e_1(t) &= x_{d1}(t) - y_1(t), \\ &\vdots \\ e_p(t) &= x_{dp}(t) - y_p(t). \end{aligned} \tag{2.4}$$

According to [3, 25], for each subsystem, one can define sliding surface as follows:

$$\begin{aligned} s_1(t) &= \left(\frac{d}{dt}+\lambda_1\right)^{(r_1-1)} e_1(t), \quad \lambda_1 > 0, \\ &\vdots \\ s_p(t) &= \left(\frac{d}{dt}+\lambda_p\right)^{(r_p-1)} e_p(t), \quad \lambda_p > 0. \end{aligned} \tag{2.5}$$

From (2.5), we can see that $e_i^{(j)}(t) \to 0$, $j = 0, 1, \ldots, r_i - 1$, $i = 1, 2, \ldots, p$ as $s_i(t) \to 0$. Then, the control duty can be transferred to design the control law such that $s_i(t) \to 0$, $i = 1, 2, \ldots, p$.

The time derivatives of the sliding surface of each subsystem are

$$\begin{aligned} \dot{s}_1(t) &= e_1^{(r_1)} + \sum_{j=1}^{r_1-1} C_{r_1-1}^{j} e_1^{(r_1-j)} \lambda_1^{(j)} = v_1 - f_1(x) - \sum_{j=1}^{p} g_{1j}(x) u_j - d_1, \\ &\vdots \\ \dot{s}_p(t) &= e_p^{(r_p)} + \sum_{j=1}^{r_p-1} C_{r_p-1}^{j} e_p^{(r_p-j)} \lambda_p^{(j)} = v_p - f_p(x) - \sum_{j=1}^{p} g_{pj}(x) u_j - d_p, \end{aligned} \tag{2.6}$$

where $C_n^k = n!/k!(n-k)!$ in which $k \le n$, and

$$\begin{aligned} v_1 &= x_{d1}^{(r_1)} + \sum_{j=1}^{r_1-1} C_{r_1-1}^{j} e_1^{(r_1-j)} \lambda_1^{(j)}, \\ &\vdots \\ v_p &= x_{dp}^{(r_p)} + \sum_{j=1}^{r_p-1} C_{r_p-1}^{j} e_p^{(r_p-j)} \lambda_p^{(j)}. \end{aligned} \tag{2.7}$$

Let $S = [s_1, s_2, \ldots, s_p]^T$ and $v = [v_1, v_2, \ldots, v_p]^T$. Equation (2.6) can be rewritten as

$$\dot{S} = v - F(x) - G(x)u - D(t). \tag{2.8}$$

The objective of this paper is to design a control law $u(t)$ such that the output vector $y(t)$ follows asymptotically the desired trajectory $x_d(t)$, with all involved signals in the closed-loop system remaining bounded. In the controller design, the following assumptions are useful for steady analysis and proof.

Assumption 2.1. $G(x)$ is a positive definite and symmetrical matrix.

Assumption 2.2. $(1/2)\|(dx/dt)G^{-1}(x)\| \le \delta(x)$, where $\delta(x)$ is bounded positive continuous function without knowing its bound.

Assumption 2.3. The ideal trajectory $x_{di}(t)$ $(i = 1,2,\ldots,p)$ are r_i-order derivable, and $x_{di}(t)$ $(i = 1,2,\ldots,p)$ and their j-order derivatives $(j = 1,2,\ldots,r_i-1)$ are continuous functions of known boundary.

Remark 2.4 (see [21]). Assumption 2.1 is useful to the stability analysis and stability proof. There are many physical systems, such as robotic systems and electrical machines, which satisfy the positive definiteness and the symmetry. Assumption 2.2 is not restrictive, since we only assume the existence of $\delta(x)$ and not its knowledge. Moreover, there are several physical systems in which the control gain matrix $G(x)$ satisfies the inequality, for example, robotic manipulators, electrical machines, inverted pendulum, and chaotic systems.

3. Variable Universe Fuzzy System

Fuzzy control emerged in decades ago is a promising way to solve nonlinear control problems. It has several excellent properties. For example, it does not require the plant model and can effectively incorporate the semantic knowledge of human experts. Since the universal approximation theorem has been put forward in [10], fuzzy system and fuzzy control evolve faster than before. Specifically, in the control area, fuzzy systems are mainly used as a nonlinear function approximation tool.

It should be emphasized that, in this paper, it is assumed that the structure and the membership function parameters of the fuzzy system are properly specified in advance by the designer. This means that the designer decision is needed to determine the structure of the fuzzy system, namely, the pertinent inputs, the number of membership functions for each input, the membership function parameters, and the number of rules.

3.1. Fuzzy System

For convenience, we will recall briefly the fuzzy system in the following. Let $X_i = [-E_i, E_i]$ $(i = 1,2,\ldots,m)$ be the universe of input variable z_i $(i = 1,2,\ldots,m)$ and $Y = [-U, U]$ the universe of output variable u_o. $\mathfrak{A}_i = \{A_{ij}\}$ $(j = 1,2,\ldots,N)$ is defined as a fuzzy partition on X_i and $\mathfrak{B} = \{B_j\}$ $(j = 1,2,\ldots,N)$ a fuzzy partition on Y, where $A_{ij} \in \mathcal{F}(X_i)$ and $B_j \in \mathcal{F}(Y)$ are termed as the base, and a_{ij} and b_j are the peak points of A_{ij} and B_j, respectively. $\mathfrak{A}_i$ and $\mathfrak{B}$ are regarded as linguistic variables so that a group of fuzzy inference rules are formed as follows:

$$\text{If } z_1 \text{ is } A_{1j}, z_2 \text{ is } A_{2j}, \ldots, z_m \text{ is } A_{mj}, \quad \text{then } u_o \text{ is } B_j \ (j = 1,2,\ldots,N), \tag{3.1}$$

where N represents the number of the rules. Singleton fuzzifier, triangle membership function (overlap law is 0.5), product inference engine, and center average defuzzifier are used in this fuzzy system. The derived output of fuzzy system can be written as

$$\hat{u}_o(z) = \xi(z)^T \theta, \tag{3.2}$$

where $z = [z_1, z_2, \ldots, z_m]^T$, $\theta = [u_1, u_2, \ldots, u_N]^T$ is a vector grouping all consequent parameters, and $\xi(z) = [\xi_1(z), \xi_2(z), \ldots, \xi_N(z)]^T$ is fuzzy basis function vector defined as

$$\xi_j(z) = \prod_{i=1}^{m} A_{ij}(z_i), \quad j = 1, 2, \ldots, N. \tag{3.3}$$

3.2. Variable Universe Fuzzy System

Adaptive fuzzy controller based on fixed universe has limited approximation accuracy according to the interpolation mechanism of fuzzy system [35]. Aiming at the problem, Li first presents the variable universe idea [36]. The core idea of variable universe fuzzy control is that the universes contracts following the decrease of error. Contraction of the universe is equivalent to the increase of the control rules. Therefore, control accuracy is improved.

The so-called variable universe means that some universes, for example, X_i and Y, respectively, can change along with changing of variables z_i and u_o. In this case, the universes are denoted by

$$\begin{aligned} X_i(z_i) &= [-\alpha_i(z_i)E_i, \alpha_i(z_i)E_i], \\ Y(u_o) &= \left[-\beta(u_o)U, \beta(u_o)U\right], \end{aligned} \tag{3.4}$$

where $\alpha_i(z_i)$ $(i = 1, 2, \ldots, m)$ and $\beta(u_o)$ are, respectively, called contraction-expansion factors of the universes X_i $(i = 1, 2, \ldots, m)$ and Y. Being relative to the variable universes, the original universes X_i and Y are naturally called initial universes. After the above changes, the output of variable universe fuzzy controller can be written as

$$\hat{u}_o(\beta, z) = \beta\zeta(z)^T\vartheta, \tag{3.5}$$

where $\vartheta = [u_2, u_2, \ldots, u_N]^T$ and $\zeta(z) = [\zeta_1(z), \zeta_2(z), \ldots, \zeta_N(z)]^T$ represent the parameter vector of inference consequence and the fuzzy base function vector, respectively, in which $\zeta_j(z) = \prod_{i=1}^{m} A_{ij}(z_i/\alpha_i(z_i))$, $j = 1, 2, \ldots, N$.

Remark 3.1. Under the framework of variable universe fuzzy control, the parameter which needs to be online adjusted is a scalar β instead of a parameter vector θ in conventional adaptive fuzzy control scheme. Therefore, variable universe fuzzy control scheme simplifies the design procedure of adaptive fuzzy control. In addition, we hardly need smart expert knowledge in the realm, but need the rough trend of control rules in the design of variable universe fuzzy controller [37]. From this point, variable universe fuzzy control reduces the design difficulty.

4. Adaptive Fuzzy SMC Design

4.1. Sliding Mode Control

In this section, we firstly consider that nonlinear function matrices $F(x)$ and $G(x)$ are known. From Assumption 2.1, the matrix $G(x)$ is reversible. Both sides of (2.8) are multiplied by $G_1(x) = G^{-1}(x)$, then we obtain that

$$G_1(x)\dot{S} = G_1(x)v - F_1(x) - u - G_1(x)D(t), \tag{4.1}$$

where $F_1(x) = G_1(x)F(x)$. The control law is designed as

$$u = G_1(x)v - F_1(x) - G_1(x)D(t) + \delta(x)I_pS + \eta\,\mathrm{sign}(S), \tag{4.2}$$

where $\mathrm{sign}(S) = [\mathrm{sign}(s_1), \mathrm{sign}(s_2), \ldots, \mathrm{sign}(s_p)]^T$ and $\eta = \mathrm{diag}(\eta_1, \eta_2, \ldots, \eta_p)$ in which $\eta_i > 0$ $(i = 1, 2, \ldots, p)$, where its aim is to meet the sliding condition. Substituting (4.2) into (4.1), we can obtain

$$G_1(x)\dot{S} = -\eta\,\mathrm{sign}(S) - \delta(x)I_pS. \tag{4.3}$$

We choose a candidate Lyapunov function $V = (1/2)S^TG_1(x)S$. For the matrix $G(x)$ being positive definite and symmetrical, $G_1(x)$ is also positive definite and symmetrical and satisfies $\dot{S}^TG_1(x)S = S^TG_1(x)\dot{S}$. Combining with Assumption 2.2, we have

$$\dot{V} = S^TG_1(x)\dot{S} + \frac{1}{2}S^T\dot{G}_1(x)S = -S^T\left(\eta\,\mathrm{sign}(S) + \delta(x)I_pS\right) + \frac{1}{2}S^T\dot{G}_1(x)S \le -\sum_{i=1}^{p}\eta_i|s_i|. \tag{4.4}$$

Therefore, $\dot{V}$ is negative definite and the control objective can be achieved. However, in engineering practice, nonlinear system matrix $F(x)$ and control gain matrix $G(x)$ are often unknown. Accordingly, the derivative function matrices $F_1(x)$ and $G_1(x)$ as well as $\delta(x)$ are also unknown. Moreover, external disturbance vector $D(t)$ is also unknown. Therefore, the control law (4.2) cannot be implemented. In the following, we employ fuzzy systems to design the control law.

4.2. Direct Adaptive Fuzzy SMC with Fuzzy Switching Term (DAFSMC with FSW)

According to the sliding mode control scheme, the control law u can be decomposed into the equivalent control and the switching control. In the sliding phase, the role of the equivalent control is to force the system dynamics to stay on the sliding surface. In the reaching phase, the switching control is designed to satisfy the sliding mode condition [3, 28, 29].

Let

$$u_{eq} \triangleq G_1(x)v - F_1(x) - G_1(x)D(t) + \delta(x)I_pS \tag{4.5}$$

and $u_{sw} \triangleq \eta\,\mathrm{sign}(S)$. Equation (4.2) can rewritten as

$$u = u_{eq} + u_{sw}. \tag{4.6}$$

It is well known that the fuzzy rules used for reasoning are not easy to extract, especially for multi-input ($m > 2$) fuzzy system. Yet, a prominent merit of adaptive fuzzy system is that it does not need initial fuzzy rules and can generate fuzzy rules online based on Lyapunov stability theory [38].

So, in what follows, adaptive fuzzy systems as (3.2) are chosen to approximate the equivalent control term u_{eq}. Therefore, we have the following format:

$$u_{eq} = \widehat{u}_{eq}(\Theta_e^*, x) + \omega = \Xi_e^T(x)\Theta_e^* + \omega, \tag{4.7}$$

where $\omega = [\omega_1, \omega_2, \ldots, \omega_p]^T$ and $\Xi_e(x) = [\mathrm{diag}(\xi_{e1}^T(x), \xi_{e2}^T(x), \ldots, \xi_{ep}^T(x))]^T$ denotes fuzzy approximate error vector and fuzzy base function matrix, respectively.

Let $\Theta_e^* = [\theta_{e1}^{*T}, \theta_{e2}^{*T}, \ldots, \theta_{ep}^{*T}]^T$ be the optimal parameter vector, where

$$\theta_{ei}^* = \arg\min_{\|\theta_{ei}\| \le M_{ei}} \left\{ \sup_{x \in D_x} \left| u_{eqi} - \widehat{u}_{eqi}(\theta_{ei}, x) \right| \right\}, \tag{4.8}$$

in which M_{ei} ($i = 1, 2, \ldots, p$) is design constant restraining parameter vector θ_{ei} ($i = 1, 2, \ldots, p$) and D_x is a compact set containing state x, and

$$\widehat{u}_{eqi}(\theta_{ei}, x) = \theta_{ei}^T \xi_{ei}(x) \tag{4.9}$$

denotes the estimate of the equivalent control law u_{eqi}. Due to unknown ideal parameter vector θ_{ei}^*, we estimate θ_{ei}^* by virtue of θ_{ei}.

Remark 4.1. In this paper, we assume that fuzzy approximation errors ω_i ($i = 1, 2, \ldots, p$) are bounded for all $x \in D_x$, that is, $|\omega_i(x)| \le \rho_i$, for all $x \in D_x$, where ρ_i is an unknown constant. The knowledge of $\rho = \mathrm{diag}(\rho_1, \rho_2, \ldots, \rho_p)$ is only required for analysis purpose.

Given the approximation error ω_i between the equivalent control u_{eqi} and the used fuzzy system $\widehat{u}_{eqi}$, the switching control term u_{sw} must be modified as $(\eta + \rho)\,\mathrm{sign}(S)$, that is, $u_{swi} = (\eta_i + \rho_i)\,\mathrm{sign}(s_i)$ ($i = 1, 2, \ldots, p$). The objective of this modification is to meet the sliding mode existing condition. In the previous literatures [23, 26], the switching gain matrix $(\eta + \rho)$ has to be determined in advance. This is difficult when the bound of the approximation error is unknown. Improper switching gain easily causes chattering problem which is undesired in practice.

Since the chattering is caused by the switching gain matrix $(\eta + \rho)$ and the discontinuous function $\mathrm{sign}(s)$, let the switching control $u_{sw} = (\eta + \rho)\,\mathrm{sign}(s)$ be replaced by a gain vector $K = [k_1, k_2, \ldots, k_p]$ [17]. Motivated by papers [28–30], in the controller design, we employ fuzzy systems in the form of (3.2) to approximate the gain vector K.

According to the switching control u_{swi} in (4.6), we can choose a single-input single-output fuzzy system $\widehat{k}_i(s_i)$ to approximate the gain k_i. Here, the fuzzy system $\widehat{k}_i$ is applied to

compensate the system uncertainty to reduce the energy of s_i and causes the sliding surface to approach zero. It is obvious that the sign of k_i is the same as that of s_i. When $|s_i|$ is away from zero, $|k_i|$ should be chosen a large value to make the system move quickly to the switching surface. When $|s_i|$ is small, $|k_i|$ should be chosen a small value to avoid overshoot. When s_i is zero, $|k_i|$ should be zero. From the above analysis, it is easy to make $s_i\dot{s}_i \leq 0$ and guarantee the sliding condition. Briefly, the fuzzy rules can be determined as follows:

$$\text{If } s_i \text{ is } A_h, \quad \text{then } k_i \text{ is } B_h, \ h = 1, 2, \ldots, i_L, \tag{4.10}$$

where s_i and k_i are the input and the output variables of the fuzzy system, respectively, and i_L represents the number of fuzzy rules. Then the estimated switching gain $\widehat{k}_i$ of the ith subsystem can be written as

$$\widehat{k}_i = \xi_{si}(s_i)^T \theta_{si}, \tag{4.11}$$

where $\xi_{si}(s_i) = [A_1(s_i/\alpha_i(s_i)), \ldots, A_{i_L}(s_i/\alpha_i(s_i))]^T$ and $\theta_{si} = [b_1, b_2, \ldots, b_{i_L}]^T$. Let

$$\theta_{si}^* = \arg\min_{\|\theta_{si}\| \leq M_{si}} \left\{ \sup_{s_i \in D_{si}} \left| k_i - \xi_{si}(s_i)^T \theta_{si} \right| \right\}, \tag{4.12}$$

be the optimal parameter vector, where M_{si} is design constant restraining parameter vector θ_{si} and D_{si} is compact set containing the variable s_i. The optimal parameter vector θ_{si}^* is unknown, so θ_{si}^* is estimated by θ_{si}.

Further, to cancel the approximation error between the equivalent control u_{eqi} and the used fuzzy system $\widehat{u}_{eqi}$, we append a compensation control term $u_c = [u_{c1}, u_{c2}, \ldots, u_{cp}]^T$ [34]. Therefore, the overall control effort can be modified as

$$u_i = \widehat{u}_{eqi} + \widehat{k}_i + u_{ci} = \xi_{ei}^T(x)\theta_{ei} + \xi_{si}^T(s_i)\theta_{si} + u_{ci} \tag{4.13}$$

or

$$u = \widehat{u}_{eq} + \widehat{K} + u_c = \Xi_e(x)^T \Theta_e + \Xi_s^T(S)\Theta_s + u_c, \tag{4.14}$$

where $\Xi_s(S) = [\mathrm{diag}(\xi_{s1}^T(s1), \xi_{s2}^T(s2), \ldots, \xi_{sp}^T(sp))]^T$ and $\Theta_s = [\theta_{s1}^T, \theta_{s2}^T, \ldots, \theta_{sp}^T]^T$.The compensation control term u_c will be designed next.

Substituting (4.14) into (4.1), we obtain

$$\begin{aligned} G_1(x)\dot{S} &= G_1(x)v - F_1(x) - \left(\Xi_e^T(x)\Theta_e + \Xi_s^T(S)\Theta_s + u_c\right) - G_1(x)D(t) \\ &= \omega - u_c - \left(\Xi_e^T(x)\Theta_e - \Xi_e^T(x)\Theta_e^*\right) - \left(\Xi_s^T(S)\Theta_s - \Xi_s^T(S)\Theta_s^*\right) - \Xi_s^T(S)\Theta_s^* - \delta(x)I_pS. \end{aligned} \tag{4.15}$$

Let $\widetilde{\Theta}_e = \Theta_e - \Theta_e^*$ and $\widetilde{\Theta}_s = \Theta_s - \Theta_s^*$. Combining the above equation, we have

$$G_1(x)\dot{S} = \omega - u_c - \Xi_e^T(x)\widetilde{\Theta}_e - \Xi_s^T(S)\widetilde{\Theta}_s - \Xi_s^T(S)\Theta_s^* - \delta(x)I_pS. \tag{4.16}$$

To derive the adaptive laws of the parameter vectors, let us consider the Lyapunov candidate function

$$V_1 = \frac{1}{2}S^TG_1(x)S + \frac{1}{2\gamma_1}\widetilde{\Theta}_e^T\widetilde{\Theta}_e + \frac{1}{2\gamma_2}\widetilde{\Theta}_s^T\widetilde{\Theta}_s + \frac{1}{2\gamma}\widetilde{\omega}^T\widetilde{\omega}, \tag{4.17}$$

where γ_1, γ_2, γ are positive constants, $\widetilde{\omega} = \omega - \widehat{\omega}$ in which the vector $\widehat{\omega} = [\widehat{\omega}_1, \widehat{\omega}_2, \ldots, \widehat{\omega}_p]^T$ denotes the estimate of the unknown approximation error vector ω.

Theorem 4.2. *For system* (2.1), *nonlinear function matrices* $F(x)$, $G(x)$, *and vector* $D(t)$ *are unknown, and Assumptions 2.1–2.3 hold. The control law is selected as* (4.13) *or* (4.14) *in which* $u_{ci} = \widehat{\omega}_i$ *with adaptation laws* (4.18) *as follows:*

$$\begin{aligned}
\dot{\theta}_{ei} &= \begin{cases} \gamma_1 s_i \xi_{ei}(x), & \|\theta_{ei}\| < M_{ei} \text{ or } \|\theta_{ei}\| = M_{ei},\ \gamma_1 s_i \theta_{ei}^T \xi_{ei}(x) \le 0, \\ \gamma_1 s_i \xi_{ei}(x) - \gamma_1 s_i \dfrac{\theta_{ei}\theta_{ei}^T}{\|\theta_{ei}\|^2}\xi_{ei}(x), & \|\theta_{ei}\| = M_{ei},\ \gamma_1 s_i \theta_{ei}^T \xi_{ei}(x) > 0, \end{cases} \\
\dot{\theta}_{si} &= \begin{cases} \gamma_2 s_i \xi_{si}(s_i), & \|\theta_{si}\| < M_{si} \text{ or } \|\theta_{si}\| = M_{si},\ \gamma_2 s_i \theta_{si}^T \xi_{si}(s_i) \le 0, \\ \gamma_2 s_i \xi_{si}(s_i) - \gamma_2 s_i \dfrac{\theta_{si}\theta_{si}^T}{\|\theta_{si}\|^2}\xi_{si}(s_i), & \|\theta_{si}\| = M_{si},\ \gamma_2 s_i \theta_{si}^T \xi_{si}(s_i) > 0, \end{cases} \\
\dot{\widehat{\omega}}_i &= \gamma s_i,
\end{aligned} \tag{4.18}$$

where M_{ei} *and* M_{si} *are defined as before. Then one can derive the performance as follows.*

(1) *The involved signals of the close loop are bounded.*

(2) *The tracking errors and their derivatives decay to zero asymptotically, in other words, when* $t \to \infty$, $e_i^{(j)} \to 0$, $j = 0, 1, \ldots, r_i - 1$, $i = 1, 2, \ldots, p$.

Proof . Differentiating (4.17) with respect to t and using (4.16), we have

$$\begin{aligned}
\dot{V}_1 &= S^T G_1(x)\dot{S} + \frac{1}{2}S^T \dot{G}_1(x)S + \frac{1}{\gamma_1}\tilde{\Theta}_e^T\dot{\tilde{\Theta}}_e + \frac{1}{\gamma_2}\tilde{\Theta}_s^T\dot{\tilde{\Theta}}_s + \frac{1}{\gamma}\tilde{\omega}^T\dot{\tilde{\omega}} \\
&= S^T\left(\omega - u_c - \Xi_e^T(x)\tilde{\Theta}_e - \Xi_s^T(S)\tilde{\Theta}_s - \Xi_s^T(S)\Theta_s^* - \delta(x)I_pS\right) \\
&\quad + \frac{1}{2}S^T\dot{G}_1(x)S + \frac{1}{\gamma_1}\tilde{\Theta}_e^T\dot{\tilde{\Theta}}_e + \frac{1}{\gamma_2}\tilde{\Theta}_s^T\dot{\tilde{\Theta}}_s + \frac{1}{\gamma}\tilde{\omega}^T\dot{\tilde{\omega}} \\
&\le \sum_{i=1}^{p} s_i\omega_i - \sum_{i=1}^{p} s_i\widehat{\omega}_i - \sum_{i=1}^{p} s_i\tilde{\theta}_{ei}^T\xi_{ei}(x) + \frac{1}{\gamma_1}\sum_{i=1}^{p}\tilde{\theta}_{ei}^T\dot{\tilde{\theta}}_{ei} + \frac{1}{2}S^T\dot{G}_1(x)S - \delta(x)\|S\|^2 \\
&\quad - \sum_{i=1}^{p} s_i\tilde{\theta}_{si}^T\xi_{si}(s_i) + \frac{1}{\gamma_2}\sum_{i=1}^{p}\tilde{\theta}_{si}^T\dot{\tilde{\theta}}_{si} - \sum_{i=1}^{p}\eta_i|s_i| - \frac{1}{\gamma}\sum_{i=1}^{p}\tilde{\omega}_i^T\dot{\tilde{\omega}}_i \\
&\le -\frac{1}{\gamma_1}\sum_{i=1}^{p}\tilde{\theta}_e^T\left(\gamma_1 s_i\xi_{ei}(x) - \dot{\theta}_e\right) - \frac{1}{\gamma_2}\sum_{i=1}^{p}\tilde{\theta}_{si}^T\left(\gamma_2 s_i\xi_{si}(s_i) - \dot{\tilde{\theta}}_{si}\right) \\
&\quad + \frac{1}{\gamma}\sum_{i=1}^{p}\left(\gamma s_i(\omega_i - \widehat{\omega}_i) - \tilde{\omega}_i^T\dot{\tilde{\omega}}_i\right) - \sum_{i=1}^{p}\eta_i|s_i|.
\end{aligned} \tag{4.19}$$

Considering the same sign between s_i and the fuzzy switching term k_i, the first inequality in the above derivation is easily established by using the inequality $\eta_i|s_i| \le s_i\theta_{si}^{*T}\xi_{si}(si) \le (\eta_i + \rho_i)|s_i|$. Noticing (4.18), we have

$$\dot{V}_1 \le -\sum_{i=1}^{p}\eta_i|s_i| < 0. \tag{4.20}$$

Consequently, all signals in the system are bounded. Obviously, if $e(0)$ is bounded, then $e(t)$ is also bounded for all t. Since the reference trajectory x_d is bounded, then the system state $x(t)$ is bounded as well.

To complete the proof and establish asymptotic convergence of the tracking error, we need to prove that $S \to 0$ as $t \to \infty$. We rearrange (4.16) as following:

$$\dot{S} = G(x)\left(\omega - \widehat{\omega} - \Xi_e^T(x)\tilde{\Theta}_e - \Xi_s^T(S)\tilde{\Theta}_s - \Xi_s^T(S)\Theta_s^* - \delta(x)I_pS\right). \tag{4.21}$$

Since $G(x)$ and $\delta(x)$ are continuous functions in a compact set D_x, they are bounded. By using the boundness of S, $\dot{\widehat{\omega}} \in L_\infty$ and in turn $\widehat{\omega} \in L_\infty$. Therefore, $\dot{S} \in L_\infty$ holds. Using Barbalat's lemma, $S \to 0$ $(t \to \infty)$ holds. This completes the proof. □

Remark 4.3. The tracking control using conventional adaptive fuzzy SMC with fuzzy switching control term [28–30] does not tackle the problem of attenuation of the effect of the fuzzy approximation error. We usually have $\dot{V} \le Sw - \eta S^T \operatorname{sign}(S)$. In this case, it can be excepted that Sw should be very small if not equal to zero in [28–30] but here we get $\dot{V} \le -\sum_{i=1}^{p}\eta_i|s_i| < 0$, which improves the stability proof. In order to overcome this restriction, we have proposed $\widehat{\omega}$ to estimate the fuzzy approximation error ω.

Remark 4.4. In conventional adaptive fuzzy SMC design [24, 39, 40], there is often an assumption that the unknown external disturbance $D(t)$ is bounded by a known positive constant. However, it is often not possible to obtain the bound in complex situations. In order to overcome this restriction, the variable $D(t)$ is incorporated into the equivalent control term u_{eq} and a fuzzy system is used to approximate u_{eq}. Therefore, knowledge of the bound of external disturbance is not necessary in the present paper.

4.3. Direct Adaptive Fuzzy SMC with Variable Universe Fuzzy Switching Term (DAFSMC with VUFSW)

As stated in Section 3.2, variable universe fuzzy system possesses high static precision by virtue of contraction-expansion factor. In this subsection, to accelerate response speed and improve the control accuracy, we consider an adaptive fuzzy SMC with VUFSW.

Similar to the analysis in Section 4.2, the variables s_i and k_i are still taken as the input and the output variables of the variable universe fuzzy system. Then the variable universe fuzzy switching control law $\widehat{k}_i$ of the ith subsystem can be written as

$$\widehat{k}_i = \beta_i \zeta_{si}(s_i)^T \theta_{si}, \tag{4.22}$$

where $\zeta_{si}(s_i) = [A_1(s_i/\alpha_i(s_i)), \ldots, A_{i_L}(s_i/\alpha_i(s_i))]^T$ and $\theta_{si} = [b_1, b_2, \ldots, b_{i_L}]^T$.

Let $\beta^* = \operatorname{diag}(\beta_1^*, \beta_2^*, \ldots, \beta_p^*)$ be the optimal parameter vector, where

$$\beta_i^* = \arg\min_{|\beta_i| \le M_i} \left\{ \sup_{s_i \in D_{si}} \left| k_i - \beta_i \zeta_{si}(s_i)^T \theta_{si} \right| \right\}, \tag{4.23}$$

in which M_i is the design constant. Similarly, since the ideal parameter β_i^* is unknown, β_i is employed to estimate β_i^*. Therefore, the overall control effort can be modified as

$$u_i = \widehat{u}_{eqi} + \widehat{k}_i + u_{ci} = \xi_{ei}^T(x)\theta_{ei} + \beta_i \zeta_{si}^T(s_i)\theta_{si} + \widehat{\omega}_i \tag{4.24}$$

or

$$u = \widehat{u}_{eq} + \widehat{K} + u_c = \Xi_e^T(x)\Theta_e + \beta \Xi_s^T(S)\Theta_s + \widehat{\omega}, \tag{4.25}$$

where $\Xi_s(S) = [\operatorname{diag}(\zeta_{s1}^T(s1), \zeta_{s2}^T(s2), \ldots, \zeta_{sp}^T(sp))]^T$ and $\Theta_s = [\theta_{s1}^T, \theta_{s2}^T, \ldots, \theta_{sp}^T]^T$.

Substituting (4.25) into (4.1), we obtain

$$\begin{aligned} G_1(x)\dot{S} &= G_1(x)v - F_1(x) - \left(\Xi_e^T\Theta_e + \beta\Xi_s^T(S)\Theta_s + \widehat{\omega}\right) - G_1(x)D(t) \\ &= (\omega - \widehat{\omega}) - \left(\Xi_e^T\Theta_e - \Xi_e^T\Theta_e^*\right) - \left(\beta\Xi_s^T(S)\Theta_s - \beta^*\Xi_s^T(S)\Theta_s\right) - \beta^*\Xi_s^T(S)\Theta_s - \delta(x)I_pS. \end{aligned} \tag{4.26}$$

Let $\widetilde{\Theta}_e = \Theta_e - \Theta_e^*$ and $\widetilde{\beta} = \beta - \beta^*$. Then

$$G_1(x)\dot{S} = \widetilde{\omega} - \Xi_e^T(x)\widetilde{\Theta}_e - \widetilde{\beta}\Xi_s^T(S)\Theta_s - \beta^*\Xi_s^T(S)\Theta_s - \delta(x)I_pS. \tag{4.27}$$

To derive the adaptive law of the parameter vectors, we consider the Lyapunov candidate function as

$$V_2 = \frac{1}{2}S^TG_1(x)S + \frac{1}{2\gamma_1}\widetilde{\Theta}_e^T\widetilde{\Theta}_e + \frac{1}{2\gamma_3}\widetilde{\beta}^T\widetilde{\beta}^T + \frac{1}{2\gamma}\widetilde{\omega}^T\widetilde{\omega}, \tag{4.28}$$

where γ_3 is a positive constant.

Theorem 4.5. *For system* (2.1), *nonlinear function matrices* $F(x)$, $G(x)$, *and vector* $D(t)$ *are unknown, and Assumptions 2.1–2.3 hold. The control law is selected as* (4.24) *or* (4.25), *with adaptation laws* (4.29) *as follows:*

$$\begin{gathered}
\dot{\theta}_{ei} = \begin{cases} \gamma_1 s_i\xi_{ei}(x), & \|\theta_{ei}\| < M_{ei} \text{ or } \|\theta_{ei}\| = M_{ei},\ \gamma_1 s_i\theta_{ei}^T\xi_{ei}(x) \le 0, \\ \gamma_1 s_i\xi_{ei}(x) - \gamma_1 s_i\dfrac{\theta_{ei}\theta_{ei}^T}{\|\theta_{ei}\|^2}\xi_{ei}(x), & \|\theta_{ei}\| = M_{ei},\ \gamma_1 s_i\theta_{ei}^T\xi_{ei}(x) > 0, \end{cases} \\
\dot{\beta}_i = \begin{cases} \gamma_3 s_i\theta_{si}^T\zeta_{si}(s_i), & |\beta_i| < M_i \text{ or } |\beta_i| = M_i,\ \gamma_3 s_i\theta_{si}^T\zeta_{si}(s_i) \le 0, \\ 0, & |\beta_i| = M_i,\ \gamma_3 s_i\theta_{si}^T\zeta_{si}(s_i) > 0, \end{cases} \\
\dot{\widetilde{\omega}} = \gamma s_i,
\end{gathered} \tag{4.29}$$

where M_{ei} *and* M_i *are defined as before. Then one can derive the performance as follows.*

(1) *The involved signals of the close loop are bounded.*

(2) *The tracking errors and their derivatives decay to zero asymptotically, in other words, when* $t \to \infty$, $e_i^{(j)} \to 0$, $j = 0, 1, \ldots, r_i - 1$, $i = 1, 2, \ldots, p$.

Proof. Differentiating (4.28) with respect to t and using (4.27), we have

$$\begin{aligned}
\dot{V}_2 &= S^TG_1(x)\dot{S} + \frac{1}{2}S^T\dot{G}_1(x)S + \frac{1}{\gamma_1}\widetilde{\Theta}_e^T\dot{\widetilde{\Theta}}_e + \frac{1}{\gamma_3}\widetilde{\beta}^T\dot{\widetilde{\beta}} + \frac{1}{\gamma}\widetilde{\omega}^T\dot{\widetilde{\omega}} \\
&= S^T\left(\widetilde{\omega} - \Xi_e^T(x)\widetilde{\Theta}_e - \widetilde{\beta}\Xi_s^T(S)\Theta_s - \beta^*\Xi_s^T(S)\Theta_s - \delta(x)I_pS\right) \\
&\quad + \frac{1}{2}S^T\dot{G}_1(x)S + \frac{1}{\gamma_1}\widetilde{\Theta}_e^T\dot{\widetilde{\Theta}}_e + \frac{1}{\gamma_3}\widetilde{\beta}^T\dot{\widetilde{\beta}} + \frac{1}{\gamma}\widetilde{\omega}^T\dot{\widetilde{\omega}}
\end{aligned}$$

$$\leq \sum_{i=1}^{p} s_i\tilde{\omega}_i - \frac{1}{\gamma}\sum_{i=1}^{p}\tilde{\omega}_i^T\dot{\hat{\omega}}_i - \sum_{i=1}^{p} s_i\tilde{\theta}_{ei}^T\xi_{ei}(x) + \frac{1}{\gamma_1}\sum_{i=1}^{p}\tilde{\theta}_{ei}^T\dot{\theta}_{ei} + \frac{1}{2}S^T\dot{G}_1(x)S - \delta(x)\|S\|^2$$
$$- \sum_{i=1}^{p} s_i\tilde{\beta}_i\theta_{si}^T\zeta_{si}(s_i) + \frac{1}{\gamma_3}\sum_{i=1}^{p}\tilde{\beta}_i\dot{\beta}_i - \sum_{i=1}^{p}\eta_i|s_i|$$
$$\leq \frac{1}{\gamma}\sum_{i=1}^{p}\tilde{\omega}_i(\gamma s_i - \dot{\hat{\omega}}_i) - \frac{1}{\gamma_1}\sum_{i=1}^{p}\tilde{\theta}_{ei}^T(\gamma_1 s_i\xi_{ei}(x) - \dot{\theta}_{ei}) - \frac{1}{\gamma_3}\sum_{i=1}^{p}\tilde{\beta}_i\left(\gamma_3 s_i\theta_{si}^T\zeta_{si}(s_i) - \dot{\beta}_i\right) - \sum_{i=1}^{p}\eta_i|s_i|. \tag{4.30}$$

Noticing that (4.29), we have

$$\dot{V}_2 \leq -\sum_{i=1}^{p}\eta_i|s_i| < 0. \tag{4.31}$$

Therefore, all signals in the system are bounded. In order to show the boundedness of $\dot{S}$, we rearrange (4.27) as follows:

$$\dot{S} = G(x)\left(\tilde{\omega} - \Xi_e^T(x)\tilde{\Theta}_e - \tilde{\beta}\ \ \Xi_s^T(S)\Theta_s - \beta^*\Xi_s^T(S)\Theta_s - \delta(x)I_pS\right). \tag{4.32}$$

Similarly, we can derive $\dot{S} \in L_\infty$. □

To summarize the above analysis, the step-by-step procedures for the two direct adaptive fuzzy SMCs are proposed as follows.

Design Procedure:

Step 1. Select proper positive coefficients $\lambda_1, \lambda_2, \ldots, \lambda_p$ and learning coefficients $\gamma_1, \gamma_2, \gamma_3$, and γ.

Step 2. Specify design constant vectors $M_e = [M_{e1}, M_{e2}, \ldots, M_{ep}]^T$, $M_s = [M_{s1}, M_{s2}, \ldots, M_{sp}]^T$ and $M = [M_1, M_2, \ldots, M_p]^T$.

Step 3. Define m_i fuzzy sets F_i for variable x_i to achieve an uniform coverage of the universe of discourse. Select the initial parameter vector $\theta_{ei}(0) = \underline{0}_{m_i\times 1}$ $(i = 1, 2, \ldots, p)$.

Step 4. Construct the fuzzy rule bases for the fuzzy system u_{swi}. Define i_L fuzzy sets A_i for variable s_i to achieve a uniform coverage of the universe of discourse. Select the initial parameter vectors $\theta_{si}(0)_{i_L\times 1}$ $(i = 1, 2, \ldots, p)$ for DAFSMC with FSW and the initial values $\beta_i(0)$ $(i = 1, 2, \ldots, p)$ for DAFSMC with VUFSW.

Step 5. Construct the fuzzy systems $\hat{u}_{eqi}$ in (4.9), and $\hat{k}_i$ in (4.11) or (4.22).

Step 6. Construct the control law (4.13) or (4.14) with the adaptive laws in (4.18) or construct the control law (4.24) or (4.25) with the adaptive laws in (4.29).

Step 7. Use the adaptive laws (4.18) or (4.29) to adjust the parameters θ_{ei}, θ_{si} or β_i, and $\hat{\omega}_i$.

5. Simulation Results and Analysis

In this section, we test the proposed control schemes on the trajectory tracking control of the two-link rigid robot manipulators moving a horizontal plane. The equations of motion of the manipulators can be expressed in matrix form as follows [21, 25]:

$$\begin{pmatrix} \ddot{q}_1 \\ \ddot{q}_2 \end{pmatrix} = -\begin{pmatrix} M_{11}, & M_{12} \\ M_{21}, & M_{22} \end{pmatrix}^{-1} \begin{pmatrix} -h\dot{q}_2, & -h(\dot{q}_1+\dot{q}_2) \\ h\dot{q}_1, & 0 \end{pmatrix} \begin{pmatrix} \dot{q}_1 \\ \dot{q}_2 \end{pmatrix} + \begin{pmatrix} M_{11}, & M_{12} \\ M_{21}, & M_{22} \end{pmatrix}^{-1} \begin{pmatrix} u_1 \\ u_2 \end{pmatrix} + \begin{pmatrix} d_1 \\ d_2 \end{pmatrix}, \quad (5.1)$$

where

$$\begin{aligned} M_{11} &= a_1 + 2a_3 \cos q_2 + 2a_4 \sin q_2, \\ M_{22} &= a_2, \\ M_{21} = M_{12} &= a_2 + a_3 \cos q_2 + a_4 \sin q_2, \\ h &= a_3 \sin q_2 - a_4 \cos q_2, \end{aligned} \quad (5.2)$$

in which

$$\begin{aligned} a_1 &= I_1 + m_1 l_{c1}^2 + I_e + m_e l_{ce}^2 + m_e l_1^2, \\ a_2 &= I_e + m_e l_{ce}^2, \\ a_3 &= m_e l_1 l_{ce} \cos \delta_e, \\ a_4 &= m_e l_1 l_{ce} \sin \delta_e. \end{aligned} \quad (5.3)$$

In the simulation, the following parameter values of the plant are used: $m_1 = 1$, $m_e = 2$, $l_1 = 1$, $l_{c1} = 0.5$, $l_{ce} = 0.6$, $I_1 = 0.12$, $I_e = 0.25$, $\delta_e = 30^o$. Let $y = [q_1, q_2]^T$, $u = [u_1, u_2]^T$, $x = [q_1, \dot{q}_1, q_2, \dot{q}_2]^T$,

$$\begin{aligned} F(x) &= \begin{pmatrix} f_1(x) \\ f_2(x) \end{pmatrix} = -\begin{pmatrix} M_{11}, & M_{12} \\ M_{21}, & M_{22} \end{pmatrix}^{-1} \begin{pmatrix} -h\dot{q}_2, & -h(\dot{q}_1+\dot{q}_2) \\ h\dot{q}_1, & 0 \end{pmatrix} \begin{pmatrix} \dot{q}_1 \\ \dot{q}_2 \end{pmatrix}, \\ G(x) &= \begin{pmatrix} g_{11}, & g_{12} \\ g_{21}, & g_{22} \end{pmatrix} = \begin{pmatrix} M_{11}, & M_{12} \\ M_{21}, & M_{22} \end{pmatrix}^{-1}, \qquad D(t) = \begin{pmatrix} d_1 \\ d_2 \end{pmatrix}. \end{aligned} \quad (5.4)$$

Then, the robotic manipulators dynamics given by (5.1) can be expressed as

$$\ddot{y} = F(x) + G(x)u + D(t). \quad (5.5)$$

The object is to design control law u to force the system output q_1 and q_2 to track the desired trajectories $y_{d1} = \sin t$ and $y_{d2} = \sin t$, respectively. The initial state is selected as $x_0 = [1, 0, 1, 0]^T$. The fuzzy system $\widehat{k}_i$ $(i = 1, 2)$ in (4.9) have $x = [q_1, \dot{q}_1, q_2, \dot{q}_2]^T$ as inputs. For each input variable, we define three triangular membership functions uniformly distributed on the interval $[-1, 1]$. s_i and k_i are the input and the output of the fuzzy system $\widehat{u}_{swi}$ $(i = 1, 2)$

Table 1: Fuzzy rule list of variable universe fuzzy switching control.

Input s_i	PB	PM	PS	ZE	NS	NM	NB
Output k_i	PB	PM	PS	ZE	NS	NM	NB

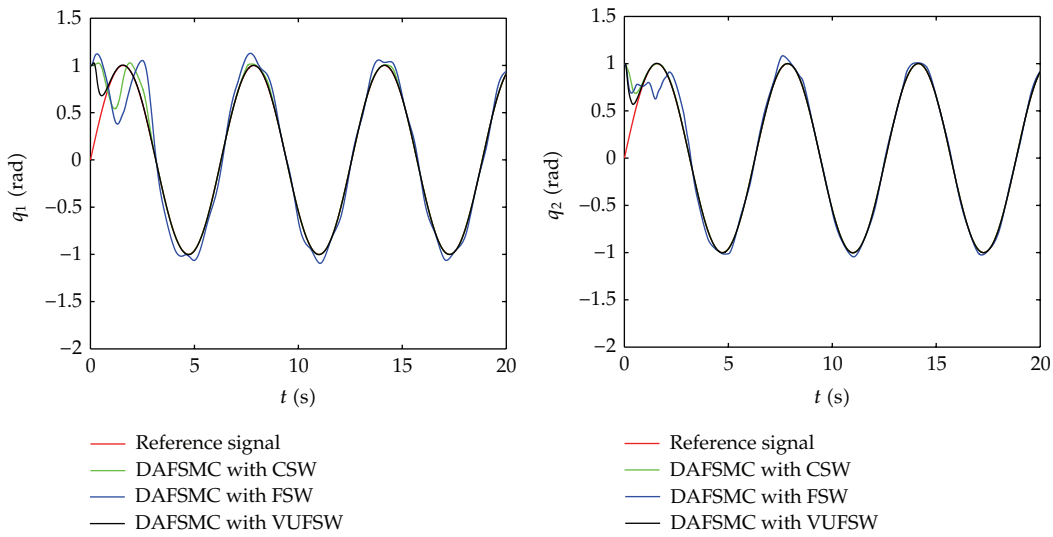

(a) Tracking curve of q_1 (b) Tracking curve of q_2

Figure 1: Angular trajectory tracking curves of robotic manipulators.

in (4.11) and (4.22), respectively. We define seven triangle membership functions uniformly distributed on the input domain $[-2, 2]$ and the output domain $[-1, 1]$, respectively. The used fuzzy rules are showed in Table 1, in which the fuzzy labels used in this study are negative big (NB), negative medium (NM), negative small (NS), zero (ZE), positive small (PS), positive medium (PM), and positive big (PB).

In this paper, we consider that the nonlinear function matrices $F(x)$ and $G(x)$ are assumed to be completely unknown, that is, the design of the proposed controller does not require the knowledge of the system's model. Moreover, the external disturbance $D(t)$ is also unknown. In fact, these functions are only required for simulation purpose. To make a fair comparison, in the simulation, we consider the direct adaptive fuzzy SMC proposed by A. Boulkroune et al. in [21] where a classical switching control term is employed to eliminate the fuzzy approximation error (hereafter referred to as a DAFSMC with CSW).

In the whole simulation, the design parameters used are chosen as follows: $\lambda_1 = \lambda_2 = 5$, $\gamma_1 = 1$, $\gamma_2 = 8$, $\gamma_3 = 8$, $\gamma = 1$, $M_{e1} = 2$, $M_{e2} = 1$, $M_{s1} = 50$, $M_{s2} = 20$, $M_1 = M_2 = 2$, $\eta_1 = 13$, $\eta_2 = 6$ and the contraction-expansion factors $\alpha_i = 1 - \lambda \exp(-k s_i^2)$ $(i = 1, 2)$ with $\lambda = 0.95$, $k = 1$. The initial conditions of the online adjustable parameter vectors are selected as $\theta_{ei} = [\underline{0}]_{81\times 1}$ $(i = 1, 2)$, $\theta_{si} = [-3, -2, -1, 0, 1, 2, 3]^T$ $(i = 1, 2)$, and $\beta(0) = \mathrm{diag}(5, 1)$.

To verify the robust stability of the proposed schemes, external disturbances are chosen as square wave signal $d_1 = d_2 = \mathrm{square}(2\pi t)$ [21]. The response curves, the tracking error curves, and sliding mode dynamic evolution curves under the aforementioned three control schemes are illustrated in Figures 1, 2, and 3, respectively. Their associated control efforts are illustrated in Figure 4. For evaluating numerically their tracking performance, the integral

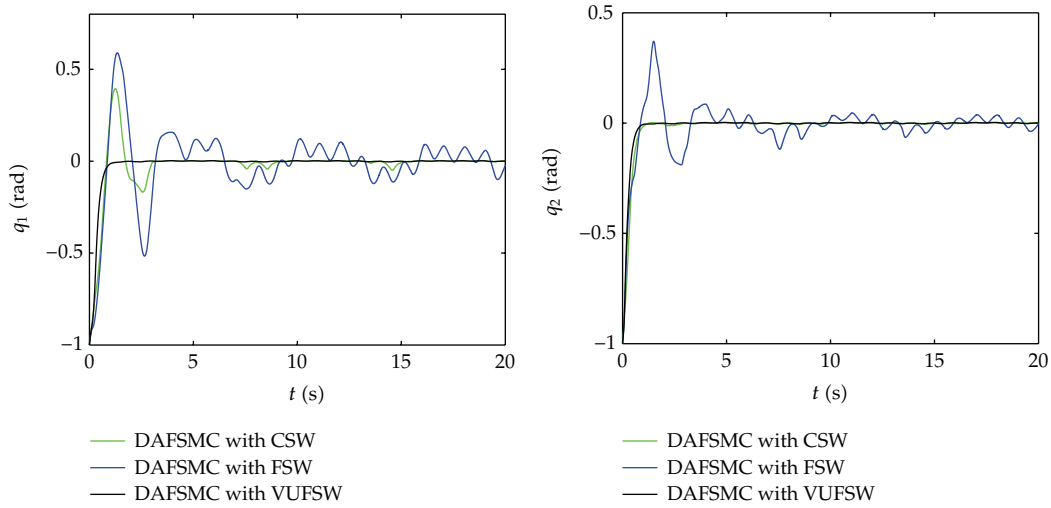

(a) Tracking error of q_1 (b) Tracking error of q_2

Figure 2: Angular trajectory tracking error curves of robotic manipulators.

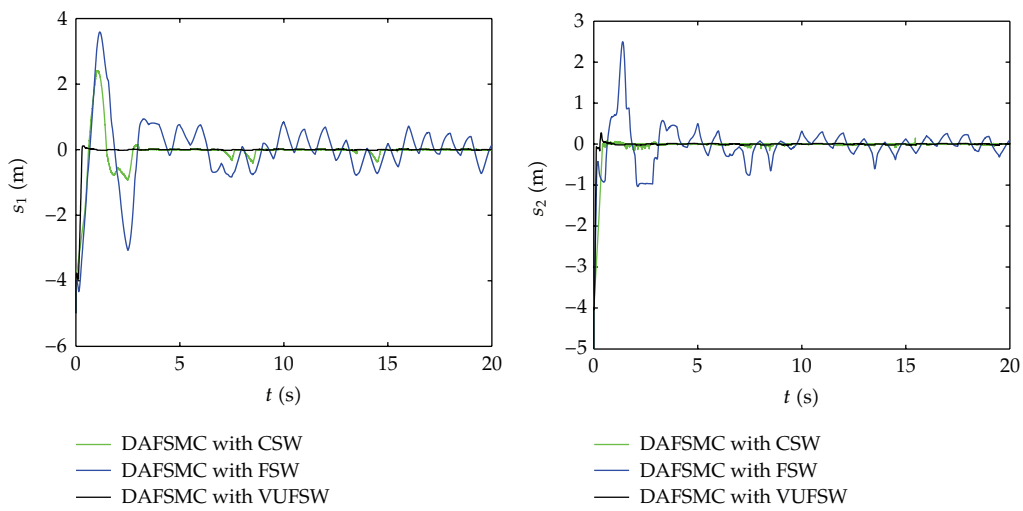

(a) Sliding surface s_1 (b) Sliding surface s_2

Figure 3: Sliding mode dynamic evolution curves.

of the absolute error (IAE), the integral of the time multiplied by the absolute error (ITAE), and the integral of square value (ISV) of the control input are also considered because mere visual observation of response curve is not always enough to make a sound comparison. The corresponding tracking performance indices in first 20 seconds and in first 100 seconds are tabulated in Tables 2 and 3, respectively.

As shown in Figures 1–4, the proposed two schemes can effectively achieve the trajectory tracking of the joint angles despite of the system uncertainties and external disturbances. Furthermore, they can effectively alleviate the chattering, which is the main

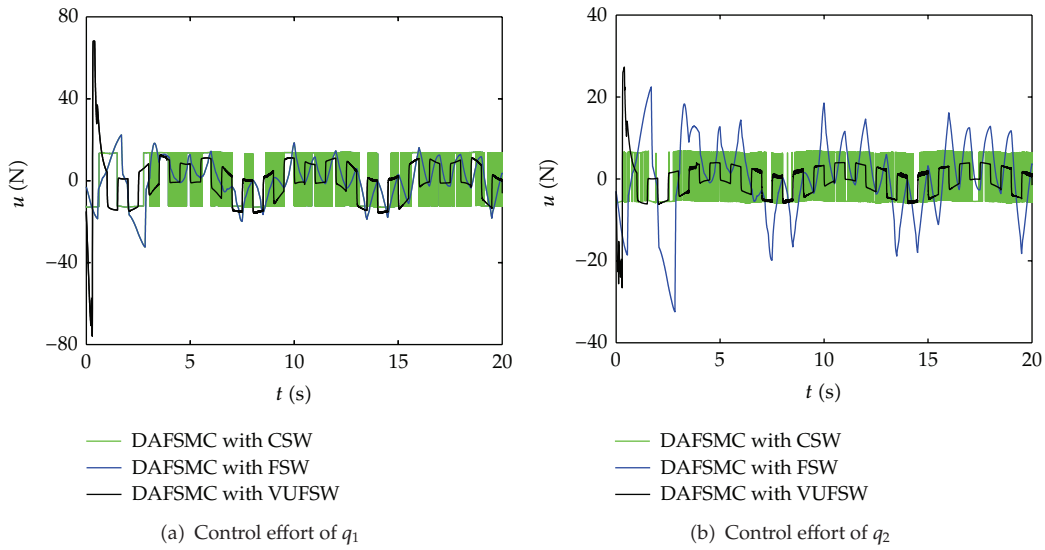

(a) Control effort of q_1 (b) Control effort of q_2

Figure 4: Control input torques of robotic manipulators.

Table 2: The performance indices in 20 seconds.

Controller	rod1			rod2		
	IAE (rad)	ITAE (rad · s)	ISV (N^2)	IAE (rad)	ITAE (rad · s)	ISV (N^2)
DAFSMC with CSW	0.8485	1.5820	$3.3838e+03$	0.4191	0.3299	704.3263
DAFSMC with FSW	2.3991	12.8742	$1.9102e+03$	1.1504	5.3901	253.8947
DAFSMC with VUFSW	0.3923	0.3867	$2.9613e+03$	0.2852	0.3180	437.4319

disadvantage of general SMC. It can also be seen from Figures 1–3, the performance specifications of DAFSMC with VUFSW are much better than those of DAFSMC with CSW and DAFSMC with FSW in terms of reaching time, steady precision.

Both IAE and ITAE are used as evaluating error performance, while the criterion ISV shows energy consumption. It is well known that there is a trade-off between error performance and energy consumption, that is, when IAE and ITAE are improved, ISV becomes worse, and vice versa. Conservative control input is often required to guarantee the stability of the control system in DAFSMC with CSW scheme. Therefore, DAFSMC with CSW expends relatively more energy to achieve the tracking task than DAFSMC with FSW. It also implies that the indices IAE and ITAE of DAFSMC with FSW become worse. But DAFSMC with VUFSW simultaneously improves IAE and ITAE as well as ISV as compared to the others as stated in Tables 2 and 3. It is undeniable that DAFSMC with VUFSW expends more energy than DAFSMC with FSW in the initial stage due to its fast response speed. However, thanks to the high precision of the variable universe fuzzy control, its energy consumption reduces quickly in the steady state.

Remark 5.1. As already stated in Section 1, in the presence of model uncertainties and external disturbances, the two disadvantages of general SMC cannot be overcome just using fuzzy switching technique or adaptive fuzzy SMC. Combining adaptive fuzzy SMC with fuzzy or variable universe fuzzy switching technique, a novel framework for designing direct

Table 3: The performance indices in 100 seconds.

Controller	rod1			rod2		
	IAE (rad)	ITAE (rad · s)	ISV (N^2)	IAE (rad)	ITAE (rad · s)	ISV (N^2)
DAFSMC with CSW	1.4397	33.2521	$1.6863e+04$	0.4722	6.6922	$3.5550e+03$
DAFSMC with FSW	3.9996	97.6183	$9.0121e+03$	2.1688	63.2731	$1.2830e+03$
DAFSMC with VUFSW	0.5073	7.2268	$8.6772e+03$	0.3844	6.1505	$1.2590e+03$

adaptive fuzzy SMC is developed for a class of MIMO nonlinear systems in this study. The derived schemes can effectively overcome these disadvantages of the general SMC.

Remark 5.2. Compared with [22, 24, 28–30, 38, 41], our proposed control schemes have several advantages as follows. (i) The proposed schemes can simultaneously solve the chattering and the calculation of the equivalent control in the presence of model uncertainties and unknown disturbances. (ii) The constraint on the control gain matrix is relaxed. In this study, the gain matrix is just required to be positive definite symmetric and the inverse of its derivative is bounded by an unknown function. (iii) An adaptive compensation term is appended to remove the assumption on fuzzy approximation error in the stability proof. (iv) The derived DAFSMC with VUFSW achieves better performances than the others in terms of response speed, steady accuracy, IAE, ITAE, and ISV.

6. Conclusion

A novel framework is developed to design a direct adaptive fuzzy SMC for a class of MIMO nonlinear systems with model uncertainties and unknown disturbances. Combining adaptive fuzzy SMC with fuzzy or variable universe fuzzy switching technique, this study proposes two novel direct adaptive fuzzy SMC schemes. The derived schemes effectively overcome the two disadvantages of general SMC. Besides, the constraint on the control gain matrix and the fuzzy approximation error are relaxed. Future works will focus on the extension of the framework to more general MIMO nonlinear systems such as the continuous-time or the discrete-time nonaffine nonlinear systems.

Acknowledgments

This work was partly supported by NSFC project (no. 61074044), Basic Scientific and Technological Frontier project of Henan province (no. 092300410178), Scientific Research key project of Henan provincial Education Department (no. 12B110007), and Specialized Research Fund for the Doctoral Program of Higher Education (no. 20090041110003).

References

[1] H. Hu and P. Y. Woo, "Fuzzy supervisory sliding-mode and neural-network control for robotic manipulators," *IEEE Transactions on Industrial Electronics*, vol. 53, no. 3, pp. 929–940, 2006.
[2] Z. S. Song, J. Q. Yi, D. B. Zhao, and X. Li, "A computed torque controller for uncertain robotic manipulator systems: fuzzy approach," *Fuzzy Sets and Systems*, vol. 154, no. 2, pp. 208–226, 2005.
[3] J. J. Slotine and W. Li, *Applied Nonlinear Control)*, Prentice-Hall, Englewood Cliffs, NJ, USA, 1991.
[4] L. G. Wu, X. J. Su, and P. Shi, "Sliding mode control with bounded L_2 gain performance of Markovian jump singular time-delay systems," *Automatica*, vol. 48, pp. 1929–1933, 2012.

[5] J. T. Fei M and Y. Xin, "Robust adaptive sliding mode controller for semi-active vehicle suspension system," *International Journal of Innovative Computing Information and Control*, vol. 8, no. 1, pp. 691–700, 2012.
[6] Q. Khan, A. I. Bhatti, M. Iqbal et al., "Dynamic integral sliding mode control for SISO uncertain nonlinear systems," *International Journal of Innovative Computing Information and Control*, vol. 8, no. 7, pp. 4621–4633, 2012.
[7] M. Ertugrul and O. Kaynak, "Neuro sliding mode control of robotic manipulators," *Mechatronics*, vol. 10, pp. 243–267, 2000.
[8] X. J. Su, P. Shi, L. G. Wu et al., "A novel control design on discrete-timeTakagi-Sugeno fuzzy systems with timevarying delays," *IEEE Transactions on Fuzzy Systems*. In press.
[9] X. J. Su, P. Shi, L. G. Wu et al., "A novel approach to filter design for T-S fuzzy discrete-time systems with timevarying delay," *IEEE Transactions on Fuzzy Systems*, vol. 20, no. 6, pp. 1114–1129, 2012.
[10] L. X. Wang and J. M. Mendel, "Fuzzy basis functions, universal approximation, and orthogonal least-squares learning," *IEEE Transactions on Neural Networks*, vol. 3, no. 5, pp. 807–814, 1992.
[11] L. G. Wu, X. J. Su, P. Shi et al., "Model approximation for discrete-time state-delay systems in the T-S fuzzy framework," *IEEE Transactions on Fuzzy Systems*, vol. 19, no. 2, pp. 366–378, 2011.
[12] Q. Zhou, P. Shi, S. Y. Xu et al., "Adaptive output feedbackcontrol for nonlinear time-delay systems by fuzzy approximation approach. IEEE," *Transactions on Fuzzy Systems*. In press.
[13] Q. Zhou, P. Shi, J. J. Lu et al., "Adaptive output-feedback fuzzy tracking control for a class of nonlinear systems," *IEEE Transactions on Fuzzy Systems*, vol. 19, no. 5, pp. 972–982, 2011.
[14] T. C. Lin, S. W. Chang, and C. H. Hsu, "Robust adaptive fuzzy sliding mode control for a class of uncertain discrete-time nonlinear systems," *International Journal of Innovative Computing Information and Control*, vol. 8, no. 1, pp. 347–359, 2012.
[15] M. Roopaei and M. Zolghadri Jahromi, "Chattering-free fuzzy sliding mode control in MIMO uncertain systems," *Nonlinear Analysis. Theory, Methods & Applications*, vol. 71, no. 10, pp. 4430–4437, 2009.
[16] H. T. Yau and C. L. Chen, "Chattering-free fuzzy sliding-mode control strategy for uncertain chaotic systems," *Chaos, Solitons and Fractals*, vol. 30, no. 3, pp. 709–718, 2006.
[17] N. Sadati and R. Ghadami, "Adaptive multi-model sliding mode control of robotic manipulators using soft computing," *Neurocomputing*, vol. 71, pp. 2702–2710, 2008.
[18] H. Lee, E. Kim, H.-J. Kang, and M. Park, "A new sliding-mode control with fuzzy boundary layer," *Fuzzy Sets and Systems*, vol. 120, no. 1, pp. 135–143, 2001.
[19] Y. R. Hwang and M. Tomizuka, "Fuzzy smoothing algorithms for variable structure systems," *IEEE Transactions on Fuzzy Systems*, vol. 2, no. 4, pp. 277–284, 1994.
[20] M. H. Korayem, R. Haghighi, A. H. Korayem et al., "Determining maximum load carrying capacity of planar flexiblelink robot: closed-loop approach," *Robotica*, vol. 28, pp. 959–973, 2010.
[21] A. Boulkroune, M. Tadjine, M. M'Saad, and M. Farza, "Fuzzy adaptive controller for MIMO nonlinear systems with known and unknown control direction," *Fuzzy Sets and Systems*, vol. 161, no. 6, pp. 797–820, 2010.
[22] J.-Y. Chen, "Rule regulation of fuzzy sliding mode controller design: direct adaptive approach," *Fuzzy Sets and Systems*, vol. 120, no. 1, pp. 159–168, 2001.
[23] Y. Byungkook and H. Woonchul, "Adaptive fuzzy sliding mode control of nonlinear system," *IEEE Transactions on Fuzzy Systems*, vol. 6, no. 2, pp. 315–321, 1998.
[24] H. F. Ho, Y. K. Wong, and A. B. Rad, "Robust fuzzy tracking control for robotic manipulators," *Simulation Modelling Practice and Theory*, vol. 15, no. 7, pp. 801–816, 2007.
[25] S. Labiod, M. S. Boucherit, and T. M. Guerra, "Adaptive fuzzy control of a class of MIMO nonlinear systems," *Fuzzy Sets and Systems*, vol. 151, no. 1, pp. 59–77, 2005.
[26] B. Yoo and W. Ham, "Adaptive fuzzy sliding mode control of nonlinear system," *IEEE Transactions on Fuzzy Systems*, vol. 6, no. 2, pp. 315–321, 1998.
[27] S. Frikha, M. Djemel, and N. Derbel, "Observer based adaptive neuro-sliding mode control for MIMO nonlinear systems," *International Journal of Control*, vol. 8, no. 2, pp. 257–265, 2010.
[28] P. T. Chan, A. B. Rad, and J. Wang, "Indirect adaptive fuzzy sliding mode control. II. Parameter projection and supervisory control," *Fuzzy Sets and Systems*, vol. 122, no. 1, pp. 31–43, 2001.
[29] J. Wang, A. B. Rad, and P. T. Chan, "Indirect adaptive fuzzy sliding mode control. I. Fuzzy switching," *Fuzzy Sets and Systems*, vol. 122, no. 1, pp. 21–30, 2001.
[30] M. Roopaei, M. Zolghadri, and S. Meshksar, "Enhanced adaptive fuzzy sliding mode control for uncertain nonlinear systems," *Communications in Nonlinear Science and Numerical Simulation*, vol. 14, no. 9-10, pp. 3670–3681, 2009.

[31] P. A. Phan and T. J. Gale, "Direct Adaptive fuzzy control with less restrictions on the control gain," *International Journal of Control Automation and Systems*, vol. 5, no. 6, pp. 621–629, 2007.
[32] S. Labiod and T. M. Guerra, "Direct adaptive fuzzy control for a class of MIMO nonlinear systems," *International Journal of Systems Science*, vol. 38, no. 8, pp. 665–675, 2007.
[33] H.-X. Li, Z.-H. Miao, and E. S. Lee, "Variable universe stable adaptive fuzzy control of a nonlinear system," *Computers & Mathematics with Applications*, vol. 44, no. 5-6, pp. 799–815, 2002.
[34] S. Aloui, O. Pages, A. El Hajjaji et al., "Improved fuzzy sliding mode control for a class of MIMO nonlinear uncertain and perturbed systems," *Applied Soft Computing*, vol. 11, pp. 820–826, 2011.
[35] H. X. Li, "Interpolation mechanism of fuzzy control," *Science in China E.*, vol. 41, no. 3, pp. 312–320, 1998.
[36] H. X. Li, "Adaptive fuzzy controllers based on variable universe," *Science in China E*, vol. 42, no. 1, pp. 10–20, 1999.
[37] H. X. Li, "Essence of fuzzy control in mathematics and design on a class of high-accuracy fuzzy controller," *Control theory and Applications*, vol. 14, no. 6, pp. 868–876, 1997.
[38] L. X. Wang, "Stable adaptive fuzzy control of nonlinear systems," *IEEE Transactions on Fuzzy Systems*, vol. 1, no. 2, pp. 146–155, 1993.
[39] M. R. Faieghi, H. Delavari, and D. Baleanu, "A novel adaptive controller for two-degree of freedom polar robot with unknown perturbations," *Communications in Nonlinear Science and Numerical Simulation*, vol. 17, no. 2, pp. 1021–1030, 2012.
[40] V. Nekoukar and A. Erfanian, "Adaptive fuzzy terminal sliding mode control for a class of MIMO uncertain nonlinear systems," *Fuzzy Sets and Systems*, vol. 179, pp. 34–49, 2011.
[41] Y. C. Chang, "Adaptive fuzzy-based tracking control for nonlinear SISO systems via VSS and approaches," *IEEE Transactions on Fuzzy Systems*, vol. 9, pp. 278–292, 2001.

Hindawi Publishing Corporation
Mathematical Problems in Engineering
Volume 2012, Article ID 432129, 12 pages
doi:10.1155/2012/432129

Research Article

Low-Speed Control of Heavy-Load Transfer Robot with Long Telescopic Boom Based on Stribeck Friction Model

Bo You, Ming Qiao, Jiazhong Xu, and Dan Liu

College of Automation, Harbin University of Science and Technology, Harbin 150080, China

Correspondence should be addressed to Ming Qiao, chrisjoe0728@gmail.com

Received 5 September 2012; Accepted 23 October 2012

Academic Editor: Hamid Reza Karimi

Copyright © 2012 Bo You et al. This is an open access article distributed under the Creative Commons Attribution License, which permits unrestricted use, distribution, and reproduction in any medium, provided the original work is properly cited.

The severe low-speed creep phenomenon occurs in the telescopic boom system of a heavy-load transfer robot with a long telescopic boom as a result of nonlinear friction. In order to improve control precision and operation performance at low speeds, we built a three-loop control nonlinear model of an AC servo motor with Stribeck friction disturbance. Traditional proportional-integral-derivative controller (PID) and fuzzy PID controls were, respectively, adopted in the position loop, and the control performance was simulated. The results showed that a system with fuzzy PID control eliminates "flat top" position tracking and "dead zone" speed tracking, which are generated by traditional PID, and thereby decreases the effect of friction on the performance of the servo system. This elimination also improved the tracking accuracy and robustness of the system.

1. Introduction

The heavy-load transfer robot with a long telescopic boom is an automatic equipment used to replace manual labour. It is widely used in situations where a small entrance leads into a large inner space, such as in installations in airplanes, space capsules, and bullet trains. The accuracy of the assembly and safety of the high-tech products installed depend on the positioning accuracy and stability of the robot when moving at low speeds. In an extensive system that bears heavy loads like this one, friction is a key factor that cannot be neglected.

Many research of adopting fuzzy control to solve the problem of stability of robot have been done, as example of [1–5]. Friction is a physical phenomenon that is complex, nonlinear, and probabilistic. It is generated between contacting surfaces that are in relative motion or tending to such motions [6, 7]. Friction significantly contributes to the effect that

low-speed creep and steady-state cyclic oscillations have on the dynamic and static properties of the system [8, 9]. In a heavy-load transfer robot system with a long telescopic boom, the quivering caused by the low-speed creep of the telescopic boom affects not only the response of the system but also its mechanical structure. Hence, eliminating the constraint of the nonlinear friction element in the mechanical system is the key to improving the performance of the control system.

The key to solving the problem of nonlinear friction is the development of an applicable friction model and the adoption of the dynamic compensation and advanced control algorithm [10]. Many scholars have done extensive research on this subject. According to nonlinear systems, Qiu et al. do some simulation studies about subsection $H\infty$ static output feedback control [11] based on fuzzy control and asynchronous output feedback control [12] based on fuzzy affine model, and the results indicate the effectiveness of this method presented. Li et al. do some simulation studies about reliable fuzzy control [13] with run time delay and fault active suspension system and adaptive sliding mode control of the nonlinear vehicle active suspension system [14] based on T-S fuzzy approaches, and the results indicate the effectiveness of control technology design. Xu and Yao put forward nonlinear dynamic friction compensation [15] and achieved self-adaption compensation control of friction. However, this method requires the foreknowledge of the structures and characteristic parameters of the friction model, and it is difficult to realise in practise. Morel proposed that adopting torque feedback control restrains friction interference [16]. This method is effective but is not widely used because the sensor that it requires is expensive and difficult to install. Besides, the flexibility of the system is increased by the installation. Xiao et al. simulated the flight simulation turntable servo system. He found that adopting the traditional PID (proportional-integral-derivative) control method was more effective when there was no friction. Highaccuracy tracking can only be achieved in a friction element by the addition of advanced PID control to traditional PID control [17].

For solving the nonlinear friction problem happening with heavy-duty servo system running slowly to improving control precision and performance of control system, in this paper, a fuzzy PID control based on a Stribeck friction model is proposed for controlling the telescopic boom of the heavy-load transfer robot with a long telescopic boom to achieve low-speed and high-precision control. We also present our three-loop control nonlinear model of an AC servo motor with Stribeck friction. Traditional PID and fuzzy PID controls were, respectively, adopted for the positioning loop, and the control performance was simulated. The results showed that traditional PID cannot be easily used to achieve the desired control performance, but adopting fuzzy PID control can yield better positioning and speed-tracking accuracy. Fuzzy-PID control algorithm fuses fuzzy control and PID control, and make up for the deficiency of the other party with their respective advantages. On the one hand, it makes PID control have the intellectuality of fuzzy control. On the other hand, it makes fuzzy control have certain structure [18]. Compared with past control algorithm, it has the advantages such as conciser algorithm, stronger robustness, wider subject range, higher control precision, overcoming nonlinear, and so on [19–21].

This paper partly removes the nonlinear rub problem of big arms-outstretched heavy-duty servo system, improving control precision and performance of control system, providing valuable reference for removing the influence of the nonlinear rub when heavy-duty servo system runs at a low speed, providing a powerful support for successfully using Fuzzy-PID control on engineering control system, and providing an another way to solve nonlinear rub problem in the control system.

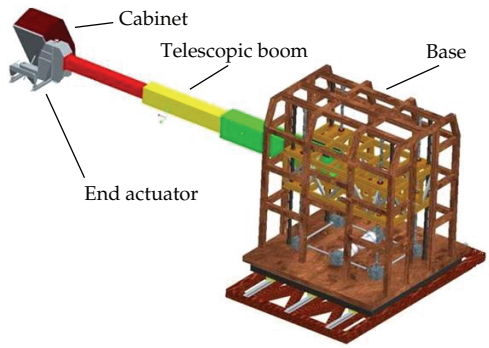

Figure 1: Three-dimensional map of a heavy loading and unloading robot with outstretched arm.

2. Control System Design of Heavy-Load Transfer Robot with Long Telescopic Boom

The structure of the heavy-load transfer robot with long telescopic boom is shown in Figure 1. It includes the base, telescopic boom, and end actuator. The telescopic boom, which has a length of 6.6 m, is moveable and bears the loads. It is an extensive and heavy-load system, so the influence of friction on its performance cannot be neglected. This is especially so when it is running at a super-low speed and bearing heavy load, which would result in a severe case of the creep phenomenon.

The control system of the robot is shown in Figure 2. It primarily consists of the motion controller, servo motor, and industrial computer. Its architecture comprises a host and lower computer with different CPUs, with the industrial computer and PMAC constituting a strong functional opening motion control system. The industrial computer serves as a user interface and medium for system state feedback, while the PMAC is used for motion and logical control. The PMAC2A-PC104 communicates in real-time with the host computer through the RS232 port. The host computer converts the operator's commands into control parameters and downloads the parameters to the PMAC through the serial port. The PMAC completes the operation and logical control and uploads the status of the machine to the display of the host computer. VC++6.0 is used in programming the host computer of the control system. The host computer, which uses a WINDOWS operating system, completes the settings of the control parameters and the status display. The control software of the lower computer includes two parts: one to write the PLC program that executes the I/O signal disposition for PMAC and the instructions of the schedule of motion control program and the other to write the motion control program for the servo motor. With these two programs, the robot can be conveniently controlled.

3. Stribeck Friction Model

Owing to its complexity, it is difficult to directly test friction. Considering that the output torsion of a motor is equal to the sum of the motor and load torque, rotor and moment of inertia of the load, friction torque and disturbance. In the experiment, the controller operated the motor smoothly and eliminated various moments of inertia. The total friction torque generated by the load and rotor could be measured approximately.

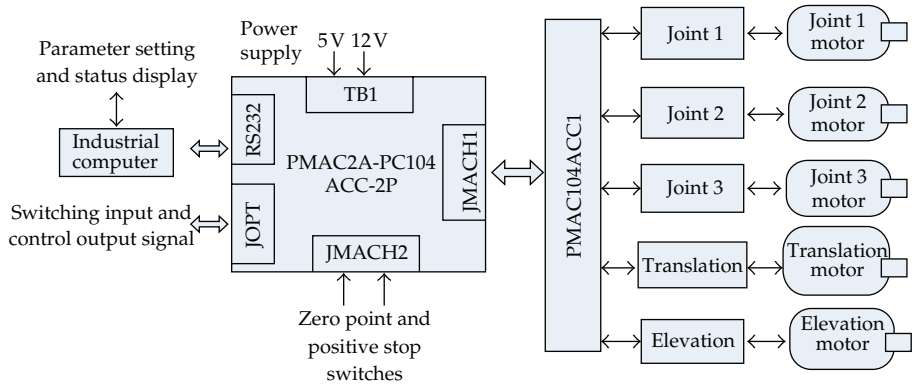

Figure 2: Control system structure of the telescopic boom.

Obviously, it is difficult to maintain uniform motion in a telescopic boom's low-speed zone in an actual system. To facilitate the development of the friction model of the telescopic boom system, we designed a test-bed of the strong stiffness [22] shrink ratio telescopic boom strove system, which included an experimental stent, servo, ball screw, and load block. They corresponded to the outriggers, servo motor, ball screw, and transportation load of an actual telescopic boom system. The friction between the load block and the test-bed corresponded to the friction between the lead screw and the ball, while the friction between the load block and the ball screw corresponded to the friction between outrigger and outrigger of an actual system.

In this system, the servo motor powered the load module through a ball screw. The weight of the load was appropriately selected to maintain a constant speed for the load block in the low-speed zone. By inputting the appropriate parameters to the servo motor driver, several types of experimental data could be collected by adjusting the value of the torsion output through the monitoring interface and the value of the actual speed of the servo drive. Table 1 lists the friction torque data for different speeds.

The curve fitting of the friction torque was done with Matlab, as shown in Figure 3.

As can be seen from the relationship between the friction torque and the speed, it is more appropriate to select the Stribeck friction model for this system. According to the research of scholars, the Stribeck friction model most appropriately describes the behaviour of friction [6] in the low-speed zone. Thus, the model was adopted in our study of the influence of friction on the long telescopic boom of a heavy-load transfer robot. Figure 4 shows the Stribeck curve [10, 23].

The Stribeck friction model can be demonstrated with the following.

When $|v(t)| < \alpha$, the static friction is

$$F_f(t) = \begin{cases} F_m & F(t) > F_m, \\ F(t) & -F_m < F(t) < F_m, \\ -F_m & F(t) < -F_m. \end{cases} \tag{3.1}$$

Table 1: Correspondence between speed and friction torque.

Speed (rad/s)	0.35	0.56	1.00	3.30	6.00	7.50	10.00
Friction torque (N·m)	−0.82	−0.88	−0.74	−0.64	−0.47	−0.53	−0.42
Speed (rad/s)	15.00	17.50	20.00	25.00	30.00	34.70	40.00
Friction torque (N·m)	−0.56	−0.54	−0.51	−0.64	−0.58	−0.56	−0.63

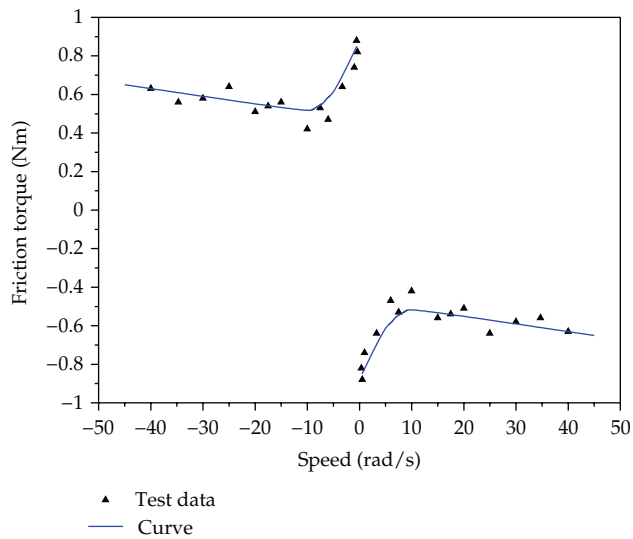

Figure 3: Friction torque curve-fitting.

When $|v(t)| > \alpha$, the dynamic friction is

$$F_f(t) = \left[F_c + (F_m - F_c)e^{-\alpha_1|v(t)|}\right]\operatorname{sgn}(v(t)) + K_v v(t),$$
$$F(t) = -Jv(t), \tag{3.2}$$

where $F(t)$ is the driving force, F_c is the coulomb friction, F_m is the maximum static friction, K_v is the viscous friction coefficient, and α and α_1 are the titchy integers.

4. Design of Fuzzy PID Controller

PID control is widely used in conventional control systems and has the advantages of simplicity of principle, ease of realisation, and high precision. It can be designed both analytically on the basis of mathematical models and by experiment and trial-and-error. However, nonlinear friction is known to increase the difficulty of control with a telescopic boom AC servo control system. It is therefore difficult to guarantee the control performance when a traditional PID control algorithm is adopted. Fuzzy control is more adaptive and performs robustly in complex nonlinear systems. However, a static error exists in fuzzy control, and it is not suitable for precision control [24–26]. The fuzzy PID control combines the advantages of fuzzy logic control and traditional PID control; it applies the control experience of human

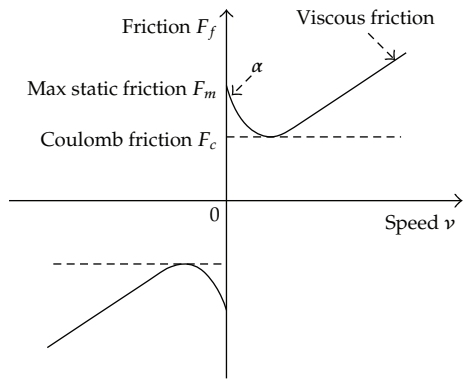

Figure 4: Friction-speed relationship curve (Stribeck curve).

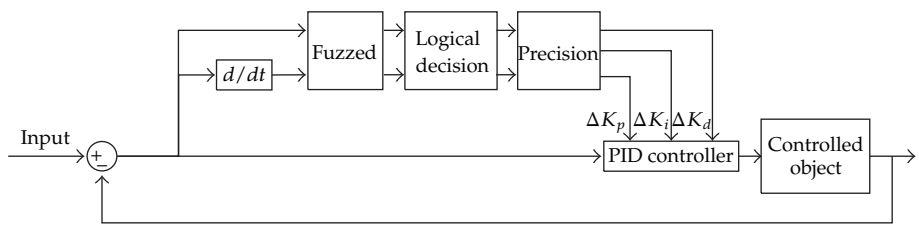

Figure 5: Structure of fuzzy adaptive PID controller.

experts, has robust performance, and is precise in handling a nonlinear complex control system.

Fuzzy PID control adopts fuzzy regulations in modifying three parameters of PID online to constitute the fuzzy adaptive PID controller, shown in Figure 5.

The process involves considering the error e and the error changing rate ec as inputs, and then blurring them. Fuzzy regulations are adopted in the blurring and deduction and eventually produce more accurate inference results, which are used to adjust the parameters of the PID controller by consulting the fuzzy matrix table [27]. The final parameters of the fuzzy PID are determined by

$$\begin{aligned} K_p &= K_{po} + \Delta K_p, \\ K_i &= K_{io} + \Delta K_i, \\ K_d &= K_{do} + \Delta K_d, \end{aligned} \tag{4.1}$$

where K_{po}, K_{io}, and K_{do} are the initial PID values.

The universe of the variables K_p, K_i, and K_d are even fuzzy subsets of $\{\mathrm{NB}, \mathrm{NM}, \mathrm{NS}, \mathrm{ZO}, \mathrm{PS}, \mathrm{PM}, \mathrm{PB}\}$, the membership function of which obeys the triangle disturbance. Figure 6 shows the distribution map of the membership function.

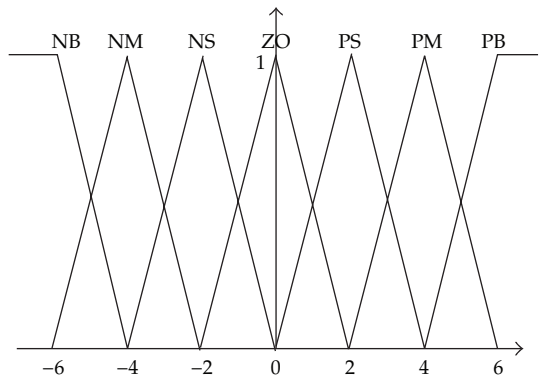

Figure 6: Distribution map of the membership function.

5. System Model Development

A three-loop control model was adopted for the AC servo system of the telescopic boom. The current loop and speed loop were achieved by a traditional PID integrated in the servo, while the position loop was achieved by a fuzzy PID integrated in the *PMAC* motion controller. The position loop was a semiclosed loop, and the feedback was the angular displacement of the servo motor shaft. The triphase AC permanent magnetic synchronous machine (PMSM) was used, and the effect of the spatial harmonics was ignored. It was assumed that the three-phase winding was symmetrical and the magnetic motive force (MMF) was distributed sinusoidally along the circumference. The magnetic saturation, eddy currents, and magnetoresistive effect were ignored. It was also assumed that the power supply voltages of the three phases were equal. Under this circumstance, the inductance parameters could be considered to be approximately equal (i.e., $L_d = L_q = L$) and the friction coefficient B to be equal to 0. With the adoption of the field orientation vector control tactics ($i_d = 0$), the linear state equation and electromagnetic torque equation were obtained.

The linear state equation was determined to be

$$\begin{bmatrix} \dfrac{di_q}{dt} \\ \dfrac{d\omega}{dt} \end{bmatrix} = \begin{bmatrix} \dfrac{-R}{L} & \dfrac{-p_n\varphi_f}{L} \\ \dfrac{3p_n\varphi_f}{2J} & 0 \end{bmatrix} \begin{bmatrix} i_q \\ \omega \end{bmatrix} + \begin{bmatrix} \dfrac{u_q}{L} \\ \dfrac{-T_l}{L} \end{bmatrix}. \tag{5.1}$$

The electromagnetic torque equation was determined to be

$$T_e = \frac{3p_n\varphi_f i_q}{2}, \tag{5.2}$$

where R is the equivalent resistance (Ω), $L_d = L_q = L$ is the equivalent inductance (H), p_n is the number of pole pairs, ω is the palstance of the rotor (rad/s), φ_f is the equivalent magnetic linkage (Wb), T_l is the load moment (N·m), i_q is the current in the q shaft (A), and J is the moment of inertia (kg·m^2).

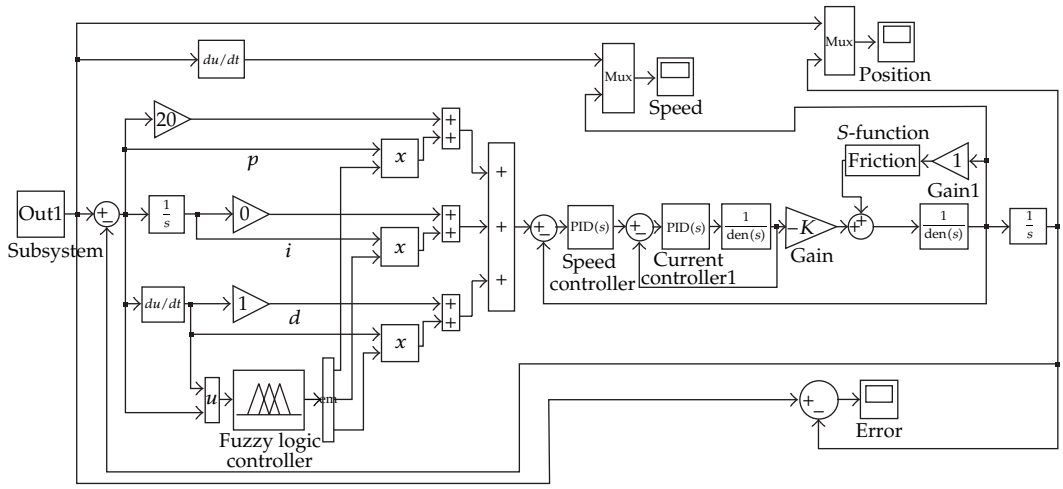

Figure 7: Simulink block diagram of the telescopic boom.

The mechanical transmission rig of the telescopic boom system comprised the driving motor, speed reducer, ball screw pairs, screw steady bearings, and moving parts. When the angular displacement of the servo motor $\theta(t)$ was the input of the mechanical transmission, the motion of the boom $X(t)$ was the output. The connection between the motor and the speed reducer was equivalent to a fixed joint. All the loads of the boom were converted to the moment of inertia J_l of the motor shaft. The friction torques and sticky connections among other parts of the boom are described by the Stribeck friction model and were added to the system model in perturbation of the speed loop. The parameters of the Stribeck friction model were adjusted. The Simulink block diagram of the telescopic boom system using fuzzy PID control with a nonlinear friction element is shown in Figure 7.

6. Results and Analysis

The sinusoidal superimposed signal was chosen as the input to the system, and is as follows:

$$r(t) = A\sin(2\pi Ft) + 0.5A\sin(1.0\pi Ft) + 0.25A\sin(0.5\pi Ft). \tag{6.1}$$

The position loop is controlled by traditional PID control and Fuzzy-PID control. Simulation results from position, speed, and error scope are shown below.

The position trailing curve, speed trailing curve, and position trailing error curve of the position loop controlled by traditional PID are shown in Figure 8. In Figure 8(a), red curve is input signal curve, blue curve is output signal curve. From the curves, output signal has obvious position trailing "flat top" phenomena and has more error following input signal, as is shown in Figure 8(c). From the curve in Figure 8(b), the wave form of output curve distorts, and speed trailing "dead zone" phenomena happens. This meant that the robustness of the low-speed servo system with friction was poor when traditional PID control was adopted, for which reason high-precision tracking could not be achieved.

The position trailing curve, speed trailing curve, and position trailing error curve of the position loop controlled with fuzzy PID control are shown in Figure 9. In Figure 9(a),

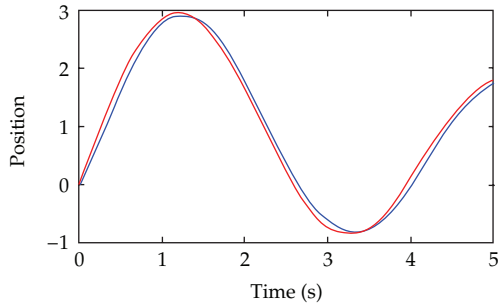

(a) Position trailing curve of traditional PID control

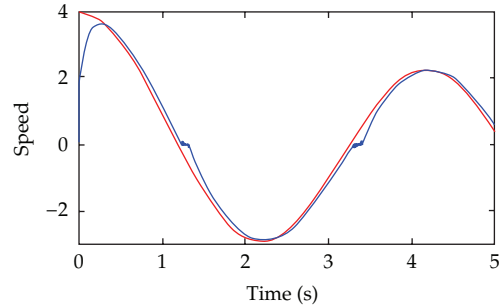

(b) Speed trailing curve of traditional PID control

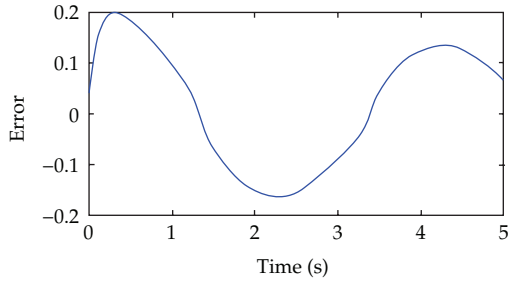

(c) Position tracking error curve of traditional PID control

Figure 8: The simulation curve of traditional PID control.

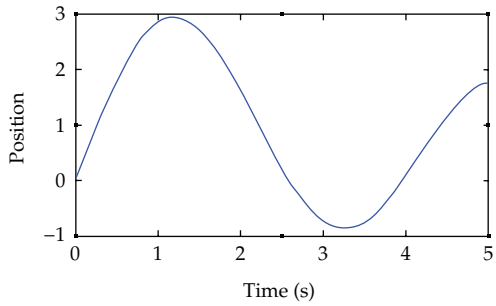

(a) Position trailing curve of fuzzy PID control

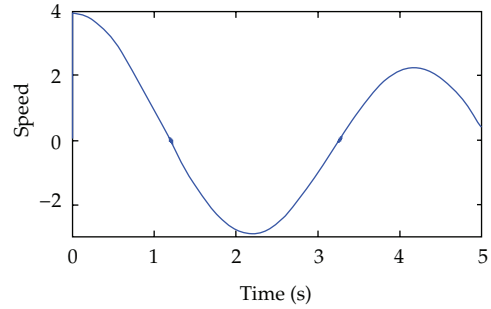

(b) Speed trailing curve of fuzzy PID control

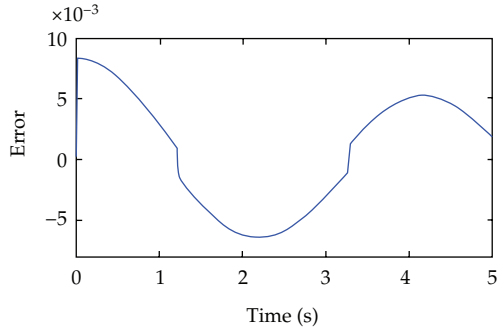

(c) Position tracking error curve of fuzzy PID control

Figure 9: The simulation curve of fuzzy PID control.

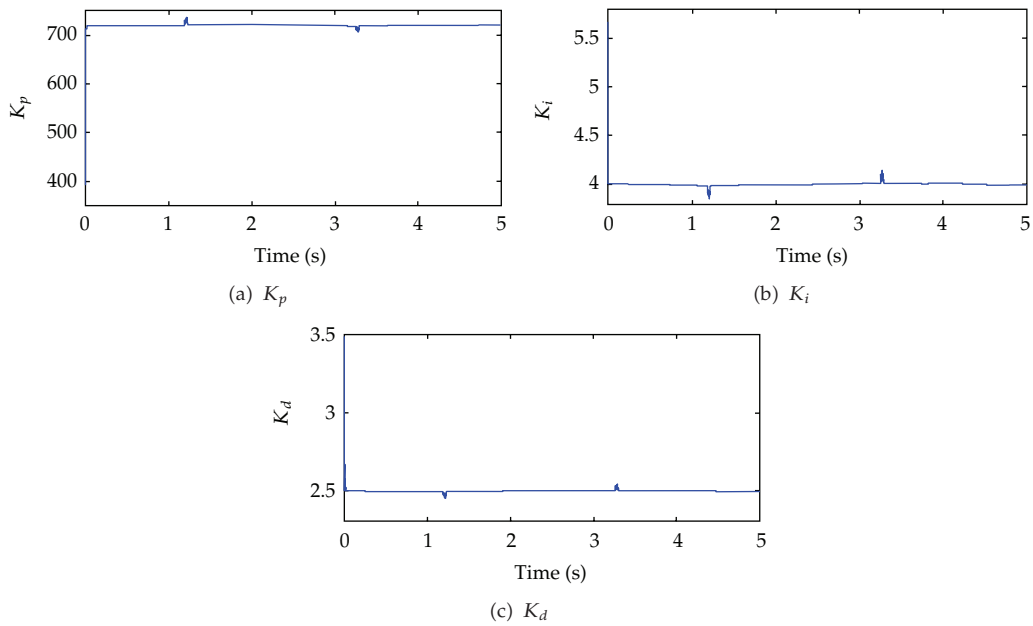

Figure 10: Self-adapting curve of fuzzy PID control.

the output curve mainly covers input curve, so using Fuzzy-PID control partly removed the position trailing "flat top" phenomena, and mainly induces position trailing error, as is shown in Figure 9(c). From the curve in Figure 9(b), output signal speed trailing "dead zone" phenomena is almost removed. It indicates that Fuzzy-PID control could achieve higher control precision and performance in slow servo system with rub.

Figure 10 shows the self-adapting curve of three parameters of fuzzy PID control. In this paper, Fuzzy-PID control means that K_p, K_i, and K_d of position loop change on line in real time to realize higher trailing precision and control performance.

7. Conclusions

The low-speed performance of the telescopic boom AC servo system of the heavy-load transfer robot with a long telescopic boom was investigated. First, we designed a scale model telescopic boom servo system experiment table with high stiffness and used it to develop a friction model of the system. Secondly, the three-loop control nonlinear model of the AC servo system was developed based on the Stribeck friction model of the actual telescopic boom. The position loops with traditional PID and fuzzy PID controls were simulated. The results showed that it was difficult to track the input signal by traditional PID control, and that the position trailing "flat top" and speed trailing "dead zone" phenomena were basically eliminated by fuzzy PID, which also produced a significant improvement in the low-speed performance and tracking precision of the servo system. Research results in this paper provide valuable control method for the accuracy control of heavy-duty servo system in low running speed.

With increasing and growing since technology, intelligent Fuzzy-PID control will become a very good development direction. Fuzzy-PID control need rules formulated by

humans expert on earth so that one certain control rule can not achieve ideal control effect in an unpredictable system running process. So more intelligent control algorithm should be input in the Fuzzy-PID control algorithm, such as neural network to form intelligent Fuzzy-PID control algorithm and remove the influence of human will in control process, to really realize the intelligent control algorithm with automatic adaptation, perfection and adjustment in system running process.

Acknowledgments

This work was supported by National Natural Science Foundation of China (Grant no. 50902039), Program for New Century Excellent Talents in Heilongjiang Provincial University (Grant no. 1155-NCET-007) and Innovative Talents Fund of Science and Technology of Harbin (grant number 2012RFXXG84).

References

[1] L. L. Liu, H. Z. Liu, Z. Y. Wu, and Z. M. Wang, "An overview of friction models in mechanical systems," *Advances in Mechanics*, vol. 38, no. 2, pp. 201–213, 2008.

[2] J. Huang and S. H. Ye, "Analysis and control offset research of servo system with rub," *Machine Science and Technology*, vol. 18, no. 1, pp. 1–4, 1999.

[3] B. Armstrong, P. Dupont, and C. C. De Wit, "A survey of models, analysis tools and compensation methods for the control of machines with friction," *Automatica*, vol. 30, no. 7, pp. 1083–1138, 1994.

[4] L. J. Ma, Y. Z. Tang, and X. B. Zhi, "Synovium variable structure control research of low-speed friction servo system," *Learned Journal of Shot and Arrow Guide*, vol. 27, no. 3, pp. 77–79, 2007.

[5] J. S. Peng, Q. Y. Su, and S. L. Song, "Application of the servo system with fuzzy PID control that base on stribeck friction model," *Electrical Engineering*, vol. 1, pp. 15–17, 2007.

[6] J. Qiu, G. Feng, and H. Gao, "Fuzzy-model-based piecewise $\mathcal{H}\infty$ static-output-feedback controller design for networked nonlinear systems," *IEEE Transactions on Fuzzy Systems*, vol. 18, no. 5, pp. 919–934, 2010.

[7] J. Qiu, G. Feng, and H. Gao, "Asynchronous output feedback control of networked nonlinear systems with multiple packet dropouts: T-S fuzzy affine model based approach," *IEEE Transactions on Fuzzy Systems*, vol. 19, no. 6, pp. 1014–1030, 2011.

[8] H. Li, H. Liu, H. Gao, and P. Shi, "Reliable fuzzy control for active suspension systems with actuator delay and fault," *IEEE Transactions on Fuzzy Systems*, vol. 20, no. 2, pp. 342–357, 2012.

[9] H. Li, J. Yu, C. Hilton, and H. Liu, "Adaptive sliding mode control for nonlinear active suspension systems using T-S fuzzy model," *IEEE Transactions on Industrial Electronics*. In press.

[10] L. Xu and B. Yao, "Adaptive robust control of mechanical systems with nonlinear dynamic friction compensation," in *Proceedings of the American Control Conference*, pp. 2595–2599, Chicago, Ill, USA, June 2000.

[11] G. Morel, K. Iagnemma, and S. Dubowsky, "Precise control of manipulators with high joint-friction using base force/torque sensing," *Automatica*, vol. 36, no. 7, pp. 931–941, 2000.

[12] B. N. Xiao, L. H. Gong, and S. Zhang, "Simulation research on friction model of a flight simulation table servo system," *Lubrication Engineering*, vol. 34, no. 3, pp. 76–80, 2009.

[13] S. Y. Li, *Neural Control and Intelligent Control Theory*, Harbin Institute of Technology Press, Harbin, China, 1996.

[14] G. Y. Li, "New fuzzy PID controller," *Journal of System Simulation*, vol. 15, no. 10, pp. 1492–1493, 2003.

[15] A. Haj-Ali and H. Ying, "Structural analysis of fuzzy controllers with nonlinear input fuzzy sets in relation to nonlinear PID control with variable gains," *Automatica*, vol. 40, no. 9, pp. 1551–1559, 2004.

[16] H. B. Zhou, H. Deng, and J. A. Duan, "Fuzzy-PID control for the motion platform of thermosonic flip-chip bonding machines," *Journal of System Simulation*, vol. 19, no. 13, pp. 2944–2954, 2007.

[17] M. Wang and L. Y. Yang, "The study of research machine tool guide crawl appearance," in *Coal Mine Machinery*, vol. 3, pp. 35–37, Harbin North Pressure Container Limited Company, Harbin, China, 2004.

[18] D. D. Guo, X. D. Liu, and Y. H. Zhang, "Repetitive control strategy of servo system with fiction offset," in *Proceedings of the 21st Chinese Control Conference*, pp. 555–558, Zhe Jiang University Press, Zhe Jiang, China, 2002.

[19] J. Zhu, *Fuzzy Control Theory and Application*, Mechanical Industry Press, 1999.

[20] Y. F. Wang and T. Y. Chai, "Adaptive fuzzy output feedback control for a class of nonlinear MIMO systems," *Journal of System Simulation*, vol. 17, no. 10, pp. 2442–2446, 2005.

[21] Y. Zhang and X. X. Yang, "Design for fuzzy immune controller based on genetic algorithm," *Journal of System Simulation*, vol. 16, no. 7, pp. 1548–1551, 2004.

[22] S. W. Yang and M. Q. Zheng, "Simulation of nonlinear friction with modeling methodology," *Journal of System Simulation*, vol. 14, no. 10, pp. 1365–1368, 2002.

[23] R. J. Lian and C. N. Huang, "Self-organizing fuzzy radial basis function neural-network controller for robotic motion control," *International Journal of Innovative Computing, Information and Control*, vol. 8, no. 3, pp. 1955–1971, 2012.

[24] M. R. Soltanpour, J. Khalilpour, and M. Soltani, "Robust nonlinear control of robot manipulator with uncertainties in kinematics. Dynamics and actuator models," *International Journal of Innovative Computing, Information and Control*, vol. 8, no. 8, pp. 5487–5498, 2012.

[25] A. Pallegedara, Y. Matsuda, T. Matsumoto, K. Tsukamoto, N. Egashira, and S. Goto, "Teleoperation of robot arms using force-free control and template matching," *International Journal of Innovative Computing, Information and Control*, vol. 8, no. 10, pp. 6869–6884, 2012.

[26] S. E. Shafiei and M. R. Soltanpour, "Neural network sliding-mode-PID controller design for electrically driven robot manipulators," *International Journal of Innovative Computing, Information and Control*, vol. 7, no. 2, pp. 511–524, 2011.

[27] M. Yue, W. Sun, and P. Hu, "Sliding mode robust control for two-wheeled mobile robot with lower center of gravity," *International Journal of Innovative Computing, Information and Control*, vol. 7, no. 2, pp. 637–646, 2011.

Hindawi Publishing Corporation
Mathematical Problems in Engineering
Volume 2012, Article ID 628295, 15 pages
doi:10.1155/2012/628295

Research Article

Fuzzy Investment Portfolio Selection Models Based on Interval Analysis Approach

Haifeng Guo,[1] BaiQing Sun,[1] Hamid Reza Karimi,[2] Yuanjing Ge,[1] and Weiquan Jin[1]

[1] *School of Management, Harbin Institute of Technology, Harbin 150001, China*
[2] *Department of Engineering, Faculty of Engineering and Science, University of Agder, 4898 Grimstad, Norway*

Correspondence should be addressed to BaiQing Sun, baiqingsun@hit.edu.cn

Received 3 November 2012; Accepted 7 November 2012

Academic Editor: Peng Shi

Copyright © 2012 Haifeng Guo et al. This is an open access article distributed under the Creative Commons Attribution License, which permits unrestricted use, distribution, and reproduction in any medium, provided the original work is properly cited.

This paper employs fuzzy set theory to solve the unintuitive problem of the Markowitz mean-variance (MV) portfolio model and extend it to a fuzzy investment portfolio selection model. Our model establishes intervals for expected returns and risk preference, which can take into account investors' different investment appetite and thus can find the optimal resolution for each interval. In the empirical part, we test this model in Chinese stocks investment and find that this model can fulfill different kinds of investors' objectives. Finally, investment risk can be decreased when we add investment limit to each stock in the portfolio, which indicates our model is useful in practice.

1. Introduction

The Markowitz mean-variance (MV) portfolio optimization theory [1] proposed by Markowitz has been widely used, which leads the investment theory to a new era. In this model, the best portfolio is a maximized profit, subjected to reaching a specified level of risk, or a minimized variance, subjected to obtaining a predetermined level of expected return [2]. However, there have been persistent doubts about the estimates' performance. Many studies indicate the model has some shortage. For example, Michaud [3] have found that MV-optimized portfolios are unintuitive, and, therefore, their estimates should be promoted [4].

In portfolio selection problem, the variables such as expected return, risk, liquidity, and so forth cannot be predicted precisely and investors generally make portfolio decision according to experience and economic wisdom; therefore, deterministic portfolio selection is not a good choice for investors. Fuzzy set theory is thought to be a good method to solve this

problem. For example, Bhattacharyya et al. [5] use fuzzy set theory to extend the investment portfolio model into a mean-variance-skewness (MVS) model, which is tested to be useful to explain the stock investment decision.

Our paper employs fuzzy set theory to extend Markowitz portfolio optimization theory by establishing return intervals and risk intervals. Because investors have difficulty to make a decision which is the best expected return or the lowest investment risk, they may set a portfolio which is in different hierarchical return and risk levels. Therefore, our paper can help investors to make investment decisions according to their return expectations level and risk preference level. Our method further minimizes the intuitive disadvantage of Markowitz mean-variance (MV) portfolio optimization method and thus can be more widely used in practice.

Our paper is structured as follows. Section 2 describes investment portfolio selection model and explain how to establish return intervals and risk intervals. Section 3 uses Chinese stock market and tests our models empirically. Section 4 makes some conclusions.

2. Fuzzy Investment Portfolio Selection Models

2.1. Markowitz MV Portfolio Optimization Model

Markowitz MV portfolio optimization theory assumes that investors are risk averse, meaning that given two portfolios that offer the same expected return, investors will prefer the less risky one. Thus, an investor will take on increased risk only if compensated by higher expected returns. Conversely, an investor who wants higher expected returns must accept more risk. The exact trade-off will be the same for all investors, but different investors will evaluate the trade-off differently based on individual risk aversion characteristics. The implication is that a rational investor will not invest in a portfolio if a second portfolio exists with a more favorable risk-expected return profile, that is, if for that level of risk an alternative portfolio exists which has better expected returns.

Markowitz MV portfolio optimization models are as follows:

$$\begin{aligned}
&\max f(x) = \sum_{i=1}^{n} E(r_i)x_i, \\
&\text{s.t.} \quad \sum_{i=1}^{n}\sum_{j=1}^{n} \sigma_{ij}x_ix_j \le \omega, \\
&\sum_{i=1}^{n} x_i = 1, \\
&0 \le x_i \le \mu_i, \quad i = 1,2,\ldots,n, \quad j = 1,2\ldots,n,
\end{aligned} \tag{2.1}$$

$$\begin{aligned}
&\min f(x) = \sum_{i=1}^{n}\sum_{j=1}^{n} \sigma_{ij}x_ix_j, \\
&\text{s.t.} \quad \sum_{i=1}^{n} E(r_i)x_i \ge r_0, \\
&\sum_{i=1}^{n} x_i = 1, \\
&0 \le x_i \le \mu_i, \quad i = 1,2,\ldots,n, \quad j = 1,2\ldots,n.
\end{aligned} \tag{2.2}$$

Model (2.1) explains a maximized expected return based on a certain risk level and model (2.2) delineates a minimized risk level conditional on a certain return level. In these two models, x_i is the investment portion of stock i in an investor's portfolio and r_i is the return of stock i. $R = (E(r_1), E(r_2), \ldots, E(r_n))^T$ is the portfolio of expected returns, where $E(r_i)$ is the expected return of stock i. $\sum_{i=1}^{n}\sum_{j=1}^{n}\sigma_{ij}x_ix_j$ is the portfolio variance, which represents investment risk, where σ_{ij} is the covariance of stocks i and j. ω is the maximum risk an investor can tolerate, μ_i is the maximum limit of stock i in investment portfolio, and r_0 is the minimum return an investor expects.

2.2. Risk Preference

Investment decisions are accompanied by much uncertainty, and risk preference varies according to an individual's personality and other reasons, such as age. Studies show that an individual's risk preference is not only affected by expected returns and risk, but also affected by gender, age, educations, wealth, health, marital factors, and so forth. In fact, investors' risk preferences are not stable; that is, different environment and social psychology can affect them as well. In general, an investor's risk appetite changes in a different environment. Therefore this section is to analyze the risk appetite.

Many investment decision models use the forms of utility function, but in some occasions, the utility function is difficult to be determined. In order to simplify the calculation and facilitate the interpretation of results, Mercurio proposes a utility function $U(W_M) = E(W_M) - A\,\mathrm{Var}(W_M)$. Based on this model, model (2.3) is constructed using risk preference coefficients, where $V = ((\sigma_{ij}^2)_{n\times n})$ is the covariance matrix of r_i, and $e = (1, 1, \ldots, 1)^T$. This model solves the single-objective optimization problem of Markowitz's mean-variance portfolio model. One has

$$\begin{aligned} \min S(X) &= (1-\beta)X^TVX - \beta X^TR, \\ \text{s.t} \quad X^Te &= 1. \end{aligned} \tag{2.3}$$

In this model, β is defined as the coefficient of risk preference and it is nonnegative. In this model, if β is bigger, investment return is more important for investors. In particular, investors focus only on the income and do not care about risk when $\beta = 1$, while, it is exactly the opposite when β approaches zero. When investors become risk averse, that is, when $\beta = 0$, model (2.3) will be simplified to the minimum variance model of portfolio:

$$\begin{aligned} \min \sigma_p^2 &= X^TVX, \\ \text{s.t} \quad X^Te &= 1. \end{aligned} \tag{2.4}$$

The optimal solution for model (2.4) is $X_g = (V^{-1}{}_e)/(e^TV^{-1}{}_e)$. Further the optimal return and optimal variance of model (2.4) are as follows:

$$\begin{aligned} R_g &= R^TX_g = \frac{R^TV^{-1}e}{e^TV^{-1}e}, \\ \sigma_g^2 &= X_g^TVX_g = \frac{1}{e^TV^{-1}e}. \end{aligned} \tag{2.5}$$

Then we define $a = e^T V^{-1} e$, $b = R^T V^{-1} e$; the solution of model (2.4) can be further simplified as follows:

$$X_g = \frac{V^{-1}e}{a}, \qquad R_g = \frac{b}{a}, \qquad \sigma_g^2 = \frac{1}{a}. \tag{2.6}$$

Properties. If the covariance matrix is positive definite, model (2.3) has a unique optimal solution:

$$X^* = \frac{V^{-1}e}{e^T V^{-1} e} + \frac{\beta}{2(1-\beta)}\left[V^{-1}R + \frac{e^T V^{-1} R}{e^T V^{-1} e} V^{-1} e\right]. \tag{2.7}$$

In (2.7), X^* indicates the optimal portfolio of model (2.3).

Proof. If V is positive definite, then model (2.3) is convex quadratic. The necessary and sufficient conditions for the solution of convex quadratic are to meet the Kuhn-tucker conditions. Kuhn-tucker conditions for model (2.3) are

$$\begin{gathered} 2(1-\beta)VX^* - \beta R - \lambda e = 0, \\ X^{*T} e = 1. \end{gathered} \tag{2.8}$$

According to (2.8), we can deduce the portfolio

$$X^* = \frac{V^{-1}e}{e^T V^{-1} e} + \frac{\beta}{2(1-\beta)}\left[V^{-1}R + \frac{e^T V^{-1} R}{e^T V^{-1} e} V^{-1} e\right]. \tag{2.9}$$

According to (2.7), we can solve the optimal return of (2.3):

$$R_p = R^T X^* = \frac{(ac - b^2)\beta}{2a(1-\beta)} + \frac{b}{a}, \tag{2.10}$$

where $c = R^T V^{-1} R$.

Discussion about $ac - b^2$.

By definition we know that $a > 0$, $c > 0$, and the covariance matrix is positive semi-definite.

According to the Cauchy-Schwarz inequality, $ac - b^2 \geq 0$, then:

(1) when securities in the portfolio have the same expected returns, according to Cauchy-Schwarz inequality, $ac - b^2 = 0$;

(2) in the portfolio, if there are at least two securities whose expected returns are different, the expected returns of all securities in the portfolio are not identical.

According to the Cauchy-Schwarz inequality, $ac - b^2 > 0$.

Based on the above two properties, combined with the actual situation, we assume that the expected returns of all securities in the portfolio are not exactly the same, so $ac - b^2 > 0$. Thus, the risk preference decision parameter β can be computed as follows:

$$\beta = \frac{2(aR_p - b)}{ac - b^2 + 2(aR_p - b)}. \tag{2.11}$$

□

2.3. Fuzzy Investment Portfolio Model

Generally, an interval linear model is expressed as the following form:

$$\begin{aligned} &\max f(x) = f(x_1, x_2, \ldots, x_n) = \sum_{i=1}^{n} K_i x_i, \\ &\text{s.t.} \quad \sum_{i=1}^{n} Z_{ij} x_i \le M_j, \quad j = 1, 2, \ldots, m, \\ &x_i \ge 0, \quad i = 1, 2, \ldots, n. \end{aligned} \tag{2.12}$$

In the above formula, K_i and Z_{ij} are interval numbers, and they are, respectively, expressed as $K_i = [\underline{k_i}, \overline{k_i}]$, $Z_{ij} = [\underline{z_{ij}}, \overline{z_{ij}}]$, where we will denote the feasible region of X by Ω, that is $X \in \Omega$.

After this, some scholars transformed the interval linear programming model into a two-goal programming problem and build a new planning model as follows:

$$\begin{aligned} &\max f_1(x) = f_1(x_1, x_2, \ldots, x_n) = \sum_{i=1}^{n} \underline{k_i} x_i, \\ &\text{s.t.} \quad X \in \Omega, \end{aligned} \tag{2.13}$$

$$\begin{aligned} &\max f_2(x) = f_2(x_1, x_2, \ldots, x_n) = \sum_{i=1}^{n} \overline{k_i} x_i, \\ &\text{s.t.} \quad X \in \Omega. \end{aligned} \tag{2.14}$$

Da and Liu [6] adopt a parameter α and use interval model to extend the above model into (2.15), which takes into account both investors' judgment and environment situation.

$$\begin{aligned} &\max f_3(x) = f_3(x_1, x_2, \ldots, x_n) = \sum_{i=1}^{n} \left[(1-\alpha) \underline{k_i} x_i + \alpha \overline{k_i} x_i \right], \\ &\text{s.t.} \quad X \in \Omega, \alpha \in [0, 1]. \end{aligned} \tag{2.15}$$

In (2.15), there are two kinds of specific situation, that is, $\alpha = 1$ and $\alpha = 0$. Further, based on investors' risk preference, there are two kinds of models: (2.16) represents a risk lover's

investment and (2.17) represents a risk adverse investor's choice, where, $v_i = [\underline{v_i}, \overline{v_i}]$ means the risk range of stock i. One has

$$\begin{aligned} &\max U(x_i) = \sum_{i=1}^{n} r_i x_i, \\ &\text{s.t.} \quad X^T e = 1, \quad X \geq 0, \end{aligned} \tag{2.16}$$

$$\begin{aligned} &\min V(x_i) = \sum_{i=1}^{n} v_i x_i, \\ &\text{s.t.} \quad X^T e = 1, X \geq 0. \end{aligned} \tag{2.17}$$

As for investors, we can naturally think of that investors want to maximize the return on investment and minimize the investment risk in the portfolio, that is, meeting the above two models at the same time, but according to practical experience, we know that this is impossible, because the higher the expected return of the portfolio, their attendant risks will also be the greater; high yield is the compensation of high risk, which requires investors to choose a balance of investment returns and risks according to their own psychology.

Since returns are uncertain, the allocation of capital in different risky assets to minimize the risk and maximize the return is the main concern of portfolio selection [5]. Therefore, it is useful to take into account returns and risks together by using the risk preference coefficient β. Thus the above multitarget interval linear function can be converted into a parametric function. By applying the risk preference coefficient β, investment flexibility can be increased because investors can decide to set different proportion of earnings targets and risks targets. It also takes into account different investors' decision-making behaviors.

However, the expected returns and risks in portfolios should be intrinsically linked and discussed together. Chen et al. [7] simplify the variance constraints using fuzzy constraints:

$$\begin{aligned} &\max U(x_i) = \sum_{i=1}^{n} E(r_i) x_i, \\ &\text{s.t.} \quad \sum_{i=1}^{n} \sigma_i x_i \leq M + d(1-\alpha), \\ &\qquad X^T e = 1, \\ &\qquad \mu \geq X \geq 0, \\ &\qquad \mu = \{\mu_1, \mu_2, \ldots, \mu_n\}. \end{aligned} \tag{2.18}$$

In (2.18), α is fuzzy membership which an investor belongs to, $\alpha \in [0,1]$; the membership function is expressed as:

$$\mu(x_i) = \begin{cases} 1, & 0 \leq \sum_{i=1}^{n} \sigma_i x_i \leq M - d, \\ \dfrac{M - \sum_{i=1}^{n} \sigma_i x_i}{d}, & M - d \leq \sum_{i=1}^{n} \sigma_i x_i \leq M, \\ 0, & \text{others}, \end{cases} \tag{2.19}$$

where d is the tolerance of investors and σ_i is the standard deviation of the stock i's return. Chen et al. [7] adopt parameters in the fuzzy interval and thus the model is transformed into a linear function:

$$\begin{aligned} &\max U(x_i) = \sum_{i=1}^{n}\left[\underline{r_i}, \overline{r_i}\right]x_i\,, \\ &\text{s.t.} \quad \sum_{i=1}^{n}\left[\underline{\sigma_i}, \overline{\sigma_i}x_i\right] \le \left[\underline{M} + d(1-\alpha), \overline{M} + d(1-\alpha)\right], \\ &\qquad X^T e = 1, \\ &\qquad \mu \ge X \ge 0, \\ &\qquad \mu = \{\mu_1, \mu_2, \ldots, \mu_n\}. \end{aligned} \tag{2.20}$$

This model can solve the calculation problems, but this model involves multiple parameters. Although parameters have the advantages in increasing flexibility, too many parameters result in decision-making errors and thereby increase uncertainty.

Risk preference is determined by the expected return and risk, which are expressed by interval numbers. We define risk preference coefficient as $\beta = [\underline{\beta}, \overline{\beta}]$ and use Markowitz method to calculate the stocks investment risk. Model (2.21) can estimate investors' risk preferences from investment decision-making behaviors, and then it compares the returns and risk together in the same model

$$\begin{aligned} \max f(x_i) &= \beta\sum_{i=1}^{n} r_i x_i - (1-\beta)\sum_{i=1}^{n} XVX^T \\ &= \left[\underline{\beta}, \overline{\beta}\right]\sum_{i=1}^{n}\left[\underline{r_i}, \overline{r_i}\right]x_i - \left[1-\overline{\beta}, 1-\underline{\beta}\right]\sum_{i=1}^{n} XVX^T \\ &= \sum_{i=1}^{n}\left[\underline{\beta}\underline{r_i}, \overline{\beta}\overline{r_i}\right]x_i - \left[1-\overline{\beta}, 1-\underline{\beta}\right]\sum_{i=1}^{n} XVX^T s. \end{aligned} \tag{2.21}$$

Covariance matrix is $V = \begin{bmatrix} \sigma_{11} & \sigma_{12} & \cdots & \sigma_{1n} \\ \vdots & & & \vdots \\ \sigma_{n1} & \sigma_{n2} & \cdots & \sigma_{nn} \end{bmatrix}$. All elements of the matrix are interval numbers, that is, $\sigma_{ij} = [\underline{\sigma_{ij}}, \overline{\sigma_{ij}}]$. So the formula $\sum_{i=1}^{n} XVX^T$ can be simplified as follows:

$$\begin{aligned} \sum_{i=1}^{n} XVX^T &= \{x_1 x_2 \cdots x_n\}\begin{bmatrix} \sigma_{11} & \sigma_{12} & \cdots & \sigma_{1n} \\ \vdots & & & \vdots \\ \sigma_{n1} & \sigma_{n2} & \cdots & \sigma_{nn} \end{bmatrix}\{x_1 x_2 \cdots x_n\}^T \\ &= \left\{\sum_{i=1}^{n}\left[\underline{\sigma_{i1}}, \overline{\sigma_{i1}}\right]x_i, \sum_{i=1}^{n}\left[\underline{\sigma_{i2}}, \overline{\sigma_{i2}}\right]x_i, \ldots, \sum_{i=1}^{n}\left[\underline{\sigma_{in}}, \overline{\sigma_{in}}\right]x_i\right\}\{x_1 x_2 \cdots x_n\}^T \end{aligned}$$

$$= x_1 \sum_{i=1}^{n} \left[\underline{\sigma_{i1}}, \overline{\sigma_{i1}}\right] x_i + x_2 \sum_{i=1}^{n} \left[\underline{\sigma_{i2}}, \overline{\sigma_{i2}}\right] x_i + \cdots + x_n \sum_{i=1}^{n} \left[\underline{\sigma_{in}}, \overline{\sigma_{in}}\right] x_i$$
$$= \sum_{j=1}^{n} x_j \sum_{i=1}^{n} \left[\underline{\sigma_{ij}}, \overline{\sigma_{ij}}\right] x_i. \tag{2.22}$$

Therefore, the portfolio model can be simplified as follows:

$$\begin{aligned} \max f(x_i) &= \beta \sum_{i=1}^{n} r_i x_i - (1-\beta) \sum_{i=1}^{n} XVX^T \\ &= \left[\underline{\beta}, \overline{\beta}\right] \sum_{i=1}^{n} \left[\underline{r_i}, \overline{r_i}\right] x_i - \left[1-\overline{\beta}, 1-\underline{\beta}\right] \sum_{j=1}^{n} x_j \sum_{i=1}^{n} \left[\underline{\sigma_{ij}}, \overline{\sigma_{ij}}\right] x_i \\ &= \sum_{i=1}^{n} \left[\underline{\beta}\underline{r_i}, \overline{\beta}\overline{r_i}\right] x_i - \sum_{j=1}^{n} x_j \sum_{i=1}^{n} \left[\left(1-\overline{\beta}\right)\underline{\sigma_{ij}}, \left(1-\underline{\beta}\right)\overline{\sigma_{ij}}\right] x_i. \end{aligned} \tag{2.23}$$

The optimal estimators of (2.23) are defined as $b = [0, 1]$, where b is the membership of the interval. A bigger b means higher expected return; that is, b reflects investor's confidence level on market expectations. Specifically when b is closer to 1, it indicates that investors are more optimistic about the market future. However, the expectation for the future market is extremely pessimistic when b is closer to 0. So the final form of the fuzzy investment portfolio model is expressed as follows:

$$\begin{aligned} \max f(x_i) &= \sum_{i=1}^{n} \left(b\overline{\beta}\overline{r_i} + (1-b)\underline{\beta}\underline{r_i}\right) x_i - \sum_{j=1}^{n} x_j \sum_{i=1}^{n} \left[b\left(1-\overline{\beta}\right)\underline{\sigma_{ij}} + (1-b)\left(1-\underline{\beta}\right)\overline{\sigma_{ij}}\right] x_i, \\ \text{s.t.} \quad & X^T e = 1, \\ & X \geq 0. \end{aligned} \tag{2.24}$$

By using (2.12), we can set an investment limit for each stock, and thus the model is expressed as follows:

$$\begin{aligned} \max f(x_i) &= \sum_{i=1}^{n} \left(b\overline{\beta}\overline{r_i} + (1-b)\underline{\beta}\underline{r_i}\right) x_i - \sum_{j=1}^{n} x_j \sum_{i=1}^{n} \left[b\left(1-\overline{\beta}\right)\underline{\sigma_{ij}} + (1-b)\left(1-\underline{\beta}\right)\overline{\sigma_{ij}}\right] x_i, \\ \text{s.t.} \quad & X^T e = 1, \\ & \mu_i \geq x_i \geq 0, \end{aligned} \tag{2.25}$$

where μ_i indicates the maximum amount of the stock i in sthe portfolio.

Based on the investment behavior analysis and clear understanding of their risk reference as well as future expectations of the market, investors can utilize this model to solve effective programs of the portfolio. Fuzzy theory is widely used to solve time varying

problems [8–18]; therefore, the following section will adopt the model we generated to solve the practice problems.

3. Empirical Study on the Stock Investment Portfolio

3.1. Data

The principle of decentralization can reduce the nonsystematic risk of the portfolio. In accordance with the principle of decentralization, we use twenty stocks which are selected from different industries. In order to provide investors with multiple choices, these stocks have different enterprise growth rates.

We use Chinese stocks to test our fuzzy investment portfolio model. The primary data come from CSMAR database produced by GTA company. We select 20 stocks and the data include each stock's weekly opening prices and weekly closing prices for the 100 weeks from June 11, 2010, to May 18, 2012.

3.2. Variables

In order to compute the expected returns, we use the historical average return to estimate the expected return. On this basis, we can make interval estimation of the returns by utilizing the fuzzy statistical method and thus construct a number of reasonable income sets.

Since many stocks distribute a little dividend to investors, the weekly dividend can be ignored because the dividend will be very small after being divided into every week. So in this paper, we discard the dividend and only take into account the stock trading prices change. We use the price change during each week. The weekly return is calculated as

$$r_{it} = \frac{p_{it} - p_{it0}}{p_{it0}}, \tag{3.1}$$

where r_{it} is stock i's return during week t ($i = 1, 2, \ldots, 20$; $t = 1, 2, \ldots, 52$). Meanwhile, p_{it0} is the opening price of stock i on week t and p_{it} is the closing price of stock i on week t.

3.3. Interval Determined by Fuzzy Statistical Method

3.3.1. Determination of Return Intervals

As for the return interval, we compute it as follows.

(1) Based on the stocks' weekly returns for 100 weeks, we divide them into 10 subintervals. Then we count the number of actual return rate contained within each subinterval.

(2) The number of returns is the degree of membership of each interval.

(3) The final return interval is the interval which the sum of each median multiplied membership degree locates in.

The stock returns are listed in Table 1.

Table 1: The stock return intervals.

Stock name	Interval lower limit	Interval upper limit
Vanke	0.005224	0.031831
Konka	−0.00596	0.021606
Victor onward Textile	0.002509	0.031017
Universe	−0.00717	0.026362
Tellus	−0.03185	0.012672
Shenxin	−0.03593	0.02052
Nonfemet	−0.03978	0.010745
Xinmao S&T	−0.00754	0.022664
INT'L Group	−0.0213	0.01444
Jinlu	−0.0273	0.00901
ZY Environment	−0.01111	0.020413
DaTong Gas	−0.00474	0.021312
Advanced Technology	−0.00708	0.024332
Fujian Electric	−0.00968	0.018596
Sinosteel	−0.01617	0.044893
Huayi Brothers	−0.0378	0.022356
China Merchants Bank	−0.00997	0.013047
Xi'An Aero Engine	−0.0003	0.031385
Ping An	−0.0124	0.01055
Petro China	−0.0207	−0.0007

3.3.2. Determination of Risks Intervals

Based on Markowitz mean-variance model, we use the variance of the stock returns to measure the level of investment risk. Stock return variance is calculated as follows.

(1) Based on the stock' weekly returns for 100 weeks, we divide the returns into 10 subintervals and count the number of returns in each subinterval.

(2) The number of returns is the degree of membership of each interval.

(3) We define that a_i and b_i are the upper and lower bounds for each interval, respectively. Thus $\widehat{\mu}_u$ and $\widehat{\mu}_l$ are, respectively, the upper and lower bounds of the interval which the product of the mean of return range and the degree of membership are in.

Denote U as a fuzzy set, where $\{x_i = [a_i, b_i], i = 1, 2, \ldots, N\}$ comprises the set U. Thus the means can be expressed as $F\mu = [\mu_l, \mu_u]$. We define that $\{x_i = [a_i, b_i], i = 1, 2, \ldots, n\}$ is a random fuzzy sample from set U, where the mean of the sample is $F\overline{X} = [\widehat{\mu}_l, \widehat{\mu}_u]$, which is the return set. Further, we denote $c_i = (a_i + b_i)/2$, $l_i = |b_i - a_i|$, $c = (\mu_l + \mu_u)/2$, and $l = |\mu_u - \mu_l|$, $\widehat{c} = (\widehat{\mu}_l + \widehat{\mu}_u)/2$, $\widehat{l} = |\widehat{\mu}_u - \widehat{\mu}_l|$, then variance of the fuzzy set can be expressed as

$$F\sigma^2 = \left\langle \frac{\sum_{i=1}^{N} (c_i - c)^2}{N}, \frac{\sum_{i=1}^{N} (l_i - l)^2}{N} \right\rangle, \tag{3.2}$$

$$FS^2 = \left\langle \frac{\sum_{i=1}^{n} (c_i - \widehat{c})^2}{n-1}, \frac{\sum_{i=1}^{N} \left(l_i - \widehat{l}\right)^2}{n-1} \right\rangle. \tag{3.3}$$

Table 2: Variance based on fuzzy method.

Stock name	Variance
Vanke	0.001959
Konka	0.002526
Victor onward Textile	0.002652
Universe	0.002953
Tellus	0.003845
Shenxin	0.0056
Nonfemet	0.004228
Xinmao S&T	0.003022
INT'L Group	0.003809
Jinlu	0.00416
ZY Environment	0.002569
DaTong Gas	0.002516
Advanced Technology	0.00328
Fujian Electric	0.003027
Sinosteel	0.007421
Huayi Brothers	0.004313
China Merchants Bank	0.001113
Xi'An Aero Engine	0.003863
Ping An	0.001489
Petro China	0.000719

(4) Then we substitute the respective values into (3.3) to calculate the variance of stocks.

The results are in Table 2.

In this model, the risk of the stock is expressed by the covariance matrix than risk losing rate. In order to determine the interval for the variance the traditional approach is to directly select the range of variance fluctuation. Then it is expressed as $\alpha^2 \pm a$, where a is a given constant. But there are no studies about the determination of covariance interval. Therefore this paper defines the covariance by determining the variance of interval numbers. By using $a = 0.0001$, the covariance interval is determined.

3.4. Empirical Results

3.4.1. Estimation without Investment Limit

Next, in order to figure out the role of the investment limit on the portfolio, we also calculate the portfolio without setting maximum investment ratio and list the results in Table 3.

3.4.2. Estimation with Investment Limit

In order to show the role of risk controlling, we set a maximum investment ratio for each stock which depends on the investor's risk preference. The investor' risk preference can be calculated in accordance with investor's risk preference decision model. Given the different

Table 3: The investment portfolio of different market expectations without limits.

Stock name	$b = 0$	$b = 0.3$	$b = 0.5$	$b = 0.8$	$b = 1$
Vanke	1.0000	0.6763	0.6950	0.2345	0
Konka	0	0	0	0	0
Victor onward Textile	0	0.3237	0.3050	0	0
Universe	0	0	0	0	0
Tellus	0	0	0	0	0
Shenxin	0	0	0	0	0
Nonfemet	0	0	0	0	0
Xinmao S&T	0	0	0	0	0
INT'L Group	0	0	0	0	0
Jinlu	0	0	0	0	0
ZY Environment	0	0	0	0	0
DaTong Gas	0	0	0	0	0
Advanced Technology	0	0	0	0	0
Fujian Electric	0	0	0	0	0
Sinosteel	0	0	0	0.7655	1.0000
Huayi Brothers	0	0	0	0	0
China Merchants Bank	0	0	0	0	0
Xi'An Aero Engine	0	0	0	0	0
Ping An	0	0	0	0	0
Petro China	0	0	0	0	0
Fval	−0.0023	−0.0074	−0.0110	−0.0185	−0.0264

expectations of the investors on the market in the future, the optimal portfolio of investors can be calculated.

Firstly, we assume that the investor's target return is $[10\%, 12\%]$. Then we calculated the interval of investors risk preference $[0.6031, 0.6454]$ using the risk preference decision parameter β. We can find that the investor is the slight risk preferences type. This paper sets the maximum investment ratio on each stock on the level of 0.2, that is, $\mu_i = 0.2$. Then the portfolio can be comprised of at least 5 stocks, which can relatively reduce investment risk. We assume the investor's market expectations are, respectively, $b = 0$, $b = 0.3$, $b = 0.5$, $b = 0.8$, and $b = 1$. The results are listed in Table 4.

Table 4 shows that the investment portfolio only includes a few stocks. Some stocks such as Tellus and ZY Environment have not been selected regardless of the market expectations. The reason is that the expected returns of selected stocks are stable and they have higher expected return range. In Table 4, we find that the investment ratios of Vanke and Victor onward Textile are 0.2, respectively, because their expected return range is positive. Meanwhile, these two stocks are less risky. Meanwhile, the investment ratio of Advanced Technology is 0.2 as well, since the investment return of the Advanced Technology is more stable than that of other stocks regardless of economic situation. Investment proportion of DaTong Gas is high in bad economic environment. However, when the economy becomes better, the investment proportion gradually declines due to its instable return. Therefore this stock is a good choice for risk-averse investor.

In the contrary, the impact of the economic situation on Sinosteel is more significant, which is reflected by the big expected return interval. So the investment ratio gradually increases when the economic situation becomes better. The value shows a decreasing trend.

Table 4: The investment portfolio of different market expectations under the conditions of limited investment ratio.

Stock name	$b = 0$	$b = 0.3$	$b = 0.5$	$b = 0.8$	$b = 1$
Vanke	0.2000	0.2000	0.2000	0.2000	0.2000
Konka	0.1672	0.0632	0	0	0
Victor onward Textile	0.2000	0.2000	0.2000	0.2000	0.2000
Universe	0	0.0919	0.1047	0.1328	0.2000
Tellus	0	0	0	0	0
Shenxin	0	0	0	0	0
Nonfemet	0	0	0	0	0
Xinmao S&T	0	0	0	0	0
INT'L Group	0	0	0	0	0
Jinlu	0	0	0	0	0
ZY Environment	0	0	0	0	0
DaTong Gas	0.2000	0.1292	0.0477	0	0
Advanced Technology	0.0328	0.0658	0.0476	0.0672	0
	0	0.0499	0.2000	0.2000	0.2000
Fujian Electric	0	0	0	0	0
Sinosteel	0	0	0	0	0
Huayi Brothers	0.2000	0.2000	0.2000	0.2000	0.2000
China Merchants Bank	0	0	0	0	0
Xi'An Aero Engine	0	0	0	0	0
Ping An	0	0	0	0	0
Petro China	0	0	0	0	0
Fval	0.0011	−0.0044	−0.0089	−0.0160	−0.0208

Therefore the maximum value of the model will show an increasing trend as the economic situation improves.

By comparing Tables 3 and 4, we find that without the investment limit, the investment portfolio consists more of Vanke and Victor onward Textile, especially in the case of a poor economic situation. But when the economy becomes better, the investment portfolio becomes to include Sinosteel. It shows that Sinosteel is more significantly influenced by the economic situation. In conclusion, we find that the expected returns and risk are both increasing without investment restrictions. Therefore, the risk can be reduced if the investment limit is set in the portfolio.

In comparison to the current research on the investment portfolio, our model's results show the optimal selection portfolio for investors with different risk preference; that is, each investor can set an expected return and risk level and thus makes his/her decision according to this level. Meanwhile, our model can set the maximum risk limit. Through this restriction, investment risk can be under control in a certain level, because it's hard for investors to always find a minimum risk.

4. Conclusions

In this paper, we use fuzzy set theory to extend Markowitz mean-variance portfolio model and test this model in Chinese stock market. The results indicates that fuzzy set theory is useful to avoid the problems of Markowitz mean-variance portfolio model and takes into

account different expected return levels and risk preference levels. The paper also uses 20 Chinese stocks to test the model's efficiency. We find that the risk can be minimized by our fuzzy investment portfolio model through adding the maximum investment portion. The model is finally proved to be useful in investment practice.

Fuzzy investment portfolio selection model can be used in many fields such as stock markets, futures market and stock index futures markets, and so forth. Further, the portfolio model can set more intervals according to investors' needs, which will be more detailed when intervals become smaller.

Acknowledgment

This study was sponsored by the National Science Foundation of China (nos. 71103049, 71271069, and 71031003), the Humanity and Social Science Research Foundation (10YJC790070), and the Research Fund for the Doctoral Program of Higher Education (20112302120038) of MoE.

References

[1] H. Markowitz, "Portfolio selection," *Journal of Finance*, vol. 7, pp. 77–91, 1952.
[2] S. Zymler, B. Rustem, and D. Kuhn, "Robust portfolio optimization with derivative insurance guarantees," *European Journal of Operational Research*, vol. 210, no. 2, pp. 410–424, 2011.
[3] R. Michaud, "The Markowitz optimization enigma: is "optimized" optimal?" *Financial Analysts Journal*, vol. 45, no. 1, pp. 31–42, 1989.
[4] P. L. Leung, H. Y. Ng, and W. K. Wong, "An improved estimation to make Markowitz's portfolio optimization theory users friendly and estimation accurate with application on the US stock market investment," *European Journal of Operational Research*, vol. 222, no. 1, pp. 85–95, 2012.
[5] R. Bhattacharyya, S. Kar, and D. D. Majumder, "Fuzzy mean-variance-skewness portfolio selection models by interval analysis," *Computers and Mathematics with Applications*, vol. 61, no. 1, pp. 126–137, 2011.
[6] Q. Da and X. Liu, "Interval linear programming and optimization," *System Engineering Theory and Practice*, vol. 4, pp. 3–7, 1999.
[7] G. Chen, S. Chen, and S. Wang, "Interval Fuzzy set investment portfolio," *System Engineering*, vol. 25, pp. 34–37, 2007.
[8] X. Su, P. Shi, L. Wu, and Y. Song, "A novel approach to filter design for T-S fuzzy discrete-time systems with time-varying delay," *IEEE Transactions on Fuzzy Systems*, vol. 20, no. 6, pp. 1114–1129, 2012.
[9] X. Su, P. Shi, L. Wu, and Y. Song, "A novel control design on discrete-time takagi-sugeno fuzzy systems with time-varying Delays," *IEEE Transactions on Fuzzy Systems*. In press.
[10] M. Nafar, G. Gharehpetian, and T. Niknam, "Using modified fuzzy particle swarm optimization algorithm for parameter estimation of surge arresters models," *International Journal of Innovative Computing Information Control*, vol. 8, no. 1 B, pp. 567–581, 2012.
[11] T. Chen, "A hybrid fuzzy and neural approach with virtual experts and partial consensus for dram price forecasting," *International Journal of Innovative Computing, Information and Control*, vol. 8, no. 1 B, pp. 583–597, 2012.
[12] L. Wu, X. Su, P. Shi, and J. Qiu, "Model approximation for discrete-time state-delay systems in the TS fuzzy framework," *IEEE Transactions on Fuzzy Systems*, vol. 19, no. 2, pp. 366–378, 2011.
[13] J. Aghaei, "Fuzzy multi-objective optimal power flow considering UPFC," *International Journal of Innovative Computing, Information and Control*, vol. 8, no. 2, pp. 1155–1166, 2012.
[14] L. Wu and W. X. Zheng, "L2-L∞ control of nonlinear fuzzy itô stochastic delay systems via dynamic output feedback," *IEEE Transactions on Systems, Man, and Cybernetics, Part B*, vol. 39, no. 5, pp. 1308–1315, 2009.
[15] H. V. Pham, T. Cao, I. Nakaoka, E. W. Cooper, and K. Kamei, "A proposal of hybrid kansei-som model for stock market investment," *International Journal of Innovative Computing, Information and Control*, vol. 7, no. 5 B, pp. 2863–2880, 2011.

[16] H. V. Pham, T. Cao, I. Nakaora, J. Kushioda, E. W. Copper, and K. Kamei, "A group decision support system using hybrid Kansei-SOM model for stock market investment strategies and its application," *International Journal of Innovative Computing, Information and Control*, vol. 7, no. 7 A, pp. 3659–3678, 2011.

[17] L. Wu and D. W. C. Ho, "Fuzzy filter design for Itô stochastic systems with application to sensor fault detection," *IEEE Transactions on Fuzzy Systems*, vol. 17, no. 1, pp. 233–242, 2009.

[18] H. Guo, R. Brooks, and R. Shami, "Detecting hot and cold cycles using a Markov regime switching model-evidence from the Chinese A-share IPO market," *International Review of Economics and Finance*, vol. 19, no. 2, pp. 196–210, 2010.

Hindawi Publishing Corporation
Mathematical Problems in Engineering
Volume 2012, Article ID 635709, 13 pages
doi:10.1155/2012/635709

Research Article

Robust Observer Design for Takagi-Sugeno Fuzzy Systems with Mixed Neutral and Discrete Delays and Unknown Inputs

Hamid Reza Karimi[1] and Mohammed Chadli[2]

[1] *Department of Engineering, Faculty of Engineering and Science, University of Agder, 4898 Grimstad, Norway*
[2] *Laboratory of Modeling, Information and Systems, University of Picardie Jules Verne, Amiens, France*

Correspondence should be addressed to Hamid Reza Karimi, hamid.r.karimi@uia.no

Received 30 September 2012; Accepted 3 November 2012

Academic Editor: Peng Shi

Copyright © 2012 H. R. Karimi and M. Chadli. This is an open access article distributed under the Creative Commons Attribution License, which permits unrestricted use, distribution, and reproduction in any medium, provided the original work is properly cited.

A robust observer design is proposed for Takagi-Sugeno fuzzy neutral models with unknown inputs. The model consists of a mixed neutral and discrete delay, and the disturbances are imposed on both state and output signals. Delay-dependent sufficient conditions for the design of an unknown input T-S observer with time delays are given in terms of linear matrix inequalities. Some relaxations are introduced by using intermediate variables. A numerical example is given to illustrate the effectiveness of the given results.

1. Introduction

In recent years, there have been rapidly growing interests in stability analysis and synthesis of fuzzy control systems; several works concerning stability and state estimation for a class of systems described by Takagi-Sugeno (T-S) fuzzy models [1–7] have been carried out. Furthermore, some recent applications of fuzzy theory in engineering are reported in [8–10]. Based on the Lyapunov method, design conditions for controllers and observers are given in linear matrix inequalities (LMIs) formulation (see among others [11–19]). In the literature of the study, all of the existing results concern T-S fuzzy models with known inputs (see, e.g., [15, 17]). However, it is well known that state estimation for dynamic systems with time delays and unknown inputs or disturbances is an interesting research topic in the fields of robust control, system supervision, and fault-tolerant control [20–23]. Recently, the problem of H_∞ model reduction for Takagi-Sugeno (TS) fuzzy stochastic systems in [24], the problem of H_∞ model approximation for discrete-time Takagi-Sugeno (T-S) fuzzy time-delay systems

in [25], and the problem of filtering for a class of discrete-time T-S fuzzy time-varying delay systems in [26] have been fully investigated.

On the other hand, stability of neutral systems proves to be a more complex issue because the system involves the derivative of the delayed state. Especially, in the past few decades, increased attention has been devoted to the problem of robust delay-dependent stability and stabilization via different approaches for linear neutral systems with delayed state and/or input and parameter uncertainties [27–30]. Recently, the problem of network-based feedback control for systems with mixed delays based on quantization and dropout compensation has been studied in [31].

However, to the best of our knowledge, the class of unknown input T-S neutral models has not yet been fully investigated in the past and remains to be important and challenging. This motivates the present study. Thus, the contributions of this paper are two-fold: (i) design of observers for T-S fuzzy models with mixed neutral and discrete time delays and unknown inputs which influence states and outputs simultaneously and (ii) for the addressed problem, the observer gains are computed by solving a convex optimization technique.

This paper is organized as follows. First, the considered observer structure for T-S fuzzy model with mixed time delays and unknown inputs is given. In Section 3, the main results are given for T-S models. Section 4 gives a numerical example to show the validity of the given results. At last, we conclude the paper in Section 5.

Notation. Throughout this paper, the notation $X > Y$, where X and Y are symmetric matrices, means that $X - Y$ is positive definite, and $\mathbf{R}^n$ and $\mathbf{R}^{n\times m}$ denote, the n-dimensional Euclidean space and the set of all $n \times m$ real matrices respectively. Superscript "T" denotes matrix transposition, I is the identity matrix with compatible dimensions, the symbol $(*)$ denotes the transpose elements in the symmetric positions, $I_M = \{1, 2, \ldots, M\}$, and Σ^+ denotes any generalized inverse of matrix Σ with $\Sigma\Sigma^+\Sigma = \Sigma$. The operator $\mathrm{diag}\{\cdots\}$ represents a block diagonal matrix, and the operator $\mathrm{sym}(A)$ represents $A + A^T$.

2. Problem Formulation

Now, consider the following T-S fuzzy models with unknown inputs and different neutral and discrete time delays:

$$\begin{gathered}\dot{x}(t) = \sum_{i=1}^{M}\mu_i(\xi(t))(A_i x(t) + A_{\tau_i}\dot{x}(t-\tau) + A_{h_i}x(t-h) + B_i u(t) + R_i d(t) + H_i w(t)) \\ x(t) = \phi(t), \quad t \in [-\kappa, 0], \\ y(t) = Cx(t) + Fd(t) + Jw(t),\end{gathered} \tag{2.1}$$

with

$$\mu_i(\xi(t)) \geq 0, \quad \sum_{i=1}^{M}\mu_i(\xi(t)) = 1, \tag{2.2}$$

where M is the number of submodels, $x(t) \in \mathbf{R}^n$ is the state vector, $u(t) \in \mathbf{R}^m$ is the input vector, $d(t) \in \mathbf{R}^{q_d}$ is the unknown input, $w(t) \in \mathbf{R}^{q_w}$ is the external disturbance vector, and

$y \in \mathbf{R}^p$ is the measured output. $A_i \in \mathbf{R}^{n\times n}$, $A_{\tau_i} \in \mathbf{R}^{n\times n}$, $B_i \in \mathbf{R}^{n\times m}$, and $C \in \mathbf{R}^{p\times n}$ define the ith local model. Matrices $R_i \in \mathbf{R}^{n\times q_d}$ and $F \in \mathbf{R}^{p\times q_d}$ represent the influence matrices of the unknown inputs, and $H_i \in \mathbf{R}^{n\times q_w}$ and $J \in \mathbf{R}^{p\times q_w}$ represent the influence matrices of the disturbances. The *activation functions* $\mu_i(\cdot)$ depend on the decision vector $\xi(t)$ assumed to depend on measurable variables. It can depend on the measurable state variables and be a function of the measurable outputs of the system and possibly of the known inputs [1, 32]. The time-varying function $\phi(t)$ is continuous vector-valued initial function, and τ and h are constant time delays with $\kappa := \max\{\tau, h\}$.

In this paper, we are concerned with the reconstruction of state variable $x(t)$ of unknown inputs T-S model (2.1) using measurable signals, that is, known input $u(t)$ and measured output $y(t)$. In order to estimate the state of the unknown input T-S fuzzy model (2.1), the considered unknown input observer structure has the following form:

$$\begin{gathered}\dot{z}(t) = \sum_{i=1}^{M}\mu_i(\xi(t))\left(N_i z(t) + N_{\tau_i}\dot{z}(t-\tau) + N_{h_i} z(t-h) + G_i u(t) + L_i y(t)\right)\\ z(t) = \varphi(t), \quad t \in [-\kappa, 0],\\ \widehat{x}(t) = z(t) - Ey(t),\end{gathered} \tag{2.3}$$

where the observer considers the same activation functions $\mu_i(\cdot)$ as used for the T-S model (2.1). The variables $N_i \in \mathbf{R}^{n\times n}$, $N_{\tau_i} \in \mathbf{R}^{n\times n}$, $G_i \in \mathbf{R}^{n\times m}$, $L_i \in \mathbf{R}^{n\times p}$, and $E \in \mathbf{R}^{n\times p}$ are the observer gains to be determined in order to estimate the state of the unknown input T-S model (2.1). The time-varying function $\varphi(t)$ is continuous vector-valued initial function. Now let us define the state estimation error

$$e(t) = x(t) - \widehat{x}(t). \tag{2.4}$$

From estimation error (2.4) with the expression of $\widehat{x}(t)$ given by the observer (2.3) and T-S model (2.1), we get

$$e(t) = (I + EC)x(t) - z(t) + EFd(t) + EJw(t). \tag{2.5}$$

The dynamic of state estimation error is then given by

$$\begin{aligned}\dot{e}(t) = \sum_{i=1}^{M}\mu_i(\xi)(&N_i e(t) + (TA_i - K_i C - N_i)x(t) + TA_{\tau_i}\dot{x}(t-\tau) - N_{\tau_i}\dot{z}(t-\tau)\\ &+ TA_{h_i}x(t-h) - N_{h_i}z(t-h) + (TB_i - G_i)u(t)\\ &+(TR_i - K_i F)d(t) + (TH_i - K_i J)w(t)) + EF\dot{d}(t) + EJ\dot{w}(t),\end{aligned} \tag{2.6}$$

with

$$T = I + EC, \qquad K_i = N_i E + L_i. \tag{2.7}$$

Then, we get

$$\dot{e}(t) = \sum_{i=1}^{M} \mu_i(\xi(t))(N_i e(t) + N_{\tau_i}\dot{e}(t-\tau) + N_{h_i} e(t-h)), \tag{2.8}$$

if the following constraints hold

$$N_i = TA_i - K_i C, \tag{2.9}$$

$$TA_{\tau_i} - N_{\tau_i} T = 0, \tag{2.10}$$

$$TA_{h_i} - N_{h_i} T = 0, \tag{2.11}$$

$$TB_i - G_i = 0, \tag{2.12}$$

$$TR_i - K_i F = 0, \tag{2.13}$$

$$E[F \;\; J] = 0, \tag{2.14}$$

$$TH_i - K_i J = 0. \tag{2.15}$$

For description brevity, (2.8) can be written as

$$\dot{e}(t) = N_\mu e(t) + N_{\mu_\tau}\dot{e}(t-\tau) + N_{\mu_h} e(t-h), \tag{2.16}$$

where $N_\mu = \sum_{i=1}^{M} \mu_i(\xi(t)) N_i$, $N_{\mu_h} = \sum_{i=1}^{M} \mu_i(\xi(t)) N_{h_i}$, and $N_{\mu_\tau} = \sum_{i=1}^{M} \mu_i(\xi(t)) N_{\tau_i}$.

Remark 2.1. It is noting that if E is determined, we get T from (2.7) and deduce directly G_i, N_{h_i}, and N_{τ_i} from (2.9)–(2.15). Then, it suffices to guarantee the stability of the dynamic system (2.8) under the constraint (2.9)–(2.15). Furthermore, (2.5) is simplified to $e(t) = (I + EC)x(t) - z(t)$.

In the following, LMIs design conditions satisfying $e(t) \to 0$ when $t \to \infty$ are given for continuous-time systems.

3. Synthesis Conditions

This section deals with the continuous-time T-S models. Sufficient LMIs conditions guaranteeing the global asymptotic convergence of state estimation error (2.4) are given by using slack variable to introduce relaxation.

Theorem 3.1. *The observer* (2.3) *converges asymptotically to the state of the continuous-time T-S model* (2.1), *if there exist matrices* $\overline{Q}_j > 0$, $j = 1, \ldots, 4$, $\overline{S}_1, \overline{U}_l > 0$, $l = 1, \ldots, 3$,

and $\overline{P}_2, \overline{P}_3, \overline{N}_i, \overline{N}_{h_i}, \overline{N}_{d_i}$ *such that the conditions* (2.9)–(2.15) *and the following hold for all* $i \in I_M$:

$$\begin{bmatrix} \widehat{\Sigma}_{11_i} & \widehat{\Sigma}_{12_i} & \widehat{\Sigma}_{13_i} & -\overline{Q}_3 + \overline{Q}_4^T & \overline{N}_{\tau_i} \\ (*) & \widehat{\Sigma}_{22} & \overline{N}_{h_i} & 0 & \overline{N}_{\tau_i} \\ (*) & (*) & \widehat{\Sigma}_{33} & 0 & 0 \\ (*) & (*) & (*) & \widehat{\Sigma}_{44} & 0 \\ (*) & (*) & (*) & (*) & -\overline{U}_2 \end{bmatrix} < 0, \tag{3.1}$$

where $\widehat{\Sigma}_{11_i} = \operatorname{sym}\{\overline{N}_i + \overline{Q}_1 + \overline{Q}_3\} + \overline{U}_1 + \overline{S}_1$, $\widehat{\Sigma}_{12_i} = -\overline{P}_2^T + \overline{N}_i^T$, $\widehat{\Sigma}_{13_i} = \overline{N}_{h_i} - \overline{Q}_1 + \overline{Q}_2^T$, $\widehat{\Sigma}_{22} = \operatorname{sym}\{-\overline{P}_3\} + \overline{U}_2 + d\overline{U}_3 + h\overline{S}_1$, $\widehat{\Sigma}_{33} = -\overline{S}_1 - \operatorname{sym}\{\overline{Q}_2\}$, *and* $\widehat{\Sigma}_{44} = -\overline{U}_1 - \operatorname{sym}\{\overline{Q}_4\}$.

Proof. To investigate the delay-dependent asymptotically stable analysis of the error system (2.8), we define a class of Lyapunov-Krasovskii functions as follows:

$$V(t) = \sum_{i=1}^{3} V_i(t), \tag{3.2}$$

where

$$\begin{aligned} V_1(t) &= e^T(t)P_1e(t), \\ V_2(t) &= \int_{t-h}^{t} e^T(\theta)S_1e(\theta)d\theta + \int_{-h}^{0}\int_{t+\tau}^{t} \dot{e}^T(\theta)S_2\dot{e}(\tau)d\theta\, d\tau, \\ V_3(t) &= \int_{t-\tau}^{t} e^T(\theta)U_1e(\theta)d\theta + \int_{t-\tau}^{t} \dot{e}^T(s)U_2\dot{e}(s)ds + \int_{-\tau}^{0}\int_{t+\tau}^{t} \dot{e}^T(\theta)U_3\dot{e}(\tau)d\theta\, d\tau. \end{aligned} \tag{3.3}$$

Time derivative of $V_1(t)$ along the system trajectory (2.16) becomes

$$\dot{V}_1(t) = 2e^T(t)P_1\big(N_\mu e(t) + N_{\mu_\tau}\dot{e}(t-\tau) + N_{\mu_h}e(t-h)\big), \tag{3.4}$$

Then by taking the time derivative of $V_2(t)$ and $V_3(t)$, one can read

$$\dot{V}_2(t) = \&e^T(t)S_1e(t) - e^T(t-h)S_1e(t-h) + h\dot{e}^T(t)S_1\dot{e}(t) - \int_{t-h}^{t} \dot{e}^T(\theta)S_1\dot{e}(\theta)d\theta, \tag{3.5}$$

$$\begin{aligned} \dot{V}_3(t) = {} & e^T(t)U_1e(t) - e^T(t-\tau)U_1e(t-\tau) + \dot{e}^T(t)U_2\dot{e}(t) - \dot{e}^T(t-\tau)U_2\dot{e}(t-\tau) \\ & + \tau\dot{e}^T(t)U_3\dot{e}(t) - \int_{t-\tau}^{t} \dot{e}^T(\tau)U_3\dot{e}(\tau)d\tau. \end{aligned} \tag{3.6}$$

Moreover, from (2.16), the following equation holds for any matrices P_2 and P_3 with appropriate dimensions:

$$2\Big(e^T(t)P_2^T + \dot{e}^T(t)P_3^T\Big) \times \big(-\dot{e}(t) + N_\mu e(t) + N_{\mu_\tau}\dot{e}(t-\tau) + N_{\mu_h}e(t-h)\big) = 0. \tag{3.7}$$

Furthermore, from the Leibniz-Newton formula, the following equations hold for any matrices $Q_j, j = 1, \ldots, 4$, with appropriate dimensions:

$$\begin{aligned} &2\left(e^T(t)Q_1 + e^T(t-h)Q_2\right)\left(e(t) - e(t-h) - \int_{t-h}^{t} \dot{e}(s)ds\right) = 0, \\ &2\left(e^T(t)Q_3 + e^T(t-\tau)Q_4\right)\left(e(t) - e(t-\tau) - \int_{t-\tau}^{t} \dot{e}(s)ds\right) = 0. \end{aligned} \tag{3.8}$$

From the obtained derivative terms in (3.4)–(3.6) and adding the left-hand side of (3.7)–(24) into $\dot{V}(t)$, we obtain the following result for $\dot{V}(t)$:

$$\begin{aligned} \dot{V}(t) = {} & \chi^T(t)\Pi\chi(t) \\ & - \int_{t-h}^{t} \left(\chi^T(t)\nu_1 + \dot{e}(s)S_1\right)\overline{S}_1\left(\chi^T(t)\nu_1 + \dot{e}(s)S_1\right)^T ds \\ & - \int_{t-\tau}^{t} \left(\chi^T(t)\nu_2 + \dot{e}(s)U_3\right)\overline{U}_3\left(\chi^T(t)\nu_2 + \dot{e}(s)U_3\right)^T ds, \end{aligned} \tag{3.9}$$

or equivalently,

$$\dot{V}(t) = \chi^T(t)\Pi\chi(t), \tag{3.10}$$

with $\Pi := \Xi + h\nu_1\overline{S}_1\nu_1^T + \tau\nu_2\overline{U}_3\nu_2^T$, $\overline{S}_1 := S_1^{-1}$, $\overline{U}_3 := U_3^{-1}$, $\chi(t) = \mathrm{col}\{e(t), \dot{e}(t), e(t-h), e(t-\tau), \dot{e}(t-\tau)\}$, $\nu_1 = \mathrm{col}\{Q_1, 0, Q_2, 0, 0\}$, $\nu_2 = \mathrm{col}\{Q_3, 0, 0, Q_4, 0\}$, and

$$\Xi = \begin{bmatrix} \Sigma_{11} & \Sigma_{12} & \Sigma_{13} & -Q_3 + Q_4^T & \Sigma_{15} \\ (*) & \Sigma_{22} & P_3^T N_{\mu_h} & 0 & P_3^T N_{\mu_\tau} \\ (*) & (*) & \Sigma_{33} & 0 & 0 \\ (*) & (*) & (*) & \Sigma_{44} & 0 \\ (*) & (*) & (*) & (*) & -U_2 \end{bmatrix}, \tag{3.11}$$

where $\Sigma_{11} = \mathrm{sym}\{(P_1 + P_2^T)N_\mu + Q_1 + Q_3\} + U_1 + S_1$, $\Sigma_{12} = -P_2^T + N_\mu^T P_3$, $\Sigma_{13} = (P_1 + P_2^T)N_{\mu_h} - Q_1 + Q_2^T$, $\Sigma_{15} = (P_1 + P_2^T)N_{\mu_\tau}$, $\Sigma_{22} = \mathrm{sym}\{-P_3\} + U_2 + \tau U_3 + hS_1$, $\Sigma_{33} = -S_1 - \mathrm{sym}\{Q_2\}$, and $\Sigma_{44} = -U_1 - \mathrm{sym}\{Q_4\}$.

If a constant scalar $\kappa > 0$ satisfies the following condition:

$$\overline{\Pi} = \Pi + \widetilde{\Pi} < 0, \tag{3.12}$$

where

$$\widetilde{\Pi} := \begin{bmatrix} \kappa I & 0 & \cdots & 0 \\ 0 & 0 & \cdots & 0 \\ \vdots & \vdots & \ddots & \vdots \\ 0 & 0 & \cdots & 0 \end{bmatrix}, \tag{3.13}$$

then

$$\begin{aligned} \dot{V}(t) &\le \chi^T(t)\Pi\chi(t) = \chi^T(t)\left(\overline{\Pi} - \widetilde{\Pi}\right)\chi(t) \\ &< -\chi^T(t)\widetilde{\Pi}\chi(t). \end{aligned} \tag{3.14}$$

From the previous inequality, we can easily obtain, for all $\widehat{e}(t) \neq 0$,

$$\dot{V}(t) < -\kappa\|\widehat{e}(t)\|^2 < 0. \tag{3.15}$$

Based on Lyapunov stability theory, the error system (2.16) is asymptotically stable.

However, the condition (3.12) is not strict LMI due to the nonconvex constraints in the matrix indices, and, thus, one always has difficulties to get solutions satisfying the constraint. In order to find the solutions of (3.12), the obtained sufficient condition is now changed by some manipulations. The inequality $\overline{\Pi} < 0$ yields (by Schur complements)

$$\sum_{i=1}^{M} \mu_i(\xi(t)) \begin{bmatrix} \Xi_i + \widetilde{\Pi} & h\nu_1 & \tau\nu_2 \\ (*) & -hS_1 & 0 \\ (*) & (*) & -\tau U_3 \end{bmatrix} < 0, \tag{3.16}$$

with

$$\Xi_i = \begin{bmatrix} \Sigma_{11_i} & \Sigma_{12_i} & \Sigma_{13_i} & -Q_3 + Q_4^T & \Sigma_{15_i} \\ (*) & \Sigma_{22} & P_3^T N_{h_i} & 0 & P_3^T N_{\tau_i} \\ (*) & (*) & \Sigma_{33} & 0 & 0 \\ (*) & (*) & (*) & \Sigma_{44} & 0 \\ (*) & (*) & (*) & (*) & -U_2 \end{bmatrix}, \tag{3.17}$$

where $\Sigma_{11_i} = \mathrm{sym}\{(P_1 + P_2^T)N_i + Q_1 + Q_3\} + U_1 + S_1$, $\Sigma_{12_i} = -P_2^T + N_i^T P_3$, $\Sigma_{13_i} = (P_1 + P_2^T)N_{h_i} - Q_1 + Q_2^T$, and $\Sigma_{15_i} = (P_1 + P_2^T)N_{\tau_i}$. It is clear that $\Xi_i < 0$ result in LMI stabilization conditions.

It can be easily seen that the matrices $(P_1 + P_2)^T$ and P_3 are nonsingular. Let $\varsigma := \mathrm{diag}\{((P_1 + P_2)^T)^{-1}, P_3^{-1}, ((P_1 + P_2)^T)^{-1}, ((P_1 + P_2)^T)^{-1}, P_3^{-1}\}$. By premultiplying ς, postmultiplying ς^T to $\Xi_i < 0$, and using the definitions $\overline{N}_i := N_i(P_1 + P_2)^{-1}$, $\overline{N}_{h_i} := N_{h_i}(P_1 + P_2)^{-1}$, $\overline{N}_{\tau_i} := N_{\tau_i}P_3^{-1}$, $\overline{Q}_i := (P_1 + P_2^T)^{-1}Q_i(P_1 + P_2)^{-1}$, $\overline{U}_1 := (P_1 + P_2^T)^{-1}U_1(P_1 + P_2)^{-1}$, $\overline{U}_2 := P_3^{-1}U_1(P_3^T)^{-1}$, $\overline{P}_2 := P_3^{-1}P_2(P_1 + P_2)^{-1}$, and $\overline{P}_3 := P_3^{-1}$, one can obtain the LMI (3.1). This completes the proof. □

Remark 3.2. The equality constraints (2.13)–(2.15) can be rewritten in the following equivalent form:

$$[E \;\; \mathbf{K}] \begin{bmatrix} C\mathbf{R} & C\mathbf{H} & [F \;\; J] \\ -\mathbf{F} & -\mathbf{J} & 0 \end{bmatrix} = [-\mathbf{R} \;\; -\mathbf{H} \;\; 0], \tag{3.18}$$

with

$$\begin{gathered} \mathbf{H} = [H_1 \;\; H_2 \;\; \cdots \;\; H_M], \qquad \mathbf{K} = [K_1 \;\; K_2 \;\; \cdots \;\; K_M], \\ \mathbf{R} = [R_1 \;\; R_2 \;\; \cdots \;\; R_M], \\ \mathbf{F} = \left.\begin{bmatrix} F & 0 & \cdots & 0 \\ 0 & F & \cdots & \vdots \\ \vdots & \vdots & \ddots & \vdots \\ 0 & \cdots & \cdots & F \end{bmatrix}\right\}, \qquad \mathbf{J} = \left.\begin{bmatrix} J & 0 & \cdots & 0 \\ 0 & J & \cdots & \vdots \\ \vdots & \vdots & \ddots & \vdots \\ 0 & \cdots & \cdots & J \end{bmatrix}\right\} M \text{ times}, \end{gathered} \tag{3.19}$$

where $\mathbf{F} \in \mathbf{R}^{M\cdot p \times M\cdot q_d}$, $\mathbf{H} \in \mathbf{R}^{n\times M\cdot q_w}$, $\mathbf{R} \in \mathbf{R}^{n\times M\cdot q_d}$, and $\mathbf{K} \in \mathbf{R}^{n\times M\cdot p}$. A necessary and sufficient condition for the existence of a solution $[E, \mathbf{K}]$ to (3.18) is [33]

$$\operatorname{rank} \begin{bmatrix} C\mathbf{R} & C\mathbf{H} & [F \;\; J] \\ -\mathbf{F} & -\mathbf{J} & 0 \\ -\mathbf{R} & -\mathbf{H} & 0 \end{bmatrix} = \operatorname{rank} \begin{bmatrix} C\mathbf{R} & C\mathbf{H} & [F \;\; J] \\ -\mathbf{F} & -\mathbf{J} & 0 \end{bmatrix}. \tag{3.20}$$

Note that under this condition, a solution is obtained by

$$\begin{aligned} [E \;\; \mathbf{K}] = {} & [-\mathbf{R} \;\; -\mathbf{H} \;\; 0] \begin{bmatrix} C\mathbf{R} & C\mathbf{H} & [F \;\; J] \\ -\mathbf{F} & -\mathbf{J} & 0 \end{bmatrix}^{+} \\ & - Z\left(I - \begin{bmatrix} C\mathbf{R} & C\mathbf{H} & [F \;\; J] \\ -\mathbf{F} & -\mathbf{J} & 0 \end{bmatrix} \begin{bmatrix} C\mathbf{R} & C\mathbf{H} & [F \;\; J] \\ -\mathbf{F} & -\mathbf{J} & 0 \end{bmatrix}^{+} \right), \end{aligned} \tag{3.21}$$

where Z is an arbitrary matrix [33].

Remark 3.3. According to Theorem 3.1, the observer parameters can be calculated in the following:

(1) calculate $N_{\tau_i} = \overline{N}_{\tau_i} P_3$,

(2) compute T by solving (2.10) and calculate E from $T = I + EC$,

(3) compute N_{h_i} by solving (2.11),

(4) compute G_i by solving (2.12),

(5) compute $N_i = \overline{N}_i \overline{N}_{h_i}^{-1} N_{h_i}$,

(6) compute K_i by solving (2.9),

(7) compute L_i from $L_i = K_i - N_i E$.

Remark 3.4. It is worth noting that the number of the variables to be determined in the LMI (3.1) is $3n^2(M+2)+4n$.

Remark 3.5. The reduced conservatism of Theorem 3.1 benefits from the construction of the Lyapunov-Krasovskii functional in (3.2), introducing some free weighting matrices to express the relationship among the system matrices, and neither the model transformation approach nor any bounding technique is needed to estimate the inner product of the involved crossing terms. It can be easily seen that results of this paper are quite different from existing results in the literature in the following perspective. The structures at most of references, for instance [20], consider a delay-free T-S fuzzy system and in comparison to our case do not center on time delays, that is, the results in the previous reference cannot be directly applied to the T-S fuzzy models with unknown inputs and different neutral and discrete-time delays.

4. Numerical Example

To show the validness of the proposed results, a numerical example is proposed for the discrete-time T-S model (2.1) with the following data:

$$
\begin{gathered}
A_1 = \begin{bmatrix} -0.4 & 0.2 & 0.3 \\ 0.3 & -0.6 & 0.3 \\ 0.4 & 0.2 & 0.6 \end{bmatrix}, \\
A_2 = \begin{bmatrix} -0.45 & 0.375 & 0.375 \\ 0.15 & -0.45 & 0 \\ 0.75 & 0.75 & -0.45 \end{bmatrix}, \\
A_{h_1} = \begin{bmatrix} -0.01 & 0.03 & 0.02 \\ 0.01 & -0.005 & 0 \\ 0.005 & 0.07 & -0.03 \end{bmatrix}, \\
A_{h_2} = \begin{bmatrix} -0.005 & 0.01 & 0.04 \\ 0.01 & -0.025 & 0.02 \\ 0.05 & 0.03 & -0.01 \end{bmatrix}, \\
A_{\tau_1} = \begin{bmatrix} 0.0045 & -0.0037 & -0.0037 \\ -0.0015 & 0.0045 & 0 \\ -0.0075 & -0.0075 & 0.0045 \end{bmatrix}, \\
A_{\tau_2} = \begin{bmatrix} 0.0170 & -0.0115 & -0.0135 \\ -0.0090 & 0.0210 & -0.0060 \\ -0.0230 & -0.0190 & -0.0030 \end{bmatrix}, \\
B_1 = \begin{bmatrix} 1.0 \\ -0.5 \\ -0.5 \end{bmatrix}, \qquad B_2 = \begin{bmatrix} -0.5 \\ 1.0 \\ -0.5 \end{bmatrix}, \qquad F = \begin{bmatrix} 1 \\ 1.2 \end{bmatrix}, \\
R_1 = \begin{bmatrix} 0.4 \\ -0.4 \\ 0.4 \end{bmatrix}, \qquad R_2 = \begin{bmatrix} 0.4 \\ 0.4 \\ -0.8 \end{bmatrix}, \; C = \begin{bmatrix} 0 & 1 & 1 \\ 1 & 0 & 1 \end{bmatrix}, \\
J = 0, \qquad H = 0, \qquad \tau = 0.05, \qquad h = 0.1, \qquad A_{\tau_1} = 0.1 I_3, \qquad A_{\tau_2} = 0.7 I_3.
\end{gathered}
\tag{4.1}
$$

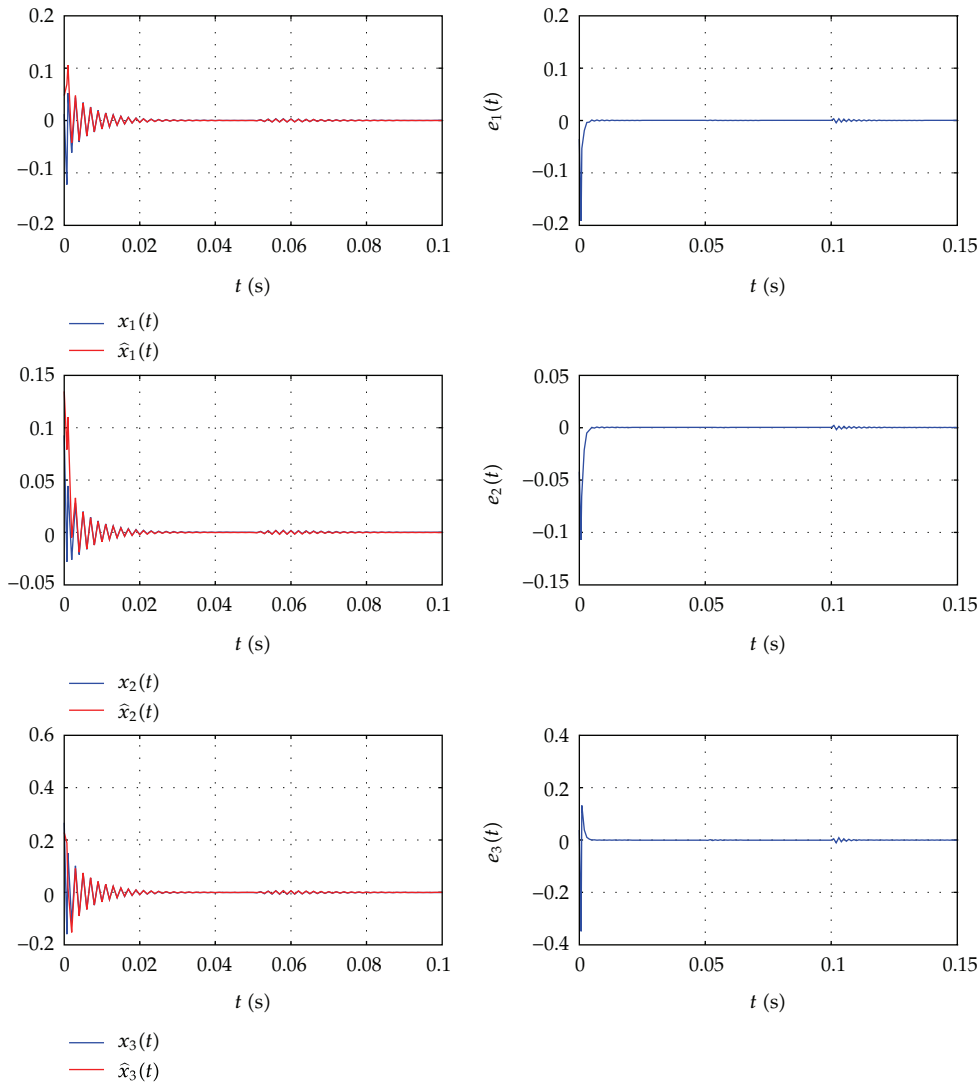

Figure 1: Time behaviour of states and corresponding error signals.

In the light of Theorem 3.1 and Remark 3.2, we solved LMIs and obtained the following observer gains by using Matlab LMI Control Toolbox [34]

$$E = \begin{bmatrix} 0.1945 & -0.1508 \\ -0.7474 & 0.6300 \\ -0.5524 & 0.4682 \end{bmatrix},$$

$$G_1 = \begin{bmatrix} 0.7363 \\ 0.5659 \\ 0.2927 \end{bmatrix}, \qquad G_2 = \begin{bmatrix} -0.2518 \\ -0.0032 \\ -1.2461 \end{bmatrix},$$

$$N_1 = \begin{bmatrix} -0.2699 & -0.2149 & 0.0543 \\ -0.2053 & -0.1778 & 0.0849 \\ -0.0775 & -0.0530 & -0.2330 \end{bmatrix},$$

$$N_2 = \begin{bmatrix} -0.2734 & -0.1996 & -0.0930 \\ -0.4198 & -0.3263 & -0.1422 \\ 1.1909 & 0.9204 & 0.3656 \end{bmatrix},$$

$$L_1 = \begin{bmatrix} 0.1565 & 0.0973 \\ 0.2284 & -0.1071 \\ 0.6159 & 0.1294 \end{bmatrix}, \qquad L_2 = \begin{bmatrix} 0.3221 & 0.0557 \\ 0.0335 & 0.3480 \\ 0.8122 & -1.3116 \end{bmatrix}. \tag{4.2}$$

For simulation purpose, we simply choose $w(t) = t/(1+t^2)$ as the disturbance, $u(t) = e^{-t}\sin(t)$ as the input signal, and $\mu_1(\xi) = (1 - \sin(x_2(t)))/2$ and $\mu_2(\xi) = (1 + \sin(x_2(t)))/2$ as activation functions. The error signals for an input are depicted in Figure 1. It is seen that the state estimation for the systems is performed as well.

5. Conclusion

In this paper, a robust observer design was proposed for Takagi-Sugeno (T-S) fuzzy neutral models with unknown inputs. The model consists of a mixed neutral and discrete delay, and the disturbances are imposed on both state and output signals. Delay-dependent sufficient conditions for the design of an unknown input T-S observer with time delays were given in terms of linear matrix inequalities (LMIs). Some relaxations were introduced by using intermediate variables. A numerical example was given to illustrate the effectiveness of the given results. Extension to the case of unmeasured decision variables is considered as a challenging problem. A numerical example has shown the effectiveness of the proposed results. Future work will investigate fault detection and Markovian jump systems for fuzzy systems with unknown inputs and time delays (see for instance [25–27, 35–37]).

Acknowledgments

The authors would like to thank the editor and anonymous reviewers for their constructive comments and suggestions to improve the quality of the paper.

References

[1] T. Takagi and M. Sugeno, "Fuzzy identification of systems and its application to modelling and control," *IEEE Transactions on Systems, Man, and Cybernetics*, vol. 15, no. 1, pp. 116–132, 1985.

[2] Y. Zhao, H. Gao, J. Lam, and B. Du, "Stability and stabilization of delayed T-S fuzzy systems: a delay partitioning approach," *IEEE Transactions on Fuzzy Systems*, vol. 17, no. 4, pp. 750–762, 2009.

[3] B. Jiang, K. Zhang, and P. Shi, "Integrated fault estimation and accommodation design for discrete-time Takagi-Sugeno fuzzy systems with actuator faults," *IEEE Trans on Fuzzy Systems*, vol. 19, no. 2, pp. 291–304, 2011.

[4] S. K. Nguang and P. Shi, "Robust H_∞ output feedback control design for Takagi- Sugeno systems with Markovian jumps: a linear matrix inequality approach," *Journal of Dynamic Systems, Measurement and Control, ASME Transaction*, vol. 128, no. 3, pp. 617–625, 2006.

[5] M. Nachidi, F. Tadeo, and A. Benzouia, "Controller design for Takagi-Sugeno systems in continuous-time," *International Journal of Innovative Computing, Information and Control*, vol. 8, no. 9, pp. 6389–6400, 2012.

[6] T.-E. Lee, J.-P. Su, K.-W. Yu, and K.-H. Hsia, "Multi-objective fuzzy optimal design of alpha-beta estimators for nonlinear variable structure control," *International Journal of Innovative Computing, Information and Control A*, vol. 7, no. 5, pp. 2123–2140, 2011.

[7] V. Kumar, K. P. S. Rana, and A. K. Sinha, "Performance, and stability analysis of a formula-based fuzzy PI controller," *International Journal of Innovative Computing, Information and ControlB*, vol. 7, no. 7, pp. 4291–4308, 2011.

[8] K. Zrar Ghafoor, K. Abu Bakar, S. Salleh et al., "Fuzzy logic-assisted geographical routing over vehicular Ad Hoc networks," *International Journal of Innovative Computing Information and Control B*, vol. 8, no. 7, pp. 5095–5120, 2012.

[9] J. Yang and J. Watada, "Fuzzy clustering analysis of data mining: application to an accident mining system," *International Journal of Innovative Computing Information and Control*, vol. 8, no. .8, pp. 5715–5724, 2012.

[10] J. Botzheim and P. Foldesi, "Parametric approximation of fuzzy exponent for computationally intensive problems," *International Journal of Innovative Computing Information and Control*, vol. 8, no. 8, pp. 5725–5744, 2012.

[11] N. Yagiz and Y. Hacioglu, "Robust control of a spatial robot using fuzzy sliding modes," *Mathematical and Computer Modelling*, vol. 49, no. 1-2, pp. 114–127, 2009.

[12] H. Gao, Y. Zhao, and T. Chen, "H_∞ Fuzzy control of nonlinear systems under unreliable communication links," *IEEE Transactions on Fuzzy Systems*, vol. 17, no. 2, pp. 265–278, 2009.

[13] H. Gao, X. Liu, and J. Lam, "Stability analysis and stabilization for discrete-time fuzzy systems with time-varying delay," *IEEE Transactions on Systems, Man and Cybernetics B*, vol. 39, no. 2, pp. 306–317, 2009.

[14] L. Wu and D. W. C. Ho, "Fuzzy filter design for Ito stochastic systems with application to sensor detection," *IEEE Trans Fuzzy Systems*, vol. 17, no. 1, pp. 233–242, 2009.

[15] L. Xiaodiong and Z. Qingling, "New approaches to H_∞ controller designs based on fuzzy observers for T-S fuzzy systems via LMIs," *Automatica*, vol. 39, no. 9, pp. 1571–1582, 2003.

[16] K. Tanaka, H. Ohtake, and H. O. Wang, "A descriptor system approach to fuzzy control system design via fuzzy lyapunov functions," *IEEE Transactions on Fuzzy Systems*, vol. 15, no. 3, pp. 333–341, 2007.

[17] W. Assawinchaichote, S. K. Nguang, and P. Shi, *Fuzzy Control and Filter Design for Uncertain Fuzzy Systems*, vol. 347, Springer, Berlin, Germany, 2006.

[18] A. Kruszewski, R. Wang, and T. M. Guerra, "Nonquadratic stabilization conditions for a class of uncertain nonlinear discrete time TS fuzzy models: a new approach," *IEEE Transactions on Automatic Control*, vol. 53, no. 2, pp. 606–611, 2008.

[19] A. Sala and C. Ariño, "Asymptotically necessary and sufficient conditions for stability and performance in fuzzy control: applications of Polya's theorem," *Fuzzy Sets and Systems*, vol. 158, no. 24, pp. 2671–2686, 2007.

[20] M. Chadli and H. R. Karimi, "Robust observer design for unknown inputs Takagi-Sugeno models," *IEEE Transactions on Fuzzy Systems*. In press.

[21] M. Blanke, M. Kinnaert, and J. M. Lunze, *Staroswiecki, Diagnosis and Fault-Tolerant Control*, Hardcover, 2nd edition, 2006.

[22] R. J. Patton, "Fault-tolerant control systems: the 1997 situation," in *IFAC Symposium on Fault Detection Supervision and Safety for Technical Processes*, vol. 3, pp. 1033–1054, 1997.

[23] M. Oudghiri, M. Chadli, and A. El Hajjaji, "Robust observer-based fault tolerant control for vehicle lateral dynamics," *International Journal of Vehicle Design*, vol. 48, no. 3-4, pp. 173–189, 2008.

[24] X. Su, L. Wu, P. Shi, and Y. D. Song, "H_∞ model reduction of T-S fuzzy stochastic systems," *IEEE Transactions on Systems, Man, and Cybernetics Part B*, vol. 42, no. 6, pp. 1574–1585, 2012.

[25] L. Wu, X. Su, P. Shi, and J. Qiu, "Model approximation for discrete-time state-delay systems in the T-S fuzzy framework," *IEEE Transactions on Fuzzy Systems*, vol. 19, no. 2, Article ID 366378, 2011.

[26] X. Su, P. Shi, L. Wu, and Y. Song, "A novel approach to filter design for T-S fuzzy discrete-time systems with time-varying delay," *IEEE Transactions on Fuzzy Systems*. In press.

[27] Y. He, M. Wu, J.-H. She, and G.-P. Liu, "Delay-dependent robust stability criteria for uncertain neutral systems with mixed delays," *Systems & Control Letters*, vol. 51, no. 1, pp. 57–65, 2004.

[28] D. Yue and Q. L. Han, "A Delay-dependent stability criterion of neutral systems and its application to a partial element equivalent circuit model," *IEEE Transactions on Circuits and Systems Part II*, vol. 51, pp. 685–680, 2004.

[29] H. R. Karimi and P. Maass, "Delay-range-dependent exponential H_∞ synchronization of a class of delayed neural networks," *Chaos, Solitons and Fractals*, vol. 41, no. 3, pp. 1125–1135, 2009.

[30] H. R. Karimi and H. Gao, "New delay-dependent exponential H_∞ synchronization for uncertain neural networks with mixed time-delays?" *IEEE Transactions on Systems, Man and Cybernetics B*, vol. 40, no. 1, pp. 173–185, 2010.

[31] R. Yang, P. Shi, G.-P. Liu, and H. Gao, "Network-based feedback control for systems with mixed delays based on quantization and dropout compensation," *Automatica*, vol. 47, no. 12, pp. 2805–2809, 2011.

[32] R. Murray-Smith and T. Johansen, *Multiple Model Approaches to Modelling and Control*, Taylor & Francis, 1999.

[33] C. R. Rao and S. K. Mitra, *Generalized Inverse of Matrices and Its Applications*, John Wiley, 1971.

[34] P. Gahinet, A. Nemirovsky, A. J. Laub, and M. Chilali, *LMI Control Toolbox: For Use with Matlab*, The MATH Works, Natik, Mass, USA, 1995.

[35] L. Zhang, E.-K. Boukas, and J. Lam, "Analysis and synthesis of Markov jump linear systems with time-varying delays and partially known transition probabilities," *IEEE Transactions on Automatic Control*, vol. 53, no. 10, pp. 2458–2464, 2008.

[36] L. Zhang, E.-K. Boukas, L. Baron, and H. R. Karimi, "Fault detection for discrete-time Markov jump linear systems with partially known transition probabilities," *International Journal of Control*, vol. 83, no. 8, pp. 1564–1572, 2010.

[37] H. R. Karimi, "Robust delay-dependent H_∞ control of uncertain time-delay systems with mixed neutral, discrete, and distributed time-delays and Markovian switching parameters," *IEEE Transactions on Circuits and Systems. I*, vol. 58, no. 8, pp. 1910–1923, 2011.

Hindawi Publishing Corporation
Mathematical Problems in Engineering
Volume 2012, Article ID 105074, 12 pages
doi:10.1155/2012/105074

Research Article

Fuzzy Variable Structure Control for Uncertain Systems with Disturbance

Bo Wang,[1,2] Peng Shi,[3,4] Hamid Reza Karimi,[5] Jun Wang,[1] and Yongduan Song[6]

[1] *School of Electrical and Information Engineering, Xihua University, Chengdu 610096, China*
[2] *School of Applied Mathematics, University of Electronic Science and Technology of China, Chengdu 610054, China*
[3] *School of Electrical and Electronic Engineering, The University of Adelaide, Adelaide SA 5005, Australia*
[4] *School of Engineering and Science, Victoria University, Melbourne, VIC 8001, Australia*
[5] *Department of Engineering, Faculty of Engineering and Science, University of Agder, 4898 Grimstad, Norway*
[6] *School of Automation, Chongqing University, Chongqing 400044, China*

Correspondence should be addressed to Peng Shi, peng.shi@vu.edu.au

Received 2 September 2012; Accepted 26 October 2012

Academic Editor: Mohammed Chadli

Copyright © 2012 Bo Wang et al. This is an open access article distributed under the Creative Commons Attribution License, which permits unrestricted use, distribution, and reproduction in any medium, provided the original work is properly cited.

This paper focuses on the fuzzy variable structure control for uncertain systems with disturbance. Specifically, the fuzzy control is introduced to estimate the control disturbance, the switching control is included to compensate for the approximation error, and they possess the characteristic of simpleness in design and effectiveness in attenuating the control chattering. Some typical numerical examples are presented to demonstrate the effectiveness and advantage of the fuzzy variable structure controller proposed.

1. Introduction

Since the pioneering works of Utkin in 1977 [1], the variable structure control (VSC) has generated considerable interests in control field. Up to now many researches on VSC have been carried out [2–16]. Based on VSC theory, [2] developed an adaptive fuzzy control system design method for uncertain Takagi-Sugeno fuzzy models with norm-bounded uncertainties. By using a high-gain observer, [3] presented an output feedback model-reference variable structure controller to achieve global exponential stability with respect to a small residual set without generating peaking in the control signal. In [4], the subordinated reachability of the sliding motion is introduced to realize the control on a class of uncertain stochastic

systems with time-varying delay. Via introducing a pseudo-inversion, the authors in [5] discussed the adaptive control for the uncertain discrete time linear systems preceded by hysteresis nonlinearity. In [6], a sufficient condition for existence of reduced-order sliding mode dynamics was derived to realize the sliding mode control of a continuous-time switched stochastic system. For VSC, one of the most intriguing properties is the insensitivity to parameter uncertainties and external disturbance for the switching action between sliding modes, which can lead to the generation of chattering phenomenon and make a difference to system control performance. Therefore how to solve this problem is always a challenging topic for VSC.

Uncertainties and disturbances exist in many kinds of systems; this makes the practical control problem complicated and has received much attention from scholars [17–22]. VSC method is one of the effective solutions, and conventionally the switching term is built based on the upper norm bound of control disturbance to satisfy the system control condition. Therefore there exists the difference between real control disturbance and its upper norm bound. The maximum switching amplitude can be double disturbance error upper bound. For ease of use, the upper norm bound sometimes is taken as a constant by experience. This may lead to the serious chattering problem. Widely acknowledged, an effective solution is to build a unit to obtain the estimate of time-varying control disturbance. Up to now, there exist some feasible methods, such as neural networks and genetic algorithm, to tackle the problem. However in real application, those approaches are too complicated and need much more control information. Corresponding control cost problem cannot be ignored.

Recently, fuzzy method gets wide attention in the control field, corresponding research can be seen in [23–33] and the references therein. It is also introduced to VSC area for its characteristic of simpleness in design, and effectiveness in attenuating chattering. In this paper, a fuzzy auxiliary controller will be built to approximate the control disturbance based on just one feedback signal and a switching control term will be designed to compensate for the approximation error. Some typical simulation examples will be concerned afterward to illustrate the effectiveness of the controller given.

Notations used in this paper are fairly standard. Let R^n be the n-dimensional Euclidean space, $R^{n\times m}$ represents the set of $n \times m$ real matrix, $(\cdot)^{(i)}$ denotes the ith derivative of $(\cdot)$, and the notation $A > 0$ means that A is real symmetric and positive definite, $\operatorname{sgn}(x)$ denotes the operator $|x|/x$, and $\operatorname{sat}(\cdot)$ denotes the saturated function.

2. Problem Statement

In this paper, the following high order uncertain single-input single-output (SISO) system with disturbance is considered:

$$\begin{aligned} \dot{x}_i(t) &= x_{i+1}(t), \quad i < n, \\ \dot{x}_n(t) &= f(x,t) + \Delta f(x,t) + p(t) + b(t)\cdot u(t), \end{aligned} \tag{2.1}$$

where $x(t) = (x_1(t), x_2(t), \ldots, x_n(t))^T \in R^n$ is the system state vector, $f(\cdot,t)$ is the nonlinear function, $\Delta f(\cdot,t)$ is the nonlinear uncertainties, $p(t)$ is the external disturbance, $b(t)$ is the nonzero coefficient of control input, and $u(t)$ is the control input.

Define the tracking error

$$E(t) = x(t) - x_r(t), \tag{2.2}$$

where $E = (e_1(t), e_2(t), \ldots, e_n(t))^T \in R^n$, $x_r(t) = (x_{r1}(t), x_{r2}(t), \ldots, x_{rn}(t))^T \in R^n$, and $x_{r1}(t)$ is the desired trajectory with

$$x_{ri}(t) = {x_{r1}}^{(i-1)}(t), \quad i \leq n, \tag{2.3}$$

where $(\cdot)^{(i-1)}$ denotes the $(i-1)$th derivative of $(\cdot)$. Then the error dynamic system can be expressed by

$$\begin{gathered} \dot{e}_i(t) = e_{i+1}(t), \\ \dot{e}_n(t) = f(x,t) - x_{rn}(t) + d(t) + b(t) \cdot u(t), \end{gathered} \tag{2.4}$$

where $d(t) = \Delta f(x,t) + p(t)$ is the control disturbance.

The problem to be addressed in this paper is to design a controller such that the tracking error variable satisfies

$$\lim_{t\to\infty} \|E(t)\| = \lim_{t\to\infty} \|x(t) - x_r(t)\| \longrightarrow 0. \tag{2.5}$$

In this paper, the following lemma is needed

Lemma 2.1 (see [34]). *If $w(t) : R \to R$ is a uniformly continuous function for $t \geq 0$ and if*

$$\lim_{t\to\infty} \int_0^t w(s)ds \tag{2.6}$$

exists and is finite, then

$$\lim_{t\to\infty} w(t) \longrightarrow 0. \tag{2.7}$$

3. Design of Fuzzy Variable Structure Controller

In this section, the FVSC method is introduced to realize the control for uncertain system with disturbance. First, the following sliding surface is introduced:

$$s(t) = C^T E(t) = e_n(t) + \sum_{i=1}^{n-1} c_i e_i(t), \tag{3.1}$$

where $C = [c_1, c_2, \ldots, c_{n-1}, 1]^T$ is chosen such that the distribution of the roots of characteristic equation $p^{n-1} + c_{n-1}p^{n-2} + \cdots + c_2 p + c_1 = 0$ is on the left side of complex plane to make the following system stable:

$$e_n(t) + \sum_{i=1}^{n-1} c_i e_i(t) = 0. \tag{3.2}$$

Then, we have

$$\begin{aligned} \dot{s}(t) &= \dot{e}_n(t) + \sum_{i=1}^{n-1} c_i e_{i+1}(t) \\ &= f(x) - x_{rn}(t) + d(t) + b(t) \cdot u(t) + \sum_{i=1}^{n-1} c_i e_{i+1}(\mathrm{t}). \end{aligned} \tag{3.3}$$

Based on Lyaponov method and VSC theory, the following theoretical result can be obtained.

First, a fuzzy auxiliary controller $D(t)$ is built to estimate the control disturbance $d(t)$. Corresponding fuzzy rules are given by

IF $Sd(t) > 0$ THEN $D(t)$ should be increased,

IF $Sd(t) < 0$ THEN $D(t)$ should be decreased,

where

$$Sd(t) = \dot{s}(t) + \varepsilon \cdot \mathrm{sgn}(s(t)). \tag{3.4}$$

The term under consideration $D(t)$ can take a greater value. If it is too big, this may lead to some serious control problem in practice. Therefore in this paper, based on the integral method, the small value $\Delta D(t)$ is recommended to replace by $D(t)$ for their relations as follows:

$$D(t) = G \int_0^t \Delta D(s) ds, \tag{3.5}$$

where G is the proportionality coefficient.

Let Sd denote the fuzzy input $Sd(t)$, and ΔD denotes the fuzzy output $\Delta D(t)$. The fuzzy sets of the input and the output are defined, respectively, as

$$\begin{aligned} Sd &= \{\mathrm{NB}, \mathrm{NM}, \mathrm{ZO}, \mathrm{PM}, \mathrm{PB}\}, \\ \Delta D &= \{\mathrm{NB}, \mathrm{NM}, \mathrm{ZO}, \mathrm{PM}, \mathrm{PB}\}, \end{aligned} \tag{3.6}$$

where NB is negative and large, NM is negative and medium, ZO is zero, PM is the positive and medium, and PB is positive and large.

Select the following fuzzy rules:

R1: IF Sd is PB THEN ΔD is PB,

R2: IF Sd is PM THEN ΔD is PM,

R3: IF Sd is ZO THEN ΔD is ZO,

R4: IF Sd is NM THEN ΔD is NM,

R5: IF Sd is PB THEN ΔD is NB.

Hence based on the proposed fuzzy auxiliary controller, the following theoretical result can be concluded.

Theorem 3.1. *For $\varepsilon > 0$, system* (2.1) *can track the desired trajectory* (2.3) *based on the following fuzzy variable structure controller:*

$$u(t) = \frac{1}{b(t)}\left[-f(x) + x_{rn}(t) - \sum_{i=1}^{n-1} c_i e_{i+1}(t) - D(t) - \varepsilon \cdot \operatorname{sgn}(s(t))\right]. \tag{3.7}$$

Proof. Choose the Lyapunov functional candidate as

$$V(t) = \frac{1}{2}s^2(t). \tag{3.8}$$

The time derivative of $V(t)$ along trajectories of error model (2.4) is as

$$\begin{aligned} \dot{V}(t) &= s(t)\dot{s}(t) \\ &= s(t)\left[f(x) - x_{rn}(t) + d(t) + b(t)\cdot u(t) + \sum_{i=1}^{n-1} c_i e_{i+1}(t)\right]. \end{aligned} \tag{3.9}$$

Substituting (3.7) into (3.9), we have

$$\begin{aligned} \dot{V}(t) &= s(t)\left[d(t) - D(t) - \varepsilon \cdot \operatorname{sgn}(s(t))\right] \\ &= -w(t), \end{aligned} \tag{3.10}$$

where $w(t) = \varepsilon|s(t)|$. For $\varepsilon > 0$, we have $\dot{V} \le 0$. Integrating both sides of (3.9) from 0 to t leads to

$$\lim_{t\to\infty} V(t) - V(0) \le -\lim_{t\to\infty}\int_0^t w(s)ds. \tag{3.11}$$

Since $V(t)$ is positive and $V(0)$ is finite, the following inequality can be concluded:

$$\lim_{t\to\infty}\int_0^t w(s)ds \le V(0) < \infty. \tag{3.12}$$

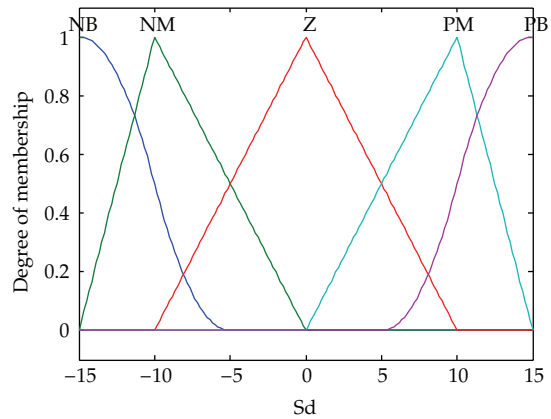

Figure 1: The membership function of the fuzzy input.

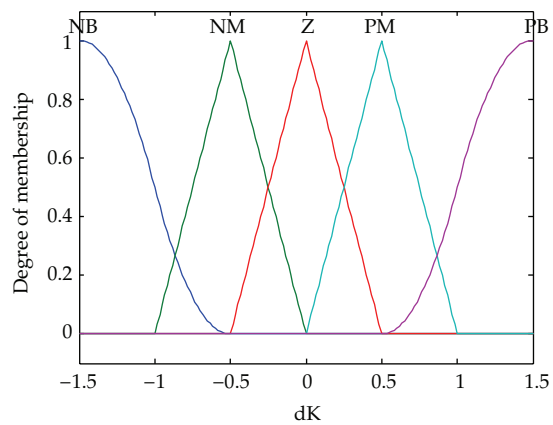

Figure 2: The membership function of the fuzzy output.

Based on Lemma 2.1, we can obtain

$$\lim_{t\to\infty} w(t) = \lim_{t\to\infty} \varepsilon|s(t)| \longrightarrow 0. \tag{3.13}$$

Hence

$$\lim_{t\to\infty} E(t) \longrightarrow 0. \tag{3.14}$$

This means the system control can be achieved based on the fuzzy VSC proposed. The proof of Theorem 3.1 is thus completed. □

Remark 3.2. The fuzzy auxiliary controller is constructed based on the feedback signal $Sd = \dot{s}(t) + \varepsilon \cdot \operatorname{sgn}(s(t))$, the employed fuzzy rule is simple, and essentially used to keep Sd at zero. Hence it can be concluded that $\dot{V}(t) = s(t)\dot{s}(t) = -\varepsilon|s(t)| \leq 0$. This completes our proof.

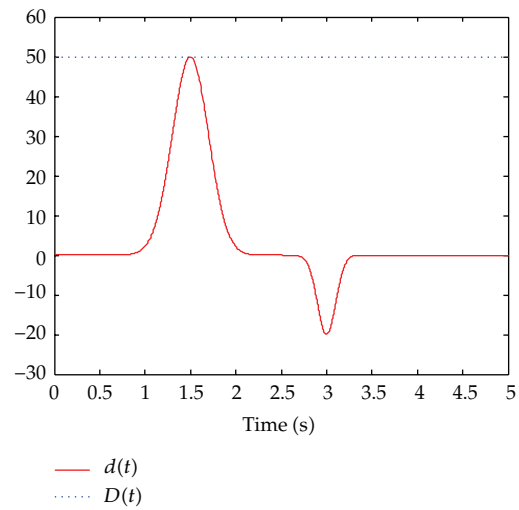

Figure 3: The time response of $d(t)$ and $D(t)$ in case 1.

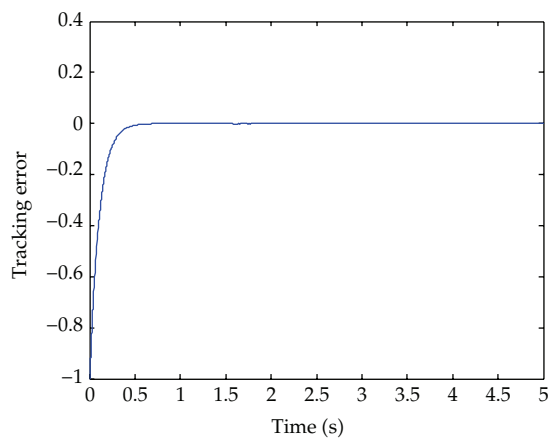

Figure 4: The time response of the tracking error in case 1.

We can see that the fuzzy auxiliary controller and the sliding mode controller come together to realize the effective control on system (2.1).

4. Numerical Example

In this section, we will verify the proposed methodology by giving an illustrative example. First consider the following disturbed system

$$\begin{aligned} \dot{x}_1(t) &= x_2(t), \\ \dot{x}_2(t) &= f(x,t) + d(t) + b(t) \cdot u(t), \end{aligned} \tag{4.1}$$

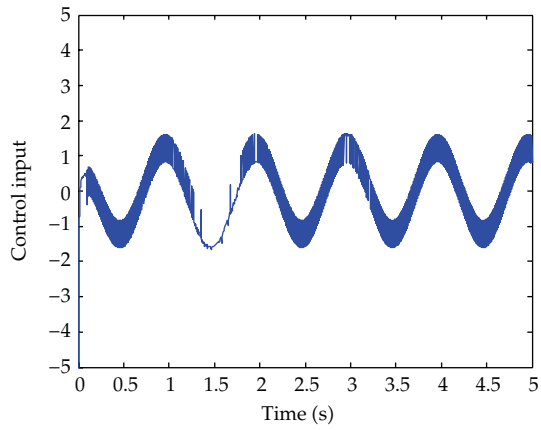

Figure 5: The time response of the control input in case 1.

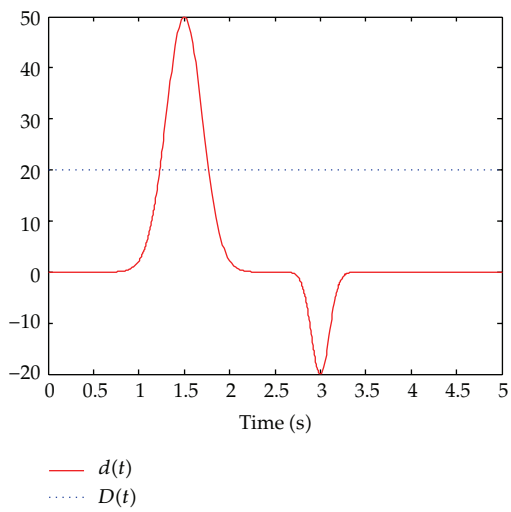

Figure 6: Time response of $d(t)$ and $D(t)$ for case 2.

where

$$f(x,t) = -0.5x_2(t) + x_1(t) - {x_1}^3(t), \quad b(t) = 133,$$
$$d(t) = 50\exp\left[-\frac{(t-1.5)^2}{2\cdot 0.2^2}\right] - 20\exp\left[-\frac{(t-3)^2}{2\cdot 0.1^2}\right]. \tag{4.2}$$

For simulation purposes, we consider the step size 0.001 second, the initial condition $x_0 = [-1,-1]^T$, the desired trajectory $x_r(t) = \sin(2\pi t)$, and the control parameters $\eta = 1.0$, $r = 1.0$, $G = 800$, $c = 150$. The membership function of the input and the output of fuzzy system are shown in Figures 1–2. First, we adopt the general VSC method via fixing $D(t) = \max\{|d(t)|\} = 50$. The simulation results are shown in Figures 3–5. Next, we adopt the general VSC method

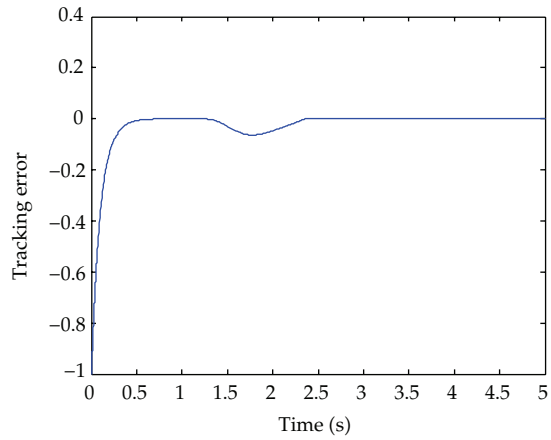

Figure 7: Time response of the tracking error for case 2.

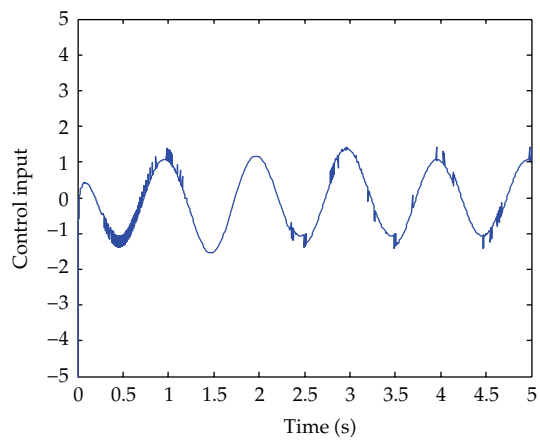

Figure 8: Time response of $u(t)$ for case 2.

via fixing $D(t) = \max\{|d(t)|\} = 20$. The simulation results are shown in Figures 6–8. Finally, we employ the given fuzzy VSC method. The simulation results are shown in Figures 9–11.

Remark 4.1. Figures 3, 6, and 9 show the time response of control disturbance $d(t)$ and its estimate $D(t)$. Figures 4, 7, and 10 show the time response of the tracking error. Figures 5, 8 and 11 show the time response of the control input. In case 1, the control disturbance $D(t)$ is fixed at 50, which is bigger than the upper bound of $d(t)$. From Figures 3–5 it can be seen, when $d(t) \neq 50$, that there is an obvious chattering phenomenon in control input for the estimation error of $d(t)$. In case 2, the control disturbance $D(t)$ is fixed at 20, which is less than the upper bound of $d(t)$. From Figures 6–8 it can be seen, when $d(t) \geq 20$, that there exists a big tracking error because the VSC can not be guaranteed at this moment. In case 3, the control disturbance $d(t)$ is estimated by the fuzzy auxiliary controller. From Figures 9–11 it can be seen that the control for the given system is realized within 1 second and the chattering phenomenon is reduced distinctly, which demonstrates the effectiveness of the presented fuzzy VSC method.

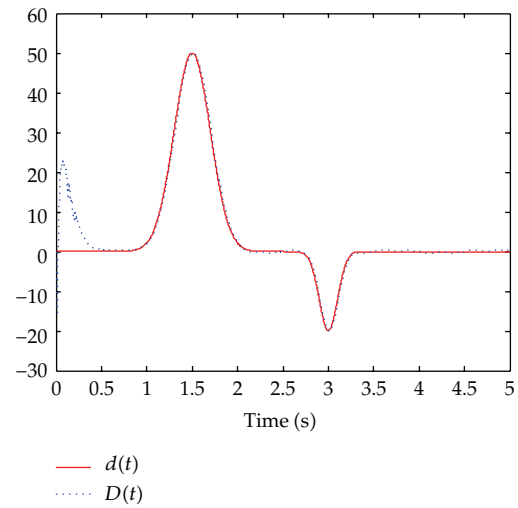

Figure 9: The time response of $d(t)$ and $D(t)$ in case 3.

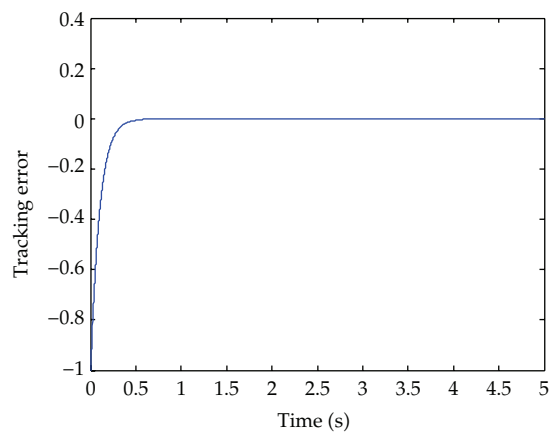

Figure 10: The time response of the tracking error in case 3.

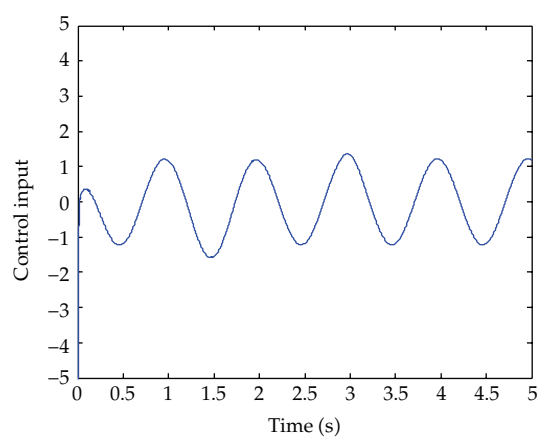

Figure 11: The time response of the control input in case 3.

Remark 4.2. From the simulation results, we can see that the chattering phenomenon is reduced effectively by using the proposed fuzzy controller however there still exists the switching term $\varepsilon \cdot \mathrm{sgn}(s(t))$ in control signal although ε is a small constant. To further overcome the control chattering phenomenon, the switching term $\varepsilon \cdot \mathrm{sgn}(s(t))$ is recommended to be substituted for $\varepsilon \cdot \mathrm{sat}(s(t))$.

5. Conclusion

In this paper, the fuzzy variable structure control problem has been studied. The fuzzy control method and the switching control method have been employed to realize the control for uncertain system with disturbance, they possess the characteristic of simpleness in design and effectiveness in attenuating the control chattering, and aresuitable for the application in engineering. Some typical numerical examples have been included afterward to demonstrate the effectiveness of the given controller.

Acknowledgments

This work was partially supported by the Key Projects of Xihua University (Z1120946), the National Key Basic Research Program (973), China (no. 2012CB215202), the 111 Project (B12018), the National Natural Science Foundation of China (nos. 61174058, and 61170030), and the Engineering and Physical Sciences Research Council, UK (EP/F029195).

References

[1] V. I. Utkin, "Variable structure systems with sliding modes," *IEEE Transactions on Automatic Control*, vol. 22, no. 2, pp. 212–222, 1977.
[2] H. H. Choi, "Adaptive controller design for uncertain fuzzy systems using variable structure control approach," *Automatica*, vol. 45, no. 11, pp. 2646–2650, 2009.
[3] J. P. V. S. Cunha, R. R. Costa, F. Lizarralde, and L. Hsu, "Peaking free variable structure control of uncertain linear systems based on a high-gain observer," *Automatica*, vol. 45, no. 5, pp. 1156–1164, 2009.
[4] H. Xing, C. C. Gao, and D. Li, "Sliding mode variable structure control for parameter uncertain stochastic systems with time-varying delay," *Journal of Mathematical Analysis and Applications*, vol. 355, no. 2, pp. 689–699, 2009.
[5] X. Chen, T. Hisayama, and C. Y. Su, "Pseudo-inverse-based adaptive control for uncertain discrete time systems preceded by hysteresis," *Automatica*, vol. 45, no. 2, pp. 469–476, 2009.
[6] L. Wu, D. W. C. Ho, and C. W. Li, "Sliding mode control of switched hybrid systems with stochastic perturbation," *Systems and Control Letters*, vol. 60, no. 8, pp. 531–539, 2011.
[7] Z. Lin, Y. Xia, P. Shi, and H. Wu, "Robust sliding mode control for uncertain linear discrete systems independent of time-delay," *International Journal of Innovative Computing, Information and Control*, vol. 7, no. 2, pp. 869–880, 2011.
[8] T. E. Lee, J. P. Su, K. W. Yu, and K. H. Hsia, "Multi-objective fuzzy optimal design of alpha-beta estimators for nonlinear variable structure control," *International Journal of Innovative Computing, Information and Control*, vol. 7, no. 5, pp. 2123–2140, 2011.
[9] S. Qu, Z. Lei, Q. Zhu, and H. Nouri, "Stabilization for a class of uncertain multi-time delays system using sliding mode controller," *International Journal of Innovative Computing, Information and Control*, vol. 7, no. 7, pp. 4195–4205, 2011.
[10] Y. Niu and D. W. C. Ho, "Stabilization of discrete-time stochastic systems via sliding mode technique," *Journal of the Franklin Institute*, vol. 349, pp. 1497–1508, 2012.
[11] T. Jia, Y. Niu, and Y. Zou, "Sliding mode control for stochastic systems subject to packet losses," *Information Sciences*, vol. 217, pp. 117–126, 2012.

[12] L. Wu and D. W. C. Ho, "Sliding mode control of singular stochastic hybrid systems," *Automatica*, vol. 46, no. 4, pp. 779–783, 2010.
[13] H. R. Karimi, "A sliding mode approach to H_∞ synchronization of master-slave time-delay systems with Markovian jumping parameters and nonlinear uncertainties," *Journal of the Franklin Institute*, vol. 349, no. 4, pp. 1480–1496, 2012.
[14] L. Wu, P. Shi, and H. Gao, "State estimation and sliding-mode control of markovian jump singular systems," *IEEE Transactions on Automatic Control*, vol. 55, no. 5, pp. 1213–1219, 2010.
[15] B. Jiang, P. Shi, and Z. Mao, "Sliding mode observer-based fault estimation for nonlinear networked control systems," *Circuits, Systems, and Signal Processing*, vol. 30, no. 1, pp. 1–16, 2011.
[16] M. Liu, P. Shi, L. Zhang, and X. Zhao, "Fault tolerant control for nonlinear Markovian jump systems via proportional and derivative sliding mode observer technique," *IEEE Transactions on Circuits and Systems*, vol. 58, pp. 2755–2764, 2011.
[17] H. R. Karimi, "Robust synchronization and fault detection of uncertain master-slave systems with mixed time-varying delays and nonlinear perturbations," *International Journal of Control, Automation and Systems*, vol. 9, no. 4, pp. 671–680, 2011.
[18] H. R. Karimi, "Adaptive H_∞ synchronization problem of uncertain master-slave systems with mixed time-varying delays and nonlinear perturbations: an LMI approach," *International Journal of Automation and Computing*, vol. 8, no. 4, pp. 381–390, 2011.
[19] H. R. Karimi, M. Zapateiro, and N. Luo, "Stability analysis and control synthesis of neutral systems with time-varying delays and nonlinear uncertainties," *Chaos, Solitons and Fractals*, vol. 42, no. 1, pp. 595–603, 2009.
[20] H. R. Karimi and P. Maass, "Delay-range-dependent exponential H_∞ synchronization of a class of delayed neural networks," *Chaos, Solitons and Fractals*, vol. 41, no. 3, pp. 1125–1135, 2009.
[21] H. R. Karimi, B. Lohmann, B. Moshiri, and P. J. Maralani, "Wavelet-based identification and control design for a class of nonlinear systems," *International Journal of Wavelets, Multiresolution and Information Processing*, vol. 4, no. 1, pp. 213–226, 2006.
[22] H. R. Karimi and H. Gao, "Mixed H_2/H_∞ output-feedback control of second-order neutral systems with time-varying state and input delays," *ISA Transactions*, vol. 47, no. 3, pp. 311–324, 2008.
[23] H. Yang, P. Shi, J. Zhang, and J. Qiu, "Robust H_∞ control for a class of discrete time fuzzy systems via delta operator approach," *Information Sciences*, vol. 184, no. 1, pp. 230–245, 2012.
[24] Z. Wu, P. Shi, H. Su, and J. Chu, "Reliable H_∞ control for discrete-time fuzzy systems with infinite-distributed delay," *IEEE Transactions on Fuzzy Systems*, vol. 20, no. 1, pp. 22–31, 2012.
[25] Q. Zhou, P. Shi, J. Lu, and S. Xu, "Adaptive output feedback fuzzy tracking control for a class of nonlinear systems," *IEEE Transactions on Fuzzy Systems*, vol. 19, no. 5, pp. 972–982, 2011.
[26] X. Su, P. Shi, and L. Wu, "A novel approach to filter design for T-S fuzzy discrete-time systems with time-varying delay," *IEEE Transactions on Fuzzy Systems*. In press.
[27] Z. Gao, B. Jiang, P. Shi, and Y. Xu, "Fault accommodation for near space vehicle attitude dynamics via T-S fuzzy models," *International Journal of Innovative Computing, Information and Control*, vol. 6, no. 11, pp. 4843–4856, 2010.
[28] Z. Pei and P. Shi, "Fuzzy risk analysis based on linguistic aggregation operations," *International Journal of Innovative Computing Information and Control*, vol. 7, no. 12, pp. 7105–7117, 2011.
[29] G. Wang, P. Shi, and C. Wen, "Fuzzy approximation relations on fuzzy n-cell number space and their applications in classification," *Information Sciences*, vol. 181, no. 18, pp. 3846–3860, 2011.
[30] J. Zhang, P. Shi, and Y. Xia, "Robust adaptive sliding-mode control for fuzzy systems with mismatched uncertainties," *IEEE Transactions on Fuzzy Systems*, vol. 18, no. 4, pp. 700–711, 2010.
[31] Q. Zhou, P. Shi, S. Xu, and H. Li, "Adaptive output feedback control for nonlinear time-delay systems by fuzzy approximation approach," *IEEE Transactions on Fuzzy Systems*. In press.
[32] X. Zhao, Y. Xu, Z. Zhang, and P. Shi, "Design of PSO fuzzy neural network control for ball and plate system," *International Journal of Innovative Computing Information and Control*, vol. 7, no. 12, pp. 7091–7103, 2011.
[33] K. Zhang, B. Jiang, and P. Shi, "Fault estimation observer design for discrete-time Takagi-Sugeno fuzzy systems based on piecewise Lyapunov functions," *IEEE Transactions on Fuzzy systems*, vol. 20, no. 1, pp. 192–200, 2012.
[34] H. Khalil, *Nonlinear Systems*, Macmillan, New York, NY, USA, 1992.

Hindawi Publishing Corporation
Mathematical Problems in Engineering
Volume 2012, Article ID 794581, 21 pages
doi:10.1155/2012/794581

Research Article

Unknown Input Observer Design for Fuzzy Bilinear System: An LMI Approach

D. Saoudi,[1] M. Chadli,[2] C. Mechmeche,[1] and N. Benhadj Braiek[1]

[1] *Laboratoire des Systèmes Avancés (LSA), Polytechnic High School of Tunisia (EPT), University of Carthage, 2078 La Marsa, Tunisia*
[2] *University of Picardie-Jules Verne, MIS 33, rue Saint-Leu,- 80039 Amiens, France*

Correspondence should be addressed to D. Saoudi, dhikra.saoudi@hotmail.com and M. Chadli, mohammed.chadli@u-picardie.fr

Received 8 September 2012; Revised 18 October 2012; Accepted 19 October 2012

Academic Editor: Peng Shi

Copyright © 2012 D. Saoudi et al. This is an open access article distributed under the Creative Commons Attribution License, which permits unrestricted use, distribution, and reproduction in any medium, provided the original work is properly cited.

A new method to design a fuzzy bilinear observer (FBO) with unknown inputs is developed for a class of nonlinear systems. The nonlinear system is modeled as a fuzzy bilinear model (FBM). This kind of T-S fuzzy model is especially suitable for a nonlinear system with a bilinear term. The proposed fuzzy bilinear observer subject to unknown inputs is developed to ensure the asymptotic convergence of the error dynamic using the Lyapunov method. The proposed design conditions are given in linear matrix inequality (LMI) formulation. The paper studies also the problem of fault detection and isolation. An unknown input fuzzy bilinear fault diagnosis observer design is proposed. This work is given for both continuous and discrete cases of fuzzy bilinear models. Illustrative examples are chosen to provide the effectiveness of the given methodology.

1. Introduction

In the recent past decades, there has been important increasing interest in the state observer design of dynamic systems subjected to unknown inputs that play an essential role in robust model-based fault detection. The case of unknown input linear system has been considered by different authors [1–4], and many types of full order and reduced order unknown input observers (UIOs) are now available.

On the other hand, since bilinear systems present the main advantage of representing an intermediate structure between linear and nonlinear models, a considerable attention has been paid for the study of this class of process [5, 6]. The observer design for bilinear systems with unknown input has been an important research topic during the last years. The works of [7, 8] have considered the design of UIO for bilinear systems in which the error

estimation dynamics is linear. Under suitable transformation, the design of UIO for bilinear systems proposed in [9, 10] is equivalent to the design of UIO for linear systems in which the unknown input links with the non measurable states.

However, many physical systems are nonlinear in nature. For such system, the use of the well-known linear techniques may reduce in bad performance and even instability. Generally, analysis for nonlinear systems is a quite involved procedure. In these last decades, a T-S fuzzy approach to represent or approximate a large class of nonlinear systems is developed [11–14]. Then, in the field of stability analysis and stabilization, many works including delay and uncertainty have been developed and applied in a lot of practical situations [15–20]. For the state estimation problems and its application in fault diagnosis for uncertain T-S fuzzy models, robust of fault detection filter is developed in LMI terms [21–25].

It is of importance to design observers for linear or nonlinear systems partially driven by unknown inputs [26–29]. Such a problem arises in systems subject to disturbances and in many applications such as robust control, fault detection and isolation (FDI), system supervision, and fault-tolerant control. The design of observers for nonlinear systems is a challenging problem and has received a considerable amount of attention in the literature. In many approaches, the transform of nonlinear systems to bilinear T-S models provides a better approximation than classical T-S models [30, 31]. Motivated by this, we consider in this work bilinear T-S fuzzy models whose consequent parts are bilinear systems with unknown inputs.

Considering the advantages of bilinear systems and fuzzy control, the fuzzy bilinear system (FBS) based on the T-S fuzzy model with bilinear rule consequence has attracted the interest of researchers [30, 32–35]. For example, robust stabilization for the T-S FBS has studied in [30, 33, 34], and extension to the T-S FBS with time delay is given in [35]. An adaptive fuzzy-bilinear-observer- (FBO-) based synchronization design for generalized Lorenz system (GLS) was also examined in [36], and in [32] an observer is designed using iterative procedure.

In this paper, we propose a novel approach of designing a fuzzy bilinear observer for a class of nonlinear system. The nonlinear system is modeled as a fuzzy bilinear model subject to unknown inputs. This kind of T-S fuzzy model is especially suitable for a nonlinear system with a bilinear term. The considered bilinear observer is obtained by a convex interpolation of unknown input bilinear observers. This interpolation is obtained throughout the same activation functions as the fuzzy bilinear model. Based on Lyapunov theory, the synthesis conditions of the given fuzzy observer are expressed in LMI terms. The design conditions lead to the resolution of linear constraints easy to solve with existing numerical tools. The given observer is then applied for fault detection. These results are provided for both continuous-time and discrete-time T-S bilinear models.

To the best of our knowledge, the FBO synthesis and fault diagnosis for fuzzy bilinear model subjected to unknown input seem not fully addressed in the past works. Moreover, in contrast with previous works, the proposed design is given in LMI formulation solved simultaneously.

This paper is organized as follows. In Section 2 the considered structure of the FBS is presented. In Section 3, the synthesis of fuzzy bilinear observers with unknown input in continuous and discrete cases is presented. Section 4 is devoted to the problem of fault detection by using unknown input fuzzy bilinear fault diagnosis observer. In Section 5, two examples to illustrate the proposed approach are proposed. The practical use of the theoretic study is illustrated by applying the proposed design to an isothermal continuous stirred tank reactor (CSTR).

Notation. In the rest of the paper, the following useful notation is used: $\Re$ denotes the set of real numbers, X^T denotes the transpose of the matrix X, $X \succ 0$ denotes symmetric positive definite matrix, X^{-1} denotes the Moore-Penrose inverse of X, and $\left(\begin{smallmatrix} A & * \\ B & C \end{smallmatrix}\right)$ denotes symmetric matrix where $(*) = B^T$. The operator δ denotes the time derivative for continuous-time models, that is, $\delta(x(t)) = \dot{x}(t)$, and the shift operator for discrete-time models, that is, $\delta(x(t)) = x(t+1)$. For simplicity, in the sequel, we will simply write $h_i(\xi(t)) = h_i(t)$.

2. General Structure of a Fuzzy Bilinear Model

In this section, fuzzy bilinear systems in the continuous and discrete-time cases are introduced. Indeed, the T-S fuzzy model is described by *if-then* rules and used to present a fuzzy bilinear system. The ith rule of the FBS for nonlinear systems is represented by the following form:

$$R^i : \text{if } \xi_1(t) \text{ is } F_{i1}, \ldots, \xi_g(t) \text{ is } F_{ig}, \tag{2.1}$$

then

$$\begin{gathered} \delta x(t) = A_i x(t) + B_i u(t) + N_i x(t) u(t), \\ y(t) = C x(t), \end{gathered} \tag{2.2}$$

where R^i denotes the ith fuzzy rule for all $i = \{1, \ldots, r\}$, r is the number of *if-then* rules, $\xi_i(t)$ are the premise variables assumed to be measurable, and $F_{ij}(\xi_j(t))$ is the membership degree of $\xi_j(t)$ in the fuzzy set F_{ij}. $x(t) \in \Re^n$ is the state vector, $u(t) \in \Re$ is the control input, and $y(t) \in \Re^p$ is the system output. The matrices $A_i \in \Re^{n\times n}, B_i \in \Re^{n\times 1}$, $N_i \in \Re^{n\times n}$, $C \in \Re^{p\times n}$ are known matrices.

Then, the overall FBS can be described as follows:

$$\begin{gathered} \delta x(t) = \sum_{i=1}^{r} h_i(t)(A_i x(t) + B_i u(t) + N_i x(t) u(t)), \\ y(t) = C x(t) \end{gathered} \tag{2.3}$$

with $h_i(\xi(t)) = \mu_i(\xi(t)) / \sum_{j=1}^{r} \mu_j(\xi(t))$, $\mu_i(\xi(t)) = \prod_{j=1}^{g} F_{ij}(\xi(t))$ and $h_i(\cdot)$ verify the following properties:

$$\begin{gathered} \sum_{i=1}^{r} h_i(\xi(t)) = 1 \\ \forall i \in \{1, 2, \ldots, r\}. \\ 0 \le h_i(\xi(t)) \le 1 \end{gathered} \tag{2.4}$$

Remark 2.1. Matrices A_i, B_i, N_i, and C can be obtained by using the polytopic transformation [37]. The advantage of this method is (i) to lead to a bilinear transformation of the nonlinear

model without any approximation error and (ii) to reduce the number of local models compared to other methods [33].

The following section is dedicated to the state estimation of the FBS (2.3), subject to unknown inputs, where the vector $\xi(t)$ is assumed depending on measurable variables.

3. Design of an Unknown Input Fuzzy Bilinear Observer

Considering an FBS subject to unknown inputs, the FBS (2.3) can be rewritten as follows:

$$\begin{gathered}\delta x(t) = \sum_{i=1}^{r} h_i(t)(A_i x(t) + B_i u(t) + N_i x(t) u(t) + F_i d(t)), \\ y(t) = Cx(t),\end{gathered} \tag{3.1}$$

where $d(t) \in \Re^q$ is the unknown inputs vector and $F_i \in \Re^{n\times q}$ is a matrix with full column rank. In order to estimate state of (3.1), we propose a full-order observer of the form

$$\begin{gathered}\delta z(t) = \sum_{i=1}^{r} h_i(t)\big(H_i z(t) + L_i y(t) + J_i u(t) + M_i y(t) u(t)\big), \\ \widehat{x}(t) = z(t) - Ey(t),\end{gathered} \tag{3.2}$$

where $\widehat{x}(t) \in \Re^n$ is the estimated state vector and the activation functions are the same as those used in FBS (3.1). H_i, M_i, L_i, J_i, and E are constant matrices with appropriate dimensions.

Our objective is to design T-S fuzzy bilinear observer of the fuzzy bilinear system (3.1) for system (3.1) subject to unknown input such that the estimation error

$$e(t) = \widehat{x}(t) - x(t) \tag{3.3}$$

converges towards zero when $t \to \infty$. Note that estimation error can be rewritten as follows:

$$e(t) = z(t) - Tx(t), \tag{3.4}$$

where $T = I_n + EC$.

The dynamics of the state estimation error is governed by

$$\delta e = \sum_{i=1}^{r} h_i(t)(H_i e + (H_i T + L_i C - TA_i)x + (M_i C - TN_i)xu + (J_i - TB_i)u - TF_i d). \tag{3.5}$$

Hence, if the following constraints are satisfied

$$H_iT + L_iC - TA_i = 0, \tag{3.6}$$

$$M_iC - TN_i = 0, \tag{3.7}$$

$$J_i - TB_i = 0, \tag{3.8}$$

$$TF_i = 0, \tag{3.9}$$

$$T = I_n + EC, \tag{3.10}$$

the estimation error becomes

$$\delta e(t) = \sum_{i=1}^{r} h_i(\xi(t))H_ie(t). \tag{3.11}$$

The parameter gains H_i, M_i, L_i, J_i, and E should be determined such that the state estimate $\widehat{x}(t)$ converges asymptotically to system state $x(t)$.

3.1. Continuous-Time Case

The estimation error for continuous case is given by

$$\dot{e}(t) = \sum_{i=1}^{r} h_i(\xi(t))H_ie(t). \tag{3.12}$$

The following theorem gives sufficient design conditions for the unknown inputs FBS (3.1).

Theorem 3.1. *If there exist a symmetric definite positive matrix P, matrices W_i, V_i, S, R_i such that the following linear conditions hold for all $i = 1, \ldots, r$:*

$$((P + SC)A_i - W_iC)^T + ((P + SC)A_i - W_iC) \prec 0, \tag{3.13}$$

$$R_i = (P + SC)B_i, \tag{3.14}$$

$$V_iC = (P + SC)N_i, \tag{3.15}$$

$$(P + SC)F_i = 0, \tag{3.16}$$

then the state estimation of the CFBO (3.2) *converges globally asymptotically to the state of the CFBS* (3.1). *The observer gains are determined by*

$$\begin{aligned} E &= P^{-1}S, \\ J_i &= P^{-1}R_i, \\ M_i &= P^{-1}V_i, \\ H_i &= (I_n + EC)A_i - P^{-1}W_iC, \\ L_i &= P^{-1}W_i - H_iE. \end{aligned} \tag{3.17}$$

Proof. In order to establish the stability of the estimation error $e(t)$, let us consider the following Lyapunov function:

$$V(t) = e^T(t)Pe(t), \quad P = P^T > 0. \tag{3.18}$$

Using (3.12), the derivative of the Lyapunov function (3.18) is given by

$$\dot{V}(t) = \sum_{i=1}^{r} h_i(t)\left(e^T(t)\left(H_i^T P + PH_i\right)e(t)\right). \tag{3.19}$$

From (3.6) and using (3.10), we get

$$H_i = TA_i - K_iC \tag{3.20}$$

with

$$K_i = H_iE + L_i. \tag{3.21}$$

Then, the derivative of the Lyapunov function is negative if

$$(TA_i - K_iC)^T P + P(TA_i - K_iC) < 0. \tag{3.22}$$

Taking into account (3.10) and considering the variable change:

$$S = PE, \tag{3.23}$$

$$W_i = PK_i, \tag{3.24}$$

we get the LMI (3.13). Taking account (3.10) and (3.23), equality (3.16) is derived from (3.9).

Similarly, using the following variable change:

$$R_i = PJ_i,$$
$$V_i = PM_i, \tag{3.25}$$

we get equalities (3.14) and (3.15) from (3.8) and (3.7), respectively, which ends the proof. □

Remark 3.2. Classical numerical tools may be used for solving the LMI problem (3.13) subject to linear equality constraints (3.14)–(3.16). Solving this linear problem allows to deduce the observer parameters from P, W_i, V_i, S, and R_i as mentioned by (3.17).

3.2. Discrete-Time Case

For discrete-time case, the estimation error is given by

$$e(t+1) = \sum_{i=1}^{r} h_i(t) H_i e(t). \tag{3.26}$$

The following result gives linear conditions to design discrete-time unknown inputs DFBS (3.1).

Theorem 3.3. *If there exists a symmetric definite positive matrix P, matrices W_i, V_i, S, R_i such that the following linear conditions hold for all $i = 1, \ldots, r$*

$$\begin{bmatrix} P & * \\ (P+SC)A_i - W_i C & P \end{bmatrix} \succ 0, \tag{3.27}$$

$$R_i = (P+SC)B_i, \tag{3.28}$$

$$V_i C = (P+SC)N_i, \tag{3.29}$$

$$(P+SC)F_i = 0, \tag{3.30}$$

then the state estimation of the DFBO (3.2) *converges globally asymptotically to the state of the DFBS* (3.1). *The observer gains are determined by* (3.17).

Proof. To prove the asymptotic convergence of the DFBS (3.1), sufficient conditions are derived using quadratic Lyapunov function (3.18). Indeed, the variation $\Delta V(t) = V(t+1) - V(t)$ along the solution of (3.26) is

$$\Delta V(t) = e^T(t)\left(H_i^T P H_i - P\right)e(t). \tag{3.31}$$

Sufficient conditions for the negativity of (3.31) are

$$H_i^T P H_i - P \prec 0. \tag{3.32}$$

Substituting (3.20) in (3.32), we obtain

$$(TA_i - K_iC)^T P(TA_i - K_iC) - P \prec 0. \tag{3.33}$$

Thus by taking account the expression of T (3.10), introducing the same variables change (3.23)-(3.24), and then applying Schur complement to (3.33), we get LMI conditions (3.27). Equality constraints (3.28)–(3.30) are obtained as previously mentioned which ends the proof. □

3.3. Design Algorithm

A design procedure to design FBO for both continuous and discrete cases is summarized as follows.

(1) Solve linear constraints (3.13)–(3.16) for continuous-time (or (3.27)–(3.30) for discrete-time) case to get W_i, V_i, S, R_i and $P > 0$.

(2) Deduce $K_i = P^{-1}W_i$.

(3) Knowing that $T = I + EC$, the observer gains are computed as follows:

$$\begin{aligned} E &= P^{-1}S, \\ H_i &= TA_i - K_iC, \\ L_i &= K_i - H_iE, \\ J_i &= TB_i, \\ M_i &= P^{-1}V_i. \end{aligned} \tag{3.34}$$

In the following, the proposed observer is used for fault detection and isolation of actuator fault.

4. Fault Detection and Isolation for Fuzzy Bilinear System

The fault detection and isolation problem for nonlinear systems is far more complicated. In this section, an unknown input fuzzy bilinear fault diagnosis observer is considered for nonlinear model in T-S fuzzy modeling. Based on proposed unknown inputs fuzzy bilinear observer, a fuzzy bilinear system affected by an actuator fault vector $f(t) \in \Re^{nf}$ is considered. In this section, a residual generation is considered in order to be sensitive to fault vector $f(t)$ and insensitive to the unknown inputs $d(t)$. Then, the considered system is as follows:

$$\begin{aligned} \delta x(t) &= \sum_{i=1}^{r} h_i(t) \begin{pmatrix} A_i x(t) + B_i u(t) + N_i x(t) u(t) \\ +F_i d(t) + G_i f(t) \end{pmatrix} \\ y(t) &= Cx(t), \end{aligned} \tag{4.1}$$

where $f(t)$ represents the vector of faults and the G_i represents matrix with appropriate dimensions.

The following unknown input fuzzy bilinear fault detection observer is proposed:

$$\begin{gathered}\delta z(t) = \sum_{i=1}^{r} h_i(t)\left(H_i z(t) + L_i y(t) + J_i u(t) + M_i y(t) u(t)\right), \\ r(t) = E_1 z(t) + E_2 y(t),\end{gathered} \tag{4.2}$$

where $z(t)$ represents the estimated vector and $r(t)$ is the output signal called the residual.

The determination of gain matrices in (4.2) will be determined to ensure the convergence of the estimated errors. In order to describe the dynamic of unknown input fuzzy bilinear fault detection observer (4.2), the state estimation error is defined by $e(t) = z(t) - \overline{T}x(t)$. Then, from (4.1) and (4.2), we have

$$\begin{gathered}\delta e(t) = \sum_{i=1}^{r} h_i(t) \begin{pmatrix} H_i e(t) + \left(H_i \overline{T} + L_i C - \overline{T} A_i\right) x(t) - \overline{T} F_i d(t) \\ \left(M_i C - \overline{T} N_i\right) x(t) u(t) + \left(J_i - \overline{T} B_i\right) u(t) - \overline{T} G_i f(t) \end{pmatrix}, \\ r(t) = E_1 e(t) + \left(E_1 \overline{T} + E_2 C\right) x(t).\end{gathered} \tag{4.3}$$

If the following conditions are satisfied:

$$H_i \overline{T} + L_i C - \overline{T} A_i = 0, \tag{4.4}$$

$$M_i C - \overline{T} N_i = 0, \tag{4.5}$$

$$J_i - \overline{T} B_i = 0, \tag{4.6}$$

$$\overline{T} F_i = 0, \tag{4.7}$$

$$E_1 \overline{T} + E_2 C = 0, \tag{4.8}$$

we get

$$\begin{gathered}\delta e(t) = \sum_{i=1}^{r} h_i(\xi(t)) \left(H_i e(t) - \overline{T} G_i f(t)\right), \\ r(t) = E_1 e(t).\end{gathered} \tag{4.9}$$

Multiplying (4.8) by F_i we get

$$E_1 \overline{T} F_i + E_2 C F_i = 0. \tag{4.10}$$

Taking into account the constraint (4.7), (4.10) becomes

$$E_2 C F_i = 0, \tag{4.11}$$

or equivalently

$$E_2 C\mathcal{F} = 0, \quad \mathcal{F} = [F_1, F_2, \ldots, F_r]. \tag{4.12}$$

Then we get

$$E_2 = \Omega\left(I_p - C\mathcal{F}(C\mathcal{F})^+\right), \tag{4.13}$$

where $(C\mathcal{F})^+$ is the pseudoinverse of $C\mathcal{F}$ and Ω is an arbitrary matrix. Substituting (4.13) into (4.8) leads to

$$E_1 T + \Omega C\left(I_n - \mathcal{F}(C\mathcal{F})^+ C\right) = 0. \tag{4.14}$$

A suitable choice of E_1 and $\overline{T}$ satisfying the relation (4.14) is

$$E_1 = -\Omega C, \tag{4.15}$$

$$\overline{T} = I_n - \mathcal{F}(C\mathcal{F})^+ C. \tag{4.16}$$

Then, the observer gains are obtained by the following result.

Theorem 4.1. *If there exist a symmetric definite positive matrix P, matrices Z_i, V_i, U_i such that the following linear conditions hold for all $i = 1, \ldots, r$*

$$Z_i^T + Z_i \prec 0 \ (\textit{for continuous case}), \tag{4.17}$$

or

$$\begin{gathered} \begin{bmatrix} P & * \\ Z_i & P \end{bmatrix} \succ 0 \ (\textit{for discrete case}), \\ Z_i \overline{T} + U_i C - P\overline{T} A_i = 0, \\ V_i C - P\overline{T} N_i = 0, \end{gathered} \tag{4.18}$$

then the state estimation of the FBO (4.2) *converges globally asymptotically to the state of the FBS* (4.1). *The observer gains are determined by*

$$\begin{gathered} H_i = P^{-1} Z_i, \\ L_i = P^{-1} U_i, \\ M_i = P^{-1} V_i, \\ J_i = \overline{T} B_i, \end{gathered} \tag{4.19}$$

where $\overline{T}$, E_1, and E_2 are given in (4.16), (4.15), *and* (4.13), *respectively.*

Proof. The proof of this result is similar to the one of Theorem 3.1. □

To illustrate the theoretical development and the design algorithm, numerical examples are proposed in the following section.

5. Simulation Examples

In this section, we consider two examples: the first is an academic example in discrete-time case, and the second is a physical model of an isothermal continuous stirred tank reactor (CSTR) for the Van de Vusse reactor system.

5.1. Example 1: Synthesis of a Discrete Fuzzy Bilinear Observer

Let us consider now the following discrete system defined by

$$\begin{aligned} x_1(t+1) &= -0.2x_2 + 0.5x_3^3 + \left(0.5x_3^2 - 0.7x_1\right)u + 0.1d, \\ x_2(t+1) &= (0.3 - x_3)x_1 - 0.1x_2 + (0.3 - 0.1x_2)u + 0.2d, \\ x_3(t+1) &= (0.3 - x_3)x_2 - 0.6x_3 + (0.4 - x_1)u + 0.3d, \\ y(t) &= Cx(t), \end{aligned} \tag{5.1}$$

where

$$C = \begin{bmatrix} 0 & 0 & 0.1 \\ -0.6 & -0.1 & -0.4 \end{bmatrix}. \tag{5.2}$$

This system can be written as

$$x(t+1) = A(x(t))x(t) + B(x(t))u(t) + Nx(t)u(t) + Fd(t) \tag{5.3}$$

with

$$\begin{gathered} A(x(t)) = \begin{bmatrix} 0 & -0.2 & 0.5x_3^2 \\ 0.3 - x_3 & -0.1 & 0 \\ 0 & 0.3 - x_3 & -0.6 \end{bmatrix}, \\ B(x(t)) = \begin{bmatrix} 0.5x_3^2 \\ 0.3 \\ 0.4 \end{bmatrix}, \qquad N = \begin{bmatrix} -0.7 & 0 & 0 \\ 0 & -0.1 & 0 \\ -1 & 0 & 0 \end{bmatrix}, \qquad F = \begin{bmatrix} 0.1 \\ 0.2 \\ 0.3 \end{bmatrix}. \end{gathered} \tag{5.4}$$

Using the polytopic transformation [37] with $-0.2 < x_3(t) < 0.2$ and $0 < x_3^2(t) < 0.33$, the DFBS can be described as (2.3)

$$x(t+1) = \sum_{i=1}^{4} h_i(x(t))(A_i x(t) + B_i u(t) + N_i x(t) u(t) + F_i d(t));$$
$$y(t) = Cx(t), \tag{5.5}$$

where

$$A_1 = \begin{bmatrix} 0 & -0.2 & 0.165 \\ 0.1 & -0.1 & 0 \\ 0 & 0.1 & -0.6 \end{bmatrix}, \qquad A_2 = \begin{bmatrix} 0 & -0.2 & 0 \\ 0.1 & -0.1 & 0 \\ 0 & 0.1 & -0.6 \end{bmatrix},$$
$$A_3 = \begin{bmatrix} 0 & -0.2 & 0.165 \\ 0.5 & -0.1 & 0 \\ 0 & 0.5 & -0.6 \end{bmatrix}, \qquad A_4 = \begin{bmatrix} 0 & -0.2 & 0 \\ 0.5 & -0.1 & 0 \\ 0 & 0.5 & -0.6 \end{bmatrix},$$
$$B_1 = B_3 = \begin{bmatrix} 0.165 \\ 0.3 \\ 0.4 \end{bmatrix}, \qquad B_2 = B_4 = \begin{bmatrix} 0 \\ 0.3 \\ 0.4 \end{bmatrix},$$
$$N_1 = N_2 = N_3 = N_4 = \begin{bmatrix} -0.7 & 0 & 0 \\ 0 & -0.1 & 0 \\ -1 & 0 & 0 \end{bmatrix},$$
$$F_1 = F_2 = F_3 = F_4 = \begin{bmatrix} 0.1 \\ 0.2 \\ 0.3 \end{bmatrix},$$
$$h_1(x(t)) = F_{11}(x_3) \cdot F_{21}(x_3), \qquad h_2(x(t)) = F_{12}(x_3) \cdot F_{21}(x_3),$$
$$h_3(x(t)) = F_{11}(x_3) \cdot F_{22}(x_3), \qquad h_4(x(t)) = F_{12}(x_3) \cdot F_{22}(x_3) \tag{5.6}$$

with

$$F_{11}(x_3) = \frac{x_3 + 1}{2}, \qquad F_{12}(x_3) = \frac{1 - x_3}{2},$$
$$F_{21}(x_3) = \frac{x_3^2}{0.33}, \qquad F_{22}(x_3) = 1 - \frac{x_3^2}{0.33}. \tag{5.7}$$

$u(t)$ is the input signal given in Figure 1, and $d(t)$ is the unknown input taken as a sine wave signal of amplitude 0.1 and frequency 50 rad/s.

Solving the design conditions (3.27)–(3.30), we get

$$P = \begin{bmatrix} 85.457 & 14.243 & 0 \\ 14.243 & 2.374 & 0 \\ 0 & 0 & 87.83 \end{bmatrix}. \tag{5.8}$$

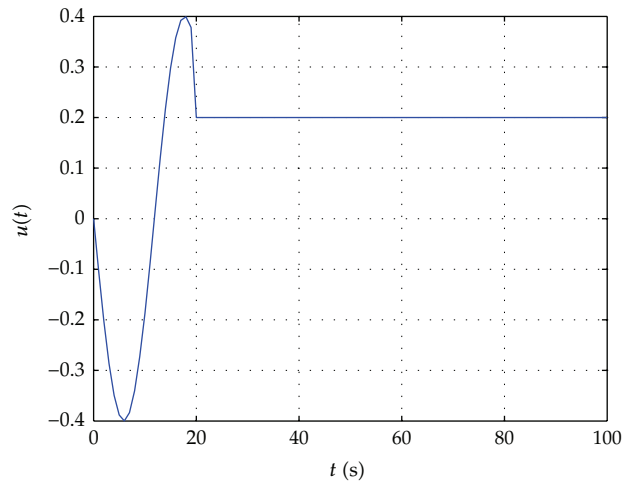

Figure 1: Input signal.

Therefore, the observer gains are computed from (3.17) as follows:

$$H_1 = H_2 = \begin{bmatrix} -0.018 & 0.07 & 0 \\ 0.107 & -0.418 & -0.001 \\ 0 & 0 & 0 \end{bmatrix},$$

$$H_3 = H_4 = \begin{bmatrix} -0.035 & 0.134 & 0 \\ 0.21 & -0.805 & -0.002 \\ 0 & 0 & 0 \end{bmatrix},$$

$$L_1 = \begin{bmatrix} 0.135 & 0.164 \\ -0.808 & -0.983 \\ 0 & 0 \end{bmatrix}, \qquad L_2 = \begin{bmatrix} 0.432 & 0.164 \\ -2.595 & -0.983 \\ 0 & 0 \end{bmatrix},$$

$$L_3 = \begin{bmatrix} 1.694 & 0.417 \\ -10.164 & -2.5 \\ 0 & 0 \end{bmatrix}, \qquad L_4 = \begin{bmatrix} 1.992 & 0.417 \\ -11.951 & -2.499 \\ 0 & 0 \end{bmatrix}, \tag{5.9}$$

$$J_1 = J_3 = \begin{bmatrix} -0.035 \\ 0.207 \\ 0 \end{bmatrix}, \qquad J_2 = J_4 = \begin{bmatrix} -0.005 \\ 0.029 \\ 0 \end{bmatrix},$$

$$M_1 = M_3 = \begin{bmatrix} 0.024 & 0.006 \\ -0.143 & -0.036 \\ 0 & 0 \end{bmatrix}, \qquad M_2 = M_4 = \begin{bmatrix} 0.024 & 0.006 \\ -0.143 & -0.036 \\ 0 & 0 \end{bmatrix},$$

$$E = \begin{bmatrix} 9.226 & 1.967 \\ -15.357 & -1.805 \\ -10 & 0 \end{bmatrix}.$$

These parameters define completely the observer

$$z(t+1) = \sum_{i=1}^{4} h_i(x_3)\big(H_i z(t) + L_i y(t) + J_i u(t) + M_i y(t) u(t)\big),$$
$$\hat{x}(t) = z(t) - Ey(t). \tag{5.10}$$

To show the effectiveness of the designed observer, simulation results are presented in Figures 2, 3, and 4 for initial conditions given by $x_0 = [0.5 \;\; 0.5 \;\; 0.5]^T$ and $\hat{x}_0 = [1 \;\; 1 \;\; 1]^T$.

It can be deduced from Figures 2, 3, and 4 that the proposed observer succeeds to track the system trajectories in spite of the presence of the unknown input.

5.2. Example 2: Synthesis of a Continuous Fuzzy Bilinear Observer

In this subsection, we intend to apply the proposed design to an isothermal continuous stirred tank reactor (CSTR) (see, e.g., [38–40]).

The dynamics of CSTR for the Van de Vusse reactor can be described by the following nonlinear second order system:

$$\dot{x}_1 = -k_1 x_1 - k_3 x_1^2 + u(C_{A0} - x_1) + 0.6d,$$
$$\dot{x}_2 = k_1 x_1 - k_2 x_2 + u(-x_2) + d, \tag{5.11}$$
$$y = x_1 + x_2,$$

where the state x_1 represents the concentration of the reactant inside the reactor (mol/L) and the state x_2 is the concentration of the product in the CSTR output stream (mol/L). The output y determines the grade of the final product. The input-feed stream to the CSTR consists of a reactant with concentration C_{A0}, and the controlled input is the dilution rate $u = F/V(\mathrm{h}^{-1})$, where F is the input flow rate to the reactor (L/h) and V is the constant volume of the CSTR (liters). In all the following discussions, the kinetic parameters are chosen to be $k_1 = 50\,\mathrm{h}^{-1}$, $k_2 = 100\,\mathrm{h}^{-1}$, $k_3 = 10\,\mathrm{L}/(\mathrm{molh})$, $C_{A0} = 10\,\mathrm{mol/L}$, and $V = 1\,\mathrm{L}$ as in [39].

The system (5.11) can be written as

$$\dot{x}(t) = A(x(t))x(t) + Bu(t) + Nx(t)u(t) + Fd(t), \tag{5.12}$$

where

$$A(x(t)) = \begin{bmatrix} -k_1 - k_3 x_1 & 0 \\ k_1 & -k_2 \end{bmatrix}, \qquad B = \begin{bmatrix} 10 \\ 0 \end{bmatrix}$$
$$N = \begin{bmatrix} -1 & 0 \\ 0 & -1 \end{bmatrix}, \qquad F = \begin{bmatrix} 0.6 \\ 1 \end{bmatrix} \tag{5.13}$$

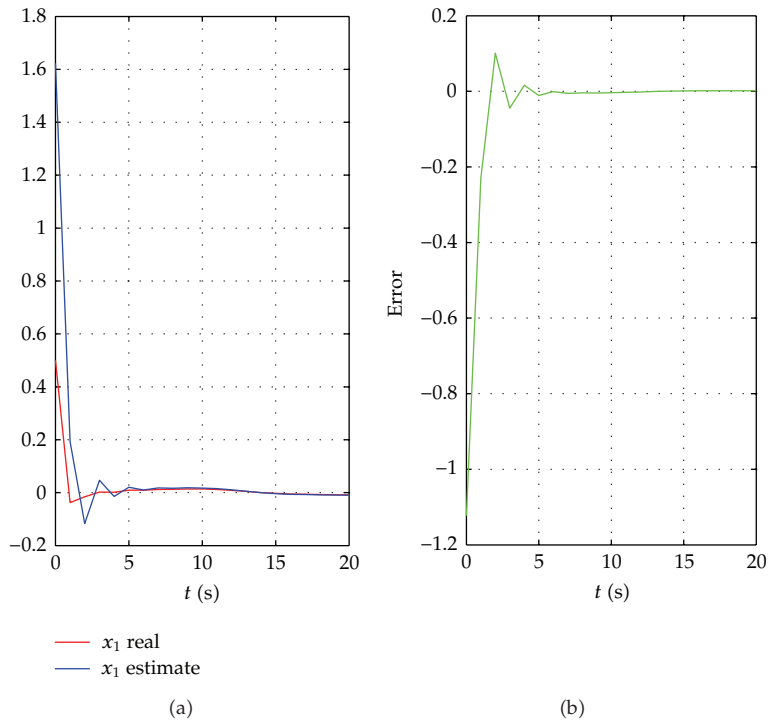

Figure 2: Trajectories of (a) x_1 and $\widehat{x}_1$, (b) $\widehat{x}_1 - x_1$.

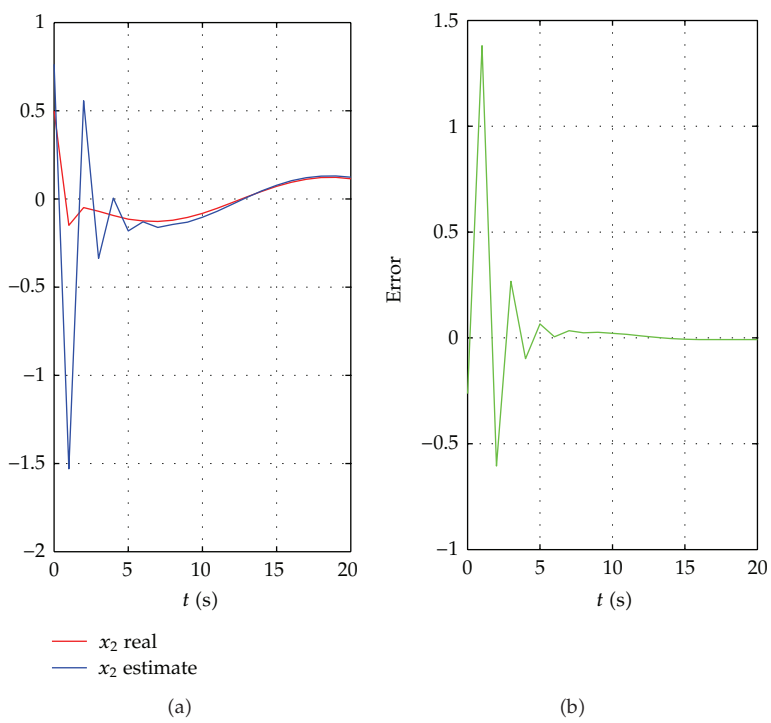

Figure 3: Trajectories of (a) x_2 and $\widehat{x}_2$, (b) $\widehat{x}_2 - x_2$.

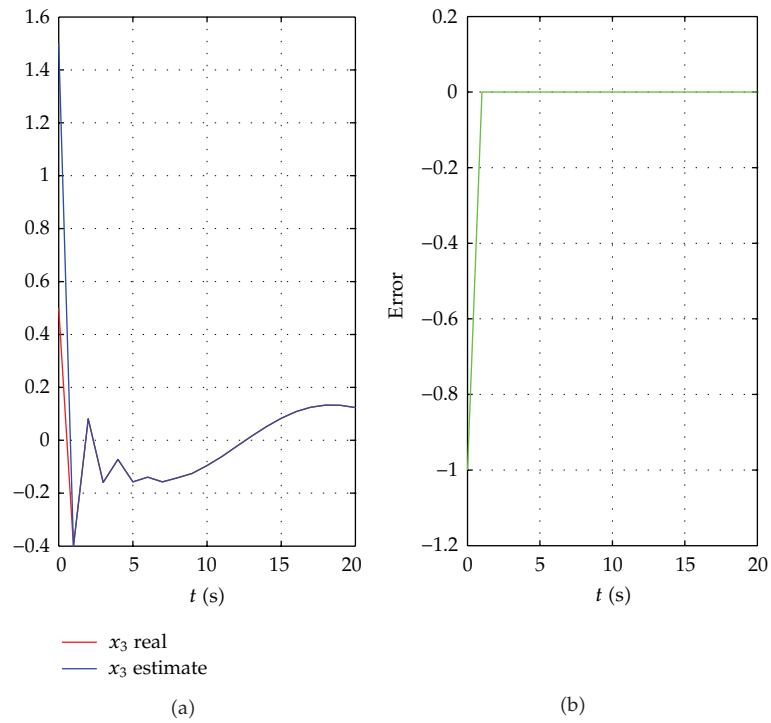

Figure 4: Trajectories of (a) x_3 and $\hat{x}_3$, (b) $\hat{x}_3 - x_3$.

with $x_1(t) \in [1, -1]$. This system can be represented using the polytopic transformation [37] as follows:

$$\dot{x}(t) = \sum_{i=1}^{2} h_i(x_1(t))(A_i x(t) + B_i u(t) + N_i x(t) u(t) + F_i d(t))$$
$$y(t) = Cx(t), \tag{5.14}$$

where

$$A_1 = \begin{bmatrix} -60 & 0 \\ 50 & -100 \end{bmatrix}, \qquad A_2 = \begin{bmatrix} -40 & 0 \\ 50 & -100 \end{bmatrix},$$
$$B_1 = B_2 = \begin{bmatrix} 10 \\ 0 \end{bmatrix}, \qquad N_1 = N_2 = \begin{bmatrix} -1 & 0 \\ 0 & -1 \end{bmatrix}, \tag{5.15}$$
$$F_1 = F_2 = \begin{bmatrix} 0.6 \\ 1 \end{bmatrix}, \qquad C = [1 \;\; 1],$$

$h_1(x_1(t)) = (1 - x_1(t))/2$, $h_2(x_1(t)) = (x_1(t) + 1)/2$.

5.2.1. Observer Design

The observer gains are obtained by solving design conditions (3.13)–(3.16), which lead to the following parameters:

$$P = \begin{bmatrix} 72.215 & 72.215 \\ 72.215 & 72.215 \end{bmatrix}. \tag{5.16}$$

Then the observer is completely defined from (3.17) by

$$\begin{gathered} H_1 = \begin{bmatrix} -57.470 & 56.231 \\ 56.970 & -56.732 \end{bmatrix}, \qquad H_2 = \begin{bmatrix} -52.743 & 52.892 \\ 52.243 & -53.392 \end{bmatrix}, \\ L_1 = \begin{bmatrix} -8.175 \\ 8.175 \end{bmatrix}, \qquad L_2 = \begin{bmatrix} -3.362 \\ 3.362 \end{bmatrix}, \\ J_1 = \begin{bmatrix} 4.063 \\ -4.063 \end{bmatrix}, \qquad J_2 = \begin{bmatrix} 4.061 \\ -4.061 \end{bmatrix}, \\ M_1 = \begin{bmatrix} 0.093 \\ -0.093 \end{bmatrix}, \qquad M_2 = \begin{bmatrix} 0.092 \\ -0.092 \end{bmatrix}, \\ E = \begin{bmatrix} -0.597 \\ -0.403 \end{bmatrix}. \end{gathered} \tag{5.17}$$

Then, the fuzzy bilinear state and their estimation are given in the following figures.

Figures 5 and 6 show, respectively, the evolution of the state variables x_1 and x_2 of the considered system and their corresponding observer estimation $\widehat{x}_1$ and $\widehat{x}_2$ with the input signal $u(t) = 4.5\sin(0.5\pi t)$ and the initial conditions $x_0 = [1 \;\; 1]^T$ and $\widehat{x}_0 = [0.5 \;\; 0.5]^T$.

5.2.2. Residual Generation

In this paragraph, we will consider the same system of isothermal stirred tank reactor subject to actuator fault:

$$\begin{gathered} \dot{x}(t) = \sum_{i=1}^{2} h_i(t)\left(A_i x(t) + B_i u(t) + N_i x(t) u(t) + F_i d(t) + G_i f(t)\right) \\ y(t) = Cx(t) \end{gathered} \tag{5.18}$$

with A_i, B_i, N_i, F_i, and C being the same previous matrices and

$$\begin{gathered} G_1 = G_2 = [0.5 \;\; 0.5], \\ f(t) = \begin{cases} 50\sin \pi t, & \text{for } t \in [6 \;\; 8], \\ 0, & \text{elsewhere.} \end{cases} \end{gathered} \tag{5.19}$$

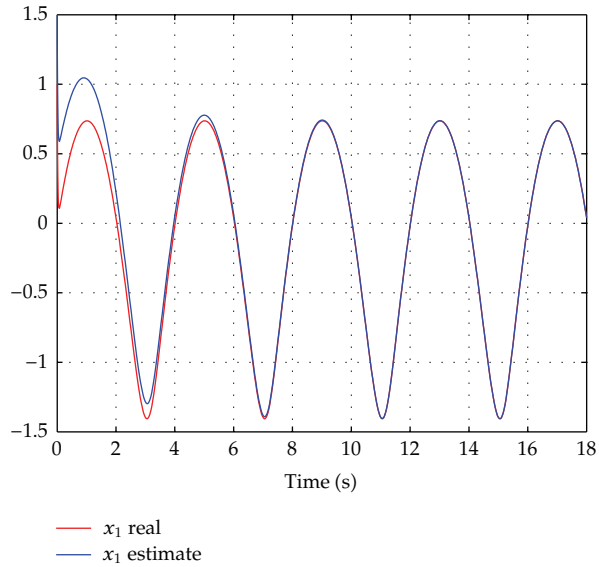

Figure 5: The state x_1 and its estimate.

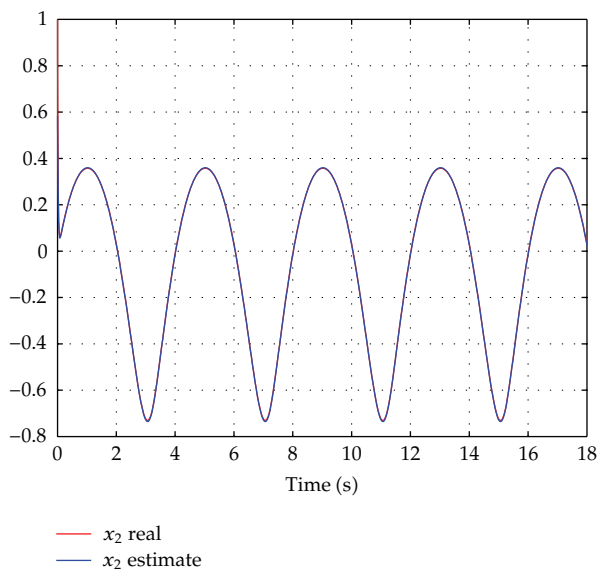

Figure 6: The state x_2 and its estimate.

Figure 7 displays the convergence of the residual corresponding to the actuator fault signal. One can see that the residual is almost zero throughout the time simulation run except at time $t = 6$ s where it appears at the actuator fault and disappears at $t = 8$ s. Figure 7 shows that the residual $r(t)$ is sensitive to $f(t)$ and insensitive to $d(t)$. So the designed unknown input fuzzy bilinear fault diagnosis observer can be efficiently used to detect faults.

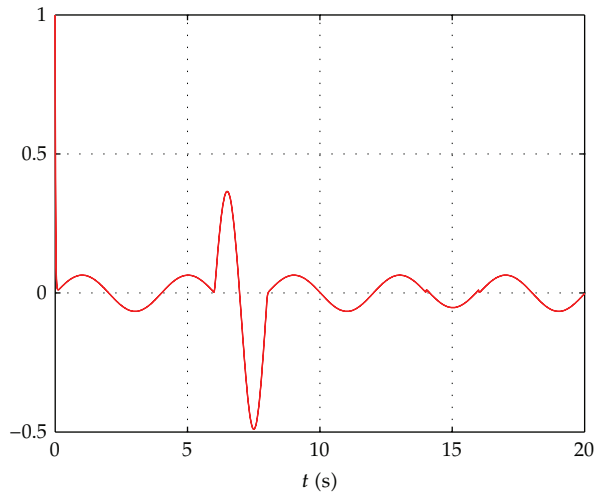

Figure 7: Residual signal $r(t)$.

6. Conclusion

In this paper, a bilinear observer design is proposed for a class of unknown inputs nonlinear system. Such design is based on a T-S fuzzy bilinear model representation, particularly suitable for a nonlinear system with a bilinear term. The proposed results are developed for both continuous-time and discrete-time cases. The synthesis conditions lead to the resolution of linear constraints easy to solve with existing numerical tools. The proposed unknown input bilinear observer structure is applied for fault detection. Two illustrative examples are also given.

Based on the results in the paper, interesting future studies may be extended the proposed technique to uncertain fuzzy bilinear systems or fuzzy bilinear systems with time-delay, and can also be considered the problem of pole placements to improve the performance of the proposed fuzzy bilinear observer.

References

[1] Y. Guan and M. Saif, "A novel approach to the design of unknown input observers," *IEEE Transactions on Automatic Control*, vol. 36, no. 5, pp. 632–635, 1991.

[2] M. Hou and P. C. Muller, "Design of observers for linear systems with unknown inputs," *IEEE Transactions on Automatic Control*, vol. 37, no. 6, pp. 871–875, 1992.

[3] M. Darouach, M. Zasadzinski, and S. J. Xu, "Full-order observers for linear systems with unknown inputs," *IEEE Transactions on Automatic Control*, vol. 39, no. 3, pp. 606–609, 1994.

[4] F. Yang and R. W. Wilde, "Observers for linear systems with unknown inputs," *IEEE Transactions on Automatic Control*, vol. 33, no. 7, pp. 677–681, 1988.

[5] R. R. Mohler, *Nonlinear Systems: Cybernetics Application To Bilinear Control*, Prentice-Hall, Englewood Cliffs, NJ, USA, 1991.

[6] M. Dong and Z. W. Gao, "H∞ fault-tolerant control for singular bilinear systems related to output feedback," *Systems Engineering and Electronics*, vol. 28, no. 12, pp. 1866–1869, 2006 (Chinese).

[7] S. Hara and K. Furuta, "Minimal order state observers for bilinear systems," *International Journal of Control*, vol. 24, no. 5, pp. 705–718, 1976.

[8] A. Hac, "Design of disturbance decoupled observer for bilinear systems," *Journal of Dynamic Systems, Measurement and Control*, vol. 114, no. 4, pp. 556–562, 1992.

[9] M. Zasadzinski, H. Rafaralahy, C. Mechmeche, and M. Darouach, "On disturbance decoupled observers for a class of bilinear systems," *Journal of Dynamic Systems, Measurement and Control*, vol. 120, no. 3, pp. 371–377, 1998.

[10] C. Mechmeche, M. Zasadzinski, H. Rafaralahy, and M. Darouach, "On unknown input observers for bilinear systems," in *Proceedings of the American Control Conference*, pp. 3212–3213, Seattle, Wash, USA, June 1995.

[11] D. Wang, W. Song, and H. Li, "Design and approximation capabilities analysis of time-variant fuzzy systems," *International Journal of Innovative Computing, Information and Control*, vol. 7, no. 3, pp. 1121–1132, 2011.

[12] X. Su, L. Wu, P. Shi, and Y.-D. Song, "H_∞ model reduction of T-S fuzzy stochastic systems," *IEEE Transactions on Fuzzy Systems. Man, and Cybernetics B*, vol. 42, no. 6, pp. 1574–1585, 2012.

[13] E. Onieva, V. Milanes, J. Perez, and T. De Perdro, "Genetic fuzzy-based steering wheel controller using a mass-produced car," *International Journal of Innovative Computing Information and Control B*, vol. 8, no. 5, pp. 3477–3494, 2012.

[14] L. Wu, X. Su, P. Shi, and J. Qiu, "Model approximation for discrete-time state-delay systems in the TS fuzzy framework," *IEEE Transactions on Fuzzy Systems*, vol. 19, no. 2, pp. 366–378, 2011.

[15] C. P. Huang, "Model based fuzzy control with affine T-S delayed models applied to nonlinear systems," *International Journal of Innovative Computing Information and Control A*, vol. 8, no. 5, pp. 2979–2993, 2012.

[16] A. Benzaouia and A. El Hajjaji, "Delay-dependent stabilization conditions of controlled positive T-S fuzzy systems with time varying delay," *International Journal of Innovative Computing, Information and Control*, vol. 7, no. 4, pp. 1533–1547, 2011.

[17] X. Song, J. Lu, S. Xu, H. Shen, and J. Lu, "Robust stabilization of state delayed TS fuzzy systems with input saturation via dynamic anti-windup fuzzy design," *International Journal of Innovative Computing, Information and Control*, vol. 7, no. 12, pp. 6665–6676, 2011.

[18] R. Yang, H. Gao, and P. Shi, "Novel robust stability criteria for stochastic Hopfield neural networks with time delays," *IEEE Transactions on Systems, Man, and Cybernetics B*, vol. 39, no. 2, pp. 467–474, 2009.

[19] R. Yang, Z. Zhang, and P. Shi, "Exponential stability on stochastic neural networks with discrete interval and distributed delays," *IEEE Transactions on Neural Networks*, vol. 21, no. 1, pp. 169–175, 2010.

[20] S. K. Nguang and P. Shi, "H∞ fuzzy output feedback control design for nonlinear systems: an LMI approach," *IEEE Transactions on Fuzzy Systems*, vol. 11, no. 3, pp. 331–340, 2003.

[21] S. K. Nguang, P. Shi, and S. Ding, "Fault detection for uncertain fuzzy systems: an LMI approach," *IEEE Transactions on Fuzzy Systems*, vol. 15, no. 6, pp. 1251–1262, 2007.

[22] X. Su, L. Wu, P. Shi, and Y.-D. Song, "A novel approach to filter design for T-S fuzzy discrete-time systems with time-varying delay," *IEEE Transactions on Fuzzy Systems*, vol. 20, no. 6, pp. 1114–1129, 2012.

[23] R. Palm and P. Bergsten, "Sliding Mode observer for a Takagi Sugeno fuzzy system," in *Proceedings of the 9th IEEE International Conference on Fuzzy Systems*, pp. 665–670, San Antonio, Tex, USA, May 2000.

[24] M. Chadli and H. R. Karimi, "Robust observer design for unknown inputs Takagi-Sugeno models," *IEEE Transactions on Fuzzy Systems*, vol. 8, no. 9, pp. 6389–6400, 2012.

[25] M. Rodrigues, D. Theilliol, M. Adam-Medina, and D. Sauter, "A fault detection and isolation scheme for industrial systems based on multiple operating models," *Control Engineering Practice*, vol. 16, no. 2, pp. 225–239, 2008.

[26] P. Bergsten, R. Palm, and D. Driankov, "Observers for Takagi-Sugeno fuzzy systems," *IEEE Transactions on Systems, Man, and Cybernetics B*, vol. 32, no. 1, pp. 114–121, 2002.

[27] M. Chadli, A. Akhenak, J. Ragot, and D. Maquin, "State and unknown input estimation for discrete time multiple model," *Journal of the Franklin Institute*, vol. 346, no. 6, pp. 593–610, 2009.

[28] M. Chadli, "An LMI approach to design observer for unknown inputs Takagi-Sugeno fuzzy models," *Asian Journal of Control*, vol. 12, no. 4, pp. 524–530, 2010.

[29] T. Zhang and M. Guay, "Adaptive control for a class of second-order nonlinear systems with unknown input nonlinearities," *IEEE Transactions on Systems, Man, and Cybernetics B*, vol. 33, no. 1, pp. 143–149, 2003.

[30] S. H. Tsai, "Robust H∞ control for Van de Vusse reactor via T-S fuzzy bilinear scheme," *Expert Systems with Applications*, vol. 38, no. 5, pp. 4935–4944, 2011.

[31] J. Baek and M. Park, "Fuzzy bilinear state feedback control design based on TS fuzzy bilinear model for DCDC converters," *Electrical Power and Energy Systems*, vol. 42, pp. 710–720, 2012.

[32] D. Saoudi, C. Mechmeche, and N. Benhadj Braeik, "T-S fuzzy bilinear observer for a class of nonlinear system," in *Proceedings of the 18th Mediterranean Conference on Control and Automation (MED '10)*, Marrakech, Maroc, June 2010.

[33] T. H. S. Li and S. H. Tsai, "T-S fuzzy bilinear model and fuzzy controller design for a class of nonlinear systems," *IEEE Transactions on Fuzzy Systems*, vol. 15, no. 3, pp. 494–506, 2007.

[34] T. H. S. Li, S. H. Tsai, J. Z. Lee, M. Y. Hsiao, and C. H. Chao, "Robust H∞ fuzzy control for a class of uncertain discrete fuzzy bilinear systems," *IEEE Transactions on Systems, Man, and Cybernetics B*, vol. 38, no. 2, pp. 510–527, 2008.

[35] S. H. Tsai and T. H. S. Li, "Robust fuzzy control of a class of fuzzy bilinear systems with time-delay," *Chaos, Solitons and Fractals*, vol. 39, no. 5, pp. 2028–2040, 2009.

[36] J. Baek, H. Lee, S. Kim, and M. Park, "Adaptive fuzzy bilinear observer based synchronization design for generalized Lorenz system," *Physics Letters A*, vol. 373, no. 47, pp. 4368–4375, 2009.

[37] K. Tanaka, T. Ikeda, and H. O. Wang, "Fuzzy regulators and fuzzy observers: relaxed stability conditions and LMI-based designs," *IEEE Transactions on Fuzzy Systems*, vol. 6, no. 2, pp. 250–265, 1998.

[38] B. Chen, X. P. Liu, C. Lin, and S. C. Tong, "Observer-based stabilization of T-S fuzzy systems with input delay," *IEEE Transactions on Fuzzy Systems*, vol. 16, no. 3, pp. 652–663, 2008.

[39] H. Perez, B. Ogunnaike, and S. Devasia, "Output tracking between operating points for nonlinear processes: Van de vusse example," *IEEE Transactions on Control Systems Technology*, vol. 10, no. 4, pp. 611–617, 2002.

[40] H. Kashiwagi and L. Rong, "Identification of Volterra kernels of nonlinear Van de Vusse reactor," *International Journal of Control Automation and Systems*, vol. 4, no. 2, pp. 109–113, 2002.

Hindawi Publishing Corporation
Mathematical Problems in Engineering
Volume 2012, Article ID 469491, 13 pages
doi:10.1155/2012/469491

Research Article

A Two-Wheeled Self-Balancing Robot with the Fuzzy PD Control Method

Junfeng Wu,[1] Wanying Zhang,[2] and Shengda Wang[1]

[1] *College of Automation, Harbin University of Science and Technology, Harbin 150080, China*
[2] *Qingdao Haier AIC Elec Corp., Ltd., Qingdao Haier Co., Ltd., Qingdao 266101, China*

Correspondence should be addressed to Wanying Zhang, zhangwy8@163.com

Received 19 September 2012; Revised 27 October 2012; Accepted 30 October 2012

Academic Editor: Peng Shi

Copyright © 2012 Junfeng Wu et al. This is an open access article distributed under the Creative Commons Attribution License, which permits unrestricted use, distribution, and reproduction in any medium, provided the original work is properly cited.

A two-wheeled self-balancing robot with a fuzzy PD control method is described and analyzed as an example of a high-order, multiple-variable, nonlinear, strong-coupling, and unstable system. Based on a system structure model, a kinetic equation is constructed using Newtonian dynamics and mechanics. After a number of simulation experiments, we get the best Q, R, and state-feedback matrices. Then a fuzzy PD controller is designed for which the position and speed of the robot are inputs and for which the angle and angle rate of the robot are controlled by a PD controller. Finally, this paper describes a real-time control platform for the two-wheeled self-balancing robot that controls the robot effectively, after some parameter debugging. The result indicates that the fuzzy PD control algorithm can successfully achieve self-balanced control of the two-wheeled robot and prevent the robot from falling.

1. Introduction

Existing research on fuzzy reasoning can be roughly divided into three overlapping categories [1]: fuzzy reasoning methods and their analysis, logical foundations of fuzzy reasoning, and applications of fuzzy reasoning. Various fuzzy methods have been proposed based mainly on three different ideas. The first idea, composition, leads to the Zadeh compositional rule of inference (CRI) method [2, 3] and its variants [4–6]. The second idea is that of analogy and similarity. The third idea, interpolation analysis of fuzzy reasoning methods, is concerned with various properties of interest, such as interpretability of fuzzy rules, consistency of new fuzzy consequences with existing fuzzy premises, and continuity of fuzzy consequences with respect to fuzzy premises and fuzzy relations [7]. Numerous different implication operators and connectives can be adopted in fuzzy reasoning methods, including an important class of methods concerned with the suitability of particular fuzzy

reasoning methods for domain-specific applications [8]. The logical foundation of fuzzy reasoning is concerned with formal systems in which various fuzzy reasoning methods can be interpreted. Several formal systems of this kind have been proposed, including basic logic, monoidal t-norm-based logic, the quasiformal deductive system of Wang [9], and possibilistic logic [10]. These formal systems are mainly generalizations of classical propositional logic and multivalued logic. On the other hand, applications of fuzzy reasoning methods are extensive and can be found in disparate areas such as complex systems modeling and control [11], pattern recognition, decision-making [12], and safety monitoring.

In recent decades, motion control of robot manipulators has received a lot of attention [13]. Motion control is needed to make each joint track a desired trajectory as closely as possible. Many control algorithms, such as the computer torque method [14], optimal control [15], adaptive control [16], variable structure control (VSC) [17], neural networks (NNs), and fuzzy systems [18], have been proposed to deal with this robotic control problem. In [19, 20], a computer torque control is developed on the basis of feedback linearization. However, these designs are possible only when the robotic dynamics are well known.

A fuzzy logic controller (FLC) makes control decisions using well-known fuzzy IF-THEN rules. FLCs can be classified into two major categories: the Mamdani-type FLC, which uses fuzzy numbers to make decisions [21], and the Takagi-Sugeno (TS)-type FLC, which generates control actions using linear functions of the input variables. In the early years, most FLCs were designed by trial and error. Since the complexity of an FLC will increase exponentially when it is used to control complex systems, it is tedious to design and tune FLCs manually for most industrial problems such as robotic systems. This is why conventional nonlinear design methods [22] such as fuzzy sliding control, fuzzy gain scheduling [8], and adaptive fuzzy control [17] were adopted in the fuzzy control field to alleviate difficulties in constructing the fuzzy rule base.

Analytical calculations show that a two-input FLC employing a proportional error signal and a velocity error signal is a nonlinear proportional-integral (PI) or proportional-derivative (PD) controller. Due to the popularity of PID controllers in industrial applications, most of the development of fuzzy controllers in the past decade has revolved around fuzzy PID controllers [13]. PI- and PD-type fuzzy controllers have gained prominence for almost two decades now because of their simple structure, ease of implementation, and inherent robustness [22]. Another possible implementation of a PID-type FC requires the development of a popular PD-type fuzzy controller in parallel with a conventional integral (I) controller. Presently, research interest in this field is focused on the development of adaptation policies that can adapt these component fuzzy controllers in a suitable and simple fashion and can further achieve a reasonably accurate and satisfactory performance. An excellent example of applying self-organized fuzzy systems to autotune the gains of a classic PID controller online and its successful application in controlling a MIMO robot arm can be found in [23].

A two-wheeled self-balancing robot [24] system is characterized as being multiple-variable, high-order, nonlinear, strong-coupling, and unstable, so it is considered a standard research target by many modern control theory researchers [25], and many abstract control concepts such as system stability, robustness, controllability, and system anti-interference properties can be displayed via two-wheeled self-balancing robot system experiments. Recently, a two-wheeled self-balancing robot, namely, Segway [26], has been widely recognized as a powerful personal transportation vehicle. It is constructed from very sophisticated and high-quality dedicated components, such as a brushless servomotor with neodymium magnets, a precision gearbox, nickel metal hydride batteries, silica-based wheels, a digital signal processor as the main controller, motor drivers, six gyroscopes,

and several safety accessories. In contrast to this kind of high-cost human transporter, many researchers have presented low-tech self-balancing transporters and claimed that such a vehicle can be built using off-the-shelf inexpensive components. Because of its simple structure, stable operation, high energy efficiency, and environmental adaptability, it has very broad application prospects in both military and civilian areas.

In this paper, the utility and effectiveness of soft computing approaches for a two-wheeled self-balancing robot with structured and unstructured uncertainties is presented. In this approach, precompensation of a hybrid fuzzy PD controller is proposed. The control scheme consists of a fuzzy logic-based precompensator followed by fuzzy PD control. Moreover, a fuzzy supervisory controller is used to supervise conventional proportional and derivative actions such that the conventional gains are adapted online through fuzzy reasoning.

We study the GBOT1001 two-wheeled self-balancing robot produced by Googol Technology (Shenzhen) Limited, and we establish the mathematical model of this system, use fuzzy PD control theory to control the robot, and, at the same time, achieve effective control.

2. System Description

2.1. Structural Analysis of the Robot System

We can develop a linear model with the following assumptions [27].

(1) The robot is a rigid body and does not distort during moving.

(2) The left- and right-hand wheels are completely analogous.

(3) Cornering forces are considered negligible.

(4) Friction is neglected during the analysis.

(5) Since the time constant of electric motors is small compared to the system's time constants, the motor dynamics have been neglected in the model.

The design of the two-wheeled self-balancing robot is based on a mobile single inverted pendulum. The robot is composed of a chassis carrying a DC motor coupled to a planetary gearbox for each wheel, the DSP board used to implement the controller, the power amplifiers for the motors, the necessary sensors to measure the robot's states, and the receiver for the radiocontrol unit, as well as a vertical bar. The wheels of the vehicle are directly coupled to the output shaft of the gearboxes. A GE laser (scanner) motion controller is the core of the embedded DSP board. This is composed of a floating-point DSP from Analog Devices, an FPGA, three 10-bit D/A converters, and four 12-bit A/D converters.

2.2. Dynamics Model of the System

Figure 1 [27] shows the chassis diagram of the robot. The linear movement of the chassis is characterized by the position x and the speed $\dot{x}$; it is also able to rotate around the axis (pitch), a movement described by the angle θ, and the corresponding angular velocity $\dot{\theta}$. In addition, the vehicle can rotate around its vertical axis (yaw) with the associated angle δ and angular velocity $\dot{\delta}$. m is the mass of rotating masses connected to the left and right wheels, M is the mass of the chassis, R is the radius of the wheel, L is the distance between the z-axis and the center of gravity of the chassis, D is the lateral distance between the contact patches

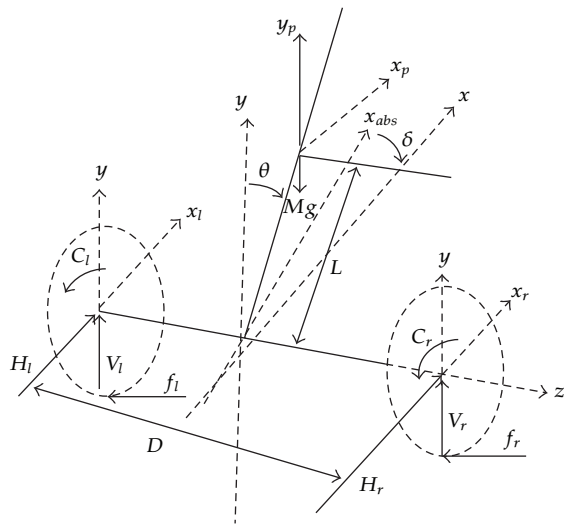

Figure 1: Chassis diagram of the robot.

of the wheels, y_p is the shift position of the wheel with respect to the y-axis, and x_p is the shift position of the chassis with respect to the x-axis.

For the left-hand wheel,

$$\begin{aligned} m\,\ddot{x}_l &= f_l - H_l \\ \frac{J_\omega}{R}\,\ddot{x}_l &= C_l - f_l R. \end{aligned} \tag{2.1}$$

For the right-hand wheel,

$$m\,\ddot{x}_r = f_r - H_r \tag{2.2}$$

$$\frac{J_\omega}{R}\,\ddot{x}_r = C_r - f_r R. \tag{2.3}$$

For the chassis,

$$\begin{aligned} M\,\ddot{x}_p &= H_l + H_r \\ J_p\,\ddot{\theta} &= (V_l + V_r)L\sin\theta - (H_l + H_r)L\cos\theta - (C_l + C_r) \\ M\,\ddot{y}_p &= V_l + V_r - Mg \\ J_\delta\,\ddot{\delta} &= \frac{D}{2}(H_l - H_r). \end{aligned} \tag{2.4}$$

For a premise,

$$x_p = x + L\sin\theta,$$
$$y_p = L\cos\theta, \tag{2.5}$$

where H_l, H_r, V_l, V_r represent reaction forces between the different free bodies [27]. Modifying the above equations and then linearizing the result around the operating point ($\theta \approx 0$, so $\sin\theta \approx \theta, \cos\theta \approx 1$), the system's state-space equations can be written in matrix form as:

$$\begin{pmatrix} \dot{x} \\ \ddot{x} \\ \dot{\theta} \\ \ddot{\theta} \\ \dot{\delta} \\ \ddot{\delta} \end{pmatrix} = \begin{pmatrix} 0 & 1 & 0 & 0 & 0 & 0 \\ 0 & 0 & a_{23} & 0 & 0 & 0 \\ 0 & 0 & 0 & 1 & 0 & 0 \\ 0 & 0 & a_{43} & 0 & 0 & 0 \\ 0 & 0 & 0 & 0 & 0 & 1 \\ 0 & 0 & 0 & 0 & 0 & 0 \end{pmatrix} \begin{pmatrix} x \\ \dot{x} \\ \theta \\ \dot{\theta} \\ \delta \\ \dot{\delta} \end{pmatrix} + \begin{pmatrix} 0 & 0 \\ b_{21} & b_{22} \\ 0 & 0 \\ b_{41} & b_{42} \\ 0 & 0 \\ b_{61} & b_{62} \end{pmatrix} \begin{pmatrix} C_l \\ C_r \end{pmatrix}. \tag{2.6}$$

In order to derive a simpler mathematical model, we need a decoupling unit (2.7) that transforms C_l and C_r into the wheel torques C_θ and C_δ as follows:

$$\begin{pmatrix} C_l \\ C_r \end{pmatrix} = \begin{pmatrix} 0.5 & 0.5 \\ 0.5 & -0.5 \end{pmatrix} \begin{pmatrix} C_\theta \\ C_\delta \end{pmatrix}. \tag{2.7}$$

Some parameters of the GBOT1001 robot are as follows:

$$M = 21\,\text{kg}, \quad m = 0.42\,\text{kg}, \quad R = 0.106\,\text{m}, \quad L = 0.3\,\text{m}, \quad D = 0.44\,\text{m}, \quad g = 9.8\,\text{m/s}^2. \tag{2.8}$$

Then the state-space equations for the vehicle can be written as two different systems [28]: one system is the model (2.9) of an inverted pendulum, which describes the rotation about the z-axis, and the other is the model (2.10) of rotation, which describes the rotation about the y-axis. Thus, we obtain

$$\begin{pmatrix} \dot{x} \\ \ddot{x} \\ \dot{\theta} \\ \ddot{\theta} \end{pmatrix} = \begin{pmatrix} 0 & 1 & 0 & 0 \\ 0 & 0 & -23.7097 & 0 \\ 0 & 0 & 0 & 1 \\ 0 & 0 & 83.7742 & 0 \end{pmatrix} \begin{pmatrix} x \\ \dot{x} \\ \theta \\ \dot{\theta} \end{pmatrix} + \begin{pmatrix} 0 \\ 1.8332 \\ 0 \\ -4.9798 \end{pmatrix} C_\theta, \tag{2.9}$$

$$\begin{pmatrix} \dot{\delta} \\ \ddot{\delta} \end{pmatrix} = \begin{pmatrix} 0 & 1 \\ 0 & 0 \end{pmatrix} \begin{pmatrix} \delta \\ \dot{\delta} \end{pmatrix} + \begin{pmatrix} 0 \\ 5.1915 \end{pmatrix} C_\delta. \tag{2.10}$$

Table 1: Fuzzy control rules.

E	Ec						
	NB	NM	NS	ZE	PS	PM	PB
NB	NB	NB	NB	NB	NM	NS	ZE
NM	NB	NB	NB	NM	NS	ZE	PS
NS	NB	NB	NM	NS	ZE	PS	PM
ZE	NB	NM	NS	ZE	PS	PM	PB
PS	NM	NS	ZE	PS	PM	PB	PB
PM	NS	ZE	PS	PM	PB	PB	PB
PB	ZE	PS	PM	PB	PB	PB	PB

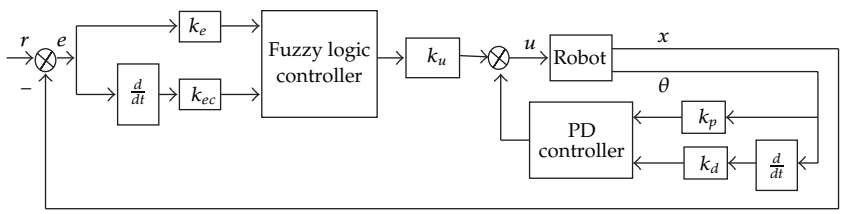

Figure 2: Structure chart of the multiple fuzzy PD controllers.

3. Controller Design

3.1. Parameters of the Fuzzy PD Controller

First, we examine the controllability of the open-loop system. After some calculations, we know that the system is controllable and the state feedback matrices can be obtained using the LQR method. After a number of simulation experiments, we choose the matrices

$$Q = \begin{pmatrix} 1000 & 0 & 0 & 0 \\ 0 & 0 & 0 & 0 \\ 0 & 0 & 1000 & 0 \\ 0 & 0 & 0 & 0 \end{pmatrix}, \qquad R = 1. \tag{3.1}$$

Then, we use the MATLAB function $K = \mathrm{lqr}(A, B, Q, R)$ to solve the optimality problem. Running $K = \mathrm{lqr}(A, B, Q, R)$ in MATLAB, we can get the state feedback matrix:

$$K = [-10.1522,\ -5.6683,\ -26.5230,\ -4.1971]. \tag{3.2}$$

Thus, the proportion parameter is 26.5230, and the differential parameter is 4.1971.

3.2. Fuzzy PD Control Method

3.2.1. Fuzzy PD Controller Design

A fuzzy logic controller is a controller that utilizes fuzzy logic to determine a course of action. The computation of the control action is composed of four steps [28]: input scaling and

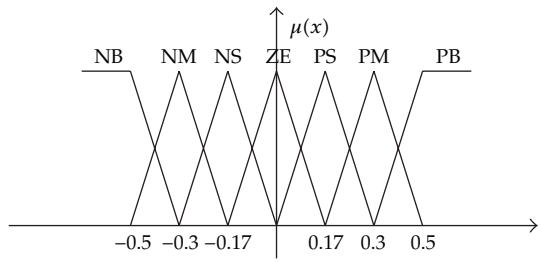

Figure 3: Membership functions of inputs.

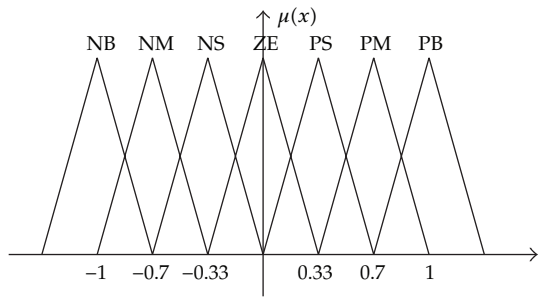

Figure 4: Membership functions of output.

shifting, fuzzification, fuzzy inference, and defuzzification. In the input scaling and shifting step, crisp inputs can be processed and scaled appropriately. In the fuzzification step, the crisp inputs are then converted into fuzzy values. After fuzzy inference, a proper control action is determined by searching through a previously established rule table. Finally, the deterministic output is defined in the defuzzification step.

In this section, a fuzzy PD controller is applied to the dynamic model of the two-wheeled self-balancing robot. Two inputs, position error $e_{(t)} = r - x$ and change of error $\dot{e}_{(t)} = \dot{r} - \dot{x}$, are fed to the fuzzy controller, while integral error is used as a conventional integral action [29]. The inputs of the fuzzy controller are the position and speed of the robot, while the angle and angle rate of the robot are controlled by the PD controller. Figure 2 shows the structure of the fuzzy PD controller.

The input $(e_{(t)}, \dot{e}_{(t)})$ and output (u) membership functions are denoted as NB, NM, NS, ZE, PS, PM, and PB. The fuzzy membership functions for inputs and output are shown in Figures 3 and 4. The control surface of the output is shown in Figure 5. Table 1 lists the fuzzy control rules.

3.2.2. Simulation Result

The control system includes a Simulink model of the feedback system [29]. The block diagram, as shown in Figure 6, consists of the subsystem 1 block with system matrices as defined in the script file. The position state is compared to a reference signal and then multiplied by its feedback gain, while the other states are simply multiplied by their respective gains, and all of these are fed back into the subsystem 1 block, which is the Simulink model of the robot, as shown in Figure 7.

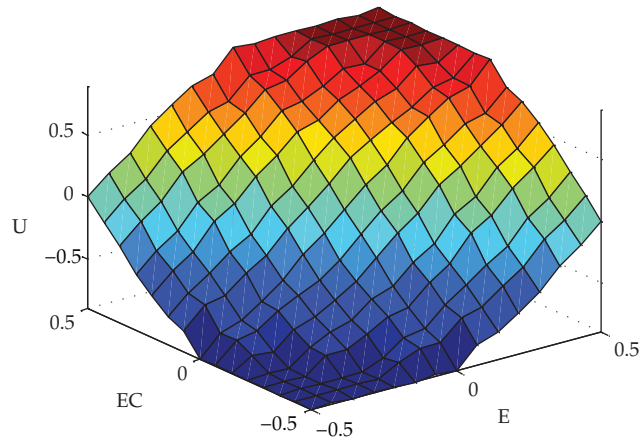

Figure 5: Control surface of output.

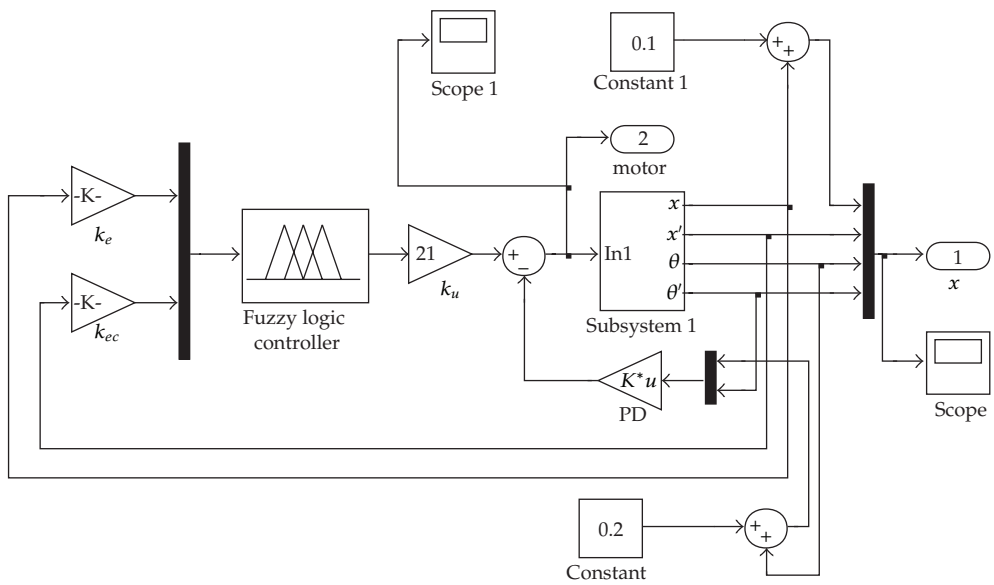

Figure 6: Block diagram of control system.

When a disturbance $x_0 = [0\ \ 0\ \ 0.2\ \ 0]$ is input to the system, the response curves become as shown in Figures 8 and 9.

As shown in Figure 8, when the disturbance of the angle is given as $\theta = 0.2$ rad, the system is successfully stabilized as required, with good dynamic performance. The robot's position, speed, angle, and angle rate return to the origin point after no more than 5 s. The system is stable throughout with good dynamic performance and robustness, showing that the fuzzy PD control method is effective. Figure 9 is the graph of the output motor torque; we can see that at time 0 the motor torque is very high, almost 5.4 N · m. 5 s later, it reduces to 0 N · m.

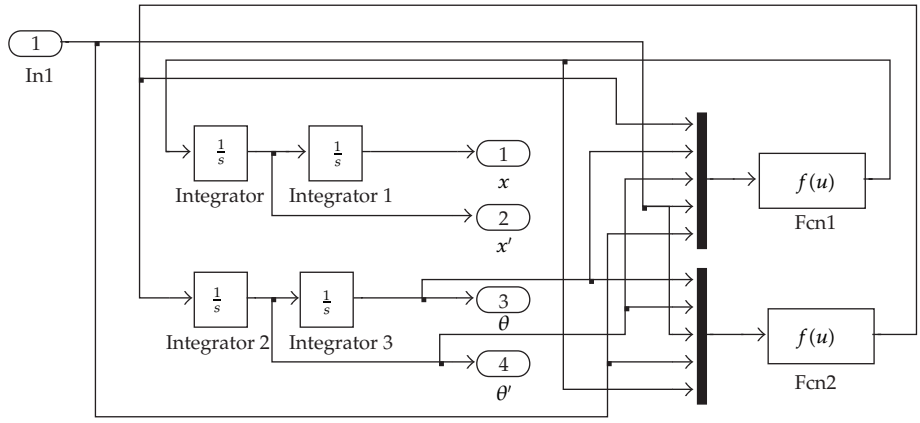

Figure 7: Simulink model of robot.

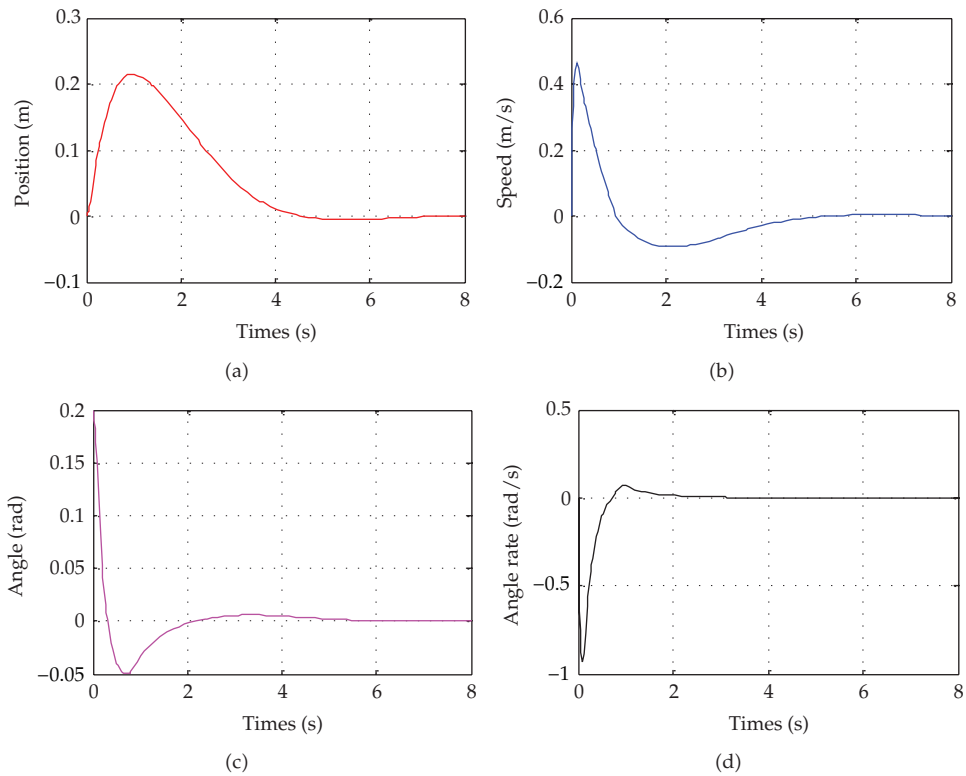

Figure 8: Graph of dip angle control.

4. Real-Time Control System

We use the fuzzy PD controller to replace the real-time control platform designed by Googol Technology Limited, so we can get the self-balancing robot's real-time control system platform, as shown in Figure 10. Compared with the simulation model, the real-time control system has a corner controller that is used to control the robot to turn around. After some

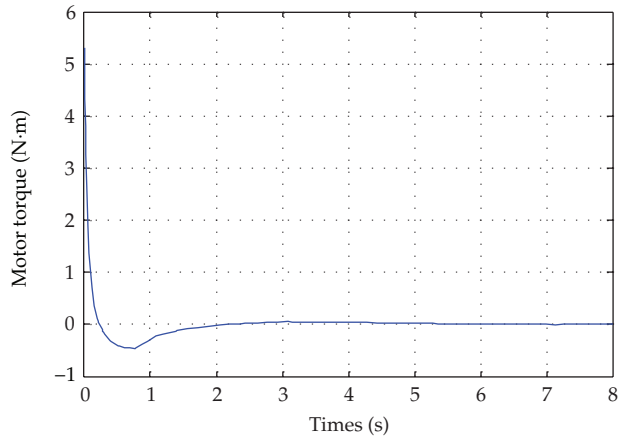

Figure 9: Graph of output motor torque.

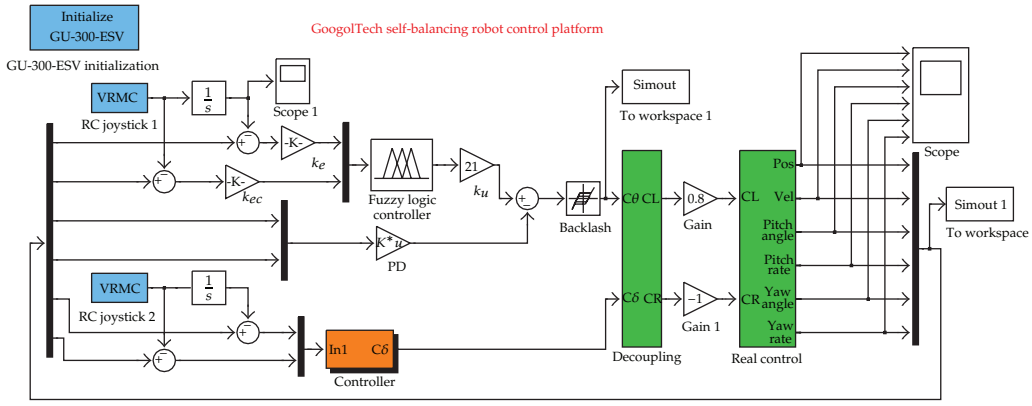

Figure 10: Actual self-balancing robot control platform.

parameter debugging, the robot is controlled effectively. Figure 11 is the robot's real-time curve; Figure 12 is its stable control photo.

From Figure 11, we can see that the robot's angle is very large at the beginning, about 0.31 rad, so the motor output torque is very high, that is, about $13\,\mathrm{N}\cdot\mathrm{m}$ with $1.7\,\mathrm{m/s}$ initial angle rate. 0.5 s later, the robot basically comes to a dynamic balance, which is 4 s faster than in the simulation. Since the ground is not flat, and there are various outside interferences, the robot does not move smoothly, and so there will be a little convulsion. After 5 s, an interference is given to the robot; from the figure we can see that the motor output torque and the angle rate increase rapidly. 0.7 s later, they all enter a stable state.

5. Conclusion

In this paper, based on the structure model of a two-wheeled self-balancing robot, a systematic mathematical model is devised according to dynamic mechanics theory. After a number of simulation experiments, we get the best Q, R, and state-feedback matrices. Based

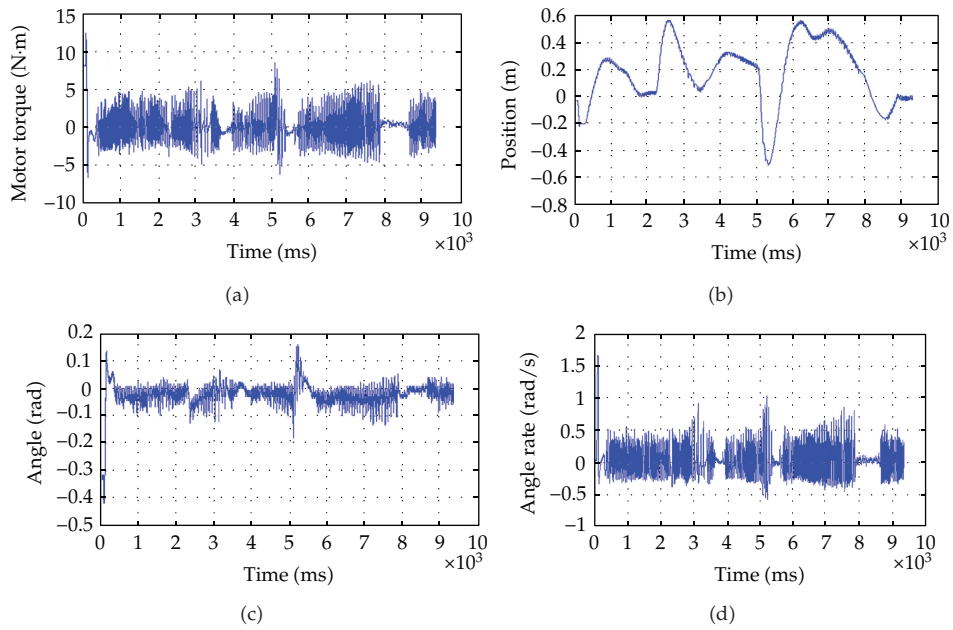

Figure 11: Real-time curve of the robot when stable.

Figure 12: Stable control photo of robot.

on traditional PD control theory and fuzzy logic control theory, a fuzzy PD controller is designed, which coordinates effectively the robust stability and speediness of the system.

Finally, a real-time control platform for the two-wheeled self-balancing robot is designed; after some parameter debugging, the robot is controlled effectively. The result indicates that the fuzzy PD control algorithm can achieve self-balanced control of the two-wheeled robot successfully and prevent the robot from falling in order to satisfy the robot's anticipated control goals and obtain a good dynamic performance.

References

[1] K. Y. Cai and L. Zhang, "Fuzzy reasoning as a control problem," *IEEE Transactions on Fuzzy Systems*, vol. 16, no. 3, pp. 600–614, 2008.

[2] L. A. Zadeh, "The concept of a linguistic variable and its application to approximate reasoning-I," *Information Sciences*, vol. 8, no. 3, pp. 199–249, 1975.

[3] L. A. Zadeh, "The concept of a linguistic variable and its application to approximate reasoning-II," *Information Sciences*, vol. 8, no. 4, pp. 301–357, 1975.

[4] D. Dubois and H. Prade, "Fuzzy sets in approximate reasoning. I. Inference with possibility distributions," *Fuzzy Sets and Systems*, vol. 40, no. 1, pp. 143–202, 1991.

[5] H. Maeda, S. Asaoka, and S. Murakami, "Dynamical fuzzy reasoning and its application to system modeling," *Fuzzy Sets and Systems*, vol. 80, no. 1, pp. 101–109, 1996.

[6] D. S. Yeung and E. C. Tsang, "Weighted fuzzy production rules," *Fuzzy Sets and Systems*, vol. 88, pp. 299–313, 1997.

[7] J. Zhang, P. Shi, and Y. Xia, "Fuzzy delay compensation control for T-S fuzzy systems over network," *IEEE Trans on Systems, Man and Cybernetics B*, no. 99, pp. 1–10, 2012.

[8] Q. Zhou, P. Shi, J. Lu, and S. Xu, "Adaptive output feedback fuzzy tracking control for a class of nonlinear systems," *IEEE Transactions on Fuzzy Systems*, vol. 19, no. 5, pp. 972–982, 2011.

[9] G.-J. Wang, "On the logic foundation of fuzzy reasoning," *Information Sciences*, vol. 117, no. 1-2, pp. 47–88, 1999.

[10] D. Dubois and H. Prade, "Possibilistic logic: a retrospective and prospective view," *Fuzzy Sets and Systems*, vol. 144, no. 1, pp. 3–23, 2004.

[11] L. Wu, X. Su, P. Shi, and J. Qiu, "Model approximation for discrete-time state-delay systems in the TS fuzzy framework," *IEEE Transactions on Fuzzy Systems*, vol. 19, no. 2, pp. 366–378, 2011.

[12] L. Wu, X. Su, P. Shi, and J. Qiu, "A new approach to stability analysis and stabilization of discrete-time T-S fuzzy time-varying delay systems," *IEEE Transactions on Systems, Man, and Cybernetics B*, vol. 41, no. 1, pp. 273–286, 2011.

[13] A. F. Amer, E. A. Sallam, and W. M. Elawady, "Fuzzy pre-compensated fuzzy self-tuning fuzzy PID controller of 3 DOF planar robot manipulators," in *Proceedings of IEEE/ASME International Conference on Advanced Intelligent Mechatronics (AIM '10)*, pp. 599–604, Montréal, Canada, July 2010.

[14] M. Nafar, G. B. Gharehpetian, and T. Niknam, "Using modified fuzzy particle swarm optimization algorithm for parameter estimation of surge arresters models," *International Journal of Innovative Computing, Information and Control*, vol. 8, no. 1, pp. 567–581, 2012.

[15] W.-H. Ho, S.-H. Chen, I.-T. Chen, J.-H. Chou, and C.-C. Shu, "Design of stable and quadratic-optimal static output feedback controllers for TS-fuzzy-model-based control systems: an integrative computational approach," *International Journal of Innovative Computing, Information and Control*, vol. 8, no. 1, pp. 403–418, 2012.

[16] K.-S. Shih, T.-H. S. Li, and S.-H. Tsai, "Observer-based adaptive fuzzy robust controller with self-adjusted membership functions for a class of uncertain MIMO nonlinear systems: a PSO-SA method," *International Journal of Innovative Computing, Information and Control*, vol. 8, no. 2, pp. 1419–1437, 2012.

[17] J. Zhang, P. Shi, and Y. Xia, "Robust adaptive sliding-mode control for fuzzy systems with mismatched uncertainties," *IEEE Transactions on Fuzzy Systems*, vol. 18, no. 4, pp. 700–711, 2010.

[18] C. Elmas, O. Deperlioglu, and H. H. Sayan, "Adaptive fuzzy logic controller for DC-DC converters," *Expert Systems with Applications*, vol. 36, no. 2, pp. 1540–1548, 2009.

[19] J. J. Craig, *Introduction to Robotics*, Addison-Wisley, Reading, Mass, USA, 2nd edition, 1989.

[20] M. W. Spong and M. Vidyasagar, *Robot Dynamics and Control*, John Wiley & Sons, New York, NY, USA, 1989.

[21] S. K. Nguang, P. Shi, and S. Ding, "Fault detection for uncertain fuzzy systems: an LMI approach," *IEEE Transactions on Fuzzy Systems*, vol. 15, no. 6, pp. 1251–1262, 2007.

[22] T.-C. Lin, S.-W. Chang, and C.-H. Hsu, "Robust adaptive fuzzy sliding mode control for a class of uncertain discrete-time nonlinear systems," *International Journal of Innovative Computing, Information and Control*, vol. 8, no. 1, pp. 347–359, 2012.

[23] H. B. Kazemian, "The SOF-PID controller for the control of a MIMO robot arm," *IEEE Transactions on Fuzzy Systems*, vol. 10, no. 4, pp. 523–532, 2002.

[24] *Googol Technology Self-Balancing Robot GBOT1001 User Manual V1.0.*, Googol Technology LTD, 2007.

[25] M. W. Spong, "Swing up control problem for the acrobot," *IEEE Control Systems Magazine*, vol. 15, no. 1, pp. 49–55, 1995.

[26] Segway Human Transporter, 2004, http://www.segway.com/.

[27] J. Wu and W. Zhang, "Research on control method of two-wheeled self-balancing robot," in *Proceedings of the 4th International Conference on Intelligent Computation Technology and Automation (ICICTA '11)*, pp. 476–479, Shenzhen, China, March 2011.
[28] M. P. Kevin and Y. Stephen, *Fuzzy Control*, Tsinghua University Press, Beijing, China, 2001.
[29] J. Wu and W. Zhang, "Design of fuzzy logic controller for two-wheeled self-balancing robot," in *Proceedings of the 6th International Forum on Strategic Technology (IFOST '11)*, pp. 1266–1270, Harbin, China, August 2011.

Hindawi Publishing Corporation
Mathematical Problems in Engineering
Volume 2012, Article ID 259494, 15 pages
doi:10.1155/2012/259494

Research Article

Approximate Analytic and Numerical Solutions to Lane-Emden Equation via Fuzzy Modeling Method

De-Gang Wang,[1] Wen-Yan Song,[2] Peng Shi,[3,4] and Hamid Reza Karimi[5]

[1] *School of Control Science and Engineering, Dalian University of Technology, Dalian 116024, China*
[2] *Department of Quantitative Economics, Dongbei University of Finance and Economics, Dalian 116025, China*
[3] *School of Electrical and Electronic Engineering, The University of Adelaide, Adelaide, SA 5005, Australia*
[4] *School of Engineering and Science, Victoria University, Melbourne, VIC 8001, Australia*
[5] *Department of Engineering, Faculty of Technology and Science, University of Agder, 4898 Grimstad, Norway*

Correspondence should be addressed to Peng Shi, peng.shi@vu.edu.au

Received 19 August 2012; Accepted 21 October 2012

Academic Editor: Mohammed Chadli

Copyright © 2012 De-Gang Wang et al. This is an open access article distributed under the Creative Commons Attribution License, which permits unrestricted use, distribution, and reproduction in any medium, provided the original work is properly cited.

A novel algorithm, called variable weight fuzzy marginal linearization (VWFML) method, is proposed. This method can supply approximate analytic and numerical solutions to Lane-Emden equations. And it is easy to be implemented and extended for solving other nonlinear differential equations. Numerical examples are included to demonstrate the validity and applicability of the developed technique.

1. Introduction

Lane-Emden equations are used to describe singular initial value problems (IVPs) relating to second-order ordinary differential equations which have been used to model several phenomena in mathematical physics, thermodynamics, fluid mechanics, and astrophysics such as the theory of stellar structure, the thermal behavior of a spherical cloud of gas, isothermal gas spheres, and theory of thermionic currents.

Lane-Emden equations, first introduced by Jonathan Homer Lane in 1870 and further explored in detail by Emden, have the following form:

$$y'' + \frac{2}{x}y' + f(y) = 0, \quad 0 < x \leq 1, \tag{1.1}$$

subject to the conditions

$$y(0) = A, \qquad y'(0) = B, \tag{1.2}$$

where A and B are constants and $f(y)$ is a continuous real valued function.

Since Lane-Emden type equations have significant applications in many scientific fields, various forms of $f(y)$ have been investigated in many research works. Among them, many attentions have been carried on the generalized Lane-Emden type equations,

$$y'' + \frac{k}{x}y' + f(x,y) = g(x), \quad 0 < x \leq 1,\ k \geq 0, \tag{1.3}$$

subject to condition (1.2), where $f(x,y)$ is a continuous real valued function, and $g \in C[0,1]$.

Many different methods have been used to obtain solutions for the generalized Lane-Emden equations. Wazwaz [1, 2] got approximate solutions by using the Adomian decomposition method (ADM) and obtained the analytic solutions of some equations. But it may be an intricate problem to calculate the so-called Adomian polynomials involved in ADM sometimes. He [3, 4] developed a more convenient analytical technique, called the homotopy perturbation method (HPM). Chowdhury and Hashim [5] and Yildirim and Öziş [6] gave the solutions for a class of singular second-order IVPs of Lane-Emden type by using HPM. Sajid et al. [7] pointed out that HPM is a special case of the homotopy analysis method (HAM) and that it is valid only for weakly nonlinear problems. Liao [8] and Van Gorder and Vajravelu [9] used HAM to increase the radius of convergence of series solutions for Lane-Emden equations. Recently, Yiğider et al. studied a numerical method for solving Lane-Emden type equations by Padé approximation in [10]. Generally, when all the above cited analytical approaches are used to solve Lane-Emden equation, a truncated power series solution of the true solution is obtained. By the methods such as HPM and HAM, a series of newly achievements on the analytical solving for some nonlinear differential equations have been proposed recently. By HAM, Ziabakhsh et al. [11, 12] studied the natural convection of a non-Newtonian fluid between two infinite parallel vertical flat plates and the effects of the non-Newtonian nature of fluid on the heat transfer. Jalaal et al. [13, 14] investigated the settling behavior of solid particles using HPM, which show the capability and effectiveness of the method and exhibit new application of it further.

Besides, many soft computing technologies are developed to deal with all types of models for dynamic systems [15–18]. It is important to note that fuzzy modeling technology can transfer data information into a mathematical model which can approximate the original system with high accuracy [19–24]. Li et al. [25] used fuzzy modeling method to approximate the solutions of a class of autonomous differential equation. In order to obtain the analytical solution of the fuzzy system, Li et al. [26] introduced fuzzy marginal linearization method. Further, Li et al. [27] proposed fuzzy inference modeling (FIM) method to approximate the time-variant system. Wang et al. [28] proposed a dynamic fuzzy inference modeling (DFIM) method and proved that fuzzy system generalized by this method was universal approximators to the solutions of some nonautonomous differential equations.

However, above fuzzy modeling technology could not be used to solve the differential equation (1.3). And when $f(x,y)$ and $g(x)$ in (1.3) are unknown and only input-output data of them are obtained, how to obtain the corresponding solution is an interesting question. Motivated by this fact, the aim of this paper is to propose a novel fuzzy modeling method to

solve the Lane-Emden equation. This paper is organized as follows. In Section 2, we introduce some preliminary knowledge. In Section 3, we propose a novel fuzzy modeling technology and use it to obtain the approximate analytical solutions of the Lane-Emden equation. Some examples are used to illustrate the validity of the proposed method in Section 4. Finally, conclusions are presented in Section 5.

2. Preliminaries and Basic Ideas of FIM

Firstly, we introduce some basic concepts which will be used in sequel.

Definition 2.1. A fuzzy set A of X is a function from the reference set X to the unit interval $[0,1]$, that is, $A : X \to [0,1]$, $x \mapsto A(x)$.

Definition 2.2. Let A_i $(i = 1,\ldots,n)$ be a group of normal fuzzy sets of X, where x_i is the peak point of A_i, that is, $A_i(x_i) = 1$. If A_i $(i = 1,\ldots,n)$ satisfies the condition: $\sum_{i=1}^{n} A_i(x) = 1$ (for all $x \in X$) and for all i, j $(i \neq j \Rightarrow x_i \neq x_j)$, then $\mathcal{A} \triangleq \{A_i\}_{1\le i\le n}$ is called a fuzzy partition of X.

Definition 2.3. The mappings w_r $(r = 1, 2)$ from $[a,b]$ to $[0,1]$ are variable weights if the following conditions hold

(a) for any $x \in [a,b]$, $w_1(x) + w_2(x) = 1$;

(b) $w_1(a) = 1$, $w_2(b) = 1$.

Example 2.4. Let $X_k = [x_k, x_{k+1}]$. The following mappings are variable weights on X_k: $w_{1k}(x) = (x_{k+1} - x)/(x_{k+1} - x_k)$, $w_{2k}(x) = (x - x_k)/(x_{k+1} - x_k)$.

In the following, we will introduce FIM method. Consider a second order ordinary differential equation

$$y'' = \phi(x, y, y'), \tag{2.1}$$

where x is the independent variable, y is the unknown function, X, Y, Y', and Y'' are the universes of x, y, y', and y'', respectively, and ϕ is a real-valued continuous function, which explicitly contains the independent variable x. Obviously (1.3) is the special case of (2.1). In this paper, we assume that X, Y, Y', and Y'' are real number intervals, that is, $X = [a_0, b_0]$, $Y = [a_1, b_1]$, $Y' = [a_2, b_2]$, and $Y'' = [a_3, b_3]$.

Let $(x_i, y_j, y'_k, y''_{ijk}) \in X \times Y \times Y' \times Y''$ $(i = 1,\ldots,n;\ j = 1,\ldots,m;\ k = 1,\ldots,l)$ be a group of known data from (2.1), which satisfy the following two conditions:

(1) $a_0 = x_1 < \cdots < x_n = b_0$, $a_1 = y_1 < \cdots < y_m = b_1$, $a_2 = y'_1 < \cdots < y'_l = b_2$;

(2) $y''_{ijk} = \phi(x_i, y_j, y'_k)$, $(i = 1,2,\ldots,n;\ j = 1,2,\ldots,m;\ k = 1,2,\ldots,l)$.

Then, we use above data information to construct fuzzy rule base. For each index i $(i = 1,\ldots,n)$, we, respectively, take y_j, y'_k, and y''_{kij} as the peak points of fuzzy sets A_j, B_k, and C_{ijk}, such that $\{A_j\}_{1\le j\le m}$ is a fuzzy partition of Y, $\{B_k\}_{1\le k\le l}$ is a fuzzy partition of Y', and $\{C_{ijk}\}_{1\le i\le n, 1\le j\le m, 1\le k\le l}$ is a fuzzy partition of Y''. Similarly, we take y''_{ijk} as peak point of fuzzy

set D_{ijk}, such that $\{D_{ijk}\}_{1\le i\le n, 1\le j\le m, 1\le k\le l}$ is a fuzzy partition of Y''. In this way, fuzzy rules based on data information are represented as follows:

$$\begin{gathered}\text{If } y \text{ is } B_j \text{ and } y' \text{ is } C_k \text{ then } y'' \text{ is } D_{ijk},\\ i = 1,\ldots,n;\ j = 1,\ldots,m;\ k = 1,\ldots,l.\end{gathered} \tag{2.2}$$

For fuzzy rules (2.2), fuzzy system generalized by FIM method can be expressed by

$$y'' = \sum_{i=1}^{n-1}\sum_{j=1}^{m}\sum_{k=1}^{l}\left(A_j(y)\cdot B_k(y')\right)\cdot y''_{ijk}\cdot \chi_i(x), \tag{2.3}$$

where the characteristic function $\chi_i(x)$ is defined as

$$\chi_i(x) \triangleq \begin{cases} 1, & x \in [x_i, x_{i+1}],\\ 0, & x \notin [x_i, x_{i+1}].\end{cases} \tag{2.4}$$

Remark 2.5. It can be seen that fuzzy system (2.3) is a nonlinear differential equation with variable coefficients. When $A_j(y)$ and $B_k(y')$ are, respectively, chosen as triangular membership functions, in each local region $[x_i, x_{i+1}] \times [y_j, y_{j+1}] \times [y'_k, y'_{k+1}]$, (2.3) is changed into an autonomous differential equation with constant coefficients. This fact means that (2.3) is a two-order differential equation with piecewise constant coefficients. In [27], it is proved that solutions of (2.3) can approximate the numerical solutions of some nonautonomous differential equations with high accuracy.

3. Approximate Analytic Solutions of the Lane-Emden Equation Based on Variable Weight Fuzzy Marginal Linearization Method

From (2.3), we find that in each local region it is still a nonlinear differential equation. Hence, it is difficult for us to get the corresponding analytical solution for it. In this section, we propose a novel fuzzy modeling method, called variable weight fuzzy marginal linearization (VMFML) method, and utilize this technology to obtain the approximate analytical solution for Lane-Emden equation. For simplicity, we introduce some denotations.

Let $\{[x_i, x_{i+1}) \times [y_j, y_{j+1}) \times [y'_k, y'_{k+1})\}$ $(i = 1,\ldots,n;\ j = 1,\ldots,m;\ k = 1,\ldots,l)$ be a partition of $X \times Y \times Y'$, where $[x_n, x_{n+1}) \triangleq \{x_n\}$, $[y_m, y_{m+1}) \triangleq \{y_m\}$ and $[y'_l, y'_{l+1}) \triangleq \{y'_l\}$. Similarly, $\{(x_{i-1}, x_i] \times [y_j, y_{j+1}) \times [y'_k, y'_{k+1})\}$ $(i = 1,\ldots,n;\ j = 1,\ldots,m;\ k = 1,\ldots,l)$ is another partition of $X \times Y \times Y'$, where $(x_0, x_1] \triangleq \{x_1\}$. Further, we, respectively, divide $[x_i, x_{i+1}) \times [y_j, y_{j+1}) \times [y'_k, y'_{k+1})$ and $(x_{i-1}, x_i] \times [y_j, y_{j+1}) \times [y'_k, y'_{k+1})$ into 4 pieces and let

$$\begin{aligned}(i,j,k)_{r_1r_2} &\triangleq [x_i, x_{i+1}) \times \left[y_{j+r_1/2}, y_{j+(r_1+1)/2}\right) \times \left[y'_{k+r_2/2}, y'_{k+(r_2+1)/2}\right),\\ \overline{(i,j,k)}_{r_1r_2} &\triangleq (x_{i-1}, x_i] \times \left[y_{j+r_1/2}, y_{j+(r_1+1)/2}\right) \times \left[y'_{k+r_2/2}, y'_{k+(r_2+1)/2}\right),\end{aligned} \tag{3.1}$$

where $r_1 = 1,\ 2$; $r_2 = 1,\ 2$; $y_{j+1/2} \triangleq (y_j + y_{j+1})/2$, $y'_{k+1/2} \triangleq (y'_k + y'_{k+1})/2$, $j = 1, \ldots, m-1$; $k = 1, \ldots, l-1$. The characteristic functions on $(i,j,k)_{r_1 r_2}$ and $\overline{(i,j,k)}_{r_1 r_2}$ are, respectively, denoted as $\chi_{(i,j,k)_{r_1 r_2}}$ and $\chi_{\overline{(i,j,k)}_{r_1 r_2}}$, that is,

$$\chi_{(i,j,k)_{r_1 r_2}}(x,y,y') \triangleq \begin{cases} 1, & (x,y,y') \in [x_i, x_{i+1}) \times [y_{j+r_1/2}, y_{j+(r_1+1)/2}) \times \left[y'_{k+r_2/2}, y'_{k+(r_2+1)/2}\right), \\ 0, & (x,y,y') \notin [x_i, x_{i+1}) \times [y_{j+r_1/2}, y_{j+(r_1+1)/2}) \times \left[y'_{k+r_2/2}, y'_{k+(r_2+1)/2}\right). \end{cases}$$

$$\chi_{\overline{(i,j,k)}_{r_1 r_2}}(x,y,y') \triangleq \begin{cases} 1, & (x,y,y') \in (x_{i-1}, x_i] \times [y_{j+r_1/2}, y_{j+(r_1+1)/2}) \times \left[y'_{k+r_2/2}, y'_{k+(r_2+1)/2}\right), \\ 0, & (x,y,y') \notin (x_{i-1}, x_i] \times [y_{j+r_1/2}, y_{j+(r_1+1)/2}) \times \left[y'_{k+r_2/2}, y'_{k+(r_2+1)/2}\right). \end{cases} \tag{3.2}$$

In the following, we will introduce the basic idea of VMFML method.

For any $(x,y,y') \in X \times Y \times Y'$, without loss of generality, we assume that $(x,y,y') \in (i,j,k)_{r_1 r_2}$. For any $j \in \{1, \ldots, m\}$ and $k \in \{1, \ldots, l\}$, by fuzzy marginal linearization technology, we take $A_j(y)$ as triangular membership function and $B_k(y')$ as rectangle-shaped membership function, then fuzzy system (2.3) can be changed into

$$y'' = \frac{y_{j+1} - y}{y_{j+1} - y_j} \cdot y''_{ij(k+r_2)} + \frac{y - y_j}{y_{j+1} - y_j} \cdot y''_{ij(k+r_2)}. \tag{3.3}$$

Similarly, when $A_j(y)$ is chosen as rectangle-shaped membership function and $B_k(y')$ is chosen as triangular membership function, fuzzy system (2.3) can be changed into

$$y'' = \frac{y'_{k+1} - y'}{y'_{k+1} - y'_k} \cdot y''_{ij(k+r_2)} + \frac{y' - y'_k}{y'_{k+1} - y'_k} \cdot y''_{ij(k+r_2)}. \tag{3.4}$$

Furthermore, we take sum of the right side of expressions (3.3) and (3.4) and subtract a constant, the corresponding fuzzy system in the local region $(i,j,k)_{r_1 r_2}$ is represented as

$$y'' = d^{(1)}_{ijk} + d^{(2)}_{ijk} y + d^{(3)}_{ijk} y', \tag{3.5}$$

where

$$d^{(1)}_{ijk} = \frac{y_{j+1} y''_{ij(k+r_2)} - y_j y''_{i(j+1)(k+r_2)}}{y_{j+1} - y_j} + \frac{y'_{(k+1)} y''_{i(j+r_1)k} - y'_k y''_{i(j+r_1)(k+1)}}{y'_{k+1} - y'_k} - y''_{i(j+r_1)(k+r_2)}, \tag{3.6}$$

$$d^{(2)}_{ijk} = \frac{y''_{i(j+1)(k+r_2)} - y''_{ij(k+r_2)}}{y_{j+1} - y_j}, \tag{3.7}$$

$$d^{(3)}_{ijk} = \frac{y''_{i(j+r_1)(k+1)} - y''_{i(j+r_1)k}}{y'_{k+1} - y'_k}. \tag{3.8}$$

By characteristic function, we can obtain fuzzy system on $X \times Y \times Y'$ as follows:

$$y'' \triangleq f(x,y,y') \triangleq \sum_{i=1}^{n}\sum_{j=1}^{m}\sum_{k=1}^{l}\left(d_{ijk}^{(1)} + d_{ijk}^{(2)}y + d_{ijk}^{(3)}y'\right) \cdot \chi_{(i,j,k)_{r_1r_2}}(x,y,y'). \tag{3.9}$$

Remark 3.1. It is easy to see that (3.9) is a piecewise linear differential equation. In each local region $(i,j,k)_{r_1r_2}$, (3.9) transfers into a linear differential equation and the corresponding coefficients can be computed by input-output data of the original system. By expressions (3.5)–(3.8), it is easy to prove that the right-hand side $f(x,y,y')$ is an interpolation function of $\phi(x,y,y')$, that is, $f(x_i,y_j,y'_k) = y''_{ijk} = \phi(x_i,y_j,y'_k)$, $i = 1,\ldots,n$; $j = 1,\ldots,m$; $k = 1,\ldots,l$. By numerical analysis theory, we know that when we obtain enough data information on (2.1), $f(x,y,y')$ can approximate $\phi(x,y,y')$ with the specified accuracy. This fact means that (3.6) can be used to describe the nonlinear differential equation (2.1).

Then, we will solve the initial value problem of (3.9).

Given an initial value problem as

$$y'' = \sum_{i=1}^{n}\sum_{j=1}^{m}\sum_{k=1}^{l}\left(d_{ijk}^{(1)} + d_{ijk}^{(2)}y + d_{ijk}^{(3)}y'\right) \cdot \chi_{(i,j,k)_{r_1r_2}}(x,y,y'), \tag{3.10}$$

subject to the conditions $y(0) = y_0$ and $y'(0) = y'_0$.

First, we can determine the local region which the initial vector $(0,y_0,y'_0)$ locates in. Suppose that $(0,y_0,y'_0) \in [x_1,x_2) \times [y_j,y_{j+1/2}) \times [y'_k,y'_{k+1/2})$. By (3.9) the corresponding piecewise equation can be written as

$$y'' = d_{1jk}^{(1)} + d_{1jk}^{(2)}y + d_{1jk}^{(3)}y', \tag{3.11}$$

and the corresponding coefficients can be computed by expressions (3.6)–(3.8). Since it is a linear ode, we can get the corresponding analytical solution and denote it as y_1. Then, we take $(x_2,y_1(x_2),y'_1(x_2))$ as the initial vector and search the next region which it moves in. And we can solve the corresponding piecewise linear equation with the initial value $(y_1(x_2),y'_1(x_2))$. In this way, by transferring initial value piece by piece and solving the corresponding piecewise linear equation, we can obtain analytical solution of (3.9).

On the other hand, if we take $\overline{(i,j,k)}_{r_1r_2}$ ($r_1 = 1, 2$; $r_2 = 1, 2$; $j = 1,\ldots,m-1$; $k = 1,\ldots,l-1$) as the local region of universe $X \times Y \times Y'$, using fuzzy marginal linearization technology, we can obtain another fuzzy system as follows:

$$y'' = \sum_{i=1}^{n}\sum_{j=1}^{m}\sum_{k=1}^{l}\left(\overline{d}_{ijk}^{(1)} + \overline{d}_{ijk}^{(2)}y + \overline{d}_{ijk}^{(3)}y'\right) \cdot \chi_{\overline{(i,j,k)}_{r_1r_2}}(x,y,y'), \tag{3.12}$$

where

$$\begin{aligned}
\overline{d}_{ijk}^{(1)} &= \frac{y_{j+1}y''_{(i+1)j(k+r_2)} - y_j y''_{(i+1)(j+1)(k+r_2)}}{y_{j+1} - y_j} + \frac{y'_{(k+1)}y''_{(i+1)(j+r_1)k} - y'_k y''_{(i+1)(j+r_1)(k+1)}}{y'_{k+1} - y'_k} \\
&\quad - y''_{(i+1)(j+r_1)(k+r_2)}, \\
\overline{d}_{ijk}^{(2)} &= \frac{y''_{(i+1)(j+1)(k+r_2)} - y''_{(i+1)j(k+r_2)}}{y_{j+1} - y_j}, \\
\overline{d}_{ijk}^{(3)} &= \frac{y''_{(i+1)(j+r_1)(k+1)} - y''_{(i+1)(j+r_1)k}}{y'_{k+1} - y'_k}.
\end{aligned} \tag{3.13}$$

Obviously, both (3.9) and (3.12) can describe (2.1) and the analytical solutions of them can be obtained. The differences between them are that the coefficients of (3.9) in the local region $[x_i, x_{i+1}] \times [y_{j+r_1/2}, y_{j+(r_1+1)/2}) \times [y'_{k+r_2/2}, y'_{k+(r_2+1)/2})$ are computed by data $(x_i, y_j, y'_k, y''_{ijk})$, $(x_i, y_j, y'_{k+1}, y''_{ij(k+1)})$, $(x_i, y_{j+1}, y'_k, y''_{i(j+1)k})$,$(x_i, y_{j+1}, y'_{k+1}, y''_{i(j+1)(k+1)})$.

On the other hand, the corresponding coefficients of (3.12) in the local region $[x_i, x_{i+1}] \times [y_{j+r_1/2}, y_{j+(r_1+1)/2}) \times [y'_{k+r_2/2}, y'_{k+(r_2+1)/2})$ are deduced by data $(x_{i+1}, y_j, y'_k, y''_{(i+1)jk})$, $(x_{i+1}, y_j, y'_{k+1}, y''_{(i+1)j(k+1)})$, $(x_{i+1}, y_{j+1}, y'_k, y''_{(i+1)(j+1)k})$, and $(x_{i+1}, y_{j+1}, y'_{k+1}, y''_{(i+1)(j+1)(k+1)})$. For a given initial value $y(0) = y_0$ and $y'(0) = y'_0$, by transferring initial value technology, we can solve the corresponding analytical solutions of (3.9) and (3.12) denote them as $\varphi_1(x)$ and $\varphi_2(x)$, respectively. In order to describe (2.1) better, we take variable weighted sum of $\varphi_1(x)$ and $\varphi_2(x)$, and denote

$$\varphi(x) = \sum_{k=1}^{n-1} \left(\omega_{1k}(x) \cdot \varphi_1(x) + \omega_{2k}(x) \cdot \varphi_2(x)\right) \cdot \chi_k(x), \tag{3.14}$$

as the approximation analytical solution of (2.1), where $w_{1k}(x) = (x_{k+1} - x)/(x_{k+1} - x_k)$ and $w_{2k}(x) = (x - x_k)/(x_{k+1} - x_k)$.

In this way, we use variable weight fuzzy marginal linearization (VWFML) technology to obtain the approximation analytical solution for (2.1).

Next, we also take (2.1) as example to summarize basic processes of VWFLM method.

Step 1. Determine the universes of x, y, and y' and denote them as X, Y, and Y'.

Step 2. Divide the universes and let x_i, y_j, y'_k be the partition points of X, Y, and Y', where $i = 1, \ldots, n$; $j = 1, \ldots, m$; $k = 1, \ldots, l$.

Step 3. By (2.1), compute the corresponding output data $y''_{ijk} = \phi(x_i, y_j, y'_k)$.

Step 4. Using expressions (3.6)–(3.8) and data information $(x_i, y_j, y'_k, y''_{ijk})$ $(i = 1, \ldots, n-1;\ j = 1, \ldots, m;\ k = 1, \ldots, l)$, deduce the coefficients of piecewise equation and construct the corresponding fuzzy system (3.9).

Step 5. For given initial value, by transferring initial value technology, solve above fuzzy system and denote the solution as $\varphi_1(x)$.

Step 6. By expression (3.13) and data information $(x_{i+1}, y_j, y'_k, y''_{(i+1)jk})$ $(i = 2, \ldots, n;\ j = 1, \ldots, m;\ k = 1, \ldots, l)$, we can also deduce the coefficients of piecewise equation and construct another fuzzy system (3.12).

Step 7. Similarly, by transferring initial value technology, we can solve this fuzzy system (3.12) and denote the solution as $\varphi_2(x)$.

Step 8. We take weighted sum of $\varphi_1(x)$ and $\varphi_2(x)$, that is,

$$\varphi(x) = \sum_{k=1}^{n-1} \left(\omega_{1k}(x) \cdot \varphi_1(x) + \omega_{2k}(x) \cdot \varphi_2(x)\right) \cdot \chi_k(x), \tag{3.15}$$

where $w_{1k}(x) = (x_{k+1} - x)/(x_{k+1} - x_k)$ and $w_{2k}(x) = (x - x_k)/(x_{k+1} - x_k)$.

Remark 3.2. In many physical problems when differential equation models are unknown and only some data information of the investigated systems are known, by VWFML method we can still set up dynamic models and obtain corresponding approximation analytical solutions for the problems.

4. Numerical Results

In this section, we will use VWFML method to solve four Lane-Emden equations. The former two equations are of original type Lane-Emden equations and the latter two are of generalized type.

Example 4.1. Consider the linear singular initial value problem:

$$y'' + \frac{2}{x} y' + y = 6 + 12x + x^2 + x^3, \tag{4.1}$$

subject to the initial conditions $y(0) = 0$ and $y'(0) = 0$. The exact solution for this equation is $y(x) = x^2 + x^3$.

The solution, which is generated from this Lane-Emden equation of classical astrophysics, has a proven physical foundation and can be used to calculate the radius of electron in an electromagnetic mass model.

Let $n = 5$, $m = 5$, and $l = 5$. Figure 1, respectively, shows curves of exact solution and approximate solutions obtained by VWFML method, DFIM method, and FIM method. Table 1 shows the coefficients of piecewise (3.9) and (3.12). In Figure 2, the absolute error curves among them are given, where "crossed line" denotes the absolute error curve between the approximate solution obtained by VWFML method and the exact solution, "$\cdots$" denotes the absolute error curve between the approximate solution obtained by FIM method and the exact solution, and "-*-" denotes the absolute error curve between the approximate solution obtained by DFIM method and the exact solution. Table 2 presents the errors among the exact solution and the approximate solutions obtained by them.

In this simulation, the approximation results are satisfying. In fact, the number of divided local regions is not large, which means that we can get all the coefficients of (3.9) and (3.12) without a great deal of computation. Accordingly, the approximate analytic solution

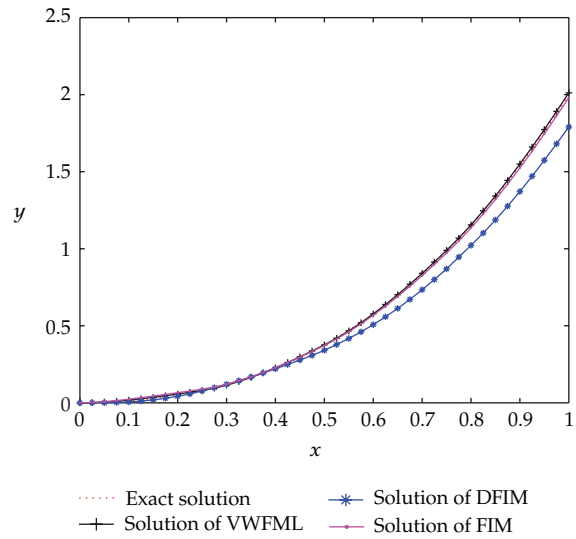

Figure 1: Solution curves of Example 4.1.

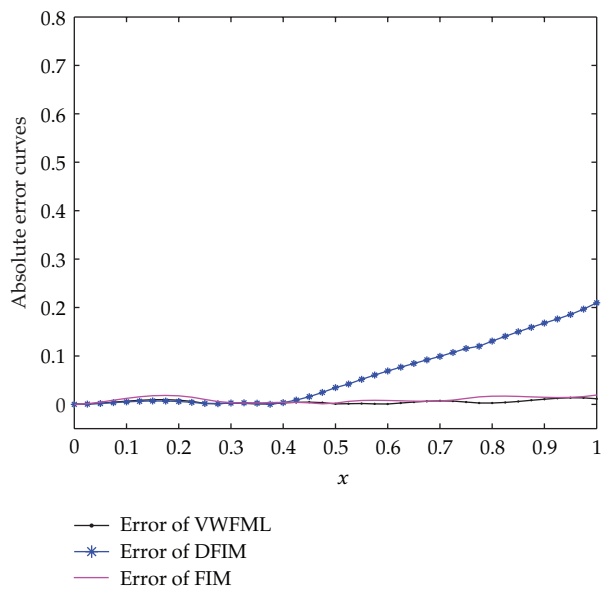

Figure 2: Error curves of Example 4.1.

can be found for Example 4.1. From Figure 2 and Table 2, it is clear that for solving this equation VWFML technology is more effective than DFIM and FIM, and the corresponding amount of error data is smaller.

Example 4.2. Consider isothermal gas spheres equation:

$$y'' + \frac{2}{x}y' + e^{y} = 0, \tag{4.2}$$

subject to the initial conditions $y(0) = 0$, $y'(0) = 0$.

Table 1: Coefficients of (3.9) and (3.12).

Example 4.1 ($n = 5,\ m = 5,\ l = 5$)							
k	x	$d_{ijk}^{(1)}$	$d_{ijk}^{(2)}$	$d_{ijk}^{(3)}$	$\overline{d}_{ijk}^{(1)}$	$\overline{d}_{ijk}^{(2)}$	$\overline{d}_{ijk}^{(3)}$
1	(0, 0.25]	0	0	0	−1	−8	9.0781
2	(0.25, 0.5]	−1.0000	−8.0000	9.0781	−1.0000	−4.0000	12.3750
3	(0.5, 0.75]	−1.0000	−4.0000	12.3750	−1.0000	−2.6667	15.9844
4	(0.75, 1]	−1.0000	−2.6667	15.9844	−1.0000	−2.0000	20.0000

Table 2: Errors of different approximate solutions for Example 4.1.

Example 4.1 ($n = 5,\ m = 5,\ l = 5$)			
x	Error of VWFML	Error of DFIM	Error of FIM
0.1	0.0067	0.0052	0.0125
0.2	0.0087	0.0059	0.0176
0.3	−0.0027	0.0028	0.0035
0.4	0.0029	−0.0035	0.0041
0.5	0.0010	−0.0345	−0.0027
0.6	0.0008	−0.0689	−0.0081
0.7	0.0072	−0.0991	−0.0070
0.8	0.0027	−0.1306	−0.0169
0.9	0.0107	−0.1678	−0.0146
1	0.0117	−0.2096	−0.0193

This type of equation has been used to model the thermal behavior of a spherical cloud of gas acting under the mutual attraction of its molecules. Isothermal gaseous sphere, in which the temperature remains constant, subjects to the classical laws of thermodynamics when one seeks to determine the density and electric force of an electron gas in the neighborhood of a hot body in thermal equilibrium. It is worthy to notice that this equation is nonlinear and has no analytic solution.

From [1, 5], we know that the 6-term series solutions of this equation obtained by ADM and HPM are the same. Obviously, in Figure 3 we find that solutions obtained by VWFML method are very close to solutions of ADM method, where "$\cdots$" denotes the solution obtained by ADM method and "crossed line" denotes the solution obtained by VWFML method.

For the consistency of the comparison and without loss of generality, chosen the same initial value and the same independent variable values, Table 3 shows the approximations of solutions for Example 4.2, respectively, obtained by ADM method and VWFML method. Further, in Figure 4, the curves obtained by the above two methods are given. Since Lane-Emden equations are singular initial value problems, the accuracy of solutions near zero point is important, whatever the solution is gotten from approximate analytical method or from numerical method. From simulation results, we can see that if the number of local regions increased in VWFML method, the accuracy of the approximation solution can be improved evidently, especially when the independent variable is near the initial value 0. Besides, the solutions of Lane-Emden equations converge rapidly in a very small region ($0 < x < 1$), and

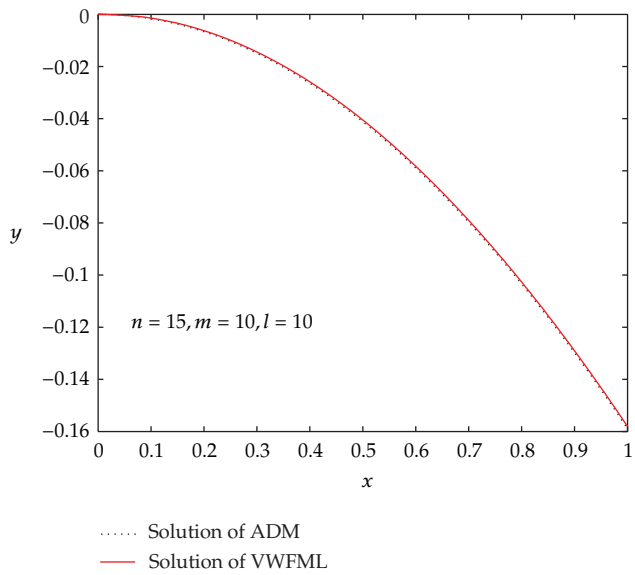

Figure 3: Solution curves of Example 4.2.

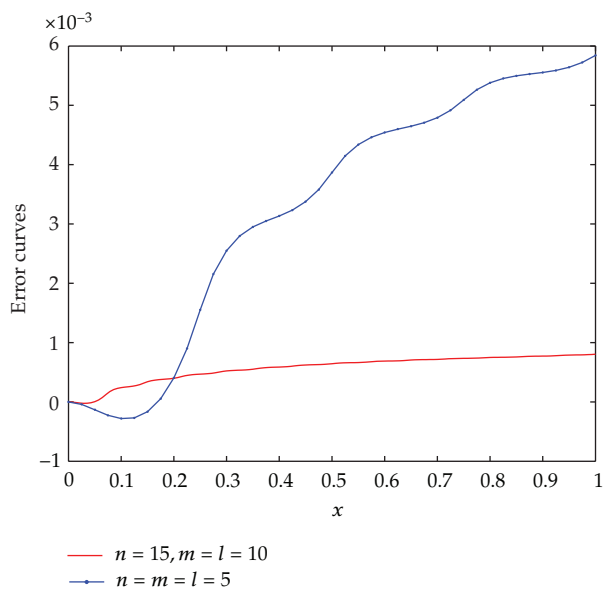

Figure 4: Error curves of Example 4.2.

in Figure 3 the approximate curve follows the trend appropriately. This implies that VWFML method can describe the isothermal gas spheres equation with high accuracy degree.

Example 4.3. Consider the linear initial value problem:

$$y'' + \frac{8}{x}y' + xy = x^5 - x^4 + 44x^2 - 30x, \tag{4.3}$$

subject to the initial conditions $y(0) = 0$, $y'(0) = 0$. The exact solution is $y(x) = x^4 - x^3$.

Table 3: Solutions of Example 4.2.

x	6-term ADM solution	VWFML solution ($n = m = l = 5$)	VWFML solution ($n = 15,\ m = l = 10$)
0.1	−0.0016658	0.0019471	0.0014253
0.2	−0.0066534	−0.0062487	−0.0062547
0.3	−0.014933	−0.012383	−0.014411
0.4	0.026456	−0.023321	−0.025868
0.5	−0.041154	−0.037287	−0.04051
0.6	−0.058945	−0.054402	−0.058256
0.7	−0.079728	−0.074936	−0.079011
0.8	−0.10339	−0.098012	−0.10264
0.9	−0.12981	−0.12426	−0.12904
1	−0.15886	−0.15302	−0.15806

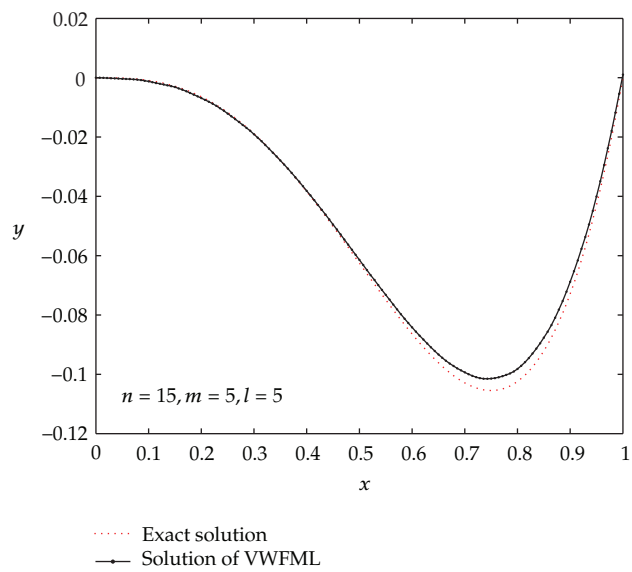

Figure 5: Solution curves of Example 4.3.

Let $n = 15$, $m = 5$, and $l = 5$. The curves of exact solution of Example 4.3 and the corresponding approximate solution obtained by VWFML method are shown in Figure 5, where "$\cdots$" denotes the exact solution and "crossed line" denotes the approximate solution obtained by VWFML method.

Example 4.4. We consider the nonlinear initial value problem:

$$y'' + \frac{6}{x}y' + 14y = -4y \ln y, \tag{4.4}$$

subject to the initial conditions $y(0) = 1$, $y'(0) = 0$. The exact solution is $y(x) = e^{-x^2}$.

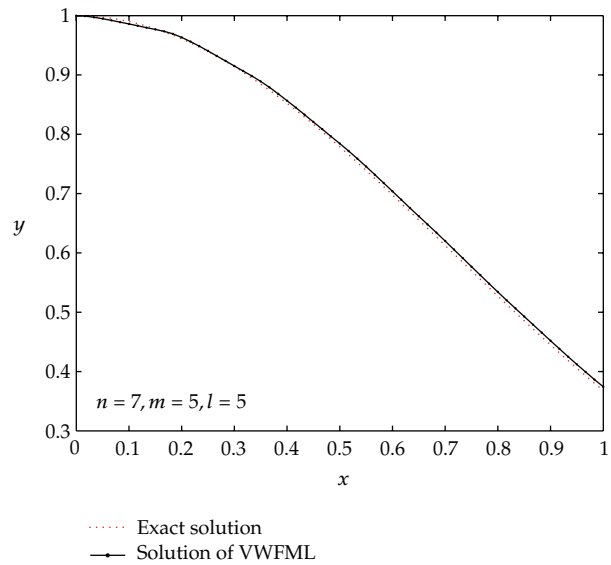

Figure 6: Solution curves of Example 4.4.

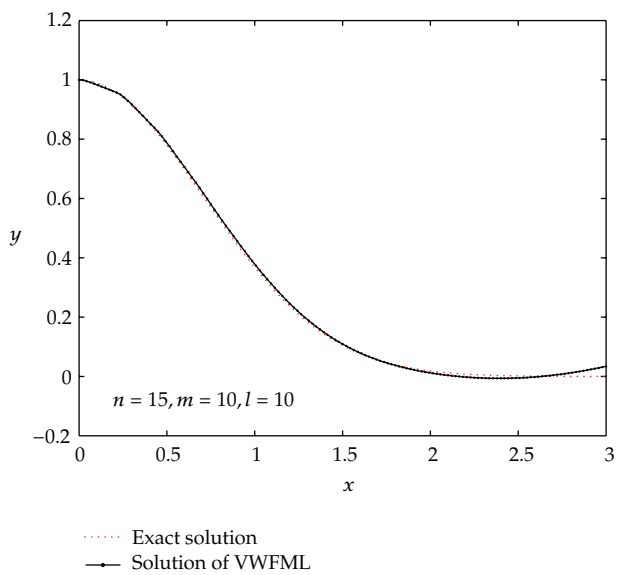

Figure 7: Solution curves of Example 4.4 ($x \in [0, 3]$).

Let $n = 7$, $m = 5$, and $l = 5$. The interval of independent variable is chosen as $[0, 1]$. The curves of exact solution of Example 4.4 and the corresponding approximate solution obtained by VWFML method are shown in Figure 6, where "$\cdots$" denotes the exact solution and "crossed line" denotes the approximate solution obtained by VWFML method. Furthermore, the interval of independent variable is extended as $[0, 3]$ and let $n = 15$, $m = 10$, and $l = 10$. The simulation result is shown in Figure 7.

Remark 4.5. From Examples 4.3 and 4.4, it can be seen that VWFML method is effective for solving generalized Lane-Emden type differential equations. Furthermore, if the solving interval is extended, VWFML method can also provide approximate solutions in the larger domains with high accuracy degree.

Remark 4.6. Comparison with some analytical solutions, solutions of VWFML methods are totally dependent on the dividing points of independent variable interval, which means that the proposed technique can be presented in a general way. In particular, when the objective equation is unknown and only some data information can be obtained, equation determined by VWFML method can be solved analytically and the corresponding solution can approximate the solution of objective equation with high accuracy.

5. Conclusion

In this paper, we apply VWFML method to obtain the approximate analytical and numerical solution for Lane-Emden type differential equation. Some numerical examples show that by relatively minor data information, solutions obtained by VWFML method can approximate the corresponding solutions of Lane-Emden type equations with high accuracy. This means that VWFML method can be utilized to solve and analyze complex nonlinear differential equations in practical application.

Acknowledgments

This work is partially supported by the National Natural Science Foundation of China (61104038, 71201019, 61074044, 61174058), the National 973 Basic Research Program of China (2009CB320602, 2012CB215202), and the 111 Project (B12018).

References

[1] A.-M. Wazwaz, "A new algorithm for solving differential equations of Lane-Emden type," *Applied Mathematics and Computation*, vol. 118, no. 2-3, pp. 287–310, 2001.

[2] A.-M. Wazwaz, "A new method for solving singular initial value problems in the second-order ordinary differential equations," *Applied Mathematics and Computation*, vol. 128, no. 1, pp. 45–57, 2002.

[3] J. H. He, "Homotopy perturbation method: a new nonlinear analytical technique," *Applied Mathematics and Computation*, vol. 135, no. 1, pp. 73–79, 2003.

[4] J. H. He, *Non-Perturbative Methods for Strongly Nonlinear Problems*, Die Deutsche Bibliothek, Germany, 2006.

[5] M. S. H. Chowdhury and I. Hashim, "Solutions of a class of singular second-order IVPs by homotopy-perturbation method," *Physics Letters A*, vol. 365, no. 5-6, pp. 439–447, 2007.

[6] A. Yildirim and T. Öziş, "Solutions of singular IVPs of Lane-Emden type by homotopy perturbation method," *Physics Letters A*, vol. 369, no. 1-2, pp. 70–76, 2007.

[7] M. Sajid, T. Hayat, and S. Asghar, "Comparison between the HAM and HPM solutions of thin film flows of non-Newtonian fluids on a moving belt," *Nonlinear Dynamics*, vol. 50, no. 1-2, pp. 27–35, 2007.

[8] S. Liao, "A new analytic algorithm of Lane-Emden type equations," *Applied Mathematics and Computation*, vol. 142, no. 1, pp. 1–16, 2003.

[9] R. A. Van Gorder and K. Vajravelu, "Analytic and numerical solutions to the Lane-Emden equation," *Physics Letters A*, vol. 372, no. 39, pp. 6060–6065, 2008.

[10] M. Yiğider, K. Tabatabaei, and E. C. Çelik, "The numerical method for solving differential equations of Lane-Emden type by Pade approximation," *Discrete Dynamics in Nature and Society*, vol. 2011, Article ID 479396, 9 pages, 2011.

[11] Z. Ziabakhsh and G. Domairry, "Analytic solution of natural convection flow of a non-Newtonian fluid between two vertical flat plates using homotopy analysis method," *Communications in Nonlinear Science and Numerical Simulation*, vol. 14, no. 5, pp. 1868–1880, 2009.

[12] Z. Ziabakhsh, G. Domairry, and H. Bararnia, "Analytical solution of non-Newtonian micropolar fluid flow with uniform suction/blowing and heat generation," *Journal of the Taiwan Institute of Chemical Engineers*, vol. 40, no. 4, pp. 443–451, 2009.

[13] M. Jalaal, D. D. Ganji, and G. Ahmadi, "Analytical investigation on acceleration motion of a vertically falling spherical particle in incompressible Newtonian media," *Advanced Powder Technology*, vol. 21, no. 3, pp. 298–304, 2010.

[14] M. Jalaal and D. D. Ganji, "On unsteady rolling motion of spheres in inclined tubes filled with incompressible Newtonian fluids," *Advanced Powder Technology*, vol. 22, no. 1, pp. 58–67, 2011.

[15] S. K. Nguang, P. Shi, and S. Ding, "Fault detection for uncertain fuzzy systems: an LMI approach," *IEEE Transactions on Fuzzy Systems*, vol. 15, no. 6, pp. 1251–1262, 2007.

[16] L. Wu, X. Su, P. Shi, and J. Qiu, "A new approach to stability analysis and stabilization of discrete-time T-S fuzzy time-varying delay systems," *IEEE Transactions on Systems, Man, and Cybernetics, Part B*, vol. 41, no. 1, pp. 273–286, 2011.

[17] M. A. Z. Raja, I. M. Qureshi, and J. A. Khan, "Swarm intelligence optimized neural networks for solving fractional differential equations," *International Journal of Innovative Computing, Information and Control*, vol. 7, no. 11, pp. 6301–6318, 2011.

[18] L. Wu, X. Su, P. Shi, and J. Qiu, "Model approximation for discrete-time state-delay systems in the TS fuzzy framework," *IEEE Transactions on Fuzzy Systems*, vol. 19, no. 2, pp. 366–378, 2011.

[19] J. Zhang, P. Shi, and Y. Xia, "Robust adaptive sliding-mode control for fuzzy systems with mismatched uncertainties," *IEEE Transactions on Fuzzy Systems*, vol. 18, no. 4, pp. 700–711, 2010.

[20] Q. Zhou, P. Shi, J. Lu, and S. Xu, "Adaptive output feedback fuzzy tracking control for a class of nonlinear systems," *IEEE Trans on Fuzzy Systems*, vol. 19, no. 5, pp. 972–982, 2011.

[21] S. Goto, T. Yamauchi, S. Katafuchi et al., "Coal type selection for power plants through fuzzy inference using coal and fly ash property," *International Journal of Innovative Computing, Information and Control*, vol. 7, no. 1, pp. 29–38, 2011.

[22] Y. Sato, T. Miki, and K. Honda, "A multi-core processor based real-time multi-modal emotion extraction system employing fuzzy inference," *International Journal of Innovative Computing, Information and Control*, vol. 7, no. 8, pp. 4603–4620, 2011.

[23] C. Y. Chang, C. H. Hsu, W. J. Wang et al., "Operation characteristic control of direct methanol fuel cell liquid feed fuel system using adaptive Neuro-Fuzzy inference system model," *International Journal of Innovative Computing, Information and Control*, vol. 8, no. 6, pp. 4177–4187, 2012.

[24] A. N. Ahmed, A. E. Shae, O. A. Karim, and A. E. Shae, "An augmented wavelet De-Noising technique with Neuro-Fuzzy inference system for water quality prediction," *International Journal of Innovative Computing, Information and Control*, vol. 8, no. 10 B, pp. 7055–7082, 2012.

[25] H. Li, J. Wang, and Z. Miao, "Modelling on fuzzy control systems," *Science in China. Series A*, vol. 45, no. 12, pp. 1506–1517, 2002.

[26] H. Li, J. Wang, and Z. Miao, "Marginal linearization method in modeling on fuzzy control systems," *Progress in Natural Science*, vol. 13, no. 7, pp. 489–496, 2003.

[27] H. X. Li, W. Y. Song, X. H. Yuan, and Y. C. Li, "Time-varying system modeling method based on fuzzy inference," *Journal of Systems Science and Mathematical Sciences*, vol. 29, no. 8, pp. 1109–1128, 2009.

[28] D.-G. Wang, W.-Y. Song, and H.-X. Li, "Analysis and design of time-variant fuzzy systems based on dynamic fuzzy inference," *Computers & Mathematics with Applications*, vol. 60, no. 3, pp. 464–489, 2010.

Hindawi Publishing Corporation
Mathematical Problems in Engineering
Volume 2012, Article ID 803912, 16 pages
doi:10.1155/2012/803912

Research Article

Fuzzy Control and Connected Region Marking Algorithm-Based SEM Nanomanipulation

Dongjie Li,[1,2] Weibin Rong,[1] Lining Sun,[1] Bo You,[2] Yu Zou,[1] and Wanzhe Xiao[1]

[1] *State Key Laboratory of Robotics and System, Harbin Institute of Technology, Harbin 150001, China*
[2] *School of Automation, Harbin University of Science and Technology, Harbin 150080, China*

Correspondence should be addressed to Weibin Rong, wbr1212@126.com

Received 14 September 2012; Accepted 18 October 2012

Academic Editor: Peng Shi

Copyright © 2012 Dongjie Li et al. This is an open access article distributed under the Creative Commons Attribution License, which permits unrestricted use, distribution, and reproduction in any medium, provided the original work is properly cited.

The interactive nanomanipulation platform is established based on fuzzy control and connected region marking (CRM) algorithm in SEM. The 3D virtual nanomanipulation model is developed to make up the insufficiency of the 2D SEM image information, which provides the operator with depth and real-time visual feedback information to guide the manipulation. The haptic device Omega3 is used as the master to control the 3D motion of the nanopositioner in master-slave mode and offer the force sensing to the operator controlled with fuzzy control algorithm. Aiming at sensing of force feedback during the nanomanipulation, the collision detection method of the virtual nanomanipulation model and the force rending model are studied to realize the force feedback of nanomanipulation. The CRM algorithm is introduced to process the SEM image which provides effective position data of the objects for updating the virtual environment (VE), and relevant issues such as calibration and update rate of VE are also discussed. Finally, the performance of the platform is validated by the ZnO nanowire manipulation experiments.

1. Introduction

As an assistant imaging tool to research nanomaterial characteristics and the visual detection device for nanomanipulation, SEM has been paid more and more attention for its real time imaging and large operation space [1, 2]. Compared with AFM, SEM is used as a tool for providing the operator with real-time visual feedback during the nanoscale manipulation although it only provides the 2D images of single view angle [3], which contains limited environment information. For example, Sitti [4] has established the SEM-based robotics systems for Microscale and nanoscale with AFM as the handle tool; Fatikow et al. [3, 5] has realized the automatic nanohandling inside SEM using the advantage of vision feedback;

Penga et al. [6] did a lot of experiments to study the probe in the SEM. In the existing SEM-based nanomanipulation system, the operator could not judge the position relationship among probe, objects, and substrate accurately only according SEM image, which would easily damage the devices and objects [7, 8] as does in open loop during manipulation. Due to the unstructured character of nanoenvironment and scale effect of nanomanipulation, micro force sensor is a possible solution compared with position sensor. On the other hand, force sensors for micro/nanomanipulation, especially for nanoscale, are difficult to manufacture and expensive, which is only suitable for force/haptic information in contact status [9]. Therefore, it is particularly important to introduce the virtual reality technology for the unstructured nanoenvironment [10]. It can guide and control the real nanomanipulation platform working in the master-slave mode with virtual nanomanipulation model and virtual force feedback information. It is a novel approach to realize the nanomanipulation with real time, accuracy, high efficiency and friendly human-machine interaction.

This work is motivated for manipulating the nanocomponent in SEM with telepresence as in macro scale. By adopting the virtual reality and haptic technology, the operator can handle the nanowire in SEM by controlling the virtual force. At the same time, although the SEM can only offer 2D image, the operator can feel the force and 3D visual information offered by virtual reality technology. The main motivation of this work is to establish a SEM-based master-slave telenanomanipulation platform having the performance of security, reliable, and real-time without force sensor.

With the aid of force feedback device (Omega 3), the nanocomponent manipulation method combined with virtual reality and SEM is studied. It can provide users with senses of force and more intuitional operation interface, as well as changeable view point and angle in virtual environment (VE) to provide more sufficient visual information of nanomanipulation in previewing and real time tracking. While updating the VE, the CRM algorithm is introduced to process the SEM image.

The slave (Attocube) needs relatively stable control variable to avoid damage of the probe, nanowire, and substrate, which is controlled by the master (controlled by the operator). But the operator's input is so unstable that it is difficult to control and accurately formalize mathematically. Fuzzy logic has become a particularly widely used methodological approach on real world applications control. Fuzzy logic-based systems do not require models, which make them especially appropriate for processes whose mathematical formalism is not clear or global for all the cases [11, 12]. The systems with fuzzy characters are studied extensively [13–16]. The fuzzy control theory and its improved theoretics have been used in many practical applications [17], such as in noisy image segmentation [18], languages character recognition [19], and prioritizing service attributes [20]. Based on this, in the literatures, the fuzzy control is adopted in the master-slave control.

The organization of the paper is as follows. Section 2 describes the designed system framework in detail, including control information and data exchanging procedure, the fuzzy control for the system. The creation method of grid model in VE as well as dynamic modeling of probe and nanowire using skeleton sphere is discussed in Section 3. Section 4 demonstrates the collision detection method using Hierarchical Bounding Volumes (BVH). Force rendering model is built to embed force information to the VE in Section 5. The region marking algorithm (CRM) used to process SEM image is introduced in Section 6, and the procedure of VE update is also illustrated in this section. In Section 7, the performance of the platform is validated on experimental results via nanowire manipulation experiments, and the results are also analysed. Section 8 is the conclusions and the novelties of our platform.

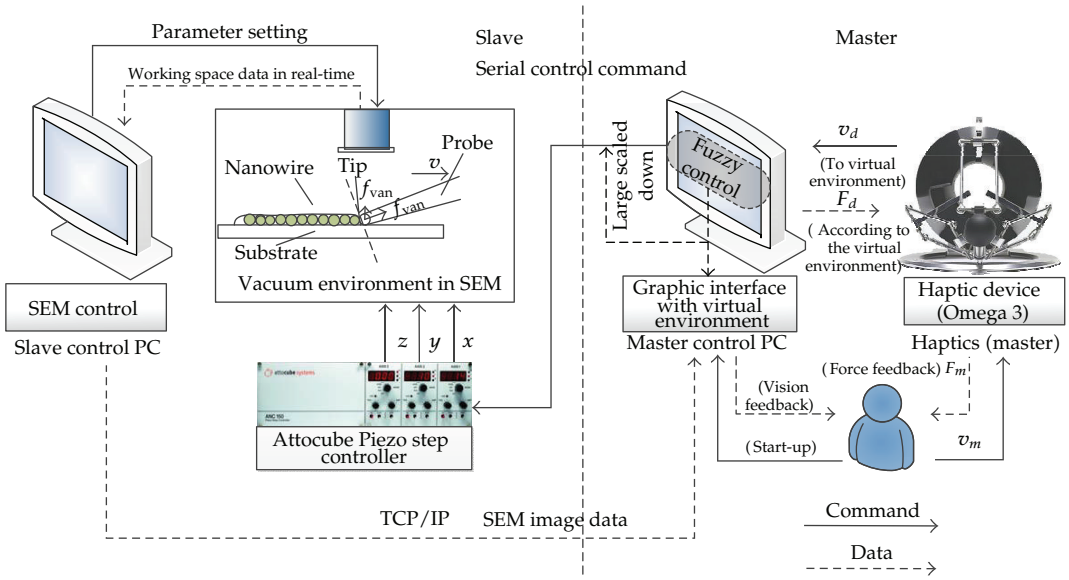

Figure 1: Structure of master-slave nanomanipulation platform.

2. System Construction

The overall structure of the master-slave nanomanipulation platform is displayed in Figure 1. The platform is mainly composed of the following components: tungsten probe, nanopositioner (Attocube), SEM vacuum manipulation environment, master haptic device (Omega 3), and the master/slave control PC. The tungsten probe is installed on the nanopositioner, working in SEM vacuum environment as the slave. The slave PC controls the imaging of SEM and communicates with the master control PC for real time image transmission via the TCP/IP. The master control PC interacts with the operator, running a 3D virtual nanomanipulation environment and the main control interface with transmitted SEM image integrated. The 3-DOF haptic device communicates with the master PC through USB. The three axes of the Attocube nanopositioner are controlled with its dedicated controller (ANC150) in remote way by the master control PC according to the information acquired from Omega 3. The nanomanipulation platform presented in this paper could accomplish multi-DOF nanomanipulation for various kinds of nanocomponents with the help of SEM real-time visual feedback.

As the master, the haptic device Omega 3 has energy output to outside. If the haptic interface composed of Omega 3 is unstable, damage will be caused to the manipulation object and the manipulation tool. Meanwhile, the transparency of manipulation process will be destroyed. For the adjustment process from the control of the operator to the suitable control variable needs time and the model of the operator is hard to establish, the robustness of the fuzzy control is considered. Therefore, fuzzy control unit is added to control the haptic interaction system, which is composed of operator, haptic interface, and the virtual environment. Energy conversion between the operator and the virtual environment is completed by the haptic interface.

The input of the fuzzy controller is the deviation e and deviation change rate ec of the output force of the operator (that is the displacement of the Omega 3). The output

is the controlled variables transmitted to virtual environment, which are transmitted to Attocube Piezo Step Controller after large scaled down. In the manipulation process, the detection of e and ec is done continuously and the parameters modification online are conducted according to the fuzzy control principle, in order to meet the requirements of the control parameters and to improve the output characteristics of virtual manipulation.

According to the characteristics of Omega 3 and the haptic control manipulation, the action range of the fuzzy controller is selected objectively. The range of the error e and error change rate ec is defined to be the universe of the fuzzy sets:

$$e, ec = \{-3, -2, -1, 0, 1, 2, 3\}. \tag{2.1}$$

Its fuzzy subset is

$$e, ec = \{\mathrm{NB}, \mathrm{NM}, \mathrm{NS}, \mathrm{Z}, \mathrm{PS}, \mathrm{PM}, \mathrm{PB}\}. \tag{2.2}$$

Assuming that they all obey normal distribution, the quantization factor of e and ec is 1.

The weighted average method with smoothing output inference rules is adopted. The crisp value of the weighted average of the output of the membership degree is picked up. The final output value of the fuzzy inference is determined. That is, the areas bounded by the fuzzy membership function cure and the horizontal ordinate are the final output value.

3. Establishment of Virtual Nanomanipulation Model

Virtual nanomanipulation is an effective way to provide the 3D visual information and simulation for real nanomanipulation, which is helpful for the operator to judge in real time, enhance their perception, and proceed off-line simulation [21–23]. The credibility of simulation interface depends on the virtual operating model. In this sense, the more realistic of the operated object model, the more actual operation scene will be reflected in the simulation interface of virtual vision. Meanwhile, the precision of operating model reduces corresponding with the increasing of modelling error in the nanoVE.

As a software interface of graphics hardware, OpenGL can satisfy modelling demands with advantages of fast getting state, good characteristics of base development, and dynamic display. Besides, it is convenient to apply in other engines with its independent hardware interface and variety library functions. Therefore, OpenGL is adopted as the base development tool to establish the basic model of nanowire in this paper. Aiming at establishing the virtual nanowire model, vertices are drawn as grid elements and formed mesh model using OpenGL functions. Although the mesh model can be edited to realize geometrical deformation, it is important to know which grid element needs to be deformed. Because of the large calculated amount of analysing each grid element, a kind of simple assistant model is needed, whose characteristics are analysed to determine the rules of deformation.

In this paper, skeleton model is adopted as the simple assistant model to research the deformation of the virtual nanowire model. Skeleton models are widely used in creating dynamic model as the role of bone in animals and plants, and the skeleton in 3D model is used to judge the motion property. A certain amount of skeleton models would be filled in the mesh model (virtual nanowire model) built with OpenGL. According to the dynamic

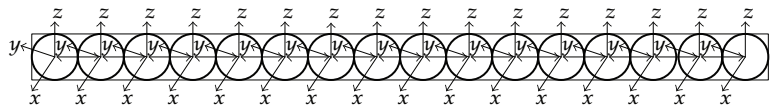

Figure 2: Perspective map of nanowire filled with skeleton spheres.

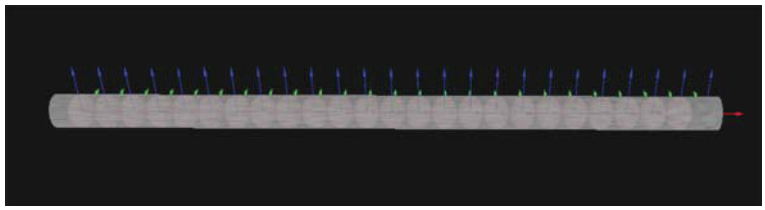

Figure 3: Modeled nanowire filled with skeleton spheres in virtual environment (VE).

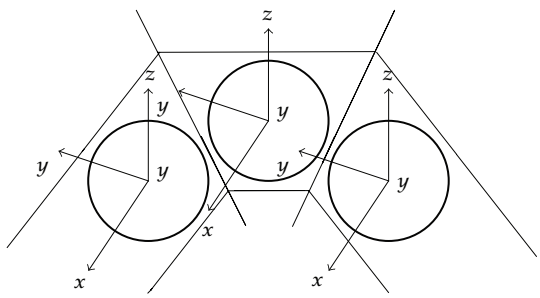

Figure 4: Deformation of skeleton spheres.

characteristic of the nanowire, skeleton spheres are suitable to fill the nanowire model. The skeleton sphere is characteristic sphere. By judging the position of every skeleton sphere in VE, the vertices is reedited to realize the dynamic deformation of the virtual objects, namely, that the mesh model (virtual nanowire model) would change its shape as the skeleton spheres. Simple perspective map of nanowire model filled with skeleton spheres is shown in Figure 2. Sketch map of modeled nanowire filled with skeleton spheres in VE is shown as Figure 3.

Figure 4 is the deformation schematic diagram of skeleton spheres in VE. It is shown that the relative coordinates of polygon grid elements also change as the coordinates of skeleton spheres change. Deformation model of skeleton spheres in VE is shown in Figure 5. In order to see the movement relationship between skeleton spheres and nanowire more clearly, the updating speed of movement is reduced; thus, the effect of nanowire motion driven by skeleton spheres is more obvious.

4. Collision Detection

In order to perceive the immersive of presence and complete interactive force in the VE, fast and accurate collision detection between different models is necessary [7]. Collision detection is to detect whether different objects in the VE have bumped into each other. In fact,

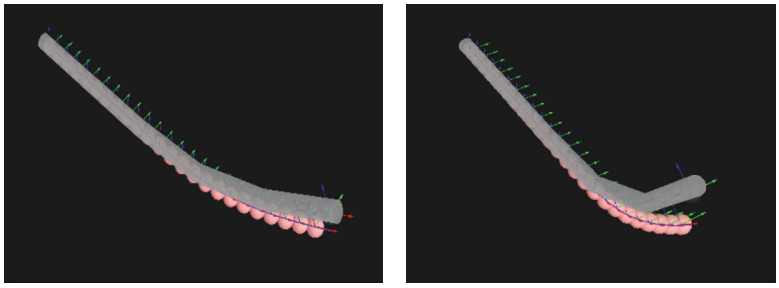

Figure 5: Motion of nanowire driven by skeleton spheres in VE.

two impenetrable objects cannot simultaneously occupy the same space in the real world; however, they can occupy the same space in the virtual world. In order to avoid regional mixed taken by the objects cross in the virtual world and offer the sense of reality, collision detection is needed [24]. Besides, the data of virtual force presence mainly comes from the collision detection among different objects. When designing a collision detection system, the design factors, namely, all aspects of developing collision detection modules, should be firstly considered in collision detection algorithm. There are many collision detection problems worthy of further research. In this paper, the structures of objects to be manipulated are relatively simple, so we only analyze the collision detection suitable for this platform. In other words, the algorithm we studied is suitable for the collision detection between single cone probe, columnar nanowire/nanotube and the substrate with smooth surface, and good rigidity. It can be used in the force presence of nanowire/nanotube manipulation handled with single probe based on adhesive control.

Among the collision detection algorithms, we usually do not adopt the "full-featured" collision detection method, while selecting the specific collision detection method is an advisable choice [25]. For the simple nanowire model in this system, BVH method is more suitable. But it is different from the collision detection algorithm of static models, the collision detection between probe and nanowire is normally dynamic and more complex. Thus, the difficulty of collision detection is greatly increased. Hence, the collision detection of nanomanipulation is divided into three parts: between probe and substrate, nanowire and substrate, and probe and nanowire, then they are integrated.

The mesh model of the probe is built with OpenGL according to the geometric parameters obtained by SEM image. Based on the virtual probe mesh model established, suitable bounding spheres which are as one category of BVH according to pyramid (the probe model) data are filled in the probe mesh model to realize the intersect detection between probe and nanowire. The arrangement method of bounding spheres filled in probe model determines the effect of collision detection between the virtual nanowire model and virtual probe model. Normally, there are three approaches to arrange the bounding spheres in probe mesh model: sphere diameter arrangement (SDA), prestack sphere center arrangement (PESCA), and poststack sphere center arrangement (POSCA) (different arrangement methods are shown as Figure 6). According to the feature of the probe (large cone height) and experimental comparison among the three arrangement method, the PESCA method is adopted since it neither leaves out a lot of empty space in probe mesh model as SDA method dose nor makes complex permutation order and larger calculated quantity as POSCA method dose. Figure 7 shows the collision detection between probe and nanowire by using PESCA method. It can be seen from Figure 7 that the probe is filled

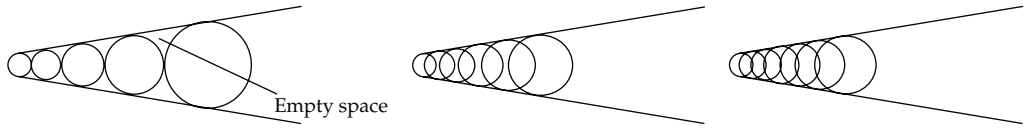

(a) Sphere diameter arrangement (SDA) (b) Prestack sphere center arrangement (PESCA) (c) Poststack sphere centre arrangement (POSCA)

Figure 6: Arrangement methods of pyramid single line balls for probe model.

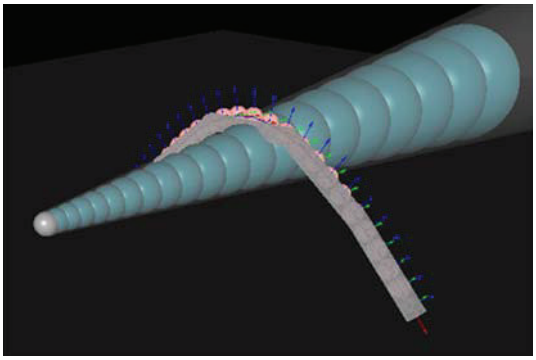

Figure 7: Collision detection between probe and nanowire.

properly, and the collision between the probe model filled with bounding spheres and the nanowire model could be detected, which prevents penetration between models.

5. Force Rendering Model

In the whole nanomanipulation process, embedding of virtual force feedback as a kind of force sensing can greatly enhance the operator's perception [26], which is important and essential for nanomanipulation and nanoassembly [27, 28]. It can allow the operator to carry out simulation of nanomanipulation better and guide real nanomanipulation more effectively.

The force rendering provides an interactive approach through which the operator could find out what kind of effects was produced between the virtual models. In nanoscale manipulation environment, the forces among operating objects, operation tools and the substrate are complicated. For SEM vacuum working space, the Van der Waals force acts as a dominated force among the nanocomponents; therefore, the force rendering is conducted based on Van der Waals force.

5.1. Force between Probe and Substrate

The shape of the probe tip is simplified as two parts [29, 30]: microsphere and microcylinder. According to Hamaker's assumption, the forces between each part and the substrate are calculated, respectively, and then added up to create a resultant force.

The interaction energy between the substrate and the microsphere molecule of the probe tip could be expressed as

$$E_{\text{single}} = -\frac{\pi C \rho_1}{6d^3}, \tag{5.1}$$

where C is Van der Waals constant, ρ_1 is the numerical density of the substrate, and d is the minimum distance between the substrate and the microsphere. And the interaction energy between the substrate and all molecules of the microsphere could be obtained via integral calculation of (5.1):

$$E = -\frac{\pi^2 C \rho_1 \rho_2}{6} \int_0^{H_1} \frac{(2R_1 - z)z}{(d+z)^3} dz, \tag{5.2}$$

where ρ_2 is the numerical density of the microsphere, and H_1 is the height of the microsphere.

The force between the substrate and the microsphere is obtained via differential calculation of (5.2):

$$\begin{aligned} F_1 &= -\frac{\pi^2 C \rho_1 \rho_2}{2} \int_0^{H_1} \frac{(2R_1 - z)z}{(d+z)^4} dz \\ &= -\frac{A_H}{2} \left[\frac{3(H_1 - R_1)(H_1 + d) + d(2R_1 + d)}{3(d + H_1)^3} - \frac{d - R_1}{3d^2} \right], \end{aligned} \tag{5.3}$$

where $A_H = \pi^2 C \rho_1 \rho_2$ is Hamaker constant.

Similarly, the force between the substrate and the microcylinder is calculated as

$$\begin{aligned} F_2 &= -\frac{\pi C \rho_1}{2} \int_0^{H_2} \frac{\pi R_2^2 \rho_2}{(d + H_1 + z)^4} \\ &= \frac{A_H R_2^2}{6} \left[\frac{1}{(d + H_1 + H_2)^3} - \frac{1}{(d + H_1)^3} \right], \end{aligned} \tag{5.4}$$

where H_2 is the height of the microcylinder.

Finally, the force between the substrate and the probe tip could be expressed as

$$F = F_1 + F_2. \tag{5.5}$$

5.2. Force between Nanowire and Substrate

The force between the substrate and the nanowire could be viewed as a kind of interaction force between serial particles and infinite plane, based on which the Van der Waals force

between a single nanowire molecule and the infinite substrate could be expressed as the following equation according to the differential of (5.1):

$$F_{\text{single}} = \frac{\pi \rho C}{2d^4}. \tag{5.6}$$

The force between unit length nanowire and the substrate could be obtained by calculating integration of (5.6):

$$\begin{aligned} F &= \int_d^{2R+d} \frac{\pi \rho_1 \rho_2 \cdot C}{r^4} \sqrt{R^2 - (R + d - r)} dr \\ &= \int_d^{2R+d} \frac{A_H}{r^4} \sqrt{R^2 - (R + d - r)} dr, \end{aligned} \tag{5.7}$$

where d is the minimum distance between the substrate and the microsphere, R is the molecule radius of the nanowire, and ρ_1 and ρ_2 are numerical densities of the nanowire and the substrate, respectively.

5.3. Force between Probe and Nanowire

The force between the probe and the nanowire could be expressed as Van der Waals force between the nanowire and microsphere of the probe tip. There exist two situations to be explained.

When the probe tip contacts with the nanowire vertically or the contacting angle is closed to 90°, the force could be expressed as the interaction between two microspheres, and the Van der Waals energy is

$$E_V = -\frac{A_H}{6d} \frac{R_1 R_2}{R_1 + R_2}, \tag{5.8}$$

where A_H is Hamaker constant, d is the minimum distance between the two microspheres, and R_1 and R_2 are the radius of the two microspheres, respectively. The force between the two microspheres is obtained by calculating differential of (5.8):

$$F_V = \frac{A_H}{6d^2} \frac{R_1 R_2}{R_1 + R_2}. \tag{5.9}$$

When the probe tip contacts with the nanowire horizontally or the contacting angle is closed to 0°, the two objects contact as parallel cylinders, and the Van der Waals energy is expressed as

$$E_H = \frac{A_H L}{12\sqrt{2} d^{3/2}} \sqrt{\frac{R_1 R_2}{R_1 + R_2}}. \tag{5.10}$$

And the calculated force is

$$F_H = -\frac{A_H L}{8\sqrt{2}d^{5/2}}\sqrt{\frac{R_1 R_2}{R_1 + R_2}}, \tag{5.11}$$

where l represents the contact length between probe and nanowire.

The forces among the virtual models are approximately simulated according to the previous expressions when different objects (nanowire, probe, and substrate) interact with one another. And these simulated forces output by CHAI 3D engine are used to strengthen the operator's perception when manipulating the nanocomponents.

6. SEM Image Processing and Virtual Environment Update

It is an essential step to acquire the position information of objects (probe and nanowire) in real nanomanipulation working space for updating the VE. Since no nanoscale sensors are installed in the vacuum space of SEM, the real time SEM image is considered as the only visual servo for the whole system, which is the source of the objects coordinates information. Therefore, it is necessary to research an effective SEM image processing approach to obtain the position data of the objects in the SEM image, which provides information for VE update.

Some researchers have proposed some novel algorithms about 2D positioning under SEM according to a single 2D SEM image [1, 12]. However, most of these have complex processing procedure which inevitably increases the calculation as well as difficulty of realization. In order to provide valid position data for VE updating, a connected region marking (CRM) algorithm for single transmitted SEM image is carried out in this paper to extract the figure of the objects, and then the desired information is obtained. After the SEM image is processed with gray-scale algorithm, dynamic threshold binarization and denoising algorithm in sequence, certain connected regions are marked with tags (such as number 1, 2, and 3). Then, the pixel number of every connected region is calculated. The essential regions of nanowire and probe are extracted respectively after setting the thresholds of pixel number according to the characteristic of nanowire and probe, which are used to calculate the key geometric parameter (position) in image. This method has the advantage of easy to be implemented.

The purpose of updating the VE or adjusting the virtual models is to realize the synchronization of real nanoworking space in slave and VE in master. It needs to calibrate the VE, namely, the relationship between a SEM image and VE should be determined. The detailed calibration process is as follow.

The size of the VE designed in this paper is set as A^3, where $A = 40$ (mm); the range of XYZ coordinates is set to $(-l, +l)$, where $l = 20$ (mm). Suppose one coordinates of the nanowire endpoint is (S, T) obtained from the processed SEM image with resolution of 1024 × 768 using CRM algorithm and define $\alpha = S/1024$, $\beta = T/768$; therefore, the coordinates of the nanowire model in VE corresponding with (S, T) is expressed as $x_v = \alpha \cdot A - l$, $y_v = \beta \cdot A - l$.

In addition, the rate of the VE needs to be discussed during the continuous operation. In this system, whether the VE should be updated depends on the processing results of the SEM image. The rate of SEM image transmission is determined in advance (transmission interval is set as 2 second). The system compares the current position data of objects acquired from the transmitted SEM image with last data acquired 2 second ago and stored in RAM. If the data changes beyond the given error range, the position data of the virtual models would

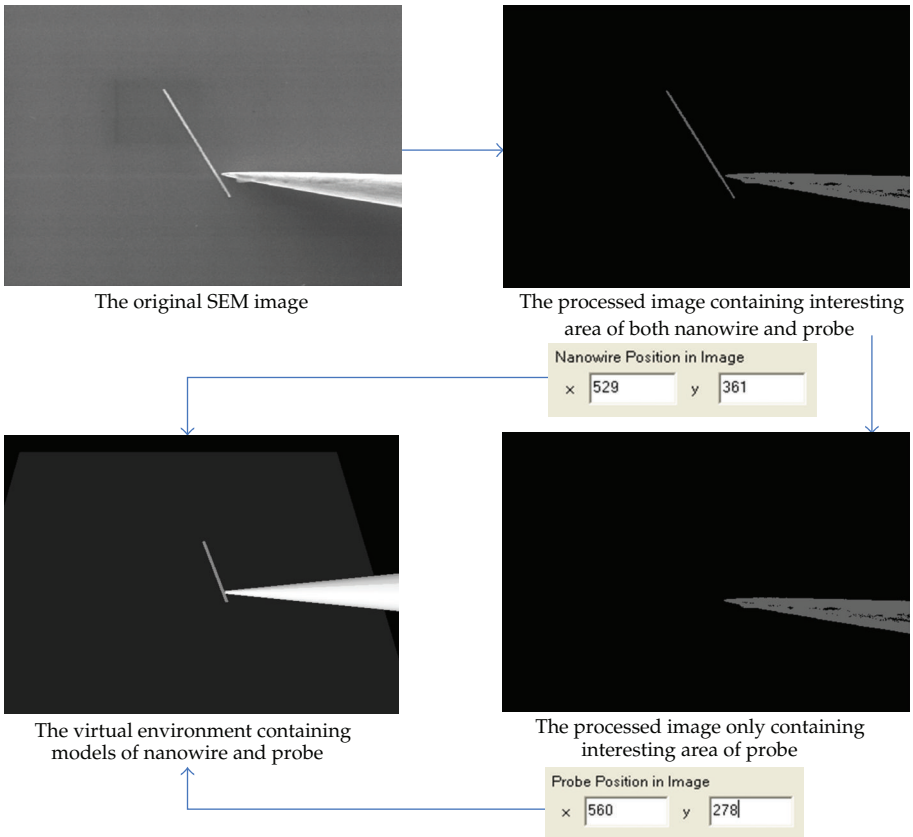

Figure 8: Detail procedure for acquiring position data of nanowire and probe from the SEM image.

be adjusted to the current data, which would be stored in the RAM for next data comparison. However, in the case that the data are same as last or change within the error range, the VE would not be updated, which could save the system resource and increase the efficiency of manipulation.

The SEM image processing procedure using CRM algorithm, as well as the update of VE, is illustrated in Figure 8. It can be seen from Figure 8 that the position of nanowire and probe in VE keeps synchronous with that in the original SEM image.

7. Experiments and Results

The experimental platform is shown in Figure 9, containing the SEM (KYKY-EM3200), Omega 3, Attocube nanopositioner and controller, and master and slave control PC. All the experiments mentioned in this paper have been done in the ten thousand level clean-room of Science Park in HIT.

The control interface of the experimental platform is shown in Figure 10. The 3D graphic interface in the master control PC is programmed with VS 2008 combined with OpenGL and CHAI 3D. The virtual nanomanipulation environment and the real SEM nanomanipulation image sent from the slave PC are displayed in the same interface. There are

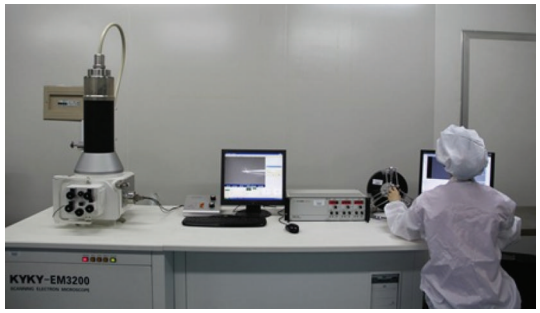

Figure 9: Experimental platform containing necessary devices in the ten thousand level clean-room.

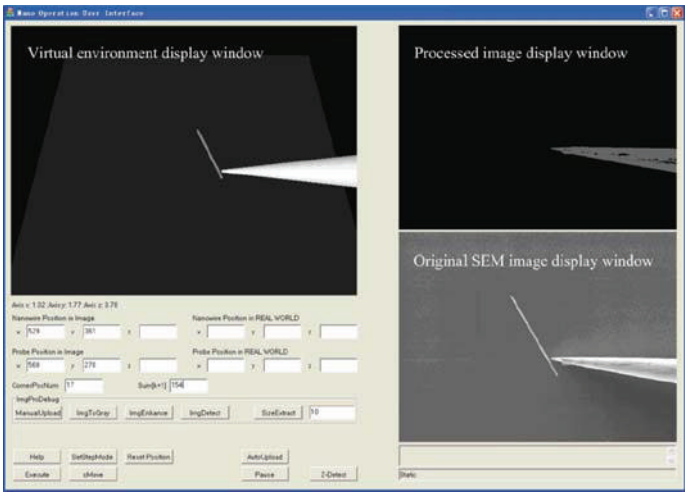

Figure 10: Control interface of the platform.

two different control modes: single-step and real time tracking. In single-step control mode, the virtual models have been controlled to move to a desired position, then the Attocube nanopositioner moves after receiving the execution commands sent by the master PC. Satisfaction test before real manipulation in single-step mode is an approach to improve the operation accuracy, although it has low efficiency. On the other hand, in real time tracking mode, the operator could manipulate Omega 3 to move Attocube nanopositioner continuously with high efficiency compared with single-step mode, but it could cause maloperation.

In the experiments, the operator pushes the bar of the 3-DOF haptic device (Omega 3) at a certain velocity to a position; the force and position information applied on the haptic device captured by the master PC is transmitted to the virtual nanoenvironment; thus, the 3D graphic interface run in the master control PC changes real time to track the movement of master; the slave Attocube positioner moves following the master as soon as receiving the position data of large scaled down. Simultaneously, the operator can feel the force in hand according to the force and position information provided by VE.

The performance of the virtual force feedback master-slave telenanomanipulation platform is tested with the ZnO nanowire (with radius of 100~200 nm) manipulation.

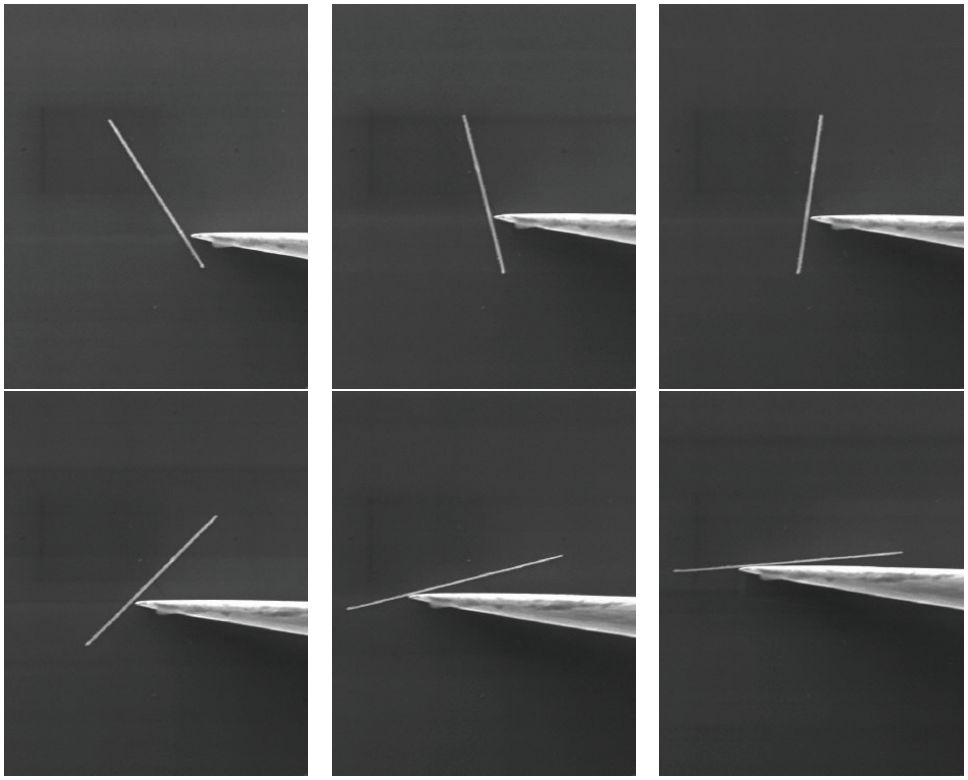

Figure 11: Procedure of ZnO nanowire shift experiment.

The experimental results are shown in Figure 11. The curves of probe position during the experiment without and with fuzzy control are shown as Figure 12.

From the curves, we can find that the trajectory of the probe controlled with fuzzy control is much smoother than that without it, and it is confined to a certain scope of the starting point. That is the redundant path of the probe is avoided, and the stability and safety (avoiding the damage of probe, nanowire, and substrate, which are expensive and need much time while replaced) of the whole manipulation process is guaranteed.

8. Conclusions

In this paper, the nanomanipulation platform with virtual 3D visual and virtual force feedback is established combined with virtual reality technology and SEM. The fuzzy control algorithm is adopted to assure the system stability and safety. The virtual models of probe and nanowire are built to provide 3D visual information of SEM-based nanomanipulation. To obtain the sense of immersion and interactive force for the operator during nanomanipulation, the collision detection model of nanomanipulation and the force rendering models are built. With employing of the VR and haptic technology, the operator can handle the nanowire by controlling virtual force, so the operator's perception to nanomanipulation is enhanced.

The CRM algorithm is proposed to process the transmitted SEM image which is the basis of VE update, and the calibration of the VE. In addition, the updating rate of VE is also

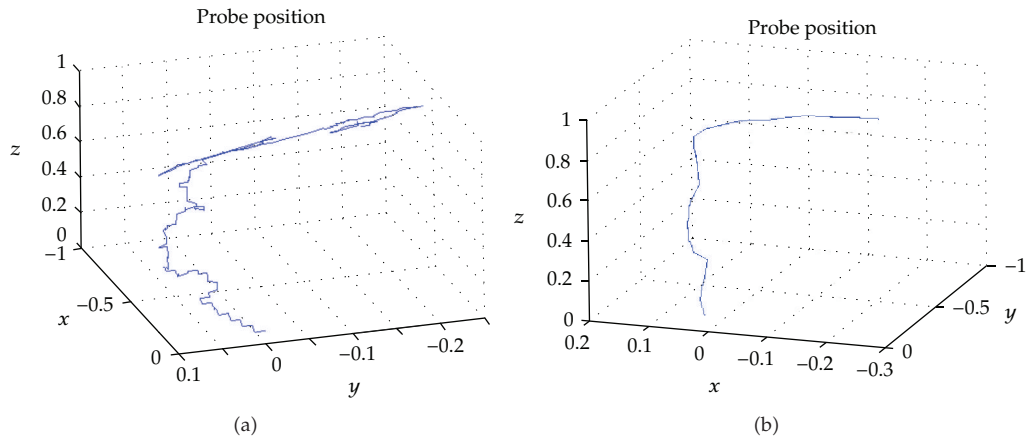

Figure 12: (a) Curves of probe position without fuzzy control; (b) Curves of probe position controlled with fuzzy control.

discussed. The 3D visualized manipulation environment cannot only provide the operator with real time image information, but also make the platform run automatically after the satisfied virtual preview result. It could reduce the research cycles and research cost of nanomanipulation.

System performance is evaluated by the ZnO nanowire manipulation experiments. The experimental studies show that the nanowire can be accurately pushed and manipulated on the substrate using the newly developed platform. The real time visual display coupled with the real time force feedback provides a telepresence environment in which the operator cannot only feel the interaction forces but also observe the real time changes of the nanoenvironment.

Through experiments, we conclude that the platform presented in this paper has the following advantages: (1) the man-machine interactive performance is enhanced with combining of virtual reality environment, SEM feedback image, and haptic device; (2) the nanomanipulation efficiency stability and safety are improved for the simultaneous monitoring and manipulating and the employing of fuzzy control; (3) the real time performance of the nanomanipulation is improved, for the dynamic refresh of VE is realized.

In future, we will do further study on automatic detection for the contact between tip and substrate based on 2D SEM image and automatic nanomanipulation based on virtual nanomanipulation model.

Acknowledgments

This work was supported by the National Natural Science Funds for Distinguished Young Scholar (Grant no. 50725518), National Natural Science Funds for Young Scholar (Grant no. 51105117), Program for New Century Excellent Talents in University (Grant no. NCET-08-0170), Program for Changjiang Scholars and Innovative Research Team in University (Grant no. IRT0915), China Postdoctoral Science Foundation funded project (Grant no. 20100471051), State Key Laboratory of Robotics and System (Grant no. SKLRS-2010-MS19) and Harbin Science & Technology Innovation Talent Study Special Fund Project (Grant no. 2012RFQXG075).

References

[1] B. E. Kratochvil, L. Dong, and B. J. Nelson, "Real-time rigid-body visual tracking in a scanning electron microscope," in *Proceedings of the 7th IEEE International Conference on Nanotechnology (IEEE-NANO '07)*, pp. 442–447, Hong Kong, China, August 2007.

[2] V. Eichhorn, S. Fatikow, T. Wich et al., "Depth-detection methods for microgripper based CNT manipulation in a scanning electron microscope," *Journal of Micro-Nano Mechatronics*, vol. 4, pp. 27–36, 2008.

[3] S. Fatikow, T. Wich, H. Hülsen, T. Sievers, and M. Jähnisch, "Microrobot system for automatic nanohandling inside a scanning electron microscope," *IEEE/ASME Transactions on Mechatronics*, vol. 12, no. 3, pp. 244–252, 2007.

[4] M. Sitti, "Microscale and nanoscale robotics systems," *IEEE Robotics and Automation Magazine*, vol. 14, no. 1, pp. 53–60, 2007.

[5] S. Fatikow, C. Dahmen, T. Wortmann, and R. Tunnell, "Vision feedback for automated nanohandling," in *Proceedings of the IEEE International Conference on Information and Automation (ICIA '09)*, pp. 806–811, Zhuhai, China, June 2009.

[6] L. M. Penga, Q. Chena, X. L. Lianga et al., "Performing probe experiments in the SEM," *Micron*, vol. 35, pp. 495–502, 2004.

[7] S. Lining, T. Fusheng, R. Weibin, Z. Jiang, and K. Minxiu, "Research on the architecture of virtual reality based on micromanipulation robot," in *Modular Machine Tool & Automatic Manufacturing Technique*, vol. 7, pp. 9–14, 2003.

[8] C. D. Onal and M. Sitti, "Teleoperated 3-D force feedback from the nanoscale with an atomic force microscope," *IEEE Transactions on Nanotechnology*, vol. 9, no. 1, pp. 46–54, 2010.

[9] J. Hua, Y. Cui, H. Li, Y. Wang, and N. Xi, "Network-based tele-robotic system with guidance functionality from virtual force," *Robot*, vol. 32, no. 4, pp. 522–528, 2010.

[10] A. Bolopion, C. Stolle, R. Tunnell, S. Haliyo, S. Régnier, and S. Fatikow, "Remote Microscale Teleoperation through Virtual Reality and Haptic Feedback," in *IEEE/RSJ International Conference on Intelligent Robots and Systems*, 2011.

[11] E. Onieva, V. Milanes, J. Perez, and T. de Pedro, "Genetic fuzzy-based steering wheel controller using a mass-produced car," *International Journal of Innovative Computing Information and Control*, vol. 8, no. 5, pp. 3477–3494, 2012.

[12] J. Zhang, P. Shi, and Y. Xia, "Fuzzy delay compensation control for t-s fuzzy systems over network," *IEEE Trans on Systems, Man and Cybernetics B*, no. 99, pp. 1–10, 2012.

[13] J. Zhang, P. Shi, and Y. Xia, "Robust adaptive sliding-mode control for fuzzy systems with mismatched uncertainties," *IEEE Transactions on Fuzzy Systems*, vol. 18, no. 4, pp. 700–711, 2010.

[14] S. K. Nguang, P. Shi, and S. Ding, "Fault detection for uncertain fuzzy systems: an LMI approach," *IEEE Transactions on Fuzzy Systems*, vol. 15, no. 6, pp. 1251–1262, 2007.

[15] L. Wu, X. Su, P. Shi, and J. Qiu, "Model approximation for discrete-time state-delay systems in the TS fuzzy framework," *IEEE Transactions on Fuzzy Systems*, vol. 19, no. 2, pp. 366–378, 2011.

[16] L. Wu, X. Su, P. Shi, and J. Qiu, "A new approach to stability analysis and stabilization of discrete-time T-S fuzzy time-varying delay systems," *IEEE Transactions on Systems, Man, and Cybernetics B*, vol. 41, no. 1, pp. 273–286, 2011.

[17] Q. Zhou, P. Shi, J. Lu, and S. Xu, "Adaptive output feedback fuzzy tracking control for a class of nonlinear systems," *IEEE Transactions on Fuzzy Systems*, vol. 19, no. 5, pp. 972–982, 2011.

[18] J. Yu, S. H. Lee, and M. Jeon, "An adaptive ACO-based fuzzy clustering algorithm for noisy image segmentation," *International Journal of Innovative Computing Information and Control*, vol. 8, no. 6, pp. 3907–3918, 2012.

[19] M. I. Razzak, S. A. Husain, A. A. Mirza, and A. Belaid, "Fuzzy based preprocessing using fusion of online and offline trait for online urdu script based languages character recognition," *International Journal of Innovative Computing Information and Control*, vol. 8, no. 5, pp. 3149–3161, 2012.

[20] H. C. Chang, G. S. Liang, C. W. Chu, and C. H. Chou, "Prioritizing service attributes for improvement using fuzzy zone of tolerance," *International Journal of Innovative Computing Information and Control A*, vol. 8, no. 1, pp. 75–89, 2012.

[21] W. Vogl, B. K. L. Ma, and M. Sitti, "Augmented reality user interface for an atomic force microscope-based nanorobotic system," *IEEE Transactions on Nanotechnology*, vol. 5, no. 4, pp. 397–406, 2006.

[22] D. Jasper, "High-speed position tracking for nanohandling inside scanning electron microscopes," in *Proceedings of the IEEE International Conference on Robotics and Automation (ICRA '09)*, pp. 508–513, Kobe, Japan, May 2009.

[23] D. Jasper and S. Fatikow, "Automated high-speed nanopositioning inside scanning electron microscopes," in *Proceedings of the IEEE International Conference on Automation Science and Engineering (CASE '10)*, pp. 704–709, Toronto, Canada, August 2010.

[24] S. M. Mousavi, M. A. Mohagheghi, A. Mousavi-Jerrahi, A. Nahvijou, and Z. Seddighi, "Outcome of breast cancer in Iran: a study of Tehran Cancer Registry data," *Asian Pacific Journal of Cancer Prevention*, vol. 9, no. 2, pp. 275–278, 2008.

[25] S. Redon, Y. J. Kim, M. C. Lin, D. Manocha, and J. Templeman, "Interactive and continuous collision detection for avatars in virtual environments," in *Proceedings of the IEEE Virtual Reality (VR '04)*, pp. 117–283, March 2004.

[26] M. A. Greminger and B. J. Nelson, "Vision-Based Force Measurement," *IEEE Transactions on Pattern Analysis and Machine Intelligence*, vol. 26, no. 3, pp. 290–298, 2004.

[27] B. Spanlang, J. M. Normand, E. Giannopoulos, and M. Slater, "GPU based detection and mapping of collisions for haptic rendering in immersive virtual reality," in *Proceedings of the 9th IEEE International Symposium on Haptic Audio-Visual Environments and Games (HAVE '10)*, pp. 41–44, Phoenix, Ariz, USA, October 2010.

[28] A. Lécuyer, M. Vidal, O. Joly, C. Mégard, and A. Berthoz, "Can haptic feedback improve the perception of self-motion in virtual reality?" in *Proceedings of the 12th International Symposium on Haptic Interfaces for Virtual Environment and Teleoperator Systems (HAPTICS '04)*, pp. 208–215, March 2004.

[29] S. H. Ahn, B. H. Son, S. W. Kim, S. Kim, J. Jeong et al., "Poor outcome of hormone receptor-positive breast cancer at very young age is due to tamoxifen resistance: Nationwide survival data in Korea—a report from the Korean Breast Cancer Society," *Journal of Clinical Oncology*, vol. 25, no. 17, pp. 2360–2368, 2007.

[30] L. F. Wang, *Research of the adhesive contact of microparts and micromanipulation methods substrated adhesion forces [Ph.D. thesis]*, Harbin Institute of Technology, 2008.

Hindawi Publishing Corporation
Mathematical Problems in Engineering
Volume 2012, Article ID 893807, 12 pages
doi:10.1155/2012/893807

Research Article

A Novel Identification Method for Generalized T-S Fuzzy Systems

Ling Huang,[1] Kai Wang,[1] Peng Shi,[1,2,3] and Hamid Reza Karimi[4]

[1] *School of Automation, Harbin University of Science and Technology, Harbin 150080, China*
[2] *Department of Computing and Mathematical Sciences, University of Glamorgan, Pontypridd CF37 1DL, UK*
[3] *School of Engineering and Science, Victoria University, Melbourne, VIC 8001, Australia*
[4] *Department of Engineering, Faculty of Engineering and Science, University of Agder, 4898 Grimstad, Norway*

Correspondence should be addressed to Ling Huang, mail_huangling@163.com

Received 1 August 2012; Accepted 17 October 2012

Academic Editor: Mohammed Chadli

Copyright © 2012 Ling Huang et al. This is an open access article distributed under the Creative Commons Attribution License, which permits unrestricted use, distribution, and reproduction in any medium, provided the original work is properly cited.

In order to approximate any nonlinear system, not just affine nonlinear systems, generalized T-S fuzzy systems, where the control variables and the state variables, are all premise variables are introduced in the paper. Firstly, fuzzy spaces and rules were determined by using ant colony algorithm. Secondly, the state-space model parameters are identified by using genetic algorithm. The simulation results show the effectiveness of the proposed algorithm.

1. Introduction

Since the presentation of Takagi-Sugeno (T-S) fuzzy model by Takagi and Sugeno in 1985, great effort has been devoted to fuzzy modeling, analysis, and design, see for example, [1–10] and the references therein. A multilayer incinerator was modeled by a T-S fuzzy model, and it was shown that the model has better accuracy compared to statistical methods in [11]. A process control rig with three subsystems, a heating element, a heat exchanger, and a compartment tank, was modeled by a T-S fuzzy model in [12], and it was shown that the proposed approach provides better modeling when compared with a linear modeling approach.

In identification of fuzzy models, an interdependent procedure for the structure determination and parameter identification is often concerned, that is, determination of the premise and consequence variables and identification of the premise and consequence parameters [13]. Structure identification of the fuzzy model is concerned with the determination of the number of rules and parameter estimation. Clustering algorithms were

widely used in the literature. The work in [14] introduced a fuzzy C-means criterion to ant clustering algorithm and analyze the partitions performance obtained from the ant-based algorithm with those from randomly initialized Hard C-means. The work in [15] focused on a global optimization strategy for the optimal clustering in compromise sum-difference linear arrays based on ant algorithm. Gath-Geva clustering algorithm [16] and subtractive clustering algorithm [17] have been applied in structure identification and premise parameter estimation.

The T-S fuzzy model is composed of linear models, and each model is according to a group of input-output data, divided by the clustering algorithm. The recursive least squares estimation can be easily used for constructing a linear system as a means for tuning the T-S fuzzy model [18, 19]. Amine et al. [20] also used T-S fuzzy model with fuzzy clustering technique to determine both the antecedent and consequent parameters of the fuzzy T-S rules. Then, recursive weighted least squares algorithm with forgetting factor is used to adapt consequent parameters. They applied the methods to model the air temperature and humidity inside the greenhouse. The other researcher, Chang-Ho et al. [21], proposed T-S fuzzy model to design adaptive fuzzy observer and controller and the proposed method is applied to the stabilization problem of a flexible joint manipulator in order to guarantee its performance.

In [22], Petridis et al. introduced a hybrid neural-genetic multimodel parameter estimation algorithm and applied it to structured system identification of nonlinear dynamical systems, and the work in [23] presented Genetic-Algorithm-Based Parameter Estimation Technique for Fragmenting Radar Meteor Head Echoes. The work in [24–27] brought an optimization methodology by using a genetic algorithm to obtain the parameters of a soil that can be represented in a multilayer structure. The method uses a curve of experimental apparent resistivity obtained from measurements made in the soil.

It is shown that a general nonlinear system can be approximated by a T-S fuzzy model to any degree of accuracy on any compact set [28]. However, it has been argued in [29] that the commonly used linear or affine T-S fuzzy models, where the control variables are not included in the premise variables, are only able to approximate affine nonlinear systems to any degree of accuracy on any compact. So the paper investigated the approximation of generalized T-S fuzzy systems, where the control variables and the state variables are all premise variables. This paper proposes application of K-Means ant-clustering algorithm to optimize the fuzzy membership function in the antecedent part. Genetic algorithm (GA) is then used in the consequent part to obtain the plant parameters and depends on the values of the membership functions in antecedent part.

The rest of this paper is structured as follows. Section 2 is devoted to the generalized T-S fuzzy model; the model description and the design principle of the idea are included. In Section 3, the algorithm for the best partition of given data and parameter estimation by using genetic algorithm are presented. Simulation results are provided in Section 4 to demonstrate the effectiveness of the proposed algorithm. Conclusion is given in Section 5.

2. Generalized T-S Fuzzy Model

Takagi-Sugeno (T-S) models are based on fuzzy rule base structures of IF…THEN rules for reasoning in which antecedents are fuzzy sets and consequents are linear functions in each rule. In this way a T-S fuzzy model can approximate a complex affine nonlinear system, general nonlinear systems exist widely in practice can be approximated by generalized T-S fuzzy model.

2.1. Model Description

The generalized T-S fuzzy model considered in this paper is as follows.

Rule i: if $z_1(t)$ is M_{i1} and $\ldots z_n(t)$ is M_{in}; $u_1(t)$ is V_{i1} and $\ldots u_m(t)$ is V_{im}, then

$$\dot{x}(t) = A_i x(t) + B_i u(t), \tag{2.1}$$

where $i = 1, 2, \ldots, r$ is the number of IF-THEN rules, $M_{i1}, M_{i2}, \ldots, M_{in}, V_{i1}, V_{i2}, \ldots, V_{im}$ are the fuzzy sets, and $Z(t) = [z_1(t), \ldots, z_n(t)]^T$ is the premise variable; $x_j (j = 1, 2, \ldots r)$ is the system input, and $x(t) \in R^n$, $u(t) \in R^m$ are the state vector and controlled input vector, respectively; $A_i \in R^{n\times n}$, $B_i \in R^{n\times m}$ are the system matrix and input matrix of the i system, respectively.

Using the parallel distributed compensation strategy, the overall fuzzy system of the model is inferred as

$$\dot{x}(t) = \sum_{i=1}^{r} h_i(z(t)) h_i(u(t)) [A_i x(t) + B_i u(t)], \tag{2.2}$$

where

$$h_i(z(t)) = \frac{w_i(z(t))}{\sum_{i=1}^{r} w_i(z(t))}, \quad h_i(z(t)) \geq 0, \qquad h_i(u(t)) = \frac{w_i(u(t))}{\sum_{i=1}^{r} w_i(u(t))}, \quad h_i(u(t)) \geq 0, \tag{2.3}$$

with

$$\begin{aligned} &\sum_{i=1}^{r} h_i(z(t)) = 1, \quad w_i(z(t)) = \prod_{j=1}^{n} M_{ij}(z_j(t)), \quad i = 1, 2, \ldots, r \\ &\sum_{i=1}^{r} h_i(u(t)) = 1, \quad w_i(u(t)) = \prod_{j=1}^{m} V_{ij}(u_j(t)), \quad i = 1, 2, \ldots, r \end{aligned} \tag{2.4}$$

and $M_{ij}(z_j(t))$ is the grade of membership of $z_j(t)$ in the fuzzy set M_{ij}; $V_{ij}(u_j(t))$ is the grade of membership of $u_j(t)$ in the fuzzy set V_{ij}.

2.2. Design Principle of Model Identification

The framework of fuzzy system models can be shown in Figure 1. During identification, fuzzy functions are fixed. The approach first clusters the given data into several overlapping fuzzy clusters, each of which is used to define a separate decision rule. During structure identification, the original input variables are used to estimate the local relations of the input-output data.

Ant-clustering model based on K-Means algorithm is used to search for the best partition of given data; genetic algorithm (GA) is used to estimate state-space model parameters. GA has been proved to be a robust approach on estimating the parameters on the time series and nonlinear functions simultaneously.

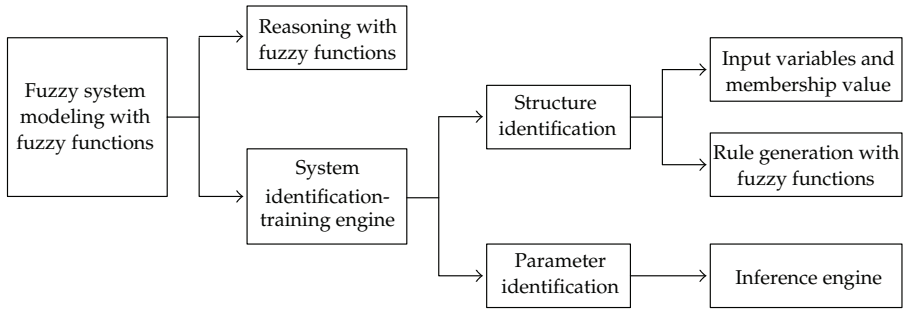

Figure 1: The framework of fuzzy system models.

3. Algorithm Implementation

3.1. The Algorithm for the Best Partition of Given Data

The single ant's action is very simple, but the group's action through the cooperation is very complex; coordinating among a group of ants it is very easy to find the shortest path from the ant nest to food source. The ants between the individual conduct information by pheromone which is a substance left by an ant when it transfers through the way. The ant clustering algorithm exactly utilizes swarm intelligence to solve combinatorial optimization problem, which has smart search, global optimization, robustness, positive feedback, distribute computing, and so forth. The ant clustering algorithm provided the powerful tool for solving complex optimization problem for many fields, which has a good effect on the traveling salesman problem (TSP), the resources, quadratic assignment problem (QAP), and telecom routing controlling such classical optimization. In addition, the classification ant eggs behavior also inspired the corresponding clustering algorithm. The core of ant clustering algorithm is first, selection mechanism: the more pheromone of the path, the greater probability selected; second, pheromones update mechanism: the shorter path, the faster the increase; third, cooperation mechanism: In communication between individual through pheromones.

Before introducing the algorithm, some definitions are given. Suppose an ant is put in the ith data of the nth state, and the data is assigned to the jth cluster centroid $z_j, j = 1, 2, \ldots, k$, the pheromone τ_{ij} is leaved when the ant goes from data i to cluster centroid j, then the ant i chooses the centroid z_j in accordance with the probability

$$p_{ij} = \frac{\tau_{ij}}{\sum_{j=1}^{n} \tau_{ij}}. \tag{3.1}$$

And the pheromone is updated based on the following equation:

$$\tau_{ij}(t+1) = \rho\tau_{ij}(t) + \frac{Q}{d_{ij}}, \tag{3.2}$$

where d_{ij} is the distance from the data i to the centroid z_j; ρ is the permanence coefficient of the pheromone, usually taken about 0.5–0.9; Q is a positive constant, which is represented as the amount of pheromone from an ant.

The algorithm flow chart is shown in Figure 2. Firstly, we sample input data of the original system, confirm the number of clusters k for every state, and then initialize

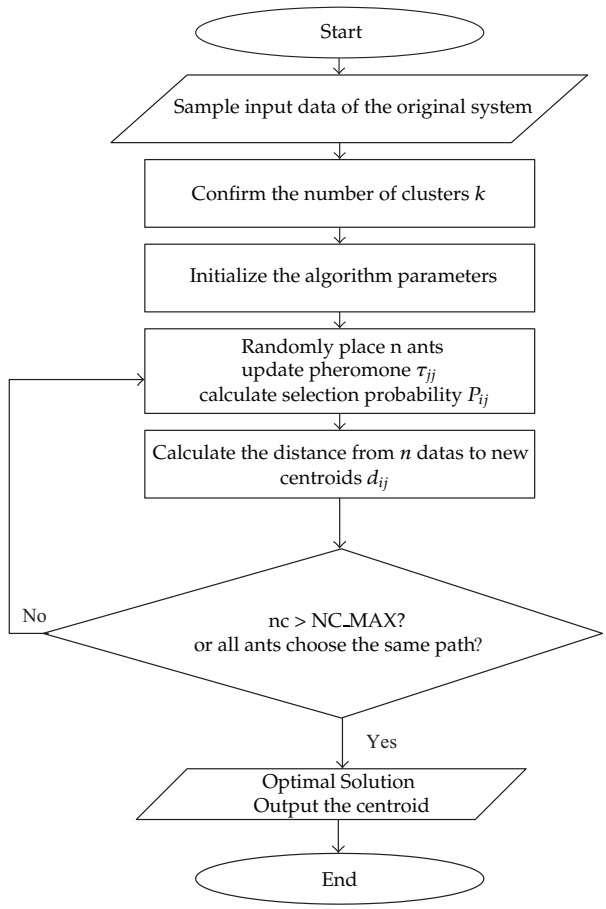

Figure 2: The K-means ant algorithm flow chart.

the algorithm parameters Q, ρ iteration counter $n_c = 0$, maximum iterations NC_MAX, the pheromone $\tau_{ij}, (i, j = 1, 2 \ldots n)$. We place n ants in n data, each of the ants chooses the next node in accordance with the probability p_{ij}, and update the pheromone τ_{ij} of every path. Then the new k centroids are calculated, the distance from n data to the new centroids d_{ij}, $i = 1, 2, \ldots, n$, $j = 1, 2, \ldots, k$ are calculated. Repeat like this until n_c is greater than the maximum iterations NC_MAX or all ants choose the same path, the optimal clustering can be given based on the pheromone. Finally, the centers of the Gaussian membership function are determined on the cluster centroid.

3.2. Parameter Estimation by Using Genetic Algorithm

Genetic algorithm (GA) is a meta-heuristic method used to find a solution based on biological evolution process. The process includes crossover, natural selection, and mutation to obtain an individual with the best gen combination. GA begins with determination of chromosome set (solution set) in terms of binary (1 and 0). Next, the selection is conducted based on the fitness value. The chromosome with the highest fitness value is retained while the rest are removed. The selected chromosomes, then, experience reproduction process to be parents.

As the aim is to minimize the error between the output of fuzzy model and output data, in the paper, the mean of squared error (MSE) is used as a proper evaluation function. MSE is given by

$$\mathrm{MSE} = \frac{1}{M}\sum_{i=1}^{M}\left[Y_i - y_i\right]^2, \tag{3.3}$$

where Y_i is output from Fuzzy model, y_i is output data, and M is number of data pairs.

Since the objective is to minimize MSE value, the fitness function is defined as follows:

$$J_k = -\mathrm{MSE}_k + \max(\mathrm{MSE}), \tag{3.4}$$

where k is the kth chromosome.

If the normalized fitness function $f_k(i)$ is used, it can be calculated by using

$$f_k(i) = \frac{J_k(i)}{\sum_{i=1}^{n} J_k(i)}, \tag{3.5}$$

where $J_k(i)$ is the fitness function for chromosome i.

The algorithm flow chart of the parameter estimation by using genetic algorithm is shown in Figure 3. Firstly, we sample output data of the original system, write the objective function based on equation and then initialize the algorithm parameters number individual NIND, maximum genetic times MAXGEN, number variable NVAR, variable precision PRECI, generation gap GGAP, and genetic counter GEN. Then the initial population $\widehat{A}, \widehat{B}, i = 1, 2, \ldots, k$ with lines NIND, columns NVAR $*$ PRECI is generated randomly. The following step is calculating fitness function value for different data in different state, then select, crossover, mutate, and calculate a new objective function value and track the performance of the solution. Selection process is used to determine two chromosomes to be the parents. Crossover is used to produce two new individuals. Generate initial population: initial solution is a randomly generated digit that has NIND line and NVAR $*$ PRECI row. We calculate fitness function value under different data in different state, then select, crossover, mutate and calculate a new objective function value and track the performance of the solution. Selection process is used to determine two chromosomes to be the parents. Crossover is used to produce two new individuals. Repeat like this until GEN > MAXGEN performance index is satisfied. Finally, the optimal $\widehat{A}, \widehat{B}, i = 1, 2, \ldots, k$ are obtained.

4. An Illustrative Example

In order to verify the effectiveness of proposed method, an example is given. Consider a system is composed of three springs and masses, see Figure 4.

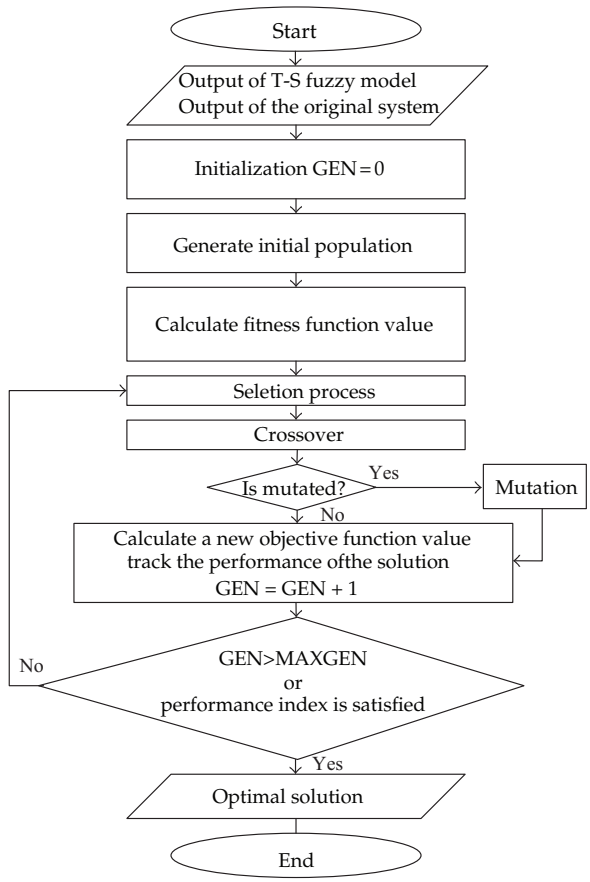

Figure 3: The genetic algorithm flow chart.

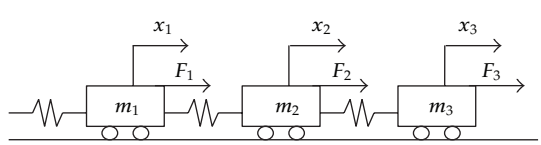

Figure 4: Spring mass system.

The dynamic characteristic of the model can be simplified as

$$
\begin{aligned}
m_1\ddot{x}_1 + (k_1 + k_2)x_1 - k_2x_2 &= F_1 \sin \omega_1 t, \\
m_2\ddot{x}_2 - k_2x_1 + (k_2 + k_3)x_2 - k_3x_3 &= F_2 \sin \omega_2 t, \\
m_3\ddot{x}_3 - k_3x_2 + k_3x_3 &= F_3 \sin \omega_3 t.
\end{aligned}
\tag{4.1}
$$

By choosing states $Z_1 = x_1$, $Z_2 = \dot{x}_1$, $Z_3 = x_2$, $Z_4 = \dot{x}_2$, $Z_5 = x_3$, $Z_6 = \dot{x}_3$ and output variables $y_1 = Z_1$, $y_2 = Z_3$, $y_3 = Z_5$, then the state-space model can be obtained:

$$\begin{bmatrix} \dot{Z}_1 \\ \dot{Z}_2 \\ \dot{Z}_3 \\ \dot{Z}_4 \\ \dot{Z}_5 \\ \dot{Z}_6 \end{bmatrix} = \begin{bmatrix} 0 & 1 & 0 & 0 & 0 & 0 \\ -\dfrac{k_1+k_2}{m_1} & 0 & \dfrac{k_2}{m_1} & 0 & 0 & 0 \\ 0 & 0 & 0 & 1 & 0 & 0 \\ \dfrac{k_2}{m_2} & 0 & -\dfrac{k_2+k_3}{m_2} & 0 & \dfrac{k_3}{m_2} & 0 \\ 0 & 0 & 0 & 0 & 0 & 1 \\ 0 & 0 & \dfrac{k_3}{m_3} & 0 & -\dfrac{k_3}{m_3} & 0 \end{bmatrix} \begin{bmatrix} Z_1 \\ Z_2 \\ Z_3 \\ Z_4 \\ Z_5 \\ Z_6 \end{bmatrix} + \begin{bmatrix} 0 & 0 & 0 \\ \dfrac{1}{m_1} & 0 & 0 \\ 0 & 0 & 0 \\ 0 & \dfrac{1}{m_2} & 0 \\ 0 & 0 & 0 \\ 0 & 0 & \dfrac{1}{m_3} \end{bmatrix} \begin{bmatrix} F_1 \sin \omega_1 t \\ F_2 \sin \omega_2 t \\ F_3 \sin \omega_3 t \end{bmatrix},$$

$$\begin{bmatrix} y_1 \\ y_2 \\ y_3 \end{bmatrix} = \begin{bmatrix} 1 & 0 & 0 & 0 & 0 & 0 \\ 0 & 0 & 1 & 0 & 0 & 0 \\ 0 & 0 & 0 & 0 & 1 & 0 \end{bmatrix} \begin{bmatrix} Z_1 \\ Z_2 \\ Z_3 \\ Z_4 \\ Z_5 \\ Z_6 \end{bmatrix}. \tag{4.2}$$

For the real system, $F_1 = F_2 = F_3 = 1500\,\mathrm{N}$, $\omega_1 = \omega_2 = \omega_3 = 260\,\mathrm{rad/s}$, $k_1 = k_2 = k_3 = 2000\,\mathrm{N/M}$, and $m_1 = m_2 = m_3 = 0.5\,\mathrm{kg}$.

Suppose the input function is sine wave, for each state sample 250 points during half a cycle, and then cluster the data by using K-means ant cluster algorithm; the parameters are setting as: the number of cluster centroids $k = 3$, the number of ants $n = 300$, the number of maximum iterations NC_MAX = 500, the permanence coefficient of the pheromone $\rho = 0.1$, the constant $Q = 0.9$, then the centroids can be optimized to

$$\begin{bmatrix} k_1 \\ k_2 \\ k_3 \end{bmatrix} = \begin{bmatrix} -1.5 & 0 & 1.5 \\ -2.3 & 0 & 2.3 \\ -2.7 & 0 & 2.7 \end{bmatrix}. \tag{4.3}$$

We sample the output data of the original system and the T-S fuzzy model and calculate T-S fuzzy model consequent parameters using genetic algorithm according to

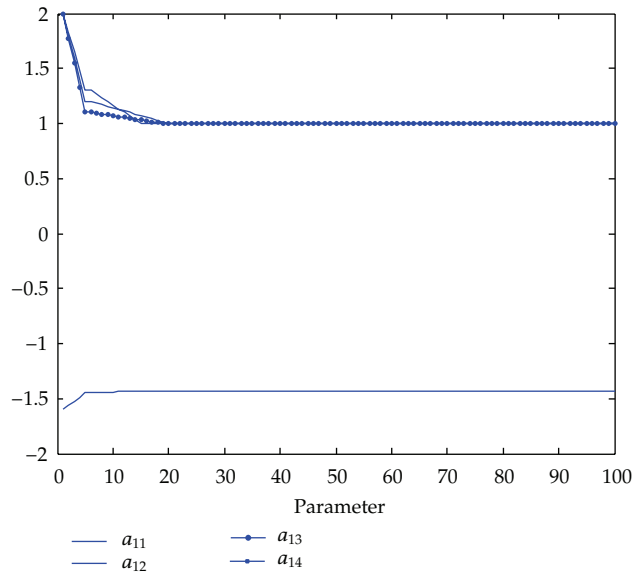

Figure 5: Optimization process.

the performance index (3.3). In order to reduce iteration times, the initialization parameters are chosen through the least square method. The consequent parameters are calculated as

$$\begin{bmatrix} a_{11} \\ a_{12} \\ a_{13} \\ a_{21} \\ a_{22} \\ a_{23} \\ a_{31} \\ a_{32} \\ a_{33} \end{bmatrix} = \begin{bmatrix} 0.0001 & 0.0001 & 0.0001 & -1.4329 \\ 0.0001 & 0.0001 & 0.0001 & -2.4251 \\ 0.0001 & 0.0001 & 0.0001 & -2.9370 \\ 0.0003 & 0.0003 & 0.0003 & -0.1127 \\ 0.0005 & 0.0005 & 0.0005 & -0.1574 \\ 0.0006 & 0.0006 & 0.0006 & -0.1703 \\ 0.0005 & 0.0005 & 0.0005 & -0.0734 \\ 0.0009 & 0.0009 & 0.0009 & -0.1475 \\ 0.0011 & 0.0011 & 0.0011 & -0.1965 \end{bmatrix}. \tag{4.4}$$

The parameter optimization process of a_{11} by using the genetic algorithm is shown in Figure 5. It can be seen from the figure that the parameters become stable when the Genetic algorithm has had 10 runs. And after a period of input simulation, the states of the original system and the T-S fuzzy model are shown in Figure 6. From the figures, we can see that the responses of the fuzzy model can approximate the original system responses very well. And the model approximation error of different methods are shown in Table 1, we can see from the table that the method proposed in the paper is more appropriate.

5. Conclusion

This paper considered the identification of T-S fuzzy model in which the control variables and the state variables are all premise variables. Ant K-means algorithm and genetic algorithm were used to determine the number of the rules and the state-space model parameters,

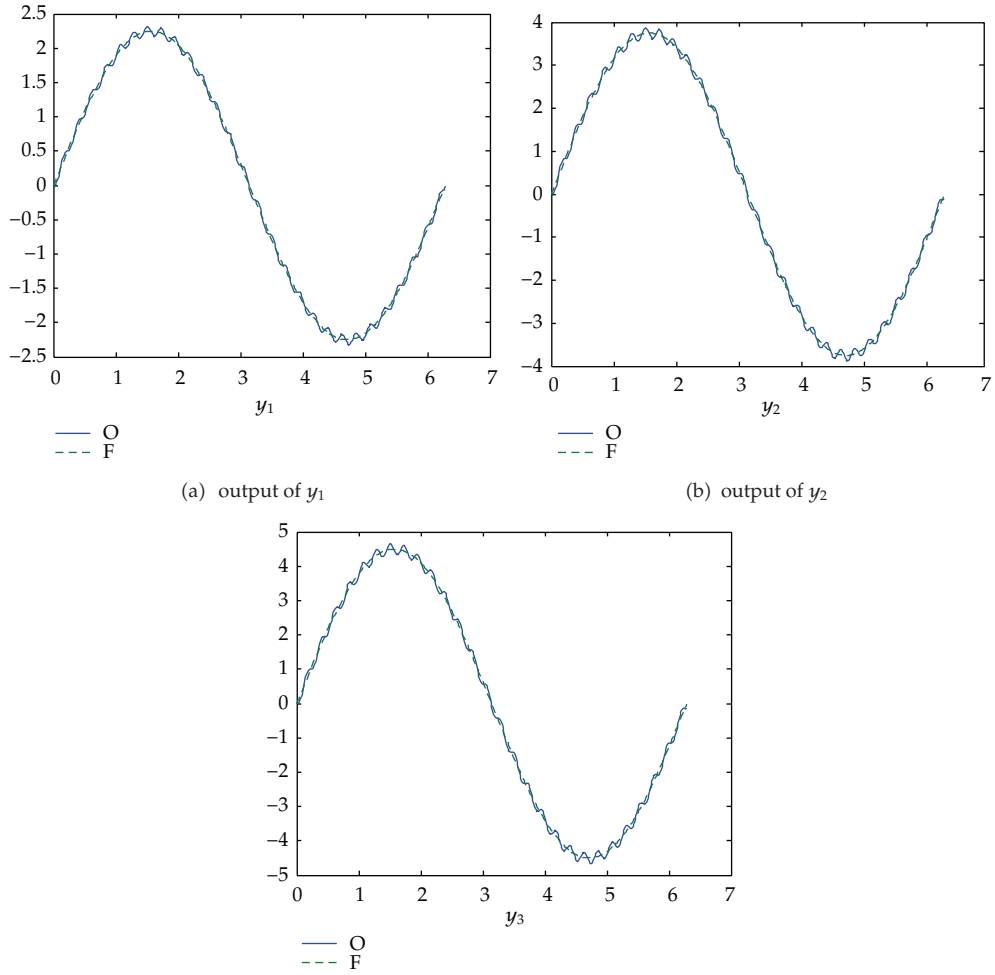

(a) output of y_1

(b) output of y_2

(c) output of y_3

Figure 6: Response curve.

Table 1: Comparison of different methods.

Methods	No. of centers	No. of parameters	MSE
Subtraction clustering algorithm and least squares algorithm	3	12	0.0202
C-means clustering and least squares algorithm	3	12	0.0133
Ant colony algorithm and genetic algorithm	3	17	0.0105

respectively. The simulation results illustrated the effectiveness of the proposed algorithm. Future work will investigate determination of the optimal cluster number for a certain amount of data.

Acknowledgments

This work was partially supported by the Heilongjiang Province Education Department under Grant no. 12511106, the National Key Basic Research Program, China (2012CB215202), the 111 Project (B12018), and the National Natural Science Foundation of China (61174058, 60974052 and 61134001). The authors also gratefully acknowledge the helpful comments and suggestions of the reviewers, which have helped greatly in improving the presentation of the paper.

References

[1] C. Sun, Y. Wang, and C. Chang, "Switching T-S fuzzy model-based guaranteed cost control for two-wheeled mobile robots," *International Journal of Innovative Computing, Information and Control A*, vol. 8, no. 5, pp. 3015–3028, 2012.

[2] C. Sun, S. Lin, and Y. Wang, "Relaxed stabilization conditions for switching T-S fuzzy systems with practical constraints, International," *Journal of Innovative Computing, Information and Control*, vol. 8, no. 6, pp. 4133–4145, 2012.

[3] A. Benzaouia and A. El-Hajjaji, "Delay-dependent stabilization conditions of controlled positive T-S fuzzy systems with time varying delay," *International Journal of Innovative Computing, Information and Control*, vol. 7, no. 4, pp. 1533–1548, 2011.

[4] Z. Wu, P. Shi, H. Su, and J. Chu, "Reliable H-infinity control for discrete-time fuzzy systems with infinite-distributed delay," *IEEE Trans on Fuzzy Systems*, vol. 20, no. 1, pp. 22–31, 2012.

[5] Q. Zhou, P. Shi, J. Lu, and S. Xu, "Adaptive output feedback fuzzy tracking control for a class of nonlinear systems," *IEEE Trans on Fuzzy Systems*, vol. 19, no. 5, pp. 972–982, 2011.

[6] L. Wu, X. Su, P. Shi, and J. Qiu, "Model approximation for discrete-time state-delay systems in the T-S fuzzy framework," *IEEE Transactions on Fuzzy Systems*, vol. 19, no. 2, pp. 366–378, 2011.

[7] L. Wu, X. Su, P. Shi, and J. Qiu, "A new approach to stability analysis and stabilization of discrete-time T-S fuzzy time-varying delay systems," *IEEE Transactions on Systems, Man, and Cybernetics B*, vol. 41, no. 1, pp. 273–286, 2011.

[8] J. Zhang, P. Shi, and Y. Xia, "Robust adaptive sliding-mode control for fuzzy systems with mismatched uncertainties," *IEEE Transactions on Fuzzy Systems*, vol. 18, no. 4, pp. 700–711, 2010.

[9] S. K. Nguang, P. Shi, and S. Ding, "Fault detection for uncertain fuzzy systems: an LMI approach," *IEEE Transactions on Fuzzy Systems*, vol. 15, no. 6, pp. 1251–1262, 2007.

[10] S. K. Nguang and P. Shi, "H-infinity Fuzzy output feedback control design for nonlinear systems: an LMI approach," *IEEE Transactions on Fuzzy Systems*, vol. 11, no. 3, pp. 331–340, 2003.

[11] T. Takagi and M. Sugeno, "Fuzzy identification of systems and its applications to modeling and control," *IEEE Transactions on Systems, Man and Cybernetics*, vol. 15, no. 1, pp. 116–132, 1985.

[12] R. Yusof, R. Z. A. Rahman, M. Khalid, and M. F. Ibrahim, "Optimization of fuzzy model using genetic algorithm for process control application," *Journal of the Franklin Institute*, vol. 348, no. 7, pp. 1717–1737, 2011.

[13] J. Q. Chen, Y. G. Xi, and Z. J. Zhang, "A clustering algorithm for fuzzy model identification," *Fuzzy Sets and Systems*, vol. 98, no. 3, pp. 319–329, 1998.

[14] P. M. Kanade and L. O. Hall, "Fuzzy ants and clustering," *IEEE Transactions on Systems, Man, and Cybernetics A*, vol. 37, no. 5, pp. 758–769, 2007.

[15] P. Rocca, L. Manica, and A. Massa, "An improved excitation matching method based on an ant colony optimization for suboptimal-free clustering in sum-difference compromise synthesis," *IEEE Transactions on Antennas and Propagation*, vol. 57, no. 8, pp. 2297–2306, 2009.

[16] I. Gath and A. B. Geva, "Unsupervised optimal fuzzy clustering," *IEEE Transactions on Pattern Analysis and Machine Intelligence*, vol. 11, no. 7, pp. 773–781, 1989.

[17] R. Yager and D. Filev, "Generation of fuzzy rules by mountain method," *Journal of Intelligent & Fuzzy Systems*, vol. 2, pp. 209–219, 1994.

[18] J. Stefan, H. Christoph, and K. Nikolaus, "Total least squares in fuzzy system identification: an application to an industrial engine," *Engineering Applications of Artificial Intelligence*, vol. 21, no. 8, pp. 1277–1288, 2008.

[19] S. Ming and R. R. Rhinehart, "A generalized TSK model with a novel rule antecedent structure: structure identification and parameter estimation," *Computers and Chemical Engineering*, vol. 34, no. 8, pp. 1199–1219, 2010.

[20] T. Amine, L. Frederic, K. Mohamed, and E. Gilles, "Fuzzy identification of a greenhouse," *Applied Soft Computing Journal*, vol. 7, no. 3, pp. 1092–1101, 2007.
[21] H. Chang-Ho, P. Chang-Woo, and K. Seungwoo, "Takagi-Sugeno fuzzy model based indirect adaptive fuzzy observer and controller design," *Information Sciences*, vol. 180, no. 11, pp. 2314–2327, 2010.
[22] V. Petridis, E. Paterakis, and A. Kehagias, "A hybrid neural-genetic multimodel parameter estimation algorithm," *IEEE Transactions on Neural Networks*, vol. 9, no. 5, pp. 862–876, 1998.
[23] A. Roy, S. J. Briczinski, J. F. Doherty, and J. D. Mathews, "Genetic-algorithm-based parameter estimation technique for fragmenting radar meteor head echoes," *IEEE Geoscience and Remote Sensing Letters*, vol. 6, no. 3, pp. 363–367, 2009.
[24] W. P. Calixto, L. M. Neto, M. Wu, K. Yamanaka, and E. Da Paz Moreira, "Parameters estimation of a horizontal multilayer soil using genetic algorithm," *IEEE Transactions on Power Delivery*, vol. 25, no. 3, pp. 1250–1257, 2010.
[25] X. Zhou and R. Wang, "Self-evolving ant colony optimization and its application to traveling salesman problem," *International Journal of Innovative Computing, Information and Control*, vol. 8, no. 12, pp. 8311–8321, 2012.
[26] J. Song and D. Kim, "Subcarrier and bit allocation scheme for the MA problem based on the ant colony optimization to minimize power consumption in OFDMA systems," *International Journal of Innovative Computing, Information and Control*, vol. 7, no. 8, pp. 4755–4764, 2011.
[27] W. Shahzad and A. Baig, "Hybrid associative classification algorithm using ant colony optimization," *International Journal of Innovative Computing, Information and Control*, vol. 7, no. 12, pp. 6815–6826, 2011.
[28] J. L. Castro, "Fuzzy logic controllers are universal approximators," *IEEE Transactions on Systems, Man and Cybernetics*, vol. 25, no. 4, pp. 629–635, 1995.
[29] Q. Gao, X. J. Zeng, G. Feng, and Y. Wang, "T-S-fuzzy-model-based approximation and controller design for general nonlinear systems," *IEEE Transactions on Man and Cybernetics B*, vol. 42, no. 4, pp. 1143–1154, 2012.

Hindawi Publishing Corporation
Mathematical Problems in Engineering
Volume 2012, Article ID 784389, 12 pages
doi:10.1155/2012/784389

Research Article

A Novel Evaluation Model for Hybrid Power System Based on Vague Set and Dempster-Shafer Evidence Theory

Dongxiao Niu,[1] Yanan Wei,[1] Yan Shi,[2] and Hamid Reza Karimi[3]

[1] *School of Economics and Management, North China Electric Power University, Beijing 102206, China*
[2] *School of Industrial Engineering, Tokai University, Kumamoto 862-8652, Japan*
[3] *Department of Engineering, Faculty of Engineering and Science, University of Agder, 4898 Grimstad, Norway*

Correspondence should be addressed to Yanan Wei, weiyanan010@163.com

Received 27 August 2012; Accepted 4 October 2012

Academic Editor: Peng Shi

Copyright © 2012 Dongxiao Niu et al. This is an open access article distributed under the Creative Commons Attribution License, which permits unrestricted use, distribution, and reproduction in any medium, provided the original work is properly cited.

Because clean energy and traditional energy have different advantages and disadvantages, it is of great significance to evaluate comprehensive benefits for hybrid power systems. Based on thorough analysis of important characters on hybrid power systems, an index system including security, economic benefit, environmental benefit, and social benefit is established in this paper. Due to advantages of processing abundant uncertain and fuzzy information, vague set is used to determine the decision matrix. Convert vague decision matrix to real one by vague combination ruleand determine uncertain degrees of different indexes by grey incidence analysis, then the mass functions of different comment set in different indexes are obtained. Information can be fused in accordance with Dempster-Shafer (D-S) combination rule and the evaluation result is got by vague set and D-S evidence theory. A simulation of hybrid power system including thermal power, wind power, and photovoltaic power in China is provided to demonstrate the effectiveness and potential of the proposed design scheme. It can be clearly seen that the uncertainties in decision making can be dramatically decreased compared with existing methods in the literature. The actual implementation results illustrate that the proposed index system and evaluation model based on vague set and D-S evidence theory are effective and practical to evaluate comprehensive benefit of hybrid power system.

1. Introduction

At present, climate warming and environmental pollution are becoming increasingly prominent, which poses a serious threat to sustainable development of human society. Developing clean energies, such as wind power and photovoltaic power, is widely accepted common choice of the world [1–5]. Clean energy and traditional energy have their own

different characteristics. As to thermal power, it has advantages of low cost and stable power, but generally causes serious pollution, especially carbon dioxide, whereas clean energy power has the disadvantages of high cost and instability, but is highly environmental friendly [6–9]. A power system usually includes thermal power, wind power, and photovoltaic power. Because of different techniques and economic influences, it is of practical significance to choose scientific, comprehensive, and reasonable indexes, and methods to evaluate comprehensive benefit of hybrid power system.

Numerous factors should be considered to evaluate the comprehensive benefit of hybrid power system, such as technique security, influence to environment, and economy [10]. Literatures [11, 12] have analyzed economic aspect of power system; security and technique aspect are considered in [13, 14]; the work in [15, 16] evaluated environmental influence of different energies. However, only a few attempts have been made on social benefit of power system, let alone comprehensive benefit including social and environmental aspects of hybrid power system.

The input indexes are critical for comprehensive evaluation and are often complex, which involves production, scheduling, dispatch, marketing, planning, and finance as well as many other aspects [17]. Because of ambiguity of characters of evaluation indexes, it is suitable for information fusion technique to evaluate comprehensive benefit of hybrid power system which allows representation of both imprecision and uncertainty [18, 19]. Information fusion technique includes several kinds of methods, such as Kalman filtering, Bayesian estimation, and D-S evidence theory. Because Kalman filtering is depending on the initial state estimation, and by measuring the noise influence such as large faults, estimate process covariance easily appears morbid, leading to filter positioning results are not stable. Bayesian is a kind of commonly used method for static environment fusion in sensor lower information, suitable for normal distribution measuring result or additive Gaussian noise system. D-S evidence theory tackles the prior probability issue by keeping track of an explicit probabilistic measure of a possible lack of information. It is suitable take into account the disparity between knowledge types [20] because it is able to provide a federative framework [21] and it combines cumulative evidence for changing prior opinions in the light of new evidence [22]. Literature [23] proposed the combined fuzzy logic/D-S evidence theory method. Although Jones et al. [24] noted that it is necessary to ensure the validity of basic probability assignment, they did not give a method to do so. Vague set is proposed to solve the problem in this paper.

Due to advantages of vague set processing abundant uncertain and fuzzy information, it is chosen to determine basic decision matrix of evaluation model [25–30]. Combining vague set with D-S evidence theory, a novel evaluation algorithm is established and applied into the comprehensive benefit evaluation of hybrid power system.

The paper is organized as follows. Section 2 proposes a systematic evaluation index system according to characters of hybrid power system. A comprehensive evaluation model based on vague set and D-S evidence theory is given in Section 3. A simulation of hybrid power system including thermal power, wind power, and photovoltaic power in China is proposed, and comparison between the proposed evaluation model with some existing works is analyzed in Section 4. The paper is conducted in Section 5.

2. Evaluation Index System

Comprehensive benefit evaluation of hybrid power generation should not only include economic benefit, but also its impact on the environment, namely, environmental benefit.

Due to the public service property of electric power, it is necessary to consider social benefit; meanwhile, because of instable clean energy generation, it is needed to consider the security of the power system. This paper establishes comprehensive benefit evaluation index system of hybrid power system from the four aspects of economic benefit, environmental benefit, social benefit, and security.

2.1. Economic Benefit

Economic benefit is the most important aspect of comprehensive benefit evaluation. It is mainly composed of the four aspects of profitability capability, solvency capability, operational capability, and development capacity.

Profitability refers to the ability to profit in a certain period. Profitability capability is determined by comprehensive consideration of gross profit margin, net profit margin, ratio of profits to cost, and return on total assets. Solvency capability refers to the ability to repay due debts which be assessed in terms of current ratio, quick ratio, asset-liability ratio, and interest coverage ratio. Operational capacity refers to enterprise's ability to make profits using existing assets. This paper mainly assesses the operational capability through current asset turnover, fixed asset turnover, and total asset turnover. Development capacity refers to the potential ability to expand scale and grow strength in the coming years which can be accessed through profit growth, sale growth, and total asset growth.

2.2. Environmental Benefit

Environmental benefit refers to the influence on living environment, which can be divided into positive benefit, negative benefit, direct benefit, and indirect benefit. Fundamentally speaking, environmental benefit is the basis of economic benefit and social benefit. Environmental benefit is a qualitative index. Comprehensively considering circumstances of hybrid power system, this paper evaluates environmental benefit from the two aspects of saving natural resources and reducing scraps.

2.3. Social Benefit

Social benefit refers to the good consequences and implications for community and society, also known as external and indirect economic benefit, mainly in forms of public reflection and social assessment system. Social benefit is a qualitative indicator. Comprehensively considering the specific circumstances of hybrid power system, this paper establishes social benefit evaluation index system from the three aspects of pulling gross domestic product, improving people's living standard and promoting social employment.

2.4. Security

Security occupies a basic position in comprehensive benefit evaluation of power grid. Combined with exiting researches and characters of hybrid power system, this paper selects four indexes to evaluate security, including integrated voltage qualification rate, grid frequency qualification rate, average loading rate of provincial grid, and power supply reliability rate.

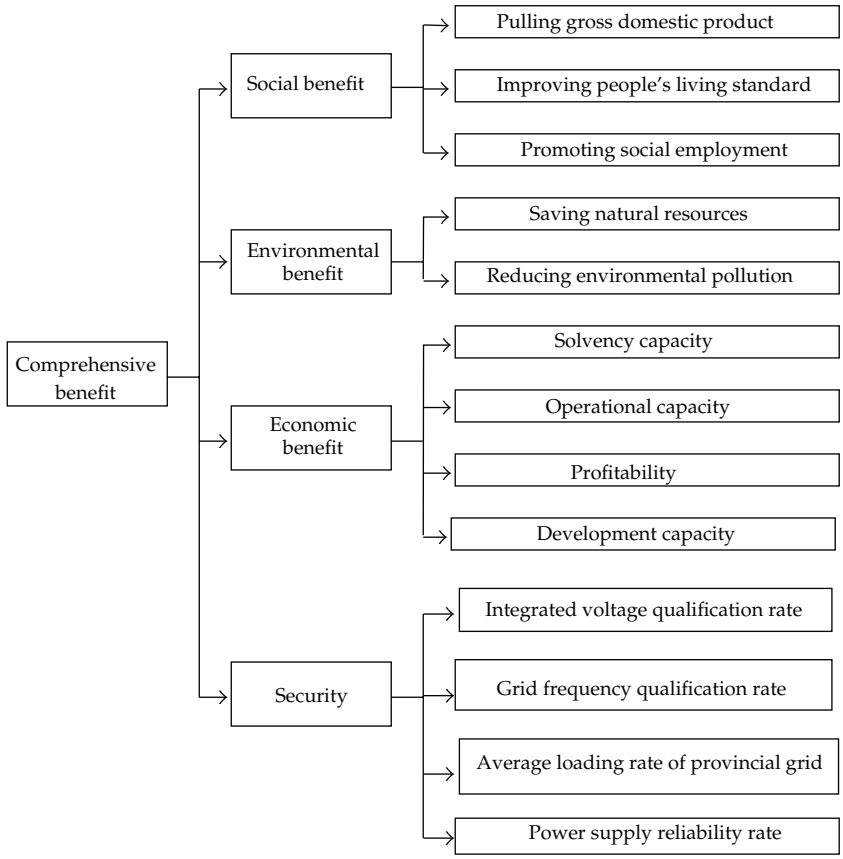

Figure 1: Comprehensive evaluation index system.

Above all, the comprehensive benefit evaluation index system of hybrid power system is shown in Figure 1.

3. Model Establishment

3.1. Decision Matrix Based on Vague Set

Vague set proposed by Gau and Buehrer [31] is a generalized form of fuzzy set. Vague set has been successfully applied in the field of fuzzy control, decision analysis and expert systems, and has achieved better results than the traditional fuzzy set theory [32–34].

Set U the universe of discourse, with a generic element u. A vague set A is characterized by a truth-membership function t_A and a false-membership function f_A, where $t_A(u)$ is a lower bound on the grade of membership of u, derived from the evidence rising for u; $f_A(u)$ is a lower bound on the negation of u, derived from the evidence against u; $0 \le t_A(u) + f_A(u) \le 1$. The grade of membership of u in vague set A is bound to a subinterval $[t_A(u), 1 - f_A(u)]$ of $[0, 1]$. The vague value $[t_A(u), 1 - f_A(u)]$ indicates that the exact grade of membership $\mu_A(u)$ of u maybe unknown, but it is bound by $t_A(u) \le \mu_A(u) \le 1 - f_A(u)$, where $0 \le t_A(u) + f_A(u) \le 1$.

When the universe of discourse U is discrete, a vague set A can be written as

$$A = \sum_{i=1}^{n} \frac{\left[t_A(u_i), 1 - f_A(u_i)\right]}{u_i}, \quad u_i \in U. \tag{3.1}$$

When the universe of discourse U is continuous, a vague set A can be written as

$$A = \frac{\int_U \left[t_A(u_i), 1 - f_A(u_i)\right]}{u_i du_i}, \quad u_i \in U. \tag{3.2}$$

The steps of determining the decision matrix is as follows.

(1) *Determination Evaluation Factors and Comment Set*

The evaluation factors are expressed as $u_1, u_2, \ldots, u_m$, then the evaluation factor set is $U = \{u_1, u_2, \ldots, u_m\}$.

set evaluation indexes of each evaluation factor be $u_{ij}, (i = 1, 2, \ldots, m; j = 1, 2 \ldots, n)$. We can get index set $u_i = \{u_{i1}, u_{i2}, \ldots, u_{ij}, \ldots, u_{im}\}, i = 1, 2, \ldots, m; j = 1, 2, \ldots, n$.

Define the comment set as $V = \{v_1, v_2, \ldots, v_p\}$.

(2) *Construct Evaluation Matrix*

Assuming the comment level of index u_{ij}, $(i = 1, 2, \ldots, m; j = 1, 2, \ldots, n)$ is $v_k (k = 1, 2, \ldots, p)$, then the relationship matrix of factor set U mapping to comment set V is R_i:

$$R_i = \begin{bmatrix} r_{i11}, r_{i12}, \ldots, r_{i1p} \\ r_{i21}, r_{i22}, \ldots, r_{i2p} \\ \vdots \quad \vdots \quad \vdots \\ r_{in1}, r_{in2}, \ldots, r_{inp} \end{bmatrix}, \tag{3.3}$$

where r_{ijk} means the comment of factor u_{ij} mapping to comment set, and r_{ijk} can be expressed as

$$r_{ijk} = \left[t_{\tilde{R}ijk}, 1 - f_{\tilde{R}ijk}\right]. \tag{3.4}$$

For qualitative index, the value can be got from experts' evaluation. For quantitative index, its quantitative value is the index value. Normalizing index value, we can get $t_{\tilde{R}ijk}$ and $1 - f_{\tilde{R}ijk}$.

The main calculations are as follows.

Multiply calculation:

$$k \cdot \tilde{A} = \left[k \cdot t_{\tilde{A}}, k \cdot \left(1 - f_{\tilde{A}}\right)\right] k, \quad k \in [0, 1]. \tag{3.5}$$

Finite sum calculation:

$$\widetilde{A} \oplus \widetilde{B} = \left[t_{\widetilde{A}} \oplus t_{\widetilde{B}}, (1 - f_{\widetilde{A}}) \oplus (1 - f_{\widetilde{B}})\right] = \left[\min\{1, t_{\widetilde{A}} + t_{\widetilde{B}}\}, \min\{1, (1 - f_{\widetilde{A}}) + (1 - f_{\widetilde{B}})\}\right], \quad (3.6)$$

$$b_{ik} = \left[\min\left\{1, \sum_{j=1}^{n} a_{ij} t_{\widetilde{R_{ijk}}}\right\}, \min\left\{1, \sum_{j=1}^{n} a_{ij}\left(1 - f_{\widetilde{R_{ijk}}}\right)\right\}\right], \quad (3.7)$$

where $\widetilde{B}_i$ is a vague subset and b_{ik} $(k = 1, 2, \ldots, p)$ is the evaluation value of k to $\widetilde{B}_i$.

3.2. D-S Evidence Theory

The evidence theory, first proposed by Harvard University mathematician A. P. Dempster in the 1960s, aims to use upper and lower probability to solve the multivalued mapping issues. G. Shafer, Dempster's student, has further developed the evidence theory by introducing the concept of belief function to form a mathematical system to deal with uncertainty reasoning based on "evidence" and "portfolio."

Definition 3.1. Suppose Θ is the frame of discernment. If set function $m : 2^{\Theta} \to [0, 1]$ (2^{Θ} is the power set of Θ) is to meet $m(\Phi) = 0$, $\sum_{A \subset \Theta} m(A) = 1$, the function m is called the basic probability assignment on Θ; for all $A \subset \Theta$, $m(A)$ is called the basic belief degree.

Definition 3.2. Suppose Θ is the frame of discernment, function $m : 2^{\Theta} \to [0, 1]$ is the basic probability assignment on Θ, then the belief function is defined as $\mathrm{Bel} : 2^{\Theta} \to [0, 1]$, where $\mathrm{Bel}(A) = \sum_{B \subset A} m(B)$, for all $A \subset \Theta$.

Definition 3.3. If $m(A) > 0$, then A is called the focal element of the belief function Bel. And all focal elements are called its core.

Definition 3.4. If function $Q : 2^{\Theta} \to [0, 1]$ is defined by $Q(A) = \sum_{A \subset B} m(B)$, for all $A \subset \Theta$, then Q is called the total belief function of Bel. For all $A \subset \Theta$, $Q(A)$ is called the total belief number of A.

Definition 3.5. Suppose $\mathrm{Bel} : 2^{\Theta} \to [0, 1]$ is a belief function on Θ. Functions $\mathrm{Dou} : 2^{\Theta} \to [0, 1]$ and $\mathrm{pl} : 2^{\Theta} \to [0, 1]$ are defined as for all $A \subset \Theta$ $\mathrm{Dou}(A) = \mathrm{Bel}(\overline{A})$ and $\mathrm{pl}(A) = 1 - \mathrm{Bel}(\overline{A})$, then Dou is called suspicion function of Bel, and pl is called plausibility function. For all $A \subset \Theta$, $\mathrm{Dou}(A)$ is called the suspicion degree of A, and $\mathrm{pl}(A)$ is called the plausibility degree.

Theorem 3.6. *Suppose m_1 and m_2 are two basic probability assignment functions formed based on information obtained from two different information sources,* Bel_1 *and* Bel_2*, in the same frame of discernment Θ. $A_1, A_2, \ldots, A_k$ and $B_1, B_2, \ldots, B_l$ are focal elements of* Bel_1 *and* Bel_2*. If $\sum_{A_i \cap B_j = \phi} m_1(A_i) m_2(B_j) < 1$, the combination of m_1 and m_2 is as follows:*

$$m(A) = \begin{cases} 0, & A = \phi, \\ \dfrac{\sum_{A_i \cap B_j = A} m_1(A_i) m_2(B_j)}{1 - \sum_{A_i \cap B_j = \phi} m_1(A_i) m_2(B_j)}, & A \neq \phi. \end{cases} \quad (3.8)$$

Theorem 3.7. *Suppose $m_1, m_2, \ldots, m_n$ are the corresponding basic probability assignment functions formed based on information obtained from different information sources $\mathrm{Bel}_1, \mathrm{Bel}_2, \ldots, \mathrm{Bel}_n$ in the same frame of discernment Θ. If $\mathrm{Bel}_1 \oplus \mathrm{Bel}_2 \oplus \cdots \oplus \mathrm{Bel}_n$ exists and m is its basic probability assignment function, then*

$$\begin{gathered}
\forall A \subseteq \Theta, \quad A \neq \phi, \\
m(A) = K_n \sum_{A_1 \cap A_2 \cap \cdots \cap A_N} m_1(A_1) m_2(A_2) \cdots m_n(A_n), \\
K_n = \frac{1}{N_n}, \\
N_n = \sum_{A_1 \cap A_2 \cap \cdots \cap A_N \neq \phi} m_1(A_1) m_2(A_2) \cdots m_n(A_n).
\end{gathered} \tag{3.9}$$

3.3. Design of Comprehensive Evaluation Model

Suppose there is a multiattribute (index) evaluation problem with comprehensive comment set $V = \{V_1, V_2, \ldots, V_m\}$ and evaluation index set $I = \{I_1, I_1, \ldots, I_n\}$. According to vague set, the decision matrix $R = (R_{ij})_{m \times n}$, $R_{ij} = [t_{ij}, 1 - f_{ij}]$ is got. By synthesis law of vague set, we can convert the vague set R into a real set $G = (g_{ij})_{m \times n}$, $g_{ij} = (t_{ij} + (1 - f_{ij}))/2$.

Different mass functions mean different evaluation results. So it is vital to determine the uncertainty degree of evidences. Theoretically, one index which matches average information better than other indexes is more beneficial for decision making, and the information uncertainty degree of the index is lower, vice versa.

Suppose the matrix G is

$$G = (g_{ij})_{m \times n}, \qquad \overline{g_i} = \frac{1}{n} \sum_{j=1}^{n} g_{ij}, \ i = 1, 2, \ldots, m. \tag{3.10}$$

Define the q-order uncertainty degree of index I_j as

$$\begin{gathered}
\mathrm{DOI}(I_j) = \frac{1}{m} \left[\sum_{i=1}^{m} (r_{ij})^q \right]^{1/q}, \\
r_{ij} = \frac{\min_i |g_{ij} - \overline{g}| + \xi \min_i |g_{ij} - \overline{g}|}{|g_{ij} - \overline{g}| + \xi \min_i |g_{ij} - \overline{g}|}, \quad i = 1, 2, \ldots, m; \ j = 1, 2, \ldots, n,
\end{gathered} \tag{3.11}$$

where r_{ij} is called gray mean correlation degree with $\xi = 0.5$ in general.

In case of negative number, the normalization method is shown as

$$\overline{g_{ij}} = \frac{g_{ij} - \min_i (g_{ij})}{\min_i (g_{ij}) - \min_i (g_{ij})}. \tag{3.12}$$

Suppose $x = (x_1, x_2, \ldots, x_t)$ is a finite difference information sequence with a length of $t(t \neq 0)$. An index set exists in the form of sequence $x_j \neq 0, j \in J, J = \{1, 2, \ldots, t\}$. The mapping function f is defined as information structure operator of finite sequence x:

$$f : x \longrightarrow yy_j = \frac{x_j}{\sum_{k=1}^{t} x_k}. \tag{3.13}$$

Here $y = (y_1, y_2, \ldots, y_t)$ is called mapping sequence of information structure.

The normalized score function matrix can be transformed into mapping sequence of information structure $Y = (y_{ij})_{m\times n}$.

Then the mass function $m_j(i)$ can be constructed:

$$m_j(i) = \left(1 - \mathrm{DOI}(I_j)\right) y_{ij}, \tag{3.14}$$

where $m_j(i)$ is a mass function of V_m to index I_j, $\sum_{i=1}^{m} m_j(i) < 1$. So the mass function of overall uncertainty with respect to the index I_j is shown as

$$m_j(i+1) = 1 - \sum_{i=1}^{m} m_j(i). \tag{3.15}$$

According to the proposed combination rule, the final evaluation results can be calculated after the combination of mass functions of comment set with respect to all indexes.

In summary, steps for comprehensive evaluation based on vague set and D-S evidence theory are as follows.

Step 1. Construct the decision-making matrix R based on the vague set theory.

Step 2. Convert R into real matrix $G = (g_{ij})_{m\times n}$ according to vague combination rule.

Step 3. Calculate the uncertainty degree $\mathrm{DOI}(I_j)$ $j = 1, 2, \ldots, n$ combined with real matrix G and (3.6).

Step 4. Establish the mapping sequence of information structure $Y = (y_{ij})_{m\times n}$.

Step 5. Build up mass function $m_j(i)$ and mass function of overall uncertainty $m_j(i+1)$ on the basis of $Y = (y_{ij})_{m\times n}$ and $\mathrm{DOI}(I_j)$.

Step 6. Fuse evidence information using the D-S combination rule.

Step 7. Make evaluation and decision in principle of the maximizing belief function.

4. Simulation Analysis

Guangdong power system in China, which includes thermal power, wind power, and solar photovoltaic power, is selected to simulation analysis. It is known from Section 2 that the comprehensive benefit evaluation index system of hybrid power system includes the four aspects of economic benefit, environmental benefit, social benefit, and security, which is

composed of 13 indexes shown in Table 1. According to data statistics and calculation, the original index value can be got as follows.

The comprehensive comment set is set to be $V = \{v_1, v_2, v_3, v_4, v_5\} = \{\text{best}, \text{better}, \text{good}, \text{worse}, \text{worst}\}$. For quantitative indexes such as voltage qualification rate, power grid frequency rate, average load rate, and power supply reliability rate, their values can be directly calculated by basic statistical data. For qualitative indicators such as debt paying ability, operation ability, saving natural resources, reducing environmental pollution, their values can be decided by comprehensive experts' opinions with specific situations.

According to vague set, we can get the vague matrix R for hybrid power system. Calculate the uncertainty degree $\mathrm{DOI}(I_j)$ and mapping sequence of information structure $Y = (y_{ij})_{m\times n}$. Then we can get mass function $m_j(i)$ and mass function of overall uncertainty $m_j(i+1)$:

$$R = \begin{array}{c} \\ I_1 \\ I_2 \\ I_3 \\ I_4 \\ I_5 \\ I_6 \\ I_7 \\ I_8 \\ I_9 \\ I_{10} \\ I_{11} \\ I_{12} \\ I_{13} \end{array} \begin{array}{c} \begin{array}{ccccc} v_1 & v_2 & v_3 & v_4 & v_5 \end{array} \\ \begin{bmatrix} [0.72, 0.86] & [0.83, 0.89] & [0.52, 0.63] & [0.24, 0.28] & [0.10, 0.16] \\ [0.68, 0.88] & [0.76, 0.80] & [0.86, 0.93] & [0.27, 0.38] & [0.34, 0.49] \\ [0.92, 0.87] & [0.80, 0.86] & [0.43, 0.49] & [0.34, 0.40] & [0.13, 0.28] \\ [0.67, 0.73] & [0.79, 0.87] & [0.64, 0.73] & [0.41, 0.56] & [0.34, 0.39] \\ [0.64, 0.73] & [0.79, 0.87] & [0.64, 0.73] & [0.41, 0.55] & [0.34, 0.39] \\ [0.71, 0.84] & [0.94, 0.98] & [0.74, 0.82] & [0.51, 0.64] & [0.14, 0.25] \\ [0.75, 0.84] & [0.77, 0.86] & [0.89, 0.90] & [0.23, 0.29] & [0.21, 0.31] \\ [0.77, 0.84] & [0.74, 0.83] & [0.91, 0.96] & [0.23, 0.32] & [0.14, 0.31] \\ [0.68, 0.76] & [0.70, 0.81] & [0.84, 0.92] & [0.18, 0.22] & [0.08, 0.16] \\ [0.82, 0.96] & [0.94, 0.97] & [0.75, 0.96] & [0.34, 0.48] & [0.18, 0.33] \\ [0.79, 0.80] & [0.94, 0.96] & [0.56, 0.63] & [0.29, 0.33] & [0.13, 0.20] \\ [0.84, 0.90] & [0.95, 0.97] & [0.34, 0.41] & [0.23, 0.26] & [0.19, 0.36] \\ [0.75, 0.69] & [0.87, 0.84] & [0.24, 0.33] & [0.17, 0.31] & [0.12, 0.24] \end{bmatrix} \end{array},$$

$$M = \begin{bmatrix} 0.14, 0.12, 0.00, 0.24, 0.11, 0.13, 0.17, 0.20, 0.17, 0.00, 0.24, 0.21, 0.17 \\ 0.32, 0.21, 0.37, 0.14, 0.37, 0.29, 0.29, 0.15, 0.15, 0.13, 0.00, 0.18, 0.24 \\ 0.14, 0.09, 0.27, 0.28, 0.17, 0.14, 0.00, 0.00, 0.16, 0.21, 0.23, 0.14, 0.00 \\ 0.00, 0.00, 0.07, 0.17, 0.19, 0.25, 0.16, 0.23, 0.00, 0.18, 0.15, 0.31, 0.18 \\ 0.24, 0.25, 0.13, 0.17, 0.16, 0.19, 0.22, 0.22, 0.39, 0.35, 0.08, 0.16, 0.31 \end{bmatrix}. \tag{4.1}$$

Set $\theta = v_1, v_2, v_3, v_4, v_5$, $2^\theta = \{\{v_1\}, \{v_2\}, \{v_3\}, \{v_4\}, \{v_5\}, \{v_1, v_2, v_3, v_4, v_5\}\}$. According to D-S combination rule, we can get belief functions of $\{v_1\}$, $\{v_2\}$, $\{v_3\}$, $\{v_4\}$, $\{v_5\}$, $\{v_1, v_2, v_3, v_4, v_5\}$ which are 0.19, 0.45, 0.13, 0.14, 0.08, 0.01, meaning $v_2 \succ v_1 \succ v_4 \succ v_3 \succ v_1$. The belief functions of v_2 is best. According to maximizing principle of belief function, the result of comprehensive benefit evaluation is "better."

In order to validate the proposed evaluation algorithm, three other commonly used algorithms including Fuzzy set theory, Vague set theory, and D-S evidence theory are calculated for comparison. According to Fuzzy set theory and the original index value, the comprehensive evaluation result of hybrid power system is $[v_1, v_2, v_3, v_4, v_5] = [0.2204, 0.2060, 0.1963, 0.1925, 0.1849]$, which means the quality of hybrid power system is "best." According to Vague set theory and the calculated vague index value, the comprehensive evaluation result is $[v_1, v_2, v_3, v_4, v_5]$

Table 1: Comprehensive benefit evaluation index system of hybrid power system.

Evaluation objective	Influence factors	Evaluation indexes	Original index value
Comprehensive benefit	Social benefit	Pulling gross domestic product (I_1)	61.24%
		Improving people's living standard (I_2)	2.99%
		Promoting social employment (I_3)	3.79%
	Environmental benefit	Saving natural resources (I_4)	17.77%
		Reducing environmental pollution (I_5)	6.70%
	Economic benefit	Solvency capacity (I_6)	4.47%
		Operational capacity (I_7)	4%
		Profitability (I_8)	4.50%
		Development capacity (I_9)	5%
	Security	Integrated voltage qualification rate (I_{10})	99.27%
		Grid frequency qualification rate (I_{11})	99.99%
		Average loading rate of provincial grid (I_{12})	80.94%
		Power supply reliability rate (I_{13})	99.81%

= [[0.7517,0.8414][0.8587,0.9067][0.6760,0.7513][0.3368,0.4229][0.1843,0.3045]], the corresponding evaluation value is 0.7966, 0.8827, 0.7137, 0.3799, 0.2444, which means the final evaluation result is "better" and the corresponding evaluation value being 0.8827. According to D-S evidence theory, the belief functions of $\{v_1\}, \{v_2\}, \{v_3\}, \{v_4\}, \{v_5\}, \{v_1, v_2, v_3, v_4, v_5\}$ are 0.19, 0.32, 0.12, 0.16, 0.07, 0.14, which means the result of comprehensive benefit evaluation is "better."

Combine the actual conditions and experts' opinions we know such that the actual comprehensive benefit of hybrid power system in Guangdong province is better, which means that the evaluation results of proposed evaluation model, vague set theory, and D-S evidence theory are all correct but fuzzy set. Therefore we know that fuzzy set has a great limitation in comprehensive evaluation compared to the proposed model. At the same time, the best result of proposed model is 0.45 which is much more than better 0.19 no less than the worst 0.01. Analyze final evaluation result sequence of proposed evaluation model, vague set theory, and D-S evidence theory; it is known that the range of result set of the proposed model is much more apparent than other evaluation algorithms. So the results from different evaluation methods validate that the proposed algorithm based on vague set and D-S evidence theory could obtain satisfying conclusion and decrease uncertainty of decision making.

5. Conclusion

The proportion of clean energy is increasing in recent years. Different power generation models have different advantages and disadvantages. It is of great significance for hybrid power system to evaluate the comprehensive benefits. Analyzing characteristics of hybrid power system, an index system of comprehensive benefit evaluation including economic benefit, environmental benefit, social benefit, and security is established in this paper. Due to advantages of processing abundant uncertain and fuzzy information, vague set is used

to determine the decision matrix. Convert vague decision matrix to real one by vague combination rule and determine uncertain degrees of different indexes by grey incidence analysis, then the mass functions of different comment set in different indexes are obtained. Information can be fused in accordance with the D-S combination rule and the evaluation result is got. A simulation of hybrid power system including thermal power, wind power, and photovoltaic power in China is simulated. In order to validate the proposed evaluation model, three other commonly used algorithms including Fuzzy set theory, Vague set theory, and D-S evidence theory are calculated for comparison. The results illustrate that a satisfying conclusion can be obtained and an obvious decrease can be observed in the uncertainty of decision making compared to other commonly used evaluation methods. The actual implementation results prove that the proposed evaluation algorithm based on vague set and D-S evidence theory is effective and practical to evaluate comprehensive benefit of hybrid power system.

Acknowledgments

This work was partially supported by the Natural Science Foundation of China (71071052, 71201057, 61174058, and 61134001), the National Key Basic Research Program, China (2012CB215202), the 111 Project (B12018), and the Fundamental Research Funds for the Central Universities (12QX22).

References

[1] R. J. Wai and C. Y. Lin, "Active low-frequency ripple control for clean-energy power-conditioning mechanism," *IEEE Transactions on Industrial Electronics*, vol. 57, no. 11, pp. 3780–3792, 2010.

[2] P. D. C. Wijayatunga and D. Prasad, "Clean energy technology and regulatory interventions for Greenhouse Gas emission mitigation: Sri Lankan power sector," *Energy Conversion and Management*, vol. 50, no. 6, pp. 1595–1603, 2009.

[3] A. Esmin and G. Lambert-Torres, "Application of particle swarm optimization to optimal power systems," *International Journal of Innovative Computing, Information and Control*, vol. 8, no. 3A, pp. 1705–1716, 2012.

[4] J. Park, T. Oh, K. Cho et al., "Reliability evaluation of interconnected power systems including wind turbine generators," *International Journal of Innovative Computing, Information and Control*, vol. 8, no. 8, pp. 5797–5808, 2012.

[5] A. Abro and J. Mohamad-Saleh, "Control of power system stability-reviewed solutions based on intelligent systems," *International Journal of Innovative Computing, Information and Control*, vol. 8, no. 10A, pp. 6643–6666, 2012.

[6] P. Tavner, "Wind power as a clean-energy contributor," *Energy Policy*, vol. 36, no. 12, pp. 4397–4400, 2008.

[7] K. Kaygusuz, "Wind power for a clean and sustainable energy future," *Energy Sources, Part B*, vol. 4, no. 1, pp. 122–133, 2009.

[8] A. Nishimura, Y. Hayashi, K. Tanaka et al., "Life cycle assessment and evaluation of energy payback time on high-concentration photovoltaic power generation system," *Applied Energy*, vol. 87, no. 9, pp. 2797–2807, 2010.

[9] K. Morison, L. Wang, and P. Kundur, "Power system security assessment," *IEEE Power and Energy Magazine*, vol. 2, no. 5, pp. 30–39, 2004.

[10] Y. Wei, D. Niu, and G. Wang, "Comprehensive benefit evaluation of thermal-wind-hydraulic power joint operation based on combined weight," *East China Electric Power*, vol. 4, pp. 1–5, 2012.

[11] C. He, F. Kai, and Z. Quan, "et al. Investment evaluation system development based on unified information platform for future smart grid," *Energy Procedia*, vol. 12, pp. 10–17, 2011.

[12] Y. Jing, H. Bai, and J. Wang, "A fuzzy multi-criteria decision-making model for CCHP systems driven by different energy sources," *Energy Policy*, vol. 42, pp. 286–296, 2012.

[13] S. Hu and L. Wang, "A comprehensive analysis of the cogeneration units to the thermal system transformation," *Energy Procedia*, vol. 17, no. B, pp. 1169–1176, 2012.

[14] Q. Sun, X. Ge, L. Liu et al., "Review of smart grid comprehensive assessment systems," *Energy Procedia*, vol. 12, pp. 219–229, 2011.

[15] A. Hepbasli, "A key review on exergetic analysis and assessment of renewable energy resources for a sustainable future," *Renewable and Sustainable Energy Reviews*, vol. 12, no. 3, pp. 593–661, 2008.

[16] R. Laleman, J. Albrecht, and J. Dewulf, "Life cycle analysis to estimate the environmental impact of residential photovoltaic systems in regions with a low solar irradiation," *Renewable and Sustainable Energy Reviews*, vol. 15, no. 1, pp. 267–281, 2011.

[17] G. Shafer, *A Mathematical Theory of Evidence*, Princeton University Press, Princeton, NJ, USA, 1976.

[18] M. Beynon, D. Cosker, and D. Marshall, "An expert system for multi-criteria decision making using Dempster Shafer theory," *Expert Systems with Applications*, vol. 20, no. 4, pp. 357–367, 2001.

[19] S. Le Hégarat-Mascle, D. Richard, and C. Ottlé, "Multi-scale data fusion using Dempster-Shafer evidence theory," *Integrated Computer-Aided Engineering*, vol. 10, no. 1, pp. 9–22, 2003.

[20] V. Kaftandjian, O. Dupuis, D. Babot, and Y. M. Zhu, "Uncertainty modelling using Dempster-Shafer theory for improving detection of weld defects," *Pattern Recognition Letters*, vol. 24, no. 1–3, pp. 547–564, 2003.

[21] S. Fabre, A. Appriou, and X. Briottet, "Presentation and description of two classification methods using data fusion based on sensor management," *Information Fusion*, vol. 2, no. 1, pp. 49–71, 2001.

[22] C. R. Parikh, M. J. Pont, and N. Barrie Jones, "Application of Dempster-Shafer theory in condition monitoring applications: a case study," *Pattern Recognition Letters*, vol. 22, no. 6-7, pp. 777–785, 2001.

[23] P. Wang, N. Propes, N. Khiripet, Y. Li, and G. Vachtsevanos, "Integrated approach to machine fault diagnosis," in *Proceedings of the IEEE Annual Textile, Fiber and Film Industry Technical Conference*, pp. 59–65, Atlanta, Ga, USA, May 1999.

[24] R. W. Jones, A. Lowe, and M. J. Harrison, "A framework for intelligent medical diagnosis using the theory of evidence," *Knowledge-Based Systems*, vol. 15, no. 1-2, pp. 77–84, 2002.

[25] X. Su, P. Shi, L. Wu et al., "A novel approach to filter design for T-S fuzzy discrete-time systems with time-varyingdelay," *IEEE Transactions on Fuzzy Systems*. In press.

[26] Q. Zhou, P. Shi, J. Lu et al., "Adaptive output feedback fuzzy tracking control for a class of nonlinear systems," *IEEE Transactions on Fuzzy Systems*, vol. 19, no. 5, pp. 972–982, 2011.

[27] L. Wu, X. Su, P. Shi, and J. Qiu, "Model approximation for discrete-time state-delay systems in the TS fuzzy framework," *IEEE Transactions on Fuzzy Systems*, vol. 19, no. 2, pp. 366–378, 2011.

[28] L. Wu, X. Su, P. Shi, and J. Qiu, "A new approach to stability analysis and stabilization of discrete-time T-S fuzzy time-varying delay systems," *IEEE Transactions on Systems, Man, and Cybernetics B*, vol. 41, no. 1, pp. 273–286, 2011.

[29] J. Zhang, P. Shi, and Y. Xia, "Robust adaptive sliding-mode control for fuzzy systems with mismatched uncertainties," *IEEE Transactions on Fuzzy Systems*, vol. 18, no. 4, pp. 700–711, 2010.

[30] S. K. Nguang, P. Shi, and S. Ding, "Fault detection for uncertain fuzzy systems: an LMI approach," *IEEE Transactions on Fuzzy Systems*, vol. 15, no. 6, pp. 1251–1262, 2007.

[31] W. L. Gau and D. J. Buehrer, "Vague sets," *IEEE Transactions on Systems, Man and Cybernetics*, vol. 23, no. 2, pp. 610–614, 1993.

[32] X. Geng, X. Chu, and Z. Zhang, "A new integrated design concept evaluation approach based on vague sets," *Expert Systems with Applications*, vol. 37, no. 9, pp. 6629–6638, 2010.

[33] D. Zhang, J. Zhang, K. K. Lai, and Y. Lu, "An novel approach to supplier selection based on vague sets group decision," *Expert Systems with Applications*, vol. 36, no. 5, pp. 9557–9563, 2009.

[34] S. Wan, "Applying interval-value vague set for multi-sensor target recognition," *International Journal of Innovative Computing, Information and Control*, vol. 7, no. 2, pp. 955–963, 2011.

Hindawi Publishing Corporation
Mathematical Problems in Engineering
Volume 2012, Article ID 836814, 18 pages
doi:10.1155/2012/836814

Review Article

Robust Stabilization for Continuous Takagi-Sugeno Fuzzy System Based on Observer Design

Yassine Manai and Mohamed Benrejeb

LA.R.A. Automatic, National Engineering School of Tunis, University of Tunis-ElManar, BP 37 Belvedere, 1002 Tunis, Tunisia

Correspondence should be addressed to Yassine Manai, yacine.manai@gmail.com

Received 30 June 2012; Revised 19 September 2012; Accepted 19 September 2012

Academic Editor: Mohammed Chadli

Copyright © 2012 Y. Manai and M. Benrejeb. This is an open access article distributed under the Creative Commons Attribution License, which permits unrestricted use, distribution, and reproduction in any medium, provided the original work is properly cited.

This paper investigates the influence of a new parallel distributed controller (PDC) on the stabilization region of continuous Takagi-Sugeno (T-S) fuzzy models. Using a nonquadratic Lyapunov function, a new sufficient stabilization criterion is established in terms of linear matrix inequality. The criterion examines the derivative membership function; an approach to determine state variables is given based on observer design. In addition, a stabilization condition for uncertain system is given. Finally, numeric simulation is given to validate the developed approach.

1. Introduction

Fuzzy control systems have experienced a big growth of industrial applications in the recent decades, because of their reliability and effectiveness. Many researches have investigated the Takagi-Sugeno models [1–3] during the last decades. Two classes of Lyapunov functions are used to analyze these systems: quadratic Lyapunov functions and nonquadratic Lyapunov ones which are less conservative than the first class. Many researches have investigated with nonquadratic Lyapunov functions [4–10].

As the information about the time derivatives of membership function is considered by the PDC fuzzy controller, it allows the introduction of slack matrices to facilitate the stability analysis. The relationship between the membership function of the fuzzy model and the fuzzy controllers is used to introduce some slack matrix variables. The boundary information of the membership functions is brought to the stability condition and thus offers some relaxed stability conditions [6]. In order to determine the state variables many approaches of observer design are given [9–11].

In this paper, new stabilization conditions for Takagi-Sugeno uncertain fuzzy models based on the use of fuzzy Lyapunov function are presented. This criterion is expressed in terms of linear matrix inequalities (LMIs) which can be efficiently solved by using various convex optimization algorithms [12, 13]. The presented method is less conservative than existing results.

The organization of the paper is as follows. In Section 2, we present the system description and problem formulation and we give some preliminaries which are needed to derive results. Section 3 will be concerned with stabilization analysis for continuous *T-S* fuzzy systems by the use of new PDC controller based on derivative membership functions. An observer approach design is derived to estimate state variables. In Section 4, a new stabilization condition for uncertain system is given. Next, a new robust PDC controller design approach is presented. Illustrative examples are given in Section 5 for a comparison of previous results to demonstrate the advantage of the proposed method. Finally Section 6 makes the conclusion.

Notation. Throughout this paper, a real symmetric matrix $S > 0$ denotes S being a positive definite matrix. The superscript "T" is used for the transpose of a matrix.

2. System Description and Preliminaries

Consider an uncertain *T-S* fuzzy continuous model for a nonlinear system as follows:

$$\begin{aligned} &\text{IF} \quad z_1(t) \text{ is } M_{i1}, \ldots, z_p(t) \text{ is } M_{ip}, \\ &\text{THEN} \quad \dot{x}(t) = (A_i + \Delta A_i)x(t) + (B_i + \Delta B_i)u(t) \quad i = 1, \ldots, r, \end{aligned} \tag{2.1}$$

where M_{ij} $(i = 1, 2, \ldots, r, j = 1, 2, \ldots, p)$ is the fuzzy set and r is the number of model rules, $x(t) \in \Re^n$ is the state vector, $u(t) \in \Re^m$ is the input vector, $A_i \in \Re^{n\times n}$, $B_i \in \Re^{n\times m}$ are constant real matrices, and $z_1(t), \ldots, z_p(t)$ are known premise variables. ΔA_i, and ΔB_i are time-varying matrices representing parametric uncertainties in the plant model. These uncertainties are admissibly norm-bound and structured.

The final outputs of the fuzzy systems are:

$$\dot{x}(t) = \sum_{i=1}^{r} h_i(z(t))\{(A_i + \Delta A_i)x(t) + (B_i + \Delta B_i)u(t)\}, \tag{2.2}$$

where

$$\begin{aligned} z(t) &= \left[z_1(t) z_2(t) \cdots z_p(t)\right], \\ h_i(z(t)) &= \frac{w_i(z(t))}{\sum_{i=1}^{r} w_i(z(t))}, \\ w_i(z(t)) &= \prod_{j=1}^{p} M_{ij}\left(z_j(t)\right) \quad \forall t. \end{aligned} \tag{2.3}$$

The term $M_{i1}(z_j(t))$ is the grade of membership of $z_j(t)$ in M_{i1}

$$\text{Since} \begin{cases} \sum_{i=1}^{r} w_i(z(t)) \succ 0 \\ w_i(z(t)) \geq 0, \quad i = 1, 2, \ldots, r \end{cases} \quad \text{we have} \begin{cases} \sum_{i=1}^{r} h_i(z(t)) = 1, \\ h_i(z(t)) \geq 0, \quad i = 1, 2, \ldots, r \end{cases} \tag{2.4}$$

for all t.

We have the following property:

$$\sum_{k=1}^{r} \dot{h}_k(z(t)) = 0. \tag{2.5}$$

This study investigates the PDC controller influence on the closed-loop stability region and gives robustness analysis of uncertain Takagi-Sugeno fuzzy system. Thus, we consider a PDC fuzzy controller which examines the derivative membership function and it is given by

$$u(t) = -\sum_{i=1}^{r} h_i(z(t)) F_i x(t) - \sum_{\rho=1}^{r} \dot{h}_\rho(z(t)) \left(K_\rho + R\right) x(t). \tag{2.6}$$

The fuzzy controller design consists to determine the local feedback gains F_i, K_ρ, and R in the consequent parts. The state variables are determined by an observer and are detailed in the next section.

The open-loop system is given by

$$\dot{x}(t) = \sum_{i=1}^{r} h_i(z(t)) (A_i + \Delta A_i) x(t). \tag{2.7}$$

By substituting (2.6) into (2.2), the closed-loop fuzzy system can be represented as:

$$\dot{x}(t) = \sum_{i=1}^{r} \sum_{j=1}^{r} h_i(z(t)) h_j(z(t)) \left\{ A_{\Delta i} - B_{\Delta i} F_j - \sum_{\rho=1}^{r} \dot{h}_\rho(z(t)) B_{\Delta i} \left(K_\rho + R\right) \right\} x(t), \tag{2.8}$$

where $A_{\Delta i} = A_i + \Delta A_i$ and $B_{\Delta i} = B_i + \Delta B_i$.

Assumption 2.1. The time derivative of the premises membership function is upper bound such that $|\dot{h}_k| \leq \phi_k$, for $k = 1, \ldots, r$, where, ϕ_k, $k = 1, \ldots, r$ are given positive constants.

Assumption 2.2. The matrices denote the uncertainties in the system and take the form of

$$\begin{aligned} \Delta A_i &= D_{a_i} F_{a_i}(t) E_{a_i}, \\ \Delta B_i &= D_{b_i} F_{b_i}(t) E_{b_i}, \end{aligned} \tag{2.9}$$

where $D_{a_i}, D_{b_i}, E_{a_i}$, and E_{b_i} are known constant matrices and $F_{a_i}(t)$ and $F_{b_i}(t)$ are unknown matrix functions satisfying:

$$\begin{aligned} F_{a_i}^T(t)F_{a_i}(t) &\leq I, \quad \forall t, \\ F_{b_i}^T(t)F_{b_i}(t) &\leq I, \quad \forall t, \end{aligned} \tag{2.10}$$

where I is an appropriately dimensioned identity matrix.

Lemma 2.3 (Boyd et al. Schur complement [12]). *Given constant matrices Ω_1, Ω_2, and Ω_3 with appropriate dimensions, where $\Omega_1 = \Omega_1^T$ and $\Omega_2 = \Omega_2^T$, then*

$$\Omega_1 + \Omega_3^T \Omega_2^{-1} \Omega_3 \prec 0 \tag{2.11}$$

if and only if

$$\begin{bmatrix} \Omega_1 & \Omega_3^T \\ & -\Omega_2 \end{bmatrix} \succ 0 \quad \text{or} \quad \begin{bmatrix} -\Omega_2 & \Omega_3 \\ & \Omega_1 \end{bmatrix} \succ 0. \tag{2.12}$$

Lemma 2.4 (Peterson and Hollot [2]). *Let $Q = Q^T, H, E$, and $F(t)$ satisfying $F^T(t)F(t) \leq I$ are appropriately dimensional matrices then the following inequality*

$$Q + HF(t)E + E^T F^T(t) H^T \prec 0 \tag{2.13}$$

is true, if and only if the following inequality holds for any $\lambda \succ 0$

$$Q + \lambda^{-1} H H^T + \lambda E^T E \prec 0. \tag{2.14}$$

The aim of the next section is to find conditions for the stabilization of the closed-loop *T-S* fuzzy system by using the Lyapunov theory.

3. Main Results

Consider the closed-loop system without uncertainties

$$\dot{x}(t) = \sum_{i=1}^{r} h_i(z(t)) \{ A_i x(t) + B_i u(t) \}. \tag{3.1}$$

In order to give stability conditions, the slack matrix variables and the membership function boundary Mozelli et al. [14] are used. Consider the following null product that will serve stability analysis purposes:

$$2\left[x^T(t)M + \dot{x}^T(t)\mu M \right] \times \left[\dot{x}(t) - \sum_{i=1}^{r} h_i(z(t)) \{ A_i x(t) + B_i u(t) \} \right] = 0. \tag{3.2}$$

3.1. A PDC Controller with Derivative Membership Function

By substituting (2.6) into (3.1), the closed-loop fuzzy system can be represented as:

$$\dot{x}(t) = \sum_{i=1}^{r}\sum_{j=1}^{r} h_i(z(t))h_j(z(t))\left\{A_i - B_iF_j - \sum_{m=1}^{r}\dot{h}_m(z(t))B_i(K_m + R)\right\}x(t). \tag{3.3}$$

The next Theorem gives sufficient conditions to guarantee stability of system (3.3).

Theorem 3.1. *Under Assumptions 2.1 and 2.2, and for $\mu \succ 0$, $\varepsilon \geq 0$, the Takagi-Sugeno fuzzy system* (3.1) *is stabilizable with the PDC controller* (2.6)*, with gains given by $F_i = S_i^T H^{-T}$, $K_\rho = V_\rho^T H^{-T}$, and $R = V^T H^{-T}$, if there exist positive definite symmetric matrices T_k, $k = 1, 2, \ldots, r$, Υ, and any matrices H, S_i, V_ρ, and V with appropriate dimensions such that the following LMIs hold.*

$$\begin{gathered} T_i \succ 0, \\ T_i + \Upsilon \succ 0 \quad (i = 1, 2, \ldots, r), \\ \Lambda_{ii} \prec 0, \\ \overline{\Lambda}_{ij} \prec 0, \end{gathered} \tag{3.4}$$

$$\overline{\Lambda}_{ij} = \Lambda_{ij} + \Lambda_{ji}, \tag{3.5}$$

where

$$\begin{gathered} \Lambda_{ij} = \begin{bmatrix} T_\phi - A_iH^T - HA_i^T + B_iS_j^T + S_jB_i^T + B_i\overline{V}_\phi^T + \overline{V}_\phi B_i^T & * \\ T_i - \mu\left(A_iH^T - B_iS_j^T - B_i\overline{V}_\phi^T\right) + H & \mu\left(H^T + H\right) \end{bmatrix}, \\ \overline{V}_\phi = \sum_{\rho=1}^{r}\phi_\rho\left(V_\rho^T + V^T\right), \\ \overline{T}_\phi = \sum_{k=1}^{r}\phi_k(T_k + \Upsilon). \end{gathered} \tag{3.6}$$

Proof of Theorem 3.1. Let's consider the fuzzy weighting-dependent Lyapunov-Krasovskii functional as:

$$V(x(t)) = \sum_{k=1}^{r} h_k(z(t)) \cdot V_k(x(t)), \tag{3.7}$$

with $V_k(x(t)) = x^T(t)(P_k + \varepsilon X)x(t)$, $k = 1, 2, \ldots, r$, where $P_k = P_k^T$, $X = X^T$, $\varepsilon \geq 0$, and $(P_k + \varepsilon X) \geq 0$.

This candidate Lyapunov function satisfies

(i) $V(x(t))$ is C^1,

(ii) $V(0) = 0$ and $V(x(t)) \geq 0$ for $x(t) \neq 0$,

(iii) $\|x(t)\| \to \infty \Rightarrow V(x(t)) \to \infty$.

The time derivative of $V(x(t))$ is given by:

$$\dot{V}(x(t)) = \sum_{k=1}^{r} \dot{h}_k(z(t)) V_k(x(t)) + \sum_{k=1}^{r} h_k(z(t)) \dot{V}_k(x(t)). \tag{3.8}$$

Adding the null product, then

$$\begin{aligned} \dot{V}(x(t)) = {} & \sum_{k=1}^{r} \dot{h}_k(z(t)) V_k(x(t)) + \sum_{k=1}^{r} h_k(z(t)) \dot{V}_k(x(t)) + 2\left[x^T(t)M + \dot{x}^T(t)\mu M\right] \\ & \times \left[\dot{x}(t) - \sum_{i=1}^{r}\sum_{j=1}^{r} h_i(z(t)) h_j(z(t)) \left\{ A_i - B_i F_j - \sum_{\rho=1}^{r} \dot{h}_\rho(z(t)) B_i (K_\rho + R) \right\} x(t)\right]. \end{aligned} \tag{3.9}$$

Equation (3.9) can be rewritten as,

$$\dot{V}(x(t)) = \Upsilon_1(x, z) + \Upsilon_2(x, z), \tag{3.10}$$

where

$$\begin{aligned} \Upsilon_1(x, z) = {} & x^T(t)\left(\sum_{k=1}^{r} \dot{h}_k(z(t)) \cdot (P_k + \varepsilon X)\right) x(t) + 2\left[x^T(t)M + \dot{x}^T(t)\mu M\right] \\ & \times \left[\sum_{i=1}^{r}\sum_{\rho=1}^{r} h_i(z(t)) \dot{h}_\rho(z(t)) B_i (K_\rho + R) x(t)\right], \\ \Upsilon_2(x, z) = {} & \sum_{i=1}^{r} h_i(z(t)) \left\{2x^T(t)(P_i + \varepsilon X)\dot{x}(t)\right\} + 2\left[x^T(t)M + \dot{x}^T(t)\mu M\right] \\ & \times \left[\dot{x}(t) - \sum_{i=1}^{r}\sum_{j=1}^{r} h_i(z(t)) h_j(z(t)) \left\{A_i - B_i F_j\right\} x(t)\right]. \end{aligned} \tag{3.11}$$

Then, based on Assumption 2.1, an upper bound of $\Upsilon_1(x, z)$ is obtained as:

$$\begin{aligned} \Upsilon_1(x, z) \leq \sum_{i=1}^{r} h_i(z(t)) \Bigg\{ & \sum_{k=1}^{r} \phi_k \cdot x(t)^T (P_k + \varepsilon X) x(t) + 2\left[x^T(t)M + \dot{x}^T(t)\mu M\right] \\ & \times \left[\sum_{\rho=1}^{r} \phi_\rho B_i (K_\rho + R) x(t)\right] \Bigg\}. \end{aligned} \tag{3.12}$$

Based on (2.5), it follows that $\sum_{k=1}^{r} \dot{h}_k(z(t))(1-\varepsilon)X = 0$ where X is any symmetric matrix of proper dimension.

Suppose that $\overline{X} = \sum_{k=1}^{r} \dot{h}_k(z(t))(1-\varepsilon)X$ and adding $\overline{X}$ to (3.12), then

$$\begin{aligned}\Upsilon_1(x,z) &\le \sum_{i=1}^{r} h_i(z(t)) \left\{ \sum_{k=1}^{r} \phi_k \cdot x(t)^T (P_k + X) x(t) + 2\left[x^T(t)M + \dot{x}^T(t)\mu M\right] \right. \\ &\qquad \left. \times \left[\sum_{\rho=1}^{r} \phi_\rho B_i (K_\rho + R) x(t) \right] \right\} \\ &= \sum_{i=1}^{r} h_i(z(t)) \left\{ x(t)^T \overline{P}_\phi x(t) + 2x^T(t) M \cdot B_i \overline{K}_\phi x(t) + 2\dot{x}^T(t)\mu M \cdot B_i \overline{K}_\phi x(t) \right\},\end{aligned} \tag{3.13}$$

where

$$\overline{P}_\phi = \sum_{k=1}^{r} \phi_k \cdot (P_k + X), \qquad \overline{K}_\phi = \sum_{\rho=1}^{r} \phi_\rho (K_\rho + R). \tag{3.14}$$

Then,

$$\begin{aligned}\dot{V}(x(t)) &\le \sum_{i=1}^{r}\sum_{j=1}^{r} h_i(z(t)) h_j(z(t)) \\ &\quad \times \left\{ x(t)^T \overline{P}_\phi x(t) + 2x^T(t) M \cdot B_i \overline{K}_\phi x(t) + 2\dot{x}^T(t)\mu M \cdot B_i \overline{K}_\phi x(t) \right. \\ &\qquad + 2x^T(t)(P_i + \varepsilon R)\dot{x}(t) + 2x^T(t) M \dot{x}(t) + 2\dot{x}^T(t)\mu M \dot{x}(t) \\ &\qquad \left. -2x^T(t) M (A_i - B_i F_j) x(t) - 2\dot{x}^T(t)\mu M (A_i - B_i F_j) x(t) \right\}.\end{aligned} \tag{3.15}$$

Using vector $\eta^T = [x^T(t) \quad \dot{x}^T(t)]^T$, (3.15) can be rewritten as

$$\begin{aligned}\dot{V}(x(t)) &\le \sum_{i=1}^{r}\sum_{j=1}^{r} h_i(z(t)) h_j(z(t)) \eta^T \Xi_{ij} \eta \\ &= \sum_{i=1}^{r} h_i^2(z(t)) \eta^T \Xi_{ii} \eta + \sum_{i=1}^{r}\sum_{i<j} h_i(z(t)) h_j(z(t)) \eta^T (\Xi_{ij} + \Xi_{ji}) \eta,\end{aligned} \tag{3.16}$$

where

$$\Xi_{ij} = \begin{bmatrix} \left\{ \overline{P}_\phi - M\left(A_i - B_i F_j - B_i \overline{K}_\phi\right) - \left(A_i - B_i F_j - B_i \overline{K}_\phi\right)^T M^T \right\} & * \\ (P_i + \varepsilon X) - \mu M\left(A_i - B_i F_j - B_i \overline{K}_\phi\right) + M^T & \mu(M + M^T) \end{bmatrix}. \tag{3.17}$$

If $\Xi_{ii} \prec 0$ and $(\Xi_{ij} + \Xi_{ji}) \prec 0$, then $\dot{V}(x(t)) \prec 0$ and (3.3) is stable. Pre- and post-multiplying $\Xi_{ii} \prec 0$ and $(\Xi_{ij} + \Xi_{ji}) \prec 0$ by nonsingular matrices $\mathrm{diag}(M^{-1}, M^{-1})$ and $\mathrm{diag}(M^{-T}, M^{-T})$, respectively, and pre- and postmultiplying by M^{-1} and M^{-T}, respectively, then we obtain

$$\begin{gathered} M^{-1}(P_i + \varepsilon X)M^{-T} \succ 0 \quad (i = 1, 2, \ldots, r), \\ M^{-1}(P_i + X)M^{-T} \succ 0 \quad (i = 1, 2, \ldots, r), \\ \Lambda_{ii} \prec 0 \quad (i = 1, 2, \ldots, r), \\ \overline{\Lambda}_{ij} \prec 0 \quad (i \prec= 1, 2, \ldots, r), \end{gathered} \tag{3.18}$$

where $\overline{\Lambda}_{ij} = \Lambda_{ij} + \Lambda_{ji}$, and

$$\Lambda_{ij} = \begin{bmatrix} \left\{ M^{-1}\overline{P}_\phi M^{-T} - \left(A_i - B_i F_j - B_i \overline{K}_\phi\right) M^{-T} \right. & \\ \left. -M^{-1}\left(A_i - B_i F_j - B_i \overline{K}_\phi\right)^T \right\} & * \\ \left\{ M^{-1}(P_i + \varepsilon X)M^{-T} - \mu\left(A_i - B_i F_j - B_i \overline{K}_\phi\right) M^{-T} + M^{-1} \right\} & \mu(M^{-T} + M^{-1}) \end{bmatrix} \tag{3.19}$$

for the following variables definition:

$$\begin{gathered} H = M^{-1}, \qquad T_i = H(P_i + \varepsilon X)H^T, \qquad T_\phi = H\overline{P}_\phi H^T, \qquad S_j = HF_j^T, \\ V_j = HK_\rho^T, \qquad V = HR^T, \qquad Y = HXH^T. \end{gathered} \tag{3.20}$$

If LMI in (3.4) holds then the closed-loop continuous fuzzy system (3.3) is asymptotically stable. The control gains are given by $F_i = S_i^T H^{-T}$, $K_\rho = V_\rho^T H^{-T}$, and $R = V^T H^{-T}$. This completes the proof. □

Remark 3.2. The selection of ϕ_k given in Assumption 2.1 is performed by using a simple procedure given in [15] .

Remark 3.3. The major contribution of the Theorem 3.1 is represented by the proposed PDC controller given by (2.6). The contribution appears in the gains $(K_\rho + R)$ introduced in the controller term based on derivative membership functions. The stabilization condition proposed is less conservative than some of those in the literature, as is shown in the example below.

3.2. Observer Design

In order to determine state variables of the system, this section gives a solution by the means of fuzzy observer design. The following condition is to be satisfied by the observer:

$$x(t) - \hat{x}(t) \longrightarrow 0 \quad \text{as } t \longrightarrow \infty, \tag{3.21}$$

where $\hat{x}(t)$ denotes the state vector estimated by a fuzzy observer. This condition guarantees that the steady-state error between $x(t)$ and $\hat{x}(t)$ converge to 0 and we denote this error by $e(t) = x(t) - \hat{x}(t)$.

A stabilizing observer-based controller can be formulated as follow:

$$\begin{gathered}\dot{\hat{x}}(t) = \sum_{j=1}^{r} h_i(z(t))\left\{A_i\hat{x}(t) + B_i u(t) + L_j\left(C_i\hat{x}(t) - y(t)\right)\right\}, \\ y(t) = -\sum_{i=1}^{r} h_i(z(t))C_i\hat{x}(t),\end{gathered} \tag{3.22}$$

where $y(t)$ denotes the output vector.

We consider the proposed PDC controller given by (2.6):

$$u(t) = -\sum_{i=1}^{r} h_i(z(t))F_i\hat{x}(t) - \sum_{\rho=1}^{r}\dot{h}_\rho(z(t))\left(K_\rho + R\right)\hat{x}(t). \tag{3.23}$$

Replacing the fuzzy controller (2.6) in fuzzy observer (3.22) we obtain the closed-loop fuzzy system as:

$$\begin{aligned}\dot{x}(t) &= \sum_{i=1}^{r}\sum_{j=1}^{r} h_i(z(t))h_j(z(t))\left\{\left(A_i - B_iF_j\right) - \sum_{\rho=1}^{r}\dot{h}_\rho(z(t))\left(K_\rho + R\right)\right\}x(t) \\ &\quad + \sum_{i=1}^{r}\sum_{j=1}^{r} h_i(z(t))h_j(z(t))\left\{B_iF_j + \sum_{\rho=1}^{r}\dot{h}_\rho(z(t))\left(K_\rho + R\right)\right\}e(t) \\ \dot{e}(t) &= \sum_{i=1}^{r}\sum_{j=1}^{r} h_i(z(t))h_j(z(t))\left\{A_i - L_iC_j\right\}e(t).\end{aligned} \tag{3.24}$$

The augmented system is represented as follows:

$$\begin{aligned}\dot{x}_a(t) &= \sum_{i=1}^{r}\sum_{j=1}^{r} h_i(z(t))h_j(z(t))\widetilde{G}_{ij}x_a(t) \\ &= \sum_{j=1}^{r} h_i(z(t))h_j(z(t))\widetilde{G}_{ii}x_a(t) + 2\sum_{i=1}^{r}\sum_{i<j}^{r} h_i(z(t))h_j(z(t))\left\{\frac{\widetilde{G}_{ij} + \widetilde{G}_{ji}}{2}\right\}x_a(t),\end{aligned} \tag{3.25}$$

where

$$x_a(t) = \begin{bmatrix} x(t) \\ e(t) \end{bmatrix},$$
$$\widetilde{G}_{ij} = \begin{bmatrix} A_i - B_iF_j - \sum_{\rho=1}^{r} \dot{h}_\rho B_i(K_\rho + R) & B_iF_j + \sum_{\rho=1}^{r} \dot{h}_\rho B_i(K_\rho + R) \\ 0 & A_i - L_iC_j \end{bmatrix}. \tag{3.26}$$

By applying Theorem 1 in [16] in the augmented system (3.25) we derive the following Theorem.

Theorem 3.4. *Under Assumptions 2.1 and 2.2, and for $0 \le \mu \le 1$, the Takagi-Sugeno fuzzy system* (3.1) *is stable if there exist positive definite symmetric matrices P_k, $k = 1, 2, \ldots, r$, and R, matrices $F_1, \ldots, F_r$ such that the following LMIs holds.*

$$P_k + R \succ 0, \quad k \in \{1, \ldots, r\},$$
$$P_j + \mu R \ge 0, \quad j = 1, 2, \ldots, r,$$
$$P_\phi + \left\{ \widetilde{G}_{ii}^T (P_k + \mu R) + (P_k + \mu R) \widetilde{G}_{ii} \right\} \prec 0, \quad i, k \in \{1, \ldots, r\},$$
$$\left\{ \frac{\widetilde{G}_{ij} + \widetilde{G}_{ji}}{2} \right\}^T (P_k + \mu R) + (P_k + \mu R) \left\{ \frac{\widetilde{G}_{ij} + \widetilde{G}_{ji}}{2} \right\} \prec 0, \quad \text{for } i, j, k = 1, 2, \ldots, r \text{ such that } i \prec j, \tag{3.27}$$

where

$$\widetilde{G}_{ij} = \begin{bmatrix} A_i - B_iF_j - \sum_{\rho=1}^{r} \dot{h}_\rho B_i(K_\rho + R) & B_iF_j + \sum_{\rho=1}^{r} \dot{h}_\rho B_i(K_\rho + R) \\ 0 & A_i - L_iC_j \end{bmatrix},$$
$$P_\phi = \sum_{k=1}^{r} \phi_k (P_k + R). \tag{3.28}$$

Proof of Theorem 3.4. The result follows immediately from the proof of Theorem 1 in [16]. □

4. Robust Stability Condition with PDC Controller

Consider the uncertain closed-loop system (2.8). A sufficient robust stability condition is given as follows.

Theorem 4.1. *Under Assumptions 2.1 and 2.2, and for $\mu \succ 0$, $\varepsilon \ge 0$, the Takagi-Sugeno fuzzy system* (2.2) *is stabilizable with the PDC controller* (2.6)*, with gains given by $F_i = S_i^T H^{-T}$, $K_\rho = V_\rho^T H^{-T}$,*

and $R = V^T H^{-T}$, if there exist positive definite symmetric matrices $T_k,\ k = 1, 2, \ldots, r,\ \Upsilon$, and any matrices H, S_i, V_ρ, and V with appropriate dimensions such that the following LMIs hold.

$$\begin{gathered} T_i \succ 0, \\ T_i + \Upsilon \succ 0 \quad (i = 1, 2, \ldots, r), \\ \sum_{ii} \prec 0, \\ \overline{\sum_{ij}} \prec 0, \end{gathered} \tag{4.1}$$

$$\begin{gathered} \overline{\sum_{ij}} = \sum_{ij} + \sum_{ji}, \\ T_\phi = \sum_{k=1}^{r} \phi_k (T_k + \Upsilon), \end{gathered} \tag{4.2}$$

where

$$\Sigma_{ij} = \begin{bmatrix} \Phi_{11} & \Phi_{12} & MD_{ai} & MD_{bi} & E_{a_i}^T & -\left(E_{bi}\left(F_i + \overline{K}_\phi\right)\right)^T \\ & \Phi_{22} & \mu MD_{ai} & \mu MD_{bi} & 0 & 0 \\ & * & -\lambda I & 0 & 0 & 0 \\ & * & * & -\lambda I & 0 & 0 \\ & * & * & * & -\lambda^{-1} I & 0 \\ & * & * & * & * & -\lambda^{-1} I \end{bmatrix}, \tag{4.3}$$

with

$$\begin{gathered} \Phi_{11} = \overline{P}_\phi + \left[M \cdot B_i \overline{K}_\phi + \overline{K}_\phi^T B_i^T M\right] - \left[M G_{ii} + G_{ii}{}^T M^T\right], \\ \Phi_{12} = (P_i + \varepsilon X) - \mu\left(G_{ii} - B_i \overline{K}_\phi\right)^T M^T + M, \\ \Phi_{22} = \mu\left(M + M^T\right), \end{gathered} \tag{4.4}$$

where $G_{ij} = A_i - B_i F_j$, $G_{ii} = A_i - B_i F_i$, and $P_\phi = \sum_{k=1}^{r} \phi_k (P_k + R)$.

Proof. [Proof of Theorem 4.1] The result follows immediately from the proof of Theorem 3.1 by replacing in the matrix inequality A_i with $A_i + D_{ai}F(t)E_{ai}$ and B_i with $B_i + D_{bi}F(t)E_{bi}$, we obtain the following inequality:

$$\begin{aligned}
\dot{V}(x(t)) \leq \sum_{i=1}^{r}\sum_{j=1}^{r} & h_i(z(t))h_j(z(t)) \\
& \times \Bigg\{ x(t)^T \overline{P}_\phi x(t) + 2x^T(t)M \cdot B_i\overline{K}_\phi x(t) + 2\dot{x}^T(t)\mu M \cdot B_i\overline{K}_\phi x(t) \\
& \quad + 2x^T(t)(P_i + \varepsilon R)\dot{x}(t) + 2x^T(t)M\dot{x}(t) + 2\dot{x}^T(t)\mu M\dot{x}(t) \\
& \quad - 2x^T(t)M\left(A_i - B_iF_j\right)x(t) - 2x^T(t)M \\
& \quad \times \left(\begin{bmatrix} D_{ai} & D_{bi} \end{bmatrix} \begin{bmatrix} F_{a_i}(t) & 0 \\ 0 & F_{b_i}(t) \end{bmatrix} \begin{bmatrix} E_{ai} \\ -E_{bi}\left(F_j + \overline{K}_\phi\right) \end{bmatrix} \right) x(t) \\
& \quad - 2\dot{x}^T(t)\mu M\left(A_i - B_iF_j\right)x(t) - 2\dot{x}^T(t)\mu M \\
& \quad \times \left(\begin{bmatrix} D_{ai} & D_{bi} \end{bmatrix} \begin{bmatrix} F_{a_i}(t) & 0 \\ 0 & F_{b_i}(t) \end{bmatrix} \begin{bmatrix} E_{ai} \\ -E_{bi}\left(F_j + \overline{K}_\phi\right) \end{bmatrix} \right) x(t) \Bigg\}.
\end{aligned} \tag{4.5}$$

Using vector $\eta^T = \left[x^T(t) \quad \dot{x}^T(t)\right]^T$, (4.5) can be rewritten as

$$\begin{aligned}
\dot{V}(x(t)) &\leq \sum_{i=1}^{r}\sum_{j=1}^{r} h_i(z(t))h_j(z(t))\eta^T\widetilde{\Xi}_{ij}\eta \\
&= \sum_{i=1}^{r} h_i^2(z(t))\eta^T\widetilde{\Xi}_{ii}\eta + \sum_{i=1}^{r}\sum_{i<j} h_i(z(t))h_j(z(t))\eta^T\left(\widetilde{\Xi}_{ij} + \widetilde{\Xi}_{ji}\right)\eta,
\end{aligned} \tag{4.6}$$

where

$$\widetilde{\Xi}_{ij} = \Xi_{ij} + \begin{bmatrix} \left\{ \begin{array}{l} M\left(\begin{bmatrix} D_{ai} & D_{bi} \end{bmatrix} \begin{bmatrix} F_{a_i}(t) & 0 \\ 0 & F_{b_i}(t) \end{bmatrix} \begin{bmatrix} E_{ai} \\ -E_{bi}\left(F_j + \overline{K}_\phi\right) \end{bmatrix} \right) \\ + \left(\begin{bmatrix} D_{ai} & D_{bi} \end{bmatrix} \begin{bmatrix} F_{a_i}(t) & 0 \\ 0 & F_{b_i}(t) \end{bmatrix} \begin{bmatrix} E_{ai} \\ -E_{bi}\left(F_j + \overline{K}_\phi\right) \end{bmatrix} \right)^T M^T \end{array} \right\} & * \\ \mu M\left(\begin{bmatrix} D_{ai} & D_{bi} \end{bmatrix} \begin{bmatrix} F_{a_i}(t) & 0 \\ 0 & F_{b_i}(t) \end{bmatrix} \begin{bmatrix} E_{ai} \\ -E_{bi}\left(F_j + \overline{K}_\phi\right) \end{bmatrix} \right) & 0 \end{bmatrix},$$

$$\begin{aligned}
\widetilde{\Xi}_{ij} = \Xi_{ij} &+ \begin{bmatrix} M\begin{bmatrix} D_{ai} & D_{bi} \end{bmatrix} \\ \mu M\begin{bmatrix} D_{ai} & D_{bi} \end{bmatrix} \end{bmatrix} \begin{bmatrix} F_{a_i}(t) & 0 \\ 0 & F_{b_i}(t) \end{bmatrix} \begin{bmatrix} E_{ai} & 0 \\ -E_{bi}\left(F_j + \overline{K}_\phi\right) & 0 \end{bmatrix} \\
&+ \begin{bmatrix} E_{a_i}^T & -\left(E_{bi}\left(F_j + \overline{K}_\phi\right)\right)^T \\ 0 & 0 \end{bmatrix} \begin{bmatrix} F_{a_i}(t) & 0 \\ 0 & F_{b_i}(t) \end{bmatrix}^T \begin{bmatrix} D_{a_i}^T M^T & \mu D_{a_i}^T M^T \\ D_{b_i}^T M^T & \mu D_{b_i}^T M^T \end{bmatrix}.
\end{aligned} \tag{4.7}$$

Then, based on Lemma 2.4, an upper bound of $\widetilde{\Xi}_{ij}$ obtained as:

$$\begin{aligned}\widetilde{\Xi}_{ij} &= \Xi_{ij} + \lambda^{-1} M \begin{bmatrix} D_{ai} & D_{bi} \\ \mu D_{ai} & \mu D_{bi} \end{bmatrix} \begin{bmatrix} D_{a_i}^T & \mu D_{a_i}^T \\ D_{b_i}^T & \mu D_{b_i}^T \end{bmatrix} M^T \\ &\quad + \lambda \begin{bmatrix} E_{a_i}^T & -\left(E_{bi}\left(F_j + \overline{K}_\phi\right)\right)^T \\ 0 & 0 \end{bmatrix} \begin{bmatrix} E_{ai} & 0 \\ -E_{bi}\left(F_j + \overline{K}_\phi\right) & 0 \end{bmatrix} \prec 0\end{aligned} \tag{4.8}$$

by Schur complement, we obtain,

$$\begin{bmatrix} \Phi_{11} & \Phi_{12} & MD_{ai} & MD_{bi} & E_{a_i}^T & -\left(E_{bi}\left(F_j + \overline{K}_\phi\right)\right)^T \\ & \Phi_{22} & \mu MD_{ai} & \mu MD_{bi} & 0 & 0 \\ & * & -\lambda I & 0 & 0 & 0 \\ & * & * & -\lambda I & 0 & 0 \\ & * & * & * & -\lambda^{-1} I & 0 \\ & * & * & * & * & -\lambda^{-1} I \end{bmatrix} \prec 0, \tag{4.9}$$

with

$$\begin{aligned}\Phi_{11} &= \overline{P}_\phi + \left[M \cdot B_i \overline{K}_\phi + \overline{K}^T{}_\phi B_i^T M\right] - \left[M\left(A_i - B_i F_j\right) + \left(A_i - B_i F_j\right)^T M^T\right], \\ \Phi_{12} &= \left(P_i + \varepsilon X\right) - \mu\left(A_i - B_i F_j - B_i \overline{K}_\phi\right)^T M^T + M, \\ \Phi_{22} &= \mu\left(M + M^T\right).\end{aligned} \tag{4.10}$$

If the LMI (4.1) holds then the system (2.8) is stable. This completes the proof. □

The following theorem gives sufficient conditions for robust PDC controller design.

Theorem 4.2. *Under Assumptions 2.1 and 2.2, and for $\mu \succ 0$, $\varepsilon \geq 0$, the Takagi-Sugeno robust fuzzy system* (2.2) *is stabilizable with the PDC controller* (2.6)*, with gains given by $F_i = \widetilde{S}_i^T \widetilde{H}^{-T}$,*

$K_\rho = \tilde{V}_\rho^T \widetilde{H}^{-T}$, and $R = \tilde{V}^T \widetilde{H}^{-T}$, if there exist positive definite symmetric matrices $\tilde{T}_k$, $k = 1, 2, \ldots, r$, $\tilde{Y}$, and any matrices $\widetilde{H}, \tilde{S}_i, \tilde{V}_\rho$, and $\tilde{V}$ with appropriate dimensions such that the following LMIs hold.

$$\begin{gathered}
\tilde{T}_i \succ 0, \\
\tilde{T}_i + \tilde{Y} \succ 0 \quad (i = 1, 2, \ldots, r), \\
\tilde{\Lambda}_{ii} \prec 0, \\
\overline{\tilde{\Lambda}}_{ij} \prec 0,
\end{gathered} \tag{4.11}$$

$$\begin{gathered}
\overline{\tilde{\Lambda}}_{ij} = \tilde{\Lambda}_{ij} + \tilde{\Lambda}_{ji}, \\
\tilde{T}_\phi = \sum_{k=1}^{r} \phi_k \left(\tilde{T}_k + \tilde{Y} \right), \\
\tilde{\overline{V}}_\phi = \sum_{\rho=1}^{r} \phi_\rho \left(\tilde{V}_\rho^T + \tilde{V}^T \right),
\end{gathered} \tag{4.12}$$

where

$$\tilde{\Lambda}_{ij} = \begin{bmatrix} \tilde{\Phi}_{11} & \tilde{\Phi}_{12} & D_{ai} & D_{bi} & HE_{a_i}^T & -\tilde{S}_j E_{bi}^T - \tilde{\overline{V}}_\phi E_{bi}^T \\ & \tilde{\Phi}_{22} & \mu D_{ai} & \mu D_{bi} & 0 & 0 \\ & * & -\lambda I & 0 & 0 & 0 \\ & * & * & -\lambda I & 0 & 0 \\ & * & * & * & -\lambda^{-1} I & 0 \\ & * & * & * & * & -\lambda^{-1} I \end{bmatrix}, \tag{4.13}$$

with

$$\begin{gathered}
\tilde{\Phi}_{11} = \tilde{T}_\phi - A_i \widetilde{H}^T - \widetilde{H} A_i^T + B_i \tilde{S}_j^T + \tilde{S}_j B_i^T + B_i \tilde{\overline{V}}_\phi^T + \tilde{\overline{V}}_\phi B_i^T, \\
\tilde{\Phi}_{12} = \tilde{T}_i - \mu \left(A_i \widetilde{H}^T - B_i \tilde{S}_j^T - B_i \tilde{\overline{V}}_\phi^T \right) + \widetilde{H}, \\
\tilde{\Phi}_{22} = \mu \left(H^T + H \right).
\end{gathered} \tag{4.14}$$

Proof of Theorem 4.2. Consider (4.8) and pre- and postmultiplying by M^{-1} and M^{-T}, respectively, then we obtain

$$\begin{aligned}
\tilde{\Lambda}_{ij} = \Lambda_{ij} &+ \lambda^{-1} \begin{bmatrix} D_{ai} & D_{bi} \\ \mu D_{ai} & \mu D_{bi} \end{bmatrix} \begin{bmatrix} D_{a_i}^T & \mu D_{a_i}^T \\ D_{b_i}^T & \mu D_{b_i}^T \end{bmatrix} \\
&+ \lambda M^{-1} \begin{bmatrix} E_{a_i}^T & -\left(E_{bi} \left(F_j + \overline{K}_\phi \right) \right)^T \\ 0 & 0 \end{bmatrix} \begin{bmatrix} E_{ai} & 0 \\ -E_{bi} \left(F_j + \overline{K}_\phi \right) & 0 \end{bmatrix} M^{-T} \prec 0,
\end{aligned} \tag{4.15}$$

with Λ_{ij} defined by (3.5).

By Schur complement, we obtain,

$$\begin{bmatrix} \widetilde{\Phi}_{11} & \widetilde{\Phi}_{12} & D_{ai} & D_{bi} & M^{-1}E_{a_i}^T & -M^{-1}\left(E_{bi}\left(F_j+\overline{K}_\phi\right)\right)^T \\ & \widetilde{\Phi}_{22} & \mu D_{ai} & \mu D_{bi} & 0 & 0 \\ & * & -\lambda I & 0 & 0 & 0 \\ & * & * & -\lambda I & 0 & 0 \\ & * & * & * & -\lambda^{-1}I & 0 \\ & * & * & * & * & -\lambda^{-1}I \end{bmatrix} \prec 0, \tag{4.16}$$

with

$$\begin{gathered} \widetilde{\Phi}_{11} = M^{-1}\overline{P}_\phi M^{-T} - \left(A_i - B_iF_j - B_i\overline{K}_\phi\right)M^{-T} - M^{-1}\left(A_i - B_iF_j - B_i\overline{K}_\phi\right)^T, \\ \widetilde{\Phi}_{12} = M^{-1}(P_i+\varepsilon X)M^{-T} - \mu\left(A_i - B_iF_j - B_i\overline{K}_\phi\right)M^{-T} + M^{-1}, \\ \widetilde{\Phi}_{22} = \mu\left(M^{-T}+M^{-1}\right) \end{gathered} \tag{4.17}$$

for the following variables definition:

$$\begin{gathered} \widetilde{H} = M^{-1}, \qquad \widetilde{T}_i = \widetilde{H}(P_i+\varepsilon X)\widetilde{H}^T, \qquad \widetilde{T}_\phi = \widetilde{H}\overline{P}_\phi\widetilde{H}^T, \\ \widetilde{S}_j = \widetilde{H}F_j^T, \qquad \widetilde{V}_j = \widetilde{H}K_\rho^T, \qquad \widetilde{V} = \widetilde{H}R^T, \qquad \widetilde{Y} = \widetilde{H}X\widetilde{H}^T. \end{gathered} \tag{4.18}$$

If LMI in (4.11) holds then the closed-loop continuous fuzzy system (2.8) is asymptotically stable.

The control gains are given by $F_i = \widetilde{S}_i^T\widetilde{H}^{-T}$, $K_\rho = \widetilde{V}_\rho^T\widetilde{H}^{-T}$, and $R = \widetilde{V}^T\widetilde{H}^{-T}$. This completes the proof. □

5. Numerical Examples

In order to show the improvements of the proposed approaches over some existing results, in this section, we present a numerical example in which we present the feasible area for a *T-S* fuzzy system. Indeed, we compare the proposed fuzzy Lyapunov approaches (Theorem 3.4) with result provided by [17], and in [14, Theorem 6]. A second example is given to improve the given gains of robust PDC controller.

Example 5.1. Consider the following continuous *T-S* fuzzy system:

$$\dot{x}(t) = \sum_{i=1}^{r} h_i(z(t))A_ix(t), \tag{5.1}$$

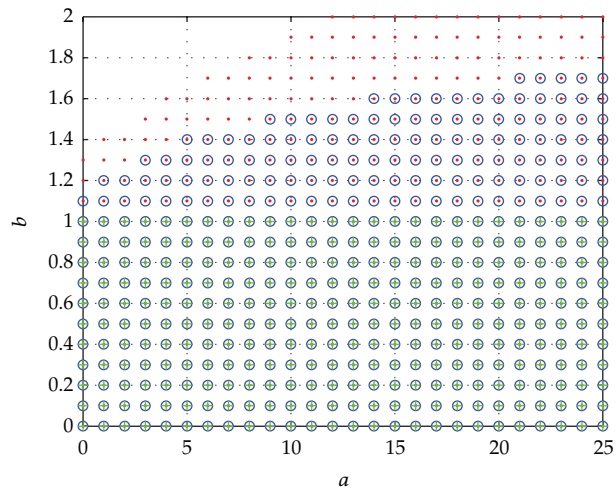

Figure 1: Feasible area provided by [17] (+), [14] (◯) and Theorem 3.1 (•).

with

$$r = 2; \qquad A_1 = \begin{bmatrix} 3.6 & -1.6 \\ 6.2 & -4.3 \end{bmatrix}, \qquad A_2 = \begin{bmatrix} -a & -1.6 \\ 6.2 & -4.3 \end{bmatrix},$$
$$B_1 = \begin{bmatrix} -0.45 \\ -3 \end{bmatrix}, \qquad B_2 = \begin{bmatrix} -b \\ -3 \end{bmatrix}, \tag{5.2}$$

where $a \in [0, 25]$, $b \in [0, 2]$, considering $\mu = 0.04$ and $\phi_{1,2} = 1$.

The proposed approach (Theorem 3.4) gives less conservative stabilization conditions (Figure 1) than some recent results provided by [14, 17].

Example 5.2. Consider the uncertain continuous *T-S* fuzzy system given by (2.8) with

$$r = 2; \qquad A_1 = \begin{bmatrix} 3.6 & -1.6 \\ 6.2 & -4.3 \end{bmatrix}, \qquad A_2 = \begin{bmatrix} -a & -1.6 \\ 6.2 & -4.3 \end{bmatrix},$$
$$B_1 = \begin{bmatrix} -0.45 \\ -3 \end{bmatrix}, \qquad B_2 = \begin{bmatrix} -b \\ -3 \end{bmatrix},$$
$$D_{a1} = E_{a1} = \begin{bmatrix} 0.3 & 0 \\ 0 & 0 \end{bmatrix}, \qquad D_{b1} = E_{b1} = \begin{bmatrix} 0.3 \\ 0 \end{bmatrix},$$
$$D_{a2} = E_{a2} = \begin{bmatrix} -0.2 & 0 \\ 0 & 0.3 \end{bmatrix}, \qquad D_{b2} = E_{b2} = \begin{bmatrix} -0.2 \\ 0.3 \end{bmatrix} \tag{5.3}$$

for $a = 1$, $b = 0.5$, considering $\mu = 0.04$, $\lambda = 0.1$ and $\phi_{1,2} = 1$, we find the following gains values:

$$\begin{gathered} F_1 = [-5.03401.5230], \qquad F_2 = [3.7868 - 0.8082], \\ K_1 = [-180.233465.7330], \qquad K_2 = [-180.949465.9073], \qquad R = [201.9216 - 71.7345]. \end{gathered} \tag{5.4}$$

6. Conclusion

This paper provided new conditions for the stabilization with a class of PDC controller of Takagi-Sugeno fuzzy systems in terms of a combination of the LMI approach and the use of nonquadratic Lyapunov function as fuzzy Lyapunov function. In addition, the time derivative of membership function is considered by the PDC fuzzy controller and the slack matrix variables are introduced in order to facilitate the stability analysis. An approach to design an observer is derived in order to estimate variable states. In addition, a new condition of the stabilization of uncertain system is given in this paper.

The stabilization condition proposed in this paper is less conservative than some of those in the literature, which has been illustrated via examples.

References

[1] T. Takagi and M. Sugeno, "Fuzzy identification of systems and its applications to modeling and control," *IEEE Transactions on Systems, Man and Cybernetics*, vol. 15, no. 1, pp. 116–132, 1985.

[2] M. A. L. Thathachar and P. Viswanath, "On the stability of fuzzy systems," *IEEE Transactions on Fuzzy Systems*, vol. 5, no. 1, pp. 145–151, 1997.

[3] L. K. Wong, F. H. F. Leung, and P. K. S. Tam, "Stability design of TS model based fuzzy systems," in *Proceedings of the 6th IEEE International Conference on Fussy Systems*, pp. 83–86, July 1997.

[4] I. Abdelmalek, N. Goléa, and M. L. Hadjili, "A new fuzzy Lyapunov approach to non-quadratic stabilization of Takagi-Sugeno fuzzy models," *International Journal of Applied Mathematics and Computer Science*, vol. 17, no. 1, pp. 39–51, 2007.

[5] C. H. Fang, Y. S. Liu, S. W. Kau, L. Hong, and C. H. Lee, "A new LMI-based approach to relaxed quadratic stabilization of T-S fuzzy control systems," *IEEE Transactions on Fuzzy Systems*, vol. 14, no. 3, pp. 386–397, 2006.

[6] H. K. Lam and F. H. Leung, *Analysis of Fuzzy Model based Control Systems*, Springer, Hong Kong, China, 2011.

[7] L. A. Mozelli, R. M. Palhares, F. O. Souza, and E. M. A. M. Mendes, "Reducing conservativeness in recent stability conditions of TS fuzzy systems," *Automatica*, vol. 45, no. 6, pp. 1580–1583, 2009.

[8] C. Hua and S. X. Ding, "Decentralized networked control system design using TS fuzzy approach," *IEEE Transactions on Fuzzy Systems*, vol. 20, no. 1, pp. 9–21, 2012.

[9] M. Chadli and T.-M. Guerra, "LMI solution for robust static output feedback control oftakagi-sugeno fuzzy models," *IEEE Transactions on Fuzzy Systems*. In press.

[10] M. Chadli and H. R. Karimi, "Robust observer design for unknown inputstakagi-sugeno models," *IEEE Transactions on Fuzzy Systems*. In press.

[11] K. Zhang, B. Jiang, and P. Shi, "Fault estimation observer design for discrete-time takagisugeno fuzzy systems based on piecewise lyapunov functions," *IEEE Transactions on Fuzzy Systems*, vol. 20, no. 1, pp. 192–200, 2012.

[12] S. Boyd, L. El Ghaoui, E. Feron, and V. Balakrishnan, *Linear Matrix Inequalities in System and Control Theory*, vol. 15, Society for Industrial and Applied Mathematics (SIAM), Philadelphia, Pa, USA, 1994.

[13] K. Tanaka and H. O. Wang, *Fuzzy Control Systems Design and Analysis: A Linear Matrix Inequality Approach*, John Wiley and Sons, 2001.

[14] L. A. Mozelli, R. M. Palhares, and G. S. C. Avellar, "A systematic approach to improve multiple Lyapunov function stability and stabilization conditions for fuzzy systems," *Information Sciences*, vol. 179, no. 8, pp. 1149–1162, 2009.

[15] K. Tanaka, T. Hori, and H. O. Wang, "A fuzzy Lyapunov approach to fuzzy control system design," in *Proceedings of the American Control Conference*, pp. 4790–4795, Arlington, Va, USA, June 2001.
[16] M. Yassine and B. Mohamed, "Condition of stabilisation for continuous takagi-sugeno fuzzy system based on fuzzy lyapunov function," *International Journal of Control and Automation*, vol. 4, no. 3, 2011.
[17] M. C. M. Teixeira, E. Assunção, and R. G. Avellar, "On relaxed LMI-based designs for fuzzy regulators and fuzzy observers," *IEEE Transactions on Fuzzy Systems*, vol. 11, no. 5, pp. 613–623, 2003.

Hindawi Publishing Corporation
Mathematical Problems in Engineering
Volume 2012, Article ID 973082, 18 pages
doi:10.1155/2012/973082

Research Article

H_∞ Fuzzy Control of DC-DC Converters with Input Constraint

D. Saifia,[1] M. Chadli,[2] S. Labiod,[1] and H. R. Karimi[3]

[1] *LAMEL, Faculty of Science and Technology, University of Jijel, BP. 98, Ouled Aissa, 18000 Jijel, Algeria*
[2] *MIS (EA 4290), Université de Picardie Jules Verne, Rue du Moulin Neuf, 80000 Amiens, France*
[3] *Department of Engineering, Faculty of Engineering and Science, University of Agder, 4898 Grimstad, Norway*

Correspondence should be addressed to M. Chadli, mohammed.chadli@u-picardie.fr

Received 6 June 2012; Accepted 9 September 2012

Academic Editor: Peng Shi

Copyright © 2012 D. Saifia et al. This is an open access article distributed under the Creative Commons Attribution License, which permits unrestricted use, distribution, and reproduction in any medium, provided the original work is properly cited.

This paper proposes a method for designing H_∞ fuzzy control of DC-DC converters under actuator saturation. Because linear control design methods do not take into account the nonlinearity of the system, a T-S fuzzy model and a controller design approach is used. The designed control not only handles the external disturbance but also the saturation of duty cycle. The input constraint is first transformed into a symmetric saturation which is represented by a polytopic model. Stabilization conditions for the H_∞ state feedback system of DC-DC converters under actuator saturation are established using the Lyapunov approach. The proposed method has been compared and verified with a simulation example.

1. Introduction

The main task of DC-DC converters is the adaptation of the voltage and current levels between sources and loads while maintaining a low power loss in the conversion [1–3]. With the extensive use of DC-DC converters in different industry applications (e.g. power supplies for personal computers, DC-motor drive, telecommunications equipment, etc.), improving their performances has become an interesting problem in recent years [1–17]. Recently, different converter circuits (buck converter, boost converter, buck-boost converter, Cuk converter, etc.) are known. According to each application purpose (increase or decrease the magnitude of the DC voltage and/or invert its polarity), the converter circuit was chosen. Among them, we consider here, the control of the basic Pulse-Width-Modulation (PWM) buck converters, but it could be easily adapted for other converters.

The DC-DC switching power converters are highly nonlinear systems [4, 5, 15, 16]. Consequently, the conventional linear controls based on averaging and linearization techniques [12, 14] will result in poor dynamic performance or system instability. In order to resolve this problem, the fuzzy logic approach has been proposed as an alternative solution [4, 5, 7, 8, 11, 13, 15, 16]. Specifically, in [4, 5], the authors have reported very significant results on the modelling and control of DC-DC converters with T-S fuzzy systems. In [4, 5, 8, 11, 15, 16], authors have proposed methods for designing fuzzy control of DC-DC converters. Nevertheless, in the aforementioned papers, they have not taken into account the inherent nonlinearity of actuator saturation (duty cycle) and the external disturbance. Motivated by this observation, our aim is to use T-S fuzzy systems in order to control a nonlinear DC-DC converter subject to external disturbances and actuator saturation.

The actuator saturation can degrade the performance of the closed-loop system and often make the stable closed-loop system unstable [1, 18–21]. The T-S fuzzy system in the presence of saturation has been receiving increasing attention for control of nonlinear systems [18–29]. In these works, the saturation effect is considered as a symmetric function. This is not the case in DC-DC converter application where the saturation function constrained is between 1 and 0. The solution of this problem proposed in linear control case [2] has been leading to complexity analysis with the nonlinearity of DC-DC converter model. Here, we proposed a simple mathematical transformation to obtain a symmetric saturation.

The H_∞ approach is used to analyze and to synthesize controllers/observers achieving an optimal level of disturbance attenuation and to guarantee the stability of the closed-loop system. To achieve this goal, the idea is to minimize the H_∞ norm which represents the maximum value ratio between the output signal energy (controlled output) and the input signal energy (disturbance input). Recently, many researchers have used this approach for control design of T-S fuzzy systems (see for example [20, 21, 30, 31] and their references). In most cases, the quadratic Lyapunov function and linear matrix inequality (LMI) techniques are used to analyze and synthesize of stabilization of T-S fuzzy systems [17–21, 30, 31]. Based on these works, we address the control problem of DC-DC converters via PDC controller with actuator saturation and external disturbance. In this paper, we will use T-S fuzzy systems to represent the DC-DC converters. The control design is based on the parallel distributed compensation (PDC) scheme [32]. The idea is that for each local linear model, a linear feedback control is designed. The control problem is formulated and solved as a LMI optimization problem [33].

This paper is organized as follows. Section 2 gives the averaged model of basic PWM buck converter. Section 3 presents the T-S fuzzy model of the DC-DC converter. Section 4 formulates the conditions for the H_∞ stabilization of fuzzy control with actuator saturation problem in terms of LMI. The simulation results to show the effectiveness of the proposed method are given in Section 4.

Notation 1. I_r denotes the set $\{1, 2, \ldots, r\}$, $\Re$ denotes the set of real number and $\Re^{n\times m}$ the set of all $n \times m$ real matrix. $M > (\geq, , <, \leq)$ is used to denote a symmetric positive definite (positive semidefinite, negative definite, negative semidefinite, resp.) matrix. * denotes the symmetric bloc matrix, $X + (^*)$ denotes $X + X^T$, $\times$ denotes the multiplication, co denotes the convex hull, and $\bigcap_{j=1}^{r}$ is used to denote the intersection of r sets.

2. Averaged Model of Basic PWM Buck Converter

Figure 1 shows the basic circuit of the nonlinear PWM buck converter proposed in [4, 5] with an external disturbance $i_{\text{load}}(t)$ as proposed in [1, 2]. R_m is the on-state resistance of the

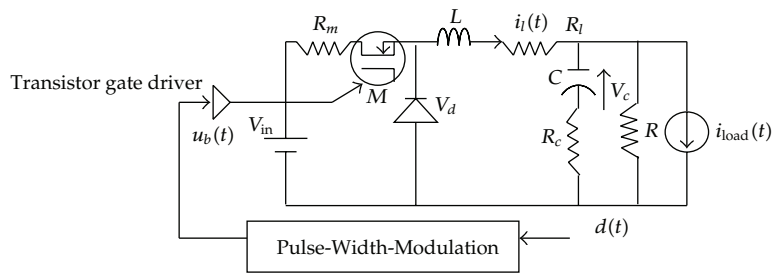

Figure 1: Schematic of a basic PWM buck converter.

MOSFET transistor, R_L is the winding resistance of inductor, V_d is the threshold voltage of the diode, and R_c is the equivalent series resistance of the filter capacitor.

By applying the Kirchhoff's voltage law (KVL) and Kirchhoff's current law (KCL) in on-state of the MOSFET transistor case, we obtain

$$\begin{bmatrix} \dot{i}_l(t) \\ \dot{v}_c(t) \end{bmatrix} = \begin{bmatrix} -\dfrac{1}{L}\left[R_l + \dfrac{RR_c}{R+R_c}\right] & -\dfrac{R}{L(R+R_c)} \\ \dfrac{R}{C(R+R_c)} & -\dfrac{1}{C(R+R_c)} \end{bmatrix} \begin{bmatrix} i_l(t) \\ v_c(t) \end{bmatrix} + \begin{bmatrix} \dfrac{1}{L}[V_{in} + R_m i_l(t)] \\ 0 \end{bmatrix} + \begin{bmatrix} \dfrac{RR_c}{L(R+R_c)} \\ -\dfrac{R}{C(R+R_c)} \end{bmatrix} i_{\text{load}}(t). \tag{2.1}$$

Now, in off-state of the MOSFET transistor case and by applying of KVL and KCL, we get

$$\begin{bmatrix} \dot{i}_l(t) \\ \dot{v}_c(t) \end{bmatrix} = \begin{bmatrix} -\dfrac{1}{L}\left[R_l + \dfrac{RR_c}{R+R_c}\right] & -\dfrac{R}{L(R+R_c)} \\ \dfrac{R}{C(R+R_c)} & -\dfrac{1}{C(R+R_c)} \end{bmatrix} \begin{bmatrix} i_l(t) \\ v_c(t) \end{bmatrix} + \begin{bmatrix} -\dfrac{V_d}{L} \\ 0 \end{bmatrix} + \begin{bmatrix} \dfrac{RR_c}{L(R+R_c)} \\ -\dfrac{R}{C(R+R_c)} \end{bmatrix} i_{\text{load}}(t). \tag{2.2}$$

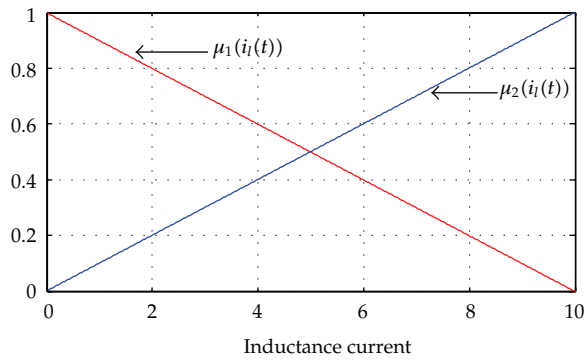

Figure 2: Membership functions of the T-S fuzzy model.

Using averaging method for one-time scale discontinuous system (AM-OTS-Ds) [9], the global dynamical behavior of the DC-DC converter is modeled as follows:

$$\begin{bmatrix} \dot{i}_l(t) \\ \dot{v}_c(t) \end{bmatrix} = \begin{bmatrix} -\dfrac{1}{L}\left[R_l + \dfrac{RR_c}{R+R_c}\right] & -\dfrac{R}{L(R+R_c)} \\ \dfrac{R}{C(R+R_c)} & -\dfrac{1}{C(R+R_c)} \end{bmatrix} \begin{bmatrix} i_l(t) \\ v_c(t) \end{bmatrix} + \begin{bmatrix} \dfrac{1}{L}[V_{in} + V_d + R_m i_l(t)] \\ 0 \end{bmatrix} d(t) + \begin{bmatrix} -\dfrac{V_d}{L} \\ 0 \end{bmatrix} + \begin{bmatrix} \dfrac{RR_c}{L(R+R_c)} \\ -\dfrac{R}{C(R+R_c)} \end{bmatrix} i_{\text{load}}(t), \tag{2.3}$$

where $d(t)$ is the duty cycle.

3. T-S Fuzzy Model of DC-DC Converter

Our control approach is based on T-S fuzzy models and the robustness of this control depends on the ability of the fuzzy model to represent the real system. In this section our objective is to show the effectiveness of T-S fuzzy model to represent the DC-DC converter.

The T-S fuzzy model has been successfully used to approximate nonlinear systems by interpolation of numerous local linear models [34].

R_i: If $\xi_1(t)$ is about M_{1i} and $\xi_q(t)$ is about M_{qi} then

$$\begin{aligned} \dot{x}(t) &= A_i x(t) + B_{1i} w(t) + B_{2i}\sigma(t) \\ z(t) &= C_{1i} x(t) + D_{1i} w(t) + D_{2i}\sigma(t) \end{aligned} \quad \text{For } i \in I_r \tag{3.1}$$

in which M_{ji} is the fuzzy set of ξ_i in rule R_i, r is the number of if-then fuzzy rules and $\xi_i(t)$ are the decision variable assumed measurable, $x(t) \in \Re^n$ is the system state vector, $\sigma(t) \in \Re^m$ is the saturate control input, $y(t) \in \Re^p$ is the measurable output, $z(t) \in \Re^{nz}$ is the controlled output variable, and $w(t) \in \Im_2$ is the disturbance variable with $\Im_2 = \{w \in \Re^{nw} \mid \|w\|_2 \leq \overline{w}, \overline{w} \succ 0\}$.

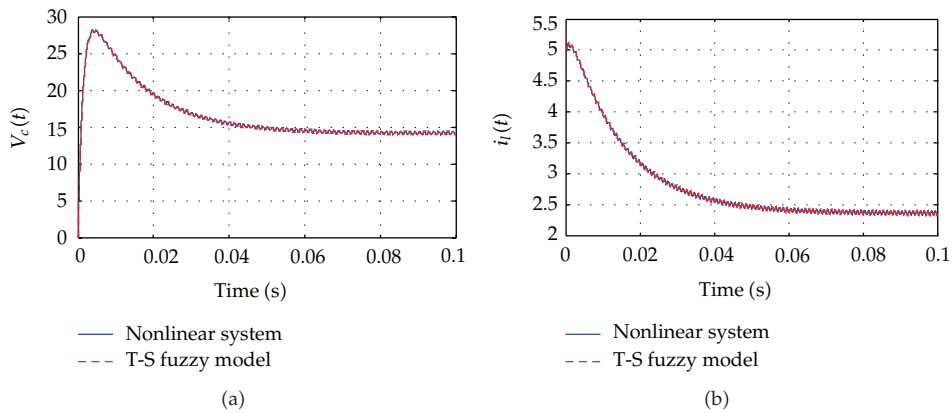

Figure 3: The nonlinear DC-DC converter responses and its T-S fuzzy representation with initial conditions $(v_c(0) = 0\,\mathrm{V},\ i_l(0) = 5\,\mathrm{A})$.

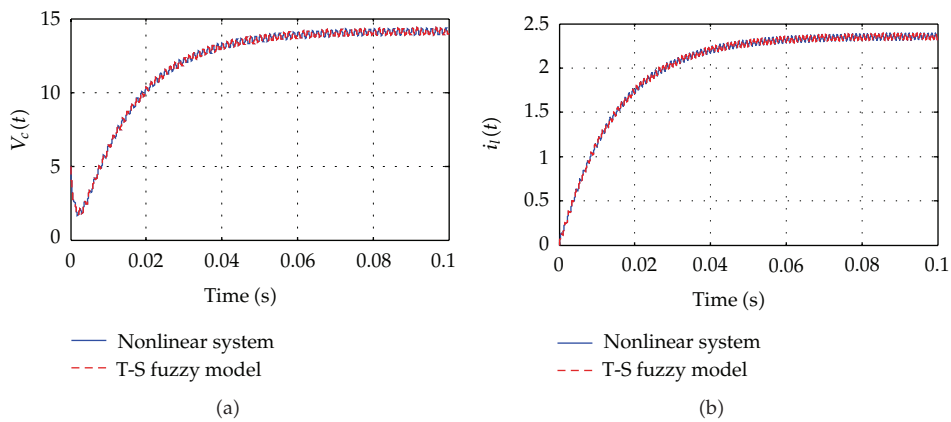

Figure 4: The nonlinear DC-DC converter responses and its T-S fuzzy representation with initial conditions $(v_c(0) = 5\,\mathrm{V},\ i_l(0) = 0\,\mathrm{A})$.

The global dynamic system is inferred as follows:

$$\begin{aligned} \dot{x}(t) &= \sum_{i=1}^{r} \mu_i(\xi(t))(A_i x(t) + B_{1i} w(t) + B_{2i}\sigma(t)), \\ z(t) &= \sum_{i=1}^{r} \mu_i(\xi(t))(C_{1i} x(t) + D_{1i} w(t) + D_{2i}\sigma(t)), \end{aligned} \tag{3.2}$$

where

$$\mu_i(\xi(t)) = \frac{\prod_{j=1}^{q} M_{ji}(\xi_j(t))}{\sum_{i=1}^{r}\left(\prod_{j=1}^{q} M_{ji}(\xi_j(t))\right)}, \tag{3.3}$$

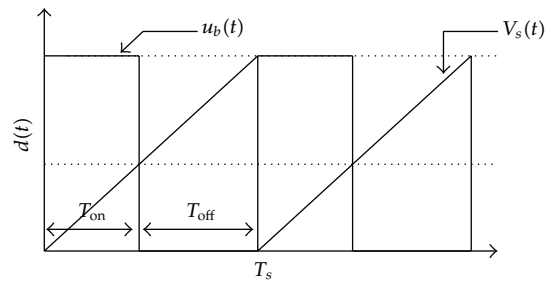

Figure 5: Waveforms of the PWM process.

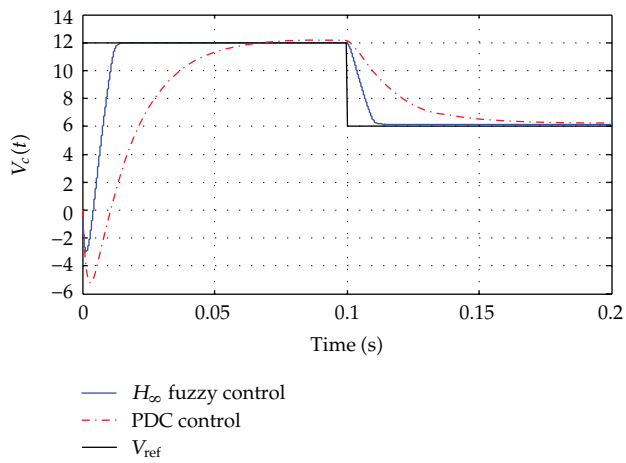

Figure 6: Response of the output voltage $v_c(t)$ of PWM buck converter.

$M_{ji}(\xi_j(t))$ is the grade of membership of $\xi_j(t)$ in M_{ji}. The normalized activation function $\mu_i(\xi(t))$ in relation with the ith submodel is such that

$$\sum_{i=1}^{r} \mu_i(\xi(t)) = 1 \quad 0 \le \mu_i(\xi(t)) \le 1 \ \forall i \in I_r, \tag{3.4}$$

Among different methods (identification method, linearization around different operating points, or by transformation in nonlinear sector), the method by transformation in nonlinear sector is based on bounded function and gives a minimum number of local models. Here we will use this method to represent the DC-DC converter.

The following Lemma will be used in the sequel of the paper.

Lemma 3.1. *Let $f(x(t)) : R \to R$ is a bounded function, it always exist tow functions, $\eta_1(x(t))$ and $\eta_2(x(t))$ and two scalars α and β such that:*

$$f(x(t)) = \alpha \times \eta_1(x(t)) + \beta \times \eta_2(x(t)) \tag{3.5}$$

with

$$\eta_1(x(t)) + \eta_2(x(t)) = 1, \quad \eta_1(x(t)) \geq 0,\ \eta_2(x(t)) \geq 0. \tag{3.6}$$

In this case, the obtained T-S fuzzy model represents exactly the nonlinear system for $x \in R^n$ with 2^{nl} locals models where nl represents the number of local models.

Assuming that, $I_{l\min} \leq i_l(t) \leq \mathrm{I}_{l\max}$ and by Lemma 3.1, the system described by (2.3) is modeled with a two-rules T-S fuzzy system as follows:

Rule 1: if $i_l(t)$ is about $I_{\min}$ then: $\dot{x}(t) = A_m x(t) + B_{m1} i_{\mathrm{load}}(t) + B_{m21} d(t) + D_m$.

Rule 2: if $i_l(t)$ is about $I_{\max}$ then: $\dot{x}(t) = A_m x(t) + B_{m1} i_{\mathrm{load}}(t) + B_{m22} d(t) + D_m$.

The overall model of T-S fuzzy system can be given by the following:

$$\dot{x}(t) = A_m x(t) + B_{m1} i_{\mathrm{load}}(t) + B_{m2\mu} d(t) + D_m, \tag{3.7}$$

with $x_1(t) = i_l(t)$, $x_2(t) = v_c(t)$, $B_{m2\mu} = \sum_{i=1}^{2} \mu_i(i_l(t)) B_{m2i}$ and

$$\begin{gathered} A_m = \begin{bmatrix} -\dfrac{1}{L}\left[R_l + \dfrac{RR_c}{R+R_c}\right] & -\dfrac{R}{L(R+R_c)} \\ \dfrac{R}{C(R+R_c)} & -\dfrac{1}{C(R+R_c)} \end{bmatrix}, \qquad B_{m21=} \begin{bmatrix} \dfrac{1}{L}(V_{in} + V_d + R_m I_{l\min}) \\ 0 \end{bmatrix}, \\ B_{m1} = \begin{bmatrix} \dfrac{RR_c}{L(R+R_c)} \\ -\dfrac{R}{C(R+R_c)} \end{bmatrix}, \qquad B_{m22=} \begin{bmatrix} \dfrac{1}{L}(V_{in} + V_d + R_m I_{l\max}) \\ 0 \end{bmatrix}, \qquad D_m = \begin{bmatrix} -\dfrac{V_d}{L} \\ 0 \end{bmatrix}. \end{gathered} \tag{3.8}$$

The membership function is such that

$$\mu_1(i_l(t)) = \frac{-i_l(t) + I_{l\max}}{I_{l\max} - I_{l\min}}, \qquad \mu_2(i_l(t)) = \frac{i_l(t) - I_{l\min}}{I_{l\max} - I_{l\min}}. \tag{3.9}$$

To show the effectiveness of the fuzzy model to represent the nonlinear system, we simulate the fuzzy model and the nonlinear system for the same inputs with different initial conditions. The simulation parameters used in this work are as follows [4]:

$$\begin{gathered} R = 6\,\Omega, \quad R_l = 48.5\,\mathrm{m}\Omega, \quad R_c = 0.16\,\Omega, \quad R_m = 0.27\,\Omega, \quad V_{in} = 30\,\mathrm{V}, \\ L = 98.58\,\mathrm{mH}, \quad C = 202.5\,\mu\mathrm{F}, \quad f = 1\,\mathrm{KH}, \quad I_{l\min} = 0\,\mathrm{A}, \quad I_{l\max} = 10\,\mathrm{A}, \end{gathered} \tag{3.10}$$

with $d(t) = 0.5$ and the input current $i_{\mathrm{load}}(t) = 0.25\sin(5000t)$.

Figure 2 shows the membership functions of the fuzzy model. The DC-DC converter responses of nonlinear system (2.3) and T-S fuzzy system (3.7) with initial conditions ($v_c(0) = 0\,\mathrm{V}$, $i_l(0) = 5\,\mathrm{A}$) and ($v_c(0) = 5\,\mathrm{V}$, $i_l(0) = 0\,\mathrm{A}$) are shown in Figures 3 and 4, respectively.

These figures demonstrate that, with different initial conditions, the T-S fuzzy system (2.3) has the same behaviour as the nonlinear system (3.7). This means the satisfactory approximation ability of the fuzzy model.

4. H_∞ Fuzzy Control of DC-DC Converter

In this section, we present an H_∞ fuzzy approach to the control design of DC-DC converter.

4.1. Saturated Control Analysis

In order to control the output voltage of the DC-DC converter, we define the following variables:

$$e_1(t) = v_c(t) - V_{\text{ref}}, \qquad e_2(t) = \dot{e}_1(t), \tag{4.1}$$

where V_{ref} is the reference voltage of $v_c(t)$.

The time-derivative of $e_2(t)$ is as follows:

$$\dot{e}_2(t) = \ddot{v}_c(t) = \frac{R}{C(R+R_c)}\dot{i}_l(t) - \frac{1}{C(R+R_c)}\dot{v}_c(t) - \frac{R}{C(R+R_c)}\dot{i}_{\text{load}}(t). \tag{4.2}$$

Using the converter's model defined in (2.3), we have

$$\begin{gathered}
\dot{x}(t) = Ax(t) + B_w w_1(t) + B_2(x)d(t) + D, \\
x_1(t) = e_1(t), \qquad x_2(t) = e_2(t), \qquad w_1(t) = \begin{bmatrix} i_{\text{load}}(t) \\ \dot{i}_{\text{load}}(t) \end{bmatrix}, \\
A = \begin{bmatrix} 0 & 1 \\ -\dfrac{(R+R_l)}{LC(R+R_c)} & -\dfrac{L + R_l C(R+R_c) + CRR_c}{LC(R+R_c)} \end{bmatrix}, \\
B_2(x) = \begin{bmatrix} 0 \\ \dfrac{R}{LC(R+R_c)}\left[V_{in} + V_d - R_m i_l(t)\right] \end{bmatrix}, \\
B_w = \begin{bmatrix} 0 & 0 \\ -\dfrac{R_l R}{LC(R+R_c)} & -\dfrac{R}{C(R+R_c)} \end{bmatrix}, \qquad D = \begin{bmatrix} 0 \\ -\dfrac{R(V_d + V_{\text{ref}}) + R_l V_{\text{ref}}}{LC(R+R_c)} \end{bmatrix}.
\end{gathered} \tag{4.3}$$

By Lemma 3.1, this system can be modeled with a two-rule T-S fuzzy system as follows:

Rule 1: if $i_l(t)$ is about $I_{\min}$ then: $\dot{x}(t) = Ax(t) + B_w w_1(t) + B_{21}d(t) + D$.

Rule 2: if $i_l(t)$ is about $I_{\max}$ then: $\dot{x}(t) = Ax(t) + B_w w_1(t) + B_{22}d(t) + D$.

and the global T-S fuzzy model can be given by the following:

$$\dot{x}(t) = Ax(t) + B_w w_1(t) + B_{2\mu}d(t) + D, \tag{4.4}$$

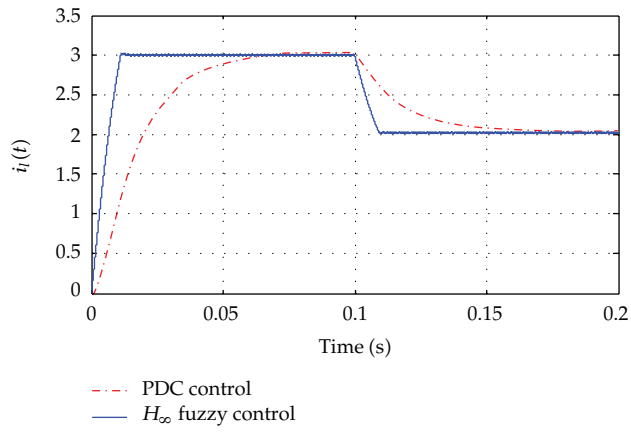

Figure 7: Response of the inductance current $i_l(t)$ of PWM buck converter.

with:

$$w_1(t) = \begin{bmatrix} i_{\text{load}}(t) \\ \dot{i}_{\text{load}}(t) \end{bmatrix}, \qquad B_{2\mu} = \sum_{i=1}^{2} \mu_i(i_l(t)) B_{2i},$$

$$B_{21} = \begin{bmatrix} 0 \\ \dfrac{R}{LC(R+R_c)}[V_{in} + V_d - R_m I_{l\min}] \end{bmatrix}, \qquad B_{22} = \begin{bmatrix} 0 \\ \dfrac{R}{LC(R+R_c)}[V_{in} + V_d - R_m I_{l\max}] \end{bmatrix}, \tag{4.5}$$

The output voltage of the DC-DC converter can be controlled by means of variation of duty cycle (Figure 1). The duty cycle is defined by the ratio T_{on}/Ts, where Ts is the frequency of the PWM circuit and T_{on} is the time when the MOSFET is on (Figure 5). A transistor gate driver (Figure 1) switches the MOSFET between the conducting (on) and blocking (off) states using a binary signal $u_b(t)$. This signal is produced by the modulator. In this operation, the duty cycle is compared with a sawtooth signal $V_s(t)$ of amplitude equals to 1. Consequently, the duty-cycle is constrained in amplitude between 0 and 1.

Thus, in this application, the control input is subject to actuator saturation with the following saturation:

$$0 \le d(t) \le 1, \tag{4.6}$$

which is not a symmetric saturation. However, most results reported in open literature have treated the controller design analysis with symmetric saturation [18–21]. To transform this saturation into a symmetric saturation, authors in [2] have proposed a change of variables to the linear converter model. This idea cannot be used in our case (nonlinear converter model) because it increases the complexity of the control analysis. Here, we will propose another idea that allows a simple analysis thereafter.

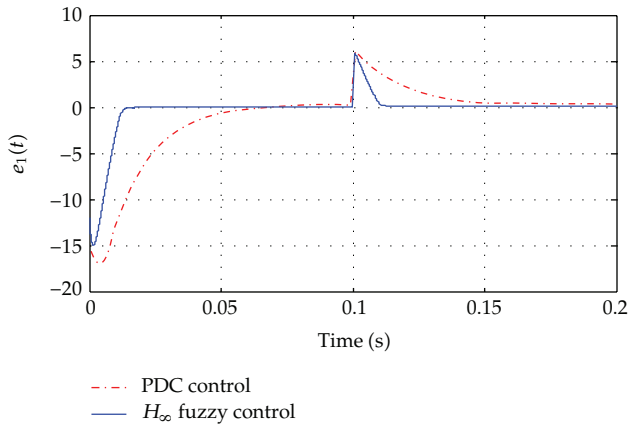

Figure 8: The trajectory of the error $e_1(t)$.

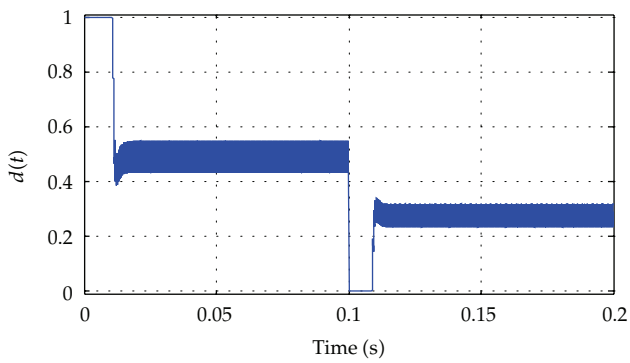

Figure 9: The trajectory of the saturated control (duty cycle $d(t)$).

The system described in (4.4) can be written as follows:

$$\begin{gathered}\dot{x}(t) = Ax(t) + B_w w_1(t) + B_2(x)\left(d(t) - \frac{1}{2}\right) + \frac{1}{2}B_2(x) + D, \\ \dot{x}(t) = Ax(t) + B_1 w(t) + B_2(x)\delta(t),\end{gathered} \tag{4.7}$$

with

$$\begin{aligned} w(t) = {} & \frac{1}{2}\frac{R}{LC(R+R_c)}[V_{in} + V_d - R_m i_l(t)] - \frac{R_l R}{LC(R+R_c)} i_{\text{load}}(t) \\ & - \frac{R}{C(R+R_c)}\dot{i}_{\text{load}}(t) - \frac{R(V_d + V_{\text{ref}}) + R_l V_{\text{ref}}}{LC(R+R_c)} \end{aligned} \tag{4.8}$$

is the external disturbance, $B_1 = [0 \;\; 1]^T$, and $\delta(t) = d(t) - 1/2$ is the new control input.

This last system can be represented with the following T-S fuzzy model:

$$\dot{x}(t) = Ax(t) + B_1 w(t) + B_{2\mu}\delta(t). \tag{4.9}$$

Thus, the new control input $\delta(t)$ is constrained as follows:

$$\frac{-1}{2} \leq \delta(t) \leq \frac{1}{2}. \tag{4.10}$$

In this work, the controller is a nonlinear state feedback which shares the same activation functions as the T-S fuzzy model (3.2) of the following form [32]:

$$\begin{gathered} u(t) = K_\mu x(t), \\ K_\mu = \sum_{j=1}^{r} \mu_j(\xi(t)) K_j, \end{gathered} \tag{4.11}$$

where and $K_j \in \Re^{m\times n}$ is the local controller matrix to be determined.

The control input is subject to actuator saturation the saturation function means:

$$\begin{gathered} \sigma(t) = \operatorname{sat}(u(t), \overline{u}) = [s_1, s_2, \ldots, s_m]^T, \\ s_i = \operatorname{sign}(u_i) \min\{\overline{u}_i, |u_i|\}, \end{gathered} \tag{4.12}$$

$\overline{u} \in R^m$ denotes the saturation level and $\overline{u}_i$ and u_i denote the ith element of $\overline{u}$ and $u(t)$. In our case:

$$\overline{u}_i = \overline{u} = 0.5. \tag{4.13}$$

The saturation obtained in (3.6) is a symmetric saturation and the following lemma can be used to the stability analysis.

Lemma 4.1 (see [18]). *Let E be the set of $m \times m$ diagonal matrices whose diagonal elements are 1 or 0. Suppose that $|v_i| \leq \overline{u}_i$ for all $i \in I_m$, where v_i and u_i denote the ith element of $v \in \Re^m$ and $u \in \Re^m$, respectively. If $x \in \bigcap_{j=1}^{r} \Im(H_j)$ for $x \in \Re^n$, then:*

$$\begin{gathered} \operatorname{sat}(u, \overline{u}) = \sum_{s=1}^{2^m} \alpha_s \left(E_s u + \overline{E}_s v\right), \\ \sum_{s=1}^{2^m} \alpha_s = 1, \quad 0 \leq \alpha_s \leq 1, \\ v = \sum_{j=1}^{r} \mu_j H_j x, \\ \Im(H_j) = \left\{x \in \Re^n \mid \left|h_i^j x\right| \leq \overline{u}_i\right\}, \end{gathered} \tag{4.14}$$

where E_s denotes all elements of E, $\overline{E}_s = I - E_s$, H_j is $m \times n$ matrix and h_i^j is the ith row of the matrix H_j.

In our case $m = 1$, $E_s \in \mathrm{co}\{0, 1\}$, $\overline{u}_1$ is the saturation level ($\overline{u}_1 = 1/2$) and $r(r = 2)$ is the number of local models. Consequently, the saturation function in (4.10) can be rewritten as follows:

$$\mathrm{sat}\left(K_\mu x(t)\right) = \left(E_\alpha K_\mu + \overline{E}_\alpha H_\mu\right) x(t), \tag{4.15}$$

with

$$\left|h_i^j x\right| \leq \frac{1}{2}, \quad \forall i \in I_m,\ j \in I_r, \tag{4.16}$$

and $H_\mu = \sum_{i=1}^{2} \mu_i H_i$, $E_\alpha = \sum_{s=1}^{2} \alpha_s E_s$ and $\overline{E}_\alpha = \sum_{s=1}^{2} \alpha_s \overline{E}_s$.

4.2. Quadratic Lyapunov Stability

For a constant $\rho > 0$ and a symmetric positive matrix P, define an ellipsoid as follows:

$$\varepsilon(P, \rho) = \left\{x \in \Re^n \mid x^T P x \leq \rho\right\}. \tag{4.17}$$

This ellipsoid can be rewritten as follows:

$$\varepsilon(P, \rho) = \left\{x \in \Re^n \mid x^T \mathbf{P} x \leq 1\right\} \tag{4.18}$$

$\rho \succ 0$, this implied that $\mathbf{P} = P/\rho \in \Re^{n \times n}$ is a symmetric positive matrix.

We define the Lyapunov function as follows:

$$V(x) = x(t)^T \mathbf{P} x(t). \tag{4.19}$$

An ellipsoid $\varepsilon(p, \rho)$ is said to be contractively invariant set if $\dot{V}(x) < 0$, for all $x \in \varepsilon(P, \rho) \mid \{0\}$. Therefore, if an ellipsoid is contractively invariant, it is inside the domain of attraction.

An ellipsoid $\varepsilon(P, \rho) = \{x \in R^n \mid x^T \mathbf{P} x \leq 1\}$ is inside $\bigcap_{j=1}^{r} \Im(H_j)$ if and only if for all $i \in I_m$, $j \in I_r$:

$$\left(h_i^j\right)^T \mathbf{P} h_i^j \leq \overline{u}_i^2 I. \tag{4.20}$$

In order to design a DC-DC converter to perform adequately in the presence of external disturbances, the H_∞ attenuation performance is chosen as the performance measure, which is defined as follows:

$$\int_0^T z(\tau)^T z(\tau) d\tau < \gamma^2 \int_0^T w(\tau)^T w(\tau) d\tau, \tag{4.21}$$

where γ is a positive scalar and small as possible, $w(t) \in L_2[0\ \ 1]$ and $x(0) = 0$.

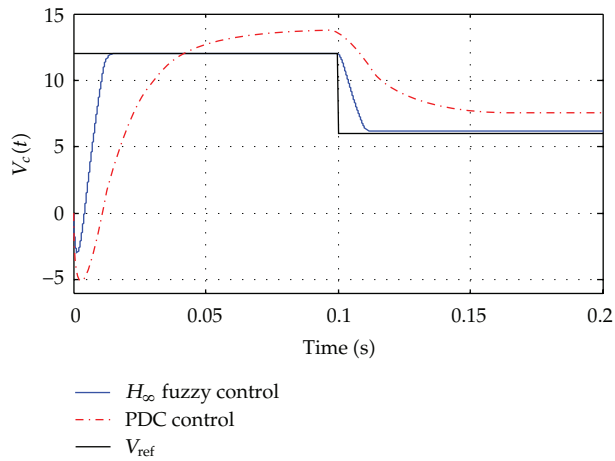

Figure 10: Response of the output voltage $v_c(t)$ of PWM buck converter for 1 kHz.

In our problem, the controlled output is the error $e_1(t)$, that is:

$$z(t) = C_1 x(t), \tag{4.22}$$

where $C_1 = [0 \;\; 1]$. The closed-loop system composed of (4.9), (4.22), and (4.15) is given by the following:

$$\begin{aligned} \dot{x}(t) &= \left(A + B_{2\mu}\left(E_\alpha K_\mu + \overline{E}_\alpha H_\mu\right)\right)x(t) + B_{m1}w(t), \\ z(t) &= C_1 x(t). \end{aligned} \tag{4.23}$$

Theorem 4.2. *The ellipsoid $\varepsilon(P,\rho)$ is contractively invariant set of the closed-loop system* (4.15) *and achieves in a disturbance rejection level γ, if there exist a symmetric positive definite matrix Q and matrices $F_j \in \Re^{m\times n}$, solutions of the following LMI problem:*

$$\min_{Q,F_j,Z_j}^{\gamma}, \tag{4.24}$$

$$\begin{bmatrix} \dfrac{1}{4} & z_i^j \\ \left(z_i^j\right)^T & Q \end{bmatrix} \geq 0, \quad \forall i \in I_m,\ j \in\ I_r \tag{4.25}$$

$$\begin{bmatrix} AQ + B_{2i}E_sF_j + B_{2i}\overline{E}_sZ_j + (*) & * & * \\ B_1^T & -\gamma I & * \\ C_1Q & 0 & -\gamma I \end{bmatrix} < 0, \quad \forall i \in I_r,\ j \in I_r. \tag{4.26}$$

Then one gets

$$K_j = F_jQ^{-1}, \qquad H_j = Z_jQ^{-1}. \tag{4.27}$$

Using Lemma 3.1 for inequality (4.20)*, one has:*

$$\left(h_i^j\right)^T \mathbf{P} h_i^j \leq \frac{1}{4}, \quad \forall i \in I_m,\ j \in I_r. \tag{4.28}$$

Let the following change of variables:

$$Q = \mathbf{P}^{-1}, \tag{4.29}$$

$$Z_j = H_j Q. \tag{4.30}$$

Consequently, the inequality (4.28) *can be rewritten as follows*

$$\frac{Q}{4} - \left(z_i^j\right)^T z_i^j \geq 0, \tag{4.31}$$

where z_i^j is the ith row of the matrix Z_j. By Schur complement [33], this last inequality can be transformed as LMI (4.25)*.*

Proposition 4.3 (see [30]). *If the Lyapunov function defined in* (4.19) *satisfies the following Hamilton-Jacobi-Bellman inequality:*

$$\dot{V}(x(t)) + \gamma^{-1} z(t)^T z(t) - \gamma w(t)^T w(t) < 0, \tag{4.32}$$

along (4.23) *for all $x(t) \neq 0$ and $w(t) \in L_2[0\ \ 1] \triangleq \{w \in \Re^{nw} \mid \int_0^T \|w\|^2 dt \leq \overline{w}, \overline{w} > 0\}$, then* (4.21) *is verified. Using* (4.23)*, one has:*

$$\begin{aligned}
&\dot{V}(x(t)) - \gamma w(t)^T w(t) + \gamma^{-1} z(t)^T z(t) \\
&\quad = \begin{bmatrix} x(t) \\ w(t) \end{bmatrix}^T \left\{ \begin{bmatrix} \left(A + B_{2\mu} E_s K_\mu + B_{2\mu} \overline{E}_s H_\mu\right)^T \mathbf{P} + (*) & * \\ B_1^T \mathbf{P} & -\gamma I \end{bmatrix} + \gamma^{-1} \begin{bmatrix} C_1^T \\ 0 \end{bmatrix} \begin{bmatrix} C_1 & 0 \end{bmatrix} \right\} \begin{bmatrix} x(t) \\ w(t) \end{bmatrix}.
\end{aligned} \tag{4.33}$$

By Schur complement [13], the condition (4.32) *holds if*

$$\Sigma_\mu = \begin{bmatrix} \mathbf{P}^T \left(A + B_{2\mu} E_s K_\mu + B_{2\mu} \overline{E}_s H_\mu\right) + (*) & * & * \\ B_1^T \mathbf{P} & -\gamma I & * \\ C_1 & 0 & -\gamma I \end{bmatrix} < 0. \tag{4.34}$$

Pre- and postmultiplying this last inequality by $\Gamma = \operatorname{diag}(Q, I, I)$ *one has*

$$\Gamma\Sigma_\mu\Gamma = \begin{bmatrix} A_iQ + B_{2i}E_sK_jQ + B_{2i}\overline{E}_sH_jQ + (*) & * & * \\ B_1^T & -\gamma I & * \\ C_1Q & 0 & -\gamma I \end{bmatrix} < 0. \tag{4.35}$$

Taking account (4.27) *and* (4.30)*, one gets the following LMI:*

$$\Gamma\Sigma_\mu\Gamma = \begin{bmatrix} A_\mu Q + B_{2\mu}F_\mu + (*) & * & * \\ B_1^T & -\gamma I & * \\ C_1Q & 0 & -\gamma I \end{bmatrix} < 0, \tag{4.36}$$

which ends the proof.

4.3. The Initial Conditions Constraint

The main purpose of the DC-DC converter control is to maintain the voltage level $v_c(t)$ equal to the desired level V_{ref}. The initial condition for the state vector is as follows:

$$x_0 = \begin{bmatrix} x_1(0) & x_2(0) \end{bmatrix}^T = \begin{bmatrix} e_1(0) & e_2(0) \end{bmatrix}^T = \begin{bmatrix} V_{\text{ref}} & 0 \end{bmatrix}^T. \tag{4.37}$$

However, it is not possible to assure that any initial condition will belong to the ellipsoid of stability given in Theorem 4.2. In this section, the objective is to guarantee the start up stability with maximum elimination of external disturbances in the presence of saturation.

The point $x_0 \in \varepsilon(P, \rho)$ is equivalent to the following:

$$x_0^T \mathbf{P} x_0 \leq 1. \tag{4.38}$$

Or in LMI form by the following:

$$\begin{bmatrix} 1 & x_0^T \\ x_0 & Q \end{bmatrix} \geq 0. \tag{4.39}$$

The optimization problem proposed in Theorem 4.2 can be formulated as follows:

$$\begin{gathered} \min_{Q, F_j, Z_j}^{\gamma}. \\ \text{LMI}(4.27),\ \text{LMI}(4.28),\ \text{LMI}(4.41) \end{gathered} \tag{4.40}$$

4.4. Simulation Results

In order to demonstrate the effectiveness of the proposed method, the DC-DC converter is controlled by the proposed H_∞-based state feedback and the PDC controller proposed in [4].

In this simulation, the current perturbation step equals to 1 A and the PWM frequency equals to 5 kHz.

Solving the optimization problem described in (4.40) for initial condition $x_0 = [12V \quad 0]^T$, we have:

$$Q = \begin{bmatrix} 817.3975 & -6.1238 \times 10^5 \\ -6.1238 \times 10^5 & 5.5691 \times 10^5 \end{bmatrix}, \quad H_1 = H_2 = [-0.0354 \quad 0],$$
$$\gamma = 0.7255, \quad K_1 = [-1.4681 \quad -0.0016], \quad K_2 = [-1.5030 \quad -0.0017]. \tag{4.41}$$

The control is defined by $d(t) = \mathrm{sat}(K_\mu x(t)) + 1/2$.

Figures 6, 7, and 8 show the DC-DC converter responses (output voltage and inductance current, resp.). Figure 9 shows the trajectory of the saturated control input signal (duty cycle $d(t)$). Figure 8 shows, with the presence of saturation, the H_∞ control can guarantee the stability of all initial conditions in the interval $e_1(0) \in [-12V \quad 12V]$ in presence of actuator saturation and external disturbances (see initial time and 0.1 s time).

Simulation results (Figures 6–8) demonstrate that our controller guarantees better stabilization performance, better perturbation rejection (see initial time in Figure 6) and better time response (see Figures 6–8) Moreover, the proposed controller is robust with respect to frequency change. Figure 10 shows the simulation results for a frequency of 1 kHz. It shows that our controller achieves better performance even with different frequency values.

Despite that we take into account not only the actuators saturation but also the external disturbance in the designing control, our controller gives better stabilization performance (perturbation rejection and better time response) of the system as reported in the open literature [4]. Moreover, with different frequency values, our saturated control gives robust control signal (guarantees the same performances despite the change of frequency). These results demonstrate the effectiveness of proposed method.

5. Conclusion

This work has presented an H_∞ controller design for DC-DC converters via state feedback under actuator saturation and external disturbances. The T-S fuzzy system is first used to describe the DC-DC converter. Then, the state controller is designed to guarantee the stability of the closed loop system with H_∞ performance. The saturation effect is represented by a polytopic model. Based on Lyapunov approach, the problem of H_∞ stabilization in the presence of actuator saturation was formulated as an LMI optimization and solved easily by using existing numerical tools. Finally, the simulation results on a DC-DC converter have demonstrated the effeteness of the proposed control.

The analysis given here is applied to the buck converter; we can extend this work to other converters (boost converter, buck-boost converter, Cuk converter, etc.). Finally, the results developed in the paper can be extended to the case that the underlying systems are involved with any switching dynamics such as a nondeterministic or stochastic switching system (see [35–37]).

References

[1] H.-S. Kim, J. H. Kim, B. D. Min, D. W. Yoo, and H. J. Kim, "A highly efficient PV system using a series connection of DC-DC converter output with a photovoltaic panel," *Renewable Energy*, vol. 34, no. 11, pp. 2432–2436, 2009.

[2] C. Olalla, I. Queinnec, R. Leyva, and A. El Aroudi, "Robust optimal control of bilinear DC-DC converters," *Control Engineering Practice*, vol. 19, no. 7, pp. 688–699, 2011.

[3] J.-K. Kaldellis, "The wind potential impact on the maximum wind energy penetration in autonomous electrical grids," *Renewable Energy*, vol. 33, no. 7, pp. 1665–1677, 2008.

[4] Y. Li and Z. Ji, "T-S modeling, simulation and control of the Buck converter," in *Proceedings of the 5th International Conference on Fuzzy Systems and Knowledge Discovery, FSKD 2008*, pp. 663–667, Schandong, China, October 2008.

[5] K. Y. Lian, J. J. Liou, and C. Y. Huang, "LMI-based integral fuzzy control of DC-DC converters," *IEEE Transactions on Fuzzy Systems*, vol. 14, no. 1, pp. 71–80, 2006.

[6] I. Gadoura, T. Suntio, and K. Zenger, "Model uncertainty and robust control of paralleled DC/DC converters," in *Proceedings of the 15th World IFAC Congress on Power Electronics, Machines and Drives*, pp. 74–79, Barcelona, Spain, April 2002.

[7] D. Alejo, P. Maussion, and J. Faucher, "Multiple model control of a Buck dc/dc converter," *Mathematics and Computers in Simulation*, vol. 63, no. 3–5, pp. 249–260, 2003.

[8] K. Guesmi, N. Essounbouli, A. Hamzaoui, J. Zaytoon, and N. Manamanni, "Shifting nonlinear phenomena in a DC-DC converter using a fuzzy logic controller," *Mathematics and Computers in Simulation*, vol. 76, no. 5-6, pp. 398–409, 2008.

[9] J. Sun and H. Grotstollen, "Averaged modelling of switching power converters: reformulation and theoretical basis," in *Proceedings of the Power electronics specialists Conference*, pp. 1165–1172, Taledo, Spain, 1992.

[10] A. Shahin, B. Huang, J. P. Martin, S. Pierfederici, and B. Davat, "New non-linear control strategy for non-isolated DC/DC converter with high voltage ratio," *Energy Conversion and Management*, vol. 51, no. 1, pp. 56–63, 2010.

[11] K. Guesmi, N. Essounbouli, and A. Hamzaoui, "Systematic design approach of fuzzy PID stabilizer for DC-DC converters," *Energy Conversion and Management*, vol. 49, no. 10, pp. 2880–2889, 2008.

[12] F. D. Tan and R. D. Middlebrook, "Unified model for current-programmed converters," *IEEE Transactions on Power Electronics*, vol. 10, no. 4, pp. 397–408, 1995.

[13] C. Elmas, O. Deperlioglu, and H. H. Sayan, "Adaptive fuzzy logic controller for DC-DC converters," *Expert Systems with Applications*, vol. 36, no. 2, pp. 1540–1548, 2009.

[14] P. R. K. Chetty, "Modelling and design of switching regulators," *IEEE Transactions on Aerospace and Electronic Systems*, vol. 18, no. 3, pp. 333–344, 1982.

[15] H. K. Lam, T. H. Lee, F. H. E. Leung, and P. K. S. Tam, "Fuzzy control of DC-DC switching converters: stability and robustness analysis," in *Proceedings of the 27th Annual Conference of the IEEE Industrial Electronics Society*, Denver, Colo, USA, December 2001.

[16] H. K. Lam and S. C. Tan, "Stability analysis of fuzzy-model-based control systems: application on regulation of switching DC-DC converter," *IET Control Theory & Applications*, vol. 3, no. 8, pp. 1093–1106, 2009.

[17] S. Bououden, M. Chadli, S. Filali, and A. El Hajjaji, "Fuzzy model based multivariable predictive control of a variable speed wind turbine: LMI approach," *Renewable Energy*, vol. 37, no. 1, pp. 434–439, 2012.

[18] Y. Y. Cao and Z. Lin, "Robust stability analysis and fuzzy-scheduling control for nonlinear systems subject to actuator saturation," *IEEE Transactions on Fuzzy Systems*, vol. 11, no. 1, pp. 57–67, 2003.

[19] D. Saifia, M. Chadli, and S. Labiod, "Static output feedback stabilization of multiple models subject to actuators saturation," in *Proceedings of the 12th IFAC Symposium on Large Scale Systems*, Villeneuve d'Ascq, France, 2011.

[20] D. Saifia, M. Chadli, and S. Labiod, "H∞ control of multiple model subject to actuator saturation: application to quarter-car suspension system," *Analog Integrated Circuits and Signal Processing*, pp. 1–10, 2011.

[21] T. Zhang, G. Feng, H. Liu, and J. Lu, "Piecewise fuzzy anti-windup dynamic output feedback control of nonlinear processes with amplitude and rate actuator saturations," *IEEE Transactions on Fuzzy Systems*, vol. 17, no. 2, pp. 253–264, 2009.

[22] C. P. Huang, "Model based fuzzy control with affine T-S delayed models applied to nonlinear systems," *International Journal of Innovative Computing*, vol. 8, no. 5, pp. 2979–2993, 2012.

[23] C.-H. Sun, Y.-T. Wang, C.-C. Chang, and T.-S. Switching, "Fuzzy model-based guaranteed cost control for two-wheeled mobile robots," *International Journal of Innovative Computing A*, vol. 8, no. 5, pp. 3015–3028, 2012.

[24] L. Wu, X. Su, P. Shi, and J. Qiu, "A new approach to stability analysis and stabilization of discrete-time T-S fuzzy time-varying delay systems," *IEEE Transactions on Systems, Man, and Cybernetics B*, vol. 41, no. 1, pp. 273–286, 2011.

[25] L. Wu, X. Su, P. Shi, and J. A. Qiu, "Novel approach to filter design for T-S fuzzy discrete-time systems with time-varying delay," *IEEE Transactions on Fuzzy Systems*, vol. PP, no. 99, p. 1, 2012.

[26] C.-H. Sun, S.-W. Lin, and Y.-T. Wang, "Relaxed stabilization conditions for switching T-S fuzzy systems with practical constraints," *International Journal of Innovative Computing*, vol. 8, no. 6, pp. 4133–4145, 2012.

[27] X. Su, L. Wu, P. Shi, and Y. D. . Song, "H_∞ model reduction of T-S fuzzy stochastic systems," *IEEE Transactions on Systems, Man, and Cybernetics B*, vol. PP, no. 99, pp. 1–12, 2012.

[28] L. Wu, X. Su, P. Shi, and J. Qiu, "Model approximation for discrete-time state-delay systems in the TS fuzzy framework," *IEEE Transactions on Fuzzy Systems*, vol. 19, no. 2, pp. 366–378, 2011.

[29] X. H. Chang and G. H. Yang, "Relaxed results on stabilization and state feedback H∞ control conditions for T-S fuzzy systems," *International Journal of Innovative Computing, Information and Control*, vol. 7, no. 4, pp. 1753–1764, 2011.

[30] H. J. Lee and D. W. Kim, "Robust stabilization of T-S fuzzy systems: fuzzy static output feedback under parametric uncertainty," *International Journal of Control, Automation and Systems*, vol. 7, no. 5, pp. 731–736, 2009.

[31] M. Chadli and P. Borne, "Design of robust static output controller for uncertain fuzzy model: an LMI formulation," *Studies in Informatics and Control*, vol. 16, pp. 421–430, 2007.

[32] K. Tanaka, T. Ikeda, and H. O. Wang, "Fuzzy regulators and fuzzy observers: relaxed stability conditions and LMI-based designs," *IEEE Transactions on Fuzzy Systems*, vol. 6, no. 2, pp. 250–265, 1998.

[33] S. Boyd, L. El Ghaoui, E. Feron, and V. Balakrishnan, *Linear Matrix Inequalities in System and Control Theory*, Society for Industrial and Applied Mathematics (SIAM), Philadelphia, Pa, USA, 1994.

[34] T. Takagi and M. Sugeno, "Fuzzy identification of systems and its applications to modeling and control," *IEEE Transactions on Systems, Man and Cybernetics*, vol. 15, no. 1, pp. 116–132, 1985.

[35] L. Zhang and J. Lam, "Necessary and sufficient conditions for analysis and synthesis of Markov jump linear systems with incomplete transition descriptions," *IEEE Transactions on Automatic Control*, vol. 55, no. 7, pp. 1695–1701, 2010.

[36] L. Zhang and P. Shi, "Stability, L2-gain and asynchronous H_∞ control of discrete-time switched systems with average dwell time," *IEEE Transactions on Automatic Control*, vol. 54, no. 9, pp. 2192–2199, 2009.

[37] L. Zhang, N. Cui, M. Liu, and Y. Zhao, "Asynchronous filtering of discrete-time switched linear systems with average dwell time," *IEEE Transactions on Circuits and Systems*, vol. 58, no. 5, pp. 1109–1118, 2011.